Title
Spectral Observations and Analyses of Low-Redshift Type Ia Supernovae

Author
Silverman, Jeffrey Michael

Publication Date
2011

Peer reviewed|Thesis/dissertation

Spectral Observations and Analyses of Low-Redshift Type Ia Supernovae

by

Jeffrey Michael Silverman

A dissertation submitted in partial satisfaction of the
requirements for the degree of
Doctor of Philosophy

in

Astrophysics

in the

Graduate Division
of the
University of California, Berkeley

Committee in charge:
Professor Alexei V. Filippenko, Chair
Professor Eliot Quataert
Professor Steven E. Boggs

Fall 2011

Spectral Observations and Analyses of Low-Redshift Type Ia Supernovae

Abstract

Spectral Observations and Analyses of Low-Redshift Type Ia Supernovae

by

Jeffrey Michael Silverman
Doctor of Philosophy in Astrophysics

University of California, Berkeley

Professor Alexei V. Filippenko, Chair

The explosive deaths of stars, known as a supernovae (SNe), have been critical to our understanding of the Universe for centuries. From the first evidence of a changing Universe beyond the Moon (Brahe 1573) to the first evidence of the accelerating expansion of the Universe (Riess et al. 1998; Perlmutter et al. 1999), SNe – and often a specific subclass of SNe called Type Ia SNe (SNe Ia) – have been integral to astronomical research. An introduction to SNe, their importance in astronomy, and how we observe them is given in Chapter 1. How SNe Ia explode, what progenitor systems give rise to them, and how different initial conditions affect the observed outcomes of these objects are understood only at a relatively basic level. In other words, a detailed understanding of the physics behind SNe Ia is still lacking. One way astronomers can begin to solve these problems, and others involving SNe Ia, is to obtain and analyze a large, self-consistent dataset of SN Ia observations. This is the goal of the Berkeley SN Ia Program (BSNIP) which comprises the majority of this Thesis.

In the second Chapter, I present the full BSNIP sample which consists of 1298 low-redshift ($z \leq 0.2$) optical spectra of 582 SNe Ia observed from 1989 through the end of 2008. Many of the SNe have well-calibrated light curves with measured distances as well as spectra which have been corrected for host-galaxy contamination. Most of the data were obtained using the Kast double spectrograph mounted on the Shane 3 m telescope at Lick Observatory with typical wavelength coverage of 3300–10400 Å, which is significantly larger than that of most previously published SN Ia spectral datasets. I also present the BSNIP observing and reduction procedures used during the two decades over which the data were collected. In addition, I describe our spectral classification scheme (using the SuperNova IDentification code, SNID; Blondin & Tonry 2007), utilizing my newly constructed set of SNID spectral templates. These templates allow me to accurately spectroscopically classify the entire BSNIP dataset, and by doing so I am able to reclassify a handful of objects as bona fide SNe Ia and a few other objects as members of some of the peculiar SN Ia subtypes. In fact, the BSNIP dataset includes spectra of nearly 90 spectroscopically peculiar SNe Ia. I also present spectroscopic host-galaxy redshifts of some SNe Ia where these values were previously unknown. The sheer size of the BSNIP dataset and the consistency of the observation and reduction methods makes this sample unique among all other published SN Ia datasets and is

complementary in many ways to the large, low-redshift SN Ia spectra presented by Matheson et al. 2008 and Blondin et al. 2011.

I present measurements of spectral features of 432 low-redshift ($z < 0.1$) optical spectra within 20 d of maximum brightness of 261 SNe Ia from the BSNIP sample in the third Chapter. I describe in detail my method of automated, robust spectral feature definition and measurement which expands upon similar previous studies. Using this procedure, I attempt to measure expansion velocities, (pseudo-)equivalent widths (pEWs), spectral feature depths, and fluxes at the center and endpoints of each of nine major spectral feature complexes. A sanity check of the consistency of the measurements is performed using the BSNIP data (as well as a separate spectral dataset). I investigate how velocity and pEW evolve with time and how they correlate with each other. Various spectral classification schemes are employed and quantitative spectral differences among the subclasses are investigated. Several ratios of pEW values are calculated and studied. Furthermore, SNe Ia that show strong evidence for interaction with circumstellar material or an aspherical explosion are found to have the largest near-maximum expansion velocities and pEWs, possibly linking extreme values of spectral observables with specific progenitor or explosion scenarios. A discussion of the relative merits of various classification schemes is presented and I find that purely spectroscopic classification schemes are useful in identifying the most peculiar SNe Ia. However, in almost all spectral parameters investigated the full sample of objects spans a nearly continuous range of values. Comparisons to previously published theoretical models of SNe Ia are made and some of the predictions of these models match the observations presented here. I conclude with a brief discussion of how these measurements and the possible correlations presented will be crucial to future SN surveys.

The fourth Chapter of this Thesis presents comparisons of spectral feature measurements to photometric properties of 115 low-redshift ($z < 0.1$) SNe Ia with optical spectra within 5 d of maximum brightness. The spectral data come from the BSNIP sample described in Chapter 2, and the photometric data come mainly from the Lick Observatory Supernova Search (LOSS) and are published by Ganeshalingam et al. (2010). The spectral measurements come from BSNIP II (Chapter 3 of this Thesis) and the light-curve fits and photometric parameters can be found in Ganeshalingam et al. (in preparation). A variety of previously proposed correlations between spectral and photometric parameters are investigated using the large and self-consistent BSNIP dataset. We also use a combination of light-curve parameters (specifically the SALT2 stretch and color parameters x_1 and c) and spectral measurements to calculate distance moduli. The residuals from these models is then compared to the standard model which only uses light-curve stretch and color. The pEW of Si II λ4000 is found to be a good indicator of light-curve width and the pEWs of the Mg II and Fe II complexes are relatively good proxies for color. However, a distance model only using these spectroscopic measurements performs worse than the standard model which uses only light-curve parameters. When using a distance model which combines the ratio of fluxes near $\sim$3600 Å and $\sim$4300 Å with both x_1 and c, the Hubble residuals are decreased by 12%, which is found to be significant at the 2.4σ level. The weighted root-mean square

of the residuals using this model is 0.130 ± 0.019 mag (as compared to 0.146 ± 0.019 mag when using the same sample with the standard model). This Hubble diagram fit has one of the smallest scatters ever published and at the highest significance ever seen in such a study. Finally, these results are discussed with regard to how they can improve the cosmological accuracy of future, large-scale SN Ia surveys.

Finally, I conclude this Thesis with an in-depth study of a quite peculiar SN Ia, not included in the BSNIP sample. Chapter 5 presents and analyzes optical photometry and spectra of the extremely luminous and slowly evolving Type Ia SN 2009dc, and offers evidence that it is a super-Chandrasekhar mass (SC) SN Ia and thus had a SC white dwarf (WD) progenitor. Optical spectra of SN 2007if, a similar object, are also shown. SN 2009dc had one of the most slowly evolving light curves ever observed for a SN Ia, with a rise time of $\sim$23 d and $\Delta m_{15}(B) = 0.72$ mag. I calculate a lower limit to the peak bolometric luminosity of $\sim 2.4 \times 10^{43}$ erg s^{-1}, though the actual value is likely almost 40% larger. Optical spectra of SNe 2009dc and 2007if obtained near maximum brightness exhibit strong C II features (indicative of a significant amount of unburned material), and the post-maximum spectra are dominated by iron-group elements. All of the spectra of SNe 2009dc and 2007if also show low expansion velocities. However, I see no strong evidence in SN 2009dc for a velocity "plateau" near maximum light like the one seen in SN 2007if (Scalzo et al. 2010). The high luminosity and low expansion velocities of SN 2009dc lead to a derived WD progenitor mass of more than 2 $M_\odot$ and a ^{56}Ni mass of about 1.4–1.7 $M_\odot$. I propose that the host galaxy of SN 2009dc underwent a gravitational interaction with a neighboring galaxy in the relatively recent past. This may have led to a sudden burst of star formation which could have produced the SC WD progenitor of SN 2009dc and likely turned the neighboring galaxy into a "post-starburst galaxy." No published model seems to match the extreme values observed in SN 2009dc, but simulations do show that such massive progenitors can exist (likely as a result of the merger of two WDs) and can possibly explode as SC SNe Ia.

For my entire family and all of my friends.
None of this would have been possible without you.

The Scientist does not study nature because it is useful to do so. He studies it because he takes pleasure in it, and he takes pleasure in it because it is beautiful. If nature were not beautiful it would not be worth knowing, and life would not be worth living.
—Jules Henri Poincaré

Contents

List of Figures

List of Tables

Acknowledgments

First and foremost thank you to $\mathcal{R}^2 + \mathcal{M}$ (Ryans Foley and Chornock plus Mohan Ganeshalingam) who taught me (almost) everything I know about supernova observations, data reduction, and cosmology. Your advice and help over the years made all of this possible and made me the astronomer I am today. Next, a big thanks to my adviser: Alex, there is never a dull moment working with you. And thank you to the rest of my committee as well: Steve Boggs, Eliot Quataert, and Josh Bloom.

My Thesis would not have been possible without a few other key members of the Flipper Group (and SuperNova Affiliated Grad Students) who helped me enormously. Thank you to Weidong Li, Dan Perley, Brad Cenko, Adam Miller, Thea Steele, Dovi Poznanski, Maryam Modjaz, Nathan Smith, and Frank Serduke for all the help, support, and guidance throughout my graduate school career. I hope that I have successfully passed along at least some of my knowledge to the younger generation of astronomers who have worked with me. Thank you to Nick Lee, Emily Miller, Chris Griffith, Io Kleiser, and Jason Kong for helping with observations, reductions, whipping the SuperNova DataBase into shape, and (among other things) for showing me how hard it is to teach people to code. I must honor my forefathers as well. Thank you to Tom Matheson, Aaron Barth, Doug Leonard, Luis Ho, and Joe Shields; your hard work over the decades was critical to much of my Thesis. Thanks also to my amazing officemates: Kristen Shapiro, Andrew Wetzel, Peter Williams, Aaron Parsons, Erik Petigura, and Katie Silverio. They let me blast my music in the office and were extremely helpful with procrastinating.

A huge thanks to all of the people who helped obtain data used in my Thesis or who have provided helpful scientific comments and conversations throughout the years: K. Alatalo, I. Arcavi, L. Armus, M. Baker, B. Barris, M. Bentz, E. Berger, M. Bershady, S. Blondin, A. Blum, A. Burgasser, N. Butler, G. Canalizo, H. Chen, J. Choi, B. Cobb, A. Coil, M. Cooper, C. DeBreuck, L.-B. Desroches, M. Dickinson, R. Eastman, M. Ellison, M. Eracleous, S. Faber, X. Fan, C. Fassnacht, P. Garnavich, E. Gates, M. George, D. Gilbank, A. Gilbert, K. Glazebrook, J. Graham, G. Graves, R. Green, J. Greene, M. Gregg, M. Hidas, K. Hiner, W. Ho, J. Hoffman, I. Hook, P. Hopkins, D. Howell, D. Hutchings, L. Jewett, S. Jha, V. Junkkarinen, M. Kandrashoff, L. Kewley, R. Kirshner, M. Kislak, D. Kocevski, S. Kulkarni, M. Lehnert, B. Leibundgut, J. Leja, K. Maeda, M. Malkan, K. Mandel, A. Martel, M. McCourt, M. Moore, E. Moran, A. Morton, R. Mostardi, P. Nandra, J. Newman, K. Noeske, P. Nugent, M. Papenkova, C. Papovich, X. Parisky, S. Park, C. Peng, S. Perlmut-

ter, M. Phillips, D. Pooley, H. Pugh, C. Reuter, J. Rex, M. Rich, M. Richmond, A. Riess, S. Rodney, K. Sandstrom, W. Sargent, J. Scala, R. Scalzo, K. Shimasaki, J. Shiode, R. Simcoe, T. Small, G. Smith, H. Smith, H. Spinrad, G. Squires, C. Steidel, D. Stern, D. Stevens, R. Street, B. Swift, C. Thornton, P. Thrasher, J. Tonry, T. Treu, B. Tucker, D. Tytler, W. van Breugel, S. Van Dyk, V. Virgilio, V. Viscomi, N. Vogt, J. Walsh, X. Wang, D. Weisz, C. Willmer, A. Wolfe, D. Wong, J.-H. Woo, and M. Yamanaka.

I am extremely grateful to the very talented staff at the Lick and Keck Observatories for their support. I specifically want to thank (former and current) Lick staff members Bernie Walp, Kris Miller, Elenor Gates, Thomas Lowe, Wayne Earthman, and Keith Baker, as well as Keck staff members Greg Wirth, Marc Kassis, and Hien Tran. Their telescope and instrument expertise was integral to this work. I also wish to recognize and acknowledge the very significant cultural role and reverence that the summit of Mauna Kea has always had within the indigenous Hawaiian community; I am most fortunate to have the opportunity to conduct observations from this mountain.

Last, but not least, I want to thank the very generous Marc J. Staley who in part supported me with the Marc J. Staley Graduate Fellowship in Astronomy. He never stopped asking the Great Questions and I hope he has found some Great Answers.

Chapter 1

Introduction

Since the beginning of time, man has yearned to destroy the Sun.
—Charles Montgomery Burns, Billionaire and Owner of the Springfield Nuclear Power Plant

Observational astronomy is unique among all other sciences. The vast majority of astronomical observations are done with telescopes that gather light which has travelled mind-boggling distances through the Universe. It is the job of the observational astronomer to observe the Cosmos and attempt to explain what they find. Nature alone presents the observational astronomer with objects to study and thus the observational astronomer has no laboratory. Other scientists often create experiments to test their hypotheses and then alter the experimental conditions in a (relatively) controlled way to investigate the outcomes of these alterations. Observational astronomers have no such luxury; they are at the mercy of whatever Nature reveals to them. I am an observational astronomer.

Furthermore, observational astronomy is one of the oldest professions. Since ancient times humans all over the planet have gazed upon the heavens in wonder and seen images in the stars (i.e., constellations). Nearly all ancient cultures associated the Moon, Sun, planets, and constellations with characters and objects from their mythology and thus observational astronomy has almost always been integral to the heritage, culture, and sociology of mankind. The *science* of observational astronomy is almost as old. Many ancient civilizations studied the motion of the Moon, Sun, planets, and stars and used this knowledge to create calendars and track the seasons, allowing these civilizations to thrive and progress technologically and culturally.

Transient astronomical phenomena were observed in ancient times as well. A cliff painting by the Ancient Pueblo Peoples known as the "Supernova Platograph" (see Figure 1.1) near Chaco Canyon, NM, USA is likely a representation of a new star that appeared in the sky in July of the year 1054. This new object was the explosive death of a star known as a supernova (SN) and these objects are the main focus of this Thesis. Despite its relative closeness, this exploding star had no detrimental impact on the Earth. However, SNe closer to Earth or other types of stellar explosions or outbursts (including some from our own Sun)

Figure 1.1: A cliff painting by the Ancient Pueblo Peoples known as the "Supernova Platograph" near Chaco Canyon, NM, USA. This is likely a representation of a new star (actually a supernova) that appeared in the sky in July of the year 1054. The supernova is represented by the starburst toward the lower left. The relative position of the Moon and its phase is represented by the crescent. The hand gives a sense of scale on the sky. *Image Credit: James Dale.*

can disable Earth-orbiting satellites, disrupt electrical power grids on the ground, damage the planet's atmosphere, and possibly destroy life on Earth.

Nonstellar astronomical objects can also have a catastrophic affect on the planet. The Chicxulub crater underneath the Yucatán Peninsula in Mexico was likely created by a meteorite that was at least 10 km in diameter and is thought to be responsible for the extinction of the dinosaurs roughly 65 million years ago (see Figure 1.2). Such a disaster may be avoided in the future through careful astronomical observations. However, observational astronomy is not just about protecting the Earth, it is also about finding our place in the Cosmos. Where do the Sun, Earth, and humans fit into the Grand Scheme of the Universe? Where did we come from and where are we going? How did it all start and how will it all end? These are just a few of the biggest and deepest questions one can ask, and observational astronomy is one of the most direct scientific ways to answer them.

Figure 1.2: An artist's conception of the impending extinction of the dinosaurs about 65 million years ago due to a 10 km meteorite. *Image Credit: Lee Krystek.*

1.1 What are Light, Photometry, and Spectroscopy?

1.1.1 Light

Electromagnetic (EM) radiation (i.e., light) is the how most observational astronomers study the Universe. Telescopes capture light from astronomical objects which is then recorded and analyzed. Light comes in a variety of flavors classified by wavelength (or, equivalently, frequency or energy) which is collectively referred to as the EM spectrum (see Figure 1.3). There is of course the familiar "visible," or optical, part of the spectrum (i.e., the colors of the rainbow that humans are able to see) and this is the main part of the EM spectrum which this Thesis is concerned with. However, much of the data presented herein cover parts of the ultraviolet and infrared regions of the EM spectrum as well. A small amount of data from other parts of the EM spectrum are also presented and discussed in this Thesis.

1.1.2 Photometry

Spectroscopy is not photometry. In astronomy, photometry is a way of measuring the intensity of EM radiation observed from an object. In essence this is currently done by attaching a camera to a telescope and taking a picture using charge-coupled devices (CCDs), which are at the heart of most digital cameras (see Figure 1.4). While some of the work herein involves photometry, that is not that main thrust this Thesis.

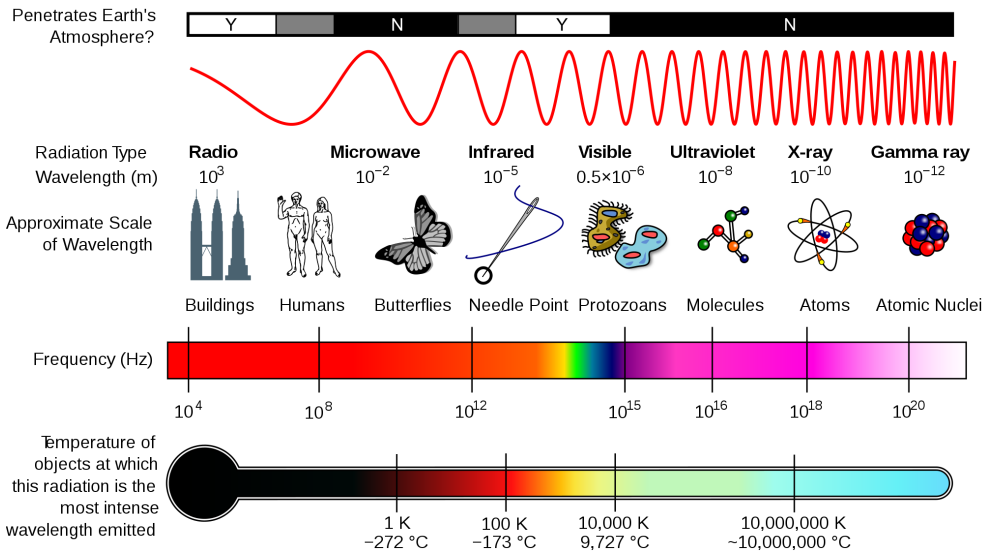

Figure 1.3: The electromagnetic spectrum showing each region and its wavelength (with size comparisons), frequency, black-body emission temperature, and whether or not the majority of the wavelength regime penetrates the Earth's atmosphere. *Image Credit: NASA.*

1.1.3 Spectroscopy

Spectroscopy is the main observational technique used in this Thesis. It involves dispersing the light from astronomical objects using a prism (or similar optical element) into its constituent wavelengths. The brightness at each wavelength is then recorded, thus producing a "spectrum." A rainbow is a crude form of spectroscopy where water droplets in the air act as the dispersive element. When looking at a rainbow with the naked eye, all colors seem to be approximately the same brightness. This is referred to as a continuous spectrum (see Figure 1.5, *Top*).

However, if one uses a more sensitive spectrometer to look at a rainbow, one would see that some very specific colors (or wavelengths) would be darker than others. These are referred to as absorption lines (see Figure 1.5, *Bottom*). The opposite case, where certain wavelengths are much brighter than others, is referred to as emission lines (see Figure 1.5, *Middle*). Each element in the Periodic Table produces a very specific set of absorption or emission lines and thus they can be used much like a fingerprint to identify which elements (or molecules) are present in an astronomical object. This is one of the biggest strengths of spectroscopy. Further information about what can be measured and inferred from astrophysical spectra is discussed in Chapter 3.

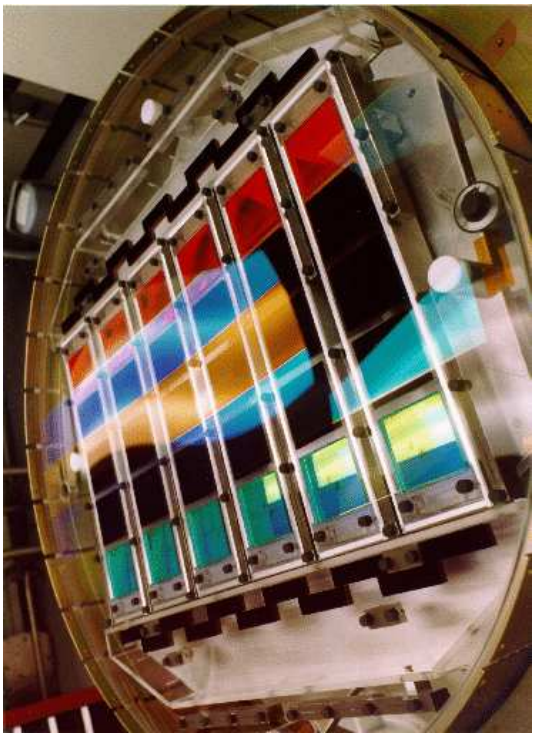

Figure 1.4: Faceplate of the CCDs on the main imaging camera of the Sloan Digital Sky Survey (SDSS) telescope. *Image Credit: SDSS.*

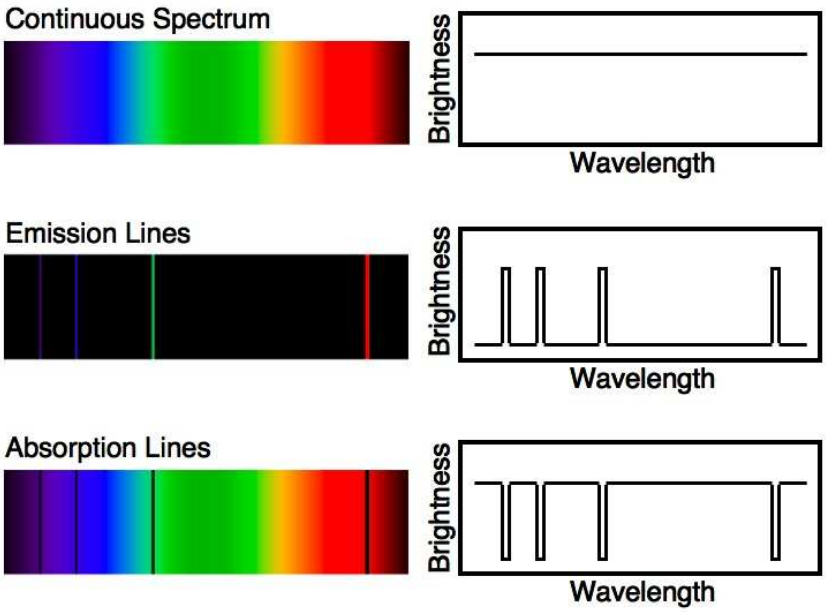

Figure 1.5: The three basic kinds of spectra. The left column shows "2-dimensional spectra" while the right column shows "1-dimensional spectra." *Image Credit: Adapted from graphics by Wikimedia Commons.*

1.2 Why Study Supernovae?

As mentioned above, SNe are the explosive deaths of stars and have been observed since ancient times. Accounts of SNe from the 16$^{\rm th}$ century demonstrated that the Heavens were not unchanging beyond the Lunar Sphere. At the end of the 20$^{\rm th}$ century, observations of SNe led to the discovery of a form of anti-gravity known as "dark energy" which is responsible for the acceleration of the expansion of the Universe. In even more recent years they have been used to accurately measure cosmological parameters of our Universe. Furthermore, the energy in SNe can trigger nearby clouds of gas to begin to collapse, which is the first step in forming new generations of stars (and planets and life). Thus the death of one star can lead to the birth of new stars, thereby completing the Cosmic Circle of Life.

Many of the elements that are built up through nuclear fusion during the life of a star are released only in a SN explosion and it is only in this explosion that most of the elements in the Periodic Table are formed naturally. Thus the Earth and all the life it supports would not exist without a generation of stars older than the Sun having already gone supernova and expelled their atoms into clouds of gas and dust, one of which would later form the Solar System. Without supernovae, we would not be here. As the great American astronomer and author Carl Sagan said, "We are made of star stuff." This statement could not be more true.

1.3 What are Supernovae?

The classification of SNe has a long and tortured past. The first distinction made between different types of SNe was based on whether the optical spectrum showed evidence for hydrogen (Type II) or not (Type I). Eventually it was noticed that many Type I SNe had spectra with strong silicon features, while some had weak or no evidence for silicon in their optical spectra. The latter were refereed to as Type I-peculiar objects. By the 1980s astronomers had further subdivided the Type I SNe into three broad categories: Ia, Ib, and Ic. The Type Ia SNe (SNe Ia) are the original Type I objects with strong silicon features and are the main focus of this Thesis. The Type Ib SNe (SNe Ib) and Type Ic SNe (SNe Ic) are the Type I-peculiar objects with little to no silicon in their spectra. Under the modern classification, SNe Ib are objects which show strong helium features, while the SNe Ic are objects that do not show evidence for helium in their spectra. As is discussed later in this Thesis, these four major subclasses can be further subdivided into many other sub-subclasses.

1.3.1 Core-Collapse Supernovae

SNe II, Ib, and Ic are collectively known as core-collapse SNe (CCSNe), and it is thought that most high-mass stars ($\gtrsim 8$ M$_\odot$, where 1 M$_\odot$ is the mass of the Sun, or $\sim 2 \times 10^{33}$ g) end their lives as CCSNe. As a high-mass star evolves it fuses heavier and heaver elements in its core until the center of the star becomes predominantly made of iron. Since iron fusion is

an endothermic process, this iron core is inert and produces no new energy, and eventually there is insufficient outward pressure to balance the inward pressure of gravity from the other layers of the star. This leads to a collapse, rebound, and explosion that we observe as a CCSN.

As discussed above, the three subclasses of CCSNe are distinguished based on the strength of hydrogen and helium in their optical spectra. If a star still has its outermost layer of hydrogen intact at the time of explosion then it is likely that strong hydrogen features will be observed in its spectrum and it would be classified as a SN II. If the star loses most or all of its outer hydrogen layer, but retains its helium layer, then helium (but little to no hydrogen) will be seen in its spectrum and it would be called a SN Ib. Finally, if the star loses both its hydrogen and helium layers before core collapse, then neither of these elements would be observed in a spectrum and it would likely be classified as a SN Ic. It is thought that stellar outflows and eruptions or mass transfer to a binary companion before explosion are responsible for the removal of the hydrogen and helium layers in SNe Ib and Ic.

1.3.2 Thermonuclear Supernovae

SNe Ia (the focus of this Thesis), sometimes called thermonuclear SNe, do *not* come from the collapse of a massive star. Broadly speaking, SNe Ia are the result of thermonuclear explosions of extremely dense stellar remnants known as white dwarfs (WDs). WDs are the end state of stellar evolution for stars $\lesssim 8$ $M_\odot$ and are composed of electron-degenerate matter. Most WDs are made mainly of carbon and oxygen, though lower mass WDs may be made primarily of helium and higher mass WDs are comprised of oxygen, neon, and magnesium. They have masses comparable to that of the Sun but volumes comparable to that of the Earth, and they glow through emission of stored thermal energy.

In 1930, Indian astrophysicist Subrahmanyan Chandrasekhar predicted that WDs should have a maximum mass, above which a WD cannot support itself against its own gravity. This so-called "Chandrasekhar Limit" is calculated today to be about 1.4 $M_\odot$. If a WD gradually gains mass through accretion from a nondegenerate binary companion, the WD will shrink and its core temperature will rise. As the mass of the WD approaches the Chandrasekhar Limit, the core becomes hot enough to ignite carbon fusion. This results in the WD undergoing a runaway thermonuclear explosion which unbinds the star and a SN Ia is born.

Instead of slowly accreting mass from a nondegenerate companion, a WD could instead merge with another degenerate object. If the combined mass is above the Chandrasekhar Limit then an explosion similar to the one described above could result. This would also give rise to a SN Ia, but perhaps with different observational signatures. Specifically, the total mass in an explosion with this type of progenitor system could be as large as almost twice the Chandrasekhar Limit (if both WDs are slightly less massive than the limit). It is possible that astronomers have seen a handful of these so-called "super-Chandrasekhar mass SNe Ia" and one such object is the focus of the last chapter of this Thesis. Despite the very

general descriptions given above for two different progenitor scenarios for SNe Ia, the exact nature of the binary companion and the details of the explosion itself are both still quite uncertain.

The cosmological utility of SNe Ia comes from the fact that they can be calibrated as precise distance indicators. To do this, astronomers need to standardize their luminosity (i.e., the amount of energy they produce). In 1993, it was shown that the width of a supernova light curve (i.e., how long it takes a supernova to brighten and then fade away) is well correlated with luminosity at peak brightness for most SNe Ia. This is the so-called "Phillips relation" and it helps astronomers calculate distances to SNe Ia. However, nearly two decades after this observation was first published, astronomers are still searching for other parameters in SN observations which could make our measurements of the distances to SNe Ia even more accurate.

1.4 Why Write this Thesis?

How most of the heavy elements are formed and disbursed through the Cosmos is intimately tied to how SNe explode. The progenitors and explosion physics of SNe Ia are still not very well understood. Distances to SNe Ia *must* be more accurate in order to perform better "precision cosmology" and to better understand dark energy and the accelerating expansion of the Universe. To make improvements on all of these fronts and to understand SNe Ia themselves better, one needs a large dataset of well-observed objects. The Berkeley SN Ia Program (BSNIP) is just such a dataset.

BSNIP is two decade's worth of spectra of SNe Ia, many of which have companion photometry. It is one of the largest datasets of its kind and the observations, data reduction, and analysis have been extremely self-consistent over the years. The data are all low redshift ($z \leq 0.2$), meaning that the SNe Ia are closer than $\sim$800 Mpc $\approx 2.5 \times 10^{27}$ cm. This may sound like a huge distance but in the world of SN research it is considered quite nearby. SNe that are further away will usually be detectable for less time than the nearer ones and thus a more complete dataset can be compiled using observations of only the nearest SNe Ia.

However, lots of data alone are not enough to make good scientific progress. One must actually analyze the data in order to gain any understanding from them. By carefully, consistently, and robustly measuring various aspects of the spectral features seen in SNe Ia one can hope to learn more about the explosions themselves and the environments in which they occur. These spectral measurements should then be combined with photometric data to paint a more complete picture of SNe Ia. While huge datasets are all well and good, one should not underestimate the importance of detailed studies of individual objects. These types of studies are invaluable when the object under investigation is peculiar, and it is often by studying the most extreme objects that one learns the most about the bulk of the population.

The construction and collation of the BSNP dataset, its analysis (both with and without photometric data), and an in-depth study of an extremely peculiar SN Ia make up this

Thesis. In Chapter 2, I present the full BSNIP sample as well as the observing and reduction procedures used to create the dataset. I also discuss the automated spectral classification scheme used to reclassify a handful of objects as bona fide SNe Ia and a few other objects as members of some of the peculiar SN Ia subtypes. Chapter 3 presents measurements of spectral features of a subset of the BSNIP data, focusing on spectra within 20 d of maximum brightness. There I also describe my method of automated, robust spectral feature definition and measurement, and I investigate how the spectral parameters evolve with time and correlate with each other. The final BSNIP chapter (Chapter 4) combines the results from Chapter 3 with photometric data and presents evidence for correlations between spectroscopic and photometric observables. I also show some of the most accurate distances to SNe Ia ever calculated and describe how this is achievable using the combination of light-curve measurements as well as spectral measurements. Finally, as mentioned previously, I conclude (Chapter 5) with a detailed study of a possible super-Chandrasekhar mass SNe Ia not included in the BSNIP sample: SN 2009dc. There I present and analyze optical photometry and spectra of this extremely luminous and slowly evolving SN Ia, and offer evidence that it is indeed a super-Chandrasekhar mass SN Ia.

Chapter 2

Berkeley Supernova Ia Program I: Spectroscopy of 582 Type Ia Supernovae

It's been said that Astronomy is a humbling, and I might add, a character-building experience.
—Carl Sagan

2.1 Introduction

Throughout the history of astronomy, supernovae have been integral to our understanding of the cosmos—from demonstrating that the Heavens were not unchanging beyond the lunar sphere (Brahe 1573) to the discovery of the acceleration of the expansion of the Universe (Riess et al. 1998; Perlmutter et al. 1999). Type Ia supernovae (SNe Ia) have been particularly useful in recent years as a way to accurately measure cosmological parameters (Astier et al. 2006; Riess et al. 2007; Wood-Vasey et al. 2007; Hicken et al. 2009a; Kessler et al. 2009; Amanullah et al. 2010). Broadly speaking, SNe Ia are the result of thermonuclear explosions of C/O white dwarfs (WDs) (e.g., Hoyle & Fowler 1960; Colgate & McKee 1969; Nomoto et al. 1984; see Hillebrandt & Niemeyer 2000 for a review). However, we still lack a detailed understanding of the progenitor systems and explosion mechanisms, as well as how differences in initial conditions create the variance in observed properties of SNe Ia. To solve these problems, and others, detailed and self-consistent observations of many hundreds of SNe Ia are required.

The cosmological application of SNe Ia as precise distance indicators relies on being able to standardize their luminosity. Phillips (1993) showed that light-curve decline is well correlated with luminosity at peak brightness for most SNe Ia, the so-called "Phillips relation". Additionally, people have searched for a "second parameter" in SN observations which would make our measurements of the distances to SNe Ia even more precise. Recently, Foley & Kasen (2011) found that the intrinsic maximum-light color of SNe Ia depends on their ejecta

velocity at maximum brightness. After accounting for this color difference, the scatter in residuals to the Hubble diagram is decreased from 0.190 mag to 0.130 mag for a subset of SNe Ia. This observation was only possible with a large set of spectroscopically observed objects, with many of the spectra coming from the sample described in this Chapter (Wang et al. 2009a).

Until now there have been several statistical samples of low-redshift SN Ia photometry (e.g., Hamuy et al. 1996b; Riess et al. 1999b; Jha et al. 2006b; Hicken et al. 2009b; Ganeshalingam et al. 2010), but only one large sample of low-redshift SN Ia spectroscopy (Matheson et al. 2008; Blondin et al. 2011). Until the publication of over 432 spectra of 32 SNe Ia by Matheson et al. (2008), large samples of SN Ia spectra were typically constructed by combining datasets published for individual objects, usually from many different groups.

The Berkeley Supernova Ia Program (BSNIP) is a large-scale effort to measure the properties of low-redshift ($z \leq 0.2$) SNe Ia, focusing on optical spectroscopy and photometry (see Ganeshalingam et al. 2010, for the companion photometry paper to much of the spectroscopic sample presented here). One aspect of our strategy for the last two decades has been to observe as many SNe Ia as possible in order to dramatically increase the number of objects with spectroscopic data. We have also attempted to obtain good temporal spectral coverage of peculiar objects as well as objects which were also being observed photometrically by our group. In addition, we strove to spectroscopically classify all SNe discovered by the 0.76 m Katzman Automatic Imaging Telescope (KAIT; Filippenko et al. 2001). By observing and reducing our spectra in a consistent manner, we avoid many of the systematic differences found in previous samples constructed from data from various groups.

In this chapter we present the low-redshift SN Ia spectral dataset. This sample consists of a total of 1298 spectra of 582 SNe Ia observed from 1989 through the end of 2008. The SNe, along with information about their host galaxies, is presented in Table 2.1. Information regarding the SN Ia spectra in the dataset is listed in Table 2.2. Many spectra presented in this chapter have complementary light curves from Hamuy et al. (1996b), Riess et al. (1999b), Jha et al. (2006b), Hicken et al. (2009b), and Ganeshalingam et al. (2010), which have all been compiled and fit by Ganeshalingam et al. (in preparation). Other spectra have complementary unfiltered light curves from Wang et al. (in preparation).

In this chapter, we describe our observations and data reduction procedure in Sections 2.2 and 2.3, respectively. We present our methods of data management and storage in Section 2.4 and our spectral classification scheme in Section 2.5. The sample of objects and spectra is described in Section 2.6, and there we also show our fully reduced spectra as well as (for the objects with multi-band SN and galaxy photometry) galaxy-subtracted spectra. In this section we also present our reclassifications of a handful of SNe as well as previously unknown spectroscopic host-galaxy redshifts. Finally, we present our conclusion in Section 2.7. Future BSNIP chapters will examine the correlations between spectroscopic properties and other observables (such as photometry and host-galaxy properties).

Table 2.1: SN Ia and Host Information

SN Name	SNID (Sub)Type[a]	Host Galaxy	Host Morp.[b]	$cz_{\rm helio}$ (km s^{-1})[c]	$E(B-V)_{\rm MW}$ (mag)[d]	Discovery Date (UT)	Discovery Reference	Classification Reference	# of Spec.	First Epoch[e]	Last Epoch[e]	$\rm JD_{max}$ Ref.[f]
SN 1989A	Ia-norm	NGC 3687	Sbc	2506	0.020	1989-01-19	IAUC 4721	IAUC 4724	1	83.80	···	1
SN 1989B	Ia-norm	NGC 3627	Sb	728	0.030	1989-01-30	IAUC 4726	IAUC 4727	4	7.54	152.19	2
SN 1989M	Ia-norm	NGC 4579	Sb	1520	0.039	1989-06-28	IAUC 4802	IAUC 4802	4	2.49	297.42	3
SN 1990G	Ia-norm	IC 2735	Sab	10727	0.021	1990-03-19	IAUC 4982	IAUC 4984	1	···	···	···
SN 1990M	Ia-norm	NGC 5493	S0	2710	0.036	1990-06-15	IAUC 5033	IAUC 5034	5	···	···	···
SN 1990O	Ia-norm	MCG +03-44-3	Sa	9192	0.095	1990-06-22	IAUC 5039	IAUC 5039	3	12.54	54.50	2
SN 1990N	Ia-norm	NGC 4639	Sbc	1019	0.025	1990-06-23	IAUC 5039	IAUC 5039	5	7.11	160.16	2
SN 1990R	Ia-norm	UGC 11699	Sd/Irr	4857	0.096	1990-06-26	IAUC 5054	IAUC 5054	3	···	···	···
SN 1990Y	Ia-norm	FCCB 1147	E	11702	0.008	1990-08-22	IAUC 5080	IAUC 5083	1	16.78	···	2
SN 1991B	Ia-norm	NGC 5426	Sc	2572	0.028	1991-01-11	IAUC 5163	IAUC 5164	3	···	···	···
SN 1991K	Ia-norm	NGC 2851	S0	5096	0.059	1991-02-20	IAUC 5196	Matheson01	2	···	···	···
SN 1991M	Ia-norm	IC 1151	Sc	2170	0.036	1991-03-12	IAUC 5207	IAUC 5207	4	18.06	152.09	2
SN 1991O	Ia-91bg	2MASX J14243792+6545294	···	···	0.012	1991-03-18	IAUC 5233	IAUC 5233	1	···	···	···
SN 1991S	Ia-norm	UGC 5691	Sb	16489	0.026	1991-04-10	IAUC 5238	IAUC 5245	1	31.05	···	2
SN 1991T	Ia-91T	NGC 4527	Sbc	1736	0.023	1991-04-13	IAUC 5239	IAUC 5251	9	−10.10	347.19	2
SN 1991am	Ia-norm	MCG +06-37-6	Sb	18353	0.018	1991-07-14	IAUC 5312	IAUC 5318	1	···	···	···
SN 1991ak	Ia-norm	NGC 5378	Sa	3043	0.013	1991-07-15	IAUC 5309	IAUC 5311	3	···	···	···
SN 1991at	Ia-norm	UGC 733	Sb	12306	0.068	1991-08-19	IAUC 5336	IAUC 5347	1	···	···	···
SN 1991as	Ia	[M91k] 224610+0754.6	···	···	0.107	1991-08-19	IAUC 5336	IAUC 5347	1	···	···	···
SN 1991ay	Ia-norm	2MASX J00471896+4032336	Sb	15289	0.062	1991-09-09	IAUC 5352	IAUC 5366	1	···	···	···
SN 1991bd	Ia-norm	UGC 2936	Sd/Irr	3813	0.449	1991-10-12	IAUC 5367	IAUC 5367	1	···	···	···
SN 1991bc	Ia-norm	UGC 2691	Sb	6401	0.071	1991-10-12	IAUC 5366	IAUC 5366	2	···	···	···
SN 1991bb	Ia-norm	UGC 2892	Sbc	7962	0.331	1991-10-13	IAUC 5365	IAUC 5365	2	···	···	···
SN 1991bf	Ia-norm	MCG -05-56-027	S0	9021	0.016	1991-11-13	IAUC 5389	IAUC 5404	1	···	···	···
SN 1991bg	Ia-91bg	NGC 4374	E	1061	0.037	1991-12-03	IAUC 5400	IAUC 5403	8	0.14	161.88	2
SN 1991bh	Ia-norm	[M91o] 024216.2+145713.4	···	···	0.102	1991-12-07	IAUC 5401	IAUC 5404	1	···	···	···
SN 1991bj	Ia-02cx	IC 344	Sb	5441	0.052	1991-12-30	IAUC 5420	IAUC 5420	1	···	···	···
SN 1992G	Ia-norm	NGC 3294	Sc	1586	0.018	1992-02-09	IAUC 5452	IAUC 5458	8	23.41	126.76	2
SN 1992M	Ia-norm	2MASX J07150996+4525556	E	15589	0.086	1992-02-25	IAUC 5473	IAUC 5473	2	···	···	···
SN 1992ah	Ia-norm	2MASX J17374476+1254168	···	···	0.149	1992-06-27	IAUC 5559	IAUC 5559	1	···	···	···
SN 1992ap	Ia-norm	UGC 10430	Sbc	8958	0.009	1992-07-29	IAUC 5573	IAUC 5601	1	···	···	···
SN 1993C	Ia-norm	NGC 2954	E	3819	0.037	1993-01-27	IAUC 5699	IAUC 5701	3	···	···	···
SN 1993Y	Ia-norm	UGC 2771	S0	5990	0.186	1993-09-18	IAUC 5870	IAUC 5870	1	28.33	···	4
SN 1993aa	Ia-91bg	APMUKS(BJ) B230046.41-063708.1	···	···	0.041	1993-09-19	IAUC 5871	IAUC 5871	1	···	···	···
SN 1993Z	Ia-norm	NGC 2775	Sab	1355	0.041	1993-09-23	IAUC 5870	IAUC 5870	9	28.92	232.69	4
SN 1993ab	Ia-norm	NGC 1164	Sab	4176	0.155	1993-09-24	IAUC 5871	IAUC 5877	1	···	···	···
SN 1993ac	Ia-norm	CGCG 307-023	E	14690	0.162	1993-10-13	IAUC 5879	IAUC 5882	2	12.68	28.66	2
SN 1993ae	Ia-norm	IC 126	Sb	5711	0.039	1993-11-07	IAUC 5888	IAUC 5888	2	18.99	68.87	2
SN 1993ai	Ia-norm	UGC 3483	Sbc	10193	0.120	1993-12-10	IAUC 5912	IAUC 5912	1	···	···	···
SN 1993aj	Ia-norm	2MFGC 09481	Sb	23264	0.025	1993-12-27	IAUC 5915	IAUC 5921	3	···	···	···
SN 1994B	Ia-norm	[P94a] 081751.35+155320.5	···	26682	0.044	1994-01-16	IAUC 5923	IAUC 5923	2	···	···	···
SN 1994E	Ia	SDSS J113207.01+552138.0	···	19148	0.010	1994-03-05	IAUC 5952	IAUC 5952	1	···	···	···
SN 1994J	···	[P94] 095815.51+544427.4	···	16788	0.013	1994-03-05	IAUC 5971	IAUC 5974	1	···	···	···
SN 1994D	Ia-norm	NGC 4526	S0	447	0.023	1994-03-07	IAUC 5946	IAUC 5946	20	−12.31	114.73	2
SN 1994Q	Ia-norm	CGCG 224-104	S0	8863	0.018	1994-06-02	IAUC 6001	IAUC 6001	3	9.68	69.79	2
SN 1994S	Ia-norm	NGC 4495	Sab	4551	0.017	1994-06-04	IAUC 6005	IAUC 6005	1	1.11	···	2
SN 1994T	Ia-norm	CGCG 016-058	Sa	10390	0.020	1994-06-11	IAUC 6007	IAUC 6007	1	33.09	···	5
SN 1994U	Ia-norm	NGC 4948	Sd/Irr	1124	0.056	1994-06-27	IAUC 6011	IAUC 6011	1	···	···	···
SN 1994X	Ia-norm	2MASX J00152051-2453337	Sb	16668	0.013	1994-08-15	IAUC 6056	IAUC 6068	1	···	···	···
SN 1994ab	Ia-norm	MCG -05-50-8	Sb	10373	0.102	1994-09-17	IAUC 6089	IAUC 6094	1	···	···	···
SN 1994ae	Ia-norm	NGC 3370	Sc	1280	0.027	1994-11-14	IAUC 6105	IAUC 6108	3	87.37	218.55	2
SN 1995A	Ia-norm	MCG +04-16-6	Sb	9476	0.085	1995-01-02	IAUC 6131	IAUC 6141	1	···	···	···
SN 1995C	Ia-norm	2MASX J12040140-3135542	···	8158	0.069	1995-02-08	IAUC 6133	IAUC 6138	1	···	···	···
SN 1995D	Ia-norm	NGC 2962	S0	1967	0.061	1995-02-10	IAUC 6134	IAUC 6135	4	3.84	92.02	2
SN 1995E	Ia-norm	NGC 2441	Sb	3472	0.026	1995-02-20	IAUC 6137	IAUC 6137	2	−2.46	53.88	2
SN 1995L	Ia-norm	NGC 5157	Sa	7321	0.011	1995-03-26	IAUC 6165	IAUC 6165	1	···	···	···
SN 1995T	Ia	SDSS J222712.66-092941.9	···	16913	0.053	1995-07-25	IAUC 6195	IAUC 6195	1	···	···	···
SN 1995ac	Ia-91T	2MFGC 17122	Sb	14960	0.042	1995-09-22	IAUC 6237	IAUC 6237	2	−6.34	24.71	2
SN 1995ak	Ia-norm	IC 1844	Sbc	6811	0.038	1995-10-27	IAUC 6254	IAUC 6254	1	26.38	···	5
SN 1995al	Ia-norm	NGC 3021	Sbc	1541	0.017	1995-11-01	IAUC 6255	IAUC 6256	2	22.15	39.06	2
SN 1996O	Ia-norm	MCG +03-41-115	Sbc	11167	0.050	1996-03-21	IAUC 6352	IAUC 6352	1	···	···	···
SN 1996P	Ia-norm	NGC 5335	Sb	4650	0.019	1996-03-25	IAUC 6357	IAUC 6357	1	···	···	···

Continued on Next Page...

Table 2.1 — Continued

SN Name	SNID (Sub)Type[a]	Host Galaxy	Host Morp.[b]	$cz_{\rm helio}$ (km s^{-1})[c]	$E(B-V)_{\rm MW}$ (mag)[d]	Discovery Date (UT)	Discovery Reference	Classification Reference	# of Spec.	First Epoch[e]	Last Epoch[e]	$\rm JD_{max}$ Ref.[f]
SN 1996ai	Ia-norm	NGC 5005	Sbc	947	0.014	1996-06-16	IAUC 6422	IAUC 6422	5	···	···	···
SN 1996bv	Ia-norm	UGC 3432	Scd	4998	0.105	1996-11-03	IAUC 6508	IAUC 6508	1	20.30	···	2
SN 1997E	Ia-norm	NGC 2258	S0	4059	0.127	1997-01-14	IAUC 6538	IAUC 6538	1	20.40	···	2
SN 1997T	Ia-norm	UGC 6896	···	12561	0.079	1997-01-19	IAUC 6543	IAUC 6557	1	···	···	···
SN 1997Y	Ia-norm	NGC 4675	Sb	4758	0.019	1997-02-02	IAUC 6556	IAUC 6557	1	1.27	···	2
SN 1997bp	Ia-norm	NGC 4680	Sd/Irr	2491	0.044	1997-04-06	IAUC 6613	IAUC 6613	1	5.49	···	2
SN 1997br	Ia-91T	ESO 576-40	Sd/Irr	2081	0.113	1997-04-10	IAUC 6623	IAUC 6623	5	−4.84	79.37	2
SN 1997cn	Ia-91bg	NGC 5490	E	4857	0.021	1997-05-14	IAUC 6661	IAUC 6667	1	18.38	···	2
SN 1997cw	Ia-norm	NGC 105	Sab	5291	0.074	1997-07-10	IAUC 6699	IAUC 6699	2	32.77	65.16	2
SN 1997do	Ia-norm	UGC 3845	Sbc	3034	0.062	1997-10-31	IAUC 6766	IAUC 6766	2	−5.67	74.35	2
SN 1997fb	Ia-norm	2MASX J05011474-3838135	Sb	16118	0.023	1997-12-31	IAUC 6807	IAUC 6809	1	···	···	···
SN 1997fc	Ia	APMUKS(BJ) B045816.80-385931.0	···	16189	0.021	1997-12-31	IAUC 6807	IAUC 6809	1	···	···	···
SN 1998V	Ia-norm	NGC 6627	Sb	5273	0.197	1998-03-10	IAUC 6841	IAUC 6844	1	7.20	···	2
SN 1998aq	Ia-norm	NGC 3982	Sb	1109	0.008	1998-04-13	IAUC 6875	IAUC 6878	3	51.34	86.13	2
SN 1998bn	Ia-norm	NGC 4462	Sab	1793	0.101	1998-04-17	IAUC 6886	IAUC 6888	3	···	···	···
SN 1998bp	Ia-91bg	NGC 6495	E	3127	0.078	1998-04-29	IAUC 6890	IAUC 6890	5	18.87	163.06	2
SN 1998bu	Ia-norm	NGC 3368	Sab	896	0.025	1998-05-09	IAUC 6899	IAUC 6905	5	29.58	338.73	2
SN 1998cd	Ia-norm	2MFGC 08366	···	7491	0.014	1998-05-17	IAUC 6909	IAUC 6945	1	···	···	···
SN 1998cl	Ia-norm	MRK 0261	Sb	9129	0.036	1998-06-03	IAUC 6934	IAUC 6946	1	···	···	···
SN 1998cm	Ia-91T	MSACSS J134412.96+030039.9	···	23983	0.018	1998-06-10	IAUC 6943	IAUC 6943	1	···	···	···
SN 1998cs	Ia-norm	UGC 10432	Sb	9761	0.012	1998-06-29	IAUC 6957	IAUC 6960	3	···	···	···
SN 1998dh	Ia-norm	NGC 7541	Sbc	2689	0.067	1998-07-20	IAUC 6978	IAUC 6980	4	18.77	71.00	2
SN 1998de	Ia-91bg	NGC 252	S0	4938	0.059	1998-07-23	IAUC 6977	IAUC 6980	3	29.49	73.56	2
SN 1998dj	Ia-norm	NGC 788	S0a	4077	0.027	1998-08-08	IAUC 6986	IAUC 6990	1	···	···	···
SN 1998dk	Ia-norm	UGC 139	Sc	3963	0.045	1998-08-19	IAUC 6991	IAUC 6997	4	−7.24	43.83	2
SN 1998dm	Ia-norm	MCG -01-4-44	Sc	1961	0.045	1998-08-22	IAUC 6993	IAUC 6997	5	−12.48	79.70	2
SN 1998dw	Ia-norm	2MASX J01091133-1529471	Sb	14787	0.026	1998-08-28	IAUC 7007	IAUC 7018	1	···	···	···
SN 1998dx	Ia-norm	UGC 11149	Sb	16255	0.040	1998-09-10	IAUC 7011	IAUC 7011	2	5.13	27.84	2
SN 1998eb	Ia-norm	NGC 1961	Sc	3933	0.124	1998-09-17	IAUC 7016	IAUC 7018	1	···	···	···
SN 1998ec	Ia-norm	UGC 3576	Sb	5966	0.084	1998-09-26	IAUC 7022	IAUC 7024	1	11.86	···	2
SN 1998ef	Ia-norm	UGC 646	Sb	5318	0.074	1998-10-18	IAUC 7032	IAUC 7032	5	−8.62	84.83	2
SN 1998eg	Ia-norm	UGC 12133	Sc	7423	0.121	1998-10-19	IAUC 7033	IAUC 7037	1	30.60	···	2
SN 1998en	Ia-norm	UGC 3645	Sbc	6386	0.070	1998-10-30	IAUC 7045	IAUC 7070	1	···	···	···
SN 1998es	Ia-99aa	NGC 632	S0	3169	0.032	1998-11-13	IAUC 7050	IAUC 7054	7	0.28	106.04	2
SN 1998fc	Ia-91bg	2MASX J02591406+0329563	···	32078	0.116	1998-12-20	IAUC 7082	IAUC 7091	1	···	···	···
SN 1999C	Ia-norm	WOOTS J100851.03+711042.9	···	37474	0.082	1999-01-14	IAUC 7088	IAUC 7092	1	···	···	···
SN 1999X	Ia-norm	CGCG 180-022	···	7546	0.034	1999-01-23	IAUC 7105	IAUC 7105	2	15.76	26.60	2
SN 1999aa	Ia-99aa	NGC 2595	Sc	4329	0.041	1999-02-11	IAUC 7108	IAUC 7108	7	−10.58	281.51	2
SN 1999aq	Ia-norm	NGSS B093540.48-045523.2	···	14990	0.033	1999-02-20	IAUC 7125	IAUC 7125	1	···	···	···
SN 1999ac	Ia-norm	NGC 6063	Scd	2848	0.044	1999-02-26	IAUC 7114	IAUC 7122	4	−3.70	116.87	2
SN 1999bh	Ia-norm	NGC 3435	Sb	5159	0.015	1999-03-29	IAUC 7135	IAUC 7138	1	···	···	···
SN 1999bv	Ia-norm	MCG +10-25-14	Sb	5594	0.030	1999-04-19	IAUC 7148	Matheson01	1	···	···	···
SN 1999by	Ia-91bg	NGC 2841	Sb	639	0.018	1999-04-30	IAUC 7156	IAUC 7158	1	183.50	···	2
SN 1999cl	Ia-norm	NGC 4501	Sb	2281	0.035	1999-05-29	IAUC 7185	IAUC 7190	4	7.90	183.95	2
SN 1999cp	Ia-norm	NGC 5468	Scd	2842	0.025	1999-06-18	IAUC 7205	IAUC 7206	2	4.91	13.85	2
SN 1999cw	Ia-norm	MCG -01-2-1	Sab	3708	0.036	1999-06-28	IAUC 7211	IAUC 7216	5	14.79	132.08	2
SN 1999da	Ia-91bg	NGC 6411	E	3804	0.051	1999-07-05	IAUC 7215	IAUC 7219	5	−2.12	66.89	2
SN 1999dg	Ia-norm	UGC 9758	S0	6613	0.033	1999-07-23	IAUC 7229	IAUC 7239	2	15.08	38.52	2
SN 1999dk	Ia-norm	UGC 1087	Sc	4485	0.050	1999-08-12	IAUC 7237	IAUC 7238	5	−6.60	72.16	2
SN 1999do	Ia-norm	MCG +05-54-3	Scd	6574	0.054	1999-08-20	IAUC 7242	IAUC 7252	1	9.96	···	6
SN 1999dq	Ia-99aa	NGC 976	Sc	4296	0.109	1999-09-02	IAUC 7247	IAUC 7250	4	−3.93	51.03	2
SN 1999ee	Ia-91T	IC 5179	Sbc	3421	0.020	1999-10-07	IAUC 7272	IAUC 7272	1	17.65	···	2
SN 1999ek	Ia-norm	UGC 3329	Sbc	5252	0.568	1999-10-20	IAUC 7286	IAUC 7300	1	5.66	···	2
SN 1999fz	Ia-norm	UGC 8164	Sbc	6637	0.041	1999-11-18	IAUC 7314	IAUC 7328	1	···	···	···
SN 1999gd	Ia-norm	NGC 2623	Sd/Irr	5549	0.042	1999-11-24	IAUC 7319	IAUC 7328	1	−1.12	···	2
SN 1999gf	Ia-norm	UGC 5515	E	13293	0.044	1999-11-27	IAUC 7321	IAUC 7328	1	···	···	···
SN 1999gh	Ia-norm	NGC 2986	E	2302	0.058	1999-12-03	IAUC 7328	IAUC 7328	4	4.12	117.97	2
SN 1999gm	Ia-norm	2MASX J08351095-0823132	S0	12706	0.041	1999-12-15	IAUC 7334	IAUC 7334	1	···	···	···
SN 2000J	Ia-norm	UGC 8510	Sbc	14369	0.014	2000-02-04	IAUC 7362	(this work)	1	···	···	···
SN 2000al	Ia-norm	SDSS J133201.08-021136.6	···	59958	0.026	2000-03-01	IAUC 7387	IAUC 7388	1	···	···	···
SN 2000Q	Ia	2MASX J16051100+6939493	···	5996	0.027	2000-03-12	IAUC 7380	IAUC 7380	2	···	···	···
SN 2000bk	Ia-norm	NGC 4520	S0	7627	0.026	2000-04-11	IAUC 7402	IAUC 7408	1	14.84	···	2

Continued on Next Page...

Table 2.1 — Continued

SN Name	SNID (Sub)Type[a]	Host Galaxy	Host Morp.[b]	$cz_{\rm helio}$ (km s^{-1})[c]	$E(B-V)_{\rm MW}$ (mag)[d]	Discovery Date (UT)	Discovery Reference	Classification Reference	# of Spec.	First Epoch[e]	Last Epoch[e]	$\rm JD_{max}$ Ref.[f]
SN 2000ce	Ia-norm	UGC 4195	Sb	4890	0.057	2000-05-08	IAUC 7417	IAUC 7422	1	27.05	···	2
SN 2000cn	Ia-norm	UGC 11064	Scd	7042	0.057	2000-06-02	IAUC 7436	IAUC 7437	2	14.25	23.09	2
SN 2000cp	Ia-norm	2MFGC 12921	Sb	10254	0.047	2000-06-21	IAUC 7441	IAUC 7442	2	2.92	11.70	2
SN 2000cv	Ia-norm	CGCG 292-085	E	6071	0.014	2000-07-11	IAUC 7456	IAUC 7464	1	···	···	···
SN 2000cu	Ia-norm	ESO 525-G004	Sa	6595	0.088	2000-07-12	IAUC 7453	IAUC 7454	2	9.63	38.87	2
SN 2000cw	Ia-norm	MCG +05-56-7	Sbc	9033	0.072	2000-07-14	IAUC 7456	IAUC 7457	2	4.81	63.02	2
SN 2000cx	Ia-pec	NGC 524	S0	2377	0.082	2000-07-17	IAUC 7458	IAUC 7463	23	−4.46	448.22	2
SN 2000dd	Ia-norm	MCG -04-48-19	S0	12726	0.042	2000-08-10	IAUC 7477	IAUC 7483	1	···	···	···
SN 2000df	Ia-norm	CGCG 051-070	E	11754	0.051	2000-08-17	IAUC 7478	IAUC 7483	1	···	···	···
SN 2000dg	Ia-norm	MCG +01-1-29	Sb	11539	0.092	2000-08-22	IAUC 7480	IAUC 7484	2	−5.09	4.66	2
SN 2000dk	Ia-norm	NGC 382	E	5228	0.070	2000-09-18	IAUC 7493	IAUC 7494	4	1.00	36.32	2
SN 2000dm	Ia-norm	UGC 11198	Sab	4506	0.185	2000-09-24	IAUC 7495	IAUC 7497	4	−1.63	33.76	2
SN 2000dn	Ia-norm	IC 1468	S0	9614	0.048	2000-09-27	IAUC 7498	IAUC 7499	2	−0.94	16.38	2
SN 2000dp	Ia-norm	NGC 1139	S0a	10349	0.038	2000-10-02	IAUC 7503	IAUC 7505	2	···	···	···
SN 2000dr	Ia-norm	IC 1610	S0	5636	0.021	2000-10-05	IAUC 7505	IAUC 7506	1	6.78	···	2
SN 2000dx	Ia-norm	UGC 1775	Sb	9108	0.039	2000-10-30	IAUC 7514	IAUC 7514	1	−9.26	···	6
SN 2000ej	Ia-91bg	IC 1371	S0	9102	0.066	2000-11-02	IAUC 7517	IAUC 7532	1	···	···	···
SN 2000ey	Ia-norm	IC 1481	Sb	6119	0.077	2000-11-11	IAUC 7531	IAUC 7531	3	7.90	61.76	6
SN 2000fa	Ia-norm	UGC 3770	Sd/Irr	6377	0.067	2000-11-30	IAUC 7533	IAUC 7535	2	−8.25	6.86	2
SN 2000fo	Ia-norm	CGCG 475-012	Sb	7152	0.068	2000-12-21	IAUC 7547	IAUC 7557	1	···	···	···
SN 2001A	Ia-91T	NGC 4261	E	2239	0.019	2001-01-01	IAUC 7554	IAUC 7579	1	···	···	···
SN 2001C	Ia-norm	CGCG 285-012	Sb	3280	0.070	2001-01-04	IAUC 7555	IAUC 7563	2	···	···	···
SN 2001E	Ia-norm	NGC 3905	Sc	5774	0.039	2001-01-05	IAUC 7557	IAUC 7566	1	15.01	···	2
SN 2001G	Ia-norm	MCG +08-17-43	···	5028	0.018	2001-01-08	IAUC 7560	IAUC 7564	1	11.57	···	2
SN 2001L	Ia-norm	MCG -01-30-11	Sb	4566	0.036	2001-01-18	IAUC 7566	IAUC 7566	1	21.57	···	6
SN 2001N	Ia-norm	NGC 3327	Sb	6302	0.025	2001-01-21	IAUC 7568	IAUC 7569	1	13.05	···	2
SN 2001P	Ia-91bg	NGC 3947	Sb	6197	0.035	2001-01-31	IAUC 7576	IAUC 7576	1	···	···	···
SN 2001U	Ia-norm	NGC 5442	Sb	8583	0.045	2001-02-15	IAUC 7583	IAUC 7604	1	···	···	···
SN 2001V	Ia-norm	NGC 3987	Sb	4503	0.013	2001-02-19	IAUC 7585	IAUC 7585	6	15.86	71.04	2
SN 2001ay	Ia-norm	IC 4423	Sb	9066	0.022	2001-04-18	IAUC 7611	IAUC 7612	2	6.79	22.72	7
SN 2001az	Ia-norm	UGC 10483	Sb	12202	0.051	2001-04-27	IAUC 7614	IAUC 7615	1	−3.24	···	2
SN 2001ba	Ia-norm	MCG -05-28-1	Sb	8820	0.064	2001-04-27	IAUC 7614	IAUC 7614	1	−4.64	···	2
SN 2001bf	Ia-norm	MCG +04-42-22	···	4647	0.099	2001-05-03	IAUC 7620	IAUC 7625	2	1.22	72.06	2
SN 2001bg	Ia-norm	NGC 2608	Sb	2135	0.042	2001-05-08	IAUC 7621	IAUC 7622	2	13.70	18.91	2
SN 2001br	Ia-norm	UGC 11260	Sa	6185	0.065	2001-05-13	IAUC 7629	IAUC 7629	2	3.47	3.48	2
SN 2001bp	Ia-norm	SDSS J160208.91+364313.8	···	28438	0.021	2001-05-15	IAUC 7626	IAUC 7626	2	0.51	12.34	2
SN 2001bs	Ia-norm	UGC 10018	Sbc	8751	0.031	2001-05-22	IAUC 7631	IAUC 7636	1	···	···	···
SN 2001cg	Ia-91bg	IC 3900	S0	7114	0.004	2001-05-28	IAUC 7637	IAUC 7637	1	···	···	···
SN 2001cj	Ia-norm	UGC 8399	Sb	7264	0.012	2001-05-30	IAUC 7640	IAUC 7640	1	23.14	···	2
SN 2001ck	Ia-norm	UGC 9425	Sb	10409	0.010	2001-06-03	IAUC 7641	IAUC 7645	2	16.39	32.77	2
SN 2001cp	Ia-norm	UGC 10738	Sbc	6715	0.157	2001-06-19	IAUC 7645	IAUC 7649	3	1.39	28.62	2
SN 2001da	Ia-norm	NGC 7780	Sab	5153	0.058	2001-07-09	IAUC 7658	IAUC 7664	2	−1.12	9.72	2
SN 2001de	Ia-91bg	UGC 12089	Sbc	9312	0.219	2001-07-13	IAUC 7664	IAUC 7671	1	···	···	···
SN 2001dd	Ia-norm	UGC 11579	Sc	5828	0.199	2001-07-13	IAUC 7663	IAUC 7663	1	···	···	···
SN 2001dl	Ia-norm	UGC 11725	Sd/Irr	6203	0.054	2001-07-30	IAUC 7675	IAUC 7680	2	13.84	33.22	2
SN 2001dm	Ia	NGC 749	S0a	4362	0.017	2001-08-07	IAUC 7679	IAUC 7685	1	···	···	···
SN 2001dn	Ia-norm	NGC 662	Sd/Irr	5654	0.054	2001-08-14	IAUC 7681	IAUC 7716	1	···	···	···
SN 2001ds	Ia-norm	UGC 1654	Sc	10870	0.054	2001-08-14	IAUC 7684	IAUC 7699	1	···	···	···
SN 2001ei	Ia-91bg	LOTOSS J235102.95+271050.6	···	···	0.038	2001-08-19	IAUC 7718	IAUC 7721	2	···	···	···
SN 2001dt	Ia-norm	UGC 12558	Scd	8946	0.208	2001-08-23	IAUC 7689	IAUC 7716	1	13.60	···	6
SN 2001dw	Ia-norm	NGC 1168	Sb	7627	0.264	2001-08-25	IAUC 7691	IAUC 7716	1	11.06	···	6
SN 2001eg	Ia-norm	UGC 3885	Sb	3807	0.049	2001-08-29	IAUC 7712	IAUC 7716	1	···	···	···
SN 2001ec	Ia-norm	KUG 0209+313A	Sb	13599	0.082	2001-08-31	IAUC 7702	IAUC 7716	1	···	···	···
SN 2001ed	Ia-norm	NGC 706	Sbc	4980	0.058	2001-09-02	IAUC 7703	IAUC 7714	1	···	···	···
SN 2001eh	Ia-99aa	UGC 1162	Sb	11104	0.064	2001-09-09	IAUC 7712	IAUC 7714	6	−5.63	59.90	2
SN 2001eu	Ia-91T	2MASX J02375888-0101390	···	40544	0.030	2001-09-21	IAUC 7731	IAUC 7754	1	···	···	···
SN 2001en	Ia-norm	NGC 523	Sd/Irr	4758	0.054	2001-09-26	IAUC 7724	IAUC 7732	3	10.09	35.64	2
SN 2001ep	Ia-norm	NGC 1699	Sb	3900	0.047	2001-10-03	IAUC 7727	IAUC 7731	7	2.83	114.91	2
SN 2001er	Ia-norm	UGC 5301	Sd/Irr	4863	0.012	2001-10-04	IAUC 7728	IAUC 7737	1	···	···	···
SN 2001es	Ia-norm	2MASX J02020834+1905246	···	20086	0.082	2001-10-07	IAUC 7729	(this work)	2	···	···	···
SN 2001ew	Ia-norm	2MASX J03125120+4122342	E	9294	0.188	2001-10-09	IAUC 7734	IAUC 7737	1	···	···	···
SN 2001fg	Ia-norm	SDSS J211245.44-005232.2	···	9324	0.061	2001-10-15	IAUC 7744	IAUC 7754	1	···	···	···

Continued on Next Page...

Table 2.1 — Continued

SN Name	SNID (Sub)Type[a]	Host Galaxy	Host Morp.[b]	$cz_{\rm helio}$ (km s^{-1})[c]	$E(B-V)_{\rm MW}$ (mag)[d]	Discovery Date (UT)	Discovery Reference	Classification Reference	# of Spec.	First Epoch[e]	Last Epoch[e]	$\rm JD_{max}$ Ref.[f]
SN 2001ex	Ia-91bg	UGC 3595	Sb	7909	0.053	2001-10-16	IAUC 7735	IAUC 7736	1	−1.82	···	2
SN 2001fe	Ia-norm	UGC 5129	Sa	4059	0.021	2001-11-02	IAUC 7742	IAUC 7752	1	−0.99	···	2
SN 2001fh	Ia-norm	2MASX J21204248+4423590	Sb	3894	0.746	2001-11-03	IAUC 7744	IAUC 7748	2	5.93	7.84	5
SN 2001fu	Ia-norm	MCG -03-23-11	S0	1694	0.195	2001-11-05	IAUC 7746	IAUC 7748	1	···	···	···
SN 2001gc	Ia-norm	UGC 3375	Sc	5783	0.210	2001-11-21	IAUC 7759	IAUC 7761	1	43.27	···	6
SN 2001ic	Ia-norm	NGC 7503	E	13263	0.068	2001-12-07	IAUC 7770	IAUC 7783	2	10.24	21.64	2
SN 2001ib	Ia-norm	NGC 7242	E	5789	0.151	2001-12-07	IAUC 7768	IAUC 7773	2	···	···	···
SN 2001iq	Ia-norm	UGC 12032	Sb	5521	0.143	2001-12-14	IAUC 7780	IAUC 7784	2	···	···	···
SN 2002G	Ia-norm	CGCG 189-024	E	10114	0.010	2002-01-18	IAUC 7797	IAUC 7802	1	19.31	···	2
SN 2002ar	Ia-norm	NGC 3746	Sb	9021	0.023	2002-02-03	IAUC 7819	IAUC 7825	1	···	···	···
SN 2002av	Ia-norm	ESO 489-G7	E	14702	0.042	2002-02-08	IAUC 7823	IAUC 7825	3	···	···	···
SN 2002bk	Ia	2MASX J09022690-0917450	···	16788	0.048	2002-02-09	IAUC 7842	IAUC 7846	1	···	···	···
SN 2002aw	Ia-norm	2MFGC 13321	Sb	7838	0.007	2002-02-15	IAUC 7831	IAUC 7834	2	2.10	15.84	2
SN 2002bf	Ia-norm	CGCG 266-031	Sb	7254	0.014	2002-02-22	IAUC 7836	IAUC 7846	2	2.97	6.90	2
SN 2002bg	Ia-norm	MCG +02-38-31	Sb	12813	0.028	2002-02-23	IAUC 7836	IAUC 7844	1	···	···	···
SN 2002bi	Ia-norm	UGC 8527	Sd/Irr	6985	0.025	2002-02-25	IAUC 7837	IAUC 7846	1	···	···	···
SN 2002bp	Ia-02cx	UGC 6332	Sa	6227	0.017	2002-03-08	IAUC 7847	(this work)	1	···	···	···
SN 2002bo	Ia-norm	NGC 3190	Sa	1271	0.024	2002-03-09	IAUC 7847	IAUC 7848	8	−11.94	227.44	2
SN 2002bs	Ia-norm	IC 4221	Sc	2890	0.081	2002-03-11	IAUC 7861	IAUC 7868	1	···	···	···
SN 2002bz	Ia-norm	MCG +05-34-33	Sb	11137	0.022	2002-04-03	IAUC 7866	IAUC 7874	1	4.92	···	2
SN 2002cc	Ia-norm	SDSS J083402.21+553906.7	···	19786	0.071	2002-04-04	IAUC 7871	IAUC 7877	1	···	···	···
SN 2002cd	Ia-norm	NGC 6916	Sbc	3100	0.405	2002-04-08	IAUC 7871	IAUC 7873	3	1.10	58.40	2
SN 2002cf	Ia-91bg	NGC 4786	E	4647	0.036	2002-04-13	IAUC 7877	IAUC 7878	2	−0.75	15.95	2
SN 2002ci	Ia-norm	UGC 10301	Sb	6664	0.032	2002-04-19	IAUC 7881	IAUC 7881	1	···	···	···
SN 2002ck	Ia-norm	UGC 10030	Sb	8952	0.092	2002-04-23	IAUC 7884	IAUC 7893	1	3.64	···	2
SN 2002cr	Ia-norm	NGC 5468	Scd	2842	0.025	2002-05-01	IAUC 7890	IAUC 7891	5	−6.78	85.98	2
SN 2002cs	Ia-norm	NGC 6702	E	4728	0.108	2002-05-05	IAUC 7891	IAUC 7894	8	−7.76	172.24	2
SN 2002cu	Ia-norm	NGC 6575	E	6991	0.063	2002-05-11	IAUC 7898	IAUC 7898	2	−5.28	16.62	2
SN 2002cx	Ia-02cx	CGCG 044-035	···	7184	0.027	2002-05-12	IAUC 7902	IAUC 7903	8	19.78	277.25	8
SN 2002cv	Ia-norm	NGC 3190	Sa	1271	0.024	2002-05-13	IAUC 7901	IAUC 7911	2	−1.40	18.53	9
SN 2002db	Ia-norm	NGC 5683	S0a	10858	0.030	2002-05-18	IAUC 7906	IAUC 7915	1	9.21	···	6
SN 2002de	Ia-norm	NGC 6104	Sd/Irr	8430	0.018	2002-06-01	IAUC 7914	IAUC 7915	2	−0.32	8.37	2
SN 2002df	Ia-norm	MCG -01-53-6	Sab	8598	0.053	2002-06-02	IAUC 7915	IAUC 7916	1	6.55	···	6
SN 2002di	Ia-91bg	MCG +05-40-2	S0	10909	0.031	2002-06-09	IAUC 7917	IAUC 7920	1	···	···	···
SN 2002dj	Ia-norm	NGC 5018	E	2815	0.095	2002-06-12	IAUC 7918	IAUC 7919	1	−7.98	···	2
SN 2002dk	Ia-91bg	NGC 6616	Sab	5555	0.146	2002-06-13	IAUC 7919	IAUC 7920	1	−1.23	···	6
SN 2002do	Ia-norm	MCG +07-41-1	E	4761	0.314	2002-06-17	IAUC 7923	IAUC 7927	1	23.09	···	2
SN 2002dp	Ia-norm	NGC 7678	Sc	3490	0.049	2002-06-18	IAUC 7924	IAUC 7927	5	15.55	134.73	2
SN 2002dr	Ia	UGC 12214	S0	6610	0.077	2002-06-24	IAUC 7927	IAUC 7953	1	···	···	···
SN 2002dx	Ia-norm	UGC 12861	Sab	7099	0.053	2002-07-08	IAUC 7933	IAUC 7953	1	···	···	···
SN 2002eb	Ia-norm	CGCG 473-011	Sb	8255	0.061	2002-07-22	IAUC 7937	IAUC 7953	3	1.68	59.75	2
SN 2002ec	Ia-norm	NGC 5910	E	12256	0.104	2002-07-23	IAUC 7937	IAUC 7946	2	···	···	···
SN 2002ef	Ia-norm	NGC 7761	S0	7189	0.032	2002-07-30	IAUC 7943	IAUC 7945	2	4.70	28.93	2
SN 2002eh	Ia-norm	NGC 917	Sab	5387	0.076	2002-08-01	IAUC 7947	IAUC 7953	1	6.88	···	6
SN 2002ep	Ia-norm	2MASX J21572200-0751253	···	16806	0.035	2002-08-06	IAUC 7959	IAUC 7964	1	···	···	···
SN 2002el	Ia-norm	NGC 6986	S0	8613	0.087	2002-08-12	IAUC 7953	IAUC 7954	3	11.82	38.94	2
SN 2002er	Ia-norm	UGC 10743	Sa	2569	0.161	2002-08-23	IAUC 7959	IAUC 7961	4	−4.58	60.64	2
SN 2002et	Ia-norm	MCG -04-47-10	Sc	8217	0.141	2002-08-24	IAUC 7959	IAUC 7967	1	11.92	···	6
SN 2002gb	Ia-norm	SDSS J224321.26-000654.5	···	22185	0.064	2002-08-28	IAUC 7983	IAUC 7988	1	···	···	···
SN 2002eu	Ia-norm	2MASXI J0149427+323730	···	11280	0.045	2002-08-30	IAUC 7963	IAUC 7965	5	−0.06	63.12	2
SN 2002ey	Ia-91bg	2MASX J23101188+0732541	···	···	0.059	2002-09-03	IAUC 7964	IAUC 7964	1	···	···	···
SN 2002fb	Ia-91bg	NGC 759	E	4668	0.089	2002-09-06	IAUC 7967	IAUC 7967	3	0.98	55.83	2
SN 2002fi	Ia-norm	MCG -04-7-10	Sa	17139	0.023	2002-09-13	IAUC 7972	IAUC 7979	1	···	···	···
SN 2002fk	Ia-norm	NGC 1309	Sbc	2138	0.040	2002-09-17	IAUC 7973	IAUC 7976	5	7.74	148.74	2
SN 2002gf	Ia-norm	2MASX J20551849-0004243	E	25853	0.093	2002-09-27	IAUC 7990	IAUC 8016	1	···	···	···
SN 2002gc	Ia-norm	UGC 1394	Sa	6389	0.105	2002-10-03	IAUC 7983	IAUC 7988	4	···	···	···
SN 2002gg	Ia-norm	NEAT J222745.65+065548.9	···	32977	0.126	2002-10-05	IAUC 7990	IAUC 8016	1	···	···	···
SN 2002gx	Ia-norm	NEAT J023144.16+401646.5	···	23983	0.055	2002-10-13	IAUC 7995	IAUC 8013	1	···	···	···
SN 2002ha	Ia-norm	NGC 6962	Sab	4212	0.102	2002-10-21	IAUC 7997	IAUC 7999	5	−0.85	63.11	2
SN 2002hd	Ia-norm	MCG -01-23-8	S0	10493	0.038	2002-10-24	IAUC 7999	IAUC 8002	2	6.48	12.72	2
SN 2002he	Ia-norm	UGC 4322	E	7363	0.040	2002-10-28	IAUC 8002	IAUC 8004	4	−5.91	3.22	2
SN 2002hl	Ia	NGC 3665	S0	2048	0.018	2002-11-05	IAUC 8008	IAUC 8011	1	···	···	···

Continued on Next Page...

Table 2.1 — Continued

SN Name	SNID (Sub)Type[a]	Host Galaxy	Host Morp.[b]	$cz_{\rm helio}$ (km s^{-1})[c]	$E(B-V)_{\rm MW}$ (mag)[d]	Discovery Date (UT)	Discovery Reference	Classification Reference	# of Spec.	First Epoch[e]	Last Epoch[e]	$\rm JD_{max}$ Ref.[f]
SN 2002hv	Ia	UGC 4974	S0	7024	0.017	2002-11-05	IAUC 8012	IAUC 8013	1	···	···	···
SN 2002hu	Ia-99aa	MCG +06-6-12	Sb	11002	0.045	2002-11-07	IAUC 8012	IAUC 8013	1	−5.81	···	2
SN 2002hw	Ia-norm	UGC 52	Sc	5255	0.105	2002-11-09	IAUC 8014	IAUC 8015	2	−6.27	24.42	2
SN 2002jg	Ia-norm	NGC 7253	Sb	4719	0.066	2002-11-23	IAUC 8022	IAUC 8023	1	10.11	···	2
SN 2002jm	Ia-91bg	IC 603	Sa	5399	0.050	2002-12-07	IAUC 8030	IAUC 8031	1	···	···	···
SN 2002jo	Ia-norm	NGC 5708	Sd/Irr	2752	0.017	2002-12-11	IAUC 8031	IAUC 8031	1	···	···	···
SN 2002jy	Ia-norm	NGC 477	Sc	5876	0.053	2002-12-17	IAUC 8035	IAUC 8037	2	11.86	39.46	2
SN 2002kf	Ia-norm	CGCG 233-023	···	5786	0.117	2002-12-27	IAUC 8040	IAUC 8041	1	6.81	···	2
SN 2003D	Ia-norm	MCG -01-25-9	E	6628	0.065	2003-01-06	IAUC 8043	IAUC 8043	2	9.98	59.88	2
SN 2003F	Ia-norm	UGC 3261	Sd/Irr	5168	0.329	2003-01-08	IAUC 8045	IAUC 8045	2	···	···	···
SN 2003K	Ia-91T	IC 1129	Scd	6541	0.028	2003-01-11	CBET 04	IAUC 8048	2	13.43	20.18	5
SN 2003M	Ia-91bg	UGC 7224	E	7267	0.022	2003-01-13	IAUC 8048	IAUC 8059	2	···	···	···
SN 2003V	Ia-norm	APMUKS(BJ) B030310.79-013550.9	···	13491	0.070	2003-01-16	IAUC 8060	IAUC 8083	1	···	···	···
SN 2003ae	Ia-norm	2MASX J09282257+2726402	···	9850	0.024	2003-01-23	IAUC 8066	IAUC 8066	1	31.69	···	5
SN 2003P	Ia-norm	MCG +09-13-107	···	10103	0.067	2003-01-23	IAUC 8057	IAUC 8060	1	···	···	···
SN 2003S	Ia-norm	MCG +09-22-94	Sb	11962	0.011	2003-01-24	IAUC 8058	IAUC 8058	1	···	···	···
SN 2003U	Ia-norm	NGC 6365	Sb	7885	0.033	2003-01-27	IAUC 8059	IAUC 8061	1	−2.55	···	2
SN 2003W	Ia-norm	UGC 5234	Sc	6017	0.049	2003-01-28	IAUC 8061	IAUC 8061	3	−5.06	56.56	2
SN 2003X	Ia-norm	UGC 11151	Sb	7018	0.090	2003-01-28	IAUC 8062	IAUC 8065	1	···	···	···
SN 2003Y	Ia-91bg	IC 522	S0	5078	0.064	2003-01-29	IAUC 8062	IAUC 8063	2	−1.74	21.63	2
SN 2003af	Ia-norm	KUG 1107+236	Sb	6157	0.014	2003-02-03	IAUC 8067	IAUC 8071	1	···	···	···
SN 2003av	Ia-norm	NEAT J080132.34+024826.7	···	41971	0.030	2003-02-04	IAUC 8077	IAUC 8083	1	···	···	···
SN 2003ai	Ia-norm	IC 4062	···	10493	0.015	2003-02-08	IAUC 8068	IAUC 8074	1	7.25	···	5
SN 2003ah	Ia-norm	LOTOSS J044309.01+004553.4	···	8994	0.092	2003-02-08	IAUC 8068	IAUC 8083	1	···	···	···
SN 2003an	Ia	MCG +05-32-22	Sb	11104	0.015	2003-02-09	IAUC 8069	IAUC 8085	1	···	···	···
SN 2003ax	Ia-norm	2MASX J08083589+0746399	···	16189	0.029	2003-02-09	IAUC 8079	IAUC 8083	1	···	···	···
SN 2003au	Ia-91bg	NGC 6095	S0	9246	0.012	2003-02-17	IAUC 8075	IAUC 8085	1	···	···	···
SN 2003bf	Ia-norm	2MASX J08082660+1219571	···	10068	0.027	2003-02-18	IAUC 8082	IAUC 8083	1	···	···	···
SN 2003ay	Ia-norm	NEAT J040726.40+280748.4	···	21885	0.592	2003-02-19	IAUC 8079	IAUC 8085	1	···	···	···
SN 2003bh	Ia-norm	NEAT J100006.84+281650.0	···	26682	0.020	2003-02-21	IAUC 8084	IAUC 8084	1	···	···	···
SN 2003bi	Ia-norm	2MASX J10440556+1231293	···	27666	0.024	2003-02-22	IAUC 8084	IAUC 8084	1	···	···	···
SN 2003cq	Ia-norm	NGC 3978	Sbc	9977	0.022	2003-03-30	IAUC 8103	IAUC 8106	1	−0.15	···	2
SN 2003du	Ia-norm	UGC 9391	Sd/Irr	1913	0.011	2003-04-22	IAUC 8121	IAUC 8122	6	17.61	80.98	2
SN 2003dw	Ia-norm	MCG +10-24-51	Sb	9003	0.018	2003-04-26	IAUC 8124	IAUC 8129	1	···	···	···
SN 2003ek	Ia-norm	FGC 2126	Sc	10804	0.023	2003-05-20	IAUC 8134	IAUC 8136	4	···	···	···
SN 2003fa	Ia-99aa	ARK 527	Sb	11800	0.039	2003-06-01	IAUC 8140	IAUC 8142	3	−8.15	39.78	2
SN 2003fd	Ia-norm	UGC 8670	Sd/Irr	18054	0.006	2003-06-09	IAUC 8147	IAUC 8158	1	···	···	···
SN 2003gj	Ia-norm	NGC 7017	S0	10118	0.065	2003-06-30	IAUC 8161	CBET 26	1	···	···	···
SN 2003gn	Ia-norm	CGCG 452-024	Sab	10328	0.050	2003-07-22	IAUC 8168	IAUC 8170	2	−5.38	3.26	2
SN 2003gq	Ia-02cx	NGC 7407	Sbc	6431	0.069	2003-07-24	IAUC 8168	IAUC 8170	2	−0.69	60.99	2
SN 2003gs	Ia-norm	NGC 936	S0	1430	0.035	2003-07-29	IAUC 8171	IAUC 8171	2	30.46	199.51	2
SN 2003gt	Ia-norm	NGC 6930	Sab	4695	0.110	2003-07-29	IAUC 8172	IAUC 8175	2	−5.07	17.61	2
SN 2003he	Ia-norm	MCG -01-1-10	Sbc	7645	0.039	2003-08-11	IAUC 8182	IAUC 8196	2	2.71	8.54	2
SN 2003hj	Ia-norm	MCG +05-36-28	···	22595	0.024	2003-08-19	IAUC 8184	IAUC 8189	1	···	···	···
SN 2003hm	Ia-norm	UGC 2295	Sb	4173	0.061	2003-08-20	IAUC 8185	IAUC 8189	1	···	···	···
SN 2003hs	Ia-norm	UGC 11149	Sb	16255	0.040	2003-08-31	IAUC 8191	IAUC 8196	1	−5.49	···	6
SN 2003hw	Ia	2MASX J03014982+3544343	···	12680	0.221	2003-09-08	IAUC 8198	IAUC 8211	1	···	···	···
SN 2003hv	Ia-norm	NGC 1201	S0	1679	0.015	2003-09-09	IAUC 8197	IAUC 8198	3	21.85	77.29	2
SN 2003hx	Ia-norm	NGC 2076	S0	2144	0.084	2003-09-12	IAUC 8199	IAUC 8200	1	21.89	···	10
SN 2003ij	Ia-99aa	UGC 3336	Sb	5510	0.099	2003-09-25	IAUC 8210	IAUC 8214	1	···	···	···
SN 2003ik	Ia-norm	MCG +11-10-56	Scd	7114	0.067	2003-09-29	IAUC 8212	IAUC 8214	1	···	···	···
SN 2003in	Ia-norm	IC 1956	Sbc	6401	0.245	2003-09-30	IAUC 8214	IAUC 8214	1	···	···	···
SN 2003im	Ia-norm	2MASX J00445922-0853228	Sa	5804	0.032	2003-09-30	IAUC 8214	IAUC 8214	1	···	···	···
SN 2003iv	Ia-norm	MCG +02-8-14	Sd/Irr	10286	0.137	2003-10-17	IAUC 8226	IAUC 8228	2	1.76	6.58	2
SN 2003iz	Ia-norm	UGC 638	···	14453	0.077	2003-10-21	IAUC 8230	IAUC 8231	1	···	···	···
SN 2003kc	Ia-norm	MCG +05-23-37	Sc	10004	0.022	2003-11-21	IAUC 8242	IAUC 8242	1	···	···	···
SN 2003kd	Ia-norm	UGC 2468	S0a	9050	0.209	2003-11-23	IAUC 8243	IAUC 8245	2	···	···	···
SN 2003kh	Ia	UGC 11491	Scd	10013	0.104	2003-11-27	IAUC 8245	IAUC 8246	1	···	···	···
SN 2003kg	Ia-norm	IC 1427	E	7804	0.044	2003-11-27	IAUC 8245	IAUC 8246	1	···	···	···
SN 2003kf	Ia-norm	MCG -02-16-2	Sb	2215	0.313	2003-11-27	CBET 53	CBET 53	2	−7.50	40.94	2
SN 2003ls	Ia-norm	APMUKS(BJ) B025836.01-110449.4	···	13011	0.069	2003-12-22	IAUC 8271	IAUC 8271	1	···	···	···
SN 2003lb	Ia-norm	UGC 2850	Sd/Irr	5426	0.226	2003-12-25	IAUC 8260	IAUC 8260	1	···	···	···

Continued on Next Page...

Table 2.1 — Continued

SN Name	SNID (Sub)Type[a]	Host Galaxy	Host Morp.[b]	$cz_{\rm helio}$ (km s^{-1})[c]	$E(B-V)_{\rm MW}$ (mag)[d]	Discovery Date (UT)	Discovery Reference	Classification Reference	# of Spec.	First Epoch[e]	Last Epoch[e]	$\rm JD_{max}$ Ref.[f]
SN 2003lc	Ia-norm	UGC 934	Sb	10493	0.054	2003-12-26	IAUC 8260	IAUC 8260	1	···	···	···
SN 2003lq	Ia-norm	UGC 5	Sbc	7270	0.040	2003-12-28	IAUC 8262	IAUC 8268	1	···	···	···
SN 2004E	Ia-norm	KUG 1314+318B	E/S0	8944	0.013	2004-01-15	IAUC 8271	IAUC 8271	1	5.26	···	2
SN 2004W	Ia-91bg	NGC 4649	E	1118	0.024	2004-01-28	IAUC 8286	IAUC 8286	1	···	···	···
SN 2004S	Ia-norm	MCG -05-16-21	Sc	2809	0.100	2004-02-03	IAUC 8282	IAUC 8283	2	8.26	311.57	2
SN 2004Y	Ia-norm	2MASX J11432825+2140266	E	20746	0.015	2004-02-12	IAUC 8288	IAUC 8288	1	···	···	···
SN 2004as	Ia-norm	SDSS J112538.81+224952.2	Sd/Irr	9300	0.011	2004-03-11	IAUC 8302	IAUC 8302	1	−4.36	···	2
SN 2004bd	Ia-norm	NGC 3786	Sa	2677	0.024	2004-04-07	IAUC 8316	IAUC 8317	3	10.76	42.68	2
SN 2004bg	Ia-norm	UGC 6363	Sb	6308	0.018	2004-04-07	IAUC 8317	IAUC 8321	2	10.34	28.01	2
SN 2004bj	Ia-norm	MCG +01-34-13	E	15035	0.026	2004-04-22	IAUC 8329	IAUC 8331	1	···	···	···
SN 2004bk	Ia-norm	NGC 5246	Sb	6931	0.022	2004-04-22	IAUC 8329	IAUC 8331	2	6.13	38.32	2
SN 2004bl	Ia-norm	MCG +00-31-42	Sd/Irr	5192	0.036	2004-04-29	IAUC 8334	IAUC 8337	2	4.61	19.38	6
SN 2004bp	Ia-91bg	MCG +06-25-14	···	8913	0.011	2004-05-03	IAUC 8335	IAUC 8339	1	···	···	···
SN 2004bq	Ia-norm	ESO 597-G32	Sa	8394	0.059	2004-05-05	IAUC 8336	IAUC 8339	1	···	···	···
SN 2004cb	Ia-norm	ESO 445-G20	Scd	4128	0.058	2004-05-12	IAUC 8350	IAUC 8353	1	···	···	···
SN 2004br	Ia-99aa	NGC 4493	E	6943	0.020	2004-05-15	IAUC 8340	IAUC 8343	3	3.50	26.90	2
SN 2004bv	Ia-91T	NGC 6907	Sbc	3181	0.063	2004-05-24	IAUC 8344	IAUC 8345	7	−7.06	161.68	2
SN 2004bw	Ia-norm	MCG +00-38-19	Scd	6356	0.142	2004-05-26	IAUC 8345	IAUC 8353	2	−10.03	6.59	2
SN 2004ca	Ia-norm	UGC 11799	Sb	5342	0.449	2004-06-02	IAUC 8350	IAUC 8350	1	···	···	···
SN 2004bz	Ia-norm	MCG +02-56-25	Sb	10232	0.058	2004-06-02	IAUC 8350	IAUC 8353	1	···	···	···
SN 2004cv	Ia-norm	MCG +03-41-120	Sbc	11017	0.044	2004-06-24	IAUC 8362	IAUC 8364	1	···	···	···
SN 2004db	Ia-norm	NGC 7377	S0	3340	0.028	2004-06-28	IAUC 8367	IAUC 8372	1	···	···	···
SN 2004da	Ia-norm	NGC 6901	Sab	4761	0.124	2004-07-06	IAUC 8370	IAUC 8371	3	···	···	···
SN 2004di	Ia-91bg	UGC 10097	S0	5963	0.017	2004-07-26	IAUC 8376	IAUC 8390	2	···	···	···
SN 2004eq	Ia-norm	ESO 404-G12	Sc	2650	0.022	2004-07-30	IAUC 8407	IAUC 8420	1	···	···	···
SN 2004dt	Ia-norm	NGC 799	Sa	5915	0.027	2004-08-11	IAUC 8386	IAUC 8387	9	−6.46	168.93	2
SN 2004ef	Ia-norm	UGC 12158	Sb	9288	0.055	2004-09-04	IAUC 8399	IAUC 8403	6	−5.52	84.60	2
SN 2004fa	Ia	MCG -05-48-5	···	···	0.088	2004-09-05	IAUC 8420	IAUC 8437	1	···	···	···
SN 2004eo	Ia-norm	NGC 6928	Sab	4707	0.108	2004-09-17	IAUC 8406	IAUC 8409	3	−5.57	44.40	2
SN 2004ev	Ia-norm	ESO 459-G13	Sc	···	0.123	2004-10-06	IAUC 8417	IAUC 8420	1	···	···	···
SN 2004ey	Ia-norm	UGC 11816	Sc	4734	0.137	2004-10-14	IAUC 8419	IAUC 8420	3	−7.58	51.39	2
SN 2004fd	Ia-norm	NGC 1060	S0	5189	0.195	2004-10-21	IAUC 8423	IAUC 8437	2	···	···	···
SN 2004fg	Ia	MCG +05-56-7	Sbc	9033	0.072	2004-10-31	IAUC 8425	IAUC 8437	1	···	···	···
SN 2004fu	Ia-norm	NGC 6949	Sc	2761	0.388	2004-11-04	IAUC 8428	IAUC 8436	3	−2.65	25.28	5
SN 2004fw	Ia-norm	UGC 4633	Sb	5777	0.031	2004-11-06	IAUC 8431	IAUC 8437	1	···	···	···
SN 2004fy	Ia-norm	MCG +15-1-10	···	···	0.257	2004-11-10	IAUC 8435	IAUC 8437	2	···	···	···
SN 2004fz	Ia-norm	NGC 783	Sc	5189	0.061	2004-11-14	IAUC 8437	IAUC 8440	3	−5.18	22.28	2
SN 2004go	Ia-norm	IC 270	S0	8745	0.041	2004-11-18	IAUC 8448	IAUC 8450	1	26.08	···	6
SN 2004gc	Ia-norm	ARP 327	Sd/Irr	9204	0.206	2004-11-18	IAUC 8442	IAUC 8449	1	31.33	···	11
SN 2004gl	Ia-norm	MCG +08-16-31	···	11782	0.032	2004-11-21	IAUC 8446	IAUC 8453	1	···	···	···
SN 2004gs	Ia-norm	MCG +03-22-20	S0	7986	0.035	2004-12-12	IAUC 8453	IAUC 8453	1	0.44	···	2
SN 2004gu	Ia-norm	FGC 175A	···	13748	0.024	2004-12-13	IAUC 8454	IAUC 8454	1	−4.65	···	11
SN 2004gw	Ia-02cx	CGCG 283-003	Sb	5102	0.305	2004-12-27	IAUC 8459	IAUC 8465	2	···	···	···
SN 2004gz	Ia-norm	MCG +10-23-45	···	···	0.014	2004-12-28	IAUC 8460	IAUC 8468	1	···	···	···
SN 2005A	Ia-norm	NGC 958	Sc	5738	0.030	2005-01-05	IAUC 8459	IAUC 8461	1	5.55	···	11
SN 2005F	Ia-norm	MCG +02-23-27	Sb	8544	0.042	2005-01-13	IAUC 8465	IAUC 8465	1	···	···	···
SN 2005G	Ia-norm	UGC 8690	Scd	6937	0.019	2005-01-14	IAUC 8465	IAUC 8468	1	···	···	···
SN 2005M	Ia-norm	NGC 2930	Sb	6598	0.032	2005-01-19	IAUC 8470	IAUC 8474	5	−1.41	35.50	2
SN 2005as	Ia-norm	NGC 3450	Sb	4026	0.056	2005-01-21	IAUC 8493	IAUC 8493	1	···	···	···
SN 2005P	Ia-02cx	NGC 5468	Scd	2842	0.025	2005-01-21	IAUC 8472	Jha06a	2	···	···	···
SN 2005X	Ia-norm	···	···	22335	0.023	2005-01-24	IAUC 8476	IAUC 8482	1	···	···	···
SN 2005W	Ia-norm	NGC 691	Sbc	2665	0.072	2005-02-01	IAUC 8475	IAUC 8479	3	0.59	28.36	11
SN 2005ag	Ia-norm	2MASX J14564322+0919361	···	23804	0.033	2005-02-10	IAUC 8484	IAUC 8484	1	0.52	···	11
SN 2005am	Ia-norm	NGC 2811	Sa	2368	0.054	2005-02-22	IAUC 8490	IAUC 8491	4	4.47	41.04	2
SN 2005ao	Ia	NGC 6462	E	11515	0.052	2005-03-07	CBET 114	IAUC 8492	2	−1.29	0.52	12
SN 2005bc	Ia-norm	NGC 5698	Sb	3678	0.012	2005-04-02	IAUC 8504	CBET 132	2	1.55	7.37	2
SN 2005be	Ia-norm	2MASX J14593310+1640070	···	10493	0.032	2005-04-05	IAUC 8506	CBET 134	2	10.96	16.71	11
SN 2005bl	Ia-91bg	NGC 4070	E	7213	0.024	2005-04-14	IAUC 8512	CBET 139	2	−5.56	18.07	2
SN 2005bo	Ia-norm	NGC 4708	Sab	4104	0.046	2005-04-17	IAUC 8514	IAUC 8517	1	27.71	···	2
SN 2005bu	Ia-norm	CGCG 117-019	···	8754	0.055	2005-04-21	CBET 144	CBET 150	1	···	···	···
SN 2005cf	Ia-norm	MCG -01-39-3	S0	1937	0.097	2005-05-28	CBET 158	CBET 160	7	−10.94	610.27	2
SN 2005de	Ia-norm	UGC 11097	Sb	4551	0.102	2005-08-02	CBET 191	CBET 193	4	−0.75	40.49	2

Continued on Next Page...

Table 2.1 — Continued

SN Name	SNID (Sub)Type[a]	Host Galaxy	Host Morp.[b]	$cz_{\rm helio}$ (km s^{-1})[c]	$E(B-V)_{\rm MW}$ (mag)[d]	Discovery Date (UT)	Discovery Reference	Classification Reference	# of Spec.	First Epoch[e]	Last Epoch[e]	$\rm JD_{max}$ Ref.[f]
SN 2005do	Ia-norm	UGC 2495	S0	9135	0.131	2005-08-08	CBET 206	CBET 206	1	...	...	...
SN 2005dh	Ia-91bg	MCG +04-37-55	Sb	4375	0.064	2005-08-10	CBET 196	CBET 199	2	...	...	...
SN 2005di	Ia-norm	MCG -04-52-46	Sb	7585	0.032	2005-08-12	CBET 198	ATEL 581	1	0.49	...	6
SN 2005dm	Ia-91bg	IC 219	E	5049	0.026	2005-08-26	CBET 203	ATEL 596	1	5.23	...	2
SN 2005dv	Ia-norm	NGC 5283	S0	3118	0.020	2005-09-04	CBET 217	CBET 218	1	−0.57	...	5
SN 2005ec	Ia	NGC 1690	E	8763	0.076	2005-09-16	CBET 228	ATEL 610	1	...	...	...
SN 2005ej	Ia-norm	CGCG 323-004	Sb	11354	0.057	2005-09-23	CBET 231	CBET 234	3	...	...	...
SN 2005el	Ia-norm	NGC 1819	S0	4470	0.114	2005-09-25	CBET 233	CBET 235	3	−6.70	8.09	2
SN 2005gj	Ia-csm	SDSS J030111.99-003313.5	...	17988	0.121	2005-09-26	CBET 247	CBET 302	5	46.32	460.35	13
SN 2005er	Ia-91bg	NGC 7385	E	7849	0.076	2005-09-29	IAUC 8608	CBET 243	3	−0.26	5.64	6
SN 2005eq	Ia-99aa	MCG -01-9-6	Scd	8688	0.074	2005-09-30	IAUC 8608	IAUC 8610	4	−6.01	51.16	2
SN 2005ew	Ia-norm	NSF J033923.74+350249.0	...	899	0.500	2005-10-04	CBET 244	CBET 244	2	18.23	40.03	5
SN 2005eu	Ia-norm	NSF J022743.32+281037.6	...	10463	0.131	2005-10-04	CBET 242	ATEL 620	4	−10.06	44.91	2
SN 2005hc	Ia	MCG +00-6-3	...	13491	0.033	2005-10-12	CBET 259	CBET 259	1	14.26	...	2
SN 2005hj	Ia-norm	SDSS J012648.45-011417.3	...	17250	0.039	2005-10-26	CBET 266	CBET 266	1	7.51	...	2
SN 2005hk	Ia-02cx	UGC 272	Sd/Irr	3894	0.023	2005-10-30	IAUC 8625	CBET 268	12	−8.29	454.74	14
SN 2005iq	Ia-norm	MCG -03-1-8	Sa	10205	0.022	2005-11-05	IAUC 8628	CBET 278	1	−5.86	...	2
SN 2005kc	Ia-norm	NGC 7311	Sab	4533	0.132	2005-11-09	IAUC 8629	CBET 286	2	10.28	12.25	5
SN 2005ke	Ia-91bg	NGC 1371	Sa	1463	0.025	2005-11-13	IAUC 8630	IAUC 8631	6	7.80	362.11	5
SN 2005ki	Ia-norm	NGC 3332	S0	5879	0.031	2005-11-18	IAUC 8632	CBET 296	3	1.62	35.80	2
SN 2005ls	Ia-norm	MCG +07-7-1	Sb	6332	0.093	2005-12-09	IAUC 8643	CBET 324	3	26.29	56.66	2
SN 2005lt	Ia-norm	MCG +03-30-51	Sbc	5975	0.012	2005-12-10	IAUC 8645	CBET 319	1	...	...	...
SN 2005lu	Ia-norm	MCG -03-07-40	Sd/Irr	9650	0.026	2005-12-11	IAUC 8645	CBET 321	1	27.88	...	11
SN 2005mc	Ia-norm	UGC 4414	S0a	7561	0.045	2005-12-23	CBET 331	CBET 334	2	6.64	25.16	2
SN 2005lz	Ia-norm	UGC 1666	Sd/Irr	11992	0.090	2005-12-24	CBET 329	CBET 337	1	0.58	...	2
SN 2005ms	Ia-norm	UGC 4614	Sb	7555	0.034	2005-12-27	CBET 343	CBET 345	2	−1.88	14.62	2
SN 2005na	Ia-norm	UGC 3634	Sa	7891	0.078	2005-12-31	CBET 350	CBET 351	5	0.03	31.19	2
SN 2006D	Ia-norm	MCG -01-33-34	Sab	2557	0.046	2006-01-11	CBET 362	CBET 366	5	3.70	126.46	2
SN 2006E	Ia-norm	NGC 5338	S0	815	0.020	2006-01-12	CBET 363	CBET 366	3	...	...	...
SN 2006H	Ia-91bg	2MASX J03260105+4041403	Sa	4195	0.206	2006-01-15	CBET 367	ATEL 699	1	7.01	...	5
SN 2006N	Ia-norm	MCG +11-8-12	...	4281	0.096	2006-01-21	CBET 375	IAUC 8661	4	−1.89	27.54	2
SN 2006S	Ia-99aa	UGC 7934	Sb	9623	0.018	2006-01-26	CBET 379	CBET 382	3	−3.93	18.45	2
SN 2006X	Ia-norm	NGC 4321	Sbc	1571	0.022	2006-02-04	IAUC 8667	CBET 393	9	3.15	358.37	2
SN 2006ac	Ia-norm	NGC 4619	Sb	6928	0.016	2006-02-09	IAUC 8669	CBET 398	2	7.96	35.39	2
SN 2006ak	Ia-norm	2MASX J11093314+2837393	Sb	11422	0.028	2006-02-17	CBET 408	CBET 408	1	8.43	...	2
SN 2006ay	Ia-norm	HCG 079:[PZH2002] 2.05	Sd/Irr	26292	0.057	2006-02-24	CBET 436	CBET 486	1	...	...	...
SN 2006ax	Ia-norm	NGC 3663	Sbc	5019	0.050	2006-03-20	CBET 435	CBET 437	3	−10.07	33.01	2
SN 2006az	Ia-norm	NGC 4172	Sb	9276	0.010	2006-03-23	IAUC 8691	CBET 447	1	26.30	...	2
SN 2006bq	Ia-norm	NGC 6685	S0	6568	0.059	2006-04-23	CBET 479	CBET 481	4	6.97	44.94	2
SN 2006br	Ia-norm	NGC 5185	Sb	7372	0.018	2006-04-25	CBET 482	CBET 487	2	3.87	10.62	2
SN 2006bt	Ia-norm	CGCG 108-013	S0a	9640	0.051	2006-04-26	CBET 485	CBET 485	5	−5.30	52.59	2
SN 2006bu	Ia-norm	2MASX J13524703+0518496	...	25183	0.019	2006-04-27	CBET 490	IAUC 8707	1	4.22	...	5
SN 2006bw	Ia-norm	SDSS J143358.05+034750.3	...	8994	0.033	2006-04-27	CBET 497	CBET 499	2	8.90	31.26	2
SN 2006bz	Ia-91bg	IC 4042A	S0	8366	0.006	2006-05-04	IAUC 8707	IAUC 8707	1	−2.44	...	2
SN 2006cc	Ia-norm	UGC 10244	Sb	9752	0.016	2006-05-06	CBET 505	CBET 506	1	17.67	...	2
SN 2006ch	Ia-norm	NGC 7753	Sbc	5168	0.099	2006-05-09	CBET 510	CBET 525	2	...	...	...
SN 2006ce	Ia-norm	NGC 908	Sc	1508	0.025	2006-05-10	IAUC 8709	CBET 541	3	...	...	...
SN 2006cf	Ia-norm	UGC 6015	Scd	12456	0.012	2006-05-11	IAUC 8710	CBET 514	3	6.28	18.69	5
SN 2006cj	Ia-norm	2MASX J12592407+2820498	...	20241	0.008	2006-05-17	CBET 515	CBET 517	1	3.43	...	2
SN 2006cm	Ia-norm	UGC 11723	Sb	4899	0.048	2006-05-24	CBET 521	CBET 526	4	−1.15	35.29	2
SN 2006ct	Ia-norm	2MASX J12095669+4705461	...	9432	0.019	2006-05-25	CBET 537	CBET 537	2	...	...	...
SN 2006cp	Ia-norm	UGC 7357	Sc	6682	0.023	2006-05-28	CBET 524	CBET 528	1	−5.30	...	2
SN 2006cq	Ia-norm	IC 4239	Sb	14492	0.013	2006-05-29	CBET 527	CBET 529	1	2.00	...	2
SN 2006cs	Ia-91bg	MCG +06-30-79	S0	7099	0.011	2006-06-03	CBET 536	CBET 539	1	2.28	...	5
SN 2006da	Ia-norm	2MASX J23274876+1428315	...	12345	0.065	2006-06-12	CBET 545	CBET 550	4	...	...	...
SN 2006cz	Ia-99aa	MCG -01-38-2	Scd	12531	0.083	2006-06-14	IAUC 8721	CBET 550	5	1.12	36.60	6
SN 2006dh	Ia-norm	UGC 8670	Sd/Irr	18054	0.006	2006-06-21	IAUC 8725	CBET 562	1	...	...	...
SN 2006di	Ia-norm	NGC 439	S0	5804	0.031	2006-06-24	IAUC 8726	CBET 587	1	...	...	...
SN 2006dm	Ia-norm	MCG -01-60-21	Sc	6601	0.039	2006-07-03	CBET 568	CBET 569	5	−7.90	36.06	2
SN 2006do	Ia	ESO 470-G18	S0a	8523	0.020	2006-07-05	CBET 572	ATEL 854	4	...	...	...
SN 2006dv	Ia-norm	UGC 12461	S0	9884	0.071	2006-07-20	IAUC 8733	CBET 585	5	...	...	...
SN 2006eb	Ia-norm	UGC 771	Sa	5165	0.029	2006-07-22	CBET 590	CBET 592	2	...	...	...

Continued on Next Page...

Table 2.1 — Continued

SN Name	SNID (Sub)Type[a]	Host Galaxy	Host Morp.[b]	$cz_{\rm helio}$ (km s^{-1})[c]	$E(B-V)_{\rm MW}$ (mag)[d]	Discovery Date (UT)	Discovery Reference	Classification Reference	# of Spec.	First Epoch[e]	Last Epoch[e]	$\rm JD_{max}$ Ref.[f]
SN 2006dw	Ia-norm	2MASX J16174359+3457534	···	8107	0.021	2006-07-23	IAUC 8733	CBET 587	4	···	···	···
SN 2006dy	Ia-norm	NGC 5587	S0a	2302	0.018	2006-07-25	CBET 586	CBET 587	5	···	···	···
SN 2006ef	Ia-norm	NGC 809	S0	5360	0.024	2006-08-18	CBET 597	CBET 604	3	3.20	34.56	2
SN 2006gr	Ia-norm	UGC 12071	Sb	10373	0.085	2006-08-21	CBET 638	CBET 642	3	−8.70	25.03	2
SN 2006ej	Ia-norm	NGC 191	Sc	6077	0.035	2006-08-23	CBET 603	CBET 604	4	−3.70	27.54	2
SN 2006em	Ia-91bg	NGC 911	E	5765	0.059	2006-08-25	CBET 605	CBET 612	3	4.16	26.70	2
SN 2006en	Ia-norm	MCG +05-54-41	Sc	9575	0.064	2006-08-26	CBET 606	CBET 608	3	8.55	30.75	2
SN 2006es	Ia-norm	UGC 2828	Sbc	12303	0.229	2006-09-01	CBET 613	CBET 613	2	···	···	···
SN 2006eu	Ia-norm	MCG +08-36-16	E	7072	0.194	2006-09-03	CBET 618	CBET 622	2	10.17	16.02	2
SN 2006et	Ia-norm	NGC 232	Sa	6646	0.019	2006-09-03	CBET 616	CBET 619	3	3.29	43.34	2
SN 2006ev	Ia-norm	UGC 11758	Sbc	8613	0.090	2006-09-12	IAUC 8747	CBET 622	2	10.54	16.36	5
SN 2006gj	Ia-norm	UGC 2650	Sab	8482	0.084	2006-09-18	CBET 631	CBET 634	1	4.70	···	2
SN 2006gt	Ia-91bg	2MASX J00561810-0137327	···	13422	0.037	2006-09-18	CBET 641	CBET 641	1	3.08	···	2
SN 2006ha	Ia-norm	IC 1461	Sc	9189	0.045	2006-09-27	CBET 649	CBET 771	1	49.55	···	2
SN 2006hb	Ia-norm	MCG -04-12-34	E	4599	0.027	2006-09-27	CBET 649	CBET 652	1	39.38	···	2
SN 2006hn	Ia-02cx	UGC 6154	Sa	5156	0.043	2006-09-28	CBET 653	CBET 694	1	···	···	···
SN 2006je	Ia-norm	IC 1735	Sb	11392	0.046	2006-10-15	CBET 675	CBET 678	2	20.18	26.02	2
SN 2006ke	Ia-91bg	UGC 3365	Sa	5150	0.188	2006-10-19	CBET 682	CBET 685	2	2.36	8.38	5
SN 2006kf	Ia-norm	UGC 2829	S0	6386	0.246	2006-10-21	CBET 686	CBET 691	3	−8.96	17.37	2
SN 2006nr	Ia-norm	UGC 3336	Sb	5510	0.098	2006-10-26	CBET 742	CBET 744	1	···	···	···
SN 2006lf	Ia-norm	UGC 3108	Sb	3960	0.954	2006-10-26	CBET 704	CBET 705	4	−6.30	43.77	2
SN 2006le	Ia-norm	UGC 3218	Sb	5225	0.408	2006-10-26	CBET 700	CBET 702	3	−8.69	41.18	2
SN 2006mo	Ia-norm	MCG +06-02-17	Sb	11092	0.045	2006-11-01	CBET 719	CBET 722	1	12.46	···	5
SN 2006mp	Ia-99aa	MCG +08-31-29	···	8094	0.035	2006-11-03	CBET 720	CBET 724	1	5.66	···	2
SN 2006ob	Ia-norm	UGC 01333	Sb	17759	0.033	2006-11-13	CBET 743	CBET 743	1	7.65	···	5
SN 2006or	Ia-norm	NGC 3891	Sbc	6218	0.036	2006-11-18	CBET 749	CBET 750	2	−2.79	4.93	5
SN 2006os	Ia-norm	UGC 2384	Sb	9836	0.146	2006-11-21	CBET 751	CBET 751	2	8.61	27.09	5
SN 2006ot	Ia-norm	ESO 544-G31	Sa	15871	0.018	2006-11-22	CBET 754	CBET 754	2	···	···	···
SN 2006ow	Ia-norm	UGC 03908	Sbc	···	0.044	2006-11-26	CBET 759	CBET 765	1	···	···	···
SN 2006qo	Ia	UGC 4133	Sc	9129	0.062	2006-11-29	CBET 763	CBET 765	1	−11.08	···	2
SN 2006sr	Ia-norm	UGC 14	Sc	7237	0.094	2006-12-12	IAUC 8784	CBET 779	2	−2.34	2.69	2
SN 2006su	Ia-norm	IC 3772	···	14030	0.015	2006-12-18	CBET 782	CBET 784	1	···	···	···
SN 2006td	Ia-norm	KUG 0155+361	Sb	4761	0.088	2006-12-24	CBET 787	CBET 790	1	22.62	···	2
SN 2006te	Ia-norm	CGCG 207-042	···	9471	0.050	2006-12-28	CBET 791	CBET 800	3	24.22	51.28	2
SN 2007A	Ia-norm	NGC 105	Sab	5290	0.074	2007-01-02	CBET 795	CBET 796	3	2.37	37.68	6
SN 2007B	Ia-norm	NGC 7315	S0	6312	0.079	2007-01-05	CBET 797	CBET 799	3	···	···	···
SN 2007E	Ia-norm	NGC 921	Sc	6778	0.030	2007-01-10	CBET 802	CBET 805	2	···	···	···
SN 2007F	Ia-norm	UGC 8162	Scd	7072	0.018	2007-01-11	CBET 803	CBET 805	4	−9.35	52.18	2
SN 2007M	Ia	NGC 4076	Sa	6214	0.038	2007-01-14	CBET 816	IAUC 8798	1	···	···	···
SN 2007N	Ia-91bg	MCG -01-33-12	Sa	3861	0.040	2007-01-21	CBET 818	CBET 818	2	0.44	23.23	2
SN 2007O	Ia-norm	UGC 9612	Sc	10856	0.023	2007-01-21	CBET 818	CBET 818	2	−0.33	25.56	2
SN 2007R	Ia-norm	UGC 4008	S0a	9219	0.059	2007-01-26	CBET 823	CBET 826	1	21.58	···	2
SN 2007S	Ia-norm	UGC 5378	Sb	4161	0.033	2007-01-29	CBET 825	CBET 829	3	5.18	61.38	2
SN 2007V	Ia-norm	LCRS B102433.3-030244	···	9100	0.040	2007-02-12	CBET 841	CBET 841	1	···	···	···
SN 2007af	Ia-norm	NGC 5584	Scd	1638	0.031	2007-03-01	CBET 863	CBET 865	9	−1.25	158.54	2
SN 2007aj	Ia-norm	SDSS J124754.53+540038.5	···	8994	0.019	2007-03-03	CBET 871	CBET 873	2	10.75	38.00	6
SN 2007al	Ia-91bg	2MASX J09591870-1928233	···	3634	0.042	2007-03-10	CBET 875	CBET 878	1	3.39	···	2
SN 2007ap	Ia-norm	MCG +03-41-3	S0	4742	0.030	2007-03-13	CBET 883	CBET 887	3	9.37	35.93	2
SN 2007ao	Ia-91bg	NGC 5532	···	7406	0.019	2007-03-13	CBET 883	CBET 892	1	···	···	···
SN 2007au	Ia-norm	UGC 3725	S0	6171	0.067	2007-03-18	CBET 895	CBET 898	2	16.11	31.85	2
SN 2007ax	Ia-91bg	NGC 2577	S0	2057	0.054	2007-03-21	CBET 904	CBET 907	1	14.93	···	5
SN 2007ba	Ia-91bg	UGC 9798	S0a	11546	0.033	2007-03-29	CBET 911	CBET 918	3	2.14	8.06	5
SN 2007bc	Ia-norm	UGC 6332	Sa	6227	0.017	2007-04-04	CBET 913	CBET 915	2	0.61	16.35	2
SN 2007bd	Ia-norm	UGC 4455	Sa	9299	0.034	2007-04-04	CBET 914	CBET 915	2	−5.79	9.70	2
SN 2007bj	Ia	NGC 6172	E	5009	0.118	2007-04-18	CBET 930	IAUC 8834	3	14.25	41.73	2
SN 2007bm	Ia-norm	NGC 3672	Sc	1862	0.041	2007-04-20	CBET 936	CBET 939	4	−7.79	40.84	5
SN 2007bz	Ia-norm	IC 3918	Sc	6529	0.031	2007-04-22	CBET 941	CBET 943	1	1.65	···	2
SN 2007ca	Ia-norm	MCG -02-34-61	Sc	4217	0.067	2007-04-25	CBET 945	CBET 947	3	−11.14	32.22	2
SN 2007cf	Ia-91bg	MCG +02-39-21	Sb	9873	0.030	2007-05-08	CBET 954	CBET 958	1	···	···	···
SN 2007cg	Ia-norm	ESO 508-G75	Sb	9952	0.082	2007-05-11	CBET 960	CBET 962	1	16.17	···	2
SN 2007ci	Ia-norm	NGC 3873	E	5434	0.019	2007-05-15	CBET 966	IAUC 8843	4	−6.57	27.75	2
SN 2007co	Ia-norm	MCG +05-43-16	···	8083	0.113	2007-06-04	CBET 977	CBET 978	8	−4.09	60.06	2

Continued on Next Page...

Table 2.1 — Continued

SN Name	SNID (Sub)Type[a]	Host Galaxy	Host Morp.[b]	$cz_{\rm helio}$ (km s^{-1})[c]	$E(B-V)_{\rm MW}$ (mag)[d]	Discovery Date (UT)	Discovery Reference	Classification Reference	# of Spec.	First Epoch[e]	Last Epoch[e]	$\rm JD_{max}$ Ref.[f]
SN 2007cp	Ia-norm	IC 807	···	10971	0.043	2007-06-13	CBET 980	CBET 981	2	···	···	···
SN 2007cq	Ia	2MASX J22144070+0504435	···	7765	0.109	2007-06-21	CBET 983	CBET 984	6	−5.82	44.79	2
SN 2007cs	Ia-norm	UGC 12798	Sb	5264	0.066	2007-06-24	CBET 986	CBET 987	4	12.15	49.42	6
SN 2007fb	Ia-norm	UGC 12859	Sbc	5405	0.056	2007-07-03	CBET 992	CBET 993	7	1.95	100.91	6
SN 2007fc	Ia-norm	ESO 538-G8	Sb	10116	0.025	2007-07-08	CBET 995	CBET 998	3	···	···	···
SN 2007fq	Ia-91bg	MCG -04-48-19	S0	12728	0.041	2007-07-14	CBET 1001	ATEL 1154	1	···	···	···
SN 2007fr	Ia-norm	UGC 11780	···	15290	0.061	2007-07-14	CBET 1001	IAUC 8864	2	−5.83	−1.25	2
SN 2007fs	Ia-norm	ESO 601-G5	Sb	5154	0.034	2007-07-15	CBET 1002	CBET 1003	6	5.03	91.35	6
SN 2007ge	Ia-norm	MCG +08-1-13	Sb	13444	0.110	2007-07-19	CBET 1012	CBET 1014	1	12.53	···	6
SN 2007gi	Ia-norm	NGC 4036	S0	1445	0.021	2007-07-31	CBET 1017	CBET 1021	5	−7.31	153.29	15
SN 2007gk	Ia-norm	MCG +11-20-27	Sb	7984	0.040	2007-08-05	CBET 1023	CBET 1025	2	−1.72	19.65	6
SN 2007if	Ia-norm	···	···	22233	0.083	2007-08-16	CBET 1059	CBET 1059	3	37.23	92.02	16
SN 2007hj	Ia-norm	NGC 7461	S0	4231	0.088	2007-09-01	CBET 1048	CBET 1048	4	−1.23	71.62	2
SN 2007hu	Ia-norm	NGC 6261	S0a	10610	0.046	2007-09-09	CBET 1056	CBET 1058	2	···	···	···
SN 2007ir	Ia-norm	UGC 02033	Sb	10548	0.050	2007-09-12	CBET 1067	CBET 1101	2	···	···	···
SN 2007is	Ia-norm	UGC 10553	Sab	8897	0.021	2007-09-14	CBET 1067	CBET 1075	2	···	···	···
SN 2007kf	Ia-norm	[K2007] J173131.76+691840.1	···	···	0.044	2007-09-22	CBET 1085	CBET 1097	1	···	···	···
SN 2007kg	Ia-norm	2MFGC 18005	···	···	0.995	2007-09-22	CBET 1086	CBET 1095	1	···	···	···
SN 2007kd	Ia-norm	MCG +6-21-36	Sc	7248	0.022	2007-09-23	CBET 1083	CBET 1094	1	···	···	···
SN 2007kk	Ia-norm	UGC 2828	Sbc	12305	0.228	2007-09-28	CBET 1096	CBET 1097	1	7.15	···	6
SN 2007le	Ia-norm	NGC 7721	Sc	2015	0.033	2007-10-13	CBET 1100	CBET 1101	9	−10.31	304.74	2
SN 2007s1[g]	Ia-norm	2MASX J00150006+1619596	···	8214	0.069	2007-10-21	Bailey09	Bailey09	2	−1.23	37.79	2
SN 2007qd	Ia-02cx	SDSS J020932.74-005959.6	···	12935	0.035	2007-10-31	CBET 1137	CBET 1137	1	···	···	···
SN 2007on	Ia-norm	NGC 1404	E	1947	0.012	2007-11-05	CBET 1121	ATEL 1261	4	−3.01	27.68	17
SN 2007qe	Ia-norm	NSF J235412.09+272432.3	···	7195	0.038	2007-11-13	CBET 1138	CBET 1138	3	−6.54	16.00	2
SN 2007sa	Ia-norm	NGC 3499	S0a	1522	0.010	2007-11-21	CBET 1161	CBET 1163	1	···	···	···
SN 2007rx	Ia-norm	BATC J234012.05+272512.23	···	8994	0.089	2007-11-28	CBET 1157	CBET 1157	1	···	···	···
SN 2007ry	Ia-norm	2MASX J03254297+4114422	Sb	11992	0.192	2007-12-08	CBET 1158	CBET 1162	1	···	···	···
SN 2007sr	Ia-norm	NGC 4038	Sd/Irr	1642	0.047	2007-12-18	CBET 1172	CBET 1173	2	32.61	135.70	2
SN 2007su	Ia-norm	SDSS J221908.85+131040.5	···	8353	0.083	2007-12-19	CBET 1178	CBET 1178	1	···	···	···
SN 2007ux	Ia-norm	2MASX J10091969+1459268	···	9268	0.044	2007-12-23	CBET 1187	CBET 1189	2	5.59	20.16	2
SN 2008A	Ia-02cx	NGC 634	Sa	4925	0.054	2008-01-02	CBET 1193	CBET 1198	6	···	···	···
SN 2008C	Ia-norm	UGC 3611	S0a	4983	0.084	2008-01-03	CBET 1195	CBET 1197	1	15.68	···	2
SN 2008L	Ia-norm	NGC 1259	S0	5816	0.159	2008-01-14	CBET 1212	CBET 1219	1	32.37	···	5
SN 2008Q	Ia-norm	NGC 524	S0	2379	0.083	2008-01-26	CBET 1228	CBET 1232	3	6.46	199.31	2
SN 2008Z	Ia-99aa	SDSS J094315.36+361709.2	···	6293	0.013	2008-02-07	CBET 1243	CBET 1246	2	−2.29	9.99	2
SN 2008af	Ia-norm	UGC 09640	E	10045	0.032	2008-02-09	CBET 1248	CBET 1253	1	24.32	···	2
SN 2008ai	Ia-91bg	MCG +06-24-39	···	10571	0.017	2008-02-13	CBET 1256	CBET 1264	2	···	···	···
SN 2008ar	Ia-norm	IC 3284	Sa	7839	0.034	2008-02-27	CBET 1273	CBET 1273	3	−8.87	49.13	2
SN 2008ca	Ia-91bg	SDSS J122901.28+122218.0	E	39423	0.019	2008-03-10	CBET 1355	CBET 1358	1	···	···	···
SN 2008cb	Ia-norm	SDSS J123118.84+082315.4	···	49571	0.018	2008-03-10	CBET 1355	CBET 1358	1	···	···	···
SN 2008bf	Ia-norm	NGC 4055	E	7203	0.030	2008-03-18	CBET 1307	CBET 1310	3	27.93	40.62	2
SN 2008bt	Ia-91bg	NGC 3404	Sab	4606	0.056	2008-04-13	CBET 1336	CBET 1337	2	−1.08	10.97	6
SN 2008bv	Ia-norm	UGC 4653	···	16748	0.035	2008-04-19	CBET 1345	CBET 1358	1	···	···	···
SN 2008bw	Ia-norm	UGC 11241	Sb	9931	0.040	2008-04-21	CBET 1346	CBET 1358	1	···	···	···
SN 2008bz	Ia-norm	2MASX J12385810+1107502	···	18071	0.024	2008-04-22	CBET 1353	CBET 1353	1	···	···	···
SN 2008cd	Ia	NGC 5038	S0	2222	0.069	2008-04-29	CBET 1360	CBET 1362	1	···	···	···
SN 2008cf	Ia-99aa	[WLF2008] J140732.38-263305.6	···	13799	0.067	2008-05-04	CBET 1365	CBET 1367	1	···	···	···
SN 2008cl	Ia-norm	UGC 10261	S0	19017	0.020	2008-05-16	CBET 1378	CBET 1380	1	4.24	···	2
SN 2008s1[h]	Ia-norm	UGC 8472	S0	6624	0.028	2008-05-16	ATEL 1532	ATEL 1532	8	−6.36	34.02	2
SN 2008ct	Ia-norm	UGC 11878	Sb	7591	0.070	2008-05-31	CBET 1394	CBET 1419	1	···	···	···
SN 2008db	Ia-norm	NGC 50	S0	5701	0.037	2008-06-13	CBET 1407	CBET 1411	3	···	···	···
SN 2008dx	Ia-91bg	NGC 4898A	E	6903	0.006	2008-06-24	CBET 1427	CBET 1427	4	2.46	28.84	2
SN 2008ds	Ia-99aa	UGC 299	Sc	6305	0.064	2008-06-28	CBET 1419	CBET 1419	11	···	···	···
SN 2008dr	Ia-norm	NGC 7222	Sb	12426	0.043	2008-06-28	CBET 1419	CBET 1419	5	···	···	···
SN 2008dt	Ia-norm	NGC 6261	S0a	10610	0.046	2008-06-30	CBET 1423	CBET 1424	3	9.27	69.95	2
SN 2008r3[i]	Ia-norm	Coma Cluster	···	6925	0.006	2008-07-12	ATEL 1615	ATEL 1617	2	···	···	···
SN 2008ec	Ia-norm	NGC 7469	Sa	4892	0.069	2008-07-14	CBET 1437	CBET 1438	7	−0.24	71.58	2
SN 2008ee	Ia-norm	NGC 307	S0	4010	0.043	2008-07-16	CBET 1440	CBET 1447	3	···	···	···
SN 2008ei	Ia-norm	UGC 11977	Sd/Irr	11284	0.084	2008-07-23	CBET 1446	CBET 1447	4	3.29	33.10	2
SN 2008er	Ia-norm	UGC 1563	E	4991	0.170	2008-08-05	CBET 1461	CBET 1465	1	···	···	···
SN 2008ez	Ia-norm	NGC 5222	E	6858	0.021	2008-08-18	CBET 1474	CBET 1477	1	···	···	···

Continued on Next Page...

Table 2.1 — Continued

SN Name	SNID (Sub)Type[a]	Host Galaxy	Host Morp.[b]	$cz_{\rm helio}$ (km s^{-1})[c]	$E(B-V)_{\rm MW}$ (mag)[d]	Discovery Date (UT)	Discovery Reference	Classification Reference	# of Spec.	First Epoch[e]	Last Epoch[e]	$\rm JD_{max}$ Ref.[f]
SN 2008ey	Ia-norm	IC 262	S0	5385	0.080	2008-08-18	CBET 1473	CBET 1478	1	···	···	···
SN 2008s3[j]	Ia-norm	2MASX J23004648+0734590	···	12291	0.056	2008-08-25	SNF[k]	SNF[k]	1	···	···	···
SN 2008s4[l]	Ia-norm	IC 144	···	12159	0.019	2008-08-26	SNF[k]	SNF[k]	1	···	···	···
SN 2008fg	Ia-norm	NGC 1268	Sb	3263	0.171	2008-08-30	CBET 1489	CBET 1503	1	···	···	···
SN 2008fj	Ia-91bg	UGC 10759	···	8138	0.018	2008-09-01	CBET 1494	CBET 1495	1	···	···	···
SN 2008s5[m]	Ia	···	···	9294	0.069	2008-09-09	SNF[k]	SNF[k]	3	1.26	15.76	2
SN 2008fr	Ia-norm	SDSS J011149.19+143826.5	···	11692	0.045	2008-09-14	CBET 1513	CBET 1513	3	···	···	···
SN 2008s8[n]	Ia-norm	···	···	···	0.025	2008-09-20	SNF[k]	SNF[k]	2	···	···	···
SN 2008gs	Ia	CRTS J012705.78+031305.7	···	···	0.023	2008-09-21	CBET 1559	CBET 1563	1	···	···	···
SN 2008fx	Ia-norm	2MASX J02113233+2353074	···	···	0.080	2008-09-23	CBET 1523	CBET 1525	1	···	···	···
SN 2008ge	Ia-02cx	NGC 1527	S0	1174	0.013	2008-10-08	CBET 1531	CBET 1540	1	···	···	···
SN 2008gh	Ia-norm	UGC 3957	E	10229	0.049	2008-10-11	CBET 1539	CBET 1585	2	···	···	···
SN 2008gt	Ia-norm	APMUKS(BJ) B224209.38-032444.7	···	···	0.044	2008-10-29	CBET 1559	CBET 1563	2	···	···	···
SN 2008gy	Ia-norm	2MASX J03100247+1913173	···	8694	0.167	2008-10-30	CBET 1565	CBET 1577	1	···	···	···
SN 2008gw	Ia-norm	2MASX J04392713+0908218	···	19187	0.225	2008-11-03	CBET 1559	CBET 1585	1	···	···	···
SN 2008hk	Ia-norm	SDSS J091243.63+095548.3	E	9025	0.083	2008-11-06	CBET 1581	CBET 1581	1	···	···	···
SN 2008ha	Ia-02cx	UGC 12682	Sd/Irr	1393	0.079	2008-11-07	CBET 1567	CBET 1576	3	7.46	22.17	18
SN 2008hj	Ia-norm	MCG -02-1-14	Sc	11360	0.036	2008-11-20	CBET 1579	CBET 1583	3	···	···	···
SN 2008hq	Ia-norm	UGC 3963	Sd/Irr	20086	0.082	2008-11-22	CBET 1593	CBET 1607	1	···	···	···
SN 2008hr	Ia-norm	2MASX J09185174+1857294	···	22725	0.030	2008-11-23	CBET 1595	CBET 1607	1	···	···	···
SN 2008hz	Ia-norm	SKHV 220	···	21900	0.078	2008-11-26	CBET 1609	ATEL 1866	1	···	···	···
SN 2008hu	Ia-norm	ESO 561-G18	Sb	···	0.107	2008-12-01	CBET 1600	CBET 1607	1	···	···	···
SN 2008hs	Ia-norm	NGC 910	E	5207	0.057	2008-12-01	CBET 1598	CBET 1599	1	−7.94	···	6
SN 2008hy	Ia-norm	IC 334	Sb	2536	0.236	2008-12-06	CBET 1608	CBET 1610	1	···	···	···

[a] See Section 2.5 for more information on our SNID classifications.

[b] Host-galaxy morphology is taken from the NASA/IPAC Extragalactic Database (NED).

[c] Heliocentric redshifts listed are from NED, except the redshift of the host of SN 1991ay (2MASX J00471896+4032336) comes from IAUC 5366, the redshift of the host of SN 1997fc (APMUKS(BJ) B045816.80-385931.0) comes from IAUC 6809, the redshift of the host of SN 2000cu (ESO 525-G004) comes from our own spectrum of the host galaxy, the redshift of the host of SN 2003V (APMUKS(BJ) B030310.79-013550.9) comes from IAUC 8085, the redshift of the host of SN 2003P (MCG +09-13-107) comes from our own spectrum of the host galaxy, the redshift of the host of SN 2003av (NEAT J080132.34+024826.7) comes from IAUC 8085, the redshift of the host of SN 2003fa (ARK 527) comes from IAUC 8146, the redshift of the host of SN 2005X comes from IAUC 8482, the redshift of the host of SN 2005ag (2MASX J14564322+0919361) comes from Contreras et al. (2010), the redshift of the host of SN 2006mp (MCG +08-31-29) comes from our own spectrum of the host galaxy, the redshift of the host of SN 2007aj comes from CBET 873, the redshift of the host of SN 2007if comes from Scalzo et al. (2010), the redshift of the host of SN 2007s1 (2MASX J00150006+1619596) comes from Bailey et al. (2009), the redshift of the host of SN 2008s3 comes from our own spectrum of the host galaxy, the redshift of the host of SN 2008s5 comes from narrow, host-galaxy emission features in our own spectra of the SN, the redshift of SN 2008s8 comes from the SNF website, and the redshift of the host of SN 2008hk comes from CBET 1581.

[d] The Milky Way (MW) reddening toward each SN as derived from the dust maps of Schlegel et al. (1998) and includes the corrections of Peek & Graves (2010).

[e] Epochs of first and last spectrum are relative to B-band maximum brightness in rest-frame days using the heliocentric redshift and date of maximum reference presented in the table. For SNe with photometric information and only one spectrum in our dataset, only a Phase of First Spectrum is listed.

[f] Julian Date of Maximum References: (1) Tsvetkov et al. (1990), (2) Ganeshalingam et al. (2010), (3) Kimeridze & Tsvetkov (1991), (4) Ho et al. (2001), (5) Hicken et al. (2009b), (6) Wang et al. in preparation, (7) Krisciunas et al. in preparation, (8) Li et al. (2003b), (9) Elias-Rosa et al. (2008), (10) Misra et al. (2008), (11) Contreras et al. (2010), (12) Wood-Vasey et al. (2008), (13) Prieto et al. (2007), (14) Phillips et al. (2007), (15) Zhang et al. (2010), (16) Scalzo et al. (2010), (17) Voss & Nelemans (2008), (18) Foley et al. (2009a).

[g] Also known as SNF20071021-000.

[h] Also known as SNF20080514-002.

[i] Also known as ROTSE3 J125642.7+273041.

[j] Also known as SNF20080825-006.

[k] This information comes from the Nearby Supernova Factory (SNF) website (`http://snfactory.lbl.gov/`, Aldering et al. 2002).

[l] Also known as SNF20080825-010.

[m] Also known as SNF20080909-030.

[n] Also known as SNF20080920-000.

Table 2.2: SN Ia Spectral Information

SN Name	UT Date[a]	MJD[b]	Phase[c]	Inst.[d]	Wavelength Range (Å)	Res.[e] (Å)	P.A.[f] (°)	Par.[g] (°)	Air.[h]	See.[i] (″)	Exp. (s)	Observer(s)[j]	Reducer[k]	Flux Corr.[l]
SN 1989A	1989-04-27.000	47643.000	83.80	1	3450–9000	12	···	···	···	2	···	1,2	1	0
SN 1989B[m]	1989-02-15.000	47572.000	7.54	2	3450–8450	7	0	···	···	···	···	1,3	1	0
SN 1989B[m]	1989-02-21.000	47578.000	13.53	2	3450–7000	7	0	···	···	···	···	1	1	0
SN 1989B	1989-04-27.000	47643.000	78.37	1	3300–9050	12	···	···	···	2	···	1,2	1	0
SN 1989B	1989-07-10.000	47717.000	152.19	1	3900–6226	12	···	···	···	3	···	1,2,3	1	0
SN 1989M	1989-07-09.000	47716.000	2.49	1	3080–10300	12	···	···	···	2.5	···	1,2,3	1	0
SN 1989M	1989-07-10.000	47717.000	3.48	1	3400–10200	12	···	···	···	3	···	1,2,3	1	0
SN 1989M	1989-12-01.000	47861.000	146.76	1	4150–9500	12	···	···	···	1.5	900	1,2	1	0
SN 1989M	1990-05-01.428	48012.428	297.42	1	3930–6980	12	54	54	2.31	2.5	2100	1,2	1	0
SN 1990G	1990-03-25.000	47975.000	···	1	3932–9800	12	···	···	···	3	···	1,2	1	0
SN 1990M	1990-04-01.000	47982.000	···	1	3932–7060	12	···	···	···	1.5	···	1,4	1	0
SN 1990M	1990-07-17.000	48089.000	···	1	3920–9860	12	···	···	···	2	···	1,2	1	0
SN 1990M	1990-07-31.255	48103.255	···	1	3900–9900	12	48	50	4.19	1.25	1200	1,2	1	0
SN 1990M	1990-08-29.171	48132.171	···	1	3940–9850	12	229	49	3.85	1.25	1300	1,2	1	0
SN 1990M	1990-08-30.000	48133.000	···	1	6720–9850	12	229	49	4.02	2.25	1300	1,2	1	0
SN 1990O	1990-07-17.000	48089.000	12.54	1	3920–7080	12	···	···	···	2	···	1,2	1	0
SN 1990O	1990-07-31.396	48103.396	26.50	1	3900–7020	12	55	56	2.67	1.25	1800	1,2	1	0
SN 1990O	1990-08-29.252	48132.252	54.50	1	3900–7020	12	235	54	1.52	1.25	1400	1,2	1	0
SN 1990N	1990-07-17.000	48089.000	7.11	1	3920–9872	12	···	···	···	2	···	1,2	1	0
SN 1990N	1990-07-31.193	48103.193	21.25	1	3900–9900	12	55	55	2.30	1.25	900	1,2	1	0
SN 1990N	1990-08-29.153	48132.153	50.11	1	3940–9850	12	234	54	3.80	1.25	500	1,2	1	0
SN 1990N	1990-08-30.000	48133.000	50.96	1	6720–9850	12	234	54	4.23	2.25	950	1,2	1	0
SN 1990N	1990-12-17.577	48242.577	160.16	1	3900–7000	12	151	331	1.14	2.5	900	1,2	1	0
SN 1990R	1990-07-17.000	48089.000	···	1	3952–7052	12	···	···	···	2	···	1,2	1	0
SN 1990R	1990-07-31.423	48103.423	···	1	3900–7020	12	32	37	1.19	1.25	1200	1,2	1	0
SN 1990R	1990-08-29.279	48132.279	···	1	3900–7020	12	180	6	1.10	1.25	2400	1,2	1	0
SN 1990Y	1990-08-30.510	48133.510	16.78	1	3940–7050	12	171	351	3.07	2.25	1200	1,2	1	0
SN 1991B	1991-01-23.586	48279.586	···	1	3900–7020	12	183	2	1.37	1.75	400	1	1	0
SN 1991B	1991-02-23.524	48310.524	···	1	3900–9800	12	188	13	1.40	2	900	1	1	0
SN 1991B	1991-03-09.466	48324.466	···	1	3900–7020	12	186	7	1.38	1	1900	1,2	1	0
SN 1991K	1991-02-23.335	48310.335	···	1	3900–7020	12	194	15	1.77	2	1800	1	1	0
SN 1991K	1991-03-09.262	48324.262	···	1	3900–7020	12	186	6	1.71	1	3600	1,2	1	0
SN 1991M	1991-04-07.000	48353.000	18.06	1	3880–7000	12	···	···	···	3.5	···	1,2	1	0
SN 1991M	1991-04-19.000	48365.000	29.97	1	3900–7000	12	···	···	···	1.5	···	1,2	1	0
SN 1991M	1991-08-05.000	48473.000	137.20	1	3920–6900	12	···	···	···	1.75	···	1,5,6	1	0
SN 1991M	1991-08-20.000	48488.000	152.09	1	3920–7000	12	···	···	···	1.25	···	1,5	1	0
SN 1991O	1991-04-07.000	48353.000	···	1	3960–7040	12	···	···	···	3.5	···	1,2	1	0
SN 1991S	1991-05-05.000	48381.000	31.05	1	3900–7000	12	···	···	···	1.25	···	1,5	1	0
SN 1991T	1991-04-18.000	48364.000	−10.10	1	4060–8360	12	···	···	···	1.5	···	1,2	1	0
SN 1991T	1991-04-19.000	48365.000	−9.11	1	3100–9840	12	···	···	···	1.5	···	1,2	1	0
SN 1991T	1991-05-05.000	48381.000	6.80	1	3110–9858	12	···	···	···	1.25	···	1,5	1	0
SN 1991T	1991-07-20.000	48457.000	82.36	1	3150–9886	12	···	···	···	1.75	···	1,2,5	1	0
SN 1991T	1991-08-19.000	48487.000	112.19	1	3924–9748	12	···	···	···	1.25	···	1,5	1	0
SN 1991T	1991-08-20.000	48488.000	113.18	1	6800–9748	12	···	···	···	1.25	···	1,5	1	0
SN 1991T	1991-10-31.000	48560.000	184.77	1	3930–7042	12	···	···	···	2.5	···	1,5	1	0

Continued on Next Page. . .

Table 2.2 — Continued

SN Name	UT Date[a]	MJD[b]	Phase[c]	Inst.[d]	Wavelength Range (Å)	Res.[e] (Å)	P.A.[f] (°)	Par.[g] (°)	Air.[h]	See.[i] (″)	Exp. (s)	Observer(s)[j]	Reducer[k]	Flux Corr.[l]
SN 1991T	1992-03-13.435	48694.435	318.43	3	3292–10188	6/11	22	14	1.27	4.75	3600	1,5,7,8	1	0
SN 1991T	1992-04-11.361	48723.361	347.19	3	3300–10450	6/11	202	16	1.29	2.25	3600	1,5,8	1	0
SN 1991am	1991-08-04.000	48472.000	···	1	3940–6920	12	···	···	···	1.75	···	1,5,6	1	0
SN 1991ak	1991-07-20.000	48457.000	···	1	3920–6980	12	···	···	···	1.75	···	1,2,5	1	0
SN 1991ak	1991-08-05.000	48473.000	···	1	3920–6900	12	···	···	···	1.75	···	1,5,6	1	0
SN 1991ak	1991-08-20.000	48488.000	···	1	3908–7060	12	···	···	···	1.25	···	1,5	1	0
SN 1991at	1991-09-16.000	48515.000	···	1	4060–7060	12	···	···	···	1.5	···	1,5	1	0
SN 1991as	1991-09-16.000	48515.000	···	1	3940–7060	12	···	···	···	1.5	···	1,5	1	0
SN 1991ay	1991-10-02.000	48531.000	···	1	3940–7040	12	···	···	···	1.5	···	1,5	1	0
SN 1991bd	1991-10-31.000	48560.000	···	1	3920–7060	12	···	···	···	2.5	···	1,5	1	0
SN 1991bc	1991-10-31.000	48560.000	···	1	3100–8900	12	···	···	···	2.5	···	1,5	1	0
SN 1991bc	1991-12-14.000	48604.000	···	1	3920–7080	12	···	···	···	1.5	···	1,5	1	0
SN 1991bb	1991-10-31.000	48560.000	···	1	3920–7060	12	···	···	···	2.5	···	1,5	1	0
SN 1991bb	1991-12-14.000	48604.000	···	1	3920–7080	12	···	···	···	1.5	···	1,5	1	0
SN 1991bf	1991-12-14.000	48604.000	···	1	3920–7000	12	···	···	···	1.5	···	1,5	1	0
SN 1991bg	1991-12-13.000	48603.000	0.14	1	3300–8680	12	···	···	···	1.5	···	1,5	1	0
SN 1991bg	1991-12-14.000	48604.000	1.14	1	3905–9900	12	···	···	···	1.5	···	1,5	1	0
SN 1991bg	1992-01-01.000	48622.000	19.07	1	3240–9910	12	···	···	···	2	···	1	1	0
SN 1991bg	1992-01-09.000	48630.000	27.04	1	3090–9905	12	···	···	···	1.75	···	1,5,7	1	0
SN 1991bg	1992-01-09.000	48630.000	27.04	1	5407–6207	···	···	···	···	1.75	···	1,5,7	1	0
SN 1991bg	1992-01-30.000	48651.000	47.97	4	3090–7005	···	25	25	1.00	1	3000	10,9	1	0
SN 1991bg	1992-03-13.493	48694.493	91.31	3	3690–9765	6/11	48	44	1.39	4.75	3900	1,5,7,8	1	0
SN 1991bg	1992-05-23.309	48765.309	161.88	3	3180–10360	6/11	51	47	1.45	1.75	3600	1,7,8	2	0
SN 1991bh	1991-12-14.000	48604.000	···	1	3920–6880	12	···	···	···	1.5	···	1,5	1	0
SN 1991bj	1992-01-01.000	48622.000	···	1	4200–7400	12	···	···	···	2	···	1	1	0
SN 1992G	1992-03-13.347	48694.347	23.41	3	3280–10200	6/11	180	86	1.02	4.75	900	1,5,7,8	1	0
SN 1992G	1992-04-11.216	48723.216	52.13	3	3130–10400	6/11	102	273	1.00	2.25	3600	1,5,8	1	0
SN 1992G	1992-04-21.225	48733.225	62.09	3	3096–10290	6/11	180	87	1.01	2.25	4500	1,5	2	0
SN 1992G	1992-05-03.000	48745.000	73.80	3	3500–10200	6/11	···	···	···	···	···	11	1	0
SN 1992G	1992-05-23.249	48765.249	93.94	3	3600–10200	6/11	74	76	1.29	1.75	3000	1,7,8	2	0
SN 1992G	1992-06-09.235	48782.235	110.84	3	3224–10214	6/11	71	73	1.50	1.5	3600	1,5,7	2	0
SN 1992G	1992-06-10.256	48783.256	111.85	3	3224–10214	6/11	67	68	1.72	1.5	1200	1,5,7	2	0
SN 1992G	1992-06-25.244	48798.244	126.76	3	4000–7400	5	63	64	2.14	2.25	1800	1,12,13	2	0
SN 1992M	1992-03-13.253	48694.253	···	3	5590–10200	11	45	101	1.10	4.75	1800	1,5,7,8	1	0
SN 1992M	1992-03-13.253	48694.253	···	3	3300–5400	6	45	101	1.10	4.75	1800	1,5,7,8	1	0
SN 1992ah	1992-07-06.383	48809.383	···	3	3232–10380	6/11	72	44	1.32	1.25	1800	1,5	2	0
SN 1992ap	1992-09-02.249	48867.249	···	3	4256–7040	3	74	75	1.47	1.75	1200	1,5,7	2	0
SN 1993C	1993-01-29.347	49016.347	···	3	3258–10200	6/11	329	322	1.11	3.5	4500	1,5	2	0
SN 1993C	1993-03-01.279	49047.279	···	3	3100–10200	6/11	161	339	1.09	1.25	1800	1,14,5	2	0
SN 1993C	1993-04-14.215	49091.215	···	3	3240–10000	6/11	200	18	1.10	1.5	1800	1,5	1	0
SN 1993Y	1993-09-25.399	49255.399	28.33	3	3200–10200	6/11	88	274	1.07	1.75	1800	1,5	1	0
SN 1993aa	1993-09-25.290	49255.290	···	3	3200–10100	6/11	180	354	1.38	1.75	3000	1,5	1	0
SN 1993Z	1993-09-25.548	49255.548	28.92	3	3200–9900	6/11	143	309	2.01	1.75	860	1,5	1	0
SN 1993Z	1993-10-22.548	49282.548	55.80	3	3130–10470	6/11	143	320	1.33	1.25	860	1,5	3	0
SN 1993Z	1993-11-17.554	49308.554	81.68	3	3240–10100	6/11	180	351	1.16	1	1200	1,5	1	0

Continued on Next Page...

Table 2.2 — Continued

SN Name	UT Date[a]	MJD[b]	Phase[c]	Inst.[d]	Wavelength Range (Å)	Res.[e] (Å)	P.A.[f] (°)	Par.[g] (°)	Air.[h]	See.[i] (″)	Exp. (s)	Observer(s)[j]	Reducer[k]	Flux Corr.[l]
SN 1993Z	1993-12-18.478	49339.478	112.47	3	3120–10380	6/11	180	352	1.16	2	2400	1,7	3	0
SN 1993Z	1994-01-07.478	49359.478	132.38	3	3300–10100	6/11	207	23	1.22	2	1800	1,5	1	0
SN 1993Z	1994-01-19.406	49371.406	144.25	3	3250–9900	6/11	187	1	1.16	1	2400	1,5	1	0
SN 1993Z	1994-02-05.416	49388.416	161.19	3	3120–10510	6/11	213	29	1.27	2	2400	1	3	0
SN 1993Z[m]	1994-03-17.236	49428.236	200.83	3	3120–10400	6/11	178	355	1.16	2	1800	1,15,5	3	0
SN 1993Z	1994-04-18.237	49460.237	232.69	3	3120–10450	6/11	218	35	1.35	1.5	2700	1,7	3	0
SN 1993ab	1993-10-22.363	49282.363	···	3	3120–10470	6/11	226	234	1.01	1.25	1200	1,5	3	0
SN 1993ac	1993-10-22.525	49282.525	12.68	3	3120–10470	6/11	169	165	1.12	1.25	1600	1,5	3	0
SN 1993ac	1993-11-08.280	49299.280	28.66	3	3220–10000	6/11	266	266	1.39	1.75	1500	1,5	1	0
SN 1993ae	1993-11-17.384	49308.384	18.99	3	3120–10100	6/11	46	42	2.07	1	2700	1,5	1	0
SN 1993ae	1994-01-07.217	49359.217	68.87	3	3300–10100	6/11	38	34	1.71	2	3600	1,5	1	0
SN 1993ai	1994-01-07.381	49359.381	···	3	3350–9850	6/11	303	129	1.08	2	2400	1,5	1	0
SN 1993aj	1994-01-07.523	49359.523	···	3	3350–10300	6/11	188	346	1.28	2	1800	1,5	1	0
SN 1993aj	1994-01-19.542	49371.542	···	3	3500–9850	6/11	179	11	1.29	1	1200	1,5	1	0
SN 1993aj	1994-02-05.451	49388.451	···	3	4270–7020	3	175	348	1.28	2	2100	1	3	0
SN 1994B	1994-01-19.506	49371.506	···	3	3250–9800	6/11	239	53	1.63	1	2700	1,5	1	0
SN 1994B	1994-02-05.364	49388.364	···	3	3140–10470	6/11	223	24	1.13	2	3600	1	3	0
SN 1994E	1994-03-13.581	49424.581	···	5	3940–8850	7	110	116	1.64	1	2100	1,5	1	0
SN 1994J	1994-04-04.455	49446.455	···	3	4250–7020	3	250	72	1.85	2.75	1200	1,15,5	3	0
SN 1994D	1994-03-09.000	49420.000	−12.31	3	3196–7372	6/5	···	···	···	···	···	16	3	0
SN 1994D	1994-03-10.000	49421.000	−11.31	3	3320–7580	6/5	···	···	···	···	···	17	3	0
SN 1994D	1994-03-12.000	49423.000	−9.32	3	3320–7760	6/5	···	···	···	···	···	17	3	0
SN 1994D	1994-03-13.644	49424.644	−7.67	5	3240–8800	4.5/7	70	71	1.90	1	800	1,5	1	0
SN 1994D	1994-03-15.000	49426.000	−6.32	3	3240–7280	6/5	···	···	···	···	···	18,19	3	0
SN 1994D	1994-03-16.000	49427.000	−5.32	3	3240–7280	6/5	···	···	···	2	···	18,19	3	0
SN 1994D[m]	1994-03-17.459	49428.459	−3.87	3	3120–9900	6/11	218	31	1.31	2	3600	1,15,5	3	0
SN 1994D[m]	1994-03-18.000	49429.000	−3.33	3	3120–9900	6/11	···	···	···	2	···	1,15,5	3	0
SN 1994D	1994-04-04.395	49446.395	14.04	3	3120–9900	6/11	36	30	1.25	2.75	1700	1,15,5	3	0
SN 1994D	1994-04-11.000	49453.000	20.64	3	3206–7384	6/5	···	···	···	···	···	16	3	0
SN 1994D	1994-04-18.402	49460.402	28.03	3	3120–9900	6/11	225	43	1.48	1.5	1500	1,7	3	0
SN 1994D	1994-04-20.000	49462.000	29.63	3	3210–10200	6/11	···	···	···	···	···	20	3	0
SN 1994D	1994-05-04.000	49476.000	43.61	3	3320–10380	6/11	···	···	···	···	···	21,22	3	0
SN 1994D	1994-05-09.000	49481.000	48.60	3	3190–7320	6/5	···	···	···	···	···	19	3	0
SN 1994D	1994-05-10.000	49482.000	49.60	3	3190–7316	6/5	···	···	···	···	···	23	3	0
SN 1994D	1994-05-12.000	49484.000	51.59	3	3140–6160	6/5	···	···	···	···	···	24	3	0
SN 1994D	1994-05-14.000	49486.000	53.59	3	3140–6160	6/5	···	···	···	···	···	24	3	0
SN 1994D	1994-06-03.310	49506.310	73.87	3	3282–10142	6/11	50	48	1.80	3	2400	1,15,5	3	0
SN 1994D	1994-06-16.294	49519.294	86.83	3	3170–10500	6/11	51	50	2.10	3	2400	1,15,5	3	0
SN 1994D	1994-07-14.232	49547.232	114.73	3	3210–10260	6/11	52	52	2.43	2.25	2400	1	3	0
SN 1994Q	1994-06-03.461	49506.461	9.68	3	3120–8040	6/5	81	83	1.20	3	1800	1,15,5	3	0
SN 1994Q	1994-07-14.370	49547.370	49.42	3	3120–10400	6/11	78	79	1.29	2.25	2200	1	3	0
SN 1994Q	1994-08-04.343	49568.343	69.79	3	3120–10360	6/11	73	74	1.48	3	1800	1,15,25	3	0
SN 1994S	1994-06-16.338	49519.338	1.11	3	3120–11300	6/11	61	61	2.19	3	1200	1,15,5	3	0
SN 1994T	1994-07-15.233	49548.233	33.09	3	3120–10400	6/11	46	45	2.33	1.5	2100	1	3	0
SN 1994U	1994-07-13.227	49546.227	···	3	3120–11400	6/11	45	43	2.70	1.75	1800	1	3	0

Continued on Next Page...

Table 2.2 — Continued

SN Name	UT Date[a]	MJD[b]	Phase[c]	Inst.[d]	Wavelength Range (Å)	Res.[e] (Å)	P.A.[f] (°)	Par.[g] (°)	Air.[h]	See.[i] (″)	Exp. (s)	Observer(s)[j]	Reducer[k]	Flux Corr.[l]
SN 1994X	1994-09-01.410	49596.410	···	3	3120–10400	6/11	175	358	2.13	2.25	1800	1,15,5	3	0
SN 1994ab	1994-10-11.226	49636.226	···	3	4260–7000	5	197	14	2.71	1.75	1800	1,5	4	0
SN 1994ae	1995-02-24.472	49772.472	87.37	3	3120–11350	6/11	52	50	1.32	1.5	2100	1,15	3	0
SN 1994ae	1995-04-22.372	49829.372	144.03	3	3130–10550	6/11	236	56	1.80	3	2100	1,15,26	4	0
SN 1994ae	1995-07-06.210	49904.210	218.55	3	3592–10450	6/11	56	56	2.76	2.75	1800	15,27	4	0
SN 1995A	1995-02-24.211	49772.211	···	3	4260–7030	3	188	7	1.02	1.5	1800	1,15	3	0
SN 1995C	1995-02-24.411	49772.411	···	3	4260–7030	3	181	358	2.78	1.5	600	1,15	3	0
SN 1995D	1995-02-24.433	49772.433	3.84	3	3120–9900	6/11	44	42	1.57	1.5	1900	1,15	3	0
SN 1995D	1995-03-25.364	49801.364	32.58	3	3140–11100	6/11	47	43	1.67	3.25	3000	1,15,27	4	0
SN 1995D	1995-04-22.265	49829.265	60.30	3	3296–10314	6/11	222	39	1.48	3	2200	1,15,26	4	0
SN 1995D	1995-05-24.195	49861.195	92.02	3	3120–10450	6/11	48	43	1.62	1.75	2100	1,15,27	4	0
SN 1995E	1995-02-24.314	49772.314	−2.46	3	3120–11340	6/11	145	149	1.27	1.5	1800	1,15	3	0
SN 1995E	1995-04-22.307	49829.307	53.88	3	3180–10550	6/11	87	89	1.62	3	1700	1,15,26	4	0
SN 1995L	1995-04-22.475	49829.475	···	3	4300–7060	5	247	68	1.46	3	1800	1,15,26	4	0
SN 1995T	1995-08-01.453	49930.453	···	3	3180–8040	6/5	70	9	1.51	1.25	3000	1,15,27	4	0
SN 1995ac	1995-09-26.406	49986.406	−6.34	3	3200–10450	6/11	231	37	2.30	2.5	3600	1,27	4	0
SN 1995ac	1995-10-29.000	50019.000	24.71	3	3340–10600	6/11	···	···	···	1.5	···	28,29	4	0
SN 1995ak	1995-11-26.477	50047.477	26.38	5	5101–10181	6	63	64	1.35	0.90	3600	1,15,30,31	3	0
SN 1995al	1995-11-30.444	50051.444	22.15	3	3160–9900	6/11	109	289	1.20	1.5	1400	1,5	4	0
SN 1995al	1995-12-17.440	50068.440	39.06	3	3180–10450	6/11	107	287	1.07	6	2700	1,27	4	0
SN 1996O	1996-04-26.626	50199.626	···	5	4835–9835	7	64	81	1.32	1.2	600	1,15,30,31	3	0
SN 1996P	1996-03-27.277	50169.277	···	3	4300–7000	3	139	318	1.60	1.5	1800	1,27	5	0
SN 1996ai	1996-06-20.000	50254.000	···	3	3700–7600	6/5	···	···	···	2	···	32	4	0
SN 1996ai	1996-06-21.000	50255.000	···	3	3600–7600	6/5	···	···	···	2	···	32	4	0
SN 1996ai	1996-06-22.331	50256.331	···	3	3160–10450	6/11	68	68	1.73	2.25	1800	1,27,33	4	0
SN 1996ai	1996-07-13.322	50277.322	···	5	4960–9820	7	92	96	1.56	1.1	1200	1,27,5,8	4	0
SN 1996ai	1996-08-10.191	50305.191	···	3	3200–10400	6/11	68	69	1.66	2.5	2100	1,27,34	4	0
SN 1996bv	1996-12-07.336	50424.336	20.30	3	4320–7040	3	90	216	1.08	3	762	1,27,34	5	0
SN 1997E	1997-02-09.272	50488.272	20.40	3	3200–10500	6/11	159	159	1.27	2	667	1,27,34,35	4	0
SN 1997T	1997-02-09.297	50488.297	···	3	4370–7050	3	107	237	1.46	2	1800	1,27,34,35	4	0
SN 1997Y	1997-02-09.351	50488.351	1.27	3	3200–9920	6/11	54	264	1.23	2	600	1,27,34,35	4	0
SN 1997bp	1997-04-16.451	50554.451	5.49	3	3160–10470	6/11	44	42	2.96	2.5	700	1,15,35	4	0
SN 1997br	1997-04-16.430	50554.430	−4.84	3	3160–10470	6/11	33	30	2.81	2.5	900	1,15,35	4	0
SN 1997br	1997-05-11.214	50579.214	19.78	3	3140–6960	6/5	186	343	2.08	1.75	1700	1,27	4	0
SN 1997br	1997-06-06.214	50605.214	45.60	3	3160–10400	6/11	186	6	2.01	4	1700	1,27	4	0
SN 1997br	1997-07-10.214	50639.214	79.36	3	4220–6960	3	37	34	3.26	3.5	900	1,27	4	0
SN 1997br	1997-07-10.221	50639.221	79.37	3	3300–10500	6/11	37	34	3.51	3.5	2100	1,27	4	0
SN 1997cn	1997-06-06.363	50605.363	18.38	3	3160–10400	6/11	235	54	1.52	4	2100	1,27	4	0
SN 1997cw	1997-08-04.452	50664.452	32.77	3	3280–10550	6/11	165	344	1.11	1.5	1500	1,27,35	5	0
SN 1997cw	1997-09-06.406	50697.406	65.16	3	3280–10450	6/11	150	14	1.11	1.75	1800	1,35	5	0
SN 1997do	1997-11-08.480	50760.480	−5.67	3	3270–10500	6/11	53	223	1.02	2	900	1,27	1	0
SN 1997do	1998-01-28.311	50841.311	74.35	3	3280–10200	6/11	93	140	1.02	2.5	1800	1,35	1	0
SN 1997fb	1998-01-17.315	50830.315	···	5	4340–6840	3	220	360	1.91	1	400	1,36	4	0
SN 1997fc	1998-01-17.322	50830.322	···	5	4340–6840	3	249	4	1.93	1	800	1,36	4	0
SN 1998V	1998-03-26.638	50898.638	7.20	5	3850–9200	4.5/7	60	286	1.05	1.15	150	1,27,37	1	0

Continued on Next Page...

Table 2.2 — Continued

SN Name	UT Date[a]	MJD[b]	Phase[c]	Inst.[d]	Wavelength Range (Å)	Res.[e] (Å)	P.A.[f] (°)	Par.[g] (°)	Air.[h]	See.[i] (″)	Exp. (s)	Observer(s)[j]	Reducer[k]	Flux Corr.[l]
SN 1998aq	1998-06-18.321	50982.321	51.34	3	3300–10400	6/11	71	71	1.81	1.25	870	1,27,38,39	1	0
SN 1998aq	1998-07-17.241	51011.241	80.15	3	3350–10400	6/11	72	71	1.81	2.5	944	1,15	1	0
SN 1998aq	1998-07-23.234	51017.234	86.13	3	3280–10200	6/11	70	70	1.86	1.5	374	27,35	1	0
SN 1998bn	1998-05-22.268	50955.268	···	3	5391–8171	5	0	22	2.43	···	900	40	6	0
SN 1998bn	1998-05-22.268	50955.268	···	3	3196–5358	6	0	22	2.43	···	900	40	6	0
SN 1998bn	1998-06-18.216	50982.216	···	3	3400–10400	6/11	30	31	2.92	1.25	1200	1,27,38,39	1	0
SN 1998bp	1998-05-22.434	50955.434	18.87	3	5391–8171	5	0	10	1.06	···	900	40	6	0
SN 1998bp	1998-05-22.434	50955.434	18.87	3	3196–5358	6	0	10	1.06	···	900	40	6	0
SN 1998bp	1998-06-18.454	50982.454	45.61	3	3300–10400	6/11	54	54	1.33	1.25	1200	1,27,38,39	1	0
SN 1998bp	1998-09-21.174	51077.174	139.35	3	3300–10200	6/11	51	51	1.25	1.5	1800	1,27,41	1	0
SN 1998bp	1998-10-15.131	51101.131	163.06	3	3474–9776	6/11	54	55	1.38	2.5	2100	1,27	1	0
SN 1998bu	1998-06-18.206	50982.206	29.58	3	3400–10400	6/11	53	53	1.84	1.25	200	1,27,38,39	1	0
SN 1998bu	1998-07-17.200	51011.200	58.49	3	3350–10400	6/11	54	54	5.06	2.5	660	1,15	1	0
SN 1998bu	1999-01-10.378	51188.378	235.13	3	3350–10300	6/11	134	316	1.30	2	1800	1,42,5	7	0
SN 1998bu	1999-02-23.420	51232.420	279.05	3	3340–10550	6/11	38	36	1.20	1.75	1800	1,42	5	0
SN 1998bu	1999-04-24.279	51292.279	338.73	3	3300–10520	6/11	45	43	1.28	2.75	1800	1,42	5	0
SN 1998cd	1998-06-18.240	50982.240	···	3	3500–10400	6/11	67	67	1.74	1.25	1200	1,27,38,39	1	0
SN 1998cl	1998-06-18.387	50982.387	···	3	3400–10400	6/11	86	85	1.64	1.25	740	1,27,38,39	1	0
SN 1998cm	1998-06-18.346	50982.346	···	3	3800–10400	6/11	50	51	2.75	1.25	1100	1,27,38,39	1	0
SN 1998cs	1998-07-17.387	51011.387	···	3	3350–10400	6/11	70	70	1.64	2.5	2150	1,15	1	0
SN 1998cs	1998-07-23.367	51017.367	···	3	3280–10200	6/11	72	71	1.58	1.5	1500	27,35	1	0
SN 1998cs	1998-09-20.182	51076.182	···	3	4300–7050	3	75	75	1.41	1.5	1800	1,27,41	1	0
SN 1998dh[m]	1998-08-23.521	51048.521	18.77	3	3300–10100	6/11	90	47	1.78	3	300	43	1	2
SN 1998dh	1998-08-31.287	51056.287	26.47	3	3396–10200	6/11	147	327	1.32	1.5	600	1,27,5	1	−6
SN 1998dh	1998-09-21.260	51077.260	47.26	3	3300–10200	6/11	161	341	1.22	1.5	1800	1,27,41	1	6
SN 1998dh	1998-10-15.218	51101.218	71.00	3	3300–10200	6/11	175	352	1.19	2.5	1500	1,27	1	5
SN 1998de	1998-08-31.492	51056.492	29.49	3	3300–10200	6/11	59	60	1.10	1.5	1800	1,27,5	1	0
SN 1998de	1998-09-20.346	51076.346	49.02	3	3300–10400	6/11	90	333	1.02	1.5	1800	1,27,41	1	0
SN 1998de	1998-10-15.294	51101.294	73.56	3	3320–10200	6/11	132	7	1.02	2.5	2700	1,27	1	0
SN 1998dj	1998-08-31.466	51056.466	···	3	3300–10200	6/11	190	358	1.39	1.5	1500	1,27,5	1	0
SN 1998dk[m]	1998-08-24.518	51049.518	−7.24	3	3300–10100	6/11	90	37	1.56	3	600	43	1	0
SN 1998dk	1998-08-31.305	51056.305	−0.54	3	3300–10200	6/11	144	324	1.53	1.5	1200	1,27,5	1	0
SN 1998dk	1998-09-21.287	51077.287	20.17	3	3300–10200	6/11	161	337	1.34	1.5	1500	1,27,41	1	0
SN 1998dk	1998-10-15.256	51101.256	43.83	3	3320–10200	6/11	171	353	1.28	2.5	2100	1,27	1	0
SN 1998dm[m]	1998-08-24.506	51049.506	−12.48	3	3300–10100	6/11	90	15	1.42	3	900	43	1	2
SN 1998dm	1998-08-31.423	51056.423	−5.61	3	3300–10200	6/11	169	350	1.39	1.5	1200	1,27,5	1	5
SN 1998dm	1998-09-20.380	51076.380	14.22	3	3300–10300	6/11	174	353	1.38	1.5	600	1,27,41	1	5
SN 1998dm	1998-10-15.335	51101.335	39.01	3	3300–10200	6/11	185	6	1.38	2.5	1800	1,27	1	6
SN 1998dm	1998-11-25.288	51142.288	79.70	3	3330–10200	6/11	209	31	1.62	2.25	2700	1,5	1	0
SN 1998dw	1998-09-21.340	51077.340	···	3	3400–10200	6/11	162	346	1.71	1.5	1300	1,27,41	1	0
SN 1998dx	1998-09-21.225	51077.225	5.13	3	3300–10200	6/11	90	90	1.26	1.5	1800	1,27,41	1	0
SN 1998dx	1998-10-15.174	51101.174	27.84	3	3300–10200	6/11	86	85	1.35	2.5	2700	1,27	1	0
SN 1998eb	1998-09-20.423	51076.423	···	3	3300–10300	6/11	77	249	1.35	1.5	1800	1,27,41	1	0
SN 1998ec	1998-10-15.463	51101.463	11.86	3	3300–10200	6/11	250	252	1.11	2.5	1800	1,27	1	0
SN 1998ef	1998-10-19.128	51105.128	−8.62	3	3200–10100	6/11	90	294	1.58	3	600	43,44	1	0

Continued on Next Page...

Table 2.2 — Continued

SN Name	UT Date[a]	MJD[b]	Phase[c]	Inst.[d]	Wavelength Range (Å)	Res.[e] (Å)	P.A.[f] (°)	Par.[g] (°)	Air.[h]	See.[i] (″)	Exp. (s)	Observer(s)[j]	Reducer[k]	Flux Corr.[l]
SN 1998ef	1998-11-25.220	51142.220	27.83	3	3330–10200	6/11	215	54	1.01	2.25	1800	1,5	1	0
SN 1998ef	1999-01-10.181	51188.181	72.99	3	3350–10300	6/11	109	70	1.20	2	1800	1,42,5	7	0
SN 1998ef	1999-01-21.212	51199.212	83.82	5	5100–8800	7	109	111	1.12	1.1	600	1,27	8	0
SN 1998ef	1999-01-22.236	51200.236	84.83	5	3500–10950	4.5/7	109	103	1.20	0.95	200	1,27	8	0
SN 1998eg	1998-11-25.166	51142.166	30.60	3	3330–10200	6/11	215	37	1.27	2.25	2550	1,5	1	0
SN 1998en	1998-11-25.341	51142.341	···	3	3340–10200	6/11	76	255	1.14	2.25	2700	1,5	1	0
SN 1998es	1998-11-25.252	51142.252	0.28	3	3330–10200	6/11	197	18	1.20	2.25	1800	1,5	1	5
SN 1998es	1999-01-10.221	51188.221	45.77	3	3350–10300	6/11	44	47	1.66	2	1800	1,42,5	7	5
SN 1998es	1999-01-18.206	51196.206	53.67	5	5420–9180	7	90	38	1.05	1.3	30	1,27,37	8	0
SN 1998es	1999-01-22.000	51200.000	57.42	5	3500–10950	4.5/7	65	66	1.29	0.95	100	1,27	8	0
SN 1998es	1999-02-12.135	51221.135	78.34	3	3300–10500	6/11	46	47	1.69	3	1800	1,27,42	5	0
SN 1998es	1999-02-23.132	51232.132	89.22	3	3300–10550	6/11	50	50	2.07	1.75	1800	1,42	5	0
SN 1998es	1999-03-12.133	51249.133	106.04	3	3700–10500	6/11	53	53	3.77	1.75	1800	1,42,5	5	0
SN 1998fc	1999-01-20.241	51198.241	···	5	5100–8850	7	51	11	1.05	2	1000	1,27,37	8	0
SN 1999C	1999-01-20.664	51198.664	···	5	5120–8840	7	126	123	1.95	2	700	1,27,37	8	0
SN 1999X	1999-02-12.168	51221.168	15.76	3	3300–10500	6/11	107	286	1.29	3	1802	1,27,42	5	0
SN 1999X	1999-02-23.278	51232.278	26.60	3	3340–10550	6/11	37	50	1.00	1.75	1800	1,42	5	0
SN 1999aa	1999-02-12.258	51221.258	−10.58	3	3300–10500	6/11	183	354	1.05	3	1800	1,27,42	5	0
SN 1999aa	1999-02-23.237	51232.237	0.24	3	3340–10550	6/11	155	336	1.05	1.75	900	1,42	5	0
SN 1999aa	1999-03-09.230	51246.230	14.04	5	3700–11000	4.5/7	93	273	1.16	1	180	1,42	8	0
SN 1999aa	1999-03-12.275	51249.275	17.04	3	3276–10500	6/11	185	46	1.10	1.75	1200	1,42,5	5	0
SN 1999aa	1999-04-24.185	51292.185	59.34	3	3300–10520	6/11	50	54	1.19	2.75	1800	1,42	5	0
SN 1999aa	1999-11-09.629	51491.629	255.94	5	4200–9600	7	3	285	1.01	1	600	1,37,45	8	0
SN 1999aa	1999-12-05.561	51517.561	281.51	5	4000–10000	7	3	285	1.01	1.85	300	1,46	8	0
SN 1999aq	1999-03-09.248	51246.248	···	5	3700–10000	4.5/7	110	301	1.54	1	300	1,42	8	0
SN 1999ac	1999-03-09.625	51246.625	−3.70	5	5050–8750	7	31	338	1.03	1	200	1,42	8	4
SN 1999ac	1999-03-12.466	51249.466	−0.89	3	3276–10500	6/11	185	327	1.25	1.75	900	1,42,5	5	2
SN 1999ac	1999-04-24.490	51292.490	41.73	3	3300–10520	6/11	213	36	1.27	2.75	1000	1,42	5	5
SN 1999ac	1999-07-09.336	51368.336	116.87	3	3290–10550	6/11	48	48	1.64	2	1800	1	5	0
SN 1999bh	1999-04-24.352	51292.352	···	3	3300–10520	6/11	100	98	1.35	2.75	1800	1,42	5	0
SN 1999bv	1999-04-24.460	51292.460	···	3	3300–10520	6/11	177	182	1.08	2.75	1800	1,42	5	0
SN 1999by	1999-11-09.645	51491.645	183.50	5	4000–9700	7	29	334	1.20	1	100	1,37,45	8	0
SN 1999cl	1999-06-21.222	51350.222	7.90	3	5130–10530	11	50	50	1.38	2.5	1200	1,42	5	−6
SN 1999cl	1999-07-09.213	51368.213	25.76	3	3290–10550	6/11	54	54	1.68	2	500	1	5	6
SN 1999cl	1999-07-18.201	51377.201	34.68	3	3360–10550	6/11	53	55	1.89	2.25	1200	1,39,5	5	5
SN 1999cl	1999-12-15.613	51527.613	183.95	5	5644–6935	3	107	284	1.23	1	900	1	1	0
SN 1999cp	1999-07-09.200	51368.200	4.91	3	3290–10550	6/11	27	28	1.54	2	600	1	5	6
SN 1999cp	1999-07-18.226	51377.226	13.85	3	3360–10550	6/11	40	41	2.01	2.25	900	1,39,5	5	6
SN 1999cw	1999-07-09.477	51368.477	14.79	3	3290–10550	6/11	153	333	1.55	2	1035	1	5	0
SN 1999cw	1999-07-18.473	51377.473	23.68	3	3360–10550	6/11	160	340	1.46	2.25	1200	1,39,5	5	0
SN 1999cw	1999-09-17.328	51438.328	83.79	3	3300–10550	6/11	172	349	1.40	1.25	1500	1,42,45	5	0
SN 1999cw	1999-10-08.369	51459.369	104.58	3	3290–10500	6/11	204	21	1.51	2.75	1800	1,47	5	0
SN 1999cw	1999-11-05.210	51487.210	132.08	3	3380–10460	6/11	175	356	1.38	2	1800	1,27,47	5	0
SN 1999da	1999-07-09.365	51368.365	−2.12	3	3290–10550	6/11	127	121	1.18	2	1200	1	5	0
SN 1999da	1999-07-18.352	51377.352	6.76	3	3360–10550	6/11	115	114	1.21	2.25	1800	1,39,5	5	0

Continued on Next Page...

Table 2.2 — Continued

SN Name	UT Date[a]	MJD[b]	Phase[c]	Inst.[d]	Wavelength Range (Å)	Res.[e] (Å)	P.A.[f] (°)	Par.[g] (°)	Air.[h]	See.[i] (″)	Exp. (s)	Observer(s)[j]	Reducer[k]	Flux Corr.[l]
SN 1999da	1999-08-17.275	51407.275	36.30	3	3340–10550	6/11	114	112	1.23	2.5	1800	1,45,47,5	5	0
SN 1999da	1999-09-10.211	51431.211	59.94	3	3300–10500	6/11	114	112	1.23	2	1500	27,47	5	0
SN 1999da[m]	1999-09-17.247	51438.247	66.89	3	3552–10174	6/11	77	92	1.42	1.25	1800	1,42,45	5	0
SN 1999dg	1999-08-17.209	51407.209	15.08	3	3340–10550	6/11	45	53	1.65	2.5	1200	1,45,47,5	5	5
SN 1999dg	1999-09-10.174	51431.174	38.52	3	3396–10500	6/11	55	55	2.18	2	1800	27,47	5	0
SN 1999dk	1999-08-17.376	51407.376	−6.60	3	3340–10550	6/11	132	309	1.39	2.5	600	1,45,47,5	5	0
SN 1999dk	1999-09-10.384	51431.384	17.06	3	3300–10500	6/11	154	335	1.11	2	1800	27,47	5	0
SN 1999dk	1999-09-17.377	51438.377	23.95	3	3300–10550	6/11	166	342	1.10	1.25	1800	1,42,45	5	0
SN 1999dk	1999-10-08.264	51459.264	44.53	3	3290–10500	6/11	137	314	1.22	2.75	1800	1,47	5	0
SN 1999dk	1999-11-05.305	51487.305	72.16	3	3380–10460	6/11	200	24	1.11	2	1800	1,27,47	5	0
SN 1999do	1999-09-10.277	51431.277	9.96	3	3300–10500	6/11	90	302	1.02	2	1800	27,47	5	0
SN 1999dq	1999-09-10.525	51431.525	−3.93	3	3300–10500	6/11	220	42	1.09	2	900	27,47	5	5
SN 1999dq	1999-09-17.521	51438.521	2.97	3	3300–10550	6/11	227	48	1.13	1.25	1200	1,42,45	5	5
SN 1999dq	1999-10-08.337	51459.337	23.49	3	3290–10500	6/11	135	312	1.11	2.75	1800	1,47	5	5
SN 1999dq	1999-11-05.271	51487.271	51.03	3	3380–10460	6/11	144	325	1.07	2	1800	1,27,47	5	0
SN 1999ee	1999-11-05.152	51487.152	17.65	3	3380–10460	6/11	183	4	3.65	2	1202	1,27,47	5	0
SN 1999ek	1999-11-05.563	51487.563	5.66	3	3564–10460	6/11	51	52	1.36	2	600	1,27,47	5	0
SN 1999fz	1999-12-05.616	51517.616	···	5	4000–10000	7	67	301	2.27	1.85	300	1,46	8	0
SN 1999gd	1999-12-05.580	51517.580	−1.12	5	4000–10000	7	23	341	1.01	1.85	100	1,46	8	0
SN 1999gf	1999-12-05.598	51517.598	···	5	4000–10000	7	138	319	1.13	1.85	200	1,46	8	0
SN 1999gh	1999-12-05.606	51517.606	4.12	5	4000–10000	7	165	346	1.35	1.85	120	1,46	8	0
SN 1999gh	1999-12-17.463	51529.463	15.89	3	3360–10250	6/11	165	344	2.02	3.5	800	27,45,47	4	0
SN 1999gh	1999-12-17.543	51529.543	15.97	3	4240–6858	5	183	358	2.00	3.5	7500	27,45,47	4	0
SN 1999gh	2000-03-29.331	51632.331	117.97	3	3300–10500	6/11	210	28	2.77	2.5	2400	47,5	5	0
SN 1999gm	1999-12-17.419	51529.419	···	3	3360–10250	6/11	164	347	1.47	3.5	900	27,45,47	4	0
SN 2000J	2000-03-15.537	51618.537	···	3	3300–10500	6/11	149	66	1.25	3	1000	1,45	5	0
SN 2000al	2000-03-15.478	51618.478	···	3	3300–10500	6/11	31	33	1.48	3	2400	1,45	5	0
SN 2000Q	2000-03-15.514	51618.514	···	3	3300–10500	6/11	183	183	1.18	3	1200	1,45	5	0
SN 2000Q	2000-03-29.527	51632.527	···	3	3300–10500	6/11	71	155	1.20	2.5	1500	47,5	5	0
SN 2000bk	2000-04-27.393	51661.393	14.84	3	3300–10350	6/11	40	42	2.29	2	1200	1,27	5	0
SN 2000ce	2000-05-31.208	51695.208	27.05	3	3290–10450	6/11	80	79	1.68	3.5	940	1,45	5	0
SN 2000cn	2000-06-27.401	51722.401	14.25	3	3290–10400	6/11	61	63	1.14	2	1800	1,45	5	6
SN 2000cn	2000-07-06.455	51731.455	23.09	3	3300–10400	6/11	63	63	1.57	3.5	1200	1,39,47	5	5
SN 2000cp	2000-06-27.322	51722.322	2.92	3	3290–10400	6/11	47	50	1.23	2	2400	1,45	5	6
SN 2000cp	2000-07-06.396	51731.396	11.70	3	3300–10400	6/11	56	57	2.10	3.5	1500	1,39,47	5	−6
SN 2000cv	2000-07-28.228	51753.228	···	3	3300–10450	6/11	83	75	1.75	1.5	900	1,47	5	0
SN 2000cu	2000-07-28.337	51753.337	9.63	3	3300–10450	6/11	192	15	2.37	1.5	900	1,47	5	5
SN 2000cu	2000-08-27.227	51783.227	38.87	3	3300–10450	6/11	176	8	2.26	1.75	1800	1,42	5	2
SN 2000cw	2000-07-28.356	51753.356	4.81	3	3300–10450	6/11	115	295	1.24	1.5	900	1,47	5	5
SN 2000cw	2000-09-26.322	51813.322	63.02	3	3300–10400	6/11	159	30	1.02	2	1800	1,42,47,48	5	−4
SN 2000cx[m]	2000-07-23.000	51748.000	−4.46	2	3832–7400	7	0	···	2.00	···	3600	49	5	0
SN 2000cx	2000-07-28.396	51753.396	0.89	3	3300–10450	6/11	130	309	1.76	1.5	200	1,47	5	0
SN 2000cx[m]	2000-08-01.000	51757.000	4.46	3	3350–10700	6/11	···	···	1.10	···	600	50	5	0
SN 2000cx[m]	2000-08-02.000	51758.000	5.46	3	3350–10700	6/11	···	···	1.10	···	600	50	5	0
SN 2000cx[m]	2000-08-03.000	51759.000	6.45	2	3950–7450	7	0	···	2.10	···	3600	49	5	0

Continued on Next Page...

Table 2.2 — Continued

SN Name	UT Date[a]	MJD[b]	Phase[c]	Inst.[d]	Wavelength Range (Å)	Res.[e] (Å)	P.A.[f] (°)	Par.[g] (°)	Air.[h]	See.[i] (″)	Exp. (s)	Observer(s)[j]	Reducer[k]	Flux Corr.[l]
SN 2000cx[m]	2000-08-05.000	51761.000	8.43	2	3950–7450	7	0	···	2.10	···	3600	49	5	0
SN 2000cx[m]	2000-08-07.000	51763.000	10.42	2	3950–7450	7	0	···	2.10	···	3600	49	5	0
SN 2000cx[m]	2000-08-10.000	51766.000	13.39	2	3950–7450	7	0	···	2.20	···	3600	49	5	0
SN 2000cx[m]	2000-08-15.000	51771.000	18.35	2	3950–7450	7	0	···	2.00	···	3600	49	5	0
SN 2000cx[m]	2000-08-18.000	51774.000	21.33	2	3950–7450	7	0	···	2.20	···	3600	49	5	0
SN 2000cx[m]	2000-08-20.000	51776.000	23.32	2	3950–7450	7	0	···	1.90	···	3600	49	5	0
SN 2000cx[m]	2000-08-22.000	51778.000	25.30	2	3950–7450	7	0	···	2.10	···	3600	49	5	0
SN 2000cx[m]	2000-08-24.000	51780.000	27.28	2	3950–7450	7	0	···	1.80	···	3600	49	5	0
SN 2000cx[m]	2000-08-26.000	51782.000	29.27	2	3950–7450	7	0	···	1.70	2	3600	49	5	0
SN 2000cx	2000-08-27.431	51783.431	30.69	3	3300–10450	6/11	160	342	1.15	1.75	450	1,42	5	0
SN 2000cx	2000-09-06.424	51793.424	40.60	3	3300–10450	6/11	174	355	1.13	3	700	1,42,47	5	0
SN 2000cx	2000-09-26.389	51813.389	60.41	3	3300–10400	6/11	185	9	1.13	2	1200	1,42,47,48	5	0
SN 2000cx	2000-10-06.359	51823.359	70.30	3	3300–10400	6/11	184	9	1.13	1.75	1800	1,47	5	0
SN 2000cx	2000-10-24.331	51841.331	88.13	3	3300–10400	6/11	197	21	1.16	1.5	1800	1,47	5	0
SN 2000cx	2000-11-01.336	51849.336	96.07	3	3300–10400	5.16/10.37	34	33	1.22	2.47	1800	1,42	5	0
SN 2000cx	2000-11-29.209	51877.209	123.73	3	3300–10500	6/11	186	6	1.13	3.5	1800	1,47	5	0
SN 2000cx	2000-12-21.173	51899.173	145.52	3	3300–10500	6/11	23	9	1.17	1.75	2700	1,39,47	5	0
SN 2000cx	2001-10-22.270	52204.270	448.22	6	3930–10198	0.5/0.5	199	288	1.60	0.70	1800	1,47	5	0
SN 2000dd	2000-08-27.256	51783.256	···	3	3300–10450	6/11	180	1	2.02	1.75	1800	1,42	5	0
SN 2000df	2000-08-26.225	51782.225	···	3	3290–10450	6/11	48	49	1.83	2	1000	27,42	5	0
SN 2000dg	2000-08-27.309	51783.309	−5.09	3	3300–10450	6/11	137	319	1.33	1.75	1500	1,42	5	0
SN 2000dg	2000-09-06.438	51793.438	4.66	3	3300–10450	6/11	210	34	1.24	3	2100	1,42,47	5	0
SN 2000dk	2000-09-26.479	51813.479	1.00	3	3300–10400	6/11	70	70	1.20	2	600	1,42,47,48	5	6
SN 2000dk	2000-10-06.487	51823.487	10.84	3	3300–10400	6/11	68	68	1.39	1.75	900	1,47	5	6
SN 2000dk	2000-10-24.361	51841.361	28.41	3	3300–10400	6/11	244	70	1.08	1.5	1200	1,47	5	4
SN 2000dk	2000-11-01.418	51849.418	36.32	3	3300–10400	7.43/9.53	66	67	1.44	2.31	1800	1,42	9	0
SN 2000dm	2000-09-26.244	51813.244	−1.63	3	3300–10400	6/11	55	56	1.78	2	1200	1,42,47,48	5	5
SN 2000dm	2000-10-06.206	51823.206	8.18	3	3300–10400	6/11	55	55	1.67	1.75	1500	1,47	5	5
SN 2000dm	2000-10-24.169	51841.169	25.88	3	3300–10400	6/11	235	56	1.86	1.5	1800	1,47	5	6
SN 2000dm	2000-11-01.166	51849.166	33.76	3	3260–10400	6/11	55	56	1.99	2.25	2400	1,42	9	5
SN 2000dn	2000-10-06.327	51823.327	−0.94	3	3300–10400	6/11	201	29	1.48	1.75	900	1,47	5	6
SN 2000dn	2000-10-24.205	51841.205	16.38	3	3300–10400	6/11	180	3	1.32	1.5	1800	1,47	5	0
SN 2000dp	2000-10-06.460	51823.460	···	3	3300–7790	6/5	201	19	1.74	1.75	1800	1,47	5	0
SN 2000dp	2000-10-24.388	51841.388	···	3	3300–10400	6/11	188	10	1.65	1.5	1200	1,47	5	0
SN 2000dr	2000-10-24.306	51841.306	6.78	3	3300–10400	6/11	186	8	1.68	1.5	1200	1,47	5	0
SN 2000dx	2000-11-01.255	51849.255	−9.26	3	3300–10400	4.55/10.68	148	332	1.25	4.99	1500	1,42	9	0
SN 2000ej	2000-11-29.126	51877.126	···	3	3300–10450	6/11	180	35	1.68	3.5	1800	1,47	5	0
SN 2000ey	2000-11-29.157	51877.157	7.90	3	3300–10450	6/11	177	29	1.21	3.5	1200	1,47	5	0
SN 2000ey	2000-12-21.000	51899.000	29.30	3	3260–10520	4.80/11.11	152	25	1.23	2.42	1200	1,39,47	5	0
SN 2000ey	2001-01-23.121	51932.121	61.76	3	3300–10600	6/11	152	50	2.03	2.5	1200	1,47	5	0
SN 2000fa	2000-12-05.566	51883.566	−8.25	3	3300–10450	6/11	240	60	1.43	1.75	1500	1,47	5	5
SN 2000fa	2000-12-21.000	51899.000	6.86	3	3260–10510	4.88/10.42	59	59	1.30	2.61	1200	1,39,47	5	5
SN 2000fo	2001-01-23.146	51932.146	···	3	3300–10600	6/11	52	60	2.06	2.5	1800	1,47	5	0
SN 2001A	2001-02-01.000	51941.000	···	3	3260–10600	5.13/10.49	200	30	1.26	1.15	1800	1,39,47	5	0
SN 2001C	2001-01-23.296	51932.296	···	3	3300–10600	6/11	174	168	1.08	2.5	1500	1,47	5	0

Continued on Next Page...

Table 2.2 — Continued

SN Name	UT Date[a]	MJD[b]	Phase[c]	Inst.[d]	Wavelength Range (Å)	Res.[e] (Å)	P.A.[f] (°)	Par.[g] (°)	Air.[h]	See.[i] (″)	Exp. (s)	Observer(s)[j]	Reducer[k]	Flux Corr.[l]
SN 2001C	2001-02-01.000	51941.000	···	3	3260–10600	5.00/10.26	167	156	1.09	2.41	900	1,39,47	5	0
SN 2001E	2001-02-01.000	51941.000	15.01	3	3260–10600	5.08/9.64	215	36	2.00	2.85	900	1,39,47	5	0
SN 2001G	2001-02-01.000	51941.000	11.57	3	3260–10600	4.91/10.65	145	220	1.04	2.33	1200	1,39,47	5	0
SN 2001L	2001-02-01.000	51941.000	21.57	3	3260–10600	5.20/9.71	220	41	2.27	2.42	500	1,39,47	5	0
SN 2001N	2001-02-01.000	51941.000	13.05	3	3260–10600	5.07/11.05	146	58	1.19	4.70	1200	1,39,47	5	0
SN 2001P	2001-02-01.000	51941.000	···	3	3260–10600	5.08/10.43	145	327	1.07	1.70	1800	1,39,47	5	0
SN 2001U	2001-03-29.450	51997.450	···	5	4350–6870	3	150	328	1.21	1.5	500	1,15	3	0
SN 2001V	2001-03-21.368	51989.368	15.86	3	3300–10400	6/11	36	38	1.04	2	900	1,39,47	5	0
SN 2001V	2001-03-29.363	51997.363	23.74	5	4350–6870	3	160	264	1.04	1.5	4800	1,15	3	0
SN 2001V	2001-03-30.282	51998.282	24.64	3	3300–10500	6/11	147	328	1.03	2	900	39,47	5	0
SN 2001V	2001-04-16.427	52015.427	41.53	5	4350–6870	3	160	108	1.08	1.75	4000	1,27	3	0
SN 2001V	2001-04-30.000	52029.000	54.91	3	3258–10600	5.07/10.37	54	56	1.12	2.22	1200	39,47	5	0
SN 2001V	2001-05-16.381	52045.381	71.04	3	3300–10450	6/11	239	59	2.19	4	1800	1,47	5	0
SN 2001ay	2001-04-30.000	52029.000	6.79	3	3260–10600	4.91/10.19	182	34	1.03	4.66	1500	39,47	5	0
SN 2001ay	2001-05-16.411	52045.411	22.72	3	3382–10206	6/11	242	62	1.34	4	1800	1,47	5	0
SN 2001az	2001-04-30.000	52029.000	−3.24	3	3260–10600	4.91/10.98	185	168	1.28	3.04	1200	39,47	5	0
SN 2001ba	2001-04-30.000	52029.000	−4.64	3	3260–10600	5.38/10.18	181	5	2.88	2.24	1200	39,47	5	0
SN 2001bf	2001-05-16.439	52045.439	1.22	3	3300–10450	6/11	147	8	1.02	4	900	1,47	5	5
SN 2001bf	2001-07-27.372	52117.372	72.06	3	3300–10400	6/11	62	62	1.37	1.5	1200	1,47	5	6
SN 2001bg	2001-05-25.000	52054.000	13.70	3	3300–10500	5.00/10.76	63	63	1.62	2.10	900	27,47	5	6
SN 2001bg	2001-05-30.247	52059.247	18.91	6	3930–10199	0.5/0.5	90	88	1.50	0.70	150	1,47	5	6
SN 2001br	2001-05-25.245	52054.245	3.47	3	3414–7850	4.97/5.59	115	293	1.62	2.88	900	27,47	5	6
SN 2001br	2001-05-25.256	52054.256	3.48	3	3334–10154	5.00/9.80	115	293	1.62	3.06	300	27,47	5	6
SN 2001bp	2001-05-16.463	52045.463	0.51	3	3300–10450	6/11	150	76	1.19	4	1200	1,47	5	0
SN 2001bp	2001-05-29.409	52058.409	12.34	6	3930–10199	0.5/0.5	240	194	1.05	0.80	400	1,47	5	0
SN 2001bs	2001-05-29.400	52058.400	···	6	3930–10200	0.5/0.5	276	181	1.49	0.80	300	1,47	5	0
SN 2001cg	2001-05-29.393	52058.393	···	6	3930–10200	0.5/0.5	183	94	1.23	0.80	300	1,47	5	0
SN 2001cj	2001-06-29.296	52089.296	23.14	3	3300–10400	6/11	246	65	1.63	2	1000	39,47,51	5	0
SN 2001ck	2001-06-29.357	52089.357	16.39	3	3300–10400	6/11	244	64	1.71	2	700	39,47,51	5	−5
SN 2001ck	2001-07-16.305	52106.305	32.77	3	3300–10400	6/11	64	64	1.69	2.5	1400	39,47	5	6
SN 2001cp	2001-06-29.422	52089.422	1.39	3	3300–10400	6/11	228	48	1.80	2	800	39,47,51	5	0
SN 2001cp	2001-07-16.406	52106.406	18.00	3	3300–10400	6/11	49	51	2.41	2.5	1200	39,47	5	0
SN 2001cp	2001-07-27.258	52117.258	28.62	3	3300–10400	6/11	50	28	1.25	1.5	1200	1,47	5	0
SN 2001da	2001-07-16.458	52106.458	−1.12	3	3300–10400	6/11	151	332	1.20	2.5	900	39,47	5	6
SN 2001da	2001-07-27.486	52117.486	9.72	3	3300–10400	6/11	181	3	1.15	1.5	900	1,47	5	6
SN 2001de	2001-07-27.446	52117.446	···	3	3300–10400	6/11	149	152	1.03	1.5	1500	1,47	5	0
SN 2001dd	2001-07-16.435	52106.435	···	3	3300–10400	6/11	25	28	1.39	2.5	1200	39,47	5	0
SN 2001dl	2001-08-23.427	52144.427	13.84	3	3300–10400	6/11	47	48	1.55	1.75	900	39,47	5	5
SN 2001dl	2001-09-12.212	52164.212	33.22	3	3300–10400	6/11	158	341	1.16	2	1200	1,42,47	9	5
SN 2001dm	2001-08-23.468	52144.468	···	3	3412–10104	6/11	171	352	2.62	1.75	600	39,47	5	0
SN 2001dn	2001-09-12.377	52164.377	···	3	3300–10400	6/11	146	274	1.03	2	900	1,42,47	9	0
SN 2001ds	2001-08-23.488	52144.488	···	3	3442–10240	6/11	99	281	1.00	1.75	1200	39,47	5	0
SN 2001ei	2001-09-20.348	52172.348	···	3	3300–10400	6/11	63	34	1.03	1.75	1800	1,47	9	0
SN 2001ei	2001-10-23.305	52205.305	···	6	3930–10199	0.5/0.5	280	241	1.03	0.90	600	1,47	5	0
SN 2001dt	2001-09-12.306	52164.306	13.60	3	3300–10400	6/11	26	204	1.03	2	1800	1,42,47	9	0

Continued on Next Page...

Table 2.2 — Continued

SN Name	UT Date[a]	MJD[b]	Phase[c]	Inst.[d]	Wavelength Range (Å)	Res.[e] (Å)	P.A.[f] (°)	Par.[g] (°)	Air.[h]	See.[i] (″)	Exp. (s)	Observer(s)[j]	Reducer[k]	Flux Corr.[l]
SN 2001dw	2001-09-12.446	52164.446	11.06	3	3300–10400	6/11	157	338	1.13	2	900	1,42,47	9	0
SN 2001eg	2001-09-12.513	52164.513	···	3	3300–10400	6/11	86	262	1.32	2	1800	1,42,47	9	0
SN 2001ec	2001-09-12.413	52164.413	···	3	3300–10400	6/11	120	306	1.02	2	1800	1,42,47	9	0
SN 2001ed	2001-09-20.418	52172.418	···	3	3300–10400	6/11	183	4	1.17	1.75	1000	1,47	9	0
SN 2001eh	2001-09-11.263	52163.263	−5.63	3	3300–10400	6/11	107	285	1.43	2.5	600	1,42,47	9	0
SN 2001eh	2001-09-12.399	52164.399	−4.53	3	3300–10400	6/11	146	243	1.01	2	600	1,42,47	9	0
SN 2001eh	2001-09-20.478	52172.478	3.26	3	3300–10400	6/11	94	92	1.08	1.75	1200	1,47	9	0
SN 2001eh	2001-10-20.367	52202.367	32.08	3	3300–10400	5.07/10.41	180	102	1.03	1.59	1200	1,47	9	0
SN 2001eh	2001-10-25.173	52207.173	36.71	3	3280–10400	6/11	99	278	1.22	1.75	2100	42,47	5	0
SN 2001eh	2001-11-18.217	52231.217	59.90	6	3930–10199	0.5/0.5	346	285	1.40	0.90	600	1,47	5	0
SN 2001eu	2001-10-22.342	52204.342	···	6	3930–10199	0.5/0.5	145	299	1.46	0.70	900	1,47	5	0
SN 2001en	2001-10-20.453	52202.453	10.09	3	3300–10400	5.35/10.26	251	70	1.31	2.15	600	1,47	9	5
SN 2001en	2001-10-25.152	52207.152	14.72	3	3280–10400	6/11	110	290	1.35	1.75	900	42,47	5	5
SN 2001en	2001-11-15.406	52228.406	35.64	3	3280–10400	6/11	69	68	1.48	2.75	900	1,47	5	0
SN 2001ep	2001-10-20.470	52202.470	2.83	3	3300–10400	5.31/10.61	182	4	1.35	2.02	600	1,47	9	6
SN 2001ep	2001-10-22.654	52204.654	4.99	6	3930–10199	0.5/0.5	143	54	1.37	0.70	210	1,47	5	3
SN 2001ep	2001-10-23.652	52205.652	5.97	6	3930–10199	0.5/0.5	143	54	1.37	0.90	300	1,47	5	3
SN 2001ep	2001-10-25.556	52207.556	7.85	3	3280–10400	6/11	46	34	1.80	1.75	900	42,47	5	3
SN 2001ep	2001-11-15.428	52228.428	28.46	3	3280–10400	6/11	195	17	1.39	2.75	900	1,47	5	0
SN 2001ep	2002-01-14.000	52288.000	87.26	3	3268–10570	4.99/10.12	25	26	1.48	3.68	2700	42,47	5	−6
SN 2001ep	2002-02-11.000	52316.000	114.91	3	3300–10400	6/11	219	37	1.75	2.2	2700	1,47	9	0
SN 2001er	2001-10-20.523	52202.523	···	3	3300–10400	5.51/10.04	100	279	1.27	1.5	1200	1,47	9	0
SN 2001es	2001-10-20.272	52202.272	···	3	3300–10400	5.27/10.44	161	317	1.12	4.33	1200	1,47	9	0
SN 2001es	2001-10-23.313	52205.313	···	6	3930–10199	0.5/0.5	250	278	1.30	0.90	300	1,47	5	0
SN 2001ew	2001-10-20.301	52202.301	···	3	3300–10400	5.20/10.08	84	268	1.09	1.5	1200	1,47	9	0
SN 2001fg	2001-11-18.251	52231.251	···	6	3930–10199	0.5/0.5	232	56	1.29	0.90	400	1,47	5	0
SN 2001ex	2001-10-20.429	52202.429	−1.82	3	3300–10400	4.95/10.00	271	253	1.18	1.5	1200	1,47	9	3
SN 2001fe	2001-11-15.444	52228.444	−0.99	3	3280–10400	6/11	119	298	1.39	2.75	600	1,47	5	0
SN 2001fh	2001-11-16.254	52229.254	5.93	3	3300–10400	6/11	253	73	1.55	1.75	1200	1,47	5	6
SN 2001fh	2001-11-18.196	52231.196	7.84	6	3930–10199	0.5/0.5	65	156	1.12	0.90	300	1,47	5	2
SN 2001fu	2001-11-16.510	52229.510	···	3	3300–10400	6/11	165	347	1.81	1.75	900	1,47	5	0
SN 2001gc	2002-01-14.000	52288.000	43.27	3	3300–10400	5.12/10.40	108	107	1.14	4.81	1500	42,47	5	0
SN 2001ic	2001-12-11.298	52254.298	10.24	3	3668–10400	6/11	54	53	4.42	4	700	1,47	9	0
SN 2001ic	2001-12-23.205	52266.205	21.64	5	3548–10300	4.5/7	58	59	1.10	1	200	1,47	5	0
SN 2001ib	2001-12-11.277	52254.277	···	3	3300–10400	6/11	62	61	2.41	4	790	1,47	9	0
SN 2001ib	2002-01-14.000	52288.000	···	3	3268–10570	5.01/10.57	72	73	1.35	2.13	1500	42,47	5	0
SN 2001iq	2001-12-23.200	52266.200	···	5	3384–10300	4.5/7	120	120	1.23	1	200	1,47	5	0
SN 2001iq	2002-01-14.000	52288.000	···	3	3268–10570	4.97/10.18	66	65	2.01	2.28	1600	42,47	5	0
SN 2002G	2002-02-11.563	52316.563	19.31	3	3300–10400	5.19/10.08	140	74	1.10	3.36	1800	1,47	9	0
SN 2002ar	2002-02-11.420	52316.420	···	3	3300–10400	5.21/10.68	98	357	1.04	2.2	1200	1,47	9	0
SN 2002av	2002-02-11.220	52316.220	···	3	3300–10400	5.40/10.62	187	9	2.12	2.41	1500	1,47	9	0
SN 2002av	2002-02-14.335	52319.335	···	5	3400–6400	9	22	23	1.48	2.5	400	1,15	4	0
SN 2002av	2002-02-14.335	52319.335	···	5	7000–10100	7	22	23	1.48	2.5	400	1,15	4	0
SN 2002bk	2002-03-07.382	52340.382	···	5	3900–8800	7	22	23	1.18	1.75	600	1,27,36	4	0
SN 2002aw	2002-02-21.558	52326.558	2.10	3	3300–10400	5.09/10.48	136	261	1.03	1.86	900	42,47	9	6

Continued on Next Page...

Table 2.2 — Continued

SN Name	UT Date[a]	MJD[b]	Phase[c]	Inst.[d]	Wavelength Range (Å)	Res.[e] (Å)	P.A.[f] (°)	Par.[g] (°)	Air.[h]	See.[i] (″)	Exp. (s)	Observer(s)[j]	Reducer[k]	Flux Corr.[l]
SN 2002aw	2002-03-07.655	52340.655	15.84	5	3900–8800	7	260	351	1.07	1.75	200	1,27,36	4	6
SN 2002bf	2002-03-07.402	52340.402	2.97	5	3900–8800	7	98	179	1.24	1.75	300	1,27,36	4	0
SN 2002bf[m]	2002-03-11.428	52344.428	6.90	3	3300–10400	5.16/10.23	98	98	1.27	2.93	1161	42,47	9	−6
SN 2002bg	2002-03-07.589	52340.589	···	5	3900–8800	7	90	339	1.01	1.75	300	1,27,36	4	0
SN 2002bi	2002-03-07.580	52340.580	···	5	3900–8800	7	90	54	1.06	1.75	300	1,27,36	4	0
SN 2002bp	2002-04-08.416	52372.416	···	3	3398–10360	5.07/9.93	58	58	1.66	1.95	1800	42,47	9	0
SN 2002bo	2002-03-11.260	52344.260	−11.94	3	3300–10400	5.35/10.46	141	333	1.05	4.83	1800	42,47	9	6
SN 2002bo	2002-03-22.167	52355.167	−1.08	3	3300–10400	6/11	126	305	1.20	3	900	42,47	9	6
SN 2002bo	2002-04-08.311	52372.311	15.99	3	3300–10400	5.16/10.43	55	55	1.21	2.58	1800	42,47	9	6
SN 2002bo	2002-04-20.308	52384.308	27.94	3	3300–10400	4.76/11.14	238	58	1.33	2.57	900	42,47	9	0
SN 2002bo	2002-05-07.269	52401.269	44.83	3	3300–10400	6/11	58	58	1.40	4.75	1500	42,47	9	6
SN 2002bo	2002-05-19.191	52413.191	56.70	3	3300–10400	6/11	123	54	1.19	1.75	1800	42,47	9	3
SN 2002bo	2002-06-08.209	52433.209	76.63	3	3188–10400	6/11	123	59	1.64	3.75	1500	1,47,52	9	−3
SN 2002bo	2002-11-06.657	52584.657	227.44	6	3950–10199	0.5/0.5	2	271	1.12	0.75	240	1,47,53	5	0
SN 2002bs	2002-04-08.341	52372.341	···	3	3300–10400	4.97/9.94	179	359	1.62	3.64	600	42,47	9	0
SN 2002bz	2002-04-08.484	52372.484	4.92	3	3300–10400	4.96/10.61	61	62	1.19	4.97	1800	42,47	9	0
SN 2002cc	2002-04-20.238	52384.238	···	3	3300–10400	6/10.97	167	99	1.26	1.33	2400	42,47	9	0
SN 2002cd	2002-04-20.510	52384.510	1.10	3	3300–10400	6/10.83	242	241	1.16	2.93	900	42,47	9	6
SN 2002cd	2002-05-07.474	52401.474	17.89	3	3300–10400	6/11	236	234	1.13	4.75	1500	42,47	9	6
SN 2002cd	2002-06-17.399	52442.399	58.40	3	3232–10400	6/11	38	213	1.09	1.75	900	1,47,52	9	0
SN 2002cf	2002-04-20.335	52384.335	−0.75	3	3300–10400	6/11	193	12	1.44	1.75	1200	42,47	9	5
SN 2002cf	2002-05-07.295	52401.295	15.95	3	3300–10400	6/11	200	21	1.49	4.75	1800	42,47	9	6
SN 2002ci	2002-04-20.456	52384.456	···	3	3300–10400	5.22/10.85	222	50	1.02	1.75	1200	42,47	9	0
SN 2002ck	2002-05-07.453	52401.453	3.64	3	3300–10400	6/11	214	35	1.51	4.75	1200	42,47	9	0
SN 2002cr	2002-05-07.354	52401.354	−6.78	3	3300–10400	6/11	202	23	1.47	4.75	900	42,47	9	6
SN 2002cr	2002-06-08.331	52433.331	24.89	3	3170–10400	6/11	222	40	1.94	3.75	600	1,47,52	9	5
SN 2002cr	2002-06-17.209	52442.209	33.69	3	3124–10400	6/11	190	10	1.38	1.75	600	1,47,52	9	0
SN 2002cr	2002-07-11.211	52466.211	57.47	3	3200–10400	7.13/11.16	33	33	1.65	2.81	900	1,47,52,54	9	5
SN 2002cr	2002-08-09.000	52495.000	85.98	3	3200–10400	6/11	45	46	2.49	1.5	1800	1,51,52,55	9	0
SN 2002cs	2002-05-07.372	52401.372	−7.76	3	3300–10400	6/11	271	270	1.18	4.75	1500	42,47	9	0
SN 2002cs	2002-06-08.389	52433.389	23.76	3	3192–10400	6/11	92	207	1.01	3.75	600	1,47,52	9	5
SN 2002cs	2002-06-17.371	52442.371	32.61	3	3186–10400	6/11	91	196	1.01	1.75	600	1,47,52	9	6
SN 2002cs	2002-07-11.325	52466.325	56.19	3	3300–10400	7.10/10.45	114	156	1.01	1.89	900	1,47,52,54	9	5
SN 2002cs[m]	2002-08-10.251	52496.251	85.65	3	3200–10400	6.55/10.19	92	144	1.02	4.27	900	1,51,52,55	9	6
SN 2002cs	2002-09-13.171	52530.171	119.04	3	3188–10400	6.80/10.66	138	124	1.03	3.42	1800	52,53,55	9	0
SN 2002cs	2002-10-08.000	52555.000	143.49	5	3061–9420	7.35/7.80	152	152	1.13	0.96	400	1,47	5	0
SN 2002cs	2002-11-06.210	52584.210	172.24	6	3950–10199	0.5/0.5	201	111	1.36	0.75	900	1,47,53	5	0
SN 2002cu	2002-05-17.000	52411.000	−5.28	7	4899–8248	6	92	52	···	···	···	56,57	9	0
SN 2002cu	2002-06-08.406	52433.406	16.62	3	3100–10400	6/11	92	52	1.02	3.75	1200	1,47,52	9	0
SN 2002cx	2002-06-10.000	52435.000	19.78	6	4001–10299	0.5/0.5	···	···	1.03	···	1200	58,9	5	5
SN 2002cx	2002-06-15.264	52440.264	24.92	5	3163–9340	6.5/7	20	26	1.03	···	900	59,60	5	−6
SN 2002cx	2002-06-16.288	52441.288	25.92	5	3040–5800	6.5	48	49	1.06	···	900	24	5	0
SN 2002cx	2002-06-17.299	52442.299	26.90	5	5470–9230	7	51	55	1.08	···	600	24	5	0
SN 2002cx	2002-07-16.280	52471.280	55.21	5	4300–9260	7	70	68	1.33	···	1200	61,62	5	0
SN 2002cx	2003-01-07.649	52646.649	226.47	5	3301–9430	4.5/7	153	309	1.05	1.2	1800	1,47	5	0

Continued on Next Page...

Table 2.2 — Continued

SN Name	UT Date[a]	MJD[b]	Phase[c]	Inst.[d]	Wavelength Range (Å)	Res.[e] (Å)	P.A.[f] (°)	Par.[g] (°)	Air.[h]	See.[i] (″)	Exp. (s)	Observer(s)[j]	Reducer[k]	Flux Corr.[l]
SN 2002cx	2003-02-28.614	52698.614	277.22	5	3161–9420	6.5/7	240	60	1.13	0.80	2200	1,47	5	0
SN 2002cx	2003-02-28.641	52698.641	277.25	5	6260–7540	3	240	60	1.24	0.80	2200	1,47	5	0
SN 2002cv	2002-05-19.191	52413.191	−1.40	3	3300–10400	6/11	123	54	1.19	1.75	1800	42,47	9	0
SN 2002cv	2002-06-08.209	52433.209	18.53	3	3332–10400	6/11	123	59	1.64	3.75	1500	1,47,52	9	0
SN 2002db	2002-06-08.346	52433.346	9.21	3	3160–10400	6/11	137	94	1.19	3.75	1200	1,47,52	9	0
SN 2002de	2002-06-08.374	52433.374	−0.32	3	3176–10400	6/11	104	78	1.07	3.75	1200	1,47,52	9	6
SN 2002de	2002-06-17.304	52442.304	8.37	3	3322–9868	6/11	104	77	1.01	1.75	1200	1,47,52	9	5
SN 2002df	2002-06-08.435	52433.435	6.55	3	3200–10400	6/11	157	341	1.42	3.75	1200	1,47,52	9	0
SN 2002di	2002-06-17.326	52442.326	···	3	3226–10400	6/11	88	51	1.02	1.75	1200	1,47,52	9	0
SN 2002dj	2002-06-17.198	52442.198	−7.98	3	3134–10400	6/11	15	16	1.95	1.75	600	1,47,52	9	5
SN 2002dk	2002-06-17.345	52442.345	−1.23	3	3174–10400	6/11	88	348	1.04	1.75	1200	1,47,52	9	0
SN 2002do	2002-07-11.455	52466.455	23.09	3	3400–10400	6.95/11.06	114	109	1.01	1	602	1,47,52,54	9	−6
SN 2002dp	2002-07-11.427	52466.427	15.55	3	3100–10400	7.23/10.53	130	307	1.15	3.29	600	1,47,52,54	9	6
SN 2002dp	2002-08-09.390	52495.390	44.18	3	3110–10400	6.53/10.39	150	325	1.06	2.22	900	1,51,52,55	9	6
SN 2002dp	2002-09-03.384	52520.384	68.88	3	3150–10400	6.75/10.26	195	26	1.05	1.64	1200	1,47,51	9	0
SN 2002dp	2002-10-08.000	52555.000	103.10	5	3071–9420	6.65/7.94	90	267	1.06	1.41	366	1,47	5	0
SN 2002dp	2002-11-09.000	52587.000	134.73	6	3950–10199	0.5/0.5	270	268	1.10	1.1	600	1,47,53,63	5	0
SN 2002dr	2002-08-09.347	52495.347	···	3	3308–10400	6.69/10.00	184	295	1.05	4.45	900	1,51,52,55	9	0
SN 2002dx	2002-08-09.369	52495.369	···	3	3202–10400	6.65/10.19	150	295	1.10	1.5	1200	1,51,52,55	9	0
SN 2002eb	2002-08-09.325	52495.325	1.68	3	3110–10400	6.56/10.10	129	312	1.07	2.20	900	1,51,52,55	9	5
SN 2002eb	2002-09-03.402	52520.402	26.08	3	3150–10400	6.44/10.38	238	57	1.16	1.74	900	1,47,51	9	5
SN 2002eb	2002-10-08.000	52555.000	59.75	5	3095–9420	7.14/7.89	265	268	1.18	0.70	400	1,47	5	0
SN 2002ec	2002-08-09.271	52495.271	···	3	3194–10400	6.66/9.75	58	58	1.93	2.79	1200	1,51,52,55	9	0
SN 2002ec	2002-09-03.187	52520.187	···	3	3372–10400	6.83/10.66	58	58	1.76	2.62	1800	1,47,51	9	0
SN 2002ef	2002-08-09.510	52495.510	4.70	3	3110–10400	7.06/9.94	202	22	1.74	2.10	400	1,51,52,55	9	6
SN 2002ef	2002-09-03.328	52520.328	28.93	3	3150–10400	6.63/10.18	163	344	1.66	2.34	1500	1,47,51	9	0
SN 2002eh	2002-08-09.405	52495.405	6.88	3	3152–10400	6.55/9.91	113	292	1.37	4.15	900	1,51,52,55	9	0
SN 2002ep	2002-09-03.290	52520.290	···	3	3242–10400	6.92/10.07	175	1	1.42	1.63	2400	1,47,51	9	0
SN 2002el	2002-09-03.263	52520.263	11.82	3	3150–10400	6.62/10.54	185	3	1.78	2.97	1200	1,47,51	9	5
SN 2002el	2002-09-13.205	52530.205	21.49	3	3190–10400	7.51/10.96	172	353	1.80	1.95	1200	52,53,55	9	6
SN 2002el	2002-10-01.162	52548.162	38.94	3	3366–10400	7.06/10.03	182	356	1.79	3.06	1800	1,52	9	−6
SN 2002er	2002-09-03.218	52520.218	−4.58	3	3127–10400	6.91/10.71	46	46	1.52	1.82	1200	1,47,51	9	6
SN 2002er	2002-09-13.142	52530.142	5.26	3	3188–10400	6.72/9.96	202	34	1.26	2.05	800	52,53,55	9	3
SN 2002er	2002-10-01.145	52548.145	23.11	3	3100–10400	7.10/10.38	45	47	1.54	2.54	900	1,52	9	6
SN 2002er	2002-11-08.000	52586.000	60.64	5	3138–9416	6.35/8.67	71	72	2.87	1.2	300	1,47,53,63	5	0
SN 2002et	2002-09-03.242	52520.242	11.92	3	3184–10400	6.93/10.44	185	7	2.21	1.52	1200	1,47,51	9	0
SN 2002gb	2002-10-08.000	52555.000	···	5	3119–9420	6.63/7.66	137	317	1.14	0.99	600	1,47	5	0
SN 2002eu	2002-09-03.442	52520.442	−0.06	3	3150–10400	6.71/10.00	101	319	1.01	2.19	1000	1,47,51	9	0
SN 2002eu	2002-09-13.231	52530.231	9.38	3	3195–10400	6/10.54	117	296	1.86	2.70	1202	52,53,55	9	6
SN 2002eu	2002-10-01.237	52548.237	26.73	3	3300–10400	6.75/9.95	113	293	1.50	1.75	1500	1,52	9	−6
SN 2002eu	2002-10-08.000	52555.000	33.25	5	3071–9420	6.60/8.34	60	238	1.08	0.77	400	1,47	5	0
SN 2002eu	2002-11-08.000	52586.000	63.12	5	3186–9266	6.38/6.33	93	86	1.75	1.90	900	1,47,53,63	5	0
SN 2002ey	2002-09-04.225	52521.225	···	3	3258–10400	7.03/10.44	134	314	1.53	1.66	900	47	9	0
SN 2002fb	2002-09-13.295	52530.295	0.98	3	3195–10400	6.92/10.10	107	287	1.31	2.27	900	52,53,55	9	5
SN 2002fb	2002-10-01.192	52548.192	18.60	3	3314–10400	7.12/10.29	115	293	1.69	1.98	1800	1,52	9	5

Continued on Next Page...

Table 2.2 — Continued

SN Name	UT Date[a]	MJD[b]	Phase[c]	Inst.[d]	Wavelength Range (Å)	Res.[e] (Å)	P.A.[f] (°)	Par.[g] (°)	Air.[h]	See.[i] (″)	Exp. (s)	Observer(s)[j]	Reducer[k]	Flux Corr.[l]
SN 2002fb	2002-11-08.000	52586.000	55.83	5	3248–9280	6.37/6.59	87	87	1.92	1.2	400	1,47,53,63	5	0
SN 2002fi	2002-10-08.000	52555.000	···	5	3163–9420	6.62/7.82	3	23	1.38	0.90	600	1,47	5	0
SN 2002fk	2002-10-08.000	52555.000	7.74	5	3013–9420	6.77/7.67	11	358	1.22	1.42	200	1,47	5	2
SN 2002fk	2002-11-09.000	52587.000	39.52	6	3950–10199	0.5/0.5	137	49	1.62	1.1	300	1,47,53,63	5	0
SN 2002fk	2002-11-11.000	52589.000	41.50	5	3136–9414	6.41/6.09	237	58	2.20	3.11	300	1,47	5	0
SN 2002fk	2002-12-12.182	52620.182	72.47	3	3100–10400	7.09/10.94	157	338	1.84	2.56	1200	52,55	9	0
SN 2002fk	2003-02-27.000	52697.000	148.74	5	3110–9416	8.42/6.10	48	51	1.67	1.00	500	1,47	5	0
SN 2002gf	2002-11-11.000	52589.000	···	5	3110–9410	8.12/6.57	44	47	1.14	1.37	720	1,47	5	0
SN 2002gc	2002-10-08.000	52555.000	···	5	3095–9420	7.16/7.60	77	255	1.55	1.06	400	1,47	5	0
SN 2002gc	2002-11-02.206	52580.206	···	3	3100–10400	6.65/10.05	76	259	1.10	2.58	1800	1,51,52	9	0
SN 2002gc	2002-11-08.000	52586.000	···	5	3146–9420	6.35/6.66	92	91	2.03	2.45	400	1,47,53,63	5	0
SN 2002gc	2003-01-07.000	52646.000	···	5	3167–9430	6.5/7	87	87	2.29	1.2	600	1,47	5	0
SN 2002gg	2002-11-11.000	52589.000	···	5	3204–9408	4.5/7.26	148	17	1.03	1.2	600	1,47	5	0
SN 2002gx	2002-11-08.000	52586.000	···	5	3160–9288	6.35/6.93	92	91	1.81	1.23	400	1,47,53,63	5	0
SN 2002ha	2002-11-02.140	52580.140	−0.85	3	3100–10400	6.55/10.02	224	24	1.33	1.88	600	1,51,52	9	2
SN 2002ha	2002-11-08.000	52586.000	4.93	5	3086–9416	6.36/6.23	54	55	1.22	2.18	150	1,47,53,63	5	6
SN 2002ha	2002-11-11.000	52589.000	7.89	5	3021–9410	8.13/7.18	43	46	1.14	1.19	200	1,47	5	0
SN 2002ha	2002-12-12.090	52620.090	38.55	3	3108–10400	7.07/10.26	210	42	1.69	2.39	1500	52,55	9	2
SN 2002ha	2003-01-06.000	52645.000	63.11	5	3127–9430	6.5/7	69	69	3.20	1.2	600	1,47	5	0
SN 2002hd	2002-11-02.539	52580.539	6.48	3	3100–10400	6.99/10.60	162	343	1.46	2.07	1800	1,51,52	9	0
SN 2002hd	2002-11-09.000	52587.000	12.72	6	3950–10199	0.5/0.5	75	350	1.13	1.1	200	1,47,53,63	5	0
SN 2002he	2002-11-01.642	52579.642	−5.91	6	3950–10199	0.5/0.5	285	192	1.38	0.90	180	47,53,63	5	0
SN 2002he	2002-11-06.649	52584.649	−1.03	6	3950–10199	0.5/0.5	270	182	1.37	0.75	240	1,47,53	5	0
SN 2002he	2002-11-08.000	52586.000	0.29	5	3070–9424	6.43/6.70	183	182	1.37	0.96	200	1,47,53,63	5	0
SN 2002he	2002-11-11.000	52589.000	3.22	5	3102–9414	7.21/5.62	190	186	1.37	1.27	200	1,47	5	0
SN 2002hl	2002-11-06.556	52584.556	···	3	3150–10400	6.89/9.66	102	282	1.21	1.5	1440	42,52	9	0
SN 2002hv	2002-11-08.000	52586.000	···	5	3124–9424	6.42/7.52	236	235	1.08	0.97	300	1,47,53,63	5	0
SN 2002hu	2002-11-08.000	52586.000	−5.81	5	3086–9420	6.38/6.51	88	88	1.88	1.12	240	1,47,53,63	5	0
SN 2002hw	2002-11-11.000	52589.000	−6.27	5	3094–9408	8.00/7.08	54	55	1.06	1.38	400	1,47	5	0
SN 2002hw	2002-12-12.230	52620.230	24.42	3	3150–10400	7.10/10.21	226	46	1.48	2.62	900	52,55	9	0
SN 2002jg	2002-12-12.166	52620.166	10.11	3	3200–10400	6.99/11.01	246	66	1.27	2.01	600	52,55	9	6
SN 2002jm	2002-12-12.465	52620.465	···	3	3142–10400	6.80/10.60	332	334	1.51	2.66	1800	52,55	9	0
SN 2002jo	2002-12-12.561	52620.561	···	3	3166–10400	6.93/10.16	105	285	1.36	3.48	1200	52,55	9	0
SN 2002jy	2003-01-07.000	52646.000	11.86	5	3089–9430	7.90/6.09	81	81	2.84	1.49	200	1,47	5	0
SN 2002jy	2003-02-04.147	52674.147	39.46	3	3136–10400	6.65/10.40	80	79	1.25	2.46	1500	51,52,64,65	9	0
SN 2002kf	2003-01-06.000	52645.000	6.81	5	3001–9430	8.39/6.13	311	128	1.29	1.29	200	1,47	5	0
SN 2003D	2003-01-07.000	52646.000	9.98	5	3153–9430	7.87/6.04	353	357	1.10	1.2	300	1,47	5	0
SN 2003D	2003-02-27.000	52697.000	59.88	5	3128–9420	8.82/6.18	308	310	1.28	0.70	500	1,47	5	0
SN 2003F	2003-01-28.275	52667.275	···	3	3218–10400	6/11	200	42	1.15	1.75	900	52,65,66	9	0
SN 2003F	2003-02-04.202	52674.202	···	3	3202–10400	6.45/10.11	199	23	1.08	3.88	1800	51,52,64,65	9	0
SN 2003K	2003-01-28.561	52667.561	13.43	3	3118–10400	6.60/9.07	216	213	1.20	2.71	1500	52,65,66	9	0
SN 2003K	2003-02-04.457	52674.457	20.18	3	3136–10400	6.72/10.38	72	252	1.36	3.10	900	51,52,64,65	9	0
SN 2003M	2003-01-28.501	52667.501	···	3	3218–10400	6.75/9.50	194	14	1.04	2.29	1200	52,65,66	9	0
SN 2003M	2003-02-28.000	52698.000	···	5	3102–9422	7.26/6.57	267	274	1.25	0.92	400	1,47	5	0
SN 2003V	2003-02-27.000	52697.000	···	5	3120–9422	7.36/6.89	346	62	1.46	0.91	300	1,47	5	0

Continued on Next Page...

Table 2.2 — Continued

SN Name	UT Date[a]	MJD[b]	Phase[c]	Inst.[d]	Wavelength Range (Å)	Res.[e] (Å)	P.A.[f] (°)	Par.[g] (°)	Air.[h]	See.[i] (″)	Exp. (s)	Observer(s)[j]	Reducer[k]	Flux Corr.[l]
SN 2003ae	2003-02-28.000	52698.000	31.69	5	3068–9422	7.28/6.25	205	197	1.01	1.37	200	1,47	5	0
SN 2003P	2003-01-28.341	52667.341	···	3	3202–10400	6.89/10.07	160	152	1.06	2.83	1800	52,65,66	9	0
SN 2003S	2003-02-04.428	52674.428	···	3	3168–10400	6.49/10.30	69	247	1.15	4.47	1800	51,52,64,65	9	0
SN 2003U	2003-02-04.552	52674.552	−2.55	3	3102–10400	6.54/10.08	71	250	1.26	2.49	1800	51,52,64,65	9	0
SN 2003W	2003-02-04.339	52674.339	−5.06	3	3102–10400	6.60/10.22	158	339	1.09	4.19	900	51,52,64,65	9	0
SN 2003W	2003-02-28.000	52698.000	18.14	5	3094–9422	7.19/6.04	337	286	1.04	0.83	200	1,47	5	0
SN 2003W	2003-04-08.199	52737.199	56.56	3	3176–10400	6.66/9.88	186	8	1.08	1	2100	52,55,67	9	0
SN 2003X	2003-02-04.510	52674.510	···	3	3302–10400	6.59/10.39	119	299	2.07	1.25	1200	51,52,64,65	9	0
SN 2003Y	2003-02-04.233	52674.233	−1.74	3	3144–10400	6.60/10.26	65	244	1.16	2.30	1200	51,52,64,65	9	0
SN 2003Y	2003-02-28.000	52698.000	21.63	5	3076–9422	7.15/6.29	176	179	1.26	1.02	300	1,47	5	0
SN 2003af	2003-02-28.000	52698.000	···	5	3042–9422	7.36/6.30	267	266	1.10	0.93	240	1,47	5	0
SN 2003av	2003-02-27.000	52697.000	···	5	3120–9420	9.01/6.30	315	321	1.08	0.64	400	1,47	5	0
SN 2003ai	2003-02-28.000	52698.000	7.25	5	3060–9422	8.92/8.00	103	101	1.43	1.26	250	1,47	5	0
SN 2003ah	2003-02-27.000	52697.000	···	5	3086–9420	8.97/6.06	54	55	1.22	0.87	300	1,47	5	0
SN 2003an	2003-02-27.000	52697.000	···	5	3086–9420	7.99/7	96	95	1.24	1.63	200	1,47	5	0
SN 2003ax	2003-02-27.000	52697.000	···	5	3052–9420	8.99/6.22	314	317	1.05	0.85	300	1,47	5	0
SN 2003au	2003-02-27.000	52697.000	···	5	3136–9420	7.64/7	198	193	1.34	0.70	300	1,47	5	0
SN 2003bf	2003-02-27.000	52697.000	···	5	3042–9420	9.10/6.27	297	301	1.04	0.84	300	1,47	5	0
SN 2003ay	2003-02-28.000	52698.000	···	5	3094–9422	7.35/6.29	96	95	1.21	1.08	400	1,47	5	0
SN 2003bh	2003-02-27.000	52697.000	···	5	3146–9422	9.03/6.32	262	259	1.14	0.76	400	1,47	5	0
SN 2003bi	2003-02-28.000	52698.000	···	5	3120–9422	7.41/6.21	288	288	1.15	1.12	300	1,47	5	0
SN 2003cq	2003-04-08.446	52737.446	−0.15	3	3134–10400	7.15/10.82	96	95	1.37	1	1500	52,55,67	9	0
SN 2003du	2003-05-24.423	52783.423	17.61	5	3220–5500	4.5	150	156	1.34	1.5	1500	1,27,47	4	0
SN 2003du	2003-05-24.423	52783.423	17.61	5	5700–9420	7	150	156	1.34	1.5	1500	1,27,47	4	4
SN 2003du	2003-05-30.397	52789.397	23.55	3	3184–10400	7.04/10.66	101	101	1.29	3.12	602	52,68,69	9	5
SN 2003du	2003-06-07.396	52797.396	31.50	3	3300–10500	5.01/11.16	96	96	1.34	2.07	700	52,70	10	5
SN 2003du	2003-07-06.343	52826.343	60.26	3	3300–10500	6/11.41	88	87	1.46	2.88	600	52,66,68	10	6
SN 2003du	2003-07-27.194	52847.194	80.98	3	3300–10400	6.73/10.01	120	117	1.18	1.87	900	1,52,68	9	0
SN 2003dw	2003-05-30.427	52789.427	···	3	3282–10400	6.94/11	127	126	1.15	1.75	900	52,68,69	9	0
SN 2003ek	2003-05-24.623	52783.623	···	5	4000–5500	···	100	102	1.49	1.5	300	1,27,47	4	0
SN 2003ek	2003-05-24.623	52783.623	···	5	5700–9420	7	100	102	1.49	1.5	300	1,27,47	4	0
SN 2003ek	2003-05-30.446	52789.446	···	3	3168–10400	6.73/11.03	91	90	1.09	4.77	1800	52,68,69	9	0
SN 2003ek	2003-06-08.421	52798.421	···	3	3640–10140	5.17/10.62	97	96	1.05	2.38	1800	52,70	10	0
SN 2003fa	2003-06-07.426	52797.426	−8.15	3	3300–10500	5.10/10.91	96	99	1.03	2.77	1800	52,70	10	0
SN 2003fa	2003-07-07.379	52827.379	20.67	3	3300–10500	6/10.61	89	88	1.10	2.79	1000	52,66,68	10	0
SN 2003fa	2003-07-27.245	52847.245	39.78	3	3300–10400	6.73/9.96	128	119	1.01	1.70	1200	1,52,68	9	0
SN 2003fd	2003-06-29.290	52819.290	···	5	3250–9200	4.5/7	135	134	1.14	1.5	240	1,47	4	0
SN 2003gj	2003-07-07.402	52827.402	···	3	5224–10156	10.55	169	350	2.25	1.38	1200	52,66,68	10	0
SN 2003gn	2003-07-27.331	52847.331	−5.38	3	3300–10400	6.63/10.26	126	307	1.19	2.35	1500	1,52,68	9	0
SN 2003gn[m]	2003-08-05.271	52856.271	3.26	3	3594–10154	5.52/11.22	124	302	1.47	3.98	1200	1,52,68	10	0
SN 2003gq	2003-07-27.294	52847.294	−0.69	3	3300–10400	7.10/10.11	112	292	1.36	3.36	1200	1,52,68	9	0
SN 2003gq	2003-09-28.302	52910.302	60.99	5	3121–9250	6.5/7	69	242	1.10	0.70	1200	1,47	5	0
SN 2003gs[m]	2003-08-28.410	52879.410	30.46	3	3300–10000	5.06/10.11	137	323	1.59	2.33	900	1,52,71	10	5
SN 2003gs	2004-02-14.264	53049.264	199.51	6	3930–10199	0.5/0.5	152	61	1.45	0.90	2000	1,47,52	5	0
SN 2003gt[m]	2003-08-05.248	52856.248	−5.07	3	3300–10500	5.44/11.17	140	321	1.27	3.95	900	1,52,68	10	5

Continued on Next Page...

Table 2.2 — Continued

SN Name	UT Date[a]	MJD[b]	Phase[c]	Inst.[d]	Wavelength Range (Å)	Res.[e] (Å)	P.A.[f] (°)	Par.[g] (°)	Air.[h]	See.[i] (″)	Exp. (s)	Observer(s)[j]	Reducer[k]	Flux Corr.[l]
SN 2003gt[m]	2003-08-28.286	52879.286	17.61	3	3300–10000	4.99/10.29	154	12	1.13	2.26	900	1,52,71	10	2
SN 2003he[m]	2003-08-28.374	52879.374	2.71	3	3300–10000	5.09/9.21	158	344	1.33	3.22	1500	1,52,71	10	5
SN 2003he	2003-09-03.358	52885.358	8.54	3	3300–10400	7.81/9.35	158	347	1.32	2.96	1800	47,52,71	9	5
SN 2003hj[m]	2003-08-28.188	52879.188	···	3	3576–9812	5.04/9.93	174	66	1.31	3.38	1500	1,52,71	10	0
SN 2003hm[m]	2003-08-28.450	52879.450	···	3	3394–9980	5.21/10.28	147	326	1.36	1.27	1200	1,52,71	10	0
SN 2003hs	2003-09-03.316	52885.316	−5.49	3	3278–10400	7.40/10.00	36	79	1.47	4.42	1800	47,52,71	9	0
SN 2003hw	2003-09-28.546	52910.546	···	5	3134–9250	6.5/7	234	171	1.04	0.70	300	1,47	5	0
SN 2003hv	2003-09-28.573	52910.573	21.85	5	3082–9250	6.5/7	191	15	1.47	0.70	240	1,47	5	5
SN 2003hv	2003-10-02.472	52914.472	25.73	3	3300–10400	6.84/10.64	190	11	2.32	2.71	300	1,52	11	6
SN 2003hv	2003-11-23.319	52966.319	77.29	3	3300–10400	4.64/9.71	192	11	2.32	2.75	1800	1,51,52	9	6
SN 2003hx	2003-10-02.547	52914.547	21.89	3	3300–10400	6/10.61	179	360	1.70	3.72	600	1,52	11	0
SN 2003ij	2003-10-02.457	52914.457	···	3	3300–10400	6.10/10.68	233	216	1.53	2.67	800	1,52	11	0
SN 2003ik	2003-10-02.536	52914.536	···	3	3300–10400	6.00/10.66	268	241	1.22	3.15	600	1,52	11	0
SN 2003in	2003-10-02.512	52914.512	···	3	3300–10400	7.39/10.61	205	27	1.25	1.10	1500	1,52	11	0
SN 2003im	2003-10-02.489	52914.489	···	3	3300–10400	7.23/10.60	224	44	2.71	3.10	1200	1,52	11	0
SN 2003iv	2003-10-23.469	52935.469	1.76	3	3312–10268	5.03/9.96	222	43	1.25	2.38	2400	1,47,53	10	0
SN 2003iv	2003-10-28.455	52940.455	6.58	3	3260–10400	4.69/9.68	48	48	1.37	2.47	1800	1,51,52	9	0
SN 2003iz	2003-10-23.357	52935.357	···	3	3586–10500	5.08/10.15	159	50	1.05	1.10	2700	1,47,53	10	0
SN 2003kc	2003-11-23.508	52966.508	···	3	3300–10400	4.97/10.05	147	298	1.05	2.75	1800	1,51,52	9	0
SN 2003kd	2003-11-29.510	52972.510	···	5	3066–9410	6.5/7	103	103	1.51	1	300	1	9	0
SN 2003kd	2004-01-17.230	53021.230	···	3	3320–10400	4.76/10.28	94	92	1.13	2.66	1800	52,71	9	0
SN 2003kh	2003-11-29.198	52972.198	···	5	3088–9420	6.5/7	115	120	1.58	1	300	1	9	0
SN 2003kg	2003-11-29.226	52972.226	···	5	3066–9420	6.5/7	75	75	1.08	1	200	1	9	0
SN 2003kf	2003-11-29.548	52972.548	−7.50	5	3000–9410	6.5/7	30	30	1.26	1	120	1	9	0
SN 2003kf	2004-01-17.343	53021.343	40.94	3	3320–10400	4.84/10.04	26	28	1.85	3.07	1500	52,71	9	0
SN 2003ls	2004-01-17.208	53021.208	···	3	3586–10400	4.86/10.00	25	26	1.71	2.97	1200	52,71	9	0
SN 2003lb	2004-01-17.315	53021.315	···	3	3320–10400	5.06/10.12	57	58	1.55	2.81	1500	52,71	9	0
SN 2003lc	2004-01-17.149	53021.149	···	3	3418–10400	5.10/10.11	67	67	1.11	2.42	1800	52,71	9	0
SN 2003lq	2004-01-17.124	53021.124	···	3	3320–10400	5.48/9.68	39	40	1.73	2.83	1500	52,71	9	0
SN 2004E	2004-01-17.517	53021.517	5.26	3	3320–10400	5.76/9.90	118	299	1.03	2.04	1500	52,71	9	0
SN 2004W	2004-02-13.587	53048.587	···	5	3134–9258	6.5/7	35	41	1.02	0.90	400	1,47,52	5	0
SN 2004S	2004-02-13.341	53048.341	8.26	5	3041–9250	6.5/7	180	17	1.64	0.90	900	1,47,52	5	0
SN 2004S	2004-12-15.491	53354.491	311.57	8	4709–7223	1.5	0	0	1.59	1	1800	1,52	9	0
SN 2004Y	2004-02-14.665	53049.665	···	6	3930–10199	0.5/0.5	172	82	1.49	0.90	360	1,47,52	5	0
SN 2004as	2004-03-16.608	53080.608	−4.36	5	3304–9230	5.49/7	79	79	2.06	1.36	300	1	11	5
SN 2004bd	2004-04-10.156	53105.156	10.76	3	3300–10400	6/9.64	109	291	1.21	2.45	800	1,68,71	11	4
SN 2004bd	2004-04-24.279	53119.279	24.76	3	3476–10600	4.99/9.54	166	64	1.03	3.18	900	66,68,71	11	5
SN 2004bd	2004-05-12.359	53137.359	42.68	3	3510–10522	5.32/10.33	66	65	1.60	4.84	1200	52,64,66	11	6
SN 2004bg	2004-04-24.256	53119.256	10.34	3	3350–10592	4.75/9.87	63	32	1.06	2.30	900	66,68,71	11	0
SN 2004bg	2004-05-12.298	53137.298	28.01	3	3544–10590	6.37/10.13	57	58	1.36	3.47	1200	52,64,66	11	0
SN 2004bj	2004-04-24.309	53119.309	···	3	3476–10600	4.86/9.93	67	5	1.16	4.25	2700	66,68,71	11	0
SN 2004bk	2004-04-24.371	53119.371	6.13	3	3400–10280	4.94/9.87	205	26	1.27	2.79	1500	66,68,71	11	6
SN 2004bk	2004-05-27.309	53152.309	38.32	3	3986–6750	7.50	35	36	1.38	3.80	1500	52,64,66	11	0
SN 2004bl	2004-05-12.189	53137.189	4.61	3	3368–10580	5.43/10.84	170	351	1.33	3.47	1200	52,64,66	11	0
SN 2004bl	2004-05-27.218	53152.218	19.38	3	3986–6750	7.37	198	21	1.39	3.80	1500	52,64,66	11	0

Continued on Next Page...

Table 2.2 — Continued

SN Name	UT Date[a]	MJD[b]	Phase[c]	Inst.[d]	Wavelength Range (Å)	Res.[e] (Å)	P.A.[f] (°)	Par.[g] (°)	Air.[h]	See.[i] (″)	Exp. (s)	Observer(s)[j]	Reducer[k]	Flux Corr.[l]
SN 2004bp	2004-05-12.329	53137.329	···	3	3436–10580	6.46/10.44	92	70	1.46	3.47	2400	52,64,66	11	0
SN 2004bq	2004-05-12.474	53137.474	···	3	3894–10532	5.85/11	161	333	2.37	1.24	1500	52,64,66	11	0
SN 2004cb	2004-06-13.197	53169.197	···	3	3320–10400	5.47/10.29	183	5	2.58	2.56	600	52,64,72	11	0
SN 2004br	2004-05-27.285	53152.285	3.50	3	3986–6750	7.04	39	39	1.58	4.15	900	52,64,66	11	0
SN 2004br	2004-06-13.219	53169.219	20.05	3	3320–10400	6.34/9.57	212	35	1.46	2.11	900	52,64,72	11	6
SN 2004br	2004-06-20.226	53176.226	26.90	3	3300–10400	6.16/10.31	41	42	1.68	2.72	900	52,66	9	6
SN 2004bv	2004-05-27.467	53152.467	−7.06	3	3988–6800	6.99	165	347	2.24	3.80	1500	52,64,66	11	0
SN 2004bv	2004-06-13.471	53169.471	9.77	3	3320–10400	4.94/9.54	182	3	2.14	3.54	600	52,64,72	11	5
SN 2004bv	2004-07-11.391	53197.391	37.39	3	3300–10400	6.74/9.69	184	4	2.15	2.07	1200	1,52,71	9	−6
SN 2004bv	2004-07-18.326	53204.326	44.26	3	3300–10400	5.06/9.96	169	349	2.21	2.98	1200	52,73	9	6
SN 2004bv	2004-08-08.305	53225.305	65.02	3	3310–10400	5.00/9.29	180	2	2.14	1.5	1500	52,66,71	9	5
SN 2004bv	2004-10-18.222	53296.222	135.19	5	3070–9400	6.5/7	6	8	1.41	1	400	1,52	9	0
SN 2004bv	2004-11-14.000	53323.000	161.68	5	3100–9400	6.25/7.71	29	34	1.61	0.66	300	1,52	9	0
SN 2004bw	2004-05-27.362	53152.362	−10.03	3	3986–6750	7.33	209	30	1.51	3.65	1800	52,64,66	11	0
SN 2004bw	2004-06-13.333	53169.333	6.59	3	3320–10400	4.90/9.59	33	35	1.61	2.41	1500	52,64,72	11	6
SN 2004ca	2004-06-13.423	53169.423	···	3	3320–10400	6.22/10.00	70	267	1.11	2.46	1500	52,64,72	11	0
SN 2004bz	2004-06-13.453	53169.453	···	3	3320–10400	4.93/9.05	134	315	1.22	1.75	1500	52,64,72	11	0
SN 2004cv	2004-07-11.317	53197.317	···	3	3300–10400	5.08/11.00	235	54	1.35	1	1500	1,52,71	9	0
SN 2004db	2004-08-08.439	53225.439	···	3	5300–10400	11	193	13	2.06	1.49	1200	52,66,71	9	0
SN 2004da	2004-07-11.438	53197.438	···	3	3300–10400	6.68/9.83	209	30	1.25	1.78	900	1,52,71	9	0
SN 2004da	2004-07-18.435	53204.435	···	3	3300–10400	5.22/10.44	214	35	1.30	2.21	900	52,73	9	0
SN 2004da	2004-08-08.365	53225.365	···	3	3310–10400	4.99/9.18	211	32	1.27	2.32	1500	52,66,71	9	0
SN 2004di	2004-08-08.279	53225.279	···	3	3310–10400	6.02/9.34	82	81	1.40	1.31	1500	52,66,71	9	0
SN 2004di	2004-08-16.301	53233.301	···	3	3320–10400	4.93/9.78	240	76	1.62	4.18	2500	1,52,66	11	0
SN 2004eq	2004-10-18.258	53296.258	···	5	3084–9400	6.5/7	354	355	1.72	1	300	1,52	9	0
SN 2004dt	2004-08-16.413	53233.413	−6.46	3	3320–10400	4.92/9.85	139	320	1.61	3.39	1300	1,52,66	11	6
SN 2004dt	2004-08-24.405	53241.405	1.38	3	4500–9800	11	150	325	1.48	3	900	1,52,66	4	6
SN 2004dt	2004-09-10.358	53258.358	18.00	3	3310–10500	6.07/9.53	145	324	1.51	2.69	900	1,66,71,74	11	5
SN 2004dt	2004-09-24.400	53272.400	31.77	3	3320–10500	4.95/9.84	177	354	1.26	1.88	1800	1,51,66	11	6
SN 2004dt[m]	2004-10-01.472	53279.472	38.71	3	3330–10400	6/11	40	34	1.46	···	1200	75	9	0
SN 2004dt[m]	2004-10-13.410	53291.410	50.42	3	3330–10500	5.05/9.19	16	17	1.29	2.49	2100	1,51,52	10	−6
SN 2004dt	2004-11-14.000	53323.000	81.39	5	3146–9400	6.17/6.43	70	68	2.45	0.97	300	1,52	9	0
SN 2004dt	2004-12-12.391	53351.391	109.24	5	3164–9320	6.5/7	57	59	1.32	1	400	1,52	9	0
SN 2004dt	2005-02-11.260	53412.260	168.93	8	5046–10201	3	64	64	1.59	0.55	540	1,52,76,77	11	0
SN 2004ef	2004-09-10.310	53258.310	−5.52	3	3310–10500	6.08/9.66	172	358	1.05	2.42	2100	1,66,71,74	11	5
SN 2004ef	2004-09-24.302	53272.302	8.05	3	3320–10500	6.20/10.32	38	17	1.06	3.67	3000	1,51,66	11	6
SN 2004ef[m]	2004-10-13.373	53291.373	26.55	3	3704–10176	4.97/9.20	56	57	1.46	2.55	2100	1,51,52	10	−6
SN 2004ef	2004-10-18.196	53296.196	31.23	5	3070–9400	6.5/7	276	276	1.24	1	300	1,52	9	5
SN 2004ef	2004-11-14.000	53323.000	57.23	5	3240–9400	6.17/7.39	266	244	1.00	0.90	500	1,52	9	0
SN 2004ef	2004-12-12.217	53351.217	84.60	5	3202–9320	4.5/7	269	86	1.08	1	700	1,52	9	0
SN 2004fa	2004-11-14.000	53323.000	···	5	3180–9400	7.74/7.71	25	27	1.70	0.89	300	1,52	9	0
SN 2004eo	2004-09-24.242	53272.242	−5.57	3	3320–10500	6.22/9.67	30	31	1.19	2.75	1000	1,51,66	11	0
SN 2004eo[m]	2004-10-13.300	53291.300	13.19	3	3410–10500	4.91/10.11	51	52	1.89	2.41	1500	1,51,52	10	0
SN 2004eo	2004-11-14.000	53323.000	44.40	5	3050–9400	6.28/7.21	66	66	1.13	0.77	300	1,52	9	0
SN 2004ev	2004-10-18.216	53296.216	···	5	3156–9400	6.5/7	22	24	1.62	1	300	1,52	9	0

Continued on Next Page...

Table 2.2 — Continued

SN Name	UT Date[a]	MJD[b]	Phase[c]	Inst.[d]	Wavelength Range (Å)	Res.[e] (Å)	P.A.[f] (°)	Par.[g] (°)	Air.[h]	See.[i] (″)	Exp. (s)	Observer(s)[j]	Reducer[k]	Flux Corr.[l]
SN 2004ey	2004-10-18.203	53296.203	−7.58	5	3040–9400	6.5/7	312	313	1.15	1	200	1,52	9	0
SN 2004ey	2004-11-14.000	53323.000	18.80	5	3050–9400	6.5/6.54	24	27	1.08	0.87	150	1,52	9	0
SN 2004ey	2004-12-17.103	53356.103	51.39	3	3320–10600	5.00/9.88	216	37	1.51	3.75	1500	51,66	11	5
SN 2004fd	2004-11-14.000	53323.000	···	5	3064–9400	6.27/7.40	90	88	1.69	1.35	300	1,52	9	0
SN 2004fd	2004-12-17.291	53356.291	···	3	3330–10392	5.15/11.45	250	70	1.10	1.77	2100	51,66	11	0
SN 2004fg	2004-11-14.000	53323.000	···	5	3094–9400	6.31/7.10	247	244	1.05	0.77	200	1,52	9	0
SN 2004fu	2004-11-14.000	53323.000	−2.65	5	3050–9400	6.35/7.01	166	157	1.45	0.81	100	1,52	9	0
SN 2004fu	2004-11-19.118	53328.118	2.43	3	3320–10500	6/11	120	130	1.19	2.5	600	1,66,71	12	0
SN 2004fu	2004-12-12.183	53351.183	25.28	5	3150–9320	6.5/7	310	127	1.66	1	200	1,52	9	0
SN 2004fw	2004-11-14.000	53323.000	···	5	3102–9400	6.33/7.29	222	221	1.28	0.79	400	1,52	9	0
SN 2004fy	2004-11-14.000	53323.000	···	5	3164–9400	6.11/6.89	246	246	2.87	0.97	200	1,52	9	0
SN 2004fy	2004-12-12.569	53351.569	···	5	3326–9320	4.5/7	225	225	2.83	1	300	1,52	9	0
SN 2004fz	2004-11-19.331	53328.331	−5.18	3	3320–10500	6/11	69	69	1.09	2.5	900	1,66,71	12	6
SN 2004fz	2004-12-12.463	53351.463	17.56	5	3300–9320	4.5/7	87	86	1.81	1	200	1,52	9	6
SN 2004fz	2004-12-17.262	53356.262	22.28	3	3320–10600	5.05/10.24	249	69	1.10	2.85	1200	51,66	11	5
SN 2004go	2004-12-17.238	53356.238	26.08	3	3320–10600	5.04/10.67	185	6	1.62	2.22	2100	51,66	11	0
SN 2004gc	2004-12-17.387	53356.387	31.33	3	3362–10258	5.04/10.14	207	35	1.26	3.82	1350	51,66	11	0
SN 2004gl	2004-12-12.543	53351.543	···	5	3264–9320	4.5/7	210	198	1.16	1	500	1,52	9	0
SN 2004gs	2004-12-17.447	53356.447	0.44	3	3354–10324	5.03/10.17	167	351	1.07	2.65	2100	51,66	11	4
SN 2004gu	2004-12-17.539	53356.539	−4.65	3	3420–10550	4.93/10.75	134	319	1.28	3.11	1375	51,66	11	0
SN 2004gw	2005-01-15.368	53385.368	···	5	3328–9250	4.5/5.44	161	160	1.38	1.47	250	29,52	11	0
SN 2004gw	2005-02-12.420	53413.420	···	5	3780–9250	4.5/7	108	106	1.95	2	400	1,52	9	0
SN 2004gz	2005-01-16.522	53386.522	···	3	3308–10500	5.89/11	98	266	1.39	3.70	1802	66,71	11	0
SN 2005A	2005-01-15.357	53385.357	5.55	5	3386–9250	4.5/6.78	64	63	1.70	1.59	200	29,52	11	0
SN 2005F	2005-01-15.373	53385.373	···	5	3354–9250	4.5/5.25	285	285	1.33	1.06	200	29,52	11	0
SN 2005G	2005-01-16.468	53386.468	···	3	3306–10500	6.47/10.56	136	316	1.59	2.32	759	66,71	11	0
SN 2005M	2005-02-01.556	53402.556	−1.41	3	3318–10500	6/10.96	60	59	1.87	3.80	1500	51,52,66	11	0
SN 2005M	2005-02-11.413	53412.413	8.23	8	5046–10201	3	255	251	1.01	1.11	200	1,52,76,77	11	0
SN 2005M	2005-02-12.430	53413.430	9.23	5	3780–9250	4.5/7	227	211	1.00	2	200	1,52	9	0
SN 2005M	2005-03-07.179	53436.179	31.49	3	3304–10500	5.78/10.93	121	303	1.21	1.58	1500	51,64,66	11	0
SN 2005M	2005-03-11.279	53440.279	35.50	5	3400–9260	4.5/7	269	269	1.14	1	200	1,52,78	9	0
SN 2005as	2005-03-11.311	53440.311	···	5	3400–9260	4.5/7	316	317	1.70	1	100	1,52,78	9	0
SN 2005P	2005-03-11.653	53440.653	···	5	3400–9260	4.5/7	54	55	1.40	1	450	1,52,78	9	0
SN 2005P	2005-05-11.536	53501.536	···	5	3126–9350	6.5/7	63	64	1.98	1	1200	1,52,79	9	0
SN 2005X	2005-02-11.433	53412.433	···	8	5046–10201	3	313	290	1.41	2.85	250	1,52,76,77	11	0
SN 2005W	2005-02-11.200	53412.200	0.59	8	5046–10201	3	88	88	1.13	1.22	120	1,52,76,77	11	0
SN 2005W	2005-03-07.155	53436.155	24.34	3	3304–10500	5.20/10.46	58	58	2.18	3.11	600	51,64,66	11	0
SN 2005W	2005-03-11.215	53440.215	28.36	5	3400–9260	4.5/7	80	79	1.91	1	100	1,52,78	9	0
SN 2005ag	2005-02-12.596	53413.596	0.52	5	3780–9250	4.5/7	298	299	1.09	2	500	1,52	9	0
SN 2005am	2005-03-11.302	53440.302	4.47	5	3400–9260	4.5/7	333	335	1.30	1	40	1,52,78	9	6
SN 2005am	2005-03-13.223	53442.223	6.37	3	4600–9800	11	155	14	1.71	1.75	600	66,71,80	4	3
SN 2005am	2005-04-11.154	53471.154	35.08	3	3310–10400	6/11	176	358	1.69	2.2	1500	51,64,66	9	5
SN 2005am	2005-04-17.161	53477.161	41.04	3	3310–10400	6/11	184	5	1.69	1.5	1200	64,66,71	9	6
SN 2005ao	2005-03-11.661	53440.661	−1.29	5	3400–9260	4.5/7	200	199	1.37	1	200	1,52,78	9	0
SN 2005ao	2005-03-13.539	53442.539	0.52	3	3320–10500	6.16/11.83	44	220	1.13	2.41	1500	66,71,80	11	0

Continued on Next Page...

Table 2.2 — Continued

SN Name	UT Date[a]	MJD[b]	Phase[c]	Inst.[d]	Wavelength Range (Å)	Res.[e] (Å)	P.A.[f] (°)	Par.[g] (°)	Air.[h]	See.[i] (″)	Exp. (s)	Observer(s)[j]	Reducer[k]	Flux Corr.[l]
SN 2005bc	2005-04-11.466	53471.466	1.55	3	3310–10400	6/11	264	83	1.09	2.2	1500	51,64,66	9	4
SN 2005bc	2005-04-17.365	53477.365	7.37	3	3310–10400	6/11	117	216	1.00	1.5	1500	64,66,71	9	6
SN 2005be	2005-04-11.440	53471.440	10.96	3	3310–10400	6/11	206	29	1.10	2.2	1500	51,64,66	9	0
SN 2005be	2005-04-17.393	53477.393	16.71	3	3310–10400	6/11	117	9	1.07	1.5	1800	64,66,71	9	0
SN 2005bl	2005-04-17.206	53477.206	−5.56	3	3500–10262	6/11	137	319	1.10	1.5	1500	64,66,71	9	0
SN 2005bl	2005-05-11.402	53501.402	18.07	5	3126–9350	6.5/7	85	84	1.22	1	500	1,52,79	9	0
SN 2005bo	2005-05-15.289	53505.289	27.71	3	3350–10400	6.66/10.47	360	23	1.67	2.23	1200	64,71	11	0
SN 2005bu	2005-05-11.239	53501.239	···	5	3134–9350	6.5/7	84	83	1.43	1	300	1,52,79	9	0
SN 2005cf	2005-06-01.385	53522.385	−10.94	3	3310–10550	6.56/9.59	360	35	1.80	2.53	600	51,64,66	11	0
SN 2005cf[m]	2005-06-10.277	53531.277	−2.11	3	3308–10500	5.39/10	186	7	1.42	3.64	300	66,71	11	0
SN 2005cf[m]	2005-06-11.205	53532.205	−1.19	3	3308–10500	6/10.98	158	340	1.49	4.62	600	71	11	0
SN 2005cf	2005-07-01.214	53552.214	18.69	3	3400–10400	5.63/11.31	360	5	1.41	1.65	300	64,66	11	0
SN 2005cf	2005-07-10.221	53561.221	27.64	3	3314–10424	4.94/11.04	192	17	1.47	2.68	500	1,71,80	11	0
SN 2005cf[m]	2006-04-27.603	53852.603	317.15	5	3242–9250	7.07/7.57	54	57	1.53	1.08	1204	1,52	11	0
SN 2005cf	2007-02-16.617	54147.617	610.27	8	4600–7238	1.5	318	328	1.32	1	6300	1,47,52,81	9	0
SN 2005de	2005-08-15.340	53597.340	−0.75	3	3304–10376	7.22/12.01	242	62	1.46	2.14	900	1,71,80	11	5
SN 2005de	2005-08-26.350	53608.350	10.10	3	3306–10370	6.14/10.02	61	61	1.90	2.53	900	71,82,83	11	6
SN 2005de	2005-09-11.236	53624.236	25.75	3	3350–10400	5.08/10.37	360	62	1.27	1.97	700	64,71,84	11	3
SN 2005de	2005-09-26.205	53639.205	40.49	3	3306–10500	5.98/9.90	62	62	1.32	3.80	1800	64,80,84	11	−6
SN 2005do	2005-08-26.480	53608.480	···	3	3450–10300	7.19/12.09	83	261	1.04	2.00	1800	71,82,83	11	0
SN 2005dh	2005-08-15.313	53597.313	···	3	3304–10374	7.14/11.96	238	58	2.44	4.13	1550	1,71,80	11	0
SN 2005dh	2005-08-26.267	53608.267	···	3	3304–10370	6/10.57	59	59	2.08	3.78	1200	71,82,83	11	0
SN 2005di	2005-08-26.406	53608.406	0.49	3	3308–10370	6.00/10.97	196	20	2.38	2.84	1500	71,82,83	11	0
SN 2005dm	2005-09-02.420	53615.420	5.23	3	3342–10500	6/10.68	151	335	1.53	2.95	1800	71,72	11	6
SN 2005dv	2005-09-11.170	53624.170	−0.57	3	3350–10400	6.44/9.86	360	78	1.70	4.73	500	64,71,84	11	0
SN 2005ec	2005-09-26.523	53639.523	···	3	3306–10500	6.33/10.70	179	358	1.23	3.02	1980	64,80,84	11	0
SN 2005ej	2005-09-26.237	53639.237	···	3	3306–10500	5.99/10.07	93	115	1.28	3.05	1720	64,80,84	11	0
SN 2005ej	2005-10-07.224	53650.224	···	5	3270–9330	4.5/7	160	156	1.49	1.3	300	5,52	9	0
SN 2005ej	2005-10-11.152	53654.152	···	3	3322–10500	5.27/9.68	136	135	1.20	1.94	2100	1,66,72	11	0
SN 2005el	2005-09-26.496	53639.496	−6.70	3	3306–10500	6.20/10.86	157	338	1.22	3.30	1200	64,80,84	11	4
SN 2005el	2005-10-04.534	53647.534	1.22	3	3318–10500	6.48/12.79	186	9	1.19	3.61	900	66,72	11	4
SN 2005el	2005-10-11.512	53654.512	8.09	3	3320–10500	5.27/10.61	185	8	1.19	2.03	1200	1,66,72	11	4
SN 2005gj	2005-12-02.403	53706.403	46.32	8	3897–9070	3	63	328	1.10	0.70	300	1,52	9	0
SN 2005gj	2005-12-04.377	53708.377	48.19	5	3280–9320	4.5/7	20	22	1.08	0.70	300	1,5,52,85,86	9	0
SN 2005gj	2006-01-01.388	53736.388	74.61	8	3900–9061	3	80	60	1.40	0.75	600	52	9	0
SN 2005gj	2006-12-23.420	54092.420	410.49	8	4483–9574	3	60	61	1.38	1.94	1500	1,52	9	0
SN 2005gj	2007-02-14.275	54145.275	460.35	5	3206–9238	6.35/7	240	61	1.39	1	1200	1,47,52,81	5	0
SN 2005er	2005-10-05.229	53648.229	−0.26	8	4901–10074	3	80	287	1.33	1.03	400	1,5,52	9	0
SN 2005er	2005-10-07.214	53650.214	1.67	5	3270–9330	4.5/7	300	287	1.39	1.3	600	5,52	9	0
SN 2005er	2005-10-11.291	53654.291	5.64	3	3320–10500	5.44/9.53	205	32	1.18	1.49	2400	1,66,72	11	0
SN 2005eq	2005-10-04.512	53647.512	−6.01	3	3322–10500	5.13/10.86	25	29	1.62	3.84	1500	66,72	11	0
SN 2005eq	2005-10-07.633	53650.633	−2.98	5	3270–9330	4.5/7	235	57	1.52	1.3	900	5,52	9	5
SN 2005eq	2005-10-11.376	53654.376	0.66	3	3320–10500	5.36/9.96	164	345	1.44	2.35	1500	1,66,72	11	6
SN 2005eq	2005-12-02.343	53706.343	51.16	8	3882–9070	3	340	344	1.14	0.70	900	1,52	9	0
SN 2005ew	2005-10-11.536	53654.536	18.23	3	3320–10500	5.41/9.29	255	75	1.15	1.90	1800	1,66,72	11	0

Continued on Next Page...

Table 2.2 — Continued

SN Name	UT Date[a]	MJD[b]	Phase[c]	Inst.[d]	Wavelength Range (Å)	Res.[e] (Å)	P.A.[f] (°)	Par.[g] (°)	Air.[h]	See.[i] (″)	Exp. (s)	Observer(s)[j]	Reducer[k]	Flux Corr.[l]
SN 2005ew	2005-11-02.402	53676.402	40.03	3	3326–10560	5.90/10.25	66	71	1.01	2.16	1800	64,71	11	0
SN 2005eu	2005-10-06.584	53649.584	−10.06	8	4922–10080	3	80	98	1.16	1.03	300	5,52	9	0
SN 2005eu	2005-10-07.622	53650.622	−9.06	5	3270–9330	4.5/7	275	89	1.40	1.3	600	5,52	9	0
SN 2005eu	2005-10-11.350	53654.350	−5.46	3	3320–10500	6.30/10.84	132	315	1.03	2.64	1500	1,66,72	11	6
SN 2005eu	2005-12-02.475	53706.475	44.91	8	3877–9070	3	88	89	1.42	0.70	400	1,52	9	0
SN 2005hc	2005-11-08.465	53682.465	14.26	8	4900–10061	3	53	54	1.22	2.84	600	1,52	9	0
SN 2005hj	2005-11-08.457	53682.457	7.51	8	4900–10061	3	54	57	1.29	2.99	600	1,52	9	0
SN 2005hk	2005-11-02.206	53676.206	−8.29	3	3326–10560	7.71/10.69	150	328	1.31	2.30	9000	64,71	11	0
SN 2005hk	2005-11-05.332	53679.332	−5.20	5	3171–9240	6.5/7	130	11	1.07	0.80	1200	1,52	5	0
SN 2005hk	2005-11-06.292	53680.292	−4.25	8	4900–10061	3	33	332	1.09	0.89	200	1,52	9	0
SN 2005hk	2005-11-07.210	53681.210	−3.35	8	4900–10061	3	300	300	1.42	0.55	300	1,52	9	0
SN 2005hk	2005-11-08.192	53682.192	−2.38	8	4900–10061	3	299	298	1.55	0.97	200	1,52	9	0
SN 2005hk	2005-12-02.756	53706.756	21.87	8	3882–10077	3	44	46	1.16	0.70	300	1,52	9	0
SN 2005hk	2005-12-04.302	53708.302	23.40	5	3280–9320	4.5/7	39	42	1.13	0.70	240	1,5,52,85,86	9	0
SN 2005hk	2006-01-01.221	53736.221	50.96	8	3900–9061	3	80	39	1.13	0.75	600	52	9	0
SN 2005hk	2006-01-24.142	53759.142	73.59	3	5176–10600	11	39	43	1.86	2.94	1800	71,82,83	11	0
SN 2005hk	2006-11-23.234	54062.234	372.79	5	3162–9250	6.27/6.60	318	324	1.14	2.06	1800	1,52	9	0
SN 2005hk	2006-12-23.216	54092.216	402.39	8	4936–10061	3	120	17	1.07	1.17	1800	1,52	9	0
SN 2005hk	2007-02-14.243	54145.243	454.74	5	5444–9238	7	248	69	2.58	1	1800	1,47,52,81	5	0
SN 2005iq	2005-11-07.215	53681.215	−5.86	8	4900–10061	3	320	320	1.54	0.60	300	1,52	9	0
SN 2005kc	2005-12-03.188	53707.188	10.28	8	3850–9068	3	18	21	1.04	0.60	300	1,5,52	9	0
SN 2005kc	2005-12-05.181	53709.181	12.25	5	3280–9320	4.5/7	16	21	1.04	0.85	240	5,52,85,86	9	0
SN 2005ke	2005-12-02.334	53706.334	7.80	8	3850–9070	3	33	337	1.50	0.70	300	1,52	9	0
SN 2005ke	2005-12-04.382	53708.382	9.83	5	3280–9320	4.5/7	2	2	1.41	0.70	150	1,5,52,85,86	9	0
SN 2005ke	2005-12-09.363	53713.363	14.79	3	3334–10600	7.39/12.72	206	28	2.88	1.35	1200	71,81	11	0
SN 2005ke	2006-01-05.242	53740.242	41.54	3	3310–10500	6.03/11	194	14	2.29	2.43	1800	64,81	11	0
SN 2005ke	2006-01-23.221	53758.221	59.43	3	3316–10600	6.98/11.91	207	23	2.57	3.32	1500	71,82,83	11	0
SN 2005ke	2006-11-23.377	54062.377	362.11	5	3066–9250	6.25/6.55	347	345	1.46	0.88	1200	1,52	9	0
SN 2005ki	2005-12-02.649	53706.649	1.62	8	3850–9068	3	136	318	1.03	0.70	200	1,52	9	0
SN 2005ki	2005-12-09.514	53713.514	8.35	3	3320–10600	7.08/12.89	146	332	1.19	1.35	1800	71,81	11	0
SN 2005ki	2006-01-06.498	53741.498	35.80	3	3310–10500	6.99/11.87	173	6	1.14	4.83	2100	64,81	11	0
SN 2005ls	2006-01-06.246	53741.246	26.29	3	3310–10500	6.65/11.49	157	94	1.09	4.26	2100	64,81	11	0
SN 2005ls	2006-01-30.220	53765.220	49.77	3	3330–10600	5.97/11	110	91	1.17	2.44	3902	71,82,83	11	0
SN 2005ls	2006-02-06.260	53772.260	56.66	3	3310–10500	5.24/11.48	81	73	1.51	3.51	1800	64,80	11	0
SN 2005lt	2006-01-05.560	53740.560	···	3	3310–10500	6.54/11	152	23	1.06	3.02	1800	64,81	11	0
SN 2005lu	2006-01-05.180	53740.180	27.88	3	3310–10500	6.43/11	191	9	1.75	4.73	2102	64,81	11	0
SN 2005mc	2006-01-05.368	53740.368	6.64	3	3310–10500	6.39/11	150	331	1.05	5.39	1500	64,81	11	0
SN 2005mc	2006-01-24.354	53759.354	25.16	3	3320–10600	7.11/11.99	192	8	1.04	2.85	1800	71,82,83	11	0
SN 2005lz	2006-01-01.381	53736.381	0.58	8	4930–10061	3	80	96	1.45	0.75	300	52	9	0
SN 2005ms	2006-01-06.400	53741.400	−1.88	3	3310–10500	6.60/12.36	145	293	1.00	3.42	1800	64,81	11	0
SN 2005ms	2006-01-23.318	53758.318	14.62	3	3316–10600	6.95/12.17	159	280	1.03	3.21	1800	71,82,83	11	0
SN 2005na	2006-01-05.335	53740.335	0.03	3	3310–10500	6.42/11	103	357	1.09	3.27	1800	64,81	11	0
SN 2005na	2006-01-06.361	53741.361	1.03	3	3310–10500	7.06/12.21	102	17	1.10	4.86	1800	64,81	11	6
SN 2005na	2006-01-23.255	53758.255	17.49	3	3316–10600	7.11/11.97	165	336	1.11	3.32	1500	71,82,83	11	6
SN 2005na	2006-01-30.320	53765.320	24.38	3	3330–10600	7.49/11	268	31	1.13	2.78	1800	71,82,83	11	−3

Continued on Next Page...

Table 2.2 — Continued

SN Name	UT Date[a]	MJD[b]	Phase[c]	Inst.[d]	Wavelength Range (Å)	Res.[e] (Å)	P.A.[f] (°)	Par.[g] (°)	Air.[h]	See.[i] (″)	Exp. (s)	Observer(s)[j]	Reducer[k]	Flux Corr.[l]
SN 2005na	2006-02-06.310	53772.310	31.19	3	3608–10600	5.61/11.16	147	35	1.15	3.34	2000	64,80	11	2
SN 2006D	2006-01-24.435	53759.435	3.70	3	3320–10600	5.48/12.10	152	328	1.84	2.81	900	71,82,83	11	0
SN 2006D	2006-02-06.539	53772.539	16.70	3	3512–9966	5.54/11.56	205	17	1.54	3.60	600	64,80	11	0
SN 2006D	2006-02-22.513	53788.513	32.54	3	3325–10300	6.90/12.27	209	23	1.61	1.15	1200	64,79,81	10	0
SN 2006D	2006-03-22.449	53816.449	60.24	3	3320–10500	5.50/12.30	202	26	1.67	2.71	1500	64,80,81	10	0
SN 2006D	2006-05-28.238	53883.238	126.46	3	3310–10400	5.21/12.30	194	17	1.54	2.37	2100	64,80	10	0
SN 2006E	2006-03-22.478	53816.478	···	3	3320–10500	7.36/10.03	204	29	1.27	2.27	1500	64,80,81	10	0
SN 2006E	2006-06-20.301	53906.301	···	3	3306–10600	5.65/11.53	222	44	1.56	3.62	2100	52,81,87	11	0
SN 2006E	2006-07-04.257	53920.257	···	3	3310–5480	5.18	84	45	1.62	1.90	2700	64,79	10	0
SN 2006H	2006-01-24.254	53759.254	7.01	3	3320–10600	6.67/11.98	84	82	1.18	2.85	1800	71,82,83	11	0
SN 2006N	2006-01-23.286	53758.286	−1.89	3	3316–10600	5.98/12.60	170	160	1.14	4.19	1500	71,82,83	11	0
SN 2006N	2006-01-24.285	53759.285	−0.90	3	3320–10600	5.41/12.13	98	159	1.14	2.85	1600	71,82,83	11	0
SN 2006N	2006-02-06.285	53772.285	11.91	3	3306–10500	5.47/10.99	147	139	1.17	3.79	1200	64,80	11	0
SN 2006N	2006-02-22.131	53788.131	27.54	3	3325–10300	6.58/12.07	219	205	1.14	2.45	1200	64,79,81	10	0
SN 2006S	2006-01-30.375	53765.375	−3.93	3	3330–10600	7.70/11	114	288	1.29	2.85	1800	71,82,83	11	0
SN 2006S	2006-02-06.517	53772.517	2.99	3	3306–10500	5.10/11.33	70	71	1.01	2.41	1500	64,80	11	0
SN 2006S	2006-02-22.476	53788.476	18.45	3	3325–10300	6.61/11.25	90	72	1.01	2.80	1800	64,79,81	10	0
SN 2006X	2006-02-22.413	53788.413	3.15	3	3325–10300	6.26/12.09	170	346	1.08	2.54	900	64,79,81	10	0
SN 2006X	2006-03-22.422	53816.422	31.01	3	3320–10500	5.45/9.95	172	40	1.16	2.54	1200	64,80,81	10	0
SN 2006X	2006-04-28.324	53853.324	67.72	3	3320–10500	5.49/9.96	90	41	1.17	2.46	1300	64,81	10	0
SN 2006X	2006-05-05.244	53860.244	74.60	3	3350–10400	7.13/12.07	129	7	1.08	2.31	1500	52,72,81	11	0
SN 2006X	2006-05-28.324	53883.324	97.56	3	3350–10500	6.88/12.32	234	55	1.65	1.37	1500	64,80	10	0
SN 2006X	2006-06-26.243	53912.243	126.33	3	3380–10586	5.81/11.67	231	54	1.51	2.20	2400	64,81,87	11	0
SN 2006X	2006-11-23.638	54062.638	275.94	5	3096–9250	6.25/6.40	283	283	1.48	0.59	500	1,52	9	0
SN 2006X	2006-12-23.665	54092.665	305.81	8	4583–7231	1.5	290	294	1.02	0.86	600	1,52	9	0
SN 2006X	2007-02-14.499	54145.499	358.37	5	3200–9238	6.41/7	310	286	1.07	2.88	1800	1,47,52,81	5	0
SN 2006ac	2006-02-22.439	53788.439	7.96	3	3325–10300	6/11.34	126	327	1.00	2.63	1500	64,79,81	10	6
SN 2006ac	2006-03-22.506	53816.506	35.39	3	3320–10500	5.53/10.18	251	72	1.31	3.04	1800	64,80,81	10	5
SN 2006ak	2006-02-22.389	53788.389	8.43	3	3325–10300	6.46/11.50	201	17	1.01	2.30	1800	64,79,81	10	0
SN 2006ay[m]	2006-04-27.623	53852.623	···	5	3156–9250	7.22/7.74	85	84	1.25	1.30	1204	1,52	11	0
SN 2006ax	2006-03-22.396	53816.396	−10.07	3	3320–10500	5.18/10.16	27	28	1.83	3.44	1800	64,80,81	10	0
SN 2006ax	2006-04-28.224	53853.224	26.16	3	3320–10500	5.73/10.68	183	4	1.55	3.04	1800	64,81	10	0
SN 2006ax	2006-05-05.191	53860.191	33.01	3	3350–10400	7.03/12.13	175	359	1.54	2.42	1800	52,72,81	11	0
SN 2006az	2006-04-28.289	53853.289	26.30	3	3320–10500	5.53/10.89	90	144	1.08	2.53	1800	64,81	10	0
SN 2006bq[m]	2006-04-27.636	53852.636	6.97	5	3096–9250	7.64/7.81	163	157	1.07	0.98	204	1,52	11	0
SN 2006bq	2006-05-05.375	53860.375	14.55	3	3350–10400	7.26/12.01	100	280	1.20	2.45	1500	52,72,81	11	0
SN 2006bq	2006-05-05.473	53860.473	14.64	3	3350–10400	6/12.35	41	249	1.01	2.45	1800	52,72,81	11	0
SN 2006bq	2006-06-05.439	53891.439	44.94	3	3310–10600	5.15/12.49	286	106	1.01	3.18	1815	72,81	10	0
SN 2006br	2006-04-28.389	53853.389	3.87	3	3320–5470	5.73	216	44	1.26	2.53	1500	64,81	10	0
SN 2006br	2006-05-05.297	53860.297	10.62	3	3350–10400	6.92/11.50	113	11	1.10	2.45	1500	52,72,81	11	0
SN 2006bt[m]	2006-04-27.629	53852.629	−5.30	5	3100–9250	7.15/7.63	82	82	1.38	1.05	304	1,52	11	0
SN 2006bt	2006-04-28.425	53853.425	−4.53	3	3320–10500	5.57/10.95	190	21	1.06	2.30	1800	64,81	10	0
SN 2006bt	2006-05-05.444	53860.444	2.27	3	3350–10400	6.85/11.47	41	44	1.11	2.09	1800	52,72,81	11	0
SN 2006bt	2006-06-05.366	53891.366	32.23	3	3310–10600	6.89/12.53	223	46	1.13	1.93	2100	72,81	10	0
SN 2006bt	2006-06-26.384	53912.384	52.59	3	3316–10600	6/11.88	274	57	1.39	1.50	2400	64,81,87	11	0

Continued on Next Page...

Table 2.2 — Continued

SN Name	UT Date[a]	MJD[b]	Phase[c]	Inst.[d]	Wavelength Range (Å)	Res.[e] (Å)	P.A.[f] (°)	Par.[g] (°)	Air.[h]	See.[i] (″)	Exp. (s)	Observer(s)[j]	Reducer[k]	Flux Corr.[l]
SN 2006bu	2006-05-05.325	53860.325	4.22	3	3350–10400	7.16/12.57	193	15	1.20	2.15	2400	52,72,81	11	0
SN 2006bw	2006-05-05.353	53860.353	8.90	3	3350–10400	7.21/12.51	193	14	1.22	2.07	1500	52,72,81	11	0
SN 2006bw	2006-05-28.383	53883.383	31.26	3	3310–10400	6.86/12.22	222	44	1.62	1.90	2400	64,80	10	0
SN 2006bz	2006-05-05.218	53860.218	−2.44	3	3350–10400	7.08/12.28	129	310	1.04	3.59	1800	52,72,81	11	0
SN 2006cc	2006-06-05.406	53891.406	17.67	3	3310–10600	5.25/12.44	270	90	1.13	3.01	2700	72,81	10	0
SN 2006ch	2006-05-28.000	53883.000	···	3	3310–10400	5.08/11	297	295	1.52	2.33	1800	64,80	10	0
SN 2006ch	2006-06-20.475	53906.475	···	3	3306–10600	6.09/12.09	113	294	1.21	1.63	600	52,81,87	11	0
SN 2006ce	2006-08-18.499	53965.499	···	3	3298–10600	5.56/12.01	166	346	2.01	2.83	1800	72,87	11	0
SN 2006ce	2006-10-24.303	54032.303	···	3	3316–10500	7.50/12.44	158	346	2.02	2.19	2400	64,72,79	11	0
SN 2006ce	2006-11-23.357	54062.357	···	5	3032–9250	6.29/6.60	359	359	1.33	0.93	400	1,52	9	0
SN 2006cf	2006-05-23.291	53878.291	6.28	3	3320–10500	5.00/9.62	84	5	1.35	4.64	1800	72,81	10	0
SN 2006cf	2006-05-28.299	53883.299	11.09	3	3310–10400	5.22/12.11	255	74	1.56	2.31	1500	64,80	10	0
SN 2006cf	2006-06-05.221	53891.221	18.69	3	3310–10500	6/11	87	86	1.24	3.18	2100	72,81	10	0
SN 2006cj	2006-05-28.349	53883.349	3.43	3	3310–10400	5.26/10.91	243	64	1.45	1.97	1800	64,80	10	0
SN 2006cm	2006-05-28.424	53883.424	−1.15	3	3310–10400	6.12/12.10	317	319	1.78	2.68	1800	64,80	10	0
SN 2006cm	2006-06-05.470	53891.470	6.77	3	3310–10600	6.93/12.84	156	338	1.36	3.18	1500	72,81	10	0
SN 2006cm	2006-06-20.410	53906.410	21.47	3	3306–10600	6.22/12.41	145	328	1.48	2.90	1800	52,81,87	11	0
SN 2006cm	2006-07-04.455	53920.455	35.29	3	3310–10700	6.23/12.48	182	5	1.29	1.17	2400	64,79	10	0
SN 2006ct	2006-06-20.328	53906.328	···	3	3366–10558	5.75/11.53	250	69	1.83	4.72	1500	52,81,87	11	0
SN 2006ct	2006-06-26.277	53912.277	···	3	3310–10600	5.93/11.85	257	76	1.51	4.46	1800	64,81,87	11	0
SN 2006cp	2006-06-05.281	53891.281	−5.30	3	3310–10600	6.83/12.50	238	59	1.39	2.52	1500	72,81	10	0
SN 2006cq	2006-06-05.307	53891.307	2.00	3	3310–10600	5.32/12.46	248	68	1.21	2.43	1800	72,81	10	0
SN 2006cs	2006-06-05.335	53891.335	2.28	3	3310–10600	6.79/11.91	241	73	1.25	4.66	2100	72,81	10	0
SN 2006da	2006-06-20.437	53906.437	···	3	3348–10600	6.30/11.62	126	307	1.57	2.58	1500	52,81,87	11	0
SN 2006da	2006-06-26.416	53912.416	···	3	3316–10600	5.59/12.81	305	306	1.63	4.70	1800	64,81,87	11	0
SN 2006da	2006-07-04.393	53920.393	···	3	3312–10698	6.23/11.06	126	307	1.54	3.15	1800	64,79	10	0
SN 2006da[m]	2006-08-02.353	53949.353	···	3	3316–10500	5.93/11.98	132	313	1.29	5.51	2400	72,87	11	0
SN 2006cz	2006-06-20.266	53906.266	1.12	3	3348–10600	5.69/11.75	194	19	1.41	2.63	1800	52,81,87	11	0
SN 2006cz	2006-06-26.304	53912.304	6.91	3	3310–10600	6.05/11.90	213	36	1.71	4.45	1500	64,81,87	11	0
SN 2006cz	2006-07-04.329	53920.329	14.62	3	3310–10648	5.08/12.12	47	46	2.61	2.28	2100	64,79	10	0
SN 2006cz	2006-07-21.244	53937.244	30.85	3	3350–10400	6.83/12.21	30	40	1.89	2.22	2100	52,81,87	11	0
SN 2006cz	2006-07-27.234	53943.234	36.60	3	3350–10500	6.25/12.13	215	41	1.97	3.29	2100	64,72,81	11	0
SN 2006dh	2006-06-26.339	53912.339	···	3	3362–10576	6.15/11.84	252	72	1.53	2.50	2100	64,81,87	11	0
SN 2006di	2006-07-25.605	53941.605	···	5	3200–9320	4.5/7	344	344	1.66	1.25	150	85,88,89	9	0
SN 2006dm	2006-07-04.421	53920.421	−7.90	3	3310–10700	6.32/10.71	138	320	1.85	3.90	1800	64,79	10	0
SN 2006dm	2006-07-21.426	53937.426	8.73	3	3350–10400	7.65/11.69	151	333	1.46	1.96	1500	52,81,87	11	5
SN 2006dm	2006-07-27.428	53943.428	14.61	3	3504–9844	6.34/10.94	152	339	1.39	4.39	2100	64,72,81	11	5
SN 2006dm[m]	2006-08-02.394	53949.394	20.44	3	3308–10500	7.19/11.77	150	333	1.46	3.27	2100	72,87	11	5
SN 2006dm	2006-08-18.357	53965.357	36.06	3	3298–10600	5.49/12.32	151	331	1.50	1.13	2400	72,87	11	5
SN 2006do	2006-07-21.477	53937.477	···	3	3744–10198	6.59/12.24	172	357	2.37	1.25	1800	52,81,87	11	0
SN 2006do	2006-07-27.476	53943.476	···	3	3520–9248	6.32/10.84	170	2	2.36	2	2100	64,72,81	11	0
SN 2006do[m]	2006-08-02.461	53949.461	···	3	3310–10490	6.26/11.89	181	2	2.36	3.2	2100	72,87	11	0
SN 2006do	2006-08-18.396	53965.396	···	3	3298–10600	5.45/11.56	171	350	2.44	1.11	2700	72,87	11	0
SN 2006dv	2006-07-25.611	53941.611	···	5	3200–9320	4.5/7	48	49	1.09	1.25	150	85,88,89	9	0
SN 2006dv	2006-07-27.357	53943.357	···	3	3350–10400	6.49/11.62	133	319	1.46	2.29	2100	64,72,81	11	0

Continued on Next Page...

Table 2.2 — Continued

SN Name	UT Date[a]	MJD[b]	Phase[c]	Inst.[d]	Wavelength Range (Å)	Res.[e] (Å)	P.A.[f] (°)	Par.[g] (°)	Air.[h]	See.[i] (″)	Exp. (s)	Observer(s)[j]	Reducer[k]	Flux Corr.[l]
SN 2006dv[m]	2006-08-02.319	53949.319	···	3	3310–10500	6.69/11.70	134	315	1.63	2.71	2400	72,87	11	0
SN 2006dv	2006-08-18.317	53965.317	···	3	3330–10576	5.43/12.31	139	320	1.43	1.92	2700	72,87	11	0
SN 2006dv	2006-08-24.277	53971.277	···	3	3320–10399	6.80/11.75	137	318	1.48	2	2700	72,81	11	0
SN 2006eb[m]	2006-08-02.431	53949.431	···	3	3308–10500	6.59/11.24	142	324	1.52	3.2	2100	72,87	11	0
SN 2006eb	2006-08-18.466	53965.466	···	3	3298–10600	5.53/12.30	165	346	1.28	3.97	2400	72,87	11	0
SN 2006dw	2006-07-27.289	53943.289	···	3	3350–10400	6.15/11.79	250	73	1.21	2.24	1500	64,72,81	11	0
SN 2006dw[m]	2006-08-02.252	53949.252	···	3	3308–10500	5.05/12.29	75	75	1.14	2.30	1500	72,87	11	0
SN 2006dw	2006-08-18.266	53965.266	···	3	3298–10600	5.03/11.87	74	71	1.35	2.04	1800	72,87	11	0
SN 2006dw	2006-08-24.233	53971.233	···	3	3320–10399	6.63/12.05	254	72	1.31	5.39	1800	72,81	11	0
SN 2006dy	2006-07-27.191	53943.191	···	3	3350–10400	6/12.30	42	47	1.30	3.32	1500	64,72,81	11	0
SN 2006dy[m]	2006-08-02.225	53949.225	···	3	3310–10500	5.00/11.66	53	54	1.68	2.21	1200	72,87	11	0
SN 2006dy	2006-08-18.202	53965.202	···	3	3296–10600	4.90/10.28	56	54	1.86	2.86	1200	72,87	11	0
SN 2006dy	2006-08-24.172	53971.172	···	3	3320–10400	6.66/11.51	236	54	1.77	2.67	1500	72,81	11	0
SN 2006dy	2006-09-02.159	53980.159	···	3	3320–10400	6.13/12.15	58	55	1.93	4.88	1500	64,66,72	11	0
SN 2006ef	2006-08-24.454	53971.454	3.20	3	3320–10400	6.57/11.75	164	342	1.51	2.26	1500	72,81	11	5
SN 2006ef[m]	2006-09-19.421	53997.421	28.71	3	3320–10600	6/11.58	169	353	1.45	2.30	1500	81,87	10	6
SN 2006ef	2006-09-25.377	54003.377	34.56	3	3310–10400	6.20/10.65	168	346	1.48	2.32	2100	64,81	11	5
SN 2006gr	2006-09-25.202	54003.202	−8.70	3	3310–10400	6.84/10.53	118	295	1.07	2.09	2100	64,81	11	0
SN 2006gr	2006-10-24.150	54032.150	19.28	3	3310–10500	7.18/11.82	122	304	1.03	2.15	2100	64,72,79	11	0
SN 2006gr	2006-10-30.101	54038.101	25.03	3	3342–10500	5.39/11.07	114	294	1.08	2.18	2100	1,66,81	11	0
SN 2006ej	2006-08-24.430	53971.430	−3.70	3	3320–10399	6.60/11.56	177	355	1.45	2.24	1800	72,81	11	0
SN 2006ej	2006-09-02.398	53980.398	5.09	3	3320–10400	6.68/11.39	173	353	1.46	4.08	1202	64,66,72	11	0
SN 2006ej[m]	2006-09-19.290	53997.290	21.65	3	3320–10600	6/12.53	149	329	1.75	2.59	1500	81,87	10	0
SN 2006ej	2006-09-25.299	54003.299	27.54	3	3310–10400	6/12.43	161	339	1.55	2.65	1500	64,81	11	0
SN 2006em	2006-09-02.440	53980.440	4.16	3	3320–10400	6.69/12.1	89	258	1.03	1.76	2100	64,66,72	11	0
SN 2006em[m]	2006-09-19.456	53997.456	20.85	3	3510–10182	6/10.92	205	181	1.00	1.65	2100	81,87	10	0
SN 2006em	2006-09-25.415	54003.415	26.70	3	3310–10400	6/10.27	237	220	1.01	2.39	2400	64,81	11	0
SN 2006en[m]	2006-09-02.319	53980.319	8.55	3	3320–10400	6.54/11	124	306	1.03	2	1200	64,66,72	11	−5
SN 2006en[m]	2006-09-19.209	53997.209	24.91	3	3592–10600	6/12.54	114	293	1.19	2.22	1500	81,87	10	5
SN 2006en	2006-09-25.232	54003.232	30.75	3	3732–10242	6.64/12.07	119	297	1.06	2.09	1800	64,81	11	−5
SN 2006es	2006-09-02.482	53980.482	···	3	3320–10400	6.89/11.86	96	270	1.05	3.62	2100	64,66,72	11	0
SN 2006es[m]	2006-09-19.499	53997.499	···	3	3364–10190	6/10.79	256	242	1.00	1.42	2400	81,87	10	0
SN 2006eu[m]	2006-09-19.155	53997.155	10.17	3	3320–10600	6/12.34	226	222	1.04	2.22	1800	81,87	10	5
SN 2006eu	2006-09-25.143	54003.143	16.02	3	3310–10400	5.19/10.64	212	206	1.03	2.30	2100	64,81	11	6
SN 2006et[m]	2006-09-19.345	53997.345	3.29	3	3320–10600	6/11.00	168	348	2.13	3.05	1500	81,87	10	0
SN 2006et	2006-09-25.321	54003.321	9.14	3	3310–10400	6.44/10.53	172	349	2.12	4.54	1500	64,81	11	0
SN 2006et	2006-10-30.278	54038.278	43.34	3	3328–10500	7.11/11.49	184	6	2.07	1	2100	1,66,81	11	0
SN 2006ev[m]	2006-09-19.183	53997.183	10.54	3	3320–10600	6/12.00	142	322	1.17	2.40	1500	81,87	10	0
SN 2006ev	2006-09-25.175	54003.175	16.36	3	3310–10400	5.26/12.61	149	329	1.13	2.69	1500	64,81	11	0
SN 2006gj	2006-09-25.482	54003.482	4.70	3	3310–10400	5.33/11.09	191	8	1.29	2.09	1500	64,81	11	0
SN 2006gt	2006-09-25.348	54003.348	3.08	3	3310–10400	6.29/11.78	174	352	1.29	2.35	2100	64,81	11	0
SN 2006ha	2006-11-24.351	54063.351	49.55	8	4792–10007	3	80	77	1.44	0.90	600	1,52,90	9	0
SN 2006hb	2006-10-30.489	54038.489	39.38	3	3328–10500	7.38/12.70	195	16	2.04	1	2100	1,66,81	11	0
SN 2006hn	2006-10-24.488	54032.488	···	3	3312–10500	7.52/11.71	92	271	1.61	2.37	1800	64,72,79	11	0
SN 2006je	2006-10-24.247	54032.247	20.18	3	3310–10500	7.13/10.16	109	288	1.09	1.48	2100	64,72,79	11	6

Continued on Next Page...

Table 2.2 — Continued

SN Name	UT Date[a]	MJD[b]	Phase[c]	Inst.[d]	Wavelength Range (Å)	Res.[e] (Å)	P.A.[f] (°)	Par.[g] (°)	Air.[h]	See.[i] (″)	Exp. (s)	Observer(s)[j]	Reducer[k]	Flux Corr.[l]
SN 2006je	2006-10-30.313	54038.313	26.02	3	3326–10500	6.84/11.62	169	17	1.00	2.26	2100	1,66,81	11	0
SN 2006ke	2006-10-24.397	54032.397	2.36	3	3312–10500	7.24/10.15	54	231	1.23	2	2400	64,72,79	11	0
SN 2006ke	2006-10-30.525	54038.525	8.38	3	3328–10500	6.80/12.61	155	152	1.17	2.11	2400	1,66,81	11	0
SN 2006kf	2006-10-24.352	54032.352	−8.96	3	3312–10500	7.51/11.68	152	334	1.20	1.65	2000	64,72,79	11	0
SN 2006kf	2006-10-30.385	54038.385	−3.05	3	3328–10500	7.00/10.24	176	360	1.14	1.94	1800	1,66,81	11	0
SN 2006kf	2006-11-20.241	54059.241	17.37	3	3314–10500	7.25/10.72	141	321	1.32	1.70	2700	81,87	11	0
SN 2006nr	2006-11-20.470	54059.470	···	3	3314–10500	6.37/10.24	164	164	1.52	1.95	1401	81,87	11	0
SN 2006lf	2006-10-30.420	54038.420	−6.30	3	3328–10500	5.16/11.80	208	191	1.01	1.92	2100	1,66,81	11	5
SN 2006lf	2006-11-20.276	54059.276	14.29	3	3314–10500	7.17/10.34	87	266	1.11	1.55	2400	81,87	11	6
SN 2006lf	2006-12-01.194	54070.194	25.06	3	3310–10500	6/11.48	96	278	1.29	1.92	2400	64,81	11	6
SN 2006lf	2006-12-20.150	54089.150	43.77	3	3310–10500	6.75/11	103	277	1.25	2.37	2400	66,72,81	11	4
SN 2006le	2006-10-30.456	54038.456	−8.69	3	3328–10500	7.28/12.85	174	169	1.11	1.60	2100	1,66,81	11	5
SN 2006le	2006-11-20.427	54059.427	11.92	3	3314–10500	6.77/11.10	177	151	1.12	1.83	2400	81,87	11	3
SN 2006le	2006-12-20.196	54089.196	41.18	3	3310–10500	6.78/11.65	69	240	1.21	1.90	2400	66,72,81	11	0
SN 2006mo	2006-11-20.174	54059.174	12.46	3	3314–10500	7.00/10.91	100	279	1.01	4.92	2400	81,87	11	0
SN 2006mp	2006-11-20.101	54059.101	5.66	3	3314–10500	6.39/11.17	71	70	1.74	1.77	2100	81,87	11	0
SN 2006ob	2006-12-01.107	54070.107	7.65	3	3310–10500	6/12.38	135	319	1.66	2	2400	64,81	11	0
SN 2006or	2006-11-23.654	54062.654	−2.79	5	3046–9250	6.23/6.23	260	259	1.19	1.26	200	1,52	9	0
SN 2006or	2006-12-01.530	54070.530	4.93	3	3310–10252	6/12.44	110	293	1.18	3.33	1500	64,81	11	0
SN 2006os	2006-12-01.142	54070.142	8.61	3	3310–10500	6.74/12.06	125	307	1.41	2.39	2100	64,81	11	0
SN 2006os	2006-12-20.233	54089.233	27.09	3	3310–10500	6.67/11	197	15	1.08	3.73	2400	66,72,81	11	0
SN 2006ot	2006-11-23.362	54062.362	···	5	3114–9250	6.43/7.00	5	5	1.32	0.99	200	1,52	9	0
SN 2006ot	2006-12-01.241	54070.241	···	3	3306–10500	6/12.12	174	1	1.89	2	2100	64,81	11	0
SN 2006ow	2006-12-01.309	54070.309	···	3	3310–10500	7.23/12.19	254	254	1.35	4.72	2100	64,81	11	0
SN 2006qo	2006-12-01.436	54070.436	−11.08	3	3310–10500	7.26/11.03	215	214	1.08	2	2700	64,81	11	0
SN 2006sr	2006-12-20.096	54089.097	−2.34	3	3310–10500	6.66/10.62	184	3	1.03	1.93	1800	66,72,81	11	0
SN 2006sr	2006-12-25.242	54094.242	2.69	5	3278–9240	4.5/6.23	93	94	1.08	1.26	200	1,52	11	0
SN 2006su	2006-12-23.672	54092.672	···	8	4473–9574	3	145	218	1.07	0.90	200	1,52	9	0
SN 2006td	2007-01-21.218	54121.218	22.62	3	3388–10588	5.21/11.66	76	75	1.22	1.20	1500	66,87	11	0
SN 2006te	2007-01-21.393	54121.393	24.22	3	3326–10600	5.30/10.73	76	108	1.02	1.05	1800	66,87	11	0
SN 2006te	2007-01-26.326	54126.326	29.00	3	3330–10500	6.75/11	43	200	1.00	3	1800	72,87	11	0
SN 2006te	2007-02-18.307	54149.307	51.28	3	3334–10140	5.88/10.10	74	115	1.01	3.09	1800	66,87	10	0
SN 2007A	2007-01-13.208	54113.208	2.37	5	3284–9254	4.5/6.59	70	71	1.10	1.11	150	52	11	0
SN 2007A	2007-01-26.140	54126.140	15.07	3	3326–10500	5.14/12.49	53	51	1.52	2.46	1500	72,87	11	0
SN 2007A	2007-02-18.144	54149.144	37.68	3	3378–10270	5.25/10.66	55	55	2.34	3.00	1800	66,87	10	0
SN 2007B	2007-01-13.203	54113.203	···	5	3284–9254	4.5/7.07	91	95	1.46	1.29	200	52	11	0
SN 2007B	2007-01-21.219	54121.219	···	5	3218–9250	5.38/7	87	87	1.90	1.17	150	1,52,81	11	0
SN 2007B	2007-01-26.116	54126.116	···	3	3326–10500	6.33/12.10	68	67	1.64	4.93	1500	72,87	11	0
SN 2007E	2007-01-13.213	54113.213	···	5	3284–9254	4.5/6.40	352	354	1.23	1.50	150	52	11	0
SN 2007E	2007-01-21.192	54121.192	···	3	3326–10600	5.20/10.65	25	26	1.97	4.43	1200	66,87	11	0
SN 2007F	2007-01-13.658	54113.658	−9.35	5	3318–9254	4.5/7.24	188	184	1.16	1.32	300	52	11	0
SN 2007F	2007-01-26.534	54126.534	3.23	3	3330–10500	6.13/11.40	186	180	1.03	2.18	1500	72,87	11	0
SN 2007F	2007-02-18.420	54149.420	25.59	3	3334–10500	6.06/11.53	65	238	1.07	2.01	1800	66,87	10	0
SN 2007F	2007-03-17.636	54176.636	52.18	8	4494–9581	3	286	107	1.58	0.80	450	47,81	9	0
SN 2007M	2007-01-22.487	54122.487	···	8	4427–9569	3	277	276	1.29	0.80	1000	1,52,81	9	0

Continued on Next Page...

Table 2.2 — Continued

SN Name	UT Date[a]	MJD[b]	Phase[c]	Inst.[d]	Wavelength Range (Å)	Res.[e] (Å)	P.A.[f] (°)	Par.[g] (°)	Air.[h]	See.[i] (″)	Exp. (s)	Observer(s)[j]	Reducer[k]	Flux Corr.[l]
SN 2007N	2007-01-22.583	54122.583	0.44	8	4448–9569	3	327	331	1.20	0.80	400	1,52,81	9	0
SN 2007N	2007-02-14.668	54145.668	23.23	5	3200–9238	6.09/7	50	51	1.44	1.12	400	1,47,52,81	5	0
SN 2007O	2007-01-22.663	54122.663	−0.33	8	4432–9569	3	220	218	1.16	0.80	200	1,52,81	9	0
SN 2007O	2007-02-18.487	54149.487	25.56	3	3334–10292	6.17/9.98	80	257	1.07	2.65	2100	66,87	10	0
SN 2007R	2007-02-18.230	54149.230	21.58	3	3472–10074	5.78/10.98	26	233	1.02	3.23	1800	66,87	10	0
SN 2007S	2007-02-18.375	54149.375	5.18	3	3334–10500	6.15/10.07	189	11	1.20	1.80	1500	66,87	10	0
SN 2007S	2007-03-18.357	54177.357	32.78	5	3450–9240	6.40/8.56	353	355	1.04	0.97	240	47,81	11	0
SN 2007S[m]	2007-04-16.352	54206.352	61.38	5	3116–9330	5.34/8.76	43	56	1.13	4.50	600	52,85,88,91	5	0
SN 2007V	2007-02-14.577	54145.577	···	5	3210–9238	6.27/7	237	58	1.41	1.80	250	1,47,52,81	5	0
SN 2007af	2007-03-13.545	54172.545	−1.25	3	3350–10500	7.24/11.06	212	33	1.46	1.87	360	1,81,87	11	6
SN 2007af	2007-03-17.653	54176.653	2.84	8	4421–9581	3	239	60	1.36	0.80	150	47,81	9	6
SN 2007af	2007-03-18.633	54177.633	3.81	5	3450–9240	6.06/7	60	56	1.27	1.16	30	47,81	11	6
SN 2007af	2007-04-10.396	54200.396	26.45	3	3314–10600	7.51/12.59	183	5	1.27	2.54	900	1,71,72	11	6
SN 2007af	2007-06-14.314	54265.314	91.02	3	3324–10500	6.81/10.12	36	39	1.61	2.35	1800	66,68,71	11	0
SN 2007af	2007-07-07.205	54288.205	113.78	3	3310–10500	7.42/11	203	25	1.36	3.13	1800	66,81,92	11	0
SN 2007af	2007-07-15.213	54296.213	121.75	3	3324–10500	5.03/11	31	35	1.49	2.89	1800	66,68,92	11	0
SN 2007af	2007-08-07.214	54319.214	144.62	3	3328–10600	5.39/10.73	224	47	2.23	2.08	1800	81,92	11	0
SN 2007af	2007-08-21.210	54333.210	158.54	3	3638–10370	5.07/12.66	48	50	2.93	1.5	1500	71,92	10	0
SN 2007aj	2007-03-13.374	54172.374	10.75	3	3350–10500	5.49/11.36	205	202	1.05	1.88	1200	1,81,87	11	0
SN 2007aj	2007-04-10.443	54200.443	38.00	3	3314–10600	7.22/12.49	189	101	1.21	2.51	1800	1,71,72	11	0
SN 2007al	2007-03-13.289	54172.289	3.39	3	3340–10500	6.30/12.40	182	3	1.83	2.47	1500	1,81,87	11	0
SN 2007ap	2007-03-17.649	54176.649	9.37	8	4442–9581	3	248	74	1.03	0.80	240	47,81	9	0
SN 2007ap	2007-04-10.502	54200.502	32.85	3	3314–10600	5.53/12.44	102	34	1.12	3.11	1500	1,71,72	11	0
SN 2007ap	2007-04-13.633	54203.633	35.93	8	4488–9574	3	79	79	1.19	0.60	200	1,52,81	9	0
SN 2007ao	2007-03-17.644	54176.644	···	8	4555–9581	3	252	71	1.23	0.80	360	47,81	9	0
SN 2007au	2007-04-10.192	54200.192	16.11	3	3324–10600	5.35/11.78	104	101	1.15	2.44	2100	1,71,72	11	6
SN 2007au	2007-04-26.255	54216.255	31.85	3	3706–9276	6.32/12.28	255	75	1.61	2.28	1800	72,87	10	0
SN 2007ax	2007-04-10.281	54200.281	14.93	3	3314–10600	5.33/12.64	60	59	1.46	3	1200	1,71,72	11	0
SN 2007ba	2007-04-10.475	54200.475	2.14	3	3314–10600	5.61/11.98	205	26	1.21	4.00	2400	1,71,72	11	0
SN 2007ba	2007-04-13.629	54203.629	5.18	8	4447–9574	3	69	69	1.37	0.60	300	1,52,81	9	0
SN 2007ba	2007-04-16.623	54206.623	8.06	8	4447–9574	3	69	69	1.38	0.70	400	11,78,93,94,95	9	0
SN 2007bc	2007-04-10.323	54200.323	0.61	3	3314–10600	6.98/10.97	46	45	1.11	2.14	1200	1,71,72	11	5
SN 2007bc	2007-04-26.387	54216.387	16.35	3	3578–10500	5.69/11.33	58	58	1.67	2.5	1500	72,87	10	−6
SN 2007bd	2007-04-10.254	54200.254	−5.79	3	3316–10600	5.21/11.84	40	40	1.68	4.23	2100	1,71,72	11	0
SN 2007bd	2007-04-26.226	54216.226	9.70	3	3614–10500	6.37/12.09	219	41	1.72	1.30	1800	72,87	10	0
SN 2007bj	2007-04-26.493	54216.493	14.25	3	3340–10500	6.11/12.19	204	26	1.39	3.76	900	72,87	10	6
SN 2007bj	2007-05-10.471	54230.471	28.00	3	3468–10600	6.51/12.16	208	30	1.45	1.5	1500	1,81,87	11	−5
SN 2007bj	2007-05-24.423	54244.423	41.73	3	3304–10600	5.73/12.00	205	30	1.44	1.5	1500	64,68,72	11	5
SN 2007bm	2007-04-26.278	54216.278	−7.79	3	3340–10500	6.57/11.97	198	19	1.56	3.83	1200	72,87	10	0
SN 2007bm	2007-05-19.239	54239.239	15.03	3	3386–10500	5.58/11.09	204	26	1.66	2	1800	64,87	10	0
SN 2007bm	2007-05-24.199	54244.199	19.96	3	3320–10500	5.86/12.17	196	17	1.54	3.65	1800	64,68,72	10	0
SN 2007bm	2007-06-14.216	54265.216	40.84	3	3324–10500	5.01/11.34	39	40	2.33	3.04	1800	66,68,71	11	0
SN 2007bz	2007-04-26.419	54216.419	1.65	3	3340–10500	5.82/12.34	58	59	1.35	4.61	1500	72,87	10	0
SN 2007ca	2007-04-26.305	54216.305	−11.14	3	3456–10500	6.57/11.15	174	356	1.64	3.77	1500	72,87	10	0
SN 2007ca	2007-05-24.291	54244.291	16.46	3	3530–10262	6.23/10.81	196	18	1.75	3.43	1500	64,68,72	10	6

Continued on Next Page...

Table 2.2 — Continued

SN Name	UT Date[a]	MJD[b]	Phase[c]	Inst.[d]	Wavelength Range (Å)	Res.[e] (Å)	P.A.[f] (°)	Par.[g] (°)	Air.[h]	See.[i] (″)	Exp. (s)	Observer(s)[j]	Reducer[k]	Flux Corr.[l]
SN 2007ca	2007-06-09.277	54260.277	32.22	3	3314–10500	5.25/12.65	27	29	2.05	2.83	2100	66,71	11	5
SN 2007cf	2007-05-10.412	54230.412	···	3	3330–10600	6.20/12.43	243	29	1.21	1.5	1800	1,81,87	11	0
SN 2007cg	2007-05-24.234	54244.234	16.17	3	3580–10486	6.12/11	176	359	2.12	1.69	1800	64,68,72	10	0
SN 2007ci	2007-05-19.316	54239.316	−6.57	3	3428–10156	5.35/10.39	57	57	1.43	3.04	1800	64,87	10	0
SN 2007ci	2007-05-24.264	54244.264	−1.71	3	3320–10500	6.30/11.10	231	52	1.22	2.65	1800	64,68,72	10	5
SN 2007ci	2007-06-09.244	54260.244	13.99	3	3310–10500	5.31/10.31	55	56	1.40	3.52	1800	66,71	11	6
SN 2007ci	2007-06-23.249	54274.249	27.75	3	3308–10500	6.66/11	58	58	1.83	2.65	2400	64,66	11	0
SN 2007co	2007-06-09.398	54260.398	−4.09	3	3310–10500	5.36/9.73	244	20	1.01	2.97	1800	66,71	11	6
SN 2007co	2007-06-14.468	54265.468	0.85	3	3324–10500	6.96/9.92	245	66	1.14	2.17	2400	66,68,71	11	5
SN 2007co	2007-06-23.408	54274.408	9.55	3	3312–10500	5.24/12.14	246	61	1.06	2.01	1800	64,66	11	6
SN 2007co	2007-07-07.316	54288.316	23.09	3	3310–10500	7.13/10.59	246	7	1.01	2.70	2400	66,81,92	11	6
SN 2007co	2007-07-15.240	54296.240	30.81	3	3600–10124	5.11/11	246	301	1.05	3.36	1800	66,68,92	11	6
SN 2007co	2007-07-20.239	54301.239	35.68	3	3320–10600	5.30/9.90	246	306	1.03	3.58	1800	1,71,92	11	5
SN 2007co	2007-08-07.277	54319.277	53.24	3	3326–10550	7.04/11	234	59	1.04	1.99	2700	81,92	11	0
SN 2007co	2007-08-14.276	54326.276	60.06	3	3600–9878	5.39/11.30	57	60	1.05	2.58	2400	66,71	10	0
SN 2007cp	2007-06-14.263	54265.263	···	3	5160–10500	10.35	31	37	2.80	1.76	1800	66,68,71	11	0
SN 2007cp	2007-06-23.217	54274.217	···	3	3308–10500	5.12/11	29	32	2.34	1.4	1800	64,66	11	0
SN 2007cq	2007-06-23.431	54274.431	−5.82	3	3310–10500	7.09/11	143	324	1.34	2.46	600	64,66	11	0
SN 2007cq	2007-07-07.439	54288.439	7.84	3	3310–10500	7.05/11.12	161	343	1.21	2.80	1500	66,81,92	11	0
SN 2007cq	2007-07-15.374	54296.374	15.57	3	3324–10500	7.25/11	144	325	1.33	3.24	1500	66,68,92	11	5
SN 2007cq	2007-07-20.319	54301.319	20.39	3	3322–10600	7.55/11	134	316	1.57	3.59	1200	1,71,92	11	5
SN 2007cq	2007-08-07.330	54319.330	37.95	3	3326–10600	5.45/11.15	149	332	1.26	3.55	2100	81,92	11	5
SN 2007cq	2007-08-14.346	54326.346	44.79	3	3610–10296	5.66/11.54	153	341	1.21	2.63	2400	66,71	10	5
SN 2007cs	2007-07-07.463	54288.463	12.15	3	3310–10500	7.53/10.03	115	295	1.09	2.66	1500	66,81,92	11	0
SN 2007cs	2007-07-20.343	54301.343	24.81	3	3322–10600	7.40/11.50	114	295	1.49	2	1300	1,71,92	11	0
SN 2007cs	2007-08-07.396	54319.396	42.55	3	3326–10600	7.08/11.51	120	298	1.06	1.5	2100	81,92	11	0
SN 2007cs	2007-08-14.384	54326.384	49.42	3	3618–10390	6.01/11.56	115	297	1.07	1	2400	66,71	10	0
SN 2007fb	2007-07-07.486	54288.486	1.95	3	3310–10500	6/11.15	150	332	1.25	2.69	1200	66,81,92	11	0
SN 2007fb	2007-07-20.396	54301.396	14.63	3	3322–10600	7.23/9.55	179	316	1.51	3.18	750	1,71,92	11	0
SN 2007fb	2007-08-07.461	54319.461	32.38	3	3326–10600	6.83/12.75	179	1	1.18	2.91	1200	81,92	11	0
SN 2007fb	2007-08-14.493	54326.493	39.28	3	3510–10500	5.79/11.41	196	28	1.22	1.77	1800	66,71	10	0
SN 2007fb	2007-08-21.274	54333.274	45.95	3	3404–10268	5.89/11	129	310	1.97	1.5	1200	71,92	10	0
SN 2007fb[m]	2007-09-05.277	54348.277	60.68	3	3310–10500	5.26/11.61	136	318	1.45	2.5	1800	81,92,96	11	0
SN 2007fb	2007-10-16.231	54389.231	100.91	5	3180–9190	7.21/7	292	292	1.53	0.87	360	1,39,52,81	11	0
SN 2007fc	2007-07-20.475	54301.475	···	3	3322–10600	7.27/9.61	167	349	2.02	3.32	1500	1,71,92	11	0
SN 2007fc	2007-08-07.432	54319.432	···	3	3324–10600	5.61/12.58	169	351	2.00	1.5	2400	81,92	11	0
SN 2007fc	2007-08-14.421	54326.421	···	3	3590–10122	5.79/11.03	168	350	2.00	1.32	1800	66,71	10	0
SN 2007fq	2007-07-15.401	54296.401	···	3	3324–10500	7.26/12.35	183	6	2.04	1.5	1800	66,68,92	11	0
SN 2007fr	2007-07-15.475	54296.475	−5.83	3	3324–10500	5.49/10.26	197	22	1.31	1.86	2100	66,68,92	11	0
SN 2007fr	2007-07-20.287	54301.287	−1.25	3	3322–10600	7.44/10.64	135	317	1.76	2.54	2400	1,71,92	11	0
SN 2007fs	2007-07-20.415	54301.415	5.03	3	3322–10600	7.45/10.53	173	356	1.93	3.39	900	1,71,92	11	0
SN 2007fs	2007-08-07.357	54319.357	22.67	3	3324–10600	7.27/12.75	171	353	1.95	2.60	1500	81,92	11	0
SN 2007fs	2007-08-14.302	54326.302	29.49	3	3314–10500	5.81/11.45	156	337	2.20	2.19	1500	66,71	10	0
SN 2007fs	2007-08-21.299	54333.299	36.37	3	3456–10500	5.76/11.91	161	344	2.06	1.5	1200	71,92	10	0
SN 2007fs[m]	2007-09-05.306	54348.306	51.13	3	3314–10500	6.95/11.20	180	2	1.93	2.11	1800	81,92,96	11	0

Continued on Next Page...

Table 2.2 — Continued

SN Name	UT Date[a]	MJD[b]	Phase[c]	Inst.[d]	Wavelength Range (Å)	Res.[e] (Å)	P.A.[f] (°)	Par.[g] (°)	Air.[h]	See.[i] (″)	Exp. (s)	Observer(s)[j]	Reducer[k]	Flux Corr.[l]
SN 2007fs	2007-10-16.225	54389.225	91.35	5	3128–9186	7.11/7	329	332	1.45	0.67	360	1,39,52,81	11	0
SN 2007ge	2007-08-07.492	54319.492	12.53	3	3326–10600	6.47/12.33	141	136	1.03	1.83	2700	81,92	11	0
SN 2007gi	2007-08-07.179	54319.179	−7.31	3	3324–10600	6.48/11	81	80	1.63	2.70	900	81,92	11	0
SN 2007gi	2007-08-14.173	54326.173	−0.35	3	3310–10500	5.48/11	78	79	1.68	2.13	900	66,71	10	0
SN 2007gi	2007-08-21.163	54333.163	6.61	3	3310–10500	7.76/11	77	74	1.75	1.5	610	71,92	10	0
SN 2007gi	2007-11-12.651	54416.651	89.70	5	3102–9180	6.63/7.52	243	243	1.72	2.53	300	1,81	11	0
SN 2007gi	2008-01-15.551	54480.551	153.29	3	3320–10500	5.23/12.15	175	167	1.10	3.78	1800	66,87,97	10	0
SN 2007gk	2007-08-14.237	54326.237	−1.72	3	3310–10500	5.40/11.78	137	135	1.22	1.85	1800	66,71	10	0
SN 2007gk[m]	2007-09-05.172	54348.172	19.65	3	3310–10500	5.11/11	135	132	1.23	2.5	2400	81,92,96	11	0
SN 2007if	2007-10-15.393	54388.393	37.23	5	3200–9216	6.59/5.18	290	295	1.03	1.26	1200	1,39,52,81	11	0
SN 2007if	2007-11-12.204	54416.204	63.12	5	3138–9170	6.69/6.56	284	283	1.49	1.34	1200	1,81	11	0
SN 2007if	2007-12-13.245	54447.245	92.02	5	3270–9150	4.33/6.57	297	308	1.01	1.07	1200	1,81,88	11	0
SN 2007hj[m]	2007-09-05.250	54348.250	−1.23	3	3310–10500	5.28/11	132	313	1.24	2.50	1200	81,92,96	11	5
SN 2007hj[m]	2007-09-19.206	54362.206	12.53	3	3320–10600	5.48/9.99	130	312	1.26	2.13	900	1,66,81	11	5
SN 2007hj	2007-10-15.315	54388.315	38.27	5	3200–9214	6.54/5.21	300	313	1.01	1.06	420	1,39,52,81	11	5
SN 2007hj	2007-11-18.132	54422.132	71.62	3	3310–10630	5.95/12.05	169	354	1.08	2.77	1800	71,92	11	4
SN 2007hu[m]	2007-09-19.184	54362.184	···	3	3320–10600	5.25/10.22	64	64	1.33	1.94	1800	1,66,81	11	0
SN 2007hu	2007-10-15.264	54388.264	···	5	3212–9210	6.36/6.73	45	82	2.02	0.58	1400	1,39,52,81	11	0
SN 2007ir[m]	2007-09-19.461	54362.461	···	3	3320–10600	5.59/11	218	97	1.00	1.42	2400	1,66,81	11	0
SN 2007ir	2007-10-14.641	54387.641	···	5	3118–8712	6.48/6.66	94	92	1.69	0.80	300	98,99	11	0
SN 2007is[m]	2007-09-19.144	54362.144	···	3	3320–10600	5.37/10.50	85	84	1.13	2.61	1200	1,66,81	11	0
SN 2007is	2007-10-15.243	54388.243	···	5	3200–9210	6.57/7.33	92	92	1.81	2.34	600	1,39,52,81	11	0
SN 2007kf	2007-10-15.286	54388.286	···	5	3270–9210	6.46/6.45	110	105	2.17	1.76	900	1,39,52,81	11	0
SN 2007kg	2007-10-15.371	54388.371	···	5	3200–9212	6.59/7.48	186	180	1.33	1.29	900	1,39,52,81	11	0
SN 2007kd	2007-11-11.652	54415.652	···	5	3140–9100	6.54/7	222	218	1.05	1.19	200	1,81	11	0
SN 2007kk	2007-10-16.639	54389.639	7.15	5	3100–9190	7.01/7	111	105	1.33	0.97	300	1,39,52,81	11	0
SN 2007le	2007-10-15.325	54388.325	−10.31	5	3200–9214	6.59/8.54	336	339	1.14	1.03	500	1,39,52,81	11	6
SN 2007le	2007-10-16.233	54389.233	−9.40	5	3100–9190	7.04/7	304	304	1.52	0.77	60	1,39,52,81	11	6
SN 2007le	2007-11-02.182	54406.182	7.43	3	3334–10620	5.86/12.67	167	349	1.41	3.13	600	66,81	11	6
SN 2007le	2007-11-11.198	54415.198	16.39	5	3050–9100	6.76/6.65	313	314	1.28	1.04	150	1,81	11	5
SN 2007le	2007-11-12.187	54416.187	17.37	5	3050–9100	7.59/7.80	310	311	1.33	1.11	150	1,81	11	5
SN 2007le	2007-11-18.182	54422.182	23.33	3	3310–10640	6.13/11.43	189	7	1.39	2.61	600	71,92	11	6
SN 2007le	2007-12-01.121	54435.121	36.18	3	3326–10630	5.58/11.11	173	356	1.39	4.28	600	71,92	11	5
SN 2007le	2007-12-12.199	54446.199	47.18	5	3090–9150	6.52/6.84	2	3	1.12	1.69	240	1,81	11	6
SN 2007le	2008-08-27.490	54705.490	304.74	5	3268–9240	4.5/7	291	5	1.12	1.56	1200	100,39	11	0
SN 2007s1[n]	2007-11-02.133	54406.133	−1.23	3	3332–10620	5.94/11.97	129	310	1.27	2.85	2700	66,81	11	5
SN 2007s1[n]	2007-12-12.221	54446.221	37.79	5	3170–9150	6.43/6.65	350	2	1.00	1.60	300	1,81	11	−6
SN 2007qd	2007-11-12.535	54416.535	···	5	3158–9170	6.62/6.66	99	66	1.78	0.90	1500	1,81	11	0
SN 2007on	2007-11-12.468	54416.468	−3.01	5	3050–9170	6.56/5.98	192	11	1.79	1.41	150	1,81	11	0
SN 2007on	2007-11-12.473	54416.473	−3.00	5	3734–6840	4.5/3.06	192	13	1.80	1.39	300	1,81	11	0
SN 2007on	2007-12-01.052	54435.053	15.46	9	4000–10399	···	298	0	1.17	2	···	101,102	9	0
SN 2007on	2007-12-13.349	54447.349	27.68	5	3312–9134	4.31/6.44	356	357	1.76	1.75	120	1,81,88	11	0
SN 2007qe	2007-11-18.104	54422.104	−6.54	3	3310–10630	5.88/11.27	196	301	1.09	1.89	1300	71,92	11	0
SN 2007qe	2007-12-01.176	54435.176	6.23	3	3326–10630	5.56/11.24	208	44	1.03	3.15	1300	71,92	11	0
SN 2007qe	2007-12-11.187	54445.187	16.00	3	3320–10500	5.48/11.53	221	57	1.08	4.32	1800	71,92	10	0

Continued on Next Page...

Table 2.2 — Continued

SN Name	UT Date[a]	MJD[b]	Phase[c]	Inst.[d]	Wavelength Range (Å)	Res.[e] (Å)	P.A.[f] (°)	Par.[g] (°)	Air.[h]	See.[i] (″)	Exp. (s)	Observer(s)[j]	Reducer[k]	Flux Corr.[l]
SN 2007sa	2007-12-13.675	54447.675	···	5	3270–9150	4.5/7	317	174	1.24	1.07	120	1,81,88	11	0
SN 2007rx	2007-12-11.156	54445.156	···	3	3320–10500	5.50/11.38	221	49	1.04	3.68	1800	71,92	10	0
SN 2007ry	2007-12-11.485	54445.485	···	3	3458–10500	5.20/10.93	67	66	1.89	3.5	1800	71,92	10	0
SN 2007sr	2008-01-15.587	54480.587	32.61	3	3320–10500	5.47/11.78	199	20	2.00	3.06	600	66,87,97	10	0
SN 2007sr	2008-04-28.243	54584.243	135.70	5	3160–9210	6.5/7	139	319	1.56	0.91	200	1,103,81,87	11	0
SN 2007su	2007-12-31.132	54465.132	···	3	3490–9888	5.12/11.42	47	51	1.49	4.49	1800	1,47,92	10	0
SN 2007ux	2007-12-31.459	54465.459	5.59	3	3528–10304	6.81/12.44	110	333	1.11	1.38	2400	1,47,92	10	0
SN 2007ux	2008-01-15.483	54480.483	20.16	3	3386–10356	5.33/11.37	197	17	1.10	2.00	1500	66,87,97	10	6
SN 2008A	2008-01-15.278	54480.278	···	3	3320–10500	5.57/11	69	68	1.70	2.03	3150	66,87,97	10	0
SN 2008A	2008-02-12.000	54508.000	···	5	3076–9340	4.07/6.54	302	90	1.66	0.98	200	39,85,88	5	0
SN 2008A	2008-02-16.228	54512.228	···	3	3370–10500	5.68/10.71	63	62	2.22	3.29	1800	66,81,87,97	10	0
SN 2008A	2008-08-03.625	54681.625	···	5	3402–9196	4.5/5.46	20	191	1.04	1.17	450	104,85,88,96	11	0
SN 2008A	2008-08-28.513	54706.513	···	5	3270–9256	4.5/7.22	157	231	1.09	0.80	1200	100,39	11	0
SN 2008A	2008-10-27.276	54766.276	···	5	3150–9160	6.5/7.22	202	261	1.42	1.12	1800	1,105,81,87	11	0
SN 2008C	2008-01-15.444	54480.444	15.68	3	3362–10600	5.31/10.84	50	57	1.41	3.53	900	66,87,97	11	0
SN 2008L	2008-02-29.000	54525.000	32.37	3	4390–9886	10.85	70	68	1.78	1.85	1200	66,81,87,97	10	0
SN 2008Q	2008-02-16.113	54512.113	6.46	3	3300–10500	5.95/11	227	47	1.48	2.31	300	66,81,87,97	10	0
SN 2008Q	2008-02-29.000	54525.000	19.25	3	4400–9888	10.42	54	54	2.65	2.19	300	66,81,87,97	10	0
SN 2008Q	2008-08-28.495	54706.495	199.31	5	3296–9256	4.5/6.85	296	299	1.10	1.28	1200	100,39	11	0
SN 2008Z	2008-02-16.463	54512.463	−2.29	3	3300–10500	5.87/11.24	255	75	1.23	1.91	1200	66,81,87,97	10	0
SN 2008Z	2008-02-29.000	54525.000	9.99	3	4400–9884	10.99	92	47	1.00	2.12	1200	66,81,87,97	10	0
SN 2008af	2008-02-29.527	54525.527	24.32	3	4430–9860	12.26	176	357	1.07	1.71	1600	66,81,87,97	10	0
SN 2008ai	2008-02-16.490	54512.490	···	3	3460–10500	5.06/11.20	256	79	1.14	1.42	1500	66,81,87,97	10	0
SN 2008ai	2008-02-29.000	54525.000	···	3	4400–9884	10.86	87	85	1.04	2.49	1800	66,81,87,97	10	0
SN 2008ar	2008-02-29.000	54525.000	−8.87	3	4428–9884	11.38	205	25	1.15	2.23	900	66,81,87,97	10	4
SN 2008ar	2008-03-12.000	54537.000	2.83	3	3300–10600	5.34/11	36	37	1.22	3.68	1800	87,92	10	5
SN 2008ar	2008-04-28.519	54584.519	49.13	5	3210–9200	4.5/5.14	125	73	1.87	0.82	600	1,103,81,87	11	−2
SN 2008ca	2008-04-28.406	54584.406	···	5	3210–9210	4.5/5.74	243	65	1.06	1.68	600	1,103,81,87	11	0
SN 2008cb	2008-04-28.416	54584.416	···	5	3192–9210	6.5/5.83	243	59	1.09	0.55	600	1,103,81,87	11	0
SN 2008bf	2008-04-27.000	54583.000	27.93	3	3300–10800	6.17/10.58	54	55	1.29	2.58	1500	106,107	10	0
SN 2008bf	2008-05-09.000	54595.000	39.65	3	3300–10800	5.37/10.81	58	58	1.81	2.02	1200	108,109,75	10	0
SN 2008bf	2008-05-10.000	54596.000	40.62	3	3300–10800	5.32/11	57	58	1.51	2.08	1200	108,109,75	10	0
SN 2008bt	2008-04-16.000	54572.000	−1.08	3	3300–10600	6.34/11	21	23	1.70	···	1800	66,87	10	0
SN 2008bt	2008-04-28.236	54584.236	10.97	5	3226–9210	4.5/7	89	332	1.24	2.42	175	1,103,81,87	11	0
SN 2008bv	2008-04-28.315	54584.315	···	5	3254–9210	4.5/5.07	177	103	1.26	2.82	400	1,103,81,87	11	0
SN 2008bw	2008-04-28.627	54584.627	···	5	3166–9200	6.34/6.46	311	165	1.17	1.75	1150	1,103,81,87	11	0
SN 2008bz	2008-04-26.000	54582.000	···	3	3300–10800	5.93/11.03	41	42	1.28	3.34	1800	106,107	10	0
SN 2008cd	2008-05-01.000	54587.000	···	3	3300–10800	6/11	193	17	1.77	4.70	1500	106,107,110	10	0
SN 2008cf	2008-05-07.000	54593.000	···	3	3622–9246	6.11/12.95	187	7	2.30	3.93	1800	108,109,110	10	0
SN 2008cl	2008-05-17.308	54603.308	4.24	3	3478–10710	6.31/10.62	60	234	1.07	4.20	1800	92,97	10	0
SN 2008s1[o]	2008-05-19.000	54605.000	−6.36	3	3300–10800	7.49/12.94	199	21	1.14	2.14	1800	111,15	10	0
SN 2008s1[o]	2008-05-21.000	54607.000	−4.40	3	3300–10800	6.12/12.60	202	22	1.14	···	1800	111,15	10	0
SN 2008s1[m,o]	2008-05-22.000	54608.000	−3.42	3	3300–10800	6.31/12.68	196	17	1.13	4.76	1800	111,15	10	0
SN 2008s1[m,o]	2008-05-26.000	54612.000	0.49	3	3298–10800	4.83/9.63	47	49	1.48	4.14	2802	112,113	10	6
SN 2008s1[o]	2008-05-30.000	54616.000	4.40	3	3300–10800	5.85/12.46	54	54	2.16	2.40	1800	111,114	10	6

Continued on Next Page...

Table 2.2 — Continued

SN Name	UT Date[a]	MJD[b]	Phase[c]	Inst.[d]	Wavelength Range (Å)	Res.[e] (Å)	P.A.[f] (°)	Par.[g] (°)	Air.[h]	See.[i] (″)	Exp. (s)	Observer(s)[j]	Reducer[k]	Flux Corr.[l]
SN 2008s1[o]	2008-05-31.000	54617.000	5.38	3	3300–10800	6.01/11.76	216	38	1.23	2.29	1800	111,114	10	6
SN 2008s1[m,o]	2008-06-10.207	54627.207	15.37	3	3300–10800	6/11	85	14	1.13	1.5	882	115	10	3
SN 2008s1[m,o]	2008-06-29.275	54646.275	34.02	3	3300–10700	5.96/10.67	51	52	1.63	1.07	900	116,117,81	10	−5
SN 2008ct[m]	2008-06-29.426	54646.426	···	3	3956–10150	6.27/11.87	133	316	1.15	1.91	2100	116,117,81	10	0
SN 2008db[m]	2008-07-07.491	54654.491	···	3	3376–10588	6/11.59	153	335	1.55	1.8	600	116,66	10	0
SN 2008db	2008-08-08.498	54686.498	···	3	3426–10800	6.76/12.21	189	13	1.43	2.12	900	66,87	11	0
SN 2008db	2008-08-26.422	54704.422	···	3	3314–10750	6.62/11.24	179	2	1.40	1.65	1500	81,87	11	0
SN 2008dx[m]	2008-06-29.219	54646.219	2.46	3	3300–10700	5.98/11.65	64	64	1.18	1.59	1500	116,117,81	10	0
SN 2008dx	2008-07-04.203	54651.203	7.33	3	3366–10152	5.76/11.15	63	63	1.18	2.11	1200	116,117,87	10	0
SN 2008dx[m]	2008-07-07.217	54654.217	10.28	3	3340–10800	6/11.57	64	64	1.26	1.8	1800	116,66	10	0
SN 2008dx[m]	2008-07-26.208	54673.208	28.84	3	3530–10760	5.81/10.70	64	63	1.65	1.64	1500	116,81	11	0
SN 2008ds[m]	2008-06-29.466	54646.466	···	3	3300–10800	6.76/12.59	113	292	1.26	2.10	900	116,117,81	10	0
SN 2008ds	2008-07-04.421	54651.421	···	3	3342–10800	5.41/11.23	115	293	1.45	3.74	900	116,117,87	10	0
SN 2008ds[m]	2008-07-07.476	54654.476	···	3	3308–10800	6/11.51	112	291	1.14	1.8	900	116,66	10	0
SN 2008ds[m]	2008-07-26.377	54673.377	···	3	3390–10780	6.49/11.07	113	292	1.31	2.36	900	116,81	11	0
SN 2008ds	2008-08-26.503	54704.503	···	3	3314–10750	6.16/11.55	67	68	1.09	2.08	1200	81,87	11	0
SN 2008ds	2008-08-31.468	54709.468	···	3	3504–10706	6.16/11.24	62	65	1.05	2.19	1500	117,92	11	0
SN 2008ds	2008-09-07.271	54716.271	···	3	3388–10724	7.51/11.44	112	292	1.25	2.21	1500	39	11	0
SN 2008ds	2008-09-22.372	54731.372	···	3	3400–10400	4.45/12.52	131	326	1.01	2.62	1800	118,87	10	0
SN 2008ds[m]	2008-09-30.294	54739.294	···	3	3408–9268	4.77/12.20	113	294	1.03	1.63	1800	118,87	11	0
SN 2008ds	2008-10-07.279	54746.279	···	3	3410–10098	4.32/10.00	113	294	1.02	2.24	2100	116,87	11	0
SN 2008ds	2008-10-22.215	54761.215	···	3	3428–6400	7.68	110	292	1.05	3.34	4200	119,120,81	11	0
SN 2008dr[m]	2008-06-29.389	54646.389	···	3	3300–10800	6.44/11.54	139	319	1.56	2.83	1200	116,117,81	10	0
SN 2008dr	2008-07-04.364	54651.364	···	3	3342–10800	5.85/10.77	137	317	1.67	2.66	1500	116,117,87	10	5
SN 2008dr[m]	2008-07-07.457	54654.457	···	3	3392–10800	6/11.11	166	351	1.23	1.8	1200	116,66	10	6
SN 2008dr	2008-08-03.000	54681.000	···	5	3568–9250	3.39/7.59	246	67	1.71	2.72	300	104,85,88,96	11	−6
SN 2008dr	2008-08-27.363	54705.363	···	5	3268–9240	4.5/5.36	307	309	1.14	1.39	450	100,39	11	0
SN 2008dt[m]	2008-07-07.395	54654.395	9.27	3	3306–10800	6/12.40	64	64	1.34	1.8	1500	116,66	10	6
SN 2008dt	2008-08-01.347	54679.347	33.37	3	3294–10800	6.05/12.02	64	64	1.48	2.58	1500	117,87	10	6
SN 2008dt	2008-09-08.228	54717.228	69.95	3	3430–10744	5.95/11.80	65	64	1.44	1.5	2100	121,81	11	0
SN 2008r3[m,p]	2008-07-26.184	54673.184	···	3	3358–10718	6/12.18	64	63	1.45	2.27	900	116,81	11	0
SN 2008r3[p]	2008-08-01.208	54679.208	···	3	3300–10800	6.02/11.69	63	62	1.79	2.59	1200	117,87	10	0
SN 2008ec[m]	2008-07-26.359	54673.359	−0.24	3	3292–10780	6.29/12.16	138	318	1.34	2.41	1200	116,81	11	5
SN 2008ec	2008-08-01.389	54679.389	5.70	3	3294–10800	6.03/11.40	151	331	1.20	1.94	1200	117,87	10	6
SN 2008ec	2008-08-08.313	54686.313	12.51	3	3306–10800	6.67/11.22	135	316	1.40	2.34	1200	66,87	11	0
SN 2008ec	2008-08-26.271	54704.271	30.18	3	3314–10750	6.69/11.11	137	317	1.36	2.10	1500	81,87	11	6
SN 2008ec	2008-08-31.256	54709.256	35.08	3	3760–10756	5.67/12.03	136	317	1.36	2.5	2100	117,92	11	−5
SN 2008ec	2008-09-08.295	54717.295	42.99	3	3430–10790	7.02/12.04	158	339	1.17	1.5	1800	121,81	11	6
SN 2008ec	2008-10-07.343	54746.343	71.58	3	3410–10750	4.37/10.93	208	33	1.32	2	2100	116,87	11	4
SN 2008ee[m]	2008-07-26.416	54673.416	···	3	3376–10790	6.49/11.83	139	320	1.73	4.07	900	116,81	11	0
SN 2008ee	2008-08-26.317	54704.317	···	3	3314–10780	6.63/11.99	137	317	1.89	3.71	1200	81,87	11	0
SN 2008ee	2008-09-07.342	54716.342	···	3	3416–10740	7.52/11.44	150	331	1.43	4.10	1200	39	11	0
SN 2008ei[m]	2008-07-26.314	54673.314	3.29	3	3382–10800	4.80/10.69	109	288	1.17	2.34	1500	116,81	11	0
SN 2008ei	2008-08-01.372	54679.372	9.13	3	3294–10800	5.97/11.94	111	292	1.03	2.18	1500	117,87	10	−6
SN 2008ei	2008-08-08.288	54686.288	15.79	3	3444–10106	5.58/10.82	108	288	1.14	1.13	1800	66,87	11	−4

Continued on Next Page...

Table 2.2 — Continued

SN Name	UT Date[a]	MJD[b]	Phase[c]	Inst.[d]	Wavelength Range (Å)	Res.[e] (Å)	P.A.[f] (°)	Par.[g] (°)	Air.[h]	See.[i] (″)	Exp. (s)	Observer(s)[j]	Reducer[k]	Flux Corr.[l]
SN 2008ei	2008-08-26.248	54704.248	33.10	3	3314–10750	6.35/11.68	109	288	1.11	2.19	1800	81,87	11	−6
SN 2008er	2008-08-08.474	54686.474	···	3	3306–10800	6.81/10.92	119	249	1.07	2.75	1800	66,87	11	0
SN 2008ez	2008-08-26.167	54704.167	···	3	3310–10700	6.13/12.48	56	55	2.40	2.84	1500	81,87	11	0
SN 2008ey	2008-08-26.393	54704.393	···	3	3330–10742	6.32/10.90	98	278	1.25	1.99	1800	81,87	11	0
SN 2008s3[q]	2008-09-08.263	54717.263	···	3	3506–10744	7.26/11.90	144	327	1.25	1.5	2100	121,81	11	0
SN 2008s4[r]	2008-09-08.422	54717.422	···	3	3318–10790	7.19/11.15	173	354	1.58	1.5	1500	121,81	11	0
SN 2008fg	2008-09-07.512	54716.512	···	3	3438–10716	7.12/11.05	38	180	1.00	1.23	1800	39	11	0
SN 2008fj	2008-09-08.200	54717.200	···	3	3414–10800	5.95/11.10	88	87	1.16	1.5	1800	121,81	11	0
SN 2008s5[s]	2008-09-22.302	54731.302	1.26	3	3400–10400	4.47/12.00	192	19	1.13	2.36	1200	118,87	10	0
SN 2008s5[m,s]	2008-09-30.235	54739.235	8.96	3	3408–10770	4.72/10.68	165	349	1.10	2.43	1800	118,87	11	0
SN 2008s5[s]	2008-10-07.245	54746.245	15.76	3	3410–10750	4.34/10.63	184	9	1.12	2.20	1800	116,87	11	0
SN 2008fr[m]	2008-09-30.422	54739.422	···	3	3408–10770	4.75/11.50	200	27	1.15	2.15	1800	118,87	11	0
SN 2008fr	2008-10-07.368	54746.368	···	3	3410–10750	4.33/11.17	182	3	1.10	2.25	1800	116,87	11	0
SN 2008fr	2008-10-22.393	54761.393	···	3	3452–6380	8.99	36	39	1.25	3.04	4200	119,120,81	11	0
SN 2008s8[t]	2008-10-07.417	54746.417	···	3	3410–10674	4.37/11.26	184	5	1.21	4.00	1500	116,87	11	0
SN 2008s8[t]	2008-10-22.448	54761.448	···	3	3512–6400	9.08	34	34	1.44	2.77	3600	119,120,81	11	0
SN 2008gs	2008-11-07.375	54777.375	···	3	3458–10800	4.54/11.55	30	34	1.53	2.33	2400	119,81	11	0
SN 2008fx	2008-10-07.399	54746.399	···	3	3410–10750	4.31/11.42	167	349	1.03	1.91	2100	116,87	11	0
SN 2008ge	2008-10-27.505	54766.505	···	5	3144–9156	6.48/7	0	1	2.62	1.73	105	1,105,81,87	11	0
SN 2008gh	2008-10-22.505	54761.505	···	3	3490–6374	9.92	65	244	1.10	2.7	4200	119,120,81	11	0
SN 2008gh	2008-11-23.542	54793.542	···	3	3420–8000	4.52/5	168	160	1.07	1.3	2100	39	10	0
SN 2008gt	2008-11-07.210	54777.210	···	3	3458–10800	4.41/11.66	191	14	1.40	1.29	1800	119,81	11	0
SN 2008gt	2008-11-23.176	54793.176	···	3	3420–8000	6.13/5	186	12	1.39	2.16	2100	39	10	0
SN 2008gy	2008-11-23.467	54793.467	···	3	3420–8000	4.59/5	236	57	1.67	3.09	1800	39	10	0
SN 2008gw	2008-11-23.505	54793.505	···	3	3420–8000	4.49/5	224	46	1.64	1.73	1800	39	10	0
SN 2008hk	2008-11-23.578	54793.578	···	3	3420–8000	4.44/5	186	9	1.14	2.05	900	39	10	0
SN 2008ha	2008-11-20.225	54790.225	7.46	3	3478–10800	4.90/11	199	23	1.11	2.76	2400	116,92	9	0
SN 2008ha	2008-11-23.000	54793.000	10.22	3	3418–8074	4.5/5	203	19	1.09	2.49	1800	39	9	0
SN 2008ha	2008-12-05.000	54805.000	22.17	3	3406–10800	4.5/11	168	56	1.27	2.3	5400	71,92	9	0
SN 2008hj	2008-11-23.283	54793.283	···	3	3420–8000	4.77/5	208	30	2.03	1.88	1500	39	10	0
SN 2008hj	2008-12-05.296	54805.296	···	3	3516–10770	4.32/10.07	184	42	3.42	3.64	1500	71,92	11	0
SN 2008hj	2008-12-31.156	54831.156	···	3	3450–10700	4.42/10.24	47	24	1.80	1.25	1500	117,87	10	0
SN 2008hq	2008-12-05.423	54805.423	···	3	3498–9914	4.78/11.05	84	231	1.04	2.3	2100	71,92	11	0
SN 2008hr	2008-12-05.534	54805.534	···	3	3482–9900	4.99/11.66	170	353	1.06	2.20	2000	71,92	11	0
SN 2008hz	2008-12-31.235	54831.235	···	3	3450–10700	4.60/11.38	87	85	1.25	1.25	1800	117,87	10	0
SN 2008hu	2008-12-05.484	54805.484	···	3	3406–10770	5.25/12.17	176	358	1.79	2.64	1800	71,92	11	0
SN 2008hs	2008-12-05.326	54805.326	−7.94	3	3406–10770	4.43/11.60	96	94	1.11	2.54	1800	71,92	11	0
SN 2008hy	2008-12-31.326	54831.326	···	3	3452–10700	4.47/10.79	143	142	1.36	1.25	1200	117,87	10	0

[a]If not rounded to the whole day, UT date at the midpoint of the observation.

[b]Modified JD (if not rounded to the whole day, modified JD at the midpoint of the observation).

[c]Phases of spectra are in rest-frame days using the heliocentric redshift and photometry reference presented in Table 2.1.

[d]Instruments: (1) UV Schmidt (Shane 3 m), (2) Stover Spectrograph (Nickel 1 m), (3) Kast (Shane 3 m), (4) Palomar Double Spectrograph (Hale 5 m at Palomar Observatory), (5) LRIS (Keck 10 m), (6) ESI (Keck 10 m), (7) R.C. Spectrograph (Kitt Peak 4 m), (8) DEIMOS (Keck 10 m), (9) LDSS-3 (Clay Magellan II 6.5 m).

Continued on Next Page...

Table 2.2 — Continued

SN Name	UT Date[a]	MJD[b]	Phase[c]	Inst.[d]	Wavelength Range (Å)	Res.[e] (Å)	P.A.[f] (°)	Par.[g] (°)	Air.[h]	See.[i] (″)	Exp. (s)	Observer(s)[j]	Reducer[k]	Flux Corr.[l]

[e]FWHM spectral resolution as measured from narrow sky emission lines. If we were unable to accurately measure the sky lines, the average resolution for that instrumental setup is displayed (see Section 2.2 for more information regarding our instrumental setups and their average resolutions).
[f]Observed position angle during observation.
[g]Average parallactic angle (Filippenko 1982) during the observation.
[h]Airmass at midpoint of exposure.
[i]Approximate atmospheric seeing as measured from the FWHM of the trace of the SN. If we were unable to accurately measure the FWHM of the trace, an estimate by the observers of the average seeing from that night is displayed with only one or two significant figures.
[j]Observers: (1) Alex Filippenko, (2) Joe Shields, (3) Michael Richmond, (4) Charles Steidel, (5) Tom Matheson, (6) Hansen Chen, (7) Luis Ho, (8) Schuyler Van Dyk, (9) Wallace Sargent, (10) Todd Small, (11) Hyron Spinrad, (12) Michael Baker, (13) Rebecca Green, (14) Bruno Leibundgut, (15) Aaron Barth, (16) Andre Martel, (17) Michael Gregg, (18) Art Wolfe, (19) Vince Virgilio, (20) Vesa Junkkarinen, (21) Matt Lehnert, (22) Lee Armus, (23) Xiaoming Fan, (24) Graeme Smith, (25) Chien Peng, (26) Dan Stevens, (27) Doug Leonard, (28) Harding Smith, (29) Adam Burgasser, (30) Saul Perlmutter, (31) Isobel Hook, (32) Nicole Vogt, (33) Jeffrey Newman, (34) Wynn Ho, (35) Andrea Gilbert, (36) Ed Moran, (37) Adam Riess, (38) Ronald Eastman, (39) Maryam Modjaz, (40) Mike Eracleous, (41) Robert Kirshner, (42) Weidong Li, (43) Carlos DeBreuck, (44) Willem van Breugel, (45) Alison Coil, (46) Peter Garnavich, (47) Ryan Chornock, (48) Mark Phillips, (49) Elinor Gates, (50) Michael Rich, (51) Brandon Swift, (52) Ryan Foley, (53) Saurabh Jha, (54) Eliot Quataert, (55) Marina Papenkova, (56) Matthew Bershady, (57) Paul Nandra, (58) Robert Simcoe, (59) Edo Berger, (60) Shrinivas Kulkarni, (61) Chris Fassnacht, (62) Gordon Squires, (63) Brian Barris, (64) Diane Wong, (65) John Graham, (66) Mohan Ganeshalingam, (67) Dan Weisz, (68) Louis Desroches, (69) Deborah Hutchings, (70) Karin Sandstrom, (71) Frank Serduke, (72) Matthew Moore, (73) Harrison Pugh, (74) Jennifer Hoffman, (75) Tommaso Treu, (76) Sandra Faber, (77) Genevieve Graves, (78) Mark Dickinson, (79) David Pooley, (80) Sung Park, (81) Jeffrey Silverman, (82) James Scala, (83) Asher Blum, (84) Katsuki Shimasaki, (85) Joshua Bloom, (86) Katherine Alatalo, (87) Thea Steele, (88) Daniel Perley, (89) Nathaniel Butler, (90) Steven Rodney, (91) Daniel Kocevski, (92) Xiaofeng Wang, (93) Daniel Stern, (94) Michael Cooper, (95) Kai Noeske, (96) Adam Miller, (97) Nicholas Lee, (98) Casey Papovich, (99) Christopher Willmer, (100) Lisa Kewley, (101) Karl Glazebrook, (102) David Gilbank, (103) Dovi Poznanski, (104) Matthew Malkan, (105) Bradley Tucker, (106) Misty Bentz, (107) Jonelle Walsh, (108) Rachel Street, (109) Marton Hidas, (110) Jong-Hak Woo, (111) Carol Thornton, (112) Gabriela Canalizo, (113) Kyle Hiner, (114) Jenny Greene, (115) David Tytler, (116) Christopher Griffith, (117) Robin Mostardi, (118) Vincent Viscomi, (119) Bethany Cobb, (120) Michael McCourt, (121) Matthew George.
[k]Reducers: (1) Tom Matheson, (2) Luis Ho, (3) Aaron Barth, (4) Doug Leonard, (5) Ryan Chornock, (6) Mike Eracleous, (7) Weidong Li, (8) Alison Coil, (9) Ryan Foley, (10) Thea Steele, (11) Jeffrey Silverman, (12) Brandon Swift.
[l]Flux Correction: (0) No correction, (2) Not parallactic, but galaxy subtracted, no contamination, (3) Not parallactic, but galaxy subtracted with contamination, (4) Parallactic and scaled, (5) Parallactic and galaxy subtracted, no contamination, (6) Parallactic and galaxy subtracted with contamination. Negative values indicate that $> 5\%$ of the corrected flux is negative.
[m]Observation has unreliable spectrophotometry due to events external to normal telescope operation and data reduction. See Section 2.3.2 for more information.
[n]Also known as SNF20071021-000.
[o]Also known as SNF20080514-002.
[p]Also known as ROTSE3 J125642.7+273041.
[q]Also known as SNF20080825-006.
[r]Also known as SNF20080825-010.
[s]Also known as SNF20080909-030.
[t]Also known as SNF20080920-000.

2.2 Observations

During the past two decades, our group has had access to several different telescopes and spectrographs for the purpose of observing SNe. The main facility for this chapter was the Shane 3 m telescope at Lick Observatory. During this period, the Shane telescope has had two low-resolution spectrographs: the UV Schmidt spectrograph until early 1992 (Miller & Stone 1987) and the Kast double spectrograph since then (Miller & Stone 1993). We also obtained a handful of spectra using the Stover spectrograph mounted on the Nickel 1 m telescope also at Lick.

We have supplemented our Lick Observatory sample with spectra obtained at Keck Observatory. When conditions were not acceptable for our faint, primary targets (typically during twilight or cloudy weather), we would use one of the 10 m Keck telescopes to obtain spectra of our relatively bright (typically $R < 18$ mag), nearby SN targets. We also obtained many late-time spectra with the Keck telescopes. We have used the Low-Resolution Imaging Spectrometer (LRIS; Oke et al. 1995, both before and after the addition of the blue arm), the DEep Imaging Multi-Object Spectrograph (DEIMOS; Faber et al. 2003), and the Echelle Spectrograph and Imager (ESI; Sheinis et al. 2002). The percentages of spectra presented in this chapter obtained using these instruments are displayed in Figure 2.1.

All of these telescopes were classically scheduled. We would typically have 1 night every two weeks on the Shane telescope (at first and last quarter moon) throughout the year and 4–10 nights per year with the Keck telescopes (typically 1–2 nights near new moon in a given lunation). Recently, we have been allotted a third night per lunar cycle on the Shane telescope near new moon. Taking into account weather and instrument problems, our coverage of any given object is typically about one spectrum every two weeks. The telescope scheduling and observing method are very different from those of Matheson et al. (2008) and Blondin et al. (2011), who observed fewer SNe Ia but with a higher cadence for each object (see Section 2.6.1 for further comparisons of the two spectral datasets).

All observations of our scheduled time were performed by members of the BSNIP group. PI Filippenko was present for an astounding 254 nights. Occasionally, as the result of a swap of time or for a particularly interesting object, an observer exterior to the BSNIP group would observe for our team. This sometimes resulted in slight variations in instrument configurations (such as a smaller wavelength range, for example). As mentioned above, the bulk of our data were obtained at Lick and Keck Observatories where our average seeing was slightly greater than 2″ and slightly greater 1″, respectively.

2.2.1 Individual Instruments

UV Schmidt on the Shane 3 m

The UV Schmidt spectrograph contained a Texas Instruments 800 × 300 pixel charge-coupled device (CCD) and our setup used a slit that was 2–3″ wide. The average resolution of our spectra from this instrument was ∼12 Å.

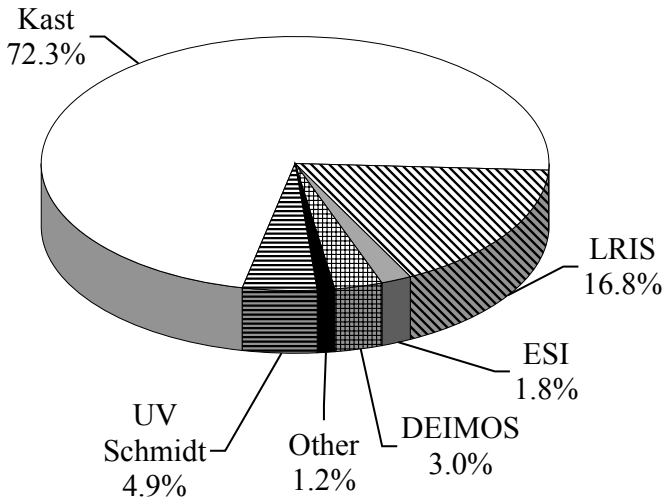

Figure 2.1: The percentages of spectra presented in this chapter obtained using various instruments. The UV Schmidt spectrograph (Miller & Stone 1987) was on the Shane 3 m telescope at Lick Observatory until early 1992 when it was replaced by the Kast double spectrograph (Miller & Stone 1993). LRIS (Oke et al. 1995), DEIMOS (Faber et al. 2003), and ESI (Sheinis et al. 2002) were all used with one of the 10 m Keck telescopes.

Kast on the Shane 3 m

Until September 2008, the Kast double spectrograph used two Reticon 1200×400 pixel CCDs with 27 μm pixels and a spatial scale of $0.78''$ per pixel, with one CCD in each of the red and blue arms of the spectrograph. Currently, the blue arm of Kast uses a Fairchild 2048×2048 pixel device with 15 μm pixels, which corresponds to $0.43''$ per pixel. For our typical setup, we would observe with a 300/7500 grating for the red side, a 600/4310 grism for the blue side, and a D55 dichroic. This results in a wavelength range of 3300–10400 Å with overlap between the two arms of 5200–5500 Å. With our typical slit of $2''$, we achieve a resolution of $\sim$11 and $\sim$6 Å on the red and blue sides, respectively.

Stover on the Nickel 1 m

The Stover spectrograph contains a Reticon 400×1200 pixel CCD with 27 μm pixels and a spatial scale of $2''$ per pixel. Our setup used a $2.9''$ wide slit with the 600/4820 grism. This yielded an average resolution of $\sim$7 Å.

LRIS on the Keck 10 m

When our dataset was obtained, the LRIS spectrograph used a Tektronik 2048×2048 pixel CCD with 21 μm pixels and a spatial scale of $0.211''$ per pixel for the red arm and two 2048×4096 pixel Marconi E2V CCDs with 15 μm pixels and a spatial scale of $0.135''$ per pixel for the blue arm. LRIS operated with only the red arm until 2002. Our typical setup would use the 400/8500 grating for the red side, either the 400/3400 or 600/4000 grism for the blue side, and the D56 dichroic resulting in a wavelength range of 3050–9200 Å and 3200–9200 Å for the respective grisms. There was typically an overlap region of 5400–5800 Å and 5400–5700 Å for the 400/3400 and 600/4000 grisms, respectively. With our typical $1''$ slit, this setup yields resolutions of $\sim$7 Å for the red side, and either $\sim$6.5 or $\sim$4.5 Å for the 400/3400 and 600/4000 grisms, respectively, for the blue side.

DEIMOS on the Keck 10 m

The DEIMOS spectrograph uses a 2×4 mosaic of 2048×4096 pixel CCDs with 15 μm pixels and a spatial scale of $0.1185''$ per pixel for a total detector array of 8192×8192 pixels. Our typical setup would use the 600/7500 grating with a GG455 order-blocking filter, resulting in a wavelength range of 4500–9000 Å. We would generally use a $1.1''$ slit which, along with our typical setup, would result in a resolution of $\sim$3 Å. Occasionally we would use the 1200/7500 grating instead, yielding a wavelength range of 4800–7400 Å and a resolution of $\sim$1.5 Å. The slit was tilted slightly to provide better sky subtraction (see Section 2.3.1 for details).

ESI on the Keck 10 m

The ESI spectrograph has an MIT-LL 2048×4096 pixel CCD with 15 μm pixels and an average spatial scale of $0.1542''$ per pixel, with the redder orders having a larger spatial scale than the bluer orders. Our observations were typically performed in the echellette mode with a $1''$ slit in 2×1 binning mode. This resulted in a resolution of 22 km s^{-1} across the entire wavelength range of 3900–11000 Å.

2.2.2 Standard Observing Procedure

Unless there was a hardware malfunction, we would observe several dome flats at the beginning of each night (and occasionally at the end). We would also observe emission-line calibration lamps ("arcs") at both the beginning of the night and often at the position of each object. Our final calibrations relied on observing standard stars throughout the night at a variety of airmasses. The goal was to obtain at least one standard star (in the case of single-beam spectrographs; both blue and red standard stars for double-beam spectrographs) at an airmass near 1.0 and at least one at an airmass comparable to or higher than the highest airmass of any SN observed during that night. The standard stars were typically from the catalogs of Oke & Gunn (1983) and Oke (1990), with the cool, metal-poor subdwarfs and hot subdwarfs calibrating the red and blue sides, respectively.

Most observations were made at the parallactic angle to reduce differential light loss (Filippenko 1982). Exceptions were usually at an airmass of < 1.2 or when the slit was positioned at a specific angle to include a second object (the host nucleus, a trace star, a second SN, etc.). In August 2007, LRIS was retrofitted with an atmospheric dispersion corrector (ADC; Phillips et al. 2006). With the ADC, differential light loss is significantly reduced regardless of position angle, even at high airmass.

2.3 Data Reduction

All data were reduced in a similar, consistent manner by only a handful of people. The percentages of spectra presented in this chapter reduced by various coauthors is displayed in Figure 2.2. There are slight differences for each instrument, but the general method is the same. Previous descriptions of our methods can be found in Matheson et al. (2000), Li et al. (2001c), Foley et al. (2003), Foley et al. (2007), and Matheson et al. (2008), but the discussion below supersedes previous descriptions.

2.3.1 Calibration

Despite differences between instruments, the general procedure for transforming raw, two-dimensional spectrograms into fully reduced, wavelength and flux calibrated, one-dimensional

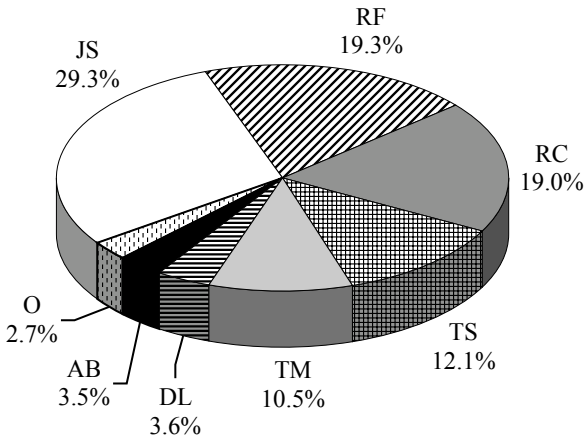

Figure 2.2: The percentages of spectra presented in this chapter reduced by various coauthors. JS, Jeffrey M. Silverman; RF, Ryan J. Foley; RC, Ryan Chornock; TS, Thea N. Steele; TM, Thomas Matheson; DL, Douglas C. Leonard; AB, Aaron J. Barth; O, Other.

spectra is similar for all of our data. We will discuss differences in the procedure for the various instruments below. The general prescription is as follows.

1. Correct for bias using an overscan region and trim the two-dimensional images to contain only the region with sky data. Our data do not typically show a bias pattern and do not have large dark currents. Therefore, we do not subtract bias frames, which would increase noise.

2. Combine and normalize flat-fields. We pay particular attention to masking emission lines from the flat-field lamps and absorption features from the air between the flat-field screen/dome and the detector. The normalizing function is generally a low-order spline.

3. Correct pixel-to-pixel variations in our spectra using our flats.

4. Extract the one-dimensional spectra. We use local background subtraction, attempting to remove as much host-galaxy contamination as possible. The spectra are typically optimally extracted using the prescription of Horne (1986).

   However, prior to mid-1997, we did not use the optimal extraction for our Kast data but, rather, employed "standard" extractions (i.e., non-optimally weighted). While

this typically had minimal impact on the signal-to-noise ratio (S/N) achieved – most SNe observed with Kast are quite bright, thus standard and optimal extractions yield similar noise levels in the final spectrum – one possible effect this has on our spectra from this era is that they may be spectrophotometrically inaccurate at the ∼5% level. This is due to time-variable "focus variations" that existed across the CCDs in the Kast spectrograph during this time. By using the optimal extraction since then we have significantly mitigated the effects of these variations in our data.

5. Calibrate the wavelength scale. Using arc-lamp spectra, we fit the wavelength scale with a low-order polynomial and linearize the wavelength solution. We then make small shifts in the wavelength scale to match the night-sky lines of each individual spectrum to a master sky template.

6. Flux calibrate the spectra. We fit splines to the continua of our standard-star spectra, producing a sensitivity function that maps CCD counts to flux at each wavelength. These sensitivity functions are then applied to each individual SN spectrum.

7. Correct for telluric absorption. Using our standard-star spectra, we interpolate over atmospheric absorption regions, providing an estimate of the atmospheric absorption at a particular time and airmass. Then, accounting for the differences in airmass, we apply these corrections to our spectra, allowing for slight wavelength shifts between the A and B telluric absorption bands.

8. Remove cosmic rays (CRs) and make other minor cosmetic changes. In the remaining one-dimensional spectra there may be unphysical features due to CRs, chip gaps, or bad, uncorrected pixels. We interpolate over these features.

9. Combine overlapping spectra. For instruments with both a red and blue side (or multiple orders in the case of ESI) we combine the spectra, scaling one side to match the other in the wavelength region where the spectra overlap. For multiple, successive observations of the same object we combine the spectra to achieve the highest S/N in the resulting spectrum, weighting each spectrum appropriately (usually by exposure time).

Through mid-1997, we used our own VISTA and Fortran routines to complete all of the steps above. For about a year after that we used a combination of generic purpose IRAF[1] routines and our own Fortran routines for our spectral reductions. Since about mid-1998, we have performed our reductions using both generic-purpose IRAF routines and our own IDL scripts. Step 1 is achieved with either IRAF or IDL depending on the instrument. Steps 2–5 are generally performed with IRAF, while steps 6–9 are performed in IDL.

[1]IRAF: The Image Reduction and Analysis Facility is distributed by the National Optical Astronomy Observatory, which is operated by the Association of Universities for Research in Astronomy (AURA), Inc., under cooperative agreement with the National Science Foundation (NSF).

We consider the resulting spectra "fully reduced." However, for a subsample of our spectra where we have multi-filtered host-galaxy photometry at the position of the SN and SN photometry near the time the spectrum was obtained, we can make additional corrections to obtain an accurate absolute flux scale as well as account for host-galaxy contamination (see Sections 2.3.2 and 2.3.3).

Kast on the Lick 3 m

Kast has large amplitude variable fringing on the red side. We observe red-side dome flats at the position of each object and we apply these flats to each object individually. As the dome moves into place to take flats, we also obtain a red-side arc exposure. Using this arc spectrum we shift the wavelength solution derived from our afternoon arc exposures (which typically have more lines and are observed with a $0.5''$ slit, yielding higher-resolution lines) and apply those wavelength solutions to the appropriate SN observations. However, we still apply a small wavelength shift based on the night-sky lines later in the reduction process.

Stover on the Nickel 1 m

The Stover spectrograph does not have the ability to rotate the slit with respect to the sky; thus, all spectra obtained with this instrument were observed with a fixed sky position angle of $0°$. When observations were at relatively large airmasses (as they were for some of the spectra presented here) this caused their continuum shape to be unreliable. The spectra in our dataset from the Stover spectrograph have been previously published (Wells et al. 1994; Li et al. 2001c), and while strange spectrophotometric calibration issues when using this instrument with our setup and reduction routines have been noted by Leonard et al. (2002), Li et al. (2001c) find no such problems.

LRIS on the Keck 10 m

The blue side of LRIS has two CCDs offset in the spatial direction (allowing a full spectrum to be on a single CCD). We typically position our objects on the slit so they will be centered on one CCD, ignoring the other CCD completely. However, in some observations circumstances dictated that objects be on the other CCD. Each CCD must be calibrated separately (different flat-field response functions, sensitivity functions, etc.). The LRIS flat-field lamp is not particularly hot, providing few photons at the bluest wavelengths of LRIS. We therefore mask this region in the flat-field response, leaving the bluest portions uncorrected for pixel-to-pixel variations.

When our dataset was obtained, the red side of the spectrograph had large fringes. We account for these fringes by applying dome flats obtained during the afternoon or morning. We occasionally obtained internal flats at the position of an object, but we have found these to typically be worse for removing pixel-to-pixel variations than the nightly dome flats. However, there are rare instances where they were used instead of dome flats.

DEIMOS on the Keck 10 m

The long slit for DEIMOS is slightly tilted, producing slightly different wavelengths for a pixel in a given column. This tilts the sky lines, providing additional sampling of the lines. Since our typical procedure is not adaptable to tilted sky lines (our background subtraction would produce dipoles for every sky line), we implement a modified version of the DEEP2 DEIMOS pipeline[2] to rectify and background-subtract our spectra. The pipeline bias-corrects, flattens, traces the slit, and fits a two-dimensional wavelength solution to the slit by modeling the sky lines. This final step provides a wavelength for each pixel. The slit is then sky subtracted (in both dimensions) and rectified, producing a rectangular two-dimensional spectrum where each pixel in a given column has the same wavelength. From this point we proceed with our normal procedure, starting with extracting the spectrum (step 4). Since the spectrum has already been sky subtracted, we do not attempt any additional sky subtraction (which would only increase the noise) unless the SN is severely contaminated by its host galaxy.

ESI on the Keck 10 m

The CCD of ESI has several large defects, which we mask before starting our reductions. These produce $\sim$50 Å gaps in our spectra, usually near 4500–4600 Å. They can also affect our measurement of the trace, but for the low-redshift, relatively bright SNe presented in this chapter, this was rarely a problem. ESI observes 9 orders; we reduce each order individually and stitch the orders together at the end (step 9), using our standard-star observations to determine the scaling and overlap regions. We weight the spectra in the overlap by their variance in each pixel before combining. For ESI we do not linearize the wavelength solution, but instead rebin to a common velocity interval, thus producing pixels of different sizes in wavelength space.

Other Instruments

In addition to the aforementioned instruments, our dataset contains a few spectra which were obtained by observers exterior to the BSNIP group at observatories aside from Lick and Keck. These data come from the Low Dispersion Survey Spectrograph 3 (LDSS-3; Mulchaey & Gladders 2005) mounted on the 6.5 m Clay Magellan II telescope, the R.C. spectrograph mounted on the Kitt Peak 4 m telescope, and the Double Spectrograph mounted on the Hale 5 m telescope at Palomar Observatory (Oke & Gunn 1982).

Additional Reduction Strategies

Occasionally our standard procedures produce non-optimal spectra. In these cases we augment our procedures to produce higher-quality spectra.

[2] `http://astro.berkeley.edu/~cooper/deep/spec2d/`.

For some spectra we perform a CR cleaning of the two-dimensional spectra before extraction (step 4). This procedure is done in IRAF and detects pixels that have significantly more counts than their surrounding pixels, replacing them with the local median. Since this procedure has the potential to remove real spectral features, it is not automatically performed on every spectrum.

We can obtain better sky subtraction on some spectra by performing a two-dimensional sky subtraction. This procedure fits each pixel in the spatial direction with a polynomial or spline function (usually constrained to the region near the SN position) and subtracts that fit from each pixel in that column. We have found, however, that local sky subtraction generally produces better results.

On rare occasions, we have multiple dithered images of a single object. With these images we can (after proper scaling) subtract one from another to remove residual fringing and sky lines. We can also shift the spectra spatially and combine the two-dimensional spectra to increase the S/N of the object. This can produce better traces.

For objects without a defined trace across the entire chip, we would create a trace function for the object either using the trace of a nearby object such as the host-galaxy nucleus or of a bright star (often an offset star) taken in the previous exposure at the same position of the SN.

2.3.2 Spectrophotometry

Using our standard reduction procedure outlined in Section 2.3.1, the spectrophotometry of our data is usually quite accurate. However, there are many ways in which the spectrophotometry of a spectrum may be corrupted. First, there are achromatic effects such as clouds that affect the absolute spectrophotometry. Absolute spectrophotometry is not necessary for many spectroscopic studies (although we will discuss absolute spectrophotometry in more detail below; see Section 2.3.2). Accurate *relative* spectrophotometry, however, is important for such studies. There are many reasons why the relative photometry of a spectrum may be incorrect, but variable atmospheric absorption, non-parallactic slit angles leading to differential light losses (Filippenko 1982), and incorrect standard-star spectrophotometry can all contribute significant errors. As shown below, after rigorous testing we find that the relative spectrophotometry of the BSNIP data is accurate to $\sim$0.05–0.1 mag across most of the wavelengths covered by the spectra.

Occasionally, events external to the normal operations of the telescope and data reduction can result in questionable spectrophotometry. Instrument failures (e.g., a broken shutter) or environmental effects (e.g., nearby wild fires) are the most troublesome. There is no clear way to fully correct the spectrophotometry in these cases. Using our detailed records as well as those of Lick Observatory, we have identified several spectra where the spectrophotometry may be affected by these external factors and exclude them from any estimates of the fidelity of our spectrophotometry. Including spectra obtained with the Stover spectrograph, which does not have a rotator and so nearly all spectra were not observed at the parallactic

angle, we have flagged 88 spectra as having possibly troublesome spectrophotometry.

Relative Spectrophotometry

Two of the key attributes of the BSNIP sample are the large wavelength range and the consistent and thorough reduction procedures. The spectra in the sample likely have similar systematic (and hopefully small) uncertainties. The large wavelength range makes the spectra ideal for comparing near-UV and near-IR features in a single spectrum, but such investigations will be limited by the accuracy of our spectrophotometry. Since most of the spectra in our sample have corresponding *BVRI* light curves (Ganeshalingam et al. 2010), we can test the spectrophotometry of a spectrum by comparing synthetic colors from the spectrum to those of the light curves at the time that the spectrum was obtained. In fact, this has previously been performed on some of the data presented here (at a somewhat less rigorous level) by Poznanski et al. (2002).

For this test, we examine only the spectra of objects that have corresponding filtered light curves. To assure that our estimates of the SN colors from the photometry are accurate, we further limit the sample to spectra that have a light-curve point within 5 d of when the spectrum was taken.

We use the light-curve fitter Multi-color Light Curve Shape (MLCS2k2, Jha et al. 2007) to model the filtered light curves, allowing us to interpolate between data points. We fit each filter individually to provide the largest degree of flexibility in each and the fits are all inspected to ensure that a good fit is obtained. In cases where the MLCS2k2 fit does not adequately reflect the data and the data are well sampled, we use a cubic spline with a Savitzky-Golay smoothing filter (Savitzky & Golay 1964).

We estimate the errors in the model light curve by running a series of Monte Carlo simulations. Light-curve realizations are generated from the original data by randomly perturbing each data point by the reported 1σ Gaussian errors and refitting the generated light curve. This process is repeated 50 times and the scatter in the derived light curves is taken as the error in the model. This process is applied to objects with MLCS2k2 and spline fits.

To determine the synthetic photometry from the spectra, we convolve each spectrum with the Bessell filter functions (Bessell 1990). We calibrate our photometry by measuring the spectrophotometry of the standard star BD+17 4708 (Oke & Gunn 1983) and applying zero-point offsets to match the standard photometry. We then apply these offsets to the synthetic photometry derived from the SN spectra. The Bessell filter functions have approximate wavelength ranges of 3700–5500, 4800–6900, 5600–8500, and 7100–9100 Å for B, V, R, and I, respectively. Most of our spectra fully cover the *BVRI* bands.

There are several effects which may reduce the accuracy of our spectrophotometry. By far, the most important is galaxy contamination. Although our reduction process removes as much galaxy light as possible from a SN spectrum (see Section 2.3.1), some of our SN spectra are still contaminated by galaxy light. The measured synthetic colors from galaxy-

contaminated spectra will likely be vastly different from the SN colors even if our spectrophotometry is excellent. For spectra with multi-color template images of the host galaxy and multi-color light curves concurrent with the spectrum, we can correct for galaxy contamination to a large degree (see Section 2.3.3). However, this correction relies on excellent relative spectrophotometry.

We have selected a subsample of SNe that are relatively isolated from their host galaxy and therefore their spectra should have minimal galaxy contamination. These objects all have template images (taken after the SN has faded) that indicate minimal galaxy light. A sample of spectra of objects from this low-contamination sample of SNe is constructed to test the fidelity of our relative spectrophotometry. For this sample, we require that the spectra have $t < 30$ d and that the spectrum was obtained at the parallactic angle or at an airmass ≤ 1.2. We present the synthetic and photometric colors for the low-contamination sample in Figure 2.3. Although the number of spectra is limited for this sample, they span a large range of color.

We present a comparison of synthetic colors derived from our low-contamination and possibly contaminated spectra to those measured from light curves at the same epoch in Figure 2.4. An estimate of the uncertainty in the spectrophotometry can be made by examining the χ^2 per degree of freedom (dof) of the residual of the synthetic to photometric colors. The uncertainty in the photometric colors is measured by examining the residuals of the photometry measurements near the epoch of the spectrum relative to the model. The uncertainty in the relative spectrophotometry is the uncertainty added to each point which causes the residuals of the synthetic to photometric colors to have $\chi^2/\mathrm{dof} = 1$. If $\chi^2/\mathrm{dof} \leq 1$ with only photometric uncertainties, then the spectrophotometry does not have uncertainties larger than the photometry itself. We present estimates of the uncertainties in Table 2.3.

Table 2.3: Relative Spectrophotometric Accuracy for the BSNIP Sample

	Additional Uncertainty to Achieve $\chi^2/\mathrm{dof} = 1$				of Spectra
Subsample	$B-V$ (mag)	$V-R$ (mag)	$R-I$ (mag)	$B-I$ (mag)	(for $V-R$)
Low contamination	0.057	0.000	0.008	0.067	23
All spectra	0.095	0.055	0.096	0.170	306
Not parallactic	0.089	0.048	0.107	0.158	48
Parallactic	0.097	0.056	0.094	0.171	258
Gal. sub. – no corr.	0.088	0.053	0.073	0.140	67
Gal. sub. – corr.	0.057	0.042	0.055	0.100	81
No gal. sub.; $t > 20$ d	0.151	0.075	0.108	0.224	47
No gal. sub.; $t \leq 20$ d	0.093	0.060	0.133	0.223	63
Airmass ≤ 1.1	0.081	0.050	0.061	0.154	24
$1.1 <$ Airmass ≤ 1.3	0.078	0.017	0.067	0.118	37
$1.3 <$ Airmass ≤ 1.5	0.076	0.048	0.056	0.080	37
Airmass > 1.5	0.064	0.060	0.067	0.126	50
S/N < 20	0.104	0.093	0.088	0.195	18
$20 \leq$ S/N < 30	0.077	0.026	0.074	0.152	16
$30 \leq$ S/N < 40	0.065	0.055	0.061	0.099	27

Continued on Next Page...

Table 2.3 — Continued

Subsample	Additional Uncertainty to Achieve $\chi^2/\mathrm{dof} = 1$				# of Spectra
	$B-V$ (mag)	$V-R$ (mag)	$R-I$ (mag)	$B-I$ (mag)	(for $V-R$)
$40 \leq$ S/N < 50	0.073	0.020	0.077	0.088	31
S/N ≥ 50	0.065	0.036	0.036	0.102	56
Reduced by T. Matheson	0.108	0.065	0.115	0.211	6
Reduced by R. Chornock	0.065	0.050	0.062	0.101	34
Reduced by R. Foley	0.058	0.041	0.040	0.107	43
Reduced by J. Silverman	0.085	0.054	0.081	0.144	51
Reduced by T. Steele	0.071	0.022	0.034	0.043	11

For the low-contamination sample, the spectrophotometry has a typical additional uncertainty of ≤ 0.07 mag across the entire spectrum, with no additional uncertainty required for $V-R$ and very little additional uncertainty (0.008 mag) required for $R-I$ across a large range of colors. Our entire sample is only slightly worse, with the additional uncertainty in $V-R$ being 0.055 mag. The accuracy of the flux calibration for the low-contamination sample is difficult to access since the uncertainties from the photometry are enough to account for the majority of the scatter (and the entire scatter for the wavelength region spanning from V to R). Nonetheless, we can place limits on the accuracy based on the additional uncertainty required and the standard deviation. From this, we find that the low-contamination sample is accurate to 5.2–6.9%, 0.0–5.8%, 0.7–4.5%, and 6.0–9.0% for the wavelength regions spanning B to V, V to R, R to I, and B to I, respectively. For the sample of objects corrected for galaxy contamination, the additional errors are similar to that of the low-contamination sample (5.3–6.5%, 3.9–4.8%, 4.9–5.1%, and 4.5–9.2% for the wavelength regions listed above), but lower than those for the entire sample (8.8%, 5.1–6.2%, 7.3–8.9%, and 12.7–15.6%), indicating that the galaxy-contamination correction works well at least for broad-band colors.

We have also split our sample by various attributes of the spectra. The spectrophotometry does not depend significantly on airmass. It does depend significantly on S/N, but the spectrophotometry does not improve as S/N increases beyond S/N ≈ 20 pixel^{-1}. The additional errors also depend slightly on the individual who reduced the spectra. However, this trend may be the result of observing and reduction techniques slowly improving over time.

We have also calculated the mean and standard deviations of the difference between the synthetic colors derived from our spectra and those measured from light curves for the various subsamples. All subsamples have a mean < 0.6 standard deviations from zero, with nearly all being < 0.3 standard deviations from zero. The means for the subsamples are also typically < 0.02 mag from zero, with no clear bias in any particular subsample.

In summary, our relative spectrophotometry is excellent. In particular, objects with little galaxy contamination or those where we are able to correct for galaxy contamination

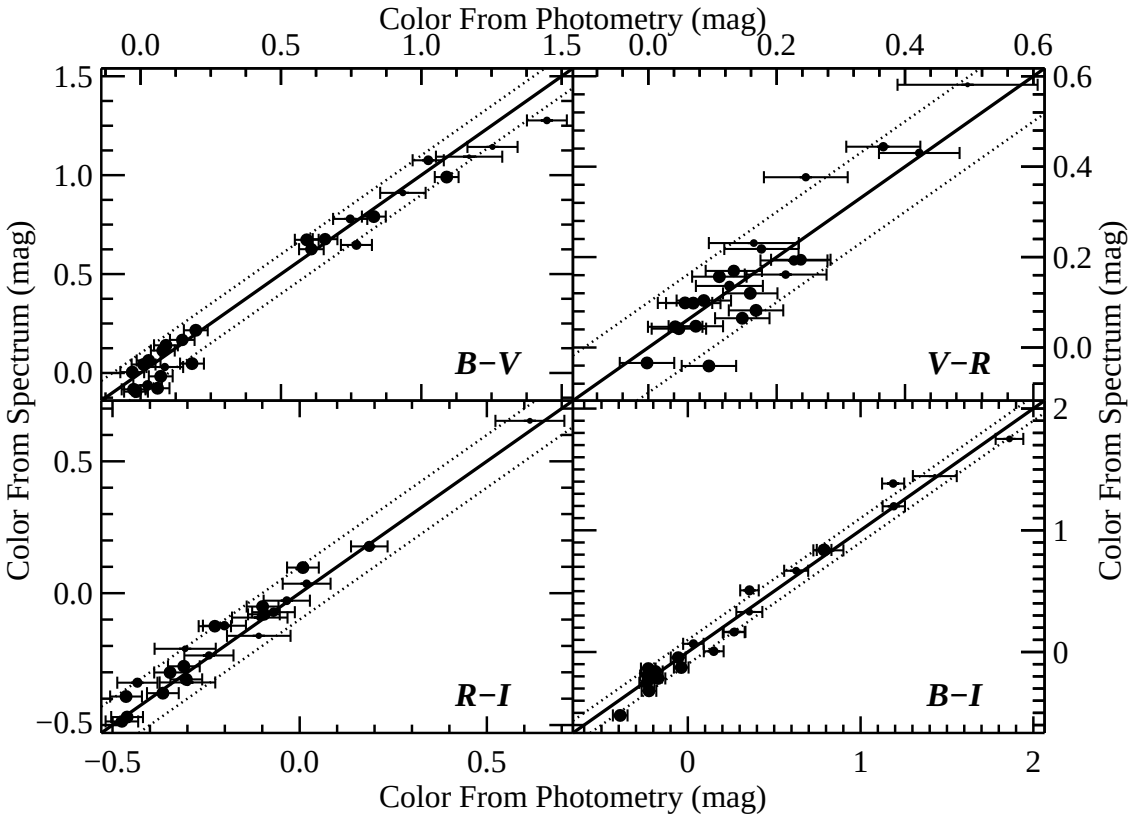

Figure 2.3: Comparison of synthetic colors derived from our spectra to those measured from light curves at the same epoch. Only spectra of objects where there is no obvious galaxy contamination at the position of the SN (from late-time imaging) are included. Clockwise from the upper-left panel, we present the $B-V$, $V-R$, $B-I$, and $R-I$ colors. The size of each circle represents the size of the photometric uncertainty, with larger circles representing smaller uncertainty. The solid line and the dotted lines in each panel are the one-to-one correspondence and the one-to-one correspondence ± 0.1 mag, respectively.

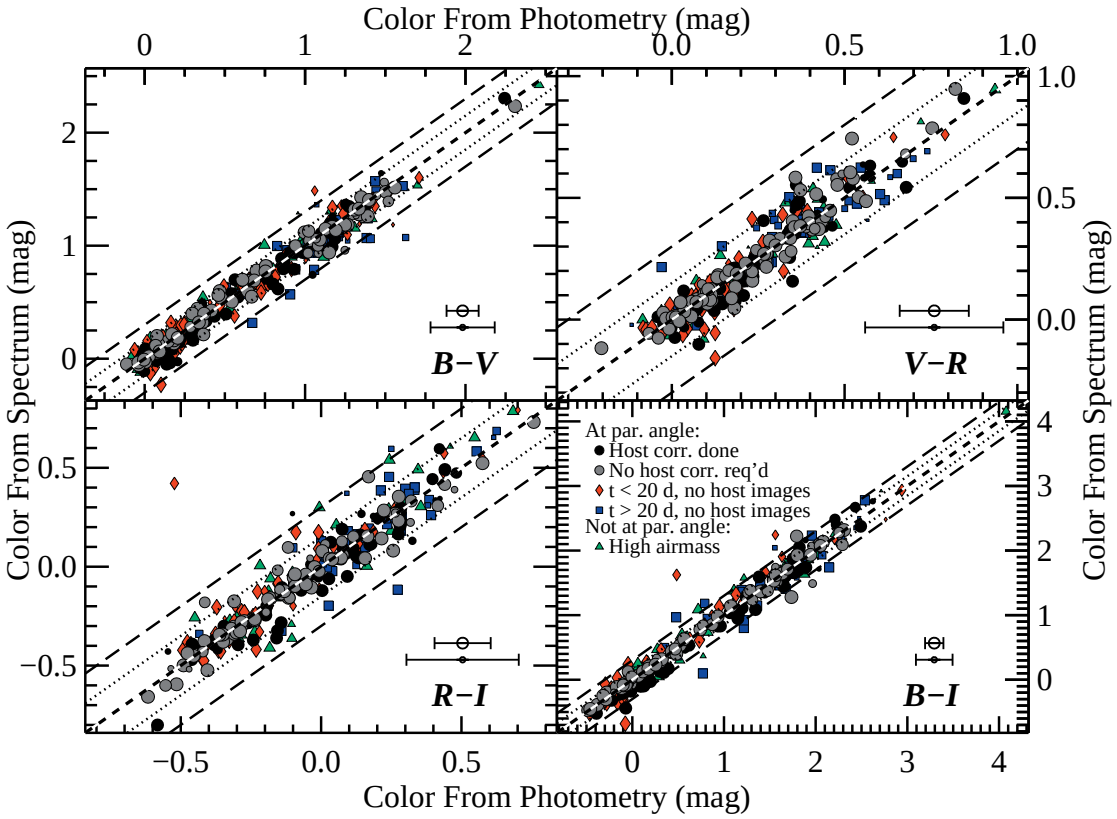

Figure 2.4: Comparison of synthetic colors derived from our spectra to those measured from light curves at the same epoch. Clockwise from the upper-left panel, we present the $B-V$, $V-R$, $B-I$, and $R-I$ colors. The green triangles, blue squares, red diamonds, gray circles, and black circles represent (respectively) spectra not observed at the parallactic angle and at high airmass; spectra with $t > 20$ d observed at the parallactic angle, but lacking host-galaxy images to perform host-galaxy subtraction; spectra with $t < 20$ d observed at the parallactic angle, but lacking host-galaxy images to perform host-galaxy subtraction; spectra observed at the parallactic angle, with host-galaxy images, but no host-galaxy subtraction is required; and spectra observed at the parallactic angle that have been corrected for host-galaxy contamination. The size of each symbol represents the size of the photometric uncertainty, with larger symbols representing smaller uncertainty. Representative sizes (0.1 and 0.2 mag) are shown with error bars in the upper-left corner of each panel. The short-dashed line, the dotted lines, and the long-dashed lines in each panel are the one-to-one correspondence, the one-to-one correspondence ± 0.15 mag, and the one-to-one correspondence ± 0.3 mag, respectively.

have extremely good relative spectrophotometry. This is achieved simply through our reduction methods and the relatively simple host-galaxy contamination correction outlined below; there is no spectral warping of any kind to achieve these results.

Absolute Spectrophotometry

As mentioned above, there are many achromatic effects which can affect our absolute spectrophotometry. We can correct for these effects if we have concurrent photometry. For these cases, we determined the synthetic photometry of our spectra and applied a multiplicative factor to scale the synthetic photometry to match our true photometry. This scaling is a byproduct of correcting for host-galaxy contamination, as described in Section 2.3.3.

2.3.3 Host-Galaxy Contamination

SNe generally do not exist in isolation. The vast majority occur within galaxies, sometimes close to or on top of complex regions such as spiral arms or H II regions. With photometry, one can correct for this by obtaining a template image after the SN has faded (or in some cases, before the star explodes), and subtracting the template from the image with the SN, leaving only the SN. Although this approach is feasible with spectroscopy (obtaining a spectrum at the position of the SN after it has faded), it is not tractable. Spectroscopy time is typically more valued, and reproducing the conditions at the time of the original SN observation is difficult. We do, however, have methods for reducing the galaxy contamination in a SN spectrum.

The first method is local background subtraction, and it is described in Section 2.3.1. Briefly, while extracting the SN spectrum, we model the underlying background by interpolating between background regions on either side of the SN. If the background is relatively smooth and monotonic between the background regions, this method works very well. However, if the SN is near the nucleus of a galaxy or on a spiral arm or other bright feature, this method can underestimate the background, leaving galaxy contamination in the SN spectrum.

We have derived a method for removing the residual galaxy contamination from our SN spectra. This approach, which we call "color matching," requires both SN photometry at the time the spectrum was obtained, and template colors for the host galaxy at the position of the SN. We use the host-galaxy colors to determine the SED of the host galaxy at the position of the SN. We then subtract the host-galaxy SED from the SN spectrum, scaled so that the synthetic photometry from the galaxy-corrected SN spectrum matches the SN photometry. This method was first presented by Foley et al. (2010a); we discuss it in detail below.

Determining the Host-Galaxy SED

The parameter space of galaxy SEDs is well known and well behaved, allowing one to reliably reconstruct galaxy SEDs with broad-band photometry (e.g., Blanton et al. 2003). Adopting the approach described by Blanton et al. (2003), but updated to include UV wavelengths by Blanton & Roweis (2007), and implemented in the IDL software package `kcorrect.v4_1_4`, we have used our *BVRI* photometry of the host galaxy at the position of the SN and the redshifts presented in Table 2.1 to reconstruct the galaxy SED at the position of the SN. We perform aperture photometry on galaxy templates obtained as part of the Lick Observatory SN Search (LOSS) follow-up photometry effort (Ganeshalingam et al. 2010) using a 3 pixel (2.4″, similar to our Kast slit size and the typical seeing at Lick Observatory) aperture and taking the median pixel value of the image to represent the sky background. Using a 3 pixel aperture for all of our galaxy templates will represent different physical sizes depending on the distance to the galaxy. An aperture significantly different from that of the slit combined with the seeing could incorporate flux from stellar populations that do not represent the SED of the galaxy at the position of SN. As a check on how aperture size affects measured galaxy color, we also used a 4 pixel aperture fixed at the SN position. We find excellent agreement between the colo)rs derived using a 3 pixel aperture with a mean difference ≤ 0.02 mag. For the typical galaxy with $z < 0.5$ (which includes all redshifts presented here), the SEDs are recovered to $\lesssim 0.02$ mag in all filters (Blanton et al. 2003; Blanton & Roweis 2007).

Color Matching

Motivation One approach to subtract galaxy contamination from a SN is to extract the SN without any local background subtraction, creating a spectrum that consists of all light at the position of the SN (including galaxy light) at the time of the spectrum. If one also has photometry at that epoch, one can, in principle, scale a galaxy SED to match the galaxy photometry, scale the spectrum to match the addition of the SN and galaxy photometry, and subtract the latter from the former to obtain a SN spectrum. The main drawbacks of this method are that (1) one must know the proper point-spread function (PSF) of the SN and galaxy when the spectrum was obtained, and (2) if there is a significant amount of galaxy contamination and the galaxy SED is incorrect, you will introduce significant errors.

When extracting our spectra, we attempt to remove as much galaxy contamination as possible during the extraction. This approach has the benefit of reducing the galaxy contamination in the SN spectrum without introducing potential errors associated with an imprecise photometrically reconstructed galaxy SED. Also, considering the lack of precise observing information for many of our spectra (which date back over two decades), it would be difficult to estimate the correct PSF to determine the exact galaxy flux (both SED and amount) entering our slit for a given observation.

Since the galaxy colors from photometry (which are easier to measure than the absolute flux entering our slit) determine the galaxy SED, if our spectrophotometry is well-calibrated,

then simply subtracting the galaxy SED until the colors of the spectrum match those of the SN photometry will result in a SN-only spectrum.

We can demonstrate this mathematically. In general, an observed SN spectrum is defined by

$$f_{\rm spec} = A\left(f_{\rm SN} + Bf_{\rm gal}\right), \tag{2.1}$$

where $f_{\rm spec}$, $f_{\rm SN}$, and $f_{\rm gal}$ are the vectors of fluxes in the observed spectrum, SN-only spectrum, and galaxy spectrum, respectively, and A and B are normalization factors. One can think of A as normalizing the spectrum in an absolute sense to account for slit losses, clouds, and other achromatic effects. The parameter B controls the amount of galaxy contamination, where $B = 0$ if there is no galaxy contamination and we impose $B \geq 0$. In principle, B could be negative in order to correct for oversubtraction of galaxy light, but our testing indicates that allowing B to have negative values produces too much overfitting of the spectra.

From our image templates, we have $p_{\rm gal}$, the broad-band photometry (in flux units) for the host galaxy at the position of the SN. Using MLCS2k2 (Jha et al. 2007) template light curves or spline interpolations (see Section 2.3.2), we are able to interpolate our SN photometry (independently in each band) to determine $p_{\rm SN}$, the broad-band photometry (in flux units) for the SN at the time of the spectrum.

We can define the function which translates spectra to synthetic broad-band photometry as P, where $P(f_{\rm SN})$ and $P(f_{\rm gal}) = p_{\rm gal}$. This function is equivalent to convolving a spectrum with a filter function. Note that we impose the first relationship, while the second relationship is required by our method of determining $f_{\rm gal}$.

From our spectrum, we are able to determine $p_{\rm spec} = P(f_{\rm spec})$, the broad-band synthetic photometry (in flux units) of the spectrum, which includes both SN and galaxy light. These vectors then obey the equation

$$P(f_{\rm spec}) = A\left(p_{\rm SN} + Bp_{\rm gal}\right). \tag{2.2}$$

For Equation 2.2 to be valid, we make two assumptions. The first assumption, which is already noted above, is that our spectra have accurate relative spectrophotometry. The second assumption is that B, the relative fraction of the galaxy and SN light, does not vary strongly with wavelength. From Section 2.3.2, we have shown that the relative spectrophotometry of our spectra is accurate to $\sim$0.05–0.1 mag across large wavelength regions, comparable to the uncertainties of our photometry (after interpolating to a given date).

Solving for $f_{\rm SN}$ in Equation 2.1, we have

$$f_{\rm SN} = A^{-1}f_{\rm spec} - Bf_{\rm gal}. \tag{2.3}$$

With a spectrum spanning at least two bands also covered by SN and galaxy photometry, one can solve for A and B from Equation 2.2. With galaxy photometry, the galaxy SED, $f_{\rm gal}$, can be properly reconstructed. It is then simple to determine the uncontaminated SN spectrum, $f_{\rm SN}$, from the galaxy-contaminated, observed spectrum, $f_{\rm spec}$. We note that if $B = 0$, then Equation 2.3 simplifies to merely scaling the spectrum to match the photometry in an absolute sense.

Testing To test this method, we have performed Monte Carlo simulations of various spectra with increasing galaxy contamination and appropriate photometric errors. To do this, we generated three linear (in f_λ) spectra having negative, zero, and positive slopes (corresponding to blue, flat, and red spectra) as well as using spectra of SN 2005cf at maximum brightness, $\sim$1 month after maximum brightness, and $\sim$1 yr after maximum brightness. To these spectra, we added 5 galaxy templates: the galaxy templates used by Sloan Digital Sky Survey (SDSS) to perform redshift cross-correlations, spanning early to late galaxy types. We measured the synthetic photometry of the spectra and galaxy templates, and for each iteration we varied the photometric data randomly using a normal distribution with width corresponding to the median error in each band for SNe and galaxies, respectively. We then performed the color-matching technique for the galaxy-contaminated spectra with the Monte Carlo based photometry.

Our recovered SN spectra were compared to our input spectra, and the *difference* between the standard deviation of the residuals of the contaminated spectra and the recovered spectra are presented in Figure 2.5. We see that the residuals for the recovered spectra are significantly lower (i.e., the recovered spectra are better at reproducing the input spectra) than the contaminated spectra for galaxy contaminations $< 70\%$. The improvement does depend somewhat on the color of the SN spectrum and the color of the galaxy template, but the differences are relatively small. At higher levels of galaxy contamination, the gains are minimal in this metric, but examining the spectra, it is obvious that this technique yields impressive results even with very large amounts of galaxy contamination.

In Figure 2.6, we present our maximum-light and nebular-phase spectra of SN 2005cf with varying amounts of galaxy contamination. At 70% galaxy contamination, where the residuals are not very large, we see that the overall shape of the spectra and spectral lines are well recovered. Even at 90% galaxy contamination, where the contaminated spectra appear to be simply galaxy spectra, the method is able to recover the overall shape of the SN spectrum.

The recovered spectra differ most at the ends of the spectral coverage. This is due to the galaxy SED reconstruction being unconstrained beyond these wavelengths. If we extended our galaxy photometry beyond *BVRI*, this would improve. The emission lines of the reconstructed galaxy spectra generally have the incorrect strength. This is difficult to model with broad-band photometry, and these regions of the spectra should be ignored. The majority of the differences between the input and recovered spectra are the result of incorrect galaxy SED reconstruction from errors in the galaxy photometry. Improving the galaxy photometry or increasing the number of bands of galaxy photometry would improve the reconstruction of the galaxy SED. As the galaxy contamination increases, the errors in the reconstructed galaxy SED are amplified.

Implementation We have applied this technique to all SN spectra that have (1) *BVRI* photometry within 5 d of when the spectrum was taken, and (2) a wavelength range which spans at least two observed bands. Spectra which cover only a single observed band are

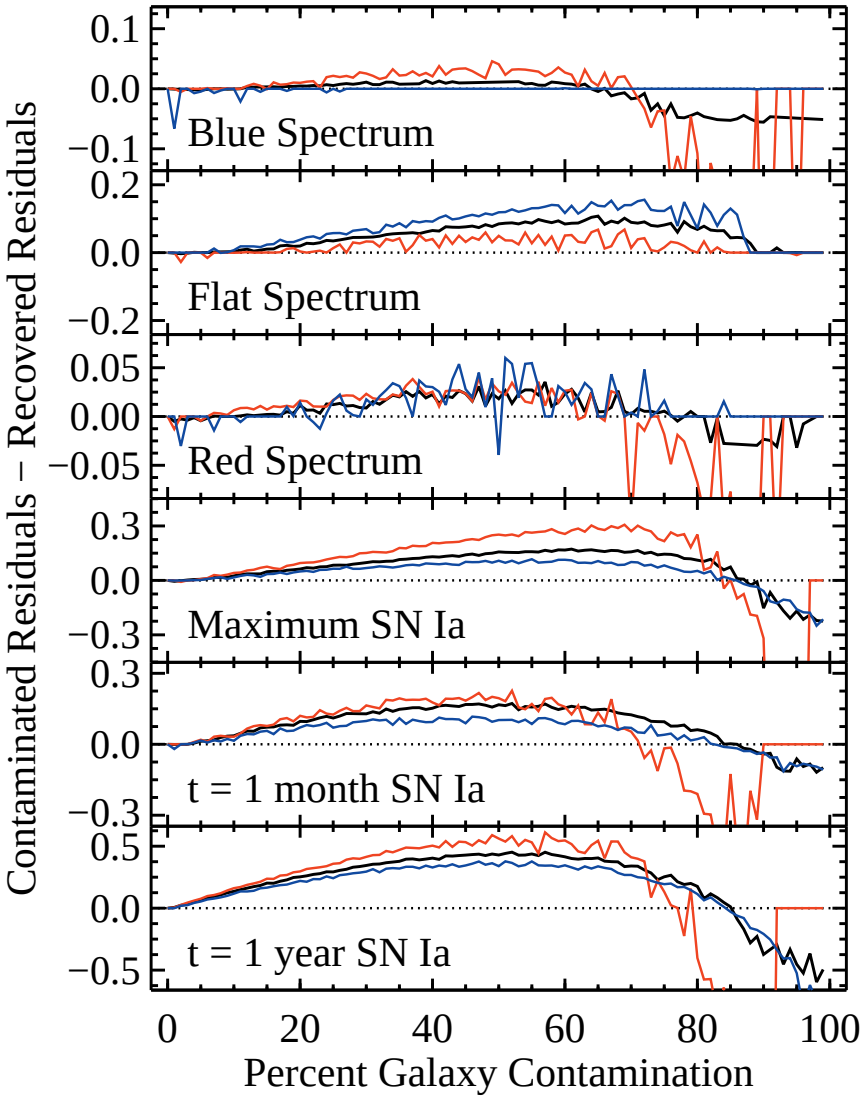

Figure 2.5: Differences between the median of the standard deviation of the residuals of contaminated spectra and recovered spectra after color-matching for different input spectra and galaxy templates with varying amounts of galaxy contamination. The top through bottom panels correspond to input spectra of a blue linear spectrum, a flat linear spectrum, a red linear spectrum, SN 2005cf at maximum brightness, SN 2005cf ∼1 month after maximum brightness, and SN 2005cf ∼1 yr after maximum brightness, respectively. Positive values imply that our color-matching technique yields spectra that are closer to the input spectra than the contaminated spectra are. The horizontal dotted line in each panel represents where the residuals of the recovered spectra are equal to those of the contaminated spectra. The blue and red lines correspond to the latest and earliest galaxy templates, respectively. The black lines correspond to the average over 5 galaxy templates.

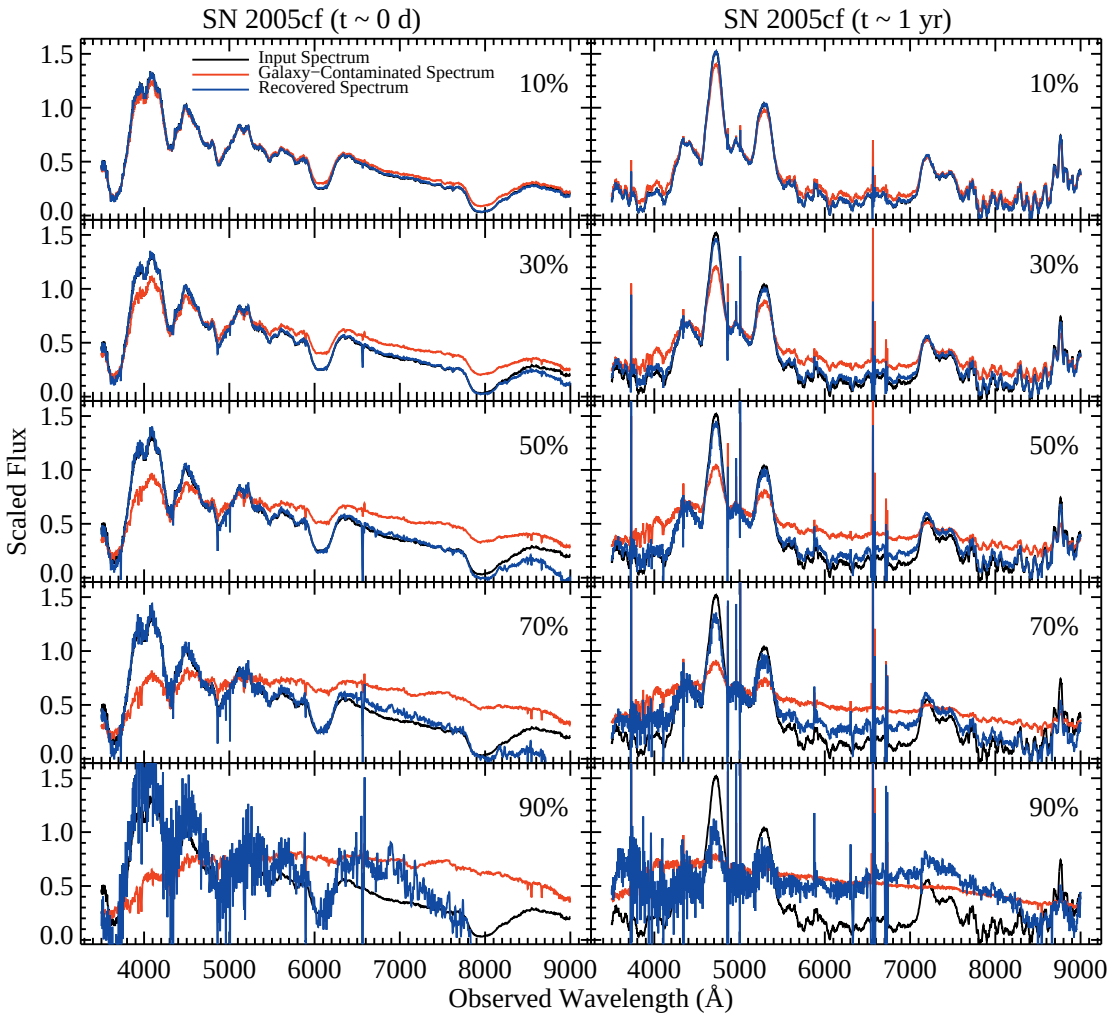

Figure 2.6: SN spectra used for testing the color-matching method. The left and right columns correspond to SN 2005cf at maximum brightness and ∼1 yr after maximum brightness, respectively. Each row represents different amounts of galaxy contamination, from 10% (*top*) to 90% (*bottom*); each panel has the percent contamination labelled. Each panel shows the input spectra (black), average galaxy-contaminated spectra (from several Monte Carlo realizations, red), and average recovered spectra (from several Monte Carlo realizations, blue). The maximum-light and nebular-phase spectra have been contaminated with early and late-type galaxy templates, respectively. The spectra are scaled to have the same median value. Comparing the black (input) spectra to the blue (recovered) spectra gives an indication of how well the color-matching method works. In the top panels, it is difficult to see the input spectra because of how closely the recovered spectra match the input spectra. However, even at low levels of contamination, residuals from narrow emission lines in the galaxy spectra are seen in the recovered SN spectra.

scaled to match the photometry at the time of the spectrum.

The procedure used to subtract galaxy light from an observed spectrum is as follows. Using `kcorrect`, the galaxy SED is reconstructed from the broad-band galaxy photometry at the position of the SN. Synthetic photometry is measured from the observed spectrum. The SN photometry at the time of the spectrum is measured from the light curves as described in Section 2.3.2. Using Equation 2.2 above, the factors A and B are determined using a χ^2 minimization technique. Using Equation 2.3, the reconstructed galaxy SED is subtracted from the observed spectrum to produce the corrected SN spectrum.

2.4 Data Management and Storage

When preparing to present a dataset as large as ours, we required some sort of internal organized storage and retrieval method. In addition, the overall utility of our dataset will be greatly increased by having a user-friendly interface to access the data.

In addition to the final data products, all other information regarding both our photometric and spectroscopic samples is stored in our SN Database (SNDB). The SNDB holds information about individual SNe (such as host-galaxy information, type, discovery information, etc.), much of which comes from external, online resources.[3] The SNDB also contains information regarding individual spectra (such as observing conditions, instrument, resolution, etc.), and individual light curves (number of points, photometric accuracy, derived light-curve parameters from various fitting routines, etc.). A complete list of all fields stored in the SNDB can be found in Table 2.4.

The SNDB contains our entire previously published spectral dataset (both SNe Ia and core-collapse SNe) as well as all of the data presented here. It also contains photometry and light-curve information which has been previously published, in addition to photometric data which have been compiled and re-fit by Ganeshalingam et al. (in preparation).

Table 2.4: SN Database (SNDB) Fields

Object Information		
SN Name	SNID-determined Subtype[a]	Host-Galaxy Name
Right Ascension	Discovery Date	Host-Galaxy Type
Declination	Discoverer	Host-Galaxy Redshift (and error)
Type	Discovery Reference	SN Redshift (and error)
Type Reference	Galactic Reddening	Other Notes
Photometry and Light Curve Information		
of Total Photometry Points	$\Delta m_{15}(B)$ (and error)	JD of B-band Maximum (and error)
of B-band Photometry Points	Maximum B-band Magnitude (and error)	Plots of MLCS2k2 Fits[b]
of V-band Photometry Points	$(B-V)_{B_{\max}}$ (and error)	MLCS2k2 Distance Modulus (and error)[b]
of R-band Photometry Points	SALT/2 Distance Modulus (and error)[c]	MLCS2k2 A_V (and error)[b]
of I-band Photometry Points	SALT/2 Light-Curve Stretch (and error)[c]	MLCS2k2 R_V (and error)[b]
of Unfiltered Photometry Points	SALT/2 c (and error)[c]	MLCS2k2 Δ (and error)[b]
Photometry Data	SALT/2 m_B (and error)[c]	MLCS2k2 m_V (and error)[b]
Light Curve Reference(s)	SALT/2 χ^2/dof[c]	MLCS2k2 χ^2/dof[b]

Continued on Next Page...

[3]For example, IAU Central Bureau for Astronomical Telegrams (`http://www.cbat.eps.harvard.edu/index.html`, `http://www.cbat.eps.harvard.edu/lists/Supernovae.html`), NASA/IPAC Extragalactic Database (NED, `http://nedwww.ipac.caltech.edu/`), and Rochester Academy of Sciences Bright Supernova List (`http://www.supernovae.net/`).

Table 2.4 — Continued

Object Information		
Spectral Information		
of Spectra of a Given SN	Exposure Time (s)	SNID Redshift (and error)[a]
UT Date of Spectrum	Position Angle (deg)	SNID Type and Subtype[a]
Filename	Parallactic Angle (deg)	SNID-Determined (Rest-Frame) Age (and error)[a]
Wavelength Range (Å)	(Observer-Frame) Age	SNID $rlap$[a]
Airmass	Observer(s)	SNID Best Matching Template[a]
Seeing (arcsec)	Reducer	Spectral Reference(s)
Spectral Resolution(s) (Å)	Instrument	Flux Standard Star(s)
S/N	Flux Correction[d]	

[a]See Section 2.5 for more information about SNID and its parameters.
[b]See Jha et al. (2007) for more information about MLCS2k2 and its parameters.
[c]See Guy et al. (2005) and Guy et al. (2007) for more information about SALT and SALT2 and their parameters.
[d]See Section 2.3.3 for more information about our flux corrections.

The SNDB uses the popular open-source software stack known as LAMP: the Linux operating system, the Apache web server, the MySQL relational database management system, and the PHP server-side scripting language. We have also implemented instances of the PHP helper classes `tar`[4] and `JpGraph`[5] as well as the JavaScript libraries `SortTable`[6] and `overLIB`[7] to improve the functionality and user-friendliness of the SNDB; we are grateful to the authors of these packages. The database is stored on machines at UC Berkeley and multiple backups exist at other locations.

The primary way of accessing the SNDB is via the SN Database Public Home Page[8]. From here, users can download pre-compiled datasets and access our public search page, where they can define various input search criteria and query the SNDB. All SNe, spectra, and light curves that match the search criteria will be returned as an HTML table. The returned information will also be written to a LaTeX table which will be linked from the Search Results Page. If spectra or photometry points are returned, users are given the option to download the actual data or plot the spectra or photometry directly in their web browser. If MLCS2k2 light-curve fits are returned, users are given the option to download a file containing the fits and probability distributions for each of the light-curve parameters.

As PI Filippenko's group at UC Berkeley publishes more spectral and photometric data of SNe of all types in the future, the SNDB will continually be updated with these newly released data. We hope that the SNDB and its free, online access will quickly become an invaluable tool to the SN community for the foreseeable future.

2.5 Classification

Optical spectra are often used to classify SNe (e.g., Filippenko 1997; Turatto 2003) into four basic types. SN II spectra are identified by strong hydrogen features which are

[4]v2.2, Josh Barger (`joshb@npt.com`)
[5]v1.27.1, Aditus Consulting (`http://www.aditus.nu/jpgraph/`)
[6]v2, Stuart Langridge (`http://www.kryogenix.org/code/browser/sorttable/`)
[7]v4.21, Erik Bosrup (`http://www.bosrup.com/web/overlib/`)
[8]`http://hercules.berkeley.edu/database/index_public.html`

absent in SN I spectra. SN Ia spectra are characterized by the presence of a strong Si II λ6355 feature typically observed in absorption near 6150 Å. SN Ib spectra lack this Si II feature but do contain strong helium features, and finally SN Ic spectra lack strong helium features and have a Si II feature that is significantly weaker than those found in SNe Ia. We performed automated spectral classification of our full spectral dataset[9] using the SuperNova IDentification code (SNID; Blondin & Tonry 2007). Details of our classification algorithm are presented below.

2.5.1 SNID Spectral Templates

SNID classifies SN spectra by cross-correlating an input spectrum with a large database of observed SN spectra (known as "templates") which have been deredshifted to the rest frame. In order to improve the accuracy of SNID classifications, we decided to create our own set of SNID spectral templates based on a combination of the default SNID templates and our own spectral dataset.

New SNID Subtypes

We began by downloading SNID v5.0[10] which includes a default set of templates consisting of nearby ($z < 0.1$) SNe of all types (Ia, Ib, Ic, II), as well as "NotSN" types, which includes galaxies, AGNs, luminous blue variables (LBVs), and M stars (see Blondin & Tonry 2007, for the complete default SNID template set). SNID further divides each basic SN type into the following subtypes: Ia-norm, Ia-91T, Ia-91bg, Ia-csm, Ia-pec, Ib-norm, Ib-pec, IIb, Ic-norm, Ic-pec, Ic-broad, IIP, II-pec, IIn, and IIL.

"Norm" and "pec" identify spectroscopically "normal" and "peculiar" SNe of their respective types. Detailed descriptions of the other subtypes can be found in Blondin & Tonry (2007) and Foley et al. (2009b). In addition to these default subtypes, we have added two new SN Ia subtypes: Ia-99aa and Ia-02cx.

"Ia-99aa" are spectra that resemble SN 1999aa-like objects (Li et al. 2001b; Strolger et al. 2002; Garavini et al. 2004). Spectra of 99aa-like SNe contain a moderately strong Si II λ6355 absorption feature before maximum brightness which is stronger than those seen in 91T-like objects, but weaker than those of "normal" SNe Ia. 99aa-like objects also exhibit strong Fe II and Fe III features at early epochs, similar to the 91T-like SNe. A comparison of early-time spectra of a 99aa-like SN, a 91T-like SN, and a "normal" SN Ia is shown in Figure 2.7. These events were previously included in the Ia-91T subtype in the default set of SNID templates, but we feel that they *perhaps* represent a spectroscopically distinct subclass and therefore deserve their own subtype in SNID.

[9] Our full dataset consists of (1) previously published SN spectra of all types, (2) SN Ia spectra which are published here for the first time, and (3) some unpublished SN spectra of non-Ia types which will be published in the future.

[10] `http://marwww.in2p3.fr/~blondin/software/snid/index.html`

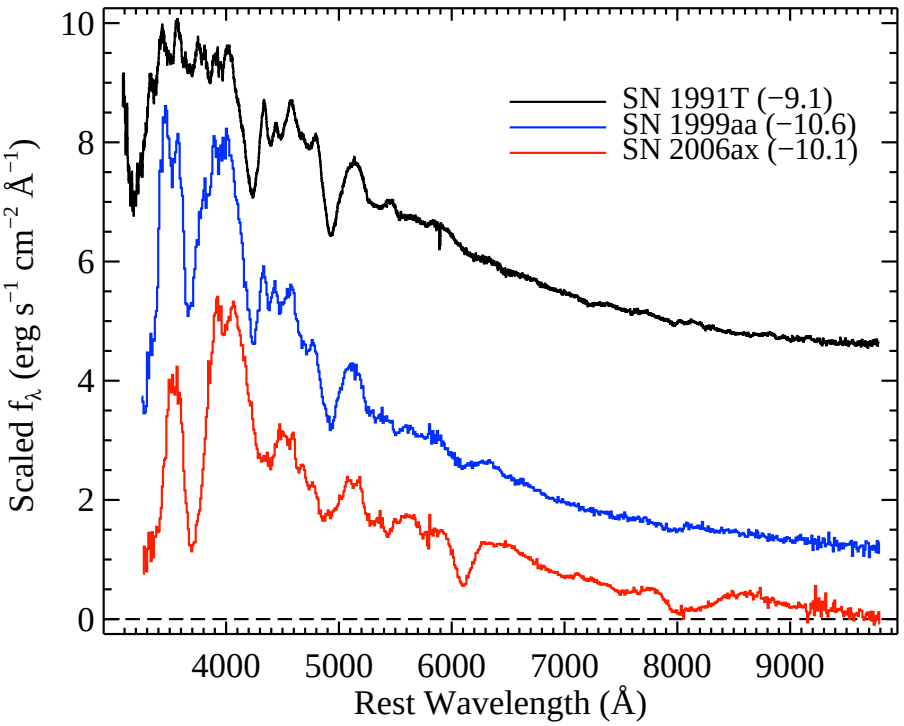

Figure 2.7: Spectra of SN 1991T, SN 1999aa, and the "normal" type Ia SN 2006ax at 9.1, 10.6, and 10.1 d before maximum brightness, respectively. All spectra in the figure (as well as all spectra plotted in this chapter) have had their host-galaxy recession velocities removed and have been corrected for MW reddening according to the values presented in Table 2.1 and assuming that the extinction follows the Cardelli et al. (1989) extinction law modified by O'Donnell (1994). Notice how the Si II λ6355 absorption feature increases in strength from SN 1991T to SN 1999aa to SN 2006ax. Also note the lack of Ca II H&K absorption in SN 1991T, which is the major difference between 91T-like and 99aa-like SNe.

Similarly, "Ia-02cx" are spectra that resemble SN 2002cx-like objects (e.g., Li et al. 2003b; Jha et al. 2006a; Foley et al. 2009a). These SNe were previously included in the Ia-pec subtype in the default set of SNID templates, but again, we believe that they represent their own subclass of events and should have their own subtype in SNID. Note that for our purposes, the "Ia-pec" category refers mainly to SN 2000cx-like objects (Li et al. 2001c).

We have made a few further changes to the classification scheme of SNID. Namely, Type IIb SNe (whose spectra evolve from a Type II SN to a Type Ib SN, as in SNe 1987K and 1993J; see Filippenko 1988; Filippenko et al. 1993; Matheson et al. 2000) are included *only* in the "Ib" SNID type (as opposed to being included in the "II" SNID type as well). We have also added two subtypes to the "NotSN" SNID type: QSOs and carbon stars. Spectra of these objects were obtained from the SDSS Data Release 6 Spectral Cross-Correlation Templates[11].

New SNID Templates, Part I

We began constructing our new set of spectral templates for SNID by performing a literature search for the best-studied and most canonical SNe in each subtype (with emphasis on the various SN Ia subtypes). Of the objects we deemed to be "the best" examples of their respective subtypes, 30 are already included in the default set of SNID v5.0 templates (Blondin & Tonry 2007) and 30 are in our full spectral dataset, with 23 found in both sets. These objects make up version 1.0 (v1.0) of our new spectral template set. Table 2.5 contains information about the objects included in v1.0, as well as the rest of our final template set. We present a summary of the number of each (sub)type of SN included in the final template set in Table 2.6. Figure 2.8 shows a histogram of the ages of our SN Ia template spectra.

[11] `http://www.sdss.org/dr6/algorithms/spectemplates/`

Table 2.5: SNID v7.0 Spectral Templates

SN Name	Subtype	Version[a]	Age(s)[b]
SN 1988Z	IIn	1	···
SN 1989B[c]	Ia-norm	1	−6,−1,4,6,8,10,[12:14],[16:25],31,37,49,50(1)
SN 1990H	IIP	3	···
SN 1990N[c]	Ia-norm	1	−13,−6,3,5,15,18,39,50(8)
SN 1990Q	IIP	3	···
SN 1991C	IIn	2	···
SN 1991T[d]	Ia-91T	1	−12,[−10:−5],0,7,11,16,19,25,[46:47],50(5)
SN 1991ao	IIP	3	···
SN 1991av	IIn	2	···
SN 1991bg[d]	Ia-91bg	1	[0:3],[15:16],[19:20],[26:27],30,[33:34],[46:48],50(10)
SN 1992A[c]	Ia-norm	1	−5,[−1:0],[2:3],[6:7],9,12,[16:17],24,28
SN 1992H	IIP	3	···
SN 1992ad	IIP	3	···
SN 1993E	IIP	3	···
SN 1993G	IIP	3	···
SN 1993J[d]	IIb	1	[−18:−16],−11,[−5:−2],1,[3:7],[11:13],17,20,24,[29:30],32,[35:39],41,50(38)
SN 1993W	IIP	3	···
SN 1993ad	IIP	3	···
SN 1994D[d]	Ia-norm	1	[−12:−2],0,[2:3],[10:17],19,21,24,26,28,30,40,[43:44],46,[48:49],50(9)
SN 1994I[d]	Ic-norm	1	−6,[−4:−3],[0:3],[21:24],26,30,36,38,40,50(1)
SN 1994S	Ia-norm	3	2
SN 1994W	IIn	1	···
SN 1994Y	IIn	2	···
SN 1994ae[d]	Ia-norm	1	[1:4],6,[9:11],30,36,40,50(6)
SN 1994ak	IIn	3	···
SN 1995D[d]	Ia-norm	1	4,6,8,[10:11],14,16,33,38,43,50(3)
SN 1995E	Ia-norm	3	−2
SN 1995G	IIn	2	···
SN 1995J	IIP	3	···
SN 1995V	IIP	3	···
SN 1995X	IIP	3	···
SN 1995ac[d]	Ia-91T	2	−6,24
SN 1996L[c]	IIn	1	8,34,42,50(4)
SN 1996ae	IIn	2	···
SN 1996an	IIP	3	···
SN 1996cc	IIP	3	···
SN 1997Y	Ia-norm	3	2
SN 1997ab	IIn	2	···
SN 1997br[d]	Ia-91T	2	[−9:−6],−4,[8:9],12,17,21,24,38,42,46,49,50(3)
SN 1997da	IIP	3	···
SN 1997dd	IIb	2	···
SN 1997ef[d]	Ic-broad	1	−14,[−12:−9],[−6:−4],7,[13:14],17,22,24,27,38,40,44,46,48,50(4)
SN 1997eg	IIn	2	···
SN 1998A	IIP	3	···
SN 1998E	IIn	2	···
SN 1998S[d]	IIn	1	−13,−2,[1:3],[10:11],[13:14],16,[31:32],[40:41],44,[46:47],50(37)
SN 1998bu[d]	Ia-norm	1	[−3:−1],1,[9:14],[28:44],50(9)
SN 1998bw[c]	Ic-broad	1	[8:9],[12:14],16,[18:19],21,24,[26:28],34,37,43,50(5)
SN 1998dl	IIP	3	···
SN 1998dt	Ib-norm	2	···
SN 1998dx	Ia-norm	3	5
SN 1998ec	Ia-norm	3	13
SN 1998ef	Ia-norm	3	−8,29,50(1)
SN 1998es	Ia-99aa	2	1,46,50(2)
SN 1999Z	IIn	2	···

Continued on Next Page...

Table 2.5 — Continued

SN Name	Subtype	Version[a]	Age(s)[b]
SN 1999aa[d]	Ia-99aa	1	[−10:−9],−4,[−1:0],3,8,[14:15],17,21,26,29,34,41,50(4)
SN 1999by[d]	Ia-91bg	1	[−5:−3],[3:8],25,29,31,33,42,50(1)
SN 1999cp	Ia-norm	3	5,14
SN 1999da	Ia-91bg	2	−2,7,37
SN 1999dk	Ia-norm	3	−7,17,24,44,50(1)
SN 1999dq	Ia-99aa	2	−3,4,24
SN 1999eb	IIn	2	···
SN 1999ed	IIP	3	···
SN 1999el	IIn	2	···
SN 1999em[d]	IIP	1	[−4:2],[5:7],9,11,16,27,[33:35],37,39,44,50(20)
SN 1999ex[c]	Ib-norm	1	−5,0,9
SN 1999gb	IIn	2	···
SN 1999gd	Ia-norm	3	0
SN 1999gi	IIP	3	···
SN 2000cn	Ia-norm	3	15
SN 2000cp	Ia-norm	3	3
SN 2000cu	Ia-norm	3	9,38
SN 2000cw	Ia-norm	3	5
SN 2000cx[d]	Ia-pec	1	[−4:2],[5:12],[14:15],19,22,24,26,28,[30:31],41,50(7)
SN 2000dg	Ia-norm	3	−5,5
SN 2000dk	Ia-norm	3	1,11,29,37
SN 2000dm	Ia-norm	3	−2,8
SN 2000dn	Ia-norm	3	−1,16
SN 2000ev	IIn	2	···
SN 2000fa	Ia-norm	3	−8,7
SN 2000fe	IIP	3	···
SN 2001K	IIP	3	···
SN 2001M	Ic-norm	2	···
SN 2001X	IIP	3	···
SN 2001ad	IIb	2	···
SN 2001bg	Ia-norm	3	14,19
SN 2001cm	IIP	3	···
SN 2001cy	IIP	3	···
SN 2001dk	IIP	3	···
SN 2001do	IIP	3	···
SN 2001dw	Ia-norm	3	11
SN 2001ef	Ic-norm	2	···
SN 2001eh	Ia-99aa	2	[−6:−5],3,32,50(1)
SN 2001en	Ia-norm	3	10,15,36
SN 2001ep	Ia-norm	3	3,[5:6],8,28,50(1)
SN 2001ey	IIn	2	···
SN 2001gd	IIb	2	···
SN 2001hg	IIP	3	···
SN 2001ir	IIn	2	···
SN 2002A	IIn	2	···
SN 2002J	Ic-norm	2	···
SN 2002an	IIP	3	···
SN 2002ap[d]	Ic-broad	1	[−6:−5],[−2:7],10,[12:13],[26:27],[30:31],50(12)
SN 2002bg	Ia-norm	3	−4
SN 2002bo[d]	Ia-norm	1	[−13:−12],[−9:0],6,[11:22],24,[28:30],39,41,44,46,50(8)
SN 2002bu	IIn	2	···
SN 2002bx	IIP	3	···
SN 2002bz	Ia-norm	3	6
SN 2002ca	IIP	3	···
SN 2002cf	Ia-91bg	2	−1

Continued on Next Page...

Table 2.5 — Continued

SN Name	Subtype	Version[a]	Age(s)[b]
SN 2002cr	Ia-norm	3	−7,25,34,50(1)
SN 2002cs	Ia-norm	3	−9,31,50(3)
SN 2002cx[d]	Ia-02cx	1	−5,−2,10,14,18,20,[23:25],50(2)
SN 2002dq	IIP	3	···
SN 2002ef	Ia-norm	3	5,29
SN 2002eg	IIb	2	···
SN 2002ei	IIP	3	···
SN 2002el	Ia-norm	3	12,21
SN 2002eo	IIP	3	···
SN 2002er[d]	Ia-norm	1	−11,[−9:−1],[2:4],6,9,[11:12],16,20,[23:24],33,50(2)
SN 2002eu	Ia-norm	3	0,33
SN 2002fb	Ia-91bg	2	1,19
SN 2002fk	Ia-norm	3	8,40,42,50(2)
SN 2002ha	Ia-norm	3	−1,5,8,39
SN 2002hd	Ia-norm	3	6
SN 2002he	Ia-norm	3	−6,[−1:0],3
SN 2002hk	IIP	3	···
SN 2002hn	Ic-norm	2	···
SN 2002ic[c]	Ia-csm	1	6,9,32,44,50(1)
SN 2002jy	Ia-norm	3	12,40
SN 2002kf	Ia-norm	3	7
SN 2002kg	IIn	2	···
SN 2003B	IIP	3	···
SN 2003G	IIn	2	···
SN 2003U	Ia-norm	3	−2
SN 2003Y	Ia-91bg	2	−3,21
SN 2003ab	IIP	3	···
SN 2003ai	Ia-norm	3	8
SN 2003cq	Ia-norm	3	0
SN 2003ei	IIn	2	···
SN 2003gd	IIP	3	···
SN 2003gg	IIP	3	···
SN 2003gq	Ia-02cx	2	50(1)
SN 2003gu	IIb	2	···
SN 2003he	Ia-norm	3	3,9
SN 2003hl	IIP	3	···
SN 2003ip	IIP	3	···
SN 2003iq	IIP	3	···
SN 2003iv	Ia-norm	3	2,7
SN 2003kb	Ic-norm	2	···
SN 2004aq	IIP	3	···
SN 2004as	Ia-norm	3	−4
SN 2004aw[c]	Ic-pec	1	−5,[−3:5],12,[18:19],21,23,[25:26],30,32,46,48,50(2)
SN 2004bg	Ia-norm	3	10
SN 2004bi	IIb	2	···
SN 2004bl	Ia-norm	3	5
SN 2004bw	Ia-norm	3	7
SN 2004cz	IIP	3	···
SN 2004dd	IIP	3	···
SN 2004dj[d]	IIP	1	0,3,5,8,[17:18],20,36,[47:48],50(4)
SN 2004dt	Ia-norm	3	−6,18,32,50(3)
SN 2004du	IIP	3	···
SN 2004ef	Ia-norm	3	−6,8,31,50(1)
SN 2004eo	Ia-norm	3	−6,13,44
SN 2004et[d]	IIP	1	[−3:−1],[1:2],4,6,[9:10],12,15,20,[23:25],27,[33:35],40,42,47,50(24)

Continued on Next Page...

Table 2.5 — Continued

SN Name	Subtype	Version[a]	Age(s)[b]
SN 2004eu	Ic-norm	2	···
SN 2004ey	Ia-norm	3	−7,19,50(1)
SN 2004ez	IIP	3	···
SN 2004fc	IIP	3	···
SN 2004fu	Ia-norm	3	−3,2,25
SN 2004fx	IIP	3	···
SN 2004fz	Ia-norm	3	−5,18,22
SN 2004gd	IIn	2	···
SN 2004gr	IIP	3	···
SN 2004gs	Ia-norm	3	0
SN 2005ad	IIP	3	···
SN 2005af	IIP	3	···
SN 2005am	Ia-norm	3	4,35,41
SN 2005aq	IIn	2	···
SN 2005ay	IIP	3	···
SN 2005bc	Ia-norm	3	2,7
SN 2005be	Ia-norm	3	11,17
SN 2005bi	IIP	3	···
SN 2005bl	Ia-91bg	2	17
SN 2005bx	IIn	2	···
SN 2005cf	Ia-norm	1	−11,[−2:−1],19,28
SN 2005cs[d]	IIP	1	[−2:5],[7:10],[26:27],50(1)
SN 2005de	Ia-norm	3	−1,10,26,40
SN 2005dv	Ia-norm	3	−1
SN 2005el	Ia-norm	3	−7,1,8
SN 2005eq	Ia-99aa	2	−3,1,50(1)
SN 2005gj[d]	Ia-csm	1	−12,−2,8,10,18,27,39,[41:42],46,48,50(13)
SN 2005hk[d]	Ia-02cx	1	[−9:−1],4,12,14,20,[22:23],[26:27],37,39,[42:43],50(3)
SN 2005ip	IIn	2	···
SN 2005kc	Ia-norm	3	10,12
SN 2005kd	IIn	2	···
SN 2005ke	Ia-91bg	2	8,10,15
SN 2005ki	Ia-norm	3	8
SN 2005ms	Ia-norm	3	−2,15
SN 2006N	Ia-norm	3	[−2:−1],12,27
SN 2006T	IIb	2	···
SN 2006ab	Ic-norm	2	···
SN 2006ac	Ia-norm	3	9
SN 2006be	IIP	3	···
SN 2006bp	IIP	3	···
SN 2006bq	Ia-norm	3	7,14
SN 2006bu	Ia-norm	3	4
SN 2006by	IIP	3	···
SN 2006bz	Ia-91bg	2	−2
SN 2006ca	IIP	3	···
SN 2006cf	Ia-norm	3	11,19
SN 2006cp	Ia-norm	3	−5
SN 2006cq	Ia-norm	3	2
SN 2006cs	Ia-91bg	2	2
SN 2006cx	IIP	3	···
SN 2006cz	Ia-99aa	2	1
SN 2006dm	Ia-norm	3	9,15,20,36
SN 2006dw	Ia-norm	3	1,7,22,28
SN 2006ef	Ia-norm	3	3,29,35
SN 2006ej	Ia-norm	3	−4,5,22,28

Continued on Next Page...

Table 2.5 — Continued

SN Name	Subtype	Version[a]	Age(s)[b]
SN 2006em	Ia-91bg	2	4,21
SN 2006et	Ia-norm	3	4,10,44
SN 2006ev	Ia-norm	3	11,17
SN 2006gt	Ia-91bg	2	2
SN 2006gy	II-pec	1	···
SN 2006ke	Ia-91bg	2	8
SN 2006kf	Ia-norm	3	−8,−2,19
SN 2006lf	Ia-norm	3	−6,14,25
SN 2006my	IIP	3	···
SN 2006or	Ia-norm	3	−3,5
SN 2006os	Ia-norm	3	9,27
SN 2006ov	IIP	3	···
SN 2006sr	Ia-norm	3	−2,3
SN 2006tf	II-pec	1	···
SN 2007A	Ia-norm	3	2,15
SN 2007C	Ib-norm	2	···
SN 2007K	IIn	2	···
SN 2007aa	IIP	3	···
SN 2007af	Ia-norm	3	−1,4,26,50(3)
SN 2007ag	Ib-norm	2	···
SN 2007al	Ia-91bg	2	5
SN 2007av	IIP	3	···
SN 2007ay	IIb	2	···
SN 2007ba	Ia-91bg	2	2,5,8
SN 2007bb	IIn	2	···
SN 2007bc	Ia-norm	3	1,16
SN 2007bd	Ia-norm	3	−6
SN 2007be	IIP	3	···
SN 2007bm	Ia-norm	3	−7,16,20,41
SN 2007ck	IIP	3	···
SN 2007cl	Ic-norm	2	···
SN 2007fb	Ia-norm	3	2,15,32,39,50(1)
SN 2007fr	Ia-norm	3	−1
SN 2007fs	Ia-norm	3	5,23,29,36,50(2)
SN 2007gk	Ia-norm	3	−2,20
SN 2007kk	Ia-norm	3	7
SN 2007oc	IIP	3	···
SN 2007od	IIP	3	···
SN 2007qe	Ia-norm	3	−7,6,16
SN 2008A	Ia-02cx	1	1
SN 2008D	Ib-norm	2	···
SN 2008aq	IIb	2	···
SN 2008aw	IIP	3	···
SN 2008be	IIn	2	···
SN 2008bj	IIP	3	···
SN 2008bl	IIP	3	···
SN 2008bt	Ia-91bg	2	11
SN 2008ds	Ia-99aa	2	−5,0,3,21,50(5)
SN 2008ec	Ia-norm	3	0,6,13,30,43,50(1)
SN 2008es	II-pec	1	···
SN 2008fq	IIP	3	···
SN 2008gf	IIP	3	···
SN 2008gj	Ic-norm	2	···
SN 2008hs	Ia-norm	3	−8
SN 2008ht	Ib-norm	2	···
SN 2008in	IIP	3	···

Continued on Next Page...

Table 2.6: Summary of SNID v7.0 Spectral Templates

Ia (Total)	134	Ib (Total)	16	Ic (Total)	14	II (Total)	113	NotSN (Total)	29
Ia-norm	101	Ib-norm	6	Ic-norm	10	IIP	76	AGN	1
Ia-91T	3	Ib-pec	0	Ic-pec	1	II-pec	3	Gal	11
Ia-91bg	16	IIb	10	Ic-broad	3	IIn	34	LBV	3
Ia-csm	2					IIL	0	M-star	7
Ia-pec	1							QSO	4
Ia-99aa	7							C-star	3
Ia-02cx	4								

Table 2.5 — Continued

SN Name	Subtype	Version[a]	Age(s)[b]
SN 2008iy	IIn	2	···

All spectral templates are solely from our full dataset, unless otherwise noted.
[a]Version of new SNID spectral templates when object was added — 1: v1.0; 2: v2.0–v2.5; 3: v3.0–v7.0.
[b]Rest-frame SN age(s), rounded to nearest whole day, in days from B-band maximum (for SNe Ia), from V-band maximum (for SNe Ib/c), or from the estimated date of explosion (for SNe II). Ages of spectral templates from our dataset are calculated from the light-curve references in Table 2.1; ages from the original SNID v5.0 set of spectral templates are from Blondin & Tonry (2007). Adjacent ages are listed in square brackets. Spectra whose age exceeds +50 days are grouped together and the number of such spectra is noted in parentheses. Many core-collapse SNe from our full spectral dataset lack age information (though we require SN Ia templates to have age information).
[c]Spectral templates are from the original SNID v5.0 (Blondin & Tonry 2007) set of templates only.
[d]Spectral templates are from both our full dataset as well as the original SNID v5.0 (Blondin & Tonry 2007) set of templates.

All templates of objects in our v1.0 that were already part of the default set of SNID templates were immediately added to our new template set. Spectra of objects in v1.0 that are only in our spectral dataset were made into SNID templates after passing certain criteria similar to the criteria used in the creation of the original SNID templates (Blondin & Tonry 2007).

For each object in v1.0, we examined only spectra that had a S/N of at least 15 pixel^{-1}, a minimum wavelength of less than 4500 Å, and a maximum wavelength of greater than 7000 Å. We also required that each SN Ia have a date of maximum brightness either from published sources or from Wang et al. (in preparation) so we can accurately calculate the age of each spectrum. Finally, each spectrum was visually inspected by multiple co-authors to be sure they truly represented their supposed subtype and were relatively free of host-galaxy contamination. If a spectrum passed the quantitative criteria and the by-eye inspection, it was cropped to 3500–10000 Å (to remove edge artefacts on both ends of the spectra). If a spectrum did not cover this entire range, 50 Å on both ends of the spectrum were removed instead. Finally, the cropped spectrum was made into a template; the result of this process was v1.0 of our new SNID templates.

To increase the number of SNe in our template set, we ran SNID (with our v1.0 templates) on our entire spectral dataset. Again, we required that a new template have a S/N

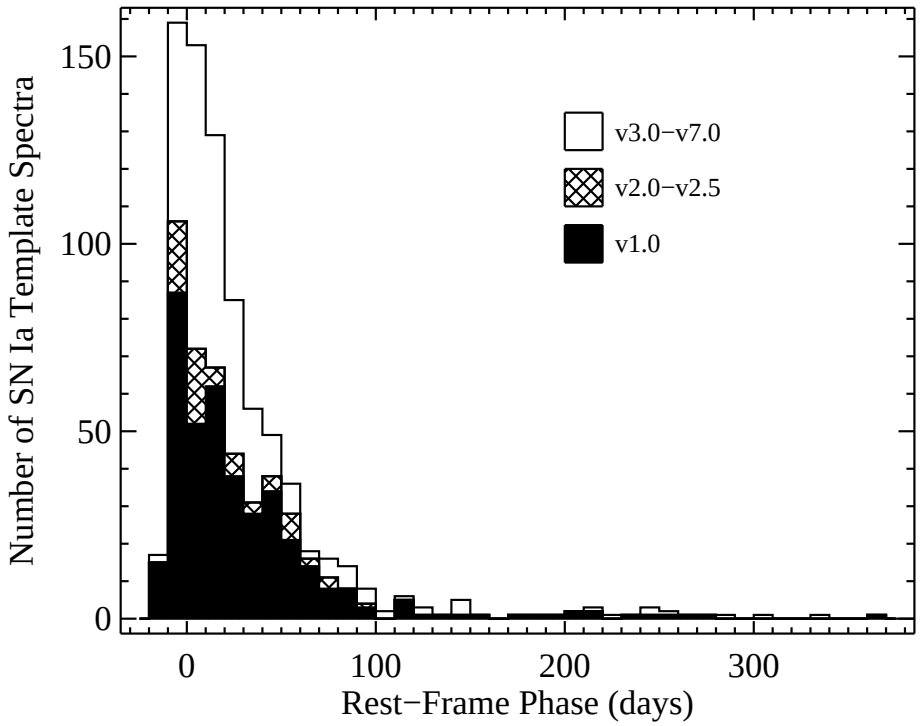

Figure 2.8: A histogram of the ages of our SN Ia template spectra separated by SNID template version.

of at least 15 pixel^{-1}, a minimum wavelength of less than or equal to 4500 Å, a maximum wavelength of greater than or equal to 7000 Å, and that each SN Ia have a known date of maximum brightness. To determine subtypes, we followed similar classification criteria to those of Blondin & Tonry (2007), requiring that the SNID $r$lap value[12] be at least 10 and the 3 best matching spectra from SNID all be of the same subtype. We also ignored any objects that were classified as "Ia-norm" or "IIP" since we wanted to concentrate on only relatively rare subtypes at this point and SNID is somewhat biased toward classifying objects as subtypes that have a large number of templates (such as "Ia-norm" and "IIP").

Again, each of the spectra was visually inspected by multiple co-authors to be sure they represented their supposed subtype and were relatively free of host-galaxy contamination. If a spectrum passed the quantitative criteria and the by-eye inspection, it was then cropped as in v1.0 and made into a template. The result of this process was v2.0 of our new SNID templates. This process was repeated iteratively, running SNID with the previously created version of our spectral templates, until no more SNe passed all of the criteria. It required 5 additional runs to reach this convergence, resulting in v2.5 of our new SNID templates.

If an object was classified and made into a template in v2.X and was already part of the default set of SNID templates, we also added the spectra of that object that came with the default set of SNID templates into our new template set. In v2.0–v2.5 there were a total of 78 new objects added, 76 of which came solely from our spectral dataset and 2 of which came from both our data and the default set of SNID templates (again, see Table 2.5 for information about the objects included in v2.0–v2.5 as well as our final SNID template set, and Figure 2.8 for a histogram of the ages of our SN Ia templates). It should be noted that upon inspection of our spectra of SN 1995ac, we reclassify this object as "Ia-91T" even though it was classified as "Ia-norm" in the default set of SNID templates (Blondin & Tonry 2007).

Initial Verification

As a sanity check we perform an initial classification verification. For this we ran all of our spectra of the objects in v2.5 through SNID and compared the (sub)type of the best-matching template to the actual (sub)type of the object. We made sure to ignore all templates of the SN currently being inspected so SNID would not match an object to itself. In addition, objects were not used in this process if their spectra made up $> 15\%$ of all the spectral templates of the object's subtype. This is necessary since if we remove $> 15\%$ of the spectral templates of a given subtype, there is little chance of successfully classifying a SN of that subtype; this would bias our classification results.

Since we are primarily discussing SNe Ia in this chapter, our first verification step was to check how well SNID can distinguish between SNe Ia and non-SNe Ia using our new templates. SNID, using v2.5 of our new templates, was able to correctly classify $\sim$97% of

[12]In SNID, the $r$lap value is a measure of the strength of the correlation between the best-matching spectrum and the input spectrum.

SN Ia spectra as one of the SN Ia subtypes and non-SN Ia spectra as one of the non-SN Ia subtypes.

It has been shown that as some of the peculiar subtypes of SNe Ia evolve and age, their optical spectra begin to resemble that of "normal" SNe Ia (e.g., Filippenko et al. 1992a; Turatto et al. 1996; Garavini et al. 2004; Branch et al. 2008) and can thus introduce an "age bias" (Li et al. 2001a). Therefore, our next verification step was to investigate how accurately SNID can distinguish between different SN Ia subtypes at various ages using our v2.5 template set. To do this, we ran our SN Ia spectra through SNID as discussed above. We found that SNID, using v2.5 of our new templates, is able to classify nearly 90% of SNe Ia spectra with ages ≤ 15 d past maximum brightness as the correct subtype (with this percentage dropping for spectra older than 15 d past maximum). Therefore, for the rest of our SNID template set creation, we require that all SNe Ia that get flagged as a possible template be less than 15 d past maximum. However, once a spectrum this young is flagged, we inspect *all* spectra of that object as possible templates.

New SNID Templates, Part II

We continued creating a new set of spectral templates by running SNID (with our v2.5 templates) on our full spectral dataset. Again, we required that a new template have a S/N of at least 15 pixel^{-1}, a maximum wavelength of greater than or equal to 7000 Å, and that each SN Ia have a known date of maximum brightness. However, we now require that the minimum wavelength be less than or equal to 4000 Å, as opposed to 4500 Å as in earlier versions. Also, as mentioned above, we require that spectra of a SN Ia be at most 15 d past maximum in order for its classification to be inspected further. We use this slightly stricter criteria since v2.5 has a reasonable number of objects and spectra in each SN type and SN Ia subtype, and we want to make sure we do not contaminate the various subtypes.

To determine subtypes, we again make our criteria slightly more stringent and require that the SNID $r$lap value be at least 15, the 8 best-matching spectra from SNID all be of the same subtype, and the 3 best-matching objects all be of the same subtype. We also now allow objects that are classified as "Ia-norm" or "IIP," which we had been ignoring in our template creation process until this point.

Each of the spectra were again visually inspected to be sure they represented their supposed subtype and were relatively free of host-galaxy contamination, and all but a few passed this inspection. If a spectrum passed the quantitative criteria and the by-eye inspection, then it was cropped as before and made into a template. The result of this process was v3.0 of our new SNID templates. For this and all higher versions of our template set, we only use spectra from our dataset and do not use any other templates that were already part of the default set of SNID templates. The process was repeated iteratively, running SNID with our previously created version of the spectral templates, until no more SNe were classified and turned into templates. This process finished with the creation of v7.0, which we consider our final set of new SNID templates and which we use to classify the remainder of our full

spectral dataset (see Table 2.5 for information regarding the entire SNID template set). v7.0 contains 1543 spectra of 277 SNe, of which 779 spectra and 134 objects are SNe Ia. Again, we show a histogram of the ages of all of our SN Ia spectral templates (separated by SNID template version) in Figure 2.8.

Final Verifications

As another sanity check, we perform final classification verifications which are basically the same as our initial classification verification (see Section 2.5.1 for details). However, this time we ran all of our spectra of the objects in v2.5 through SNID using our v7.0 templates, and then we ran all of our spectra of the objects in v7.0 through SNID (again using our v7.0 templates). As before, we compare the (sub)type of the best-matching template to the actual (sub)type of the object and make sure to ignore all templates of the SN currently being inspected. Again, SNe are not used in this process if their spectra make up $> 15\%$ of all the spectra in the object's subtype.

Using only objects from v2.5 (v7.0) we find that SNID, using v7.0 of our new templates, is able to correctly classify $\sim$97% ($\sim$99%) of SN Ia spectra as one of the SN Ia subtypes and non-Ia SN spectra as one of the non-Ia SN subtypes. We also find that SNID is able to correctly classify $\sim$85% ($\sim$95%) of SN Ia spectra with ages ≤ 15 d past maximum brightness as the correct subtype.

The fact that these percentages increase with the addition of more templates and more input objects is reassuring. This seems to indicate that SNID, using our v7.0 templates, is robustly classifying the vast majority of objects correctly as SNe Ia or non-Ia as well as correctly classifying the various subtypes of SNe Ia (as long as their spectra are younger than about 15 d past maximum brightness). It also indicates that the templates added between v2.5 and v7.0 have improved the accuracy of our SNID classifications.

We compared the classification results of our full dataset using our v7.0 templates to the results using the default set of SNID templates. The average difference between $z_{\rm gal}$ (the actual redshift of the host galaxy) and $z_{\rm SNID}$ (the redshift of the SN as determined by SNID) was found to decrease using our v7.0 templates. Furthermore, the discrepancies between $t_{\rm LC}$ (the spectral age derived from photometry) and $t_{\rm SNID}$ (the SNID-determined spectral age) improved drastically when using our v7.0 templates. Our template set also markedly suppressed the SNID-determined age bias seen near maximum brightness and +30 d (see Östman et al. 2011, and Section 2.5.3 for more on this bias). Finally, with the significant increase in the number of templates of peculiar SNe Ia and our two additional SN Ia subtypes, SNID (using our v7.0 template set) can distinguish between the various spectroscopic subtypes much better than when using the default templates. The SNID-determined subtype of $\sim$15% ($\sim$26%) of the spectra (SNe Ia) presented here is different when using SNID with our v7.0 templates versus using SNID with the default templates.

2.5.2 Classification of Spectra

Using our v7.0 SNID templates, we can attempt to classify all of the spectra in our full dataset using criteria similar to those of Miknaitis et al. (2007) and Foley et al. (2009b). To do this we execute a series of SNID runs to separately determine the type, subtype, redshift, and age of the input spectrum. For all of the SNID runs we ignore all templates of the SN currently being inspected so SNID will not match an object to itself, and we truncate all spectra at 10000 Å to avoid any possible second-order light contamination. Besides these, we use the default parameters of SNID unless specifically noted below. If a spectrum was obtained within 10° of the parallactic angle (or was obtained at an airmass < 1.1) and corrected for host-galaxy contamination via our color-matching technique (as described in Section 2.3.3), then we use the galaxy-subtracted spectrum in all of the SNID runs. The results of the classification algorithm presented below can be found in Table 2.7.

Table 2.7: SNID Classification Information

SN Name	Type	Subtype	$z_{\rm SNID}$[a]	$t_{\rm SNID}$[b]	$r$lap	Best Match[c]
SN 1989A	Ia	Ia-norm	0.0087 (0.0014)	85.5 (8.2)	13.1	sn99dk (Ia-norm) 0.0088 (0.0044) 71.83 (8.18500)
SN 1989B	Ia	Ia-norm	0.0055 (0.0039)	7.7 (0.0)	10.6	sn02fk (Ia-norm) 0.0023 (0.0046) 7.74 (0.00000)
SN 1989B	Ia	Ia-norm	0.0046 (0.0041)	22.7 (0.0)	10.8	sn07fs (Ia-norm) 0.0026 (0.0047) 22.67 (0.00000)
SN 1989B	Ia	···	0.0047 (0.0043)	83.0 (3.0)	15.1	sn98es (Ia-99aa) 0.0025 (0.0034) 78.70 (12.3380)
SN 1989B	Ia	Ia-norm	0.0029 (0.0015)	216.9 (6.3)	12.2	sn98bu (Ia-norm) 0.0024 (0.0047) 208.00 (6.29300)
SN 1989M	Ia	Ia-norm	0.0014 (0.0053)	−3.5 (7.5)	15.3	sn02er (Ia-norm) 0.0050 (0.0039) −3.50 (7.52800)
SN 1989M	Ia	Ia-norm	0.0022 (0.0054)	−0.1 (2.4)	12.8	sn02er (Ia-norm) 0.0053 (0.0046) −3.50 (5.43200)
SN 1989M	Ia	···	0.0077 (0.0014)	246.2 (30.1)	5.8	sn90N (Ia-norm) 0.0047 (0.0095) 246.20 (30.0640)
SN 1989M	Ia	Ia-norm	0.0061 (0.0000)	332.5 (0.0)	8.0	sn90N (Ia-norm) 0.0061 (0.0073) 332.50 (0.00000)
SN 1990G	Ia	Ia-norm	0.0365 (0.0047)	9.3 (0.8)	24.1	sn98bu (Ia-norm) 0.0359 (0.0022) 9.30 (3.25200)
SN 1990M	Ia	Ia-norm	0.0082 (0.0000)	216.9 (6.3)	10.4	sn98bu (Ia-norm) 0.0082 (0.0057) 208.00 (6.29300)
SN 1990M	Ia	Ia-norm	0.0077 (0.0019)	31.3 (0.0)	12.5	sn02cs (Ia-norm) 0.0091 (0.0046) 31.28 (0.00000)
SN 1990M	Ia	Ia-norm	0.0081 (0.0020)	29.0 (10.4)	9.9	sn04fz (Ia-norm) 0.0095 (0.0059) 17.56 (8.56600)
SN 1990M	Ia	Ia-norm	0.0070 (0.0010)	59.1 (0.0)	10.8	sn98bu (Ia-norm) 0.0082 (0.0050) 59.12 (0.00000)
SN 1990M	···	···	···	···	···	···
SN 1990O	Ia	Ia-norm	0.0291 (0.0025)	15.1 (1.0)	25.6	sn07qe (Ia-norm) 0.0318 (0.0024) 16.00 (1.65300)
SN 1990O	Ia	···	0.0287 (0.0042)	22.7 (2.9)	20.0	sn99dq (Ia-99aa) 0.0310 (0.0026) 24.09 (12.0700)
SN 1990O	Ia	Ia-norm	0.0299 (0.0017)	55.1 (5.0)	16.1	sn02bo (Ia-norm) 0.0284 (0.0032) 56.35 (7.53600)
SN 1990N	Ia	Ia-norm	0.0052 (0.0054)	5.5 (1.8)	12.8	sn02er (Ia-norm) 0.0035 (0.0041) 5.50 (1.83800)
SN 1990N	Ia	Ia-norm	0.0033 (0.0019)	18.9 (2.8)	16.7	sn06dw (Ia-norm) 0.0032 (0.0034) 22.47 (2.77100)
SN 1990N	Ia	Ia-norm	0.0031 (0.0008)	43.1 (6.4)	15.4	sn00cu (Ia-norm) 0.0031 (0.0036) 38.25 (8.09400)
SN 1990N	···	···	···	···	···	···
SN 1990N	Ia	Ia-norm	0.0043 (0.0012)	235.8 (58.2)	12.0	sn94ae (Ia-norm) 0.0033 (0.0046) 153.40 (75.6390)
SN 1990R	Ia	Ia-norm	0.0175 (0.0010)	41.3 (1.3)	17.5	sn94D (Ia-norm) 0.0178 (0.0029) 43.20 (3.94600)
SN 1990R	Ia	···	0.0183 (0.0042)	56.8 (6.5)	16.0	sn08ds (Ia-99aa) 0.0165 (0.0031) 51.91 (15.0150)
SN 1990R	Ia	Ia-norm	0.0150 (0.0013)	87.9 (7.3)	18.2	sn94D (Ia-norm) 0.0172 (0.0030) 74.23 (14.3320)
SN 1990Y	Ia	Ia-norm	0.0410 (0.0013)	16.1 (7.1)	12.7	sn02bg (Ia-norm) 0.0397 (0.0045) −3.65 (7.14200)
SN 1991B	Ia	Ia-norm	0.0096 (0.0021)	40.5 (0.0)	11.3	sn05de (Ia-norm) 0.0089 (0.0045) 40.49 (0.00000)
SN 1991B	Ia	Ia-norm	0.0098 (0.0009)	61.0 (7.0)	15.0	sn02er (Ia-norm) 0.0092 (0.0037) 60.98 (9.07100)
SN 1991B	Ia	···	0.0133 (0.0045)	83.0 (4.3)	14.8	sn98es (Ia-99aa) 0.0087 (0.0033) 78.70 (20.7630)
SN 1991K	···	···	···	···	···	···
SN 1991K	Ia	Ia-norm	0.0189 (0.0007)	84.6 (18.6)	10.3	sn07af (Ia-norm) 0.0182 (0.0050) 113.82 (18.5570)
SN 1991M	Ia	Ia-norm	0.0055 (0.0010)	18.9 (0.0)	10.6	sn01bg (Ia-norm) 0.0066 (0.0051) 18.91 (0.00000)
SN 1991M	Ia	Ia-norm	0.0066 (0.0014)	30.2 (6.8)	8.5	sn01en (Ia-norm) 0.0067 (0.0060) 35.64 (7.92500)
SN 1991M	Ia	···	0.0093 (0.0018)	245.2 (28.1)	7.5	sn91bg (Ia-91bg) 0.0079 (0.0066) 202.70 (51.2400)
SN 1991M	Ia	Ia-norm	0.0094 (0.0016)	255.9 (18.2)	8.0	sn90N (Ia-norm) 0.0075 (0.0068) 255.90 (18.2110)
SN 1991O	Ia	Ia-91bg	0.0365 (0.0028)	21.0 (0.0)	12.4	sn06em (Ia-91bg) 0.0391 (0.0060) 20.95 (0.00000)
SN 1991S	Ia	Ia-norm	0.0556 (0.0021)	38.5 (9.7)	8.7	sn94D (Ia-norm) 0.0556 (0.0051) 43.20 (11.5040)
SN 1991T	Ia	Ia-91T	0.0029 (0.0012)	−5.6 (0.0)	8.6	sn95ac (Ia-91T) 0.0053 (0.0057) −5.61 (0.00000)
SN 1991T	Ia	Ia-91T	0.0034 (0.0012)	−9.0 (0.0)	9.4	sn97br (Ia-91T) 0.0057 (0.0056) −9.00 (0.00000)

Continued on Next Page...

Table 2.7 — Continued

SN Name	Type	Subtype	$z_{\rm SNID}$[a]	$t_{\rm SNID}$[b]	$r$lap	Best Match[c]
SN 1991T	Ia	Ia-norm	0.0041 (0.0015)	9.4 (0.0)	16.1	sn94ae (Ia-norm) 0.0052 (0.0037) 9.40 (0.00000)
SN 1991T	Ia	···	0.0081 (0.0042)	78.7 (13.3)	14.8	sn98es (Ia-99aa) 0.0057 (0.0038) 78.70 (17.0070)
SN 1991T	Ia	Ia-norm	0.0061 (0.0011)	87.3 (3.0)	12.4	sn98ef (Ia-norm) 0.0056 (0.0046) 85.52 (2.99500)
SN 1991T	···	···	···	···	···	···
SN 1991T	Ia	Ia-norm	0.0079 (0.0098)	245.2 (74.5)	8.9	sn90N (Ia-norm) 0.0061 (0.0068) 255.90 (74.5330)
SN 1991T	···	···	···	···	···	···
SN 1991T	···	···	···	···	···	···
SN 1991am	Ia	Ia-norm	0.0604 (0.0022)	16.4 (2.6)	16.6	sn89B (Ia-norm) 0.0602 (0.0030) 13.40 (3.79300)
SN 1991ak	Ia	Ia-norm	0.0114 (0.0010)	41.3 (2.1)	13.7	sn02fk (Ia-norm) 0.0104 (0.0033) 41.50 (2.13500)
SN 1991ak	Ia	Ia-norm	0.0112 (0.0016)	57.5 (3.1)	19.3	sn02cr (Ia-norm) 0.0100 (0.0023) 57.47 (3.13400)
SN 1991ak	Ia	···	0.0124 (0.0042)	71.6 (5.0)	20.8	sn08ds (Ia-99aa) 0.0103 (0.0023) 63.44 (18.2730)
SN 1991at	Ia	Ia-norm	0.0429 (0.0021)	36.4 (8.4)	12.2	sn04dt (Ia-norm) 0.0416 (0.0036) 31.97 (8.38400)
SN 1991as	Ia	···	0.0135 (0.0042)	92.9 (3.9)	17.4	sn00cx (Ia-pec) 0.0140 (0.0034) 88.93 (44.2430)
SN 1991ay	Ia	Ia-norm	0.0487 (0.0016)	14.5 (1.5)	17.8	sn95D (Ia-norm) 0.0471 (0.0033) 16.10 (4.14000)
SN 1991bd	Ia	Ia-norm	0.0144 (0.0044)	23.6 (0.0)	11.6	sn99dk (Ia-norm) 0.0139 (0.0049) 23.62 (0.00000)
SN 1991bc	Ia	Ia-norm	0.0223 (0.0026)	17.7 (2.4)	24.0	sn90N (Ia-norm) 0.0219 (0.0024) 17.70 (4.23700)
SN 1991bc	Ia	···	0.0233 (0.0039)	59.4 (9.8)	14.4	sn91T (Ia-91T) 0.0201 (0.0036) 75.20 (18.2740)
SN 1991bb	Ia	Ia-norm	0.0259 (0.0032)	10.2 (1.3)	25.6	sn02er (Ia-norm) 0.0270 (0.0023) 12.40 (2.20200)
SN 1991bb	Ia	Ia-norm	0.0249 (0.0006)	50.0 (5.8)	12.7	sn94D (Ia-norm) 0.0259 (0.0041) 48.00 (5.78700)
SN 1991bf	Ia	Ia-norm	0.0324 (0.0051)	28.5 (0.0)	10.8	sn01ep (Ia-norm) 0.0323 (0.0046) 28.46 (0.00000)
SN 1991bg	Ia	Ia-91bg	0.0020 (0.0027)	2.1 (3.5)	12.8	sn03Y (Ia-91bg) 0.0031 (0.0044) −2.82 (3.46800)
SN 1991bg	Ia	···	0.0025 (0.0045)	−0.6 (0.7)	12.4	sn02cf (Ia-91bg) 0.0026 (0.0042) −0.65 (4.03900)
SN 1991bg	Ia	Ia-91bg	0.0013 (0.0010)	21.0 (0.0)	10.6	sn06em (Ia-91bg) 0.0027 (0.0051) 20.95 (0.00000)
SN 1991bg	Ia	Ia-91bg	0.0020 (0.0028)	18.6 (8.8)	9.4	sn06em (Ia-91bg) 0.0036 (0.0060) 20.95 (6.75600)
SN 1991bg	···	···	···	···	···	···
SN 1991bg	Ia	Ia-norm	0.0027 (0.0038)	53.9 (7.1)	5.9	sn02er (Ia-norm) 0.0026 (0.0081) 60.98 (7.11700)
SN 1991bg	Ic	Ic-broad	0.0151 (0.0070)	29.5 (0.0)	5.2	sn02ap (Ic-broad) 0.0032 (0.0121) 29.50 (0.00000)
SN 1991bg	···	···	···	···	···	···
SN 1991bh	Ia	Ia-norm	0.0280 (0.0028)	51.5 (6.7)	9.6	sn02bo (Ia-norm) 0.0257 (0.0051) 56.35 (19.0350)
SN 1991bj	Ia	Ia-02cx	0.0175 (0.0013)	23.0 (3.5)	15.6	sn02cx (Ia-02cx) 0.0184 (0.0022) 18.20 (4.19800)
SN 1992G	Ia	Ia-norm	0.0057 (0.0021)	41.1 (10.8)	14.5	sn89B (Ia-norm) 0.0057 (0.0034) 20.40 (11.5400)
SN 1992G	Ia	Ia-norm	0.0060 (0.0011)	49.0 (8.2)	36.5	sn94D (Ia-norm) 0.0057 (0.0014) 48.96 (8.21800)
SN 1992G	Ia	Ia-norm	0.0058 (0.0011)	70.0 (7.7)	17.8	sn08ec (Ia-norm) 0.0049 (0.0029) 71.57 (12.9950)
SN 1992G	Ia	Ia-norm	0.0052 (0.0013)	70.0 (5.7)	15.6	sn94ae (Ia-norm) 0.0051 (0.0032) 70.00 (10.6040)
SN 1992G	Ia	Ia-norm	0.0051 (0.0012)	87.9 (0.1)	17.0	sn94ae (Ia-norm) 0.0056 (0.0029) 87.80 (19.2960)
SN 1992G	Ia	Ia-norm	0.0054 (0.0012)	123.6 (28.6)	18.9	sn94ae (Ia-norm) 0.0052 (0.0028) 123.60 (28.6380)
SN 1992G	Ia	Ia-norm	0.0053 (0.0013)	123.6 (28.6)	18.1	sn94ae (Ia-norm) 0.0053 (0.0029) 123.60 (21.4020)
SN 1992G	Ia	Ia-norm	0.0070 (0.0028)	87.3 (7.7)	8.3	sn07fs (Ia-norm) 0.0052 (0.0058) 91.35 (16.9970)
SN 1992M	Ia	Ia-norm	0.0527 (0.0023)	12.5 (5.5)	8.2	sn06N (Ia-norm) 0.0532 (0.0085) 11.87 (8.20000)
SN 1992M	Ia	Ia-norm	0.0529 (0.0000)	16.1 (0.0)	5.0	sn95D (Ia-norm) 0.0529 (0.0078) 16.10 (0.00000)
SN 1992ah	Ia	Ia-norm	0.0218 (0.0032)	8.9 (1.2)	22.6	sn06ev (Ia-norm) 0.0229 (0.0026) 11.03 (2.50300)
SN 1992ap	Ia	Ia-norm	0.0327 (0.0017)	50.0 (4.0)	20.8	sn94D (Ia-norm) 0.0320 (0.0023) 48.96 (8.09200)
SN 1993C	Ia	Ia-norm	0.0108 (0.0008)	41.0 (19.8)	14.2	sn02ha (Ia-norm) 0.0120 (0.0039) 38.55 (18.2020)
SN 1993C	Ia	Ia-norm	0.0114 (0.0011)	87.8 (1.4)	13.8	sn94ae (Ia-norm) 0.0119 (0.0037) 87.80 (1.36100)
SN 1993C	Ia	Ia-norm	0.0122 (0.0001)	153.4 (21.1)	10.6	sn94ae (Ia-norm) 0.0121 (0.0052) 153.40 (21.0720)
SN 1993Y	Ia	Ia-norm	0.0181 (0.0017)	23.4 (7.5)	18.1	sn07fs (Ia-norm) 0.0181 (0.0033) 29.49 (9.64500)
SN 1993aa	Ia	Ia-91bg	0.0253 (0.0022)	8.0 (7.4)	12.1	sn07ba (Ia-91bg) 0.0250 (0.0047) 8.01 (7.43600)
SN 1993Z	Ia	Ia-norm	−0.0001 (0.0033)	18.7 (7.5)	8.3	sn04ef (Ia-norm) 0.0047 (0.0074) 8.05 (4.67400)
SN 1993Z	Ia	Ia-norm	0.0049 (0.0029)	54.6 (7.2)	9.9	sn02bo (Ia-norm) 0.0046 (0.0060) 54.60 (17.0840)
SN 1993Z	Ia	Ia-norm	0.0059 (0.0007)	71.8 (0.0)	11.5	sn99dk (Ia-norm) 0.0050 (0.0052) 71.83 (0.00000)
SN 1993Z	Ia	Ia-norm	0.0081 (0.0042)	84.6 (5.9)	9.0	sn04ef (Ia-norm) 0.0044 (0.0068) 84.60 (5.87600)
SN 1993Z	Ia	Ia-norm	0.0049 (0.0000)	84.6 (0.0)	10.2	sn04ef (Ia-norm) 0.0048 (0.0061) 84.60 (0.00000)
SN 1993Z	Ia	Ia-norm	0.0081 (0.0035)	84.6 (5.9)	9.7	sn04ef (Ia-norm) 0.0048 (0.0064) 84.60 (5.87600)
SN 1993Z	Ia	Ia-norm	0.0077 (0.0018)	84.6 (9.0)	7.5	sn04ef (Ia-norm) 0.0046 (0.0078) 84.60 (9.02600)
SN 1993Z	Ia	Ia-norm	0.0079 (0.0025)	113.8 (22.8)	6.2	sn98ef (Ia-norm) 0.0040 (0.0091) 85.52 (22.8000)
SN 1993Z	Ia	Ia-norm	0.0096 (0.0029)	71.8 (0.0)	6.0	sn99dk (Ia-norm) 0.0041 (0.0101) 71.83 (0.00000)
SN 1993ab	Ia	Ia-norm	0.0151 (0.0008)	87.3 (3.4)	15.3	sn07fs (Ia-norm) 0.0153 (0.0034) 91.35 (6.15900)
SN 1993ac	Ia	Ia-norm	0.0457 (0.0031)	10.1 (2.6)	24.7	sn01en (Ia-norm) 0.0482 (0.0026) 10.09 (2.90600)
SN 1993ac	Ia	Ia-norm	0.0482 (0.0021)	29.4 (2.6)	17.6	sn02bo (Ia-norm) 0.0492 (0.0037) 29.40 (7.06000)
SN 1993ae	Ia	Ia-norm	0.0184 (0.0019)	20.4 (7.3)	19.0	sn04fz (Ia-norm) 0.0194 (0.0031) 17.56 (11.7370)

Continued on Next Page...

Table 2.7 — Continued

SN Name	Type	Subtype	$z_{\rm SNID}$[a]	$t_{\rm SNID}$[b]	$r$lap	Best Match[c]
SN 1993ae	Ia	Ia-norm	0.0197 (0.0014)	59.1 (8.7)	13.3	sn94ae (Ia-norm) 0.0185 (0.0038) 70.00 (8.68900)
SN 1993ai	Ia	Ia-norm	0.0363 (0.0020)	18.7 (1.7)	24.8	sn07bm (Ia-norm) 0.0361 (0.0025) 20.45 (10.0860)
SN 1993aj	Ia	Ia-norm	0.0788 (0.0020)	14.5 (3.4)	11.8	sn05kc (Ia-norm) 0.0795 (0.0040) 12.19 (3.43400)
SN 1993aj	Ia	Ia-norm	0.0747 (0.0000)	49.2 (0.0)	10.2	sn89B (Ia-norm) 0.0746 (0.0048) 49.20 (0.00000)
SN 1993aj	Ia	Ia-pec	0.0811 (0.0000)	30.4 (0.2)	10.9	sn00cx (Ia-pec) 0.0811 (0.0048) 30.40 (0.239000)
SN 1994B	Ia	Ia-norm	0.0875 (0.0063)	3.3 (5.7)	14.2	sn94ae (Ia-norm) 0.0865 (0.0037) 2.30 (5.03100)
SN 1994B	Ia	Ia-norm	0.0886 (0.0024)	14.1 (2.4)	12.6	sn98bu (Ia-norm) 0.0890 (0.0043) 14.30 (2.41100)
SN 1994E	Ia	···	0.0649 (0.0040)	49.1 (9.8)	9.5	sn91T (Ia-91T) 0.0633 (0.0058) 67.60 (12.4130)
SN 1994J	···	···	···	···	···	···
SN 1994D	Ia	Ia-norm	−0.0070 (0.0046)	−6.0 (2.7)	8.4	sn02bo (Ia-norm) 0.0011 (0.0075) −6.00 (2.74700)
SN 1994D	Ia	Ia-norm	−0.0065 (0.0049)	−4.4 (0.0)	6.7	sn02bo (Ia-norm) 0.0015 (0.0091) −4.40 (0.00000)
SN 1994D	Ia	Ia-norm	−0.0039 (0.0049)	−1.0 (3.0)	8.8	sn02he (Ia-norm) 0.0011 (0.0060) −1.03 (3.02300)
SN 1994D	Ia	Ia-norm	−0.0006 (0.0054)	−7.5 (3.3)	9.1	sn04ey (Ia-norm) 0.0012 (0.0067) −7.48 (3.14900)
SN 1994D	Ia	Ia-norm	0.0055 (0.0050)	−1.8 (0.0)	11.7	sn06kf (Ia-norm) 0.0014 (0.0042) −1.75 (0.00000)
SN 1994D	Ia	Ia-norm	0.0009 (0.0049)	−0.9 (4.1)	9.9	sn06N (Ia-norm) 0.0014 (0.0049) −0.95 (3.56500)
SN 1994D	Ia	Ia-norm	0.0026 (0.0044)	−1.7 (4.0)	11.6	sn07bm (Ia-norm) 0.0015 (0.0043) −7.30 (3.95800)
SN 1994D	Ia	Ia-norm	0.0023 (0.0043)	3.3 (6.3)	14.2	sn94ae (Ia-norm) 0.0013 (0.0036) 3.30 (4.78000)
SN 1994D	Ia	Ia-norm	0.0026 (0.0023)	18.9 (0.0)	25.5	sn04ey (Ia-norm) 0.0015 (0.0021) 18.90 (0.00000)
SN 1994D	Ia	Ia-norm	0.0013 (0.0014)	25.8 (2.1)	12.9	sn05de (Ia-norm) 0.0014 (0.0041) 25.75 (2.12200)
SN 1994D	Ia	Ia-norm	0.0019 (0.0011)	36.2 (5.3)	13.8	sn05cf (Ia-norm) 0.0014 (0.0041) 27.64 (6.44600)
SN 1994D	Ia	Ia-norm	0.0017 (0.0011)	33.4 (0.3)	20.6	sn95D (Ia-norm) 0.0014 (0.0027) 33.05 (5.25200)
SN 1994D	Ia	Ia-norm	0.0020 (0.0019)	41.5 (10.9)	16.4	sn02fk (Ia-norm) 0.0015 (0.0032) 41.50 (10.1610)
SN 1994D	Ia	Ia-norm	0.0021 (0.0013)	61.0 (6.7)	19.8	sn04ey (Ia-norm) 0.0016 (0.0024) 51.49 (10.1680)
SN 1994D	Ia	Ia-norm	0.0013 (0.0012)	61.0 (6.5)	19.7	sn04ey (Ia-norm) 0.0014 (0.0024) 51.49 (10.1680)
SN 1994D	Ia	Ia-norm	0.0034 (0.0030)	56.3 (9.4)	8.9	sn08ec (Ia-norm) 0.0014 (0.0049) 42.99 (15.5240)
SN 1994D	Ia	Ia-norm	0.0012 (0.0015)	44.4 (0.0)	10.3	sn04eo (Ia-norm) 0.0014 (0.0042) 44.40 (0.00000)
SN 1994D	Ia	Ia-norm	0.0036 (0.0040)	70.0 (8.2)	9.7	sn94ae (Ia-norm) 0.0016 (0.0050) 70.00 (8.19600)
SN 1994D	Ia	Ia-norm	0.0011 (0.0008)	123.6 (0.0)	12.8	sn94ae (Ia-norm) 0.0016 (0.0042) 123.60 (0.00000)
SN 1994D	Ia	Ia-norm	0.0023 (0.0017)	153.4 (44.1)	9.8	sn94ae (Ia-norm) 0.0015 (0.0056) 153.40 (62.9220)
SN 1994Q	Ia	Ia-norm	0.0304 (0.0022)	10.2 (1.4)	15.7	sn05kc (Ia-norm) 0.0292 (0.0034) 10.22 (1.89800)
SN 1994Q	Ia	Ia-norm	0.0313 (0.0016)	42.1 (7.4)	17.8	sn98bu (Ia-norm) 0.0316 (0.0031) 43.10 (11.1430)
SN 1994Q	Ia	···	0.0341 (0.0040)	71.9 (8.1)	17.3	sn91T (Ia-91T) 0.0304 (0.0031) 75.20 (19.7210)
SN 1994S	Ia	Ia-norm	0.0171 (0.0042)	3.3 (0.7)	25.1	sn94ae (Ia-norm) 0.0162 (0.0020) 3.30 (1.65200)
SN 1994T	Ia	Ia-norm	0.0345 (0.0008)	38.2 (7.1)	13.3	sn94ae (Ia-norm) 0.0330 (0.0043) 40.10 (7.06400)
SN 1994U	Ia	Ia-norm	0.0079 (0.0052)	7.7 (0.0)	21.5	sn02fk (Ia-norm) 0.0034 (0.0024) 7.74 (1.70800)
SN 1994X	Ia	Ia-norm	0.0566 (0.0018)	29.2 (7.8)	14.3	sn02er (Ia-norm) 0.0608 (0.0045) 33.20 (7.58800)
SN 1994ab	Ia	Ia-norm	0.0343 (0.0016)	20.4 (1.7)	13.5	sn89B (Ia-norm) 0.0337 (0.0033) 20.40 (1.73000)
SN 1994ae	Ia	Ia-norm	0.0034 (0.0014)	74.2 (10.1)	12.7	sn98ef (Ia-norm) 0.0043 (0.0043) 85.52 (10.0800)
SN 1994ae	Ia	Ia-norm	0.0047 (0.0026)	208.0 (83.6)	8.0	sn98bu (Ia-norm) 0.0044 (0.0068) 208.00 (83.6140)
SN 1994ae	···	···	···	···	···	···
SN 1995A	Ia	Ia-norm	0.0299 (0.0000)	72.5 (0.0)	10.3	sn02bo (Ia-norm) 0.0299 (0.0048) 72.50 (0.00000)
SN 1995C	Ia	Ia-norm	0.0263 (0.0012)	25.8 (3.1)	23.4	sn02er (Ia-norm) 0.0287 (0.0022) 23.44 (8.25800)
SN 1995D	Ia	Ia-norm	0.0093 (0.0043)	2.3 (2.4)	15.8	sn00dn (Ia-norm) 0.0065 (0.0035) −1.04 (1.75300)
SN 1995D	Ia	Ia-norm	0.0072 (0.0012)	30.2 (5.1)	20.4	sn94D (Ia-norm) 0.0065 (0.0028) 29.99 (6.64200)
SN 1995D	Ia	Ia-norm	0.0075 (0.0012)	50.0 (2.6)	23.0	sn94D (Ia-norm) 0.0067 (0.0021) 48.96 (7.70100)
SN 1995D	Ia	Ia-norm	0.0050 (0.0012)	87.8 (7.4)	13.9	sn94ae (Ia-norm) 0.0064 (0.0038) 87.95 (7.39600)
SN 1995E	Ia	Ia-norm	0.0127 (0.0045)	1.3 (0.2)	26.2	sn06dw (Ia-norm) 0.0118 (0.0021) 1.07 (3.05600)
SN 1995E	Ia	Ia-norm	0.0103 (0.0013)	46.2 (0.0)	11.1	sn94D (Ia-norm) 0.0112 (0.0044) 46.20 (0.00000)
SN 1995L	Ia	Ia-norm	0.0255 (0.0012)	121.8 (5.2)	14.9	sn07af (Ia-norm) 0.0250 (0.0035) 113.82 (18.2930)
SN 1995T	Ia	···	0.0561 (0.0075)	9.6 (1.7)	13.0	sn91T (Ia-91T) 0.0560 (0.0043) 10.90 (3.75000)
SN 1995ac	Ia	Ia-91T	0.0480 (0.0012)	−6.4 (1.7)	15.0	sn97br (Ia-91T) 0.0462 (0.0038) −4.00 (1.74700)
SN 1995ac	Ia	Ia-norm	0.0492 (0.0016)	27.6 (4.3)	14.1	sn98ef (Ia-norm) 0.0502 (0.0046) 28.51 (5.43700)
SN 1995ak	Ia	Ia-norm	0.0236 (0.0011)	28.8 (3.7)	13.6	sn06dw (Ia-norm) 0.0244 (0.0054) 28.28 (4.16800)
SN 1995al	Ia	Ia-norm	0.0029 (0.0026)	18.9 (1.5)	11.4	sn06ev (Ia-norm) 0.0049 (0.0052) 16.85 (1.45700)
SN 1995al	Ia	Ia-norm	0.0047 (0.0010)	38.5 (6.8)	14.6	sn05am (Ia-norm) 0.0048 (0.0040) 35.08 (9.09700)
SN 1996O	Ia	Ia-norm	0.0361 (0.0005)	64.0 (6.7)	21.6	sn94D (Ia-norm) 0.0370 (0.0024) 59.10 (7.24100)
SN 1996P	Ia	Ia-norm	0.0153 (0.0011)	57.1 (4.6)	17.4	sn04ey (Ia-norm) 0.0156 (0.0027) 51.49 (7.08600)
SN 1996ai	Ia	Ia-norm	0.0022 (0.0010)	3.3 (0.0)	10.0	sn94ae (Ia-norm) 0.0032 (0.0050) 3.30 (0.00000)
SN 1996ai	Ia	Ia-99aa	0.0033 (0.0000)	−0.1 (0.0)	10.9	sn08ds (Ia-99aa) 0.0033 (0.0050) −0.08 (0.00000)
SN 1996ai	Ia	Ia-norm	0.0039 (0.0053)	2.3 (2.8)	9.9	sn02ha (Ia-norm) 0.0031 (0.0051) −0.85 (2.59900)

Continued on Next Page...

Table 2.7 — Continued

SN Name	Type	Subtype	$z_{\rm SNID}$[a]	$t_{\rm SNID}$[b]	$r$lap	Best Match[c]
SN 1996ai	Ia	Ia-norm	0.0026 (0.0007)	51.5 (0.0)	10.3	sn04ey (Ia-norm) 0.0033 (0.0065) 51.49 (0.00000)
SN 1996ai	Ia	Ia-norm	0.0041 (0.0007)	44.2 (0.0)	10.2	sn99dk (Ia-norm) 0.0034 (0.0056) 44.20 (0.00000)
SN 1996bv	Ia	Ia-norm	0.0158 (0.0004)	18.9 (2.2)	12.4	sn05cf (Ia-norm) 0.0158 (0.0039) 18.69 (2.23600)
SN 1997E	Ia	Ia-norm	0.0126 (0.0012)	28.5 (6.7)	16.8	sn98bu (Ia-norm) 0.0126 (0.0036) 30.22 (8.33800)
SN 1997T	Ia	Ia-norm	0.0423 (0.0020)	18.4 (2.7)	14.5	sn07fs (Ia-norm) 0.0420 (0.0034) 22.67 (2.60600)
SN 1997Y	Ia	Ia-norm	0.0190 (0.0045)	1.2 (1.6)	24.3	sn00dn (Ia-norm) 0.0151 (0.0023) −1.04 (2.99400)
SN 1997bp	Ia	Ia-norm	−0.0024 (0.0065)	−3.4 (4.2)	9.8	sn02bo (Ia-norm) 0.0086 (0.0064) −3.40 (4.22000)
SN 1997br	Ia	Ia-91T	0.0066 (0.0000)	−0.2 (0.0)	16.9	sn91T (Ia-91T) 0.0065 (0.0034) −0.20 (0.00000)
SN 1997br	Ia	···	0.0040 (0.0047)	22.5 (1.3)	10.9	sn99dq (Ia-99aa) 0.0067 (0.0046) 24.09 (5.69700)
SN 1997br	Ia	···	0.0085 (0.0041)	40.5 (3.5)	17.0	sn91T (Ia-91T) 0.0073 (0.0031) 45.70 (11.9030)
SN 1997br	Ia	Ia-norm	0.0080 (0.0005)	42.8 (1.9)	10.7	sn02jy (Ia-norm) 0.0072 (0.0047) 39.90 (1.91100)
SN 1997br	Ia	Ia-norm	0.0066 (0.0012)	64.0 (9.7)	12.4	sn02bo (Ia-norm) 0.0063 (0.0046) 51.60 (9.66300)
SN 1997cn	Ia	···	0.0169 (0.0051)	18.6 (8.1)	14.7	sn05ke (Ia-91bg) 0.0161 (0.0037) 14.85 (12.1070)
SN 1997cw	Ia	···	0.0166 (0.0046)	36.1 (8.4)	14.5	sn01eh (Ia-99aa) 0.0177 (0.0042) 32.08 (15.2240)
SN 1997cw	Ia	Ia-norm	0.0173 (0.0021)	72.5 (17.4)	16.6	sn02bo (Ia-norm) 0.0153 (0.0035) 72.50 (17.3500)
SN 1997do	Ia	Ia-norm	0.0002 (0.0063)	−10.6 (2.0)	7.1	sn02er (Ia-norm) 0.0102 (0.0077) −7.40 (2.60700)
SN 1997do	Ia	Ia-norm	0.0113 (0.0009)	79.4 (6.6)	19.3	sn02bo (Ia-norm) 0.0107 (0.0029) 79.40 (6.59100)
SN 1997fb	Ia	Ia-norm	0.0506 (0.0024)	10.1 (1.3)	13.8	sn06dm (Ia-norm) 0.0496 (0.0040) 8.73 (1.61700)
SN 1997fc	Ia	···	0.0582 (0.0046)	−0.1 (1.1)	22.9	sn08ds (Ia-99aa) 0.0550 (0.0022) −0.08 (3.75500)
SN 1998V	Ia	Ia-norm	0.0171 (0.0039)	9.3 (1.3)	14.1	sn05ki (Ia-norm) 0.0164 (0.0039) 7.96 (1.45800)
SN 1998aq	Ia	Ia-norm	0.0022 (0.0009)	39.3 (26.2)	14.2	sn02ha (Ia-norm) 0.0034 (0.0036) 38.55 (26.2170)
SN 1998aq	Ia	Ia-norm	0.0015 (0.0014)	59.1 (0.0)	11.7	sn98bu (Ia-norm) 0.0034 (0.0042) 59.12 (0.00000)
SN 1998aq	Ia	···	0.0025 (0.0039)	71.0 (12.6)	9.7	sn98bu (Ia-norm) 0.0035 (0.0050) 59.12 (29.5940)
SN 1998bn	Ia	Ia-norm	0.0034 (0.0023)	18.7 (6.5)	7.5	sn01bg (Ia-norm) 0.0059 (0.0084) 18.91 (7.66700)
SN 1998bn	Ib	IIb	0.0026 (0.0041)	···	5.7	sn03gu (IIb) 0.0055 (0.0082) −999.00 (0.00000)
SN 1998bn	Ia	Ia-norm	0.0041 (0.0008)	39.3 (33.7)	13.1	sn07fb (Ia-norm) 0.0059 (0.0041) 39.28 (33.6900)
SN 1998bp	···	···	···	···	···	···
SN 1998bp	Ia	Ia-norm	0.0094 (0.0023)	28.5 (7.3)	6.6	sn00cu (Ia-norm) 0.0097 (0.0064) 38.25 (7.30600)
SN 1998bp	Ia	Ia-91bg	0.0108 (0.0024)	42.1 (9.0)	17.1	sn99by (Ia-91bg) 0.0108 (0.0031) 42.10 (8.99400)
SN 1998bp	Ia	Ia-norm	0.0125 (0.0015)	245.2 (72.1)	7.8	sn07af (Ia-norm) 0.0110 (0.0065) 121.79 (72.0890)
SN 1998bp	Ia	Ia-99aa	0.0092 (0.0000)	256.0 (0.0)	5.0	sn99aa (Ia-99aa) 0.0092 (0.0107) 256.03 (0.00000)
SN 1998bu	Ia	Ia-norm	0.0025 (0.0011)	28.3 (3.6)	15.7	sn06N (Ia-norm) 0.0027 (0.0037) 27.49 (4.45200)
SN 1998bu	Ia	Ia-norm	0.0019 (0.0009)	59.1 (14.5)	13.9	sn94D (Ia-norm) 0.0031 (0.0036) 59.10 (14.5320)
SN 1998bu	Ia	Ia-norm	0.0031 (0.0012)	153.4 (0.0)	14.4	sn94ae (Ia-norm) 0.0031 (0.0039) 153.40 (0.00000)
SN 1998bu	Ia	Ia-norm	0.0033 (0.0006)	213.4 (0.0)	20.7	sn90N (Ia-norm) 0.0029 (0.0029) 213.40 (0.00000)
SN 1998bu	Ia	Ia-norm	0.0034 (0.0046)	213.4 (138.5)	7.7	sn90N (Ia-norm) 0.0030 (0.0074) 213.40 (115.269)
SN 1998cd	Ia	Ia-norm	0.0248 (0.0018)	39.3 (8.6)	19.0	sn07bm (Ia-norm) 0.0251 (0.0032) 20.45 (10.3420)
SN 1998cl	Ia	Ia-norm	0.0303 (0.0028)	13.2 (0.9)	24.1	sn98bu (Ia-norm) 0.0304 (0.0024) 13.20 (3.85000)
SN 1998cm	Ia	Ia-91T	0.0688 (0.0000)	8.5 (0.0)	11.7	sn97br (Ia-91T) 0.0691 (0.0050) 8.50 (0.00000)
SN 1998cs	Ia	Ia-norm	0.0315 (0.0056)	−3.5 (3.6)	26.4	sn02er (Ia-norm) 0.0327 (0.0023) −3.50 (3.56500)
SN 1998cs	Ia	Ia-norm	0.0306 (0.0041)	11.2 (0.7)	25.9	sn98bu (Ia-norm) 0.0310 (0.0022) 10.20 (3.85000)
SN 1998cs	Ia	Ia-norm	0.0322 (0.0019)	72.5 (3.8)	22.8	sn02bo (Ia-norm) 0.0309 (0.0023) 72.50 (10.9420)
SN 1998dh	Ia	···	0.0059 (0.0051)	41.4 (12.0)	11.6	sn95ac (Ia-91T) 0.0082 (0.0046) 24.40 (8.43700)
SN 1998dh	Ia	Ia-norm	0.0107 (0.0000)	39.5 (0.0)	10.1	sn02fk (Ia-norm) 0.0107 (0.0058) 39.52 (0.00000)
SN 1998dh	Ia	Ia-norm	0.0089 (0.0009)	41.3 (3.8)	17.8	sn05am (Ia-norm) 0.0093 (0.0032) 41.04 (7.63700)
SN 1998dh	Ia	Ia-norm	0.0088 (0.0013)	70.0 (4.8)	16.6	sn02er (Ia-norm) 0.0094 (0.0033) 60.98 (13.1900)
SN 1998de	Ia	···	0.0198 (0.0038)	36.9 (12.9)	15.3	sn99da (Ia-91bg) 0.0169 (0.0038) 36.91 (12.8940)
SN 1998de	Ia	Ia-91bg	0.0196 (0.0016)	50.5 (4.0)	15.1	sn91bg (Ia-91bg) 0.0196 (0.0038) 46.50 (4.00000)
SN 1998de	Ib	IIb	0.0191 (0.0014)	68.0 (19.7)	6.2	sn93J (IIb) 0.0166 (0.0087) 70.00 (0.00000)
SN 1998dj	Ia	Ia-norm	0.0129 (0.0011)	41.5 (3.1)	15.5	sn04eo (Ia-norm) 0.0125 (0.0034) 44.40 (7.98700)
SN 1998dk	Ia	Ia-norm	0.0025 (0.0060)	−7.0 (1.6)	7.9	sn92A (Ia-norm) 0.0127 (0.0068) −5.00 (3.06400)
SN 1998dk	Ia	Ia-norm	0.0086 (0.0045)	−6.4 (2.2)	23.9	sn02er (Ia-norm) 0.0140 (0.0026) −6.40 (2.19700)
SN 1998dk	Ia	Ia-norm	0.0118 (0.0024)	17.7 (5.1)	14.5	sn90N (Ia-norm) 0.0121 (0.0037) 17.70 (4.46900)
SN 1998dk	Ia	Ia-norm	0.0126 (0.0010)	41.0 (2.7)	19.0	sn99dk (Ia-norm) 0.0128 (0.0031) 44.20 (10.5370)
SN 1998dm	Ia	Ia-norm	0.0008 (0.0055)	−4.4 (2.3)	9.9	sn04as (Ia-norm) 0.0072 (0.0067) −4.36 (1.66700)
SN 1998dm	Ia	Ia-norm	0.0064 (0.0039)	−3.0 (3.3)	13.5	sn06dw (Ia-norm) 0.0062 (0.0037) 1.07 (3.28700)
SN 1998dm	Ia	Ia-norm	0.0069 (0.0020)	15.1 (2.5)	39.9	sn07A (Ia-norm) 0.0071 (0.0014) 15.07 (2.54100)
SN 1998dm	Ia	···	0.0078 (0.0041)	42.8 (4.2)	23.1	sn98es (Ia-99aa) 0.0063 (0.0023) 46.13 (12.4220)
SN 1998dm	Ia	Ia-norm	0.0061 (0.0013)	87.8 (9.4)	18.7	sn94ae (Ia-norm) 0.0064 (0.0027) 87.80 (11.2910)
SN 1998dw	II	IIP	0.0477 (0.0030)	119.0 (28.6)	9.0	sn99em (IIP) 0.0450 (0.0062) 119.80 (0.00000)

Continued on Next Page...

Table 2.7 — Continued

SN Name	Type	Subtype	$z_{\rm SNID}$[a]	$t_{\rm SNID}$[b]	$r$lap	Best Match[c]
SN 1998dx	Ia	Ia-norm	0.0547 (0.0049)	3.2 (4.1)	35.4	sn02he (Ia-norm) 0.0569 (0.0016) 3.22 (4.11700)
SN 1998dx	Ia	Ia-norm	0.0517 (0.0029)	31.4 (6.0)	16.9	sn89B (Ia-norm) 0.0503 (0.0034) 31.40 (5.95300)
SN 1998eb	Ia	Ia-norm	0.0134 (0.0013)	72.5 (8.1)	19.5	sn02bo (Ia-norm) 0.0124 (0.0029) 72.50 (10.2240)
SN 1998ec	Ia	Ia-norm	0.0171 (0.0029)	11.9 (1.5)	21.1	sn98bu (Ia-norm) 0.0183 (0.0028) 11.20 (2.62000)
SN 1998ef	Ia	Ia-norm	0.0077 (0.0040)	−5.0 (0.2)	16.9	sn92A (Ia-norm) 0.0180 (0.0031) −5.00 (0.174000)
SN 1998ef	Ia	Ia-norm	0.0168 (0.0012)	28.4 (4.8)	17.5	sn06N (Ia-norm) 0.0169 (0.0035) 27.49 (7.68100)
SN 1998ef	Ia	Ia-norm	0.0152 (0.0007)	74.2 (0.0)	11.1	sn94D (Ia-norm) 0.0162 (0.0047) 74.23 (0.00000)
SN 1998ef	Ia	Ia-norm	0.0184 (0.0011)	87.2 (25.6)	8.7	sn94D (Ia-norm) 0.0183 (0.0059) 74.23 (25.5760)
SN 1998ef	Ia	Ia-norm	0.0167 (0.0010)	91.3 (2.5)	18.5	sn07fs (Ia-norm) 0.0167 (0.0031) 91.35 (13.3560)
SN 1998eg	Ia	Ia-norm	0.0256 (0.0016)	29.5 (6.9)	21.3	sn06os (Ia-norm) 0.0259 (0.0028) 27.16 (7.37000)
SN 1998en	Ia	Ia-norm	0.0228 (0.0010)	27.5 (2.8)	11.7	sn06lf (Ia-norm) 0.0229 (0.0055) 25.06 (2.76100)
SN 1998es	Ia	Ia-99aa	0.0144 (0.0057)	0.7 (0.0)	12.9	sn05eq (Ia-99aa) 0.0099 (0.0039) 0.66 (0.00000)
SN 1998es	Ia	Ia-norm	0.0116 (0.0016)	41.0 (2.5)	22.3	sn94ae (Ia-norm) 0.0110 (0.0023) 40.10 (8.14500)
SN 1998es	Ia	Ia-99aa	0.0113 (0.0000)	59.4 (0.0)	11.3	sn99aa (Ia-99aa) 0.0112 (0.0048) 59.43 (0.00000)
SN 1998es	Ia	···	0.0137 (0.0040)	67.6 (15.4)	24.7	sn91T (Ia-91T) 0.0113 (0.0021) 67.60 (15.4110)
SN 1998es	Ia	Ia-norm	0.0110 (0.0014)	87.3 (9.5)	16.6	sn99dk (Ia-norm) 0.0101 (0.0035) 71.83 (12.6500)
SN 1998es	Ia	Ia-norm	0.0110 (0.0013)	87.8 (2.8)	15.3	sn94ae (Ia-norm) 0.0116 (0.0033) 87.80 (7.30200)
SN 1998es	Ia	Ia-norm	0.0121 (0.0009)	91.3 (0.0)	10.3	sn07fs (Ia-norm) 0.0115 (0.0052) 91.35 (0.00000)
SN 1998fc	Ia	Ia-91bg	0.1009 (0.0016)	33.1 (4.0)	6.8	sn99by (Ia-91bg) 0.1002 (0.0077) 33.10 (4.62000)
SN 1999C	Ia	Ia-norm	0.1308 (0.0022)	14.5 (0.9)	9.6	sn07qe (Ia-norm) 0.1335 (0.0062) 16.00 (2.37900)
SN 1999X	Ia	Ia-norm	0.0260 (0.0027)	14.6 (3.0)	15.9	sn02el (Ia-norm) 0.0266 (0.0038) 11.82 (4.15900)
SN 1999X	Ia	Ia-norm	0.0248 (0.0018)	26.5 (7.1)	24.4	sn02er (Ia-norm) 0.0271 (0.0026) 23.44 (8.31100)
SN 1999aa	Ia	Ia-pec	0.0126 (0.0031)	−2.4 (0.7)	9.3	sn00cx (Ia-pec) 0.0135 (0.0065) −2.40 (0.669000)
SN 1999aa	Ia	Ia-99aa	0.0142 (0.0023)	0.7 (3.1)	16.1	sn05eq (Ia-99aa) 0.0130 (0.0032) 0.66 (2.63600)
SN 1999aa	Ia	Ia-norm	0.0144 (0.0029)	14.1 (0.6)	15.6	sn95D (Ia-norm) 0.0142 (0.0035) 14.10 (1.18200)
SN 1999aa	Ia	Ia-norm	0.0142 (0.0020)	16.1 (2.8)	22.1	sn95D (Ia-norm) 0.0132 (0.0024) 16.10 (2.78500)
SN 1999aa	Ia	Ia-norm	0.0153 (0.0013)	57.1 (4.9)	20.4	sn02er (Ia-norm) 0.0150 (0.0027) 60.98 (9.17900)
SN 1999aa	Ia	Ia-norm	0.0175 (0.0014)	246.2 (0.0)	10.7	sn90N (Ia-norm) 0.0157 (0.0058) 246.20 (0.00000)
SN 1999aa	Ia	Ia-norm	0.0181 (0.0018)	309.8 (45.0)	6.9	sn90N (Ia-norm) 0.0158 (0.0090) 246.20 (44.9720)
SN 1999aq	Ia	Ia-norm	0.0489 (0.0017)	19.6 (4.4)	25.9	sn04fz (Ia-norm) 0.0492 (0.0024) 17.56 (9.20600)
SN 1999ac	Ia	Ia-norm	0.0098 (0.0051)	−0.7 (3.8)	8.9	sn98bu (Ia-norm) 0.0099 (0.0052) −2.80 (4.13400)
SN 1999ac	Ia	Ia-norm	0.0134 (0.0066)	3.2 (2.3)	13.7	sn00cp (Ia-norm) 0.0099 (0.0043) 3.21 (2.25400)
SN 1999ac	Ia	Ia-norm	0.0110 (0.0019)	38.3 (4.4)	15.9	sn07bm (Ia-norm) 0.0100 (0.0035) 41.34 (4.71100)
SN 1999ac	Ia	Ia-norm	0.0129 (0.0025)	113.8 (20.4)	6.8	sn02bo (Ia-norm) 0.0098 (0.0070) 79.40 (20.4210)
SN 1999bh	Ia	Ia-norm	0.0245 (0.0010)	28.7 (0.2)	11.5	sn01ep (Ia-norm) 0.0229 (0.0051) 28.46 (0.161000)
SN 1999bv	Ia	Ia-norm	0.0178 (0.0023)	91.3 (5.7)	11.7	sn02bo (Ia-norm) 0.0178 (0.0053) 83.30 (5.69500)
SN 1999by	Ia	Ia-91bg	0.0037 (0.0012)	117.2 (0.0)	7.1	sn91bg (Ia-91bg) 0.0017 (0.0062) 117.20 (0.00000)
SN 1999cl	Ia	···	0.0040 (0.0029)	41.3 (5.7)	9.0	sn00cx (Ia-pec) 0.0078 (0.0085) 31.40 (21.1220)
SN 1999cl	Ia	Ia-norm	0.0068 (0.0010)	29.4 (3.1)	15.2	sn04ef (Ia-norm) 0.0071 (0.0042) 31.23 (4.53300)
SN 1999cl	Ia	···	0.0082 (0.0035)	40.1 (5.7)	13.7	sn97br (Ia-91T) 0.0074 (0.0041) 49.10 (11.6590)
SN 1999cl	···	···	···	···	···	···
SN 1999cp	Ia	Ia-norm	0.0122 (0.0046)	4.9 (1.4)	24.9	sn94D (Ia-norm) 0.0092 (0.0021) 2.90 (2.21400)
SN 1999cp	Ia	Ia-norm	0.0102 (0.0022)	14.1 (0.6)	24.3	sn98bu (Ia-norm) 0.0102 (0.0022) 13.20 (2.16500)
SN 1999cw	Ia	Ia-norm	0.0103 (0.0024)	14.8 (1.7)	12.0	sn98bu (Ia-norm) 0.0118 (0.0047) 13.20 (1.66200)
SN 1999cw	Ia	···	0.0102 (0.0045)	41.3 (11.7)	13.6	sn00cx (Ia-pec) 0.0131 (0.0048) 41.40 (8.36200)
SN 1999cw	Ia	Ia-norm	0.0121 (0.0010)	79.4 (7.4)	18.0	sn02bo (Ia-norm) 0.0112 (0.0030) 79.40 (7.35900)
SN 1999cw	Ia	Ia-norm	0.0128 (0.0012)	84.6 (7.3)	13.4	sn04ef (Ia-norm) 0.0117 (0.0044) 84.60 (7.29900)
SN 1999cw	Ia	Ia-norm	0.0138 (0.0026)	213.4 (81.8)	8.4	sn04ef (Ia-norm) 0.0121 (0.0067) 84.60 (76.6890)
SN 1999da	Ia	Ia-91bg	0.0084 (0.0017)	1.4 (1.4)	11.5	sn02cf (Ia-91bg) 0.0095 (0.0046) −0.65 (1.43500)
SN 1999da	Ia	Ia-91bg	0.0140 (0.0030)	19.3 (6.7)	10.5	sn05ke (Ia-91bg) 0.0118 (0.0058) 9.87 (6.67500)
SN 1999da	Ia	···	0.0161 (0.0041)	31.1 (2.0)	16.4	sn99by (Ia-91bg) 0.0145 (0.0032) 33.10 (17.4930)
SN 1999da	Ia	Ia-91bg	0.0158 (0.0000)	53.5 (0.1)	11.3	sn91bg (Ia-91bg) 0.0158 (0.0054) 53.30 (0.141000)
SN 1999da	Ia	···	0.0127 (0.0016)	53.5 (35.3)	9.5	sn91bg (Ia-91bg) 0.0135 (0.0057) 53.50 (22.4590)
SN 1999dg	Ia	Ia-norm	0.0220 (0.0025)	14.3 (3.0)	30.6	sn06ev (Ia-norm) 0.0215 (0.0020) 16.85 (4.51800)
SN 1999dg	Ia	···	0.0212 (0.0038)	40.3 (6.8)	20.4	sn00cx (Ia-pec) 0.0237 (0.0027) 30.06 (15.2090)
SN 1999dk	Ia	Ia-norm	0.0028 (0.0050)	−5.5 (1.6)	11.8	sn04ef (Ia-norm) 0.0139 (0.0057) −5.52 (1.59100)
SN 1999dk	Ia	Ia-norm	0.0136 (0.0027)	13.7 (3.4)	18.2	sn01bg (Ia-norm) 0.0143 (0.0034) 13.70 (2.75300)
SN 1999dk	Ia	Ia-norm	0.0126 (0.0025)	21.7 (0.7)	15.2	sn02bo (Ia-norm) 0.0157 (0.0039) 21.70 (3.59800)
SN 1999dk	Ia	Ia-norm	0.0152 (0.0011)	44.4 (4.2)	19.7	sn02bo (Ia-norm) 0.0151 (0.0030) 44.48 (6.99200)
SN 1999dk	Ia	Ia-norm	0.0157 (0.0014)	79.4 (5.5)	21.8	sn02bo (Ia-norm) 0.0157 (0.0026) 72.50 (12.3480)

Continued on Next Page...

Table 2.7 — Continued

SN Name	Type	Subtype	$z_{\rm SNID}$[a]	$t_{\rm SNID}$[b]	$r$lap	Best Match[c]
SN 1999do	Ia	Ia-norm	0.0197 (0.0058)	9.4 (0.1)	18.2	sn94ae (Ia-norm) 0.0198 (0.0028) 9.30 (0.0710000)
SN 1999dq	Ia	Ia-99aa	0.0183 (0.0068)	−4.5 (1.1)	15.6	sn05eq (Ia-99aa) 0.0122 (0.0033) −2.98 (2.84200)
SN 1999dq	Ia	Ia-norm	0.0161 (0.0060)	6.1 (5.9)	15.0	sn07A (Ia-norm) 0.0123 (0.0034) 2.37 (4.88700)
SN 1999dq	Ia	Ia-norm	0.0128 (0.0026)	19.4 (13.1)	15.7	sn07bc (Ia-norm) 0.0127 (0.0037) 16.35 (13.5960)
SN 1999dq	Ia	···	0.0158 (0.0040)	44.5 (9.4)	18.4	sn98es (Ia-99aa) 0.0128 (0.0029) 57.79 (19.1650)
SN 1999ee	Ia	Ia-91T	0.0109 (0.0000)	18.6 (0.0)	10.9	sn91T (Ia-91T) 0.0109 (0.0055) 18.60 (0.00000)
SN 1999ek	Ia	Ia-norm	0.0220 (0.0054)	7.7 (1.9)	21.1	sn07af (Ia-norm) 0.0191 (0.0025) 3.85 (2.44300)
SN 1999fz	Ia	Ia-norm	0.0224 (0.0027)	38.5 (19.8)	16.7	sn94D (Ia-norm) 0.0238 (0.0034) 17.40 (17.0360)
SN 1999gd	Ia	Ia-norm	0.0215 (0.0045)	0.6 (1.9)	24.5	sn07bc (Ia-norm) 0.0173 (0.0022) 0.61 (3.28100)
SN 1999gf	Ia	Ia-norm	0.0409 (0.0015)	29.4 (3.0)	31.1	sn02bo (Ia-norm) 0.0407 (0.0022) 29.40 (5.50600)
SN 1999gh	Ia	Ia-norm	0.0101 (0.0050)	7.9 (2.0)	17.4	sn00dm (Ia-norm) 0.0075 (0.0035) 8.18 (1.79500)
SN 1999gh	Ia	Ia-norm	0.0070 (0.0010)	28.5 (6.4)	16.0	sn04ef (Ia-norm) 0.0079 (0.0039) 31.23 (5.82900)
SN 1999gh	Ia	Ia-norm	0.0053 (0.0015)	19.6 (2.5)	9.9	sn07gk (Ia-norm) 0.0082 (0.0053) 19.65 (3.34700)
SN 1999gh	Ia	Ia-norm	0.0119 (0.0019)	246.2 (0.0)	5.3	sn90N (Ia-norm) 0.0078 (0.0103) 246.20 (0.00000)
SN 1999gm	Ia	Ia-norm	0.0458 (0.0047)	−0.8 (2.9)	28.1	sn07af (Ia-norm) 0.0438 (0.0019) −1.21 (3.54000)
SN 2000J	Ia	Ia-norm	0.0492 (0.0009)	55.1 (2.8)	15.1	sn94D (Ia-norm) 0.0500 (0.0036) 55.10 (8.44000)
SN 2000al	Ia	Ia-norm	0.1899 (0.0059)	3.5 (5.0)	8.9	sn92A (Ia-norm) 0.2036 (0.0056) −5.00 (4.87500)
SN 2000Q	Ia	Ia-norm	0.0223 (0.0029)	−1.0 (1.6)	19.1	sn07fr (Ia-norm) 0.0210 (0.0028) −1.15 (3.30800)
SN 2000Q	Ia	Ia-91bg	0.0239 (0.0012)	8.4 (10.0)	12.0	sn91bg (Ia-91bg) 0.0247 (0.0051) 27.28 (9.95200)
SN 2000bk	Ia	Ia-norm	0.0253 (0.0024)	16.4 (2.7)	20.2	sn04eo (Ia-norm) 0.0252 (0.0031) 13.19 (8.21400)
SN 2000ce	Ia	Ia-norm	0.0155 (0.0011)	30.0 (8.0)	16.9	sn06os (Ia-norm) 0.0152 (0.0036) 27.16 (8.54800)
SN 2000cn	Ia	Ia-norm	0.0213 (0.0019)	21.5 (8.9)	15.9	sn04fz (Ia-norm) 0.0220 (0.0037) 17.56 (9.67200)
SN 2000cn	Ia	Ia-norm	0.0236 (0.0018)	28.5 (2.5)	24.4	sn04fu (Ia-norm) 0.0255 (0.0026) 25.15 (6.89300)
SN 2000cp	Ia	Ia-norm	0.0363 (0.0050)	0.6 (1.9)	23.3	sn97Y (Ia-norm) 0.0328 (0.0024) 2.31 (3.58800)
SN 2000cp	Ia	Ia-norm	0.0350 (0.0032)	11.5 (2.8)	16.0	sn89B (Ia-norm) 0.0326 (0.0035) 12.40 (4.03300)
SN 2000cv	Ia	Ia-norm	0.0215 (0.0026)	15.5 (3.0)	21.2	sn04eo (Ia-norm) 0.0215 (0.0028) 13.19 (15.0960)
SN 2000cu	Ia	Ia-norm	0.0204 (0.0029)	10.1 (0.8)	21.5	sn05kc (Ia-norm) 0.0204 (0.0027) 10.22 (3.31100)
SN 2000cu	Ia	Ia-norm	0.0208 (0.0012)	40.5 (3.2)	17.8	sn04eo (Ia-norm) 0.0196 (0.0031) 44.40 (8.46800)
SN 2000cw	Ia	Ia-norm	0.0331 (0.0054)	2.8 (3.1)	33.6	sn01ep (Ia-norm) 0.0293 (0.0017) 2.83 (3.05200)
SN 2000cw	Ia	Ia-norm	0.0311 (0.0008)	57.1 (6.5)	16.6	sn94D (Ia-norm) 0.0322 (0.0032) 55.10 (7.22400)
SN 2000cx	Ia	···	0.0041 (0.0050)	−5.6 (1.3)	7.5	sn99dq (Ia-99aa) 0.0053 (0.0070) −3.33 (2.33700)
SN 2000cx	Ia	···	0.0043 (0.0053)	−3.3 (0.8)	7.9	sn01eh (Ia-99aa) 0.0082 (0.0064) −4.53 (3.23800)
SN 2000cx	Ia	···	0.0018 (0.0054)	−1.2 (2.0)	6.9	sn06cz (Ia-99aa) 0.0072 (0.0070) 1.12 (3.78400)
SN 2000cx	Ia	Ia-norm	0.0017 (0.0036)	−1.2 (5.1)	6.5	sn02bo (Ia-norm) 0.0082 (0.0084) −1.20 (5.12500)
SN 2000cx	Ia	···	0.0030 (0.0076)	−0.6 (1.9)	5.4	sn99dq (Ia-99aa) 0.0076 (0.0095) −3.33 (1.91900)
SN 2000cx	···	···	···	···	···	···
SN 2000cx	···	···	···	···	···	···
SN 2000cx	···	···	···	···	···	···
SN 2000cx	Ia	Ia-norm	0.0055 (0.0025)	16.0 (1.7)	9.1	sn07qe (Ia-norm) 0.0085 (0.0065) 16.00 (1.68200)
SN 2000cx	Ia	Ia-norm	0.0066 (0.0019)	13.8 (0.6)	10.9	sn02bo (Ia-norm) 0.0072 (0.0056) 14.80 (0.608000)
SN 2000cx	Ia	Ia-norm	0.0053 (0.0035)	15.7 (1.7)	9.7	sn02bo (Ia-norm) 0.0073 (0.0060) 17.80 (2.43300)
SN 2000cx	Ia	Ia-norm	0.0038 (0.0027)	18.7 (4.1)	6.5	sn02bo (Ia-norm) 0.0072 (0.0086) 18.70 (4.09700)
SN 2000cx	Ia	Ia-norm	0.0043 (0.0020)	18.7 (2.0)	9.8	sn02bo (Ia-norm) 0.0072 (0.0059) 19.80 (3.46900)
SN 2000cx	Ia	Ia-norm	0.0054 (0.0017)	21.7 (1.5)	9.3	sn02bo (Ia-norm) 0.0078 (0.0062) 21.70 (3.22500)
SN 2000cx	Ia	Ia-norm	0.0048 (0.0023)	21.7 (8.6)	9.0	sn02bo (Ia-norm) 0.0087 (0.0064) 21.70 (8.62100)
SN 2000cx	Ia	Ia-norm	0.0058 (0.0024)	18.9 (5.3)	7.4	sn01bg (Ia-norm) 0.0079 (0.0084) 18.91 (5.28900)
SN 2000cx	Ia	Ia-norm	0.0078 (0.0033)	59.1 (15.4)	8.9	sn02fk (Ia-norm) 0.0072 (0.0060) 72.46 (17.4360)
SN 2000cx	Ia	Ia-norm	0.0060 (0.0010)	87.9 (0.0)	11.0	sn94ae (Ia-norm) 0.0072 (0.0051) 87.95 (0.00000)
SN 2000cx	Ia	Ia-norm	0.0066 (0.0008)	85.5 (0.0)	12.5	sn98ef (Ia-norm) 0.0072 (0.0046) 85.52 (0.00000)
SN 2000cx	Ia	Ia-norm	0.0078 (0.0006)	87.2 (1.2)	10.9	sn98ef (Ia-norm) 0.0078 (0.0052) 85.52 (1.18400)
SN 2000cx	Ia	Ia-norm	0.0079 (0.0007)	115.1 (19.7)	10.7	sn94D (Ia-norm) 0.0074 (0.0053) 115.09 (19.7260)
SN 2000cx	Ia	Ia-norm	0.0080 (0.0000)	115.1 (0.0)	10.8	sn94D (Ia-norm) 0.0080 (0.0051) 115.09 (0.00000)
SN 2000cx	···	···	···	···	···	···
SN 2000dd	Ia	Ia-norm	0.0363 (0.0015)	17.3 (0.0)	10.1	sn92A (Ia-norm) 0.0412 (0.0060) 17.30 (0.00000)
SN 2000df	Ia	Ia-norm	0.0381 (0.0013)	14.9 (7.1)	21.6	sn01dw (Ia-norm) 0.0389 (0.0030) 11.06 (8.03600)
SN 2000dg	Ia	Ia-norm	0.0387 (0.0041)	−5.2 (3.0)	28.2	sn04fz (Ia-norm) 0.0364 (0.0017) −5.18 (3.02600)
SN 2000dg	Ia	Ia-norm	0.0408 (0.0052)	7.7 (1.6)	22.4	sn02er (Ia-norm) 0.0405 (0.0024) 5.50 (2.94400)
SN 2000dk	Ia	Ia-norm	0.0195 (0.0047)	1.6 (3.4)	32.1	sn05bc (Ia-norm) 0.0173 (0.0017) 1.65 (3.44200)
SN 2000dk	Ia	Ia-norm	0.0193 (0.0030)	13.2 (2.3)	19.1	sn04eo (Ia-norm) 0.0174 (0.0031) 13.19 (3.25800)
SN 2000dk	Ia	Ia-norm	0.0184 (0.0015)	33.7 (1.4)	24.4	sn02eu (Ia-norm) 0.0180 (0.0023) 33.44 (6.95000)

Continued on Next Page...

Table 2.7 — Continued

SN Name	Type	Subtype	$z_{\rm SNID}$[a]	$t_{\rm SNID}$[b]	$r$lap	Best Match[c]
SN 2000dk	Ia	Ia-norm	0.0185 (0.0010)	41.5 (5.0)	20.3	sn04eo (Ia-norm) 0.0170 (0.0027) 44.40 (7.76400)
SN 2000dm	Ia	Ia-norm	0.0170 (0.0046)	−1.8 (2.7)	21.6	sn94D (Ia-norm) 0.0152 (0.0023) −1.80 (3.14300)
SN 2000dm	Ia	Ia-norm	0.0166 (0.0038)	7.9 (2.4)	34.8	sn02ha (Ia-norm) 0.0156 (0.0015) 7.89 (2.37600)
SN 2000dm	Ia	Ia-norm	0.0155 (0.0012)	30.0 (4.0)	20.0	sn02eu (Ia-norm) 0.0151 (0.0028) 33.44 (7.12600)
SN 2000dm	Ia	Ia-norm	0.0145 (0.0011)	36.1 (7.8)	11.5	sn02eu (Ia-norm) 0.0150 (0.0046) 33.44 (7.81200)
SN 2000dn	Ia	Ia-norm	0.0355 (0.0044)	1.3 (2.8)	23.2	sn02cr (Ia-norm) 0.0331 (0.0024) −6.78 (3.06300)
SN 2000dn	Ia	Ia-norm	0.0347 (0.0029)	14.3 (3.0)	27.0	sn94D (Ia-norm) 0.0349 (0.0021) 13.40 (16.6010)
SN 2000dp	Ia	Ia-norm	0.0355 (0.0048)	4.8 (1.7)	39.5	sn97Y (Ia-norm) 0.0325 (0.0014) 2.31 (3.66200)
SN 2000dp	Ia	···	0.0346 (0.0049)	17.4 (4.3)	29.8	sn99dq (Ia-99aa) 0.0357 (0.0021) 24.09 (17.8520)
SN 2000dr	Ia	Ia-norm	0.0207 (0.0034)	7.8 (0.6)	17.8	sn01ep (Ia-norm) 0.0194 (0.0032) 7.85 (2.43900)
SN 2000dx	Ia	Ia-norm	0.0276 (0.0033)	−6.0 (1.6)	15.9	sn02bo (Ia-norm) 0.0291 (0.0041) −6.00 (2.50100)
SN 2000ej	Ia	···	0.0358 (0.0064)	39.5 (4.1)	7.8	sn91bg (Ia-91bg) 0.0314 (0.0080) 33.70 (7.09100)
SN 2000ey	Ia	Ia-norm	0.0168 (0.0051)	3.7 (3.7)	11.4	sn05ms (Ia-norm) 0.0217 (0.0052) −1.51 (3.69500)
SN 2000ey	Ia	Ia-norm	0.0179 (0.0013)	11.1 (0.0)	10.9	sn01dw (Ia-norm) 0.0199 (0.0059) 11.06 (0.00000)
SN 2000ey	NotSN	Gal	0.0219 (0.0000)	···	7.0	kcSa (Gal) 0.0219 (0.0030) −99.90 (0.00000)
SN 2000fa	Ia	Ia-norm	0.0077 (0.0082)	−5.5 (3.1)	9.9	sn04ef (Ia-norm) 0.0192 (0.0063) −5.52 (2.51100)
SN 2000fa	Ia	Ia-norm	0.0178 (0.0046)	7.1 (2.1)	17.5	sn06bu (Ia-norm) 0.0214 (0.0034) 4.24 (3.97500)
SN 2000fo	Ia	Ia-norm	0.0275 (0.0017)	28.5 (5.2)	9.6	sn06lf (Ia-norm) 0.0245 (0.0059) 25.06 (7.50900)
SN 2001A	Ia	Ia-91T	0.0224 (0.0113)	112.8 (0.0)	6.3	sn91T (Ia-91T) 0.0096 (0.0086) 112.82 (0.00000)
SN 2001C	Ia	Ia-norm	0.0103 (0.0030)	17.4 (3.4)	13.2	sn05cf (Ia-norm) 0.0109 (0.0044) 18.69 (3.43600)
SN 2001C	Ia	Ia-norm	0.0107 (0.0010)	36.2 (9.9)	17.4	sn94ae (Ia-norm) 0.0101 (0.0032) 36.20 (7.03400)
SN 2001E	Ia	Ia-norm	0.0126 (0.0035)	10.8 (2.3)	8.6	sn02bo (Ia-norm) 0.0182 (0.0067) 10.80 (2.26400)
SN 2001G	Ia	Ia-norm	0.0146 (0.0033)	12.3 (1.9)	27.5	sn02jy (Ia-norm) 0.0153 (0.0020) 12.30 (1.89700)
SN 2001L	Ia	Ia-norm	0.0147 (0.0019)	21.4 (8.5)	17.4	sn04fz (Ia-norm) 0.0158 (0.0031) 17.56 (11.2130)
SN 2001N	Ia	Ia-norm	0.0160 (0.0046)	11.9 (2.7)	9.0	sn04ef (Ia-norm) 0.0209 (0.0069) 8.05 (4.04200)
SN 2001P	Ia	Ia-91bg	0.0226 (0.0017)	11.0 (3.8)	15.1	sn05ke (Ia-91bg) 0.0217 (0.0041) 9.87 (7.15700)
SN 2001U	Ia	Ia-norm	0.0295 (0.0011)	59.1 (8.0)	16.5	sn98bu (Ia-norm) 0.0297 (0.0025) 57.10 (7.89600)
SN 2001V	Ia	Ia-norm	0.0142 (0.0024)	13.7 (3.0)	19.6	sn01bg (Ia-norm) 0.0150 (0.0031) 13.70 (2.98300)
SN 2001V	Ia	Ia-norm	0.0146 (0.0026)	22.7 (1.5)	16.7	sn07fs (Ia-norm) 0.0139 (0.0029) 22.67 (1.73900)
SN 2001V	Ia	···	0.0134 (0.0046)	24.1 (5.4)	18.0	sn99dq (Ia-99aa) 0.0150 (0.0033) 24.09 (12.2770)
SN 2001V	Ia	Ia-norm	0.0138 (0.0011)	44.1 (15.3)	12.1	sn98bu (Ia-norm) 0.0149 (0.0037) 44.10 (15.2670)
SN 2001V	Ia	Ia-norm	0.0156 (0.0020)	51.1 (5.6)	20.3	sn07fs (Ia-norm) 0.0144 (0.0027) 51.13 (7.81800)
SN 2001V	Ia	Ia-norm	0.0157 (0.0014)	69.6 (6.1)	16.4	sn02er (Ia-norm) 0.0156 (0.0035) 60.98 (10.7010)
SN 2001ay	Ia	Ia-norm	0.0272 (0.0054)	2.3 (4.6)	8.5	sn92A (Ia-norm) 0.0304 (0.0067) 8.90 (4.76800)
SN 2001ay	Ia	Ia-norm	0.0290 (0.0023)	12.5 (2.7)	18.4	sn00dk (Ia-norm) 0.0291 (0.0035) 11.19 (13.1250)
SN 2001az	Ia	Ia-norm	0.0378 (0.0045)	−2.8 (2.9)	16.5	sn06N (Ia-norm) 0.0386 (0.0032) −1.94 (2.47700)
SN 2001ba	Ia	Ia-norm	0.0271 (0.0063)	−2.5 (2.2)	9.4	sn90N (Ia-norm) 0.0317 (0.0085) −6.40 (3.07900)
SN 2001bf	Ia	Ia-norm	0.0176 (0.0044)	−2.1 (2.8)	7.7	sn94D (Ia-norm) 0.0159 (0.0071) −5.96 (3.23000)
SN 2001bf	Ia	Ia-norm	0.0179 (0.0000)	81.6 (0.0)	13.5	sn04dt (Ia-norm) 0.0179 (0.0039) 81.59 (0.00000)
SN 2001bg	Ia	Ia-norm	0.0059 (0.0029)	11.0 (5.4)	19.6	sn06or (Ia-norm) 0.0067 (0.0031) 4.80 (3.89900)
SN 2001bg	Ia	Ia-norm	0.0069 (0.0018)	16.9 (2.3)	13.1	sn06ev (Ia-norm) 0.0067 (0.0046) 16.85 (2.29900)
SN 2001br	Ia	Ia-99aa	0.0218 (0.0021)	3.3 (0.0)	10.1	sn01eh (Ia-99aa) 0.0203 (0.0057) 3.26 (0.00000)
SN 2001br	Ia	Ia-norm	0.0173 (0.0043)	−1.5 (3.5)	13.5	sn89B (Ia-norm) 0.0195 (0.0045) −6.30 (3.52500)
SN 2001bp	Ia	Ia-norm	0.0927 (0.0067)	2.4 (4.3)	12.2	sn94ae (Ia-norm) 0.0928 (0.0041) 2.30 (4.33000)
SN 2001bp	Ia	Ia-norm	0.0925 (0.0013)	10.3 (1.9)	10.3	sn03he (Ia-norm) 0.0943 (0.0053) 8.53 (1.88500)
SN 2001bs	Ia	Ia-norm	0.0253 (0.0034)	−6.3 (2.5)	7.1	sn02he (Ia-norm) 0.0320 (0.0064) −5.91 (2.67500)
SN 2001cg	Ia	Ia-91bg	0.0248 (0.0023)	3.1 (0.8)	20.4	sn99by (Ia-91bg) 0.0240 (0.0028) 3.10 (2.26000)
SN 2001cj	Ia	Ia-norm	0.0243 (0.0024)	17.4 (3.1)	22.4	sn07fs (Ia-norm) 0.0239 (0.0027) 22.67 (15.1290)
SN 2001ck	Ia	Ia-norm	0.0354 (0.0022)	14.3 (2.1)	30.6	sn98bu (Ia-norm) 0.0350 (0.0019) 14.30 (2.10600)
SN 2001ck	Ia	···	0.0355 (0.0045)	29.5 (5.1)	28.8	sn01eh (Ia-99aa) 0.0369 (0.0022) 32.08 (14.7380)
SN 2001cp	Ia	Ia-norm	0.0224 (0.0044)	2.4 (2.0)	19.4	sn94ae (Ia-norm) 0.0220 (0.0027) 2.30 (2.20400)
SN 2001cp	Ia	Ia-norm	0.0225 (0.0028)	14.3 (3.0)	21.1	sn98bu (Ia-norm) 0.0233 (0.0027) 13.20 (3.95200)
SN 2001cp	Ia	Ia-norm	0.0223 (0.0023)	22.7 (14.3)	19.2	sn07fs (Ia-norm) 0.0233 (0.0031) 22.67 (14.4860)
SN 2001da	Ia	Ia-norm	0.0176 (0.0061)	−1.7 (1.3)	14.2	sn98bu (Ia-norm) 0.0162 (0.0038) −0.70 (1.46400)
SN 2001da	Ia	Ia-norm	0.0170 (0.0033)	10.2 (1.5)	25.4	sn05kc (Ia-norm) 0.0165 (0.0024) 10.22 (3.68800)
SN 2001de	Ia	···	0.0314 (0.0062)	2.1 (1.9)	23.2	sn07ba (Ia-91bg) 0.0298 (0.0023) 2.09 (6.62700)
SN 2001dd	Ia	Ia-norm	0.0207 (0.0041)	7.7 (0.2)	26.9	sn03ai (Ia-norm) 0.0182 (0.0020) 7.73 (2.61600)
SN 2001dl	Ia	Ia-norm	0.0210 (0.0027)	13.7 (1.1)	20.7	sn95D (Ia-norm) 0.0210 (0.0025) 14.10 (2.32800)
SN 2001dl	Ia	Ia-norm	0.0210 (0.0013)	39.3 (6.7)	15.2	sn94D (Ia-norm) 0.0202 (0.0036) 43.96 (7.60400)
SN 2001dm	Ia	···	0.0172 (0.0045)	44.4 (8.2)	8.3	sn05eq (Ia-99aa) 0.0142 (0.0065) 51.16 (8.25300)

Continued on Next Page...

Table 2.7 — Continued

SN Name	Type	Subtype	$z_{\rm SNID}$[a]	$t_{\rm SNID}$[b]	$r$lap	Best Match[c]
SN 2001dn	Ia	Ia-norm	0.0198 (0.0011)	33.0 (6.7)	16.0	sn01dw (Ia-norm) 0.0198 (0.0039) 11.06 (7.46000)
SN 2001ds	Ia	Ia-norm	0.0341 (0.0015)	28.5 (5.2)	6.9	sn94D (Ia-norm) 0.0379 (0.0111) 26.20 (5.00600)
SN 2001ei	Ia	···	0.0287 (0.0043)	18.6 (1.7)	22.2	sn05bl (Ia-91bg) 0.0302 (0.0026) 17.19 (14.0400)
SN 2001ei	Ia	Ia-91bg	0.0282 (0.0001)	53.5 (0.1)	13.1	sn91bg (Ia-91bg) 0.0282 (0.0046) 53.50 (0.141000)
SN 2001dt	Ia	Ia-norm	0.0295 (0.0024)	14.8 (3.4)	17.6	sn06ev (Ia-norm) 0.0283 (0.0038) 16.85 (3.30600)
SN 2001dw	Ia	Ia-norm	0.0250 (0.0016)	27.2 (6.3)	20.2	sn94ae (Ia-norm) 0.0241 (0.0027) 30.20 (8.00300)
SN 2001eg	Ia	Ia-norm	0.0134 (0.0010)	85.5 (8.2)	13.2	sn98ef (Ia-norm) 0.0140 (0.0047) 85.52 (8.22600)
SN 2001ec	Ia	Ia-norm	0.0470 (0.0016)	13.4 (10.1)	23.8	sn98bu (Ia-norm) 0.0467 (0.0024) 14.30 (4.08800)
SN 2001ed	Ia	Ia-norm	0.0165 (0.0006)	38.3 (5.7)	13.5	sn02bo (Ia-norm) 0.0162 (0.0041) 44.40 (6.69400)
SN 2001eh	Ia	Ia-99aa	0.0343 (0.0066)	−3.0 (1.0)	19.5	sn05eq (Ia-99aa) 0.0343 (0.0028) −2.98 (1.04000)
SN 2001eh	Ia	Ia-99aa	0.0354 (0.0066)	−3.0 (1.0)	21.2	sn05eq (Ia-99aa) 0.0354 (0.0026) −2.98 (1.04000)
SN 2001eh	Ia	···	0.0367 (0.0054)	0.7 (3.9)	22.6	sn05eq (Ia-99aa) 0.0353 (0.0024) 0.66 (3.86000)
SN 2001eh	Ia	Ia-norm	0.0359 (0.0012)	26.5 (5.0)	33.0	sn07fs (Ia-norm) 0.0354 (0.0020) 29.49 (8.85200)
SN 2001eh	Ia	Ia-norm	0.0368 (0.0017)	28.5 (3.6)	24.0	sn02bo (Ia-norm) 0.0380 (0.0028) 27.59 (7.96500)
SN 2001eh	Ia	···	0.0398 (0.0037)	75.2 (17.8)	23.9	sn91T (Ia-91T) 0.0369 (0.0024) 75.20 (21.9740)
SN 2001eu	Ia	Ia-91T	0.1294 (0.0039)	37.6 (9.8)	7.3	sn97br (Ia-91T) 0.1322 (0.0074) 23.70 (9.82900)
SN 2001en	Ia	Ia-norm	0.0131 (0.0028)	11.0 (2.5)	16.9	sn04ef (Ia-norm) 0.0152 (0.0035) 8.05 (2.73100)
SN 2001en	Ia	Ia-norm	0.0148 (0.0025)	13.2 (3.5)	21.9	sn01bg (Ia-norm) 0.0157 (0.0028) 13.70 (2.82300)
SN 2001en	Ia	Ia-norm	0.0157 (0.0016)	37.2 (5.3)	16.4	sn02jy (Ia-norm) 0.0155 (0.0034) 39.90 (6.95400)
SN 2001ep	Ia	Ia-norm	0.0165 (0.0050)	3.8 (2.8)	25.8	sn07af (Ia-norm) 0.0125 (0.0021) 3.85 (2.84900)
SN 2001ep	Ia	Ia-norm	0.0164 (0.0050)	6.1 (0.2)	22.4	sn02hd (Ia-norm) 0.0141 (0.0026) 6.05 (1.25900)
SN 2001ep	Ia	Ia-norm	0.0160 (0.0039)	7.7 (1.4)	16.3	sn02ha (Ia-norm) 0.0140 (0.0034) 7.89 (1.29800)
SN 2001ep	Ia	Ia-norm	0.0157 (0.0037)	8.7 (1.5)	15.2	sn05de (Ia-norm) 0.0127 (0.0036) 10.10 (1.53700)
SN 2001ep	Ia	Ia-norm	0.0150 (0.0012)	32.0 (5.7)	16.2	sn02eu (Ia-norm) 0.0142 (0.0034) 33.44 (4.83000)
SN 2001ep	Ia	Ia-norm	0.0145 (0.0013)	84.6 (8.3)	15.5	sn07fs (Ia-norm) 0.0132 (0.0036) 91.35 (7.97500)
SN 2001ep	Ia	Ia-norm	0.0161 (0.0015)	113.8 (15.9)	12.7	sn07af (Ia-norm) 0.0137 (0.0041) 113.82 (15.9480)
SN 2001er	Ia	Ia-norm	0.0169 (0.0004)	50.0 (6.6)	13.6	sn94D (Ia-norm) 0.0169 (0.0037) 53.90 (6.60900)
SN 2001es	NotSN	M-star	0.0664 (0.0000)	···	5.6	mstar (M-star) 0.0664 (0.0080) 0.00 (0.00000)
SN 2001es	Ia	Ia-norm	0.0675 (0.0013)	28.5 (6.6)	7.7	sn04fz (Ia-norm) 0.0672 (0.0074) 22.28 (7.94400)
SN 2001ew	Ia	Ia-norm	0.0318 (0.0044)	5.6 (2.0)	33.2	sn01ep (Ia-norm) 0.0292 (0.0018) 2.83 (3.09900)
SN 2001fg	Ia	Ia-norm	0.0321 (0.0003)	79.4 (5.5)	11.3	sn02bo (Ia-norm) 0.0323 (0.0049) 72.50 (5.46900)
SN 2001ex	Ia	···	0.0301 (0.0053)	2.1 (4.1)	19.0	sn06gt (Ia-91bg) 0.0272 (0.0026) 2.09 (4.10000)
SN 2001fe	Ia	Ia-norm	0.0126 (0.0014)	2.3 (3.1)	12.9	sn94ae (Ia-norm) 0.0123 (0.0039) 2.30 (3.10900)
SN 2001fh	Ia	Ia-norm	0.0154 (0.0053)	4.9 (0.8)	23.1	sn02ha (Ia-norm) 0.0134 (0.0023) 4.93 (2.41200)
SN 2001fh	Ia	Ia-norm	0.0158 (0.0049)	8.2 (0.2)	24.1	sn02ha (Ia-norm) 0.0140 (0.0023) 7.89 (1.64000)
SN 2001fu	Ia	Ia-norm	0.0068 (0.0009)	36.2 (3.9)	15.6	sn06dm (Ia-norm) 0.0061 (0.0037) 36.06 (4.95100)
SN 2001gc	Ia	Ia-norm	0.0178 (0.0006)	44.4 (0.1)	16.0	sn02bo (Ia-norm) 0.0176 (0.0039) 44.48 (2.66500)
SN 2001ic	NotSN	···	0.0449 (0.0013)	1.0 (52.8)	7.8	kcE (Gal) 0.0436 (0.0029) −99.90 (0.00000)
SN 2001ic	Ia	Ia-norm	0.0389 (0.0023)	19.6 (6.0)	30.7	sn07gk (Ia-norm) 0.0408 (0.0023) 19.65 (6.01500)
SN 2001ib	Ia	Ia-norm	0.0232 (0.0044)	7.7 (1.8)	18.6	sn02ha (Ia-norm) 0.0209 (0.0026) 4.93 (2.42900)
SN 2001ib	Ia	Ia-norm	0.0210 (0.0013)	30.2 (5.5)	17.7	sn02cr (Ia-norm) 0.0190 (0.0033) 33.69 (6.10100)
SN 2001iq	Ia	Ia-norm	0.0168 (0.0047)	−6.4 (0.8)	16.8	sn02er (Ia-norm) 0.0201 (0.0037) −6.40 (2.04300)
SN 2001iq	Ia	Ia-norm	0.0204 (0.0024)	16.4 (3.4)	11.7	sn07bc (Ia-norm) 0.0175 (0.0054) 16.35 (3.43500)
SN 2002G	Ia	Ia-norm	0.0299 (0.0022)	18.7 (3.8)	19.0	sn00cn (Ia-norm) 0.0318 (0.0035) 14.95 (9.37300)
SN 2002ar	Ia	Ia-norm	0.0332 (0.0056)	−5.0 (1.2)	9.2	sn94D (Ia-norm) 0.0278 (0.0057) −5.96 (4.26000)
SN 2002av	Ia	Ia-norm	0.0444 (0.0052)	7.2 (1.6)	26.8	sn06bu (Ia-norm) 0.0470 (0.0025) 4.24 (3.76700)
SN 2002av	Ia	Ia-norm	0.0443 (0.0045)	9.6 (1.6)	26.5	sn00fa (Ia-norm) 0.0490 (0.0023) 7.34 (1.55300)
SN 2002av	···	···	···	···	···	···
SN 2002bk	Ia	···	0.0554 (0.0045)	37.8 (5.0)	21.6	sn91T (Ia-91T) 0.0541 (0.0026) 45.70 (12.8450)
SN 2002aw	Ia	Ia-norm	0.0290 (0.0044)	−0.2 (4.1)	16.3	sn00cp (Ia-norm) 0.0283 (0.0033) 3.21 (3.72700)
SN 2002aw	Ia	Ia-norm	0.0279 (0.0021)	15.3 (0.6)	31.3	sn89B (Ia-norm) 0.0266 (0.0018) 14.40 (4.51000)
SN 2002bf	Ia	Ia-norm	0.0218 (0.0041)	−1.5 (0.9)	12.5	sn02bo (Ia-norm) 0.0220 (0.0050) −1.20 (0.930000)
SN 2002bf	Ia	Ia-norm	0.0144 (0.0039)	6.7 (4.7)	13.4	sn06bq (Ia-norm) 0.0223 (0.0046) 6.69 (4.74100)
SN 2002bg	Ia	Ia-norm	0.0446 (0.0027)	16.1 (1.9)	30.0	sn95D (Ia-norm) 0.0438 (0.0019) 16.10 (2.70300)
SN 2002bi	Ia	Ia-norm	0.0249 (0.0012)	33.7 (6.5)	16.1	sn02cr (Ia-norm) 0.0247 (0.0035) 24.90 (6.57800)
SN 2002bp	Ia	Ia-02cx	0.0280 (0.0020)	32.1 (10.7)	7.0	sn05hk (Ia-02cx) 0.028 (0.005) 27.2 (0.00000)
SN 2002bo	···	···	···	···	···	···
SN 2002bo	Ia	Ia-norm	−0.0016 (0.0051)	−2.8 (4.2)	16.0	sn02er (Ia-norm) 0.0054 (0.0039) −6.40 (3.54500)
SN 2002bo	Ia	Ia-norm	0.0023 (0.0026)	11.0 (3.7)	14.2	sn01bg (Ia-norm) 0.0036 (0.0043) 13.70 (3.32800)
SN 2002bo	Ia	Ia-norm	0.0026 (0.0009)	28.5 (7.0)	13.6	sn04fu (Ia-norm) 0.0043 (0.0044) 25.15 (7.02500)

Continued on Next Page...

Table 2.7 — Continued

SN Name	Type	Subtype	$z_{\rm SNID}$[a]	$t_{\rm SNID}$[b]	$r$lap	Best Match[c]
SN 2002bo	Ia	Ia-norm	0.0040 (0.0008)	51.1 (4.9)	17.0	sn99dk (Ia-norm) 0.0040 (0.0034) 44.20 (11.4910)
SN 2002bo	Ia	···	0.0069 (0.0037)	61.0 (8.7)	14.6	sn99aa (Ia-99aa) 0.0049 (0.0039) 59.43 (19.1100)
SN 2002bo	Ia	···	0.0077 (0.0034)	87.3 (14.1)	8.4	sn98es (Ia-99aa) 0.0053 (0.0063) 57.79 (25.8820)
SN 2002bo	Ia	···	0.0072 (0.0016)	256.0 (26.7)	7.8	sn90N (Ia-norm) 0.0048 (0.0074) 246.20 (34.4280)
SN 2002bs	Ia	Ia-norm	0.0126 (0.0027)	12.4 (2.1)	11.0	sn06ev (Ia-norm) 0.0101 (0.0054) 16.85 (2.08600)
SN 2002bz	Ia	Ia-norm	0.0375 (0.0043)	2.2 (3.8)	28.0	sn03iv (Ia-norm) 0.0358 (0.0017) 2.16 (3.75000)
SN 2002cc	Ia	Ia-norm	0.0700 (0.0021)	14.5 (4.7)	15.6	sn94D (Ia-norm) 0.0696 (0.0033) 15.30 (3.96900)
SN 2002cd	Ia	Ia-norm	−0.0019 (0.0053)	5.9 (7.3)	12.8	sn92A (Ia-norm) 0.0099 (0.0044) 5.90 (7.25300)
SN 2002cd	Ia	Ia-norm	0.0049 (0.0020)	14.3 (1.3)	12.1	sn07qe (Ia-norm) 0.0080 (0.0049) 16.00 (1.28500)
SN 2002cd	Ia	Ia-norm	0.0109 (0.0000)	72.5 (0.0)	11.2	sn02bo (Ia-norm) 0.0109 (0.0050) 72.50 (0.00000)
SN 2002cf	Ia	···	0.0165 (0.0056)	2.1 (1.9)	21.5	sn06gt (Ia-91bg) 0.0134 (0.0023) 2.09 (5.17400)
SN 2002cf	Ia	Ia-91bg	0.0127 (0.0000)	14.9 (0.0)	13.3	sn05ke (Ia-91bg) 0.0127 (0.0045) 14.85 (0.00000)
SN 2002ci	Ia	Ia-norm	0.0223 (0.0045)	2.3 (2.3)	18.1	sn02he (Ia-norm) 0.0244 (0.0030) 3.22 (3.22100)
SN 2002ck	Ia	Ia-norm	0.0314 (0.0052)	6.4 (1.8)	19.1	sn95D (Ia-norm) 0.0298 (0.0029) 6.10 (3.45100)
SN 2002cr	Ia	Ia-norm	0.0115 (0.0040)	2.3 (0.6)	23.6	sn07A (Ia-norm) 0.0088 (0.0023) 2.37 (2.50000)
SN 2002cr	Ia	Ia-norm	0.0101 (0.0017)	38.3 (4.5)	17.6	sn95D (Ia-norm) 0.0088 (0.0028) 37.80 (6.24500)
SN 2002cr	Ia	Ia-norm	0.0115 (0.0011)	39.5 (3.9)	16.9	sn06dm (Ia-norm) 0.0103 (0.0032) 36.06 (4.14600)
SN 2002cr	Ia	Ia-norm	0.0101 (0.0010)	53.9 (10.5)	18.2	sn94D (Ia-norm) 0.0104 (0.0026) 53.90 (12.6110)
SN 2002cr	Ia	Ia-norm	0.0104 (0.0017)	87.3 (8.5)	12.8	sn01ep (Ia-norm) 0.0090 (0.0043) 87.26 (8.50600)
SN 2002cs	Ia	Ia-norm	0.0018 (0.0039)	−6.3 (1.0)	11.9	sn99dk (Ia-norm) 0.0128 (0.0047) −6.92 (0.976000)
SN 2002cs	Ia	Ia-norm	0.0099 (0.0013)	27.2 (5.5)	14.3	sn06ej (Ia-norm) 0.0129 (0.0041) 21.65 (5.41100)
SN 2002cs	Ia	Ia-norm	0.0127 (0.0010)	25.1 (0.0)	12.5	sn04fu (Ia-norm) 0.0145 (0.0047) 25.15 (0.00000)
SN 2002cs	Ia	Ia-norm	0.0139 (0.0011)	27.6 (4.8)	17.3	sn90N (Ia-norm) 0.0146 (0.0030) 38.50 (6.70100)
SN 2002cs	Ia	Ia-norm	0.0143 (0.0010)	49.6 (7.0)	12.3	sn98bu (Ia-norm) 0.0152 (0.0045) 59.12 (6.99100)
SN 2002cs	Ia	Ia-norm	0.0139 (0.0011)	87.9 (1.7)	11.2	sn98ef (Ia-norm) 0.0146 (0.0052) 85.52 (1.71600)
SN 2002cs	Ia	Ia-norm	0.0144 (0.0013)	92.5 (4.9)	10.8	sn98ef (Ia-norm) 0.0145 (0.0055) 85.52 (4.92800)
SN 2002cs	Ia	···	0.0168 (0.0031)	113.2 (94.1)	5.9	sn94ae (Ia-norm) 0.0152 (0.0114) 367.70 (94.0990)
SN 2002cu	Ia	Ia-norm	0.0180 (0.0041)	−5.6 (1.8)	12.4	sn07bd (Ia-norm) 0.0221 (0.0046) −5.58 (1.84400)
SN 2002cu	Ia	Ia-norm	0.0200 (0.0022)	16.9 (3.8)	13.0	sn06ev (Ia-norm) 0.0218 (0.0049) 16.85 (3.78600)
SN 2002cx	Ia	Ia-02cx	0.0232 (0.0016)	23.4 (4.4)	16.5	sn05hk (Ia-02cx) 0.0249 (0.0026) 14.30 (4.73000)
SN 2002cx	Ia	Ia-02cx	0.0240 (0.0011)	23.4 (0.9)	20.6	sn05hk (Ia-02cx) 0.0243 (0.0019) 21.87 (8.16400)
SN 2002cx	Ia	Ia-02cx	0.0237 (0.0011)	23.4 (0.0)	16.4	sn05hk (Ia-02cx) 0.0242 (0.0023) 23.40 (2.19500)
SN 2002cx	Ia	Ia-02cx	0.0241 (0.0002)	23.4 (0.9)	13.5	sn05hk (Ia-02cx) 0.0241 (0.0026) 23.40 (0.882000)
SN 2002cx	Ia	Ia-02cx	0.0248 (0.0005)	51.0 (5.7)	18.3	sn05hk (Ia-02cx) 0.0244 (0.0018) 50.96 (6.31800)
SN 2002cx	II	IIP	0.0240 (0.0013)	236.8 (89.0)	7.4	sn04et (IIP) 0.0236 (0.0033) 229.70 (0.00000)
SN 2002cx	II	IIP	0.0243 (0.0011)	242.8 (84.2)	8.9	sn04et (IIP) 0.0242 (0.0026) 229.70 (0.00000)
SN 2002cx	···	···	···	···	···	···
SN 2002cv	···	···	···	···	···	···
SN 2002cv	Ia	Ia-norm	0.0046 (0.0003)	54.6 (25.2)	9.8	sn04ey (Ia-norm) 0.0044 (0.0064) 18.90 (28.6800)
SN 2002db	Ia	Ia-norm	0.0314 (0.0044)	7.3 (0.1)	15.6	sn07kk (Ia-norm) 0.0386 (0.0036) 7.15 (1.77200)
SN 2002de	Ia	Ia-norm	0.0265 (0.0044)	−1.5 (3.8)	16.2	sn89B (Ia-norm) 0.0274 (0.0038) −6.30 (3.04700)
SN 2002de	Ia	Ia-norm	0.0253 (0.0042)	8.1 (1.8)	13.7	sn94ae (Ia-norm) 0.0257 (0.0038) 9.30 (3.50800)
SN 2002df	Ia	Ia-norm	0.0301 (0.0034)	7.8 (1.9)	16.6	sn05bc (Ia-norm) 0.0276 (0.0034) 7.47 (2.15500)
SN 2002di	Ic	Ic-norm	0.0406 (0.0051)	···	13.5	sn08gj (Ic-norm) 0.0387 (0.0042) −999.00 (0.00000)
SN 2002dj	Ia	Ia-norm	−0.0015 (0.0054)	−6.5 (1.4)	13.3	sn00fa (Ia-norm) 0.0074 (0.0051) −7.77 (1.38700)
SN 2002dk	Ia	Ia-91bg	0.0145 (0.0000)	−1.5 (0.0)	10.6	sn99da (Ia-91bg) 0.0174 (0.0057) −1.52 (0.00000)
SN 2002do	Ia	Ia-norm	0.0172 (0.0024)	29.0 (4.7)	10.0	sn02cr (Ia-norm) 0.0152 (0.0055) 33.69 (6.38600)
SN 2002dp	Ia	Ia-norm	0.0140 (0.0024)	14.4 (2.1)	20.3	sn05cf (Ia-norm) 0.0119 (0.0029) 18.69 (10.5300)
SN 2002dp	Ia	Ia-norm	0.0130 (0.0008)	41.5 (4.3)	19.3	sn02fk (Ia-norm) 0.0128 (0.0027) 41.50 (7.78400)
SN 2002dp	Ia	Ia-norm	0.0131 (0.0011)	76.3 (9.1)	14.0	sn94ae (Ia-norm) 0.0126 (0.0036) 70.00 (9.62100)
SN 2002dp	Ia	Ia-norm	0.0118 (0.0013)	87.2 (22.3)	14.8	sn94ae (Ia-norm) 0.0124 (0.0035) 123.60 (15.5890)
SN 2002dp	Ia	Ia-norm	0.0132 (0.0015)	213.0 (34.5)	10.3	sn94ae (Ia-norm) 0.0123 (0.0052) 153.40 (34.5260)
SN 2002dr	Ia	···	0.0249 (0.0050)	46.5 (13.6)	7.0	sn91bg (Ia-91bg) 0.0238 (0.0078) 46.50 (16.6860)
SN 2002dx	Ia	Ia-norm	0.0252 (0.0012)	91.3 (4.8)	12.6	sn07fs (Ia-norm) 0.0252 (0.0041) 91.35 (4.77900)
SN 2002eb	Ia	···	0.0295 (0.0055)	0.7 (0.0)	23.7	sn05eq (Ia-99aa) 0.0272 (0.0022) 0.66 (4.68100)
SN 2002eb	Ia	Ia-norm	0.0272 (0.0016)	25.8 (7.7)	24.3	sn05cf (Ia-norm) 0.0265 (0.0025) 27.64 (9.31700)
SN 2002eb	Ia	Ia-norm	0.0295 (0.0013)	51.1 (4.7)	26.5	sn94D (Ia-norm) 0.0295 (0.0020) 50.10 (17.2190)
SN 2002ec	Ia	Ia-norm	0.0344 (0.0023)	14.3 (2.4)	18.5	sn02bo (Ia-norm) 0.0371 (0.0034) 10.80 (2.55000)
SN 2002ec	Ia	Ia-norm	0.0393 (0.0016)	28.5 (2.2)	19.7	sn98ef (Ia-norm) 0.0396 (0.0033) 28.51 (6.84400)
SN 2002ef	Ia	Ia-norm	0.0236 (0.0046)	3.2 (2.2)	18.5	sn06sr (Ia-norm) 0.0257 (0.0029) 2.73 (3.18900)

Continued on Next Page...

Table 2.7 — Continued

SN Name	Type	Subtype	$z_{\rm SNID}$[a]	$t_{\rm SNID}$[b]	$r$lap	Best Match[c]
SN 2002ef	Ia	Ia-norm	0.0240 (0.0013)	28.5 (4.9)	20.3	sn98ef (Ia-norm) 0.0249 (0.0030) 28.51 (7.53300)
SN 2002eh	Ia	Ia-norm	0.0165 (0.0019)	26.5 (10.6)	14.8	sn04fz (Ia-norm) 0.0173 (0.0038) 17.56 (9.72300)
SN 2002ep	Ia	Ia-norm	0.0549 (0.0014)	28.5 (2.0)	21.0	sn06ej (Ia-norm) 0.0563 (0.0032) 27.54 (6.94600)
SN 2002el	Ia	Ia-norm	0.0282 (0.0027)	13.2 (1.5)	31.2	sn90N (Ia-norm) 0.0284 (0.0019) 14.50 (3.35500)
SN 2002el	Ia	Ia-norm	0.0265 (0.0016)	26.5 (9.1)	23.4	sn07bm (Ia-norm) 0.0270 (0.0027) 20.45 (9.60200)
SN 2002el	Ia	···	0.0285 (0.0045)	40.3 (5.6)	18.4	sn00cx (Ia-pec) 0.0298 (0.0030) 30.06 (14.4920)
SN 2002er	Ia	Ia-norm	0.0046 (0.0045)	−1.4 (0.6)	13.3	sn06sr (Ia-norm) 0.0090 (0.0041) −2.30 (1.03600)
SN 2002er	Ia	Ia-norm	0.0086 (0.0056)	8.7 (1.1)	24.6	sn02kf (Ia-norm) 0.0085 (0.0023) 7.14 (3.43600)
SN 2002er	Ia	Ia-norm	0.0062 (0.0010)	25.1 (5.8)	12.6	sn04fu (Ia-norm) 0.0082 (0.0047) 25.15 (15.7060)
SN 2002er	Ia	Ia-norm	0.0085 (0.0010)	56.3 (7.9)	15.4	sn94D (Ia-norm) 0.0093 (0.0033) 57.10 (8.56800)
SN 2002et	Ia	Ia-norm	0.0286 (0.0018)	15.5 (3.4)	16.6	sn07bm (Ia-norm) 0.0282 (0.0035) 15.52 (16.3970)
SN 2002gb	Ia	Ia-norm	0.0744 (0.0013)	33.0 (5.2)	20.3	sn06dm (Ia-norm) 0.0734 (0.0026) 36.06 (7.93700)
SN 2002eu	Ia	Ia-norm	0.0382 (0.0047)	1.4 (2.9)	24.0	sn04fu (Ia-norm) 0.0398 (0.0023) 2.30 (3.81400)
SN 2002eu	Ia	Ia-norm	0.0370 (0.0023)	11.0 (2.7)	16.3	sn00dk (Ia-norm) 0.0350 (0.0035) 11.19 (4.22300)
SN 2002eu	Ib	IIb	0.0398 (0.0001)	5.5 (1.2)	5.6	sn93J (IIb) 0.0397 (0.0081) 3.80 (0.00000)
SN 2002eu	Ia	Ia-norm	0.0375 (0.0016)	32.4 (3.5)	36.7	sn06dm (Ia-norm) 0.0367 (0.0016) 36.06 (8.34700)
SN 2002eu	Ia	Ia-norm	0.0378 (0.0016)	87.9 (9.1)	17.9	sn01ep (Ia-norm) 0.0360 (0.0030) 87.26 (13.6890)
SN 2002ey	Ia	···	0.0397 (0.0057)	1.0 (2.1)	17.8	sn06gt (Ia-91bg) 0.0365 (0.0029) 2.09 (4.12000)
SN 2002fb	Ia	Ia-91bg	0.0161 (0.0020)	2.4 (0.7)	17.1	sn06cs (Ia-91bg) 0.0161 (0.0029) 2.41 (2.50000)
SN 2002fb	Ia	Ia-91bg	0.0154 (0.0019)	20.5 (5.8)	14.0	sn06em (Ia-91bg) 0.0166 (0.0040) 20.95 (5.66900)
SN 2002fb	Ia	Ia-91bg	0.0131 (0.0012)	48.2 (0.0)	10.8	sn91bg (Ia-91bg) 0.0157 (0.0048) 48.21 (0.00000)
SN 2002fi	Ia	Ia-norm	0.0568 (0.0041)	28.5 (8.0)	13.6	sn01ep (Ia-norm) 0.0557 (0.0042) 28.46 (6.37700)
SN 2002fk	Ia	Ia-norm	0.0122 (0.0050)	7.7 (1.9)	15.3	sn03ai (Ia-norm) 0.0070 (0.0033) 7.73 (2.19400)
SN 2002fk	Ia	···	0.0082 (0.0038)	44.0 (3.8)	18.1	sn97br (Ia-91T) 0.0068 (0.0030) 49.10 (11.1360)
SN 2002fk	Ia	Ia-norm	0.0078 (0.0018)	42.8 (3.0)	19.7	sn08ec (Ia-norm) 0.0066 (0.0027) 42.99 (8.18400)
SN 2002fk	Ia	Ia-norm	0.0070 (0.0012)	71.6 (14.3)	14.8	sn08ec (Ia-norm) 0.0066 (0.0035) 71.57 (12.7740)
SN 2002fk	Ia	Ia-norm	0.0071 (0.0013)	123.6 (20.1)	20.0	sn94ae (Ia-norm) 0.0069 (0.0027) 123.60 (20.1170)
SN 2002gf	Ia	Ia-norm	0.0889 (0.0019)	29.2 (7.0)	9.6	sn98bu (Ia-norm) 0.0896 (0.0051) 30.20 (7.88400)
SN 2002gc	Ia	Ia-norm	0.0269 (0.0060)	0.6 (2.8)	13.0	sn00dk (Ia-norm) 0.0213 (0.0041) 1.36 (2.72800)
SN 2002gc	Ia	Ia-91bg	0.0282 (0.0027)	36.9 (0.0)	12.3	sn99da (Ia-91bg) 0.0217 (0.0044) 36.91 (0.00000)
SN 2002gc	Ia	Ia-norm	0.0273 (0.0020)	28.5 (6.1)	15.9	sn89B (Ia-norm) 0.0273 (0.0031) 24.40 (5.81700)
SN 2002gc	Ia	Ia-norm	0.0264 (0.0009)	81.6 (32.3)	14.5	sn04dt (Ia-norm) 0.0267 (0.0036) 81.59 (32.2860)
SN 2002gg	Ia	Ia-norm	0.1072 (0.0019)	36.4 (12.6)	15.3	sn04fz (Ia-norm) 0.1084 (0.0033) 17.56 (12.0150)
SN 2002gx	Ia	Ia-norm	0.0806 (0.0014)	28.5 (4.6)	14.8	sn94D (Ia-norm) 0.0809 (0.0034) 24.20 (5.39800)
SN 2002ha	Ia	Ia-norm	0.0146 (0.0041)	1.1 (1.9)	23.6	sn06dw (Ia-norm) 0.0146 (0.0022) 1.07 (3.24900)
SN 2002ha	Ia	Ia-norm	0.0166 (0.0048)	1.6 (0.2)	32.1	sn00dk (Ia-norm) 0.0154 (0.0017) 1.36 (3.41100)
SN 2002ha	Ia	Ia-norm	0.0165 (0.0042)	8.1 (0.3)	33.1	sn05bc (Ia-norm) 0.0128 (0.0016) 7.47 (2.83400)
SN 2002ha	Ia	Ia-norm	0.0131 (0.0007)	41.5 (6.4)	17.7	sn02fk (Ia-norm) 0.0130 (0.0029) 41.50 (11.2170)
SN 2002ha	Ia	Ia-norm	0.0124 (0.0015)	87.9 (11.0)	20.3	sn02fk (Ia-norm) 0.0128 (0.0026) 72.46 (15.3160)
SN 2002hd	Ia	Ia-norm	0.0356 (0.0041)	7.0 (1.6)	20.8	sn02ha (Ia-norm) 0.0346 (0.0025) 7.89 (3.05600)
SN 2002hd	Ia	Ia-norm	0.0336 (0.0022)	15.3 (2.7)	25.0	sn05be (Ia-norm) 0.0363 (0.0025) 10.96 (4.85100)
SN 2002he	Ia	Ia-norm	0.0181 (0.0040)	−3.7 (2.3)	19.6	sn07bd (Ia-norm) 0.0255 (0.0027) −5.58 (1.98000)
SN 2002he	Ia	Ia-norm	0.0213 (0.0041)	−2.3 (4.0)	13.3	sn06sr (Ia-norm) 0.0259 (0.0039) −2.30 (4.00000)
SN 2002he	Ia	Ia-norm	0.0217 (0.0048)	2.7 (3.6)	37.0	sn06sr (Ia-norm) 0.0230 (0.0015) 2.73 (3.62000)
SN 2002he	Ia	Ia-norm	0.0226 (0.0049)	2.7 (0.3)	25.6	sn06sr (Ia-norm) 0.0247 (0.0021) 2.73 (3.77800)
SN 2002hl	Ia	···	0.0097 (0.0038)	57.8 (13.9)	13.3	sn02bo (Ia-norm) 0.0075 (0.0039) 51.60 (21.2670)
SN 2002hv	Ia	···	0.0248 (0.0042)	44.0 (7.9)	18.4	sn99da (Ia-91bg) 0.0216 (0.0030) 36.91 (15.9830)
SN 2002hu	Ia	···	0.0371 (0.0064)	0.7 (0.3)	21.0	sn05eq (Ia-99aa) 0.0342 (0.0025) 0.66 (3.79200)
SN 2002hw	Ia	Ia-norm	0.0168 (0.0037)	−1.1 (1.6)	23.4	sn07fr (Ia-norm) 0.0167 (0.0022) −1.15 (3.47200)
SN 2002hw	Ia	Ia-norm	0.0173 (0.0008)	28.4 (3.5)	10.1	sn94D (Ia-norm) 0.0171 (0.0059) 28.39 (3.52500)
SN 2002jg	Ia	Ia-norm	0.0170 (0.0037)	11.0 (1.4)	13.4	sn89B (Ia-norm) 0.0144 (0.0041) 12.40 (1.38300)
SN 2002jm	Ia	Ia-91bg	0.0178 (0.0026)	8.4 (0.0)	10.1	sn06ke (Ia-91bg) 0.0196 (0.0056) 8.43 (0.00000)
SN 2002jo	Ia	Ia-norm	0.0086 (0.0010)	30.2 (6.2)	14.9	sn07af (Ia-norm) 0.0083 (0.0041) 26.49 (7.05600)
SN 2002jy	Ia	Ia-norm	0.0192 (0.0035)	11.2 (1.6)	24.0	sn04bg (Ia-norm) 0.0188 (0.0024) 10.34 (2.77700)
SN 2002jy	Ia	Ia-norm	0.0202 (0.0016)	37.8 (4.2)	21.3	sn07fs (Ia-norm) 0.0190 (0.0026) 36.37 (9.74700)
SN 2002kf	Ia	Ia-norm	0.0202 (0.0053)	4.5 (2.5)	25.5	sn00dk (Ia-norm) 0.0186 (0.0022) 1.36 (3.11100)
SN 2003D	Ia	Ia-norm	0.0227 (0.0023)	12.5 (3.6)	15.5	sn00dk (Ia-norm) 0.0213 (0.0036) 11.19 (4.31200)
SN 2003D	Ia	···	0.0227 (0.0045)	54.5 (15.6)	14.5	sn91bg (Ia-91bg) 0.0211 (0.0036) 54.50 (19.6550)
SN 2003F	Ia	Ia-norm	0.0178 (0.0023)	13.7 (5.1)	19.7	sn04ey (Ia-norm) 0.0161 (0.0028) 18.90 (4.05500)
SN 2003F	Ia	Ia-norm	0.0171 (0.0028)	17.4 (1.5)	19.4	sn94D (Ia-norm) 0.0175 (0.0029) 17.40 (8.94400)

Continued on Next Page...

Table 2.7 — Continued

SN Name	Type	Subtype	$z_{\rm SNID}$[a]	$t_{\rm SNID}$[b]	$r$lap	Best Match[c]
SN 2003K	Ia	···	0.0166 (0.0063)	7.8 (4.5)	18.5	sn97br (Ia-91T) 0.0204 (0.0033) 7.80 (4.47900)
SN 2003K	Ia	···	0.0188 (0.0047)	15.9 (1.1)	19.0	sn91T (Ia-91T) 0.0206 (0.0031) 15.90 (3.79800)
SN 2003M	···	···	···	···	···	···
SN 2003M	Ia	···	0.0228 (0.0039)	61.2 (11.1)	9.6	sn91bg (Ia-91bg) 0.0220 (0.0060) 46.50 (20.6650)
SN 2003V	Ia	Ia-norm	0.0449 (0.0015)	54.6 (19.2)	27.5	sn02bo (Ia-norm) 0.0431 (0.0021) 54.60 (19.1970)
SN 2003ae	Ia	Ia-norm	0.0356 (0.0012)	29.4 (4.3)	12.4	sn05de (Ia-norm) 0.0360 (0.0054) 25.75 (4.25300)
SN 2003P	Ia	Ia-norm	0.0320 (0.0016)	30.2 (3.7)	26.4	sn98bu (Ia-norm) 0.0322 (0.0022) 33.20 (8.27500)
SN 2003S	Ia	Ia-norm	0.0400 (0.0013)	10.2 (0.7)	16.2	sn98bu (Ia-norm) 0.0401 (0.0036) 10.20 (1.18100)
SN 2003U	Ia	Ia-norm	0.0272 (0.0048)	−0.9 (2.7)	29.9	sn02ha (Ia-norm) 0.0255 (0.0018) −0.85 (3.83200)
SN 2003W	Ia	Ia-norm	0.0002 (0.0068)	−10.7 (2.4)	9.5	sn94D (Ia-norm) 0.0189 (0.0080) −10.70 (2.41800)
SN 2003W	Ia	Ia-norm	0.0189 (0.0000)	8.1 (0.0)	10.2	sn04ef (Ia-norm) 0.0189 (0.0064) 8.05 (0.00000)
SN 2003W	Ia	···	0.0237 (0.0040)	51.1 (8.5)	11.5	sn01eh (Ia-99aa) 0.0217 (0.0049) 59.90 (20.1380)
SN 2003X	Ia	Ia-norm	0.0211 (0.0016)	27.5 (3.5)	16.3	sn04fu (Ia-norm) 0.0223 (0.0039) 25.15 (5.98200)
SN 2003Y	Ia	Ia-91bg	0.0153 (0.0032)	1.0 (1.0)	12.7	sn06cs (Ia-91bg) 0.0166 (0.0042) 2.41 (1.04200)
SN 2003Y	Ia	Ia-91bg	0.0163 (0.0016)	18.6 (5.0)	13.2	sn02fb (Ia-91bg) 0.0173 (0.0046) 18.60 (4.97200)
SN 2003af	Ia	Ia-norm	0.0179 (0.0025)	20.7 (3.3)	16.9	sn99dk (Ia-norm) 0.0200 (0.0037) 23.62 (3.22800)
SN 2003av	Ia	Ia-norm	0.1472 (0.0010)	14.1 (0.7)	17.3	sn07A (Ia-norm) 0.1472 (0.0030) 15.07 (1.90500)
SN 2003ai	Ia	Ia-norm	0.0381 (0.0043)	11.1 (2.5)	28.3	sn06cf (Ia-norm) 0.0347 (0.0020) 11.12 (2.48600)
SN 2003ah	Ia	Ia-norm	0.0324 (0.0029)	12.5 (1.5)	23.0	sn07A (Ia-norm) 0.0325 (0.0025) 15.07 (2.66900)
SN 2003an	Ia	···	0.0330 (0.0048)	18.7 (3.6)	28.4	sn99dq (Ia-99aa) 0.0348 (0.0021) 24.09 (9.80400)
SN 2003ax	Ia	Ia-norm	0.0504 (0.0028)	15.6 (6.6)	37.4	sn02bo (Ia-norm) 0.0520 (0.0017) 15.65 (3.95200)
SN 2003au	Ia	Ia-91bg	0.0325 (0.0017)	17.2 (7.9)	24.9	sn05bl (Ia-91bg) 0.0326 (0.0023) 17.19 (7.89900)
SN 2003bf	Ia	Ia-norm	0.0291 (0.0041)	−3.5 (2.3)	18.7	sn05ms (Ia-norm) 0.0307 (0.0032) −1.51 (2.30200)
SN 2003ay	Ia	Ia-norm	0.0755 (0.0019)	14.7 (3.3)	12.9	sn94D (Ia-norm) 0.0751 (0.0038) 14.40 (3.28900)
SN 2003bh	Ia	Ia-norm	0.0892 (0.0013)	28.4 (2.8)	19.7	sn06N (Ia-norm) 0.0893 (0.0027) 27.49 (6.50300)
SN 2003bi	Ia	Ia-norm	0.0956 (0.0043)	1.1 (2.7)	20.2	sn06bu (Ia-norm) 0.0974 (0.0027) 4.24 (3.89800)
SN 2003cq	Ia	Ia-norm	0.0310 (0.0051)	−1.5 (1.5)	27.6	sn02er (Ia-norm) 0.0333 (0.0023) −1.50 (3.41200)
SN 2003du	Ia	···	0.0052 (0.0049)	18.9 (3.1)	13.5	sn08ds (Ia-99aa) 0.0059 (0.0033) 21.43 (10.0970)
SN 2003du	Ia	Ia-norm	0.0047 (0.0008)	54.6 (25.2)	12.2	sn04ey (Ia-norm) 0.0061 (0.0054) 18.90 (25.2420)
SN 2003du	Ia	Ia-norm	0.0059 (0.0022)	17.4 (3.4)	16.7	sn89B (Ia-norm) 0.0060 (0.0030) 17.40 (3.36700)
SN 2003du	Ia	Ia-norm	0.0067 (0.0016)	33.0 (5.5)	19.9	sn95D (Ia-norm) 0.0063 (0.0028) 33.05 (6.35800)
SN 2003du	Ia	Ia-norm	0.0060 (0.0010)	57.1 (4.7)	22.0	sn94D (Ia-norm) 0.0062 (0.0022) 53.90 (10.2190)
SN 2003du	Ia	Ia-norm	0.0059 (0.0014)	87.8 (10.6)	18.2	sn94ae (Ia-norm) 0.0060 (0.0027) 87.80 (10.6140)
SN 2003dw	Ia	Ia-norm	0.0306 (0.0029)	29.4 (3.4)	7.6	sn02bo (Ia-norm) 0.0289 (0.0078) 29.40 (9.28700)
SN 2003ek	···	···	···	···	···	···
SN 2003ek	Ia	Ia-norm	0.0422 (0.0005)	−1.2 (0.9)	10.2	sn02bo (Ia-norm) 0.0425 (0.0053) −2.50 (0.919000)
SN 2003ek	Ic	Ic-broad	0.0413 (0.0000)	···	5.5	sn97ef (Ic-broad) 0.0413 (0.0032) −999.00 (0.00000
SN 2003ek	Ia	Ia-norm	0.0358 (0.0006)	25.1 (2.6)	11.5	sn04fz (Ia-norm) 0.0358 (0.0064) 22.28 (2.60800)
SN 2003fa	Ia	Ia-99aa	0.0386 (0.0024)	−4.5 (1.1)	15.4	sn08ds (Ia-99aa) 0.0366 (0.0036) −4.93 (1.10700)
SN 2003fa	Ia	Ia-norm	0.0410 (0.0027)	18.9 (16.8)	31.2	sn04ey (Ia-norm) 0.0399 (0.0018) 18.90 (16.7550)
SN 2003fa	Ia	···	0.0418 (0.0045)	36.2 (3.8)	35.2	sn98es (Ia-99aa) 0.0401 (0.0016) 46.13 (15.3680)
SN 2003fd	Ia	Ia-norm	0.0589 (0.0026)	15.1 (1.1)	24.8	sn07A (Ia-norm) 0.0584 (0.0021) 15.07 (2.65500)
SN 2003gj	Ia	Ia-norm	0.0331 (0.0031)	27.2 (4.7)	8.6	sn02er (Ia-norm) 0.0364 (0.0084) 19.50 (4.94900)
SN 2003gn	Ia	Ia-norm	0.0309 (0.0054)	−4.0 (1.8)	25.6	sn02bo (Ia-norm) 0.0364 (0.0024) −5.10 (2.52000)
SN 2003gn	Ia	Ia-norm	0.0378 (0.0022)	5.5 (0.0)	10.6	sn98dx (Ia-norm) 0.0363 (0.0050) 5.50 (0.00000)
SN 2003gq	Ia	Ia-02cx	0.0232 (0.0005)	−3.3 (1.5)	15.9	sn05hk (Ia-02cx) 0.0230 (0.0028) −3.30 (1.53300)
SN 2003gq	Ia	Ia-02cx	0.0222 (0.0000)	65.5 (0.0)	12.0	sn05hk (Ia-02cx) 0.0222 (0.0027) 65.50 (0.00000)
SN 2003gs	Ia	Ia-norm	0.0052 (0.0009)	41.3 (3.0)	12.1	sn00dk (Ia-norm) 0.0048 (0.0046) 36.68 (3.02200)
SN 2003gs	Ia	Ia-91bg	0.0029 (0.0011)	182.3 (0.0)	5.4	sn99by (Ia-91bg) 0.0044 (0.0097) 182.26 (0.00000)
SN 2003gt	Ia	Ia-norm	0.0137 (0.0023)	−1.9 (3.6)	16.6	sn00dg (Ia-norm) 0.0145 (0.0027) −5.00 (2.70000)
SN 2003gt	Ia	Ia-norm	0.0147 (0.0017)	13.4 (1.8)	16.9	sn95D (Ia-norm) 0.0145 (0.0031) 16.10 (2.66700)
SN 2003he	Ia	Ia-norm	0.0261 (0.0058)	0.3 (4.4)	16.1	sn89B (Ia-norm) 0.0266 (0.0038) −6.30 (4.77300)
SN 2003he	Ia	Ia-norm	0.0231 (0.0039)	10.1 (1.3)	16.8	sn94ae (Ia-norm) 0.0232 (0.0032) 11.30 (2.41600)
SN 2003hj	Ia	Ia-norm	0.0746 (0.0046)	12.4 (1.9)	11.8	sn89B (Ia-norm) 0.0744 (0.0042) 11.50 (30.6020)
SN 2003hm	Ia	Ia-norm	0.0134 (0.0041)	57.1 (2.1)	9.6	sn94D (Ia-norm) 0.0138 (0.0053) 59.10 (31.5710)
SN 2003hs	Ia	Ia-norm	0.0485 (0.0044)	−4.4 (3.1)	17.7	sn02er (Ia-norm) 0.0525 (0.0040) −4.40 (3.20900)
SN 2003hw	Ia	···	0.0421 (0.0041)	51.5 (4.9)	24.6	sn98es (Ia-99aa) 0.0387 (0.0021) 57.79 (17.8980)
SN 2003hv	Ia	Ia-norm	0.0040 (0.0011)	32.4 (13.0)	13.4	sn07fb (Ia-norm) 0.0053 (0.0041) 32.38 (10.5680)
SN 2003hv	Ia	Ia-norm	0.0048 (0.0010)	30.2 (5.9)	16.2	sn98bu (Ia-norm) 0.0051 (0.0036) 30.22 (6.42400)
SN 2003hv	Ia	···	0.0041 (0.0039)	71.0 (16.6)	8.6	sn98bu (Ia-norm) 0.0051 (0.0059) 59.12 (23.2790)

Continued on Next Page...

Table 2.7 — Continued

SN Name	Type	Subtype	$z_{\rm SNID}$[a]	$t_{\rm SNID}$[b]	$r$lap	Best Match[c]
SN 2003hx	Ia	Ia-norm	0.0056 (0.0011)	27.5 (2.1)	16.1	sn04fu (Ia-norm) 0.0073 (0.0037) 25.15 (2.33200)
SN 2003ij	Ia	Ia-99aa	0.0148 (0.0038)	−5.6 (0.0)	11.6	sn01eh (Ia-99aa) 0.0174 (0.0051) −5.63 (0.00000)
SN 2003ik	Ia	Ia-norm	0.0253 (0.0039)	2.3 (3.3)	17.9	sn07A (Ia-norm) 0.0236 (0.0029) 2.37 (3.67500)
SN 2003in	Ia	Ia-norm	0.0207 (0.0036)	18.9 (0.0)	10.2	sn04ey (Ia-norm) 0.0232 (0.0053) 18.90 (0.00000)
SN 2003im	Ia	Ia-norm	0.0206 (0.0013)	40.5 (2.5)	21.6	sn04eo (Ia-norm) 0.0191 (0.0025) 44.40 (8.15700)
SN 2003iv	Ia	Ia-norm	0.0363 (0.0048)	4.9 (2.8)	21.5	sn02bz (Ia-norm) 0.0356 (0.0022) 5.60 (3.12800)
SN 2003iv	Ia	Ia-norm	0.0373 (0.0051)	5.7 (2.6)	25.7	sn04gs (Ia-norm) 0.0370 (0.0021) 0.44 (3.16200)
SN 2003iz	Ia	Ia-norm	0.0470 (0.0051)	7.9 (1.4)	22.0	sn05am (Ia-norm) 0.0482 (0.0026) 4.47 (2.65200)
SN 2003kc	Ia	Ia-norm	0.0191 (0.0071)	−7.0 (0.8)	28.0	sn02bo (Ia-norm) 0.0332 (0.0023) −8.10 (2.28700)
SN 2003kd	Ia	Ia-norm	0.0301 (0.0041)	5.6 (2.0)	26.2	sn06sr (Ia-norm) 0.0322 (0.0020) 2.73 (3.78900)
SN 2003kd	Ia	···	0.0348 (0.0111)	14.2 (20.3)	6.7	sn02cx (Ia-02cx) 0.0216 (0.0058) 14.20 (20.2790)
SN 2003kh	Ia	···	0.0369 (0.0054)	0.4 (0.8)	25.7	sn02cf (Ia-91bg) 0.0359 (0.0020) −0.65 (4.94500)
SN 2003kg	Ia	Ia-norm	0.0226 (0.0064)	−1.7 (2.2)	12.1	sn04as (Ia-norm) 0.0277 (0.0051) −4.36 (2.16900)
SN 2003kf	Ia	Ia-norm	0.0060 (0.0038)	−6.4 (0.0)	12.1	sn02er (Ia-norm) 0.0069 (0.0050) −6.40 (0.00000)
SN 2003kf	Ia	Ia-norm	0.0068 (0.0008)	41.5 (3.1)	15.9	sn02bo (Ia-norm) 0.0068 (0.0036) 44.48 (7.69600)
SN 2003ls	Ia	Ia-norm	0.0443 (0.0018)	18.9 (19.6)	13.6	sn94D (Ia-norm) 0.0448 (0.0049) 14.40 (19.6300)
SN 2003lb	Ia	Ia-norm	0.0192 (0.0020)	15.5 (2.5)	14.5	sn06ev (Ia-norm) 0.0193 (0.0044) 16.85 (3.03300)
SN 2003lc	Ia	Ia-norm	0.0347 (0.0019)	20.5 (1.3)	29.7	sn07bm (Ia-norm) 0.0352 (0.0021) 20.45 (10.9050)
SN 2003lq	Ia	Ia-norm	0.0246 (0.0035)	10.2 (1.3)	20.9	sn05kc (Ia-norm) 0.0240 (0.0026) 10.22 (2.59600)
SN 2004E	Ia	Ia-norm	0.0285 (0.0039)	9.3 (2.6)	17.6	sn94ae (Ia-norm) 0.0294 (0.0029) 9.40 (2.70400)
SN 2004W	Ia	Ia-91bg	0.0051 (0.0024)	117.2 (16.8)	6.0	sn91bg (Ia-91bg) 0.0027 (0.0093) 117.20 (16.8010)
SN 2004S	Ia	Ia-norm	0.0129 (0.0062)	5.0 (0.0)	12.4	sn01ep (Ia-norm) 0.0088 (0.0046) 4.99 (0.00000)
SN 2004S	···	···	···	···	···	···
SN 2004Y	Ia	Ia-norm	0.0680 (0.0020)	27.2 (8.0)	14.7	sn04fz (Ia-norm) 0.0687 (0.0039) 17.56 (7.81800)
SN 2004as	Ia	Ia-norm	0.0231 (0.0057)	−4.5 (1.3)	22.2	sn02er (Ia-norm) 0.0282 (0.0029) −6.40 (2.35300)
SN 2004bd	Ia	···	0.0092 (0.0063)	8.0 (1.7)	10.3	sn07ba (Ia-91bg) 0.0086 (0.0056) 8.01 (9.59800)
SN 2004bd	Ia	Ia-norm	0.0109 (0.0010)	28.5 (0.0)	12.1	sn01ep (Ia-norm) 0.0090 (0.0049) 28.46 (0.00000)
SN 2004bd	Ia	···	0.0123 (0.0041)	46.3 (5.9)	9.6	sn05eq (Ia-99aa) 0.0087 (0.0056) 51.16 (11.0650)
SN 2004bg	Ia	Ia-norm	0.0229 (0.0042)	11.3 (3.0)	37.5	sn94ae (Ia-norm) 0.0221 (0.0014) 11.30 (2.99100)
SN 2004bg	Ia	Ia-norm	0.0219 (0.0019)	40.5 (8.8)	13.6	sn04eo (Ia-norm) 0.0202 (0.0041) 44.40 (8.72500)
SN 2004bj	Ia	Ia-norm	0.0496 (0.0046)	−1.1 (3.7)	20.6	sn07fr (Ia-norm) 0.0502 (0.0025) −1.15 (3.73400)
SN 2004bk	Ia	Ia-norm	0.0192 (0.0051)	7.2 (4.7)	23.4	sn07kk (Ia-norm) 0.0238 (0.0025) 7.15 (4.70700)
SN 2004bk	Ia	Ia-pec	0.0248 (0.0000)	30.1 (0.0)	11.8	sn00cx (Ia-pec) 0.0248 (0.0043) 30.06 (0.00000)
SN 2004bl	Ia	Ia-norm	0.0179 (0.0051)	4.2 (0.6)	26.7	sn95D (Ia-norm) 0.0161 (0.0020) 4.20 (2.67600)
SN 2004bl	Ia	Ia-norm	0.0181 (0.0018)	17.7 (1.1)	23.5	sn95D (Ia-norm) 0.0173 (0.0022) 16.10 (5.03200)
SN 2004bp	Ia	Ia-91bg	0.0291 (0.0020)	16.4 (6.0)	7.0	sn91bg (Ia-91bg) 0.0291 (0.0074) 18.60 (4.78200)
SN 2004bq	Ia	Ia-norm	0.0287 (0.0048)	17.2 (2.1)	11.5	sn94D (Ia-norm) 0.0287 (0.0047) 17.20 (2.05100)
SN 2004cb	Ia	Ia-norm	0.0140 (0.0014)	39.2 (12.2)	12.7	sn07bc (Ia-norm) 0.0143 (0.0047) 16.35 (12.2030)
SN 2004br	Ia	Ia-99aa	0.0246 (0.0000)	−4.9 (0.0)	10.1	sn08ds (Ia-99aa) 0.0246 (0.0054) −4.93 (0.00000)
SN 2004br	Ia	···	0.0198 (0.0048)	18.6 (4.6)	17.6	sn91T (Ia-91T) 0.0211 (0.0033) 18.60 (4.58700)
SN 2004br	Ia	···	0.0209 (0.0046)	20.5 (3.8)	15.7	sn99dq (Ia-99aa) 0.0231 (0.0039) 24.09 (12.5390)
SN 2004bv	Ia	Ia-91T	0.0101 (0.0012)	−4.3 (2.5)	8.6	sn97br (Ia-91T) 0.0084 (0.0061) −4.00 (2.27600)
SN 2004bv	Ia	Ia-norm	0.0102 (0.0035)	11.1 (2.4)	17.4	sn03ai (Ia-norm) 0.0085 (0.0032) 7.73 (1.90400)
SN 2004bv	Ia	Ia-norm	0.0113 (0.0012)	30.2 (6.3)	11.2	sn06et (Ia-norm) 0.0104 (0.0049) 43.76 (6.27400)
SN 2004bv	Ia	Ia-norm	0.0130 (0.0011)	37.8 (4.6)	22.2	sn94ae (Ia-norm) 0.0119 (0.0024) 36.20 (7.07900)
SN 2004bv	Ia	Ia-norm	0.0132 (0.0011)	53.9 (4.8)	21.5	sn02er (Ia-norm) 0.0129 (0.0026) 60.98 (8.75400)
SN 2004bv	Ia	Ia-norm	0.0127 (0.0014)	121.8 (16.8)	17.8	sn94D (Ia-norm) 0.0132 (0.0033) 87.19 (17.8920)
SN 2004bv	Ia	Ia-norm	0.0137 (0.0014)	123.6 (17.8)	17.4	sn94ae (Ia-norm) 0.0138 (0.0032) 123.60 (41.4470)
SN 2004bw	Ia	Ia-norm	0.0165 (0.0054)	−5.9 (3.1)	9.6	sn02he (Ia-norm) 0.0220 (0.0052) −5.91 (3.94100)
SN 2004bw	Ia	Ia-norm	0.0230 (0.0053)	5.7 (1.4)	26.1	sn02kf (Ia-norm) 0.0229 (0.0022) 7.14 (2.80100)
SN 2004ca	Ia	Ia-norm	0.0133 (0.0042)	−6.4 (0.8)	18.0	sn02er (Ia-norm) 0.0177 (0.0035) −6.40 (2.25900)
SN 2004bz	Ia	Ia-norm	0.0355 (0.0015)	51.1 (5.8)	24.4	sn04ey (Ia-norm) 0.0353 (0.0022) 51.49 (14.9890)
SN 2004cv	Ia	Ia-norm	0.0338 (0.0030)	13.8 (1.5)	23.0	sn02bo (Ia-norm) 0.0350 (0.0029) 13.80 (1.86200)
SN 2004db	Ia	Ia-norm	0.0149 (0.0012)	91.1 (0.0)	5.1	sn07af (Ia-norm) 0.0111 (0.0103) 91.06 (0.00000)
SN 2004da	Ic	···	0.0113 (0.0070)	−1.7 (2.8)	9.9	sn04aw (Ic-pec) 0.0150 (0.0060) −0.20 (0.00000)
SN 2004da	Ia	···	0.0076 (0.0048)	14.5 (4.3)	9.5	sn00cx (Ia-pec) 0.0135 (0.0068) 19.40 (4.38100)
SN 2004da	Ia	Ia-norm	0.0142 (0.0039)	44.4 (15.3)	8.8	sn02bo (Ia-norm) 0.0144 (0.0061) 44.40 (22.5730)
SN 2004di	Ia	···	0.0188 (0.0056)	25.1 (8.3)	7.4	sn02fb (Ia-91bg) 0.0216 (0.0070) 18.60 (9.34700)
SN 2004di	Ia	Ia-91bg	0.0209 (0.0018)	17.2 (4.6)	12.2	sn03Y (Ia-91bg) 0.0210 (0.0047) 20.55 (4.64700)
SN 2004eq	Ia	Ia-norm	0.0092 (0.0012)	79.4 (7.4)	14.1	sn99dk (Ia-norm) 0.0094 (0.0043) 71.83 (7.40700)

Continued on Next Page...

Table 2.7 — Continued

SN Name	Type	Subtype	$z_{\rm SNID}$[a]	$t_{\rm SNID}$[b]	$r$lap	Best Match[c]
SN 2004dt	Ia	Ia-norm	0.0095 (0.0052)	−9.1 (1.0)	9.8	sn02cs (Ia-norm) 0.0216 (0.0060) −9.09 (0.990000)
SN 2004dt	Ia	Ia-norm	0.0191 (0.0044)	−2.1 (4.5)	8.5	sn94D (Ia-norm) 0.0188 (0.0069) −8.96 (3.86800)
SN 2004dt	Ia	Ia-norm	0.0192 (0.0023)	16.7 (5.7)	13.1	sn89B (Ia-norm) 0.0181 (0.0037) 14.40 (5.73100)
SN 2004dt	Ia	Ia-norm	0.0210 (0.0018)	30.2 (5.3)	20.1	sn98bu (Ia-norm) 0.0210 (0.0026) 29.20 (6.79600)
SN 2004dt	Ia	Ia-norm	0.0209 (0.0019)	43.6 (7.3)	17.3	sn02bo (Ia-norm) 0.0190 (0.0030) 45.60 (9.62600)
SN 2004dt	Ia	Ia-norm	0.0197 (0.0015)	57.5 (7.7)	16.1	sn02cr (Ia-norm) 0.0191 (0.0032) 57.47 (11.0430)
SN 2004dt	Ia	Ia-norm	0.0206 (0.0007)	142.2 (35.1)	11.3	sn02cs (Ia-norm) 0.0211 (0.0056) 142.16 (35.1220)
SN 2004dt	Ia	···	0.0190 (0.0019)	142.2 (38.9)	9.1	sn02cs (Ia-norm) 0.0195 (0.0069) 142.16 (20.0610)
SN 2004dt	Ia	Ia-norm	0.0199 (0.0014)	228.1 (56.1)	5.3	sn90N (Ia-norm) 0.0189 (0.0124) 228.10 (56.1170)
SN 2004ef	Ia	Ia-norm	0.0306 (0.0034)	−4.0 (3.0)	17.1	sn02bo (Ia-norm) 0.0314 (0.0037) −5.10 (2.80900)
SN 2004ef	Ia	Ia-norm	0.0298 (0.0036)	11.0 (0.6)	24.7	sn05kc (Ia-norm) 0.0288 (0.0024) 10.22 (2.20800)
SN 2004ef	Ia	Ia-norm	0.0320 (0.0008)	29.4 (3.0)	20.2	sn04fu (Ia-norm) 0.0321 (0.0034) 25.15 (3.68500)
SN 2004ef	Ia	Ia-norm	0.0304 (0.0015)	28.5 (2.9)	27.8	sn04fu (Ia-norm) 0.0317 (0.0023) 25.15 (7.73400)
SN 2004ef	Ia	Ia-norm	0.0325 (0.0014)	69.6 (7.9)	20.3	sn95D (Ia-norm) 0.0325 (0.0028) 69.60 (13.7420)
SN 2004ef	Ia	Ia-norm	0.0327 (0.0022)	113.8 (18.8)	23.8	sn94D (Ia-norm) 0.0326 (0.0025) 87.19 (15.2900)
SN 2004fa	Ia	···	0.0218 (0.0043)	63.4 (13.6)	13.2	sn91bg (Ia-91bg) 0.0233 (0.0038) 48.21 (23.2710)
SN 2004eo	Ia	Ia-norm	0.0165 (0.0046)	−1.7 (2.2)	19.2	sn07bm (Ia-norm) 0.0159 (0.0028) −7.30 (3.01200)
SN 2004eo	Ia	Ia-norm	0.0170 (0.0026)	16.4 (2.9)	17.5	sn08ec (Ia-norm) 0.0151 (0.0033) 12.51 (3.06200)
SN 2004eo	Ia	Ia-norm	0.0169 (0.0018)	42.1 (2.5)	20.4	sn08ec (Ia-norm) 0.0160 (0.0027) 42.99 (7.17100)
SN 2004ev	Ia	Ia-norm	0.0292 (0.0026)	16.7 (4.2)	19.7	sn06ev (Ia-norm) 0.0296 (0.0031) 16.85 (4.54900)
SN 2004ey	Ia	Ia-norm	0.0143 (0.0052)	−6.4 (1.5)	15.6	sn02er (Ia-norm) 0.0143 (0.0042) −4.40 (1.50500)
SN 2004ey	Ia	Ia-norm	0.0172 (0.0024)	16.4 (3.2)	19.0	sn94D (Ia-norm) 0.0172 (0.0029) 15.30 (5.14100)
SN 2004ey	Ia	Ia-norm	0.0160 (0.0014)	53.9 (4.9)	23.6	sn94D (Ia-norm) 0.0156 (0.0021) 49.96 (9.22300)
SN 2004fd	Ia	Ia-norm	0.0162 (0.0027)	17.4 (5.8)	16.7	sn89B (Ia-norm) 0.0156 (0.0030) 17.40 (4.89200)
SN 2004fd	Ia	Ia-norm	0.0166 (0.0007)	50.0 (8.7)	12.3	sn94D (Ia-norm) 0.0168 (0.0042) 43.96 (8.65300)
SN 2004fg	Ia	···	0.0314 (0.0055)	2.9 (2.1)	26.9	sn08ds (Ia-99aa) 0.0286 (0.0020) 2.91 (3.65500)
SN 2004fu	Ia	Ia-norm	0.0038 (0.0045)	−5.6 (0.6)	20.4	sn02er (Ia-norm) 0.0084 (0.0030) −6.40 (1.87000)
SN 2004fu	Ia	Ia-norm	0.0073 (0.0050)	0.3 (3.3)	20.1	sn02he (Ia-norm) 0.0091 (0.0028) 0.29 (3.28000)
SN 2004fu	Ia	Ia-norm	0.0079 (0.0010)	29.4 (1.8)	17.7	sn04ef (Ia-norm) 0.0087 (0.0034) 31.23 (6.03500)
SN 2004fw	Ia	Ia-norm	0.0304 (0.0050)	7.7 (0.0)	14.5	sn02fk (Ia-norm) 0.0256 (0.0036) 7.74 (2.19400)
SN 2004fy	Ia	Ia-norm	0.0207 (0.0032)	10.2 (1.1)	34.0	sn05kc (Ia-norm) 0.0199 (0.0016) 10.22 (3.82400)
SN 2004fy	Ia	Ia-norm	0.0187 (0.0012)	36.1 (5.4)	20.9	sn06dm (Ia-norm) 0.0178 (0.0027) 36.06 (7.59600)
SN 2004fz	Ia	Ia-norm	0.0194 (0.0045)	−0.9 (1.4)	22.5	sn95E (Ia-norm) 0.0188 (0.0023) −1.70 (2.57700)
SN 2004fz	Ia	Ia-norm	0.0166 (0.0018)	30.2 (9.8)	16.9	sn06kf (Ia-norm) 0.0180 (0.0034) 18.67 (9.72800)
SN 2004fz	Ia	Ia-norm	0.0177 (0.0016)	28.8 (7.0)	21.2	sn02eu (Ia-norm) 0.0176 (0.0027) 33.44 (7.08200)
SN 2004go	Ia	Ia-norm	0.0315 (0.0014)	27.5 (4.4)	12.8	sn98ef (Ia-norm) 0.0321 (0.0050) 28.51 (4.40300)
SN 2004gc	Ia	Ia-norm	0.0337 (0.0022)	31.4 (2.1)	11.0	sn01ep (Ia-norm) 0.0337 (0.0058) 28.46 (2.08000)
SN 2004gl	Ia	Ia-norm	0.0425 (0.0029)	72.5 (6.5)	13.1	sn02fk (Ia-norm) 0.0431 (0.0040) 72.46 (6.52800)
SN 2004gs	Ia	Ia-norm	0.0280 (0.0055)	4.5 (3.2)	30.4	sn05am (Ia-norm) 0.0280 (0.0018) 4.47 (3.23200)
SN 2004gu	Ia	Ia-norm	0.0428 (0.0061)	−6.4 (2.8)	15.4	sn90N (Ia-norm) 0.0466 (0.0046) −6.40 (2.76500)
SN 2004gw	Ia	Ia-02cx	0.0146 (0.0005)	18.2 (0.0)	11.8	sn02cx (Ia-02cx) 0.0157 (0.0032) 18.20 (0.00000)
SN 2004gw	Ia	Ia-02cx	0.0150 (0.0003)	42.9 (4.9)	17.0	sn05hk (Ia-02cx) 0.0150 (0.0022) 42.90 (7.28900)
SN 2004gz	Ia	Ia-norm	0.0155 (0.0010)	38.2 (4.5)	18.1	sn05de (Ia-norm) 0.0148 (0.0031) 40.49 (7.59300)
SN 2005A	Ia	Ia-norm	0.0363 (0.0018)	−12.1 (0.7)	13.6	sn02bo (Ia-norm) 0.0376 (0.0050) −13.10 (0.707000)
SN 2005F	Ia	Ia-norm	0.0297 (0.0031)	14.9 (2.8)	16.6	sn00cn (Ia-norm) 0.0297 (0.0037) 14.95 (6.74700)
SN 2005G	Ia	Ia-norm	0.0249 (0.0030)	12.3 (2.4)	31.8	sn02jy (Ia-norm) 0.0249 (0.0018) 12.30 (2.44500)
SN 2005M	Ia	Ia-99aa	0.0333 (0.0049)	−3.0 (0.0)	10.9	sn05eq (Ia-99aa) 0.0304 (0.0048) −2.98 (0.00000)
SN 2005M	Ia	Ia-norm	0.0323 (0.0042)	1.9 (4.1)	7.4	sn94D (Ia-norm) 0.0340 (0.0059) −5.60 (3.96600)
SN 2005M	Ia	···	0.0294 (0.0061)	2.3 (4.4)	13.8	sn91T (Ia-91T) 0.0254 (0.0039) 7.43 (11.8020)
SN 2005M	Ia	Ia-norm	0.0258 (0.0017)	31.1 (7.5)	21.2	sn01dw (Ia-norm) 0.0267 (0.0029) 11.06 (8.71800)
SN 2005M	Ia	Ia-norm	0.0266 (0.0018)	30.2 (4.0)	21.2	sn02eu (Ia-norm) 0.0258 (0.0027) 33.44 (7.54300)
SN 2005as	Ia	Ia-norm	0.0161 (0.0013)	37.8 (2.9)	8.3	sn95D (Ia-norm) 0.0144 (0.0065) 37.80 (4.88000)
SN 2005P	II	IIP	0.0085 (0.0013)	242.8 (26.2)	5.5	sn04et (IIP) 0.0090 (0.0069) 236.80 (0.00000)
SN 2005P	II	IIP	0.0115 (0.0009)	284.8 (68.8)	5.9	sn04et (IIP) 0.0128 (0.0056) 411.50 (0.00000)
SN 2005X	Ia	Ia-norm	0.0761 (0.0014)	15.3 (2.3)	12.2	sn90N (Ia-norm) 0.0761 (0.0049) 17.70 (2.25100)
SN 2005W	Ia	Ia-norm	0.0102 (0.0027)	4.5 (3.1)	18.9	sn05am (Ia-norm) 0.0094 (0.0028) 4.47 (3.13500)
SN 2005W	Ia	Ia-norm	0.0091 (0.0011)	33.0 (5.5)	16.8	sn02eu (Ia-norm) 0.0087 (0.0033) 33.44 (6.92700)
SN 2005W	Ia	Ia-norm	0.0102 (0.0011)	28.8 (6.3)	17.1	sn01ep (Ia-norm) 0.0085 (0.0033) 28.46 (5.27000)
SN 2005ag	Ia	Ia-norm	0.0767 (0.0032)	1.2 (3.9)	14.4	sn95D (Ia-norm) 0.0745 (0.0038) 4.20 (3.81600)
SN 2005am	Ia	Ia-norm	0.0072 (0.0047)	0.1 (2.2)	20.4	sn02eu (Ia-norm) 0.0079 (0.0026) 0.14 (2.97100)

Continued on Next Page...

Table 2.7 — Continued

SN Name	Type	Subtype	$z_{\rm SNID}$[a]	$t_{\rm SNID}$[b]	$r$lap	Best Match[c]
SN 2005am	Ia	Ia-norm	0.0090 (0.0073)	5.5 (3.4)	13.9	sn98dx (Ia-norm) 0.0083 (0.0037) 5.50 (3.39100)
SN 2005am	Ia	Ia-norm	0.0072 (0.0009)	33.0 (4.2)	16.8	sn90N (Ia-norm) 0.0077 (0.0031) 38.50 (6.81500)
SN 2005am	Ia	Ia-norm	0.0074 (0.0009)	40.5 (4.2)	17.0	sn00cu (Ia-norm) 0.0074 (0.0033) 38.25 (5.96200)
SN 2005ao	Ia	···	0.0382 (0.0051)	2.9 (2.1)	26.9	sn08ds (Ia-99aa) 0.0349 (0.0020) 2.91 (3.83600)
SN 2005ao	Ia	···	0.0382 (0.0053)	3.3 (1.9)	17.7	sn08ds (Ia-99aa) 0.0361 (0.0032) −0.08 (3.83000)
SN 2005bc	Ia	Ia-norm	0.0139 (0.0047)	1.4 (1.8)	20.8	sn07fr (Ia-norm) 0.0122 (0.0026) −1.15 (3.28500)
SN 2005bc	Ia	Ia-norm	0.0146 (0.0039)	7.9 (0.3)	23.7	sn02ha (Ia-norm) 0.0133 (0.0022) 7.89 (1.59300)
SN 2005be	Ia	Ia-norm	0.0335 (0.0031)	12.2 (3.2)	34.2	sn05kc (Ia-norm) 0.0334 (0.0016) 12.19 (3.23300)
SN 2005be	Ia	Ia-norm	0.0319 (0.0018)	18.7 (1.5)	27.2	sn06kf (Ia-norm) 0.0330 (0.0023) 18.67 (8.22500)
SN 2005bl	Ia	Ia-norm	0.0271 (0.0071)	4.5 (3.8)	7.8	sn02kf (Ia-norm) 0.0242 (0.0064) 7.14 (3.94800)
SN 2005bl	Ia	Ia-91bg	0.0250 (0.0034)	20.5 (3.3)	18.6	sn03Y (Ia-91bg) 0.0250 (0.0033) 20.55 (6.60300)
SN 2005bo	Ia	Ia-norm	0.0151 (0.0012)	28.8 (3.6)	19.4	sn02eu (Ia-norm) 0.0147 (0.0029) 33.44 (5.66300)
SN 2005bu	Ia	Ia-norm	0.0305 (0.0016)	31.2 (2.0)	30.6	sn04ef (Ia-norm) 0.0315 (0.0021) 31.23 (6.01900)
SN 2005cf	Ia	Ia-norm	−0.0014 (0.0063)	−5.1 (3.1)	7.3	sn94D (Ia-norm) 0.0060 (0.0092) −10.60 (3.00300)
SN 2005cf	Ia	Ia-norm	0.0068 (0.0055)	−3.0 (3.1)	8.4	sn06kf (Ia-norm) 0.0059 (0.0061) −1.75 (3.25700)
SN 2005cf	Ia	Ia-99aa	0.0063 (0.0000)	−4.5 (0.0)	10.1	sn01eh (Ia-99aa) 0.0063 (0.0054) −4.53 (0.00000)
SN 2005cf	Ia	Ia-norm	0.0075 (0.0022)	14.4 (1.4)	16.2	sn07bm (Ia-norm) 0.0060 (0.0035) 15.52 (1.57600)
SN 2005cf	Ia	Ia-norm	0.0071 (0.0011)	33.4 (5.7)	16.5	sn02eu (Ia-norm) 0.0068 (0.0033) 33.44 (7.19200)
SN 2005cf	Ia	Ia-norm	0.0085 (0.0018)	246.2 (105.7)	6.8	sn07af (Ia-norm) 0.0061 (0.0078) 121.79 (101.255)
SN 2005cf	···	···	···	···	···	···
SN 2005de	Ia	Ia-norm	0.0165 (0.0044)	1.3 (2.3)	18.4	sn07af (Ia-norm) 0.0146 (0.0029) −1.21 (3.02000)
SN 2005de	Ia	Ia-norm	0.0162 (0.0034)	9.5 (1.0)	25.7	sn05kc (Ia-norm) 0.0158 (0.0021) 10.22 (3.33100)
SN 2005de	Ia	Ia-norm	0.0153 (0.0016)	30.0 (6.6)	17.3	sn07af (Ia-norm) 0.0150 (0.0034) 26.49 (7.40000)
SN 2005de	Ia	Ia-norm	0.0159 (0.0016)	38.5 (3.0)	20.4	sn06dm (Ia-norm) 0.0150 (0.0028) 36.06 (8.13200)
SN 2005do	Ia	Ia-norm	0.0324 (0.0015)	40.1 (2.2)	32.1	sn94ae (Ia-norm) 0.0312 (0.0016) 40.10 (8.83900)
SN 2005dh	Ia	Ia-91bg	0.0160 (0.0020)	2.1 (0.6)	15.2	sn06cs (Ia-91bg) 0.0156 (0.0030) 2.41 (0.644000)
SN 2005dh	Ia	Ia-91bg	0.0162 (0.0015)	14.9 (4.4)	11.8	sn05ke (Ia-91bg) 0.0155 (0.0050) 9.87 (4.37900)
SN 2005di	Ia	Ia-norm	0.0284 (0.0043)	1.1 (1.9)	8.6	sn94D (Ia-norm) 0.0268 (0.0052) −1.80 (3.20500)
SN 2005dm	Ia	Ia-91bg	0.0156 (0.0036)	4.3 (6.7)	9.2	sn91bg (Ia-91bg) 0.0163 (0.0067) 19.31 (8.13500)
SN 2005dv	Ia	Ia-norm	0.0061 (0.0048)	−0.3 (4.8)	16.7	sn06bq (Ia-norm) 0.0104 (0.0036) 6.69 (4.66700)
SN 2005ec	NotSN	Gal	0.0277 (0.0005)	···	9.1	kcE (Gal) 0.0282 (0.0032) −99.90 (0.00000)
SN 2005ej	Ia	Ia-norm	0.0427 (0.0048)	6.4 (2.8)	21.9	sn07A (Ia-norm) 0.0398 (0.0024) 2.37 (4.03000)
SN 2005ej	Ia	Ia-norm	0.0391 (0.0027)	14.3 (1.2)	33.1	sn98bu (Ia-norm) 0.0382 (0.0018) 14.30 (7.67000)
SN 2005ej	Ia	Ia-norm	0.0398 (0.0026)	18.9 (2.5)	40.1	sn04ey (Ia-norm) 0.0391 (0.0014) 18.90 (16.5800)
SN 2005el	Ia	Ia-norm	0.0134 (0.0037)	−3.8 (1.5)	13.9	sn94D (Ia-norm) 0.0137 (0.0039) −3.80 (2.27700)
SN 2005el	Ia	Ia-norm	0.0167 (0.0043)	−1.8 (3.0)	25.6	sn94D (Ia-norm) 0.0161 (0.0020) −1.80 (2.98300)
SN 2005el	Ia	Ia-norm	0.0164 (0.0042)	7.9 (2.7)	32.0	sn02ha (Ia-norm) 0.0145 (0.0016) 7.89 (2.71900)
SN 2005gj	Ia	···	0.0643 (0.0040)	46.1 (5.4)	11.6	sn02ic (Ia-csm) 0.0621 (0.0046) 44.10 (11.7960)
SN 2005gj	Ia	Ia-91T	0.0629 (0.0017)	49.1 (2.0)	11.5	sn97br (Ia-91T) 0.0600 (0.0055) 50.50 (1.97600)
SN 2005gj	II	IIP	0.0598 (0.0003)	146.9 (0.0)	10.6	sn04et (IIP) 0.0596 (0.0033) 146.90 (0.00000)
SN 2005gj	II	IIn	0.0601 (0.0005)	323.8 (0.7)	11.6	sn96L (IIn) 0.0595 (0.0021) 322.80 (0.00000)
SN 2005gj	II	IIn	0.0592 (0.0009)	323.8 (0.7)	10.8	sn96L (IIn) 0.0592 (0.0022) 322.80 (0.00000)
SN 2005er	Ia	Ia-91bg	0.0233 (0.0029)	1.4 (1.4)	14.1	sn91bg (Ia-91bg) 0.0267 (0.0040) 1.38 (1.43500)
SN 2005er	Ia	Ia-91bg	0.0251 (0.0000)	1.5 (0.0)	10.3	sn91bg (Ia-91bg) 0.0251 (0.0064) 1.50 (0.00000)
SN 2005er	Ia	Ia-91bg	0.0243 (0.0027)	19.3 (6.1)	8.5	sn91bg (Ia-91bg) 0.0238 (0.0066) 16.40 (8.72900)
SN 2005eq	Ia	Ia-99aa	0.0303 (0.0069)	−4.5 (0.8)	17.7	sn01eh (Ia-99aa) 0.0298 (0.0031) −4.53 (0.965000)
SN 2005eq	Ia	Ia-99aa	0.0296 (0.0056)	−4.5 (0.8)	25.8	sn01eh (Ia-99aa) 0.0303 (0.0022) −4.53 (2.92500)
SN 2005eq	Ia	Ia-99aa	0.0323 (0.0054)	1.1 (1.4)	12.7	sn98es (Ia-99aa) 0.0291 (0.0039) 0.64 (1.43400)
SN 2005eq	Ia	Ia-norm	0.0307 (0.0013)	41.5 (2.1)	23.0	sn98bu (Ia-norm) 0.0310 (0.0024) 43.10 (11.4830)
SN 2005ew	Ia	Ia-norm	0.0002 (0.0029)	10.1 (2.5)	8.6	sn98ec (Ia-norm) 0.0031 (0.0068) 13.49 (2.40700)
SN 2005ew	Ia	···	0.0109 (0.0049)	7.4 (1.8)	6.3	sn99da (Ia-91bg) 0.0032 (0.0111) 7.36 (1.81300)
SN 2005eu	Ia	Ia-norm	0.0393 (0.0055)	−6.4 (1.6)	7.9	sn90N (Ia-norm) 0.0345 (0.0064) −6.40 (1.60800)
SN 2005eu	Ia	Ia-norm	0.0349 (0.0055)	−0.1 (4.4)	9.6	sn00dg (Ia-norm) 0.0327 (0.0055) −5.00 (4.17900)
SN 2005eu	Ia	···	0.0342 (0.0045)	1.1 (3.3)	9.4	sn99aa (Ia-99aa) 0.0325 (0.0061) 0.33 (3.60900)
SN 2005eu	Ia	Ia-norm	0.0346 (0.0014)	20.5 (5.6)	12.1	sn06dw (Ia-norm) 0.0346 (0.0048) 28.28 (5.55300)
SN 2005hc	Ia	···	0.0451 (0.0034)	19.1 (2.3)	18.2	sn91T (Ia-91T) 0.0452 (0.0038) 15.90 (28.8100)
SN 2005hj	Ia	Ia-norm	0.0556 (0.0018)	9.3 (1.0)	21.5	sn94ae (Ia-norm) 0.0573 (0.0021) 9.30 (0.982000)
SN 2005hk	···	···	···	···	···	···
SN 2005hk	Ia	Ia-02cx	0.0135 (0.0011)	−2.4 (2.1)	8.8	sn02cx (Ia-02cx) 0.0127 (0.0045) −2.40 (2.05100)
SN 2005hk	···	···	···	···	···	···

Continued on Next Page...

Table 2.7 — Continued

SN Name	Type	Subtype	$z_{\rm SNID}$[a]	$t_{\rm SNID}$[b]	$r$lap	Best Match[c]
SN 2005hk	...	...	...	...	...	...
SN 2005hk	...	...	...	...	...	...
SN 2005hk	Ia	Ia-02cx	0.0129 (0.0007)	23.0 (3.5)	20.8	sn02cx (Ia-02cx) 0.0125 (0.0018) 24.97 (2.88900)
SN 2005hk	Ia	Ia-02cx	0.0131 (0.0006)	25.0 (1.4)	25.7	sn02cx (Ia-02cx) 0.0127 (0.0014) 24.97 (2.88900)
SN 2005hk	Ia	Ia-02cx	0.0127 (0.0002)	55.3 (1.4)	16.2	sn02cx (Ia-02cx) 0.0125 (0.0020) 55.26 (1.38300)
SN 2005hk	...	...	...	...	...	...
SN 2005hk	II	IIP	0.1282 (0.0017)	411.5 (33.0)	5.5	sn04et (IIP) 0.0129 (0.0040) 411.50 (0.00000)
SN 2005hk	...	...	...	...	...	...
SN 2005hk	...	...	...	...	...	...
SN 2005iq	Ia	Ia-norm	0.0331 (0.0039)	−2.1 (2.4)	23.2	sn03U (Ia-norm) 0.0320 (0.0022) −2.14 (3.02400)
SN 2005kc	Ia	Ia-norm	0.0168 (0.0035)	10.1 (1.1)	18.4	sn00cu (Ia-norm) 0.0152 (0.0030) 8.95 (2.01700)
SN 2005kc	Ia	Ia-norm	0.0162 (0.0031)	12.4 (2.9)	21.7	sn06ev (Ia-norm) 0.0152 (0.0027) 16.85 (3.95100)
SN 2005ke	Ia	...	0.0025 (0.0052)	25.1 (8.4)	8.6	sn91bg (Ia-91bg) 0.0042 (0.0060) 18.60 (9.48900)
SN 2005ke	Ia	Ia-91bg	0.0070 (0.0011)	17.2 (4.4)	13.7	sn08bt (Ia-91bg) 0.0064 (0.0043) 10.97 (4.39900)
SN 2005ke	Ia	Ia-91bg	0.0085 (0.0042)	18.6 (0.0)	10.9	sn91bg (Ia-91bg) 0.0056 (0.0047) 18.60 (0.00000)
SN 2005ke	Ia	Ia-91bg	0.0063 (0.0017)	46.5 (8.6)	14.7	sn91bg (Ia-91bg) 0.0065 (0.0033) 34.40 (6.19100)
SN 2005ke	Ia	Ia-91bg	0.0079 (0.0014)	50.5 (0.0)	11.7	sn91bg (Ia-91bg) 0.0065 (0.0041) 50.50 (0.00000)
SN 2005ke	Ic	Ic-broad	0.0072 (0.0016)	30.5 (0.0)	5.3	sn02ap (Ic-broad) 0.0059 (0.0112) 30.50 (0.00000)
SN 2005ki	Ia	Ia-norm	0.0208 (0.0045)	−1.6 (3.3)	18.6	sn07A (Ia-norm) 0.0186 (0.0027) 2.37 (3.76700)
SN 2005ki	Ia	Ia-norm	0.0207 (0.0043)	7.9 (0.3)	28.7	sn02ha (Ia-norm) 0.0192 (0.0019) 7.89 (2.61500)
SN 2005ki	Ia	Ia-norm	0.0184 (0.0009)	36.2 (5.5)	22.6	sn95D (Ia-norm) 0.0180 (0.0024) 42.80 (11.3320)
SN 2005ls	Ia	Ia-norm	0.0199 (0.0014)	20.5 (10.6)	12.3	sn06kf (Ia-norm) 0.0208 (0.0053) 18.67 (10.6190)
SN 2005ls	Ia	...	0.0253 (0.0042)	74.5 (10.2)	5.8	sn98es (Ia-99aa) 0.0231 (0.0100) 57.79 (19.3280)
SN 2005ls	Ia	Ia-norm	0.0246 (0.0024)	50.0 (0.0)	10.8	sn94D (Ia-norm) 0.0229 (0.0061) 50.00 (0.00000)
SN 2005lt	Ia	Ia-norm	0.0235 (0.0018)	41.3 (5.5)	17.7	sn02cr (Ia-norm) 0.0216 (0.0032) 33.69 (4.67700)
SN 2005lu	Ia	Ia-norm	0.0324 (0.0010)	26.5 (3.1)	11.9	sn05de (Ia-norm) 0.0326 (0.0054) 25.75 (3.12800)
SN 2005mc	Ia	Ia-norm	0.0274 (0.0028)	7.5 (1.2)	16.3	sn01ep (Ia-norm) 0.0249 (0.0035) 7.85 (1.82000)
SN 2005mc	Ia	Ia-norm	0.0262 (0.0011)	28.7 (8.9)	11.7	sn04fu (Ia-norm) 0.0267 (0.0054) 25.15 (8.91600)
SN 2005lz	Ia	Ia-norm	0.0436 (0.0039)	−1.0 (2.4)	27.7	sn98bu (Ia-norm) 0.0435 (0.0017) −2.80 (3.32900)
SN 2005ms	Ia	Ia-norm	0.0245 (0.0049)	−1.7 (2.8)	19.0	sn02er (Ia-norm) 0.0260 (0.0032) −3.50 (2.93200)
SN 2005ms	Ia	Ia-norm	0.0259 (0.0030)	13.2 (1.2)	29.6	sn98bu (Ia-norm) 0.0267 (0.0020) 13.20 (3.84100)
SN 2005na	Ia	...	0.0294 (0.0048)	2.4 (1.6)	21.3	sn08ds (Ia-99aa) 0.0264 (0.0025) −0.08 (3.54600)
SN 2005na	Ia	Ia-norm	0.0287 (0.0042)	2.4 (3.0)	19.1	sn07A (Ia-norm) 0.0273 (0.0028) 2.37 (3.01900)
SN 2005na	Ia	Ia-norm	0.0260 (0.0024)	18.9 (4.2)	31.5	sn04ey (Ia-norm) 0.0256 (0.0018) 18.90 (4.21200)
SN 2005na	Ia	Ia-norm	0.0246 (0.0018)	21.5 (7.7)	20.1	sn04fz (Ia-norm) 0.0259 (0.0028) 17.56 (8.52200)
SN 2005na	Ia	Ia-norm	0.0278 (0.0010)	28.5 (3.0)	14.2	sn06lf (Ia-norm) 0.0279 (0.0044) 25.06 (3.98700)
SN 2006D	Ia	Ia-norm	0.0091 (0.0023)	1.4 (1.6)	11.1	sn05bc (Ia-norm) 0.0091 (0.0045) 1.65 (1.57100)
SN 2006D	Ia	Ia-norm	0.0060 (0.0027)	15.1 (1.9)	11.9	sn06ev (Ia-norm) 0.0080 (0.0049) 16.85 (1.94300)
SN 2006D	Ia	Ia-norm	0.0103 (0.0018)	40.5 (9.0)	7.4	sn02cr (Ia-norm) 0.0091 (0.0074) 33.69 (6.41100)
SN 2006D	Ia	Ia-norm	0.0054 (0.0012)	48.0 (0.0)	12.2	sn94D (Ia-norm) 0.0080 (0.0039) 48.00 (0.00000)
SN 2006D	Ia	Ia-norm	0.0067 (0.0013)	100.9 (0.0)	12.6	sn07fb (Ia-norm) 0.0090 (0.0045) 100.91 (0.00000)
SN 2006E	Ia	Ia-norm	0.0023 (0.0010)	87.9 (1.7)	13.0	sn98ef (Ia-norm) 0.0026 (0.0042) 85.52 (1.71600)
SN 2006E	Ia	Ia-norm	0.0034 (0.0011)	153.4 (63.2)	18.8	sn94ae (Ia-norm) 0.0030 (0.0030) 153.40 (63.2150)
SN 2006E	...	...	...	...	...	...
SN 2006H	...	...	...	...	...	...
SN 2006N	Ia	Ia-norm	0.0135 (0.0043)	−5.0 (2.5)	19.4	sn06kf (Ia-norm) 0.0134 (0.0026) −1.75 (3.17300)
SN 2006N	Ia	Ia-norm	0.0131 (0.0043)	−3.6 (3.8)	18.7	sn06sr (Ia-norm) 0.0148 (0.0028) 2.73 (3.05100)
SN 2006N	Ia	Ia-norm	0.0138 (0.0026)	11.0 (2.9)	28.3	sn05be (Ia-norm) 0.0147 (0.0020) 10.96 (2.88200)
SN 2006N	Ia	Ia-norm	0.0141 (0.0012)	29.0 (6.5)	19.9	sn02eu (Ia-norm) 0.0137 (0.0029) 33.44 (6.89200)
SN 2006S	Ia	Ia-99aa	0.0291 (0.0040)	−4.5 (0.8)	21.1	sn01eh (Ia-99aa) 0.0310 (0.0026) −4.53 (0.775000)
SN 2006S	Ia	Ia-norm	0.0322 (0.0051)	1.3 (2.3)	18.9	sn06cq (Ia-norm) 0.0316 (0.0030) 1.91 (2.51600)
SN 2006S	Ia	Ia-norm	0.0321 (0.0022)	16.1 (1.6)	23.0	sn95D (Ia-norm) 0.0307 (0.0023) 16.10 (2.72600)
SN 2006X	Ia	Ia-norm	−0.0069 (0.0048)	−3.4 (0.7)	10.7	sn02bo (Ia-norm) 0.0043 (0.0060) −3.40 (0.677000)
SN 2006X	Ia	Ia-norm	0.0025 (0.0015)	29.4 (0.0)	10.3	sn02bo (Ia-norm) 0.0037 (0.0059) 29.40 (0.00000)
SN 2006X	Ia	Ia-norm	0.0065 (0.0004)	79.4 (4.9)	13.9	sn02bo (Ia-norm) 0.0068 (0.0040) 72.50 (4.87900)
SN 2006X	Ia	Ia-norm	0.0100 (0.0039)	71.8 (10.5)	9.2	sn99dk (Ia-norm) 0.0068 (0.0065) 71.83 (11.8550)
SN 2006X	Ia	Ia-norm	0.0072 (0.0013)	83.3 (8.1)	11.0	sn02bo (Ia-norm) 0.0067 (0.0055) 83.30 (8.11000)
SN 2006X	Ia	Ia-norm	0.0086 (0.0040)	85.5 (6.5)	7.9	sn98ef (Ia-norm) 0.0070 (0.0068) 85.52 (19.3080)
SN 2006X	...	...	...	...	...	...
SN 2006X	...	...	...	...	...	...

Continued on Next Page...

Table 2.7 — Continued

SN Name	Type	Subtype	$z_{\rm SNID}$[a]	$t_{\rm SNID}$[b]	$r$lap	Best Match[c]
SN 2006X	Ia	Ia-norm	0.1485 (0.0020)	17.7 (3.9)	5.3	sn90N (Ia-norm) 0.0036 (0.0117) 17.70 (3.88900)
SN 2006ac	Ia	Ia-norm	0.0191 (0.0039)	8.7 (3.5)	24.3	sn06os (Ia-norm) 0.0211 (0.0024) 8.68 (3.49600)
SN 2006ac	Ia	Ia-norm	0.0220 (0.0012)	28.5 (6.9)	16.5	sn01en (Ia-norm) 0.0222 (0.0038) 35.64 (7.30300)
SN 2006ak	Ia	Ia-norm	0.0348 (0.0052)	5.5 (5.9)	20.3	sn02er (Ia-norm) 0.0349 (0.0029) 5.50 (3.33200)
SN 2006ay	Ia	Ia-norm	0.0896 (0.0010)	51.1 (5.5)	13.2	sn04ey (Ia-norm) 0.0903 (0.0036) 51.49 (5.45800)
SN 2006ax	Ia	Ia-norm	0.0126 (0.0058)	−2.5 (1.2)	14.2	sn04fu (Ia-norm) 0.0178 (0.0044) −2.77 (2.26700)
SN 2006ax	Ia	Ia-norm	0.0173 (0.0019)	40.1 (11.2)	17.7	sn02fk (Ia-norm) 0.0160 (0.0032) 41.50 (12.5580)
SN 2006ax	Ia	Ia-norm	0.0187 (0.0012)	37.8 (6.3)	23.1	sn95D (Ia-norm) 0.0172 (0.0022) 37.80 (6.25600)
SN 2006az	Ia	Ia-norm	0.0326 (0.0017)	27.5 (2.8)	31.1	sn06lf (Ia-norm) 0.0326 (0.0021) 25.06 (6.28800)
SN 2006bq	Ia	Ia-norm	0.0166 (0.0045)	−0.6 (3.2)	20.5	sn92A (Ia-norm) 0.0213 (0.0028) 6.30 (4.04300)
SN 2006bq	Ia	Ia-norm	0.0186 (0.0031)	12.8 (2.3)	16.0	sn04ef (Ia-norm) 0.0207 (0.0039) 8.05 (2.31300)
SN 2006bq	Ia	Ia-norm	0.0185 (0.0028)	12.8 (1.5)	15.1	sn01en (Ia-norm) 0.0203 (0.0042) 10.09 (2.72600)
SN 2006bq	Ia	Ia-norm	0.0243 (0.0010)	28.3 (0.0)	10.2	sn06dw (Ia-norm) 0.0235 (0.0062) 28.28 (0.00000)
SN 2006br	Ia	Ia-norm	0.0190 (0.0052)	−1.7 (2.1)	6.8	sn02bo (Ia-norm) 0.0264 (0.0091) −3.40 (2.11300)
SN 2006br	Ia	Ia-norm	0.0204 (0.0017)	8.7 (0.1)	11.4	sn06ac (Ia-norm) 0.0241 (0.0053) 8.54 (0.0960000)
SN 2006bt	Ia	Ia-norm	0.0292 (0.0044)	0.3 (4.4)	17.0	sn08hs (Ia-norm) 0.0301 (0.0031) −7.94 (3.22600)
SN 2006bt	Ia	Ia-norm	0.0299 (0.0043)	−0.9 (2.8)	16.6	sn08hs (Ia-norm) 0.0308 (0.0032) −7.94 (3.01100)
SN 2006bt	Ia	Ia-norm	0.0319 (0.0044)	1.4 (4.5)	19.5	sn07fr (Ia-norm) 0.0307 (0.0029) −1.15 (3.49000)
SN 2006bt	Ia	Ia-norm	0.0337 (0.0024)	28.8 (4.6)	16.4	sn01ep (Ia-norm) 0.0320 (0.0037) 28.46 (7.30900)
SN 2006bt	Ia	Ia-91bg	0.0326 (0.0025)	34.4 (0.5)	10.7	sn91bg (Ia-91bg) 0.0346 (0.0046) 34.40 (0.495000)
SN 2006bu	Ia	Ia-norm	0.0812 (0.0041)	4.3 (2.7)	19.1	sn89B (Ia-norm) 0.0798 (0.0028) 3.50 (4.23300)
SN 2006bw	Ia	Ia-norm	0.0311 (0.0033)	6.1 (1.5)	20.8	sn01ep (Ia-norm) 0.0296 (0.0028) 5.97 (1.89600)
SN 2006bw	Ia	Ia-norm	0.0298 (0.0015)	28.7 (7.4)	25.0	sn02er (Ia-norm) 0.0322 (0.0025) 23.44 (8.28900)
SN 2006bz	Ia	Ia-91bg	0.0246 (0.0017)	0.4 (2.6)	13.4	sn91bg (Ia-91bg) 0.0263 (0.0043) 0.38 (2.63600)
SN 2006cc	Ia	Ia-norm	0.0322 (0.0023)	16.1 (4.0)	34.0	sn95D (Ia-norm) 0.0310 (0.0016) 16.10 (3.95800)
SN 2006ch	Ia	Ia-norm	0.0178 (0.0011)	40.1 (3.9)	16.9	sn94D (Ia-norm) 0.0173 (0.0033) 43.96 (7.77900)
SN 2006ch	Ia	Ia-norm	0.0176 (0.0016)	70.0 (10.8)	13.6	sn94D (Ia-norm) 0.0171 (0.0036) 74.23 (11.6760)
SN 2006ce	Ia	Ia-norm	0.0040 (0.0009)	87.8 (3.3)	11.9	sn94D (Ia-norm) 0.0046 (0.0045) 83.10 (3.32300)
SN 2006ce	Ia	Ia-norm	0.0049 (0.0010)	179.1 (56.7)	14.0	sn98bu (Ia-norm) 0.0054 (0.0041) 179.10 (56.7160)
SN 2006ce	Ia	Ia-norm	0.0056 (0.0011)	213.4 (35.0)	15.5	sn90N (Ia-norm) 0.0051 (0.0037) 213.40 (30.9410)
SN 2006cf	Ia	Ia-norm	0.0448 (0.0047)	4.2 (2.2)	20.4	sn95D (Ia-norm) 0.0437 (0.0026) 4.20 (3.16000)
SN 2006cf	Ia	Ia-norm	0.0441 (0.0041)	7.7 (2.8)	29.8	sn03ai (Ia-norm) 0.0417 (0.0018) 7.73 (2.81700)
SN 2006cf	Ia	Ia-norm	0.0446 (0.0027)	18.9 (2.5)	27.2	sn04ey (Ia-norm) 0.0432 (0.0020) 18.90 (14.6130)
SN 2006cj	Ia	Ia-norm	0.0669 (0.0039)	4.2 (1.6)	15.9	sn07A (Ia-norm) 0.0663 (0.0035) 2.37 (3.17900)
SN 2006cm	Ia	···	0.0159 (0.0047)	0.6 (4.0)	8.1	sn01eh (Ia-99aa) 0.0173 (0.0072) −4.53 (3.36300)
SN 2006cm	Ia	Ia-norm	0.0152 (0.0046)	9.3 (0.8)	16.4	sn94ae (Ia-norm) 0.0155 (0.0030) 9.30 (0.778000)
SN 2006cm	Ia	Ia-norm	0.0151 (0.0000)	17.4 (0.0)	10.1	sn94D (Ia-norm) 0.0151 (0.0054) 17.40 (0.00000)
SN 2006cm	II	II-pec	0.0178 (0.0018)	···	10.8	sn06gy (II-pec) 0.0185 (0.0025) −999.00 (0.00000)
SN 2006ct	···	···	···	···	···	···
SN 2006ct	II	···	0.0287 (0.0040)	34.5 (10.9)	6.1	sn04et (IIP) 0.0286 (0.0099) 39.50 (0.00000)
SN 2006cp	Ia	Ia-norm	0.0118 (0.0051)	−5.0 (1.5)	16.5	sn98ef (Ia-norm) 0.0224 (0.0038) −7.93 (2.81100)
SN 2006cq	Ia	Ia-norm	0.0508 (0.0048)	−1.5 (2.0)	25.9	sn94D (Ia-norm) 0.0520 (0.0020) −3.60 (2.87000)
SN 2006cs	Ia	Ia-91bg	0.0235 (0.0024)	2.5 (1.1)	22.0	sn02fb (Ia-91bg) 0.0234 (0.0024) 0.98 (2.02700)
SN 2006da	Ia	Ia-norm	0.0373 (0.0030)	10.1 (2.5)	12.9	sn06cf (Ia-norm) 0.0371 (0.0042) 11.12 (2.49300)
SN 2006da	Ia	Ia-norm	0.0403 (0.0020)	15.3 (12.1)	15.4	sn94D (Ia-norm) 0.0395 (0.0038) 15.30 (5.85500)
SN 2006da	Ia	Ia-norm	0.0397 (0.0018)	28.3 (7.1)	21.0	sn94D (Ia-norm) 0.0400 (0.0031) 15.20 (7.83600)
SN 2006da	Ia	Ia-norm	0.0412 (0.0010)	39.3 (9.6)	13.4	sn94D (Ia-norm) 0.0406 (0.0040) 43.96 (9.19800)
SN 2006cz	Ia	···	0.0388 (0.0063)	−1.5 (3.1)	15.8	sn01eh (Ia-99aa) 0.0433 (0.0039) −4.53 (4.07300)
SN 2006cz	Ia	Ia-norm	0.0397 (0.0062)	3.7 (2.8)	8.8	sn06or (Ia-norm) 0.0422 (0.0064) −2.91 (3.88900)
SN 2006cz	Ia	Ia-norm	0.0403 (0.0023)	12.8 (1.6)	12.1	sn02bo (Ia-norm) 0.0413 (0.0053) 12.80 (1.56600)
SN 2006cz	Ia	Ia-norm	0.0406 (0.0018)	27.6 (8.1)	14.9	sn07gk (Ia-norm) 0.0432 (0.0050) 19.65 (7.13100)
SN 2006cz	Ia	Ia-91bg	0.0481 (0.0106)	7.8 (0.0)	5.6	sn05ke (Ia-91bg) 0.0406 (0.0114) 7.82 (0.00000)
SN 2006dh	Ia	Ia-norm	0.0578 (0.0042)	−1.7 (2.9)	19.9	sn05ms (Ia-norm) 0.0581 (0.0031) −1.51 (2.76600)
SN 2006di	Ia	Ia-norm	0.0188 (0.0022)	41.5 (2.9)	19.6	sn00dk (Ia-norm) 0.0180 (0.0028) 36.68 (9.28600)
SN 2006dm	Ia	Ia-norm	0.0173 (0.0036)	−4.3 (2.3)	13.6	sn02er (Ia-norm) 0.0209 (0.0040) −4.25 (2.30800)
SN 2006dm	Ia	Ia-norm	0.0232 (0.0033)	8.9 (1.1)	21.6	sn01ep (Ia-norm) 0.0218 (0.0026) 7.85 (3.19000)
SN 2006dm	Ia	Ia-norm	0.0230 (0.0026)	15.5 (3.3)	21.3	sn04eo (Ia-norm) 0.0222 (0.0028) 13.19 (10.5280)
SN 2006dm	Ia	Ia-norm	0.0217 (0.0017)	27.2 (3.6)	23.5	sn05de (Ia-norm) 0.0217 (0.0026) 25.75 (8.00800)
SN 2006dm	Ia	Ia-norm	0.0229 (0.0015)	38.2 (4.1)	21.0	sn05de (Ia-norm) 0.0225 (0.0028) 40.49 (7.96200)
SN 2006do	Ia	···	0.0171 (0.0071)	17.9 (13.6)	5.4	sn05gj (Ia-csm) 0.0205 (0.0113) 17.90 (13.6470)

Continued on Next Page...

Table 2.7 — Continued

SN Name	Type	Subtype	$z_{\rm SNID}$[a]	$t_{\rm SNID}$[b]	$r$lap	Best Match[c]
SN 2006do	NotSN	Gal	0.0273 (0.0002)	···	18.3	kcS0 (Gal) 0.0275 (0.0018) −99.90 (0.00000)
SN 2006do	Ia	Ia-norm	0.0261 (0.0020)	25.1 (6.0)	12.8	sn04ef (Ia-norm) 0.0261 (0.0049) 31.23 (6.01400)
SN 2006do	NotSN	Gal	0.0288 (0.0004)	···	8.3	kcS0 (Gal) 0.0293 (0.0035) −99.90 (0.00000)
SN 2006dv	Ia	Ia-norm	0.0342 (0.0045)	2.2 (2.5)	25.8	sn94D (Ia-norm) 0.0313 (0.0020) 2.90 (3.60000)
SN 2006dv	Ia	Ia-norm	0.0342 (0.0045)	4.9 (3.3)	38.0	sn02ha (Ia-norm) 0.0320 (0.0014) 4.93 (3.30100)
SN 2006dv	Ia	Ia-norm	0.0326 (0.0031)	11.0 (1.3)	22.9	sn06dm (Ia-norm) 0.0314 (0.0025) 8.73 (3.16100)
SN 2006dv	Ia	Ia-norm	0.0316 (0.0018)	28.4 (4.3)	28.1	sn06N (Ia-norm) 0.0319 (0.0023) 27.49 (7.43800)
SN 2006dv	Ia	Ia-norm	0.0329 (0.0032)	28.5 (6.5)	7.8	sn94D (Ia-norm) 0.0332 (0.0078) 24.20 (8.16100)
SN 2006eb	Ia	Ia-norm	0.0173 (0.0009)	57.1 (6.5)	14.5	sn02er (Ia-norm) 0.0177 (0.0039) 60.98 (7.42000)
SN 2006eb	Ia	Ia-norm	0.0180 (0.0014)	79.4 (4.9)	22.3	sn02bo (Ia-norm) 0.0159 (0.0025) 79.40 (11.6820)
SN 2006dw	Ia	Ia-norm	0.0269 (0.0043)	1.3 (3.5)	26.9	sn94ae (Ia-norm) 0.0264 (0.0019) 1.30 (3.52900)
SN 2006dw	Ia	Ia-norm	0.0284 (0.0047)	3.8 (3.5)	34.6	sn07af (Ia-norm) 0.0252 (0.0015) 3.85 (3.46100)
SN 2006dw	Ia	Ia-norm	0.0263 (0.0029)	15.5 (2.1)	27.4	sn07bm (Ia-norm) 0.0258 (0.0022) 15.52 (4.51100)
SN 2006dw	Ia	Ia-norm	0.0267 (0.0013)	30.0 (7.5)	16.0	sn07fb (Ia-norm) 0.0280 (0.0038) 32.38 (8.22400)
SN 2006dy	Ia	Ia-norm	0.0063 (0.0064)	−4.4 (0.0)	21.3	sn04as (Ia-norm) 0.0075 (0.0032) −4.36 (0.00000)
SN 2006dy	Ia	Ia-norm	0.0084 (0.0039)	−1.8 (3.2)	17.8	sn05ms (Ia-norm) 0.0083 (0.0031) −1.51 (2.92300)
SN 2006dy	Ia	Ia-norm	0.0102 (0.0041)	7.7 (2.0)	22.8	sn03ai (Ia-norm) 0.0082 (0.0023) 7.73 (2.49000)
SN 2006dy	Ia	Ia-norm	0.0095 (0.0026)	18.9 (3.7)	21.9	sn99cp (Ia-norm) 0.0083 (0.0025) 13.70 (6.34900)
SN 2006dy	Ia	Ia-norm	0.0081 (0.0018)	39.9 (7.4)	16.5	sn02fk (Ia-norm) 0.0071 (0.0032) 41.50 (7.23000)
SN 2006ef	Ia	Ia-norm	0.0177 (0.0048)	0.1 (3.1)	17.4	sn06sr (Ia-norm) 0.0179 (0.0031) 2.73 (3.34800)
SN 2006ef	Ia	Ia-norm	0.0185 (0.0010)	28.8 (7.9)	19.9	sn02eu (Ia-norm) 0.0180 (0.0029) 33.44 (7.39100)
SN 2006ef	Ia	Ia-norm	0.0187 (0.0016)	39.9 (3.3)	20.1	sn00cu (Ia-norm) 0.0181 (0.0029) 38.25 (7.02800)
SN 2006gr	Ia	Ia-norm	0.0224 (0.0081)	−13.2 (0.0)	14.0	sn90N (Ia-norm) 0.0349 (0.0051) −13.20 (0.00000)
SN 2006gr	Ia	Ia-norm	0.0311 (0.0032)	17.8 (1.0)	20.9	sn02bo (Ia-norm) 0.0333 (0.0030) 17.80 (4.02500)
SN 2006gr	Ia	Ia-norm	0.0307 (0.0024)	21.7 (0.7)	22.7	sn02bo (Ia-norm) 0.0346 (0.0028) 21.70 (8.51300)
SN 2006ej	Ia	Ia-norm	0.0153 (0.0045)	−2.3 (3.1)	23.6	sn02he (Ia-norm) 0.0186 (0.0023) 0.29 (1.73800)
SN 2006ej	Ia	Ia-norm	0.0194 (0.0052)	5.5 (0.7)	30.0	sn98dx (Ia-norm) 0.0195 (0.0019) 5.50 (3.05900)
SN 2006ej	Ia	Ia-norm	0.0175 (0.0017)	23.4 (8.0)	19.2	sn02er (Ia-norm) 0.0199 (0.0033) 23.44 (10.0640)
SN 2006ej	Ia	Ia-norm	0.0193 (0.0011)	28.5 (3.2)	21.0	sn04fu (Ia-norm) 0.0210 (0.0030) 25.15 (7.86300)
SN 2006em	Ia	Ia-91bg	0.0205 (0.0032)	8.4 (2.4)	14.3	sn07al (Ia-91bg) 0.0192 (0.0039) 5.04 (3.46500)
SN 2006em	Ia	Ia-91bg	0.0184 (0.0000)	8.4 (0.0)	10.6	sn06ke (Ia-91bg) 0.0184 (0.0052) 8.43 (0.00000)
SN 2006em	Ia	Ia-91bg	0.0149 (0.0000)	29.5 (0.0)	10.1	sn91bg (Ia-91bg) 0.0149 (0.0060) 29.50 (0.00000)
SN 2006en	Ia	Ia-norm	0.0333 (0.0043)	10.2 (2.3)	17.1	sn95D (Ia-norm) 0.0325 (0.0029) 10.10 (2.04700)
SN 2006en	Ia	Ia-norm	0.0318 (0.0019)	17.2 (10.6)	22.2	sn94D (Ia-norm) 0.0344 (0.0026) 17.20 (10.5710)
SN 2006en	Ia	Ia-norm	0.0322 (0.0012)	33.0 (6.7)	23.0	sn95D (Ia-norm) 0.0318 (0.0026) 33.05 (7.91800)
SN 2006es	Ia	Ia-norm	0.0401 (0.0024)	16.4 (1.8)	28.4	sn07bc (Ia-norm) 0.0391 (0.0022) 16.35 (13.9870)
SN 2006es	Ia	Ia-norm	0.0417 (0.0011)	33.0 (7.4)	21.6	sn07af (Ia-norm) 0.0413 (0.0031) 26.49 (8.49000)
SN 2006eu	Ia	···	0.0230 (0.0058)	29.4 (10.9)	12.0	sn99da (Ia-91bg) 0.0226 (0.0057) 7.36 (13.7180)
SN 2006eu	Ia	Ia-norm	0.0249 (0.0017)	29.4 (7.1)	12.8	sn04fu (Ia-norm) 0.0259 (0.0054) 25.15 (7.14600)
SN 2006et	Ia	Ia-norm	0.0255 (0.0056)	4.2 (1.6)	13.7	sn94ae (Ia-norm) 0.0208 (0.0041) 6.40 (1.54000)
SN 2006et	Ia	Ia-norm	0.0205 (0.0046)	7.7 (0.4)	22.0	sn03ai (Ia-norm) 0.0177 (0.0027) 7.73 (2.97900)
SN 2006et	Ia	Ia-norm	0.0238 (0.0016)	28.8 (3.7)	19.2	sn05am (Ia-norm) 0.0240 (0.0032) 35.08 (6.58200)
SN 2006ev	Ia	Ia-norm	0.0285 (0.0050)	7.5 (1.6)	20.0	sn01ep (Ia-norm) 0.0268 (0.0030) 5.97 (2.17600)
SN 2006ev	Ia	Ia-norm	0.0296 (0.0028)	13.7 (3.7)	16.4	sn89B (Ia-norm) 0.0276 (0.0035) 12.40 (4.18500)
SN 2006gj	Ia	Ia-norm	0.0312 (0.0054)	5.0 (2.6)	19.9	sn03iv (Ia-norm) 0.0282 (0.0026) 6.99 (2.72500)
SN 2006gt	Ia	Ia-norm	0.0475 (0.0047)	1.6 (2.5)	21.4	sn00dk (Ia-norm) 0.0470 (0.0024) 1.36 (3.19800)
SN 2006ha	Ia	Ia-norm	0.0322 (0.0002)	29.4 (3.1)	13.3	sn04fu (Ia-norm) 0.0325 (0.0053) 25.15 (3.11700)
SN 2006hb	Ia	Ia-norm	0.0159 (0.0010)	41.3 (3.0)	20.8	sn00dk (Ia-norm) 0.0153 (0.0027) 36.68 (7.38600)
SN 2006hn	Ia	Ia-02cx	0.0170 (0.0020)	22.4 (3.6)	10.8	sn05hk (Ia-02cx) 0.017 (0.005) 14.3 (0.0000)
SN 2006je	Ia	Ia-norm	0.0379 (0.0019)	27.5 (1.7)	24.9	sn01ep (Ia-norm) 0.0362 (0.0026) 28.46 (6.96400)
SN 2006je	Ia	···	0.0390 (0.0048)	28.5 (8.8)	13.9	sn05ke (Ia-91bg) 0.0378 (0.0043) 14.85 (10.0660)
SN 2006ke	Ia	Ia-91bg	0.0179 (0.0020)	1.5 (2.4)	14.4	sn91bg (Ia-91bg) 0.0176 (0.0041) 2.50 (2.35500)
SN 2006ke	Ia	Ia-91bg	0.0190 (0.0022)	21.0 (11.3)	15.8	sn06em (Ia-91bg) 0.0177 (0.0037) 20.95 (8.59100)
SN 2006kf	Ia	Ia-norm	0.0212 (0.0038)	−5.9 (4.3)	16.4	sn02he (Ia-norm) 0.0231 (0.0033) −5.91 (3.88400)
SN 2006kf	Ia	Ia-norm	0.0217 (0.0042)	−3.5 (1.4)	23.7	sn94D (Ia-norm) 0.0202 (0.0021) −2.97 (3.13200)
SN 2006kf	Ia	Ia-norm	0.0197 (0.0018)	20.5 (9.4)	17.3	sn04fz (Ia-norm) 0.0209 (0.0033) 17.56 (9.85600)
SN 2006nr	Ia	Ia-norm	0.0168 (0.0016)	18.7 (12.5)	12.6	sn01dw (Ia-norm) 0.0177 (0.0046) 11.06 (12.4970)
SN 2006lf	Ia	Ia-norm	0.0120 (0.0044)	−1.9 (3.4)	21.9	sn06N (Ia-norm) 0.0126 (0.0024) −1.94 (2.93100)
SN 2006lf	Ia	Ia-norm	0.0147 (0.0024)	14.6 (7.0)	16.8	sn04ey (Ia-norm) 0.0131 (0.0033) 18.90 (4.93700)
SN 2006lf	Ia	Ia-norm	0.0129 (0.0012)	30.0 (5.8)	16.5	sn02eu (Ia-norm) 0.0128 (0.0034) 33.44 (5.80700)

Continued on Next Page...

Table 2.7 — Continued

SN Name	Type	Subtype	$z_{\rm SNID}$[a]	$t_{\rm SNID}$[b]	$r$lap	Best Match[c]
SN 2006lf	Ia	Ia-norm	0.0122 (0.0010)	44.1 (7.3)	13.0	sn98bu (Ia-norm) 0.0123 (0.0038) 44.10 (7.29500)
SN 2006le	Ia	Ia-norm	0.0142 (0.0057)	−6.5 (0.0)	11.3	sn07qe (Ia-norm) 0.0180 (0.0069) −6.54 (0.00000)
SN 2006le	Ia	Ia-norm	0.0144 (0.0030)	12.3 (2.3)	14.8	sn02bo (Ia-norm) 0.0176 (0.0040) 11.90 (2.26200)
SN 2006le	Ia	Ia-norm	0.0173 (0.0016)	41.0 (3.3)	20.3	sn99dk (Ia-norm) 0.0168 (0.0030) 44.20 (11.7350)
SN 2006mo	Ia	Ia-norm	0.0377 (0.0034)	16.4 (2.1)	19.0	sn89B (Ia-norm) 0.0353 (0.0028) 16.40 (3.34500)
SN 2006mp	Ia	···	0.0303 (0.0060)	4.2 (2.3)	15.2	sn05eq (Ia-99aa) 0.0288 (0.0034) 0.66 (3.20400)
SN 2006ob	Ia	Ia-norm	0.0614 (0.0050)	10.1 (2.0)	7.6	sn94ae (Ia-norm) 0.0632 (0.0062) 10.40 (3.06200)
SN 2006or	Ia	Ia-norm	0.0225 (0.0059)	0.2 (3.2)	15.9	sn99gd (Ia-norm) 0.0190 (0.0035) 0.17 (3.33400)
SN 2006or	Ia	Ia-norm	0.0198 (0.0030)	14.3 (1.7)	17.3	sn02bo (Ia-norm) 0.0225 (0.0036) 13.80 (2.30200)
SN 2006os	Ia	Ia-norm	0.0328 (0.0052)	6.1 (1.8)	28.8	sn02er (Ia-norm) 0.0328 (0.0020) 5.59 (3.15700)
SN 2006os	Ia	Ia-norm	0.0324 (0.0018)	27.5 (2.4)	29.9	sn02er (Ia-norm) 0.0346 (0.0022) 23.44 (8.02100)
SN 2006ot	Ia	Ia-norm	0.0487 (0.0048)	−2.5 (4.2)	14.2	sn02bo (Ia-norm) 0.0505 (0.0045) −1.40 (3.96200)
SN 2006ot	Ia	Ia-norm	0.0520 (0.0060)	−1.5 (4.1)	9.0	sn02er (Ia-norm) 0.0540 (0.0081) −2.50 (3.86500)
SN 2006ow	Ia	Ia-norm	0.0411 (0.0025)	18.7 (2.4)	24.1	sn94D (Ia-norm) 0.0423 (0.0025) 15.30 (12.8220)
SN 2006qo	Ia	···	0.0298 (0.0077)	−2.5 (3.7)	8.1	sn01eh (Ia-99aa) 0.0302 (0.0082) −4.53 (3.79500)
SN 2006sr	Ia	Ia-norm	0.0198 (0.0041)	−2.8 (2.2)	22.9	sn02he (Ia-norm) 0.0265 (0.0023) −5.91 (2.69600)
SN 2006sr	Ia	Ia-norm	0.0226 (0.0047)	0.3 (3.6)	35.2	sn02he (Ia-norm) 0.0255 (0.0016) 0.29 (3.56800)
SN 2006su	Ia	Ia-norm	0.0469 (0.0012)	23.4 (9.8)	22.0	sn07bm (Ia-norm) 0.0470 (0.0025) 20.45 (8.42600)
SN 2006td	Ia	Ia-norm	0.0149 (0.0010)	28.2 (6.6)	14.1	sn01dw (Ia-norm) 0.0151 (0.0043) 11.06 (6.78600)
SN 2006te	Ia	Ia-norm	0.0312 (0.0018)	19.2 (5.6)	20.8	sn06dw (Ia-norm) 0.0324 (0.0029) 28.28 (8.33600)
SN 2006te	Ia	Ia-norm	0.0323 (0.0018)	28.4 (4.3)	9.8	sn94D (Ia-norm) 0.0324 (0.0065) 24.20 (8.06800)
SN 2006te	Ia	Ia-norm	0.0330 (0.0012)	40.1 (10.2)	21.0	sn06dw (Ia-norm) 0.0342 (0.0028) 28.28 (8.48100)
SN 2007A	Ia	Ia-norm	0.0196 (0.0043)	1.5 (3.0)	21.4	sn00dn (Ia-norm) 0.0167 (0.0025) −1.04 (3.26100)
SN 2007A	Ia	Ia-norm	0.0172 (0.0028)	13.2 (1.1)	25.8	sn05kc (Ia-norm) 0.0163 (0.0021) 12.19 (3.09000)
SN 2007A	Ia	Ia-norm	0.0182 (0.0017)	35.6 (6.3)	19.3	sn02jy (Ia-norm) 0.0174 (0.0028) 39.90 (7.71500)
SN 2007B	Ia	Ia-norm	0.0202 (0.0045)	−0.9 (1.8)	27.4	sn06sr (Ia-norm) 0.0214 (0.0019) 2.73 (3.34700)
SN 2007B	Ia	Ia-norm	0.0213 (0.0045)	8.1 (0.1)	28.8	sn05ki (Ia-norm) 0.0193 (0.0019) 7.96 (3.10000)
SN 2007B	Ia	Ia-norm	0.0194 (0.0026)	11.0 (2.8)	30.0	sn05be (Ia-norm) 0.0203 (0.0019) 10.96 (2.80900)
SN 2007E	Ia	Ia-norm	0.0262 (0.0046)	7.5 (1.6)	26.0	sn02hd (Ia-norm) 0.0246 (0.0020) 6.05 (1.81900)
SN 2007E	Ia	Ia-norm	0.0226 (0.0023)	18.4 (2.5)	17.5	sn89B (Ia-norm) 0.0216 (0.0029) 17.40 (10.2920)
SN 2007F	Ia	Ia-norm	0.0212 (0.0054)	−6.4 (0.8)	12.5	sn02er (Ia-norm) 0.0230 (0.0048) −6.40 (0.763000)
SN 2007F	Ia	Ia-norm	0.0243 (0.0041)	3.3 (1.0)	23.0	sn07A (Ia-norm) 0.0230 (0.0023) 2.37 (2.90100)
SN 2007F	Ia	Ia-norm	0.0223 (0.0025)	22.5 (3.0)	22.4	sn07fs (Ia-norm) 0.0233 (0.0027) 22.67 (13.6580)
SN 2007F	Ia	···	0.0252 (0.0036)	57.8 (5.7)	21.4	sn08ds (Ia-99aa) 0.0249 (0.0026) 56.77 (17.0410)
SN 2007M	Ia	···	0.0197 (0.0022)	92.8 (0.2)	20.3	sn08ds (Ia-99aa) 0.0209 (0.0027) 92.83 (24.0970)
SN 2007N	Ia	Ia-91bg	0.0088 (0.0016)	−1.5 (0.0)	10.4	sn99da (Ia-91bg) 0.0101 (0.0053) −1.52 (0.00000)
SN 2007N	Ia	Ia-91bg	0.0141 (0.0018)	18.6 (4.2)	13.8	sn91bg (Ia-91bg) 0.0167 (0.0042) 19.31 (4.22200)
SN 2007O	Ia	Ia-norm	0.0430 (0.0046)	1.3 (3.3)	14.8	sn94ae (Ia-norm) 0.0378 (0.0032) 4.40 (3.47900)
SN 2007O	Ia	Ia-norm	0.0369 (0.0018)	30.0 (6.9)	32.7	sn07fb (Ia-norm) 0.0379 (0.0019) 32.38 (8.48900)
SN 2007R	Ia	Ia-norm	0.0277 (0.0024)	17.2 (4.1)	13.5	sn04fz (Ia-norm) 0.0287 (0.0044) 17.56 (5.09500)
SN 2007S	Ia	Ia-norm	0.0142 (0.0060)	3.7 (1.4)	13.4	sn98bu (Ia-norm) 0.0142 (0.0043) 1.20 (1.36900)
SN 2007S	Ia	Ia-norm	0.0139 (0.0011)	29.0 (8.2)	17.3	sn06et (Ia-norm) 0.0128 (0.0034) 43.76 (6.47500)
SN 2007S	Ia	Ia-norm	0.0153 (0.0009)	51.6 (3.9)	18.7	sn02er (Ia-norm) 0.0148 (0.0030) 60.98 (7.93600)
SN 2007V	Ia	Ia-norm	0.0295 (0.0016)	28.5 (3.6)	28.1	sn06N (Ia-norm) 0.0295 (0.0022) 27.49 (7.65000)
SN 2007af	Ia	Ia-norm	0.0069 (0.0043)	1.6 (1.8)	19.0	sn05de (Ia-norm) 0.0057 (0.0028) −0.75 (2.51800)
SN 2007af	Ia	Ia-norm	0.0080 (0.0044)	4.9 (3.1)	20.4	sn07bc (Ia-norm) 0.0050 (0.0025) 0.61 (2.15300)
SN 2007af	Ia	Ia-norm	0.0091 (0.0048)	2.8 (2.2)	24.0	sn01ep (Ia-norm) 0.0058 (0.0023) 2.83 (2.15300)
SN 2007af	Ia	Ia-norm	0.0056 (0.0011)	30.2 (4.8)	19.0	sn95D (Ia-norm) 0.0052 (0.0029) 33.05 (6.52600)
SN 2007af	Ia	Ia-norm	0.0073 (0.0012)	84.6 (4.2)	15.8	sn04ef (Ia-norm) 0.0055 (0.0036) 84.60 (4.19800)
SN 2007af	Ia	Ia-norm	0.0080 (0.0011)	84.6 (0.0)	13.7	sn04ef (Ia-norm) 0.0058 (0.0040) 84.60 (0.00000)
SN 2007af	Ia	Ia-norm	0.0083 (0.0023)	83.3 (100.8)	5.9	sn02bo (Ia-norm) 0.0053 (0.0087) 83.30 (100.795)
SN 2007af	Ia	Ia-norm	0.0078 (0.0018)	280.7 (27.0)	6.8	sn90N (Ia-norm) 0.0059 (0.0081) 255.90 (26.9790)
SN 2007af	Ia	Ia-norm	0.0080 (0.0015)	255.9 (117.6)	7.4	sn90N (Ia-norm) 0.0057 (0.0075) 255.90 (117.592)
SN 2007aj	Ia	Ia-norm	0.0304 (0.0030)	14.5 (1.6)	33.3	sn98bu (Ia-norm) 0.0310 (0.0017) 12.20 (2.99200)
SN 2007aj	Ia	Ia-norm	0.0312 (0.0016)	31.1 (3.2)	25.1	sn98bu (Ia-norm) 0.0310 (0.0022) 32.10 (7.51800)
SN 2007al	Ia	Ia-91bg	0.0156 (0.0026)	4.3 (1.2)	15.6	sn91bg (Ia-91bg) 0.0131 (0.0036) 2.50 (0.709000)
SN 2007ap	Ia	Ia-norm	0.0161 (0.0031)	8.1 (1.3)	15.9	sn05ki (Ia-norm) 0.0161 (0.0035) 7.96 (1.31000)
SN 2007ap	Ia	Ia-norm	0.0156 (0.0011)	36.1 (4.2)	19.8	sn06dm (Ia-norm) 0.0148 (0.0030) 36.06 (8.02500)
SN 2007ap	Ia	Ia-norm	0.0156 (0.0009)	40.5 (2.7)	16.8	sn00cu (Ia-norm) 0.0154 (0.0036) 38.25 (4.88200)
SN 2007ao	Ia	Ia-91bg	0.0265 (0.0021)	2.4 (2.9)	5.9	sn06bz (Ia-91bg) 0.0265 (0.0094) −1.67 (2.88100)

Continued on Next Page...

Table 2.7 — Continued

SN Name	Type	Subtype	$z_{\rm SNID}$[a]	$t_{\rm SNID}$[b]	$r$lap	Best Match[c]
SN 2007au	Ia	Ia-norm	0.0209 (0.0017)	27.5 (2.2)	18.5	sn04ef (Ia-norm) 0.0219 (0.0034) 31.23 (5.56300)
SN 2007au	Ia	Ia-norm	0.0228 (0.0013)	36.4 (5.7)	14.8	sn00dk (Ia-norm) 0.0217 (0.0040) 36.68 (5.62600)
SN 2007ax	Ia	Ia-91bg	0.0085 (0.0025)	16.4 (1.1)	12.7	sn05ke (Ia-91bg) 0.0064 (0.0042) 14.85 (1.09400)
SN 2007ba	Ia	Ia-91bg	0.0388 (0.0033)	0.4 (2.2)	20.4	sn99by (Ia-91bg) 0.0388 (0.0027) −2.80 (2.82500)
SN 2007ba	Ia	Ia-91bg	0.0403 (0.0024)	2.5 (2.0)	16.3	sn99by (Ia-91bg) 0.0381 (0.0034) 3.10 (1.64900)
SN 2007ba	Ia	Ia-norm	0.0381 (0.0040)	18.4 (4.4)	13.4	sn02bo (Ia-norm) 0.0389 (0.0045) 21.70 (4.35300)
SN 2007bc	Ia	Ia-norm	0.0245 (0.0045)	1.6 (2.1)	25.4	sn05bc (Ia-norm) 0.0225 (0.0021) 1.65 (3.12900)
SN 2007bc	Ia	Ia-norm	0.0221 (0.0027)	16.4 (2.6)	16.9	sn04eo (Ia-norm) 0.0222 (0.0035) 13.19 (14.3040)
SN 2007bd	Ia	Ia-norm	0.0243 (0.0044)	−2.3 (2.5)	27.6	sn06sr (Ia-norm) 0.0284 (0.0020) −2.30 (2.51300)
SN 2007bd	Ia	Ia-norm	0.0287 (0.0032)	10.1 (1.8)	17.1	sn01en (Ia-norm) 0.0302 (0.0035) 10.09 (2.56800)
SN 2007bj	Ia	Ia-pec	0.0172 (0.0000)	19.4 (0.0)	14.5	sn00cx (Ia-pec) 0.0173 (0.0042) 19.40 (0.00000)
SN 2007bj	Ia	Ia-norm	0.0150 (0.0026)	29.5 (9.5)	14.0	sn99dk (Ia-norm) 0.0181 (0.0046) 23.62 (9.50100)
SN 2007bj	Ia	Ia-norm	0.0172 (0.0017)	44.2 (2.2)	18.4	sn02bo (Ia-norm) 0.0172 (0.0032) 44.48 (12.3110)
SN 2007bm	Ia	Ia-norm	0.0063 (0.0041)	−1.9 (2.2)	18.3	sn06N (Ia-norm) 0.0068 (0.0028) −1.94 (2.50100)
SN 2007bm	Ia	Ia-norm	0.0073 (0.0025)	13.2 (3.4)	21.6	sn05cf (Ia-norm) 0.0061 (0.0027) 18.69 (3.03500)
SN 2007bm	Ia	Ia-norm	0.0057 (0.0018)	39.2 (9.6)	16.0	sn07bc (Ia-norm) 0.0065 (0.0036) 16.35 (10.2820)
SN 2007bm	Ia	Ia-norm	0.0073 (0.0009)	40.5 (2.9)	21.4	sn04eo (Ia-norm) 0.0059 (0.0025) 44.40 (6.93400)
SN 2007bz	Ia	Ia-norm	0.0208 (0.0050)	3.3 (3.5)	14.3	sn94ae (Ia-norm) 0.0197 (0.0036) 3.30 (3.50100)
SN 2007ca	Ia	Ia-norm	0.0085 (0.0059)	−8.4 (0.4)	9.1	sn02er (Ia-norm) 0.0135 (0.0070) −8.40 (5.23500)
SN 2007ca	Ia	Ia-norm	0.0144 (0.0027)	14.1 (1.8)	26.1	sn95D (Ia-norm) 0.0148 (0.0020) 14.10 (2.75800)
SN 2007ca	Ia	···	0.0155 (0.0046)	38.3 (5.0)	17.7	sn98es (Ia-99aa) 0.0137 (0.0031) 46.13 (12.3300)
SN 2007cf	Ia	Ia-91bg	0.0368 (0.0036)	7.8 (2.8)	12.5	sn99by (Ia-91bg) 0.0350 (0.0052) 3.10 (2.83700)
SN 2007cg	Ia	Ia-norm	0.0301 (0.0020)	11.0 (3.5)	11.3	sn06ev (Ia-norm) 0.0301 (0.0055) 16.85 (3.49900)
SN 2007ci	Ia	Ia-norm	0.0142 (0.0044)	−1.4 (1.7)	16.8	sn06ej (Ia-norm) 0.0187 (0.0030) −3.69 (3.44900)
SN 2007ci	Ia	Ia-norm	0.0171 (0.0046)	−0.5 (3.6)	18.0	sn03cq (Ia-norm) 0.0199 (0.0030) −0.05 (3.51000)
SN 2007ci	Ia	Ia-norm	0.0163 (0.0013)	27.5 (7.1)	15.7	sn06N (Ia-norm) 0.0166 (0.0040) 27.49 (8.73400)
SN 2007ci	Ia	Ia-norm	0.0184 (0.0011)	28.5 (2.0)	17.3	sn01ep (Ia-norm) 0.0166 (0.0035) 28.46 (5.11100)
SN 2007co	Ia	Ia-norm	0.0215 (0.0055)	−4.4 (1.5)	21.1	sn04as (Ia-norm) 0.0283 (0.0031) −4.36 (1.97000)
SN 2007co	Ia	Ia-norm	0.0248 (0.0055)	−3.5 (3.6)	31.7	sn02er (Ia-norm) 0.0271 (0.0020) −3.50 (3.58700)
SN 2007co	Ia	Ia-norm	0.0247 (0.0034)	10.8 (1.2)	20.9	sn04ef (Ia-norm) 0.0265 (0.0029) 8.05 (2.83000)
SN 2007co	Ia	Ia-norm	0.0252 (0.0019)	23.6 (2.8)	22.5	sn07gk (Ia-norm) 0.0278 (0.0030) 19.65 (9.18400)
SN 2007co	Ia	Ia-norm	0.0281 (0.0011)	27.6 (3.7)	21.1	sn02bo (Ia-norm) 0.0289 (0.0032) 27.59 (7.77600)
SN 2007co	Ia	Ia-norm	0.0278 (0.0010)	31.1 (6.3)	19.3	sn02bo (Ia-norm) 0.0286 (0.0034) 27.59 (7.93300)
SN 2007co	Ia	Ia-norm	0.0288 (0.0012)	51.1 (5.1)	21.5	sn02bo (Ia-norm) 0.0278 (0.0026) 49.60 (8.81900)
SN 2007co	Ia	Ia-norm	0.0292 (0.0017)	61.0 (10.0)	23.8	sn02er (Ia-norm) 0.0285 (0.0024) 60.98 (9.95400)
SN 2007cp	Ia	Ia-norm	0.0343 (0.0036)	−6.3 (2.8)	13.1	sn94D (Ia-norm) 0.0366 (0.0039) −8.70 (2.83300)
SN 2007cp	Ia	Ia-norm	0.0363 (0.0059)	3.2 (4.8)	15.3	sn00dk (Ia-norm) 0.0343 (0.0035) 1.36 (3.71400)
SN 2007cq	Ia	···	0.0263 (0.0031)	2.1 (0.7)	9.8	sn02fb (Ia-91bg) 0.0261 (0.0058) 0.98 (3.47400)
SN 2007cq	Ia	Ia-91bg	0.0254 (0.0019)	−2.8 (3.2)	13.6	sn06cs (Ia-91bg) 0.0260 (0.0037) 2.41 (3.15000)
SN 2007cq	Ib	Ib-norm	0.0252 (0.0009)	9.3 (0.0)	10.4	sn99ex (Ib-norm) 0.0246 (0.0061) 9.30 (0.00000)
SN 2007cq	Ia	Ia-91bg	0.0247 (0.0000)	27.3 (0.0)	10.1	sn91bg (Ia-91bg) 0.0247 (0.0062) 27.28 (0.00000)
SN 2007cq	Ia	Ia-norm	0.0241 (0.0017)	21.5 (9.5)	16.9	sn07fb (Ia-norm) 0.0247 (0.0033) 39.28 (9.75200)
SN 2007cq	Ia	Ia-norm	0.0241 (0.0017)	40.1 (2.1)	23.0	sn98bu (Ia-norm) 0.0248 (0.0023) 42.10 (14.2620)
SN 2007cs	Ia	Ia-norm	0.0147 (0.0027)	39.3 (4.2)	7.8	sn95D (Ia-norm) 0.0166 (0.0073) 42.80 (7.87200)
SN 2007cs	Ia	Ia-norm	0.0144 (0.0037)	44.1 (3.0)	9.9	sn02bo (Ia-norm) 0.0162 (0.0057) 45.60 (13.5240)
SN 2007cs	Ia	Ia-norm	0.0184 (0.0017)	51.6 (11.0)	15.2	sn02bo (Ia-norm) 0.0177 (0.0039) 51.60 (11.1950)
SN 2007cs	Ia	Ia-norm	0.0189 (0.0025)	51.6 (1.4)	15.7	sn02bo (Ia-norm) 0.0184 (0.0037) 49.60 (11.0150)
SN 2007fb	Ia	Ia-norm	0.0182 (0.0044)	1.1 (2.2)	22.1	sn94D (Ia-norm) 0.0176 (0.0023) −1.80 (3.44700)
SN 2007fb	Ia	Ia-norm	0.0182 (0.0025)	11.9 (5.5)	23.1	sn05be (Ia-norm) 0.0193 (0.0024) 10.96 (4.51000)
SN 2007fb	Ia	Ia-norm	0.0168 (0.0015)	29.2 (4.8)	19.9	sn94D (Ia-norm) 0.0175 (0.0028) 21.00 (8.13000)
SN 2007fb	Ia	Ia-norm	0.0169 (0.0016)	39.2 (5.5)	19.3	sn02ha (Ia-norm) 0.0175 (0.0028) 38.55 (8.55700)
SN 2007fb	Ia	Ia-norm	0.0161 (0.0011)	43.1 (9.2)	16.1	sn94ae (Ia-norm) 0.0174 (0.0030) 30.20 (16.2500)
SN 2007fb	Ia	···	0.0172 (0.0043)	59.1 (9.8)	17.1	sn08ds (Ia-99aa) 0.0168 (0.0032) 78.23 (22.7500)
SN 2007fb	Ia	Ia-norm	0.0161 (0.0009)	87.2 (39.8)	16.4	sn94D (Ia-norm) 0.0167 (0.0034) 87.19 (39.8070)
SN 2007fc	Ia	Ia-norm	0.0364 (0.0024)	18.9 (9.9)	38.9	sn04ey (Ia-norm) 0.0347 (0.0015) 18.90 (9.90000)
SN 2007fc	Ia	Ia-norm	0.0353 (0.0013)	27.6 (2.9)	22.4	sn02bo (Ia-norm) 0.0364 (0.0029) 27.59 (7.29300)
SN 2007fc	Ia	Ia-norm	0.0354 (0.0012)	35.6 (5.2)	22.8	sn07af (Ia-norm) 0.0352 (0.0027) 26.49 (7.55000)
SN 2007fq	Ia	Ia-91bg	0.0468 (0.0000)	16.4 (0.0)	5.7	sn91bg (Ia-91bg) 0.0466 (0.0126) 16.40 (0.00000)
SN 2007fr	Ia	Ia-norm	0.0513 (0.0046)	−0.9 (3.4)	13.4	sn06dw (Ia-norm) 0.0512 (0.0039) 1.07 (3.36200)
SN 2007fr	Ia	Ia-norm	0.0520 (0.0045)	4.8 (1.9)	26.5	sn05bc (Ia-norm) 0.0509 (0.0021) 1.65 (3.80900)

Continued on Next Page...

Table 2.7 — Continued

SN Name	Type	Subtype	$z_{\rm SNID}$[a]	$t_{\rm SNID}$[b]	$r$lap	Best Match[c]
SN 2007fs	Ia	Ia-norm	0.0190 (0.0053)	6.1 (1.4)	24.8	sn94ae (Ia-norm) 0.0176 (0.0021) 6.40 (2.44100)
SN 2007fs	Ia	Ia-norm	0.0177 (0.0026)	16.4 (2.6)	18.3	sn89B (Ia-norm) 0.0165 (0.0028) 17.40 (12.1320)
SN 2007fs	Ia	Ia-norm	0.0177 (0.0015)	35.1 (6.1)	19.2	sn95D (Ia-norm) 0.0160 (0.0026) 37.80 (7.53300)
SN 2007fs	Ia	Ia-norm	0.0183 (0.0015)	38.3 (2.9)	20.8	sn02jy (Ia-norm) 0.0180 (0.0026) 39.90 (6.82000)
SN 2007fs	Ia	Ia-norm	0.0183 (0.0021)	55.1 (5.0)	26.6	sn02bo (Ia-norm) 0.0171 (0.0020) 49.60 (9.41400)
SN 2007fs	Ia	Ia-norm	0.0177 (0.0012)	87.9 (2.3)	22.1	sn07af (Ia-norm) 0.0164 (0.0025) 91.06 (16.9730)
SN 2007ge	Ia	Ia-norm	0.0474 (0.0038)	13.4 (0.7)	26.8	sn89B (Ia-norm) 0.0456 (0.0020) 12.40 (4.65500)
SN 2007gi	Ia	Ia-norm	−0.0094 (0.0023)	−7.8 (2.8)	7.9	sn02cs (Ia-norm) −0.0040 (0.0070) −9.09 (2.81900)
SN 2007gi	Ia	Ia-norm	−0.0065 (0.0039)	−1.4 (4.6)	14.6	sn02bo (Ia-norm) −0.0019 (0.0043) −1.40 (4.43800)
SN 2007gi	Ia	Ia-norm	−0.0040 (0.0034)	6.7 (1.6)	18.5	sn06bq (Ia-norm) 0.0030 (0.0033) 6.69 (3.98500)
SN 2007gi	Ia	Ia-norm	0.0059 (0.0002)	85.5 (9.7)	10.7	sn98ef (Ia-norm) 0.0060 (0.0058) 85.52 (9.67900)
SN 2007gi	Ia	Ia-norm	0.0084 (0.0015)	208.0 (38.1)	8.6	sn98bu (Ia-norm) 0.0093 (0.0068) 208.00 (67.4890)
SN 2007gk	Ia	Ia-norm	0.0196 (0.0048)	−1.4 (2.0)	19.0	sn02bo (Ia-norm) 0.0269 (0.0033) −3.40 (2.30600)
SN 2007gk	Ia	Ia-norm	0.0245 (0.0018)	23.6 (7.5)	15.1	sn02er (Ia-norm) 0.0262 (0.0044) 23.44 (7.21000)
SN 2007if	Ia	Ia-norm	0.0748 (0.0021)	35.2 (7.9)	8.8	sn05de (Ia-norm) 0.0740 (0.0058) 40.49 (10.5030)
SN 2007if	Ia	Ia-norm	0.0728 (0.0007)	59.1 (1.2)	14.4	sn02cr (Ia-norm) 0.0728 (0.0034) 57.47 (4.97100)
SN 2007if	Ia	Ia-norm	0.0727 (0.0019)	72.5 (13.1)	13.4	sn02fk (Ia-norm) 0.0730 (0.0037) 72.46 (13.1090)
SN 2007hj	Ia	Ia-norm	0.0124 (0.0049)	0.3 (3.9)	17.2	sn08hs (Ia-norm) 0.0137 (0.0031) −7.94 (3.60500)
SN 2007hj	Ia	Ia-norm	0.0120 (0.0015)	25.1 (7.2)	10.9	sn00cn (Ia-norm) 0.0138 (0.0054) 14.95 (7.21400)
SN 2007hj	Ia	Ia-norm	0.0158 (0.0009)	41.3 (3.5)	18.0	sn00cu (Ia-norm) 0.0155 (0.0031) 38.25 (5.61700)
SN 2007hj	Ia	Ia-norm	0.0154 (0.0010)	91.1 (3.2)	13.8	sn01ep (Ia-norm) 0.0153 (0.0041) 87.26 (6.16700)
SN 2007hu	Ia	Ia-norm	0.0329 (0.0054)	5.1 (1.4)	31.7	sn05am (Ia-norm) 0.0339 (0.0018) 4.47 (3.08400)
SN 2007hu	Ia	Ia-norm	0.0331 (0.0016)	28.5 (1.9)	33.0	sn06ej (Ia-norm) 0.0339 (0.0019) 27.54 (7.48000)
SN 2007ir	Ia	Ia-norm	0.0330 (0.0019)	6.0 (2.7)	5.4	sn01ep (Ia-norm) 0.0336 (0.0122) 5.97 (2.71200)
SN 2007ir	Ia	Ia-norm	0.0331 (0.0029)	28.5 (7.7)	7.4	sn02cs (Ia-norm) 0.0340 (0.0082) 31.28 (9.23400)
SN 2007is	Ia	Ia-norm	0.0309 (0.0060)	−4.4 (2.3)	16.0	sn98bu (Ia-norm) 0.0273 (0.0035) −0.70 (2.50700)
SN 2007is	Ia	Ia-norm	0.0285 (0.0019)	19.6 (7.8)	26.0	sn07gk (Ia-norm) 0.0312 (0.0025) 19.65 (9.74200)
SN 2007kf	Ia	Ia-norm	0.0451 (0.0011)	43.2 (6.8)	17.1	sn94D (Ia-norm) 0.0454 (0.0031) 43.20 (7.35100)
SN 2007kg	Ia	Ia-norm	0.0072 (0.0020)	71.6 (11.9)	13.0	sn08ec (Ia-norm) 0.0067 (0.0043) 71.57 (11.9280)
SN 2007kd	Ia	Ia-norm	0.0233 (0.0015)	72.5 (4.2)	23.3	sn02bo (Ia-norm) 0.0229 (0.0024) 72.50 (10.2490)
SN 2007kk	Ia	Ia-norm	0.0355 (0.0046)	7.3 (4.0)	28.8	sn00fa (Ia-norm) 0.0382 (0.0020) 7.34 (3.99800)
SN 2007le	Ia	Ia-norm	−0.0020 (0.0030)	−5.1 (2.7)	11.5	sn94D (Ia-norm) −0.0031 (0.0057) −8.96 (2.68600)
SN 2007le	Ia	Ia-norm	−0.0022 (0.0030)	−7.8 (1.9)	13.4	sn00fa (Ia-norm) −0.0015 (0.0052) −7.77 (1.87500)
SN 2007le	Ia	Ia-norm	0.0026 (0.0049)	7.3 (3.4)	16.4	sn89B (Ia-norm) 0.0008 (0.0033) 7.50 (3.66800)
SN 2007le	Ia	Ia-norm	0.0045 (0.0022)	13.4 (2.8)	13.5	sn90N (Ia-norm) 0.0043 (0.0040) 17.70 (2.96500)
SN 2007le	Ia	Ia-norm	0.0049 (0.0021)	13.4 (4.6)	13.8	sn02bo (Ia-norm) 0.0072 (0.0042) 14.80 (4.39100)
SN 2007le	Ia	···	0.0043 (0.0047)	31.5 (11.6)	14.4	sn99dq (Ia-99aa) 0.0052 (0.0040) 24.09 (17.3150)
SN 2007le	Ia	Ia-norm	0.0056 (0.0009)	39.9 (6.0)	17.0	sn02bo (Ia-norm) 0.0058 (0.0031) 44.40 (8.56600)
SN 2007le	Ia	Ia-norm	0.0070 (0.0012)	49.6 (4.4)	16.2	sn99dk (Ia-norm) 0.0071 (0.0034) 44.20 (13.7680)
SN 2007le	Ia	Ia-norm	0.0117 (0.0034)	216.9 (57.9)	8.5	sn94ae (Ia-norm) 0.0104 (0.0068) 153.40 (81.2870)
SN 2007s1[d]	Ia	Ia-norm	0.0259 (0.0051)	−4.3 (1.6)	20.3	sn02er (Ia-norm) 0.0293 (0.0032) −4.40 (2.47800)
SN 2007s1[d]	Ia	Ia-norm	0.0279 (0.0012)	36.4 (4.5)	31.1	sn01en (Ia-norm) 0.0275 (0.0018) 35.64 (8.51800)
SN 2007qd	Ia	Ia-02cx	0.0499 (0.0037)	51.0 (8.0)	9.0	sn03gq (Ia-02cx) 0.0442 (0.0030) 57.96 (9.19700)
SN 2007on	Ia	Ia-norm	0.0053 (0.0038)	−0.9 (3.7)	13.3	sn06N (Ia-norm) 0.0062 (0.0038) −0.95 (3.47700)
SN 2007on	Ia	Ia-norm	0.0068 (0.0040)	−3.8 (3.5)	16.1	sn07fb (Ia-norm) 0.0059 (0.0028) 1.95 (2.91700)
SN 2007on	Ia	Ia-norm	0.0060 (0.0010)	27.5 (5.3)	12.3	sn98bu (Ia-norm) 0.0062 (0.0048) 30.22 (5.27300)
SN 2007on	Ia	Ia-norm	0.0066 (0.0016)	33.4 (3.3)	20.2	sn02eu (Ia-norm) 0.0064 (0.0028) 33.44 (4.71300)
SN 2007qe	Ia	Ia-norm	0.0104 (0.0062)	−5.0 (5.8)	9.1	sn92A (Ia-norm) 0.0220 (0.0063) −5.00 (2.89300)
SN 2007qe	Ia	Ia-norm	0.0179 (0.0057)	6.7 (5.6)	20.5	sn02bo (Ia-norm) 0.0261 (0.0030) −1.20 (4.31000)
SN 2007qe	Ia	Ia-norm	0.0204 (0.0029)	13.5 (1.5)	15.6	sn98bu (Ia-norm) 0.0219 (0.0038) 12.20 (1.56300)
SN 2007sa	Ia	Ia-norm	0.0045 (0.0009)	35.6 (4.3)	16.9	sn01en (Ia-norm) 0.0048 (0.0033) 35.64 (6.41400)
SN 2007rx	Ia	Ia-norm	0.0368 (0.0043)	2.3 (1.9)	13.5	sn07bc (Ia-norm) 0.0323 (0.0040) 0.61 (2.10100)
SN 2007ry	Ia	Ia-norm	0.0437 (0.0000)	18.7 (0.0)	10.6	sn06cf (Ia-norm) 0.0434 (0.0050) 18.72 (0.00000)
SN 2007sr	Ia	Ia-norm	0.0049 (0.0009)	29.0 (7.6)	13.6	sn04ef (Ia-norm) 0.0058 (0.0043) 31.23 (7.24300)
SN 2007sr	Ia	Ia-norm	0.0078 (0.0010)	84.6 (0.0)	11.4	sn04ef (Ia-norm) 0.0060 (0.0051) 84.60 (0.00000)
SN 2007su	Ia	Ia-norm	0.0293 (0.0079)	−2.9 (3.7)	14.4	sn06or (Ia-norm) 0.0267 (0.0040) −2.91 (3.68400)
SN 2007ux	Ia	Ia-norm	0.0329 (0.0039)	3.4 (2.7)	13.9	sn00dk (Ia-norm) 0.0323 (0.0035) 1.36 (3.21200)
SN 2007ux	Ia	Ia-norm	0.0306 (0.0017)	20.5 (7.9)	24.1	sn06kf (Ia-norm) 0.0321 (0.0027) 18.67 (9.09800)
SN 2008A	Ia	Ia-02cx	0.0109 (0.0000)	3.6 (0.0)	13.2	sn05hk (Ia-02cx) 0.0109 (0.0038) 3.60 (0.00000)
SN 2008A	Ia	Ia-02cx	0.0114 (0.0006)	23.0 (2.5)	14.2	sn05hk (Ia-02cx) 0.0113 (0.0028) 23.40 (2.53900)

Continued on Next Page...

Table 2.7 — Continued

SN Name	Type	Subtype	$z_{\rm SNID}$[a]	$t_{\rm SNID}$[b]	$r$lap	Best Match[c]
SN 2008A	Ia	Ia-02cx	0.0125 (0.0011)	19.8 (1.8)	11.6	sn02cx (Ia-02cx) 0.0131 (0.0034) 18.20 (1.84000)
SN 2008A	...	...	...	...	...	...
SN 2008A	...	...	...	...	...	...
SN 2008A	...	...	...	...	...	...
SN 2008C	Ia	Ia-norm	0.0175 (0.0026)	14.6 (5.5)	16.5	sn90N (Ia-norm) 0.0171 (0.0032) 17.70 (4.42700)
SN 2008L	Ia	Ia-norm	0.0175 (0.0009)	32.4 (6.8)	16.3	sn98bu (Ia-norm) 0.0175 (0.0034) 34.20 (8.28800)
SN 2008Q	Ia	Ia-norm	0.0085 (0.0047)	5.5 (3.0)	24.8	sn98dx (Ia-norm) 0.0087 (0.0021) 5.50 (3.02200)
SN 2008Q	Ia	Ia-norm	0.0039 (0.0015)	21.7 (0.0)	10.2	sn02bo (Ia-norm) 0.0073 (0.0056) 21.70 (0.00000)
SN 2008Q	Ia	...	0.0087 (0.0028)	146.4 (42.9)	13.6	sn00cx (Ia-pec) 0.0085 (0.0045) 146.40 (67.2450)
SN 2008Z	Ia	Ia-99aa	0.0178 (0.0037)	−0.1 (2.7)	13.9	sn08ds (Ia-99aa) 0.0162 (0.0038) −0.08 (3.12700)
SN 2008Z	Ia	Ia-norm	0.0187 (0.0000)	11.3 (1.3)	13.3	sn94ae (Ia-norm) 0.0188 (0.0039) 11.30 (1.34400)
SN 2008af	Ia	Ia-norm	0.0271 (0.0010)	23.4 (1.3)	18.4	sn06ej (Ia-norm) 0.0292 (0.0039) 21.65 (5.37000)
SN 2008ai	Ia	Ia-91bg	0.0366 (0.0029)	5.1 (2.5)	16.9	sn07ba (Ia-91bg) 0.0367 (0.0034) 5.12 (5.30500)
SN 2008ai	Ia	Ia-norm	0.0354 (0.0016)	27.5 (2.2)	11.0	sn01ep (Ia-norm) 0.0336 (0.0054) 28.46 (7.33300)
SN 2008ar	Ia	Ia-norm	0.0267 (0.0005)	−7.8 (1.3)	12.5	sn94D (Ia-norm) 0.0270 (0.0053) −9.60 (1.29500)
SN 2008ar	Ia	Ia-norm	0.0283 (0.0053)	3.2 (0.9)	20.7	sn06cq (Ia-norm) 0.0257 (0.0028) 1.91 (2.69600)
SN 2008ar	Ia	Ia-norm	0.0286 (0.0029)	45.6 (3.5)	5.1	sn02bo (Ia-norm) 0.0267 (0.0087) 40.60 (3.53600)
SN 2008ca	Ia	Ia-91bg	0.1418 (0.0000)	20.2 (0.0)	5.1	sn91bg (Ia-91bg) 0.1417 (0.0119) 20.20 (0.00000)
SN 2008cb	Ia	Ia-norm	0.1679 (0.0011)	32.0 (6.7)	11.5	sn05cf (Ia-norm) 0.1673 (0.0045) 27.64 (6.71000)
SN 2008bf	Ia	Ia-norm	0.0210 (0.0017)	21.5 (8.9)	19.1	sn07fb (Ia-norm) 0.0217 (0.0030) 39.28 (9.24800)
SN 2008bf	Ia	Ia-norm	0.0219 (0.0019)	41.5 (13.8)	11.9	sn01bg (Ia-norm) 0.0258 (0.0055) 18.91 (13.7640)
SN 2008bf	Ia	Ia-norm	0.0216 (0.0013)	35.1 (7.5)	18.7	sn98bu (Ia-norm) 0.0217 (0.0029) 40.10 (9.32500)
SN 2008bt	Ia	Ia-91bg	0.0158 (0.0025)	1.5 (2.0)	13.5	sn06cs (Ia-91bg) 0.0160 (0.0034) 2.41 (1.96300)
SN 2008bt	Ia	Ia-91bg	0.0159 (0.0018)	18.6 (5.1)	12.7	sn02fb (Ia-91bg) 0.0163 (0.0046) 18.60 (5.08400)
SN 2008bv	Ia	Ia-norm	0.0524 (0.0053)	7.3 (0.1)	30.0	sn07kk (Ia-norm) 0.0570 (0.0020) 7.15 (3.99400)
SN 2008bw	Ia	Ia-norm	0.0305 (0.0024)	17.3 (10.7)	29.3	sn92A (Ia-norm) 0.0393 (0.0020) 17.30 (10.6650)
SN 2008bz	Ia	Ia-norm	0.0608 (0.0043)	−0.9 (3.1)	20.8	sn02he (Ia-norm) 0.0639 (0.0026) 0.29 (3.71900)
SN 2008cd	NotSN	Gal	0.7739 (0.0025)	...	6.4	kcSa (Gal) 0.0077 (0.0029) −99.90 (0.00000)
SN 2008cf	Ia	Ia-99aa	0.0451 (0.0000)	2.9 (0.0)	10.5	sn08ds (Ia-99aa) 0.0451 (0.0052) 2.91 (0.00000)
SN 2008cl	Ia	Ia-norm	0.0638 (0.0048)	−0.2 (2.2)	22.1	sn02he (Ia-norm) 0.0661 (0.0025) 0.29 (3.63300)
SN 2008s1[e]	Ia	Ia-norm	0.0221 (0.0038)	−1.2 (2.9)	21.2	sn04fz (Ia-norm) 0.0200 (0.0022) −5.18 (3.26500)
SN 2008s1[e]	Ia	Ia-norm	0.0224 (0.0026)	−0.2 (2.8)	18.2	sn04fz (Ia-norm) 0.0208 (0.0025) −5.18 (3.34900)
SN 2008s1[e]	Ia	Ia-norm	0.0231 (0.0042)	−1.9 (2.4)	29.0	sn04fz (Ia-norm) 0.0208 (0.0016) −5.18 (3.06900)
SN 2008s1[e]	Ia	Ia-norm	0.0241 (0.0042)	−0.2 (2.8)	30.5	sn06dw (Ia-norm) 0.0241 (0.0016) 1.07 (3.36400)
SN 2008s1[e]	Ia	Ia-norm	0.0244 (0.0041)	3.8 (2.7)	28.1	sn07fr (Ia-norm) 0.0237 (0.0019) −1.15 (3.24700)
SN 2008s1[e]	Ia	Ia-norm	0.0245 (0.0045)	3.8 (3.2)	30.4	sn07fr (Ia-norm) 0.0240 (0.0017) −1.15 (3.33300)
SN 2008s1[e]	Ia	Ia-norm	0.0220 (0.0027)	18.9 (3.2)	26.1	sn04ey (Ia-norm) 0.0215 (0.0021) 18.90 (4.28100)
SN 2008s1[e]	Ia	Ia-norm	0.0215 (0.0013)	30.2 (7.1)	15.1	sn07fb (Ia-norm) 0.0235 (0.0039) 32.38 (8.18100)
SN 2008ct	Ia	Ia-norm	0.0244 (0.0025)	123.6 (25.3)	9.9	sn94ae (Ia-norm) 0.0238 (0.0048) 87.80 (32.4980)
SN 2008db	Ia	Ia-norm	0.0189 (0.0009)	32.4 (6.6)	14.0	sn98bu (Ia-norm) 0.0192 (0.0038) 28.20 (7.21000)
SN 2008db	Ia	Ia-norm	0.0204 (0.0016)	61.0 (14.1)	12.9	sn94ae (Ia-norm) 0.0196 (0.0037) 70.00 (14.0660)
SN 2008db	Ia	Ia-norm	0.0199 (0.0023)	72.5 (10.5)	6.2	sn94ae (Ia-norm) 0.0191 (0.0075) 87.80 (10.4750)
SN 2008dx	Ia	Ia-91bg	0.0261 (0.0025)	2.5 (0.8)	21.6	sn91bg (Ia-91bg) 0.0250 (0.0025) 2.50 (1.28800)
SN 2008dx	Ia	Ia-91bg	0.0228 (0.0025)	7.8 (1.1)	15.7	sn05ke (Ia-91bg) 0.0224 (0.0038) 7.82 (5.84000)
SN 2008dx	Ia	Ia-91bg	0.0243 (0.0013)	14.9 (3.4)	16.5	sn05ke (Ia-91bg) 0.0234 (0.0036) 9.87 (6.20500)
SN 2008dx	Ia	Ia-91bg	0.0233 (0.0000)	29.5 (0.0)	10.6	sn91bg (Ia-91bg) 0.0233 (0.0054) 29.50 (0.00000)
SN 2008ds	Ia	Ia-99aa	0.0241 (0.0057)	−3.3 (1.2)	15.3	sn01eh (Ia-99aa) 0.0235 (0.0038) −4.53 (3.85200)
SN 2008ds	Ia	Ia-99aa	0.0241 (0.0051)	0.7 (2.9)	13.9	sn05eq (Ia-99aa) 0.0219 (0.0040) 0.66 (2.64400)
SN 2008ds	Ia	Ia-norm	0.0223 (0.0042)	2.4 (2.2)	16.9	sn95D (Ia-norm) 0.0195 (0.0034) 6.10 (3.52100)
SN 2008ds	Ia	Ia-norm	0.0220 (0.0026)	18.9 (16.5)	26.2	sn04ey (Ia-norm) 0.0209 (0.0022) 18.90 (16.5210)
SN 2008ds	Ia	Ia-norm	0.0223 (0.0017)	50.0 (0.6)	28.5	sn94D (Ia-norm) 0.0221 (0.0018) 50.10 (16.7210)
SN 2008ds	Ia	Ia-norm	0.0211 (0.0017)	57.1 (4.6)	23.5	sn94D (Ia-norm) 0.0215 (0.0022) 57.10 (19.7420)
SN 2008ds	Ia	Ia-norm	0.0210 (0.0011)	59.1 (5.9)	20.1	sn94ae (Ia-norm) 0.0208 (0.0025) 70.00 (12.5010)
SN 2008ds	Ia	Ia-norm	0.0196 (0.0013)	87.8 (7.9)	15.8	sn07fs (Ia-norm) 0.0186 (0.0034) 91.35 (10.4910)
SN 2008ds	Ia	Ia-norm	0.0194 (0.0011)	91.1 (2.3)	22.5	sn95D (Ia-norm) 0.0204 (0.0023) 92.49 (14.0000)
SN 2008ds	Ia	Ia-norm	0.0191 (0.0010)	87.8 (2.4)	12.9	sn94ae (Ia-norm) 0.0209 (0.0039) 87.80 (2.40900)
SN 2008ds	Ia	Ia-norm	0.0203 (0.0011)	91.1 (14.2)	19.6	sn07af (Ia-norm) 0.0182 (0.0026) 121.79 (23.5990)
SN 2008dr	Ia	Ia-norm	0.0296 (0.0043)	−6.9 (1.3)	14.4	sn98ef (Ia-norm) 0.0400 (0.0043) −7.93 (4.95800)
SN 2008dr	Ia	Ia-norm	0.0342 (0.0044)	−1.4 (1.1)	25.8	sn02bo (Ia-norm) 0.0408 (0.0025) −1.40 (3.33500)
SN 2008dr	Ia	Ia-norm	0.0378 (0.0051)	−1.4 (3.1)	20.3	sn02bo (Ia-norm) 0.0444 (0.0030) −2.50 (3.74800)

Continued on Next Page...

Table 2.7 — Continued

SN Name	Type	Subtype	$z_{\rm SNID}$[a]	$t_{\rm SNID}$[b]	$r$lap	Best Match[c]
SN 2008dr	Ia	Ia-norm	0.0415 (0.0001)	28.6 (1.0)	13.2	sn02bo (Ia-norm) 0.0415 (0.0047) 28.60 (1.00200)
SN 2008dr	Ia	Ia-norm	0.0410 (0.0017)	61.0 (10.0)	17.3	sn99dk (Ia-norm) 0.0390 (0.0035) 71.83 (10.2500)
SN 2008dt	Ia	Ia-norm	0.0339 (0.0030)	−2.9 (0.0)	10.3	sn06or (Ia-norm) 0.0362 (0.0060) −2.91 (0.00000)
SN 2008dt	Ia	Ia-norm	0.0381 (0.0018)	28.5 (0.6)	11.4	sn01ep (Ia-norm) 0.0363 (0.0065) 28.46 (0.614000)
SN 2008dt	Ia	Ia-norm	0.0380 (0.0007)	44.4 (2.1)	10.1	sn04eo (Ia-norm) 0.0375 (0.0056) 44.40 (2.05000)
SN 2008r3[f]	Ia	Ia-norm	0.0250 (0.0044)	5.7 (0.6)	32.4	sn98dx (Ia-norm) 0.0250 (0.0016) 5.50 (3.05100)
SN 2008r3[f]	Ia	Ia-norm	0.0233 (0.0031)	12.2 (0.9)	38.9	sn05be (Ia-norm) 0.0244 (0.0015) 10.96 (4.09800)
SN 2008ec	Ia	Ia-norm	0.0188 (0.0045)	−0.9 (2.6)	26.6	sn02ha (Ia-norm) 0.0176 (0.0020) −0.85 (3.25800)
SN 2008ec	Ia	Ia-norm	0.0202 (0.0053)	6.6 (2.1)	22.9	sn07af (Ia-norm) 0.0172 (0.0023) 3.85 (2.52300)
SN 2008ec	Ia	Ia-norm	0.0187 (0.0031)	14.6 (2.3)	19.3	sn06lf (Ia-norm) 0.0174 (0.0030) 14.29 (12.3180)
SN 2008ec	Ia	Ia-norm	0.0177 (0.0012)	33.4 (2.4)	22.6	sn02eu (Ia-norm) 0.0173 (0.0025) 33.44 (5.85200)
SN 2008ec	Ia	Ia-norm	0.0161 (0.0012)	39.5 (3.6)	17.2	sn02fk (Ia-norm) 0.0160 (0.0031) 39.52 (3.58300)
SN 2008ec	Ia	Ia-norm	0.0177 (0.0018)	43.1 (4.4)	20.5	sn98bu (Ia-norm) 0.0179 (0.0026) 43.10 (7.89400)
SN 2008ec	Ia	Ia-norm	0.0174 (0.0015)	72.5 (13.7)	17.3	sn94ae (Ia-norm) 0.0169 (0.0029) 70.00 (13.8060)
SN 2008ee	Ia	Ia-norm	0.0162 (0.0019)	71.8 (11.2)	13.5	sn99dk (Ia-norm) 0.0130 (0.0042) 71.83 (11.1750)
SN 2008ee	Ia	Ia-norm	0.0156 (0.0039)	91.1 (13.7)	8.4	sn07af (Ia-norm) 0.0122 (0.0064) 91.06 (18.9960)
SN 2008ee	Ia	Ia-norm	0.0146 (0.0009)	81.6 (0.0)	13.6	sn04dt (Ia-norm) 0.0139 (0.0039) 81.59 (0.00000)
SN 2008ei	Ia	Ia-norm	0.0286 (0.0056)	−1.2 (3.3)	28.6	sn02bo (Ia-norm) 0.0349 (0.0022) −1.20 (3.28600)
SN 2008ei	Ia	Ia-norm	0.0294 (0.0034)	6.2 (1.2)	20.1	sn07qe (Ia-norm) 0.0370 (0.0033) 6.23 (1.15400)
SN 2008ei	Ia	Ia-norm	0.0338 (0.0017)	13.5 (2.0)	14.3	sn06bq (Ia-norm) 0.0355 (0.0050) 14.26 (1.86000)
SN 2008ei	Ia	Ia-norm	0.0372 (0.0012)	27.6 (7.8)	26.3	sn02bo (Ia-norm) 0.0376 (0.0027) 27.59 (7.82300)
SN 2008er	Ia	Ia-norm	0.0185 (0.0025)	28.5 (7.1)	14.6	sn01ep (Ia-norm) 0.0168 (0.0040) 28.46 (7.08500)
SN 2008ez	Ia	Ia-norm	0.0230 (0.0018)	27.5 (2.5)	13.1	sn02cs (Ia-norm) 0.0246 (0.0047) 31.28 (2.53400)
SN 2008ey	Ia	Ia-norm	0.0194 (0.0010)	43.0 (6.2)	15.4	sn99dk (Ia-norm) 0.0197 (0.0041) 44.20 (7.35800)
SN 2008s3[g]	Ia	Ia-norm	0.0423 (0.0016)	27.5 (5.0)	24.3	sn06ej (Ia-norm) 0.0447 (0.0028) 21.65 (7.89000)
SN 2008s4[h]	Ia	Ia-norm	0.0424 (0.0051)	4.9 (2.2)	25.6	sn02ha (Ia-norm) 0.0394 (0.0021) 4.93 (3.58600)
SN 2008fg	Ia	Ia-norm	0.0126 (0.0012)	91.1 (3.8)	13.0	sn04ef (Ia-norm) 0.0104 (0.0046) 84.60 (3.81900)
SN 2008fj	Ia	Ia-91bg	0.0298 (0.0033)	5.0 (2.7)	19.8	sn91bg (Ia-91bg) 0.0297 (0.0029) 2.50 (7.05400)
SN 2008s5[i]	Ia	Ia-99aa	0.0358 (0.0048)	0.7 (0.4)	22.7	sn05eq (Ia-99aa) 0.0332 (0.0023) 0.66 (0.420000)
SN 2008s5[i]	Ia	Ia-norm	0.0352 (0.0055)	7.7 (2.1)	17.7	sn95D (Ia-norm) 0.0327 (0.0032) 6.10 (2.96100)
SN 2008s5[i]	Ia	Ia-norm	0.0331 (0.0027)	13.7 (5.5)	15.4	sn98bu (Ia-norm) 0.0335 (0.0036) 14.30 (4.59800)
SN 2008fr	Ia	Ia-norm	0.0407 (0.0049)	0.3 (3.5)	20.7	sn02bo (Ia-norm) 0.0504 (0.0029) −3.40 (4.04100)
SN 2008fr	Ia	Ia-99aa	0.0385 (0.0080)	15.4 (4.0)	21.6	sn99aa (Ia-99aa) 0.0527 (0.0029) 15.40 (4.03100)
SN 2008fr	Ia	Ia-norm	0.0386 (0.0020)	19.2 (4.2)	19.5	sn94D (Ia-norm) 0.0401 (0.0026) 14.30 (10.0680)
SN 2008s8[j]	Ia	Ia-norm	0.0337 (0.0033)	11.1 (2.3)	19.6	sn06cf (Ia-norm) 0.0325 (0.0030) 11.12 (2.87000)
SN 2008s8[j]	Ia	Ia-norm	0.0375 (0.0031)	50.6 (0.0)	10.6	sn04dt (Ia-norm) 0.0308 (0.0047) 50.61 (0.00000)
SN 2008gs	Ia	···	0.0633 (0.0045)	41.0 (6.6)	14.8	sn97br (Ia-91T) 0.0622 (0.0043) 46.13 (14.2100)
SN 2008fx	Ia	Ia-norm	0.0544 (0.0032)	13.7 (3.0)	18.1	sn90N (Ia-norm) 0.0546 (0.0038) 14.50 (11.9270)
SN 2008ge	Ia	Ia-02cx	0.0028 (0.0010)	19.8 (3.9)	13.1	sn05hk (Ia-02cx) 0.0042 (0.0034) 14.30 (3.90700)
SN 2008gh	Ia	Ia-norm	0.0253 (0.0034)	8.9 (0.1)	16.8	sn92A (Ia-norm) 0.0325 (0.0035) 8.90 (1.64800)
SN 2008gh	Ia	Ia-91bg	0.0345 (0.0033)	48.2 (4.6)	8.9	sn91bg (Ia-91bg) 0.0328 (0.0063) 46.50 (7.50900)
SN 2008gt	Ia	Ia-norm	0.0759 (0.0050)	7.3 (2.1)	11.2	sn94ae (Ia-norm) 0.0724 (0.0045) 9.40 (2.12800)
SN 2008gt	Ia	Ia-norm	0.0668 (0.0010)	51.1 (10.5)	12.2	sn07fs (Ia-norm) 0.0662 (0.0040) 51.13 (10.5050)
SN 2008gy	Ia	Ia-norm	0.0290 (0.0023)	21.6 (1.9)	19.9	sn07gk (Ia-norm) 0.0316 (0.0031) 19.65 (6.99700)
SN 2008gw	Ia	Ia-norm	0.0645 (0.0021)	16.4 (2.9)	17.5	sn05cf (Ia-norm) 0.0627 (0.0031) 18.69 (3.56000)
SN 2008hk	Ia	Ia-norm	0.0318 (0.0025)	16.1 (3.7)	33.0	sn95D (Ia-norm) 0.0298 (0.0016) 16.10 (3.65400)
SN 2008ha	II	IIP	0.0069 (0.0040)	71.2 (0.0)	8.8	sn99em (IIP) 0.0047 (0.0034) 71.20 (0.00000)
SN 2008ha	II	IIP	0.0054 (0.0024)	71.2 (7.6)	6.1	sn99em (IIP) 0.0046 (0.0045) 71.20 (0.00000)
SN 2008ha	II	IIP	0.0063 (0.0023)	146.9 (53.5)	8.1	sn04et (IIP) 0.0042 (0.0031) 146.90 (0.00000)
SN 2008hj	Ia	Ia-norm	0.0342 (0.0044)	−6.9 (2.4)	17.0	sn04as (Ia-norm) 0.0347 (0.0039) −4.36 (2.14500)
SN 2008hj	Ia	Ia-norm	0.0376 (0.0048)	2.3 (3.0)	27.8	sn99gd (Ia-norm) 0.0355 (0.0021) 0.17 (3.89000)
SN 2008hj	Ia	Ia-norm	0.0371 (0.0015)	25.8 (5.2)	27.9	sn07af (Ia-norm) 0.0368 (0.0023) 26.49 (8.81900)
SN 2008hq	Ia	Ia-norm	0.0744 (0.0045)	4.4 (0.0)	11.6	sn02er (Ia-norm) 0.0713 (0.0043) 4.40 (0.00000)
SN 2008hr	Ia	Ia-norm	0.0833 (0.0046)	−0.5 (2.4)	17.5	sn08ec (Ia-norm) 0.0810 (0.0028) −0.24 (3.19600)
SN 2008hz	Ia	Ia-norm	0.0695 (0.0028)	16.4 (1.4)	15.1	sn92A (Ia-norm) 0.0795 (0.0033) 16.30 (14.2680)
SN 2008hu	Ia	Ia-norm	0.0461 (0.0047)	2.7 (1.7)	31.6	sn06sr (Ia-norm) 0.0467 (0.0018) 2.73 (3.60600)
SN 2008hs	Ia	Ia-norm	0.0153 (0.0046)	−0.5 (2.9)	16.7	sn06lf (Ia-norm) 0.0163 (0.0031) −6.30 (2.87800)
SN 2008hy	Ia	Ia-norm	0.0070 (0.0011)	37.8 (8.4)	32.9	sn95D (Ia-norm) 0.0056 (0.0016) 37.80 (8.40700)

The entries in this table match one-to-one with the entries in Table 2.2.

Continued on Next Page...

Table 2.7 — Continued

SN Name	Type	Subtype	$z_{\rm SNID}$[a]	$t_{\rm SNID}$[b]	$r$lap	Best Match[c]

[a]The redshift error is in parentheses.
[b]Phases of spectra are in rest-frame days. The phase error is in parentheses.
[c]The best matching SNID template in the form: "template SN" (subtype) $z_{\rm SNID}$ (error) $t_{\rm SNID}$ (error)
[d]Also known as SNF20071021-000.
[e]Also known as SNF20080514-002.
[f]Also known as ROTSE3 J125642.7+273041.
[g]Also known as SNF20080825-006.
[h]Also known as SNF20080825-010.
[i]Also known as SNF20080909-030.
[j]Also known as SNF20080920-000.

SNID Type

If the object's redshift is known *a priori* (from the host galaxy, usually via NED), we force SNID to use this redshift, otherwise we do not use any redshift prior. For the first attempt to determine a type, the minimum $r$lap value is set to 10. A spectrum is determined to be of a given type if the fraction of "good" correlations that correspond to this type exceeds 50%. In addition, we require the best-matching SN template to be of this same type. If the spectrum's type cannot be determined using these criteria we perform another SNID run, this time using a minimum $r$lap value of 5. This resulted in 1259 of our 1298 spectra receiving a SNID type. If the type of the input spectrum is successfully determined (using either $r$lap value), an attempt is made to determine its subtype.

SNID Subtype

Again, we adopt the host-galaxy redshift when available and the minimum $r$lap used to determine if the subtype is the same as was used to successfully determine the type (either 5 or 10). We also force SNID to only consider templates of the previously determined SN type. A spectrum is determined to be of a given subtype if the fraction of "good" correlations that correspond to this subtype exceeds 50%. In addition, we require the best-matching SN template to be of this same subtype. If the spectrum's subtype cannot be determined using these criteria, *and* a minimum $r$lap of 10 was used, we perform another SNID run, this time using a minimum $r$lap value of 5. This resulted in 1151 of our 1298 spectra receiving a SNID subtype. Regardless of whether SNID determines a subtype, a third run is executed to determine the redshift.

SNID Redshift

The SNID redshift is calculated by taking the median of all "good" template redshifts and the redshift error is the standard deviation of these redshifts. If a subtype has been successfully determined, we force SNID to only use templates of that subtype, otherwise we only use templates of the previously determined type. For this SNID run no *a priori* redshift information is used. 1259 of our 1298 spectra received a SNID redshift. If a redshift

is successfully determined in this run, a fourth run is executed to calculate the age of the spectrum.

SNID Age

The SNID age is calculated by taking the median of all "good" template ages that have an $r$lap value larger than 75% of the $r$lap value of the best-matching template. The age error is the standard deviation of these ages. Again, if a subtype has been successfully determined, we force SNID to only use templates of that subtype, otherwise we only use templates of the previously determined type. For this run, we again force SNID to adopt the host-galaxy redshift when available. If no host-galaxy redshift is known, we use the previously determined SNID redshift instead. 1249 of our 1298 spectra received a SNID age.

2.5.3 Verifying Redshifts and Ages from SNID

It has been shown previously that SNID-determined redshifts correlate extremely well with actual redshifts of SN host galaxies (e.g., Foley et al. 2009b; Östman et al. 2011). Figure 2.9 shows that the SNID-determined redshifts (using v7.0 of our templates) agree well with the host-galaxy redshifts of our data. The dispersion about the one-to-one correspondence is only $\sim$0.005 for the 1206 spectra for which the redshift is known and which SNID determined were SNe Ia and calculated a redshift. This is as good as or better than what has been found previously using much smaller samples of higher-redshift SNe (Foley et al. 2009b; Östman et al. 2011). However, as seen in Figure 2.9, the majority of the largest outliers appear to have SNID redshifts that are lower than the host-galaxy redshifts. The normalized median absolute deviation (i.e., a measure of the precision of our redshifts; Ilbert et al. 2006), defined as

$$\sigma \equiv 1.48 \times \text{ median} \left[\frac{|z_{\rm SNID} - z_{\rm gal}|}{1 + z_{\rm gal}} \right], \tag{2.4}$$

is 0.002.

One spectrum is a fairly significant outlier (seen in the top left of the top panel of Fig. 2.9). This spectrum is 360 d past maximum brightness (according to the light curve) and we only have a small number of SN Ia templates that are this old (only 3 older than 300 d). The relative lack of good matches with old SN Ia spectra, as opposed to much younger spectra at much higher redshifts, is most likely the cause of the erroneous redshift (and age) from SNID.

The original SNID template spectra have ages which have been corrected for the $1/(1+z)$ time-dilation factor which we expect to observe in an expanding universe (e.g., Riess et al. 1997; Blondin et al. 2008). Thus, SNID templates should have ages in the rest frame of the SNe.[13] We compare the SNID-determined ages of our SN Ia spectra to their actual

[13]When creating our own SNID templates, we transformed our SN ages to the rest frame (using the redshift of the SN or the host galaxy).

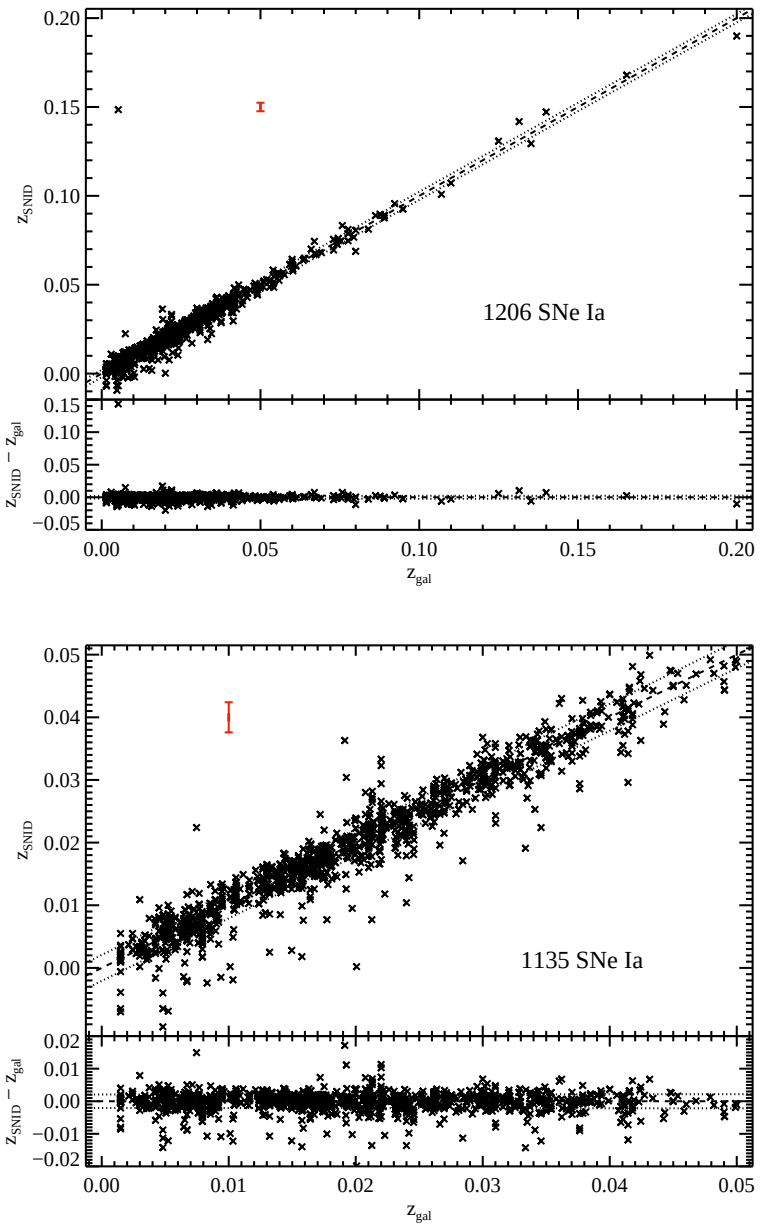

Figure 2.9: Comparison of galaxy redshifts ($z_{\rm gal}$) and SNID-determined redshifts ($z_{\rm SNID}$) using our SNID classification scheme. All 1206 spectra for which the redshift is known and which SNID determined were SNe Ia (*top*) and a zoom-in on the 1135 SN Ia spectra with $z_{\rm gal} \leq 0.05$ and $z_{\rm SNID} \leq 0.05$ (*bottom*). The median error bar in both directions for the entire sample is shown in red in the top left of each plot. The bottom of each plot shows the residuals versus $z_{\rm gal}$. In all plots the short-dashed line is the one-to-one correspondence and the dotted lines are $z_{\rm SNID} = z_{\rm gal} \pm 0.002\,(1 + z_{\rm gal})$ (representing the average precision). See the text for more information on the extreme outlier in the top left of the top panel.

(rest-frame) ages as derived from their light curves and redshifts as presented in Table 2.1; the result is shown in Figure 2.10. There are 869 total spectra that SNID determined were SNe Ia (and 704 with light-curve ages ≤ 50 d) which have both SNID-determined ages and light-curve ages. The dispersion about the one-to-one correspondence for the total sample is approximately 21 d, and the dispersion for the sample with light-curve ages ≤ 50 d is $\sim$6.0 d. Foley et al. (2009b) calculated a dispersion of 1.8 d for 59 SN Ia spectra with light-curve ages between -11 and 19.4 d at moderate to high redshift ($0.100 \leq z \leq 0.807$). We have 451 spectra in this range and calculate a dispersion of $\sim$5.3 d for these data. Östman et al. (2011) obtained a dispersion of 4 d for 127 SN Ia spectra with light-curve ages between -11.7 and 67.9 d at moderate redshift ($0.03 \leq z \leq 0.32$). We have 757 spectra in this range and calculate a dispersion of $\sim$6.3 d for these data. The significantly larger number of spectra in our sample is likely responsible for the increase in the dispersions as compared to previous work.

The samples used by Foley et al. (2009b) and Östman et al. (2011) were at higher redshift than our data, and the way in which they determined spectral ages using SNID was slightly different; both studies used the median age of all "good" template ages. We initially used this same method for our spectra, but we soon found a significant bias in our SNID-determined ages (as compared to ages derived from the SN light curves). The bias was causing SNID-determined ages to be artificially skewed toward about +30 d for spectra which are (according to their photometry) in the range of about 23–33 d. We also observed a similar, yet weaker, version of this bias for spectra whose photometric ages were near maximum brightness as well as spectra with light-curve ages near $\sim$100 d (still visible in the top panel of Fig. 2.10). The bias near maximum brightness is seen in the higher-redshift data presented by Östman et al. (2011), and we suggest that the bias near ages of $\sim$30 d (and perhaps the one near 100 d as well) *would* have been observed in their data if their dataset had contained spectra at these epochs. It should be noted, however, that despite these biases, half of our SNID-derived ages are within 1σ of the one-to-one correspondence with light-curve age.

Despite this, we thoroughly investigated the phenomenon but unfortunately found no simple explanation for the apparent bias. In order to characterize and explain the strongest bias (near photometric ages of one month past maximum brightness), we used the default set of SNID templates, instead of our own, and re-ran all of our spectra through our classification routine, only to have the bias appear even stronger than before. We examined the age and light-curve shape (as characterized by the MLCS2k2 Δ parameter; Jha et al. 2007) distributions of our v7.0 templates, the default set of SNID templates, and the light-curve ages of our entire dataset, and none of these showed any deviation at or near +30 d that might affect SNID's age determinations. For example, Figure 2.8 shows a histogram of the ages of all of our SN Ia spectral templates (separated by SNID template version), and there does not appear to be any obvious bias near +30 d. Furthermore, we investigated how the strength of the bias changed with SNID-determined subtype, best-matching subtype, and $r$lap but saw no strong correlations. Finally, we altered the way in which we used SNID to

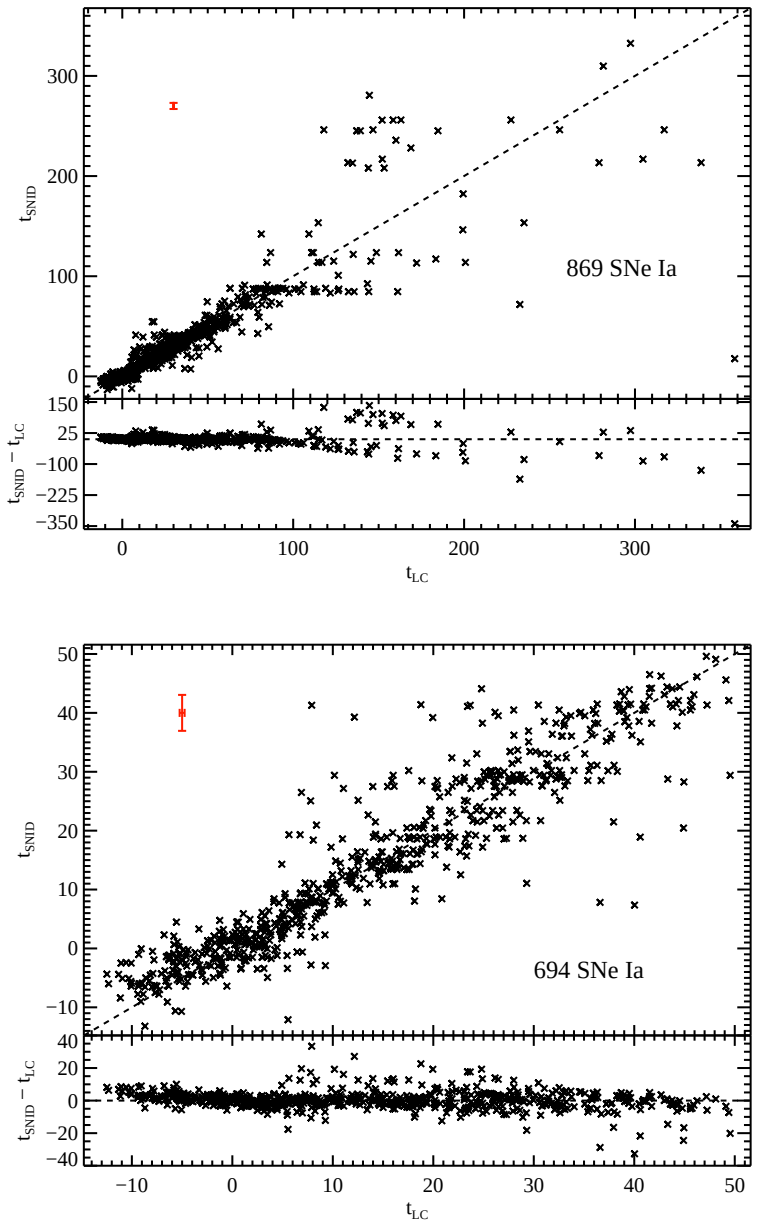

Figure 2.10: Comparison of rest-frame light-curve ages ($t_{\rm LC}$) and SNID-determined ages ($t_{\rm SNID}$) using our SNID classification scheme. All 869 spectra which SNID determined were SNe Ia and that have both SNID-determined ages and light-curve ages (*top*), and a zoom-in on the 694 SN Ia spectra with $t_{\rm LC} \leq 50$ d and $t_{\rm SNID} \leq 50$ d (*bottom*). The median error bar in both directions for the entire sample is shown in red in the top left of each plot. The bottom of both plots shows the residuals versus $t_{\rm LC}$.

actually determine the spectral age. Instead of using the median age of *all* "good" templates, we tried using the median of various subsamples of "good" templates. We found that using the median of all "good" template ages with an $r$lap value larger than 75% of the largest $r$lap value decreased the bias most effectively.

One possible explanation for this bias is that templates with ages near +30 d were being considered "good" by SNID (i.e., they had $r$lap values above the minimum $r$lap for a given SNID run), but they were not actually all that well correlated with the input spectrum. Thus, the median age of all "good" templates was being unphysically skewed toward +30 d. We avoid this by effectively having a variable minimum $r$lap value that is scaled to the $r$lap of the best-matching template. This allows us to take a median age of only a subset of templates that are all relatively strongly correlated with the input spectrum. Furthermore, the fact that we are using the median of a set of template ages ensures that no single template will dominate the age determination.

Even though this new method of determining SNID ages reduces the bias near +30 d, the bias near maximum brightness (mentioned above and seen in Östman et al. 2011) is still present. This is almost certainly caused by the fact that we have many more SNID templates within a couple days of maximum brightness than we do a week (or more) before maximum. Thus, for example, a spectrum that was actually observed 10 d before maximum brightness will get artificially skewed toward older SNID ages closer to maximum.

2.5.4 Classification of Objects

After classifying (or attempting to classify) all of the spectra in our dataset using the method described in Section 2.5.2, we use the SNID information for all spectra of a given object to determine the SN's (sub)type.

Classification Accuracy

To investigate the accuracy of our SN Ia classification scheme, we attempt to find correlations between the accuracy of our SN Ia subtype determination and the $r$lap value of the best-match template, the SNID-determined age of the input spectrum, and the S/N of the input spectrum. We find that our accuracy is similarly correlated with both $r$lap and S/N, which is unsurprising since S/N is one of the factors which determines the $r$lap value during a SNID run. Thus, we attempt to correlate our classification accuracy with only $r$lap and spectral age, simultaneously.

To do this, we compare the subtype we determined using our classification scheme (Section 2.5.2) for each SN Ia template spectrum in v7.0 to the actual subtype of the template object. If our multiple SNID runs correctly classified a given spectrum, we assigned it an "accuracy percentage" (P) of 1, and if it was misclassified it received an accuracy classification of 0. We then used the $r$lap value of the best-matching template (r) and the SNID-determined

(rest-frame) age (t, in days) of each spectrum to fit a two-dimensional surface of the form

$$P = c_1 + c_2 t + c_3 r \tag{2.5}$$

to the SNID classifications of our v7.0 SN Ia template spectra. This function was fit on a grid of phases from −20 to 200 d (in steps of 2 d) and $r$lap values from 5 to 40 (in steps of 1). Our best-fitting values for the constants were $c_1 = 0.48 \pm 0.05$, $c_2 = -0.0004 \pm 0.0002$, and $c_3 = 0.028 \pm 0.002$, and our resulting contours are shown in Figure 2.11. Using our values for c_1, c_2, and c_3, we can now calculate an "accuracy percentage" (P) for *any* SN Ia spectrum that has a SNID-determined age and $r$lap (by using Equation 2.5).

As expected, our accuracy increases with increased $r$lap value since $r$lap is a measure of the strength of the correlation of the input spectrum with the best-matching SNID template. In addition, our accuracy decreases slightly with increased age since, as noted earlier, as some subtypes of SNe Ia evolve and age their optical spectra begin to resemble those of "normal SNe Ia." We have also shown previously that our classification accuracy decreases markedly for spectra that are older than a few weeks past maximum brightness.

Final Object Classification

For SNe with multiple spectra, we must consider each spectrum's classification when obtaining a final classification for a given object. To do this we first determine an object's type by counting the total number of spectra of each type for the given object. The object is then classified as the type with the highest count. If there is more than one type with the same highest count, we compare the spectra of those types only and use the type of the spectrum with the largest $r$lap (though we add a "?" to the type to denote our uncertainty regarding the classification).

For each object whose definite type has been determined (i.e., no trailing "?") and that *is not* a SN Ia, we assign a subtype by counting the total number of spectra of each subtype for the given object. The SN is then classified as the subtype with the highest count. If there is more than one subtype with the same highest count, we cannot accurately determine the subtype and thus classify the object as simply the previously determined type.

For each object that we have determined is a definite SN Ia (i.e., no trailing "?"), we calculate the "accuracy percentage" (P) for each spectrum of that object using Equation 2.5. We then combine the "accuracy percentages" of all of the spectra of the given SN to calculate the *maximum* probability that it is of each subtype. For example, if a spectrum has an "accuracy percentage" of P, then that is a measure of the probability that the spectrum is of subtype m (where subtype m is the subtype determined by our classification scheme in Section 2.5.2). This means that $1-P$ is the probability that this spectrum is any of the other SN Ia subtypes, and it is in fact the *maximum* probability that the spectrum is of subtype n for any $n \neq m$. Therefore, we can combine the "accuracy percentages" for multiple spectra

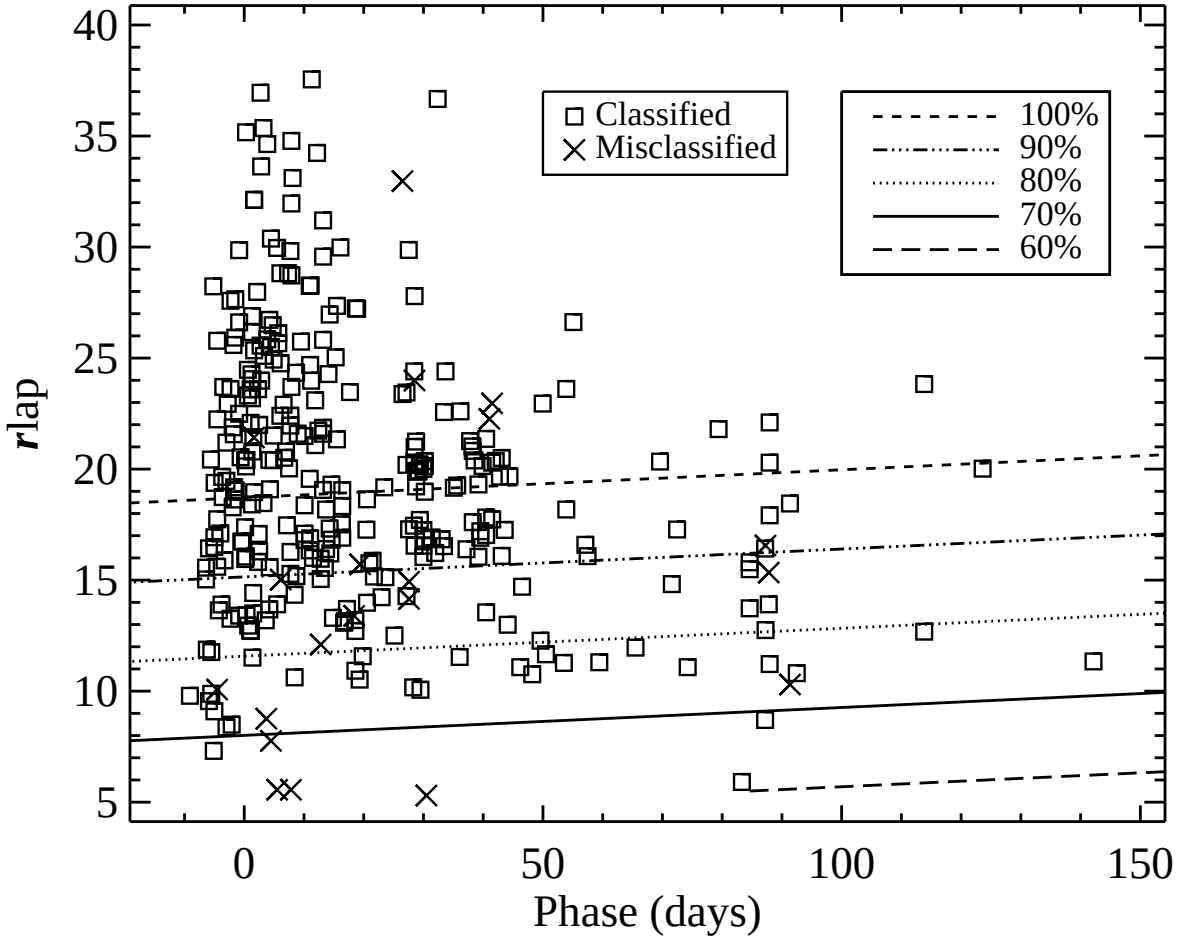

Figure 2.11: Accuracy of our SNID-determined SN Ia subtypes (using our classification scheme described in Section 2.5.2) versus SNID-determined (rest-frame) phase (in days) and *r*lap. □ are correctly classified spectra from our v7.0 SNID templates; × are misclassified spectra from our v7.0 SNID templates. The contours (from bottom to top) represent 60%, 70%, 80%, 90%, and 100% accuracy.

of different subtypes to calculate a maximum probability for each subtype,

$$\widetilde{P}_m = \frac{\prod_{n=m} P_n \times \prod_{n\neq m} (1 - P_n)}{k_m}, \tag{2.6}$$

where $\widetilde{P}_m$ is the maximum probability the given object is of subtype m, the first product is over all spectra whose subtype (n) is equal to m, the second product is over all spectra whose subtype (n) is not equal to m, and k_m is a normalization constant for subtype m defined as

$$k_m = \prod_{n=m} P_n \times \prod_{n\neq m} (1 - P_n) + \prod_{n=m} (1 - P_n) \times \prod_{n\neq m} P_n. \tag{2.7}$$

Once we calculate the maximum probability for each subtype, we classify the given object as the subtype with the largest such probability.

SNID is merely a tool, albeit a useful one for determining spectral subtypes of SNe, but ultimately humans classify SN spectra. Thus, we visually inspected any objects in our dataset that were classified as "Ia" or "Ia?" (with no subtype) or as any of the non-SN Ia subtypes, in addition to any object that had spectra that were classified as more than one SN Ia subtype. From these visual inspections we changed a handful of the final object classifications from what our SNID-based classification algorithm would have yielded. We also forced all objects that were v7.0 SNID templates to be their actual subtype. These final (sub)type determinations can be found in Table 2.1; we also present a summary of the final (sub)type determinations from SNID, as well as our adjusted classifications, in Table 2.8.

Of all of the v7.0 template objects, 95% were classified as the correct type by SNID and 86% were classified as the correct subtype by SNID. We were unable to determine a type (subtype) for 2% (7%) of the v7.0 template objects using our aforementioned SNID-based classification scheme. Of solely the SNe Ia that are v7.0 template objects, 99% received the correct type classification from SNID and 92% the correct subtype classification, and we could determine a type and subtype from SNID for all of the v7.0 template SNe Ia. These are more informative and more accurate percentages than those from the simple sanity checks that were discussed in Section 2.5.1.

Of the 582 SNe Ia that are presented in this chapter, our SNID-based algorithm classifies 98.1% of them as SN Ia, 1.6% as other SN types, and we are unable to classify 0.3%. Over half of the spectra of objects that are classified by SNID as non-Ia types or that are unclassified are relatively old and/or noisy, and thus it is not surprising that our classification scheme failed on these observations. A few spectra of these objects are heavily contaminated by host-galaxy light and lacked sufficient photometry for us to apply our galaxy-correction algorithm (Section 2.3.3), and so again it is reasonable that these are not correctly classified. In addition, some of these objects are well-known, peculiar SNe Ia (including a couple of our v7.0 SNID templates), but we do not have enough templates of other objects of their subtype at similar ages for SNID to get good matches to our observations. This is most likely responsible for many of SNID's "Ia" (with no definitive subtype) and "Ia?" classifications as well, and is partially why we visually re-inspected these objects.

Table 2.8: Summary of Final SN Classifications

SNID		Adjusted	
(Sub)Type	#	(Sub)Type	#
Ia	28	Ia	26
Ia?	2	Ia?	0
Ia-norm	477	Ia-norm	467
Ia-91T	6	Ia-91T	9
Ia-91bg	41	Ia-91bg	50
Ia-csm	0	Ia-csm	1
Ia-pec	0	Ia-pec	1
Ia-99aa	7	Ia-99aa	15
Ia-02cx	10	Ia-02cx	12
Ic-norm	1	Ic-norm	0
II	1	II	0
IIP	3	IIP	0
IIn	1	IIn	0
NotSN?	1	NotSN?	0
Gal	2	Gal	0
Unknown	2	Unknown	1

Relative Fractions of Subtypes

Even though our SN Ia spectral sample is not complete by any rigorous definition and suffers from multiple observational biases, it is still illuminating to calculate the relative fractions of SN Ia subtypes (as determined by SNID) in our dataset. Of the objects for which SNID determines a SN Ia subtype, 88.2% are normal, 7.6% are 91bg-like, 1.1% are 91T-like, 1.3% are 99aa-like, and 1.8% are 02cx-like. For the purposes of comparing these percentages to values in the literature, we will follow Li et al. (2011a) and combine 99aa-like objects with 91T-like objects, yielding 2.4% for this group. If, as we did when creating our new SNID templates in order to get more accurate subtype classifications, we require spectra to have ages less than 15 d past maximum brightness and S/N > 15 pixel^{-1}, then we find that of these objects 88.1% are normal, 8.0% are 91bg-like, 3.1% are 91T/99aa-like, and 0.9% are 02cx-like.

In the volume-limited sample of Li et al. (2011a), 70% of SN Ia were normal, while 15% were 91bg-like, 9% were 91T/99aa-like (only a lower limit, however), and 5% were 02cx-like. The slightly higher redshift ($\overline{z} = 0.17$) sample of Östman et al. (2011) detected only a few probable peculiar SNe Ia, but they calculate that 7–32% of local SNe Ia should be 91T/99aa-like. The even higher redshift ($\overline{z} \approx 0.35$) sample of Foley et al. (2009b) found that 4–19%

were 91T/99aa-like, while they had no 91bg-like objects in their dataset.[14] However, an analysis of the companion photometry to much of the spectroscopic sample presented here (Ganeshalingam et al. 2010) finds that 80.6% of their SNe Ia are normal, 10.9% are 91bg-like, 5.5% are 91T/99aa-like, 2.4% are 02cx-like, and 0.6% are 00cx-like (i.e., just SN 2000cx, which SNID classified as a Ia-norm since we have no other SNID templates of 00cx-like objects). These percentages are much closer to our fractions of subtypes than the complete sample presented by Li et al. (2011a). This likely comes from the fact that for most of the project's lifetime, BSNIP has had a strong focus on spectroscopically monitoring SNe Ia that were being concurrently observed photometrically as part of the sample presented by Ganeshalingam et al. (2010).

The main differences between our SNID-determined fractions of SN Ia subtypes and those found in the complete sample of Li et al. (2011a) is that we classify too many objects as normal and not enough as 91T/99aa-like. This can possibly be explained by the fact that spectra of 91T/99aa-like SNe Ia resemble spectra of normal SNe Ia within a week or two after maximum brightness (introducing the so-called "age bias"; Li et al. 2001a). Thus, some of our Ia-norm objects may in fact be 91T/99aa-like SNe Ia, but the spectra in our dataset are too old to distinguish between the two subtypes. Since there are many more normal SNID templates than 91T-like and 99aa-like templates, these objects will ultimately get classified as normal. Furthermore, it is possible that some objects have essentially normal spectra and are classified as Ia-norm by SNID, but have slowly declining light curves and are thus *photometrically* classified as 91T/99aa-like by Li et al. (2011a). This interesting possibility will be investigated further in future BSNIP analyses.

Many of the non-normal SNe Ia that we classify in our dataset have already been noted as peculiar in the literature (either in unrefereed circulars or published papers). However, there are still a few peculiar classifications that we publish here for the first time. Details regarding these interesting individual objects can be found in Section 2.6.2.

2.6 The BSNIP Sample

Our SN Ia spectral dataset consists of a total of 1298 spectra of 582 SNe Ia observed from 1989 through the end of 2008. 1159 spectra of 563 objects are published here for the first time. In Figures 2.12 through 2.16 we show examples of our most recent, fully reduced spectra from each of our commonly used instruments (Kast, LRIS, UV Schmidt, DEIMOS, and ESI, respectively). Plots of all of the fully reduced spectra as well as (for the objects with multi-band SN and galaxy photometry) galaxy-subtracted spectra (as discussed in Section 2.3.3) presented in this chapter are available on the SNDB Home Page[15]. Figure 2.17 shows an example of a spectral sequence, obtained for SN 2007le (spectral sequences for all objects in

[14] Foley et al. (2009b), after correcting for various biases, expected only 1–4 91bg-like objects based on the Li et al. (2001b) percentages.

[15] `http://hercules.berkeley.edu/database/`

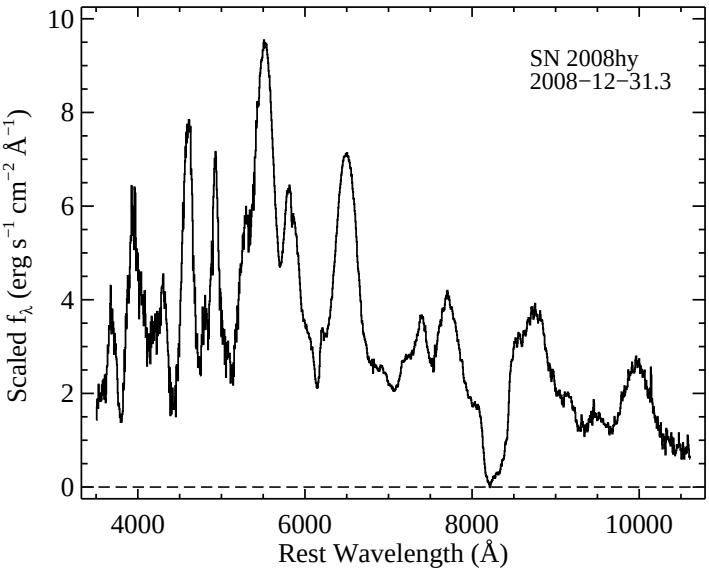

Figure 2.12: Spectrum of SN 2008hy taken on 2008 Dec. 31 (UT dates are used throughout this chapter) using Kast. This spectrum is classified as "Ia-norm" by SNID. Clipped bad residuals along with host-galaxy emission lines and telluric absorptions (if present) are plotted in light grey.

our dataset with more than 7 spectra can be found on the SNDB Home Page).

2.6.1 Sample Characteristics

If we remove objects where we have no light-curve information, leaving only spectra with phase (and light-curve shape) information, the sample is reduced to 914 (770) spectra of 321 (251) SNe Ia. If we further restrict ourselves to objects with relatively well-sampled, filtered light curves, retaining only those objects with precise distance measurements, our dataset contains 584 spectra of 199 SNe Ia. Finally, if we only count spectra which have reasonable estimates of multi-filtered SN magnitudes at the time of the spectrum and measurements of the host-galaxy colors at the position of the SN, providing accurate flux-calibrated, galaxy-subtracted spectra (see Section 2.3.3 for more information), our sample contains 234 spectra of 95 SNe Ia.

This dataset has ∼3 times the number of spectra and ∼18 times the number of objects in the sample of Matheson et al. (2008). Due to the scheduling of their telescope time, their dataset mainly consisted of well-sampled spectroscopic time series of a handful of SNe Ia, averaging 13.5 spectra per object. By contrast, the BSNIP sample consists of ∼2.2 spectra per object, showing our emphasis on the total number of objects rather than the number of spectra per object. The histogram of the number of spectra per object for our sample can be seen in Figure 2.18. Thus, our sample (emphasizing the total number of objects) and

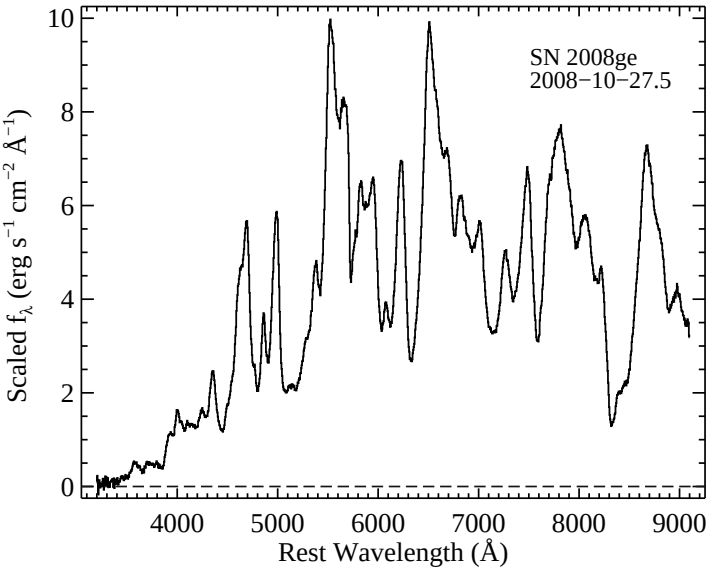

Figure 2.13: Spectrum of SN 2008ge taken on 2008 Oct. 28 using LRIS. This spectrum is classified as "Ia-02cx" by SNID and "Ia-02cx" by Foley et al. (2010c). Clipped bad residuals along with host-galaxy emission lines and telluric absorptions (if present) are plotted in light grey.

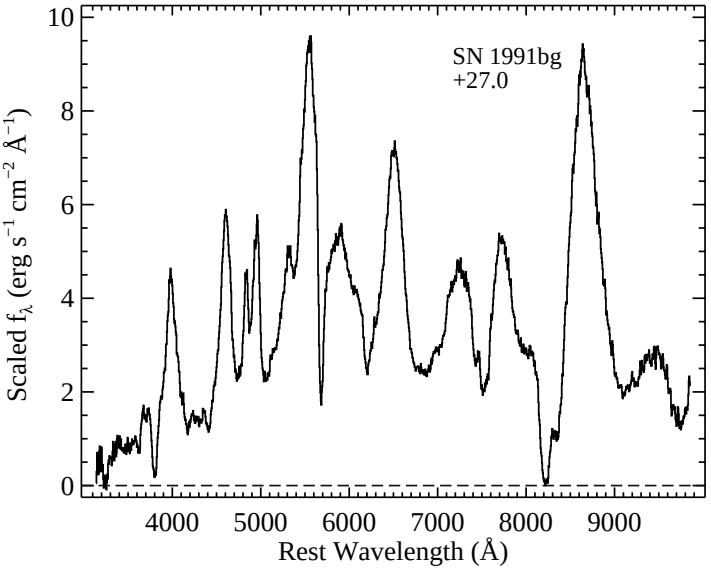

Figure 2.14: Spectrum of SN 1991bg taken 27 d (rest frame) past maximum brightness using the UV Schmidt spectrograph. This spectrum is classified as "Ia-91bg" by SNID. Clipped bad residuals along with host-galaxy emission lines and telluric absorptions (if present) are plotted in light grey.

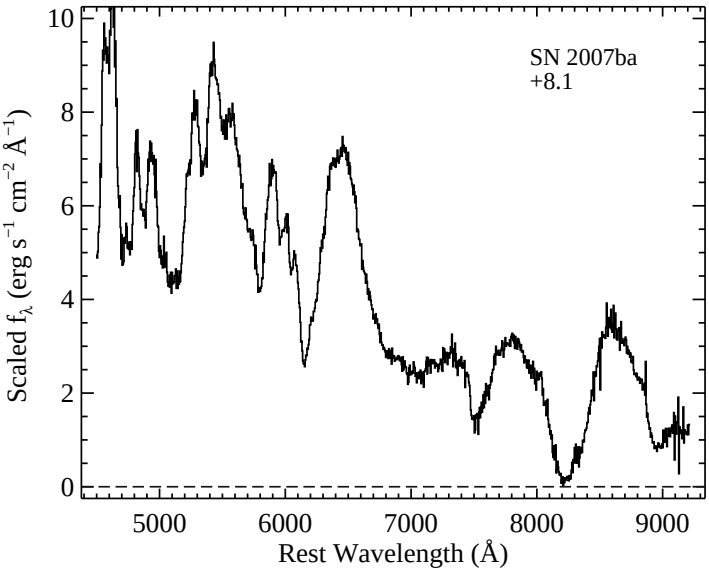

Figure 2.15: Spectrum of SN 2007ba taken 8 d (rest frame) past maximum brightness using DEIMOS. This spectrum is classified as "Ia-norm" by SNID. Clipped bad residuals along with host-galaxy emission lines and telluric absorptions (if present) are plotted in light grey.

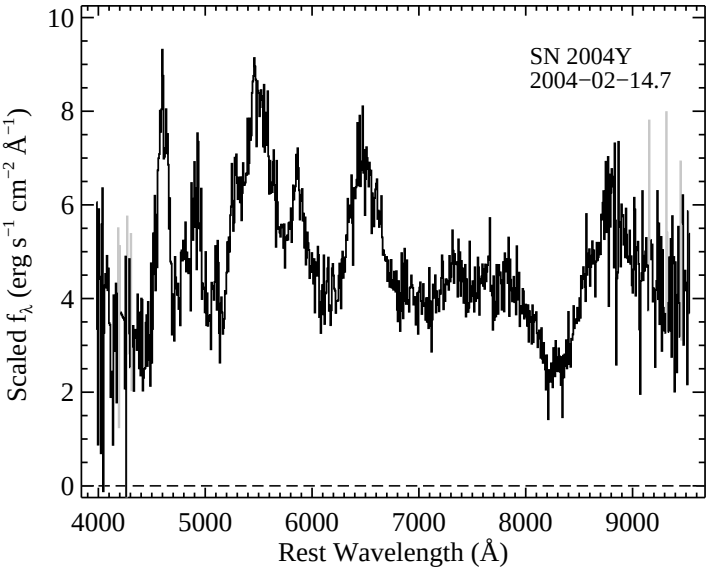

Figure 2.16: Spectrum of SN 2004Y taken on 2004 Feb. 15 using ESI. This spectrum is classified as "Ia-norm" by SNID. Clipped bad residuals along with host-galaxy emission lines and telluric absorptions (if present) are plotted in light grey.

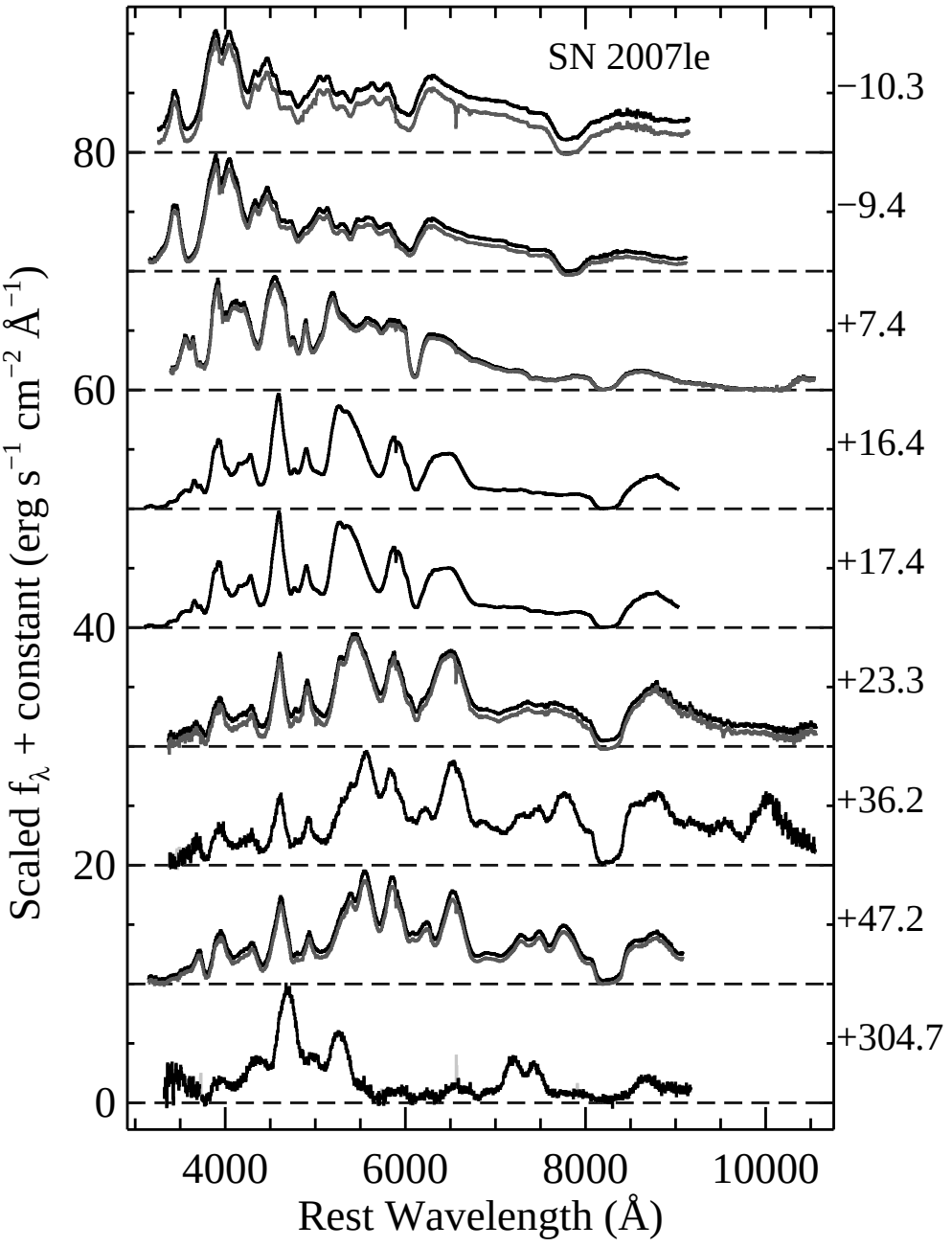

Figure 2.17: Spectral sequence of SN 2007le, classified as "Ia-norm" by SNID. Each spectrum is labelled with its rest-frame age relative to maximum brightness. Clipped bad residuals along with host-galaxy emission lines and telluric absorptions (if present) are plotted in light gray. The galaxy-subtracted spectra are overplotted in dark gray. The horizontal dashed lines correspond to zero flux for each spectrum.

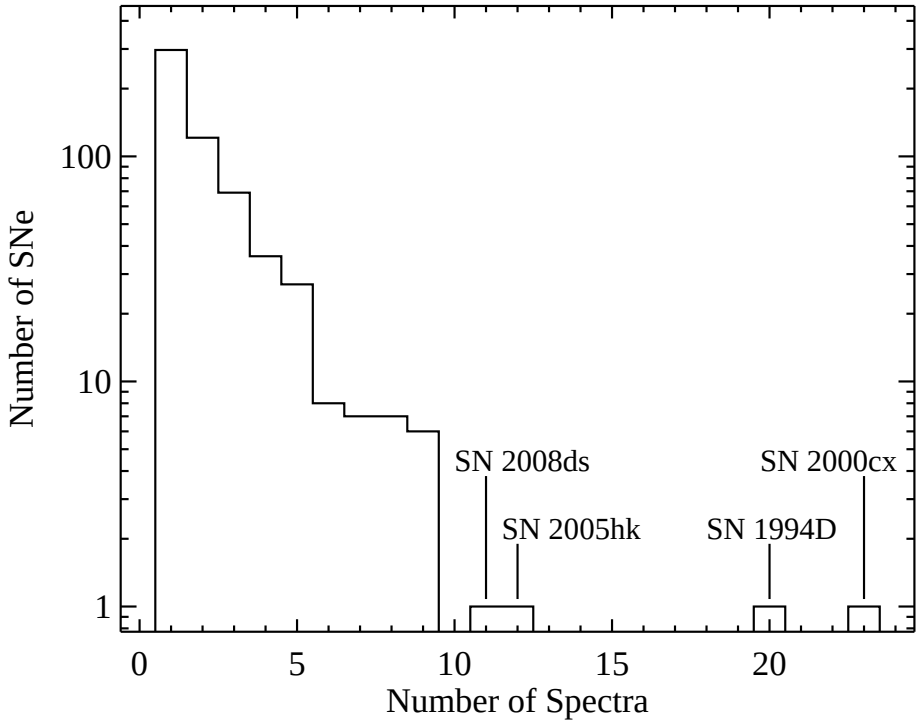

Figure 2.18: A histogram of the number of spectra versus the number of objects in our SN Ia sample. Our average is ∼2.2 spectra per object.

the sample of Matheson et al. (2008) and Blondin et al. (2011) (emphasiszing the number of spectra per object) are complementary. Furthermore, as mentioned in Section 2.2, our spectra typically cover 3300–10400 Å, compared to the typical 3700–7400 Å wavelength range of the spectra from Matheson et al. (2008).

All of the SNe Ia in our dataset have $z \leq 0.2$, and the vast majority (∼89.5%) have $z \leq 0.05$. The distribution of redshifts for all of our SNe Ia (as well as just those with phase information) is shown in Figure 2.19. The average redshift of the full sample of objects presented here is about 0.0283 and the median uncertainty is 0.00004. About 78.0% of our SNe Ia have $z \geq 0.015$ (which is approximately the redshift above which peculiar velocities can be ignored in cosmological calculations; see, e.g., Astier et al. 2006). 18 of our objects have unknown host-galaxy redshifts, but all of the spectra of these objects received a redshift from our SNID classification scheme (Section 2.5.2).

As mentioned above, many of our spectra have phase information from photometric observations; the distribution of phases for all of our spectra is shown in Figure 2.20. We have 147 spectra of 114 SNe Ia before maximum brightness, and 245 (107) spectra of 181 (96) objects within 7 d (3 d) of maximum brightness. Our sample also contains 34 spectra of 20 SNe Ia older than 180 d past maximum brightness. The median uncertainty of our phases is 0.38 d, though the practical uncertainty is more like 0.5 d (Ganeshalingam et al.

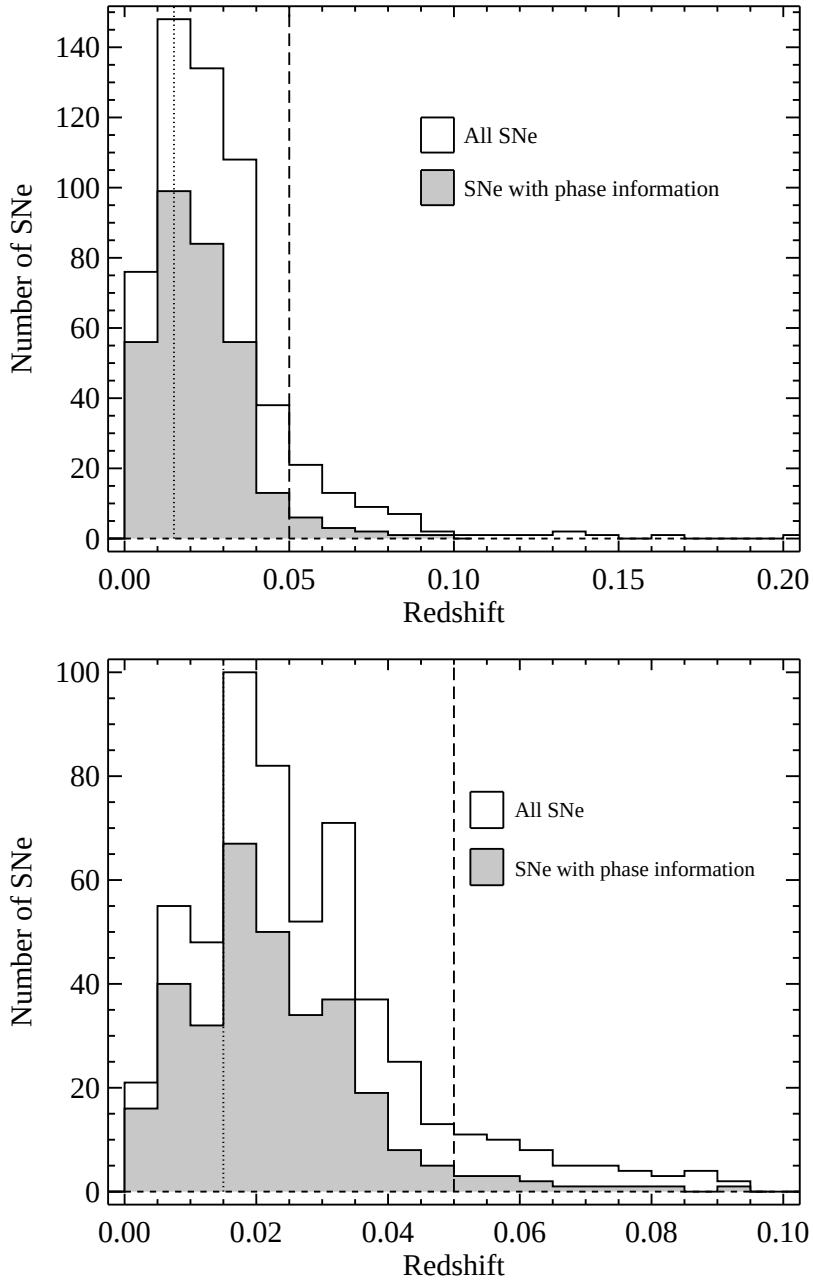

Figure 2.19: A histogram of the redshifts of all of the SNe Ia in our sample (*top*) and a zoom-in on those objects with $z \leq 0.1$ (*bottom*). The shaded regions represent objects for which we have phase information (i.e., a date of maximum brightness). The dotted vertical line ($z = 0.015$) is approximately the redshift above which peculiar velocities can be ignored in cosmological calculations (see, e.g., Astier et al. 2006). The dashed vertical line ($z = 0.05$) represents our approximate 90% cutoff; i.e., $\sim$90% of our SNe Ia have redshifts less than 0.05. Our average redshift is about 0.0283 and our median uncertainty is 0.00004.

2010). Figure 2.21 shows the distribution of the phase of each SN Ia at the time of its first spectrum.

Also mentioned above, many of our SNe have light-curve shape information (as characterized here by the MLCS2k2 Δ parameter; Jha et al. 2007); the distribution of Δ values for all of these objects is shown in Figure 2.22. In the histogram we also denote each object's final SNID classification (Section 2.5.4). The Δ values come from previously published photometric data which have all been compiled and fit by Ganeshalingam et al. (in preparation). The average Δ for our dataset is $\sim$0.12, and the median Δ and uncertainty are about -0.03 and 0.035, respectively. Our SNe Ia span most of the standard range of Δ values (about -0.4 to 1.6, e.g., Hicken et al. 2009b).

Figure 2.23 presents the host-galaxy redshift of our SNe Ia versus their Δ values. Our dataset covers most of the range of Δ values at the lowest redshifts, but our coverage decreases at higher redshifts. SNe Ia with large Δ are the fainter, faster-evolving objects (Jha et al. 2007), and thus we have fewer of those (relative to smaller Δ objects) in our sample at higher redshifts. Figure 2.24 presents the phase of each spectrum versus their Δ values. Analogous to Figure 2.23, our sample spans most of the standard range of Δ values at early times, but the coverage begins to drop off at about 40 d past maximum brightness. Once again, we lack large-Δ objects at the latest times, while we still have a handful of SNe Ia with small Δ values at these epochs. This is unsurprising since objects with large Δ values are fainter and have faster-evolving light curves, and thus we are not able to follow them spectroscopically for as long as their small-Δ brethren. It is interesting to note that there are relatively few SNe Ia with $0.5 \leq \Delta \leq 0.7$ or $1.1 \leq \Delta \leq 1.3$; these possible anomalies will be investigated further in future BSNIP work.

2.6.2 Object (Re-)Classification

Some of the SNe Ia presented here were originally classified as other types of SNe or remained unclassified prior to this chapter. Using our SNID classification scheme we have reclassified these objects as bona fide SNe Ia. Similarly, there are a few objects in our dataset that, again after applying our spectral classification procedure, were found to be examples of some of the peculiar SN Ia subtypes. All of the objects for which (re-)classifications were made are described below.

SN 1991O

This SN was discovered on 1991 Mar. 18, by Mueller & Filippenko (1991), and classified as a SN Ia "about 1–2 months past maximum brightness" (Mueller & Filippenko 1991). Our SNID classification reveals that SN 1991O is 91bg-like. Figure 2.25 shows this SN compared to its best-matching SNID template, the 91bg-like SN 2006em $\sim$21 d past maximum brightness.

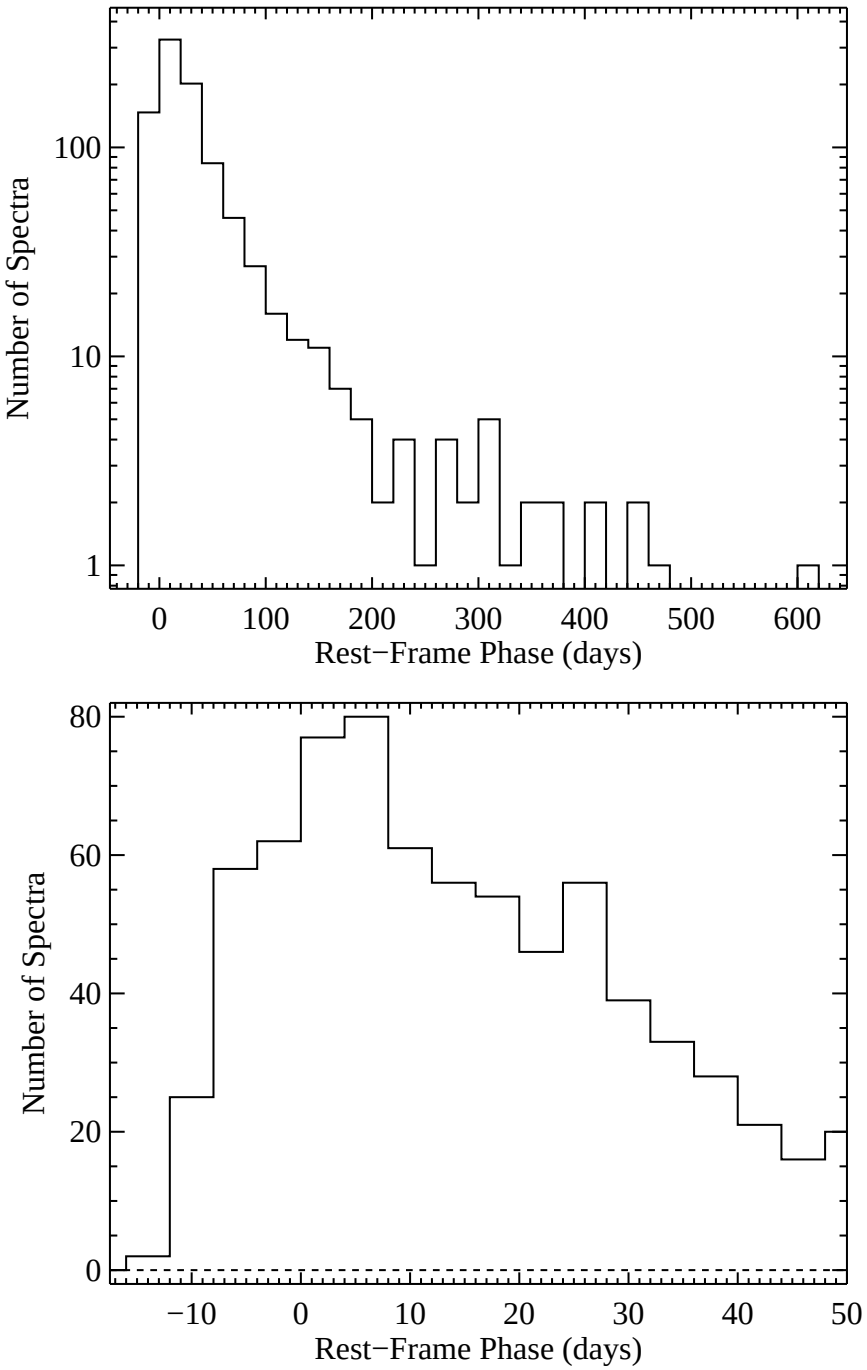

Figure 2.20: A histogram of the phases of all of the spectra in our sample for which we have phase information (*top*) and a zoom-in on those spectra with $t \leq 50$ d (*bottom*). Our median uncertainty is 0.38 d.

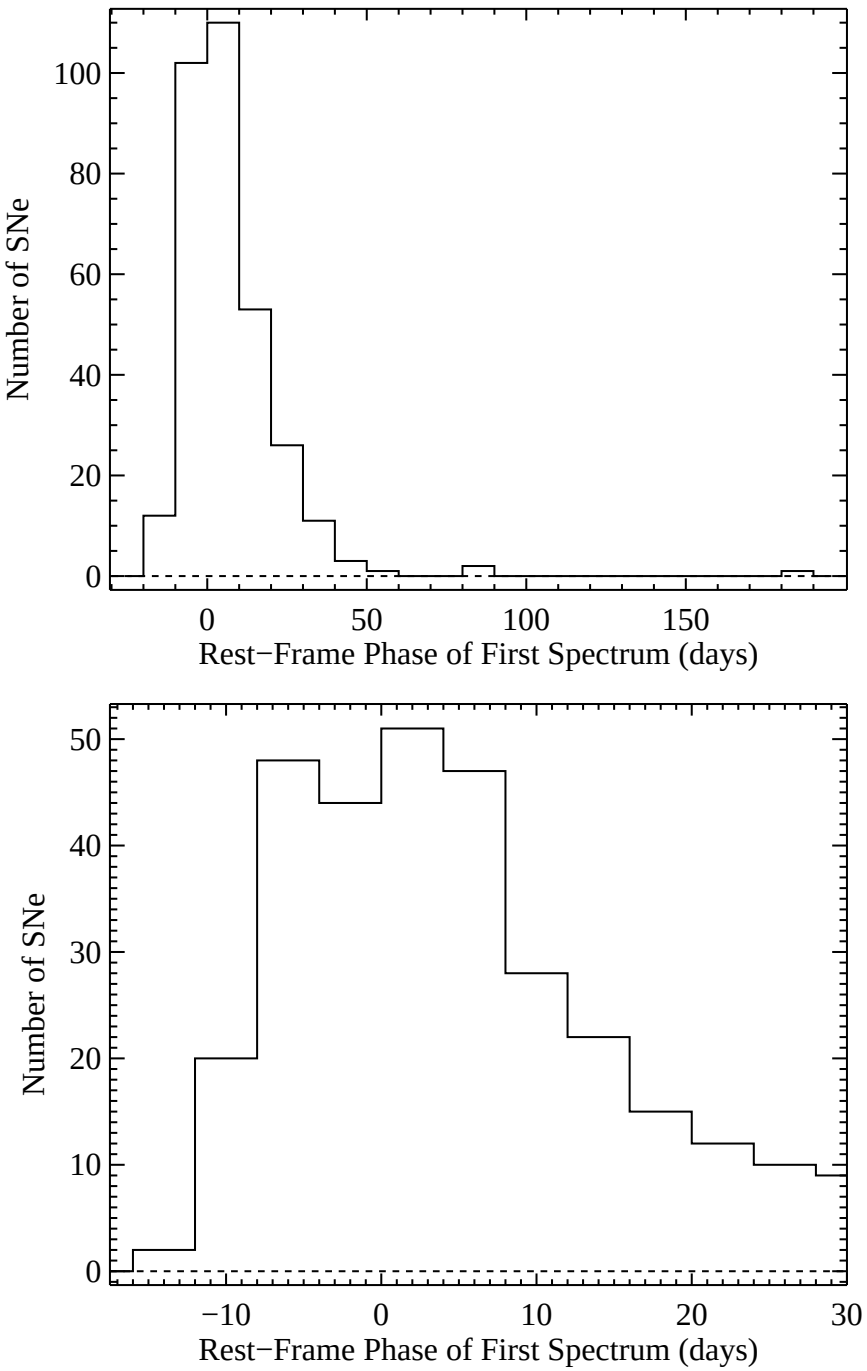

Figure 2.21: A histogram of the phase of each SN Ia (for which we have phase information) at the time of our first spectrum (*top*) and a zoom-in on those spectra with $t_{\rm first} \leq 30$ d (*bottom*). Our median uncertainty is 0.38 d.

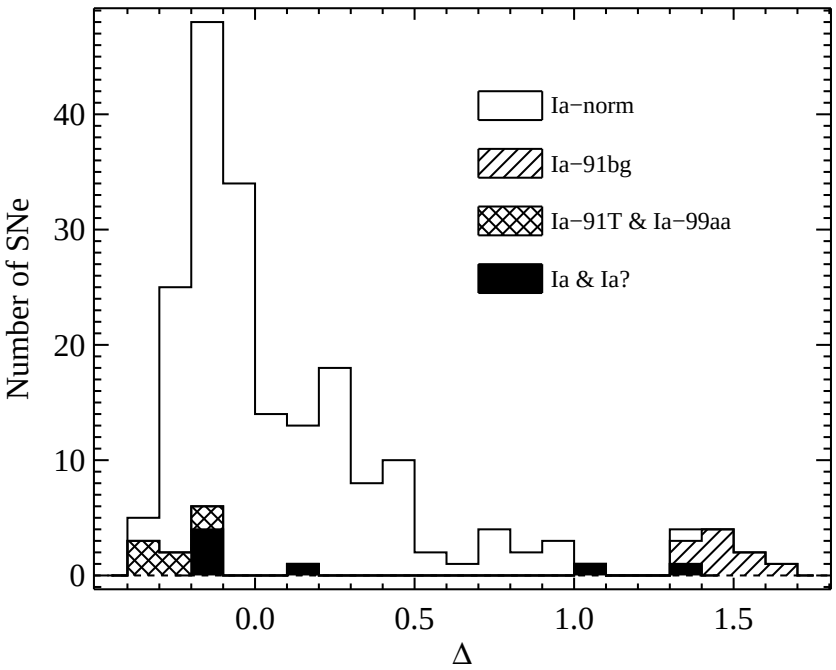

Figure 2.22: A histogram of the MLCS2k2 Δ value (which is a measurement of the light-curve shape) of each SN Ia (for which we have light-curve shape information). Our average Δ is about 0.12 and our median Δ and uncertainty is about -0.03 and 0.035. The different shadings correspond to each object's final SNID classification (Section 2.5.4)

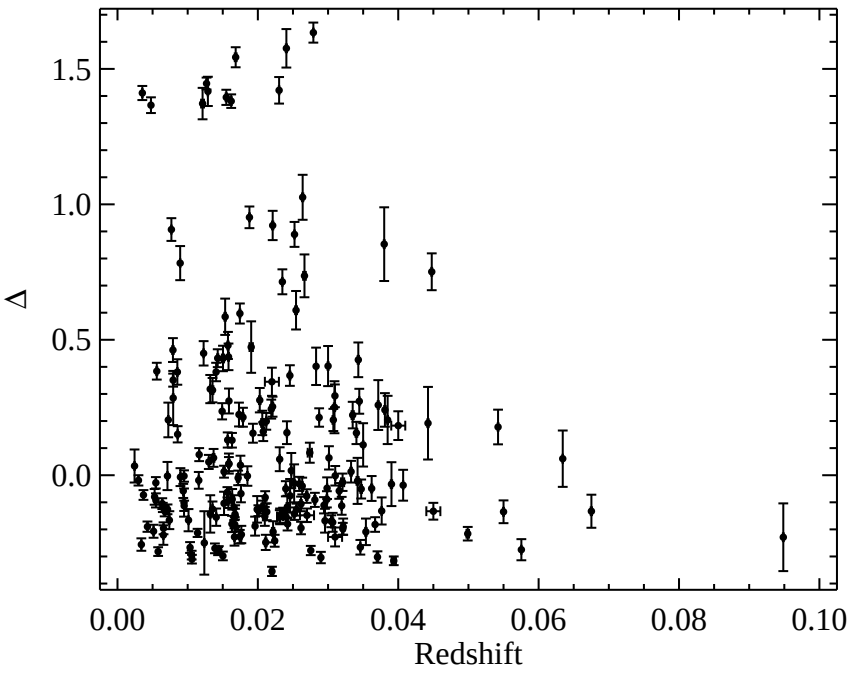

Figure 2.23: The host-galaxy redshift versus the MLCS2k2 Δ value of each SN Ia (for which we have light-curve shape information).

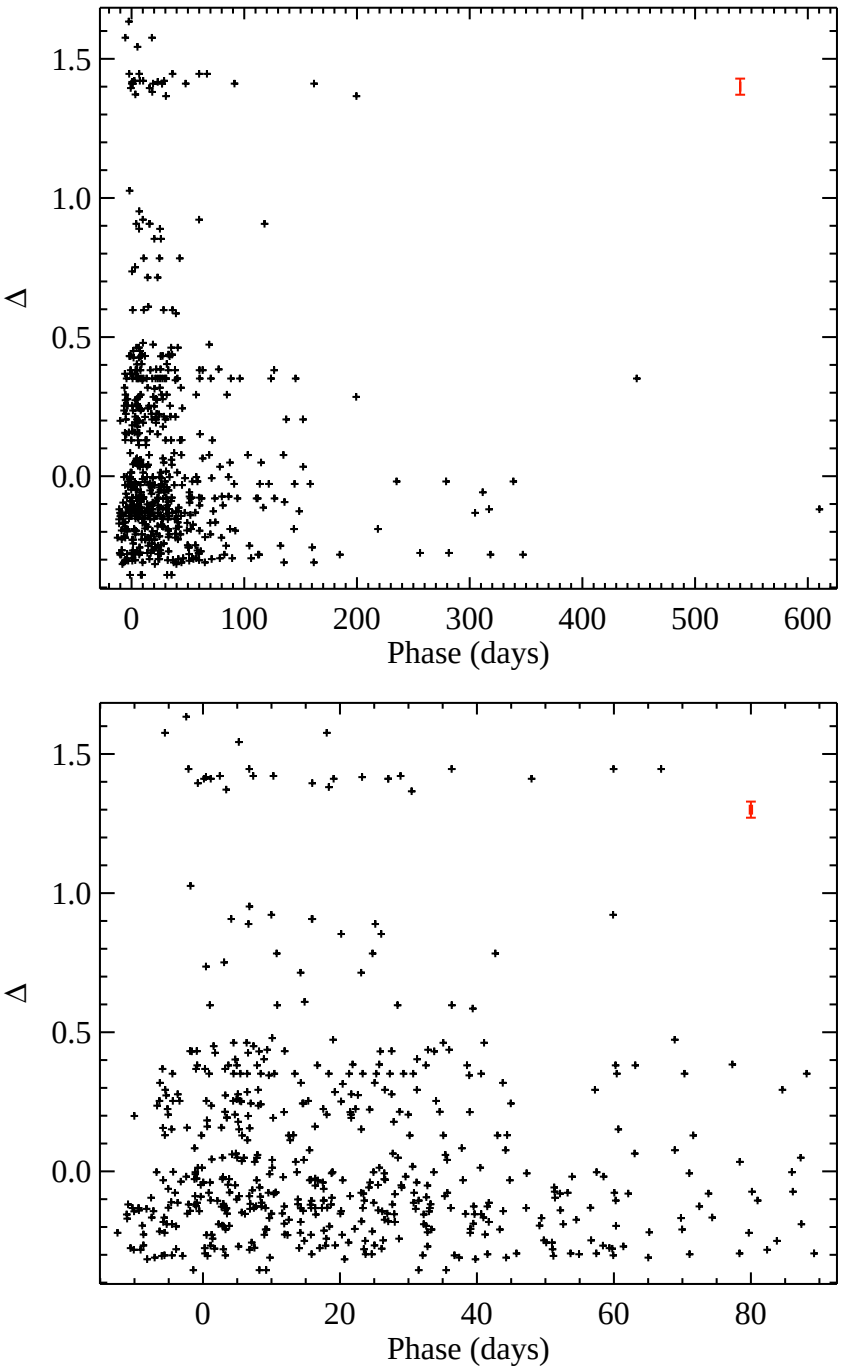

Figure 2.24: The phase versus the MLCS2k2 Δ value of each spectrum for which we have light-curve shape information (*top*) and a zoom-in on those spectra with $t \leq 90$ d (*bottom*). The median error bar in both directions is shown in red in the top-right corner of each plot.

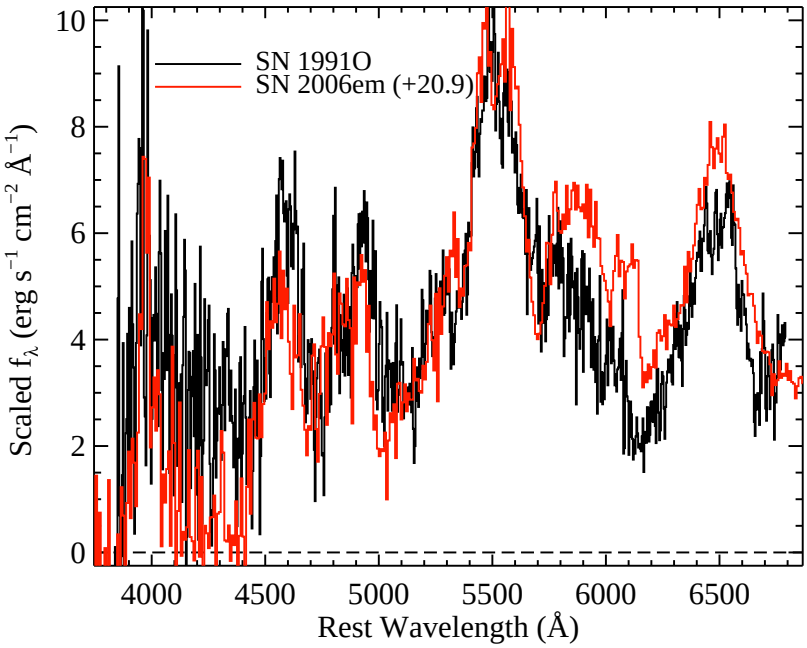

Figure 2.25: Our spectrum of SN 1991O (*black*) compared to the 91bg-like SN 2006em (*red*) ∼21 d past maximum brightness.

SN 1993aa

This SN was discovered on 1993 Sep. 19, by Pollas et al. (1993), and classified as a SN Ia "probably about 1 month past maximum brightness" (Pollas et al. 1993). Our SNID classification reveals that SN 1993aa is also 91bg-like. Figure 2.26 shows this SN compared to its best-matching SNID template, the 91bg-like SN 2007ba ∼8 d past maximum brightness.

SN 1998cm

This SN was discovered on 1998 Jun. 10, by Germany et al. (1998), and classified as a SN Ia "within a week or two of maximum brightness" (Germany et al. 1998). Our SNID classification reveals that SN 1998cm is 91T-like. Figure 2.27 shows this SN compared to its best-matching SNID template, the 91T-like SN 1997br ∼8 d past maximum brightness.

SN 2000J

This SN was discovered on 2000 Feb. 4, by Puckett et al. (2000). Nearly 6 weeks later it was classified as a SN II based on the noisy spectrum presented in this chapter (Filippenko & Coil 2000). However, a SNID fit to the same spectrum reveals that it is more likely a normal SN Ia. Figure 2.28 shows this SN compared to its best-matching SNID template, the normal type Ia SN 1994D ∼54 d past maximum brightness.

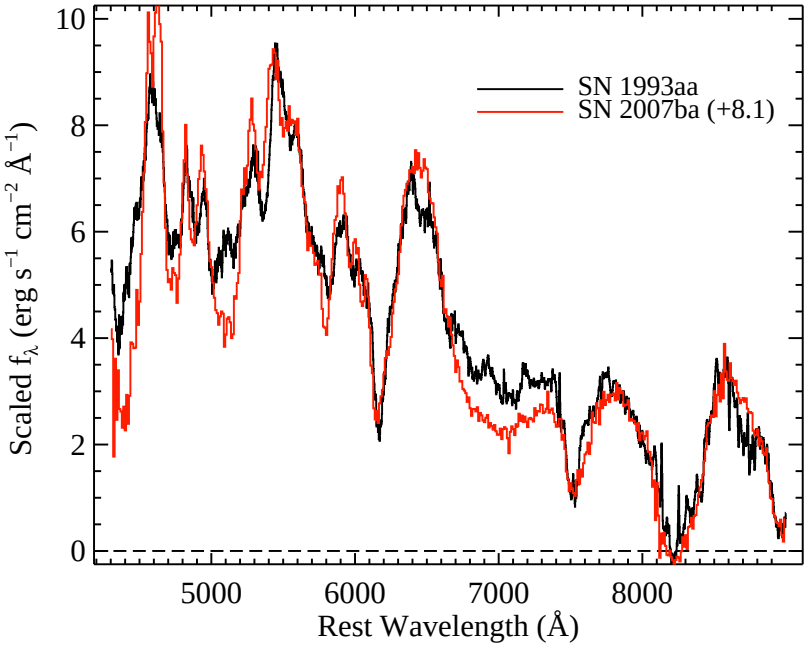

Figure 2.26: Our spectrum of SN 1993aa (*black*) compared to the 91bg-like SN 2007ba (*red*) ∼8 d past maximum brightness.

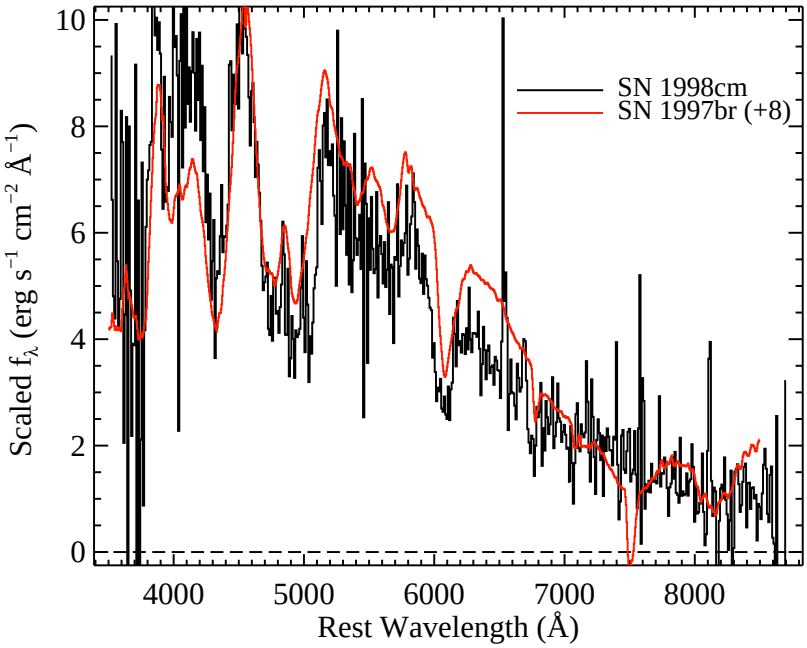

Figure 2.27: Our spectrum of SN 1998cm (*black*) compared to the 91T-like SN 1997br (*red*) ∼8 d past maximum brightness.

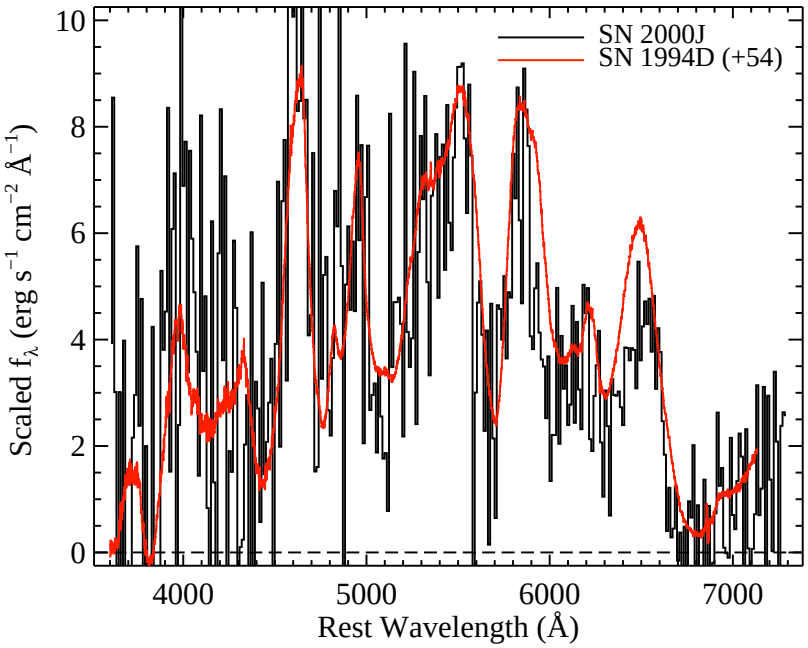

Figure 2.28: Our spectrum of the previously misclassified SN 2000J (*black*) compared to the normal type Ia SN 1994D (*red*) ∼54 d past maximum brightness.

SN 2001es

This SN was discovered on 2001 Oct. 7, by Li (2001), but it has remained unclassified until now. From a SNID fit to one of the spectra presented in this chapter, we determine that it is likely a normal SN Ia. Figure 2.29 shows this SN compared to its best-matching SNID template, the normal type Ia SN 2004fz ∼22 d past maximum brightness.

SN 2002bp

This SN was discovered on 2002 Mar. 8, by Puckett & Langoussis (2002), but it too has remained unclassified until now. From a SNID fit to our spectrum presented here, we determine that it is a SN 2002cx-like object. Upon further inspection, it seems to be a better match to the quite peculiar SN 2008ha (Foley et al. 2009a) than to the more "normal" members of the SN 2002cx-like class (e.g., Jha et al. 2006a). A comparison between our spectrum of SN 2002bp and our spectrum of SN 2008ha from 7.5 d past maximum brightness (previously published by Foley et al. 2009a) is shown in Figure 2.30. We include SNe 2002bp and 2008ha here in our SN Ia sample even though there is uncertainty regarding whether SN 2008ha was in fact a SN Ia (e.g., Valenti et al. 2009).

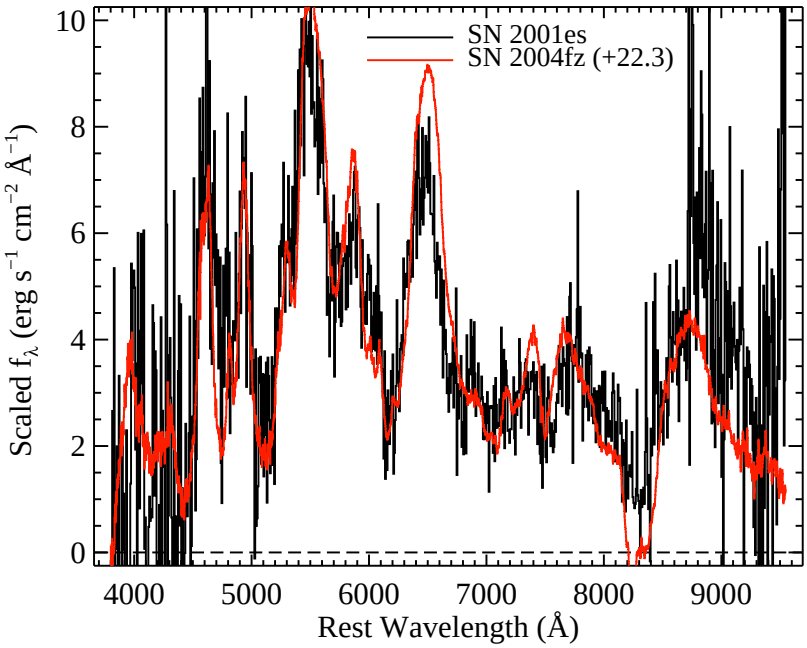

Figure 2.29: Our spectrum of the previously unclassified SN 2001es (*black*) compared to the normal type Ia SN 2004fz (*red*) ∼22 d past maximum brightness.

SN 2004br

This SN was discovered on 2004 May 15, by Graham & Foley (2004), and classified as "an unusual type Ia supernova, similar to the spectrum of SN 2000cx" (Gerardy et al. 2004). The SNID classification of our earliest spectrum of SN 2004br reveals that it is likely 99aa-like. Figure 2.31 shows this spectrum compared to its best-matching SNID template, the 99aa-like SN 2008ds ∼5 d before maximum brightness. We are unable to confidently determine the subtype of the two older (both >2 weeks past maximum brightness) spectra of SN 2004br in our dataset. The best-matching template of one of these other spectra is another 99aa-like SN, and the best-matching template of the other is a 91T-like SN. Furthermore, Ganeshalingam et al. (in preparation) have determined that the MLCS2k2 Δ parameter of SN 2004br is -0.152. This spectral and photometric information increases our confidence in the 99aa-like classification of SN 2004br, though it is still uncertain. As seen in Figure 2.31, there are a few obvious differences between its spectrum and that of SN 2008ds; further study of this object is warranted.

SN 2005dh

This SN was discovered on 2005 Aug. 10, by Moore & Li (2005), and classified as a SN Ia "near maximum light" (Salvo et al. 2005). The SNID classifications of both spectra

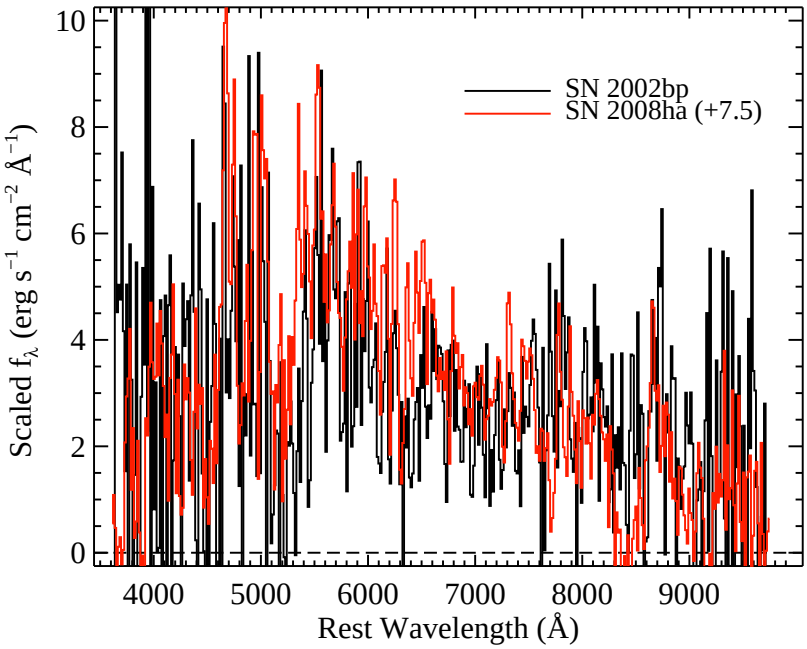

Figure 2.30: Our spectrum of the previously unclassified SN 2002bp (*black*) compared to the peculiar (possible) type Ia SN 2008ha (*red*) 7.5 d past maximum brightness, which was previously published by Foley et al. (2009a).

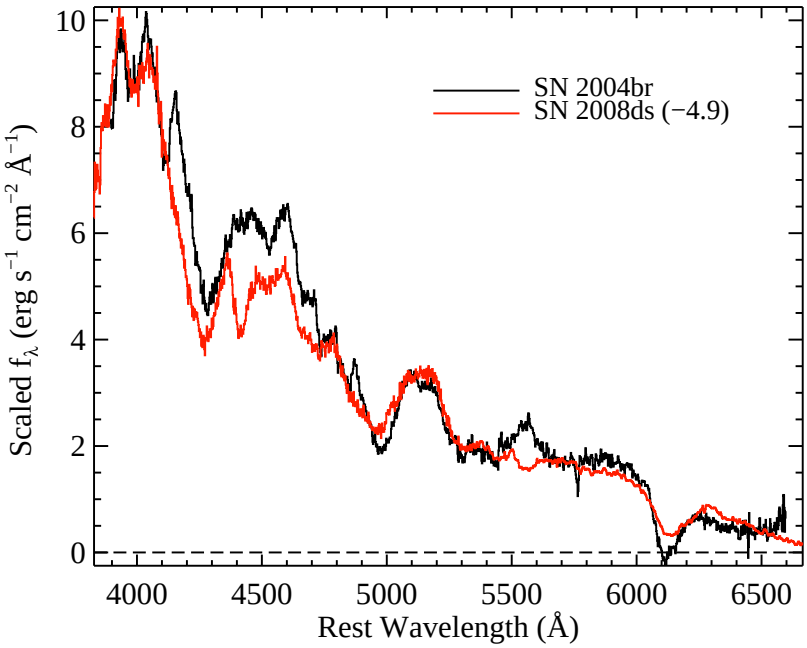

Figure 2.31: Our spectrum of SN 2004br (*black*) compared to the 99aa-like SN 2008ds (*red*) ∼5 d before maximum brightness.

of SN 2005dh in our sample reveal it to be 91bg-like. Figure 2.32 shows our earlier spectrum of this SN compared to its best-matching SNID template, the 91bg-like SN 2006cs ∼2 d past maximum brightness. This object was specifically noted to have an "unusually high" expansion velocity of 16000–16600 km s^{-1} (based on the minimum of the Si II λ6355 absorption feature; Salvo et al. 2005; Gal-Yam et al. 2005). However, both Salvo et al. (2005) and Gal-Yam et al. (2005) used the host-galaxy redshift presented by Falco et al. (1999), $z = 0.038$, as opposed to the actual host-galaxy redshift of $z = 0.015$ (Adelman-McCarthy et al. 2008). Using the correct redshift, we calculate a relatively normal expansion velocity of ∼9300 km s^{-1} for our spectrum of SN 2005dh from a similar epoch.

SN 2008Z

This SN was discovered on 2008 Feb. 7, by Puckett et al. (2008), and classified as a type Ia (Blondin & Calkins 2008). The SNID classification of our earliest spectrum of SN 2008Z reveals that it is 99aa-like. Figure 2.33 shows this spectrum compared to its best-matching SNID template, the 99aa-like SN 2008ds at maximum brightness. Ganeshalingam et al. (in preparation) have determined that the MLCS2k2 Δ parameter of SN 2008Z is −0.152.

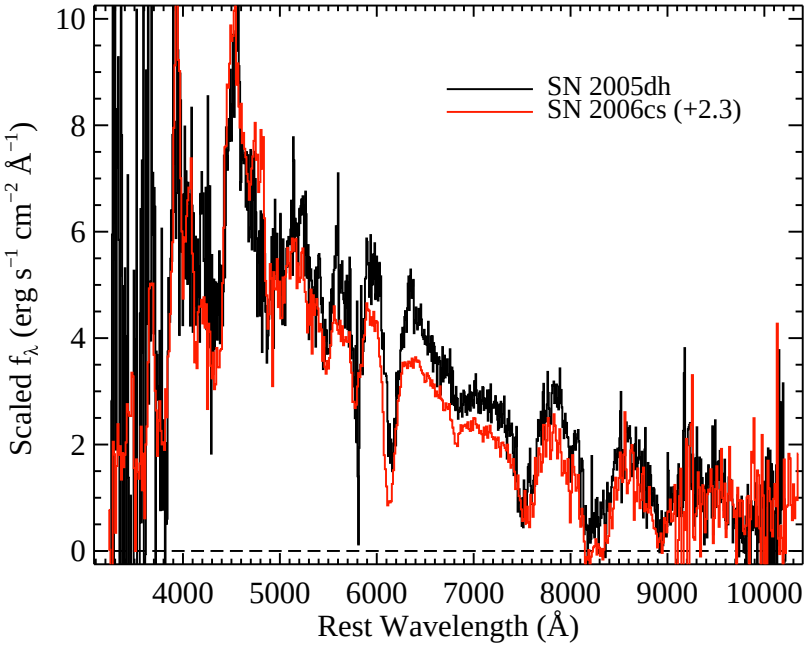

Figure 2.32: Our spectrum of SN 2005dh (*black*) compared to the 91bg-like SN 2006cs (*red*) ∼2 d past maximum brightness.

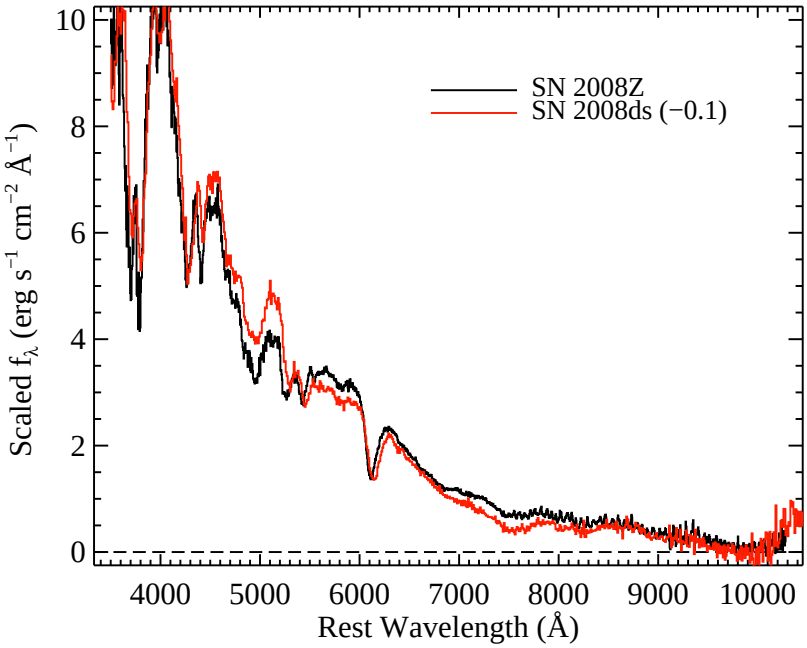

Figure 2.33: Our spectrum of SN 2008Z (*black*) compared to the 99aa-like SN 2008ds (*red*) at maximum brightness.

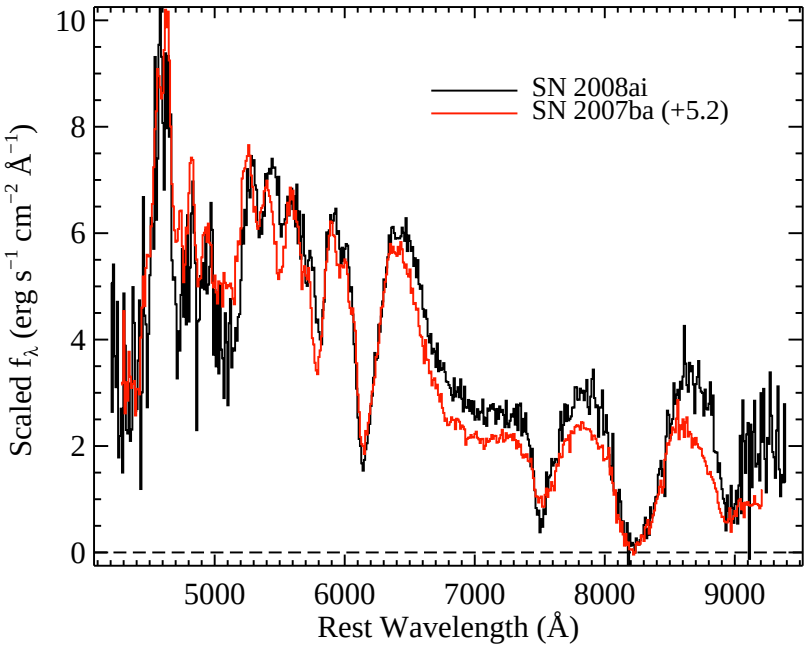

Figure 2.34: Our spectrum of SN 2008ai (*black*) compared to the 91bg-like SN 2007ba (*red*) ∼5 d past maximum brightness.

SN 2008ai

This SN was discovered on 2008 Feb. 13, by Boles & Li (2008), and classified as a type Ia (Silverman et al. 2008) using the earliest spectrum of this object presented in this chapter. Our SNID classification of this same spectrum reveals that it is actually 91bg-like. Figure 2.34 shows this spectrum compared to its best-matching SNID template, the 91bg-like SN 2007ba ∼5 d past maximum brightness.

2.6.3 New Redshifts for Individual Objects

Some of the objects in our dataset do not have published spectroscopic host-galaxy redshifts. Therefore, we have obtained host-galaxy spectra of a few of the SNe presented in this chapter in order to determine their redshift. Furthermore, we have calculated the host-galaxy redshift of some of these objects with no published redshift based on narrow features present in our SN spectra. The SNe for which this was done, their host galaxies, the redshifts themselves, and basic information about the spectrum from which the redshift was determined can be found in Table 2.9.

Table 2.9: Previously Unpublished Spectroscopic Host-Galaxy Redshifts

SN Name	Host Galaxy	$cz_{\rm helio}$ (km s^{-1})[a]	UT Date of spectrum[b]	SN/Gal[c]	Abs/Emis[d]
SN 2000cu	ESO 525-G004	0.022 (0.001)	2006-07-21	Gal	Abs
SN 2003P	MCG +09-13-107	0.034 (0.003)	2003-01-23	Gal	Abs & Emis
SN 2006mp	MCG +08-31-29	0.027 (0.001)	2006-11-03	Gal	Emis
SN 2008s3[e]	2MASX J23004648+0734590	0.041 (0.001)	2008-09-08	Gal	Abs
SN 2008s5[f]	···	0.031 (0.001)	2008-09-22	SN	Emis

[a]The redshift uncertainty is in parentheses.
[b]UT date of the spectrum from which we determined the redshift.
[c] "SN" = Spectrum from which we determined the redshift was of the SN but contained narrow host-galaxy spectral features; "Gal" = Spectrum from which we determined the redshift was of the host galaxy itself.
[d] "Abs" = Absorption features were used to determine the redshift; "Emis" = Emission features were used to determine the redshift.
[e]Also known as SNF20080825-006.
[f]Also known as SNF20080909-030.

2.7 Conclusion

In this first BSNIP chapter we have presented a large, homogeneous set of low-redshift ($z \leq 0.2$) optical spectra of SNe Ia. Many of the SNe have well-calibrated light curves with measured distance moduli as well as host-galaxy corrections. We have also presented our observing and reduction procedures used during the two decades over which we collected these data, as well as our "color matching" method for removing residual galaxy contamination. Our relative spectrophotometry was shown to be extremely accurate for the vast majority of our dataset. How the data are currently stored and will eventually be made accessible to the astronomical community is also discussed.

In addition, we described the construction of our own set of SNID spectral templates as well as our classification scheme which utilizes these new templates. Using our classification procedure we were able to classify for the first time (as well as re-classify) a handful of objects as bona fide SNe Ia. Furthermore, we present classifications of objects as members of some of the peculiar SN Ia subtypes that were heretofore assumed to be "normal." In total our dataset includes spectra of nearly 90 spectroscopically peculiar SNe Ia. We also determine spectroscopic host-galaxy redshifts of some objects where these values were previously unknown.

The sheer size of the BSNIP sample and the consistency of our observation and reduction methods makes this sample unique among all other published SN Ia datasets. In future BSNIP chapters we will use these data to examine the relationships between spectroscopic characteristics and other observables (such as photometric and host-galaxy properties).

Our sample is also a preview of coming attractions; new large transient searches such as the Palomar Transient Factory (PTF; Rau et al. 2009; Law et al. 2009) and Pan-STARRS (Kaiser et al. 2002) will compile datasets similar in size to ours in just a few years.

Chapter 3

Berkeley Supernova Ia Program II: Initial Analysis of Spectra Obtained Near Maximum Brightness

Bright points in the sky or a blow on the head will equally cause one to see stars.
—Percival Lawrence Lowell

3.1 Introduction

Type Ia supernovae (SNe Ia) have been particularly useful in recent years as a way to accurately measure cosmological parameters (e.g. Astier et al. 2006; Riess et al. 2007; Wood-Vasey et al. 2007; Hicken et al. 2009a; Kessler et al. 2009; Amanullah et al. 2010; Suzuki et al. 2011), and led to the discovery of the accelerating expansion of the Universe (Riess et al. 1998; Perlmutter et al. 1999). Broadly speaking, SNe Ia are the result of thermonuclear explosions of C/O white dwarfs (WDs) (e.g., Hoyle & Fowler 1960; Colgate & McKee 1969; Nomoto et al. 1984; see Hillebrandt & Niemeyer 2000 for a review). However, we still lack a detailed understanding of the progenitor systems and explosion mechanisms, as well as how differences in initial conditions create the variance in observed properties of SNe Ia. To solve these problems, and others, detailed and self-consistent observations of many hundreds of SNe Ia are required.

The cosmological application of SNe Ia as precise distance indicators relies on being able to standardize their luminosity. Phillips (1993) showed that the light-curve decline rate is well correlated with luminosity at peak brightness for most SNe Ia, the so-called "Phillips relation." However, this simple empirical relation relies on photometry alone and it may be possible to refine the relation with the addition of spectral observations. Many comparisons of spectral features and studies of the temporal evolution of these features in low-redshift SN Ia have been performed in the past (e.g., Barbon et al. 1990; Branch & van den Bergh 1993; Nugent et al. 1995; Hatano et al. 2000; Folatelli 2004; Benetti et al. 2005; Bongard

et al. 2006; Hachinger et al. 2006; Bronder et al. 2008; Foley et al. 2008; Branch et al. 2009; Wang et al. 2009a; Walker et al. 2011; Nordin et al. 2011b; Blondin et al. 2011; Konishi et al. 2011). In addition, there has been similar work with SNe Ia at higher redshifts (e.g., Hook et al. 2005; Blondin et al. 2006; Altavilla et al. 2009; Garavini et al. 2007; Bronder et al. 2008; Walker et al. 2011; Konishi et al. 2011). Many of these studies aimed to find a "second parameter" in SN Ia spectra which would make our measurements of the distances to SNe Ia even more precise.

However, most of these studies utilized relatively small and heterogenous datasets. Using the self-consistently observed and reduced low-redshift ($z \leq 0.2$) optical SN Ia spectra from the Berkeley Supernova Ia Program (BSNIP; Chapter 2), we can accurately and robustly measure various spectral features. These measurements can then be used to investigate how the spectral observables correlate with each other and with the objects' previously determined spectral subclasses based on different classification schemes.

We provide an overview of the dataset used for this analysis in Section 3.2, and we describe in detail our automated and robust procedure for measuring multiple aspects of each spectral feature in Section 3.3. Our resulting measurements are described in Section 3.4, and how these measured values evolve with time and how they correlate with each other and with previously determined spectral classifications is presented in Section 3.5. We discuss our conclusions in Section 3.6, specifically summarizing the main results from our analysis in Section 3.6.1. Finally, we attempt to answer questions regarding how SNe Ia should be spectroscopically classified (Section 3.6.2), whether or not theoretical models can explain the spectra of SNe Ia and the correlations we find (Section 3.6.3), and how our analysis of spectral features will be critical for future SN surveys (Section 3.6.4). Forthcoming BSNIP chapters will utilize the spectral measurements described here and examine the correlations between these and other observables (such as photometry and host-galaxy properties).

3.2 Spectral Dataset

The SN Ia spectra that are used in this study all come from BSNIP and are published in BSNIP I (Chapter 2). The majority of the spectra were obtained using the Shane 3 m telescope at Lick Observatory with the Kast double spectrograph (Miller & Stone 1993). The typical wavelength coverage is 3300–10400 Å with resolutions of ∼11 and ∼6 Å on the red and blue sides, respectively (crossover wavelength ∼5500 Å). The relative spectrophotometry of the BSNIP data is quite accurate, though the absolute spectrophometry is only correct in a handful of spectra. Thus, flux measurements alone may be inaccurate, but *ratios* of flux values should be quite precise. Some of the spectra examined here have had residual host-galaxy contamination removed using our "color matching" technique. This method uses photometry of the host galaxy of a SN to correct for any contamination that remains after our normal data reduction procedure (which often removes the majority of host-galaxy light). Further information regarding the observations, data reduction, spectrophotometric accuracy, and host-galaxy corrections can be found in BSNIP I.

For this study we required that a spectrum be within 20 d (rest frame) of maximum brightness, using the redshift and JD of maximum presented in Table 1 of BSNIP I. The only SNe which we ignored *a priori* were the extremely peculiar SN 2000cx (e.g., Li et al. 2001c), SN 2002cx (e.g., Li et al. 2003b; Jha et al. 2006a), SN 2005hk (e.g., Chornock et al. 2006; Phillips et al. 2007), and SN 2008ha (e.g., Foley et al. 2009a; Valenti et al. 2009). After removing these objects, we were left with 458 spectra (147 of which were corrected for host-galaxy contamination) of 271 SNe Ia, and we attempted to measure their spectral features.

Of these, there were some spectra which did not pass our minimum signal-to-noise ratio (S/N) cut (see Section 3.3.3), or whose wavelength range did not sufficiently cover any of the features we attempted to measure (see Section 3.3.1). In addition, the endpoints of each feature sometimes fell outside our allowed boundaries (see Section 3.3.2), or every spectral feature that was measured was deemed to have a poorly defined continuum (see Section 3.3.6). After removing these data there remain 432 spectra of 261 SNe Ia with a "good" fit for at least one spectral feature. The largest redshift of these observations is $\sim$0.1 (even though the full BSNIP dataset contains SNe with $0.1 < z < 0.2$). The earliest spectrum successfully fit in this chapter has a rest-frame age of about -12.7 d. A summary of these SNe Ia, their ages, and spectral classifications based on various classification schemes can be found in Section 3.7.1.

3.3 Measurement Procedure

3.3.1 Measured Features

Previous studies similar to this one have split optical SN Ia spectra near maximum brightness into nine major absorption feature complexes (e.g., Folatelli 2004; Hachinger et al. 2006). All of these are features are, in actuality, blends of multiple spectral transitions, but each absorption complex itself is often distinct enough from the others for its properties to be measured independently. We follow previous studies' naming convention for the measured features by referring to each one by an ion or spectral line responsible for the majority of the absorption. The nine features we attempt to fit in each observation are labelled on a spectrum of the "normal" type Ia SN 2002ha (taken 1 d before maximum brightness) in Figure 3.1. Each feature's name and reference number, along with its rest wavelength (used to determine expansion velocities), is presented in Table 3.1.

Table 3.1: Spectral Features and Boundaries

Name	Feature #	Rest Wavelength[a] (Å)	Blue Boundary[b] (Å)	Red Boundary[b] (Å)
Ca II H&K	f1	3945.28	3400–3800	3800–4100
Si II λ4000	f2	4129.73	3850–4000	4000–4150
Mg II	f3	...[c]	4000–4150	4350–4700

Continued on Next Page...

Table 3.1 — Continued

Name	Feature #	Rest Wavelength[a] (Å)	Blue Boundary[b] (Å)	Red Boundary[b] (Å)
Fe II	f4	...[c]	4350–4700	5050–5550
S II "W"[d]	f5	5624.32	5100–5300	5450–5700
Si II λ5972	f6	5971.85	5400–5700	5750–6000
Si II λ6355	f7	6355.21	5750–6060	6200–6600
O I Triplet	f8	7773.37	6800–7450	7600–8000
Ca II Near-IR Triplet	f9	8578.75	7500–8100	8200–8900

[a]The rest wavelengths are weighted averages of the strongest spectral lines that give rise to each absorption feature.
[b]These boundaries are necessary in order to account for variations in spectral feature width and expansion velocity among SNe, as well as the temporal evolution of these values.
[c]This feature is a blend of so many spectral lines that a single reference wavelength is practically meaningless (and thus an expansion velocity cannot be accurately determined).
[d]Both broad absorptions that make up the S II "W" are fit as a single feature, but we calculate the expansion velocity of the absorption complex using the minimum of the redder of the two features relative to its rest wavelength.

There have been a significant number of spectroscopically peculiar SNe Ia observed whose spectra near maximum brightness do not contain some of the nine features or contain extremely weak absorptions from certain features (for a review of these objects, see Filippenko 1997). We consider an object "spectroscopically normal" if it is classified as "Ia-norm" by the SuperNova IDentification code (SNID; Blondin & Tonry 2007) as implemented in BSNIP I. In the current study we have 351 Ia-norm objects and 10 "Ia" objects for which we were unable to determine a definitive subtype in BSNIP I. There are 39 SN 1991bg-like objects ("Ia-91bg," e.g., Filippenko et al. 1992b; Leibundgut et al. 1993) which represent the usually underluminous SNe Ia. We also have 9 SN 1991T-like objects ("Ia-91T," e.g., Filippenko et al. 1992a; Phillips et al. 1992) and 23 SN 1999aa-like objects ("Ia-99aa," e.g., Li et al. 2001b; Strolger et al. 2002; Garavini et al. 2004) which together represent the often overluminous SNe Ia. These classifications are listed in the "SNID (Sub)Type" column of Table 3.5. See BSNIP I for more information regarding our implementation of SNID and the various spectroscopic subtype classifications. We include these peculiar objects in our study in an attempt to better quantify the extent of the spectral peculiarities among these types of SNe Ia. However, as mentioned in Section 3.2, there are some objects which are so spectroscopically peculiar (compared with "normal" SNe Ia) that we have removed them from our sample.

3.3.2 Allowed Boundaries

As in previous studies, we require that the endpoints for each feature, as determined on a SN-by-SN basis by our fitting algorithm (see Section 3.3.4), be within pre-determined boundaries (e.g., Folatelli 2004; Nordin et al. 2011b). These boundaries are necessary in

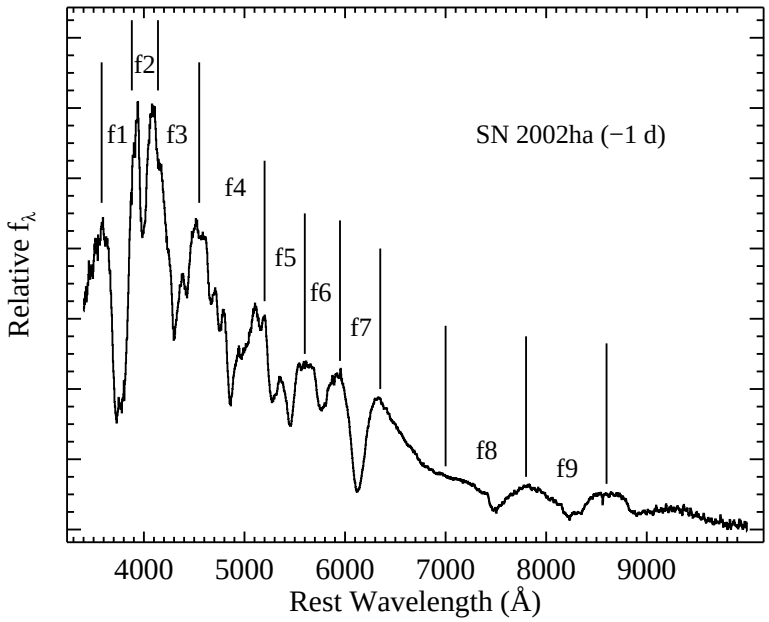

Figure 3.1: The nine features we attempt to fit in each observation shown on a spectrum of the "normal" type Ia SN 2002ha, taken 1 d before maximum brightness, from BSNIP I. The spectrum has had its host-galaxy recession velocity removed and has been corrected for Milky Way reddening according to the values presented in Table 1 of BSNIP I and assuming that the extinction follows the Cardelli et al. (1989) extinction law modified by O'Donnell (1994). See Table 3.1 for more information regarding each feature.

order to account for variations in spectral feature width and expansion velocity among SNe, as well as the temporal evolution of these values. Even though the formal boundaries of neighboring features (among the totality of SN spectra) may overlap, the actual endpoints of neighboring features in a *given* spectrum will not.

The boundaries used here are slightly modified from those in previous studies; our boundaries tend to be wider than those of our predecessors (e.g., Folatelli 2004; Nordin et al. 2011b). The final values of our boundaries were a result of extensive testing and represent a compromise between including as many fits as possible (by accounting for differences in spectral feature width and velocity) while making sure that no endpoints overlap with a neighboring feature. The boundaries used in this chapter for each spectral feature can be found in Table 3.1.

3.3.3 Initial Steps

For each spectrum we begin by removing the host-galaxy recession velocity and correcting for Milky Way (MW) reddening according to the values presented in Table 1 of BSNIP I and assuming that the extinction follows the Cardelli et al. (1989) extinction law modified by O'Donnell (1994). The spectrum is then smoothed using a Savitzky–Golay smoothing filter (Savitzky & Golay 1964). From this point in the procedure we only focus on the spectral region near the current feature being measured. The S/N is then calculated and no attempt is made to measure the spectral feature if the S/N is less than 6.5 pixel^{-1} over the entire feature. This cutoff is based on the fact that no data with S/N $<$ 6.5 pixel^{-1} yielded reasonable spectral fits. We also calculate the uncertainties in the measured flux at each pixel by taking the root-mean square error (RMSE) of wavelength bins centered on each pixel.

3.3.4 The (Pseudo-)Continuum

One of the most difficult aspects of a study such as this is defining suitable continua for the spectral features. Since SN Ia spectra consist of broad, heavily blended absorption features, the physical spectral continuum is nearly impossible to define accurately (Nordin et al. 2011b). However, we can define a pseudo-continuum for each feature which will allow us to measure spectral features accurately and consistently, although the direct physical interpretation of such measurements is complicated and beyond the scope of this chapter (Folatelli 2004).

In order to define the pseudo-continuum, the local minimum of the data for the current spectral feature is determined. The local slope of the data is then calculated in wavelength bins to either side of this minimum until the slope changes sign (i.e., we have reached a local maximum). The Mg II, Fe II, and S II "W" features consistently have local maxima within the features themselves and thus our usual method will determine the endpoints incorrectly. Therefore, we began calculating the slope of these features just inside the inner edges of their allowable ranges (see Table 3.1). Furthermore, the flux blueward of the O I triplet rarely

reached a local maximum before entering the region surrounding the Si II λ6355 feature. Again, this would lead to an inaccurate pseudo-continuum definition. To remedy this, we allowed the blue endpoint of the pseudo-continuum of this feature to be defined where the slope of the flux is $\gtrsim 0.002$ (since it rarely actually changes sign, which is the endpoint criterion for all other spectral features).

Once these two endpoints are determined, a quadratic function is fit to the data in wavelength bins centered on each endpoint. If either fit results in a concave upward parabola, we consider the endpoints to be ill-determined and no further attempt to fit the feature is made. In addition, if either parabola's peak is outside the allowed boundary range for the feature being measured (see Table 3.1), we consider the pseudo-continuum to be incorrectly defined and again no further attempt to fit the feature is made. However, if both fits resulted in concave downward parabolas, with peaks within the allowed boundary range for the spectral feature in question, we connect the peaks of each parabola with a line and define this as the pseudo-continuum.

This method is similar to those used in previous studies (e.g., Blondin et al. 2011; Nordin et al. 2011b), though our use of a quadratic fit to the region near each endpoint is somewhat unique. This extra step can be thought of as an additional local smoothing function to ensure that the pseudo-continuum endpoints truly represent a local maximum in the flux and not simply the top of a noise spike that remains in the data even after our initial smoothing. Also, note that our pseudo-continuum definition is completely automated (i.e., the endpoints are not manually chosen).

When a pseudo-continuum is determined for a given spectral feature, we record the flux at the blue and red endpoints of the feature (F_b and F_r, respectively), which are effectively the peaks of the two parabolas mentioned above. These values correspond to $h_{\rm blue}$ and $h_{\rm peak}$ (respectively) from Blondin et al. (2011). The uncertainties of these values are simply the calculated RMSE at these pixels. An example of F_b and F_r (along with the pseudo-continuum and the rest of our spectral measurements) is shown in Figure 3.2.

For all features with a well determined pseudo-continuum, we also calculate the pseudo-equivalent width (pEW; e.g., Garavini et al. 2007) defined as

$$\mathrm{pEW} = \sum_{i=0}^{N-1} \Delta\lambda_i \left(\frac{f_c(\lambda_i) - f(\lambda_i)}{f_c(\lambda_i)} \right), \tag{3.1}$$

where λ_i are the wavelengths of each pixel in the spectrum ranging from the blue endpoint to the red endpoint (as defined by the pseudo-continuum), $\Delta\lambda_i$ is the width of the $i^{\rm th}$ pixel, $f(\lambda_i)$ is the data's flux at λ_i, and $f_c(\lambda_i)$ is the flux of the pseudo-continuum at λ_i. The 1σ uncertainty on the pEW was calculated by error propagation of the uncertainty in the measured flux at each pixel. Somewhat surprisingly, varying the exact choice of pseudo-continuum endpoints added negligibly to the uncertainty of the pEW (as well as all of the other values measured). The pEW is represented schematically in the bottom panel of Figure 3.2.

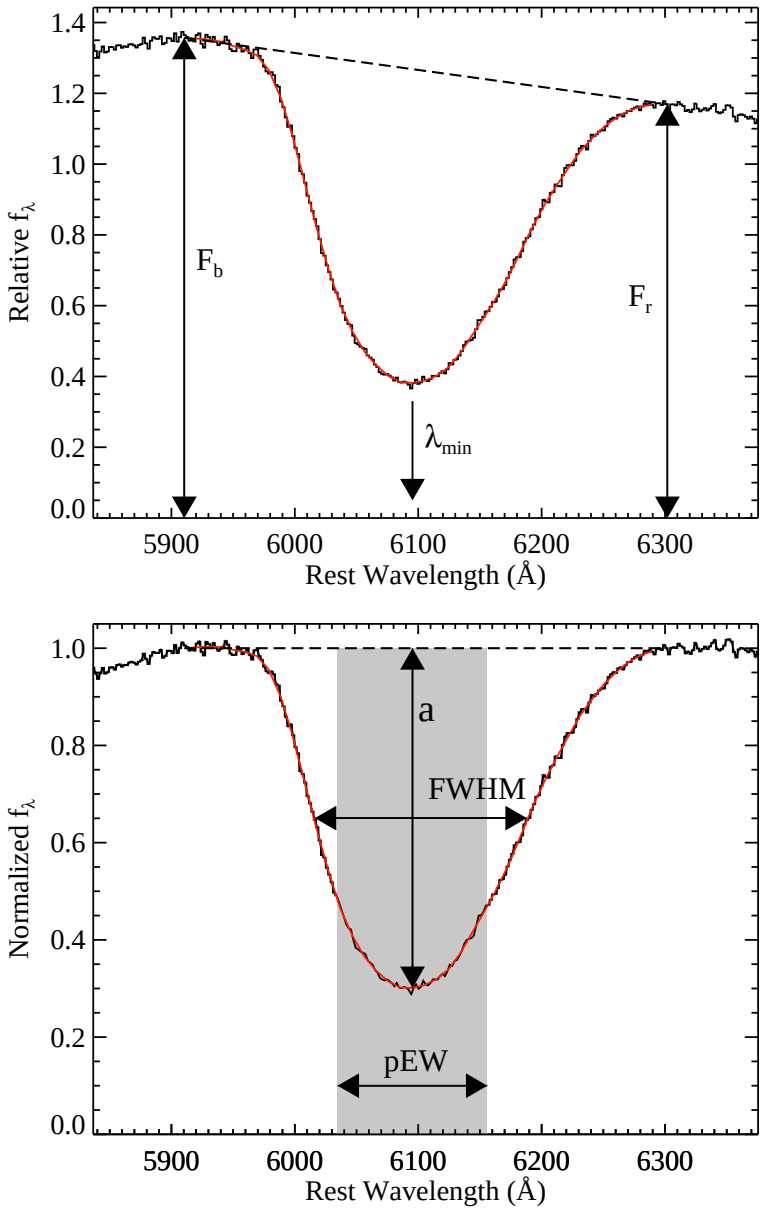

Figure 3.2: An example of the spectral measurements used in this study. The feature shown is Si II λ6355 from a spectrum of SN 2002he at maximum brightness. In both panels the data are the solid black curve, the spline fit is the solid red curve, and the pseudo-continuum is the dashed black line. The top panel shows the SN spectrum along with the flux at the endpoints of the feature (F_b and F_r) as well as the minimum of the spline fit ($\lambda_{\rm min}$) which is used to calculate the expansion velocity (v). The bottom panel shows the spectrum normalized to the pseudo-continuum, in addition to the relative depth (a) and FWHM of the feature, and a schematic representation of the pEW.

3.3.5 Spline Fits

Once a pseudo-continuum is calculated for a given spectral feature, a cubic spline is fit to the smoothed data between the endpoints previously determined. However, no attempt is made to fit any of the Mg II or Fe II features in this manner. These complexes consist of so many blended spectral lines that it is unclear which reference wavelength to use when attempting to define an expansion velocity (which is one of the main reasons for fitting a function to the data in the first place).

Other functional forms were considered before the spline was chosen. This included the Gauss-Hermite (van der Marel & Franx 1993) , Gaussian, and sixth-order polynomial. In many cases all of these functions matched the data relatively well, though the spline fits matched the data better in more cases than the other functions. The Gauss-Hermite and Gaussian parameters calculated from spectra of astrophysical sources can be directly related to physical properties of the source in question (e.g., van der Marel & Franx 1993). Unfortunately, such an interpretation is unrealistic since a true continuum is not being measured in SN spectra and the features that are measured are actually blends of many spectral lines.

Using the wavelength at which the spline fit reaches its minimum ($\lambda_{\rm min}$, labelled in the top panel of Figure 3.2) along with the reference rest wavelength (listed in Table 3.1) and the relativistic Doppler equation, we calculate the expansion velocity (v). Thus, all velocities used in this study are relative to the *deepest* component of each spectral feature. As mentioned previously, varying the pseudo-continuum endpoints did not significantly change the measured values of $\lambda_{\rm min}$ and thus we impose a 2 Å uncertainty on the wavelength at which the spline fit reaches its minimum. We then propagate this error through the relativistic Doppler equation to calculate the uncertainty in the expansion velocity.

The spectral feature being measured is then normalized to the pseudo-continuum and the relative depth of the feature (a) and the full width at half-maximum intensity (FWHM) of the feature are both computed. The bottom panel of Figure 3.2 shows both a and the FWHM. The uncertainty of a is taken directly from the calculated RMSE (normalized to the pseudo-continuum). The uncertainty of the FWHM is the standard deviation of the FWHM values when varying the half-maximum level.

3.3.6 Final Inspection

While the aforementioned automated fitting procedure is quite robust, we felt it was wise for each spectral feature in each spectrum (for which a pseudo-continuum was determined) to be visually inspected by more than one co-author. Thus, 3141 spectral features and their fits were examined by eye.

About 10–40% of the time (depending on the feature) the pseudo-continuum endpoints passed the automated fitting criteria but did not accurately reflect the actual edges of the spectral feature in question. This was usually due to the measured feature being blended with a neighboring spectral feature. In these cases we simply removed these fits from the

Table 3.2: Number of Spectra and Objects Measured Per Feature

Feature	Good Pseudo-Continuum		Good Spline Fit	
	Spectra	SNe	Spectra	SNe
Ca II H&K	281	191	172	128
Si II λ4000	188	137	172	129
Mg II	219	163	0	0
Fe II	313	217	0	0
S II "W"	240	179	240	179
Si II λ5972	204	156	166	129
Si II λ6355	366	239	360	235
O I triplet	192	139	109	84
Ca II near-IR triplet	301	201	129	103

rest of our analysis since if the pseudo-continuum was unreliable then any of the other measurements would be as well.

Of the features determined to have accurate pseudo-continua, sometimes the spline fit did not accurately reproduce the actual minimum of the flux. This meant that the calculated expansion velocities, relative spectral feature depths, and FWHM would be inaccurate. In cases such as this, these spectral measurements are ignored, but F_b, F_r, and the pEW are recorded since these values are based on the accuracy of the pseudo-continuum alone and are unaffected by the spline fit to the data. As mentioned previously, all Mg II and Fe II data fall into this category since we do not even attempt a spline fit for these features. About 30–50% of the Ca II H&K, O I triplet, and Ca II near-IR triplet features were found to have unreliable spline fits. Less than 12% of each of the three Si II features and none of the S II "W" data had untrustworthy spline fits.

3.4 Results

The dataset used in this analysis, after the aforementioned automated cuts were applied and the spectra were visually inspected, contains 432 spectra of 261 SNe Ia. Each of these has a measured pseudo-continuum for at least one spectral feature. A summary of the number of spectra and objects with well-defined pseudo-continua and the number with "good" spline fits can be found in Table 3.2. As described in Section 3.3.6, a feature in a given spectrum that has a "good" spline fit will have a well-defined pseudo-continuum by construction, though the opposite is not necessarily true. All measured values for each feature can be found in the tables in Section 3.7.2.

3.4.1 Comments on Individual Spectral Features

Ca II H&K

The Ca II H&K feature usually falls completely within our data and we are able to accurately measure it in many of our spectra. Sometimes the left edge of this feature is not well-defined due to either noise at the bluest end of our data or the complex spectral shape. The velocity of this feature may be somewhat uncertain (especially at the earliest epochs) due to detached, high-velocity absorption that is sometimes observed in Ca II H&K (e.g., Branch et al. 2005). The measured values for the Ca II H&K feature can be found in Table 3.6.

Si II λ4000

The Si II λ4000 feature is measurable in many of our spectra before and near maximum brightness. By about 7 d past maximum, it often weakens to the point where it becomes indistinguishable from the complex blend of spectral lines we refer to as the Mg II feature. In spectra where it is unclear whether Si II λ4000 is a distinct feature or blended with Mg II, we consider the continuum to be ill-defined for both spectral features. The measured values for the Si II λ4000 feature are presented in Table 3.7.

Mg II

As mentioned previously, we did not attempt to fit any of the Mg II features with a spline function. This is mainly due to the fact that this feature is actually made up of blends of many iron-group element (IGE) spectral lines and thus was extremely complex to fit (even with something as generic as a spline function). In cases where a spline would have fit the data fairly well, we did not record its velocity since it is unclear which rest wavelength to use when attempting to define an expansion velocity for such a complex spectral region. The measured values for the Mg II feature are shown in Table 3.8.

Fe II

The Fe II feature suffers from the same blending issues as the Mg II feature, and thus we again do not attempt to fit any of these features with a spline. Another similarity with the Mg II feature is that after about 7 d past maximum brightness the red edge of the Fe II feature becomes difficult to distinguish from the blue edge of the S II "W". As in the case of Mg II and Si II λ4000, we consider the continuum to be ill-defined for both Fe II and S II "W" when it is unclear if the two features are distinct. The measured values for the Fe II feature can be viewed in Table 3.9.

S II "W"

After about 7 d past maximum, the S II "W" weakens significantly and becomes blended with both Fe II (as mentioned above) and Si II λ5972. The two broad features that make up the tell-tale "W" shape of this S II feature are sometimes so broadened (at the highest expansion velocities) that they are almost indistinguishable. Note that all velocities derived for the S II "W" are with respect to the redder of the two broad features ($\sim$5624 Å). The measured values for the S II "W" feature are displayed in Table 3.10.

Si II λ5972

The Si II λ5972 feature, as stated previously, becomes blended with the S II "W" after about 7 d past maximum brightness. It also becomes blended with the usually much stronger Si II λ6355 feature near this epoch as well. Furthermore, this feature can sometimes be contaminated by Ti II absorption, especially in Ia-91bg objects (Filippenko et al. 1992b). The spectral range over which we fit the Si II λ5972 feature also includes Na I D at rest (i.e., from the Milky Way) and, for most of the objects presented here, at the redshift of the SN host galaxy. The vast majority of our data do not show strong Na I D absorption from either source, but there are a few spectra where it is detected. No attempt is made to correct for this absorption or interpolate over it; we simply point out that our measured pEW of the Si II λ5972 is perhaps larger than the actual value in a few cases due to the added absorption from Na I D. The measured values for the Si II λ5972 feature are listed in Table 3.11.

Si II λ6355

The characteristic spectral feature of SN Ia spectra near maximum brightness is the Si II λ6355 trough. Unsurprisingly, this is the feature for which the most "good" fits were obtained (see Table 3.2). As we have already pointed out, the nearby (though usually weaker) Si II λ5972 feature becomes somewhat blended with Si II λ6355 by about 7 d past maximum. However, the Si II λ6355 feature is usually so much stronger than Si II λ5972 that we are still able to obtain "good" fits to Si II λ6355 well after 7 d past maximum brightness. The measured values for the Si II λ6355 feature can be found in Table 3.12.

O I Triplet

Perhaps the most uncertain feature we attempt to fit is the O I triplet (notice its relatively low numbers in Table 3.2). Even though this is not at the reddest edge of most of our spectra, it is in a region that is often contaminated by large-amplitude fringing due to the spectrograph. In addition, it is usually found in a part of the spectrum that is strongly affected by telluric absorption. Even though corrections are made for both the fringing and the telluric absorption (see BSNIP I for more information on how these correction are made), there often remains significant noise in this wavelength region. However, the O I

triplet is important for us to investigate here, since it has been often neglected in previous measurements of SN Ia spectra. For example, one of the largest pre-BSNIP SN Ia spectral datasets had an average wavelength coverage of 3700–7400 Å (Matheson et al. 2008). Despite the aforementioned sources of uncertainty, we attempt to measure this spectral feature and are successful for a significant number of spectra. However, we do caution that the measured properties of the O I triplet are more uncertain than the rest of the features inspected. The measured values for the O I triplet are given in Table 3.13.

Ca II Near-IR Triplet

Finally, the Ca II near-IR triplet often falls completely within our data which, as mentioned above, has rarely been the case for previous studies similar to this one. This feature is difficult to measure accurately due to fringing at the reddest end of many of the BSNIP spectra. Like the Ca II H&K feature, the velocity of the Ca II near-IR triplet may be somewhat uncertain (especially at the earliest epochs) due to detached, high-velocity absorption that has been observed (e.g., Mazzali et al. 2005). The measured values for the Ca II near-IR triplet are compiled in Table 3.14.

3.4.2 Self-Consistency of the Measurements

To investigate how self-consistent and reliable the measurement procedure used in this study is, values measured from spectra of the same SN obtained on consecutive nights were compared. Since the spectra of SNe Ia should not evolve much over the course of one day, any differences in the values measured should come mainly from the measurement procedure itself (in addition to the uncertainty in the spectrum itself). There are about 10–20 pairs of spectra with "good" fits (depending on the feature) separated by one day in the data analyzed here. We find that the median relative difference between each pair is slightly larger than or about equal to the median uncertainty of the measurements themselves. Thus, the measured change in an object's spectrum over the course of one day is consistent with the uncertainties we report for each measurement.

This test was redone with pairs of spectra that were observed within 0.5 d of each other, but there were very few data which met this criterion and thus no useful results could be obtained. It was also run with pairs of spectra within 2 d of each other. This adds about 20 pairs to the test, but also increases the median relative difference between consecutive spectra. The difference was still on the order of the uncertainties reported, though the difference in expansion velocities was often larger than our calculated uncertainties. This is not as enlightening as the test with spectral pairs separated by one day since over the course of two days (near maximum brightness) the expansion velocity of SNe Ia can change by almost 100 km s^{-1} d^{-1} (see Section 3.5.1), which is on the same order as the median of our reported expansion-velocity uncertainties.

Another, similar test was conducted using the SN Ia spectra presented by Matheson et al. (2008). Due to the scheduling of their telescope time, their dataset mainly consists of well-

sampled spectroscopic time series of a handful of SNe Ia, averaging more spectra per object than BSNIP (Chapter 2). When applying our measurements procedure to the Matheson et al. (2008) data, there are about 40–70 pairs of spectra with "good" fits (depending on the feature) separated by one day. Again, the median relative difference between pairs is larger than or about equal to the median uncertainty of the measurements themselves. This supports the idea that the measurement procedure is reliable and any measured spectral changes are indeed physical. In addition, this indicates that the uncertainties calculated by the measurement procedure are representative of the actual uncertainties.

3.5 Analysis

3.5.1 Temporal Evolution of Expansion Velocities

Much work has been done previously on studying the expansion velocities of the ejecta of low-z SNe Ia as they decrease with time (e.g., Barbon et al. 1990; Branch & van den Bergh 1993; Benetti et al. 2005; Wang et al. 2009a). It has been claimed that there exist a population of spectroscopically normal SNe Ia (i.e., Ia-norm) that have higher-than-normal expansion velocities (as determined by the Si II λ6355 feature) near maximum brightness, and that these objects might have photometric peculiarities as well (Wang et al. 2009a; Foley & Kasen 2011). Wang et al. (2009a) defined high-velocity (HV) objects as spectroscopically normal SNe Ia with velocities greater than 3σ above the average (i.e., $\gtrsim 11,800$ km s^{-1}) within 7 d of maximum brightness.

As will be shown below, the scatter in Si II λ6355 velocity increases drastically at ages earlier than 5 d before maximum, so this is the lower age boundary in the investigation of HV objects. A histogram of the Si II λ6355 velocities for spectra within 5 d of maximum is shown in Figure 3.3. The vertical dashed line at $v = 11,800$ km s^{-1} is the cutoff between normal and HV objects. While there is likely a distinct population of SNe Ia with $v > 11,800$ km s^{-1}, it is also interesting to note that there might exist a third population of SNe with even higher velocities ($v \gtrsim 13,000$ km s^{-1}).

The average velocity of spectra with velocities less than 11,800 km s^{-1} and within 5 d of maximum is $\sim 10,700 \pm 700$ km s^{-1}, which is consistent with what Wang et al. (2009a) found.[1] The average (linear) change in velocity with time of all spectra with velocities less than 11,800 km s^{-1} and $t > -5$ d is 38 km s^{-1} d^{-1}, again consistent with the findings of Wang et al. (2009a).

To determine if an object should be considered HV or normal, the cutoff from Wang et al. (2009a), 11,800 km s^{-1}, is applied at $t = 0$. The average change in velocity with time is then used to extrapolate that cutoff value from $t = -5$ d to $t = 10$ d. The lower age boundary was mentioned above, while the upper age boundary comes from the fact that the

[1] Even though most of the spectra used here were also in Wang et al. (2009a), they used data from non-BSNIP sources as well. In addition, the method of measuring expansion velocities is different between the two studies (see Section 3.3 for more information on the measurements procedure adopted here).

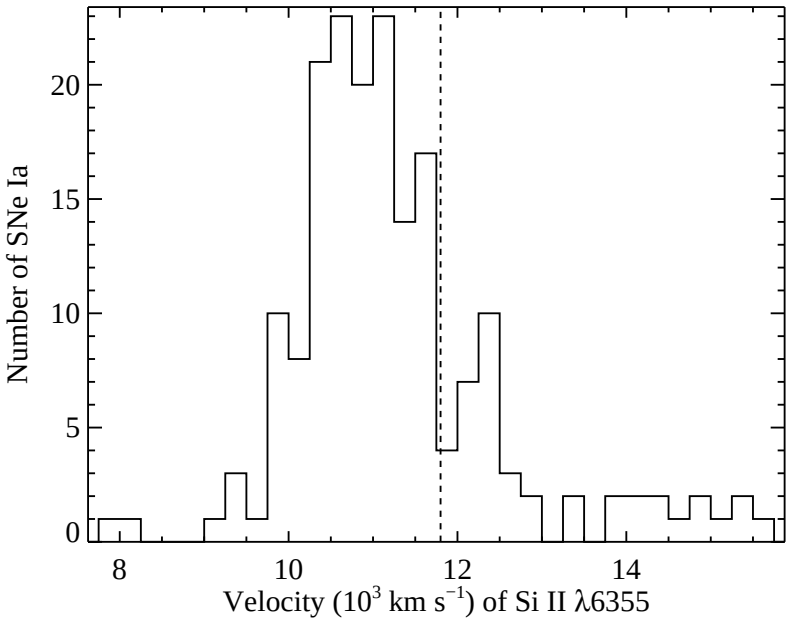

Figure 3.3: A histogram of the velocities of the Si II λ6355 feature for spectra within 5 d of maximum brightness. The vertical dashed line at $v = 11,800$ km s^{-1} is the cutoff between normal and HV objects.

velocities of HV and normal SNe begin to significantly overlap by about 10 d past maximum. Three SNe, all with velocities close to the cutoff between HV and normal, had one spectrum with a velocity that was above the cutoff and one below the cutoff. These were ultimately classified using the velocity of the spectrum closest to maximum brightness. The results of this classification can be found in the "Wang Type" column of Table 3.5. Objects for which a "Wang Type" could not be determined are either spectroscopically peculiar (according to SNID) or have no Si II λ6355 velocity in the range $-5 < t < 10$ d. Of the 140 SNe for which a "Wang Type" is determined, about 27% are HV (for comparison, $\sim$35% of the 158 objects in the sample of Wang et al. 2009a, were found to be HV).

The temporal evolution of the expansion velocities for each of the seven spectral features with measured velocities is shown in Figures 3.4–3.10. The color of each data point corresponds to whether it is a normal or high-velocity SN (or undetermined), while the shape of each data point corresponds to its "SNID type."

Ca II

The evolution of the two Ca II features (Figures 3.4 and 3.5) are quite similar to each other. Both have a large range of velocities at $t < -5$ d, reaching values as high as 26,000–30,000 km s^{-1}, which is likely due to detached, high-velocity absorption that has been observed in these features (e.g., Branch et al. 2005; Mazzali et al. 2005). However, these

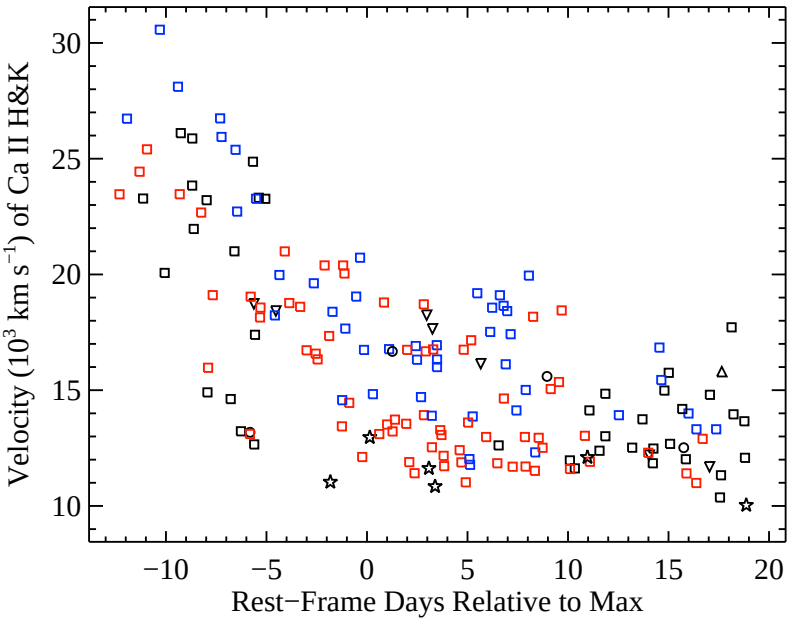

Figure 3.4: The velocity of Ca II H&K versus rest-frame age relative to maximum of 172 spectra of 128 SNe. Blue points are high-velocity (HV) objects, red points are normal-velocity objects, and black points are objects for which we could not determine whether the SN was normal or high velocity (see the text for further details regarding how HV SNe are defined). Squares are Ia-norm objects, stars are Ia-91bg objects, upward-pointing triangles are Ia-91T objects, downward-pointing triangles are Ia-99aa objects, and circles are objects which do not have a spectroscopic subclass (see BSNIP I for further details regarding how these subclasses are defined). Uncertainties in the velocities are smaller than the size of the data points.

highest velocities decrease rather quickly. For $-5 < t < 20$ d the velocities of both features are quite constant (at ∼12,000–16,000 km s^{-1}) with only a hint of decreasing with time. For both of these features, the HV SNe have higher typical post-maximum velocities, but the difference is not too significant, and the ranges of velocities spanned by the normal and HV objects are highly overlapping. Similarly, Ia-91T/99aa objects have slightly higher than average velocities near maximum brightness and Ia-91bg objects tend to have normal to low velocities.

Si II

As mentioned above, the velocities of the Si II λ6355 feature (Figure 3.6) span a huge range of values at $t < -5$ d. However, at $t > -5$ d, the velocities decline relatively linearly with time. The typical velocity near maximum brightness for the Ia-norm is ∼11,000 km s^{-1}. By construction, the HV objects have higher velocities than the normal objects for $-5 <$

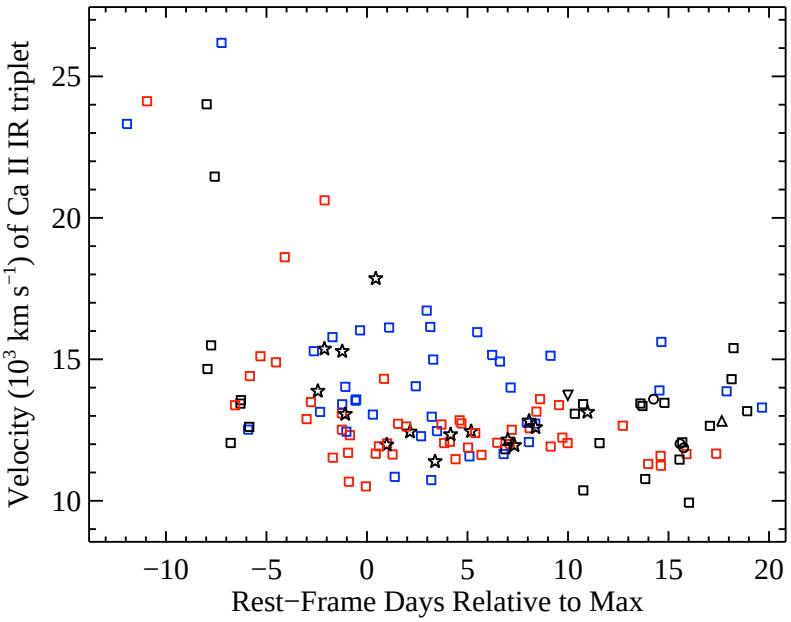

Figure 3.5: The velocity of the Ca II near-IR triplet versus rest-frame age relative to maximum brightness of 129 spectra of 103 SNe. Colors and shapes of data points are the same as in Figure 3.4. Uncertainties in the velocities are smaller than the size of the data points.

$t < 10$ d, but this also appears to hold at earlier times. At later times, the velocities of HV and Ia-norm objects become quite similar. Most of the spectroscopically peculiar objects from all subclasses (Ia-91bg, Ia-91T, and Ia-99aa) have lower than average velocities near maximum brightness, with the Ia-91bg SNe having the lowest velocities measured.

The Si II λ4000 feature (Figure 3.7) has a very similar temporal evolution to the Si II λ6355 feature, except it has less velocity scatter at $t < -5$ d. In fact, for $-10 \lesssim t \lesssim 10$ d the Si II λ4000 feature appears to have a linear decline and the normal and HV objects remain well separated during those epochs. The typical velocity of the Si II λ4000 feature for all objects matches that of the Si II λ6355 feature for only the normal-velocity objects. Furthermore, the highest velocities seen in Si II λ6355 are not see in the Si II λ4000 feature. These are both most likely due to the fact that we are unable to measure such high velocities for Si II λ4000 since at these values the Si II λ4000 feature becomes blended into the much stronger Ca II H&K feature.

Conversely, the Si II λ5972 feature (Figure 3.8) shows a large velocity scatter at $t < -5$ d *and* a significant overlap between the normal and HV SNe at $t > 5$ d. The typical Si II λ5972 velocity, as well as the range spanned, match well with the Si II λ6355 feature, though perhaps also lacking some of the highest velocities. The upturn in many of the velocities near $t = 5$ d is likely due to blending between the Si II λ5972 feature and the Na I D line which can appear in SN Ia spectra near this epoch (e.g., Branch et al. 2005).

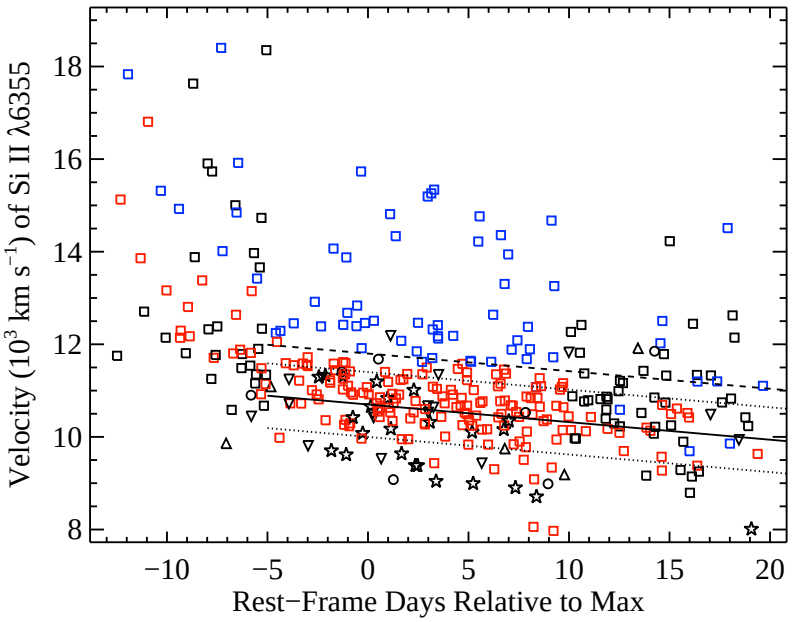

Figure 3.6: The velocity of Si II λ6355 versus rest-frame age relative to maximum brightness of 360 spectra of 235 SNe. Colors and shapes of data points are the same as in Figure 3.4. The solid line is the mean evolution of the normal-velocity SNe with $t > -5$ d, the dotted lines are the 1σ uncertainties, and the dashed line is the cutoff between HV and normal velocity objects (see the text for further details regarding how HV SNe are defined). Uncertainties in the velocities are smaller than the size of the data points.

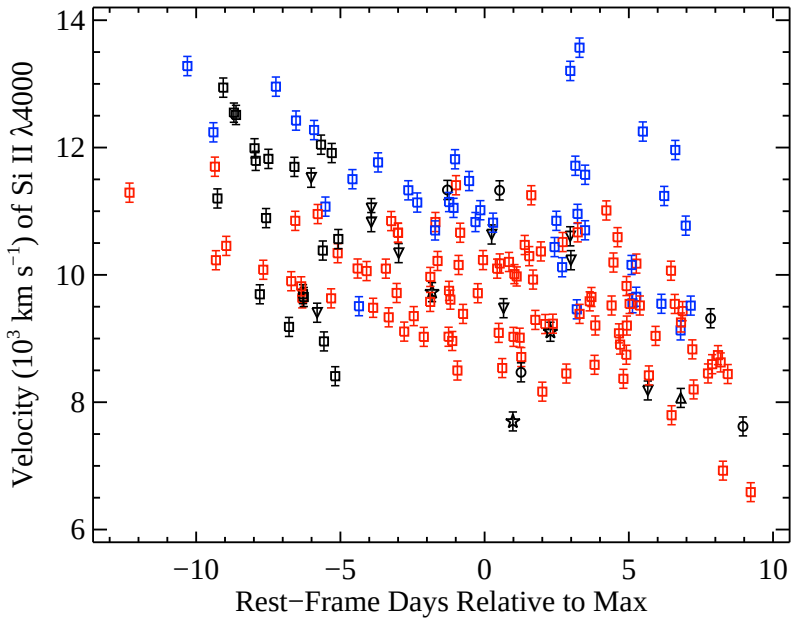

Figure 3.7: The velocity of Si II λ4000 versus rest-frame age relative to maximum brightness of 172 spectra of 129 SNe. Colors and shapes of data points are the same as in Figure 3.4.

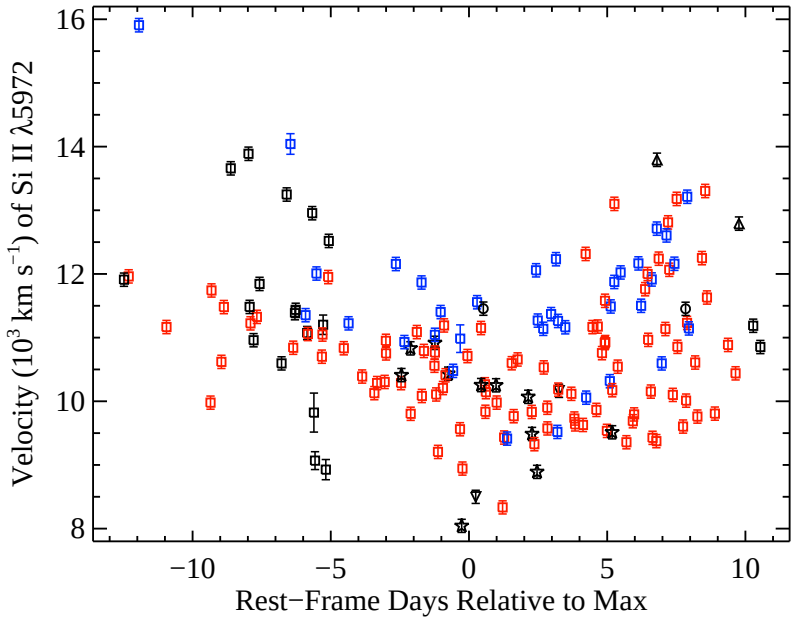

Figure 3.8: The velocity of Si II λ5972 versus rest-frame age relative to maximum brightness of 166 spectra of 129 SNe. Colors and shapes of data points are the same as in Figure 3.4.

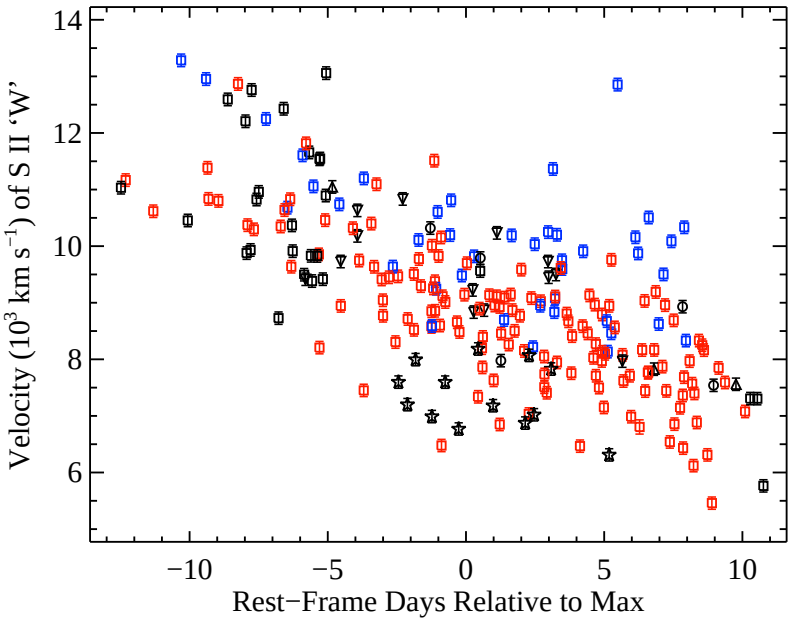

Figure 3.9: The velocity of the S II "W" feature versus rest-frame age relative to maximum brightness of 240 spectra of 179 SNe. Colors and shapes of data points are the same as in Figure 3.4.

S II

The temporal evolution of the S II "W" velocity (Figure 3.9) is quite linear from about 10 d before maximum brightness through 10 d after maximum. At about 5 d before maximum the typical velocity is ∼10,000 km s^{-1}, and by 5 d after maximum the typical velocity is ∼8000 km s^{-1}. As expected, the HV objects have larger velocities on average than the normal objects, but again there is significant overlap between the two subclasses. In addition, it seems that some of the HV objects decrease in velocity more quickly than the normal objects such that they have about the same velocity as the Ia-norm at the time of maximum brightness (see Section 3.5.2 for more information regarding the change of velocities with time). The Ia-91T/99aa objects have relatively large velocities for the S II "W" feature, similar to the HV SNe. Like the velocities of the Si II λ6355 feature, the Ia-91bg objects have many of the lowest velocities measured.

O I

The O I triplet (Figure 3.10) behaves in a manner similar to the Ca II features. The velocities remain constant in most of our spectra. However, the typical post-maximum velocity, ∼11,000 km s^{-1}, is lower than that of the Ca II features and has less scatter. The cluster of 6 spectra at extremely low velocities all have relatively weak O I triplets,

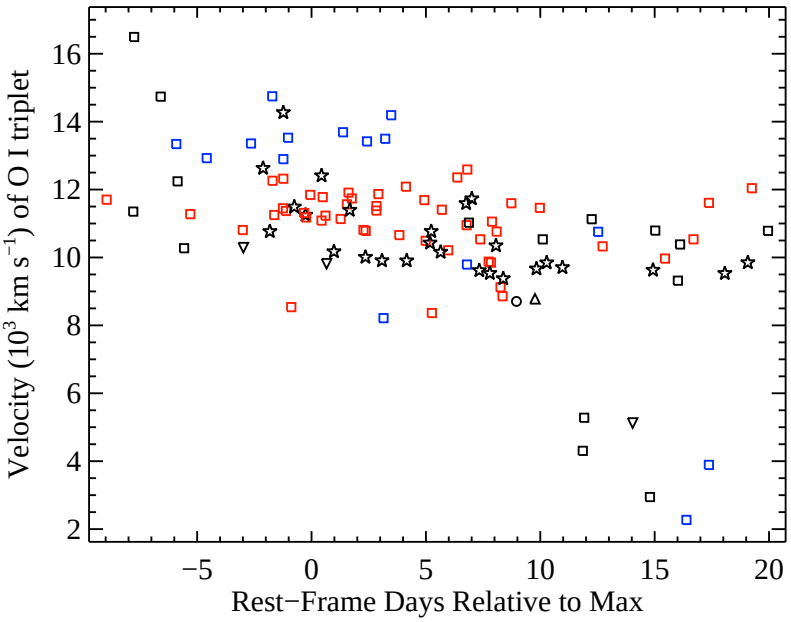

Figure 3.10: The velocity of the O I triplet versus rest-frame age relative to maximum brightness of 109 spectra of 84 SNe. Colors and shapes of data points are the same as in Figure 3.4. Uncertainties in the velocities are smaller than the size of the data points.

and since this feature is so broad, determining the exact minimum when it is weak can be somewhat inaccurate. That being said, the visual checks of these fits reveal that they should be considered "good" fits. Here again the HV SNe have higher velocities on average before and near maximum brightness, but they appear to have lower velocities than the normal objects after maximum. Like the Si II λ6355 feature, most of the spectroscopically peculiar objects from all subclasses (Ia-91bg, Ia-91T, and Ia-99aa) have lower than average velocities, although there is much scatter in the velocities of the Ia-91bg SNe.

Summary of Velocity Evolution

Within a few days of maximum brightness, the typical velocities of the Ca II features are 12,000–15,000 km s^{-1}, the typical velocities of the Si II and O I features are 10,000-11,000 km s^{-1}, and the typical velocity of the S II feature is ∼9000 km s^{-1}. These differences in velocities support the idea of the layered structure of SN Ia ejecta, with Ca II predominantly found in the outermost (i.e., fastest expanding) layers and O I, Si II, and S II mainly found in the inner (i.e., slower expanding) layers. Ca II shows the largest velocity scatter and is likely well-mixed from the outermost layers into moderately deeper layers of the ejecta. O I, Si II, and S II all show velocity scatter similar to each other (and smaller than that of Ca II), implying that they are probably not as thoroughly mixed throughout the ejecta.

When comparing the velocities of most of the features investigated here, the typical near-

maximum velocity of the normal SNe is in fact lower than that of the HV objects. However, this difference in velocities is relatively small in most cases, and there is significant overlap in the velocities spanned by the normal and HV SNe. By construction, the normal and HV objects have significantly different Si II λ6355 velocities, but even in the other Si II features there is a fair amount of overlap among the two subclasses. Furthermore, in Figure 3.6, there does not appear to be a strong distinction between the normal and HV objects, and thus a sharp cut to define these subclasses does not seem all that well-motivated.

Ia-91bg objects tend to have expansion velocities lower than those of spectroscopically normal SNe, with the Si II λ6355 velocities being the most extreme case, though there is much overlap among the velocities for these subclasses. Ia-91T/99aa objects, on the other hand, are much more complicated. While there is significant scatter in the velocities calculated for these SNe, they are sometimes found to have higher than average velocities (in the Ca II and S II features) and sometimes smaller than average velocities (in the Si II λ6355 and O I features).

Even though we question the idea of two distinct velocity populations of spectroscopically normal SNe Ia, it has been shown that normal and HV objects may have different intrinsic reddening or colors (Wang et al. 2009a; Foley & Kasen 2011). The BSNIP data seem to indicate, however, that instead of two distinct populations with two different intrinsic colors, there is likely a (nearly) continuous distribution of near-maximum velocities which may be *correlated* with intrinsic color (or reddening). This is supported by recent theoretical models and interpretations of these models that explain the existence of normal and HV SNe Ia based on different viewing angles to the SNe (Kasen & Plewa 2007; Kasen et al. 2009; Maeda et al. 2010; Foley & Kasen 2011). Further investigations into these models and the photometric differences between HV and normal-velocity objects will be conducted in future BSNIP studies.

3.5.2 Velocity Gradients

One way to quantify how expansion velocities of SNe Ia evolve with time is to calculate their velocity gradient. Benetti et al. (2005) defined the velocity gradient, $\dot{v} = -\Delta v/\Delta t$, as the "average daily rate of decrease of the expansion velocity" of the Si II λ6355 feature. Note that the BSNIP sample is not the best suited to this kind of study since the average number of spectra per object is relatively low ($\sim$2; Chapter 2). Therefore, the majority of the objects in our dataset have only a single near-maximum spectrum and we do not attempt to determine a velocity gradient for these objects. Despite this limitation, there are still quite a few SNe with multiple spectra in the sample analyzed here for which we can calculate a velocity gradient.

While previous studies have mainly used post-maximum velocities only, for our $\dot{v}$ calculations we utilize velocities from spectra with $t \geq -5$ d. This is reasonable since, as can be seen in Figure 3.6, the velocities of the Si II λ6355 feature decay linearly starting at $t \approx -5$ d, and this allows us to add more SNe to our $\dot{v}$ investigation. The velocity gradient is

calculated using a linear least-squares fit to all the velocities of a given SN Ia measured from spectra with $-5 \leq t \leq 20$ d. For objects with more than two velocities, the uncertainty in $\dot{v}$ is computed from the linear fit. For objects with only two velocities, the uncertainty in $\dot{v}$ is calculated by propagating the uncertainties in the two velocity measurements themselves.

Using the velocity gradient, Benetti et al. (2005) found that their sample of 26 SNe Ia could be divided into three subclasses. The high velocity gradient (HVG) group had the largest velocity gradients ($\dot{v} \gtrsim 70$ km s^{-1} d^{-1}) and consisted of Ia-norm, while the low velocity gradient (LVG) group had the smallest velocity gradients and included Ia-norm as well as Ia-91T/99aa. The third subclass (FAINT) had the lowest expansion velocities, yet moderately large velocity gradients, and consisted of subluminous SNe Ia (i.e., Ia-91bg) with $\Delta m_{15}(B) \gtrsim 1.6$ mag. The same subclasses and criteria for membership are used in the study presented here. Note that the largest velocity gradient presented by Benetti et al. (2005) or Hachinger et al. (2006) is 125 km s^{-1} d^{-1}, while the BSNIP data contain 12 SNe with $\dot{v} \gtrsim 200$ km s^{-1} d^{-1}.

Despite the fact that the BSNIP dataset only averages about two spectra per object, a velocity gradient can be calculated for 61 of the SNe Ia. The computed values of $\dot{v}$ (and their uncertainties), along with the photometric references which are the sources of the Δm_{15} values used to determine whether or not a SN is FAINT, are presented in Table 3.3. The classification (i.e., Type) of each of these objects is also shown in Table 3.3 as well as in the "Benetti Type" column of Table 3.5.

Table 3.3: Velocity Gradients and Interpolated/Extrapolated Velocities

SN Name	Type[a]	LC Ref.[b]	$\dot{v}$[c]	v_0[d]	v_{10}[d]
SN 1989M	HVG	Ganeshalingam et al. (2010)	291.84 (139.49)	13.19 (0.42)	10.27 (0.98)
SN 1991bg†	FAINT	Hicken et al. (2009b)	131.31 (6.44)	10.50 (0.07)	9.19 (0.10)
SN 1994D†	LVG	Hicken et al. (2009b)	33.43 (6.77)	10.60 (0.06)	10.27 (0.09)
SN 1999ac	HVG	Ganeshalingam et al. (2010)	445.41 (49.10)	9.90 (0.13)	5.45 (0.61)
SN 1999cp	LVG	Ganeshalingam et al. (2010)	32.36 (15.43)	10.65 (0.16)	10.32 (0.07)
SN 1999da	FAINT	Ganeshalingam et al. (2010)	131.17 (15.56)	11.05 (0.08)	9.73 (0.14)
SN 1999dq	HVG	Ganeshalingam et al. (2010)	83.64 (20.04)	10.92 (0.07)	10.08 (0.22)
SN 1999gh†	FAINT	Jha et al. (2006b)	46.49 (10.13)	11.21 (0.13)	10.74 (0.17)
SN 2000dk	FAINT	Ganeshalingam et al. (2010)	108.19 (14.04)	11.30 (0.11)	10.21 (0.09)
SN 2000dm	HVG	Ganeshalingam et al. (2010)	97.14 (14.08)	11.28 (0.08)	10.31 (0.12)
SN 2000dn	LVG	Ganeshalingam et al. (2010)	49.24 (7.95)	10.18 (0.09)	9.69 (0.07)
SN 2001bg	HVG*	Ganeshalingam et al. (2010)	228.90 (26.52)	14.56 (0.44)	12.27 (0.18)
SN 2001da	HVG	Ganeshalingam et al. (2010)	88.17 (12.75)	11.50 (0.09)	10.62 (0.10)
SN 2001en	HVG	Ganeshalingam et al. (2010)	103.48 (29.98)	13.31 (0.38)	12.28 (0.10)
SN 2001ep†	HVG	Ganeshalingam et al. (2010)	96.18 (26.92)	10.45 (0.15)	9.49 (0.31)
SN 2002bo	HVG	Ganeshalingam et al. (2010)	245.14 (8.12)	13.61 (0.09)	11.16 (0.07)
SN 2002cd	LVG	Ganeshalingam et al. (2010)	17.91 (8.33)	14.83 (0.11)	14.65 (0.07)
SN 2002de	HVG	Ganeshalingam et al. (2010)	96.88 (15.94)	11.89 (0.09)	10.92 (0.12)
SN 2002eu	HVG?	···	119.97 (14.63)	11.07 (0.10)	9.87 (0.10)
SN 2002ha†	LVG	Ganeshalingam et al. (2010)	15.54 (15.55)	10.90 (0.08)	10.74 (0.18)
SN 2002hd	HVG*	Ganeshalingam et al. (2010)	116.29 (22.08)	11.17 (0.22)	10.01 (0.07)
SN 2002he†	HVG	Ganeshalingam et al. (2010)	81.01 (31.94)	12.57 (0.06)	11.76 (0.33)
SN 2003he	LVG	Ganeshalingam et al. (2010)	14.49 (23.71)	11.39 (0.15)	11.25 (0.12)
SN 2003iv	HVG?	···	98.60 (28.67)	11.42 (0.14)	10.43 (0.18)
SN 2004bl	HVG?	···	70.91 (9.33)	11.01 (0.13)	10.30 (0.07)
SN 2004dt	HVG	Ganeshalingam et al. (2010)	269.45 (8.34)	14.71 (0.11)	12.01 (0.07)

Continued on Next Page...

Table 3.3 — Continued

SN Name	Type[a]	LC Ref.[b]	$\dot{v}$[c]	v_0[d]	v_{10}[d]
SN 2004fu	HVG?	···	211.06 (27.37)	12.36 (0.07)	10.25 (0.29)
SN 2005M	HVG	Ganeshalingam et al. (2010)	86.36 (137.62)	8.77 (1.20)	7.90 (0.19)
SN 2005am	FAINT	Ganeshalingam et al. (2010)	61.11 (72.62)	11.74 (0.40)	11.13 (0.34)
SN 2005bc	LVG	Ganeshalingam et al. (2010)	64.63 (23.70)	11.01 (0.13)	10.37 (0.15)
SN 2005cf	HVG	Ganeshalingam et al. (2010)	106.69 (149.59)	10.14 (0.26)	9.07 (1.74)
SN 2005de	HVG	Ganeshalingam et al. (2010)	70.45 (12.73)	10.86 (0.09)	10.15 (0.10)
SN 2005el	LVG	Ganeshalingam et al. (2010)	13.46 (20.10)	10.95 (0.12)	10.81 (0.13)
SN 2005er	HVG?	···	228.72 (71.21)	10.02 (0.09)	7.73 (0.67)
SN 2005eq	HVG	Ganeshalingam et al. (2010)	76.47 (37.84)	9.58 (0.08)	8.82 (0.43)
SN 2005ki	LVG	Ganeshalingam et al. (2010)	24.19 (20.54)	11.27 (0.12)	11.03 (0.12)
SN 2005ms	HVG	Hicken et al. (2009b)	115.00 (8.36)	10.95 (0.09)	9.80 (0.08)
SN 2005na	HVG	Ganeshalingam et al. (2010)	288.79 (138.17)	10.93 (0.10)	8.04 (1.31)
SN 2006N†	HVG	Hicken et al. (2009b)	84.84 (8.96)	11.20 (0.06)	10.35 (0.11)
SN 2006S†	LVG	Hicken et al. (2009b)	35.46 (6.02)	10.60 (0.07)	10.25 (0.09)
SN 2006bq†	HVG*	Ganeshalingam et al. (2010)	219.70 (15.82)	15.47 (0.20)	13.27 (0.25)
SN 2006bt	HVG	Ganeshalingam et al. (2010)	223.70 (20.34)	11.04 (0.07)	8.80 (0.24)
SN 2006dm	HVG	Ganeshalingam et al. (2010)	131.21 (23.46)	11.49 (0.28)	10.18 (0.08)
SN 2006ej	HVG	Ganeshalingam et al. (2010)	92.24 (15.78)	12.11 (0.07)	11.19 (0.16)
SN 2006et	LVG	Ganeshalingam et al. (2010)	16.07 (23.52)	9.49 (0.16)	9.32 (0.11)
SN 2006eu	HVG	Ganeshalingam et al. (2010)	356.38 (23.54)	14.50 (0.32)	10.94 (0.10)
SN 2006ev	HVG?	···	82.46 (23.77)	12.69 (0.33)	11.86 (0.11)
SN 2006ke	HVG?	···	111.91 (22.80)	9.65 (0.14)	8.53 (0.13)
SN 2006sr	HVG	Hicken et al. (2009b)	152.37 (27.60)	12.03 (0.07)	10.51 (0.28)
SN 2007A	LVG?	···	22.10 (10.87)	10.83 (0.12)	10.61 (0.07)
SN 2007af†	HVG	Ganeshalingam et al. (2010)	72.01 (25.73)	10.91 (0.07)	10.19 (0.27)
SN 2007co†	LVG	Ganeshalingam et al. (2010)	41.96 (10.01)	11.43 (0.06)	11.01 (0.12)
SN 2007fb	LVG?	···	52.78 (10.90)	11.46 (0.11)	10.93 (0.07)
SN 2007gi	HVG?	···	197.68 (20.12)	15.66 (0.09)	13.69 (0.15)
SN 2007gk	HVG?	···	138.74 (6.50)	13.83 (0.09)	12.44 (0.07)
SN 2007hj	FAINT	Ganeshalingam et al. (2010)	133.27 (10.06)	12.26 (0.09)	10.92 (0.08)
SN 2007le†	HVG	Ganeshalingam et al. (2010)	93.35 (12.65)	12.78 (0.18)	11.84 (0.22)
SN 2008dx	FAINT*	Ganeshalingam et al. (2010)	97.91 (28.21)	9.62 (0.15)	8.64 (0.16)
SN 2008ec†	LVG	Ganeshalingam et al. (2010)	68.61 (10.82)	11.01 (0.09)	10.33 (0.14)
SN 2008ei	HVG*	Ganeshalingam et al. (2010)	114.40 (23.97)	15.72 (0.16)	14.57 (0.11)
SN 2008s5[e]	LVG*	Ganeshalingam et al. (2010)	11.86 (17.85)	9.09 (0.11)	8.97 (0.11)

Uncertainties are given in parentheses.
†This object has more than two near-maximum spectra that were used to calculate $\dot{v}$.
[a]Classification based on the velocity gradient of the Si II λ6355 line (Benetti et al. 2005). "HVG" = high velocity gradient; "LVG" = low velocity gradient; "FAINT" = faint/underluminous. Classifications marked with a "?" are uncertain since light-curve shape information is unavailable. Classifications marked with a "*" use the MLCS2k2 Δ parameter (Jha et al. 2007) as a proxy for Δm_{15}.
[b]Source of Δm_{15} (or MLCS2k2 Δ) value.
[c]The velocity gradient is in units of km s^{-1} day^{-1}.
[d]The velocity is calculated from the Si II λ6355 line and is in units of 1000 km s^{-1}.
[e]Also known as SNF20080909-030.

The 11 objects in Table 3.3 that have classifications marked with a "?" are uncertain since light-curve shape information is unavailable, so their classification is based only on their velocity gradient. As we will show below, FAINT objects have similar $\dot{v}$ values to HVG objects, thus some of the HVG? could in fact be part of the FAINT subclass. The 6 SNe in Table 3.3 that have classifications marked with a '*' use the MLCS2k2 Δ parameter (Jha et al. 2007) as a proxy for Δm_{15}.[2]

[2]A SN with $\Delta m_{15} = 1.1$ is defined to have $\Delta = 1$ (Jha et al. 2007), and the relationship between Δm_{15}

Most LVG and FAINT objects are also normal velocity (as opposed to HV) objects and have the lowest velocities observed (specifically in the Si II and Ca II features). This confirms what was observed by Benetti et al. (2005). The HVG subclass contains both normal and HV objects. Many HVG objects have relatively high velocities at early times, but then evolve to have normal to somewhat low velocities by about 10 d past maximum brightness. This confirms what was seen in at least one previous study (Pignata et al. 2008), but differs from what has been seen (and assumed) in other previous work (Benetti et al. 2005; Wang et al. 2009a; Foley & Kasen 2011). In these studies, HVG objects were claimed to have higher velocities than LVG and FAINT objects from before maximum through $t \approx 10$ d. While most HVG SNe start out at high velocities before and near maximum brightness, our data are in agreement with Pignata et al. (2008) and show that they evolve to average (or even relatively low) velocities by only a few days after maximum.

The objects in the BSNIP data with the highest velocity gradients, which have not been seen previously, appear to follow this paradigm of having high velocities before maximum through $t \approx 10$ d. These observations can be explained using the off-center explosion models of Maeda et al. (2010). In their models, different viewing angles will result in a wide range of observed velocities and velocity gradients. Furthermore, before maximum the highest velocity objects have the largest velocity gradients, but the velocities of all of their models become quite similar by 10 d after maximum, much like what is observed in our data. It is also interesting to note that Maeda et al. (2010) have at least one model that we would classify with $\dot{v} \approx 300$–400 km s^{-1} d^{-1}.

In Table 3.4 we present the averages and standard deviations of Δm_{15} and $\dot{v}$ for each subclass (with and without SNe having uncertain classifications due to a lack of photometric data), as well as the number of SNe in each subclass. HVG is the largest group and only a few SNe fall into the FAINT subclass. Comparing these numbers to those of Benetti et al. (2005), we find a similar number of LVG and FAINT objects, but significantly more HVG SNe. These differences are interesting to note, but may not have any physical significance since the sample used by Benetti et al. (2005) contained only well-observed SNe Ia which perhaps biased the sample to contain more peculiar or bright or nearby objects since these have historically been better observed. They also used spectra from a variety of sources which could introduce systematic biases into their analysis, and they measure velocities from their first epoch until the last epoch in which the Si II λ6355 feature is detected. The BSNIP dataset used here consists of an effectively random sample of SNe Ia with spectra having $t < 20$ d obtained using a small number of instruments and reduced by only a few people (see BSNIP I for more on the homogeneity of the BSNIP dataset).

and Δ is roughly linear over most of the range of observed values of Δ (e.g., Hicken et al. 2009b). In addition, many of our objects with a velocity gradient have both Δ and Δm_{15} values known, and using these we are able to confirm which subclass an object belongs to based solely on $\dot{v}$ and Δ.

Table 3.4: Summary of Velocity Gradient Subtypes

Type	Δm_{15} (mag)	$\dot{v}$ (km s^{-1} d^{-1})	v_0 (10^3 km s^{-1})	v_{10} (10^3 km s^{-1})	# of Objects
LVG	1.16 (0.24)	31.37 (18.91)	10.96 (1.30)	10.64 (1.32)	14
LVG + LVG?	···	32.13 (18.59)	10.98 (1.22)	10.66 (1.23)	16
HVG	1.23 (0.22)	156.12 (98.23)	11.98 (1.78)	10.42 (1.75)	29
HVG + HVG?	···	152.30 (89.92)	11.98 (1.78)	10.46 (1.75)	38
FAINT	1.80 (0.13)	101.35 (35.34)	11.10 (0.85)	10.08 (0.93)	7

Average values are shown and standard deviations are given in parentheses.
Average Δm_{15} values are undefined for the rows that include objects with no light-curve shape information.
Note that the average Δm_{15} values do not include the 6 objects that use Δ as a proxy for Δm_{15}.

The average Δm_{15} is about the same for all of the subclasses except FAINT. This is partially by construction since all SNe with $\Delta m_{15} > 1.6$ mag are considered FAINT. However, the fact that LVG and HVG objects all have effectively the same average Δm_{15} value implies that $\dot{v}$ and Δm_{15} are *not* correlated. This has been seen before, and previous similar studies found nearly identical average Δm_{15} values for each subclass (e.g., Benetti et al. 2005).

By construction, the velocity gradients of LVG objects are significantly lower than those of HVG objects. Perhaps somewhat surprisingly, HVG and FAINT SNe have similar values of $\dot{v}$. The average value of $\dot{v}$ for each subclass is effectively unchanged when objects with uncertain classifications are included, implying that the LVG? objects are almost certainly all bona fide LVG SNe. However, it is unclear whether the HVG? are truly HVG or if they are actually part of the FAINT subclass. While the average $\dot{v}$ for the LVG and HVG objects is nearly equal to those from Benetti et al. (2005), the average velocity gradient for the FAINT SNe is somewhat larger in our sample (although they *are* within one standard deviation of each other). Also, the average velocity gradient of the HVG objects is larger than that of Benetti et al. (2005), due to the handful of SNe with significantly larger $\dot{v}$ values than what has been seen previously.

As stated earlier, the BSNIP sample is not the best suited to this kind of study since the average number of spectra per object is relatively low. If we restrict ourselves to only objects with more than two near-maximum spectra (i.e., SNe marked with a "†" in Table 3.3), we are left with 6 HVG objects, 5 LVG objects, and 2 FAINT objects (which used Δ as a proxy for Δm_{15}). One might worry, based on these numbers, that many of our HVG objects are a result of the large uncertainty introduced when calculating the velocity gradient using only two data points. However, the average Δm_{15} and $\dot{v}$ for each subclass is consistent with that of the entire sample when only using objects with more than two spectra. It should be noted that the average velocity gradient for the HVG subclass does decrease when applying this cut and actually becomes smaller than the one calculated by Benetti et al. (2005). Similarly, the FAINT subclass' average $\dot{v}$ becomes approximately equal to the one in Benetti et al. (2005) when only using SNe with more than two spectra. One caveat is that the fact that there are more than two spectra of these objects in the BSNIP dataset may imply that they are particularly interesting objects that are peculiar, intrinsically bright, nearby, or well-separated from their host galaxy. While these may be true and could lead to a bias in this subsample, all of these objects *are* Ia-norm except for one Ia-91bg and one Ia-99aa.

3.5.3 Interpolated/Extrapolated Velocities

Once a velocity gradient is calculated for a SN Ia, one can interpolate/extrapolate that gradient to determine the expansion velocity at a specified epoch. Benetti et al. (2005) defined v_{10} as the expansion velocity of Si II λ6355 at 10 d past maximum brightness. Similarly, Hachinger et al. (2006) interpolate/extrapolate their expansion velocities to the time of maximum brightness (i.e., $t = 0$ d), and so v_0 is defined here as the expansion velocity of Si II λ6355 at maximum brightness. For each SN where $\dot{v}$ is calculated, v_0 and v_{10} are also calculated. The uncertainties of these two velocities are computed by propagating the uncertainties in the linear fit (when more than two spectra are used) or, when only two spectra are used to determine the velocity gradient, by propagating the uncertainties in the two velocity measurements themselves. The computed values of v_0 and v_{10} (and their uncertainties) are presented in Table 3.3, and the averages and standard deviations of these velocities for each subclass are displayed in Table 3.4.

This interpolation/extrapolation calculation allows a more self-consistent comparison of the expansion velocities of different objects. By the sheer fact that we calculate non-zero velocity gradients, the expansion velocities are changing with time and not all of our objects were observed at exactly the same epochs. This procedure also enables us to make more quantitative statements regarding the differences in expansion velocities among various subclasses of SNe Ia.

As expected, at maximum brightness all objects determined to be HV do in fact have $v_0 > 11,800$ km s^{-1} and the opposite is true for objects determined to have normal velocities. This can be seen in the top panel of Figure 3.11, where we plot v_0 versus $\dot{v}$ for all SNe having a measured velocity gradient. All blue points (HV SNe) are to the right of the vertical line at $v_0 = 11,800$ km s^{-1} and all red points (normal velocity SNe) are to the left of it. This sanity check is encouraging and implies that our HV determination (as outlined in Section 3.5.1) is relatively robust at maximum brightness.

While there does not appear to be a strong correlation between $\dot{v}$ and v_0, it does at least seem that, on average, objects with larger velocity gradients tend to have larger velocities at maximum light, though there are plenty of SNe Ia that do not follow this correlation. The solid line in Figure 3.11 is a linear least-squares fit to the "moderate decliners" (i.e., $1 < \Delta m_{15} < 1.5$ mag, whose data points are circled in the Figure) of the form

$$\dot{v} = \alpha v_0 + \beta. \tag{3.2}$$

We calculate $\alpha = 55.0 \pm 1.8$ and $\beta = -539 \pm 22$ for v_0 in units of 10^3 km s^{-1} and $\dot{v}$ in units of km s^{-1} d^{-1}. Foley et al. (2011) fit a similar relationship to their data in order to derive a family of functions. This allows them to calculate a velocity of the Si II λ6355 feature at maximum brightness given a spectral age and velocity at that age. They find $\alpha = 32.2$ and $\beta = -285$, which are both significantly different than what is calculated for the BSNIP data. The large amount of scatter around the solid line in Figure 3.11 casts doubt on how useful the family of functions proposed by Foley et al. (2011) can actually be in calculating velocities at maximum brightness.

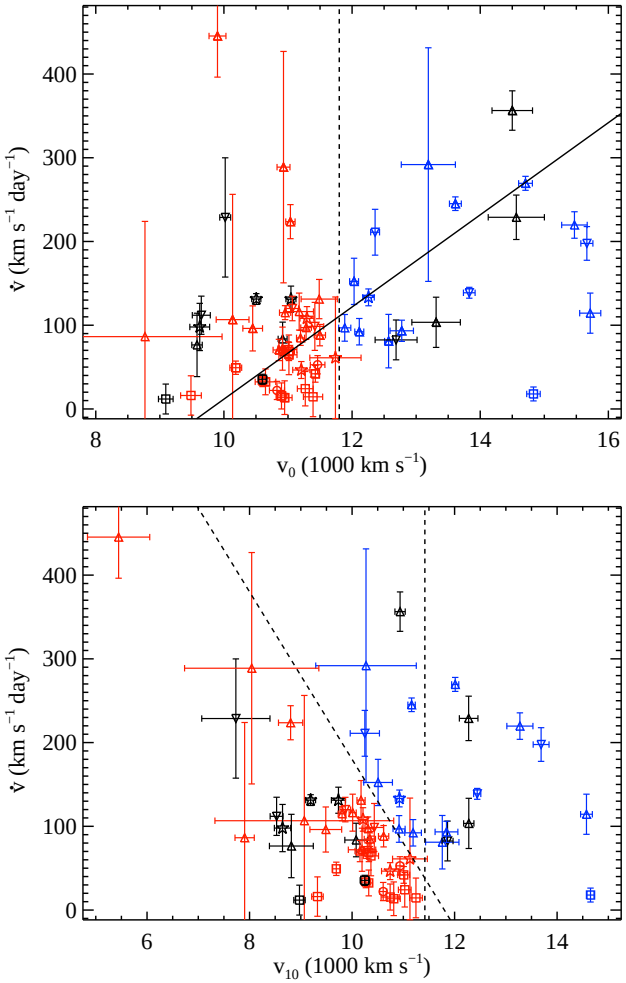

Figure 3.11: v_0 versus $\dot{v}$ (*top*) and v_{10} versus $\dot{v}$ (*bottom*) for all SNe where we calculate a velocity gradient. Blue points are HV objects, red points are normal-velocity objects, and black points are objects for which we could not determine whether the SN was normal or high velocity (see Section 3.5.1 for further details regarding how HV SNe are defined). Squares are low velocity gradient (LVG) objects, circles are possible LVG objects, stars are FAINT objects, upward-pointing triangles are high velocity gradient (HVG) objects, and downward-pointing triangles are possible HVG objects (see Section 3.5.2 for further details regarding how these subclasses are defined). The vertical dashed line in the top panel is our HV cutoff ($v_0 = 11,800$ km s^{-1}). The solid line is a linear fit to the "moderate decliners" ($1 < \Delta m_{15} < 1.5$ mag, whose data points are circled). The vertical dashed line in the bottom panel is our HV cutoff at $t = 0$ d (11,8000 km s^{-1}) decreased by the average velocity gradient for the normal-velocity SNe (38 km s^{-1} d^{-1}) for 10 d (i.e., $v_{10} = 11,420$ km s^{-1}= $11,800 - 10 \times 38$). The slanted dashed line in the bottom panel is our HV cutoff at $t = 10$ d *as a function of* $\dot{v}$ (i.e., $v_{10} = 11,8000 - 10 \times \dot{v}$).

In Figure 3.12 we plot histograms of v_0 values coded by "Benetti type" for secure classifications (*top*) and all objects (*bottom*). As seen in both panels of Figure 3.12, the majority of LVG and FAINT objects have low values of v_0, and the HVG objects fall mainly toward the middle and extend to high v_0 values. This is a graphical way of presenting what is shown in the fourth column of Table 3.4, namely that the average v_0 for LVG and FAINT SNe is lower than the average v_0 for HVG SNe.

Somewhat surprising, however, is the wide range of v_0 values spanned by each of the subclasses. Even at maximum brightness, where the difference between HV and normal objects is defined, a HVG SN may have normal (or even relatively low) velocity. This is contrary to many previous studies that often assume a one-to-one correlation between HV and HVG and, similarly, between normal velocities and LVG (e.g., Hachinger et al. 2006; Pignata et al. 2008; Wang et al. 2009a). Kolmogorov–Smirnov tests were performed on the v_0 values of LVG and HVG SNe (both including and excluding objects with uncertain classifications) and we find that they likely come from different parent populations ($p \approx 0.03$). Thus, it is still reasonable to associate LVG SNe with normal velocities at maximum and HVG SNe with HV objects, but we caution that this may not be as robust an association as was previously thought.

The connection between HVG and HV is even more tenuous by 10 d after maximum brightness. In the bottom panel of Figure 3.11 we velocity gradient. The vertical line is our HV cutoff value at $t = 0$ d (11,8000 km s^{-1}) decreased by the average velocity gradient for the normal-velocity SNe (38 km s^{-1} d^{-1}) for 10 d (i.e., $v_{10} = 11,420$ km s^{-1}= $11,800 - 10 \times 38$). Naively, if one measured $v_{10} \lesssim 11420$ km s^{-1} for a given SN, they might classify it as a normal velocity object. However, about half of our HV SNe fall in this regime. This is actually expected since our HV definition only included velocities within 5 d of maximum, so extrapolating this analysis to 10 d past maximum may not be valid. If we instead plot our HV cutoff at $t = 10$ d *as a function of* $\dot{v}$ (i.e., $v_{10} = 11,8000 - 10 \times \dot{v}$), then we get the slanted line in the bottom panel of Figure 3.11. Now, the HV SNe all fall above this line while the normal-velocity objects are all below it. Effectively, some of the HVG objects have decreased their velocity fast enough to "catch up" with the velocities of the normal-velocity objects by this epoch. By 10 d past maximum brightness, a single velocity measurement alone is not sufficient to determine whether an objects should be considered HV or not.

Another way of looking at this is in Figure 3.13, where all four velocity gradient subclasses span nearly the full range of v_{10} values. Once again this is a graphical way of presenting what is seen in the fifth column of Table 3.4: the average v_{10} is effectively the same for all subclasses. Kolmogorov–Smirnov tests were performed on the v_{10} values of LVG and HVG (both including and excluding objects with uncertain classifications), and we find no evidence that they come from different parent populations. Thus, by 10 d past maximum brightness the distribution of expansion velocities among LVG and HVG objects are consistent with each other.

As mentioned in Section 3.5.2, the off-center explosion models of Maeda et al. (2010) may naturally explain the existence of HVG SNe. They also show that models with the

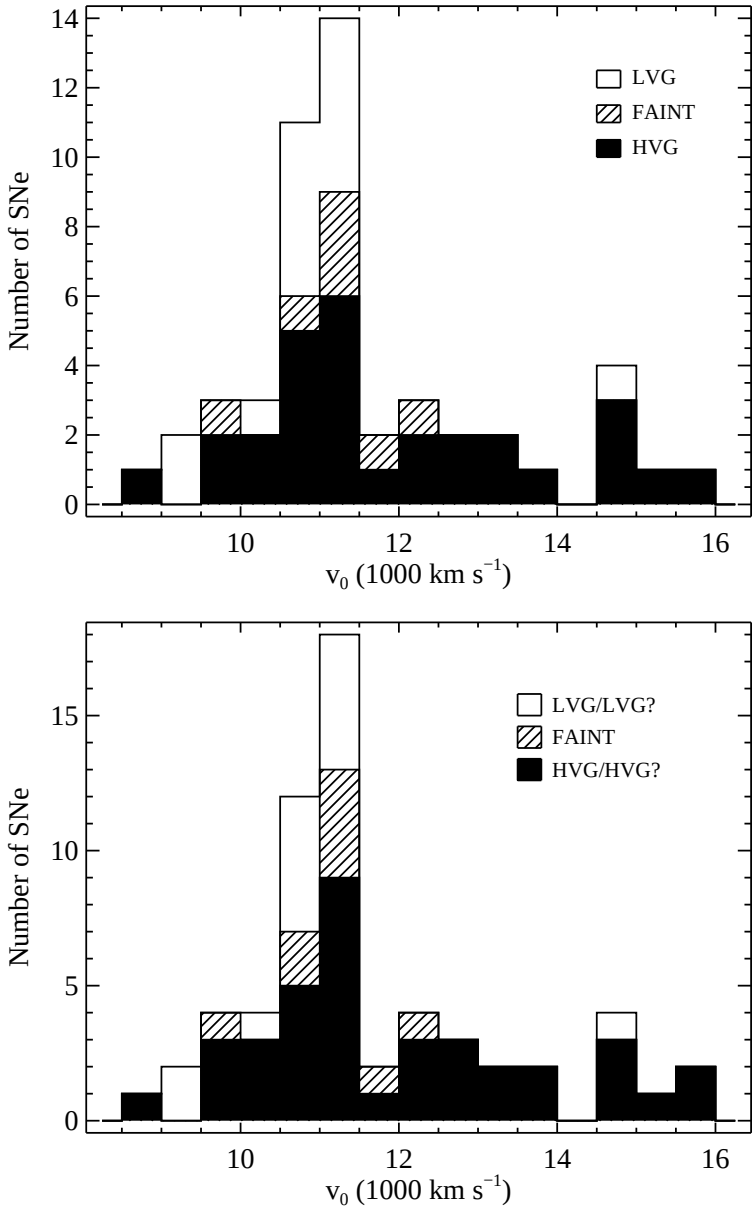

Figure 3.12: Histograms of v_0 for all SNe where we calculate a velocity gradient, separated by subclass, excluding uncertain classifications due to a lack of photometric information (*top*) and including uncertain classifications (*bottom*).

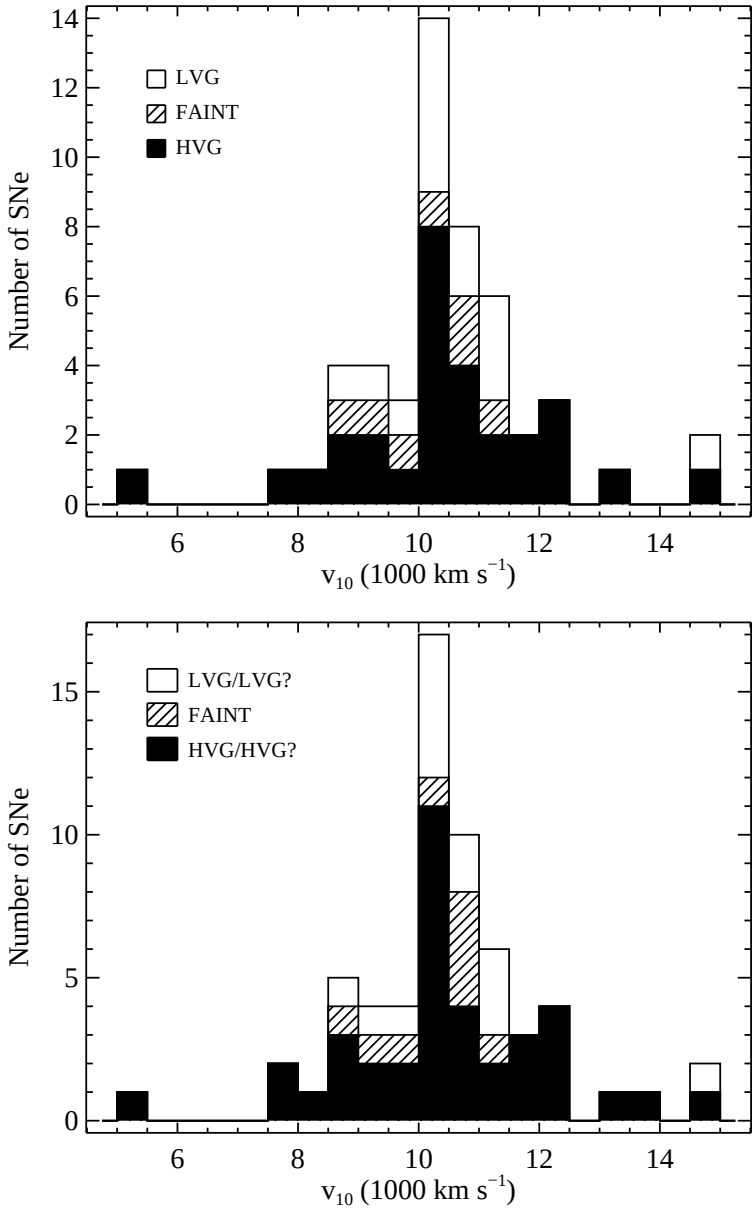

Figure 3.13: Histograms of v_{10} for all SNe where we calculate a velocity gradient, separated by subclass, excluding uncertain classifications due to a lack of photometric information (*top*) and including uncertain classifications (*bottom*).

largest velocity gradients have the highest velocities near maximum brightness, but by about 10 d after maximum the expansion velocities of almost all of their models become quite similar (independent of initial velocities or velocity gradients). These models seem to have observational grounding in the data we present here. Further comparisons to the models and predictions of Maeda et al. (2010), especially at later epochs, will be made in future BSNIP chapters. Also, the velocity gradients, classifications, and interpolated/extrapolated velocities discussed here will be compared to photometric properties (such as light-curve shape and decline rate) in BSNIP III.

3.5.4 Temporal Evolution of Pseudo-Equivalent Widths

As with expansion velocities of SNe Ia, much work has been done previously on studying the (pseudo-)equivalent widths of various spectral features as they change in time (e.g., Folatelli 2004; Garavini et al. 2007; Bronder et al. 2008; Walker et al. 2011; Nordin et al. 2011b; Konishi et al. 2011). The temporal evolution of the pEW for each of the nine spectral features is shown in Figures 3.14–3.17 and Figures 3.19–3.23. The color of each data point represents its "Wang type" (see Section 3.5.1) while the shape of each data point represents its spectroscopic subtype (as determined by SNID, see BSNIP I). The "SNID type" is displayed rather than the "Benetti type" (see Section 3.5.2) in the pEW figures because the velocity gradient of an object does not appear to be well-correlated with its pEW measurements.

Also shown in Figures 3.14–3.17 and Figures 3.19–3.23 are fits to the pEW evolution for each spectral feature (solid line) along with the standard error of the fit (gray region), using *only* Ia-norm (with normal velocities). For features whose pEW appears to evolve linearly with time a linear function is fit to the data, while features whose pEW have a sharp change in their temporal evolution have a quadratic function fit to them. This differs from previous studies which have modeled the behavior of pEWs with time either using cubic splines (e.g., Garavini et al. 2007) or logistic functions instead of quadratic ones (Nordin et al. 2011b). As seen in the figures, the pEW temporal evolution for each spectral feature can be fit relatively well with either a linear or quadratic function. Experiments with fitting the pEW evolution with cubic splines and logistic functions were carried out, but the fits were either worse or comparable to the linear and quadratic functions (which have fewer free parameters).

Following Nordin et al. (2011b), we use our fits of the temporal evolution of the pEW for each spectral feature to attempt to "remove" the age dependence of the pEW. To do this, an epoch-independent quantity called the "pEW difference" (ΔpEW) is defined; it is simply the measured pEW minus the expected pEW at the same epoch using the linear or quadratic fit. The uncertainty in ΔpEW comes from combining the uncertainty of the pEW measurement with the standard error of the fit. The ΔpEW values and their uncertainties can be found in Tables 3.6–3.14. Note that while the fits were defined using only Ia-norm, ΔpEW values are calculated for SNe of all spectral types.

Ca II

The Ca II H&K feature and the Ca II near-IR triplet show a cluster of spectra with relatively large pEW at $t < -5$ d in Figures 3.14 and 3.15. This is perhaps due to detached, high-velocity absorption blending with the normal-velocity component (e.g., Branch et al. 2005). For $t \gtrsim -5$ d, the pEW of the Ca II H&K feature decreases slightly and the scatter in the pEW values decreases markedly near $t \gtrsim 10$ d. This feature is fit with a quadratic in order to encompass the relatively large number of objects with high pEW values at the earliest times as well as the decrease and eventual flattening out at later times. It is interesting to note that the typical pEW for the HV objects is larger than that of the normal-velocity objects (for $t \lesssim 10$ d).

Despite the fact that there are not that many spectroscopically peculiar objects plotted in Figure 3.14, it seems that Ia-91bg follow the evolution of the Ia-norm objects while Ia-91T/99aa are below the typical pEW values (and thus have negative values of ΔpEW). This matches what has been observed previously in other low-redshift datasets (Garavini et al. 2007; Bronder et al. 2008).

On the other hand, the Ca II near-IR triplet pEW values increase linearly with time after about 5 d before maximum (which is why the evolution of this feature is fit with a linear function). Also distinct from the Ca II H&K feature, the typical pEW of the HV and normal objects is about the same. While the Ia-91T/99aa objects are certainly below the normal pEW values, the Ia-91bg objects have pEWs that are well above the normal evolution. Once again, this has been noted previously, though the few large pEW values at early times have not been seen and our sample has far more data points than earlier work (Folatelli 2004).

Si II

The pEW of the Si II λ6355 feature (Figure 3.16) linearly increases with time before $t \approx 10$ d and shows a hint of a sharp upturn after this (however, this is likely due to the feature becoming blended with Si II λ5972 at these later epochs). Also, before $\sim$10 d past maximum the HV objects have a larger typical pEW than the normal-velocity objects. Like the Ca II H&K feature, the Ia-91T/99aa objects fall well below the normal evolution while the Ia-91bg span a large range of pEW values (from well below to well above the average evolution). This behavior is similar to that seen in the low-z (and moderate-z) samples of Folatelli (2004) and Konishi et al. (2011).

The temporal evolution of the pEWs of the Si II λ4000 feature (Figure 3.17) is quite unique. There is evidence for two distinct evolutionary tracks: one rising until 2–3 d past maximum and then declining, and one constant (and lower) until 2–3 d past maximum and then rising. The two groups are effectively blended into one another by $\sim$5 d past maximum. This creates a gap at relatively low values of pEW from a few days before maximum until a few days after maximum. The two-component evolution has been seen in other datasets, but the gap in the present sample is not nearly as pronounced as in some of the earlier studies which used many fewer data points (Folatelli 2004; Bronder et al. 2008).

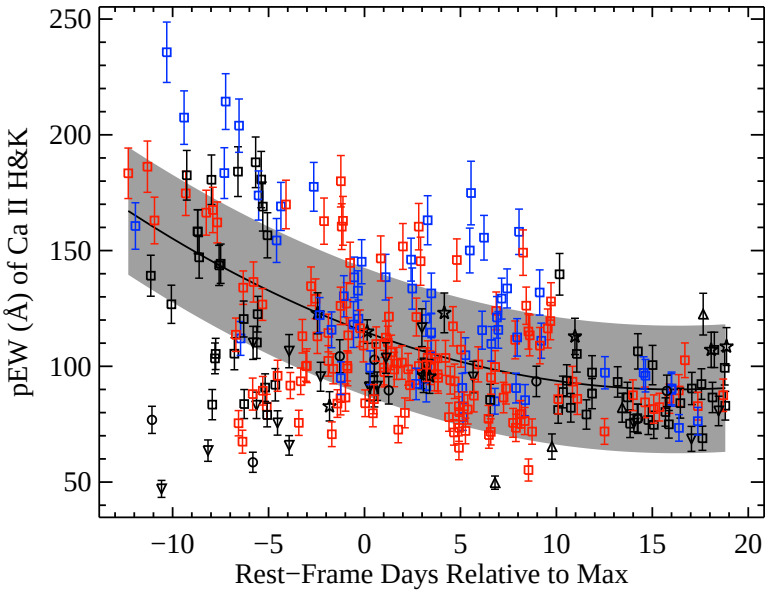

Figure 3.14: The pEW of Ca II H&K versus rest-frame age relative to maximum brightness of 281 spectra of 191 SNe. Colors and shapes of data points are the same as in Figure 3.4. The solid curve is a quadratic fit to the data using *only* Ia-norm; the gray region is the standard error of the fit.

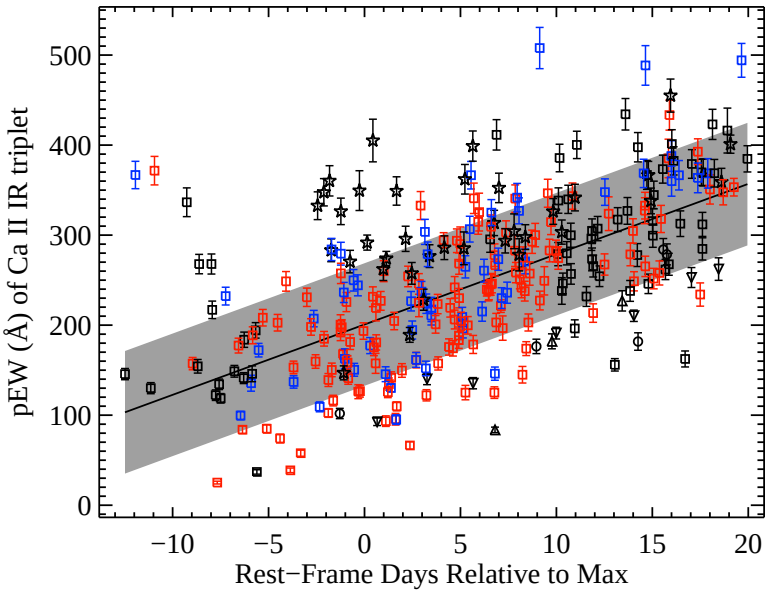

Figure 3.15: The pEW of the Ca II near-IR triplet versus rest-frame age relative to maximum brightness of 301 spectra of 201 SNe. Colors and shapes of data points are the same as in Figure 3.4. The solid line is a linear fit to the data using *only* Ia-norm; the gray region is the standard error of the fit.

There is no significant difference in pEW of the Si II λ4000 feature between HV and normal-velocity objects, though almost all of the HV objects are found in the "upper evolutionary track." While there are only a small number of Ia-91bg objects for which we measure a pEW for the Si II λ4000 feature, they also fall well within the "upper evolutionary track." The Ia-91T/99aa SNe are found *only* in the "lower evolutionary track." Note that Ia-norm objects are found in both tracks.

The ΔpEW values of the Si II λ4000 have been found to correlate with SN color as well as velocity gradient (Nordin et al. 2011a). In BSNIP III the relationship between both ΔpEW and pEW and SN color for this feature will be investigated. In Figure 3.18 we plot ΔpEW of Si II λ4000 against $-\dot{v}$ (the minus sign is used here in order to match the velocity gradient definition of Nordin et al. 2011a) for all objects with $0 \leq t \leq 8$ d. Our plot contains 31 SNe Ia as compared to the 20 objects shown in Figure 3 of Nordin et al. (2011a), and we also follow their convention of taking the mean ΔpEW value for objects with multiple spectra in the epoch range studied.

The basic trends seen in Figure 3.18 are unchanged if we use pEW instead of ΔpEW, and are similar to what was observed by Nordin et al. (2011a). The biggest difference between the two studies is that Nordin et al. (2011a) use only spectroscopically normal SNe (thus they would not have the four black points in the bottom-right of Figure 3.18), and they do not see the most extreme HVG objects which appear in our dataset (i.e., the two left-most points in Figure 3.18). Nordin et al. (2011a) claim a "strong correlation" between ΔpEW values of Si II λ4000 and velocity gradient (quoting a Spearman rank coefficient of -0.73). A fit to the BSNIP data (excluding the 6 aforementioned outlier objects which are ignored or not seen in their sample) yields a Spearman rank coefficient of -0.54, which implies that the supposed correlation may not actually be all that significant.

There is a relatively large scatter in the pEW values measured for the Si II λ5972 feature (Figure 3.19). Evidence suggests that the pEW values are trending slightly upward with time; however, this is driven mainly by points at $t \gtrsim 5$ d where we might expect the Si II λ5972 feature to start blending with the Na I D line which can appear in SN Ia spectra near this epoch (e.g., Branch et al. 2005). Ignoring points at $t > 5$ d, the temporal evolution is relatively constant, although the HV objects are perhaps decreasing slightly with time. Once again, the Ia-91T/99aa objects have relatively small pEW values while the Ia-91bg SNe lie well above the average evolution. This matches the trends seen in the low-z data presented by Folatelli (2004) and Konishi et al. (2011).

Mg II

The temporal evolution of the pEW of the Mg II complex (Figure 3.20) has relatively small scatter and linearly increases slightly with time. The HV objects have larger pEW values (and more scatter) than the normal-velocity objects. Interestingly, this evolution is markedly different from what has been seen in some other low-z samples (Folatelli 2004; Garavini et al. 2007). While the BSNIP data match these previous studies until $t \approx 10$ d,

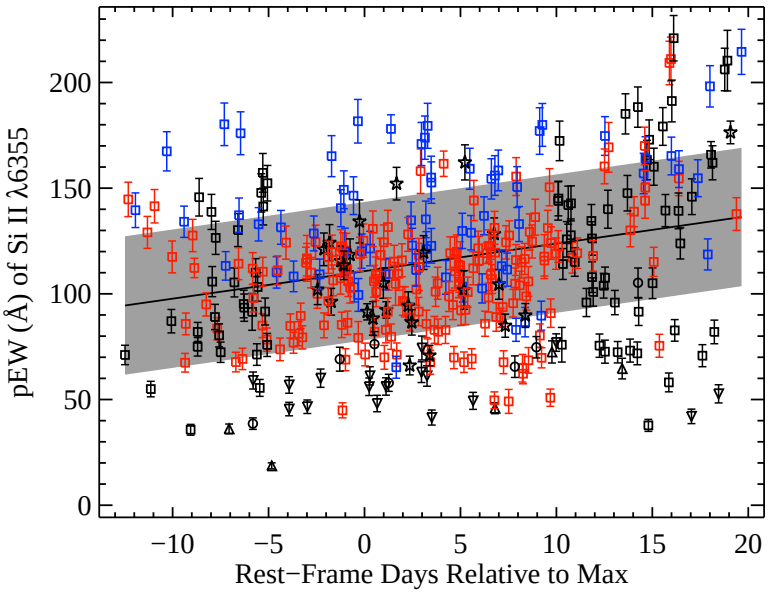

Figure 3.16: The pEW of Si II λ6355 versus rest-frame age relative to maximum brightness of 366 spectra of 239 SNe. Colors and shapes of data points are the same as in Figure 3.4. The solid line is a linear fit to the data using *only* Ia-norm; the gray region is the standard error of the fit.

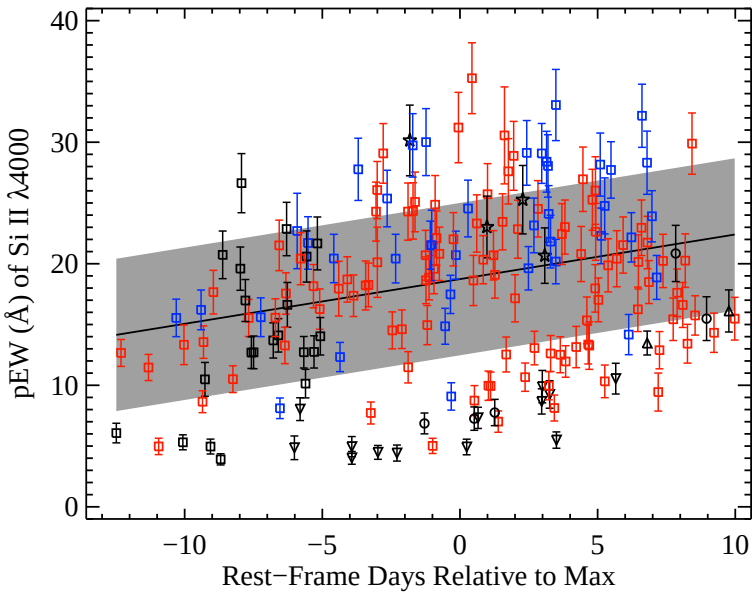

Figure 3.17: The pEW of Si II λ4000 versus rest-frame age relative to maximum brightness of 188 spectra of 137 SNe. Colors and shapes of data points are the same as in Figure 3.4. The solid line is a linear fit to the data using *only* Ia-norm; the gray region is the standard error of the fit.

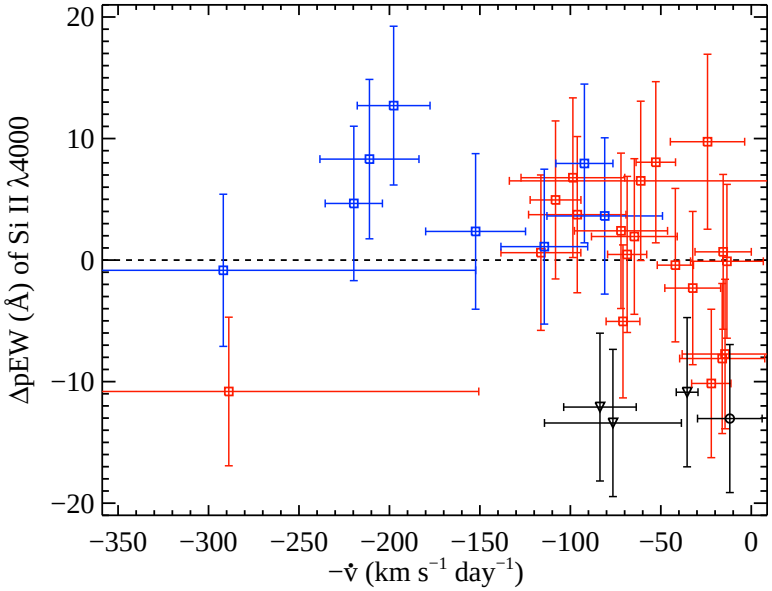

Figure 3.18: The ΔpEW of Si II λ4000 versus $-\dot{v}$ (the minus sign is used here in order to match the velocity-gradient definition of Nordin et al. 2011a) for all 31 objects with $0 \leq t \leq 8$ d. Colors and shapes of data points are the same as in Figure 3.4.

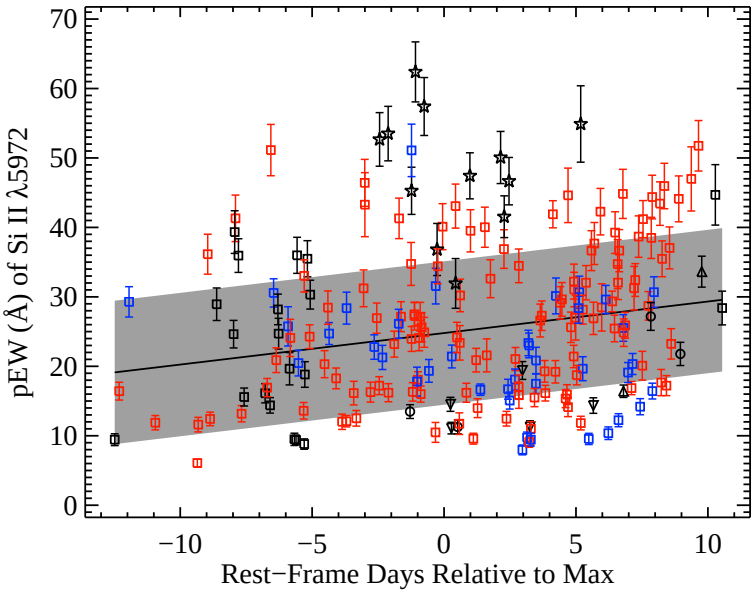

Figure 3.19: The pEW of Si II λ5972 versus rest-frame age relative to maximum brightness of 204 spectra of 156 SNe. Colors and shapes of data points are the same as in Figure 3.4. The solid line is a linear fit to the data using *only* Ia-norm; the gray region is the standard error of the fit.

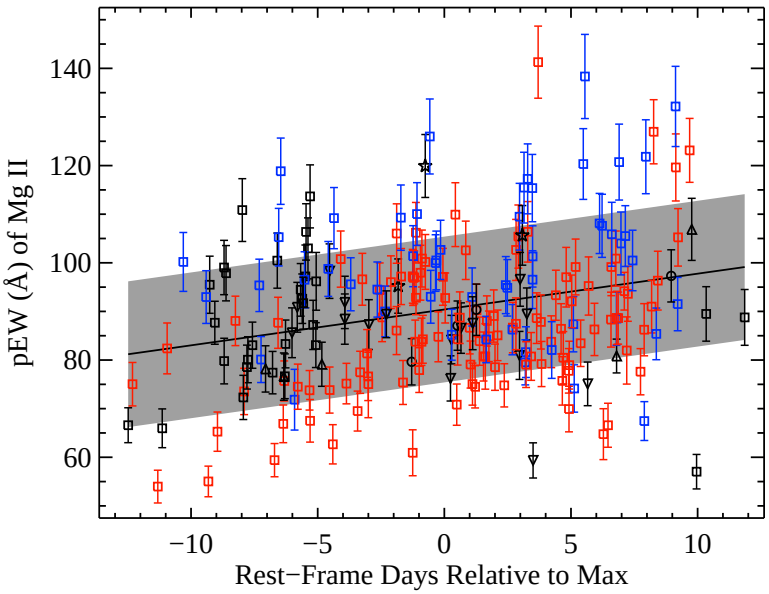

Figure 3.20: The pEW of the Mg II complex versus rest-frame age relative to maximum brightness of 219 spectra of 163 SNe. Colors and shapes of data points are the same as in Figure 3.4. The solid line is a linear fit to the data using *only* Ia-norm; the gray region is the standard error of the fit.

there is no evidence for the sudden increase in pEW values for this feature. In fact, no attempt is made to measure the pEW of the Mg II complex beyond $t \approx 10$ d because it becomes too blended with the Si II λ4000 feature (as pointed out by Garavini et al. 2007). Folatelli (2004) simply define a larger wavelength range at these epochs (see their Fig. 1, feature 3) which will certainly increase the measured pEW. Our temporal evolution does, however, match what was seen by Walker et al. (2011).

The Ia-91T/99aa objects are yet again found to have lower than average pEW values, though not too low. On the other hand, the Ia-91bg objects have somewhat higher than average pEW values, but there are very few of these types of objects for which a pEW is successfully measured. This is due to the fact that when the Mg II complex is strong before and near maximum brightness, as it often is for Ia-91bg SNe due to additional absorption from Ti II (e.g., Bronder et al. 2008), it becomes severely blended with Si II λ4000, and thus no attempt is made to measure its pEW. This is further supported by the fact that we see no objects with pEW of Mg II $\gtrsim$140 Å, while data in Garavini et al. (2007) and the low-z sample presented by Bronder et al. (2008) contain several objects with such large pEW values.

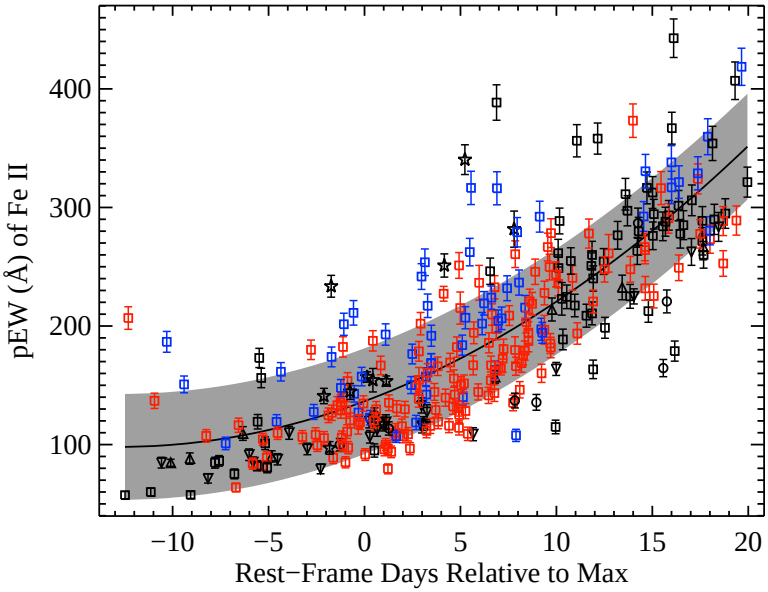

Figure 3.21: The pEW of the Fe II complex versus rest-frame age relative to maximum brightness of 313 spectra of 217 SNe. Colors and shapes of data points are the same as in Figure 3.4. The solid curve is a quadratic fit to the data using *only* Ia-norm; the gray region is the standard error of the fit.

Fe II

While the Mg II complex has a fairly tight linear pEW evolution, the pEW of the Fe II complex (Figure 3.21) shows an extremely tight temporal evolution which is almost certainly nonlinear (thus we fit it with a quadratic function). Another difference between these two features is that the Mg II complex pEW values are nearly constant for $-10 \lesssim t \lesssim 10$ d (increasing by < 20 Å over that range) while the Fe II complex pEWs increase dramatically during the same span of time ($\sim$130 Å). Despite these differences, the data for both the Mg II and Fe II complexes fall almost completely within the standard error of their respective fits. Furthermore, the HV objects in both features have larger pEW values, as well as more scatter, than the normal-velocity objects.

As with the pEWs of the Mg II feature, the Ia-91T/99aa objects are all below the fit to the Ia-norm. It is even more apparent for the Fe II complex than it was for the Mg II complex that the Ia-91bg objects are all found above the fit to the data. These differences, as well as the overall trends, have been recognized in numerous previous studies of both low-z and moderate-z SNe Ia (e.g., Folatelli 2004; Garavini et al. 2007; Nordin et al. 2011b; Konishi et al. 2011).

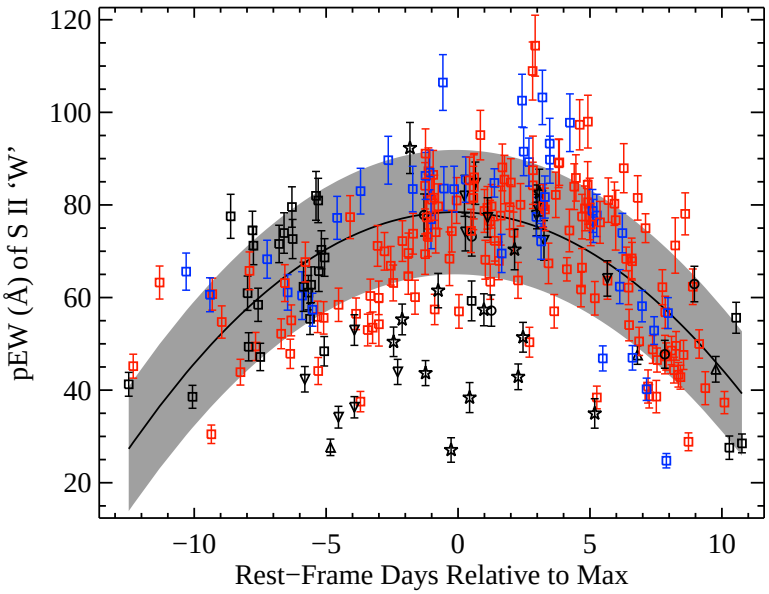

Figure 3.22: The pEW of the S II "W" versus rest-frame age relative to maximum brightness of 240 spectra of 179 SNe. Colors and shapes of data points are the same as in Figure 3.4. The solid curve is a quadratic fit to the data using *only* Ia-norm; the gray region is the standard error of the fit.

S II

The temporal evolution of the pEW values for the S II "W" feature (Figure 3.22) is unique. The pEW of the majority of objects increases until maximum brightness and then decreases in a nearly symmetric way. A quadratic function centered near $t = 0$ d fits the data (especially the Ia-norm objects) very well. There is a possibility that the HV objects have higher pEW values before maximum (with equal pEW values after maximum), but the significance of this difference is relatively low. The Ia-91T/99aa objects have even lower pEW values than the normal-velocity objects before maximum, though they also seem to evolve to more average values after maximum brightness. The Ia-91bg objects, on the other hand, are almost all significantly below the average evolution at all epochs (though there are a few with relatively normal pEWs). The temporal evolution seen here confirms what was found by Nordin et al. (2011b) and Konishi et al. (2011) in their low-z and moderate-z data.

O I

The O I triplet's average pEW values evolve in much the same way as those of the S II "W" with the normal pEW values rising until ∼4 d past maximum and then declining. There is a hint that the HV objects might have smaller pEW values than the normal-velocity objects, though the scatter in both of these subclasses is quite large. As mentioned

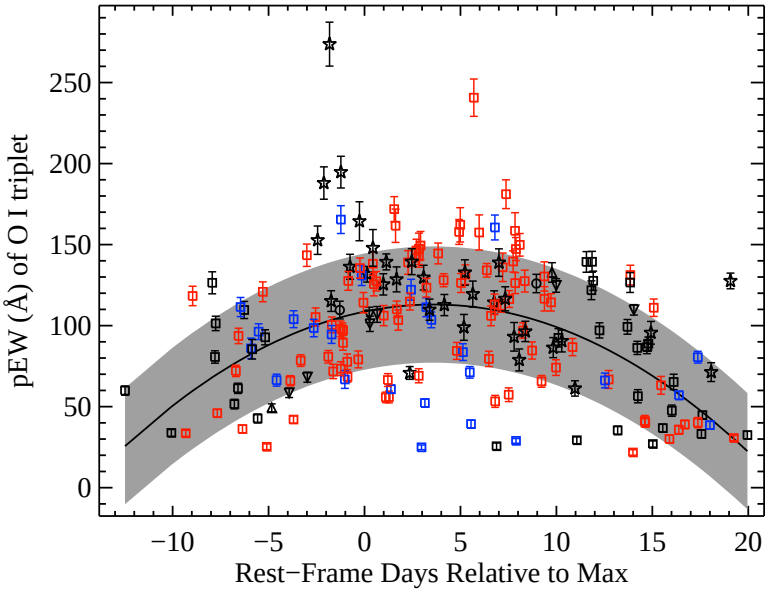

Figure 3.23: The pEW of the O I triplet versus rest-frame age relative to maximum brightness of 192 spectra of 139 SNe. Colors and shapes of data points are the same as in Figure 3.4. The solid curve is a quadratic fit to the data using *only* Ia-norm; the gray region is the standard error of the fit.

in Section 3.4.1, this feature is often strongly affected by telluric absorption, and thus some of the points which lie significantly away from the average evolution could be explained by imperfect telluric absorption corrections. This could also explain why we are able to measure pEWs of the O I triplet for relatively few Ia-91T/99aa objects. As was see in the Ca II features, the Ia-91T/99aa SNe have relatively low pEW values, and if their O I triplet pEWs are also small, then the feature could get "lost in the noise" after an inaccurate telluric absorption correction. The Ia-91bg objects, however, have large pEW values for $t \lesssim 2$ d, but quickly decrease to more average values at later epochs.

Summary of pEW Evolution

As mentioned above, we chose to present the "SNID type" rather than the "Benetti type" in the pEW versus time figures because the velocity gradient of an object is not well-correlated with any pEW measurements. The one species with a possible correlation is Si II. In all three of its features, while the LVG and HVG objects show very little difference in pEW values, there is an indication that the pEWs of the FAINT objects are larger than the average values at each epoch. This is unsurprising since the Ia-91bg objects also have larger-than-average pEW values for the Si II λ4000 and Si II λ5972 features, and these SNe are also often underluminous (which is exactly how the FAINT subclass is defined).

When comparing the pEW values of normal and HV objects, for most of the features investigated here the typical pEWs of the HV SNe are larger than those of the normal-velocity objects. The HV SNe also tend to have more scatter in their pEW values. These two points are most noticeable in the Ca II H&K, Mg II, Fe II, and Si II λ6355 features. However, some of the features do show very similar pEW values between HV and normal-velocity objects, and the O I triplet's typical pEW for HV SNe is perhaps *smaller* than that of normal-velocity objects. By $t \approx 10$ d the average pEW values of HV and normal-velocity SNe are nearly equal in almost all of the spectral features measured.

The velocity of the Si II λ6355 feature is used to differentiate between HV and normal objects, so it may be unsurprising that the pEW of this same feature shows a marked split between these two subclasses. Somewhat more interesting is the fact that the other three features which exhibit a strong split in pEW between HV and normal-velocity objects are three of the four *bluest* features we measure (Ca II H&K, Mg II, and Fe II).[3] HV SNe may have different intrinsic colors which could be caused by line blanketing due to their relatively large velocities, especially at the shortest optical wavelengths (Foley & Kasen 2011). This is exactly where the greatest pEW difference between HV and normal-velocity SNe is observed. An alternative, yet related, explanation for increased pEWs for HV objects at the blue end of the optical regime is that a change in metallicity can alter the effective optical depth at these wavelengths, especially for IGEs such as Fe and Mg (Domínguez et al. 2001; Timmes et al. 2003). This may hint at a possible correlation between expansion velocity and pEW (at least for the four spectral features mentioned), and we investigate this possibility further in Section 3.5.8. Correlations between the pEWs of HV and normal-velocity SNe and their intrinsic colors (and reddening) as well as host-galaxy metallicities will be investigated in future BSNIP studies.

Ia-91T/99aa objects consistently have the lowest pEW (and ΔpEW) values at all epochs of any of the SN Ia spectral subtypes, with the exception of the S II "W" where they are the lowest for $t < 0$ d but increase to more average values after maximum. This generic trend of Ia-91T/99aa objects having small pEWs has been seen before (e.g., Folatelli 2004; Bronder et al. 2008). The relative weakness of the spectral features in these SNe can be attributed to the fact that they tend to be overluminous and have higher inferred temperatures (e.g., Nugent et al. 1995).

On the other hand, the Ia-91bg SNe usually have the largest pEWs (and ΔpEWs) at all epochs (though the S II "W" feature is again the exception in that the Ia-91bg SNe have *below average* pEW values at all epochs). This basic trend is most readily explained (partially) by a temperature effect since Ia-91bg object are usually underluminous and often found to be cooler than Ia-norm and Ia-91T/99aa SNe (e.g., Nugent et al. 1995). As mentioned above, there is often evidence for Ti II absorption in Ia-91bg objects which will blend with what has been defined here as the Mg II complex. However, when Mg II is observed to be

[3]The second bluest feature we measure, Si II λ4000, is relatively weak and has a large scatter in pEW values (perhaps even showing evidence for two separate evolutionary tracks). Thus, it is reasonable that the difference between HV and normal-velocity objects is difficult to observe in the pEW values of this feature.

this strong, it is often also blended with the Si II λ4000 feature and a pEW would not be measured for that spectrum. This explains the low number of Ia-91bg objects for which a pEW is measured for Mg II. Comparisons of spectroscopic subtypes and their pEW values to light-curve shapes and luminosities will be undertaken in BSNIP III.

3.5.5 Spectral Classification Using Pseudo-Equivalent Widths

The differences among the various spectroscopic subtypes can be more quantitatively investigated by directly comparing pEW values of different spectral features. Branch et al. (2006) presented a means of spectroscopically classifying SNe Ia using near-maximum ($-3 \leq t \leq 3$ d) pEWs of Si II λ6355 and Si II λ5972 ($W(6100)$ and $W(5750)$ in their notation, respectively). This original sample has since been updated by Branch et al. (2009). Based on their EW measurements they split their sample into four distinct groups: core normal (CN), broad line (BL), cool (CL), and shallow silicon (SS). However, they point out that the SNe seem to have a continuous distribution of pEW values and so how the exact boundaries are defined is not critical.

The pEW values we measure for Si II λ6355 and Si II λ5972 for $-5 \leq t \leq 5$ d, along with the boundaries from Branch et al. (2009) and the median pEW value for each feature, are shown in Figure 3.24. The color of each data point represents its "Wang type" (see Section 3.5.1) while the shape of each data point represents its "SNID type." The median uncertainty in both directions is shown in the upper-right corner of the figure. Our plot of 89 SNe Ia covers a parameter space similar to that of the 59 SNe Ia plotted in Figure 2 of Branch et al. (2009), and ten of the eleven SNe in both datasets are classified as the same subclass (the lone disagreement is SN 1999ac, which is a borderline case between CN and SS). Classifications for the SNe shown in Figure 3.24 can be found in Table 3.5 in the "Branch Type" column.

A slightly larger range of spectral ages than what was used by Branch et al. (2009) is adopted here in order to increase the number of objects studied. The classifications and general trends seen when using only spectra within 3 d of maximum brightness are preserved when spectra within 5 d of maximum are used. Conversely, if a larger range of ages is used, the pEWs of the Si II λ5972 and Si II λ5972 features begin to evolve noticeably. The trends seen in Figure 3.24 are also seen at similar levels when plotting ΔpEW values (instead of pEW values), but by definition ΔpEW relies on a fit to the measurements as opposed to the measurements themselves. Finally, when the BSNIP dataset contains multiple spectra of a given object within 5 d of maximum, only the spectrum nearest maximum brightness is used. This also has little to no effect on the classification of any SNe, nor on the trends seen in Figure 3.24.

One distinction between the two studies is that the BSNIP sample is lacking some of the most extreme members of the SS subclass. Most of these objects are the extremely peculiar SN 2000cx and SN 2002cx-like objects which are ignored in this study *a priori*. Other SNe in the bottom-left corner of Figure 2 of Branch et al. (2009) are Ia-91T, and even though

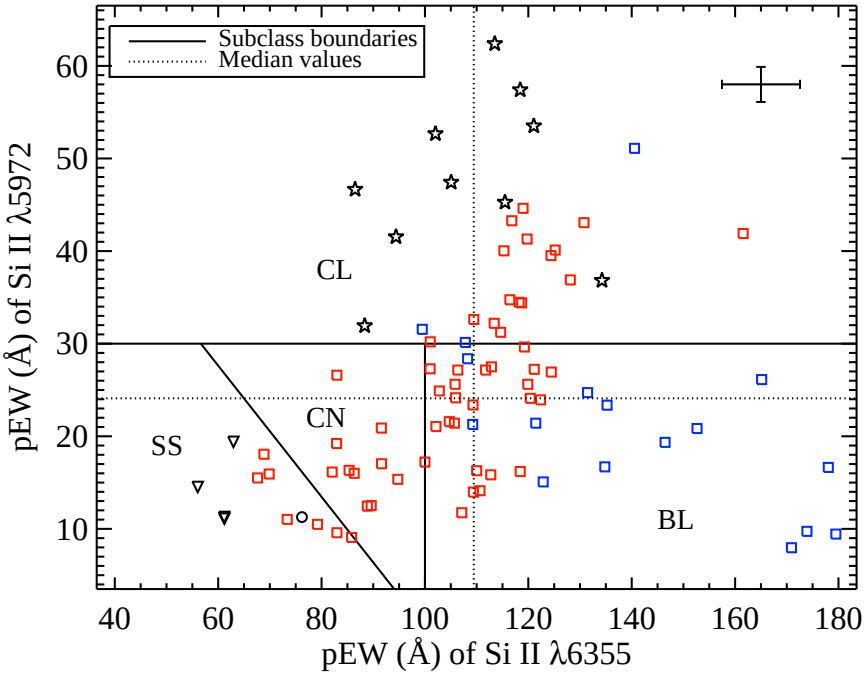

Figure 3.24: The pEW of Si II λ5972 versus the pEW of Si II λ6355 of 89 SNe. Colors and shapes of data points are the same as in Figure 3.4. The solid lines are the boundaries between the four classes as inferred from Branch et al. (2009). CN = core normal, BL = broad line, CL = cool, SS = shallow silicon. The dotted lines are the median values of the two features' pEWs. The median uncertainty in both directions is shown in the upper-right corner.

there are a handful of Ia-91T SNe in the dataset presented here, the BSNIP sample does not contain spectra of any of these objects within 4 d of maximum. It does, however, include four Ia-99aa objects plotted in Figure 3.24 (SNe 1998es, 1999aa, 1999dq, 2001eh) which are thought to be intermediate objects between Ia-91T and Ia-norm (e.g., Garavini et al. 2004). They are much less clustered than they are in Branch et al. (2009), even though SN 1998es and SN 2001eh lie nearly on top of each other in Figure 3.24. The other major difference between this sample and that of Branch et al. (2009) is the relative number of objects in each class. Even though the total number of SNe is comparable in the two datasets, the BSNIP sample has significantly more CL and BL objects, mostly at the expense of CN objects (if one accounts for the fact that we are biased against some of the extreme SS SNe as mentioned above).

One of the most striking trends seen in Figure 3.24 is that all of the data seem to form a nearly continuous, fairly well-correlated distribution with the most spectroscopically peculiar objects lying at the extreme edges of the distribution. We have no Ia-91T objects in the figure, but they *would* fall in the bottom-left corner. From there, as the pEW of Si II λ6355 increases at approximately constant Si II λ5972 pEW, we find the Ia-99aa, then Ia-norm, and finally the HV SNe. Similarly, if we start at the median pEW values for the two features (where the dotted lines cross in Figure 3.24), and increase Si II λ5972 pEW at constant Si II λ6355, we first find (mostly) Ia-norm and then we find the Ia-91bg objects. This amount of separation between SN Ia subclasses is not seen when comparing the pEWs of any other pair of features measured here. However, a somewhat weaker version of this separation is seen when comparing the pEW of Si II λ6355 to the pEW of both Ca II H&K and the S II "W." In addition, Ia-91bg objects are found to distinguish themselves from the other subclasses mentioned here when comparing pEW values from a few pairs of spectral features.

The subtypes used here (excluding HV) come from SNID, which cross-correlates the entire input spectrum with a library of SN spectra of various subtypes. However, it appears that we can classify the vast majority of SNe Ia using only the pEWs of these two Si II features, as opposed to a spectrum covering a much wider wavelength range. The fact that there seems to be a continuous distribution in these pEW values with the "most" spectroscopically peculiar objects on the edges of the distribution[4] indicates that the often-used spectral classification scheme based on Ia-91bg, Ia-norm, and Ia-91T objects may only accurately represent the most extreme objects. In other words, an object spectrally classified as Ia-norm might in reality have some observables in common with Ia-norm and some in common with one of the peculiar subtypes. This classification scheme, while being somewhat qualitative in nature, is still useful, however, since any object spectroscopically classified as peculiar will be an outlier in the population of all SNe Ia and it is often by studying the most extreme cases that one learns the most. A deeper, quantitative investigation into the

[4]In fact, most of the Ia-91bg and all of the Ia-99aa objects that appear in Figure 3.24 were used as SNID templates in BSNIP I. This indicates that they are indeed some of the "most" spectroscopically peculiar objects in the BSNIP dataset, and that their spectra most closely resemble their subclass' namesakes (SN 1991bg and SN 1999aa, respectively).

photometric and host-galaxy properties of these *spectroscopically* determined subclasses will be undertaken in BSNIP III and other papers in this series.

3.5.6 The Si II Ratio

The so-called "Si II ratio", $\Re$(Si II), was defined by Nugent et al. (1995) as the ratio of the depth of the Si II λ5972 feature to the depth of the Si II λ6355 feature. In our notation this is a(Si II λ5972) / a(Si II λ6355). They present a spectroscopic and photometric sequence of SNe Ia based on temperature differences which they attribute to differences in the total amount of ^{56}Ni produced in the explosion. The Si II ratio has been previously found to correlate with absolute B-band magnitude (Nugent et al. 1995), Δm_{15} (Benetti et al. 2005; Hachinger et al. 2006), $(B-V)_0$ (Altavilla et al. 2009), and color-corrected Hubble residual (Blondin et al. 2011). We will explore some of these relationships in BSNIP III.

While Nugent et al. (1995) originally defined the Si II ratio using the *depths* of spectral features, Hachinger et al. (2006) define the Si II ratio using the pEWs of the Si II λ5972 and Si II λ6355 lines. With their redefined Si II ratio, Hachinger et al. (2006) observe a similar trend to what was found by Nugent et al. (1995): brighter SNe Ia with broader light curves have smaller Si II ratios. In Figure 3.25 we investigate how consistent the Si II ratio is when defined using spectral feature depths (ordinate) versus pEWs (abscissa). The color of each data point represents its "Wang type" (see Section 3.5.1) while the shape of each data point represents its "SNID type." The linear least-squares fit to all 162 points is shown as a solid line while the standard error of the fit is shown as the dashed lines.

The two different ways to define the Si II ratio appear to be well correlated; the Spearman rank coefficient is $\sim$0.86. According to the fit, the zero-point offset between the two is $\sim$0.06, though this should formally be zero since if the pEW is zero then the feature's depth is also zero. To measure the spectral feature depth one must determine the minimum of the spectral feature (either by smoothing the data or fitting a function to the flux, in order to avoid local, unphysical minima due to noise) and then define the feature's endpoints and a pseudo-continuum to compare to the flux at the minimum. However, to measure a pEW, one only needs to define the endpoints and a pseudo-continuum. Therefore, the pEW is a more robust and easier to measure parameter than the spectral feature depth, and since they are well correlated we will follow Hachinger et al. (2006) and define the Si II ratio as

$$\Re\left(\text{Si II}\right) \equiv \frac{\text{pEW}\left(\text{Si II } \lambda5972\right)}{\text{pEW}\left(\text{Si II } \lambda6355\right)}. \tag{3.3}$$

The temporal evolution of the Si II ratio is shown in Figure 3.26 where we have once again color-coded the data based on their HV or normal-velocity classification and shape-coded the data based on their SNID classification. There is a significant amount of scatter in $\Re$(Si II) and thus it is difficult to discern whether or not there is much temporal evolution for any of the subclasses of SNe Ia. The one point that can be fairly robustly made from inspecting Figure 3.26 is that Ia-91bg objects consistently have the largest Si II ratios. This

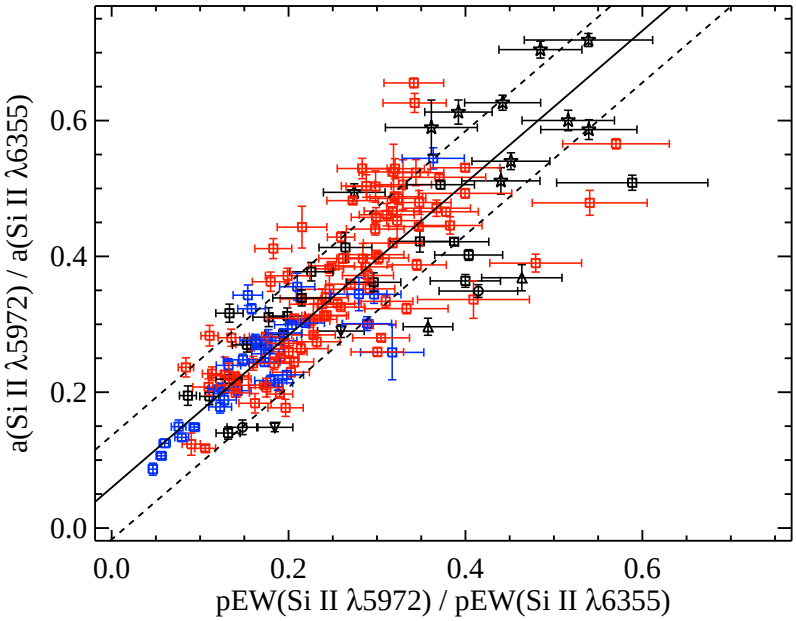

Figure 3.25: The Si II ratio defined using spectral feature depth versus the Si II ratio defined using pEWs for 162 SNe. Colors and shapes of data points are the same as in Figure 3.4. The solid line is the linear least-squares fit and the dashed lines are the standard error of the fit. The Spearman rank coefficient is ∼0.86.

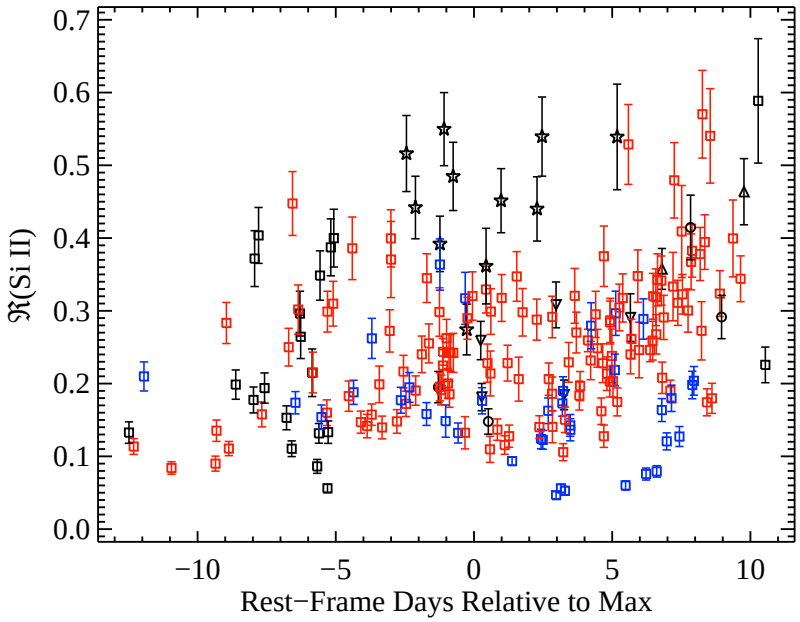

Figure 3.26: The Si II ratio versus rest-frame age relative to maximum brightness of 200 spectra of 154 SNe Ia. Colors and shapes of data points are the same as in Figure 3.4.

partially matches what has been previously seen in that fainter SNe Ia with narrow light curves (oftentimes spectroscopically resembling SN 1991bg) tend to have large $\Re$(Si II) values (e.g., Nugent et al. 1995; Benetti et al. 2005; Hachinger et al. 2006). However, these previous results also show that brighter objects with broader light curves have the smallest Si II ratios, which is not readily apparent in the current study. There are only a few Ia-91T/99aa SNe plotted in Figure 3.26, but they all have average values of $\Re$(Si II).

Figure 3.26 also suggests that HV objects may have, on average, lower Si II ratios than SNe with normal velocities, although the large scatter renders this conclusion tentative at best. When color-coding the data by "Benetti type," as expected the FAINT objects have the highest values of $\Re$(Si II) (since they are defined as SNe having the narrowest light curves). Somewhat different than previous studies is that LVG and HVG objects all have approximately the same values of the Si II ratio. Furthermore, while we only have a handful of objects with a measured $\Re$(Si II) at $t < -5$ d, a few are LVG and a few are HVG, and they all have approximately average values of the Si II ratio. This is markedly different than Benetti et al. (2005), whose data show that HVG objects have larger than average $\Re$(Si II) values at these earliest epochs (though they do decrease to more typical values at later times).

Hatano et al. (2000) plot Si II ratio versus the expansion velocity (as determined by the Si II λ6355 feature) in their Figure 1. They point out that it is unclear whether or not these two observables are correlated, as one might expect if the diversity of SNe Ia only depended on

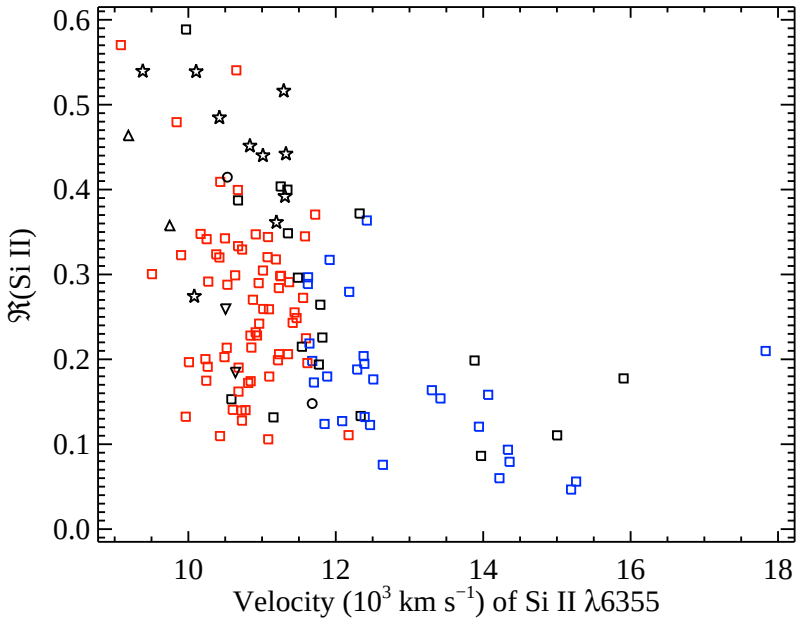

Figure 3.27: The Si II ratio versus velocity of the Si II λ6355 feature of 127 SNe Ia. Colors and shapes of data points are the same as in Figure 3.4.

one parameter (^{56}Ni, for example), even if you ignore the spectroscopically peculiar objects. Their basic observation (using many more data points) is confirmed in Figure 3.27. If the current dataset had multiple spectra of a given object for which $\Re$(Si II) and the velocity of the Si II λ6355 feature was calculated, the observation closest to maximum brightness was used.

In actuality, Hatano et al. (2000) plot $\Re$(Si II) versus the velocity of the Si II λ6355 feature at 10 d after maximum brightness (v_{10} in our notation). A plot of the Si II ratio versus v_{10} for our data looks qualitatively similar to Figure 3.27. The main difference is that there is more overlap between HV and normal-velocity objects, which is expected since it was shown above that v_{10} is a poor discriminant between HV and normal-velocity SNe (Section 3.5.3). Unsurprisingly, a plot of $\Re$(Si II) versus v_0 is extremely similar to Figure 3.27, but with significantly fewer data points. Furthermore, if only spectra within 5 d of maximum brightness are used, the trends seen in Figure 3.27 are unchanged. This is likely due to the fact that the Si II ratio does not change much with time and the Si II λ6355 velocity is decreasing relatively slowly over the epochs where $\Re$(Si II) is measured.

In Figure 3.27, Ia-91bg objects again distinguish themselves by having large values of $\Re$(Si II) and low expansion velocities, while the Ia-91T/99aa objects are fairly well mixed in with the Ia-norm. Unsurprisingly, the HV objects are found at the highest velocities and once again point toward a continuous distribution of expansion velocities (and Si II ratios) when combined with the normal-velocity SNe. However, it is interesting to note that the

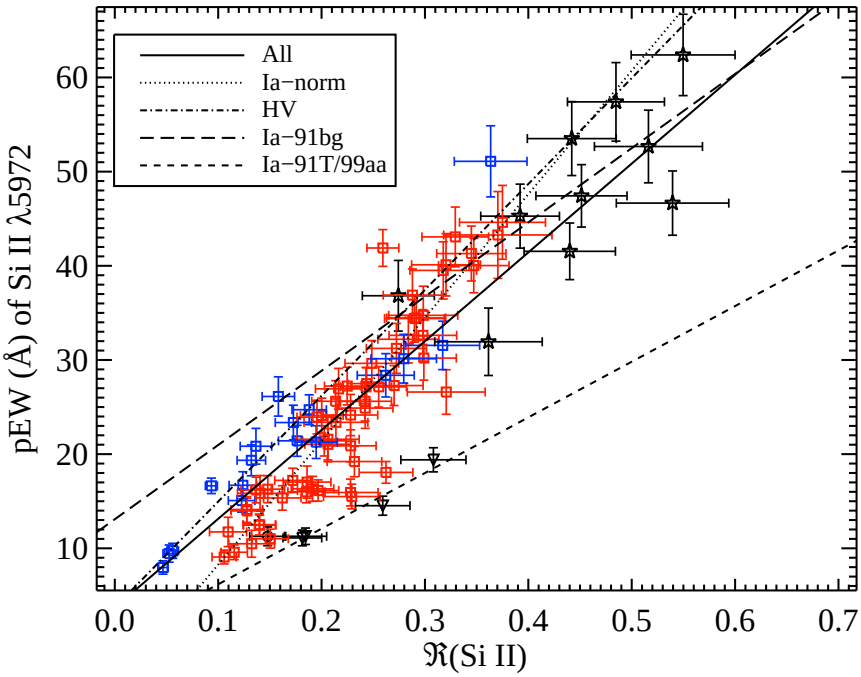

Figure 3.28: The pEW of the Si II λ5972 feature versus Si II ratio for 89 SNe Ia. Colors and shapes of data points are the same as in Figure 3.4. The various lines are fits to all of the data (solid), only Ia-norm objects (dotted), only HV objects (dot-dashed), only Ia-91bg objects (long-dashed), and only Ia-91T/99aa objects (short-dashed). All of the fits have Spearman rank coefficients of > 0.89 except the Ia-91bg objects (which have a coefficient of $\sim$0.79).

scatter in Si II ratio values decreases dramatically for velocities $\gtrsim 13,000$ km s^{-1}.

The pEW of the Si II λ5972 feature and the Si II ratio have both been found to correlate well with Δm_{15} (e.g., Nugent et al. 1995; Hachinger et al. 2006). Hachinger et al. (2006) point out (from their Fig. 10) that each of these correlations implies the other's existence based on the relationship between the near-maximum values of pEW of Si II λ5972 and $\Re$(Si II). In Figure 3.28 the pEW of the Si II λ5972 feature versus the Si II ratio is plotted for objects within 5 d of maximum, confirming this correlation. Our plot contains 89 SNe Ia, which are again color-coded based on their HV or normal-velocity classification and shape-coded based on their SNID classification. As before, if multiple spectra of a given object have a calculated pEW of Si II λ5972 and $\Re$(Si II), the observation closest to maximum brightness is used.

In Figure 3.28 the current study's definition of $\Re$(Si II) is used (i.e., the ratio of pEWs) as opposed to the original definition (i.e., the ratio of depths; Nugent et al. 1995). Figure 10 of Hachinger et al. (2006) uses the original definition on the abscissa. When the original definition is used with the BSNIP data, results qualitatively similar to those of Figure 3.28

are seen. Hachinger et al. (2006) interpolate/extrapolate their pEW measurements to $t = 0$ d, while spectra within 5 d of maximum brightness (as in Section 3.5.5) are used in Figure 3.28 since the pEWs of the Si II λ5972 and Si II λ5972 features do not change much during these epochs. If the few objects with spectra earlier than 5 d before maximum are included, they fall along the linear correlation. However, if objects with spectra later than 5 d after maximum are added, they mainly fall *below* the linear correlation. This is due to the fact that the Si II λ5972 pEW values remain relatively constant for $t \lesssim 5$ d but begin to increase at later times, as seen in Figure 3.19.

As mentioned above, Ia-91bg objects have large Si II ratios and large Si II λ5972 pEWs and are thus found in the upper right of the linear correlation in Figure 3.28. Conversely, it was shown that Ia-91T/99aa SNe have low values of Si II λ6355 pEWs and low-to-average values of Si II λ5972 pEWs, so one may expect them to lie at the bottom left of the correlation, and in fact it appears that these objects lie somewhat below the main correlation. The HV SNe perhaps make up the upper part of the main correlation, with the normal-velocity objects making up the lower part, though these two groups are fairly well-mixed. Similarly, if we code the points in Figure 3.28 by velocity gradient, we see that the HVG objects usually lie slightly above the LVG objects (as seen in Hachinger et al. 2006), but with a significant amount of overlap. The FAINT objects in the BSNIP sample are found at the upper right of the correlation, as seen previously (Hachinger et al. 2006), and reiterate the connection between Ia-91bg SNe and FAINT SNe.

To investigate whether the various subclasses have distinct correlations, linear functions were fit to all of the data in Figure 3.28 as well as each individual subclass. All of the fits have Spearman rank coefficients of > 0.89 except the Ia-91bg objects (which have a coefficient of $\sim$0.79), implying that each subclass, and the data as a whole, are well fit by a linear function (though Ia-91bg SNe have a fair amount of scatter). The linear fit to all of the data and the linear fits to the Ia-norm, HV, and Ia-91bg objects are all consistent with each other at the 2σ level. As mentioned above, the Ia-91T/99aa SNe fall below the main correlation and appear to lie on their own relationship. However, since there are only four points in the fit, it is difficult to say if this difference is statistically significant. Previous work has indicated that the pEW of the Si II λ5972 feature and Si II ratio are both luminosity indicators (e.g., Hachinger et al. 2006). The scatter in the relationship between these two parameters may be related to differences in luminosity or light-curve shape (i.e., Ia-norm versus Ia-91bg versus Ia-91T) or differences in velocity (i.e., HV versus normal velocity), which might also be related to differences in color (Foley & Kasen 2011). Adding photometric observables such as these into this analysis will be done in BSNIP III.

The pEW of the Si II λ4000 feature has also been used as a luminosity indicator (Arsenijevic et al. 2008; Walker et al. 2011; Blondin et al. 2011; Chotard et al. 2011). Therefore, one might expect it to also correlate well with the Si II ratio. Figure 3.29 shows the pEW of the Si II λ4000 feature versus $\Re$(Si II) for objects within 5 d of maximum. The plot contains 66 SNe Ia, which are again color-coded by "Wang type" and shape-coded by "SNID type." As before, the observation closest to maximum brightness is used if there are multiple spectra

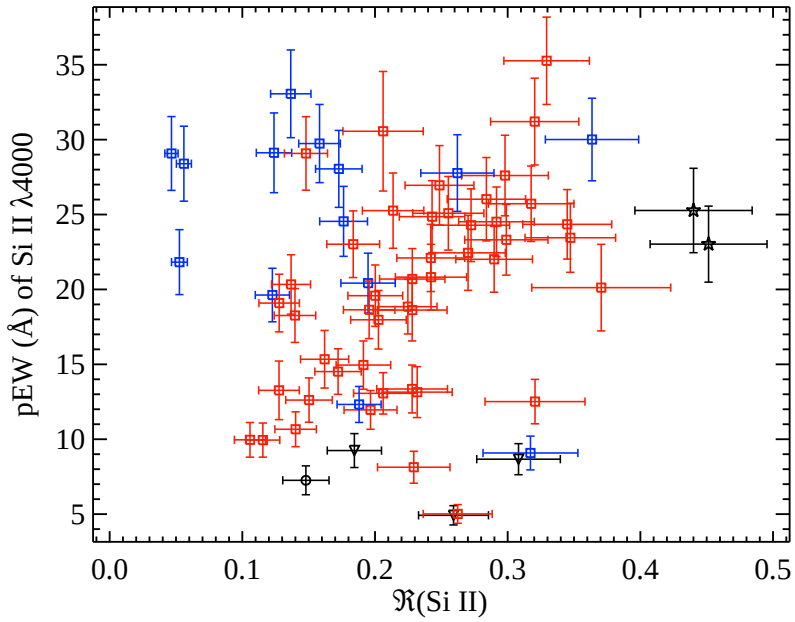

Figure 3.29: The pEW of the Si II λ4000 feature versus Si II ratio for 66 SNe Ia. Colors and shapes of data points are the same as in Figure 3.4.

of a given object with measured values of the pEW of Si II λ4000 and the Si II ratio.

Figure 3.29 shows no obvious correlation between pEWs of the Si II λ4000 feature and $\Re$(Si II). As in Figure 3.28, Ia-91bg are found to have the highest Si II ratio and are thus toward the right of the figure, while the Ia-91T/99aa SNe have small pEWs in general and are thus found toward the bottom of the plot. The HV objects have higher-than-average Si II λ4000 pEW values with relatively low Si II ratios, but they overlap quite a bit with the normal-velocity objects. The Ia-norm SNe show the most consistent relationship between these two parameters, although they have a large scatter and a Spearman rank coefficient of only $\sim$0.51. The fact that these two spectroscopic observables are both used as luminosity indicators (e.g., Blondin et al. 2011) and yet they are seemingly uncorrelated is curious. Further investigation into this discrepancy (with the addition of luminosity information for some of the SNe presented here) will take place in BSNIP III.

3.5.7 Other pEW and Flux Ratios

The Ca II Ratio

Similar to the Si II ratio, Nugent et al. (1995) defined the Ca II ratio as the ratio of the flux at the red edge of the Ca II H&K feature to the flux at the blue edge of that feature.

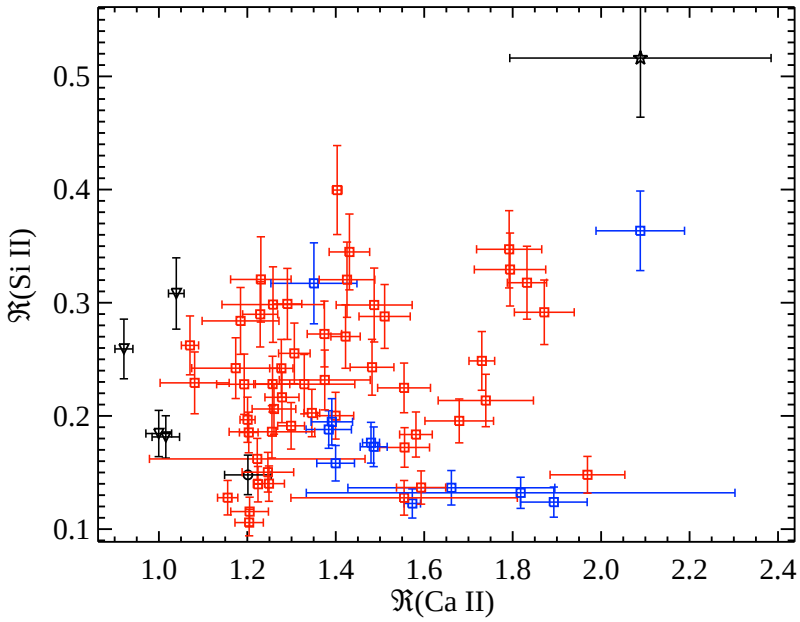

Figure 3.30: The Si II ratio versus the Ca II ratio for 68 SNe Ia. Colors and shapes of data points are the same as in Figure 3.4.

In our notation this is defined as

$$\Re\,(\text{Ca II}) \equiv \frac{F_r\,(\text{Ca II H\&K})}{F_b\,(\text{Ca II H\&K})}. \tag{3.4}$$

They found that this parameter scaled with absolute B-band magnitude in the same way as $\Re$(Si II). The Ca II ratio has been investigated further in more recent studies, and while there is not much temporal evolution of the parameter within 5 d of maximum brightness (Bongard et al. 2006), it is unclear if this spectral parameter is all that well correlated with luminosity (Blondin et al. 2011).

Since the Si II ratio and the Ca II ratio have both been shown to correlate with absolute B-band magnitude (Nugent et al. 1995; Bongard et al. 2006), one might expect the two ratios to correlate with each other. However, we find no significant correlation. Figure 3.30 shows the 68 SNe (within 5 d of maximum) for which we measure both $\Re$(Ca II) and $\Re$(Si II). The data are color-coded by "Wang type" and shape-coded by "SNID type." As above, if multiple spectra of a given object have these two ratios calculated for them, the observation closest to maximum brightness is used.

Both increasing and decreasing the age range investigated does not change the basic trends seen in Figure 3.30. While there is significant scatter and no obvious linear trend, there are still some clear separations among the various subclasses. The lone Ia-91bg object in the plot is separated from the rest of the SNe and the four Ia-99aa objects also occupy one of the extreme edges of the distribution. Furthermore, while is there some overlap between

Ia-norm and HV objects, the bulk of the HV objects have the lowest values of $\Re$(Si II) and higher-than-average $\Re$(Ca II) values. Whether the Ca II ratio is a good luminosity indicator will be investigated further in BSNIP III.

Bongard et al. (2006) introduced an integral flux ratio, $\Re$(CaS), defined as the flux integral over 3887–4012 Å divided by the flux integral over 3620–3716 Å. They state that the wavelength regions were chosen "in order to produce a spectral index that is well correlated to luminosity." Aside from seeming somewhat contrived, the fact that a wavelength range is effectively "hard-coded" into this flux ratio is disconcerting. SNe have a wide range of expansion velocities (especially the Ca II H&K feature; see Figure 3.4) and thus these pre-specified wavelength ranges, which are meant to encompass only the blue and red edges of the spectral feature, may end up including part of the absorption feature itself at some of the most extreme expansion velocities.

One advantage to an integral flux ratio, however, is that it can "smooth over" any spurious noise spikes that might be mistaken for the local maximum – which is how Nugent et al. (1995) defined the fluxes used when calculating $\Re$(Ca II). This is not an added advantage for the current study since our fitting procedure uses locally defined quadratic functions at the blue and red edges of each spectral feature to effectively smooth the flux and measure robust peaks (see Section 3.3.4 for more information on how the endpoints are defined and how the peaks are determined). Therefore, $\Re$(CaS) is not calculated for the BSNIP data.

One may expect the Ca II ratio to be related to the pEW of the Ca II H&K feature, but we see no evidence for such a relationship. Figure 3.31 presents 96 SNe within 5 d of maximum brightness for which we measure $\Re$(Ca II). As done previously, the data are color-coded based on their "Wang type" and shape-coded based on their "SNID type." Once again, the observation closest to maximum light is used. Changing the age range investigated does not alter the basic trends seen in Figure 3.31. As in Figure 3.30, Ia-91bg and Ia-99aa objects tend to lie on the outskirts of the distribution, but there is much more overlap in Figure 3.31. Similarly, the HV objects are well separated from the Ia-norm objects, but again there is a significant amount of overlap.

The "SiS" Ratio

Somewhat analogous to the Ca II ratio, Bongard et al. (2006) defined the "SiS ratio" as the ratio of the flux at the red edge of the S II "W" feature to the flux at the red edge of the Si II λ6355 feature. This is defined using our notation as

$$\Re\left(\text{SiS}\right) \equiv \frac{F_r\left(\text{S II "W"}\right)}{F_r\left(\text{Si II } \lambda 6355\right)}. \tag{3.5}$$

This parameter was shown to scale with absolute B-band magnitude in the same way as $\Re$(Ca II). Even though Bongard et al. (2006) make a time-dependent correction to yield this correlation, they state that the existence of a universal time correction for this ratio is doubtful. In fact, very little temporal evolution of $\Re$(SiS) near maximum brightness is seen

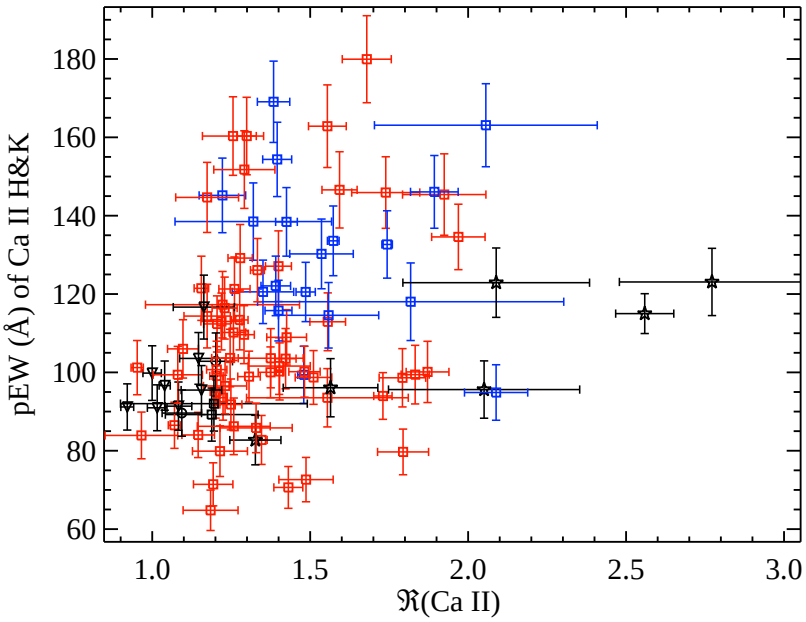

Figure 3.31: The pEW of the Ca II H&K feature versus Ca II ratio for 96 SNe Ia. Colors and shapes of data points are the same as in Figure 3.4.

in the BSNIP data. The SiS ratio has been measured for more objects in recent work, but it does not appear to correlate as well with luminosity as initially claimed (Blondin et al. 2011).

Since the SiS ratio and the Si II ratio have both been shown to correlate with absolute B-band magnitude (Bongard et al. 2006), one might expect the two ratios to correlate with each other. Only marginal evidence for such correlation is found in the current dataset. Figure 3.32 shows the 85 SNe (within 5 d of maximum) for which both $\Re$(SiS) and $\Re$(Si II) is measured. The data are color-coded based by "Wang type" and shape-coded by "SNID type." As before, if multiple spectra of a given object have these two ratios measured, the observation closest to maximum brightness is used.

Decreasing the age range investigated does not change the basic trends seen in Figure 3.32, while increasing the age range adds substantial scatter to the plot. There possibly exists a linear trend for Ia-norm objects and perhaps includes the Ia-99aa objects as well, though there are only three such objects in the Figure and they occupy the lower end of the supposed relationship. The HV and Ia-91bg SNe are found significantly off the purported trend. In BSNIP III we will investigate the efficacy of $\Re$(SiS) as a luminosity indicator. Bongard et al. (2006) also introduced an integral flux ratio, $\Re$(SiSS), analogous to $\Re$(CaS), defined as the flux integral over 5500–5700 Å divided by the flux integral over 6200–6450 Å. For the same reasons given above for $\Re$(CaS), $\Re$(SiSS) is not calculated for the BSNIP data.

One may expect the SiS ratio to be related to the pEW of the S II "W" feature or

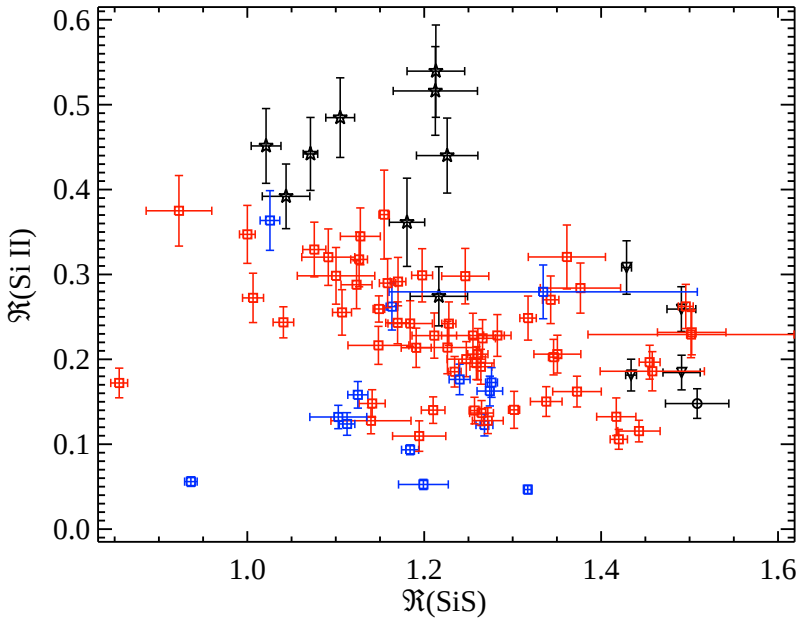

Figure 3.32: The Si II ratio versus the SiS ratio for 85 SNe Ia. Colors and shapes of data points are the same as in Figure 3.4.

the Si II λ6355 feature (or perhaps the ratio of the two). We find no evidence for such a correlation with the pEW of the S II "W" alone, but a possible relationship exists between $\Re$(SiS) and the pEW of the Si II λ6355 feature as well as the ratio of the pEW of the S II "W" to that of Si II λ6355. Figure 3.33 presents 110 SNe within 5 d of maximum brightness for which we measure $\Re$(SiS). As above, the data are color-coded by their "Wang type" and shape-coded by their "SNID type." Only the closest spectra to maximum brightness are once again used. Increasing or decreasing the age range investigated does not change the basic trends seen in Figure 3.33.

It is possible that the SiS ratio is linearly (or quadratically) related to the ratio of pEWs, but there is a significant amount of scatter in Figure 3.33. Interestingly, Ia-91bg and Ia-99aa objects once again tend to lie on the outskirts of the distribution, but there is a lot of overlap with the HV and Ia-norm objects (which are nearly indistinguishable in this parameter space). There are also a few extreme outliers in Figure 3.33, including the lone Ia-91T object plotted. When comparing $\Re$(SiS) to the pEW of Si II λ6355 alone, the same separations, or lack thereof, between the different subclasses once again appear, as do the same outliers. The only difference is that the two values are (possibly) linearly *anti*-correlated.

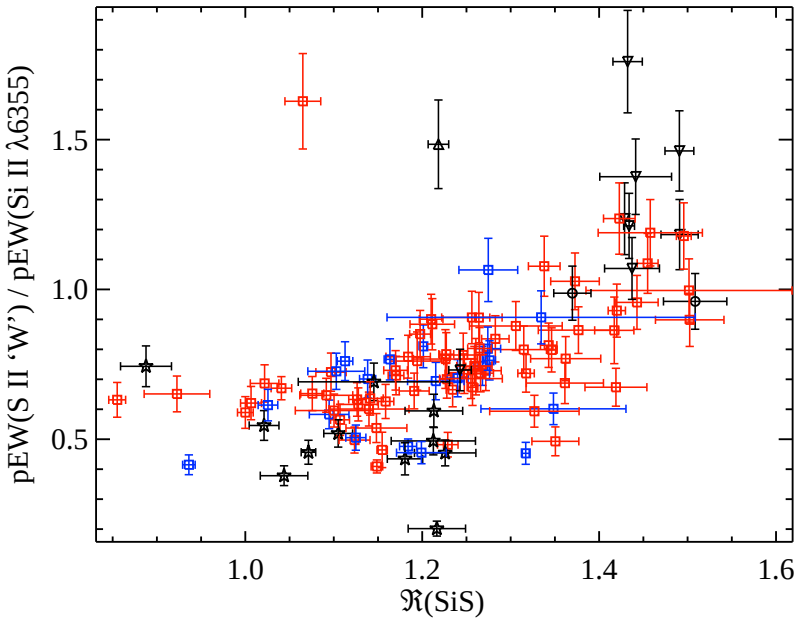

Figure 3.33: The ratio of the pEW of S II "W" to that of Si II λ6355 versus SiS ratio for 110 SNe Ia. Colors and shapes of data points are the same as in Figure 3.4.

The "SSi" Ratio

Another parameter that has been proposed as a spectroscopic luminosity indicator is the ratio of the pEW of the S II "W" to that of the Si II λ5972 feature (Hachinger et al. 2006). They found that this ratio, dubbed $\Re$(S,Si), is linearly anti-correlated with Δm_{15} (which is opposite the relationship between $\Re$(Si II) and Δm_{15}). Following Hachinger et al. (2006), we define the "SSi ratio" as

$$\Re\,(\mathrm{S,Si}) \equiv \frac{\mathrm{pEW}\,(\mathrm{S\ II\ ``W"})}{\mathrm{pEW}\,(\mathrm{Si\ II}\ \lambda 5972)}. \tag{3.6}$$

There is strong evidence for an anti-correlation between the Si II ratio and the SSi ratio in Figure 3.34, which presents the 85 SNe (within 5 d of maximum) for which both $\Re$(S,Si) and $\Re$(Si II) are measured. As usual, data are color-coded by "Wang type" and shape-coded by "SNID type" and only observations closest to maximum light are used.

Interestingly, the overall correlation (and differences between different subclasses) is unchanged when we include data from all epochs studied in this chapter. It is also unchanged when a narrower age range is used. The overall anti-correlation seen in Figure 3.34 suggests that $\Re$(S,Si) may indeed be as good a luminosity indicator as $\Re$(Si II), though recent work suggests otherwise (Blondin et al. 2011). While the trend for all objects shown in Figure 3.34 may not be linear, they do appear well correlated, with a Spearman rank coefficient of about -0.89. A linear fit to all 85 SNe in Figure 3.34 is shown by the solid line. A linear fit to only

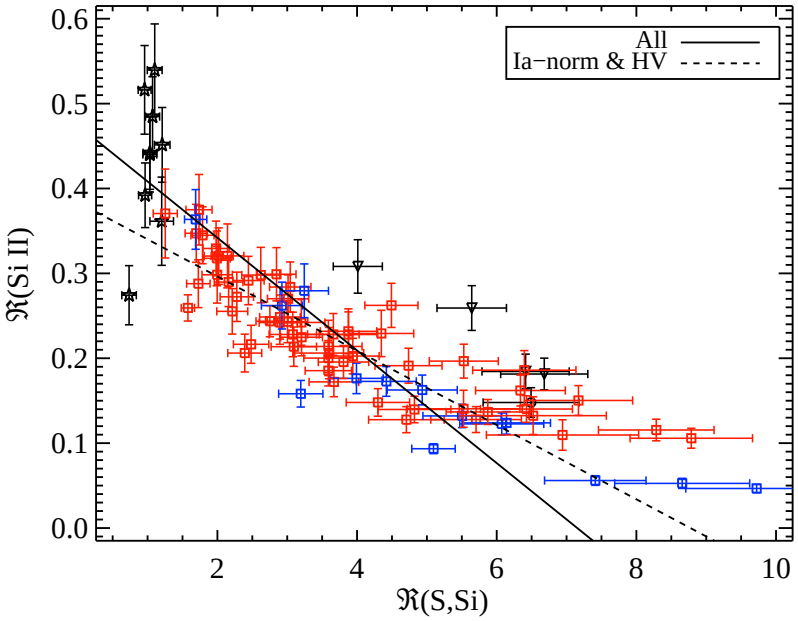

Figure 3.34: The Si II ratio versus the SSi ratio for 85 SNe Ia. Colors and shapes of data points are the same as in Figure 3.4. The solid line is a linear fit to all of the data and the dashed line is a linear fit to only the Ia-norm and HV objects. The Spearman rank coefficient for both fits is approximately -0.89.

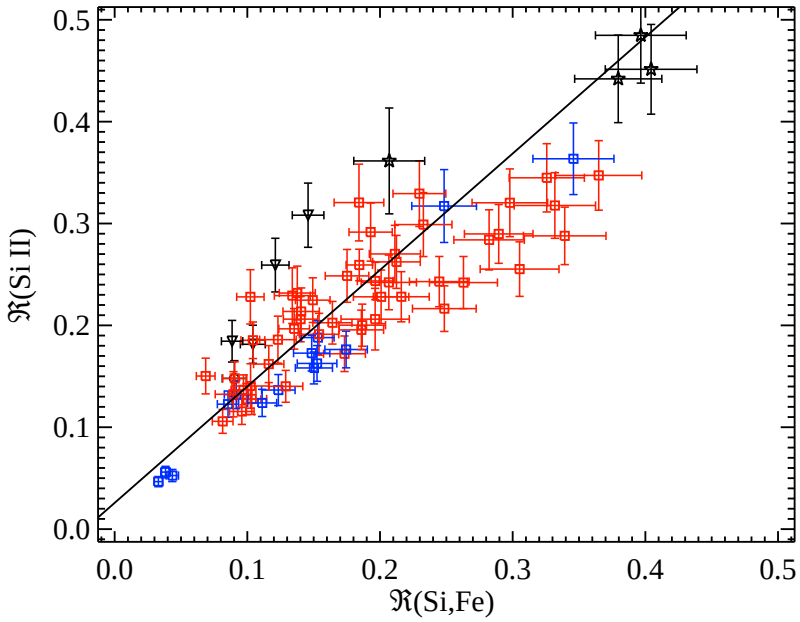

Figure 3.35: The Si II ratio versus the SiFe ratio for 72 SNe Ia. Colors and shapes of data points are the same as in Figure 3.4. The solid line is a linear fit to all of the data and the Spearman rank coefficient is ∼0.86.

the Ia-norm and HV objects (shown by the dashed line in Figure 3.34) has a nearly identical Spearman rank coefficient to that of the entire sample. The tantalizing possibility that ℜ(S,Si) is yet another spectral luminosity indicator will be explored further in BSNIP III.

The "SiFe" Ratio

Similar to the SSi ratio, Hachinger et al. (2006) also found that the ratio of the pEW of the Si II λ5972 feature to that of the Fe II complex can be used as a spectroscopic luminosity indicator since it scaled linearly with Δm_{15}. They referred to this as the "SiFe ratio," defined as

$$\Re\,(\text{Si,Fe}) \equiv \frac{\text{pEW}\,(\text{Si II}\ \lambda5972)}{\text{pEW}\,(\text{Fe II})}. \tag{3.7}$$

There is also strong evidence for a correlation between the Si II ratio and the SiFe ratio in Figure 3.35, where the 72 SNe (within 5 d of maximum) are shown for which both ℜ(Si,Fe) and ℜ(Si II) are measured. Again the data are color-coded based on their "Wang type" and shape-coded based on their "SNID type," and only spectra closest to maximum brightness are used.

The scatter in the relationship between the Si II ratio and the SiFe ratio increases when including data from all epochs studied here. The overall correlation seen in Figure 3.35 suggests that ℜ(Si,Fe) may also be an accurate luminosity indicator, though Blondin et al.

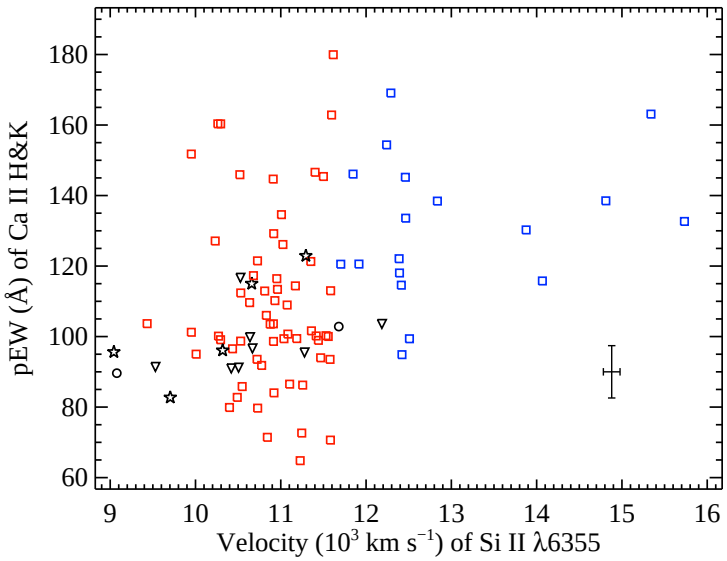

Figure 3.36: The pEW of Ca II H&K versus the velocity of Si II λ6355 for 92 SNe Ia. Colors and shapes of data points are the same as in Figure 3.4. The median uncertainty in both directions is shown in the lower-right corner.

(2011) report that it does not significantly improve the accuracy of their luminosity determinations. The data are well fit by a linear function and are highly correlated (Spearman rank coefficient of $\sim$0.86); a linear fit to all 72 SNe in Figure 3.34 is shown by the solid line. The Ia-91bg objects distinguish themselves quite prominently except the lone point that appears to be closer to the Ia-99aa objects, which are also found at an outer edge of the main relationship. The HV SNe tend to be at the bottom of the relationship, with a handful of significant outliers. The use of $\Re$(Si,Fe) as a luminosity indicator will be investigated further in BSNIP III.

3.5.8 Comparing Expansion Velocities to Pseudo-Equivalent Widths

In Section 3.5.4 the possibility of a correlation between expansion velocity and pEW was mentioned, at least for the Ca II H&K, Mg II, Fe II, and Si II λ6355 features. The pEW for these four features is plotted versus the expansion velocity of Si II λ6355 in Figures 3.36–3.39. They contain all objects within 5 d of maximum brightness and as above, if there are multiple spectra of a given object, only the observation closest to maximum brightness is shown. The data are color-coded by "Wang type" and shape-coded by "SNID type." In all cases, decreasing the age range investigated does not change the basic trends seen in Figures 3.36–3.39, though increasing the age range increases the overlap among the various subclasses.

If the pEW of a given feature is instead plotted versus its *own* expansion velocity, similar

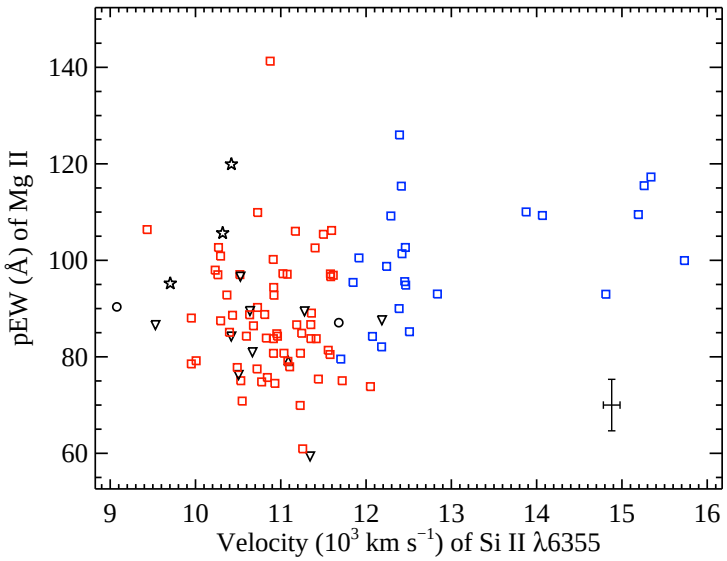

Figure 3.37: The pEW of the Mg II complex versus the velocity of Si II λ6355 for 99 SNe Ia. Colors and shapes of data points are the same as in Figure 3.4. The median uncertainty in both directions is shown in the lower-right corner.

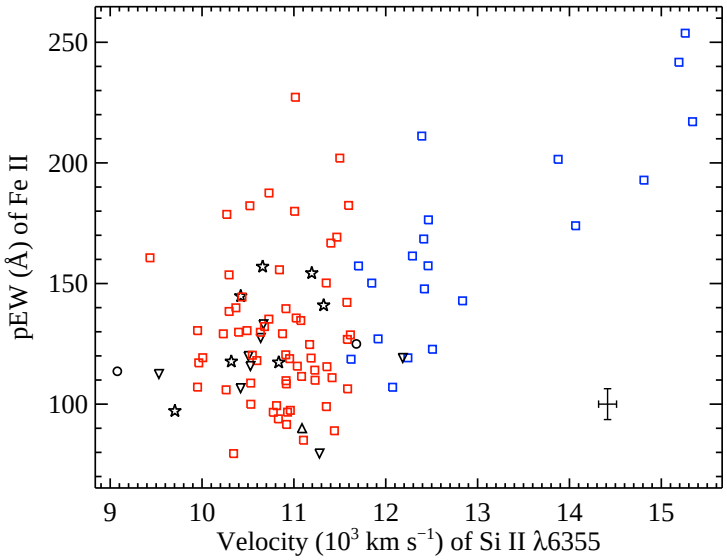

Figure 3.38: The pEW of the Fe II complex versus the velocity of Si II λ6355 for 99 SNe Ia. Colors and shapes of data points are the same as in Figure 3.4. The median uncertainty in both directions is shown in the lower-right corner.

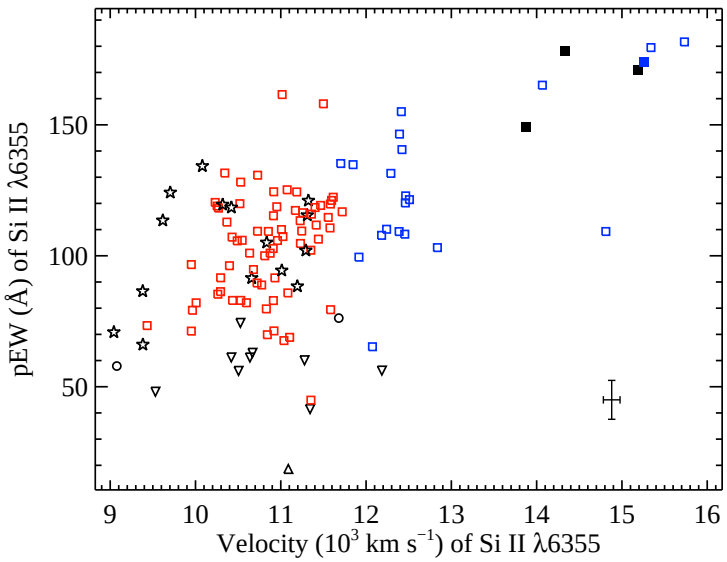

Figure 3.39: The pEW of Si II λ6355 versus the velocity of Si II λ6355 for 120 SNe Ia. Colors and shapes of data points are the same as in Figure 3.4. The median uncertainty in both directions is shown in the lower-right corner. The filled blue square is the HV object SN 2006X which shows evidence for interaction with circumstellar material (Patat et al. 2007). The filled black squares are the HV objects SNe 2002bf, 2002bo, and 2004dt, all of which show evidence for an aspherical explosion via large Si II polarizations (Wang et al. 2006).

trends are observed. However, pEWs versus the expansion velocity of only the Si II λ6355 feature are shown since HV objects are defined using this velocity, and this spectral feature has the most measured velocities of any other feature in our dataset (not to mention the fact that we *never* measure the velocity of the Mg II or Fe II complexes). Furthermore, when investigating ΔpEW versus velocity, trends nearly identical to those seen in Figures 3.36–3.39 are found.

By construction, HV objects are always found toward the right-hand side of plots of pEW versus Si II λ6355 velocity. But, as hinted at in Section 3.5.4, they also have higher-than-average pEW values for most of the spectral features investigated. The features showing the greatest differentiation between Ia-norm and HV objects in this parameter space are the four mentioned above and plotted in Figures 3.36–3.39.

As discussed in Section 3.5.1, spectroscopically peculiar SNe have the lowest Si II λ6355 expansion velocities, with the Ia-91bg objects having even lower velocities than the Ia-91T/99aa objects. This is clearly seen in Figure 3.39 (and to a lesser extent in the other three pEW versus velocity figures). As mentioned in Section 3.5.4, Ia-91bg objects tend to have large pEW values for most features investigated, while the Ia-91T/99aa objects tend to have lower-than-average pEWs. This is also seen (to various extents) in Figures 3.36–3.39.

In each of these four Figures there is significant overlap among spectroscopically peculiar objects and Ia-norm, while the HV SNe tend to be fairly well separated. However, there is a large scatter, and thus it is difficult to say whether or not there is any real correlation between pEW and Si II λ6355 velocity for the Ia-norm and the HV objects. The Spearman rank coefficients for Figures 3.36–3.38 are all about 0.21–0.35. Using only the Ia-norm and HV objects, the Spearman rank coefficients improve only moderately for these spectral features (0.28–0.33).

Figure 3.39 shows the largest difference between the various subclasses of SNe Ia, although there is still significant overlap (mostly between Ia-norm and Ia-91bg objects). There is a more significant correlation between the pEW of Si II λ6355 and the expansion velocity derived from that same feature, though it is still not too significant (Spearman rank coefficient of 0.43 for all objects in Figure 3.39 and 0.51 for Ia-norm and HV SNe only). The basic trend seen in this figure has also been seen previously by Wang et al. (2009a) with some of the same spectra used in this study. Their plot shows only SNe Ia within 3 d of maximum while Figure 3.39 presents objects within 5 d as maximum. Wang et al. (2009a) point out that HV objects typically have pEW values greater than $\sim$100 Å, which is also observed here.

The observation of a strong Si II λ6355 feature at high velocities may indicate an enhancement in the abundance or density in the outermost layers of HV objects. This could be caused by an extended burning front, different degrees of mixing in the ejecta, or interaction with circumstellar material (CSM; Benetti et al. 2004; Wang et al. 2009a). In fact, two SNe Ia with some of the best direct observational evidence for CSM interaction, SN 2006X (Patat et al. 2007, the filled blue square in Figure 3.39) and SN 2007le (Simon et al. 2009), are both in the current sample and are found to be HV objects.

Wang et al. (2009a) also point out that the distribution of pEWs and velocities between Ia-norm and HV objects is continuous, and therefore it is likely that the proposed enhancement occurs at a wide range of values (with the majority of SNe Ia showing relatively low levels of this enhancement). They suggest that this could be a result of viewing angle effects if HV objects are associated with asymmetric structures. There is both observational (Leonard et al. 2005; Wang et al. 2006) and theoretical (Maeda et al. 2010) evidence that HV SNe may be associated with certain viewing angles of aspherical explosions.

Leonard et al. (2005) and Wang et al. (2007) discuss spectropolarimetric data on SNe 1997bp, 2002bf, 2002bo, 2004dt, and 2004ef which show large Si II polarizations, implying an asymmetric explosion. All of these objects are found to be HV SNe in the BSNIP data; SNe 2002bf, 2002bo, and 2004dt are plotted as filled black squares in Figure 3.39. Building on the work of Leonard et al. (2005), Maund et al. (2010) found a correlation between the level of Si II polarization and $\dot{v}$. Of the five aforementioned HV SNe with large polarizations, the two for which we measure a velocity gradient are both HVG objects. Si II λ6355 velocity, $\dot{v}$, and level of polarization may all also be correlated with velocity offsets of nebular lines in late-time spectra (Maeda et al. 2010). Comparisons of spectra at later epochs to models such as those presented by Maeda et al. (2010) will be made in future BSNIP studies.

3.6 Conclusions

This chapter presents spectral feature measurements of 432 low-redshift ($z < 0.1$) optical spectra within 20 d of maximum brightness of 261 SNe Ia. These data all come from BSNIP I (Chapter 2) and were obtained from 1989 through the end of 2008. We have outlined in detail our automated and robust procedure for spectral feature definition and measurement which has expanded upon the work of previous studies. Using this algorithm we attempted to measure expansion velocities, pEWs, spectral feature depths, and fluxes at the center and endpoints of each of nine major spectral feature complexes. The raw numbers measured from the data are also presented. A sanity check of the consistency of our measurements was performed using the BSNIP data in addition to the spectra presented by Matheson et al. (2008). Even though the current study utilizes spectral data almost exclusively, future BSNIP papers will incorporate photometric data and host-galaxy properties into the measurements discussed in this chapter.

3.6.1 Summary of Spectral Feature Measurements

The temporal evolution of the expansion velocity of each of the spectral features (except for the Mg II and Fe II complexes) was explored. The observed differences in velocities support the layered structure of SN Ia ejecta, with Ca II found in the outermost (i.e., fastest expanding) layers and O I, Si II, and S II found in the inner (i.e., slower expanding) layers. Many of the basic trends seen previously are confirmed by the current analysis, including evidence of a HV population of spectroscopically normal SNe (Wang et al. 2009a). However,

a handful of extremely high velocity objects ($v > 13,000$ km s^{-1} near maximum brightness) which have not been found in previous data exist in the BSNIP sample. A *sharp* cutoff between normal-velocity and HV objects is not well motivated by the data analyzed here, though there are some differences between spectroscopically normal SNe Ia with the lowest and highest velocities near maximum brightness (which is discussed in more detail below).

Following Benetti et al. (2005), velocity gradients are calculated and then used (along with light-curve shape, for those that have that information) in order to classify the SNe. The BSNIP dataset is not the best suited to this kind of study due to the relatively low number of spectra per object. However, $\dot{v}$ is still measured for 61 objects.

The interpolated/extrapolated velocity at maximum brightness (v_0) and at 10 d past maximum (v_{10}) was calculated for each SN with a $\dot{v}$. Effectively no correlation is found between v_{10} and velocity-gradient classification, and only a weak correlation is found between v_0 and velocity gradient. In previous work HV and HVG objects have been used almost interchangeably, as have normal-velocity and LVG objects (e.g., Hachinger et al. 2006; Pignata et al. 2008; Wang et al. 2009a). However, the data presented here cast serious doubt on these associations.

The temporal evolution of the pEW of each spectral feature was also examined. As in Nordin et al. (2011b), ΔpEW was calculated by subtracting a fit to the data from the measurements themselves. Unlike previous work, only linear and quadratic functions were used to fit the temporal evolution. ΔpEW is supposed to effectively remove the age dependence on pEW measurements (Nordin et al. 2011b), though the scatter in the pEWs of most features is large enough in the BSNIP data that there is still some level of temporal evolution in ΔpEW. Furthermore, the ΔpEW values rely on defining a fit (either linear or quadratic) to the measurements which adds another assumption to the analysis. No correlation between velocity gradient and pEW or ΔpEW is seen in the data presented here, even though there has been evidence presented previously for a relationship between ΔpEW of the Si II λ4000 feature and $\dot{v}$ (Nordin et al. 2011a).

We use pEW values of Si II λ6355 and Si II λ5972 were used the BSNIP data according to the four groups defined by Branch et al. (2006). The boundaries between these groups appear to be arbitrary in the context of the spectral measurements presented here. That being said, spectroscopically peculiar SNe Ia and HV objects occupy the outermost edges of the nearly continuous parameter space filled in by the Ia-norm objects. Thus, the "SNID types" seem to be the most extreme versions of the three non-CN "Branch types." Furthermore, both of these classification schemes are quasi-arbitrary cuts in what appears to be a continuous distribution of pEW values.

It was shown that the Si II ratio can be equivalently defined as a ratio of spectral feature depths or pEW values and the latter is used as the definition for the present study. This quantity has been shown to correlate with a variety of photometric observables (e.g., Nugent et al. 1995; Hachinger et al. 2006; Altavilla et al. 2009; Blondin et al. 2011) and these proposed relationships will be investigated further in BSNIP III. We do confirm the observation that Ia-91bg objects (often underluminous) have the largest $\Re$(Si II) values. On

the other hand, the Ia-91T/99aa objects (often overluminous) seem to have average $\Re$(Si II) values, which is different than what has been seen before (e.g., Hachinger et al. 2006).

Benetti et al. (2005) presented evidence of HVG objects having the largest measured Si II ratios at $t < -5$ d, though the few objects for which we measure $\Re$(Si II) at these early epochs all have quite typical Si II ratios and represent the LVG and HVG classes. The pEW of the Si II λ5972 feature and $\Re$(Si II) have both been found to correlate well with Δm_{15} (e.g., Nugent et al. 1995; Hachinger et al. 2006), and the BSNIP data show strong evidence of a linear correlation between these spectral parameters. While the HV and Ia-norm objects show quite a bit of overlap in this parameter space, the Ia-91bg objects lie at the upper-most end of the correlation and the Ia-91T/99aa objects are well below the main trend (and perhaps form there own, distinct relationship).

Four other pEW and flux ratios were also calculated and discussed. Two of these, the Ca II ratio and SiS ratio, have been previously seen to be correlated with B-band magnitude in the same way as the Si II ratio (Nugent et al. 1995; Bongard et al. 2006, respectively). However, no relationship between $\Re$(Si II) and $\Re$(Ca II) is seen here and only a weak relationship is observed between $\Re$(Si II) and $\Re$(SiS). The various "SNID types" and "Wang types" all have similar ranges of Ca II and SiS ratios. The other two ratios investigated, the SSi ratio and the SiFe ratio, were shown by Hachinger et al. (2006) to be anti-correlated and correlated with Δm_{15}, respectively. There is strong evidence for both of these trends in the BSNIP data. Most of the "SNID types" and "Wang types" have a high degree of overlap in the plots of Si II ratio versus SSi ratio and SiFe ratio, and the Ia-91bg objects occupy the extreme upper end of both of these correlations.

Finally, a possible correlation between the expansion velocity of Si II λ6355 and pEWs of Ca II H&K, Mg II, Fe II, and Si II λ6355 was explored. Spectroscopically peculiar objects mostly overlap with Ia-norm objects in these plots, while the HV SNe show both higher expansion velocities and pEW values. CSM interaction and asymmetric explosions have been proposed to explain the existence of SNe Ia with high velocities and large pEWs (Benetti et al. 2005; Wang et al. 2006, respectively). Interestingly, four of the points at the upper-most end of the Si II λ6355 velocity-pEW relationship show evidence for CSM interaction (SN 2006X) or an aspherical explosion (SNe 2002bf, 2002bo, and 2004dt).

3.6.2 How Should One Spectroscopically Classify SNe Ia?

Throughout this chapter, various SN Ia spectral classification schemes have been used, but which is "best" or the most illustrative? The "Benetti types" based on velocity gradient measurements are not only difficult to determine, requiring velocity measurements of multiple spectra near maximum brightness, but the various subclasses do not show many obvious observable differences (aside from $\dot{v}$ and Δm_{15} values, which is how the groups are defined). As mentioned above, the "SNID types" are merely the most extreme objects of the non-CN "Branch types," though the delineation between the different subclasses is fuzzy at best. Finally, the distinction between HV and normal-velocity objects is somewhat arbitrary as

well.

Despite the ambiguity in subclass determination, we prefer to use the "SNID types" (Ia-norm, Ia-91bg, Ia-91T, and Ia-99aa) as defined in BSNIP I. We also favor splitting the Ia-norm objects into HV and normal-velocity objects as defined in Section 3.5.1. It should be made clear that these distinctions may merely be a naming convention used for the most extreme SNe Ia (according to some measured observable), and in reality all of these objects represent a continuous distribution of observables.

One can ask "How Ia-91bg is an object?" if measurements of some spectral parameters are similar to Ia-91bg objects and some parameters are more similar to Ia-norm. We suggest that this is an ill-posed question and that one should be less concerned with naming conventions and more concerned with how the various spectral measurements correlate with luminosity (or other observables). One might respond to this with the question "Why keep the naming conventions at all?" The spectroscopically peculiar SNID types and the HV objects are the extreme members of the SN Ia population and it is often by studying the most extreme objects that one understands the more typical specimen. This is why we prefer the classification scheme outlined above.

3.6.3 Can a Theoretical Model of SNe Ia Explain Their Spectra?

Many of the spectral measurements investigated in this study show a continuous (or nearly so) range of values. This is perhaps evidence that all of the SN Ia subclasses considered here can be described by one, self-consistent physical model that only varies in one or two intrinsic parameters. It was suggested well over a decade ago that the Ia-91bg, Ia-norm, and Ia-91T/99aa objects can be naturally linked through a continuous increase in temperature, presumably by a smoothly increasing amount of ^{56}Ni produced in the explosion (e.g., Nugent et al. 1995). More recently, it has been suggested that continuous variations in viewing angle can give rise to HV and normal-velocity objects (Kasen & Plewa 2007; Kasen et al. 2009; Maeda et al. 2010). Any model that hopes to reflect reality must match the observed spectral properties near maximum brightness (as presented here), as well as the photometric observations of SNe Ia (as shown by Ganeshalingam et al. 2010, and discussed further in BSNIP III).

Perhaps by varying both the amount of ^{56}Ni produced and the viewing angle, one can self-consistently explain all of the subclasses of SNe Ia (and their measured spectral parameters). Though tantalizing, a deeper investigation of this possibility is beyond the scope of this chapter. Furthermore, if one (or more) of the subclasses of SNe Ia are in reality fundamentally different, then discussing only a single theoretical model does not make sense. At least two distinct progenitor channels (possibly resulting in different observed spectra) have been suggested for SNe Ia: the single degenerate (e.g., Whelan & Iben 1973) and the double degenerate (e.g., Iben & Tutukov 1984; Webbink 1984). Similarly, different types of SNe Ia may be found in different host galaxies (perhaps related to host-galaxy type, mass, metallicity, or stellar age; e.g., Gallagher et al. 2008; Hicken et al. 2009b; Howell et al. 2009),

which may also point to multiple models being required to explain all of the observed spectra.

3.6.4 What About Future SN Surveys?

Surveys which are much larger than BSNIP and tuned to discovering the bulk of their SNe Ia at higher redshifts than BSNIP are already underway (e.g., Rau et al. 2009; Law et al. 2009; Kaiser et al. 2002), with many more planned for the future (e.g., LSST, WFIRST). With such large numbers of objects being discovered, it will be extremely difficult to obtain high-quality light curves and/or multiple spectra of most SNe. Instead, one will need to rely on only a handful of photometric points and perhaps one, often relatively low S/N, spectrum. Thus, spectral indicators of luminosity that can be measured in one low-quality spectrum will be of the utmost importance.

For higher-z surveys in particular, useful spectral features that are found toward the blue end of the optical range will be even more critical. For $z \gtrsim 0.6$, the red wing of the typical, near-maximum Si II λ6355 feature becomes redshifted beyond $\sim$1 μm. The Ca II ratio is promising in this regard, though no relation between it and the Si II ratio was seen in the BSNIP data. The SiFe ratio does correlate well the Si II ratio, and the Fe II complex is easier to measure and bluer than the Si II λ5972 feature, but it still requires a measurement of the pEW of Si II λ6355.

The accuracy as luminosity indicators of these and other spectral observables discussed herein will be explored in the next chapter in this series, BSNIP III. It will utilize the measured values and relationships described in this chapter, examining the correlations between spectroscopic observables and photometric properties, with an eye toward using a single spectrum to determine the luminosity (and possibly other intrinsic characteristics) of a SN Ia.

3.7 Appendix

3.7.1 Summary of Spectral Dataset

Table 3.5 presents each SN Ia which had a measured pseudo-continuum for at least one spectral feature. Also listed is the (rest-frame) spectral age for each observation that was fit, and spectral classifications based on various classification schemes.

Table 3.5: Summary of Spectral Dataset

SN Name	Phase[a]	SNID (Sub)Type[b]	Benetti Type[c]	Branch Type[d]	Wang Type[e]
SN 1989B	7.54	Ia-norm	···	···	N
SN 1989M	2.49,3.48	Ia-norm	HVG	BL	HV
SN 1990O	12.54	Ia-norm	···	···	···
SN 1990N	7.11	Ia-norm	···	···	N
SN 1991M	18.06	Ia-norm	···	···	···

Continued on Next Page...

Table 3.5 — Continued

SN Name	Phase[a]	SNID (Sub)Type[b]	Benetti Type[c]	Branch Type[d]	Wang Type[e]
SN 1991T	−10.10,−9.11,6.80	Ia-91T	···	···	···
SN 1991bg	0.14,1.14,19.07	Ia-91bg	FAINT	···	···
SN 1993ac	12.68	Ia-norm	···	···	···
SN 1994D	−12.31,−11.31,−9.32,−7.67,−6.32,−5.32,−3.87,−3.33,14.04	Ia-norm	LVG	CN	N
SN 1994Q	9.68	Ia-norm	···	···	N
SN 1994S	1.11	Ia-norm	···	SS	N
SN 1995D	3.84	Ia-norm	···	CN	N
SN 1995E	−2.46	Ia-norm	···	CN	N
SN 1995ac	−6.34	Ia-91T	···	···	···
SN 1997Y	1.27	Ia-norm	···	BL	N
SN 1997bp	5.49	Ia-norm	···	···	HV
SN 1997br	−4.84	Ia-91T	···	···	···
SN 1997do	−5.67	Ia-norm	···	···	···
SN 1998V	7.20	Ia-norm	···	···	N
SN 1998bp	18.87	Ia-91bg	···	···	···
SN 1998dh	18.77	Ia-norm	···	···	···
SN 1998dk	−7.24,−0.54	Ia-norm	···	···	HV
SN 1998dm	−12.48,−5.61,14.22	Ia-norm	···	···	···
SN 1998dx	5.13	Ia-norm	···	···	HV
SN 1998ec	11.86	Ia-norm	···	···	···
SN 1998ef	−8.62	Ia-norm	···	···	···
SN 1998es	0.28	Ia-99aa	···	SS	···
SN 1999aa	−10.58,0.24,14.04,17.04	Ia-99aa	···	SS	···
SN 1999ac	−3.70,−0.89	Ia-norm	HVG	CN	N
SN 1999cl	7.90	Ia-norm	···	···	N
SN 1999cp	4.91,13.85	Ia-norm	LVG	BL	N
SN 1999cw	14.79	Ia-norm	···	···	···
SN 1999da	−2.12,6.76	Ia-91bg	FAINT	CL	···
SN 1999dg	15.08	Ia-norm	···	···	···
SN 1999dk	−6.60,17.06	Ia-norm	···	···	···
SN 1999do	9.96	Ia-norm	···	···	···
SN 1999dq	−3.93,2.97	Ia-99aa	HVG	SS	···
SN 1999ee	17.65	Ia-91T	···	···	···
SN 1999ek	5.66	Ia-norm	···	···	N
SN 1999gd	−1.12	Ia-norm	···	BL	N
SN 1999gh	4.12,15.89,15.97	Ia-norm	FAINT	CL	N
SN 2000bk	14.84	Ia-norm	···	···	···
SN 2000cn	14.25	Ia-norm	···	···	···
SN 2000cp	2.92,11.70	Ia-norm	···	···	N
SN 2000cu	9.64	Ia-norm	···	···	N
SN 2000cw	4.81	Ia-norm	···	BL	N
SN 2000dg	−5.09,4.66	Ia-norm	···	SS	N
SN 2000dk	1.00,10.84	Ia-norm	FAINT	CL	N
SN 2000dm	−1.63,8.18	Ia-norm	HVG	BL	N
SN 2000dn	−0.94,16.38	Ia-norm	LVG	BL	N
SN 2000dr	6.78	Ia-norm	···	···	N
SN 2000dx	−9.26	Ia-norm	···	···	···
SN 2000ey	7.90	Ia-norm	···	···	HV
SN 2000fa	−8.25,6.86	Ia-norm	···	···	N
SN 2001E	15.01	Ia-norm	···	···	···
SN 2001G	11.57	Ia-norm	···	···	···
SN 2001N	13.05	Ia-norm	···	···	···
SN 2001V	15.86	Ia-norm	···	···	···
SN 2001ay	6.79	Ia-norm	···	···	HV
SN 2001az	−3.24	Ia-norm	···	···	N
SN 2001bf	1.22	Ia-norm	···	···	N
SN 2001bg	13.70,18.91	Ia-norm	HVG*	···	···
SN 2001br	3.47,3.48	Ia-norm	···	BL	HV
SN 2001bp	0.51	Ia-norm	···	···	···

Continued on Next Page...

Table 3.5 — Continued

SN Name	Phase[a]	SNID (Sub)Type[b]	Benetti Type[c]	Branch Type[d]	Wang Type[e]
SN 2001cp	1.39,18.00	Ia-norm	···	···	N
SN 2001da	−1.12,9.72	Ia-norm	HVG	BL	N
SN 2001dl	13.84	Ia-norm	···	···	···
SN 2001dt	13.60	Ia-norm	···	···	···
SN 2001dw	11.06	Ia-norm	···	···	···
SN 2001eh	−5.63,−4.53,3.26	Ia-99aa	···	SS	···
SN 2001en	10.09,14.72	Ia-norm	HVG	···	···
SN 2001ep	2.83,4.99,5.97,7.85	Ia-norm	HVG	CL	N
SN 2001ex	−1.82	Ia-91bg	···	···	···
SN 2001fe	−0.99	Ia-norm	···	SS	N
SN 2001fh	5.93,7.84	Ia-norm	···	···	N
SN 2002G	19.31	Ia-norm	···	···	···
SN 2002aw	2.10,15.84	Ia-norm	···	···	N
SN 2002bf	2.97,6.90	Ia-norm	···	BL	HV
SN 2002bo	−11.94,−1.08,15.99	Ia-norm	HVG	···	HV
SN 2002bz	4.92	Ia-norm	···	CL	N
SN 2002cd	1.10,17.89	Ia-norm	LVG	···	HV
SN 2002cf	−0.75,15.95	Ia-91bg	···	CL	···
SN 2002ck	3.64	Ia-norm	···	CN	N
SN 2002cr	−6.78	Ia-norm	···	···	···
SN 2002cs	−7.76	Ia-norm	···	···	···
SN 2002cu	−5.28,16.62	Ia-norm	···	···	···
SN 2002db	9.21	Ia-norm	···	···	HV
SN 2002de	−0.32,8.37	Ia-norm	HVG	CL	HV
SN 2002df	6.55	Ia-norm	···	···	···
SN 2002dj	−7.98	Ia-norm	···	···	···
SN 2002dk	−1.23	Ia-91bg	···	CL	···
SN 2002dp	15.55	Ia-norm	···	···	···
SN 2002eb	1.68	Ia-norm	···	···	N
SN 2002ef	4.70	Ia-norm	···	BL	N
SN 2002eh	6.88	Ia-norm	···	···	···
SN 2002el	11.82	Ia-norm	···	···	···
SN 2002er	−4.58,5.26	Ia-norm	···	···	HV
SN 2002et	11.92	Ia-norm	···	···	···
SN 2002eu	−0.06,9.38	Ia-norm	HVG?	CL	N
SN 2002fb	0.98,18.60	Ia-91bg	···	CL	···
SN 2002fk	7.74	Ia-norm	···	···	N
SN 2002ha	−0.85,4.93,7.89	Ia-norm	LVG	BL	N
SN 2002hd	6.48,12.72	Ia-norm	HVG*	···	N
SN 2002he	−5.91,−1.03,0.29,3.22	Ia-norm	HVG	BL	HV
SN 2002hu	−5.81	Ia-99aa	···	···	···
SN 2002hw	−6.27	Ia-norm	···	···	···
SN 2002jg	10.11	Ia-norm	···	···	···
SN 2002jy	11.86	Ia-norm	···	···	···
SN 2002kf	6.81	Ia-norm	···	···	N
SN 2003D	9.98	Ia-norm	···	···	N
SN 2003K	13.43	Ia-91T	···	···	···
SN 2003U	−2.55	Ia-norm	···	BL	N
SN 2003W	−5.06,18.14	Ia-norm	···	···	···
SN 2003Y	−1.74	Ia-91bg	···	···	···
SN 2003ai	7.25	Ia-norm	···	···	N
SN 2003cq	−0.15	Ia-norm	···	···	HV
SN 2003du	17.61	Ia-norm	···	···	···
SN 2003fa	−8.16	Ia-99aa	···	···	···
SN 2003gn	−5.38	Ia-norm	···	···	···
SN 2003gt	−5.07,17.61	Ia-norm	···	···	···
SN 2003he	2.71,8.54	Ia-norm	LVG	BL	N
SN 2003hs	−5.49	Ia-norm	···	···	···
SN 2003iv	1.76,6.58	Ia-norm	HVG?	CL	N

Continued on Next Page...

Table 3.5 — Continued

SN Name	Phase[a]	SNID (Sub)Type[b]	Benetti Type[c]	Branch Type[d]	Wang Type[e]
SN 2003kf	−7.50	Ia-norm	···	···	···
SN 2004E	5.26	Ia-norm	···	···	N
SN 2004S	8.26	Ia-norm	···	···	N
SN 2004as	−4.36	Ia-norm	···	BL	HV
SN 2004bd	10.76	Ia-norm	···	···	···
SN 2004bg	10.34	Ia-norm	···	···	···
SN 2004bk	6.13	Ia-norm	···	···	HV
SN 2004bl	4.61,19.38	Ia-norm	HVG?	CN	N
SN 2004br	3.50	Ia-99aa	···	···	···
SN 2004bv	−7.06,9.77	Ia-91T	···	···	···
SN 2004bw	−10.03,6.59	Ia-norm	···	···	N
SN 2004dt	−6.46,1.38,18.00	Ia-norm	HVG	BL	HV
SN 2004ef	−5.52,8.05	Ia-norm	···	···	HV
SN 2004eo	−5.57,13.19	Ia-norm	···	···	···
SN 2004ey	−7.58,18.80	Ia-norm	···	···	···
SN 2004fu	−2.65,2.43	Ia-norm	HVG?	BL	HV
SN 2004fz	−5.18,17.56	Ia-norm	···	···	···
SN 2004gs	0.44	Ia-norm	···	CL	N
SN 2004gu	−4.65	Ia-norm	···	···	···
SN 2005A	5.55	Ia-norm	···	···	HV
SN 2005M	−1.41,8.23,9.23	Ia-norm	HVG	···	N
SN 2005W	0.59	Ia-norm	···	BL	N
SN 2005ag	0.53	Ia-norm	···	···	N
SN 2005am	4.47,6.37	Ia-norm	FAINT	BL	N
SN 2005ao	−1.29,0.52	Ia	···	SS	···
SN 2005bc	1.55,7.37	Ia-norm	LVG	CL	N
SN 2005be	10.96,16.71	Ia-norm	···	···	···
SN 2005bl	18.07	Ia-91bg	···	···	···
SN 2005cf	−10.94,−2.11,−1.19,18.69	Ia-norm	HVG	CN	N
SN 2005de	−0.75,10.10	Ia-norm	HVG	BL	N
SN 2005dm	5.23	Ia-91bg	···	···	···
SN 2005dv	−0.57	Ia-norm	···	BL	HV
SN 2005el	−6.70,1.22,8.09	Ia-norm	LVG	CN	N
SN 2005er	−0.26,1.67,5.64	Ia-91bg	HVG?	CL	···
SN 2005eq	−6.01,−2.98,0.66	Ia-99aa	HVG	···	···
SN 2005ew	18.23	Ia-norm	···	···	···
SN 2005eu	−9.06,−5.46	Ia-norm	···	···	···
SN 2005hj	7.51	Ia-norm	···	···	N
SN 2005iq	−5.86	Ia-norm	···	···	···
SN 2005kc	10.28,12.25	Ia-norm	···	···	···
SN 2005ke	7.80,9.83,14.79	Ia-91bg	···	···	···
SN 2005ki	1.62,8.35	Ia-norm	LVG	BL	N
SN 2005mc	6.64	Ia-norm	···	···	N
SN 2005lz	0.58	Ia-norm	···	BL	N
SN 2005ms	−1.88,14.62	Ia-norm	HVG	···	N
SN 2005na	0.03,1.03,17.49	Ia-norm	HVG	···	N
SN 2006D	3.70,16.70	Ia-norm	···	BL	N
SN 2006H	7.01	Ia-91bg	···	···	···
SN 2006N	−1.89,−0.90,11.91	Ia-norm	HVG	BL	N
SN 2006S	−3.93,2.99,18.45	Ia-99aa	LVG	···	···
SN 2006X	3.15	Ia-norm	···	BL	HV
SN 2006ac	7.96	Ia-norm	···	···	HV
SN 2006ak	8.43	Ia-norm	···	···	N
SN 2006ax	−10.07	Ia-norm	···	···	···
SN 2006bq	6.97,14.55,14.64	Ia-norm	HVG*	···	HV
SN 2006br	10.62	Ia-norm	···	···	···
SN 2006bt	−5.30,−4.53,2.27	Ia-norm	HVG	CL	N
SN 2006bu	4.22	Ia-norm	···	CN	N
SN 2006bw	8.90	Ia-norm	···	···	N

Continued on Next Page...

Table 3.5 — Continued

SN Name	Phase[a]	SNID (Sub)Type[b]	Benetti Type[c]	Branch Type[d]	Wang Type[e]
SN 2006bz	−2.44	Ia-91bg	···	CL	···
SN 2006cc	17.67	Ia-norm	···	···	···
SN 2006cf	6.28,11.09,18.69	Ia-norm	···	···	N
SN 2006cj	3.43	Ia-norm	···	SS	N
SN 2006cm	−1.15,6.77	Ia-norm	···	···	N
SN 2006cp	−5.30	Ia-norm	···	···	···
SN 2006cq	2.00	Ia-norm	···	···	N
SN 2006cs	2.28	Ia-91bg	···	CL	···
SN 2006cz	1.12	Ia-99aa	···	···	···
SN 2006dm	−7.90,8.73,14.61	Ia-norm	HVG	···	N
SN 2006ef	3.20	Ia-norm	···	BL	HV
SN 2006gr	−8.70	Ia-norm	···	···	···
SN 2006ej	−3.70,5.09	Ia-norm	HVG	BL	HV
SN 2006em	4.16	Ia-91bg	···	···	···
SN 2006en	8.55	Ia-norm	···	···	N
SN 2006eu	10.17,16.02	Ia-norm	HVG	···	···
SN 2006et	3.29,9.14	Ia-norm	LVG	SS	N
SN 2006ev	10.54,16.36	Ia-norm	HVG?	···	···
SN 2006gt	3.08	Ia-91bg	···	···	···
SN 2006gj	4.70	Ia-norm	···	CL	N
SN 2006ke	2.36,8.38	Ia-91bg	HVG?	···	···
SN 2006kf	−8.96,−3.05,17.37	Ia-norm	···	CL	N
SN 2006le	−8.69,11.92	Ia-norm	···	···	···
SN 2006lf	−6.30,14.29	Ia-norm	···	···	···
SN 2006mo	12.46	Ia-norm	···	···	···
SN 2006mp	5.66	Ia-99aa	···	···	···
SN 2006or	−2.79,4.93	Ia-norm	···	BL	N
SN 2006os	8.61	Ia-norm	···	···	N
SN 2006qo	−11.08	Ia	···	···	···
SN 2006sr	−2.34,2.69	Ia-norm	HVG	BL	HV
SN 2007A	2.37,15.07	Ia-norm	LVG?	CN	N
SN 2007F	−9.35,3.23	Ia-norm	···	SS	N
SN 2007N	0.44	Ia-91bg	···	CL	···
SN 2007O	−0.33	Ia-norm	···	SS	N
SN 2007S	5.18	Ia-norm	···	···	N
SN 2007af	−1.25,2.84,3.81	Ia-norm	HVG	BL	N
SN 2007aj	10.75	Ia-norm	···	···	···
SN 2007al	3.39	Ia-91bg	···	···	···
SN 2007ap	9.37	Ia-norm	···	···	N
SN 2007au	16.11	Ia-norm	···	···	···
SN 2007ax	14.93	Ia-91bg	···	···	···
SN 2007ba	2.14,5.18,8.06	Ia-91bg	···	···	···
SN 2007bc	0.61	Ia-norm	···	CL	N
SN 2007bd	−5.79,9.70	Ia-norm	···	···	N
SN 2007bj	14.25	Ia	···	···	···
SN 2007bm	−7.79,15.03,19.96	Ia-norm	···	···	···
SN 2007bz	1.65	Ia-norm	···	···	HV
SN 2007ca	−11.14,16.46	Ia-norm	···	···	···
SN 2007cg	16.17	Ia-norm	···	···	···
SN 2007ci	−6.57,−1.71,13.99	Ia-norm	···	CL	N
SN 2007co	−4.09,0.85,9.55	Ia-norm	LVG	BL	N
SN 2007cq	−5.82,7.84,15.57	Ia	···	···	···
SN 2007cs	12.15	Ia-norm	···	···	···
SN 2007fb	1.95,14.63	Ia-norm	LVG?	···	N
SN 2007fr	−5.83,−1.25	Ia-norm	···	CL	N
SN 2007fs	5.03	Ia-norm	···	···	N
SN 2007ge	12.53	Ia-norm	···	···	···
SN 2007gi	−7.31,−0.35,6.61	Ia-norm	HVG?	···	HV
SN 2007gk	−1.72,19.65	Ia-norm	HVG?	BL	HV

Continued on Next Page...

Table 3.5 — Continued

SN Name	Phase[a]	SNID (Sub)Type[b]	Benetti Type[c]	Branch Type[d]	Wang Type[e]
SN 2007hj	−1.23,12.53	Ia-norm	FAINT	CL	HV
SN 2007kk	7.15	Ia-norm	···	···	HV
SN 2007le	−10.31,−9.40,7.43,16.39,17.37	Ia-norm	HVG	···	HV
SN 2007s1[f]	−1.23	Ia-norm	···	BL	N
SN 2007on	−3.01,−3.00,15.45	Ia-norm	···	CL	N
SN 2007qe	−6.54,6.23,16.00	Ia-norm	···	···	HV
SN 2007ux	5.59	Ia-norm	···	···	N
SN 2008C	15.68	Ia-norm	···	···	···
SN 2008Q	6.46,19.25	Ia-norm	···	···	N
SN 2008Z	−2.29,9.99	Ia-99aa	···	···	···
SN 2008ar	−8.87,2.83	Ia-norm	···	CN	N
SN 2008bt	−1.08,10.97	Ia-91bg	···	CL	···
SN 2008cl	4.24	Ia-norm	···	CL	HV
SN 2008s1[g]	−6.36,−4.40,−3.42,0.49,4.40,5.38,15.37	Ia-norm	···	BL	N
SN 2008dx	2.46,7.33,10.28	Ia-91bg	FAINT*	CL	···
SN 2008dt	9.27	Ia-norm	···	···	HV
SN 2008ec	−0.24,5.70,12.51	Ia-norm	LVG	CL	N
SN 2008ei	3.29,9.13	Ia-norm	HVG*	BL	HV
SN 2008s5[h]	1.26,8.96,15.76	Ia	LVG*	···	···
SN 2008hs	−7.94	Ia-norm	···	···	···

[a]Phases of spectra are in rest-frame days using the heliocentric redshift and photometry reference presented in table 1 of Silverman et al. (submitted).
[b]Spectral classification using the SuperNova IDentification code (SNID; Blondin & Tonry 2007) taken from section 5 of Silverman et al. (submitted).
[c]Classification based on the velocity gradient of the Si II λ6355 line (Benetti et al. 2005). 'HVG' = high velocity gradient; 'LVG' = low velocity gradient; 'FAINT' = faint/underluminous. Classifications marked with a '?' are uncertain since light-curve shape information is unavailable. Classifications marked with a '*' use the MLCS2k2 Δ parameter (Jha et al. 2007) as a proxy for Δm_{15}.
[d]Classification based on the (pseduo-)equivalent widths of the Si II λ6355 and Si II λ5972 lines (Branch et al. 2009). 'CN' = core normal; 'BL' = broad line; 'CL' = cool; 'SS' = shallow silicon.
[e]Classifcation based on the velocity of the Si II λ6355 line (Wang et al. 2009a). 'HV' = high velocity; 'N' = normal.
[f]Also known as SNF20071021-000.
[g]Also known as SNF20080514-002.
[h]Also known as SNF20080909-030.

3.7.2 Measured Values

Tables 3.6 through 3.14 present the measured values for each feature (and their uncertainties), along with their rest-frame spectral ages.

Table 3.6: Measured Values for Ca II H&K

SN Name	Phase[a]	F_b[b]	F_r[b]	pEW[c]	ΔpEW[c,d]	v[e]	a	FWHM[c]
SN 1989M	2.49	27.45 (0.30)	43.18 (0.17)	133.6 (8.9)	25.6 (29.0)	16.32 (0.16)	0.749 (0.028)	179.1 (2.4)
SN 1989M	3.48	35.28 (0.33)	55.18 (0.42)	131.5 (8.8)	26.0 (28.9)	16.00 (0.16)	0.749 (0.029)	177.1 (2.4)
SN 1991T	6.80	26.79 (0.40)	29.81 (0.52)	49.7 (2.9)	-48.7 (27.7)	···	···	···
SN 1991bg	0.14	5.84 (0.16)	14.95 (0.33)	115.0 (5.1)	0.4 (28.0)	12.96 (0.16)	0.716 (0.050)	175.0 (6.1)
SN 1994D	−12.31	15.84 (0.21)	23.91 (0.15)	183.4 (10.9)	16.3 (29.6)	23.46 (0.16)	0.801 (0.020)	235.6 (2.4)
SN 1994D	−11.31	23.25 (0.41)	27.06 (0.26)	186.2 (11.1)	24.4 (29.7)	24.44 (0.16)	0.836 (0.007)	231.7 (2.4)
SN 1994D	−9.32	59.59 (0.47)	60.09 (0.40)	174.7 (9.6)	22.9 (29.2)	23.47 (0.16)	0.700 (0.007)	253.6 (2.4)
SN 1994D	−7.67	74.40 (0.73)	74.88 (0.68)	162.1 (8.8)	18.0 (28.9)	19.11 (0.16)	0.659 (0.008)	253.6 (2.4)
SN 1994D	−6.32	107.22 (1.00)	106.98 (0.99)	134.0 (7.2)	-4.2 (28.5)	···	···	···
SN 1994D	−5.32	96.89 (1.01)	105.74 (0.88)	126.7 (6.9)	-7.3 (28.4)	18.14 (0.16)	0.567 (0.016)	229.7 (2.4)
SN 1994D	−3.87	127.51 (0.54)	156.59 (1.04)	91.7 (5.6)	-36.6 (28.1)	18.76 (0.16)	0.495 (0.011)	195.7 (2.4)
SN 1994D	−3.33	126.36 (0.44)	154.68 (1.13)	93.5 (5.7)	-32.7 (28.1)	18.60 (0.16)	0.502 (0.012)	193.7 (2.4)
SN 1994Q	9.68	1.44 (0.06)	2.46 (0.09)	119.5 (8.0)	25.4 (28.7)	18.45 (0.16)	0.676 (0.020)	205.9 (2.4)

Continued on Next Page...

Table 3.6 — Continued

SN Name	Phase[a]	F_b[b]	F_r[b]	pEW[c]	ΔpEW[c,d]	v[e]	a	FWHM[c]
SN 1994S	1.11	21.38 (0.59)	25.76 (0.56)	112.4 (7.2)	0.6 (28.5)	...	...	...
SN 1995D	3.84	36.68 (0.26)	44.03 (0.54)	95.0 (6.7)	-9.6 (28.4)	11.72 (0.16)	0.573 (0.009)	172.9 (2.4)
SN 1995E	−2.46	1.00 (0.03)	1.55 (0.04)	112.9 (7.4)	-10.2 (28.5)	16.33 (0.16)	0.604 (0.019)	181.9 (2.4)
SN 1997Y	1.27	9.16 (0.10)	10.59 (0.17)	121.5 (8.2)	10.2 (28.7)	13.22 (0.16)	0.671 (0.009)	175.2 (2.4)
SN 1997bp	5.49	5.52 (0.39)	14.13 (0.33)	150.0 (9.7)	49.0 (29.2)	19.19 (0.16)	0.774 (0.034)	206.3 (2.4)
SN 1997do	−5.67	8.12 (0.12)	10.60 (0.16)	188.1 (10.9)	52.7 (29.6)	24.87 (0.16)	0.810 (0.015)	241.6 (2.4)
SN 1998bp	18.87	0.09 (0.01)	0.35 (0.02)	108.6 (8.2)	17.9 (28.7)	10.03 (0.16)	0.788 (0.056)	132.1 (2.2)
SN 1998dh	18.77	2.13 (0.15)	3.39 (0.10)	99.3 (7.4)	8.8 (28.5)	13.66 (0.16)	0.774 (0.034)	122.9 (2.4)
SN 1998dk	−7.24	1.77 (0.10)	5.58 (0.19)	214.4 (12.0)	72.2 (30.1)	25.94 (0.16)	0.861 (0.034)	266.5 (2.4)
SN 1998dk	−0.54	6.73 (0.08)	9.58 (0.20)	138.4 (8.7)	21.7 (28.9)	19.05 (0.16)	0.702 (0.011)	193.4 (2.4)
SN 1998dm	−5.61	8.13 (0.09)	9.84 (0.26)	110.3 (6.9)	-24.9 (28.4)	12.66 (0.16)	0.558 (0.007)	196.7 (2.4)
SN 1998dm	14.22	2.71 (0.07)	3.74 (0.11)	77.6 (6.1)	-12.8 (28.2)	11.84 (0.16)	0.646 (0.058)	113.3 (2.4)
SN 1998dx	5.13	0.83 (0.03)	1.16 (0.02)	78.1 (5.8)	-23.7 (28.1)	11.78 (0.16)	0.501 (0.019)	170.7 (2.3)
SN 1998ec	11.86	0.76 (0.02)	1.56 (0.03)	88.2 (6.5)	-3.7 (28.3)	14.85 (0.16)	0.597 (0.023)	151.0 (2.4)
SN 1998ef	−8.62	5.13 (0.15)	6.68 (0.06)	147.1 (9.0)	-1.4 (29.0)	21.97 (0.16)	0.770 (0.010)	206.3 (2.4)
SN 1998es	0.28	23.76 (0.32)	24.14 (0.66)	91.0 (5.9)	-23.2 (28.2)	...	...	...
SN 1999aa	−10.58	3.55 (0.09)	3.67 (0.08)	47.0 (3.7)	-111.0 (27.8)	...	...	...
SN 1999aa	0.24	3.78 (0.07)	3.48 (0.05)	91.2 (5.9)	-23.1 (28.2)	...	...	...
SN 1999aa	14.04	7.38 (0.22)	11.66 (0.17)	75.4 (3.7)	-15.0 (27.8)	12.19 (0.16)	0.532 (0.016)	142.9 (6.0)
SN 1999aa	17.04	2.61 (0.08)	3.96 (0.06)	68.6 (5.4)	-21.4 (28.1)	11.69 (0.16)	0.557 (0.027)	130.1 (2.4)
SN 1999ac	−0.89	16.50 (0.19)	19.85 (0.26)	99.1 (7.5)	-18.7 (28.6)	14.45 (0.16)	0.677 (0.028)	156.5 (2.4)
SN 1999cp	4.91	15.19 (0.13)	20.44 (0.20)	82.8 (6.2)	-19.4 (28.3)	11.02 (0.16)	0.580 (0.016)	160.5 (2.4)
SN 1999cw	14.79	5.97 (0.21)	10.87 (0.18)	76.8 (6.3)	-13.4 (28.3)	14.98 (0.16)	0.648 (0.013)	128.4 (2.4)
SN 1999dg	15.08	0.60 (0.04)	0.92 (0.05)	74.7 (5.9)	-15.4 (28.2)	12.68 (0.16)	0.588 (0.087)	131.1 (2.4)
SN 1999dk	−6.60	8.03 (0.12)	9.70 (0.14)	184.1 (10.7)	44.7 (29.6)	21.00 (0.16)	0.798 (0.007)	234.5 (2.4)
SN 1999dk	17.06	3.10 (0.06)	5.77 (0.08)	90.4 (7.0)	0.4 (28.4)	14.80 (0.16)	0.695 (0.019)	132.0 (2.4)
SN 1999dq	−3.93	9.72 (0.23)	10.08 (0.19)	65.8 (4.2)	-62.7 (27.9)	...	...	...
SN 1999dq	2.97	9.19 (0.11)	9.55 (0.11)	96.6 (6.3)	-10.1 (28.3)	18.24 (0.16)	0.545 (0.016)	195.2 (2.4)
SN 1999ee	17.65	1.88 (0.27)	4.54 (0.20)	122.5 (9.0)	32.4 (29.0)	15.80 (0.20)	0.777 (0.048)	158.2 (2.4)
SN 1999gh	15.89	0.92 (0.07)	1.64 (0.06)	86.0 (6.3)	-4.0 (28.3)	11.41 (0.16)	0.597 (0.021)	146.9 (2.4)
SN 2000cn	14.25	0.26 (0.02)	0.42 (0.02)	106.5 (7.6)	16.1 (28.6)	12.48 (0.16)	0.723 (0.054)	152.4 (2.4)
SN 2000cp	2.92	0.26 (0.01)	0.49 (0.02)	145.4 (10.4)	38.6 (29.4)	16.68 (0.16)	0.891 (0.039)	172.1 (2.4)
SN 2000cw	4.81	0.83 (0.05)	1.45 (0.03)	145.9 (9.1)	43.5 (29.0)	16.75 (0.16)	0.723 (0.011)	213.6 (2.4)
SN 2000dg	−5.09	0.97 (0.02)	1.18 (0.03)	82.6 (5.3)	-50.5 (28.1)	...	...	...
SN 2000dg	4.66	0.79 (0.03)	0.95 (0.03)	71.4 (5.5)	-31.3 (28.1)	...	...	...
SN 2000dk	1.00	3.02 (0.07)	5.54 (0.06)	99.4 (7.5)	-12.6 (28.5)	13.52 (0.16)	0.670 (0.017)	161.2 (2.4)
SN 2000dk	10.84	1.16 (0.03)	2.00 (0.04)	93.4 (6.6)	0.6 (28.3)	13.03 (0.16)	0.626 (0.050)	157.3 (2.4)
SN 2000dm	−1.63	3.27 (0.07)	4.27 (0.07)	98.9 (6.5)	-21.3 (28.3)	...	...	...
SN 2000dm	8.18	2.11 (0.04)	2.70 (0.04)	79.3 (5.8)	-16.9 (28.2)	...	...	...
SN 2000dn	−0.94	1.38 (0.03)	1.94 (0.03)	127.1 (9.0)	9.1 (29.0)	...	...	...
SN 2000dn	16.38	0.35 (0.02)	0.45 (0.01)	89.6 (6.8)	-0.4 (28.4)	10.99 (0.16)	0.690 (0.055)	139.5 (2.4)
SN 2000dx	−9.26	0.21 (0.03)	0.45 (0.03)	182.5 (10.7)	31.0 (29.6)	26.10 (0.16)	0.720 (0.025)	269.8 (2.4)
SN 2000ey	7.90	2.79 (0.05)	5.04 (0.19)	90.6 (6.4)	-6.0 (28.3)	15.01 (0.16)	0.601 (0.033)	164.6 (2.4)
SN 2000fa	−8.25	1.67 (0.04)	2.01 (0.04)	166.4 (9.7)	19.6 (29.2)	22.67 (0.16)	0.782 (0.021)	191.9 (2.4)
SN 2000fa	6.86	1.76 (0.05)	2.70 (0.05)	123.9 (8.2)	25.5 (28.7)	...	...	...
SN 2001E	15.01	0.40 (0.09)	0.70 (0.06)	100.5 (8.5)	10.4 (28.8)	15.75 (0.16)	0.751 (0.038)	143.2 (2.4)
SN 2001G	11.57	3.92 (0.05)	6.00 (0.08)	79.2 (6.3)	-12.9 (28.3)	12.39 (0.16)	0.620 (0.036)	139.7 (2.4)
SN 2001V	15.86	4.96 (0.08)	7.02 (0.21)	74.9 (6.0)	-15.1 (28.2)	12.02 (0.16)	0.623 (0.028)	122.2 (2.4)
SN 2001ay	6.79	1.19 (0.04)	1.60 (0.04)	84.9 (5.6)	-13.6 (28.1)	18.64 (0.16)	0.498 (0.009)	188.3 (2.4)
SN 2001az	−3.24	1.02 (0.05)	1.25 (0.03)	113.0 (7.3)	-13.0 (28.5)	...	...	...
SN 2001bg	13.70	4.51 (0.09)	8.35 (0.14)	86.6 (6.5)	-4.1 (28.3)	13.74 (0.16)	0.628 (0.029)	145.0 (2.4)
SN 2001br	3.47	1.41 (0.13)	2.19 (0.08)	114.6 (8.4)	9.1 (28.8)	16.94 (0.16)	0.760 (0.040)	166.6 (2.4)
SN 2001br	3.48	1.23 (0.16)	2.05 (0.11)	104.4 (8.0)	-1.1 (28.7)	16.33 (0.16)	0.730 (0.056)	176.4 (2.4)
SN 2001bp	0.51	0.30 (0.03)	0.36 (0.03)	89.2 (6.8)	-24.2 (28.4)	...	...	...
SN 2001cp	1.39	1.29 (0.05)	1.42 (0.03)	106.0 (7.4)	-4.9 (28.5)	13.73 (0.19)	0.626 (0.012)	174.1 (2.4)
SN 2001da	−1.12	3.07 (0.10)	4.77 (0.10)	162.8 (10.5)	44.3 (29.5)	20.04 (0.16)	0.857 (0.009)	202.5 (2.4)
SN 2001da	9.72	1.26 (0.03)	3.00 (0.05)	128.0 (8.1)	34.0 (28.7)	...	...	...
SN 2001dl	13.84	0.44 (0.04)	0.54 (0.05)	75.2 (6.0)	-15.4 (28.2)	...	...	...
SN 2001dw	11.06	0.14 (0.03)	0.31 (0.02)	105.3 (7.8)	12.8 (28.6)	14.13 (0.16)	0.738 (0.041)	134.6 (2.4)
SN 2001eh	−5.63	9.50 (0.44)	8.63 (0.45)	83.1 (5.7)	-52.1 (28.1)	18.73 (0.16)	0.510 (0.019)	167.8 (2.4)
SN 2001eh	−4.53	2.16 (0.07)	2.14 (0.05)	75.5 (5.3)	-55.3 (28.0)	18.42 (0.16)	0.483 (0.017)	177.4 (2.4)
SN 2001eh	3.26	1.41 (0.03)	1.41 (0.03)	99.8 (7.0)	-6.2 (28.4)	17.65 (0.16)	0.630 (0.022)	181.3 (2.4)
SN 2001en	10.09	2.47 (0.06)	4.59 (0.11)	81.1 (5.7)	-12.5 (28.1)	11.97 (0.16)	0.524 (0.026)	177.2 (2.4)
SN 2001ep	2.83	4.92 (0.09)	9.21 (0.28)	100.1 (7.8)	-7.0 (28.6)	13.92 (0.16)	0.729 (0.016)	148.1 (2.4)
SN 2001ep	7.85	3.23 (0.09)	5.70 (0.13)	111.4 (8.2)	14.7 (28.7)	12.98 (0.16)	0.773 (0.031)	150.0 (2.4)
SN 2001ex	−1.82	0.55 (0.03)	0.73 (0.02)	82.7 (6.3)	-38.2 (28.3)	11.03 (0.16)	0.613 (0.024)	152.0 (2.4)
SN 2001fe	−0.99	11.31 (0.11)	12.10 (0.19)	86.5 (5.9)	-31.7 (28.2)	...	...	...
SN 2001fh	5.93	0.51 (0.09)	0.84 (0.06)	100.8 (7.6)	0.7 (28.6)	12.98 (0.16)	0.641 (0.035)	173.7 (2.4)
SN 2002aw	2.10	2.52 (0.13)	3.06 (0.16)	79.9 (6.5)	-29.1 (28.3)	11.89 (0.16)	0.597 (0.016)	157.9 (2.4)
SN 2002bf	6.90	0.90 (0.25)	2.07 (0.10)	121.1 (9.0)	22.8 (29.0)	16.12 (0.34)	0.736 (0.063)	167.9 (2.4)
SN 2002bo	−11.94	0.66 (0.10)	2.55 (0.08)	160.6 (10.0)	-4.5 (29.3)	26.73 (0.16)	0.766 (0.053)	217.1 (2.4)
SN 2002bo	−1.08	12.86 (0.61)	19.75 (0.90)	130.2 (8.9)	11.8 (29.0)	17.66 (0.16)	0.761 (0.020)	185.2 (2.4)
SN 2002bo	15.99	2.96 (0.16)	5.91 (0.22)	89.8 (7.0)	-0.2 (28.4)	13.99 (0.16)	0.684 (0.028)	135.4 (2.4)
SN 2002bz	4.92	0.68 (0.04)	0.81 (0.04)	64.8 (5.2)	-37.4 (28.0)	...	...	...
SN 2002cd	1.10	0.62 (0.10)	0.82 (0.08)	138.5 (9.9)	26.7 (29.3)	16.77 (0.16)	0.807 (0.031)	184.1 (2.4)
SN 2002ck	3.64	1.02 (0.05)	1.26 (0.04)	96.5 (7.1)	-8.5 (28.5)	13.27 (0.16)	0.632 (0.014)	153.4 (2.4)
SN 2002cr	−6.78	10.02 (0.20)	11.92 (0.16)	105.4 (6.9)	-34.7 (28.4)	14.62 (0.16)	0.586 (0.007)	172.4 (2.4)
SN 2002cs	−7.76	2.09 (0.07)	2.26 (0.06)	105.3 (6.7)	-39.2 (28.4)	...	...	...
SN 2002db	9.21	0.52 (0.04)	0.89 (0.04)	111.1 (7.6)	16.3 (28.6)	...	...	...
SN 2002de	−0.32	1.40 (0.08)	1.89 (0.08)	120.6 (8.1)	4.6 (28.7)	...	...	...
SN 2002de	8.37	0.86 (0.04)	1.39 (0.03)	85.4 (6.7)	-10.5 (28.4)	12.31 (0.16)	0.631 (0.014)	149.8 (2.4)
SN 2002df	6.55	0.18 (0.03)	0.36 (0.03)	85.5 (6.8)	-13.5 (28.4)	12.62 (0.16)	0.625 (0.020)	145.8 (2.4)

Continued on Next Page...

Table 3.6 — Continued

SN Name	Phase[a]	F_b[b]	F_r[b]	pEW[c]	ΔpEW[c,d]	v[e]	a	FWHM[c]
SN 2002dj	−7.98	7.44 (0.26)	9.36 (0.20)	180.6 (10.7)	35.1 (29.6)	23.21 (0.16)	0.813 (0.008)	229.8 (2.4)
SN 2002eb	1.68	2.88 (0.05)	2.74 (0.03)	101.2 (6.9)	-8.9 (28.4)	···	···	···
SN 2002ef	4.70	0.93 (0.12)	1.45 (0.15)	93.5 (7.4)	-9.1 (28.5)	11.88 (0.16)	0.628 (0.038)	152.3 (2.4)
SN 2002er	−4.58	6.75 (0.06)	9.42 (0.30)	154.4 (9.5)	23.3 (29.1)	18.23 (0.16)	0.743 (0.016)	212.2 (2.4)
SN 2002er	5.26	4.70 (0.08)	9.10 (0.28)	104.8 (7.5)	3.3 (28.6)	13.87 (0.16)	0.676 (0.024)	164.6 (2.4)
SN 2002eu	−0.06	0.80 (0.03)	1.14 (0.03)	108.9 (7.1)	-6.2 (28.4)	···	···	···
SN 2002fk	7.74	23.16 (0.17)	32.00 (0.43)	75.6 (6.2)	-21.3 (28.2)	···	···	···
SN 2002ha	−0.85	6.41 (0.07)	8.18 (0.14)	113.4 (7.6)	-4.3 (28.6)	···	···	···
SN 2002ha	4.93	3.99 (0.05)	6.98 (0.13)	80.2 (6.6)	-22.0 (28.3)	···	···	···
SN 2002ha	7.89	8.74 (0.10)	12.60 (0.18)	73.4 (5.9)	-23.2 (28.2)	11.70 (0.16)	0.563 (0.045)	151.9 (2.4)
SN 2002hd	6.48	1.46 (0.04)	2.27 (0.03)	70.3 (5.7)	-28.8 (28.1)	11.84 (0.16)	0.588 (0.040)	139.1 (2.4)
SN 2002he	0.29	2.16 (0.02)	3.19 (0.02)	99.4 (7.3)	-14.7 (28.5)	14.83 (0.16)	0.635 (0.014)	173.7 (2.4)
SN 2002he	3.22	4.09 (0.05)	6.45 (0.05)	91.4 (6.8)	-14.7 (28.4)	13.90 (0.16)	0.614 (0.024)	167.9 (2.4)
SN 2002hu	−5.81	1.37 (0.02)	1.42 (0.01)	110.1 (7.1)	-25.9 (28.5)	···	···	···
SN 2002hw	−6.27	0.77 (0.02)	1.06 (0.03)	83.7 (6.3)	-54.3 (28.3)	13.22 (0.16)	0.577 (0.022)	151.3 (2.4)
SN 2002jy	11.86	1.65 (0.03)	2.12 (0.03)	97.3 (7.3)	5.4 (28.5)	13.01 (0.16)	0.685 (0.024)	149.1 (2.4)
SN 2002kf	6.81	1.57 (0.02)	3.85 (0.03)	99.7 (7.1)	1.2 (28.4)	14.64 (0.16)	0.622 (0.029)	164.8 (2.4)
SN 2003K	13.43	0.98 (0.07)	1.46 (0.04)	82.1 (6.2)	-8.7 (28.3)	···	···	···
SN 2003U	−2.55	1.33 (0.03)	1.70 (0.03)	129.2 (8.6)	5.7 (28.9)	16.58 (0.16)	0.710 (0.008)	181.2 (2.4)
SN 2003W	−5.06	0.94 (0.03)	1.22 (0.02)	156.6 (9.7)	23.6 (29.2)	23.27 (0.16)	0.816 (0.018)	186.3 (2.4)
SN 2003W	18.14	0.33 (0.01)	1.11 (0.02)	86.5 (6.5)	-3.8 (28.3)	17.72 (0.16)	0.620 (0.027)	143.1 (2.4)
SN 2003ai	7.25	1.08 (0.03)	1.50 (0.03)	86.5 (6.6)	-11.2 (28.3)	11.69 (0.16)	0.601 (0.014)	150.7 (2.4)
SN 2003cq	−0.15	0.81 (0.04)	0.99 (0.03)	145.2 (9.5)	29.7 (29.2)	16.74 (0.16)	0.771 (0.015)	183.9 (2.4)
SN 2003du	17.61	5.91 (0.03)	9.44 (0.05)	68.9 (5.2)	-21.2 (28.0)	11.32 (0.16)	0.564 (0.060)	107.3 (2.4)
SN 2003fa	−8.16	0.91 (0.04)	0.82 (0.03)	63.6 (4.6)	-82.8 (27.9)	···	···	···
SN 2003gn	−5.38	0.25 (0.07)	0.34 (0.04)	180.7 (12.2)	46.4 (30.1)	23.31 (0.16)	0.939 (0.027)	195.3 (2.4)
SN 2003gt	−5.07	4.52 (0.21)	5.48 (0.18)	79.0 (5.1)	-54.0 (28.0)	···	···	···
SN 2003he	2.71	1.81 (0.06)	2.28 (0.05)	121.3 (8.2)	13.9 (28.7)	···	···	···
SN 2003he	8.54	1.44 (0.06)	2.19 (0.05)	115.0 (7.6)	19.4 (28.6)	12.94 (0.16)	0.641 (0.018)	171.6 (2.4)
SN 2003iv	1.76	0.05 (0.00)	0.07 (0.00)	72.6 (5.7)	-37.3 (28.1)	···	···	···
SN 2003iv	6.58	0.20 (0.02)	0.32 (0.02)	71.7 (5.7)	-27.2 (28.1)	···	···	···
SN 2003kf	−7.50	8.91 (0.06)	12.07 (0.23)	144.3 (8.5)	1.0 (28.8)	···	···	···
SN 2004E	5.26	2.75 (0.13)	3.05 (0.08)	72.1 (5.5)	-29.4 (28.1)	···	···	···
SN 2004S	8.26	5.15 (0.02)	10.10 (0.08)	149.1 (9.8)	53.0 (29.2)	18.17 (0.16)	0.806 (0.010)	194.2 (2.4)
SN 2004as	−4.36	0.98 (0.03)	1.36 (0.02)	169.1 (10.4)	38.9 (29.4)	19.98 (0.16)	0.788 (0.011)	228.9 (2.4)
SN 2004bg	10.34	2.21 (0.12)	3.21 (0.08)	88.9 (6.8)	-4.4 (28.4)	11.62 (0.16)	0.662 (0.033)	141.0 (2.4)
SN 2004bk	6.13	2.47 (0.18)	3.37 (0.10)	115.6 (8.2)	15.9 (28.7)	17.52 (0.16)	0.780 (0.020)	158.3 (2.4)
SN 2004bl	4.61	3.94 (0.72)	4.82 (0.38)	117.3 (8.5)	14.4 (28.8)	12.41 (0.16)	0.790 (0.030)	149.4 (2.4)
SN 2004bv	9.77	9.25 (0.31)	13.38 (0.32)	65.3 (5.5)	-28.7 (28.1)	···	···	···
SN 2004bw	6.59	0.94 (0.04)	2.13 (0.06)	95.2 (7.2)	-3.7 (28.5)	···	···	···
SN 2004dt	−6.46	4.95 (0.14)	3.83 (0.11)	112.0 (7.3)	-26.8 (28.5)	22.72 (0.22)	0.624 (0.022)	149.1 (2.4)
SN 2004ef	−5.52	0.88 (0.02)	1.09 (0.02)	173.8 (10.6)	39.0 (29.5)	23.27 (0.16)	0.836 (0.012)	203.7 (2.4)
SN 2004ef	8.05	0.45 (0.09)	0.95 (0.06)	158.1 (9.8)	61.7 (29.2)	19.95 (0.16)	0.746 (0.044)	248.3 (2.4)
SN 2004eo	−5.57	2.12 (0.08)	2.85 (0.08)	122.5 (7.7)	-12.5 (28.6)	17.39 (0.16)	0.623 (0.018)	198.9 (2.4)
SN 2004eo	13.19	0.66 (0.06)	1.02 (0.05)	93.3 (6.6)	2.3 (28.3)	12.52 (0.16)	0.628 (0.045)	165.4 (2.4)
SN 2004ey	−7.58	5.55 (0.04)	6.35 (0.06)	143.6 (8.7)	-0.1 (28.9)	···	···	···
SN 2004ey	18.80	1.09 (0.01)	1.68 (0.02)	83.0 (6.2)	-7.6 (28.2)	12.08 (0.16)	0.635 (0.056)	137.8 (2.4)
SN 2004fu	−2.65	3.12 (0.06)	4.91 (0.10)	177.5 (10.5)	53.7 (29.5)	19.62 (0.16)	0.796 (0.016)	233.8 (2.4)
SN 2004fu	2.43	2.87 (0.08)	5.43 (0.15)	146.1 (9.3)	38.0 (29.1)	16.91 (0.16)	0.756 (0.034)	194.2 (2.4)
SN 2004fz	−5.18	6.14 (0.09)	6.86 (0.09)	90.8 (6.0)	-42.6 (28.2)	···	···	···
SN 2004fz	17.56	0.84 (0.03)	1.50 (0.02)	92.3 (6.6)	2.2 (28.3)	10.37 (0.16)	0.692 (0.046)	112.1 (2.4)
SN 2004gs	0.44	0.62 (0.02)	1.11 (0.03)	79.7 (5.8)	-34.0 (28.2)	···	···	···
SN 2004gu	−4.65	0.21 (0.05)	0.25 (0.02)	92.0 (7.0)	-39.3 (28.4)	···	···	···
SN 2005A	5.55	0.04 (0.03)	0.14 (0.01)	174.9 (13.7)	74.0 (30.8)	···	···	···
SN 2005M	−1.41	3.95 (0.28)	3.82 (0.36)	83.9 (6.0)	-35.6 (28.2)	···	···	···
SN 2005am	4.47	13.38 (0.17)	23.15 (0.26)	94.0 (6.0)	-9.2 (28.2)	···	···	···
SN 2005ao	−1.29	1.20 (0.03)	1.28 (0.03)	104.3 (7.1)	-14.8 (28.5)	···	···	···
SN 2005ao	0.52	0.91 (0.03)	1.10 (0.03)	102.8 (7.2)	-10.6 (28.5)	···	···	···
SN 2005bc	1.55	1.50 (0.05)	2.69 (0.06)	98.6 (7.4)	-11.9 (28.5)	···	···	···
SN 2005bc	7.37	1.00 (0.07)	1.66 (0.05)	90.4 (6.7)	-7.1 (28.4)	···	···	···
SN 2005bl	18.07	0.03 (0.00)	0.06 (0.00)	107.1 (7.6)	16.8 (28.6)	···	···	···
SN 2005cf	−10.94	2.66 (0.15)	6.58 (0.11)	163.0 (10.1)	3.1 (29.3)	25.40 (0.16)	0.773 (0.012)	220.6 (2.4)
SN 2005cf	−2.11	211.51 (4.47)	274.45 (4.95)	162.7 (10.0)	40.8 (29.3)	20.39 (0.16)	0.824 (0.014)	216.6 (2.4)
SN 2005cf	−1.19	42.14 (0.76)	54.74 (0.82)	160.3 (9.9)	41.5 (29.3)	20.39 (0.16)	0.809 (0.016)	218.6 (2.4)
SN 2005de	−0.75	4.41 (0.32)	5.18 (0.22)	144.7 (8.9)	27.3 (29.0)	···	···	···
SN 2005de	10.10	1.43 (0.10)	2.60 (0.09)	85.8 (6.4)	-7.8 (28.3)	11.60 (0.16)	0.622 (0.056)	147.8 (2.4)
SN 2005dv	−0.57	0.64 (0.16)	1.16 (0.10)	118.0 (9.9)	1.2 (29.3)	···	···	···
SN 2005el	−6.70	3.67 (0.08)	4.34 (0.10)	113.6 (7.2)	-26.2 (28.5)	···	···	···
SN 2005el	1.22	5.50 (0.14)	6.91 (0.12)	110.2 (7.2)	-1.2 (28.5)	···	···	···
SN 2005el	8.09	3.44 (0.06)	4.93 (0.08)	79.2 (5.9)	-17.1 (28.2)	···	···	···
SN 2005eq	0.66	1.98 (0.06)	2.14 (0.05)	91.4 (6.2)	-21.7 (28.2)	···	···	···
SN 2005ew	18.23	1.28 (0.04)	3.66 (0.06)	107.1 (7.6)	16.7 (28.6)	13.96 (0.16)	0.697 (0.019)	159.5 (2.4)
SN 2005ki	8.35	2.28 (0.16)	3.57 (0.14)	76.4 (5.9)	-19.6 (28.2)	11.52 (0.16)	0.566 (0.028)	156.9 (2.4)
SN 2005ms	−1.88	5.91 (0.30)	6.94 (0.25)	114.4 (8.1)	-6.8 (28.7)	17.34 (0.16)	0.703 (0.020)	183.4 (2.4)
SN 2005ms	14.62	0.57 (0.04)	1.02 (0.05)	84.4 (6.6)	-5.8 (28.3)	···	···	···
SN 2005na	0.03	2.26 (0.09)	2.58 (0.06)	84.0 (5.8)	-30.9 (28.2)	···	···	···
SN 2005na	1.03	2.98 (0.16)	3.32 (0.12)	97.5 (6.4)	-14.5 (28.3)	···	···	···
SN 2006D	3.70	32.26 (0.60)	45.88 (0.64)	103.5 (7.7)	-1.4 (28.6)	13.07 (0.16)	0.705 (0.017)	152.7 (2.4)
SN 2006D	16.70	1.56 (0.16)	2.03 (0.09)	102.6 (7.5)	12.6 (28.6)	12.90 (0.16)	0.713 (0.037)	136.8 (2.4)
SN 2006N	−1.89	3.62 (0.14)	5.10 (0.09)	102.3 (6.6)	-18.8 (28.3)	···	···	···
SN 2006N	−0.90	3.33 (0.09)	4.94 (0.10)	100.2 (6.5)	-17.7 (28.3)	···	···	···
SN 2006S	−3.93	22.94 (1.61)	25.62 (0.90)	106.5 (7.2)	-22.0 (28.5)	···	···	···

Continued on Next Page...

Table 3.6 — Continued

SN Name	Phase[a]	F_b[b]	F_r[b]	pEW[c]	ΔpEW[c,d]	v[e]	a	FWHM[c]
SN 2006S	2.99	1.12 (0.08)	1.30 (0.05)	116.7 (8.2)	10.0 (28.7)	...	...	...
SN 2006S	18.45	0.27 (0.02)	0.48 (0.02)	80.7 (6.4)	-9.7 (28.3)	...	...	...
SN 2006ac	7.96	1.36 (0.09)	2.50 (0.05)	112.5 (8.1)	15.9 (28.7)	...	...	...
SN 2006ak	8.43	0.38 (0.02)	0.76 (0.02)	126.2 (8.0)	30.3 (28.7)	...	...	...
SN 2006ax	−10.07	1.42 (0.07)	1.89 (0.03)	126.8 (8.2)	-28.7 (28.8)	20.07 (0.16)	0.678 (0.014)	192.8 (2.4)
SN 2006bq	6.97	4.86 (0.09)	8.33 (0.10)	115.7 (7.9)	17.5 (28.7)	18.42 (0.16)	0.662 (0.014)	178.1 (2.4)
SN 2006bq	14.55	0.54 (0.04)	1.24 (0.04)	97.2 (6.9)	6.9 (28.4)	16.84 (0.16)	0.596 (0.020)	160.5 (2.4)
SN 2006bq	14.64	0.46 (0.04)	1.11 (0.03)	95.9 (7.0)	5.7 (28.4)	15.44 (0.16)	0.644 (0.027)	150.7 (2.4)
SN 2006bt	−5.30	0.77 (0.01)	0.96 (0.01)	89.4 (6.2)	-44.5 (28.2)	18.57 (0.16)	0.516 (0.019)	189.9 (2.4)
SN 2006bt	−4.53	0.81 (0.03)	1.06 (0.03)	95.9 (6.7)	-34.9 (28.4)	...	...	...
SN 2006bt	2.27	0.56 (0.02)	0.85 (0.02)	98.7 (6.9)	-9.8 (28.4)	...	...	...
SN 2006bu	4.22	0.20 (0.01)	0.27 (0.01)	103.6 (7.6)	-0.1 (28.6)	...	...	...
SN 2006bz	−2.44	0.27 (0.03)	0.55 (0.04)	122.9 (8.9)	-0.2 (28.9)	...	...	...
SN 2006cf	11.09	0.63 (0.03)	0.81 (0.02)	86.0 (6.8)	-6.6 (28.4)	11.91 (0.16)	0.636 (0.027)	151.7 (2.4)
SN 2006cf	18.69	0.18 (0.02)	0.24 (0.02)	87.5 (7.0)	-3.1 (28.4)	...	...	...
SN 2006cj	3.43	0.35 (0.02)	0.38 (0.02)	99.4 (7.3)	-6.2 (28.5)	...	...	...
SN 2006cp	−5.30	1.85 (0.06)	2.39 (0.05)	169.0 (10.6)	35.1 (29.5)	...	...	...
SN 2006cq	2.00	0.55 (0.04)	0.70 (0.03)	151.8 (9.9)	42.5 (29.3)	16.74 (0.16)	0.809 (0.014)	206.0 (2.3)
SN 2006cz	1.12	0.71 (0.03)	0.82 (0.03)	103.6 (6.6)	-8.1 (28.3)	...	...	...
SN 2006dm	−7.90	0.50 (0.06)	0.71 (0.05)	167.5 (9.8)	22.4 (29.2)	15.97 (0.16)	0.706 (0.037)	258.3 (2.4)
SN 2006dm	8.73	0.93 (0.03)	1.65 (0.03)	71.8 (5.5)	-23.6 (28.1)	12.51 (0.16)	0.552 (0.067)	123.3 (2.4)
SN 2006ef	3.20	3.85 (0.06)	5.72 (0.08)	120.5 (7.6)	14.4 (28.6)	...	...	...
SN 2006gr	−8.70	0.66 (0.04)	0.79 (0.03)	158.3 (9.4)	9.4 (29.1)	23.84 (0.16)	0.738 (0.013)	193.3 (2.4)
SN 2006ej	5.09	1.51 (0.04)	2.15 (0.03)	90.7 (6.3)	-11.2 (28.3)	12.02 (0.16)	0.565 (0.029)	184.3 (2.4)
SN 2006em	4.16	0.11 (0.01)	0.32 (0.01)	123.1 (8.6)	19.2 (28.9)	...	...	...
SN 2006en	8.55	0.85 (0.06)	1.02 (0.06)	55.2 (4.8)	-40.5 (28.0)	...	...	...
SN 2006eu	10.17	0.12 (0.02)	0.23 (0.02)	139.7 (9.0)	46.2 (29.0)	...	...	...
SN 2006et	3.29	1.82 (0.07)	2.27 (0.07)	103.7 (7.3)	-2.3 (28.5)	16.76 (0.16)	0.656 (0.016)	174.1 (2.4)
SN 2006et	9.14	0.87 (0.05)	1.53 (0.05)	108.9 (7.8)	14.1 (28.6)	15.05 (0.16)	0.721 (0.024)	164.4 (2.4)
SN 2006ev	10.54	0.23 (0.03)	0.76 (0.03)	93.8 (6.9)	0.7 (28.4)	...	...	...
SN 2006gt	3.08	0.26 (0.02)	0.41 (0.02)	96.1 (7.4)	-10.4 (28.5)	11.63 (0.16)	0.702 (0.020)	145.5 (2.3)
SN 2006kf	−3.05	1.18 (0.03)	1.62 (0.02)	100.0 (6.5)	-25.2 (28.3)	...	...	...
SN 2006kf	17.37	0.08 (0.01)	0.12 (0.01)	82.8 (6.0)	-7.3 (28.2)	...	...	...
SN 2006lf	−6.30	0.28 (0.02)	0.40 (0.01)	120.4 (7.8)	-17.7 (28.6)	...	...	...
SN 2006le	−8.69	0.90 (0.03)	1.19 (0.02)	158.1 (9.6)	9.3 (29.2)	25.87 (0.16)	0.781 (0.019)	192.6 (2.4)
SN 2006mp	5.66	1.77 (0.02)	1.97 (0.04)	95.4 (6.8)	-5.3 (28.4)	16.14 (0.16)	0.622 (0.020)	175.3 (2.4)
SN 2006or	−2.79	0.50 (0.01)	0.99 (0.03)	134.6 (8.4)	10.3 (28.8)	...	...	...
SN 2006or	4.93	0.14 (0.01)	0.28 (0.02)	73.4 (5.8)	-28.8 (28.2)	...	...	...
SN 2006os	8.61	0.16 (0.03)	0.34 (0.03)	113.4 (8.8)	17.8 (28.9)	...	...	...
SN 2006qo	−11.08	0.18 (0.02)	0.22 (0.02)	76.9 (5.9)	-83.7 (28.2)	...	...	...
SN 2006sr	−2.34	1.26 (0.04)	1.75 (0.03)	122.1 (7.6)	-0.6 (28.6)	...	...	...
SN 2006sr	2.69	1.61 (0.04)	2.48 (0.04)	92.4 (6.8)	-15.0 (28.4)	14.70 (0.16)	0.562 (0.018)	177.7 (2.4)
SN 2007A	2.37	2.99 (0.04)	3.73 (0.09)	91.8 (6.5)	-16.5 (28.3)	11.41 (0.16)	0.572 (0.015)	161.2 (2.4)
SN 2007A	15.07	1.23 (0.05)	1.67 (0.05)	81.5 (6.1)	-8.6 (28.2)	...	...	...
SN 2007F	3.23	2.51 (0.05)	3.02 (0.05)	100.7 (7.2)	-5.4 (28.5)	12.53 (0.16)	0.650 (0.012)	158.3 (2.4)
SN 2007S	5.18	1.76 (0.05)	2.14 (0.05)	82.7 (6.2)	-18.9 (28.2)	17.16 (0.16)	0.567 (0.016)	167.7 (2.4)
SN 2007af	−1.25	36.39 (0.38)	48.50 (0.62)	126.1 (8.1)	7.1 (28.7)	13.44 (0.16)	0.673 (0.016)	173.1 (2.4)
SN 2007af	3.81	27.05 (0.41)	42.78 (0.76)	96.6 (7.2)	-8.1 (28.5)	12.17 (0.16)	0.673 (0.030)	159.1 (2.4)
SN 2007aj	10.75	0.65 (0.02)	0.97 (0.03)	82.1 (6.2)	-10.8 (28.2)	...	...	...
SN 2007al	3.39	0.31 (0.04)	0.64 (0.02)	95.6 (7.3)	-10.1 (28.5)	10.85 (0.16)	0.722 (0.025)	156.1 (2.4)
SN 2007bd	−5.79	1.01 (0.06)	1.31 (0.05)	136.4 (8.7)	0.5 (28.9)	19.04 (0.16)	0.650 (0.019)	207.6 (2.4)
SN 2007bc	0.61	3.37 (0.07)	4.35 (0.06)	109.6 (7.4)	-3.5 (28.5)	13.11 (0.16)	0.617 (0.019)	166.5 (2.4)
SN 2007bj	14.25	2.49 (0.10)	3.30 (0.07)	77.3 (6.3)	-13.1 (28.3)	...	...	...
SN 2007bm	−7.79	5.66 (0.25)	7.62 (0.29)	103.4 (6.6)	-41.3 (28.3)	...	...	...
SN 2007ca	−11.14	0.86 (0.12)	1.36 (0.08)	139.1 (8.8)	-21.8 (28.9)	23.28 (0.16)	0.715 (0.022)	218.9 (2.4)
SN 2007ca	16.46	0.73 (0.08)	1.15 (0.07)	84.1 (6.4)	-5.9 (28.3)	...	...	...
SN 2007ci	−6.57	1.86 (0.08)	2.44 (0.08)	75.4 (5.5)	-63.8 (28.1)	...	...	...
SN 2007ci	−1.71	2.50 (0.06)	3.58 (0.07)	70.6 (5.3)	-49.9 (28.1)	...	...	...
SN 2007ci	13.99	0.40 (0.03)	0.70 (0.04)	87.5 (6.6)	-3.0 (28.3)	12.30 (0.16)	0.711 (0.053)	106.1 (2.4)
SN 2007co	−4.09	0.91 (0.06)	1.47 (0.05)	169.9 (10.5)	40.7 (29.5)	20.99 (0.19)	0.834 (0.033)	206.4 (2.4)
SN 2007co	0.85	1.16 (0.03)	1.85 (0.04)	146.6 (9.7)	34.1 (29.2)	18.79 (0.16)	0.831 (0.024)	183.1 (2.4)
SN 2007co	9.55	0.43 (0.02)	1.01 (0.02)	116.3 (8.4)	22.1 (28.8)	15.35 (0.16)	0.750 (0.017)	161.6 (2.4)
SN 2007cq	−5.82	1.40 (0.05)	1.83 (0.04)	58.5 (4.3)	-77.5 (27.9)	13.18 (0.16)	0.415 (0.013)	150.1 (2.4)
SN 2007fb	1.95	3.67 (0.24)	5.14 (0.13)	101.6 (7.2)	-7.8 (28.5)	13.55 (0.16)	0.630 (0.007)	165.0 (2.4)
SN 2007fr	−5.83	0.23 (0.02)	0.32 (0.02)	88.0 (6.9)	-48.1 (28.4)	13.11 (0.16)	0.668 (0.012)	131.3 (2.3)
SN 2007fr	−1.25	0.32 (0.03)	0.41 (0.02)	86.2 (7.2)	-32.8 (28.5)	...	...	...
SN 2007fs	5.03	4.48 (0.17)	7.44 (0.11)	107.2 (7.6)	5.2 (28.6)	13.60 (0.16)	0.663 (0.028)	165.2 (2.4)
SN 2007gi	−7.31	28.02 (0.39)	36.14 (0.20)	183.5 (11.0)	41.0 (29.7)	26.74 (0.16)	0.822 (0.017)	236.9 (2.4)
SN 2007gi	−0.35	30.24 (0.27)	52.73 (0.19)	132.7 (8.6)	16.6 (28.9)	20.72 (0.16)	0.705 (0.026)	201.0 (2.4)
SN 2007gi	6.61	9.98 (0.15)	22.67 (0.32)	109.7 (7.5)	10.9 (28.6)	19.10 (0.16)	0.640 (0.033)	179.1 (2.4)
SN 2007gk	−1.72	0.91 (0.02)	1.27 (0.02)	115.8 (7.7)	-4.8 (28.6)	18.39 (0.16)	0.654 (0.015)	181.2 (2.4)
SN 2007hj	−1.23	2.04 (0.09)	4.26 (0.08)	94.9 (7.1)	-24.1 (28.4)	14.57 (0.16)	0.650 (0.026)	153.8 (2.4)
SN 2007hj	12.53	0.50 (0.03)	0.95 (0.03)	97.2 (7.0)	5.9 (28.4)	13.92 (0.16)	0.663 (0.029)	142.0 (2.4)
SN 2007kk	7.15	2.35 (0.04)	3.64 (0.05)	129.2 (8.8)	31.4 (28.9)	17.42 (0.16)	0.733 (0.021)	178.7 (2.4)
SN 2007le	−10.31	3.72 (0.08)	9.05 (0.10)	235.7 (13.0)	79.0 (30.5)	30.57 (0.17)	0.906 (0.033)	262.2 (2.4)
SN 2007le	−9.40	5.94 (0.07)	10.28 (0.14)	207.4 (11.6)	55.2 (29.9)	28.11 (0.17)	0.814 (0.016)	262.2 (2.4)
SN 2007le	7.43	8.81 (0.16)	17.57 (0.41)	133.6 (8.4)	36.2 (28.8)	14.13 (0.16)	0.684 (0.024)	180.8 (2.4)
SN 2007le	16.39	3.15 (0.04)	7.86 (0.15)	73.4 (5.7)	-16.6 (28.1)	13.31 (0.16)	0.611 (0.060)	117.2 (2.4)
SN 2007le	17.37	2.73 (0.04)	6.86 (0.14)	76.3 (6.0)	-13.8 (28.2)	13.31 (0.16)	0.634 (0.058)	117.2 (2.4)
SN 2007s1[f]	−1.23	1.11 (0.05)	1.86 (0.04)	179.9 (11.1)	61.0 (29.7)	...	...	...
SN 2007on	−3.01	36.19 (0.14)	50.78 (0.33)	100.2 (7.3)	-24.9 (28.5)	16.72 (0.16)	0.636 (0.005)	162.9 (2.4)
SN 2007qe	−6.54	2.00 (0.06)	2.79 (0.03)	204.0 (11.5)	64.8 (29.9)	25.38 (0.16)	0.779 (0.016)	277.3 (2.4)

Continued on Next Page...

Table 3.6 — Continued

SN Name	Phase[a]	F_b[b]	F_r[b]	pEW[c]	ΔpEW[c,d]	v[e]	a	FWHM[c]
SN 2007qe	6.23	1.70 (0.07)	3.36 (0.06)	155.6 (9.6)	56.0 (29.2)	18.56 (0.16)	0.749 (0.031)	197.3 (2.4)
SN 2007qe	16.00	0.56 (0.06)	1.41 (0.09)	90.4 (7.1)	0.4 (28.4)	...	...	...
SN 2008C	15.68	1.13 (0.07)	1.76 (0.10)	80.2 (6.1)	-9.8 (28.2)	14.19 (0.16)	0.565 (0.022)	151.5 (2.4)
SN 2008Q	6.46	19.16 (0.68)	24.31 (0.46)	77.3 (5.8)	-21.8 (28.2)	...	...	...
SN 2008Z	−2.29	2.79 (0.13)	3.22 (0.10)	95.5 (6.3)	-27.1 (28.3)	...	...	...
SN 2008ar	2.83	2.51 (0.18)	3.15 (0.10)	160.3 (10.0)	53.2 (29.3)	18.71 (0.16)	0.781 (0.028)	216.3 (2.4)
SN 2008bt	10.97	0.13 (0.01)	0.25 (0.01)	112.9 (7.8)	20.2 (28.6)	12.10 (0.16)	0.691 (0.035)	173.3 (2.4)
SN 2008s1[g]	−6.36	2.04 (0.08)	2.52 (0.05)	67.4 (5.0)	-70.9 (28.0)	...	...	...
SN 2008s1[g]	−3.42	2.44 (0.13)	2.99 (0.10)	75.6 (5.4)	-51.1 (28.1)	...	...	...
SN 2008s1[g]	0.49	2.63 (0.21)	3.49 (0.12)	85.8 (6.3)	-27.7 (28.3)	...	...	...
SN 2008s1[g]	4.40	2.56 (0.09)	3.39 (0.05)	78.0 (6.1)	-25.3 (28.2)	...	...	...
SN 2008s1[g]	5.38	2.53 (0.05)	3.23 (0.04)	81.4 (6.3)	-19.9 (28.3)	...	...	...
SN 2008s1[g]	15.37	0.72 (0.04)	1.11 (0.03)	82.4 (6.0)	-7.7 (28.2)	...	...	...
SN 2008ec	−0.24	3.67 (0.10)	4.51 (0.07)	116.4 (7.9)	0.7 (28.7)	12.11 (0.16)	0.650 (0.011)	177.1 (2.4)
SN 2008ec	5.70	2.17 (0.05)	4.11 (0.06)	87.3 (7.0)	-13.2 (28.4)	...	...	...
SN 2008ec	12.51	0.96 (0.03)	1.55 (0.04)	71.9 (5.6)	-19.5 (28.1)	...	...	...
SN 2008ei	3.29	0.25 (0.04)	0.52 (0.03)	163.1 (10.6)	57.2 (29.5)	...	...	...
SN 2008ei	9.13	0.16 (0.05)	0.43 (0.02)	131.9 (9.8)	37.1 (29.2)	...	...	...
SN 2008s5[h]	1.26	2.51 (0.09)	2.75 (0.12)	89.6 (5.9)	-21.7 (28.2)	16.68 (0.16)	0.503 (0.010)	190.1 (2.4)
SN 2008s5[h]	8.96	1.40 (0.03)	1.74 (0.04)	93.5 (6.6)	-1.6 (28.3)	15.60 (0.16)	0.592 (0.016)	168.8 (2.4)
SN 2008s5[h]	15.76	0.54 (0.02)	0.88 (0.03)	89.4 (6.8)	-0.7 (28.4)	12.52 (0.16)	0.649 (0.025)	141.6 (2.4)
SN 2008hs	−7.94	0.92 (0.03)	1.31 (0.02)	83.4 (6.5)	-61.9 (28.3)	14.91 (0.16)	0.587 (0.016)	155.3 (2.4)

Uncertainties for each measured value are given in parentheses.
[a]Phases of spectra are in rest-frame days using the heliocentric redshift and photometry reference presented in table 1 of Silverman et al. (submitted).
[b]Fluxes are in units of 10^{-15} erg s^{-1} cm^{-2} Å^{-1}.
[c]The pEW, ΔpEW, and FWHM are in units of Å.
[d]ΔpEW is the measured pEW minus the expected pEW at the same epoch using our linear or quadratic fit (see Section 3.5.4 for more information).
[e]The expansion velocity is in units of 1000 km s^{-1}.
[f]Also known as SNF20071021-000.
[g]Also known as SNF20080514-002.
[h]Also known as SNF20080909-030.

Table 3.7: Measured Values for Si II λ4000

SN Name	Phase[a]	F_b[b]	F_r[b]	pEW[c]	ΔpEW[c,d]	v[e]	a	FWHM[c]
SN 1989M	2.49	43.62 (0.17)	42.08 (0.19)	19.6 (1.8)	-1.2 (6.3)	10.85 (0.15)	0.220 (0.001)	95.5 (2.4)
SN 1989M	3.48	55.41 (0.41)	50.14 (0.34)	20.2 (1.8)	-0.5 (6.3)	10.70 (0.15)	0.226 (0.003)	95.5 (2.4)
SN 1991T	6.80	30.63 (0.51)	29.66 (0.31)	13.5 (1.0)	-5.9 (6.1)	8.07 (0.15)	0.164 (0.003)	75.6 (4.9)
SN 1994D	−12.31	23.98 (0.14)	22.41 (0.08)	12.7 (1.1)	4.6 (6.1)	11.29 (0.15)	0.124 (0.002)	99.9 (2.4)
SN 1994D	−11.31	27.21 (0.26)	26.28 (0.24)	11.5 (1.1)	1.7 (6.1)	...	...	...
SN 1994D	−9.32	60.43 (0.39)	58.43 (0.23)	13.6 (1.3)	0.7 (6.1)	10.23 (0.15)	0.165 (0.001)	79.9 (2.4)
SN 1994D	−7.67	75.13 (0.68)	71.19 (0.33)	15.5 (1.5)	0.5 (6.2)	10.08 (0.15)	0.195 (0.003)	79.9 (2.4)
SN 1994D	−6.32	108.09 (1.01)	101.88 (0.49)	17.5 (1.7)	1.0 (6.2)	9.63 (0.15)	0.219 (0.002)	79.9 (2.4)
SN 1994D	−5.32	106.83 (0.86)	100.50 (0.67)	18.2 (1.8)	0.7 (6.3)	9.63 (0.15)	0.232 (0.003)	79.9 (2.4)
SN 1994D	−3.87	158.72 (1.04)	146.52 (0.35)	17.4 (1.7)	-1.3 (6.2)	9.48 (0.15)	0.221 (0.002)	79.9 (2.4)
SN 1994D	−3.33	156.68 (1.13)	144.21 (0.34)	18.3 (1.8)	-0.8 (6.3)	9.33 (0.15)	0.235 (0.003)	81.9 (2.4)
SN 1994S	1.11	26.37 (0.57)	24.88 (0.26)	9.9 (1.1)	-10.8 (6.1)	9.98 (0.15)	0.158 (0.004)	65.0 (2.4)
SN 1995D	3.84	44.53 (0.52)	41.74 (0.11)	12.0 (1.3)	-8.6 (6.1)	9.20 (0.15)	0.184 (0.003)	65.6 (2.4)
SN 1995E	−2.46	1.56 (0.04)	1.66 (0.02)	14.5 (1.5)	-5.1 (6.2)	9.35 (0.15)	0.209 (0.004)	69.2 (2.4)
SN 1997Y	1.27	10.87 (0.19)	10.34 (0.09)	19.1 (1.9)	-1.7 (6.3)	8.71 (0.15)	0.246 (0.004)	76.8 (2.4)
SN 1997bp	5.49	14.37 (0.23)	14.07 (0.15)	27.7 (2.3)	7.7 (6.4)	12.25 (0.15)	0.242 (0.002)	117.0 (2.4)
SN 1997do	−5.67	10.96 (0.16)	10.29 (0.07)	12.7 (1.3)	-4.5 (6.1)	12.05 (0.15)	0.183 (0.003)	75.2 (2.4)
SN 1998V	7.20	7.02 (0.07)	6.24 (0.05)	9.4 (1.6)	-9.7 (6.2)	8.83 (0.15)	0.164 (0.005)	59.0 (1.2)
SN 1998dk	−7.24	5.54 (0.19)	5.64 (0.06)	15.6 (1.6)	0.1 (6.2)	12.96 (0.15)	0.215 (0.007)	77.0 (2.4)
SN 1998dk	−0.54	9.66 (0.20)	9.87 (0.06)	14.9 (1.5)	-5.6 (6.2)	11.47 (0.15)	0.202 (0.004)	73.0 (2.4)
SN 1998dm	−12.48	1.30 (0.03)	1.69 (0.03)	6.1 (0.8)	-1.7 (6.0)	...	...	...
SN 1998dm	−5.61	9.84 (0.26)	9.99 (0.06)	10.1 (1.2)	-7.1 (6.1)	10.38 (0.15)	0.162 (0.002)	61.6 (2.4)
SN 1998dx	5.13	1.18 (0.02)	0.99 (0.01)	22.3 (2.3)	2.1 (6.4)	9.55 (0.15)	0.302 (0.005)	72.1 (2.3)
SN 1998ef	−8.62	6.68 (0.06)	7.16 (0.07)	20.7 (2.0)	6.9 (6.3)	12.51 (0.15)	0.247 (0.002)	84.5 (2.4)
SN 1999aa	0.24	3.48 (0.05)	3.65 (0.04)	4.9 (0.6)	-15.7 (6.0)	10.63 (0.15)	0.105 (0.002)	45.3 (2.4)
SN 1999cp	4.91	20.86 (0.18)	19.52 (0.11)	18.0 (2.0)	-2.3 (6.3)	8.75 (0.15)	0.279 (0.004)	67.4 (2.4)
SN 1999dk	−6.60	9.71 (0.14)	10.04 (0.08)	14.1 (1.4)	-2.1 (6.1)	11.70 (0.15)	0.173 (0.001)	82.8 (2.4)
SN 1999dq	−3.93	10.08 (0.19)	10.30 (0.10)	4.0 (0.5)	-14.6 (6.0)	11.05 (0.15)	0.080 (0.001)	45.4 (2.4)
SN 1999dq	2.97	9.89 (0.11)	10.04 (0.07)	8.7 (1.0)	-12.1 (6.1)	10.61 (0.15)	0.157 (0.002)	59.2 (2.4)
SN 2000cw	4.81	1.48 (0.03)	1.20 (0.03)	25.3 (2.5)	4.9 (6.5)	8.37 (0.15)	0.341 (0.006)	71.8 (2.4)
SN 2000dg	−5.09	1.17 (0.03)	1.05 (0.01)	16.3 (1.7)	-1.4 (6.2)	10.34 (0.15)	0.220 (0.005)	69.3 (2.4)
SN 2000dg	4.66	1.02 (0.03)	0.87 (0.01)	13.4 (1.6)	-7.0 (6.2)	9.08 (0.15)	0.206 (0.007)	67.4 (2.4)
SN 2000dk	1.00	5.56 (0.06)	5.01 (0.05)	25.7 (2.5)	4.9 (6.5)	9.03 (0.15)	0.306 (0.003)	84.5 (2.4)
SN 2000dm	−1.63	4.41 (0.07)	4.17 (0.05)	25.1 (2.5)	5.1 (6.5)	10.22 (0.15)	0.313 (0.003)	78.8 (2.4)
SN 2000dm	8.18	2.83 (0.04)	2.39 (0.04)	20.3 (2.2)	1.9 (6.4)	8.62 (0.15)	0.301 (0.005)	70.9 (2.4)
SN 2000dn	−0.94	1.97 (0.03)	1.89 (0.02)	19.6 (2.1)	-0.7 (6.3)	8.50 (0.15)	0.268 (0.002)	73.6 (2.4)
SN 2000dx	−9.26	0.45 (0.03)	0.44 (0.02)	10.5 (1.4)	-2.4 (6.2)	11.20 (0.15)	0.171 (0.002)	66.0 (2.4)
SN 2000fa	−8.25	2.03 (0.04)	1.93 (0.02)	10.5 (1.1)	-3.8 (6.1)	...	...	...

Continued on Next Page...

Table 3.7 — Continued

SN Name	Phase[a]	F_b[b]	F_r[b]	pEW[c]	ΔpEW[c,d]	v[e]	a	FWHM[c]
SN 2000fa	6.86	2.73 (0.05)	2.32 (0.04)	18.5 (1.8)	-0.8 (6.2)	9.43 (0.15)	0.206 (0.005)	90.1 (2.4)
SN 2001ay	6.79	1.60 (0.04)	1.42 (0.02)	28.3 (2.6)	9.0 (6.5)	9.13 (0.15)	0.317 (0.004)	87.4 (2.4)
SN 2001az	−3.24	1.27 (0.03)	1.25 (0.03)	7.7 (0.9)	-11.4 (6.1)	10.85 (0.15)	0.122 (0.002)	65.3 (2.4)
SN 2001br	3.48	2.23 (0.10)	2.36 (0.11)	33.1 (2.9)	12.4 (6.7)	11.57 (0.15)	0.316 (0.006)	99.9 (2.4)
SN 2001cp	1.39	1.47 (0.03)	1.52 (0.03)	7.0 (0.9)	-13.8 (6.1)	10.47 (0.15)	0.109 (0.003)	66.5 (2.4)
SN 2001da	−1.12	4.78 (0.10)	4.82 (0.10)	18.8 (1.8)	-1.4 (6.3)	8.96 (0.15)	0.224 (0.002)	82.6 (2.4)
SN 2001eh	3.26	1.43 (0.02)	1.48 (0.02)	9.2 (1.1)	-11.5 (6.1)	...	...	...
SN 2001ep	2.83	9.60 (0.28)	7.97 (0.06)	24.5 (2.3)	3.7 (6.4)	8.45 (0.15)	0.290 (0.006)	80.9 (2.4)
SN 2001ex	−1.82	0.74 (0.02)	0.72 (0.01)	30.1 (2.9)	10.2 (6.7)	9.73 (0.15)	0.344 (0.003)	91.6 (2.4)
SN 2001fe	−0.99	12.39 (0.18)	12.68 (0.08)	5.0 (0.6)	-15.3 (6.0)	11.41 (0.15)	0.096 (0.002)	51.3 (2.4)
SN 2001fh	5.93	0.84 (0.06)	0.77 (0.03)	21.5 (2.3)	1.7 (6.4)	9.04 (0.15)	0.266 (0.008)	75.0 (2.4)
SN 2002aw	2.10	3.27 (0.16)	3.05 (0.09)	22.8 (2.4)	2.0 (6.5)	9.23 (0.15)	0.301 (0.010)	74.1 (2.4)
SN 2002bf	2.97	2.45 (0.01)	2.93 (0.01)	29.1 (2.5)	8.3 (6.5)	13.20 (0.15)	0.248 (0.004)	121.1 (2.4)
SN 2002bo	−1.08	20.35 (0.75)	22.74 (0.33)	21.5 (2.0)	1.3 (6.3)	11.05 (0.15)	0.220 (0.002)	101.6 (2.4)
SN 2002bz	4.92	0.85 (0.03)	0.80 (0.03)	26.0 (2.8)	5.7 (6.6)	9.82 (0.15)	0.354 (0.002)	75.2 (2.4)
SN 2002ck	3.64	1.27 (0.04)	1.24 (0.04)	12.5 (1.5)	-8.1 (6.2)	9.58 (0.15)	0.202 (0.004)	66.0 (2.4)
SN 2002cr	−6.78	12.06 (0.16)	11.09 (0.10)	13.7 (1.4)	-2.3 (6.2)	9.18 (0.15)	0.190 (0.003)	73.3 (2.4)
SN 2002de	−0.32	1.91 (0.07)	1.97 (0.05)	9.1 (1.1)	-11.4 (6.1)	10.83 (0.15)	0.161 (0.003)	58.4 (2.4)
SN 2002dj	−7.98	9.36 (0.19)	10.34 (0.12)	19.6 (1.8)	5.0 (6.3)	11.99 (0.15)	0.210 (0.003)	89.2 (2.4)
SN 2002eb	1.68	2.90 (0.03)	2.89 (0.02)	12.5 (1.4)	-8.3 (6.2)	9.93 (0.15)	0.214 (0.001)	62.3 (2.4)
SN 2002ef	4.70	1.47 (0.13)	1.40 (0.09)	13.3 (2.0)	-7.1 (6.3)	8.90 (0.15)	0.234 (0.008)	58.6 (2.4)
SN 2002er	−4.58	9.64 (0.30)	9.21 (0.03)	20.4 (2.0)	2.3 (6.3)	11.50 (0.15)	0.241 (0.002)	87.3 (2.4)
SN 2002er	5.26	9.10 (0.28)	7.23 (0.06)	24.8 (2.3)	4.6 (6.4)	9.66 (0.15)	0.292 (0.006)	85.3 (2.4)
SN 2002eu	−0.06	1.17 (0.02)	1.13 (0.03)	31.2 (2.9)	10.6 (6.7)	10.23 (0.15)	0.334 (0.004)	90.6 (2.4)
SN 2002fb	0.98	1.48 (0.04)	1.05 (0.02)	23.0 (2.5)	2.3 (6.5)	7.70 (0.15)	0.319 (0.012)	74.8 (2.4)
SN 2002fk	7.74	33.32 (0.40)	29.17 (0.14)	15.4 (1.7)	-3.3 (6.2)	8.45 (0.15)	0.260 (0.004)	59.6 (2.4)
SN 2002ha	−0.85	8.68 (0.13)	8.67 (0.08)	22.1 (2.2)	1.8 (6.4)	10.66 (0.15)	0.287 (0.002)	74.9 (2.4)
SN 2002ha	4.93	7.14 (0.12)	6.50 (0.05)	22.6 (2.3)	2.4 (6.4)	9.20 (0.15)	0.314 (0.004)	73.0 (2.4)
SN 2002ha	7.89	13.21 (0.19)	11.28 (0.07)	17.6 (2.0)	-1.0 (6.3)	8.60 (0.15)	0.269 (0.006)	69.0 (2.4)
SN 2002hd	6.48	2.33 (0.03)	1.71 (0.03)	20.1 (2.2)	0.6 (6.4)	7.80 (0.15)	0.286 (0.006)	71.5 (2.4)
SN 2002he	−5.91	1.49 (0.19)	1.55 (0.05)	22.7 (3.1)	5.8 (6.7)	12.28 (0.15)	0.274 (0.008)	88.0 (1.2)
SN 2002he	−1.03	3.34 (0.15)	3.62 (0.08)	21.5 (2.9)	1.2 (6.7)	11.82 (0.15)	0.267 (0.004)	76.0 (1.2)
SN 2002he	0.29	3.19 (0.02)	3.16 (0.02)	24.5 (2.3)	3.9 (6.4)	10.82 (0.15)	0.291 (0.001)	85.9 (2.4)
SN 2002he	3.22	6.48 (0.05)	6.00 (0.04)	24.1 (2.3)	3.4 (6.4)	10.96 (0.15)	0.295 (0.002)	82.0 (2.4)
SN 2002hu	−5.81	1.43 (0.01)	1.33 (0.01)	8.0 (0.9)	-9.0 (6.1)	9.41 (0.15)	0.132 (0.003)	59.8 (2.4)
SN 2002hw	−6.27	1.07 (0.03)	1.02 (0.02)	16.6 (1.8)	0.0 (6.3)	9.65 (0.15)	0.235 (0.003)	72.7 (2.4)
SN 2002kf	6.81	3.85 (0.03)	3.37 (0.02)	21.7 (2.2)	2.4 (6.4)	9.25 (0.15)	0.280 (0.003)	78.5 (2.4)
SN 2003D	9.98	0.88 (0.01)	0.65 (0.01)	15.5 (1.8)	-1.3 (6.2)	...	...	...
SN 2003ai	7.25	1.52 (0.04)	1.24 (0.03)	12.9 (1.5)	-6.2 (6.2)	8.20 (0.15)	0.206 (0.006)	61.8 (2.4)
SN 2003cq	−0.15	0.99 (0.03)	0.97 (0.01)	20.7 (2.0)	0.2 (6.3)	11.02 (0.15)	0.236 (0.002)	79.4 (2.4)
SN 2003gt	−5.07	5.52 (0.18)	5.23 (0.14)	14.0 (1.5)	-3.7 (6.2)	10.56 (0.15)	0.205 (0.002)	67.0 (2.4)
SN 2003he	2.71	2.34 (0.05)	2.36 (0.05)	13.1 (1.4)	-7.7 (6.2)	10.52 (0.15)	0.198 (0.002)	58.5 (2.4)
SN 2003he	8.54	2.18 (0.05)	1.73 (0.04)	15.7 (1.6)	-2.4 (6.2)	...	...	...
SN 2003iv	1.76	0.07 (0.00)	0.07 (0.00)	27.6 (2.7)	6.8 (6.6)	9.29 (0.15)	0.334 (0.004)	85.1 (2.4)
SN 2003kf	−7.50	12.07 (0.23)	11.70 (0.05)	12.7 (1.3)	-2.5 (6.1)	11.82 (0.15)	0.200 (0.002)	61.5 (2.4)
SN 2004E	5.26	3.09 (0.08)	2.82 (0.09)	10.3 (1.3)	-9.8 (6.1)	10.18 (0.15)	0.202 (0.003)	52.4 (2.4)
SN 2004S	8.26	10.72 (0.07)	8.97 (0.03)	13.4 (1.6)	-4.9 (6.2)	6.92 (0.15)	0.234 (0.006)	59.4 (2.4)
SN 2004as	−4.36	1.35 (0.02)	1.41 (0.02)	12.3 (1.2)	-6.0 (6.1)	9.51 (0.15)	0.150 (0.002)	75.7 (2.4)
SN 2004bk	6.13	3.50 (0.12)	3.15 (0.11)	14.2 (1.7)	-5.6 (6.2)	9.55 (0.15)	0.218 (0.005)	70.4 (2.4)
SN 2004bl	4.61	4.79 (0.33)	4.81 (0.26)	15.3 (1.9)	-5.0 (6.3)	10.59 (0.15)	0.241 (0.004)	62.9 (2.4)
SN 2004br	3.50	4.23 (0.06)	4.39 (0.06)	5.5 (0.7)	-15.2 (6.0)	...	...	...
SN 2004bv	9.77	13.02 (0.32)	12.29 (0.20)	16.1 (1.7)	-0.9 (6.2)	...	...	...
SN 2004bw	−10.03	0.43 (0.02)	0.43 (0.02)	13.3 (1.6)	1.5 (6.2)	...	...	...
SN 2004bw	6.59	2.13 (0.05)	1.85 (0.04)	23.0 (2.3)	3.5 (6.4)	9.54 (0.15)	0.305 (0.005)	70.5 (2.4)
SN 2004ef	−5.52	1.14 (0.03)	1.06 (0.02)	21.7 (2.2)	4.4 (6.4)	11.07 (0.15)	0.265 (0.004)	87.3 (2.4)
SN 2004eo	−5.57	2.87 (0.08)	2.67 (0.05)	20.6 (2.1)	3.3 (6.4)	8.95 (0.15)	0.273 (0.004)	80.7 (2.4)
SN 2004ey	−7.58	6.45 (0.06)	6.17 (0.03)	12.7 (1.3)	-2.4 (6.1)	10.89 (0.15)	0.173 (0.003)	70.9 (2.4)
SN 2004fu	−2.65	4.93 (0.10)	5.72 (0.04)	25.4 (2.3)	5.9 (6.4)	11.33 (0.15)	0.273 (0.002)	95.1 (2.4)
SN 2004fu	2.43	5.46 (0.15)	5.55 (0.06)	29.1 (2.7)	8.3 (6.6)	10.44 (0.15)	0.311 (0.002)	99.1 (2.4)
SN 2004fz	−5.18	7.02 (0.08)	6.30 (0.07)	21.7 (2.2)	4.0 (6.4)	8.41 (0.15)	0.262 (0.004)	80.6 (2.4)
SN 2004gs	0.44	1.13 (0.03)	1.05 (0.02)	35.3 (2.9)	14.6 (6.7)	10.10 (0.15)	0.316 (0.003)	111.0 (2.4)
SN 2005M	9.23	2.28 (0.02)	2.39 (0.02)	14.3 (1.6)	-3.2 (6.2)	6.59 (0.15)	0.227 (0.002)	64.6 (2.4)
SN 2005ag	0.53	0.08 (0.00)	0.08 (0.00)	8.7 (1.2)	-12.0 (6.1)	10.18 (0.15)	0.151 (0.004)	61.2 (2.3)
SN 2005am	4.47	23.67 (0.26)	20.36 (0.08)	27.0 (2.7)	6.5 (6.6)	10.19 (0.15)	0.340 (0.004)	77.4 (2.4)
SN 2005ao	−1.29	1.30 (0.03)	1.35 (0.02)	6.9 (0.9)	-13.3 (6.1)	11.33 (0.15)	0.122 (0.002)	53.9 (2.4)
SN 2005ao	0.52	1.09 (0.03)	1.10 (0.02)	7.3 (1.0)	-13.4 (6.1)	11.33 (0.15)	0.152 (0.001)	44.3 (2.4)
SN 2005bc	1.55	2.69 (0.06)	2.60 (0.03)	23.4 (2.3)	2.6 (6.4)	10.29 (0.15)	0.280 (0.001)	83.0 (2.4)
SN 2005bc	7.37	1.73 (0.05)	1.43 (0.04)	20.2 (2.2)	1.2 (6.4)	...	...	...
SN 2005cf	−10.94	6.63 (0.11)	7.27 (0.09)	5.0 (0.7)	-5.4 (6.0)	...	...	...
SN 2005cf	−2.11	281.00 (4.26)	256.89 (1.95)	14.6 (1.6)	-5.2 (6.2)	9.03 (0.15)	0.222 (0.002)	67.6 (2.4)
SN 2005cf	−1.19	57.08 (0.79)	52.64 (0.49)	15.0 (1.6)	-5.3 (6.2)	9.61 (0.15)	0.224 (0.004)	67.6 (2.4)
SN 2005de	−0.75	5.39 (0.24)	5.26 (0.10)	20.8 (2.2)	0.4 (6.4)	9.39 (0.15)	0.291 (0.005)	76.8 (2.4)
SN 2005el	−6.70	4.35 (0.09)	4.18 (0.06)	15.6 (1.6)	-0.6 (6.2)	9.90 (0.15)	0.184 (0.004)	80.8 (2.4)
SN 2005el	1.22	7.06 (0.12)	6.87 (0.09)	20.7 (2.0)	-0.1 (6.3)	9.01 (0.15)	0.262 (0.003)	74.9 (2.4)
SN 2005el	8.09	5.09 (0.09)	4.18 (0.04)	16.6 (1.9)	-1.9 (6.3)	8.74 (0.15)	0.255 (0.006)	69.0 (2.4)
SN 2005eq	−6.01	0.88 (0.05)	0.85 (0.03)	4.9 (1.0)	-12.0 (6.1)	11.53 (0.15)	0.120 (0.005)	38.9 (2.4)
SN 2005eq	−2.98	2.18 (0.05)	2.21 (0.01)	4.5 (0.6)	-14.8 (6.0)	10.34 (0.15)	0.088 (0.001)	48.6 (2.4)
SN 2005eq	0.66	2.15 (0.05)	2.24 (0.03)	7.3 (0.9)	-13.4 (6.1)	9.48 (0.15)	0.128 (0.003)	56.4 (2.4)
SN 2005eu	−9.06	0.74 (0.01)	0.71 (0.01)	5.0 (0.6)	-8.2 (6.0)	12.94 (0.15)	0.094 (0.002)	52.2 (2.4)
SN 2005ki	1.62	24.02 (0.80)	20.18 (0.25)	30.6 (4.0)	9.7 (7.2)	11.25 (0.15)	0.340 (0.011)	92.0 (1.2)
SN 2005ms	−1.88	7.00 (0.23)	7.81 (0.15)	11.5 (1.3)	-8.4 (6.1)	9.97 (0.15)	0.161 (0.005)	74.1 (2.4)
SN 2005na	1.03	3.32 (0.12)	3.13 (0.09)	10.0 (1.2)	-10.8 (6.1)	10.01 (0.15)	0.166 (0.004)	54.6 (2.4)

Continued on Next Page...

Table 3.7 — Continued

SN Name	Phase[a]	F_b[b]	F_r[b]	pEW[c]	ΔpEW[c,d]	v[e]	a	FWHM[c]
SN 2006D	3.70	47.23 (0.64)	38.68 (0.34)	22.4 (2.5)	1.8 (6.5)	9.65 (0.15)	0.346 (0.007)	67.4 (2.4)
SN 2006N	−1.89	5.28 (0.08)	5.35 (0.08)	24.3 (2.4)	4.4 (6.4)	9.58 (0.15)	0.280 (0.003)	84.8 (2.4)
SN 2006N	−0.90	5.10 (0.11)	5.10 (0.06)	24.9 (2.4)	4.5 (6.5)	10.16 (0.15)	0.305 (0.002)	82.8 (2.4)
SN 2006S	−3.93	25.99 (0.90)	24.86 (0.77)	4.9 (0.8)	-13.7 (6.1)	10.83 (0.15)	0.138 (0.005)	36.8 (2.4)
SN 2006S	2.99	1.32 (0.05)	1.36 (0.05)	9.9 (1.3)	-10.9 (6.1)	10.23 (0.15)	0.187 (0.006)	56.2 (2.4)
SN 2006X	3.15	2.55 (0.05)	3.57 (0.04)	28.4 (2.5)	7.7 (6.5)	11.71 (0.15)	0.272 (0.006)	107.4 (2.4)
SN 2006ak	8.43	0.77 (0.02)	0.64 (0.01)	29.9 (2.5)	11.7 (6.5)	8.44 (0.15)	0.256 (0.003)	109.8 (2.4)
SN 2006ax	−10.07	1.92 (0.03)	1.92 (0.02)	5.3 (0.6)	-6.4 (6.0)	...	...	...
SN 2006bq	6.97	8.35 (0.10)	8.57 (0.08)	23.9 (2.1)	4.7 (6.4)	10.77 (0.15)	0.229 (0.001)	107.6 (2.4)
SN 2006bu	4.22	0.27 (0.01)	0.25 (0.01)	13.1 (1.7)	-7.4 (6.2)	11.01 (0.15)	0.240 (0.004)	55.4 (2.3)
SN 2006cj	3.43	0.39 (0.02)	0.41 (0.01)	8.1 (1.1)	-12.6 (6.1)	...	...	...
SN 2006cp	−5.30	2.42 (0.06)	2.72 (0.03)	12.7 (1.3)	-4.8 (6.1)	11.91 (0.15)	0.163 (0.007)	74.3 (2.4)
SN 2006cq	2.00	0.74 (0.03)	0.72 (0.02)	17.2 (1.9)	-3.7 (6.3)	8.17 (0.15)	0.260 (0.003)	63.0 (2.3)
SN 2006cs	2.28	0.57 (0.03)	0.44 (0.02)	25.3 (2.8)	4.4 (6.6)	9.11 (0.15)	0.395 (0.009)	64.5 (2.4)
SN 2006ef	3.20	5.71 (0.08)	5.22 (0.04)	28.0 (2.6)	7.3 (6.5)	9.46 (0.15)	0.323 (0.003)	90.4 (2.4)
SN 2006ej	−3.70	3.77 (0.04)	3.82 (0.04)	27.8 (2.6)	8.9 (6.5)	11.77 (0.15)	0.294 (0.002)	94.1 (2.4)
SN 2006ej	5.09	2.15 (0.03)	1.82 (0.03)	28.2 (2.6)	8.0 (6.5)	10.16 (0.15)	0.332 (0.004)	92.1 (2.4)
SN 2006et	3.29	2.28 (0.09)	2.39 (0.06)	12.6 (1.5)	-8.1 (6.2)	9.39 (0.15)	0.198 (0.005)	66.5 (2.4)
SN 2006gt	3.08	0.41 (0.02)	0.32 (0.01)	20.7 (2.3)	-0.1 (6.4)	...	...	...
SN 2006kf	−8.96	0.47 (0.01)	0.47 (0.01)	17.7 (1.8)	4.3 (6.3)	10.46 (0.15)	0.216 (0.002)	88.1 (2.4)
SN 2006kf	−3.05	1.68 (0.02)	1.67 (0.02)	24.3 (2.4)	5.0 (6.5)	9.72 (0.15)	0.306 (0.002)	80.3 (2.4)
SN 2006lf	−6.30	0.40 (0.01)	0.44 (0.01)	22.9 (2.2)	6.3 (6.4)	9.70 (0.15)	0.265 (0.004)	88.8 (2.4)
SN 2006le	−8.69	1.24 (0.02)	1.24 (0.01)	3.9 (0.5)	-9.8 (6.0)	12.55 (0.15)	0.065 (0.002)	57.0 (2.4)
SN 2006mp	5.66	2.06 (0.04)	2.06 (0.02)	10.5 (1.3)	-9.4 (6.1)	8.18 (0.15)	0.171 (0.001)	58.4 (2.4)
SN 2006or	−2.79	1.00 (0.03)	0.91 (0.01)	29.1 (2.5)	9.7 (6.5)	9.11 (0.15)	0.262 (0.004)	107.8 (2.4)
SN 2006sr	−2.34	1.75 (0.02)	1.87 (0.02)	20.4 (2.0)	0.8 (6.3)	11.14 (0.15)	0.255 (0.002)	82.0 (2.4)
SN 2006sr	2.69	2.48 (0.05)	2.56 (0.02)	23.2 (2.2)	2.4 (6.4)	10.12 (0.15)	0.286 (0.002)	82.0 (2.4)
SN 2007A	2.37	3.78 (0.09)	3.83 (0.03)	10.7 (1.2)	-10.2 (6.1)	9.23 (0.15)	0.157 (0.002)	66.8 (2.4)
SN 2007F	−9.35	2.02 (0.02)	2.00 (0.02)	8.6 (0.9)	-4.1 (6.1)	11.70 (0.15)	0.127 (0.002)	68.4 (2.4)
SN 2007F	3.23	3.11 (0.05)	3.14 (0.03)	10.0 (1.2)	-10.8 (6.1)	10.67 (0.15)	0.169 (0.002)	60.6 (2.4)
SN 2007af	−1.25	49.60 (0.62)	46.60 (0.23)	20.7 (2.0)	0.5 (6.3)	9.03 (0.15)	0.263 (0.002)	75.6 (2.4)
SN 2007af	3.81	43.00 (0.76)	36.43 (0.24)	23.0 (2.2)	2.4 (6.4)	8.59 (0.15)	0.280 (0.004)	83.5 (2.4)
SN 2007bd	−5.79	1.31 (0.05)	1.27 (0.05)	20.4 (2.1)	3.4 (6.4)	10.96 (0.15)	0.273 (0.002)	77.6 (2.4)
SN 2007bc	0.61	4.67 (0.06)	4.17 (0.04)	23.3 (2.4)	2.6 (6.4)	8.54 (0.15)	0.301 (0.005)	76.4 (2.4)
SN 2007bm	−7.79	7.62 (0.29)	8.37 (0.17)	17.0 (1.7)	2.1 (6.2)	9.70 (0.15)	0.218 (0.005)	75.5 (2.4)
SN 2007ci	−6.57	2.42 (0.08)	2.65 (0.05)	21.5 (2.1)	5.2 (6.3)	10.85 (0.15)	0.247 (0.003)	92.3 (2.4)
SN 2007ci	−1.71	3.70 (0.07)	3.66 (0.03)	24.3 (2.3)	4.4 (6.4)	10.83 (0.15)	0.280 (0.002)	84.5 (2.4)
SN 2007co	−4.09	1.48 (0.05)	1.47 (0.03)	18.7 (1.9)	0.2 (6.3)	10.06 (0.15)	0.233 (0.003)	76.0 (2.4)
SN 2007co	0.85	1.85 (0.04)	1.79 (0.02)	20.3 (2.0)	-0.4 (6.3)	10.20 (0.15)	0.262 (0.002)	72.1 (2.4)
SN 2007cq	7.84	3.47 (0.07)	2.71 (0.06)	20.8 (2.3)	2.2 (6.4)	9.32 (0.15)	0.306 (0.016)	72.1 (2.4)
SN 2007fb	1.95	5.18 (0.14)	5.43 (0.14)	28.9 (2.8)	8.0 (6.6)	10.37 (0.15)	0.350 (0.003)	84.5 (2.4)
SN 2007fs	5.03	7.45 (0.12)	6.87 (0.09)	17.0 (1.8)	-3.2 (6.3)	9.54 (0.15)	0.266 (0.004)	61.0 (2.4)
SN 2007gi	−0.35	53.99 (0.20)	66.06 (0.21)	17.5 (1.6)	-3.0 (6.2)	...	...	...
SN 2007gi	6.61	22.74 (0.32)	22.94 (0.12)	32.2 (2.6)	12.7 (6.5)	11.96 (0.15)	0.271 (0.002)	123.4 (2.4)
SN 2007gk	−1.72	1.28 (0.02)	1.45 (0.02)	29.7 (2.6)	9.8 (6.5)	10.70 (0.15)	0.280 (0.003)	109.1 (2.4)
SN 2007hj	−1.23	4.27 (0.08)	3.73 (0.04)	30.0 (2.8)	9.8 (6.6)	11.14 (0.15)	0.326 (0.002)	96.6 (2.4)
SN 2007kk	7.15	3.64 (0.05)	3.21 (0.04)	18.9 (1.8)	-0.3 (6.3)	9.52 (0.15)	0.204 (0.003)	94.1 (2.4)
SN 2007le	−10.31	9.07 (0.13)	8.82 (0.07)	15.5 (1.5)	4.2 (6.2)	13.28 (0.15)	0.200 (0.002)	73.5 (2.4)
SN 2007le	−9.40	10.32 (0.21)	10.12 (0.04)	16.2 (1.6)	3.5 (6.2)	12.24 (0.15)	0.208 (0.002)	77.5 (2.4)
SN 2007s1[f]	−1.23	1.91 (0.04)	1.78 (0.02)	18.6 (1.9)	-1.6 (6.3)	9.75 (0.15)	0.243 (0.003)	77.9 (2.4)
SN 2007on	−3.01	51.12 (0.33)	42.56 (0.09)	26.1 (2.4)	6.8 (6.4)	10.66 (0.15)	0.289 (0.005)	87.4 (2.4)
SN 2007on	−3.00	39.45 (0.27)	32.65 (0.07)	20.1 (2.9)	0.8 (6.7)	10.66 (0.15)	0.271 (0.002)	80.0 (1.2)
SN 2007qe	−6.54	2.83 (0.03)	3.05 (0.04)	8.1 (0.8)	-8.2 (6.1)	12.42 (0.15)	0.110 (0.003)	74.2 (2.4)
SN 2007qe	6.23	3.41 (0.06)	3.11 (0.05)	22.2 (2.0)	2.5 (6.3)	11.24 (0.15)	0.228 (0.003)	95.7 (2.4)
SN 2008Q	6.46	25.17 (0.49)	21.25 (0.27)	16.2 (1.8)	-3.3 (6.3)	10.07 (0.15)	0.263 (0.005)	63.5 (2.4)
SN 2008Z	−2.29	3.28 (0.11)	3.31 (0.07)	4.4 (0.7)	-15.3 (6.0)	...	...	...
SN 2008s1[g]	−6.36	2.54 (0.05)	2.37 (0.06)	13.3 (1.5)	-3.2 (6.2)	9.82 (0.15)	0.198 (0.003)	68.5 (2.4)
SN 2008s1[g]	−4.40	2.90 (0.32)	2.76 (0.13)	17.9 (2.3)	-0.3 (6.4)	10.10 (0.15)	0.298 (0.006)	58.7 (2.4)
SN 2008s1[g]	−3.42	3.09 (0.10)	2.90 (0.07)	18.2 (2.0)	-0.8 (6.3)	10.10 (0.15)	0.265 (0.003)	70.4 (2.4)
SN 2008s1[g]	0.49	3.67 (0.11)	3.53 (0.12)	18.6 (2.1)	-2.1 (6.3)	9.09 (0.15)	0.270 (0.003)	68.5 (2.4)
SN 2008s1[g]	4.40	3.60 (0.06)	3.31 (0.05)	20.8 (2.3)	0.3 (6.4)	9.52 (0.15)	0.294 (0.005)	74.4 (2.4)
SN 2008s1[g]	5.38	3.41 (0.04)	2.99 (0.05)	19.9 (2.2)	-0.2 (6.4)	9.52 (0.15)	0.294 (0.006)	70.4 (2.4)
SN 2008ec	−0.24	4.61 (0.07)	4.65 (0.05)	22.0 (2.2)	1.5 (6.4)	9.71 (0.15)	0.275 (0.002)	78.7 (2.4)
SN 2008ec	5.70	4.24 (0.06)	3.28 (0.05)	20.4 (2.3)	0.5 (6.4)	8.42 (0.15)	0.316 (0.009)	66.9 (2.4)
SN 2008ei	3.29	0.52 (0.03)	0.57 (0.02)	21.8 (2.2)	1.1 (6.4)	13.57 (0.15)	0.196 (0.008)	111.8 (2.4)
SN 2008s5[h]	1.26	2.76 (0.11)	2.75 (0.09)	7.8 (1.1)	-13.0 (6.1)	8.47 (0.15)	0.145 (0.002)	52.4 (2.4)
SN 2008s5[h]	8.96	1.83 (0.03)	1.73 (0.03)	15.5 (1.8)	-2.3 (6.3)	7.62 (0.15)	0.264 (0.002)	58.2 (2.4)
SN 2008hs	−7.94	1.35 (0.02)	1.25 (0.02)	26.6 (2.4)	11.9 (6.5)	11.79 (0.15)	0.274 (0.002)	100.3 (2.4)

Uncertainties for each measured value are given in parentheses.
[a]Phases of spectra are in rest-frame days using the heliocentric redshift and photometry reference presented in table 1 of Silverman et al. (submitted).
[b]Fluxes are in units of 10^{-15} erg s^{-1} cm^{-2} Å^{-1}.
[c]The pEW, ΔpEW, and FWHM are in units of Å.
[d]ΔpEW is the measured pEW minus the expected pEW at the same epoch using our linear or quadratic fit (see Section 3.5.4 for more information).
[e]The expansion velocity is in units of 1000 km s^{-1}.
[f]Also known as SNF20071021-000.
[g]Also known as SNF20080514-002.
[h]Also known as SNF20080909-030.

Table 3.8: Measured Values for Mg II

SN Name	Phase[a]	F_b[b]	F_r[b]	pEW[c]	ΔpEW[c,d]
SN 1989M	2.49	41.95 (0.16)	38.42 (0.14)	94.9 (5.8)	1.8 (16.1)
SN 1989M	3.48	50.14 (0.35)	46.18 (0.16)	96.5 (5.9)	3.0 (16.1)
SN 1990N	7.11	53.35 (0.44)	50.93 (0.41)	94.2 (3.9)	-0.6 (15.5)
SN 1991T	6.80	29.65 (0.28)	31.24 (0.28)	80.8 (3.5)	-13.9 (15.4)
SN 1994D	−12.31	22.35 (0.08)	19.50 (0.27)	75.0 (4.5)	-2.5 (15.6)
SN 1994D	−11.31	26.23 (0.24)	19.65 (0.14)	54.0 (3.4)	-25.1 (15.4)
SN 1994D	−9.32	58.43 (0.23)	39.77 (0.14)	55.0 (3.2)	-26.8 (15.3)
SN 1994D	−6.32	101.74 (0.48)	70.48 (0.51)	75.7 (4.1)	-9.9 (15.5)
SN 1994D	−5.32	100.15 (0.67)	71.84 (0.27)	73.8 (4.1)	-12.9 (15.5)
SN 1994D	−3.87	146.03 (0.35)	106.07 (0.22)	75.2 (4.2)	-13.1 (15.6)
SN 1994D	−3.33	143.85 (0.34)	101.34 (0.21)	77.5 (4.3)	-11.3 (15.6)
SN 1994Q	9.68	2.17 (0.04)	2.44 (0.02)	123.1 (6.6)	28.0 (16.4)
SN 1994S	1.11	24.89 (0.26)	16.64 (0.10)	75.0 (4.3)	-17.2 (15.6)
SN 1995D	3.84	41.76 (0.11)	31.42 (0.08)	79.2 (4.6)	-14.5 (15.7)
SN 1995E	−2.46	1.66 (0.02)	1.58 (0.02)	88.8 (5.0)	-0.8 (15.8)
SN 1995ac	−6.34	0.48 (0.02)	0.37 (0.01)	76.6 (4.9)	-9.0 (15.8)
SN 1997Y	1.27	10.34 (0.09)	7.45 (0.05)	90.2 (5.4)	-2.1 (15.9)
SN 1997bp	5.49	14.06 (0.15)	15.01 (0.08)	120.3 (7.3)	26.0 (16.7)
SN 1997br	−4.84	17.64 (0.14)	14.78 (0.09)	79.1 (4.5)	-8.1 (15.7)
SN 1997do	−5.67	10.29 (0.07)	7.40 (0.04)	94.4 (5.4)	8.1 (15.9)
SN 1998V	7.20	6.14 (0.05)	6.16 (0.02)	82.0 (6.9)	-12.8 (16.5)
SN 1998dk	−7.24	5.56 (0.06)	4.67 (0.05)	80.1 (4.7)	-4.4 (15.7)
SN 1998dk	−0.54	9.87 (0.06)	7.73 (0.04)	93.0 (5.4)	1.9 (15.9)
SN 1998dm	−12.48	1.68 (0.03)	2.22 (0.02)	66.6 (3.6)	-10.6 (15.4)
SN 1998dm	−5.61	9.94 (0.06)	7.25 (0.05)	92.6 (5.1)	6.2 (15.8)
SN 1998dx	5.13	0.99 (0.01)	0.93 (0.02)	74.1 (4.9)	-20.1 (15.8)
SN 1998ef	−8.62	7.15 (0.07)	4.93 (0.04)	97.9 (5.7)	15.1 (16.0)
SN 1998es	0.28	25.19 (0.16)	18.08 (0.10)	84.2 (5.0)	-7.5 (15.8)
SN 1999aa	0.24	3.64 (0.04)	2.67 (0.02)	76.2 (4.6)	-15.4 (15.7)
SN 1999ac	−0.89	19.80 (0.12)	15.19 (0.08)	100.9 (5.9)	10.1 (16.1)
SN 1999cp	4.91	19.53 (0.11)	15.48 (0.07)	77.8 (4.6)	-16.4 (15.7)
SN 1999dk	−6.60	10.03 (0.08)	7.08 (0.06)	100.4 (5.7)	15.2 (16.0)
SN 1999do	9.96	1.56 (0.04)	1.59 (0.02)	57.0 (3.5)	-38.1 (15.4)
SN 1999dq	−3.93	10.29 (0.09)	7.36 (0.09)	91.9 (5.4)	3.7 (15.9)
SN 1999dq	2.97	10.01 (0.08)	8.06 (0.06)	80.9 (4.9)	-12.3 (15.8)
SN 1999gd	−1.12	1.52 (0.02)	1.31 (0.02)	92.8 (3.5)	2.2 (15.4)
SN 2000cp	2.92	0.48 (0.03)	0.46 (0.01)	105.4 (6.5)	12.1 (16.3)
SN 2000cw	4.81	1.19 (0.03)	1.17 (0.02)	97.0 (6.1)	2.9 (16.2)
SN 2000dg	4.66	0.84 (0.02)	0.86 (0.01)	75.7 (5.0)	-18.3 (15.8)
SN 2000dk	1.00	5.01 (0.05)	4.29 (0.04)	86.6 (5.4)	-5.5 (15.9)
SN 2000dm	−1.63	4.12 (0.05)	3.07 (0.03)	75.4 (4.5)	-14.8 (15.7)
SN 2000dm	8.18	2.38 (0.04)	2.74 (0.03)	91.0 (5.4)	-4.0 (15.9)
SN 2000dn	−0.94	1.88 (0.02)	1.31 (0.01)	98.0 (5.6)	7.2 (16.0)
SN 2000dx	−9.26	0.43 (0.02)	0.36 (0.01)	95.5 (5.9)	13.6 (16.1)
SN 2000ey	7.90	4.68 (0.06)	4.53 (0.03)	67.4 (4.0)	-27.5 (15.5)
SN 2000fa	−8.25	1.92 (0.02)	1.37 (0.02)	88.1 (5.1)	4.8 (15.8)
SN 2000fa	6.86	2.32 (0.04)	2.34 (0.02)	88.6 (5.4)	-6.1 (15.9)
SN 2001ay	6.79	1.42 (0.02)	1.55 (0.02)	88.5 (5.5)	-6.2 (16.0)
SN 2001az	−3.24	1.25 (0.03)	0.77 (0.01)	96.6 (5.3)	7.8 (15.9)
SN 2001br	3.47	2.51 (0.09)	2.21 (0.06)	115.4 (6.9)	21.8 (16.5)
SN 2001br	3.48	2.31 (0.11)	2.12 (0.06)	101.3 (6.3)	7.8 (16.3)
SN 2001cp	1.39	1.52 (0.03)	1.04 (0.02)	83.9 (5.0)	-8.5 (15.8)
SN 2001da	−1.12	4.82 (0.10)	4.09 (0.05)	106.2 (6.2)	15.6 (16.2)
SN 2001eh	−4.53	2.16 (0.03)	1.39 (0.03)	98.3 (5.6)	10.7 (16.0)
SN 2001eh	3.26	1.48 (0.02)	1.12 (0.01)	89.5 (5.3)	-3.9 (15.9)
SN 2001ep	2.83	7.93 (0.07)	7.29 (0.04)	102.7 (6.3)	9.4 (16.3)
SN 2001ex	−1.82	0.72 (0.01)	0.63 (0.02)	95.2 (5.6)	5.1 (16.0)
SN 2001fe	−0.99	12.66 (0.08)	8.35 (0.05)	77.9 (4.6)	-12.8 (15.7)
SN 2001fh	5.93	0.76 (0.03)	1.03 (0.02)	86.3 (5.4)	-8.2 (15.9)
SN 2002aw	2.10	3.05 (0.08)	2.14 (0.06)	85.1 (5.2)	-7.7 (15.9)
SN 2002bf	2.97	2.92 (0.01)	3.16 (0.01)	109.5 (6.9)	16.2 (16.5)
SN 2002bf	6.90	1.80 (0.11)	2.17 (0.11)	120.7 (7.8)	26.0 (16.9)
SN 2002bo	−1.08	22.69 (0.33)	20.58 (0.31)	110.0 (6.5)	19.4 (16.3)
SN 2002bz	4.92	0.80 (0.03)	0.67 (0.02)	69.9 (4.7)	-24.2 (15.7)
SN 2002cd	1.10	1.06 (0.08)	1.10 (0.06)	93.0 (6.0)	0.8 (16.1)
SN 2002cf	−0.75	1.37 (0.03)	1.70 (0.03)	119.9 (6.5)	29.0 (16.3)
SN 2002ck	3.64	1.24 (0.04)	0.97 (0.02)	88.6 (5.2)	-5.0 (15.9)
SN 2002cr	−6.78	11.03 (0.10)	7.44 (0.09)	77.4 (4.4)	-7.7 (15.6)
SN 2002cs	−7.76	2.47 (0.04)	1.84 (0.02)	80.1 (4.7)	-3.8 (15.7)
SN 2002db	9.21	0.76 (0.02)	0.76 (0.02)	91.5 (5.5)	-3.6 (16.0)
SN 2002de	−0.32	1.95 (0.05)	1.32 (0.04)	100.5 (6.0)	9.2 (16.2)
SN 2002de	8.37	1.15 (0.03)	1.27 (0.01)	85.4 (5.3)	-9.6 (15.9)
SN 2002dj	−7.98	10.28 (0.12)	7.90 (0.10)	110.8 (6.5)	27.2 (16.3)
SN 2002eb	1.68	2.89 (0.03)	2.11 (0.03)	88.0 (5.2)	-4.5 (15.9)
SN 2002ef	4.70	1.41 (0.09)	1.35 (0.08)	80.5 (5.4)	-13.6 (15.9)
SN 2002er	−4.58	9.21 (0.03)	7.20 (0.03)	98.7 (5.6)	11.2 (16.0)
SN 2002eu	−0.06	1.13 (0.03)	1.04 (0.03)	97.1 (5.9)	5.7 (16.1)

Continued on Next Page...

Table 3.8 — Continued

SN Name	Phase[a]	F_b[b]	F_r[b]	pEW[c]	ΔpEW[c,d]
SN 2002fk	7.74	29.02 (0.14)	25.85 (0.13)	77.6 (4.8)	-17.3 (15.7)
SN 2002ha	−0.85	8.65 (0.08)	6.18 (0.04)	84.3 (4.9)	-6.6 (15.8)
SN 2002ha	4.93	6.49 (0.05)	5.69 (0.04)	78.9 (4.9)	-15.2 (15.8)
SN 2002ha	7.89	11.16 (0.08)	12.44 (0.07)	86.2 (5.4)	-8.7 (15.9)
SN 2002he	−5.91	1.56 (0.05)	1.08 (0.04)	71.8 (6.2)	-14.2 (16.2)
SN 2002he	0.29	3.15 (0.02)	2.45 (0.01)	85.2 (5.2)	-6.5 (15.9)
SN 2002he	3.22	6.00 (0.04)	5.44 (0.04)	81.6 (5.2)	-11.8 (15.9)
SN 2002hu	−5.81	1.32 (0.01)	0.82 (0.01)	90.9 (5.1)	4.7 (15.8)
SN 2002hw	−6.27	1.02 (0.02)	1.11 (0.01)	83.3 (4.9)	-2.4 (15.8)
SN 2002jy	11.86	1.62 (0.02)	2.03 (0.02)	88.8 (5.7)	-6.3 (16.1)
SN 2002kf	6.81	3.35 (0.02)	3.34 (0.02)	88.7 (5.5)	-6.0 (16.0)
SN 2003U	−2.55	1.81 (0.03)	1.15 (0.02)	94.4 (5.6)	4.9 (16.0)
SN 2003W	−5.06	1.21 (0.03)	1.00 (0.02)	96.2 (5.9)	9.2 (16.1)
SN 2003ai	7.25	1.24 (0.03)	1.30 (0.03)	93.6 (5.7)	-1.2 (16.0)
SN 2003cq	−0.15	0.97 (0.01)	0.71 (0.02)	102.7 (6.1)	11.3 (16.2)
SN 2003gn	−5.38	0.35 (0.02)	0.23 (0.02)	103.0 (6.3)	16.3 (16.2)
SN 2003gt	−5.07	5.23 (0.14)	3.61 (0.08)	83.1 (4.6)	-3.9 (15.7)
SN 2003he	2.71	2.36 (0.05)	1.80 (0.03)	86.7 (5.2)	-6.5 (15.9)
SN 2003hs	−5.49	0.28 (0.02)	0.25 (0.02)	97.2 (6.5)	10.7 (16.3)
SN 2003iv	1.76	0.07 (0.00)	0.05 (0.00)	84.9 (5.2)	-7.7 (15.9)
SN 2003iv	6.58	0.26 (0.01)	0.28 (0.01)	88.3 (5.6)	-6.3 (16.0)
SN 2004S	8.26	8.94 (0.03)	9.52 (0.01)	127.0 (6.6)	32.0 (16.4)
SN 2004as	−4.36	1.41 (0.02)	1.10 (0.02)	109.2 (6.3)	21.5 (16.3)
SN 2004bg	10.34	2.56 (0.05)	2.82 (0.05)	89.5 (5.6)	-5.6 (16.0)
SN 2004bk	6.13	3.13 (0.11)	2.83 (0.05)	108.1 (6.2)	13.6 (16.2)
SN 2004bl	4.61	4.78 (0.26)	3.57 (0.17)	86.4 (5.2)	-7.6 (15.9)
SN 2004br	3.50	4.38 (0.06)	3.13 (0.04)	59.3 (3.6)	-34.2 (15.4)
SN 2004bv	−7.06	10.99 (0.07)	8.17 (0.06)	78.2 (4.8)	-6.6 (15.7)
SN 2004bv	9.77	12.07 (0.21)	13.93 (0.12)	106.9 (6.4)	11.8 (16.3)
SN 2004bw	6.59	1.85 (0.04)	1.81 (0.04)	99.1 (5.9)	4.5 (16.1)
SN 2004dt	−6.46	5.41 (0.07)	4.02 (0.06)	118.8 (6.8)	33.4 (16.5)
SN 2004ef	−5.52	1.06 (0.02)	0.86 (0.01)	96.5 (5.8)	10.0 (16.1)
SN 2004eo	−5.57	2.67 (0.05)	2.01 (0.04)	91.7 (5.3)	5.2 (15.9)
SN 2004ey	−7.58	6.10 (0.03)	4.10 (0.02)	83.1 (4.7)	-1.1 (15.7)
SN 2004fu	−2.65	5.72 (0.04)	4.51 (0.03)	94.5 (5.7)	5.1 (16.0)
SN 2004fu	2.43	5.54 (0.06)	5.12 (0.06)	95.4 (5.9)	2.4 (16.1)
SN 2004fz	−5.18	6.24 (0.07)	4.67 (0.05)	87.2 (5.1)	0.4 (15.8)
SN 2004gs	0.44	1.05 (0.02)	1.13 (0.01)	109.9 (6.6)	18.1 (16.4)
SN 2005A	5.55	0.13 (0.01)	0.26 (0.01)	138.3 (8.7)	44.0 (17.3)
SN 2005M	9.23	2.37 (0.02)	2.14 (0.02)	105.2 (5.9)	10.1 (16.1)
SN 2005ag	0.53	0.08 (0.00)	0.05 (0.00)	84.3 (5.3)	-7.6 (15.9)
SN 2005ao	−1.29	1.35 (0.02)	0.93 (0.02)	79.6 (4.8)	-10.9 (15.7)
SN 2005ao	0.52	1.11 (0.02)	0.80 (0.02)	87.1 (5.1)	-4.8 (15.8)
SN 2005bc	1.55	2.59 (0.03)	2.48 (0.03)	80.7 (5.0)	-11.8 (15.8)
SN 2005cf	−10.94	7.27 (0.09)	5.46 (0.06)	82.4 (5.2)	2.8 (15.9)
SN 2005cf	−2.11	256.89 (1.97)	173.22 (1.68)	96.0 (5.4)	6.2 (15.9)
SN 2005cf	−1.19	52.69 (0.50)	35.99 (0.28)	97.0 (5.4)	6.4 (15.9)
SN 2005de	−0.75	5.24 (0.09)	3.68 (0.07)	100.2 (5.6)	9.3 (16.0)
SN 2005dv	−0.57	1.47 (0.09)	1.38 (0.08)	126.0 (7.7)	34.9 (16.9)
SN 2005el	−6.70	4.14 (0.06)	2.95 (0.05)	59.4 (3.4)	-25.8 (15.4)
SN 2005el	1.22	6.83 (0.09)	5.05 (0.06)	74.5 (4.4)	-17.8 (15.6)
SN 2005eq	−6.01	0.84 (0.04)	0.58 (0.03)	85.6 (5.1)	-0.3 (15.8)
SN 2005eq	−2.98	2.21 (0.01)	1.57 (0.01)	87.3 (5.1)	-1.8 (15.8)
SN 2005eq	0.66	2.24 (0.03)	1.61 (0.02)	86.6 (5.2)	-5.4 (15.9)
SN 2005eu	−9.06	0.71 (0.01)	0.50 (0.01)	87.7 (4.4)	5.5 (15.6)
SN 2005eu	−5.46	1.24 (0.05)	0.90 (0.03)	106.4 (5.8)	19.8 (16.1)
SN 2005ki	1.62	20.18 (0.25)	14.88 (0.12)	80.7 (6.7)	-11.8 (16.4)
SN 2005ms	−1.88	7.81 (0.14)	5.15 (0.17)	106.0 (6.1)	16.0 (16.2)
SN 2005na	0.03	2.59 (0.06)	1.77 (0.03)	92.8 (5.1)	1.3 (15.8)
SN 2005na	1.03	3.07 (0.10)	2.06 (0.07)	79.1 (4.8)	-13.1 (15.8)
SN 2006D	3.70	38.68 (0.34)	35.73 (0.27)	141.3 (7.4)	47.6 (16.7)
SN 2006N	−1.89	5.33 (0.08)	3.80 (0.05)	86.1 (4.9)	-4.0 (15.8)
SN 2006N	−0.90	5.10 (0.06)	3.67 (0.04)	83.8 (4.9)	-7.0 (15.8)
SN 2006S	−3.93	25.29 (0.79)	17.20 (0.40)	88.4 (5.2)	0.3 (15.9)
SN 2006S	2.99	1.35 (0.05)	0.97 (0.03)	96.6 (5.5)	3.3 (16.0)
SN 2006X	3.15	3.57 (0.04)	5.83 (0.04)	115.5 (7.3)	22.1 (16.7)
SN 2006ac	7.96	2.08 (0.04)	2.61 (0.03)	121.8 (7.6)	26.9 (16.8)
SN 2006ak	8.43	0.64 (0.01)	0.78 (0.01)	96.3 (6.0)	1.3 (16.2)
SN 2006bq	6.97	8.57 (0.08)	8.34 (0.06)	104.0 (6.5)	9.2 (16.3)
SN 2006bt	−5.30	0.76 (0.01)	0.75 (0.01)	67.5 (4.4)	-19.2 (15.6)
SN 2006bt	−4.53	0.84 (0.02)	0.79 (0.02)	73.8 (4.7)	-13.7 (15.7)
SN 2006bu	4.22	0.25 (0.01)	0.20 (0.01)	83.8 (5.3)	-10.1 (15.9)
SN 2006cf	6.28	0.44 (0.04)	0.36 (0.03)	64.8 (5.2)	-29.8 (15.9)
SN 2006cj	3.43	0.40 (0.01)	0.29 (0.01)	80.7 (4.9)	-12.8 (15.8)
SN 2006cm	−1.15	0.30 (0.02)	0.40 (0.01)	83.8 (4.4)	-6.8 (15.6)
SN 2006cm	6.77	0.28 (0.02)	0.33 (0.02)	100.9 (5.7)	6.2 (16.0)
SN 2006cp	−5.30	2.71 (0.03)	1.98 (0.03)	113.7 (6.5)	26.9 (16.3)
SN 2006cq	2.00	0.71 (0.02)	0.53 (0.02)	78.5 (4.8)	-14.2 (15.7)
SN 2006cz	1.12	0.81 (0.03)	0.63 (0.02)	87.6 (5.4)	-4.7 (15.9)
SN 2006dm	−7.90	0.62 (0.03)	0.49 (0.02)	73.5 (4.8)	-10.2 (15.7)
SN 2006ef	3.20	5.22 (0.03)	4.54 (0.03)	79.5 (4.6)	-13.9 (15.7)
SN 2006gr	−8.70	0.73 (0.02)	0.43 (0.01)	99.0 (5.6)	16.3 (16.0)

Continued on Next Page...

Table 3.8 — Continued

SN Name	Phase[a]	F_b[b]	F_r[b]	pEW[c]	ΔpEW[c,d]
SN 2006ej	−3.70	3.82 (0.04)	2.87 (0.06)	95.6 (5.5)	7.2 (16.0)
SN 2006ej	5.09	1.80 (0.03)	1.93 (0.02)	87.4 (5.7)	-6.8 (16.0)
SN 2006et	3.29	2.39 (0.06)	2.03 (0.02)	106.4 (6.2)	12.9 (16.2)
SN 2006et	9.14	1.33 (0.03)	1.76 (0.03)	119.6 (6.9)	24.5 (16.5)
SN 2006gt	3.08	0.32 (0.01)	0.33 (0.01)	105.6 (6.1)	12.3 (16.2)
SN 2006kf	−8.96	0.47 (0.01)	0.35 (0.01)	65.3 (4.0)	-17.1 (15.5)
SN 2006kf	−3.05	1.67 (0.02)	1.33 (0.02)	81.4 (4.9)	-7.6 (15.8)
SN 2006le	−8.69	1.24 (0.01)	0.85 (0.01)	79.8 (4.7)	-2.9 (15.7)
SN 2006lf	−6.30	0.44 (0.01)	0.39 (0.01)	76.7 (4.6)	-9.0 (15.7)
SN 2006mp	5.66	2.06 (0.02)	1.59 (0.01)	75.1 (4.5)	-19.3 (15.6)
SN 2006sr	−2.34	1.87 (0.02)	1.27 (0.02)	90.0 (5.2)	0.4 (15.9)
SN 2006sr	2.69	2.56 (0.02)	1.91 (0.02)	86.2 (5.2)	-6.9 (15.9)
SN 2007A	2.37	3.82 (0.03)	2.86 (0.03)	74.8 (4.4)	-18.2 (15.6)
SN 2007F	3.23	3.13 (0.03)	2.20 (0.02)	79.1 (4.7)	-14.3 (15.7)
SN 2007S	5.18	2.50 (0.03)	2.44 (0.02)	99.1 (5.7)	4.9 (16.1)
SN 2007af	−1.25	46.60 (0.24)	34.13 (0.17)	97.2 (5.5)	6.7 (16.0)
SN 2007af	3.81	36.12 (0.22)	34.25 (0.18)	87.8 (5.6)	-5.8 (16.0)
SN 2007bc	0.61	4.14 (0.04)	3.08 (0.03)	88.7 (5.3)	-3.2 (15.9)
SN 2007bd	−5.79	1.26 (0.05)	0.84 (0.03)	74.5 (4.6)	-11.7 (15.7)
SN 2007bm	−7.79	8.36 (0.17)	6.93 (0.12)	78.5 (4.5)	-5.3 (15.7)
SN 2007bz	1.65	2.11 (0.05)	1.73 (0.04)	84.2 (4.8)	-8.3 (15.7)
SN 2007ca	−11.14	1.51 (0.08)	1.06 (0.06)	66.0 (4.0)	-13.3 (15.5)
SN 2007ci	−6.57	2.63 (0.05)	2.13 (0.05)	87.7 (5.2)	2.3 (15.9)
SN 2007ci	−1.71	3.64 (0.03)	2.88 (0.03)	97.2 (5.8)	7.0 (16.1)
SN 2007co	−4.09	1.47 (0.03)	1.17 (0.02)	100.8 (5.8)	12.8 (16.1)
SN 2007co	0.85	1.79 (0.02)	1.43 (0.02)	102.6 (6.0)	10.5 (16.1)
SN 2007fb	1.95	5.38 (0.14)	4.11 (0.08)	89.1 (5.4)	-3.7 (15.9)
SN 2007fr	−1.25	0.33 (0.02)	0.32 (0.01)	60.9 (4.7)	-29.6 (15.7)
SN 2007fs	5.03	6.86 (0.09)	5.58 (0.06)	92.1 (5.4)	-2.1 (15.9)
SN 2007gi	−7.31	50.07 (0.22)	34.17 (0.13)	95.4 (5.4)	10.9 (15.9)
SN 2007gi	−0.35	66.11 (0.21)	48.15 (0.16)	100.0 (5.8)	8.7 (16.1)
SN 2007gi	6.61	22.85 (0.11)	23.72 (0.10)	105.9 (6.6)	11.2 (16.4)
SN 2007gk	−1.72	1.45 (0.02)	1.26 (0.02)	109.3 (6.7)	19.1 (16.4)
SN 2007hj	−1.23	3.75 (0.04)	3.84 (0.04)	101.4 (6.3)	10.8 (16.3)
SN 2007kk	7.15	3.21 (0.04)	3.20 (0.04)	105.5 (6.3)	10.7 (16.2)
SN 2007le	−10.31	8.81 (0.07)	6.25 (0.06)	100.2 (6.1)	19.7 (16.2)
SN 2007le	−9.40	10.10 (0.04)	7.41 (0.04)	93.0 (5.4)	11.2 (15.9)
SN 2007le	7.43	14.47 (0.15)	18.20 (0.10)	100.5 (6.2)	5.6 (16.2)
SN 2007s1[e]	−1.23	1.77 (0.02)	1.39 (0.02)	96.9 (5.7)	6.4 (16.0)
SN 2007on	−3.01	42.40 (0.10)	36.15 (0.07)	76.6 (5.0)	-12.4 (15.8)
SN 2007on	−3.00	33.44 (0.07)	28.86 (0.05)	75.0 (6.9)	-14.0 (16.5)
SN 2007qe	−6.54	3.05 (0.04)	1.85 (0.02)	105.3 (5.9)	19.9 (16.1)
SN 2007qe	6.23	3.11 (0.06)	3.04 (0.04)	107.6 (6.5)	13.1 (16.3)
SN 2008Q	6.46	21.06 (0.30)	20.95 (0.33)	66.6 (4.5)	-28.0 (15.7)
SN 2008Z	−2.29	3.30 (0.07)	2.42 (0.06)	89.4 (4.8)	-0.3 (15.7)
SN 2008ar	2.83	2.93 (0.12)	2.35 (0.06)	87.5 (5.3)	-5.7 (15.9)
SN 2008s1[f]	−6.36	2.36 (0.06)	1.72 (0.03)	66.9 (3.9)	-18.7 (15.5)
SN 2008s1[f]	−4.40	2.73 (0.14)	2.08 (0.14)	62.7 (4.0)	-25.0 (15.5)
SN 2008s1[f]	−3.42	2.89 (0.07)	2.35 (0.06)	69.5 (4.1)	-19.1 (15.5)
SN 2008s1[f]	0.49	3.47 (0.13)	3.30 (0.07)	70.8 (4.2)	-21.0 (15.6)
SN 2008s1[f]	4.40	3.30 (0.05)	2.74 (0.03)	93.3 (5.1)	-0.6 (15.8)
SN 2008s1[f]	5.38	2.97 (0.05)	2.60 (0.02)	83.5 (4.8)	-10.8 (15.7)
SN 2008cl	4.24	0.23 (0.03)	0.18 (0.02)	82.1 (5.8)	-11.8 (16.1)
SN 2008ec	−0.24	4.65 (0.05)	3.53 (0.03)	84.8 (5.1)	-6.5 (15.8)
SN 2008ec	5.70	3.26 (0.05)	3.37 (0.03)	95.2 (6.0)	0.8 (16.1)
SN 2008ei	3.29	0.57 (0.02)	0.52 (0.01)	117.3 (7.2)	23.8 (16.6)
SN 2008ei	9.13	0.37 (0.02)	0.46 (0.01)	132.2 (8.2)	37.1 (17.1)
SN 2008s5[g]	1.26	2.75 (0.09)	2.04 (0.06)	90.3 (5.3)	-2.0 (15.9)
SN 2008s5[g]	8.96	1.72 (0.03)	1.48 (0.03)	97.3 (5.4)	2.2 (15.9)
SN 2008hs	−7.94	1.25 (0.02)	0.97 (0.02)	72.3 (4.5)	-11.4 (15.7)

Uncertainties for each measured value are given in parentheses.
[a]Phases of spectra are in rest-frame days using the heliocentric redshift and photometry reference presented in table 1 of Silverman et al. (submitted).
[b]Fluxes are in units of 10^{-15} erg s^{-1} cm^{-2} $Å^{-1}$.
[c]The pEW and ΔpEW are in units of Å.
[d]ΔpEW is the measured pEW minus the expected pEW at the same epoch using our linear or quadratic fit (see Section 3.5.4 for more information).
[e]Also known as SNF20071021-000.
[f]Also known as SNF20080514-002.
[g]Also known as SNF20080909-030.

Table 3.9: Measured Values for Fe II

SN Name	Phase[a]	F_b[b]	F_r[b]	pEW[c]	ΔpEW[c,d]
SN 1989B	7.54	435.78 (2.00)	311.99 (1.05)	208.8 (8.3)	13.3 (45.4)

Continued on Next Page...

Table 3.9 — Continued

SN Name	Phase[a]	F_b[b]	F_r[b]	pEW[c]	ΔpEW[c,d]
SN 1989M	2.49	38.42 (0.14)	31.16 (0.07)	176.4 (8.3)	23.3 (45.4)
SN 1989M	3.48	46.53 (0.15)	35.13 (0.09)	191.8 (8.9)	31.3 (45.5)
SN 1990N	7.11	50.99 (0.41)	42.91 (0.19)	164.2 (5.4)	-27.2 (45.0)
SN 1991T	−10.10	86.40 (0.36)	64.16 (0.18)	84.7 (2.9)	-15.1 (44.7)
SN 1991T	−9.11	57.61 (0.24)	45.11 (0.28)	88.2 (4.8)	-13.0 (44.9)
SN 1991T	6.80	31.26 (0.29)	24.42 (0.14)	157.1 (5.2)	-31.5 (44.9)
SN 1991bg	0.14	15.58 (0.32)	12.38 (0.10)	157.0 (4.3)	19.6 (44.8)
SN 1991bg	1.14	18.36 (0.43)	15.78 (0.14)	153.6 (4.3)	9.8 (44.8)
SN 1994D	−12.31	19.63 (0.25)	14.00 (0.06)	206.7 (9.5)	108.6 (45.6)
SN 1994D	−5.32	69.32 (0.30)	45.31 (0.19)	82.1 (4.4)	-29.0 (44.9)
SN 1994Q	9.68	2.43 (0.02)	1.81 (0.02)	185.3 (8.4)	-32.0 (45.4)
SN 1994S	1.11	16.64 (0.10)	12.30 (0.06)	100.0 (5.1)	-43.6 (44.9)
SN 1995D	3.84	31.31 (0.08)	22.51 (0.10)	119.2 (5.8)	-44.0 (45.0)
SN 1995E	−2.46	1.55 (0.02)	1.52 (0.02)	99.4 (5.1)	-23.8 (44.9)
SN 1995ac	−6.34	0.38 (0.01)	0.28 (0.01)	109.4 (5.8)	1.6 (45.0)
SN 1997Y	1.27	7.63 (0.05)	5.03 (0.04)	135.2 (6.7)	-9.4 (45.1)
SN 1997bp	5.49	15.12 (0.08)	12.44 (0.08)	262.3 (11.6)	85.5 (46.1)
SN 1997br	−4.84	14.89 (0.08)	12.39 (0.08)	90.0 (4.7)	-22.9 (44.9)
SN 1998V	7.20	6.16 (0.03)	5.16 (0.02)	172.4 (11.5)	-19.9 (46.1)
SN 1998dk	−7.24	4.67 (0.05)	3.39 (0.04)	101.0 (5.3)	-4.3 (44.9)
SN 1998dk	−0.54	7.71 (0.04)	5.89 (0.03)	142.8 (6.9)	9.4 (45.2)
SN 1998dm	−12.48	2.19 (0.02)	2.30 (0.02)	57.3 (3.1)	-40.7 (44.7)
SN 1998dm	−5.61	7.24 (0.05)	5.80 (0.03)	82.1 (4.2)	-28.0 (44.8)
SN 1998dm	14.22	5.61 (0.05)	4.96 (0.05)	263.3 (11.4)	-6.9 (46.1)
SN 1998dx	5.13	0.93 (0.02)	0.56 (0.01)	140.1 (6.7)	-33.7 (45.1)
SN 1998ec	11.86	1.88 (0.02)	1.62 (0.01)	259.9 (11.5)	18.5 (46.1)
SN 1998es	0.28	17.97 (0.11)	13.90 (0.09)	106.6 (5.3)	-31.7 (45.0)
SN 1999aa	−10.58	2.53 (0.04)	1.86 (0.04)	84.8 (4.5)	-14.4 (44.9)
SN 1999aa	0.24	2.67 (0.02)	1.84 (0.02)	119.9 (5.9)	-18.1 (45.0)
SN 1999aa	14.04	12.76 (0.11)	10.07 (0.04)	225.0 (6.4)	-43.0 (45.1)
SN 1999aa	17.04	5.21 (0.03)	3.89 (0.02)	262.5 (11.3)	-45.6 (46.0)
SN 1999ac	−0.89	15.14 (0.08)	10.12 (0.06)	153.6 (7.1)	22.2 (45.2)
SN 1999cp	4.91	15.48 (0.07)	10.95 (0.06)	130.5 (6.4)	-41.5 (45.1)
SN 1999cp	13.85	10.94 (0.06)	8.45 (0.04)	247.9 (10.8)	-17.8 (45.9)
SN 1999cw	14.79	11.99 (0.16)	7.67 (0.07)	212.6 (9.4)	-65.1 (45.6)
SN 1999da	−2.12	2.05 (0.02)	1.54 (0.01)	141.0 (6.5)	16.1 (45.1)
SN 1999dg	15.08	1.46 (0.04)	1.12 (0.02)	294.3 (12.5)	13.0 (46.4)
SN 1999dk	17.06	7.70 (0.05)	6.72 (0.03)	306.0 (12.9)	-2.4 (46.5)
SN 1999do	9.96	1.58 (0.02)	1.35 (0.02)	114.9 (5.8)	-105.3 (45.0)
SN 1999dq	−3.93	7.34 (0.09)	5.75 (0.07)	109.9 (5.5)	-6.6 (45.0)
SN 1999dq	2.97	8.31 (0.06)	5.97 (0.03)	133.1 (6.4)	-23.5 (45.1)
SN 1999ee	17.65	6.93 (0.08)	5.79 (0.09)	266.8 (11.0)	-50.0 (46.0)
SN 1999ek	5.66	1.16 (0.12)	1.16 (0.05)	166.9 (8.1)	-11.4 (45.4)
SN 1999gd	−1.12	1.32 (0.02)	1.06 (0.01)	139.9 (4.4)	9.8 (44.9)
SN 1999gh	4.12	11.45 (0.09)	7.95 (0.06)	227.2 (6.2)	61.7 (45.1)
SN 2000cp	2.92	0.47 (0.01)	0.36 (0.01)	202.0 (9.5)	45.7 (45.6)
SN 2000cp	11.70	0.36 (0.02)	0.32 (0.03)	278.0 (12.3)	38.5 (46.3)
SN 2000cu	9.64	1.94 (0.02)	1.47 (0.02)	249.7 (10.8)	32.9 (45.9)
SN 2000cw	4.81	1.18 (0.02)	0.77 (0.01)	182.2 (8.6)	11.1 (45.5)
SN 2000dg	−5.09	0.78 (0.01)	0.54 (0.01)	89.0 (4.9)	-22.9 (44.9)
SN 2000dg	4.66	0.87 (0.01)	0.69 (0.01)	155.7 (7.3)	-14.1 (45.2)
SN 2000dk	1.00	4.29 (0.04)	2.93 (0.02)	119.1 (6.1)	-23.8 (45.1)
SN 2000dk	10.84	2.75 (0.03)	2.09 (0.02)	240.6 (10.4)	10.8 (45.8)
SN 2000dm	−1.63	3.03 (0.03)	2.31 (0.02)	89.0 (5.0)	-38.4 (44.9)
SN 2000dm	8.18	2.73 (0.03)	2.26 (0.02)	168.7 (7.7)	-33.1 (45.3)
SN 2000dn	−0.94	1.29 (0.01)	0.93 (0.01)	129.1 (7.0)	-1.9 (45.2)
SN 2000dn	16.38	0.63 (0.01)	0.47 (0.01)	249.1 (10.8)	-49.8 (45.9)
SN 2000dr	6.78	2.54 (0.03)	1.83 (0.01)	232.7 (9.8)	44.3 (45.7)
SN 2000ey	7.90	4.54 (0.03)	3.81 (0.05)	107.7 (5.1)	-91.2 (44.9)
SN 2000fa	−8.25	1.38 (0.02)	0.94 (0.02)	107.3 (5.3)	4.5 (45.0)
SN 2000fa	6.86	2.35 (0.02)	1.79 (0.02)	197.5 (9.2)	8.3 (45.6)
SN 2001E	15.01	1.09 (0.05)	1.09 (0.03)	312.6 (13.4)	32.1 (46.6)
SN 2001G	11.57	5.44 (0.03)	4.04 (0.02)	208.7 (9.7)	-29.3 (45.7)
SN 2001V	15.86	8.80 (0.06)	6.79 (0.06)	293.4 (12.5)	1.5 (46.4)
SN 2001ay	6.79	1.54 (0.02)	1.14 (0.01)	163.0 (7.4)	-25.5 (45.3)
SN 2001az	−3.24	0.78 (0.01)	0.53 (0.01)	106.3 (5.5)	-13.2 (45.0)
SN 2001bf	1.22	6.19 (0.05)	4.93 (0.04)	79.5 (4.2)	-64.8 (44.8)
SN 2001bg	13.70	11.32 (0.05)	8.98 (0.04)	297.2 (12.7)	33.5 (46.4)
SN 2001br	3.47	2.20 (0.06)	1.44 (0.07)	168.4 (8.3)	8.1 (45.4)
SN 2001br	3.48	2.11 (0.06)	1.46 (0.05)	168.9 (7.8)	8.4 (45.3)
SN 2001bp	0.51	0.27 (0.02)	0.18 (0.01)	95.0 (5.6)	-44.7 (45.0)
SN 2001cp	1.39	1.06 (0.02)	0.85 (0.02)	93.9 (4.9)	-51.5 (44.9)
SN 2001cp	18.00	0.71 (0.03)	0.60 (0.02)	273.2 (11.9)	-48.7 (46.2)
SN 2001da	−1.12	4.07 (0.05)	2.72 (0.04)	182.4 (8.6)	52.3 (45.5)
SN 2001da	9.72	3.42 (0.02)	2.76 (0.03)	278.3 (12.1)	60.8 (46.3)
SN 2001dl	13.84	0.77 (0.02)	0.70 (0.02)	225.0 (10.1)	-40.4 (45.8)
SN 2001dt	13.60	0.16 (0.01)	0.17 (0.01)	311.2 (13.3)	48.7 (46.6)
SN 2001dw	11.06	0.48 (0.02)	0.65 (0.01)	356.2 (13.6)	123.9 (46.7)
SN 2001eh	−4.53	1.37 (0.03)	0.95 (0.02)	87.6 (4.7)	-26.4 (44.9)
SN 2001eh	3.26	1.14 (0.01)	0.79 (0.01)	127.4 (6.1)	-31.3 (45.1)
SN 2001en	10.09	4.83 (0.05)	3.80 (0.03)	261.5 (11.7)	39.9 (46.1)
SN 2001en	14.72	3.58 (0.02)	2.93 (0.03)	316.5 (13.4)	39.8 (46.6)

Continued on Next Page...

Table 3.9 — Continued

SN Name	Phase[a]	F_b[b]	F_r[b]	pEW[c]	ΔpEW[c,d]
SN 2001ep	2.83	7.38 (0.04)	5.00 (0.03)	178.6 (8.3)	23.1 (45.4)
SN 2001ep	4.99	6.75 (0.19)	4.78 (0.09)	215.2 (13.5)	42.6 (46.6)
SN 2001ep	5.97	6.42 (0.11)	4.84 (0.05)	236.5 (14.7)	55.4 (47.0)
SN 2001ep	7.85	6.05 (0.05)	4.98 (0.04)	260.6 (11.3)	62.0 (46.0)
SN 2001ex	−1.82	0.62 (0.02)	0.45 (0.01)	97.2 (5.3)	-29.2 (45.0)
SN 2001fe	−0.99	8.36 (0.05)	6.24 (0.04)	85.0 (4.7)	-45.8 (44.9)
SN 2001fh	5.93	1.03 (0.02)	0.90 (0.02)	144.4 (6.8)	-36.3 (45.1)
SN 2001fh	7.84	0.91 (0.03)	0.89 (0.02)	179.8 (11.2)	-18.7 (46.0)
SN 2002G	19.31	0.31 (0.03)	0.37 (0.04)	406.9 (15.8)	65.5 (47.4)
SN 2002aw	2.10	2.15 (0.06)	1.44 (0.06)	129.8 (6.6)	-20.5 (45.1)
SN 2002aw	15.84	1.53 (0.01)	1.19 (0.01)	290.8 (12.5)	-0.8 (46.4)
SN 2002bf	2.97	3.20 (0.01)	2.51 (0.00)	241.7 (10.8)	85.1 (45.9)
SN 2002bf	6.90	2.20 (0.11)	1.69 (0.05)	316.2 (13.9)	126.7 (46.8)
SN 2002bo	−1.08	20.21 (0.30)	15.22 (0.20)	201.5 (9.3)	71.2 (45.6)
SN 2002bo	15.99	10.88 (0.08)	11.47 (0.10)	338.0 (14.1)	44.4 (46.8)
SN 2002bz	4.92	0.66 (0.02)	0.44 (0.01)	114.1 (6.0)	-57.9 (45.0)
SN 2002cd	1.10	1.18 (0.06)	1.27 (0.04)	192.8 (9.0)	49.4 (45.5)
SN 2002cd	17.89	0.58 (0.02)	1.05 (0.02)	359.7 (15.2)	39.4 (47.1)
SN 2002cf	−0.75	1.71 (0.03)	1.25 (0.02)	144.8 (6.7)	12.6 (45.1)
SN 2002ck	3.64	1.02 (0.03)	0.84 (0.02)	144.4 (7.1)	-17.3 (45.2)
SN 2002cr	−6.78	7.36 (0.09)	5.17 (0.06)	75.3 (4.1)	-31.2 (44.8)
SN 2002cu	16.62	1.08 (0.05)	1.17 (0.06)	285.1 (12.2)	-17.2 (46.3)
SN 2002db	9.21	0.76 (0.02)	0.70 (0.03)	197.2 (9.3)	-15.0 (45.6)
SN 2002de	−0.32	1.29 (0.04)	1.01 (0.06)	127.0 (7.0)	-7.6 (45.2)
SN 2002de	8.37	1.26 (0.01)	1.02 (0.01)	215.5 (10.3)	11.8 (45.8)
SN 2002df	6.55	0.40 (0.02)	0.36 (0.03)	246.2 (11.1)	60.0 (46.0)
SN 2002dp	15.55	6.07 (0.09)	4.70 (0.05)	284.1 (12.1)	-3.5 (46.2)
SN 2002eb	1.68	2.11 (0.03)	1.63 (0.02)	130.5 (6.5)	-16.9 (45.1)
SN 2002ef	4.70	1.35 (0.08)	1.18 (0.05)	142.2 (7.3)	-28.0 (45.2)
SN 2002eh	6.88	0.33 (0.02)	0.51 (0.02)	388.5 (14.9)	199.2 (47.1)
SN 2002el	11.82	1.43 (0.02)	1.01 (0.01)	250.7 (10.9)	9.7 (46.0)
SN 2002er	−4.58	7.21 (0.03)	5.36 (0.03)	119.2 (6.1)	5.3 (45.0)
SN 2002er	5.26	8.72 (0.06)	6.98 (0.06)	207.0 (9.3)	32.1 (45.6)
SN 2002et	11.92	0.48 (0.03)	0.43 (0.03)	163.4 (7.8)	-78.6 (45.3)
SN 2002eu	−0.06	1.03 (0.03)	0.57 (0.01)	134.7 (6.5)	-1.6 (45.1)
SN 2002eu	9.38	0.49 (0.02)	0.33 (0.01)	227.8 (10.0)	13.8 (45.7)
SN 2002fb	0.98	1.48 (0.03)	0.93 (0.02)	117.3 (5.8)	-25.4 (45.0)
SN 2002fk	7.74	25.74 (0.13)	19.52 (0.13)	135.2 (6.6)	-62.4 (45.1)
SN 2002ha	−0.85	6.20 (0.04)	4.52 (0.04)	97.4 (5.2)	-34.2 (44.9)
SN 2002ha	4.93	5.69 (0.04)	4.22 (0.04)	125.0 (6.3)	-47.1 (45.1)
SN 2002ha	7.89	12.42 (0.07)	10.01 (0.05)	166.1 (7.6)	-32.8 (45.3)
SN 2002hd	6.48	2.12 (0.02)	1.26 (0.02)	185.8 (8.4)	0.1 (45.4)
SN 2002hd	12.72	0.62 (0.04)	0.49 (0.03)	261.3 (15.8)	9.6 (47.4)
SN 2002he	0.29	2.42 (0.01)	1.75 (0.01)	122.7 (6.1)	-15.6 (45.1)
SN 2002he	3.22	5.42 (0.04)	3.91 (0.03)	142.2 (6.8)	-16.3 (45.2)
SN 2002hu	−5.81	0.86 (0.01)	0.58 (0.01)	85.1 (4.4)	-24.4 (44.9)
SN 2002jg	10.11	0.69 (0.03)	0.69 (0.02)	248.9 (11.0)	27.2 (46.0)
SN 2002jy	11.86	2.03 (0.02)	1.59 (0.02)	210.6 (9.6)	-30.8 (45.7)
SN 2002kf	6.81	3.37 (0.02)	2.58 (0.02)	162.3 (7.6)	-26.3 (45.3)
SN 2003D	9.98	1.35 (0.01)	1.12 (0.01)	243.5 (10.5)	23.2 (45.9)
SN 2003K	13.43	1.50 (0.03)	1.12 (0.02)	232.5 (10.4)	-27.8 (45.8)
SN 2003U	−2.55	1.16 (0.02)	0.82 (0.01)	108.4 (5.8)	-14.3 (45.0)
SN 2003W	18.14	1.76 (0.01)	2.00 (0.01)	354.0 (14.4)	30.1 (46.9)
SN 2003Y	−1.74	0.66 (0.02)	0.52 (0.01)	233.5 (9.2)	106.7 (45.6)
SN 2003ai	7.25	1.30 (0.03)	1.00 (0.02)	180.5 (8.4)	-12.2 (45.4)
SN 2003cq	−0.15	0.72 (0.02)	0.49 (0.01)	157.3 (7.8)	21.7 (45.3)
SN 2003du	17.61	13.63 (0.02)	10.14 (0.01)	271.5 (11.5)	-44.8 (46.1)
SN 2003fa	−8.16	0.50 (0.01)	0.36 (0.01)	71.4 (3.9)	-31.6 (44.8)
SN 2003gn	−5.38	0.25 (0.02)	0.16 (0.01)	156.2 (8.2)	45.3 (45.4)
SN 2003gt	−5.07	3.61 (0.08)	2.64 (0.07)	80.7 (4.4)	-31.4 (44.9)
SN 2003gt	17.61	2.70 (0.04)	2.41 (0.02)	288.7 (12.0)	-27.5 (46.2)
SN 2003he	2.71	1.82 (0.03)	1.36 (0.02)	150.2 (7.3)	-4.4 (45.2)
SN 2003he	8.54	1.81 (0.04)	1.26 (0.02)	194.5 (9.1)	-10.9 (45.6)
SN 2003hs	−5.49	0.25 (0.02)	0.24 (0.01)	173.1 (8.1)	62.5 (45.4)
SN 2003iv	6.58	0.28 (0.01)	0.21 (0.01)	154.0 (7.3)	-32.6 (45.2)
SN 2004E	5.26	2.30 (0.12)	1.65 (0.03)	128.3 (6.4)	-46.6 (45.1)
SN 2004S	8.26	9.31 (0.01)	7.34 (0.01)	175.0 (7.8)	-27.6 (45.3)
SN 2004as	−4.36	1.08 (0.01)	0.69 (0.01)	161.4 (7.7)	46.6 (45.3)
SN 2004bg	10.34	2.82 (0.05)	2.07 (0.05)	188.7 (8.7)	-35.6 (45.5)
SN 2004bk	6.13	2.85 (0.05)	2.29 (0.03)	202.0 (9.4)	19.6 (45.6)
SN 2004bl	4.61	3.62 (0.17)	2.42 (0.09)	132.2 (6.6)	-37.3 (45.1)
SN 2004bl	19.38	3.04 (0.03)	2.37 (0.02)	289.0 (12.3)	-53.5 (46.3)
SN 2004bv	9.77	13.80 (0.11)	10.94 (0.07)	214.0 (9.7)	-4.2 (45.7)
SN 2004bw	6.59	1.80 (0.04)	1.37 (0.01)	166.8 (7.8)	-19.9 (45.3)
SN 2004dt	18.00	2.71 (0.04)	1.71 (0.02)	280.3 (11.9)	-41.6 (46.2)
SN 2004ef	8.05	0.98 (0.05)	0.76 (0.03)	236.7 (10.6)	36.1 (45.9)
SN 2004eo	−5.57	2.01 (0.04)	1.35 (0.03)	119.3 (6.1)	9.0 (45.1)
SN 2004eo	13.19	1.60 (0.03)	1.18 (0.02)	276.5 (11.7)	19.1 (46.1)
SN 2004ey	−7.58	4.12 (0.02)	2.79 (0.02)	86.3 (4.4)	-18.1 (44.9)
SN 2004ey	18.80	2.62 (0.02)	2.12 (0.02)	294.9 (12.5)	-38.9 (46.4)
SN 2004fu	−2.65	4.58 (0.03)	3.83 (0.03)	127.5 (6.3)	5.3 (45.1)
SN 2004fu	2.43	5.14 (0.06)	4.32 (0.04)	150.2 (7.2)	-2.4 (45.2)

Continued on Next Page...

Table 3.9 — Continued

SN Name	Phase[a]	F_b[b]	F_r[b]	pEW[c]	ΔpEW[c,d]
SN 2004fz	−5.18	4.61 (0.05)	2.94 (0.04)	101.1 (5.3)	-10.6 (45.0)
SN 2004gs	0.44	1.13 (0.01)	0.69 (0.01)	187.5 (8.6)	48.3 (45.5)
SN 2005A	5.55	0.26 (0.01)	0.33 (0.01)	316.5 (14.1)	139.1 (46.8)
SN 2005M	−1.41	2.16 (0.20)	1.74 (0.09)	133.2 (7.2)	4.7 (45.2)
SN 2005M	9.23	2.08 (0.02)	1.48 (0.02)	160.1 (7.7)	-52.3 (45.3)
SN 2005ag	0.53	0.06 (0.00)	0.04 (0.00)	118.0 (6.3)	-21.8 (45.1)
SN 2005am	4.47	21.01 (0.07)	14.44 (0.04)	169.2 (7.8)	1.0 (45.3)
SN 2005ao	−1.29	0.93 (0.02)	0.66 (0.01)	99.9 (5.2)	-29.3 (44.9)
SN 2005ao	0.52	0.81 (0.02)	0.51 (0.01)	125.0 (6.1)	-14.8 (45.0)
SN 2005bc	1.55	2.51 (0.03)	1.99 (0.02)	109.7 (5.7)	-36.8 (45.0)
SN 2005be	10.96	0.51 (0.01)	0.38 (0.01)	217.3 (9.5)	-13.8 (45.6)
SN 2005cf	−10.94	5.59 (0.06)	4.34 (0.05)	136.9 (6.5)	38.1 (45.1)
SN 2005cf	−2.11	171.87 (1.76)	115.85 (0.94)	105.5 (5.4)	-19.4 (45.0)
SN 2005cf	−1.19	35.69 (0.28)	24.69 (0.24)	105.9 (5.5)	-23.8 (45.0)
SN 2005cf	18.69	11.89 (0.12)	9.57 (0.06)	288.5 (12.2)	-43.6 (46.3)
SN 2005de	−0.75	3.57 (0.07)	2.31 (0.05)	120.4 (6.2)	-11.7 (45.1)
SN 2005de	10.10	2.89 (0.03)	2.47 (0.03)	235.6 (10.2)	14.0 (45.8)
SN 2005dm	5.23	0.37 (0.01)	0.57 (0.01)	340.3 (12.5)	165.7 (46.4)
SN 2005dv	−0.57	1.36 (0.07)	1.18 (0.06)	211.1 (10.4)	77.9 (45.8)
SN 2005el	−6.70	2.97 (0.05)	2.17 (0.03)	63.8 (3.6)	-42.9 (44.8)
SN 2005el	1.22	4.91 (0.06)	3.62 (0.03)	96.7 (5.2)	-47.6 (44.9)
SN 2005el	8.09	4.35 (0.02)	3.36 (0.03)	146.2 (6.9)	-54.7 (45.2)
SN 2005eq	−6.01	0.59 (0.03)	0.42 (0.02)	91.4 (4.9)	-17.4 (44.9)
SN 2005eq	−2.98	1.57 (0.01)	1.19 (0.01)	96.3 (4.9)	-24.4 (44.9)
SN 2005eq	0.66	1.67 (0.02)	1.25 (0.02)	112.5 (5.5)	-28.2 (45.0)
SN 2005eu	−9.06	0.50 (0.01)	0.37 (0.00)	57.5 (2.9)	-43.7 (44.7)
SN 2005ew	18.23	4.76 (0.03)	4.91 (0.02)	289.9 (12.7)	-35.3 (46.4)
SN 2005kc	10.28	0.16 (0.00)	0.14 (0.00)	222.9 (13.7)	-0.7 (46.7)
SN 2005ke	7.80	3.11 (0.05)	4.59 (0.04)	281.7 (15.2)	83.7 (47.2)
SN 2005ki	1.62	14.88 (0.12)	10.78 (0.08)	109.9 (7.8)	-37.0 (45.3)
SN 2005ki	8.35	3.13 (0.08)	2.31 (0.04)	179.3 (8.1)	-24.2 (45.4)
SN 2005mc	6.64	0.98 (0.03)	0.81 (0.02)	209.7 (9.0)	22.6 (45.5)
SN 2005ms	−1.88	4.98 (0.17)	3.58 (0.07)	124.7 (6.2)	-1.3 (45.1)
SN 2005ms	14.62	1.29 (0.03)	0.97 (0.02)	264.1 (11.6)	-11.3 (46.1)
SN 2005na	0.03	1.79 (0.04)	1.23 (0.03)	91.6 (4.9)	-45.2 (44.9)
SN 2005na	1.03	2.12 (0.06)	1.40 (0.05)	96.0 (5.4)	-47.1 (45.0)
SN 2005na	17.49	1.22 (0.04)	0.90 (0.03)	277.7 (12.0)	-36.9 (46.2)
SN 2006D	3.70	36.44 (0.24)	24.01 (0.15)	129.2 (6.1)	-33.0 (45.1)
SN 2006N	−0.90	3.66 (0.04)	2.49 (0.04)	111.0 (5.8)	-20.3 (45.0)
SN 2006N	11.91	2.27 (0.04)	1.69 (0.03)	220.7 (9.7)	-21.4 (45.7)
SN 2006S	2.99	0.92 (0.03)	0.71 (0.02)	115.8 (6.0)	-41.0 (45.0)
SN 2006S	18.45	0.69 (0.01)	0.51 (0.01)	283.6 (12.2)	-45.0 (46.3)
SN 2006X	3.15	5.86 (0.04)	8.10 (0.03)	253.8 (11.2)	95.9 (46.0)
SN 2006ac	7.96	2.62 (0.03)	1.98 (0.02)	279.1 (12.4)	79.5 (46.3)
SN 2006ak	8.43	0.78 (0.01)	0.57 (0.00)	203.2 (9.0)	-1.0 (45.5)
SN 2006bq	6.97	8.38 (0.07)	6.27 (0.06)	204.4 (9.2)	14.2 (45.6)
SN 2006bq	14.55	1.60 (0.02)	1.36 (0.02)	292.4 (12.6)	17.9 (46.4)
SN 2006bq	14.64	1.28 (0.02)	1.07 (0.01)	330.5 (14.2)	54.8 (46.9)
SN 2006bt	−5.30	0.76 (0.01)	0.58 (0.01)	104.4 (5.1)	-6.8 (44.9)
SN 2006bt	−4.53	0.80 (0.02)	0.55 (0.01)	109.6 (5.3)	-4.4 (44.9)
SN 2006bt	2.27	0.67 (0.01)	0.50 (0.01)	108.7 (5.7)	-42.8 (45.0)
SN 2006bu	4.22	0.20 (0.01)	0.14 (0.00)	139.6 (7.2)	-26.7 (45.2)
SN 2006bw	8.90	0.65 (0.01)	0.46 (0.01)	245.8 (10.7)	36.8 (45.9)
SN 2006cc	17.67	0.47 (0.01)	0.36 (0.01)	260.1 (11.3)	-57.1 (46.0)
SN 2006cf	11.09	0.76 (0.01)	0.59 (0.01)	193.7 (9.0)	-38.9 (45.5)
SN 2006cf	18.69	0.30 (0.02)	0.23 (0.01)	252.7 (10.8)	-79.4 (45.9)
SN 2006cj	3.43	0.29 (0.01)	0.20 (0.01)	115.7 (6.4)	-44.3 (45.1)
SN 2006cm	−1.15	0.38 (0.01)	0.45 (0.01)	99.0 (5.1)	-31.0 (44.9)
SN 2006cm	6.77	0.33 (0.02)	0.38 (0.01)	143.5 (7.1)	-44.8 (45.2)
SN 2006cq	2.00	0.52 (0.02)	0.33 (0.01)	107.1 (5.5)	-42.5 (45.0)
SN 2006cz	1.12	0.64 (0.02)	0.49 (0.01)	119.1 (6.0)	-24.5 (45.0)
SN 2006dm	8.73	1.94 (0.02)	1.49 (0.01)	218.8 (9.5)	11.5 (45.6)
SN 2006dm	14.61	1.48 (0.06)	1.06 (0.04)	266.6 (11.5)	-8.6 (46.1)
SN 2006ef	3.20	4.56 (0.03)	3.17 (0.03)	157.3 (7.5)	-1.0 (45.3)
SN 2006ej	5.09	1.95 (0.02)	1.31 (0.02)	183.9 (8.5)	10.4 (45.4)
SN 2006em	4.16	0.34 (0.01)	0.44 (0.00)	251.0 (9.8)	85.3 (45.7)
SN 2006en	8.55	1.24 (0.04)	0.72 (0.02)	187.3 (9.0)	-18.1 (45.5)
SN 2006eu	10.17	0.30 (0.01)	0.40 (0.01)	288.6 (10.9)	66.2 (45.9)
SN 2006eu	16.02	0.16 (0.01)	0.32 (0.01)	366.9 (13.4)	72.9 (46.6)
SN 2006et	3.29	2.04 (0.02)	1.57 (0.02)	160.7 (7.6)	1.6 (45.3)
SN 2006ev	10.54	0.76 (0.02)	0.64 (0.01)	224.6 (9.9)	-1.9 (45.7)
SN 2006ev	16.36	0.53 (0.02)	0.46 (0.01)	301.5 (12.8)	2.8 (46.4)
SN 2006gt	3.08	0.34 (0.01)	0.22 (0.00)	117.7 (5.8)	-39.7 (45.0)
SN 2006kf	17.37	0.22 (0.01)	0.29 (0.00)	324.1 (12.7)	11.3 (46.4)
SN 2006le	11.92	1.61 (0.03)	1.43 (0.02)	240.1 (10.6)	-2.0 (45.9)
SN 2006lf	14.29	0.47 (0.02)	0.52 (0.02)	279.8 (11.8)	8.7 (46.2)
SN 2006mo	12.46	0.48 (0.01)	0.29 (0.01)	254.4 (10.9)	5.9 (45.9)
SN 2006mp	5.66	1.63 (0.02)	1.24 (0.01)	108.8 (5.5)	-69.5 (45.0)
SN 2006or	−2.79	1.03 (0.01)	0.87 (0.01)	179.9 (8.2)	58.4 (45.4)
SN 2006or	4.93	0.51 (0.01)	0.43 (0.01)	251.1 (10.9)	79.0 (45.9)
SN 2006os	8.61	0.34 (0.02)	0.33 (0.01)	220.8 (10.3)	14.8 (45.8)
SN 2006sr	2.69	1.92 (0.02)	1.47 (0.02)	118.6 (6.0)	-35.9 (45.0)

Continued on Next Page...

Table 3.9 — Continued

SN Name	Phase[a]	F_b[b]	F_r[b]	pEW[c]	ΔpEW[c,d]
SN 2007A	2.37	2.86 (0.03)	2.26 (0.02)	96.6 (5.1)	-55.6 (44.9)
SN 2007A	15.07	1.97 (0.03)	1.66 (0.02)	225.3 (10.0)	-56.0 (45.7)
SN 2007F	3.23	2.19 (0.02)	1.70 (0.02)	111.5 (5.7)	-47.0 (45.0)
SN 2007O	−0.33	22.93 (0.33)	15.73 (0.20)	117.1 (8.2)	-17.5 (45.4)
SN 2007N	0.44	5.07 (0.10)	4.08 (0.06)	154.3 (9.9)	15.0 (45.7)
SN 2007S	5.18	2.46 (0.02)	2.07 (0.02)	151.6 (7.2)	-22.7 (45.2)
SN 2007af	−1.25	34.27 (0.17)	22.85 (0.12)	135.7 (6.7)	6.3 (45.1)
SN 2007af	2.84	35.07 (0.18)	25.13 (0.09)	154.6 (10.4)	-1.0 (45.8)
SN 2007af	3.81	34.64 (0.17)	24.05 (0.18)	166.0 (7.8)	3.0 (45.3)
SN 2007aj	10.75	1.09 (0.02)	0.82 (0.01)	254.8 (11.2)	26.0 (46.0)
SN 2007ap	9.37	46.73 (0.51)	36.11 (0.33)	196.8 (12.1)	-17.1 (46.3)
SN 2007au	16.11	0.45 (0.02)	0.72 (0.01)	442.7 (16.2)	147.5 (47.5)
SN 2007bc	0.61	3.10 (0.03)	1.98 (0.02)	129.8 (6.5)	-10.5 (45.1)
SN 2007bd	9.70	0.97 (0.07)	0.77 (0.04)	181.9 (8.6)	-35.5 (45.5)
SN 2007bj	14.25	4.05 (0.05)	3.16 (0.05)	286.8 (12.7)	16.1 (46.4)
SN 2007bm	−7.79	6.85 (0.11)	5.75 (0.07)	84.7 (4.6)	-19.2 (44.9)
SN 2007bm	15.03	4.55 (0.08)	4.38 (0.03)	276.1 (11.7)	-4.6 (46.1)
SN 2007bm	19.96	3.55 (0.04)	4.80 (0.02)	321.4 (12.7)	-29.9 (46.4)
SN 2007bz	1.65	1.72 (0.04)	1.31 (0.03)	107.0 (5.2)	-40.2 (44.9)
SN 2007ca	−11.14	1.04 (0.05)	0.96 (0.03)	59.9 (3.5)	-38.8 (44.8)
SN 2007ca	16.46	1.72 (0.03)	1.55 (0.02)	277.8 (12.0)	-22.3 (46.2)
SN 2007cg	16.17	0.23 (0.03)	0.26 (0.02)	178.8 (8.5)	-117.2 (45.4)
SN 2007ci	−6.57	2.13 (0.05)	1.12 (0.02)	116.3 (6.0)	9.2 (45.0)
SN 2007ci	−1.71	2.88 (0.03)	1.63 (0.02)	126.8 (6.5)	-0.1 (45.1)
SN 2007ci	13.99	1.33 (0.02)	1.45 (0.03)	373.2 (14.1)	105.9 (46.8)
SN 2007co	0.85	1.42 (0.02)	0.93 (0.01)	166.8 (7.8)	24.9 (45.3)
SN 2007co	9.55	1.10 (0.01)	0.91 (0.01)	266.6 (11.7)	50.8 (46.2)
SN 2007cq	7.84	2.87 (0.06)	1.89 (0.05)	137.1 (6.2)	-61.3 (45.1)
SN 2007cq	15.57	1.09 (0.02)	0.96 (0.02)	164.5 (7.3)	-123.4 (45.2)
SN 2007cs	12.15	0.52 (0.03)	1.11 (0.01)	358.1 (13.1)	113.2 (46.5)
SN 2007fb	1.95	4.06 (0.08)	3.11 (0.04)	115.5 (6.0)	-33.7 (45.0)
SN 2007fb	14.63	1.42 (0.02)	1.18 (0.02)	231.7 (10.0)	-43.8 (45.8)
SN 2007fr	−5.83	0.24 (0.01)	0.16 (0.01)	83.9 (4.7)	-25.5 (44.9)
SN 2007fs	5.03	5.58 (0.06)	4.11 (0.05)	150.0 (7.2)	-22.9 (45.2)
SN 2007ge	12.53	0.30 (0.01)	0.23 (0.00)	198.5 (8.8)	-50.9 (45.5)
SN 2007gi	6.61	24.10 (0.09)	19.29 (0.11)	224.0 (9.8)	37.1 (45.7)
SN 2007gk	−1.72	1.26 (0.02)	0.85 (0.01)	173.9 (8.3)	47.0 (45.4)
SN 2007gk	19.65	0.31 (0.01)	0.45 (0.01)	418.6 (15.7)	72.1 (47.3)
SN 2007hj	−1.23	3.90 (0.04)	2.30 (0.03)	147.8 (7.1)	18.3 (45.2)
SN 2007kk	7.15	3.22 (0.04)	2.57 (0.03)	206.5 (9.5)	14.7 (45.6)
SN 2007le	−10.31	6.55 (0.06)	4.76 (0.05)	186.7 (8.8)	87.2 (45.5)
SN 2007le	−9.40	7.66 (0.04)	5.54 (0.03)	150.8 (7.1)	50.0 (45.2)
SN 2007le	7.43	18.20 (0.10)	16.01 (0.08)	231.9 (10.5)	37.4 (45.9)
SN 2007le	16.39	13.28 (0.05)	11.92 (0.04)	321.4 (13.7)	22.3 (46.7)
SN 2007le	17.37	12.25 (0.05)	11.16 (0.05)	328.8 (14.0)	16.0 (46.8)
SN 2007s1[e]	−1.23	1.36 (0.02)	0.92 (0.02)	128.7 (6.5)	-0.8 (45.1)
SN 2007on	15.45	45.57 (0.82)	70.78 (0.51)	316.3 (13.9)	30.0 (46.8)
SN 2007qe	6.23	3.04 (0.04)	2.35 (0.04)	219.1 (9.9)	35.8 (45.7)
SN 2007qe	16.00	1.86 (0.04)	1.57 (0.03)	316.9 (13.7)	23.1 (46.7)
SN 2008C	15.68	2.64 (0.04)	2.03 (0.02)	288.0 (12.2)	-1.5 (46.3)
SN 2008Q	6.46	20.92 (0.33)	15.91 (0.19)	141.5 (6.8)	-44.0 (45.1)
SN 2008Z	−2.29	2.43 (0.06)	1.78 (0.03)	79.5 (4.1)	-44.5 (44.8)
SN 2008Z	9.99	1.05 (0.01)	0.89 (0.01)	163.8 (5.5)	-56.7 (45.0)
SN 2008ar	2.83	2.34 (0.06)	1.30 (0.05)	138.4 (6.9)	-17.1 (45.2)
SN 2008s1[f]	0.49	3.29 (0.07)	1.65 (0.05)	120.3 (6.1)	-19.3 (45.1)
SN 2008s1[f]	4.40	2.74 (0.03)	1.65 (0.04)	115.9 (5.8)	-51.8 (45.0)
SN 2008s1[f]	5.38	2.59 (0.02)	1.58 (0.02)	109.1 (5.6)	-66.8 (45.0)
SN 2008dt	9.27	0.37 (0.03)	0.36 (0.02)	194.3 (8.8)	-18.5 (45.5)
SN 2008ec	−0.24	3.59 (0.03)	2.40 (0.04)	118.9 (6.1)	-16.3 (45.1)
SN 2008ec	5.70	3.37 (0.03)	2.71 (0.03)	194.3 (9.2)	15.6 (45.6)
SN 2008ec	12.51	2.30 (0.03)	1.82 (0.03)	247.8 (10.7)	-1.3 (45.9)
SN 2008ei	3.29	0.53 (0.01)	0.39 (0.01)	217.1 (9.9)	58.1 (45.7)
SN 2008ei	9.13	0.46 (0.01)	0.41 (0.01)	292.2 (13.0)	80.8 (46.5)
SN 2008s5[g]	1.26	1.98 (0.06)	1.52 (0.06)	113.6 (5.6)	-31.0 (45.0)
SN 2008s5[g]	8.96	1.46 (0.03)	1.13 (0.02)	135.6 (6.7)	-74.0 (45.1)
SN 2008s5[g]	15.76	0.99 (0.02)	0.77 (0.01)	220.7 (9.7)	-69.7 (45.7)

Uncertainties for each measured value are given in parentheses.
[a]Phases of spectra are in rest-frame days using the heliocentric redshift and photometry reference presented in table 1 of Silverman et al. (submitted).
[b]Fluxes are in units of 10^{-15} erg s^{-1} cm^{-2} Å^{-1}.
[c]The pEW and ΔpEW are in units of Å.
[d]ΔpEW is the measured pEW minus the expected pEW at the same epoch using our linear or quadratic fit (see Section 3.5.4 for more information).
[e]Also known as SNF20071021-000.
[f]Also known as SNF20080514-002.
[g]Also known as SNF20080909-030.

Table 3.10: Measured Values for S II "W"

SN Name	Phase[a]	F_b[b]	F_r[b]	pEW[c]	ΔpEW[c,d]	v[e]	a	FWHM[c]
SN 1989B	7.54	315.52 (0.97)	226.66 (1.80)	46.5 (2.6)	-12.6 (13.7)	6.85 (0.11)	0.282 (0.007)	241.9 (3.1)
SN 1989M	2.49	31.44 (0.08)	29.48 (0.09)	91.5 (5.2)	15.3 (14.4)	10.03 (0.11)	0.393 (0.002)	274.6 (2.4)
SN 1989M	3.48	35.49 (0.11)	32.33 (0.12)	89.8 (5.1)	15.6 (14.4)	9.60 (0.11)	0.397 (0.003)	270.6 (2.4)
SN 1990N	7.11	44.46 (0.22)	34.88 (0.19)	75.0 (3.1)	13.8 (13.8)	7.87 (0.11)	0.348 (0.008)	259.1 (4.9)
SN 1991T	6.80	24.83 (0.14)	20.75 (0.12)	47.6 (2.0)	-15.1 (13.6)	7.83 (0.11)	0.204 (0.005)	258.5 (4.9)
SN 1994D	−12.31	14.25 (0.07)	10.80 (0.06)	45.2 (2.6)	16.5 (13.7)	11.17 (0.11)	0.225 (0.005)	253.6 (2.4)
SN 1994D	−11.31	14.33 (0.14)	10.25 (0.11)	63.2 (3.6)	26.7 (13.9)	10.62 (0.11)	0.275 (0.005)	273.6 (2.4)
SN 1994D	−9.32	28.76 (0.10)	23.48 (0.10)	60.7 (3.5)	10.6 (13.9)	10.83 (0.11)	0.276 (0.005)	261.6 (2.4)
SN 1994D	−7.67	32.60 (0.07)	24.61 (0.09)	49.4 (3.0)	-9.9 (13.8)	10.30 (0.11)	0.240 (0.004)	251.6 (2.4)
SN 1994D	−6.32	45.59 (0.17)	35.46 (0.14)	55.1 (3.3)	-10.5 (13.8)	9.64 (0.11)	0.265 (0.005)	253.6 (2.4)
SN 1994D	−5.32	46.56 (0.22)	36.13 (0.18)	55.8 (3.4)	-13.5 (13.9)	9.86 (0.11)	0.265 (0.006)	257.6 (2.4)
SN 1994D	−3.87	66.48 (0.18)	53.56 (0.24)	56.5 (3.4)	-17.2 (13.9)	9.75 (0.11)	0.264 (0.004)	257.6 (2.4)
SN 1994D	−3.33	63.65 (0.14)	51.73 (0.18)	60.3 (3.6)	-14.6 (13.9)	9.64 (0.11)	0.284 (0.004)	257.6 (2.4)
SN 1994S	1.11	12.00 (0.07)	9.99 (0.10)	79.4 (4.6)	1.4 (14.2)	9.11 (0.11)	0.341 (0.003)	269.9 (2.4)
SN 1995D	3.84	23.16 (0.09)	19.13 (0.08)	89.2 (4.9)	15.9 (14.3)	8.41 (0.11)	0.376 (0.002)	272.2 (2.4)
SN 1995E	−2.46	1.61 (0.02)	1.53 (0.01)	63.1 (3.9)	-13.4 (14.0)	9.47 (0.11)	0.316 (0.008)	110.7 (2.4)
SN 1997Y	1.27	5.26 (0.03)	4.42 (0.04)	79.7 (4.7)	1.9 (14.2)	8.46 (0.11)	0.378 (0.005)	263.8 (2.4)
SN 1997bp	5.49	12.47 (0.08)	10.22 (0.06)	46.9 (2.7)	-21.3 (13.7)	12.85 (0.11)	0.196 (0.004)	259.8 (2.4)
SN 1997br	−4.84	12.44 (0.09)	9.86 (0.05)	27.6 (1.8)	-43.3 (13.6)	11.05 (0.11)	0.100 (0.005)	236.4 (2.4)
SN 1997do	−5.67	4.81 (0.05)	3.88 (0.02)	61.1 (3.7)	-7.0 (13.9)	11.66 (0.11)	0.279 (0.005)	257.4 (2.4)
SN 1998V	7.20	5.18 (0.02)	4.06 (0.02)	40.8 (3.6)	-20.0 (13.9)	8.96 (0.11)	0.232 (0.003)	100.0 (1.2)
SN 1998dk	−7.24	3.64 (0.05)	2.75 (0.01)	68.3 (4.1)	6.8 (14.1)	12.25 (0.11)	0.325 (0.009)	138.2 (2.4)
SN 1998dk	−0.54	5.99 (0.03)	5.44 (0.01)	83.5 (4.7)	5.2 (14.2)	10.81 (0.11)	0.352 (0.003)	270.4 (2.4)
SN 1998dm	−12.48	2.46 (0.02)	1.90 (0.01)	41.3 (2.6)	13.9 (13.7)	11.03 (0.11)	0.231 (0.004)	168.9 (2.4)
SN 1998dm	−5.61	5.92 (0.03)	4.56 (0.01)	55.4 (3.4)	-12.9 (13.9)	9.83 (0.11)	0.240 (0.005)	262.3 (2.4)
SN 1998dx	5.13	0.57 (0.01)	0.46 (0.01)	76.5 (4.7)	7.1 (14.2)	8.14 (0.11)	0.371 (0.012)	254.2 (2.3)
SN 1998ef	−8.62	2.54 (0.03)	1.88 (0.02)	77.5 (4.8)	23.3 (14.3)	12.59 (0.11)	0.386 (0.008)	249.6 (2.4)
SN 1998es	0.28	14.08 (0.09)	11.59 (0.04)	74.2 (4.1)	-4.2 (14.1)	8.83 (0.11)	0.290 (0.003)	287.0 (2.4)
SN 1999aa	0.24	1.94 (0.03)	1.55 (0.01)	82.0 (4.4)	3.5 (14.1)	9.23 (0.11)	0.318 (0.003)	281.9 (2.4)
SN 1999ac	−3.70	8.32 (0.08)	5.70 (0.03)	37.5 (2.2)	-36.6 (13.6)	7.45 (0.11)	0.158 (0.004)	275.4 (2.4)
SN 1999ac	−0.89	10.24 (0.05)	7.19 (0.03)	57.4 (3.3)	-20.8 (13.8)	6.48 (0.11)	0.258 (0.003)	255.6 (2.4)
SN 1999cp	4.91	10.49 (0.06)	9.71 (0.02)	84.4 (5.0)	14.2 (14.3)	7.97 (0.11)	0.408 (0.004)	261.5 (2.4)
SN 1999da	−2.12	1.58 (0.01)	1.40 (0.01)	55.3 (3.3)	-21.8 (13.8)	7.20 (0.11)	0.294 (0.003)	244.9 (2.4)
SN 1999dk	−6.60	4.53 (0.03)	3.81 (0.02)	73.9 (4.4)	9.6 (14.1)	12.43 (0.11)	0.330 (0.004)	271.9 (2.4)
SN 1999dq	−3.93	5.80 (0.07)	4.35 (0.02)	36.3 (2.3)	-37.2 (13.6)	10.18 (0.11)	0.153 (0.013)	252.4 (2.4)
SN 1999dq	2.97	6.08 (0.02)	5.60 (0.02)	77.8 (4.5)	2.5 (14.2)	9.73 (0.11)	0.370 (0.003)	264.2 (2.4)
SN 1999ek	5.66	1.20 (0.05)	1.14 (0.03)	63.6 (4.0)	-3.8 (14.0)	8.08 (0.11)	0.335 (0.006)	110.1 (2.4)
SN 1999gd	−1.12	1.08 (0.01)	1.00 (0.01)	75.6 (2.9)	-2.4 (13.7)	8.86 (0.11)	0.359 (0.005)	142.4 (6.0)
SN 1999gh	4.12	8.01 (0.06)	6.65 (0.03)	66.1 (2.5)	-6.4 (13.7)	6.47 (0.11)	0.363 (0.005)	248.1 (6.1)
SN 2000cp	2.92	0.39 (0.01)	0.33 (0.00)	114.4 (6.6)	39.0 (15.0)	7.41 (0.11)	0.488 (0.007)	266.9 (2.4)
SN 2000cw	4.81	0.80 (0.01)	0.65 (0.01)	79.3 (4.8)	8.8 (14.3)	7.50 (0.11)	0.408 (0.008)	106.8 (2.4)
SN 2000dg	−5.09	0.55 (0.01)	0.43 (0.00)	55.6 (3.5)	-14.5 (13.9)	10.46 (0.11)	0.268 (0.007)	115.6 (2.4)
SN 2000dg	4.66	0.70 (0.01)	0.60 (0.01)	61.7 (3.7)	-9.2 (13.9)	8.97 (0.11)	0.327 (0.004)	246.5 (2.4)
SN 2000dk	1.00	2.92 (0.02)	2.34 (0.01)	78.7 (4.6)	0.6 (14.2)	7.63 (0.11)	0.384 (0.008)	263.4 (2.4)
SN 2000dm	−1.63	2.32 (0.02)	1.83 (0.01)	60.1 (3.7)	-17.6 (13.9)	9.29 (0.11)	0.312 (0.004)	116.3 (2.4)
SN 2000dm	8.18	2.28 (0.02)	1.65 (0.02)	44.3 (2.8)	-11.3 (13.7)	7.57 (0.11)	0.270 (0.006)	244.3 (2.4)
SN 2000dn	−0.94	0.89 (0.01)	0.70 (0.01)	86.5 (5.3)	8.3 (14.4)	8.60 (0.11)	0.420 (0.008)	263.5 (2.4)
SN 2000ey	7.90	3.83 (0.05)	3.32 (0.02)	24.8 (1.6)	-32.5 (13.5)	10.33 (0.11)	0.127 (0.005)	184.2 (2.4)
SN 2000fa	−8.25	0.98 (0.01)	0.73 (0.01)	43.9 (2.8)	-12.4 (13.7)	12.87 (0.11)	0.219 (0.011)	88.1 (2.4)
SN 2000fa	6.86	1.80 (0.02)	1.32 (0.01)	50.5 (3.0)	-11.8 (13.8)	9.19 (0.11)	0.204 (0.007)	256.5 (2.4)
SN 2001az	−3.24	0.54 (0.01)	0.42 (0.01)	53.5 (3.4)	-21.7 (13.9)	11.09 (0.11)	0.250 (0.004)	255.6 (2.4)
SN 2001bf	1.22	4.43 (0.04)	4.01 (0.03)	63.4 (3.8)	-14.5 (14.0)	6.85 (0.11)	0.308 (0.004)	139.8 (2.4)
SN 2001br	3.47	1.42 (0.07)	1.41 (0.07)	93.2 (5.5)	19.0 (14.5)	9.75 (0.11)	0.425 (0.008)	262.6 (2.4)
SN 2001bp	0.51	0.18 (0.01)	0.15 (0.01)	59.3 (4.3)	-19.1 (14.1)	9.56 (0.11)	0.312 (0.014)	180.8 (2.2)
SN 2001cp	1.39	0.87 (0.02)	0.73 (0.02)	72.3 (4.4)	-5.5 (14.1)	9.09 (0.11)	0.318 (0.004)	105.6 (2.4)
SN 2001da	−1.12	2.79 (0.03)	2.70 (0.02)	87.3 (5.0)	9.2 (14.4)	9.38 (0.11)	0.391 (0.003)	269.4 (2.4)
SN 2001eh	−4.53	0.92 (0.03)	0.77 (0.02)	34.2 (2.3)	-37.7 (13.6)	9.73 (0.11)	0.150 (0.016)	77.1 (2.4)
SN 2001eh	3.26	0.79 (0.01)	0.73 (0.01)	72.3 (4.3)	-2.4 (14.1)	9.50 (0.11)	0.337 (0.005)	258.4 (2.4)
SN 2001ep	2.83	5.12 (0.03)	4.19 (0.02)	84.2 (5.0)	8.6 (14.3)	7.51 (0.11)	0.415 (0.005)	146.1 (2.4)
SN 2001ep	4.99	5.02 (0.09)	3.94 (0.08)	79.1 (6.6)	9.3 (15.0)	7.15 (0.11)	0.424 (0.009)	162.0 (1.2)
SN 2001ep	5.97	4.99 (0.05)	3.94 (0.04)	76.7 (6.5)	10.5 (14.9)	6.99 (0.11)	0.419 (0.006)	164.0 (1.2)
SN 2001ep	7.85	5.08 (0.04)	3.97 (0.03)	56.8 (3.5)	-0.6 (13.9)	6.43 (0.11)	0.329 (0.006)	250.7 (2.4)
SN 2001ex	−1.82	0.45 (0.01)	0.34 (0.01)	92.3 (5.5)	14.8 (14.5)	8.00 (0.11)	0.440 (0.013)	257.2 (2.4)
SN 2001fe	−0.99	6.35 (0.04)	5.64 (0.02)	81.1 (4.5)	3.0 (14.2)	9.83 (0.11)	0.307 (0.002)	280.2 (2.4)
SN 2001fh	5.93	0.95 (0.01)	0.90 (0.02)	80.3 (4.7)	13.9 (14.2)	7.71 (0.11)	0.393 (0.006)	144.1 (2.4)
SN 2001fh	7.84	0.91 (0.01)	0.76 (0.01)	47.7 (4.2)	-9.8 (14.1)	7.36 (0.11)	0.279 (0.007)	167.0 (1.2)
SN 2002aw	2.10	1.50 (0.06)	1.46 (0.03)	74.0 (4.5)	-2.9 (14.2)	8.15 (0.11)	0.362 (0.003)	142.3 (2.4)
SN 2002bf	2.97	2.51 (0.00)	2.16 (0.00)	77.4 (4.2)	2.1 (14.1)	10.25 (0.11)	0.296 (0.002)	287.1 (2.4)
SN 2002bo	−1.08	15.25 (0.20)	14.29 (0.22)	87.0 (4.9)	8.8 (14.3)	9.25 (0.11)	0.367 (0.006)	276.8 (2.4)
SN 2002bz	4.92	0.44 (0.01)	0.39 (0.01)	98.0 (5.7)	27.9 (14.6)	8.79 (0.11)	0.448 (0.012)	258.4 (2.4)
SN 2002cf	−0.75	1.32 (0.03)	1.15 (0.01)	61.5 (3.7)	-16.8 (13.9)	7.60 (0.11)	0.316 (0.006)	157.6 (2.4)
SN 2002ck	3.64	0.83 (0.02)	0.70 (0.02)	57.0 (3.6)	-16.8 (13.9)	8.81 (0.11)	0.308 (0.005)	248.6 (2.4)
SN 2002cr	−6.78	5.43 (0.06)	4.38 (0.04)	71.6 (4.0)	8.0 (14.0)	8.73 (0.11)	0.330 (0.005)	134.7 (2.4)
SN 2002cs	−7.76	1.30 (0.02)	1.12 (0.01)	71.2 (4.1)	12.3 (14.1)	12.76 (0.11)	0.339 (0.005)	155.5 (2.4)
SN 2002cu	−5.28	1.07 (0.03)	0.96 (0.02)	65.7 (4.4)	-3.8 (14.1)	11.55 (0.11)	0.353 (0.004)	127.2 (2.1)
SN 2002dj	−7.98	4.97 (0.08)	3.94 (0.06)	60.9 (3.7)	3.2 (13.9)	12.21 (0.11)	0.298 (0.005)	120.9 (2.4)
SN 2002dk	−1.23	0.29 (0.00)	0.32 (0.01)	43.7 (2.7)	-34.3 (13.7)	6.99 (0.11)	0.238 (0.010)	125.7 (2.4)
SN 2002eb	1.68	1.56 (0.02)	1.26 (0.01)	88.1 (5.1)	10.7 (14.4)	8.87 (0.11)	0.389 (0.006)	268.6 (2.4)
SN 2002ef	4.70	1.25 (0.04)	1.00 (0.04)	66.5 (4.1)	-4.4 (14.1)	8.27 (0.11)	0.309 (0.009)	257.8 (2.4)
SN 2002er	−4.58	5.54 (0.03)	4.99 (0.03)	77.2 (4.6)	5.5 (14.2)	10.74 (0.11)	0.366 (0.005)	126.9 (2.4)
SN 2002er	5.26	7.11 (0.06)	5.99 (0.02)	77.7 (4.6)	8.8 (14.2)	8.46 (0.11)	0.354 (0.005)	261.8 (2.4)
SN 2002eu	−0.06	0.61 (0.01)	0.54 (0.01)	81.0 (4.9)	2.5 (14.3)	9.14 (0.11)	0.383 (0.011)	262.1 (2.4)

Continued on Next Page...

Table 3.10 — Continued

SN Name	Phase[a]	F_b[b]	F_r[b]	pEW[c]	ΔpEW[c,d]	v[e]	a	FWHM[c]
SN 2002fb	0.98	1.08 (0.02)	0.78 (0.01)	57.4 (3.5)	-20.7 (13.9)	7.18 (0.11)	0.288 (0.006)	249.1 (2.4)
SN 2002fk	7.74	20.58 (0.11)	14.99 (0.12)	62.2 (3.8)	4.2 (14.0)	7.14 (0.11)	0.341 (0.006)	145.0 (2.4)
SN 2002ha	−0.85	4.46 (0.03)	3.61 (0.01)	74.1 (4.5)	-4.1 (14.2)	9.11 (0.11)	0.374 (0.007)	153.8 (2.4)
SN 2002ha	4.93	4.45 (0.04)	3.79 (0.04)	80.6 (4.7)	10.5 (14.3)	8.13 (0.11)	0.391 (0.007)	258.4 (2.4)
SN 2002ha	7.89	10.16 (0.05)	7.30 (0.05)	47.3 (2.9)	-10.0 (13.8)	7.69 (0.11)	0.270 (0.007)	92.7 (2.4)
SN 2002hd	6.48	1.30 (0.02)	0.91 (0.01)	54.0 (3.4)	-10.0 (13.9)	7.44 (0.11)	0.306 (0.007)	100.5 (2.4)
SN 2002he	−5.91	0.79 (0.02)	0.62 (0.02)	60.4 (5.2)	-6.8 (14.4)	11.60 (0.11)	0.310 (0.003)	250.0 (1.2)
SN 2002he	−1.03	1.91 (0.04)	1.67 (0.03)	76.9 (6.4)	-1.3 (14.9)	10.60 (0.11)	0.353 (0.008)	269.0 (1.2)
SN 2002he	0.29	1.69 (0.01)	1.45 (0.01)	85.5 (4.9)	7.1 (14.3)	9.82 (0.11)	0.373 (0.001)	275.2 (2.4)
SN 2002he	3.22	3.93 (0.03)	3.15 (0.04)	79.9 (4.6)	5.1 (14.2)	9.07 (0.11)	0.354 (0.006)	271.3 (2.4)
SN 2002hu	−5.81	0.60 (0.01)	0.44 (0.01)	42.3 (2.8)	-25.2 (13.7)	9.42 (0.11)	0.219 (0.008)	137.0 (2.4)
SN 2002hw	−6.27	0.93 (0.01)	0.90 (0.01)	72.6 (4.2)	6.9 (14.1)	9.91 (0.11)	0.348 (0.007)	253.6 (2.4)
SN 2002kf	6.81	2.66 (0.02)	2.18 (0.02)	81.5 (4.8)	18.9 (14.3)	8.17 (0.11)	0.387 (0.005)	261.0 (2.4)
SN 2003U	−2.55	0.81 (0.01)	0.68 (0.02)	66.9 (4.2)	-9.6 (14.1)	8.30 (0.11)	0.353 (0.007)	93.5 (2.4)
SN 2003W	−5.06	0.66 (0.01)	0.62 (0.02)	68.6 (4.1)	-1.6 (14.0)	13.06 (0.11)	0.275 (0.005)	284.3 (2.4)
SN 2003ai	7.25	1.00 (0.02)	0.72 (0.02)	38.7 (2.5)	-21.9 (13.7)	7.44 (0.11)	0.205 (0.008)	79.2 (2.4)
SN 2003cq	−0.15	0.51 (0.01)	0.42 (0.01)	83.4 (4.9)	5.0 (14.3)	9.48 (0.11)	0.370 (0.004)	133.6 (2.4)
SN 2003gn	−5.38	0.19 (0.01)	0.16 (0.01)	82.0 (5.3)	12.8 (14.4)	9.83 (0.11)	0.399 (0.021)	257.1 (2.4)
SN 2003gt	−5.07	2.70 (0.06)	2.39 (0.03)	48.4 (3.2)	-21.8 (13.8)	10.89 (0.11)	0.191 (0.006)	108.3 (2.4)
SN 2003he	2.71	1.34 (0.02)	1.38 (0.02)	50.3 (3.2)	-25.5 (13.8)	9.03 (0.11)	0.303 (0.004)	187.2 (2.4)
SN 2003iv	1.76	0.03 (0.00)	0.02 (0.00)	85.5 (5.2)	8.2 (14.4)	8.50 (0.11)	0.473 (0.014)	166.3 (2.4)
SN 2003iv	6.58	0.21 (0.01)	0.18 (0.01)	68.5 (4.4)	4.8 (14.1)	7.76 (0.11)	0.385 (0.004)	197.2 (2.4)
SN 2003kf	−7.50	6.86 (0.04)	5.52 (0.03)	47.2 (3.0)	-13.0 (13.8)	10.96 (0.11)	0.232 (0.005)	87.4 (2.4)
SN 2004E	5.26	1.66 (0.02)	1.44 (0.01)	38.4 (2.5)	-30.5 (13.7)	9.76 (0.11)	0.230 (0.004)	97.1 (2.4)
SN 2004S	8.26	7.38 (0.01)	5.80 (0.01)	49.6 (3.1)	-5.7 (13.8)	7.40 (0.11)	0.304 (0.005)	83.2 (2.4)
SN 2004bd	10.76	2.99 (0.04)	2.52 (0.02)	28.5 (2.0)	-10.8 (13.6)	5.76 (0.11)	0.212 (0.004)	71.4 (2.4)
SN 2004bk	6.13	2.29 (0.03)	1.74 (0.01)	62.4 (3.7)	-3.2 (13.9)	10.16 (0.11)	0.293 (0.006)	248.3 (2.4)
SN 2004bl	4.61	2.43 (0.09)	1.94 (0.03)	97.3 (5.4)	26.2 (14.5)	8.03 (0.11)	0.394 (0.004)	265.4 (2.4)
SN 2004bv	9.77	11.02 (0.08)	7.99 (0.06)	44.5 (2.8)	-1.6 (13.7)	7.56 (0.11)	0.270 (0.009)	126.7 (2.4)
SN 2004bw	6.59	1.39 (0.01)	1.14 (0.02)	67.8 (4.1)	4.3 (14.0)	7.77 (0.11)	0.361 (0.005)	205.6 (2.4)
SN 2004dt	−6.46	2.35 (0.04)	1.90 (0.02)	61.1 (3.8)	-3.8 (14.0)	10.68 (0.11)	0.321 (0.006)	107.9 (2.4)
SN 2004dt	1.38	3.66 (0.02)	2.83 (0.02)	84.7 (3.1)	7.0 (13.8)	8.70 (0.11)	0.363 (0.005)	127.5 (6.0)
SN 2004ef	−5.52	0.48 (0.01)	0.43 (0.01)	57.4 (3.6)	-11.3 (13.9)	11.06 (0.11)	0.297 (0.006)	252.2 (2.4)
SN 2004eo	−5.57	1.42 (0.03)	1.11 (0.01)	62.8 (3.9)	-5.7 (14.0)	9.38 (0.11)	0.322 (0.008)	250.1 (2.4)
SN 2004ey	−7.58	2.97 (0.02)	2.34 (0.02)	58.4 (3.6)	-1.4 (13.9)	10.82 (0.11)	0.290 (0.007)	145.7 (2.4)
SN 2004fu	−2.65	3.87 (0.03)	3.70 (0.03)	89.7 (5.2)	13.4 (14.4)	9.64 (0.11)	0.389 (0.004)	271.5 (2.4)
SN 2004fu	2.43	4.42 (0.05)	4.01 (0.02)	102.5 (5.7)	26.2 (14.6)	8.22 (0.11)	0.432 (0.002)	275.5 (2.4)
SN 2004fz	−5.18	3.06 (0.05)	2.46 (0.02)	70.3 (4.1)	0.5 (14.1)	9.42 (0.11)	0.362 (0.007)	159.2 (2.4)
SN 2004gs	0.44	0.72 (0.01)	0.60 (0.01)	85.3 (5.0)	7.0 (14.3)	7.34 (0.11)	0.388 (0.004)	270.8 (2.4)
SN 2005M	8.23	0.48 (0.01)	0.38 (0.01)	71.2 (6.0)	15.8 (14.7)	6.12 (0.11)	0.379 (0.008)	99.0 (1.2)
SN 2005W	0.59	3.33 (0.08)	3.38 (0.07)	83.9 (6.9)	5.6 (15.1)	7.86 (0.11)	0.391 (0.005)	134.0 (1.2)
SN 2005am	4.47	14.74 (0.05)	12.86 (0.08)	85.8 (5.0)	14.3 (14.3)	9.13 (0.11)	0.410 (0.004)	265.9 (2.4)
SN 2005am	6.37	13.90 (0.09)	11.27 (0.03)	68.3 (2.5)	3.8 (13.7)	8.16 (0.11)	0.335 (0.005)	143.9 (6.1)
SN 2005ao	−1.29	0.65 (0.01)	0.60 (0.01)	77.8 (4.5)	-0.1 (14.2)	10.32 (0.11)	0.340 (0.004)	269.6 (2.4)
SN 2005ao	0.52	0.51 (0.01)	0.44 (0.01)	73.2 (4.2)	-5.2 (14.1)	9.79 (0.11)	0.307 (0.008)	258.1 (2.4)
SN 2005bc	1.55	2.01 (0.02)	1.82 (0.01)	67.9 (4.1)	-9.6 (14.0)	8.26 (0.11)	0.336 (0.006)	116.6 (2.4)
SN 2005bc	7.37	1.95 (0.03)	1.61 (0.01)	48.8 (3.0)	-11.1 (13.8)	6.54 (0.11)	0.271 (0.005)	247.0 (2.4)
SN 2005cf	−2.11	120.15 (0.90)	103.17 (0.60)	72.2 (4.4)	-4.9 (14.1)	8.71 (0.11)	0.367 (0.007)	155.0 (2.4)
SN 2005cf	−1.19	25.29 (0.21)	21.12 (0.15)	77.3 (4.7)	-0.7 (14.2)	9.25 (0.11)	0.381 (0.007)	123.2 (2.4)
SN 2005de	−0.75	2.38 (0.06)	2.09 (0.03)	79.7 (4.9)	1.4 (14.3)	9.01 (0.11)	0.382 (0.008)	151.7 (2.4)
SN 2005de	10.10	2.48 (0.02)	1.67 (0.02)	37.3 (2.4)	-6.6 (13.7)	7.08 (0.11)	0.247 (0.007)	165.5 (2.4)
SN 2005dv	−0.57	1.35 (0.06)	1.22 (0.03)	106.4 (6.0)	28.1 (14.7)	10.20 (0.11)	0.436 (0.011)	277.1 (2.4)
SN 2005el	−6.70	2.22 (0.02)	1.74 (0.02)	52.2 (3.2)	-11.7 (13.8)	10.35 (0.11)	0.269 (0.006)	254.2 (2.4)
SN 2005el	1.22	3.51 (0.05)	3.09 (0.03)	76.5 (4.5)	-1.4 (14.2)	8.93 (0.11)	0.372 (0.006)	122.2 (2.4)
SN 2005el	8.09	3.42 (0.03)	2.46 (0.01)	48.5 (3.1)	-7.6 (13.8)	7.97 (0.11)	0.287 (0.006)	88.7 (2.4)
SN 2005er	−0.26	0.00 (0.00)	0.00 (0.00)	27.1 (2.6)	-51.4 (13.7)	6.77 (0.11)	0.144 (0.003)	266.0 (1.2)
SN 2005eq	0.66	1.30 (0.02)	1.04 (0.01)	84.7 (4.6)	6.4 (14.2)	8.87 (0.11)	0.324 (0.004)	276.0 (2.4)
SN 2005hj	7.51	0.54 (0.02)	0.46 (0.01)	38.6 (3.5)	-20.6 (13.9)	8.69 (0.11)	0.208 (0.007)	244.0 (1.2)
SN 2005iq	−5.86	8.91 (0.12)	6.99 (0.08)	62.3 (5.3)	-5.1 (14.5)	9.50 (0.11)	0.301 (0.007)	257.0 (1.2)
SN 2005kc	10.28	0.14 (0.00)	0.11 (0.00)	27.6 (2.5)	-15.1 (13.7)	7.31 (0.11)	0.194 (0.007)	182.0 (1.2)
SN 2005ki	1.62	10.16 (0.08)	8.85 (0.06)	77.7 (6.4)	0.2 (14.9)	9.14 (0.11)	0.357 (0.002)	267.0 (1.2)
SN 2005ki	8.35	2.33 (0.04)	1.70 (0.04)	43.3 (2.7)	-11.4 (13.7)	6.88 (0.11)	0.199 (0.011)	141.2 (2.4)
SN 2005lz	0.58	6.62 (0.12)	5.82 (0.09)	81.5 (6.8)	3.2 (15.1)	8.20 (0.11)	0.374 (0.007)	263.0 (1.2)
SN 2005ms	−1.88	3.49 (0.07)	3.14 (0.10)	69.6 (4.3)	-7.8 (14.1)	8.52 (0.11)	0.346 (0.006)	99.5 (2.4)
SN 2005na	0.03	1.20 (0.03)	0.95 (0.02)	57.0 (3.6)	-21.4 (13.9)	9.70 (0.11)	0.275 (0.004)	120.8 (2.4)
SN 2005na	1.03	1.48 (0.04)	1.27 (0.04)	68.2 (4.2)	-9.9 (14.1)	8.95 (0.11)	0.325 (0.011)	91.6 (2.4)
SN 2006D	3.70	23.23 (0.11)	17.51 (0.10)	82.2 (4.9)	8.5 (14.3)	8.67 (0.11)	0.399 (0.005)	259.8 (2.4)
SN 2006N	−1.89	2.77 (0.04)	2.34 (0.02)	64.6 (3.9)	-12.8 (14.0)	9.51 (0.11)	0.290 (0.005)	266.2 (2.4)
SN 2006N	−0.90	2.50 (0.04)	2.01 (0.01)	81.6 (4.9)	3.3 (14.3)	10.15 (0.11)	0.371 (0.006)	272.1 (2.4)
SN 2006S	−3.93	12.57 (0.36)	10.16 (0.41)	53.0 (3.3)	-20.6 (13.8)	10.63 (0.11)	0.244 (0.013)	250.0 (2.4)
SN 2006S	2.99	0.71 (0.02)	0.65 (0.01)	79.6 (4.7)	4.3 (14.2)	9.45 (0.11)	0.358 (0.004)	255.8 (2.4)
SN 2006X	3.15	8.11 (0.03)	9.89 (0.04)	72.1 (3.9)	-2.8 (14.0)	11.36 (0.11)	0.257 (0.002)	304.4 (2.4)
SN 2006ac	7.96	1.98 (0.02)	1.50 (0.01)	56.6 (3.3)	-0.3 (13.8)	8.33 (0.11)	0.278 (0.007)	261.9 (2.4)
SN 2006ak	8.43	0.57 (0.00)	0.46 (0.00)	42.8 (2.6)	-11.5 (13.7)	8.33 (0.11)	0.226 (0.003)	129.1 (2.4)
SN 2006ax	−10.07	0.92 (0.01)	0.70 (0.01)	38.6 (2.5)	-6.8 (13.7)	10.45 (0.11)	0.188 (0.004)	112.1 (2.4)
SN 2006bq	6.97	6.29 (0.06)	4.74 (0.04)	58.1 (3.4)	-3.7 (13.9)	8.62 (0.11)	0.255 (0.004)	270.1 (2.4)
SN 2006bt	−5.30	0.49 (0.01)	0.42 (0.00)	44.1 (2.9)	-25.3 (13.8)	8.21 (0.11)	0.259 (0.007)	255.8 (2.4)
SN 2006bt	−4.53	0.47 (0.01)	0.39 (0.01)	58.4 (3.6)	-13.5 (13.9)	8.94 (0.11)	0.307 (0.010)	129.8 (2.4)
SN 2006bt	2.27	0.48 (0.00)	0.39 (0.01)	63.7 (3.9)	-12.9 (14.0)	7.03 (0.11)	0.325 (0.008)	139.5 (2.4)
SN 2006bu	4.22	0.14 (0.00)	0.12 (0.00)	74.5 (4.6)	2.2 (14.2)	8.59 (0.11)	0.362 (0.009)	125.5 (2.3)
SN 2006bw	8.90	0.47 (0.01)	0.38 (0.00)	62.3 (3.8)	10.8 (14.0)	5.46 (0.11)	0.359 (0.006)	207.8 (2.4)
SN 2006bz	−2.44	0.34 (0.02)	0.29 (0.01)	50.4 (3.2)	-26.2 (13.8)	7.60 (0.11)	0.272 (0.004)	223.8 (2.4)

Continued on Next Page...

Table 3.10 — Continued

SN Name	Phase[a]	F_b[b]	F_r[b]	pEW[c]	ΔpEW[c,d]	v[e]	a	FWHM[c]
SN 2006cf	6.28	0.36 (0.03)	0.33 (0.03)	87.9 (5.3)	23.0 (14.4)	6.81 (0.13)	0.357 (0.012)	88.3 (2.4)
SN 2006cj	3.43	0.20 (0.01)	0.17 (0.01)	67.4 (4.4)	-7.0 (14.1)	9.61 (0.11)	0.339 (0.015)	254.8 (2.3)
SN 2006cm	−1.15	0.44 (0.01)	0.57 (0.01)	73.1 (4.2)	-5.0 (14.1)	11.51 (0.11)	0.307 (0.006)	261.7 (2.4)
SN 2006cp	−5.30	1.19 (0.02)	0.98 (0.01)	81.0 (4.8)	11.5 (14.3)	11.54 (0.11)	0.355 (0.004)	271.9 (2.4)
SN 2006cq	2.00	0.33 (0.01)	0.29 (0.01)	84.8 (5.1)	7.9 (14.4)	9.58 (0.11)	0.372 (0.005)	265.2 (2.3)
SN 2006cs	2.28	0.33 (0.01)	0.28 (0.01)	42.9 (2.8)	-33.7 (13.7)	8.07 (0.11)	0.243 (0.008)	218.8 (2.4)
SN 2006cz	1.12	0.50 (0.01)	0.43 (0.01)	77.3 (4.3)	-0.7 (14.1)	10.23 (0.11)	0.283 (0.007)	274.5 (2.4)
SN 2006dm	−7.90	0.35 (0.02)	0.30 (0.01)	65.8 (4.1)	7.6 (14.0)	10.37 (0.11)	0.320 (0.013)	144.8 (2.4)
SN 2006dm	8.73	1.50 (0.01)	1.01 (0.01)	28.8 (1.9)	-23.7 (13.6)	6.31 (0.11)	0.189 (0.009)	182.0 (2.4)
SN 2006ef	3.20	3.19 (0.03)	2.28 (0.01)	103.2 (5.9)	28.4 (14.7)	8.83 (0.11)	0.431 (0.005)	273.1 (2.4)
SN 2006ej	−3.70	1.81 (0.02)	1.46 (0.01)	83.0 (4.9)	8.9 (14.3)	11.20 (0.11)	0.367 (0.006)	271.5 (2.4)
SN 2006ej	5.09	1.30 (0.02)	1.10 (0.01)	78.7 (4.6)	9.2 (14.2)	8.68 (0.11)	0.376 (0.004)	156.8 (2.4)
SN 2006en	8.55	0.73 (0.02)	0.51 (0.01)	47.6 (3.1)	-6.0 (13.8)	8.25 (0.11)	0.288 (0.011)	116.3 (2.4)
SN 2006et	3.29	1.58 (0.02)	1.39 (0.02)	79.0 (4.6)	4.4 (14.2)	7.94 (0.11)	0.364 (0.005)	256.3 (2.4)
SN 2006et	9.14	1.48 (0.01)	1.08 (0.04)	50.0 (3.1)	-0.1 (13.8)	7.85 (0.11)	0.270 (0.009)	242.6 (2.4)
SN 2006ev	10.54	0.64 (0.01)	0.48 (0.01)	55.6 (3.3)	14.8 (13.8)	7.30 (0.11)	0.276 (0.007)	112.8 (2.4)
SN 2006gj	4.70	0.24 (0.01)	0.24 (0.01)	77.5 (4.8)	6.7 (14.3)	7.71 (0.11)	0.395 (0.012)	245.1 (2.4)
SN 2006gt	3.08	0.23 (0.01)	0.20 (0.01)	82.7 (5.1)	7.6 (14.4)	7.83 (0.11)	0.403 (0.013)	252.7 (2.3)
SN 2006kf	−8.96	0.26 (0.02)	0.26 (0.01)	54.7 (3.5)	2.4 (13.9)	10.80 (0.11)	0.316 (0.008)	180.2 (2.4)
SN 2006kf	−3.05	0.83 (0.02)	0.69 (0.01)	71.2 (4.4)	-4.4 (14.1)	9.41 (0.11)	0.345 (0.004)	256.5 (2.4)
SN 2006lf	−6.30	0.42 (0.01)	0.41 (0.00)	79.6 (4.4)	13.9 (14.1)	10.37 (0.11)	0.335 (0.004)	264.5 (2.4)
SN 2006mp	5.66	1.23 (0.02)	1.08 (0.01)	64.1 (3.8)	-3.3 (14.0)	7.97 (0.11)	0.319 (0.004)	251.2 (2.4)
SN 2006or	−2.79	0.88 (0.01)	0.81 (0.01)	70.0 (4.1)	-6.0 (14.0)	9.45 (0.11)	0.324 (0.004)	264.5 (2.4)
SN 2006os	8.61	0.34 (0.01)	0.29 (0.01)	78.1 (4.5)	24.8 (14.2)	8.16 (0.11)	0.381 (0.006)	129.7 (2.4)
SN 2006sr	2.69	1.44 (0.02)	1.30 (0.01)	89.3 (5.2)	13.4 (14.4)	8.95 (0.11)	0.402 (0.005)	267.5 (2.4)
SN 2007A	2.37	2.31 (0.03)	2.09 (0.02)	80.0 (4.6)	3.6 (14.2)	9.08 (0.11)	0.357 (0.004)	269.2 (2.4)
SN 2007F	−9.35	0.97 (0.01)	0.71 (0.01)	30.5 (2.0)	-19.4 (13.6)	11.38 (0.11)	0.165 (0.007)	248.1 (2.4)
SN 2007F	3.23	1.68 (0.02)	1.51 (0.01)	79.7 (4.6)	5.0 (14.2)	9.11 (0.11)	0.356 (0.003)	263.8 (2.4)
SN 2007N	0.44	4.10 (0.05)	3.99 (0.05)	38.4 (3.2)	-40.0 (13.8)	8.18 (0.11)	0.183 (0.003)	177.0 (1.2)
SN 2007O	−0.33	16.46 (0.20)	13.23 (0.13)	68.4 (5.8)	-10.1 (14.6)	8.66 (0.11)	0.313 (0.007)	263.0 (1.2)
SN 2007S	5.18	2.15 (0.01)	2.15 (0.04)	59.8 (3.6)	-9.4 (13.9)	8.94 (0.11)	0.296 (0.004)	248.6 (2.4)
SN 2007af	−1.25	23.55 (0.14)	19.77 (0.10)	84.1 (5.0)	6.1 (14.3)	8.85 (0.11)	0.388 (0.006)	121.3 (2.4)
SN 2007af	2.84	25.11 (0.10)	21.44 (0.08)	87.5 (7.4)	11.9 (15.3)	7.73 (0.11)	0.425 (0.006)	145.0 (1.2)
SN 2007af	3.81	24.45 (0.14)	20.66 (0.13)	89.0 (5.2)	15.6 (14.4)	7.75 (0.11)	0.431 (0.005)	151.2 (2.4)
SN 2007ap	9.37	36.23 (0.34)	25.44 (0.22)	40.4 (3.6)	-8.2 (13.9)	7.59 (0.11)	0.257 (0.004)	180.0 (1.2)
SN 2007ba	2.14	0.57 (0.02)	0.49 (0.02)	70.4 (4.4)	-6.4 (14.1)	6.87 (0.11)	0.372 (0.008)	238.8 (2.4)
SN 2007ba	5.18	4.39 (0.07)	3.85 (0.08)	35.0 (3.2)	-34.2 (13.8)	6.31 (0.11)	0.219 (0.006)	180.0 (1.2)
SN 2007bc	0.61	2.08 (0.02)	1.58 (0.01)	86.0 (5.2)	7.7 (14.4)	8.40 (0.11)	0.397 (0.007)	260.6 (2.4)
SN 2007bd	−5.79	0.61 (0.02)	0.48 (0.02)	67.7 (4.3)	0.0 (14.1)	11.82 (0.11)	0.318 (0.021)	147.4 (2.4)
SN 2007bm	−7.79	6.32 (0.07)	5.38 (0.06)	74.5 (4.1)	15.8 (14.1)	9.93 (0.11)	0.326 (0.007)	264.4 (2.4)
SN 2007bz	1.65	1.31 (0.03)	1.16 (0.03)	69.5 (4.1)	-7.9 (14.1)	10.19 (0.11)	0.282 (0.006)	262.3 (2.4)
SN 2007ci	−6.57	1.20 (0.02)	0.95 (0.02)	63.1 (4.0)	-1.4 (14.0)	10.64 (0.11)	0.312 (0.012)	139.5 (2.4)
SN 2007ci	−1.71	1.75 (0.02)	1.39 (0.02)	73.8 (4.4)	-3.8 (14.1)	9.77 (0.11)	0.350 (0.005)	263.2 (2.4)
SN 2007co	−4.09	0.74 (0.01)	0.67 (0.01)	77.4 (4.6)	4.2 (14.2)	10.32 (0.11)	0.352 (0.004)	266.8 (2.4)
SN 2007co	0.85	0.95 (0.01)	0.84 (0.01)	95.1 (5.3)	16.9 (14.5)	9.13 (0.11)	0.383 (0.005)	280.4 (2.4)
SN 2007cq	7.84	1.93 (0.04)	1.57 (0.02)	47.7 (3.0)	-9.8 (13.8)	8.93 (0.11)	0.290 (0.008)	171.6 (2.4)
SN 2007fb	1.95	2.93 (0.03)	2.75 (0.03)	79.5 (4.8)	2.5 (14.3)	8.77 (0.11)	0.384 (0.005)	115.9 (2.4)
SN 2007fr	−1.25	0.20 (0.01)	0.15 (0.01)	69.4 (4.4)	-8.6 (14.1)	8.57 (0.11)	0.384 (0.014)	123.7 (2.3)
SN 2007fs	5.03	4.09 (0.05)	3.22 (0.03)	75.8 (4.6)	6.0 (14.2)	8.10 (0.11)	0.373 (0.003)	257.6 (2.4)
SN 2007gi	6.61	19.42 (0.11)	15.34 (0.03)	47.0 (2.7)	-16.5 (13.7)	10.51 (0.11)	0.202 (0.004)	258.8 (2.4)
SN 2007gk	−1.72	0.84 (0.01)	0.80 (0.01)	83.4 (4.9)	5.9 (14.3)	10.11 (0.11)	0.380 (0.003)	268.8 (2.4)
SN 2007hj	−1.23	2.34 (0.02)	1.83 (0.01)	86.3 (5.1)	8.3 (14.4)	8.59 (0.11)	0.413 (0.004)	266.2 (2.4)
SN 2007kk	7.15	2.57 (0.03)	1.95 (0.03)	40.2 (2.4)	-20.8 (13.7)	9.50 (0.11)	0.171 (0.011)	265.1 (2.4)
SN 2007le	−10.31	5.17 (0.05)	4.01 (0.06)	65.6 (4.0)	21.9 (14.0)	13.28 (0.11)	0.331 (0.006)	246.3 (2.4)
SN 2007le	−9.40	5.91 (0.03)	4.94 (0.04)	60.6 (3.7)	11.0 (13.9)	12.95 (0.11)	0.297 (0.005)	252.3 (2.4)
SN 2007le	7.43	16.01 (0.08)	12.17 (0.04)	52.9 (3.0)	-6.7 (13.8)	10.09 (0.11)	0.211 (0.004)	284.1 (2.4)
SN 2007s1[f]	−1.23	0.97 (0.02)	0.90 (0.01)	91.1 (5.3)	13.1 (14.5)	10.01 (0.11)	0.394 (0.006)	270.6 (2.4)
SN 2007on	−3.01	21.94 (0.05)	18.56 (0.10)	59.9 (3.6)	-15.7 (13.9)	9.04 (0.11)	0.307 (0.005)	258.3 (2.4)
SN 2007on	−3.00	18.57 (0.05)	15.58 (0.06)	54.2 (4.7)	-21.4 (14.2)	8.77 (0.11)	0.288 (0.004)	115.0 (1.2)
SN 2007qe	6.23	2.35 (0.04)	1.72 (0.02)	73.9 (4.3)	8.8 (14.1)	9.87 (0.11)	0.293 (0.008)	261.7 (2.4)
SN 2008Q	6.46	16.52 (0.16)	14.94 (0.09)	62.1 (3.7)	-2.0 (13.9)	9.03 (0.11)	0.313 (0.004)	144.9 (2.4)
SN 2008Z	−2.29	1.83 (0.03)	1.75 (0.01)	43.9 (2.7)	-32.9 (13.7)	10.83 (0.11)	0.206 (0.004)	96.0 (2.4)
SN 2008ar	2.83	1.29 (0.05)	0.73 (0.02)	108.9 (6.3)	33.3 (14.8)	8.05 (0.11)	0.427 (0.012)	272.9 (2.4)
SN 2008s1[g]	−6.36	1.04 (0.03)	0.84 (0.01)	47.8 (3.2)	-17.5 (13.8)	10.83 (0.11)	0.305 (0.007)	92.0 (2.4)
SN 2008s1[g]	−3.42	1.32 (0.04)	1.09 (0.02)	53.0 (3.4)	-21.8 (13.9)	10.40 (0.11)	0.273 (0.008)	103.7 (2.4)
SN 2008s1[g]	0.49	1.62 (0.06)	1.38 (0.03)	74.4 (4.7)	-4.0 (14.2)	8.90 (0.11)	0.380 (0.007)	105.7 (2.4)
SN 2008s1[g]	4.40	1.72 (0.03)	1.36 (0.01)	83.9 (4.9)	12.2 (14.3)	8.46 (0.11)	0.390 (0.007)	260.2 (2.4)
SN 2008s1[g]	5.38	1.62 (0.02)	1.35 (0.01)	76.2 (4.5)	7.8 (14.2)	8.56 (0.11)	0.395 (0.004)	125.2 (2.4)
SN 2008cl	4.24	0.11 (0.01)	0.09 (0.01)	97.8 (6.2)	25.5 (14.8)	9.91 (0.11)	0.468 (0.014)	252.0 (2.3)
SN 2008dx	2.46	0.36 (0.02)	0.34 (0.01)	51.4 (3.2)	-24.9 (13.8)	7.02 (0.11)	0.280 (0.007)	250.2 (2.4)
SN 2008ec	−0.24	2.55 (0.03)	2.22 (0.01)	74.3 (4.5)	-4.1 (14.2)	8.48 (0.11)	0.382 (0.004)	106.3 (2.4)
SN 2008ec	5.70	2.82 (0.03)	2.44 (0.01)	81.0 (4.8)	13.7 (14.3)	7.62 (0.11)	0.414 (0.006)	118.1 (2.4)
SN 2008ei	3.29	0.39 (0.01)	0.34 (0.01)	81.7 (4.6)	7.1 (14.2)	10.20 (0.11)	0.322 (0.006)	287.2 (2.4)
SN 2008s5[h]	1.26	1.56 (0.07)	1.30 (0.01)	57.2 (3.4)	-20.7 (13.9)	7.98 (0.11)	0.266 (0.008)	118.3 (2.4)
SN 2008s5[h]	8.96	1.16 (0.02)	0.90 (0.01)	62.9 (3.8)	11.7 (14.0)	7.54 (0.11)	0.329 (0.004)	106.7 (2.4)
SN 2008hs	−7.94	0.66 (0.02)	0.54 (0.01)	49.4 (3.0)	-8.6 (13.8)	9.88 (0.11)	0.240 (0.005)	261.5 (2.4)

Uncertainties for each measured value are given in parentheses.
[a]Phases of spectra are in rest-frame days using the heliocentric redshift and photometry reference presented in table 1 of Silverman et al. (submitted).
[b]Fluxes are in units of 10^{-15} erg s^{-1} cm^{-2} Å^{-1}.
[c]The pEW, ΔpEW, and FWHM are in units of Å.

Continued on Next Page...

Table 3.10 — Continued

SN Name	Phase[a]	F_b[b]	F_r[b]	pEW[c]	ΔpEW[c,d]	v[e]	a	FWHM[c]

[d] ΔpEW is the measured pEW minus the expected pEW at the same epoch using our linear or quadratic fit (see Section 3.5.4 for more information).
[e] The expansion velocity is in units of 1000 km s^{-1}.
[f] Also known as SNF20071021-000.
[g] Also known as SNF20080514-002.
[h] Also known as SNF20080909-030.

Table 3.11: Measured Values for Si II λ5972

SN Name	Phase[a]	F_b[b]	F_r[b]	pEW[c]	ΔpEW[c,d]	v[e]	a	FWHM[c]
SN 1989B	7.54	216.73 (1.84)	221.50 (4.84)	41.2 (2.7)	11.7 (10.6)	10.86 (0.10)	0.303 (0.017)	134.7 (3.1)
SN 1989M	2.49	29.47 (0.10)	25.77 (0.14)	15.1 (1.2)	-9.7 (10.3)	11.27 (0.10)	0.125 (0.006)	121.4 (2.4)
SN 1989M	3.48	32.32 (0.12)	28.34 (0.14)	17.5 (1.4)	-8.0 (10.3)	11.16 (0.10)	0.143 (0.005)	121.4 (2.4)
SN 1990N	7.11	34.83 (0.19)	33.95 (0.37)	16.9 (1.0)	-12.2 (10.3)	11.13 (0.10)	0.130 (0.002)	127.6 (4.9)
SN 1991T	6.80	20.72 (0.12)	20.03 (0.38)	16.4 (0.9)	-12.3 (10.3)	13.79 (0.10)	0.121 (0.005)	143.2 (4.9)
SN 1994D	−12.31	10.73 (0.06)	9.31 (0.05)	16.4 (1.3)	-8.5 (10.3)	11.96 (0.10)	0.136 (0.006)	111.8 (2.4)
SN 1994D	−9.32	23.26 (0.08)	21.14 (0.07)	11.6 (1.1)	-11.5 (10.3)	11.74 (0.10)	0.121 (0.005)	101.8 (2.4)
SN 1994D	−7.67	26.18 (0.08)	23.32 (0.08)	13.2 (1.2)	-9.4 (10.3)	11.33 (0.10)	0.128 (0.005)	105.8 (2.4)
SN 1994D	−5.32	37.84 (0.22)	33.24 (0.27)	13.6 (1.2)	-8.6 (10.3)	10.70 (0.10)	0.128 (0.005)	115.8 (2.4)
SN 1994D	−3.87	55.62 (0.21)	49.90 (0.33)	12.0 (1.1)	-10.2 (10.3)	10.39 (0.10)	0.114 (0.004)	119.8 (2.4)
SN 1994D	−3.33	53.70 (0.19)	47.60 (0.21)	12.5 (1.1)	-9.8 (10.3)	10.29 (0.10)	0.122 (0.004)	111.8 (2.4)
SN 1994S	1.11	9.99 (0.10)	8.57 (0.09)	9.6 (0.8)	-14.3 (10.3)	...	...	...
SN 1995D	3.84	19.12 (0.09)	16.25 (0.17)	16.1 (1.1)	-9.7 (10.3)	9.64 (0.10)	0.106 (0.008)	137.1 (2.4)
SN 1995E	−2.46	1.63 (0.01)	1.71 (0.01)	17.2 (1.3)	-5.2 (10.3)	10.28 (0.10)	0.132 (0.001)	128.5 (2.4)
SN 1997Y	1.27	4.48 (0.04)	3.76 (0.11)	14.0 (1.4)	-10.0 (10.3)	9.43 (0.10)	0.156 (0.018)	90.6 (2.4)
SN 1997bp	5.49	10.15 (0.07)	9.81 (0.15)	9.5 (0.8)	-17.7 (10.3)	12.02 (0.10)	0.097 (0.005)	93.2 (2.4)
SN 1997do	−5.67	3.93 (0.01)	3.61 (0.04)	9.5 (0.9)	-12.7 (10.3)	12.95 (0.10)	0.106 (0.008)	85.1 (2.4)
SN 1998V	7.20	4.03 (0.02)	4.15 (0.01)	31.2 (3.1)	2.1 (10.7)	12.81 (0.10)	0.213 (0.005)	136.0 (1.2)
SN 1998dm	−12.48	1.86 (0.01)	1.65 (0.01)	9.4 (0.8)	-15.6 (10.3)	11.91 (0.10)	0.097 (0.006)	101.3 (2.4)
SN 1998dm	−5.61	4.64 (0.01)	4.45 (0.01)	9.4 (0.7)	-12.8 (10.3)	9.82 (0.31)	0.072 (0.005)	145.1 (2.4)
SN 1998dx	5.13	0.46 (0.01)	0.42 (0.00)	30.7 (2.3)	3.7 (10.5)	11.49 (0.10)	0.224 (0.008)	108.1 (2.3)
SN 1998ef	−8.62	1.72 (0.01)	1.58 (0.01)	28.9 (2.3)	6.1 (10.5)	13.66 (0.10)	0.224 (0.008)	141.5 (2.4)
SN 1998es	0.28	11.44 (0.05)	10.43 (0.04)	11.1 (0.8)	-12.3 (10.3)	...	...	...
SN 1999aa	0.24	1.55 (0.01)	1.34 (0.01)	14.5 (1.0)	-8.9 (10.3)	8.50 (0.10)	0.127 (0.004)	90.7 (2.4)
SN 1999ac	−3.70	5.91 (0.03)	5.30 (0.02)	12.1 (0.8)	-10.1 (10.3)	...	...	...
SN 1999ac	−0.89	7.24 (0.02)	6.61 (0.02)	16.0 (1.2)	-6.9 (10.3)	...	...	...
SN 1999cp	4.91	9.68 (0.02)	8.84 (0.03)	21.4 (1.6)	-5.3 (10.4)	10.91 (0.10)	0.163 (0.005)	124.8 (2.4)
SN 1999da	−2.12	1.40 (0.01)	1.33 (0.01)	53.5 (3.9)	31.0 (11.0)	10.83 (0.10)	0.403 (0.007)	118.5 (2.4)
SN 1999dk	−6.60	3.95 (0.02)	3.69 (0.03)	14.4 (1.1)	-7.9 (10.3)	13.25 (0.10)	0.121 (0.008)	98.5 (2.4)
SN 1999dq	2.97	5.59 (0.02)	5.03 (0.03)	19.4 (1.3)	-5.7 (10.3)	...	...	...
SN 1999ek	5.66	1.19 (0.03)	1.19 (0.05)	26.9 (2.3)	-0.6 (10.5)	...	...	...
SN 1999gd	−1.12	1.01 (0.01)	0.96 (0.04)	27.5 (1.7)	4.7 (10.4)	...	...	...
SN 1999gh	4.12	6.65 (0.03)	5.95 (0.04)	41.9 (2.0)	15.9 (10.4)	9.63 (0.10)	0.305 (0.005)	138.9 (6.1)
SN 2000cu	9.64	1.07 (0.03)	1.10 (0.01)	51.8 (3.6)	19.5 (10.9)	10.44 (0.10)	0.372 (0.014)	137.3 (2.4)
SN 2000cw	4.81	0.65 (0.01)	0.60 (0.01)	25.6 (2.2)	-1.0 (10.5)	10.76 (0.10)	0.240 (0.005)	102.9 (2.4)
SN 2000dg	−5.09	0.44 (0.01)	0.40 (0.01)	24.3 (1.7)	2.1 (10.4)	11.95 (0.10)	0.173 (0.004)	132.9 (2.4)
SN 2000dg	4.66	0.61 (0.01)	0.55 (0.01)	15.9 (1.4)	-10.6 (10.3)	11.17 (0.10)	0.154 (0.012)	123.3 (2.4)
SN 2000dk	1.00	2.35 (0.01)	2.28 (0.01)	39.5 (3.0)	15.7 (10.7)	9.98 (0.10)	0.334 (0.003)	106.1 (2.4)
SN 2000dm	−1.63	1.93 (0.01)	1.89 (0.01)	27.1 (2.2)	4.5 (10.5)	10.79 (0.10)	0.223 (0.003)	106.4 (2.4)
SN 2000dm	8.18	1.64 (0.02)	1.73 (0.02)	43.4 (3.1)	13.1 (10.7)	10.61 (0.10)	0.313 (0.004)	137.9 (2.4)
SN 2000dn	−0.94	0.71 (0.01)	0.64 (0.01)	24.1 (1.9)	1.2 (10.4)	10.21 (0.10)	0.198 (0.007)	98.8 (2.4)
SN 2000dr	6.78	1.31 (0.01)	1.26 (0.01)	44.8 (3.5)	16.2 (10.8)	9.37 (0.10)	0.417 (0.005)	98.2 (2.4)
SN 2000ey	7.90	3.32 (0.02)	3.42 (0.03)	16.4 (1.1)	-13.5 (10.3)	13.21 (0.10)	0.113 (0.001)	166.6 (2.4)
SN 2000fa	6.86	1.32 (0.01)	1.38 (0.01)	25.9 (1.9)	-2.9 (10.4)	12.24 (0.10)	0.198 (0.003)	115.5 (2.4)
SN 2001ay	6.79	0.88 (0.01)	0.99 (0.01)	25.5 (1.9)	-3.2 (10.4)	12.71 (0.10)	0.194 (0.006)	122.3 (2.4)
SN 2001br	3.48	1.26 (0.03)	1.25 (0.04)	20.8 (1.9)	-4.7 (10.4)	...	...	...
SN 2001da	−1.12	2.67 (0.02)	2.37 (0.03)	27.2 (2.0)	4.4 (10.4)	9.20 (0.10)	0.208 (0.007)	121.9 (2.4)
SN 2001eh	3.26	0.72 (0.01)	0.65 (0.01)	11.3 (0.9)	-14.0 (10.3)	10.16 (0.10)	0.081 (0.003)	136.9 (2.4)
SN 2001ep	2.83	4.15 (0.02)	3.71 (0.02)	34.5 (2.4)	9.5 (10.5)	9.90 (0.10)	0.249 (0.005)	116.5 (2.4)
SN 2001ep	4.99	4.03 (0.07)	3.33 (0.15)	27.0 (3.2)	0.2 (10.7)	9.53 (0.10)	0.234 (0.016)	109.0 (1.2)
SN 2001ep	5.97	3.92 (0.04)	3.36 (0.15)	28.5 (3.4)	0.7 (10.8)	9.79 (0.10)	0.257 (0.015)	108.0 (1.2)
SN 2001ep	7.85	3.97 (0.03)	3.63 (0.05)	38.5 (3.0)	8.6 (10.7)	10.01 (0.10)	0.314 (0.008)	114.5 (2.4)
SN 2001fe	−0.99	5.63 (0.02)	4.91 (0.03)	18.1 (1.2)	-4.8 (10.3)	...	...	...
SN 2001fh	5.93	0.90 (0.02)	0.90 (0.01)	42.3 (3.3)	14.5 (10.8)	9.69 (0.10)	0.344 (0.012)	106.6 (2.4)
SN 2002bf	2.97	2.15 (0.00)	1.88 (0.01)	8.0 (0.7)	-17.1 (10.3)	11.37 (0.10)	0.067 (0.007)	119.1 (2.4)
SN 2002bo	−11.94	2.24 (0.03)	2.19 (0.04)	29.3 (2.2)	4.7 (10.5)	15.91 (0.11)	0.216 (0.012)	135.4 (2.4)
SN 2002bz	4.92	0.38 (0.01)	0.33 (0.01)	32.2 (2.5)	5.4 (10.6)	11.58 (0.10)	0.279 (0.016)	104.1 (2.4)
SN 2002cf	−0.75	1.13 (0.01)	1.11 (0.02)	57.4 (4.2)	34.4 (11.1)	10.43 (0.10)	0.456 (0.008)	108.3 (2.4)
SN 2002ck	3.64	0.69 (0.02)	0.65 (0.02)	26.6 (2.4)	1.0 (10.5)	...	...	...
SN 2002cr	−6.78	4.35 (0.03)	3.94 (0.04)	16.1 (1.4)	-6.2 (10.3)	10.59 (0.10)	0.163 (0.006)	112.9 (2.4)
SN 2002cu	−5.28	0.99 (0.02)	0.91 (0.02)	18.8 (1.8)	-3.4 (10.4)	11.20 (0.15)	0.194 (0.008)	89.9 (2.1)
SN 2002de	−0.32	1.10 (0.06)	0.95 (0.06)	31.5 (2.6)	8.4 (10.6)	10.98 (0.22)	0.201 (0.031)	130.3 (2.4)
SN 2002dj	−7.98	4.07 (0.04)	3.65 (0.06)	24.6 (2.0)	2.0 (10.4)	13.89 (0.10)	0.204 (0.009)	118.9 (2.4)
SN 2002dk	−1.23	0.32 (0.01)	0.29 (0.01)	45.3 (3.4)	22.5 (10.8)	10.92 (0.10)	0.359 (0.010)	113.9 (2.4)
SN 2002ef	4.70	1.03 (0.03)	1.03 (0.03)	14.1 (1.4)	-12.4 (10.3)	...	...	...
SN 2002er	5.26	5.98 (0.02)	5.23 (0.10)	19.7 (1.7)	-7.4 (10.4)	11.87 (0.10)	0.205 (0.017)	95.2 (2.4)

Continued on Next Page...

Table 3.11 — Continued

SN Name	Phase[a]	F_b[b]	F_r[b]	pEW[c]	ΔpEW[c,d]	v[e]	a	FWHM[c]
SN 2002eu	−0.06	0.51 (0.01)	0.52 (0.01)	40.1 (3.3)	16.8 (10.8)	10.71 (0.10)	0.346 (0.009)	98.3 (2.4)
SN 2002fb	0.98	0.78 (0.01)	0.89 (0.01)	47.4 (3.3)	23.6 (10.8)	10.25 (0.10)	0.358 (0.008)	96.5 (2.4)
SN 2002fk	7.74	14.99 (0.12)	14.15 (0.09)	28.7 (2.1)	-1.1 (10.5)	9.60 (0.10)	0.171 (0.004)	172.3 (2.4)
SN 2002ha	−0.85	3.61 (0.03)	3.35 (0.04)	25.6 (2.1)	2.7 (10.5)	10.41 (0.10)	0.220 (0.004)	110.4 (2.4)
SN 2002ha	4.93	3.79 (0.04)	3.51 (0.06)	31.1 (2.5)	4.3 (10.5)	10.93 (0.10)	0.272 (0.012)	108.5 (2.4)
SN 2002ha	7.89	7.25 (0.05)	7.77 (0.12)	44.4 (3.1)	14.4 (10.7)	11.23 (0.10)	0.301 (0.008)	149.9 (2.4)
SN 2002hd	6.48	0.90 (0.01)	0.85 (0.01)	39.3 (3.0)	10.9 (10.7)	10.97 (0.10)	0.324 (0.004)	125.6 (2.4)
SN 2002he	−5.91	0.67 (0.02)	0.61 (0.02)	25.8 (2.8)	3.5 (10.6)	11.35 (0.10)	0.215 (0.006)	107.0 (1.2)
SN 2002he	−1.03	1.69 (0.03)	1.59 (0.03)	17.8 (2.1)	-5.1 (10.5)	11.40 (0.10)	0.171 (0.006)	102.0 (1.2)
SN 2002he	0.29	1.45 (0.01)	1.36 (0.01)	21.4 (1.6)	-2.0 (10.4)	11.56 (0.10)	0.184 (0.002)	109.3 (2.4)
SN 2002he	3.22	3.15 (0.03)	2.82 (0.02)	23.0 (1.8)	-2.3 (10.4)	11.26 (0.10)	0.195 (0.003)	115.2 (2.4)
SN 2002hw	−6.27	0.89 (0.02)	0.91 (0.04)	24.7 (2.2)	2.4 (10.5)	11.44 (0.10)	0.245 (0.013)	102.2 (2.4)
SN 2002kf	6.81	2.18 (0.02)	2.11 (0.02)	24.8 (2.0)	-3.8 (10.4)	...	...	...
SN 2003U	−2.55	0.69 (0.01)	0.65 (0.01)	26.9 (2.2)	4.5 (10.5)	...	...	...
SN 2003ai	7.25	0.71 (0.02)	0.73 (0.01)	32.4 (2.4)	3.2 (10.5)	12.07 (0.10)	0.225 (0.007)	135.3 (2.4)
SN 2003gt	−5.07	2.37 (0.03)	2.12 (0.03)	30.3 (2.1)	8.1 (10.5)	12.52 (0.10)	0.198 (0.005)	153.6 (2.4)
SN 2003he	2.71	1.38 (0.02)	1.30 (0.02)	21.1 (1.7)	-3.9 (10.4)	10.53 (0.10)	0.178 (0.005)	122.9 (2.4)
SN 2003iv	1.76	0.02 (0.00)	0.02 (0.00)	32.6 (2.7)	8.4 (10.6)	10.66 (0.10)	0.310 (0.005)	108.3 (2.4)
SN 2003iv	6.58	0.18 (0.01)	0.19 (0.01)	34.7 (3.5)	6.3 (10.8)	10.15 (0.10)	0.343 (0.027)	110.2 (2.4)
SN 2004E	5.26	1.44 (0.01)	1.33 (0.01)	28.2 (2.1)	1.1 (10.5)	13.10 (0.10)	0.200 (0.003)	139.8 (2.4)
SN 2004S	8.26	5.78 (0.01)	5.62 (0.04)	35.5 (2.6)	5.1 (10.6)	9.76 (0.10)	0.286 (0.004)	107.0 (2.4)
SN 2004as	−4.36	0.56 (0.01)	0.46 (0.00)	24.7 (1.6)	2.5 (10.4)	11.22 (0.10)	0.136 (0.007)	174.6 (2.4)
SN 2004bk	6.13	1.74 (0.01)	1.75 (0.03)	29.6 (2.0)	1.7 (10.4)	12.17 (0.10)	0.216 (0.007)	105.6 (2.4)
SN 2004bl	4.61	1.94 (0.03)	1.73 (0.03)	15.3 (1.3)	-11.1 (10.3)	9.86 (0.10)	0.123 (0.010)	135.7 (2.4)
SN 2004bv	9.77	8.00 (0.03)	7.90 (0.09)	33.6 (2.2)	1.2 (10.5)	12.79 (0.10)	0.207 (0.011)	158.3 (2.4)
SN 2004bw	6.59	1.15 (0.02)	1.18 (0.01)	32.0 (2.4)	3.6 (10.5)	...	...	...
SN 2004dt	−6.46	1.91 (0.02)	1.69 (0.03)	30.6 (2.0)	8.3 (10.5)	14.04 (0.16)	0.180 (0.008)	213.8 (2.4)
SN 2004dt	1.38	2.82 (0.02)	2.59 (0.02)	16.6 (0.8)	-7.4 (10.3)	9.41 (0.10)	0.111 (0.003)	152.0 (6.0)
SN 2004ef	−5.52	0.43 (0.00)	0.39 (0.01)	20.5 (1.8)	-1.7 (10.4)	12.01 (0.10)	0.209 (0.009)	95.1 (2.4)
SN 2004eo	−5.57	1.12 (0.01)	1.05 (0.01)	36.0 (2.6)	13.8 (10.6)	9.07 (0.14)	0.250 (0.009)	135.9 (2.4)
SN 2004ey	−7.58	2.29 (0.01)	2.05 (0.01)	15.6 (1.3)	-7.0 (10.3)	11.84 (0.10)	0.151 (0.002)	108.3 (2.4)
SN 2004fu	−2.65	4.09 (0.04)	3.95 (0.04)	22.8 (1.8)	0.4 (10.4)	12.16 (0.10)	0.189 (0.008)	111.0 (2.4)
SN 2004fu	2.43	3.97 (0.02)	3.72 (0.03)	16.7 (1.4)	-8.0 (10.3)	12.06 (0.10)	0.146 (0.005)	146.6 (2.4)
SN 2004fz	−5.18	2.45 (0.02)	2.36 (0.02)	35.5 (2.6)	13.3 (10.6)	8.93 (0.16)	0.258 (0.003)	129.8 (2.4)
SN 2004gs	0.44	0.59 (0.01)	0.55 (0.02)	43.1 (3.2)	19.6 (10.7)	11.15 (0.10)	0.342 (0.025)	111.0 (2.4)
SN 2005M	8.23	0.38 (0.01)	0.35 (0.00)	17.7 (1.9)	-12.7 (10.4)	...	...	...
SN 2005W	0.59	3.42 (0.06)	3.02 (0.06)	23.4 (2.5)	-0.2 (10.5)	9.84 (0.10)	0.185 (0.006)	106.0 (1.2)
SN 2005am	4.47	12.86 (0.08)	11.40 (0.07)	29.6 (2.4)	3.3 (10.5)	11.17 (0.10)	0.265 (0.002)	107.2 (2.4)
SN 2005am	6.37	11.26 (0.04)	10.86 (0.03)	29.3 (1.5)	1.1 (10.4)	11.76 (0.10)	0.261 (0.004)	104.2 (6.1)
SN 2005ao	−1.29	0.60 (0.01)	0.51 (0.01)	13.5 (1.0)	-9.3 (10.3)	...	...	...
SN 2005ao	0.52	0.44 (0.01)	0.40 (0.01)	11.3 (1.0)	-12.3 (10.3)	11.45 (0.10)	0.092 (0.006)	125.2 (2.4)
SN 2005bc	1.55	1.84 (0.01)	1.91 (0.01)	40.0 (2.9)	15.9 (10.6)	10.60 (0.10)	0.305 (0.003)	116.6 (2.4)
SN 2005bc	7.37	1.58 (0.01)	1.69 (0.02)	38.7 (3.0)	9.3 (10.7)	10.10 (0.10)	0.327 (0.012)	106.7 (2.4)
SN 2005cf	−10.94	3.29 (0.02)	2.86 (0.03)	11.9 (1.0)	-12.1 (10.3)	11.17 (0.10)	0.127 (0.008)	75.5 (2.4)
SN 2005cf	−2.11	101.04 (0.45)	88.16 (0.46)	16.2 (1.3)	-6.3 (10.3)	9.80 (0.10)	0.143 (0.004)	107.3 (2.4)
SN 2005cf	−1.19	20.49 (0.11)	18.71 (0.12)	16.3 (1.3)	-6.5 (10.3)	10.11 (0.10)	0.147 (0.002)	107.3 (2.4)
SN 2005de	−0.75	2.05 (0.04)	1.87 (0.03)	24.9 (2.2)	1.9 (10.5)	...	...	...
SN 2005dv	−0.57	1.20 (0.03)	1.12 (0.04)	19.3 (1.6)	-3.7 (10.4)	10.48 (0.10)	0.176 (0.007)	114.8 (2.4)
SN 2005el	−6.70	1.80 (0.02)	1.60 (0.01)	16.9 (1.3)	-5.4 (10.3)	...	...	...
SN 2005el	1.22	3.09 (0.03)	2.86 (0.03)	20.9 (1.7)	-3.0 (10.4)	8.33 (0.10)	0.173 (0.002)	104.4 (2.4)
SN 2005er	−0.26	0.00 (0.00)	0.00 (0.00)	36.8 (3.8)	13.6 (10.9)	8.04 (0.10)	0.295 (0.007)	119.0 (1.2)
SN 2005hj	7.51	0.45 (0.01)	0.46 (0.01)	20.1 (2.1)	-9.4 (10.5)	13.18 (0.10)	0.153 (0.012)	190.0 (1.2)
SN 2005iq	−5.86	7.14 (0.06)	6.54 (0.10)	19.7 (2.3)	-2.6 (10.5)	11.07 (0.10)	0.194 (0.007)	100.0 (1.2)
SN 2005kc	10.28	0.11 (0.00)	0.12 (0.00)	44.7 (4.4)	11.5 (11.1)	11.19 (0.10)	0.293 (0.006)	152.0 (1.2)
SN 2005ki	1.62	8.85 (0.06)	8.18 (0.06)	21.6 (2.4)	-2.6 (10.5)	9.77 (0.10)	0.207 (0.003)	96.0 (1.2)
SN 2005ki	8.35	1.69 (0.04)	1.79 (0.04)	46.0 (3.3)	15.4 (10.8)	...	...	...
SN 2005mc	6.64	0.68 (0.02)	0.61 (0.01)	36.7 (3.0)	8.1 (10.7)	9.43 (0.10)	0.355 (0.006)	97.5 (2.4)
SN 2005lz	0.58	5.95 (0.08)	5.47 (0.10)	11.7 (1.6)	-11.8 (10.4)	10.27 (0.10)	0.141 (0.008)	82.0 (1.2)
SN 2006D	3.70	17.01 (0.11)	15.26 (0.05)	27.3 (2.1)	1.6 (10.5)	10.12 (0.10)	0.234 (0.005)	99.2 (2.4)
SN 2006N	−1.89	2.37 (0.02)	2.35 (0.02)	23.2 (1.9)	0.6 (10.4)	11.09 (0.10)	0.183 (0.004)	128.2 (2.4)
SN 2006N	−0.90	2.08 (0.02)	1.97 (0.01)	27.1 (2.1)	4.2 (10.5)	11.19 (0.10)	0.215 (0.004)	122.3 (2.4)
SN 2006X	3.15	9.89 (0.04)	9.64 (0.04)	9.7 (0.8)	-15.5 (10.3)	12.23 (0.10)	0.083 (0.003)	121.4 (2.4)
SN 2006ac	7.96	1.50 (0.01)	1.43 (0.01)	30.7 (2.2)	0.6 (10.5)	11.14 (0.10)	0.235 (0.005)	115.3 (2.4)
SN 2006ak	8.43	0.46 (0.00)	0.44 (0.00)	17.2 (1.4)	-13.4 (10.4)	12.25 (0.10)	0.161 (0.003)	98.3 (2.4)
SN 2006bq	6.97	4.72 (0.04)	4.38 (0.03)	19.1 (1.4)	-9.8 (10.4)	10.59 (0.10)	0.151 (0.002)	121.3 (2.4)
SN 2006bt	−5.30	0.41 (0.01)	0.37 (0.00)	33.0 (2.3)	10.8 (10.5)	11.05 (0.10)	0.250 (0.008)	100.8 (2.4)
SN 2006bt	−4.53	0.36 (0.01)	0.35 (0.00)	20.3 (1.9)	-1.9 (10.4)	10.83 (0.10)	0.234 (0.008)	100.8 (2.4)
SN 2006bt	2.27	0.37 (0.01)	0.36 (0.00)	36.9 (2.8)	12.3 (10.6)	9.83 (0.10)	0.327 (0.011)	91.1 (2.4)
SN 2006bu	4.22	0.12 (0.00)	0.11 (0.00)	19.2 (1.6)	-6.9 (10.4)	12.31 (0.10)	0.165 (0.006)	112.5 (2.3)
SN 2006bw	8.90	0.38 (0.00)	0.35 (0.00)	44.1 (3.3)	12.9 (10.8)	9.81 (0.10)	0.328 (0.006)	124.3 (2.4)
SN 2006bz	−2.44	0.29 (0.01)	0.28 (0.01)	52.7 (3.9)	30.2 (11.0)	10.41 (0.10)	0.400 (0.009)	118.7 (2.4)
SN 2006cj	3.43	0.18 (0.01)	0.15 (0.00)	15.5 (1.3)	-10.0 (10.3)	...	...	...
SN 2006cp	−5.30	0.95 (0.01)	0.90 (0.01)	8.8 (0.7)	-13.4 (10.3)	...	...	...
SN 2006cs	2.28	0.27 (0.01)	0.28 (0.00)	41.5 (3.0)	16.9 (10.7)	9.49 (0.10)	0.319 (0.012)	113.3 (2.4)
SN 2006dm	−7.90	0.30 (0.01)	0.29 (0.02)	41.3 (3.3)	18.7 (10.8)	11.22 (0.10)	0.342 (0.012)	115.5 (2.4)
SN 2006ef	3.20	2.28 (0.01)	1.95 (0.01)	23.4 (1.8)	-1.9 (10.4)	9.52 (0.10)	0.171 (0.004)	133.6 (2.4)
SN 2006ej	−3.70	1.43 (0.01)	1.36 (0.01)	28.4 (2.3)	6.1 (10.5)	...	...	...
SN 2006ej	5.09	1.10 (0.01)	1.00 (0.01)	28.4 (2.2)	1.5 (10.5)	10.32 (0.10)	0.210 (0.003)	117.6 (2.4)
SN 2006en	8.55	0.48 (0.02)	0.52 (0.01)	37.0 (3.0)	6.3 (10.7)	13.30 (0.10)	0.325 (0.012)	129.9 (2.4)
SN 2006et	3.29	1.39 (0.02)	1.23 (0.02)	11.0 (1.0)	-14.3 (10.3)	...	...	...
SN 2006ev	10.54	0.48 (0.01)	0.49 (0.01)	28.4 (2.4)	-5.2 (10.5)	10.85 (0.10)	0.262 (0.008)	103.0 (2.4)
SN 2006gj	4.70	0.23 (0.01)	0.24 (0.01)	44.6 (3.9)	18.1 (11.0)	...	...	...

Continued on Next Page...

Table 3.11 — Continued

SN Name	Phase[a]	F_b[b]	F_r[b]	pEW[c]	ΔpEW[c,d]	v[e]	a	FWHM[c]
SN 2006kf	−8.96	0.26 (0.01)	0.26 (0.00)	36.1 (2.9)	13.2 (10.6)	10.62 (0.10)	0.331 (0.009)	99.9 (2.4)
SN 2006kf	−3.05	0.69 (0.01)	0.69 (0.01)	31.2 (2.6)	8.9 (10.6)	10.30 (0.10)	0.315 (0.003)	96.0 (2.4)
SN 2006lf	−6.30	0.41 (0.00)	0.43 (0.00)	28.2 (2.2)	5.9 (10.5)	11.38 (0.10)	0.217 (0.008)	136.2 (2.4)
SN 2006mp	5.66	1.08 (0.01)	1.01 (0.01)	14.3 (1.1)	-13.1 (10.3)	···	···	···
SN 2006or	−2.79	0.81 (0.01)	0.78 (0.02)	16.3 (1.4)	-6.1 (10.3)	···	···	···
SN 2006os	8.61	0.29 (0.01)	0.27 (0.01)	23.2 (2.2)	-7.6 (10.5)	11.63 (0.10)	0.270 (0.011)	91.0 (2.4)
SN 2006sr	−2.34	0.80 (0.01)	0.75 (0.01)	21.3 (1.7)	-1.2 (10.4)	10.93 (0.10)	0.179 (0.004)	119.1 (2.4)
SN 2006sr	2.69	1.29 (0.01)	1.15 (0.01)	18.1 (1.5)	-6.8 (10.4)	11.14 (0.10)	0.182 (0.006)	99.6 (2.4)
SN 2007A	2.37	2.12 (0.01)	2.00 (0.02)	12.5 (1.1)	-12.2 (10.3)	9.33 (0.10)	0.123 (0.004)	82.5 (2.4)
SN 2007F	−9.35	0.71 (0.01)	0.63 (0.00)	6.1 (0.6)	-17.1 (10.3)	9.98 (0.10)	0.053 (0.007)	105.5 (2.4)
SN 2007F	3.23	1.51 (0.01)	1.34 (0.01)	9.1 (0.7)	-16.2 (10.3)	10.18 (0.10)	0.077 (0.003)	129.0 (2.4)
SN 2007N	0.44	3.95 (0.04)	3.31 (0.11)	31.9 (3.6)	8.4 (10.9)	10.25 (0.10)	0.298 (0.020)	94.0 (1.2)
SN 2007O	−0.33	13.14 (0.13)	11.37 (0.14)	10.5 (1.4)	-12.7 (10.3)	9.56 (0.10)	0.122 (0.010)	91.0 (1.2)
SN 2007S	5.18	2.16 (0.04)	2.03 (0.04)	11.8 (1.0)	-15.2 (10.3)	10.17 (0.10)	0.104 (0.007)	128.2 (2.4)
SN 2007af	2.84	21.40 (0.07)	18.34 (0.11)	15.8 (1.9)	-9.2 (10.4)	9.57 (0.10)	0.152 (0.006)	101.0 (1.2)
SN 2007af	3.81	20.63 (0.12)	18.52 (0.11)	19.3 (1.6)	-6.5 (10.4)	9.73 (0.10)	0.168 (0.006)	109.4 (2.4)
SN 2007ap	9.37	25.42 (0.22)	26.18 (0.21)	47.0 (4.6)	15.1 (11.2)	10.89 (0.10)	0.320 (0.004)	152.0 (1.2)
SN 2007ba	2.14	0.47 (0.02)	0.43 (0.01)	50.1 (3.8)	25.6 (10.9)	10.07 (0.10)	0.365 (0.014)	171.4 (2.4)
SN 2007ba	5.18	3.86 (0.08)	3.60 (0.06)	54.9 (5.5)	27.9 (11.6)	9.51 (0.10)	0.419 (0.005)	102.0 (1.2)
SN 2007bc	0.61	1.56 (0.01)	1.48 (0.01)	30.2 (2.3)	6.6 (10.5)	10.14 (0.10)	0.269 (0.002)	92.1 (2.4)
SN 2007bm	−7.79	5.40 (0.06)	5.32 (0.03)	35.9 (2.4)	13.3 (10.5)	10.96 (0.10)	0.226 (0.004)	194.8 (2.4)
SN 2007ci	−6.57	0.97 (0.03)	0.92 (0.02)	51.1 (3.7)	28.8 (10.9)	···	···	···
SN 2007ci	−1.71	1.34 (0.01)	1.31 (0.01)	41.3 (2.9)	18.7 (10.7)	10.08 (0.10)	0.267 (0.005)	151.3 (2.4)
SN 2007co	−4.09	0.67 (0.01)	0.63 (0.01)	18.3 (1.5)	-3.9 (10.4)	···	···	···
SN 2007co	0.85	0.84 (0.01)	0.74 (0.01)	16.2 (1.4)	-7.5 (10.3)	···	···	···
SN 2007cq	7.84	1.55 (0.02)	1.48 (0.02)	27.2 (2.0)	-2.7 (10.4)	11.45 (0.10)	0.192 (0.005)	140.4 (2.4)
SN 2007fr	−5.83	0.12 (0.01)	0.12 (0.00)	24.1 (2.7)	1.9 (10.6)	11.06 (0.10)	0.299 (0.021)	89.4 (2.3)
SN 2007fr	−1.25	0.15 (0.01)	0.15 (0.00)	34.7 (3.1)	12.0 (10.7)	10.56 (0.10)	0.355 (0.015)	99.0 (2.3)
SN 2007fs	5.03	3.23 (0.03)	3.04 (0.03)	18.7 (1.4)	-8.1 (10.3)	···	···	···
SN 2007gi	6.61	15.35 (0.03)	14.84 (0.07)	12.2 (0.9)	-16.2 (10.3)	11.91 (0.10)	0.102 (0.004)	117.4 (2.4)
SN 2007gk	−1.72	0.77 (0.01)	0.73 (0.00)	26.1 (2.1)	3.5 (10.5)	11.87 (0.10)	0.232 (0.005)	116.9 (2.4)
SN 2007hj	−1.23	1.77 (0.01)	1.80 (0.01)	51.1 (3.8)	28.3 (10.9)	11.04 (0.10)	0.387 (0.011)	124.2 (2.4)
SN 2007kk	7.15	1.93 (0.02)	1.94 (0.03)	20.3 (1.5)	-8.7 (10.4)	12.61 (0.10)	0.150 (0.005)	103.7 (2.4)
SN 2007le	7.43	12.10 (0.04)	11.80 (0.09)	14.2 (1.2)	-15.2 (10.3)	12.16 (0.10)	0.136 (0.006)	97.3 (2.4)
SN 2007s1[f]	−1.23	0.89 (0.01)	0.80 (0.01)	23.9 (1.8)	1.1 (10.4)	10.77 (0.10)	0.190 (0.004)	105.1 (2.4)
SN 2007on	−3.01	18.69 (0.10)	17.12 (0.05)	46.4 (3.4)	24.1 (10.8)	10.95 (0.10)	0.362 (0.003)	117.2 (2.4)
SN 2007on	−3.00	15.36 (0.07)	14.54 (0.06)	43.3 (4.6)	20.9 (11.2)	10.75 (0.10)	0.353 (0.003)	116.0 (1.2)
SN 2007qe	6.23	1.70 (0.01)	1.71 (0.02)	10.4 (0.9)	-17.7 (10.3)	11.50 (0.10)	0.112 (0.007)	84.0 (2.4)
SN 2007ux	5.59	0.82 (0.03)	0.85 (0.03)	36.7 (2.9)	9.3 (10.6)	···	···	···
SN 2008Q	6.46	14.96 (0.09)	14.98 (0.09)	25.4 (1.9)	-2.9 (10.4)	12.00 (0.10)	0.211 (0.002)	107.1 (2.4)
SN 2008ar	−8.87	0.42 (0.01)	0.36 (0.00)	12.4 (1.0)	-10.5 (10.3)	11.48 (0.10)	0.137 (0.007)	97.5 (4.8)
SN 2008ar	2.83	0.73 (0.02)	0.62 (0.02)	17.0 (1.7)	-8.0 (10.4)	···	···	···
SN 2008bt	−1.08	1.20 (0.10)	1.16 (0.05)	62.4 (4.3)	39.5 (11.1)	···	···	···
SN 2008s1[g]	−6.36	0.86 (0.01)	0.78 (0.01)	20.9 (1.8)	-1.4 (10.4)	10.84 (0.10)	0.201 (0.004)	105.7 (2.4)
SN 2008s1[g]	−4.40	1.16 (0.04)	1.04 (0.04)	28.5 (2.4)	6.3 (10.5)	···	···	···
SN 2008s1[g]	−3.42	1.08 (0.01)	1.00 (0.01)	16.1 (1.7)	-6.1 (10.4)	10.13 (0.10)	0.204 (0.006)	93.9 (2.4)
SN 2008s1[g]	0.49	1.37 (0.02)	1.31 (0.02)	24.2 (2.2)	0.6 (10.5)	···	···	···
SN 2008s1[g]	4.40	1.36 (0.01)	1.17 (0.01)	29.1 (2.3)	2.9 (10.5)	···	···	···
SN 2008s1[g]	5.38	1.35 (0.01)	1.16 (0.00)	32.0 (2.5)	4.8 (10.5)	10.54 (0.10)	0.287 (0.004)	90.0 (2.4)
SN 2008cl	4.24	0.09 (0.00)	0.09 (0.00)	30.1 (2.6)	4.0 (10.6)	10.06 (0.10)	0.263 (0.018)	148.6 (2.3)
SN 2008dx	2.46	0.33 (0.01)	0.32 (0.00)	46.7 (3.4)	21.9 (10.8)	8.89 (0.10)	0.353 (0.008)	101.7 (2.4)
SN 2008ec	−0.24	2.25 (0.01)	2.11 (0.01)	34.4 (2.5)	11.2 (10.6)	8.94 (0.10)	0.268 (0.006)	116.1 (2.4)
SN 2008ec	5.70	2.43 (0.01)	2.20 (0.02)	37.7 (3.0)	10.2 (10.7)	9.36 (0.10)	0.338 (0.006)	102.3 (2.4)
SN 2008ei	3.29	0.33 (0.01)	0.30 (0.01)	9.4 (0.9)	-15.9 (10.3)	···	···	···
SN 2008s5[h]	8.96	0.90 (0.01)	0.92 (0.01)	21.8 (1.7)	-9.5 (10.4)	···	···	···
SN 2008hs	−7.94	0.56 (0.01)	0.56 (0.01)	39.3 (3.1)	16.7 (10.7)	11.48 (0.10)	0.326 (0.004)	110.1 (2.4)

Uncertainties for each measured value are given in parentheses.
[a]Phases of spectra are in rest-frame days using the heliocentric redshift and photometry reference presented in table 1 of Silverman et al. (submitted).
[b]Fluxes are in units of 10^{-15} erg s^{-1} cm^{-2} Å^{-1}.
[c]The pEW, ΔpEW, and FWHM are in units of Å.
[d]ΔpEW is the measured pEW minus the expected pEW at the same epoch using our linear or quadratic fit (see Section 3.5.4 for more information).
[e]The expansion velocity is in units of 1000 km s^{-1}.
[f]Also known as SNF20071021-000.
[g]Also known as SNF20080514-002.
[h]Also known as SNF20080909-030.

Table 3.12: Measured Values for Si II λ6355

SN Name	Phase[a]	F_b[b]	F_r[b]	pEW[c]	ΔpEW[c,d]	v[e]	a	FWHM[c]
SN 1989B	7.54	208.47 (4.96)	152.53 (0.64)	127.6 (6.9)	12.3 (32.7)	9.90 (0.10)	0.668 (0.008)	169.6 (3.1)
SN 1989M	2.49	24.67 (0.22)	23.25 (0.16)	122.9 (8.2)	15.5 (33.0)	12.46 (0.10)	0.700 (0.001)	175.1 (2.4)
SN 1989M	3.48	27.34 (0.25)	25.26 (0.11)	122.7 (8.2)	14.2 (33.0)	12.17 (0.10)	0.708 (0.002)	169.1 (2.4)
SN 1990O	12.54	1.00 (0.02)	0.57 (0.01)	107.6 (5.0)	-21.2 (32.4)	11.21 (0.10)	0.648 (0.010)	147.5 (4.8)
SN 1990N	7.11	34.03 (0.37)	23.46 (0.17)	88.7 (4.6)	-25.8 (32.3)	10.68 (0.10)	0.661 (0.005)	119.6 (4.9)

Continued on Next Page...

Table 3.12 — Continued

SN Name	Phase[a]	F_b[b]	F_r[b]	pEW[c]	ΔpEW[c,d]	v[e]	a	FWHM[c]
SN 1991M	18.06	6.35 (0.08)	5.22 (0.06)	165.8 (6.3)	15.5 (32.6)	10.83 (0.10)	0.664 (0.003)	238.3 (4.9)
SN 1991T	6.80	18.57 (0.39)	14.37 (0.07)	45.9 (2.6)	-67.9 (32.1)	9.75 (0.10)	0.407 (0.005)	107.4 (4.9)
SN 1991bg	0.14	10.08 (0.16)	9.71 (0.05)	91.5 (3.8)	-14.2 (32.2)	10.66 (0.10)	0.579 (0.007)	150.0 (6.1)
SN 1991bg	1.14	13.59 (0.26)	13.60 (0.16)	92.4 (3.9)	-13.9 (32.2)	10.17 (0.10)	0.582 (0.006)	150.0 (6.1)
SN 1991bg	19.07	3.26 (0.06)	4.14 (0.03)	176.4 (5.4)	21.4 (32.4)	8.01 (0.10)	0.600 (0.004)	290.0 (6.1)
SN 1993ac	12.68	0.13 (0.00)	0.10 (0.00)	140.0 (9.0)	10.7 (33.2)	11.16 (0.10)	0.726 (0.006)	184.9 (2.3)
SN 1994D	−12.31	9.33 (0.06)	8.95 (0.04)	144.7 (8.1)	27.3 (33.0)	15.13 (0.10)	0.600 (0.001)	237.6 (2.4)
SN 1994D	−11.31	9.06 (0.11)	8.15 (0.10)	129.1 (7.6)	13.9 (32.9)	13.86 (0.10)	0.561 (0.005)	235.6 (2.4)
SN 1994D	−9.32	21.15 (0.07)	18.64 (0.08)	85.8 (5.1)	-25.6 (32.4)	12.29 (0.10)	0.432 (0.002)	195.7 (2.4)
SN 1994D	−7.67	23.32 (0.08)	20.21 (0.08)	83.5 (5.3)	-25.4 (32.4)	11.71 (0.10)	0.474 (0.002)	165.8 (2.4)
SN 1994D	−5.32	33.58 (0.27)	29.69 (0.22)	85.0 (5.7)	-21.5 (32.5)	10.92 (0.10)	0.527 (0.003)	153.8 (2.4)
SN 1994D	−3.87	50.63 (0.31)	43.18 (0.21)	84.8 (5.7)	-20.8 (32.5)	10.72 (0.10)	0.520 (0.002)	153.8 (2.4)
SN 1994D	−3.33	48.12 (0.19)	41.16 (0.14)	89.6 (6.0)	-15.8 (32.5)	10.72 (0.10)	0.547 (0.002)	153.8 (2.4)
SN 1994D	14.04	32.85 (0.14)	26.07 (0.11)	138.9 (7.1)	4.9 (32.7)	10.13 (0.10)	0.554 (0.002)	229.7 (2.4)
SN 1994Q	9.68	1.08 (0.02)	0.98 (0.02)	50.9 (4.1)	-69.6 (32.2)	10.15 (0.10)	0.471 (0.005)	103.0 (2.4)
SN 1994S	1.11	8.58 (0.10)	6.92 (0.09)	83.0 (6.2)	-23.3 (32.6)	10.53 (0.10)	0.607 (0.003)	132.0 (2.4)
SN 1995D	3.84	16.29 (0.16)	13.15 (0.09)	82.0 (6.0)	-26.9 (32.5)	10.01 (0.10)	0.600 (0.003)	133.1 (2.4)
SN 1995E	−2.46	1.71 (0.01)	1.79 (0.01)	100.0 (6.8)	-5.2 (32.7)	10.81 (0.10)	0.625 (0.002)	156.2 (2.4)
SN 1997Y	1.27	3.97 (0.04)	3.48 (0.04)	109.4 (7.6)	3.0 (32.9)	10.73 (0.10)	0.690 (0.001)	155.5 (2.4)
SN 1997bp	5.49	9.78 (0.15)	7.99 (0.07)	159.2 (9.7)	47.8 (33.4)	14.22 (0.10)	0.780 (0.004)	196.4 (2.4)
SN 1997br	−4.84	9.77 (0.07)	8.09 (0.07)	18.6 (1.4)	-87.5 (32.0)	11.09 (0.10)	0.144 (0.005)	135.1 (2.4)
SN 1997do	−5.67	3.66 (0.04)	3.36 (0.01)	110.0 (6.6)	3.2 (32.6)	13.97 (0.10)	0.544 (0.002)	190.1 (2.4)
SN 1998V	7.20	4.16 (0.01)	2.90 (0.01)	93.7 (9.3)	-20.9 (33.3)	10.67 (0.10)	0.660 (0.004)	127.0 (1.2)
SN 1998dh	18.77	6.88 (0.03)	4.97 (0.03)	206.2 (10.0)	52.6 (33.5)	10.42 (0.10)	0.673 (0.004)	339.0 (2.4)
SN 1998dk	−7.24	2.20 (0.05)	1.75 (0.01)	113.2 (6.7)	4.8 (32.7)	14.01 (0.10)	0.558 (0.005)	185.5 (2.4)
SN 1998dk	−0.54	5.07 (0.03)	4.53 (0.01)	103.1 (7.0)	-2.3 (32.7)	12.84 (0.10)	0.631 (0.001)	157.9 (2.4)
SN 1998dm	−12.48	1.71 (0.01)	1.51 (0.01)	71.1 (4.6)	-46.7 (32.3)	11.75 (0.10)	0.442 (0.005)	143.1 (2.4)
SN 1998dm	−5.61	4.45 (0.01)	4.08 (0.03)	71.3 (5.1)	-35.5 (32.4)	11.15 (0.10)	0.516 (0.004)	129.2 (2.4)
SN 1998dm	14.22	2.74 (0.01)	2.85 (0.01)	71.8 (5.4)	-62.8 (32.4)	10.07 (0.10)	0.543 (0.004)	123.2 (2.4)
SN 1998dx	5.13	0.42 (0.00)	0.33 (0.00)	103.4 (7.2)	-7.4 (32.8)	11.62 (0.10)	0.650 (0.003)	151.8 (2.3)
SN 1998ec	11.86	1.22 (0.01)	0.82 (0.01)	126.2 (7.9)	-0.5 (32.9)	10.87 (0.10)	0.643 (0.005)	188.3 (2.4)
SN 1998ef	−8.62	1.59 (0.01)	1.44 (0.01)	145.7 (8.9)	35.4 (33.2)	13.88 (0.10)	0.717 (0.004)	194.5 (2.4)
SN 1998es	0.28	10.42 (0.04)	8.08 (0.02)	61.2 (4.3)	-44.6 (32.3)	10.42 (0.10)	0.439 (0.005)	132.6 (2.4)
SN 1999aa	0.24	1.34 (0.01)	1.04 (0.01)	56.0 (4.1)	-49.7 (32.2)	10.50 (0.10)	0.438 (0.005)	122.2 (2.4)
SN 1999aa	17.04	1.84 (0.02)	1.71 (0.01)	42.0 (3.4)	-103.8 (32.2)	10.48 (0.10)	0.425 (0.009)	78.9 (2.4)
SN 1999ac	−3.70	5.30 (0.02)	4.99 (0.01)	76.9 (5.0)	-28.7 (32.4)	11.55 (0.10)	0.438 (0.001)	168.4 (2.4)
SN 1999ac	−0.89	6.64 (0.02)	5.82 (0.02)	86.3 (5.5)	-19.0 (32.4)	10.29 (0.10)	0.473 (0.002)	176.3 (2.4)
SN 1999cl	7.90	12.61 (0.49)	12.48 (0.27)	155.5 (9.0)	39.4 (33.2)	10.11 (0.10)	0.695 (0.007)	200.5 (2.4)
SN 1999cp	4.91	8.86 (0.03)	7.21 (0.03)	105.7 (7.5)	-4.8 (32.8)	10.49 (0.10)	0.711 (0.002)	142.6 (2.4)
SN 1999cp	13.85	6.83 (0.04)	4.01 (0.02)	130.1 (7.8)	-3.3 (32.9)	10.20 (0.10)	0.692 (0.006)	144.6 (2.4)
SN 1999cw	14.79	3.73 (0.03)	3.42 (0.01)	37.8 (2.8)	-99.0 (32.1)	10.74 (0.10)	0.314 (0.008)	134.3 (2.4)
SN 1999da	−2.12	1.33 (0.01)	1.31 (0.01)	121.1 (7.7)	15.8 (32.9)	11.32 (0.10)	0.643 (0.001)	193.5 (2.4)
SN 1999da	6.76	0.99 (0.01)	1.24 (0.00)	128.3 (7.6)	14.6 (32.9)	10.16 (0.10)	0.598 (0.004)	227.1 (2.4)
SN 1999dg	15.08	0.80 (0.01)	0.66 (0.01)	160.1 (8.8)	22.3 (33.2)	10.25 (0.10)	0.700 (0.004)	191.8 (2.4)
SN 1999dk	−6.60	3.72 (0.03)	3.49 (0.02)	130.2 (7.8)	22.5 (32.9)	15.00 (0.10)	0.623 (0.001)	206.9 (2.4)
SN 1999dk	17.06	5.15 (0.01)	3.63 (0.01)	146.0 (8.5)	0.0 (33.1)	11.33 (0.10)	0.684 (0.003)	195.1 (2.4)
SN 1999dq	−3.93	4.08 (0.04)	3.18 (0.03)	45.5 (3.2)	-60.2 (32.1)	11.24 (0.10)	0.328 (0.004)	132.1 (2.4)
SN 1999dq	2.97	5.04 (0.04)	3.92 (0.01)	62.9 (4.9)	-45.0 (32.3)	10.67 (0.10)	0.527 (0.004)	116.3 (2.4)
SN 1999ek	5.66	1.20 (0.04)	1.20 (0.03)	112.1 (7.8)	0.4 (32.9)	10.16 (0.10)	0.699 (0.006)	157.2 (2.4)
SN 1999gd	−1.12	0.97 (0.04)	0.96 (0.00)	112.9 (4.9)	7.6 (32.3)	10.37 (0.10)	0.683 (0.005)	162.0 (6.0)
SN 1999gh	4.12	5.95 (0.04)	5.79 (0.02)	161.6 (6.0)	52.2 (32.5)	11.02 (0.10)	0.711 (0.001)	233.2 (6.1)
SN 1999gh	15.89	2.78 (0.04)	3.55 (0.02)	209.2 (10.3)	68.2 (33.6)	10.52 (0.10)	0.701 (0.004)	309.6 (2.4)
SN 1999gh	15.97	2.74 (0.04)	3.47 (0.02)	211.1 (10.4)	69.7 (33.6)	10.42 (0.10)	0.697 (0.006)	319.5 (2.4)
SN 2000bk	14.84	0.31 (0.01)	0.32 (0.00)	172.9 (9.4)	36.0 (33.3)	11.32 (0.10)	0.705 (0.008)	237.9 (2.4)
SN 2000cn	14.25	0.43 (0.01)	0.50 (0.01)	188.3 (9.5)	53.6 (33.4)	10.85 (0.10)	0.692 (0.003)	265.8 (2.4)
SN 2000cp	2.92	0.31 (0.01)	0.30 (0.00)	158.0 (10.5)	50.2 (33.7)	11.50 (0.10)	0.903 (0.004)	177.9 (2.4)
SN 2000cu	9.64	1.10 (0.01)	0.88 (0.01)	150.4 (8.8)	30.1 (33.2)	11.08 (0.10)	0.711 (0.002)	192.2 (2.4)
SN 2000cw	4.81	0.60 (0.01)	0.55 (0.00)	119.9 (8.0)	9.6 (33.0)	10.52 (0.10)	0.711 (0.003)	157.3 (2.4)
SN 2000dg	−5.09	0.40 (0.01)	0.37 (0.00)	78.3 (5.5)	-28.0 (32.4)	11.14 (0.10)	0.518 (0.004)	140.6 (2.4)
SN 2000dg	4.66	0.50 (0.01)	0.50 (0.01)	69.9 (5.3)	-40.3 (32.4)	10.84 (0.10)	0.502 (0.004)	136.7 (2.4)
SN 2000dk	1.00	2.28 (0.01)	2.08 (0.01)	124.4 (8.2)	18.2 (33.0)	11.19 (0.10)	0.717 (0.001)	174.9 (2.4)
SN 2000dk	10.84	1.26 (0.01)	1.45 (0.01)	117.0 (7.2)	-6.6 (32.8)	10.12 (0.10)	0.629 (0.003)	174.9 (2.4)
SN 2000dm	−1.63	1.89 (0.01)	1.66 (0.01)	106.4 (7.3)	1.1 (32.8)	11.44 (0.10)	0.675 (0.002)	149.7 (2.4)
SN 2000dm	8.18	1.73 (0.02)	1.39 (0.01)	114.9 (7.3)	-1.9 (32.8)	10.49 (0.10)	0.671 (0.002)	151.7 (2.4)
SN 2000dn	−0.94	0.64 (0.01)	0.56 (0.01)	120.4 (8.3)	15.0 (33.0)	10.23 (0.10)	0.762 (0.005)	147.3 (2.4)
SN 2000dn	16.38	0.38 (0.00)	0.27 (0.00)	154.6 (8.1)	11.5 (33.0)	9.38 (0.10)	0.642 (0.005)	242.2 (2.4)
SN 2000dr	6.78	1.26 (0.01)	1.14 (0.01)	131.2 (7.8)	17.5 (32.9)	10.25 (0.10)	0.636 (0.001)	186.5 (2.4)
SN 2000ey	7.90	3.29 (0.07)	3.09 (0.06)	83.0 (5.4)	-33.1 (32.4)	11.68 (0.10)	0.502 (0.012)	143.1 (2.4)
SN 2000fa	−8.25	0.69 (0.01)	0.67 (0.01)	95.0 (5.5)	-14.7 (32.4)	13.38 (0.10)	0.451 (0.007)	197.8 (2.4)
SN 2000fa	6.86	1.31 (0.02)	0.99 (0.01)	89.0 (6.7)	-24.9 (32.7)	11.37 (0.10)	0.659 (0.006)	129.3 (2.4)
SN 2001E	15.01	0.81 (0.02)	0.59 (0.02)	105.0 (7.3)	-32.6 (32.8)	14.23 (0.10)	0.650 (0.024)	164.8 (2.4)
SN 2001G	11.57	2.72 (0.02)	1.68 (0.01)	95.9 (6.7)	-29.9 (32.7)	10.82 (0.10)	0.662 (0.006)	120.0 (2.4)
SN 2001N	13.05	0.27 (0.01)	0.22 (0.00)	95.9 (5.7)	-34.6 (32.5)	...	...	...
SN 2001V	15.86	3.04 (0.04)	3.12 (0.02)	58.1 (4.5)	-82.8 (32.3)	...	...	...
SN 2001ay	6.79	0.99 (0.01)	0.75 (0.01)	156.0 (9.4)	42.2 (33.3)	13.30 (0.10)	0.712 (0.005)	211.6 (2.4)
SN 2001az	−3.24	0.38 (0.01)	0.30 (0.01)	79.4 (5.5)	-26.0 (32.4)	11.58 (0.10)	0.526 (0.002)	134.5 (2.4)
SN 2001bf	1.22	3.68 (0.02)	3.26 (0.02)	131.6 (7.9)	25.3 (32.9)	10.34 (0.10)	0.619 (0.002)	212.7 (2.4)
SN 2001bg	13.70	6.72 (0.09)	4.78 (0.02)	147.6 (8.4)	14.8 (33.1)	11.43 (0.10)	0.683 (0.009)	192.6 (2.4)
SN 2001bg	18.91	5.82 (0.21)	5.03 (0.09)	210.3 (14.3)	56.1 (35.0)	10.23 (0.10)	0.702 (0.006)	295.0 (1.2)
SN 2001br	3.47	1.20 (0.06)	1.04 (0.04)	155.0 (10.1)	46.5 (33.5)	12.41 (0.10)	0.811 (0.010)	194.0 (2.4)
SN 2001br	3.48	1.18 (0.04)	1.05 (0.02)	152.6 (9.8)	44.1 (33.4)	12.13 (0.10)	0.784 (0.005)	196.0 (2.4)
SN 2001cp	1.39	0.69 (0.01)	0.58 (0.01)	79.7 (6.0)	-26.7 (32.5)	10.83 (0.10)	0.602 (0.006)	129.1 (2.4)

Continued on Next Page...

Table 3.12 — Continued

SN Name	Phase[a]	F_b[b]	F_r[b]	pEW[c]	ΔpEW[c,d]	v[e]	a	FWHM[c]
SN 2001da	−1.12	2.35 (0.02)	2.13 (0.02)	121.1 (7.8)	15.9 (32.9)	11.60 (0.10)	0.682 (0.003)	169.1 (2.4)
SN 2001da	9.72	1.89 (0.02)	1.54 (0.01)	124.0 (7.7)	3.5 (32.9)	10.64 (0.10)	0.634 (0.003)	171.1 (2.4)
SN 2001dl	13.84	0.41 (0.01)	0.40 (0.01)	73.1 (5.4)	-60.1 (32.4)	9.16 (0.10)	0.559 (0.010)	117.6 (2.4)
SN 2001dt	13.60	0.16 (0.00)	0.16 (0.00)	185.1 (9.5)	52.7 (33.4)	10.52 (0.10)	0.672 (0.005)	269.9 (2.4)
SN 2001eh	3.26	0.63 (0.01)	0.49 (0.00)	61.2 (4.8)	-47.1 (32.3)	10.64 (0.10)	0.549 (0.007)	104.1 (2.4)
SN 2001en	10.09	2.49 (0.03)	1.89 (0.01)	143.9 (9.1)	22.4 (33.2)	12.27 (0.10)	0.741 (0.009)	181.1 (2.4)
SN 2001en	14.72	2.18 (0.03)	1.64 (0.01)	163.3 (9.3)	26.8 (33.3)	11.79 (0.10)	0.737 (0.007)	198.8 (2.4)
SN 2001ep	2.83	3.71 (0.02)	3.58 (0.02)	118.2 (8.0)	10.4 (33.0)	10.27 (0.10)	0.707 (0.002)	159.9 (2.4)
SN 2001ep	4.99	3.19 (0.06)	3.41 (0.05)	113.4 (11.2)	2.8 (33.9)	9.83 (0.10)	0.710 (0.003)	160.0 (1.2)
SN 2001ep	5.97	3.09 (0.03)	3.35 (0.05)	115.7 (11.5)	3.4 (34.0)	9.83 (0.10)	0.732 (0.001)	158.0 (1.2)
SN 2001ep	7.85	2.97 (0.02)	3.23 (0.02)	104.8 (7.4)	-11.2 (32.8)	9.78 (0.10)	0.666 (0.001)	157.9 (2.4)
SN 2001ex	−1.82	0.40 (0.01)	0.39 (0.01)	124.2 (8.6)	18.9 (33.1)	9.70 (0.10)	0.813 (0.008)	144.2 (2.4)
SN 2001fe	−0.99	4.92 (0.03)	3.77 (0.01)	68.9 (5.2)	-36.5 (32.4)	11.10 (0.10)	0.536 (0.004)	124.3 (2.4)
SN 2001fh	5.93	0.90 (0.01)	0.87 (0.01)	121.6 (8.1)	9.4 (33.0)	10.17 (0.10)	0.717 (0.005)	167.8 (2.4)
SN 2002aw	2.10	1.23 (0.03)	1.08 (0.02)	96.2 (7.1)	-10.8 (32.8)	10.40 (0.12)	0.655 (0.007)	148.1 (2.4)
SN 2002bf	2.97	1.88 (0.01)	1.64 (0.00)	170.9 (10.2)	63.0 (33.6)	15.19 (0.10)	0.774 (0.002)	216.8 (2.4)
SN 2002bo	−11.94	2.23 (0.07)	2.39 (0.02)	139.6 (8.2)	23.0 (33.0)	17.83 (0.10)	0.609 (0.008)	233.0 (2.4)
SN 2002bo	−1.08	12.95 (0.59)	13.06 (0.18)	149.2 (8.9)	43.9 (33.2)	13.88 (0.10)	0.711 (0.008)	213.1 (2.4)
SN 2002bo	15.99	9.38 (0.25)	8.28 (0.06)	165.2 (8.9)	23.8 (33.2)	9.69 (0.10)	0.662 (0.008)	235.0 (2.4)
SN 2002bz	4.92	0.33 (0.01)	0.28 (0.01)	113.4 (7.8)	2.9 (32.9)	11.23 (0.10)	0.704 (0.005)	148.5 (2.4)
SN 2002cd	1.10	1.44 (0.03)	1.39 (0.02)	109.3 (7.3)	3.0 (32.8)	14.81 (0.10)	0.666 (0.010)	160.3 (2.4)
SN 2002cd	17.89	0.97 (0.02)	0.79 (0.01)	118.6 (7.4)	-30.9 (32.8)	14.51 (0.10)	0.658 (0.017)	170.2 (2.4)
SN 2002cf	−0.75	1.08 (0.01)	1.04 (0.01)	118.4 (7.6)	13.1 (32.9)	10.42 (0.10)	0.647 (0.004)	181.2 (2.4)
SN 2002ck	3.64	0.59 (0.01)	0.51 (0.01)	83.0 (6.4)	-25.8 (32.6)	10.43 (0.10)	0.643 (0.008)	126.2 (2.4)
SN 2002cr	−6.78	3.92 (0.04)	3.54 (0.02)	105.4 (6.9)	-2.5 (32.7)	10.58 (0.10)	0.604 (0.004)	174.3 (2.4)
SN 2002cs	−7.76	1.07 (0.02)	1.01 (0.01)	126.5 (7.8)	17.4 (32.9)	15.73 (0.10)	0.620 (0.002)	198.9 (2.4)
SN 2002cu	−5.28	0.90 (0.02)	0.85 (0.02)	141.3 (8.7)	34.8 (33.1)	12.34 (0.10)	0.614 (0.003)	237.4 (2.1)
SN 2002db	9.21	0.36 (0.01)	0.27 (0.02)	89.7 (6.9)	-29.6 (32.7)	11.72 (0.10)	0.702 (0.006)	115.8 (2.4)
SN 2002de	−0.32	0.83 (0.04)	0.68 (0.02)	99.5 (7.8)	-6.0 (32.9)	11.92 (0.10)	0.779 (0.013)	118.7 (2.4)
SN 2002de	8.37	0.72 (0.01)	0.63 (0.01)	86.6 (7.0)	-30.6 (32.7)	11.07 (0.10)	0.722 (0.005)	114.8 (2.4)
SN 2002dj	−7.98	3.42 (0.06)	3.89 (0.04)	138.8 (8.3)	29.4 (33.0)	15.90 (0.10)	0.655 (0.005)	210.0 (2.4)
SN 2002dk	−1.23	0.27 (0.01)	0.31 (0.01)	115.5 (7.1)	10.2 (32.8)	11.31 (0.10)	0.587 (0.007)	212.1 (2.4)
SN 2002dp	15.55	3.57 (0.03)	3.04 (0.01)	179.2 (8.9)	39.5 (33.2)	9.29 (0.10)	0.651 (0.003)	274.8 (2.4)
SN 2002eb	1.68	1.07 (0.01)	0.88 (0.01)	71.2 (5.5)	-35.4 (32.4)	9.95 (0.10)	0.565 (0.003)	118.7 (2.4)
SN 2002ef	4.70	1.00 (0.02)	0.88 (0.02)	110.6 (7.9)	0.5 (32.9)	11.58 (0.10)	0.734 (0.003)	144.5 (2.4)
SN 2002el	11.82	0.66 (0.01)	0.45 (0.01)	134.5 (7.8)	7.9 (32.9)	10.39 (0.10)	0.648 (0.006)	176.9 (2.4)
SN 2002er	−4.58	4.71 (0.07)	4.38 (0.03)	110.1 (7.4)	4.1 (32.8)	12.24 (0.10)	0.678 (0.001)	154.7 (2.4)
SN 2002eu	−0.06	0.53 (0.01)	0.49 (0.01)	125.2 (7.9)	19.6 (32.9)	11.07 (0.10)	0.653 (0.005)	181.2 (2.4)
SN 2002eu	9.38	0.23 (0.01)	0.23 (0.00)	115.7 (7.3)	-3.9 (32.8)	9.94 (0.10)	0.638 (0.014)	181.2 (2.4)
SN 2002fb	0.98	0.89 (0.01)	0.76 (0.01)	105.1 (7.2)	-1.1 (32.8)	10.83 (0.10)	0.664 (0.002)	155.6 (2.4)
SN 2002fk	7.74	14.13 (0.09)	10.40 (0.07)	95.6 (6.5)	-20.2 (32.6)	9.51 (0.10)	0.661 (0.004)	121.1 (2.4)
SN 2002ha	−0.85	3.36 (0.04)	2.94 (0.02)	105.8 (7.1)	0.5 (32.7)	10.96 (0.10)	0.650 (0.006)	151.9 (2.4)
SN 2002ha	4.93	3.43 (0.06)	2.85 (0.03)	108.3 (7.5)	-2.3 (32.8)	10.68 (0.10)	0.707 (0.003)	145.9 (2.4)
SN 2002ha	7.89	7.72 (0.12)	5.41 (0.03)	116.0 (7.3)	-0.1 (32.8)	10.87 (0.10)	0.675 (0.007)	145.9 (2.4)
SN 2002hd	6.48	0.86 (0.01)	0.66 (0.01)	122.7 (7.6)	9.5 (32.9)	10.42 (0.10)	0.663 (0.004)	168.1 (2.4)
SN 2002hd	12.72	0.41 (0.02)	0.34 (0.02)	169.3 (11.8)	39.9 (34.1)	9.69 (0.10)	0.607 (0.013)	342.0 (1.2)
SN 2002he	−1.03	1.60 (0.03)	1.37 (0.03)	119.9 (11.2)	14.6 (33.9)	12.68 (0.10)	0.691 (0.004)	173.0 (1.2)
SN 2002he	0.29	1.36 (0.01)	1.17 (0.01)	121.4 (8.2)	15.7 (33.0)	12.51 (0.10)	0.699 (0.002)	171.8 (2.4)
SN 2002he	3.22	2.80 (0.02)	2.39 (0.02)	121.2 (8.2)	13.0 (33.0)	12.32 (0.10)	0.707 (0.002)	171.8 (2.4)
SN 2002hu	−5.81	0.41 (0.01)	0.35 (0.00)	59.0 (4.0)	-47.9 (32.2)	10.44 (0.10)	0.400 (0.003)	137.0 (2.4)
SN 2002hw	−6.27	0.95 (0.01)	0.89 (0.01)	93.5 (6.4)	-13.9 (32.6)	11.79 (0.10)	0.593 (0.003)	147.4 (2.4)
SN 2002jg	10.11	0.67 (0.02)	0.64 (0.02)	145.1 (8.2)	23.5 (33.0)	...	...	...
SN 2002jy	11.86	1.18 (0.02)	0.73 (0.01)	107.9 (7.3)	-18.8 (32.8)	10.59 (0.10)	0.684 (0.009)	131.4 (2.4)
SN 2002kf	6.81	2.11 (0.02)	1.73 (0.01)	119.5 (7.9)	5.6 (32.9)	10.79 (0.10)	0.701 (0.002)	160.9 (2.4)
SN 2003D	9.98	0.75 (0.01)	0.88 (0.01)	119.0 (7.4)	-2.2 (32.8)	10.44 (0.10)	0.629 (0.003)	180.0 (2.4)
SN 2003K	13.43	0.75 (0.02)	0.52 (0.01)	64.6 (4.9)	-67.2 (32.3)	11.91 (0.10)	0.534 (0.016)	103.7 (2.4)
SN 2003U	−2.55	0.65 (0.01)	0.59 (0.01)	124.4 (8.1)	19.2 (33.0)	10.92 (0.10)	0.688 (0.003)	179.3 (2.4)
SN 2003W	−5.06	0.53 (0.01)	0.61 (0.01)	152.3 (8.4)	46.0 (33.1)	18.35 (0.10)	0.587 (0.004)	258.8 (2.4)
SN 2003W	18.14	1.44 (0.02)	1.34 (0.01)	162.0 (8.1)	11.4 (33.0)	12.62 (0.10)	0.548 (0.004)	286.3 (2.4)
SN 2003Y	−1.74	0.49 (0.01)	0.43 (0.01)	96.2 (6.3)	-9.0 (32.6)	...	...	...
SN 2003ai	7.25	0.59 (0.02)	0.54 (0.02)	67.6 (5.4)	-47.1 (32.4)	9.84 (0.10)	0.576 (0.005)	112.1 (2.4)
SN 2003cq	−0.15	0.38 (0.01)	0.34 (0.01)	120.2 (8.1)	14.6 (33.0)	12.46 (0.10)	0.686 (0.005)	180.0 (2.4)
SN 2003gn	−5.38	0.14 (0.01)	0.14 (0.00)	147.8 (9.1)	41.2 (33.2)	13.66 (0.10)	0.712 (0.017)	210.7 (2.4)
SN 2003gt	−5.07	2.12 (0.03)	1.93 (0.02)	75.8 (5.4)	-30.5 (32.4)	11.34 (0.10)	0.543 (0.005)	133.9 (2.4)
SN 2003gt	17.61	1.29 (0.01)	1.45 (0.01)	70.7 (5.2)	-77.6 (32.4)	10.74 (0.10)	0.523 (0.012)	137.8 (2.4)
SN 2003he	2.71	1.25 (0.02)	1.02 (0.01)	102.1 (7.5)	-5.5 (32.8)	11.35 (0.10)	0.727 (0.004)	138.5 (2.4)
SN 2003he	8.54	0.98 (0.02)	0.63 (0.01)	105.9 (7.0)	-11.7 (32.7)	11.27 (0.10)	0.656 (0.005)	142.4 (2.4)
SN 2003iv	1.76	0.02 (0.00)	0.01 (0.00)	109.4 (7.7)	2.7 (32.9)	11.25 (0.10)	0.705 (0.008)	150.8 (2.4)
SN 2003iv	6.58	0.16 (0.01)	0.14 (0.00)	108.9 (7.4)	-4.5 (32.8)	10.77 (0.10)	0.654 (0.003)	156.6 (2.4)
SN 2003kf	−7.50	5.44 (0.10)	5.29 (0.05)	72.4 (4.8)	-36.3 (32.3)	12.39 (0.10)	0.469 (0.007)	137.0 (2.4)
SN 2004E	5.26	1.33 (0.01)	1.00 (0.01)	92.4 (7.0)	-18.6 (32.7)	11.01 (0.10)	0.714 (0.004)	120.4 (2.4)
SN 2004S	8.26	4.18 (0.01)	4.19 (0.00)	62.2 (4.8)	-54.7 (32.3)	9.08 (0.10)	0.505 (0.002)	118.9 (2.4)
SN 2004as	−4.36	0.46 (0.00)	0.44 (0.00)	131.5 (8.0)	25.6 (33.0)	12.29 (0.10)	0.637 (0.001)	205.6 (2.4)
SN 2004bd	10.76	2.39 (0.04)	2.46 (0.02)	142.8 (8.3)	19.4 (33.0)	11.37 (0.10)	0.623 (0.001)	224.0 (2.4)
SN 2004bg	10.34	1.59 (0.01)	1.08 (0.01)	114.1 (7.3)	-8.1 (32.8)	9.96 (0.10)	0.663 (0.004)	145.0 (2.4)
SN 2004bk	6.13	1.75 (0.03)	1.28 (0.01)	102.6 (6.9)	-10.0 (32.7)	11.62 (0.10)	0.719 (0.006)	113.4 (2.4)
SN 2004bl	4.61	1.66 (0.03)	1.41 (0.02)	94.7 (6.9)	-15.3 (32.7)	10.68 (0.10)	0.672 (0.004)	137.6 (2.4)
SN 2004bl	19.38	1.86 (0.02)	1.15 (0.02)	137.7 (7.8)	-18.7 (32.9)	9.63 (0.10)	0.641 (0.006)	202.5 (2.4)
SN 2004br	3.50	1.89 (0.03)	1.44 (0.03)	41.5 (3.6)	-67.1 (32.2)	11.34 (0.10)	0.408 (0.007)	101.6 (2.4)
SN 2004bv	−7.06	4.27 (0.05)	3.55 (0.06)	36.1 (2.3)	-72.1 (32.1)	9.86 (0.10)	0.199 (0.005)	201.9 (2.4)
SN 2004bv	9.77	7.40 (0.08)	5.75 (0.04)	72.5 (5.2)	-48.1 (32.4)	9.19 (0.10)	0.562 (0.007)	112.8 (2.4)
SN 2004bw	−10.03	0.18 (0.01)	0.18 (0.01)	117.5 (7.5)	4.9 (32.8)	13.16 (0.10)	0.639 (0.014)	182.1 (2.4)

Continued on Next Page...

Table 3.12 — Continued

SN Name	Phase[a]	F_b[b]	F_r[b]	pEW[c]	ΔpEW[c,d]	v[e]	a	FWHM[c]
SN 2004bw	6.59	1.18 (0.01)	0.90 (0.01)	119.7 (8.1)	6.3 (33.0)	11.15 (0.10)	0.702 (0.005)	164.5 (2.4)
SN 2004dt	−6.46	1.68 (0.02)	1.57 (0.02)	176.0 (10.1)	68.4 (33.5)	15.92 (0.10)	0.703 (0.003)	251.0 (2.4)
SN 2004dt	1.38	2.59 (0.02)	2.39 (0.01)	178.0 (6.7)	71.6 (32.7)	14.34 (0.10)	0.750 (0.002)	235.4 (6.0)
SN 2004dt	18.00	1.71 (0.02)	1.39 (0.02)	198.2 (9.8)	48.1 (33.4)	9.86 (0.10)	0.730 (0.002)	239.3 (2.4)
SN 2004ef	−5.52	0.39 (0.01)	0.38 (0.01)	132.9 (7.9)	26.2 (32.9)	13.42 (0.10)	0.609 (0.003)	219.2 (2.4)
SN 2004ef	8.05	0.58 (0.02)	0.42 (0.01)	133.0 (8.3)	16.6 (33.0)	11.89 (0.10)	0.695 (0.008)	172.7 (2.4)
SN 2004eo	−5.57	1.06 (0.01)	0.99 (0.01)	103.2 (6.7)	-3.5 (32.7)	11.35 (0.10)	0.592 (0.005)	163.4 (2.4)
SN 2004eo	13.19	0.61 (0.01)	0.83 (0.01)	72.4 (5.1)	-58.6 (32.4)	...	...	...
SN 2004ey	−7.58	2.05 (0.01)	1.89 (0.01)	80.4 (5.5)	-28.5 (32.4)	11.77 (0.10)	0.529 (0.001)	135.9 (2.4)
SN 2004fu	−2.65	3.96 (0.04)	3.79 (0.03)	128.6 (8.2)	23.3 (33.0)	12.92 (0.10)	0.673 (0.004)	192.2 (2.4)
SN 2004fu	2.43	3.79 (0.03)	3.60 (0.02)	134.8 (8.7)	27.4 (33.1)	11.85 (0.10)	0.708 (0.002)	192.2 (2.4)
SN 2004fz	−5.18	2.36 (0.02)	2.22 (0.01)	91.6 (6.4)	-14.8 (32.6)	10.67 (0.10)	0.613 (0.002)	141.5 (2.4)
SN 2004gs	0.44	0.56 (0.01)	0.56 (0.00)	130.8 (8.4)	24.9 (33.1)	10.73 (0.10)	0.677 (0.005)	196.8 (2.4)
SN 2005A	5.55	0.29 (0.02)	0.29 (0.00)	128.9 (8.1)	17.4 (33.0)	14.76 (0.10)	0.655 (0.018)	196.2 (2.4)
SN 2005M	8.23	0.35 (0.01)	0.25 (0.00)	64.8 (6.5)	-52.1 (32.6)	8.06 (0.10)	0.491 (0.003)	124.0 (1.2)
SN 2005M	9.23	1.11 (0.01)	0.79 (0.01)	69.7 (4.8)	-49.5 (32.3)	7.97 (0.10)	0.497 (0.005)	123.3 (2.4)
SN 2005W	0.59	2.95 (0.05)	2.76 (0.06)	109.3 (10.7)	3.4 (33.7)	10.85 (0.10)	0.702 (0.003)	157.0 (1.2)
SN 2005ag	0.53	0.03 (0.00)	0.02 (0.00)	82.1 (6.2)	-23.8 (32.6)	10.60 (0.10)	0.579 (0.007)	135.4 (2.3)
SN 2005am	4.47	11.40 (0.07)	9.76 (0.03)	119.2 (7.7)	9.4 (32.9)	11.47 (0.10)	0.686 (0.002)	162.7 (2.4)
SN 2005am	6.37	10.87 (0.03)	8.67 (0.01)	119.2 (4.9)	6.2 (32.3)	11.35 (0.10)	0.683 (0.004)	163.7 (6.1)
SN 2005ao	−1.29	0.51 (0.01)	0.39 (0.01)	69.1 (5.7)	-36.2 (32.5)	11.41 (0.10)	0.593 (0.005)	115.6 (2.4)
SN 2005ao	0.52	0.38 (0.01)	0.29 (0.00)	76.2 (5.9)	-29.7 (32.5)	11.68 (0.10)	0.617 (0.011)	117.5 (2.4)
SN 2005bc	1.55	1.92 (0.01)	1.82 (0.01)	115.3 (7.7)	8.7 (32.9)	10.91 (0.10)	0.686 (0.001)	164.0 (2.4)
SN 2005bc	7.37	1.73 (0.02)	1.50 (0.02)	124.4 (7.9)	9.4 (32.9)	10.54 (0.10)	0.709 (0.005)	164.0 (2.4)
SN 2005be	10.96	0.26 (0.00)	0.21 (0.00)	115.1 (6.8)	-8.9 (32.7)	10.79 (0.10)	0.573 (0.006)	166.2 (2.4)
SN 2005cf	−10.94	2.85 (0.03)	3.08 (0.02)	141.5 (7.9)	27.1 (32.9)	16.81 (0.10)	0.538 (0.003)	262.3 (2.4)
SN 2005cf	−2.11	87.99 (0.47)	75.21 (0.42)	85.1 (5.9)	-20.1 (32.5)	10.36 (0.10)	0.569 (0.001)	137.1 (2.4)
SN 2005cf	−1.19	18.71 (0.12)	16.71 (0.12)	85.3 (6.0)	-20.0 (32.5)	10.26 (0.10)	0.586 (0.001)	135.1 (2.4)
SN 2005de	−0.75	1.88 (0.03)	1.76 (0.03)	102.8 (7.1)	-2.6 (32.7)	10.91 (0.10)	0.666 (0.005)	145.8 (2.4)
SN 2005de	10.10	1.75 (0.01)	1.34 (0.01)	122.4 (7.5)	0.9 (32.8)	10.15 (0.10)	0.670 (0.004)	149.7 (2.4)
SN 2005dm	5.23	0.45 (0.01)	0.51 (0.01)	162.2 (8.3)	51.2 (33.0)	9.00 (0.10)	0.595 (0.002)	275.4 (2.4)
SN 2005dv	−0.57	1.15 (0.05)	1.11 (0.02)	146.5 (8.9)	41.0 (33.2)	12.39 (0.10)	0.734 (0.008)	199.9 (2.4)
SN 2005el	−6.70	1.60 (0.01)	1.41 (0.01)	67.7 (4.6)	-40.1 (32.3)	11.80 (0.10)	0.444 (0.003)	141.9 (2.4)
SN 2005el	1.22	2.87 (0.03)	2.41 (0.02)	91.6 (6.5)	-14.8 (32.6)	10.93 (0.10)	0.609 (0.002)	145.8 (2.4)
SN 2005el	8.09	2.55 (0.02)	1.80 (0.01)	104.0 (6.7)	-12.6 (32.7)	10.84 (0.10)	0.630 (0.004)	143.9 (2.4)
SN 2005er	−0.26	0.00 (0.00)	0.00 (0.00)	134.3 (10.2)	28.7 (33.6)	10.08 (0.10)	0.597 (0.004)	200.0 (1.2)
SN 2005er	1.67	0.15 (0.00)	0.17 (0.00)	152.1 (7.7)	45.5 (32.9)	9.64 (0.10)	0.585 (0.002)	253.4 (2.4)
SN 2005eq	−2.98	0.75 (0.01)	0.61 (0.00)	46.6 (3.2)	-58.8 (32.1)	9.81 (0.10)	0.321 (0.003)	132.2 (2.4)
SN 2005eq	0.66	0.93 (0.01)	0.73 (0.00)	48.1 (3.9)	-57.9 (32.2)	9.53 (0.10)	0.412 (0.003)	112.7 (2.4)
SN 2005ew	18.23	3.98 (0.02)	2.72 (0.01)	82.0 (5.6)	-69.1 (32.5)	12.14 (0.10)	0.519 (0.005)	153.5 (2.4)
SN 2005eu	−9.06	0.24 (0.00)	0.20 (0.00)	35.7 (2.5)	-75.3 (32.1)	11.81 (0.10)	0.226 (0.003)	150.7 (2.4)
SN 2005eu	−5.46	0.47 (0.01)	0.36 (0.01)	55.5 (4.0)	-51.1 (32.2)	11.90 (0.10)	0.380 (0.004)	146.9 (2.4)
SN 2005hj	7.51	0.44 (0.01)	0.36 (0.01)	49.1 (5.7)	-66.2 (32.5)	10.43 (0.10)	0.454 (0.007)	104.0 (1.2)
SN 2005iq	−5.86	6.57 (0.09)	5.91 (0.08)	91.5 (8.7)	-15.5 (33.1)	11.54 (0.10)	0.573 (0.003)	153.0 (1.2)
SN 2005kc	10.28	0.09 (0.00)	0.09 (0.00)	75.9 (8.2)	-46.1 (33.0)	9.97 (0.10)	0.576 (0.005)	131.0 (1.2)
SN 2005kc	12.25	1.56 (0.02)	1.70 (0.01)	75.5 (5.5)	-52.4 (32.4)	10.29 (0.10)	0.529 (0.012)	137.9 (2.4)
SN 2005ki	1.62	8.18 (0.06)	7.02 (0.04)	104.7 (10.1)	-1.9 (33.5)	11.23 (0.10)	0.669 (0.001)	152.0 (1.2)
SN 2005ki	8.35	1.78 (0.04)	1.21 (0.03)	116.5 (7.3)	-0.6 (32.8)	11.07 (0.10)	0.661 (0.009)	155.0 (2.4)
SN 2005mc	6.64	0.60 (0.01)	0.63 (0.01)	107.0 (6.8)	-6.5 (32.7)	10.50 (0.10)	0.567 (0.009)	183.4 (2.4)
SN 2005lz	0.58	5.50 (0.11)	4.87 (0.09)	107.1 (10.3)	1.2 (33.6)	10.43 (0.10)	0.677 (0.004)	154.0 (1.2)
SN 2005ms	−1.88	2.72 (0.05)	2.36 (0.05)	117.3 (7.6)	12.1 (32.9)	11.17 (0.10)	0.646 (0.005)	181.4 (2.4)
SN 2005ms	14.62	0.71 (0.01)	0.49 (0.01)	144.1 (8.4)	8.0 (33.0)	9.27 (0.10)	0.682 (0.005)	185.3 (2.4)
SN 2005na	0.03	0.90 (0.02)	0.72 (0.01)	71.3 (5.4)	-34.3 (32.4)	10.92 (0.10)	0.542 (0.011)	126.7 (2.4)
SN 2005na	1.03	1.00 (0.04)	0.89 (0.02)	70.0 (5.6)	-36.2 (32.5)	10.63 (0.10)	0.574 (0.006)	120.8 (2.4)
SN 2006D	3.70	15.29 (0.05)	13.04 (0.05)	101.0 (6.9)	-7.8 (32.7)	10.88 (0.10)	0.652 (0.003)	150.7 (2.4)
SN 2006H	7.01	0.28 (0.01)	0.39 (0.01)	104.5 (7.0)	-9.8 (32.7)	10.34 (0.10)	0.611 (0.005)	171.6 (2.4)
SN 2006N	−1.89	2.36 (0.02)	2.13 (0.02)	96.5 (6.4)	-8.7 (32.6)	11.22 (0.10)	0.587 (0.002)	157.7 (2.4)
SN 2006N	−0.90	1.97 (0.01)	1.72 (0.02)	111.7 (7.5)	6.4 (32.8)	11.42 (0.10)	0.685 (0.002)	155.8 (2.4)
SN 2006N	11.91	1.31 (0.02)	0.96 (0.02)	118.0 (7.3)	-8.9 (32.8)	10.17 (0.10)	0.617 (0.004)	163.7 (2.4)
SN 2006S	−3.93	8.98 (0.27)	7.35 (0.15)	56.9 (3.9)	-48.8 (32.2)	10.72 (0.10)	0.374 (0.005)	137.6 (2.4)
SN 2006S	2.99	0.58 (0.01)	0.45 (0.01)	74.4 (5.7)	-33.6 (32.5)	10.53 (0.10)	0.592 (0.003)	114.3 (2.4)
SN 2006S	18.45	0.25 (0.01)	0.25 (0.00)	52.7 (4.3)	-99.4 (32.3)	9.94 (0.10)	0.493 (0.015)	95.0 (2.4)
SN 2006X	3.15	9.64 (0.07)	10.56 (0.07)	173.9 (10.2)	65.8 (33.6)	15.26 (0.10)	0.784 (0.002)	212.9 (2.4)
SN 2006ac	7.96	1.42 (0.01)	1.06 (0.01)	150.5 (9.7)	34.3 (33.4)	12.38 (0.10)	0.786 (0.004)	185.7 (2.4)
SN 2006ak	8.43	0.44 (0.00)	0.36 (0.00)	98.8 (6.5)	-18.5 (32.6)	10.84 (0.10)	0.571 (0.004)	169.5 (2.4)
SN 2006ax	−10.07	0.66 (0.01)	0.58 (0.00)	87.1 (5.5)	-25.6 (32.4)	12.14 (0.10)	0.487 (0.002)	169.2 (2.4)
SN 2006bq	6.97	4.38 (0.03)	3.61 (0.03)	158.4 (9.6)	44.2 (33.4)	13.94 (0.10)	0.741 (0.002)	217.2 (2.4)
SN 2006bq	14.55	0.97 (0.01)	0.73 (0.01)	156.9 (9.6)	21.1 (33.4)	12.02 (0.10)	0.755 (0.006)	207.5 (2.4)
SN 2006bq	14.64	0.78 (0.01)	0.51 (0.01)	164.0 (10.3)	27.8 (33.6)	12.50 (0.10)	0.835 (0.009)	195.7 (2.4)
SN 2006br	10.62	0.22 (0.01)	0.20 (0.01)	142.0 (9.0)	19.0 (33.2)	12.42 (0.10)	0.759 (0.011)	197.2 (2.4)
SN 2006bt	−5.30	0.37 (0.00)	0.34 (0.00)	110.5 (6.8)	4.0 (32.7)	11.48 (0.10)	0.547 (0.001)	197.6 (2.4)
SN 2006bt	−4.53	0.35 (0.00)	0.33 (0.00)	111.1 (6.9)	5.1 (32.7)	12.05 (0.10)	0.568 (0.005)	189.9 (2.4)
SN 2006bt	2.27	0.36 (0.00)	0.34 (0.00)	128.1 (8.0)	20.9 (33.0)	10.53 (0.10)	0.650 (0.002)	191.8 (2.4)
SN 2006bu	4.22	0.11 (0.00)	0.08 (0.00)	82.9 (6.4)	-26.6 (32.6)	10.91 (0.10)	0.602 (0.005)	134.7 (2.3)
SN 2006bw	8.90	0.35 (0.00)	0.35 (0.00)	136.3 (8.5)	17.9 (33.1)	10.38 (0.10)	0.675 (0.002)	203.9 (2.4)
SN 2006bz	−2.44	0.28 (0.01)	0.24 (0.01)	102.0 (7.1)	-3.2 (32.8)	11.29 (0.10)	0.666 (0.005)	151.8 (2.4)
SN 2006cf	6.28	0.27 (0.02)	0.24 (0.01)	85.8 (5.9)	-27.0 (32.5)	9.30 (0.10)	0.595 (0.014)	134.4 (2.4)
SN 2006cf	11.09	0.44 (0.01)	0.29 (0.00)	119.2 (7.2)	-5.1 (32.8)	10.43 (0.10)	0.653 (0.005)	149.8 (2.4)
SN 2006cj	3.43	0.14 (0.00)	0.11 (0.00)	67.6 (5.7)	-40.8 (32.5)	11.04 (0.10)	0.590 (0.006)	116.2 (2.3)
SN 2006cm	−1.15	0.62 (0.01)	0.53 (0.01)	44.9 (3.6)	-60.4 (32.2)	11.35 (0.10)	0.389 (0.007)	116.1 (2.4)
SN 2006cm	6.77	0.47 (0.01)	0.38 (0.01)	49.6 (4.0)	-64.1 (32.2)	11.45 (0.10)	0.492 (0.005)	86.6 (2.4)
SN 2006cp	−5.30	0.91 (0.01)	0.87 (0.01)	157.2 (9.2)	50.8 (33.3)	14.73 (0.10)	0.696 (0.004)	232.8 (2.4)

Continued on Next Page...

Table 3.12 — Continued

SN Name	Phase[a]	F_b[b]	F_r[b]	pEW[c]	ΔpEW[c,d]	v[e]	a	FWHM[c]
SN 2006cq	2.00	0.26 (0.00)	0.22 (0.00)	96.6 (6.8)	-10.3 (32.7)	9.95 (0.10)	0.662 (0.006)	137.4 (2.3)
SN 2006cs	2.28	0.28 (0.00)	0.23 (0.00)	94.4 (6.6)	-12.8 (32.6)	11.01 (0.10)	0.625 (0.004)	138.7 (2.4)
SN 2006cz	1.12	0.37 (0.01)	0.30 (0.00)	56.2 (4.1)	-50.1 (32.2)	12.19 (0.10)	0.413 (0.006)	124.8 (2.4)
SN 2006dm	8.73	1.07 (0.01)	0.79 (0.01)	124.8 (7.8)	6.7 (32.9)	10.34 (0.10)	0.659 (0.003)	178.1 (2.4)
SN 2006dm	14.61	0.70 (0.01)	0.60 (0.01)	170.0 (8.9)	33.9 (33.2)	9.57 (0.10)	0.662 (0.005)	254.4 (2.4)
SN 2006ef	3.20	1.95 (0.01)	1.78 (0.01)	135.2 (8.7)	27.1 (33.1)	11.70 (0.10)	0.701 (0.002)	192.6 (2.4)
SN 2006gr	−8.70	0.23 (0.00)	0.22 (0.00)	74.9 (4.4)	-35.5 (32.3)	17.63 (0.10)	0.308 (0.003)	264.8 (2.4)
SN 2006ej	−3.70	1.36 (0.01)	1.25 (0.00)	108.3 (7.3)	2.7 (32.8)	12.45 (0.10)	0.626 (0.003)	170.5 (2.4)
SN 2006ej	5.09	1.01 (0.01)	0.87 (0.01)	129.8 (8.4)	19.0 (33.0)	11.64 (0.10)	0.695 (0.003)	178.4 (2.4)
SN 2006en	8.55	0.42 (0.01)	0.37 (0.01)	68.5 (6.0)	-49.1 (32.5)	10.65 (0.10)	0.679 (0.007)	102.7 (2.4)
SN 2006et	3.29	1.21 (0.01)	1.04 (0.01)	73.3 (5.3)	-34.9 (32.4)	9.43 (0.10)	0.524 (0.003)	133.1 (2.4)
SN 2006et	9.14	0.90 (0.03)	0.68 (0.01)	80.3 (5.5)	-38.8 (32.4)	9.34 (0.10)	0.569 (0.009)	115.4 (2.4)
SN 2006eu	10.17	0.27 (0.01)	0.36 (0.00)	172.4 (9.4)	50.6 (33.3)	10.88 (0.10)	0.679 (0.008)	263.8 (2.4)
SN 2006eu	16.02	0.20 (0.00)	0.29 (0.00)	191.2 (9.9)	49.7 (33.5)	8.79 (0.10)	0.673 (0.006)	298.9 (2.4)
SN 2006ev	10.54	0.50 (0.01)	0.37 (0.02)	125.8 (8.4)	3.0 (33.0)	11.82 (0.10)	0.694 (0.011)	184.7 (2.4)
SN 2006ev	16.36	0.33 (0.03)	0.27 (0.01)	139.3 (8.5)	-3.7 (33.1)	11.34 (0.10)	0.685 (0.004)	192.5 (2.4)
SN 2006gj	4.70	0.25 (0.01)	0.27 (0.00)	119.0 (8.0)	8.8 (33.0)	10.25 (0.10)	0.701 (0.009)	167.3 (2.4)
SN 2006gt	3.08	0.19 (0.00)	0.18 (0.00)	119.5 (8.0)	11.5 (33.0)	10.32 (0.10)	0.720 (0.004)	162.7 (2.3)
SN 2006ke	2.36	0.15 (0.00)	0.16 (0.00)	66.1 (4.4)	-41.2 (32.3)	9.38 (0.10)	0.411 (0.002)	159.3 (2.4)
SN 2006ke	8.38	0.12 (0.00)	0.15 (0.00)	89.8 (5.7)	-27.4 (32.5)	8.71 (0.10)	0.515 (0.010)	184.8 (2.4)
SN 2006kf	−8.96	0.26 (0.00)	0.24 (0.00)	127.6 (7.6)	16.8 (32.9)	12.81 (0.10)	0.624 (0.004)	197.8 (2.4)
SN 2006kf	−3.05	0.69 (0.01)	0.68 (0.00)	114.6 (7.4)	9.3 (32.8)	11.56 (0.10)	0.653 (0.001)	162.5 (2.4)
SN 2006lf	−6.30	0.43 (0.00)	0.43 (0.00)	95.2 (6.5)	-12.2 (32.6)	11.49 (0.10)	0.599 (0.002)	157.9 (2.4)
SN 2006lf	14.29	0.32 (0.01)	0.45 (0.01)	91.5 (6.5)	-43.4 (32.6)	10.22 (0.10)	0.604 (0.010)	150.0 (2.4)
SN 2006le	−8.69	0.52 (0.01)	0.52 (0.00)	82.0 (4.5)	-28.4 (32.3)	...	...	...
SN 2006le	11.92	1.14 (0.01)	0.81 (0.01)	100.9 (6.7)	-26.0 (32.7)	10.81 (0.10)	0.640 (0.004)	137.6 (2.4)
SN 2006mo	12.46	0.24 (0.00)	0.24 (0.00)	103.8 (5.8)	-24.8 (32.5)	10.99 (0.10)	0.481 (0.006)	190.9 (2.4)
SN 2006mp	5.66	1.02 (0.01)	0.74 (0.01)	49.4 (4.0)	-62.4 (32.2)	9.43 (0.10)	0.444 (0.004)	109.1 (2.4)
SN 2006or	−2.79	0.78 (0.03)	0.71 (0.01)	110.0 (7.2)	4.7 (32.8)	11.01 (0.10)	0.616 (0.008)	168.5 (2.4)
SN 2006or	4.93	0.31 (0.01)	0.28 (0.00)	104.7 (6.5)	-5.8 (32.6)	11.39 (0.10)	0.550 (0.004)	176.3 (2.4)
SN 2006os	8.61	0.27 (0.01)	0.25 (0.01)	129.3 (8.6)	11.5 (33.1)	11.10 (0.10)	0.746 (0.003)	178.2 (2.4)
SN 2006sr	−2.34	0.75 (0.01)	0.69 (0.00)	109.2 (7.2)	4.0 (32.8)	12.39 (0.10)	0.623 (0.002)	171.9 (2.4)
SN 2006sr	2.69	1.16 (0.01)	1.02 (0.01)	111.3 (7.6)	3.6 (32.9)	11.62 (0.10)	0.660 (0.002)	167.9 (2.4)
SN 2007A	2.37	2.02 (0.02)	1.73 (0.01)	88.8 (6.4)	-18.4 (32.6)	10.78 (0.10)	0.619 (0.002)	137.6 (2.4)
SN 2007A	15.07	1.39 (0.01)	0.95 (0.01)	115.1 (6.9)	-22.7 (32.7)	10.49 (0.10)	0.632 (0.005)	139.5 (2.4)
SN 2007F	−9.35	0.63 (0.01)	0.59 (0.00)	67.4 (4.4)	-44.0 (32.3)	12.14 (0.10)	0.428 (0.002)	144.6 (2.4)
SN 2007F	3.23	1.32 (0.01)	1.06 (0.01)	85.8 (6.5)	-22.4 (32.6)	11.08 (0.10)	0.657 (0.003)	123.1 (2.4)
SN 2007O	−0.33	11.47 (0.14)	9.34 (0.11)	79.2 (7.7)	-26.3 (32.9)	9.96 (0.10)	0.543 (0.005)	130.0 (1.2)
SN 2007N	0.44	3.39 (0.04)	3.38 (0.04)	88.3 (8.0)	-17.5 (32.9)	11.19 (0.10)	0.506 (0.002)	171.0 (1.2)
SN 2007S	5.18	1.98 (0.02)	1.59 (0.02)	67.6 (4.8)	-43.3 (32.3)	10.24 (0.10)	0.502 (0.004)	124.3 (2.4)
SN 2007af	−1.25	17.40 (0.07)	16.11 (0.08)	107.3 (7.5)	2.1 (32.8)	11.02 (0.10)	0.694 (0.002)	149.2 (2.4)
SN 2007af	2.84	18.20 (0.07)	16.47 (0.05)	112.7 (11.2)	5.0 (33.9)	10.60 (0.10)	0.722 (0.002)	154.0 (1.2)
SN 2007af	3.81	17.08 (0.08)	16.56 (0.07)	105.0 (7.6)	-3.9 (32.9)	10.73 (0.10)	0.691 (0.002)	153.2 (2.4)
SN 2007aj	10.75	0.54 (0.01)	0.37 (0.00)	127.7 (7.7)	4.4 (32.9)	10.77 (0.10)	0.688 (0.006)	147.6 (2.4)
SN 2007al	3.39	0.63 (0.01)	0.59 (0.01)	70.8 (4.8)	-37.6 (32.3)	9.04 (0.10)	0.465 (0.006)	144.3 (2.4)
SN 2007ap	9.37	26.16 (0.21)	19.21 (0.14)	117.6 (10.4)	-2.0 (33.6)	10.67 (0.10)	0.649 (0.004)	164.0 (1.2)
SN 2007au	16.11	0.49 (0.01)	0.61 (0.02)	220.9 (10.7)	79.0 (33.7)	9.14 (0.10)	0.716 (0.003)	337.1 (2.4)
SN 2007ba	5.18	3.26 (0.05)	3.43 (0.05)	101.8 (9.2)	-9.1 (33.3)	10.11 (0.10)	0.583 (0.003)	168.0 (1.2)
SN 2007bc	0.61	1.47 (0.01)	1.32 (0.01)	101.0 (7.1)	-4.9 (32.8)	10.63 (0.10)	0.667 (0.003)	145.0 (2.4)
SN 2007bd	−5.79	0.43 (0.01)	0.42 (0.01)	98.0 (6.6)	-8.9 (32.6)	13.15 (0.10)	0.577 (0.005)	168.8 (2.4)
SN 2007bd	9.70	0.53 (0.03)	0.37 (0.01)	90.8 (6.7)	-29.6 (32.7)	11.16 (0.10)	0.627 (0.019)	143.5 (2.4)
SN 2007bj	14.25	2.57 (0.03)	1.34 (0.01)	105.2 (7.0)	-29.5 (32.7)	11.85 (0.10)	0.734 (0.012)	106.2 (2.4)
SN 2007bm	−7.79	5.32 (0.04)	5.26 (0.05)	89.0 (6.0)	-20.0 (32.5)	11.25 (0.10)	0.562 (0.003)	151.1 (2.4)
SN 2007bz	1.65	1.08 (0.02)	0.91 (0.01)	65.3 (5.2)	-41.4 (32.4)	12.07 (0.10)	0.554 (0.005)	113.5 (2.4)
SN 2007ca	−11.14	0.72 (0.02)	0.71 (0.02)	55.0 (3.7)	-59.8 (32.2)	12.71 (0.10)	0.341 (0.010)	147.9 (2.4)
SN 2007ca	16.46	1.33 (0.03)	0.85 (0.02)	123.8 (7.4)	-19.5 (32.8)	9.25 (0.10)	0.645 (0.014)	153.8 (2.4)
SN 2007cg	16.17	0.26 (0.01)	0.21 (0.01)	82.7 (5.1)	-59.5 (32.4)	12.44 (0.10)	0.445 (0.007)	170.3 (2.4)
SN 2007ci	−6.57	0.92 (0.02)	0.89 (0.01)	114.3 (7.6)	6.6 (32.9)	12.64 (0.10)	0.669 (0.003)	172.9 (2.4)
SN 2007ci	−1.71	1.31 (0.01)	1.23 (0.01)	119.8 (8.0)	14.5 (33.0)	11.58 (0.10)	0.688 (0.001)	172.9 (2.4)
SN 2007co	−4.09	0.63 (0.01)	0.58 (0.00)	124.2 (7.8)	18.5 (32.9)	11.59 (0.10)	0.646 (0.003)	185.0 (2.4)
SN 2007co	0.85	0.74 (0.01)	0.66 (0.01)	118.4 (7.8)	12.3 (32.9)	11.40 (0.10)	0.690 (0.001)	163.6 (2.4)
SN 2007co	9.55	0.70 (0.01)	0.51 (0.00)	131.1 (8.4)	11.0 (33.1)	11.02 (0.10)	0.729 (0.005)	163.6 (2.4)
SN 2007cq	−5.82	0.67 (0.01)	0.59 (0.01)	38.6 (2.7)	-68.3 (32.1)	10.90 (0.10)	0.272 (0.004)	150.1 (2.4)
SN 2007cq	7.84	1.48 (0.03)	1.07 (0.01)	65.5 (5.1)	-50.4 (32.4)	10.53 (0.10)	0.550 (0.006)	109.2 (2.4)
SN 2007fb	1.95	2.83 (0.03)	2.69 (0.03)	115.9 (7.8)	9.0 (32.9)	11.36 (0.10)	0.689 (0.004)	165.0 (2.4)
SN 2007fb	14.63	0.94 (0.01)	0.79 (0.01)	150.2 (8.0)	14.1 (33.0)	10.69 (0.10)	0.650 (0.005)	186.6 (2.4)
SN 2007fr	−5.83	0.12 (0.00)	0.11 (0.00)	111.9 (7.6)	5.0 (32.8)	11.82 (0.10)	0.675 (0.004)	165.6 (2.3)
SN 2007fr	−1.25	0.15 (0.00)	0.14 (0.00)	116.4 (7.9)	11.2 (32.9)	11.26 (0.10)	0.706 (0.011)	161.8 (2.3)
SN 2007fs	5.03	2.92 (0.02)	2.30 (0.01)	92.2 (7.0)	-18.5 (32.7)	10.36 (0.10)	0.689 (0.004)	129.8 (2.4)
SN 2007ge	12.53	0.15 (0.00)	0.17 (0.00)	72.6 (5.4)	-56.2 (32.4)	10.23 (0.10)	0.499 (0.012)	145.5 (2.3)
SN 2007gi	−7.31	16.24 (0.05)	16.75 (0.07)	180.2 (10.1)	71.7 (33.5)	18.40 (0.10)	0.713 (0.002)	250.8 (2.4)
SN 2007gi	−0.35	25.92 (0.14)	22.76 (0.05)	181.7 (10.3)	76.2 (33.6)	15.73 (0.10)	0.753 (0.001)	234.9 (2.4)
SN 2007gi	6.61	14.81 (0.07)	11.23 (0.06)	154.4 (9.5)	40.9 (33.4)	14.36 (0.10)	0.767 (0.005)	195.1 (2.4)
SN 2007gk	−1.72	0.73 (0.00)	0.71 (0.00)	165.1 (9.7)	59.9 (33.4)	14.07 (0.10)	0.719 (0.002)	233.8 (2.4)
SN 2007gk	19.65	0.34 (0.01)	0.36 (0.00)	214.5 (10.7)	56.7 (33.7)	11.10 (0.10)	0.713 (0.006)	315.6 (2.4)
SN 2007hj	−1.23	1.81 (0.01)	1.78 (0.01)	140.5 (8.8)	35.3 (33.1)	12.42 (0.10)	0.710 (0.005)	195.2 (2.4)
SN 2007hj	12.53	1.14 (0.01)	1.24 (0.01)	174.7 (9.2)	45.9 (33.3)	10.59 (0.10)	0.676 (0.002)	254.4 (2.4)
SN 2007kk	7.15	1.94 (0.03)	1.44 (0.02)	113.1 (7.7)	-1.4 (32.9)	11.88 (0.10)	0.689 (0.006)	157.5 (2.4)
SN 2007le	−10.31	4.54 (0.04)	5.21 (0.06)	167.4 (9.3)	54.3 (33.3)	15.32 (0.10)	0.662 (0.004)	254.3 (2.4)
SN 2007le	−9.40	4.60 (0.04)	5.06 (0.05)	134.1 (7.4)	22.6 (32.8)	14.92 (0.10)	0.552 (0.003)	258.3 (2.4)
SN 2007le	7.43	11.74 (0.12)	9.54 (0.05)	111.5 (7.8)	-3.6 (32.9)	12.09 (0.10)	0.722 (0.009)	149.0 (2.4)
SN 2007le	16.39	8.08 (0.24)	6.75 (0.03)	159.0 (8.7)	15.9 (33.1)	11.20 (0.10)	0.688 (0.008)	210.6 (2.4)

Continued on Next Page...

Table 3.12 — Continued

SN Name	Phase[a]	F_b[b]	F_r[b]	pEW[c]	ΔpEW[c,d]	v[e]	a	FWHM[c]
SN 2007le	17.37	8.43 (0.21)	6.61 (0.02)	154.7 (8.7)	7.5 (33.1)	11.20 (0.10)	0.705 (0.007)	196.7 (2.4)
SN 2007s1[f]	−1.23	0.80 (0.01)	0.71 (0.01)	122.4 (8.0)	17.1 (32.9)	11.61 (0.10)	0.698 (0.004)	165.5 (2.4)
SN 2007on	−3.01	17.11 (0.05)	15.54 (0.04)	116.2 (7.7)	10.8 (32.9)	11.53 (0.10)	0.683 (0.002)	166.9 (2.4)
SN 2007on	−3.00	14.54 (0.06)	13.49 (0.04)	116.8 (10.9)	11.5 (33.8)	11.72 (0.10)	0.683 (0.001)	167.0 (1.2)
SN 2007qe	−6.54	0.91 (0.01)	0.87 (0.01)	137.2 (8.1)	29.6 (33.0)	14.85 (0.10)	0.622 (0.002)	214.8 (2.4)
SN 2007qe	6.23	1.71 (0.02)	1.30 (0.02)	136.9 (9.0)	24.2 (33.2)	12.64 (0.10)	0.752 (0.005)	173.8 (2.4)
SN 2007ux	5.59	0.80 (0.03)	0.82 (0.03)	69.3 (4.7)	-42.3 (32.3)	10.73 (0.10)	0.459 (0.009)	157.1 (2.4)
SN 2008C	15.68	1.43 (0.01)	1.17 (0.01)	139.4 (7.6)	-0.8 (32.9)	9.90 (0.10)	0.588 (0.004)	218.4 (2.4)
SN 2008Q	6.46	14.98 (0.09)	11.55 (0.05)	98.2 (6.9)	-14.9 (32.7)	11.09 (0.10)	0.648 (0.002)	146.8 (2.4)
SN 2008Z	−2.29	1.76 (0.02)	1.41 (0.01)	60.1 (4.3)	-45.1 (32.3)	11.28 (0.10)	0.441 (0.004)	127.3 (2.4)
SN 2008Z	9.99	0.74 (0.01)	0.51 (0.00)	76.9 (4.1)	-44.3 (32.2)	11.83 (0.10)	0.618 (0.005)	109.7 (4.8)
SN 2008ar	−8.87	0.36 (0.00)	0.37 (0.01)	112.2 (4.6)	1.6 (32.3)	12.17 (0.10)	0.485 (0.002)	237.8 (4.8)
SN 2008ar	2.83	0.57 (0.02)	0.50 (0.01)	91.6 (6.7)	-16.2 (32.7)	10.29 (0.10)	0.643 (0.012)	140.3 (2.4)
SN 2008bt	−1.08	1.18 (0.05)	1.10 (0.03)	113.5 (6.8)	8.2 (32.7)	9.62 (0.10)	0.608 (0.012)	179.2 (2.4)
SN 2008s1[g]	−6.36	0.79 (0.01)	0.69 (0.01)	69.2 (5.1)	-38.2 (32.4)	11.88 (0.10)	0.505 (0.005)	135.0 (2.4)
SN 2008s1[g]	−4.40	1.04 (0.04)	0.88 (0.03)	73.7 (5.4)	-32.2 (32.4)	9.98 (0.10)	0.505 (0.004)	144.8 (2.4)
SN 2008s1[g]	−3.42	1.02 (0.02)	0.88 (0.01)	81.1 (5.7)	-24.3 (32.5)	11.22 (0.10)	0.550 (0.006)	140.9 (2.4)
SN 2008s1[g]	0.49	1.33 (0.03)	1.10 (0.02)	105.9 (7.5)	0.0 (32.8)	10.55 (0.10)	0.724 (0.003)	138.9 (2.4)
SN 2008s1[g]	4.40	1.17 (0.01)	1.03 (0.01)	98.7 (7.1)	-11.0 (32.7)	10.64 (0.10)	0.678 (0.005)	140.9 (2.4)
SN 2008s1[g]	5.38	1.16 (0.00)	0.96 (0.00)	100.8 (7.1)	-10.4 (32.7)	10.46 (0.10)	0.684 (0.002)	137.0 (2.4)
SN 2008s1[g]	15.37	0.52 (0.01)	0.67 (0.01)	75.4 (5.4)	-63.5 (32.4)	10.61 (0.10)	0.545 (0.006)	140.9 (2.4)
SN 2008cl	4.24	0.08 (0.01)	0.07 (0.00)	107.8 (8.0)	-1.7 (33.0)	12.18 (0.10)	0.762 (0.012)	139.2 (2.3)
SN 2008dx	2.46	0.29 (0.01)	0.28 (0.01)	86.5 (6.0)	-20.9 (32.5)	9.38 (0.10)	0.601 (0.008)	129.0 (2.4)
SN 2008dx	7.33	0.22 (0.01)	0.24 (0.00)	84.9 (5.5)	-30.0 (32.4)	8.90 (0.10)	0.532 (0.009)	138.8 (2.4)
SN 2008dt	9.27	0.28 (0.01)	0.30 (0.01)	179.9 (10.1)	60.6 (33.5)	13.26 (0.10)	0.717 (0.012)	272.4 (2.4)
SN 2008ec	−0.24	2.11 (0.01)	1.92 (0.01)	118.7 (8.1)	13.2 (33.0)	10.95 (0.10)	0.721 (0.003)	159.4 (2.4)
SN 2008ec	5.70	2.25 (0.02)	1.87 (0.01)	144.2 (9.5)	32.4 (33.4)	10.77 (0.10)	0.852 (0.005)	163.3 (2.4)
SN 2008ec	12.51	1.58 (0.01)	1.27 (0.01)	160.3 (8.2)	31.6 (33.0)	10.09 (0.10)	0.630 (0.005)	249.9 (2.4)
SN 2008ei	3.29	0.30 (0.01)	0.28 (0.00)	179.5 (10.7)	71.2 (33.7)	15.34 (0.10)	0.797 (0.004)	217.8 (2.4)
SN 2008ei	9.13	0.32 (0.00)	0.27 (0.00)	177.0 (11.0)	58.0 (33.8)	14.67 (0.10)	0.890 (0.005)	188.9 (2.4)
SN 2008s5[h]	1.26	1.18 (0.01)	0.95 (0.01)	57.9 (4.0)	-48.5 (32.2)	9.08 (0.10)	0.403 (0.004)	130.0 (2.4)
SN 2008s5[h]	8.96	0.92 (0.01)	0.64 (0.00)	74.7 (5.1)	-43.9 (32.4)	8.99 (0.10)	0.526 (0.007)	114.5 (2.4)
SN 2008hs	−7.94	0.56 (0.01)	0.50 (0.01)	105.8 (7.1)	-3.5 (32.8)	12.32 (0.10)	0.646 (0.003)	161.2 (2.4)

Uncertainties for each measured value are given in parentheses.
[a]Phases of spectra are in rest-frame days using the heliocentric redshift and photometry reference presented in table 1 of Silverman et al. (submitted).
[b]Fluxes are in units of 10^{-15} erg s^{-1} cm^{-2} Å^{-1}.
[c]The pEW, ΔpEW, and FWHM are in units of Å.
[d]ΔpEW is the measured pEW minus the expected pEW at the same epoch using our linear or quadratic fit (see Section 3.5.4 for more information).
[e]The expansion velocity is in units of 1000 km s^{-1}.
[f]Also known as SNF20071021-000.
[g]Also known as SNF20080514-002.
[h]Also known as SNF20080909-030.

Table 3.13: Measured Values for the O I Triplet

SN Name	Phase[a]	F_b[b]	F_r[b]	pEW[c]	ΔpEW[c,d]	v[e]	a	FWHM[c]
SN 1989B	7.54	59.30 (0.70)	47.12 (0.42)	116.4 (5.2)	8.7 (36.2)	...	...	...
SN 1989M	3.48	9.28 (0.09)	8.02 (0.05)	103.6 (4.9)	-9.4 (36.2)	14.19 (0.08)	0.342 (0.002)	348.2 (2.4)
SN 1990N	7.11	9.61 (0.10)	7.64 (0.07)	112.2 (4.0)	3.4 (36.1)	...	...	...
SN 1991bg	0.14	6.21 (0.07)	7.01 (0.14)	131.7 (4.8)	22.7 (36.2)	...	...	...
SN 1991bg	1.14	8.09 (0.07)	8.53 (0.13)	139.3 (4.9)	28.4 (36.2)	...	...	...
SN 1991bg	19.07	2.50 (0.05)	3.35 (0.06)	127.6 (4.8)	95.5 (36.2)	9.85 (0.08)	0.648 (0.010)	175.0 (6.1)
SN 1994D	−9.32	12.70 (0.08)	9.73 (0.07)	33.6 (1.9)	-23.1 (35.9)	...	...	...
SN 1994D	−7.67	13.04 (0.07)	10.45 (0.05)	45.9 (2.4)	-24.1 (36.0)	...	...	...
SN 1994D	−3.87	24.26 (0.19)	20.13 (0.38)	66.0 (3.2)	-28.2 (36.0)	...	...	...
SN 1994D	−3.33	20.57 (0.14)	17.20 (0.08)	78.4 (3.6)	-18.4 (36.1)	...	...	...
SN 1994S	1.11	2.00 (0.03)	2.08 (0.03)	55.7 (3.2)	-55.2 (36.0)	...	...	...
SN 1995D	3.84	5.59 (0.05)	4.48 (0.05)	144.5 (6.4)	31.5 (36.4)	10.66 (0.08)	0.396 (0.003)	387.5 (2.4)
SN 1997Y	1.27	1.38 (0.04)	1.02 (0.03)	56.0 (3.7)	-55.2 (36.1)	11.13 (0.08)	0.350 (0.016)	124.0 (2.4)
SN 1997bp	5.49	3.27 (0.05)	2.13 (0.03)	71.2 (3.6)	-40.6 (36.0)	...	...	...
SN 1997br	−4.84	5.77 (0.07)	4.50 (0.02)	49.3 (2.4)	-39.7 (36.0)	...	...	...
SN 1998V	7.20	1.23 (0.01)	0.98 (0.01)	136.0 (8.8)	27.4 (36.9)	...	...	...
SN 1998dm	−12.48	1.04 (0.01)	0.83 (0.01)	59.9 (2.9)	34.3 (36.0)	...	...	...
SN 1998dm	14.22	1.26 (0.01)	1.19 (0.01)	86.2 (4.1)	11.4 (36.1)	...	...	...
SN 1998dx	5.13	0.13 (0.01)	0.10 (0.00)	83.7 (5.2)	-28.6 (36.2)	...	...	...
SN 1998es	0.28	3.22 (0.02)	2.85 (0.02)	101.1 (4.7)	-8.2 (36.2)	...	...	...
SN 1999aa	0.24	0.50 (0.01)	0.40 (0.01)	106.6 (4.8)	-2.6 (36.2)	...	...	...
SN 1999aa	14.04	1.90 (0.01)	1.47 (0.01)	109.7 (3.2)	33.6 (36.0)	5.12 (0.08)	0.263 (0.004)	428.8 (6.0)
SN 1999ac	−3.70	2.63 (0.01)	2.32 (0.01)	42.0 (2.2)	-53.0 (35.9)	...	...	...
SN 1999ac	−0.89	2.84 (0.02)	2.29 (0.02)	68.4 (3.2)	-37.8 (36.0)	8.54 (0.08)	0.233 (0.006)	319.0 (2.4)
SN 1999cp	13.85	1.57 (0.02)	0.88 (0.02)	131.2 (6.1)	53.8 (36.4)	...	...	...
SN 1999cw	14.79	1.55 (0.01)	1.07 (0.02)	88.9 (4.1)	18.3 (36.1)	2.94 (0.08)	0.228 (0.005)	405.0 (2.4)
SN 1999da	−2.12	0.68 (0.01)	0.71 (0.01)	188.0 (10.0)	86.0 (37.2)	12.63 (0.08)	0.720 (0.008)	268.6 (2.4)

Continued on Next Page...

Table 3.13 — Continued

SN Name	Phase[a]	F_b[b]	F_r[b]	pEW[c]	ΔpEW[c,d]	v[e]	a	FWHM[c]
SN 1999da	6.76	0.66 (0.00)	0.71 (0.01)	114.3 (7.2)	4.6 (36.6)	11.59 (0.08)	0.660 (0.009)	158.0 (2.4)
SN 1999dk	−6.60	1.97 (0.02)	1.44 (0.02)	61.3 (3.2)	-16.6 (36.0)	14.74 (0.08)	0.237 (0.015)	279.8 (2.4)
SN 1999dq	−3.93	1.60 (0.02)	1.46 (0.02)	58.5 (2.9)	-35.4 (36.0)	...	...	...
SN 1999gd	−1.12	0.50 (0.00)	0.46 (0.01)	97.2 (2.9)	-8.3 (36.0)	11.37 (0.08)	0.317 (0.002)	270.0 (6.0)
SN 1999gh	4.12	2.29 (0.01)	2.15 (0.02)	128.0 (4.0)	15.1 (36.1)	12.08 (0.08)	0.441 (0.002)	267.9 (6.1)
SN 1999gh	15.89	1.80 (0.01)	2.00 (0.03)	30.1 (2.4)	-31.8 (35.9)	...	...	...
SN 2000cn	14.25	0.23 (0.00)	0.22 (0.01)	56.4 (4.1)	-18.2 (36.1)	...	...	...
SN 2000cp	2.92	0.11 (0.00)	0.10 (0.01)	149.4 (8.6)	36.6 (36.9)	11.87 (0.08)	0.749 (0.018)	179.8 (2.4)
SN 2000cw	4.81	0.21 (0.00)	0.15 (0.00)	84.4 (5.2)	-28.1 (36.3)	...	...	...
SN 2000dg	−5.09	0.18 (0.00)	0.18 (0.00)	25.2 (1.8)	-62.3 (35.9)	...	...	...
SN 2000dk	1.00	0.67 (0.01)	0.81 (0.01)	106.2 (6.2)	-4.6 (36.4)	...	...	...
SN 2000dk	10.84	0.49 (0.01)	0.51 (0.01)	86.8 (5.3)	-8.5 (36.3)	...	...	...
SN 2000dm	−1.63	0.69 (0.01)	0.77 (0.01)	71.7 (4.4)	-32.1 (36.1)	11.25 (0.08)	0.422 (0.009)	153.7 (2.4)
SN 2000dn	16.38	0.10 (0.00)	0.09 (0.00)	35.7 (2.7)	-22.0 (36.0)	...	...	...
SN 2000dr	6.78	0.42 (0.00)	0.43 (0.01)	113.1 (6.3)	3.5 (36.4)	10.95 (0.08)	0.524 (0.008)	196.3 (2.4)
SN 2000ey	7.90	1.98 (0.02)	1.80 (0.02)	28.9 (1.5)	-77.9 (35.9)	...	...	...
SN 2001G	11.57	0.66 (0.01)	0.51 (0.01)	139.3 (6.4)	47.8 (36.4)	...	...	...
SN 2001ay	6.79	0.35 (0.01)	0.31 (0.01)	160.6 (7.7)	51.0 (36.7)	9.79 (0.08)	0.516 (0.010)	312.5 (2.4)
SN 2001bg	13.70	1.69 (0.02)	1.43 (0.01)	99.2 (4.5)	20.8 (36.2)	...	...	...
SN 2001da	−1.12	0.89 (0.01)	0.75 (0.02)	89.4 (4.6)	-16.1 (36.2)	...	...	...
SN 2001da	9.72	0.64 (0.01)	0.53 (0.01)	114.4 (5.3)	14.0 (36.3)	...	...	...
SN 2001dl	13.84	0.16 (0.00)	0.14 (0.01)	126.6 (6.1)	49.1 (36.4)	...	...	...
SN 2001dw	11.06	0.31 (0.01)	0.31 (0.01)	29.3 (2.1)	-64.9 (35.9)	...	...	...
SN 2001en	14.72	0.52 (0.01)	0.43 (0.01)	86.7 (4.0)	15.5 (36.1)	...	...	...
SN 2001ep	2.83	1.48 (0.02)	1.27 (0.01)	142.7 (6.7)	29.9 (36.5)	11.38 (0.08)	0.496 (0.012)	236.9 (2.4)
SN 2001ep	4.99	1.45 (0.07)	1.22 (0.04)	162.2 (10.6)	49.8 (37.4)	10.49 (0.09)	0.539 (0.010)	270.0 (1.2)
SN 2001ep	5.97	1.35 (0.05)	1.17 (0.03)	157.5 (10.8)	46.4 (37.5)	10.21 (0.08)	0.567 (0.005)	246.0 (1.2)
SN 2001ep	7.85	1.22 (0.02)	1.05 (0.02)	126.2 (6.5)	19.4 (36.5)	...	...	...
SN 2001ex	−1.82	0.19 (0.01)	0.20 (0.01)	273.7 (13.6)	170.6 (38.3)	10.77 (0.08)	0.963 (0.018)	263.1 (2.4)
SN 2001fh	7.84	0.37 (0.01)	0.43 (0.01)	158.5 (11.2)	51.6 (37.6)	9.85 (0.08)	0.601 (0.005)	219.0 (1.2)
SN 2002bf	2.97	0.50 (0.01)	0.52 (0.00)	24.9 (1.4)	-88.0 (35.9)	...	...	...
SN 2002cf	−0.75	0.57 (0.01)	0.52 (0.01)	136.3 (7.7)	29.7 (36.7)	11.49 (0.08)	0.649 (0.005)	220.6 (2.4)
SN 2002cr	−6.78	2.06 (0.02)	1.86 (0.02)	51.6 (3.0)	-25.0 (36.0)	...	...	...
SN 2002cs	−7.76	0.63 (0.01)	0.50 (0.01)	101.4 (4.5)	31.9 (36.1)	16.49 (0.10)	0.289 (0.006)	350.5 (2.4)
SN 2002dk	−1.23	0.20 (0.00)	0.21 (0.01)	194.7 (9.8)	89.6 (37.2)	14.27 (0.10)	0.693 (0.012)	278.8 (2.4)
SN 2002dp	15.55	1.12 (0.02)	0.95 (0.02)	36.7 (2.5)	-28.0 (36.0)	...	...	...
SN 2002eb	1.68	0.40 (0.01)	0.32 (0.00)	110.1 (5.1)	-1.7 (36.2)	...	...	...
SN 2002eh	6.88	0.24 (0.01)	0.23 (0.01)	25.5 (2.1)	-83.8 (35.9)	11.03 (0.08)	0.224 (0.008)	94.3 (2.4)
SN 2002el	11.82	0.17 (0.00)	0.16 (0.01)	121.8 (5.8)	31.7 (36.3)	...	...	...
SN 2002er	−4.58	2.53 (0.02)	2.10 (0.02)	66.3 (3.7)	-24.1 (36.1)	12.93 (0.08)	0.332 (0.004)	162.6 (2.4)
SN 2002eu	−0.06	0.21 (0.01)	0.23 (0.01)	114.2 (6.3)	5.7 (36.4)	11.84 (0.08)	0.507 (0.007)	198.5 (2.4)
SN 2002eu	9.38	0.09 (0.00)	0.08 (0.00)	116.5 (7.5)	14.8 (36.6)	...	...	...
SN 2002fb	0.98	0.45 (0.01)	0.46 (0.01)	125.5 (6.6)	14.8 (36.5)	10.17 (0.08)	0.494 (0.008)	216.6 (2.4)
SN 2002fk	7.74	4.54 (0.04)	3.58 (0.04)	139.6 (6.6)	32.4 (36.5)	9.88 (0.08)	0.480 (0.004)	280.0 (2.4)
SN 2002ha	−0.85	1.46 (0.01)	1.20 (0.01)	127.6 (5.8)	21.3 (36.3)	...	...	...
SN 2002ha	4.93	1.18 (0.02)	1.00 (0.02)	157.8 (7.7)	45.4 (36.7)	11.69 (0.08)	0.563 (0.002)	252.5 (2.4)
SN 2002ha	7.89	2.13 (0.02)	2.00 (0.02)	147.2 (7.1)	40.5 (36.6)	11.05 (0.08)	0.500 (0.002)	278.1 (2.4)
SN 2002hd	6.48	0.27 (0.01)	0.20 (0.01)	79.5 (4.7)	-30.7 (36.2)	...	...	...
SN 2002hd	12.72	0.15 (0.02)	0.15 (0.02)	66.8 (5.5)	-18.1 (36.3)	10.33 (0.08)	0.311 (0.022)	180.0 (1.2)
SN 2002he	−5.91	0.34 (0.01)	0.28 (0.01)	86.0 (6.3)	3.5 (36.4)	13.34 (0.08)	0.338 (0.007)	229.0 (1.2)
SN 2002he	−1.03	0.48 (0.02)	0.58 (0.02)	66.8 (5.5)	-39.0 (36.3)	13.53 (0.08)	0.333 (0.030)	193.0 (1.2)
SN 2002he	3.22	0.86 (0.01)	0.82 (0.01)	111.4 (5.9)	-1.6 (36.3)	13.50 (0.08)	0.435 (0.014)	230.3 (2.4)
SN 2002hw	−6.27	0.65 (0.01)	0.62 (0.01)	109.7 (5.3)	29.5 (36.3)	...	...	...
SN 2002jg	10.11	0.29 (0.01)	0.28 (0.01)	92.5 (5.6)	-6.2 (36.3)	10.53 (0.08)	0.524 (0.011)	163.4 (2.4)
SN 2002jy	11.86	0.28 (0.01)	0.22 (0.01)	139.4 (6.4)	49.5 (36.4)	4.31 (0.08)	0.345 (0.008)	423.7 (2.4)
SN 2002kf	6.81	0.55 (0.01)	0.48 (0.01)	53.3 (3.7)	-56.3 (36.1)	12.59 (0.08)	0.346 (0.012)	157.0 (2.4)
SN 2003D	9.98	0.33 (0.00)	0.29 (0.01)	74.1 (4.8)	-25.1 (36.2)	11.46 (0.08)	0.481 (0.006)	156.5 (2.4)
SN 2003U	−2.55	0.30 (0.01)	0.26 (0.01)	105.3 (5.6)	5.1 (36.3)	...	...	...
SN 2003Y	−1.74	0.30 (0.00)	0.32 (0.01)	115.1 (6.4)	11.7 (36.4)	...	...	...
SN 2003cq	−0.15	0.16 (0.01)	0.13 (0.00)	130.9 (6.2)	22.7 (36.4)	...	...	...
SN 2003du	17.61	2.32 (0.00)	1.81 (0.00)	44.8 (2.3)	-1.9 (35.9)	...	...	...
SN 2003he	2.71	0.38 (0.01)	0.28 (0.01)	146.3 (7.0)	33.6 (36.5)	...	...	...
SN 2003iv	1.76	0.01 (0.00)	0.01 (0.00)	103.4 (6.3)	-8.4 (36.4)	11.74 (0.08)	0.519 (0.014)	152.8 (2.4)
SN 2004E	5.26	0.36 (0.01)	0.30 (0.00)	131.5 (6.0)	19.4 (36.4)	8.36 (0.08)	0.372 (0.019)	409.8 (2.4)
SN 2004S	8.26	1.80 (0.01)	1.40 (0.00)	97.0 (4.7)	-8.7 (36.2)	9.12 (0.08)	0.310 (0.003)	350.7 (2.4)
SN 2004bv	9.77	2.54 (0.04)	2.03 (0.03)	132.8 (6.0)	32.7 (36.4)	8.78 (0.08)	0.360 (0.011)	381.9 (2.4)
SN 2004bw	6.59	0.36 (0.01)	0.26 (0.01)	106.0 (6.1)	-3.9 (36.4)	...	...	...
SN 2004dt	−6.46	0.87 (0.02)	0.67 (0.01)	111.5 (5.9)	32.6 (36.4)	...	...	...
SN 2004dt	1.38	0.94 (0.01)	0.73 (0.01)	60.8 (2.6)	-50.6 (36.0)	13.69 (0.08)	0.314 (0.009)	186.3 (6.0)
SN 2004dt	18.00	0.79 (0.01)	0.76 (0.01)	38.6 (2.3)	-4.2 (35.9)	...	...	...
SN 2004ef	−5.52	0.23 (0.00)	0.19 (0.00)	96.3 (4.9)	11.4 (36.2)	...	...	...
SN 2004eo	−5.57	0.46 (0.01)	0.48 (0.01)	42.7 (2.8)	-41.9 (36.0)	10.27 (0.08)	0.235 (0.007)	187.1 (2.4)
SN 2004eo	13.19	0.35 (0.01)	0.30 (0.01)	35.4 (2.6)	-46.5 (36.0)	...	...	...
SN 2004fu	−2.65	2.01 (0.01)	1.70 (0.01)	98.5 (5.4)	-1.3 (36.3)	13.36 (0.08)	0.427 (0.003)	212.0 (2.4)
SN 2004fu	2.43	1.45 (0.01)	1.23 (0.01)	122.1 (6.5)	9.6 (36.4)	13.42 (0.08)	0.499 (0.006)	214.0 (2.4)
SN 2004fz	−5.18	1.25 (0.02)	1.03 (0.01)	92.8 (4.7)	5.8 (36.2)	...	...	...
SN 2004fz	17.56	0.89 (0.01)	0.86 (0.01)	33.1 (2.5)	-14.0 (36.0)	...	...	...
SN 2004gs	0.44	0.27 (0.00)	0.20 (0.01)	138.2 (7.1)	28.5 (36.6)	11.09 (0.08)	0.533 (0.022)	222.1 (2.4)
SN 2005A	5.55	0.15 (0.00)	0.11 (0.00)	39.2 (2.4)	-72.5 (36.0)	...	...	...
SN 2005M	9.23	0.26 (0.01)	0.26 (0.00)	65.6 (3.6)	-36.7 (36.1)	...	...	...
SN 2005am	6.37	3.29 (0.01)	2.99 (0.01)	134.2 (4.2)	23.7 (36.1)	12.36 (0.08)	0.474 (0.004)	248.0 (6.1)
SN 2005ao	−1.29	0.16 (0.01)	0.13 (0.01)	109.6 (5.5)	4.7 (36.3)	...	...	...

Continued on Next Page...

Table 3.13 — Continued

SN Name	Phase[a]	F_b[b]	F_r[b]	pEW[c]	ΔpEW[c,d]	v[e]	a	FWHM[c]
SN 2005bc	1.55	0.94 (0.01)	0.84 (0.01)	171.9 (7.7)	60.3 (36.7)	11.57 (0.08)	0.570 (0.005)	231.2 (2.4)
SN 2005bc	7.37	0.63 (0.01)	0.63 (0.02)	181.1 (8.9)	72.9 (37.0)	10.53 (0.08)	0.652 (0.010)	215.4 (2.4)
SN 2005bl	18.07	0.08 (0.00)	0.11 (0.00)	71.3 (5.8)	29.1 (36.3)	9.53 (0.08)	0.613 (0.012)	111.3 (2.4)
SN 2005dm	5.23	0.28 (0.01)	0.35 (0.01)	132.8 (7.8)	20.7 (36.7)	10.77 (0.08)	0.658 (0.012)	181.0 (2.4)
SN 2005el	−6.70	0.95 (0.01)	0.78 (0.00)	72.1 (3.5)	-5.1 (36.0)	...	...	...
SN 2005el	1.22	0.76 (0.01)	0.88 (0.02)	66.4 (4.0)	-44.7 (36.1)	...	...	...
SN 2005el	8.09	0.72 (0.01)	0.63 (0.01)	149.9 (7.0)	43.7 (36.5)	10.76 (0.08)	0.511 (0.011)	262.1 (2.4)
SN 2005er	−0.26	0.00 (0.00)	0.00 (0.00)	164.4 (12.0)	56.4 (37.8)	11.25 (0.08)	0.663 (0.006)	217.0 (1.2)
SN 2005er	1.67	0.10 (0.00)	0.12 (0.00)	128.5 (7.7)	16.8 (36.7)	11.40 (0.08)	0.642 (0.004)	173.5 (2.4)
SN 2005er	5.64	0.06 (0.00)	0.09 (0.00)	119.5 (8.0)	7.9 (36.8)	10.16 (0.08)	0.714 (0.025)	181.3 (2.4)
SN 2005eq	−2.98	0.35 (0.00)	0.27 (0.00)	68.1 (3.1)	-30.2 (36.0)	10.29 (0.08)	0.211 (0.006)	307.1 (2.4)
SN 2005eq	0.66	0.34 (0.01)	0.27 (0.01)	106.9 (4.9)	-3.2 (36.2)	9.82 (0.08)	0.308 (0.004)	361.5 (2.4)
SN 2005hj	7.51	0.21 (0.01)	0.18 (0.01)	57.4 (4.2)	-50.5 (36.1)	...	...	...
SN 2005iq	−5.86	3.53 (0.07)	2.86 (0.05)	85.4 (6.0)	2.6 (36.4)	12.24 (0.08)	0.334 (0.006)	255.0 (1.2)
SN 2005kc	12.25	0.74 (0.01)	0.67 (0.01)	97.1 (4.7)	9.3 (36.2)	11.13 (0.08)	0.299 (0.002)	340.8 (2.4)
SN 2005ke	7.80	2.42 (0.02)	2.49 (0.02)	93.1 (8.8)	-13.9 (36.9)	9.53 (0.08)	0.603 (0.003)	137.0 (1.2)
SN 2005ke	9.83	3.69 (0.02)	3.83 (0.03)	86.4 (6.2)	-13.4 (36.4)	9.67 (0.08)	0.621 (0.004)	129.4 (2.4)
SN 2005ki	1.62	2.89 (0.03)	2.70 (0.03)	161.6 (10.3)	49.9 (37.3)	11.91 (0.08)	0.505 (0.004)	284.0 (1.2)
SN 2005ki	8.35	0.41 (0.02)	0.40 (0.02)	127.5 (6.7)	22.1 (36.5)	8.86 (0.08)	0.480 (0.020)	178.5 (2.4)
SN 2006D	16.70	0.99 (0.02)	0.85 (0.03)	39.0 (2.6)	-16.0 (36.0)	10.53 (0.14)	0.224 (0.012)	160.6 (2.4)
SN 2006H	7.01	0.18 (0.00)	0.19 (0.01)	138.9 (8.5)	29.8 (36.9)	11.73 (0.08)	0.710 (0.005)	173.6 (2.4)
SN 2006N	−1.89	1.17 (0.01)	1.01 (0.02)	80.8 (3.9)	-22.1 (36.1)	...	...	...
SN 2006N	−0.90	0.51 (0.01)	0.54 (0.01)	77.7 (4.8)	-28.5 (36.2)	...	...	...
SN 2006X	3.15	5.20 (0.04)	4.72 (0.03)	52.2 (2.5)	-60.7 (36.0)	8.21 (0.40)	0.149 (0.012)	380.0 (2.4)
SN 2006ax	−10.07	0.35 (0.01)	0.30 (0.00)	33.8 (2.1)	-16.1 (35.9)	...	...	...
SN 2006bt	−5.30	0.20 (0.00)	0.19 (0.00)	120.9 (6.1)	34.6 (36.4)	11.28 (0.08)	0.469 (0.005)	226.7 (2.4)
SN 2006bt	2.27	0.15 (0.00)	0.15 (0.00)	139.0 (7.3)	26.6 (36.6)	10.81 (0.08)	0.573 (0.004)	232.5 (2.4)
SN 2006bz	−2.44	0.15 (0.00)	0.16 (0.01)	152.7 (8.8)	52.0 (36.9)	...	...	...
SN 2006cm	−1.15	0.34 (0.01)	0.35 (0.01)	97.0 (4.6)	-8.4 (36.2)	...	...	...
SN 2006dm	8.73	0.29 (0.00)	0.22 (0.01)	84.6 (5.3)	-19.4 (36.3)	11.60 (0.08)	0.470 (0.008)	156.6 (2.4)
SN 2006dm	14.61	0.22 (0.01)	0.18 (0.02)	41.2 (3.4)	-30.9 (36.0)	...	...	...
SN 2006ej	−3.70	0.66 (0.01)	0.56 (0.01)	104.0 (5.2)	8.9 (36.2)	...	...	...
SN 2006em	4.16	0.22 (0.00)	0.25 (0.00)	112.7 (6.5)	-0.2 (36.5)	9.90 (0.08)	0.501 (0.005)	225.7 (2.4)
SN 2006eu	16.02	0.16 (0.00)	0.21 (0.00)	47.5 (3.5)	-13.4 (36.0)	9.32 (0.08)	0.388 (0.013)	107.5 (2.4)
SN 2006gt	3.08	0.08 (0.00)	0.10 (0.01)	129.6 (7.6)	16.7 (36.7)	9.91 (0.08)	0.635 (0.041)	189.5 (2.3)
SN 2006ke	2.36	0.14 (0.00)	0.16 (0.01)	70.8 (3.9)	-41.7 (36.1)	10.01 (0.08)	0.314 (0.009)	200.6 (2.4)
SN 2006ke	8.38	0.12 (0.00)	0.15 (0.00)	96.4 (6.3)	-8.8 (36.4)	9.38 (0.08)	0.580 (0.009)	127.8 (2.4)
SN 2006kf	−8.96	0.17 (0.00)	0.15 (0.00)	118.3 (6.0)	58.6 (36.4)	11.70 (0.08)	0.408 (0.013)	264.4 (2.4)
SN 2006kf	17.37	0.14 (0.00)	0.14 (0.00)	40.1 (3.2)	-8.7 (36.0)	11.61 (0.08)	0.339 (0.016)	103.8 (2.4)
SN 2006le	11.92	0.34 (0.01)	0.26 (0.01)	127.7 (6.0)	38.1 (36.4)	5.28 (0.08)	0.375 (0.010)	385.3 (2.4)
SN 2007A	2.37	0.78 (0.01)	0.68 (0.01)	114.9 (5.2)	2.4 (36.3)	10.78 (0.08)	0.364 (0.003)	340.0 (2.4)
SN 2007A	15.07	0.39 (0.01)	0.32 (0.01)	111.1 (5.4)	42.6 (36.3)	...	...	...
SN 2007F	3.23	0.40 (0.01)	0.36 (0.00)	123.4 (5.8)	10.4 (36.3)	...	...	...
SN 2007N	0.44	2.33 (0.03)	2.21 (0.03)	148.0 (11.3)	38.3 (37.6)	12.41 (0.08)	0.595 (0.003)	260.0 (1.2)
SN 2007O	−0.33	4.34 (0.06)	3.67 (0.07)	79.2 (5.2)	-28.7 (36.2)	11.31 (0.08)	0.265 (0.005)	324.0 (1.2)
SN 2007af	−1.25	7.57 (0.05)	6.22 (0.06)	98.1 (4.8)	-7.0 (36.2)	11.45 (0.08)	0.378 (0.005)	202.9 (2.4)
SN 2007af	2.84	6.58 (0.06)	5.62 (0.04)	147.4 (9.7)	34.6 (37.1)	11.51 (0.08)	0.494 (0.005)	279.0 (1.2)
SN 2007al	3.39	0.38 (0.01)	0.43 (0.01)	109.8 (6.5)	-3.2 (36.5)	...	...	...
SN 2007ap	9.37	7.32 (0.12)	6.94 (0.11)	130.4 (9.0)	28.6 (37.0)	...	...	...
SN 2007au	16.11	0.31 (0.01)	0.35 (0.01)	65.2 (4.8)	5.2 (36.2)	10.38 (0.08)	0.451 (0.014)	141.1 (2.4)
SN 2007ax	14.93	0.90 (0.01)	1.25 (0.03)	95.6 (7.0)	26.0 (36.5)	9.63 (0.08)	0.681 (0.012)	147.0 (2.4)
SN 2007ba	5.18	1.46 (0.05)	1.63 (0.04)	98.9 (8.0)	-13.2 (36.7)	10.43 (0.08)	0.479 (0.008)	185.0 (1.2)
SN 2007ba	8.06	0.91 (0.04)	0.99 (0.02)	78.8 (6.8)	-27.4 (36.5)	10.35 (0.08)	0.452 (0.010)	154.0 (1.2)
SN 2007bc	0.61	0.54 (0.01)	0.46 (0.01)	127.4 (6.0)	17.4 (36.4)	11.23 (0.08)	0.471 (0.003)	182.2 (2.4)
SN 2007bm	−7.79	3.50 (0.03)	2.97 (0.02)	80.6 (3.8)	11.5 (36.1)	11.35 (0.08)	0.278 (0.005)	272.3 (2.4)
SN 2007bm	15.03	1.82 (0.02)	1.60 (0.02)	26.9 (1.9)	-41.9 (35.9)	10.79 (0.08)	0.180 (0.006)	141.1 (2.4)
SN 2007bm	19.96	2.69 (0.02)	2.73 (0.02)	32.5 (2.3)	9.9 (35.9)	10.78 (0.08)	0.252 (0.005)	119.3 (2.4)
SN 2007ci	−6.57	0.45 (0.01)	0.38 (0.01)	93.6 (4.8)	15.5 (36.2)	...	...	...
SN 2007ci	−1.71	0.57 (0.01)	0.46 (0.01)	100.4 (4.9)	-3.1 (36.2)	12.26 (0.08)	0.338 (0.006)	261.3 (2.4)
SN 2007ci	13.99	0.53 (0.01)	0.56 (0.01)	21.7 (1.7)	-54.8 (35.9)	...	...	...
SN 2007fb	14.63	0.30 (0.00)	0.26 (0.01)	40.2 (2.9)	-31.6 (36.0)	...	...	...
SN 2007fs	5.03	0.91 (0.01)	0.68 (0.01)	126.3 (5.9)	14.0 (36.3)	...	...	...
SN 2007gk	−1.72	0.32 (0.00)	0.28 (0.00)	94.6 (5.5)	-8.9 (36.3)	14.75 (0.08)	0.457 (0.004)	198.7 (2.4)
SN 2007hj	−1.23	0.87 (0.01)	0.81 (0.01)	165.4 (8.6)	60.3 (36.9)	12.90 (0.08)	0.626 (0.005)	244.5 (2.4)
SN 2007hj	12.53	0.58 (0.00)	0.57 (0.01)	66.2 (4.6)	-19.9 (36.2)	10.76 (0.08)	0.453 (0.010)	136.1 (2.4)
SN 2007le	16.39	2.48 (0.02)	1.97 (0.02)	57.0 (2.6)	-0.7 (36.0)	2.27 (0.08)	0.149 (0.007)	445.0 (2.4)
SN 2007le	17.37	2.40 (0.01)	1.91 (0.01)	80.5 (3.6)	31.6 (36.1)	3.89 (0.08)	0.211 (0.002)	441.0 (2.4)
SN 2007s1[f]	−1.23	0.32 (0.00)	0.24 (0.01)	73.4 (4.3)	-31.7 (36.1)	12.32 (0.08)	0.389 (0.023)	169.4 (2.4)
SN 2007on	−3.01	9.21 (0.02)	8.47 (0.07)	143.4 (6.9)	45.2 (36.5)	10.81 (0.08)	0.515 (0.004)	228.5 (2.4)
SN 2007on	15.45	35.06 (0.37)	36.52 (0.39)	63.2 (5.5)	-2.3 (36.3)	9.97 (0.08)	0.508 (0.006)	114.8 (1.8)
SN 2008Q	19.25	3.99 (0.03)	3.81 (0.04)	30.6 (1.6)	0.4 (35.9)	12.04 (0.08)	0.227 (0.003)	142.9 (4.9)
SN 2008Z	9.99	0.24 (0.00)	0.19 (0.01)	124.7 (4.2)	25.6 (36.1)	...	...	...
SN 2008ar	2.83	0.21 (0.01)	0.16 (0.01)	69.1 (4.4)	-43.7 (36.1)	...	...	...
SN 2008bt	10.97	0.42 (0.00)	0.43 (0.01)	61.2 (4.7)	-33.4 (36.2)	9.71 (0.08)	0.517 (0.007)	112.3 (2.4)
SN 2008s1[g]	−6.36	0.36 (0.00)	0.36 (0.00)	36.2 (2.4)	-43.3 (36.0)	...	...	...
SN 2008s1[g]	0.49	0.43 (0.02)	0.38 (0.03)	125.6 (7.2)	15.8 (36.6)	11.78 (0.08)	0.598 (0.019)	146.8 (2.4)
SN 2008dx	2.46	0.17 (0.00)	0.17 (0.00)	139.5 (8.0)	26.9 (36.8)	...	...	...
SN 2008dx	7.33	0.17 (0.00)	0.18 (0.01)	116.6 (7.4)	8.3 (36.6)	9.62 (0.08)	0.696 (0.006)	187.7 (2.4)
SN 2008dx	10.28	0.25 (0.01)	0.29 (0.01)	90.5 (6.7)	-7.4 (36.5)	9.85 (0.08)	0.681 (0.021)	123.2 (2.4)
SN 2008ec	−0.24	0.90 (0.01)	0.79 (0.01)	135.5 (6.3)	27.4 (36.4)	11.18 (0.08)	0.480 (0.007)	226.3 (2.4)
SN 2008ec	5.70	0.61 (0.01)	0.48 (0.01)	240.7 (11.5)	129.1 (37.7)	11.41 (0.08)	0.854 (0.010)	230.2 (2.4)

Continued on Next Page...

Table 3.13 — Continued

SN Name	Phase[a]	F_b[b]	F_r[b]	pEW[c]	ΔpEW[c,d]	v[e]	a	FWHM[c]
SN 2008s5[h]	8.96	0.30 (0.00)	0.22 (0.00)	126.0 (5.7)	22.7 (36.3)	8.71 (0.08)	0.380 (0.019)	384.1 (2.4)
SN 2008hs	−7.94	0.30 (0.00)	0.31 (0.01)	126.4 (6.8)	58.4 (36.5)	...	...	...

Uncertainties for each measured value are given in parentheses.
[a]Phases of spectra are in rest-frame days using the heliocentric redshift and photometry reference presented in table 1 of Silverman et al. (submitted).
[b]Fluxes are in units of 10^{-15} erg s^{-1} cm^{-2} Å^{-1}.
[c]The pEW, ΔpEW, and FWHM are in units of Å.
[d]ΔpEW is the measured pEW minus the expected pEW at the same epoch using our linear or quadratic fit (see Section 3.5.4 for more information).
[e]The expansion velocity is in units of 1000 km s^{-1}.
[f]Also known as SNF20071021-000.
[g]Also known as SNF20080514-002.
[h]Also known as SNF20080909-030.

Table 3.14: Measured Values for the Ca II Near-IR Triplet

SN Name	Phase[a]	F_b[b]	F_r[b]	pEW[c]	ΔpEW[c,d]	v[e]	a	FWHM[c]
SN 1989M	2.49	9.32 (0.12)	9.98 (0.07)	194.6 (10.0)	-10.6 (66.5)	...	...	...
SN 1989M	3.48	8.03 (0.05)	9.09 (0.04)	210.6 (10.4)	-1.3 (66.5)	12.46 (0.07)	0.656 (0.006)	316.4 (2.4)
SN 1990N	7.11	7.64 (0.07)	9.79 (0.11)	221.1 (7.0)	-19.8 (66.1)	12.00 (0.07)	0.617 (0.006)	386.7 (4.9)
SN 1991T	6.80	4.38 (0.06)	4.78 (0.05)	83.7 (3.0)	-154.6 (65.8)	...	...	...
SN 1991bg	0.14	7.02 (0.14)	6.44 (0.24)	291.7 (8.4)	100.0 (66.3)	...	...	...
SN 1991bg	1.14	8.48 (0.14)	6.53 (0.14)	274.0 (7.9)	77.0 (66.2)	...	...	...
SN 1991bg	19.07	3.33 (0.06)	4.68 (0.06)	401.0 (10.1)	10.8 (66.5)	...	...	...
SN 1994D	−7.67	8.58 (0.08)	8.97 (0.03)	25.1 (1.5)	-144.3 (65.7)	...	...	...
SN 1994D	−3.87	17.53 (0.19)	16.33 (0.17)	38.7 (2.5)	-137.2 (65.8)	...	...	...
SN 1994D	−3.33	15.58 (0.15)	15.58 (0.24)	57.8 (3.4)	-119.8 (65.8)	...	...	...
SN 1994D	14.04	9.49 (0.09)	13.30 (0.09)	248.7 (10.7)	-68.8 (66.6)	...	...	...
SN 1994S	1.11	2.07 (0.11)	1.98 (0.07)	93.4 (5.9)	-103.5 (66.0)	...	...	...
SN 1995D	3.84	4.48 (0.05)	4.41 (0.05)	157.5 (7.3)	-56.9 (66.1)	12.04 (0.07)	0.491 (0.006)	327.8 (2.4)
SN 1997Y	1.27	1.19 (0.02)	1.14 (0.03)	134.6 (6.7)	-63.2 (66.1)	11.64 (0.07)	0.461 (0.008)	259.9 (2.4)
SN 1997bp	5.49	2.16 (0.02)	2.82 (0.03)	306.6 (14.3)	79.6 (67.3)	15.96 (0.07)	0.874 (0.013)	368.9 (2.4)
SN 1997do	−5.67	1.43 (0.02)	1.27 (0.01)	194.2 (8.6)	22.4 (66.3)	...	...	...
SN 1998V	7.20	0.98 (0.01)	1.06 (0.01)	196.7 (13.5)	-45.1 (67.1)	12.51 (0.07)	0.635 (0.004)	296.0 (1.2)
SN 1998dk	−7.24	0.52 (0.01)	0.46 (0.01)	232.3 (9.9)	62.5 (66.5)	26.18 (0.16)	0.601 (0.049)	420.4 (2.4)
SN 1998dk	−0.54	1.71 (0.01)	1.72 (0.01)	150.4 (7.1)	-38.0 (66.1)	13.58 (0.07)	0.467 (0.011)	284.2 (2.4)
SN 1998dm	−12.48	0.75 (0.01)	0.78 (0.01)	145.6 (6.2)	-27.4 (66.0)	...	...	...
SN 1998dm	−5.61	1.96 (0.01)	2.02 (0.01)	36.9 (2.4)	-135.0 (65.8)	...	...	...
SN 1998dm	14.22	1.18 (0.01)	2.16 (0.03)	277.9 (12.7)	-41.9 (66.9)	...	...	...
SN 1998dx	5.13	0.11 (0.00)	0.11 (0.00)	196.2 (10.4)	-27.9 (66.5)	...	...	...
SN 1998ec	11.86	0.27 (0.00)	0.44 (0.01)	304.4 (13.7)	13.9 (67.1)	...	...	...
SN 1998ef	−8.62	0.66 (0.01)	0.50 (0.02)	267.9 (10.8)	98.8 (66.6)	...	...	...
SN 1999aa	14.04	1.47 (0.01)	2.27 (0.02)	210.4 (6.3)	-107.0 (66.0)	...	...	...
SN 1999aa	17.04	0.52 (0.01)	0.90 (0.01)	252.9 (11.1)	-106.2 (66.7)	...	...	...
SN 1999ac	−3.70	2.32 (0.01)	2.09 (0.01)	153.0 (7.0)	-23.4 (66.1)	...	...	...
SN 1999ac	−0.89	2.33 (0.02)	2.19 (0.02)	158.4 (7.4)	-28.4 (66.1)	...	...	...
SN 1999cp	4.91	2.00 (0.02)	2.21 (0.02)	183.4 (9.2)	-39.1 (66.4)	...	...	...
SN 1999cp	13.85	0.90 (0.02)	1.98 (0.02)	278.6 (12.6)	-36.5 (66.9)	...	...	...
SN 1999cw	14.79	1.09 (0.02)	1.79 (0.03)	245.9 (10.8)	-81.6 (66.6)	13.46 (0.07)	0.663 (0.014)	375.4 (2.4)
SN 1999da	−2.12	0.69 (0.01)	0.63 (0.01)	347.6 (15.2)	165.9 (67.5)	15.37 (0.07)	0.832 (0.014)	428.6 (2.4)
SN 1999da	6.76	0.67 (0.01)	0.69 (0.01)	313.5 (14.0)	75.7 (67.2)	...	...	...
SN 1999dg	15.08	0.21 (0.01)	0.31 (0.01)	344.6 (15.4)	13.3 (67.5)	...	...	...
SN 1999dk	17.06	1.08 (0.02)	2.23 (0.02)	379.1 (15.9)	19.7 (67.6)	12.65 (0.07)	0.867 (0.024)	417.8 (2.4)
SN 1999ee	17.65	1.21 (0.03)	2.20 (0.04)	369.7 (15.0)	1.5 (67.4)	12.82 (0.07)	0.820 (0.021)	429.1 (2.4)
SN 1999ek	5.66	0.55 (0.04)	0.70 (0.03)	178.6 (10.0)	-49.9 (66.5)	...	...	...
SN 1999gd	−1.12	0.46 (0.01)	0.48 (0.01)	167.7 (5.3)	-18.1 (65.9)	...	...	...
SN 1999gh	4.12	2.15 (0.02)	2.48 (0.03)	294.3 (8.4)	77.8 (66.3)	12.09 (0.07)	0.752 (0.003)	397.0 (6.1)
SN 1999gh	15.89	1.93 (0.03)	2.22 (0.04)	433.4 (16.7)	90.8 (67.8)	11.65 (0.07)	0.881 (0.023)	450.5 (2.4)
SN 2000cn	14.25	0.22 (0.01)	0.27 (0.01)	397.6 (16.3)	77.5 (67.7)	...	...	...
SN 2000cp	2.92	0.11 (0.01)	0.14 (0.01)	332.8 (15.6)	124.8 (67.5)	...	...	...
SN 2000cu	9.64	0.29 (0.01)	0.41 (0.02)	282.9 (12.6)	17.1 (66.9)	...	...	...
SN 2000cw	4.81	0.18 (0.01)	0.21 (0.01)	293.8 (13.1)	72.1 (67.0)	...	...	...
SN 2000dg	−5.09	0.16 (0.01)	0.15 (0.00)	84.9 (4.6)	-88.0 (65.9)	...	...	...
SN 2000dk	1.00	0.80 (0.01)	0.77 (0.01)	260.0 (11.6)	63.6 (66.7)	12.03 (0.07)	0.707 (0.023)	355.8 (2.4)
SN 2000dk	10.84	0.50 (0.01)	0.79 (0.01)	343.3 (14.6)	64.6 (67.3)	...	...	...
SN 2000dm	−1.63	0.76 (0.01)	0.57 (0.02)	116.2 (5.9)	-67.4 (66.0)	...	...	...
SN 2000dm	8.18	0.51 (0.01)	0.63 (0.01)	241.6 (11.1)	-9.5 (66.7)	...	...	...
SN 2000dn	−0.94	0.21 (0.01)	0.19 (0.01)	225.7 (10.6)	39.1 (66.6)	11.70 (0.07)	0.700 (0.024)	306.2 (2.4)
SN 2000dr	6.78	0.43 (0.01)	0.47 (0.01)	277.7 (12.6)	39.7 (66.9)	...	...	...
SN 2000dx	−9.26	0.07 (0.01)	0.06 (0.01)	336.5 (16.0)	167.4 (67.6)	...	...	...
SN 2000fa	6.86	0.32 (0.01)	0.41 (0.01)	203.0 (10.1)	-35.8 (66.5)	...	...	...
SN 2001E	15.01	0.18 (0.01)	0.40 (0.02)	315.6 (14.0)	-14.7 (67.2)	...	...	...
SN 2001G	11.57	0.51 (0.01)	0.67 (0.01)	231.8 (11.0)	-55.2 (66.6)	12.04 (0.13)	0.701 (0.010)	302.9 (2.4)
SN 2001N	13.05	0.12 (0.01)	0.16 (0.01)	155.9 (6.9)	-148.9 (66.1)	...	...	...
SN 2001V	15.86	1.09 (0.01)	1.62 (0.03)	267.6 (12.2)	-74.5 (66.8)	...	...	...
SN 2001ay	6.79	0.31 (0.01)	0.34 (0.01)	146.1 (7.3)	-92.0 (66.1)	11.65 (0.07)	0.474 (0.023)	314.5 (2.4)

Continued on Next Page...

Table 3.14 — Continued

SN Name	Phase[a]	F_b[b]	F_r[b]	pEW[c]	ΔpEW[c,d]	v[e]	a	FWHM[c]
SN 2001bg	13.70	1.43 (0.01)	2.40 (0.03)	326.9 (14.8)	13.8 (67.4)	13.35 (0.07)	0.852 (0.013)	373.3 (2.4)
SN 2001bg	18.91	1.50 (0.05)	3.17 (0.04)	416.2 (24.9)	28.5 (70.3)	13.17 (0.07)	0.978 (0.009)	397.0 (1.2)
SN 2001br	3.48	0.28 (0.02)	0.27 (0.04)	217.4 (13.5)	5.5 (67.1)	...	...	...
SN 2001cp	1.39	0.23 (0.01)	0.22 (0.01)	141.6 (6.5)	-56.9 (66.0)	...	...	...
SN 2001cp	18.00	0.08 (0.01)	0.22 (0.02)	350.7 (16.2)	-22.8 (67.7)	...	...	...
SN 2001da	9.72	0.54 (0.01)	0.71 (0.01)	314.4 (13.8)	47.9 (67.2)	12.23 (0.07)	0.796 (0.009)	399.1 (2.4)
SN 2001dl	13.84	0.13 (0.01)	0.26 (0.01)	238.0 (11.6)	-76.9 (66.7)	10.77 (0.07)	0.745 (0.029)	303.7 (2.4)
SN 2001dt	13.60	0.07 (0.00)	0.14 (0.01)	434.3 (17.5)	122.4 (68.0)	13.44 (0.10)	0.925 (0.029)	497.2 (2.4)
SN 2001dw	11.06	0.31 (0.01)	0.36 (0.01)	400.2 (15.2)	118.9 (67.5)	...	...	...
SN 2001eh	3.26	0.15 (0.00)	0.18 (0.00)	140.2 (6.3)	-70.1 (66.0)	...	...	...
SN 2001en	10.09	0.53 (0.01)	0.85 (0.01)	278.9 (12.9)	8.3 (67.0)	...	...	...
SN 2001en	14.72	0.43 (0.01)	0.89 (0.02)	366.8 (16.0)	40.4 (67.6)	...	...	...
SN 2001ep	2.83	1.24 (0.01)	1.39 (0.01)	245.8 (11.5)	38.3 (66.7)	...	...	...
SN 2001ep	4.99	1.19 (0.05)	1.57 (0.04)	290.1 (19.0)	67.0 (68.4)	...	...	...
SN 2001ep	5.97	1.17 (0.02)	1.66 (0.03)	325.6 (21.0)	94.5 (69.0)	...	...	...
SN 2001ep	7.85	1.06 (0.01)	1.46 (0.02)	340.5 (15.2)	92.6 (67.5)	...	...	...
SN 2001ex	−1.82	0.20 (0.01)	0.17 (0.01)	360.3 (16.8)	177.5 (67.8)	...	...	...
SN 2001fh	5.93	0.42 (0.01)	0.50 (0.01)	314.8 (13.8)	84.1 (67.2)	...	...	...
SN 2001fh	7.84	0.43 (0.01)	0.64 (0.01)	282.8 (17.6)	34.9 (68.0)	...	...	...
SN 2002aw	15.84	0.07 (0.01)	0.21 (0.01)	385.2 (21.4)	43.3 (69.1)	...	...	...
SN 2002bf	2.97	0.52 (0.00)	0.55 (0.00)	237.2 (11.3)	28.9 (66.7)	16.72 (0.07)	0.667 (0.004)	367.1 (2.4)
SN 2002bo	−11.94	1.10 (0.02)	1.28 (0.02)	366.8 (15.2)	194.9 (67.5)	23.32 (0.08)	0.826 (0.035)	454.1 (2.4)
SN 2002bo	−1.08	5.00 (0.12)	5.28 (0.19)	236.3 (11.2)	50.4 (66.7)	14.03 (0.07)	0.725 (0.014)	354.5 (2.4)
SN 2002bo	15.99	2.79 (0.04)	4.65 (0.09)	387.8 (17.0)	43.8 (67.9)	...	...	...
SN 2002bz	4.92	0.09 (0.01)	0.12 (0.01)	188.4 (9.5)	-34.1 (66.4)	...	...	...
SN 2002cd	1.10	0.67 (0.01)	0.79 (0.04)	145.5 (8.3)	-51.3 (66.2)	16.12 (0.07)	0.607 (0.018)	249.4 (2.4)
SN 2002cd	17.89	0.31 (0.01)	0.81 (0.02)	368.6 (16.4)	-3.2 (67.7)	13.87 (0.07)	0.986 (0.019)	350.4 (2.4)
SN 2002cf	−0.75	0.53 (0.01)	0.39 (0.01)	270.6 (12.5)	83.2 (66.9)	...	...	...
SN 2002cf	15.95	0.53 (0.03)	0.47 (0.06)	455.0 (18.4)	111.6 (68.2)	...	...	...
SN 2002cr	−6.78	1.87 (0.02)	1.51 (0.03)	148.8 (6.5)	-21.5 (66.0)	12.04 (0.07)	0.416 (0.010)	380.4 (2.4)
SN 2002cs	−7.76	0.50 (0.01)	0.37 (0.01)	122.2 (5.9)	-47.1 (66.0)	15.49 (0.07)	0.406 (0.009)	259.9 (2.4)
SN 2002de	8.37	0.13 (0.01)	0.20 (0.01)	270.8 (13.9)	17.9 (67.2)	12.73 (0.07)	0.996 (0.021)	268.5 (2.4)
SN 2002df	6.55	0.11 (0.02)	0.15 (0.02)	295.3 (14.4)	59.3 (67.3)	...	...	...
SN 2002dj	−7.98	1.56 (0.03)	1.47 (0.02)	267.9 (11.1)	98.7 (66.7)	24.01 (0.08)	0.579 (0.010)	491.4 (2.4)
SN 2002dk	−1.23	0.21 (0.01)	0.16 (0.01)	326.4 (14.7)	141.1 (67.4)	15.29 (0.07)	0.842 (0.028)	398.6 (2.4)
SN 2002dp	15.55	0.95 (0.02)	1.64 (0.04)	373.3 (15.5)	35.6 (67.5)	11.46 (0.07)	0.872 (0.008)	391.4 (2.4)
SN 2002eb	1.68	0.32 (0.01)	0.30 (0.01)	109.8 (4.9)	-90.4 (65.9)	...	...	...
SN 2002ef	4.70	0.31 (0.02)	0.34 (0.02)	206.2 (10.4)	-14.6 (66.5)	12.73 (0.07)	0.742 (0.020)	289.1 (2.4)
SN 2002eh	6.88	0.20 (0.01)	0.36 (0.01)	411.4 (16.9)	172.4 (67.9)	11.82 (0.07)	0.940 (0.032)	412.6 (2.4)
SN 2002el	11.82	0.15 (0.01)	0.23 (0.01)	296.2 (13.2)	6.1 (67.0)	...	...	...
SN 2002er	5.26	1.69 (0.03)	2.16 (0.02)	264.8 (12.3)	39.6 (66.9)	...	...	...
SN 2002eu	−0.06	0.23 (0.01)	0.21 (0.01)	193.5 (9.1)	2.7 (66.4)	10.51 (0.29)	0.529 (0.032)	366.2 (2.4)
SN 2002fb	0.98	0.46 (0.01)	0.37 (0.01)	262.2 (12.6)	66.0 (66.9)	11.98 (0.07)	0.794 (0.012)	324.9 (2.4)
SN 2002fb	18.60	0.25 (0.01)	0.30 (0.00)	359.0 (15.2)	-23.8 (67.5)	...	...	...
SN 2002ha	−0.85	1.20 (0.01)	1.04 (0.03)	141.1 (6.8)	-45.9 (66.1)	12.32 (0.07)	0.485 (0.024)	276.1 (2.4)
SN 2002ha	4.93	1.00 (0.02)	1.05 (0.02)	230.0 (10.8)	7.4 (66.6)	...	...	...
SN 2002ha	7.89	2.00 (0.02)	2.44 (0.02)	258.4 (11.3)	10.2 (66.7)	...	...	...
SN 2002hd	6.48	0.22 (0.01)	0.25 (0.01)	239.3 (11.1)	3.9 (66.7)	12.05 (0.07)	0.701 (0.014)	324.6 (2.4)
SN 2002hd	12.72	0.15 (0.02)	0.21 (0.02)	323.8 (18.7)	22.9 (68.3)	12.65 (0.07)	0.791 (0.020)	422.0 (1.2)
SN 2002he	−5.91	0.28 (0.01)	0.23 (0.01)	135.5 (8.9)	-35.9 (66.3)	12.52 (0.07)	0.431 (0.011)	281.0 (1.2)
SN 2002he	−1.03	0.58 (0.02)	0.58 (0.02)	162.6 (11.1)	-23.6 (66.7)	12.44 (0.07)	0.518 (0.007)	286.0 (1.2)
SN 2002he	0.29	0.41 (0.01)	0.39 (0.01)	177.3 (8.9)	-15.2 (66.3)	13.05 (0.07)	0.571 (0.007)	300.6 (2.4)
SN 2002he	3.22	0.83 (0.01)	0.83 (0.02)	223.8 (10.8)	13.7 (66.6)	12.97 (0.07)	0.663 (0.007)	318.2 (2.4)
SN 2002hw	−6.27	0.61 (0.01)	0.51 (0.01)	183.8 (8.5)	13.0 (66.3)	13.56 (0.07)	0.536 (0.009)	316.5 (2.4)
SN 2002jg	10.11	0.30 (0.02)	0.51 (0.03)	338.4 (14.1)	67.7 (67.2)	...	...	...
SN 2002jy	11.86	0.22 (0.01)	0.33 (0.02)	273.0 (12.7)	-17.4 (66.9)	...	...	...
SN 2002kf	6.81	0.55 (0.01)	0.71 (0.01)	266.6 (12.1)	28.3 (66.8)	...	...	...
SN 2003D	9.98	0.29 (0.01)	0.33 (0.01)	282.3 (12.1)	13.0 (66.8)	12.04 (0.07)	0.731 (0.012)	362.0 (2.4)
SN 2003K	13.43	0.14 (0.01)	0.20 (0.01)	227.0 (11.3)	-82.6 (66.7)	...	...	...
SN 2003U	−2.55	0.26 (0.01)	0.22 (0.01)	159.6 (7.5)	-20.5 (66.2)	...	...	...
SN 2003W	18.14	0.48 (0.01)	0.69 (0.01)	423.0 (16.8)	47.4 (67.8)	14.30 (0.07)	0.873 (0.005)	458.8 (2.4)
SN 2003Y	−1.74	0.31 (0.01)	0.25 (0.01)	283.1 (12.6)	100.0 (66.9)	...	...	...
SN 2003du	17.61	1.80 (0.00)	3.29 (0.01)	311.9 (13.4)	-55.7 (67.1)	...	...	...
SN 2003gt	17.61	0.46 (0.01)	0.89 (0.01)	284.7 (12.3)	-82.9 (66.9)	...	...	...
SN 2003he	2.71	0.28 (0.01)	0.33 (0.02)	161.1 (8.6)	-45.5 (66.3)	...	...	...
SN 2003he	8.54	0.27 (0.01)	0.26 (0.01)	203.0 (9.5)	-51.6 (66.4)	...	...	...
SN 2003iv	6.58	0.05 (0.01)	0.06 (0.01)	245.3 (12.1)	9.1 (66.8)	...	...	...
SN 2003kf	−7.50	2.97 (0.02)	2.59 (0.02)	118.7 (5.3)	-50.8 (65.9)	...	...	...
SN 2004E	5.26	0.26 (0.01)	0.31 (0.01)	125.1 (8.0)	-100.1 (66.2)	...	...	...
SN 2004S	8.26	1.40 (0.00)	2.01 (0.01)	275.2 (11.7)	23.4 (66.8)	...	...	...
SN 2004bg	10.34	0.32 (0.01)	0.44 (0.01)	246.4 (11.5)	-26.9 (66.7)	13.08 (0.09)	0.690 (0.015)	331.0 (2.4)
SN 2004bd	10.76	1.06 (0.01)	1.24 (0.02)	256.9 (11.4)	-21.0 (66.7)	10.37 (0.07)	0.652 (0.017)	392.5 (2.4)
SN 2004bk	6.13	0.31 (0.01)	0.40 (0.01)	215.1 (10.8)	-17.3 (66.6)	...	...	...
SN 2004bl	4.61	0.47 (0.02)	0.56 (0.02)	174.3 (8.6)	-45.9 (66.3)	12.84 (0.07)	0.582 (0.017)	277.2 (2.4)
SN 2004bv	9.77	2.02 (0.03)	2.04 (0.02)	182.0 (8.3)	-85.1 (66.2)	...	...	...
SN 2004bw	6.59	0.31 (0.00)	0.41 (0.01)	309.4 (13.0)	73.0 (67.0)	...	...	...
SN 2004dt	−6.46	0.68 (0.01)	0.46 (0.01)	99.6 (4.7)	-71.0 (65.9)	...	...	...
SN 2004dt	1.38	0.87 (0.01)	0.79 (0.01)	130.3 (4.2)	-68.2 (65.9)	10.85 (0.07)	0.437 (0.005)	308.9 (6.0)
SN 2004ef	−5.52	0.18 (0.00)	0.15 (0.00)	172.2 (7.5)	0.1 (66.2)	...	...	...
SN 2004ef	8.05	0.14 (0.01)	0.18 (0.01)	327.0 (14.4)	77.2 (67.3)	12.08 (0.07)	0.864 (0.031)	298.7 (2.4)
SN 2004eo	13.19	0.32 (0.01)	0.44 (0.01)	317.3 (13.2)	10.6 (67.0)	...	...	...
SN 2004ey	−7.58	0.93 (0.01)	0.78 (0.01)	134.3 (5.8)	-35.2 (66.0)	21.46 (0.07)	0.359 (0.004)	313.1 (2.4)

Continued on Next Page...

Table 3.14 — Continued

SN Name	Phase[a]	F_b[b]	F_r[b]	pEW[c]	ΔpEW[c,d]	v[e]	a	FWHM[c]
SN 2004fu	−2.65	1.69 (0.01)	1.81 (0.02)	207.3 (9.1)	27.5 (66.4)	15.29 (0.07)	0.521 (0.004)	402.3 (2.4)
SN 2004fu	2.43	1.29 (0.01)	1.59 (0.02)	226.6 (10.8)	21.8 (66.6)	14.05 (0.07)	0.657 (0.007)	352.8 (2.4)
SN 2004fz	17.56	0.86 (0.01)	1.10 (0.01)	369.7 (14.6)	2.9 (67.3)	...	...	...
SN 2004gs	0.44	0.21 (0.00)	0.22 (0.00)	231.5 (11.0)	38.3 (66.6)	11.67 (0.07)	0.694 (0.034)	348.7 (2.4)
SN 2005A	5.55	0.11 (0.00)	0.18 (0.01)	366.5 (15.3)	139.0 (67.5)	...	...	...
SN 2005M	8.23	0.09 (0.00)	0.11 (0.00)	144.9 (9.2)	-106.6 (66.4)	...	...	...
SN 2005W	0.59	0.98 (0.04)	1.08 (0.05)	219.1 (14.3)	25.0 (67.3)	11.93 (0.07)	0.642 (0.012)	336.0 (1.2)
SN 2005am	4.47	3.29 (0.02)	3.45 (0.02)	219.2 (10.2)	0.2 (66.5)	...	...	...
SN 2005am	6.37	2.99 (0.01)	3.29 (0.05)	239.4 (7.0)	4.9 (66.1)	...	...	...
SN 2005ao	−1.29	0.13 (0.01)	0.13 (0.01)	101.9 (5.7)	-83.2 (66.0)	...	...	...
SN 2005bc	1.55	0.84 (0.01)	0.85 (0.01)	204.6 (9.7)	5.2 (66.4)	12.72 (0.07)	0.608 (0.008)	339.8 (2.4)
SN 2005bc	7.37	0.62 (0.02)	0.79 (0.01)	302.8 (13.1)	59.4 (67.0)	...	...	...
SN 2005be	10.96	0.08 (0.00)	0.11 (0.01)	196.3 (9.6)	-83.8 (66.4)	...	...	...
SN 2005be	16.71	0.06 (0.00)	0.08 (0.01)	162.5 (8.9)	-191.8 (66.3)	...	...	...
SN 2005cf	−10.94	1.32 (0.03)	1.53 (0.02)	371.6 (15.8)	201.2 (67.6)	24.12 (0.08)	0.877 (0.017)	419.3 (2.4)
SN 2005cf	−2.11	17.96 (0.42)	19.94 (0.30)	184.9 (8.1)	3.2 (66.2)	20.62 (0.07)	0.516 (0.034)	222.6 (2.4)
SN 2005cf	−1.19	7.60 (0.16)	7.58 (0.10)	197.7 (8.4)	12.2 (66.3)	...	...	...
SN 2005cf	18.69	2.13 (0.02)	3.77 (0.03)	347.6 (14.0)	-36.6 (67.2)	...	...	...
SN 2005de	−0.75	0.66 (0.02)	0.62 (0.01)	181.3 (8.3)	-6.1 (66.2)	...	...	...
SN 2005de	10.10	0.42 (0.01)	0.65 (0.01)	274.5 (12.5)	3.9 (66.9)	...	...	...
SN 2005dm	5.23	0.35 (0.01)	0.28 (0.00)	362.1 (16.4)	137.1 (67.7)	...	...	...
SN 2005dv	−0.57	0.52 (0.02)	0.50 (0.02)	249.8 (11.9)	61.6 (66.8)	13.54 (0.07)	0.754 (0.014)	342.4 (2.4)
SN 2005el	1.22	0.87 (0.01)	0.83 (0.02)	125.5 (6.0)	-72.0 (66.0)	...	...	...
SN 2005el	8.09	0.62 (0.01)	0.79 (0.03)	251.0 (10.6)	0.8 (66.6)	12.57 (0.07)	0.653 (0.021)	386.2 (2.4)
SN 2005er	−0.26	0.00 (0.00)	0.00 (0.00)	349.5 (22.1)	159.8 (69.3)	...	...	...
SN 2005er	1.67	0.12 (0.00)	0.11 (0.00)	349.0 (15.8)	148.9 (67.6)	...	...	...
SN 2005er	5.64	0.10 (0.00)	0.11 (0.01)	398.9 (16.8)	170.6 (67.8)	...	...	...
SN 2005eq	0.66	0.27 (0.01)	0.28 (0.01)	92.7 (4.2)	-101.8 (65.9)	...	...	...
SN 2005ew	18.23	0.68 (0.01)	1.87 (0.01)	368.8 (15.3)	-8.3 (67.5)	15.40 (0.17)	0.857 (0.029)	408.8 (2.4)
SN 2005iq	−5.86	2.84 (0.05)	2.33 (0.05)	146.0 (8.8)	-25.5 (66.3)	12.61 (0.07)	0.398 (0.016)	413.0 (1.2)
SN 2005kc	10.28	0.03 (0.00)	0.03 (0.00)	238.0 (14.8)	-34.6 (67.4)	...	...	...
SN 2005kc	12.25	0.67 (0.01)	0.98 (0.01)	254.3 (11.5)	-40.7 (66.7)	...	...	...
SN 2005ke	7.80	2.48 (0.02)	2.13 (0.01)	304.3 (19.3)	56.9 (68.5)	...	...	...
SN 2005ke	9.83	3.82 (0.03)	3.75 (0.02)	326.3 (14.3)	58.5 (67.3)	...	...	...
SN 2005ke	14.79	2.36 (0.04)	2.40 (0.02)	366.6 (15.3)	39.2 (67.5)	...	...	...
SN 2005ki	1.62	2.69 (0.03)	2.75 (0.03)	95.5 (6.5)	-104.4 (66.0)	...	...	...
SN 2005ki	8.35	0.41 (0.02)	0.47 (0.03)	237.8 (11.0)	-14.9 (66.6)	...	...	...
SN 2005mc	6.64	0.28 (0.02)	0.33 (0.02)	246.2 (10.3)	9.4 (66.5)	...	...	...
SN 2005lz	0.58	1.88 (0.05)	2.09 (0.17)	157.6 (11.1)	-36.4 (66.7)	...	...	...
SN 2005ms	−1.88	0.88 (0.04)	0.84 (0.08)	139.1 (7.2)	-43.5 (66.1)	...	...	...
SN 2005ms	14.62	0.15 (0.01)	0.25 (0.02)	332.8 (14.8)	7.6 (67.4)	11.24 (0.07)	0.915 (0.026)	390.2 (2.4)
SN 2005na	17.49	0.13 (0.01)	0.32 (0.01)	234.0 (12.9)	-131.8 (67.0)	...	...	...
SN 2006D	3.70	4.62 (0.03)	4.27 (0.04)	200.9 (9.8)	-12.6 (66.4)	12.70 (0.07)	0.660 (0.009)	313.3 (2.4)
SN 2006H	7.01	0.19 (0.01)	0.20 (0.01)	352.4 (16.4)	112.4 (67.7)	12.15 (0.21)	0.945 (0.016)	366.9 (2.4)
SN 2006N	−1.89	1.00 (0.02)	0.92 (0.02)	102.4 (4.9)	-80.1 (65.9)	...	...	...
SN 2006N	−0.90	0.52 (0.01)	0.54 (0.01)	158.3 (8.0)	-28.4 (66.2)	10.67 (0.07)	0.522 (0.019)	272.1 (2.4)
SN 2006N	11.91	0.34 (0.02)	0.58 (0.02)	213.4 (10.3)	-77.7 (66.5)	...	...	...
SN 2006S	18.45	0.08 (0.00)	0.15 (0.01)	262.3 (12.5)	-118.2 (66.9)	...	...	...
SN 2006X	3.15	4.65 (0.02)	7.19 (0.03)	303.6 (13.9)	94.0 (67.2)	16.14 (0.07)	0.816 (0.009)	372.1 (2.4)
SN 2006ac	7.96	0.28 (0.00)	0.39 (0.01)	341.6 (15.8)	92.8 (67.6)	12.76 (0.07)	0.924 (0.010)	365.6 (2.4)
SN 2006ak	8.43	0.15 (0.00)	0.17 (0.00)	173.9 (7.7)	-79.5 (66.2)	13.15 (0.07)	0.458 (0.019)	369.9 (2.4)
SN 2006bq	6.97	1.16 (0.02)	1.37 (0.02)	273.2 (12.3)	33.5 (66.9)	...	...	...
SN 2006bq	14.55	0.21 (0.01)	0.40 (0.01)	368.6 (15.7)	44.4 (67.6)	13.90 (0.07)	0.844 (0.028)	436.4 (2.4)
SN 2006bq	14.64	0.07 (0.01)	0.20 (0.02)	488.5 (22.0)	163.1 (69.3)	15.61 (0.30)	1.251 (0.060)	397.3 (2.4)
SN 2006br	10.62	0.09 (0.01)	0.16 (0.01)	339.8 (15.7)	63.5 (67.6)	...	...	...
SN 2006bt	−5.30	0.19 (0.00)	0.14 (0.00)	208.3 (9.2)	35.8 (66.4)	15.11 (0.07)	0.515 (0.011)	418.5 (2.4)
SN 2006bt	−4.53	0.17 (0.00)	0.13 (0.01)	202.7 (9.2)	28.5 (66.4)	14.89 (0.07)	0.532 (0.022)	397.2 (2.4)
SN 2006bt	2.27	0.15 (0.00)	0.13 (0.00)	254.1 (11.4)	50.2 (66.7)	...	...	...
SN 2006bw	8.90	0.12 (0.00)	0.15 (0.01)	300.1 (13.0)	42.0 (67.0)	...	...	...
SN 2006bz	−2.44	0.16 (0.01)	0.12 (0.01)	332.7 (15.4)	152.2 (67.5)	13.88 (0.07)	0.966 (0.021)	346.3 (2.4)
SN 2006cm	6.77	0.23 (0.01)	0.30 (0.01)	125.1 (6.4)	-112.9 (66.0)	...	...	...
SN 2006dm	8.73	0.26 (0.00)	0.37 (0.01)	292.7 (12.9)	36.2 (67.0)	...	...	...
SN 2006dm	14.61	0.19 (0.01)	0.25 (0.01)	327.1 (14.4)	2.2 (67.3)	11.59 (0.16)	0.847 (0.045)	362.0 (2.4)
SN 2006ef	3.20	0.43 (0.01)	0.52 (0.01)	151.9 (8.1)	-58.0 (66.2)	10.73 (0.07)	0.546 (0.014)	279.0 (2.4)
SN 2006ej	−3.70	0.54 (0.01)	0.43 (0.00)	136.9 (6.9)	-39.5 (66.1)	...	...	...
SN 2006ej	5.09	0.22 (0.01)	0.24 (0.01)	209.1 (10.7)	-14.8 (66.6)	11.57 (0.07)	0.677 (0.027)	319.5 (2.4)
SN 2006em	4.16	0.25 (0.00)	0.19 (0.00)	286.0 (13.2)	69.3 (67.0)	12.34 (0.13)	0.806 (0.013)	323.8 (2.4)
SN 2006eu	10.17	0.20 (0.01)	0.23 (0.01)	385.7 (15.3)	114.3 (67.5)	...	...	...
SN 2006eu	16.02	0.21 (0.00)	0.20 (0.00)	401.2 (15.9)	56.9 (67.6)	9.93 (0.07)	0.814 (0.016)	537.3 (2.4)
SN 2006et	9.14	0.19 (0.00)	0.24 (0.01)	227.3 (10.4)	-33.2 (66.5)	11.92 (0.07)	0.648 (0.008)	322.8 (2.4)
SN 2006ev	10.54	0.13 (0.00)	0.17 (0.01)	279.8 (12.9)	4.4 (67.0)	...	...	...
SN 2006gj	4.70	0.13 (0.01)	0.16 (0.01)	242.0 (11.9)	21.2 (66.8)	...	...	...
SN 2006gt	3.08	0.10 (0.01)	0.07 (0.01)	228.2 (11.7)	19.1 (66.8)	...	...	...
SN 2006ke	2.36	0.16 (0.01)	0.15 (0.00)	189.2 (8.2)	-15.2 (66.2)	...	...	...
SN 2006ke	8.38	0.15 (0.00)	0.15 (0.00)	297.8 (13.8)	44.8 (67.1)	12.59 (0.07)	0.837 (0.015)	342.1 (2.4)
SN 2006kf	−8.96	0.15 (0.00)	0.14 (0.00)	157.3 (6.8)	-11.8 (66.1)	...	...	...
SN 2006kf	17.37	0.14 (0.00)	0.17 (0.01)	392.7 (14.3)	28.7 (67.3)	11.67 (0.07)	0.777 (0.021)	518.9 (2.4)
SN 2006le	−8.69	0.27 (0.00)	0.24 (0.00)	154.3 (7.6)	-14.8 (66.2)	...	...	...
SN 2006le	11.92	0.26 (0.01)	0.46 (0.02)	265.6 (12.1)	-25.6 (66.8)	...	...	...
SN 2006lf	−6.30	0.37 (0.01)	0.33 (0.00)	141.2 (6.1)	-29.7 (66.0)	13.43 (0.07)	0.390 (0.015)	329.6 (2.4)
SN 2006mp	5.66	0.25 (0.00)	0.28 (0.01)	135.5 (6.2)	-93.0 (66.0)	...	...	...
SN 2006or	−2.79	0.26 (0.00)	0.32 (0.01)	198.0 (9.2)	18.7 (66.4)	13.49 (0.07)	0.535 (0.008)	366.4 (2.4)

Continued on Next Page...

Table 3.14 — Continued

SN Name	Phase[a]	F_b[b]	F_r[b]	pEW[c]	ΔpEW[c,d]	v[e]	a	FWHM[c]
SN 2006or	4.93	0.10 (0.00)	0.19 (0.01)	268.4 (11.8)	45.8 (66.8)	...	...	...
SN 2006os	8.61	0.09 (0.00)	0.11 (0.00)	257.3 (12.9)	2.1 (67.0)	13.59 (0.07)	0.837 (0.018)	350.5 (2.4)
SN 2006sr	−2.34	0.29 (0.01)	0.24 (0.00)	109.3 (5.5)	-71.6 (66.0)	13.14 (0.07)	0.398 (0.019)	251.9 (2.4)
SN 2006sr	2.69	0.34 (0.01)	0.36 (0.01)	161.4 (8.2)	-45.1 (66.2)	12.28 (0.07)	0.538 (0.006)	294.9 (2.4)
SN 2007A	2.37	0.58 (0.01)	0.63 (0.01)	66.4 (4.1)	-138.1 (65.9)	...	...	...
SN 2007A	15.07	0.33 (0.01)	0.53 (0.01)	251.7 (11.4)	-79.5 (66.7)	...	...	...
SN 2007F	3.23	0.35 (0.00)	0.37 (0.01)	122.1 (6.2)	-88.0 (66.0)	...	...	...
SN 2007O	−0.33	3.71 (0.07)	3.71 (0.10)	126.1 (7.8)	-63.3 (66.2)	...	...	...
SN 2007N	0.44	2.21 (0.03)	2.28 (0.03)	405.1 (23.7)	211.8 (69.9)	17.86 (0.07)	0.857 (0.006)	492.0 (1.2)
SN 2007af	−1.25	6.26 (0.06)	6.01 (0.03)	191.8 (9.0)	6.6 (66.3)	12.51 (0.07)	0.578 (0.008)	288.4 (2.4)
SN 2007af	2.84	5.63 (0.03)	6.59 (0.05)	224.8 (15.4)	17.3 (67.5)	...	...	...
SN 2007af	3.81	5.51 (0.04)	6.17 (0.06)	223.5 (10.7)	9.2 (66.6)	...	...	...
SN 2007aj	10.75	0.11 (0.00)	0.19 (0.01)	299.9 (13.4)	22.1 (67.1)	13.42 (0.07)	0.760 (0.014)	351.5 (2.4)
SN 2007al	3.39	0.43 (0.01)	0.34 (0.01)	276.7 (12.6)	65.4 (66.9)	11.39 (0.07)	0.772 (0.007)	345.8 (2.4)
SN 2007ap	9.37	6.83 (0.11)	9.05 (0.16)	249.3 (15.7)	-13.7 (67.6)	...	...	...
SN 2007au	16.11	0.35 (0.01)	0.34 (0.01)	382.5 (15.7)	36.8 (67.6)	...	...	...
SN 2007ax	14.93	1.21 (0.03)	1.31 (0.02)	338.0 (14.3)	8.7 (67.3)	...	...	...
SN 2007ba	2.14	0.17 (0.01)	0.17 (0.01)	295.9 (14.0)	92.9 (67.2)	12.44 (0.07)	0.829 (0.029)	352.4 (2.4)
SN 2007ba	5.18	1.64 (0.05)	1.66 (0.12)	285.4 (18.2)	60.8 (68.2)	12.46 (0.07)	0.789 (0.011)	353.0 (1.2)
SN 2007ba	8.06	0.98 (0.02)	1.04 (0.06)	278.1 (17.8)	28.2 (68.1)	12.82 (0.07)	0.782 (0.012)	342.0 (1.2)
SN 2007bc	0.61	0.46 (0.01)	0.44 (0.01)	180.8 (8.4)	-13.3 (66.3)	...	...	...
SN 2007bj	14.25	0.30 (0.01)	0.51 (0.02)	181.8 (9.7)	-138.5 (66.4)	13.59 (0.07)	0.650 (0.040)	304.9 (2.4)
SN 2007bm	15.03	1.64 (0.02)	2.50 (0.02)	299.4 (12.9)	-31.2 (67.0)	...	...	...
SN 2007bm	19.96	2.73 (0.02)	3.41 (0.03)	384.7 (14.6)	-19.7 (67.3)	...	...	...
SN 2007bz	1.65	0.34 (0.01)	0.34 (0.01)	95.1 (5.3)	-105.0 (65.9)	...	...	...
SN 2007ca	−11.14	0.40 (0.01)	0.41 (0.01)	130.0 (6.1)	-40.7 (66.0)	...	...	...
SN 2007ca	16.46	0.31 (0.01)	0.72 (0.05)	312.7 (14.2)	-37.9 (67.2)	...	...	...
SN 2007ci	−6.57	0.36 (0.01)	0.31 (0.01)	177.3 (8.2)	6.9 (66.2)	13.38 (0.07)	0.522 (0.018)	375.2 (2.4)
SN 2007ci	−1.71	0.46 (0.01)	0.41 (0.01)	150.3 (7.5)	-33.0 (66.2)	11.52 (0.07)	0.527 (0.010)	257.3 (2.4)
SN 2007ci	13.99	0.55 (0.01)	0.57 (0.01)	304.6 (13.5)	-12.2 (67.1)	11.30 (0.07)	0.788 (0.013)	339.8 (2.4)
SN 2007co	−4.09	0.25 (0.01)	0.23 (0.01)	248.7 (10.9)	73.3 (66.6)	18.61 (0.07)	0.656 (0.012)	426.5 (2.4)
SN 2007co	0.85	0.21 (0.00)	0.23 (0.01)	227.0 (10.4)	31.5 (66.5)	14.31 (0.07)	0.621 (0.007)	397.3 (2.4)
SN 2007co	9.55	0.13 (0.00)	0.21 (0.01)	346.5 (15.5)	81.7 (67.5)	13.38 (0.07)	0.884 (0.011)	395.3 (2.4)
SN 2007cq	15.57	0.18 (0.01)	0.31 (0.01)	284.0 (12.2)	-54.1 (66.9)	12.02 (0.07)	0.754 (0.016)	349.0 (2.4)
SN 2007cs	12.15	0.88 (0.01)	0.84 (0.01)	307.3 (13.5)	13.3 (67.1)	...	...	...
SN 2007fb	1.95	0.91 (0.02)	0.91 (0.02)	149.7 (7.6)	-52.2 (66.2)	12.63 (0.07)	0.531 (0.018)	257.4 (2.4)
SN 2007fb	14.63	0.28 (0.01)	0.45 (0.01)	265.3 (11.3)	-60.0 (66.7)	...	...	...
SN 2007fr	−5.83	0.07 (0.00)	0.04 (0.01)	188.7 (9.4)	17.2 (66.4)	14.41 (0.11)	0.599 (0.040)	329.2 (2.3)
SN 2007fr	−1.25	0.06 (0.00)	0.05 (0.01)	200.5 (11.0)	15.3 (66.6)	13.09 (0.07)	0.799 (0.041)	353.9 (2.3)
SN 2007fs	5.03	0.69 (0.01)	0.79 (0.01)	204.4 (10.0)	-19.0 (66.5)	11.88 (0.07)	0.648 (0.009)	302.8 (2.4)
SN 2007gi	−0.35	6.94 (0.04)	7.24 (0.04)	244.2 (11.7)	54.9 (66.8)	16.02 (0.07)	0.726 (0.003)	344.3 (2.4)
SN 2007gi	6.61	3.33 (0.03)	4.19 (0.04)	324.9 (14.5)	88.4 (67.3)	14.92 (0.07)	0.823 (0.013)	412.0 (2.4)
SN 2007gk	−1.72	0.29 (0.00)	0.26 (0.01)	284.1 (12.3)	100.8 (66.9)	15.78 (0.07)	0.693 (0.012)	444.2 (2.4)
SN 2007gk	19.65	0.18 (0.01)	0.22 (0.01)	494.2 (18.8)	94.7 (68.4)	13.29 (0.07)	0.946 (0.017)	551.3 (2.4)
SN 2007hj	−1.23	0.81 (0.01)	0.73 (0.01)	279.4 (12.7)	94.1 (66.9)	13.41 (0.07)	0.731 (0.009)	374.7 (2.4)
SN 2007hj	12.53	0.57 (0.01)	0.73 (0.01)	347.8 (14.7)	49.3 (67.4)	...	...	...
SN 2007kk	7.15	0.44 (0.02)	0.56 (0.02)	230.1 (11.5)	-11.3 (66.7)	14.00 (0.07)	0.711 (0.013)	343.9 (2.4)
SN 2007le	7.43	3.10 (0.03)	3.96 (0.03)	236.1 (11.7)	-7.9 (66.8)	...	...	...
SN 2007le	16.39	1.97 (0.02)	4.15 (0.04)	366.5 (16.3)	16.9 (67.7)	...	...	...
SN 2007le	17.37	1.91 (0.01)	3.98 (0.03)	363.6 (16.5)	-0.4 (67.8)	...	...	...
SN 2007s1[f]	−1.23	0.25 (0.00)	0.26 (0.01)	257.5 (11.3)	72.2 (66.7)	...	...	...
SN 2007on	−3.01	8.45 (0.07)	6.33 (0.04)	231.0 (10.2)	52.4 (66.5)	12.89 (0.07)	0.627 (0.011)	365.6 (2.4)
SN 2007on	15.45	35.29 (0.36)	35.53 (0.30)	318.0 (15.1)	-18.5 (67.4)	...	...	...
SN 2007qe	6.23	0.36 (0.01)	0.48 (0.01)	260.6 (12.6)	27.3 (66.9)	15.15 (0.07)	0.778 (0.020)	339.8 (2.4)
SN 2007qe	16.00	0.19 (0.02)	0.42 (0.02)	359.9 (16.7)	15.8 (67.8)	...	...	...
SN 2008C	15.68	0.47 (0.01)	0.73 (0.01)	261.8 (11.2)	-77.9 (66.7)	12.07 (0.07)	0.634 (0.013)	389.5 (2.4)
SN 2008Q	6.46	5.03 (0.06)	5.37 (0.04)	237.5 (10.6)	2.3 (66.6)	...	...	...
SN 2008Q	19.25	3.81 (0.04)	4.48 (0.07)	353.2 (9.8)	-39.7 (66.4)	...	...	...
SN 2008Z	9.99	0.19 (0.01)	0.25 (0.01)	191.2 (6.5)	-78.3 (66.0)	13.73 (0.07)	0.590 (0.011)	286.0 (4.8)
SN 2008bt	−1.08	0.65 (0.03)	0.55 (0.03)	147.0 (7.7)	-38.9 (66.2)	13.06 (0.07)	0.520 (0.019)	321.1 (2.4)
SN 2008bt	10.97	0.44 (0.01)	0.41 (0.01)	341.7 (14.8)	61.5 (67.4)	13.14 (0.07)	0.862 (0.007)	358.5 (2.4)
SN 2008s1[g]	−6.36	0.36 (0.00)	0.27 (0.00)	83.9 (4.2)	-86.9 (65.9)	...	...	...
SN 2008s1[g]	−4.40	0.43 (0.03)	0.36 (0.02)	74.1 (4.8)	-100.4 (65.9)	...	...	...
SN 2008s1[g]	0.49	0.39 (0.02)	0.37 (0.03)	175.3 (9.3)	-18.2 (66.4)	...	...	...
SN 2008s1[g]	4.40	0.30 (0.01)	0.31 (0.01)	175.8 (9.0)	-42.8 (66.3)	11.47 (0.07)	0.605 (0.018)	295.5 (2.4)
SN 2008s1[g]	5.38	0.30 (0.01)	0.31 (0.01)	199.8 (9.7)	-26.4 (66.4)	12.40 (0.07)	0.652 (0.015)	309.2 (2.4)
SN 2008s1[g]	15.37	0.14 (0.01)	0.32 (0.01)	258.0 (13.4)	-77.3 (67.1)	...	...	...
SN 2008dx	2.46	0.17 (0.00)	0.14 (0.01)	257.5 (12.1)	52.5 (66.8)	...	...	...
SN 2008dx	7.33	0.17 (0.01)	0.16 (0.02)	293.7 (13.5)	50.6 (67.1)	11.96 (0.07)	0.904 (0.053)	306.9 (2.4)
SN 2008dx	10.28	0.29 (0.01)	0.25 (0.01)	303.4 (13.4)	30.8 (67.1)	...	...	...
SN 2008ec	−0.24	0.76 (0.01)	0.69 (0.01)	126.7 (6.6)	-63.1 (66.1)	...	...	...
SN 2008ec	5.70	0.46 (0.01)	0.56 (0.02)	340.9 (16.9)	112.1 (67.9)	11.62 (0.07)	1.139 (0.017)	289.3 (2.4)
SN 2008ec	12.51	0.46 (0.01)	0.65 (0.01)	267.4 (11.8)	-30.9 (66.8)	...	...	...
SN 2008ei	3.29	0.09 (0.00)	0.10 (0.01)	278.7 (13.7)	68.2 (67.1)	14.99 (0.07)	0.838 (0.023)	366.2 (2.4)
SN 2008ei	9.13	0.06 (0.01)	0.09 (0.01)	507.8 (22.9)	247.4 (69.6)	15.13 (0.07)	1.344 (0.046)	391.3 (2.4)
SN 2008s5[h]	8.96	0.21 (0.00)	0.28 (0.01)	176.4 (8.0)	-82.3 (66.2)	...	...	...
SN 2008s5[h]	15.76	0.13 (0.00)	0.24 (0.01)	278.7 (11.6)	-62.0 (66.7)	11.87 (0.07)	0.664 (0.026)	444.2 (2.4)
SN 2008hs	−7.94	0.31 (0.01)	0.22 (0.01)	217.0 (9.7)	47.7 (66.4)	14.66 (0.07)	0.625 (0.018)	330.3 (2.4)

Uncertainties for each measured value are given in parentheses.
[a]Phases of spectra are in rest-frame days using the heliocentric redshift and photometry reference presented in table 1 of Silverman et al. (submitted).

Continued on Next Page...

Table 3.14 — Continued

SN Name	Phase[a]	F_b[b]	F_r[b]	pEW[c]	ΔpEW[c,d]	v[e]	a	FWHM[c]

[b] Fluxes are in units of 10^{-15} erg s^{-1} cm^{-2} Å^{-1}.
[c] The pEW, ΔpEW, and FWHM are in units of Å.
[d] ΔpEW is the measured pEW minus the expected pEW at the same epoch using our linear or quadratic fit (see Section 3.5.4 for more information).
[e] The expansion velocity is in units of 1000 km s^{-1}.
[f] Also known as SNF20071021-000.
[g] Also known as SNF20080514-002.
[h] Also known as SNF20080909-030.

Chapter 4

Berkeley Supernova Ia Program III: Analysis of Spectra Obtained Near Maximum Brightness and Photometry, or, Spectra Improve the Accuracy of Distances to Type Ia Supernovae

If I have seen a little further it is by standing on the shoulders of Giants.
—Sir Isaac Newton

4.1 Introduction

Type Ia supernovae (SNe Ia) have been used in the recent past to measure cosmological parameters (e.g., Astier et al. 2006; Riess et al. 2007; Wood-Vasey et al. 2007; Hicken et al. 2009a; Kessler et al. 2009; Amanullah et al. 2010; Suzuki et al. 2011), as well as discover the accelerating expansion of the Universe (Riess et al. 1998; Perlmutter et al. 1999). In the most general terms, thermonuclear explosions of C/O white dwarfs (WDs) are thought to give rise to SNe Ia (e.g., Hoyle & Fowler 1960; Colgate & McKee 1969; Nomoto et al. 1984; see Hillebrandt & Niemeyer 2000 for a review). However, after decades of observations and theoretical work, a detailed understanding of both the SN progenitors and explosion mechanisms is still missing. In addition, there is very little known how the differences in initial conditions in SNe Ia give rise to the measured range of observables. A large, self-consistent dataset is needed in order to solve these problems.

The ability to do precision cosmology using SNe Ia requires that one is able to calibrate

or standardize their luminosity. Phillips (1993) showed a tight correlation between light-curve decline rate and luminosity at peak brightness for the majority of SNe Ia, the so-called "Phillips relation." However, the addition of spectral observations to the light-curve data complicates the picture far beyond the simple assumption underlying the "Phillips relation." Many comparisons of spectral and photometric data of low-redshift SNe Ia have been performed in the past (e.g., Nugent et al. 1995; Benetti et al. 2005; Bongard et al. 2006; Hachinger et al. 2006; Arsenijevic et al. 2008; Walker et al. 2011; Nordin et al. 2011b; Blondin et al. 2011; Chotard et al. 2011). In addition, there has been similar work with SNe Ia at higher redshifts (e.g., Blondin et al. 2006; Altavilla et al. 2009; Nordin et al. 2011b; Walker et al. 2011). These studies often aimed to find a "second parameter" in SN Ia spectral or photometric data which would increase the accuracy of their distance measurements.

Most of these previous studies utilized relatively small and heterogeneous datasets. The data studied here were self-consistently observed and reduced, and constitute one of the largest datasets to be analyzed in this manner. Low-redshift ($z \leq 0.1$) optical SN Ia spectra from the Berkeley Supernova Ia Program (BSNIP; Chapter 2) are used along with complementary photometric data, largely from Ganeshalingam et al. (2010). The spectral features have been accurately and robustly measured (BSNIP II; Chapter 3) and the light curves have been fit using a variety of methods (Ganeshalingam et al. in preparation).

We summarize both the spectral and photometric datasets used for this analysis in Section 4.2 and we describe our procedure for measuring spectral features, fitting light curves, and producing Hubble diagrams in Section 4.3. How these measured values correlate with each other and with previously determined classifications is presented in Section 4.4, along with our Hubble diagram results using various models for the distances to SNe Ia. We present our conclusions in Section 4.5 where the main results of our analysis are summarized and the most accurate and useful spectral indicators are discussed. Other BSNIP papers in the near future will expand on the analysis performed here with the addition of host-galaxy properties and late-time SN spectra.

4.2 Dataset

4.2.1 Spectral Data

The same SN Ia spectral data are used in the current study as were used in BSNIP II. The spectra are all originally published in BSNIP I. Most of the spectra were obtained using the Shane 3 m telescope at Lick Observatory with the Kast double spectrograph (Miller & Stone 1993), and the typical wavelength coverage is 3300–10,400 Å with resolutions of ∼11 and ∼6 Å on the red and blue sides (crossover wavelength ∼5500 Å), respectively. For more information regarding the observations and data reduction, see BSNIP I.

In BSNIP II, we required that a spectrum be within 20 d (rest frame) of maximum brightness and we *a priori* ignored the extremely peculiar SN 2000cx (e.g., Li et al. 2001c), SN 2002cx (e.g., Li et al. 2003b; Jha et al. 2006a), SN 2005hk (e.g., Chornock et al. 2006;

Phillips et al. 2007), and SN 2008ha (e.g., Foley et al. 2009a; Valenti et al. 2009). BSNIP II contains 432 spectra of 261 SNe Ia with a "good" fit for at least one spectral feature. However, only a subset of these data are used in the current study since not all of them have reliable photometric observations and we are currently only considering spectra within 5 d of maximum brightness. It was shown in BSNIP II that the spectral measurements do not evolve significantly during these epochs. For the 11 SNe Ia that had more than one spectrum within 5 d of maximum brightness and photometric information, we only use the spectrum closest to the date of maximum in the current analysis.

4.2.2 Photometric Data

A majority of the SNe in our spectral sample were discovered as part of the Lick Observatory Supernova Search (LOSS). LOSS is a transient survey utilizing the 0.76-m Katzman Automatic Imaging Telescope (KAIT) at Lick Observatory (Li et al. 2000; Filippenko et al. 2001; see also Filippenko, Li, & Treffers 2012, in preparation). KAIT is a robotic telescope that monitors a sample of ∼15,000 galaxies in the nearby Universe (redshift $z < 0.05$) with the goal of finding transients within days of explosion. Fields are imaged every 3–10 d and compared to archived template images, after which potential new transients are flagged. These images are examined by human image checkers and the best candidates are reobserved the following night. Candidates that are present on two consecutive nights are reported to the community using the International Astronomical Union Circulars (IAUCs) and the Central Bureau of Electronic Telegrams (CBETs). The statistical power of the LOSS sample is well demonstrated by the series of papers deriving the nearby SN rates (Leaman et al. 2011; Li et al. 2011a,b).

In addition to the SN search, KAIT monitors active SNe of all types in broad-band *BVRI* filters. The first data release of *BVRI* light curves for 165 SNe Ia along with details about the reduction procedure have been published by Ganeshalingam et al. (2010). In summary, point-spread function (PSF) fitting photometry is performed on images from which the host galaxy has been subtracted using templates obtained > 1 yr after explosion. Photometry is transformed to the Landolt system (Landolt 1983, 1992) using averaged color terms determined over many photometric nights. Calibrations for each SN field are obtained on photometric nights with an average of 5 calibrations per field.

We also include SN Ia light curves obtained from the literature to maximise the overlap between our photometric and spectroscopic samples. We include 29 objects from the Calán-Tololo sample (Hamuy et al. 1996b), 22 objects from the CfA1 sample (Riess et al. 1999b), 44 objects from CfA2 (Jha et al. 2006b), and 185 objects from CfA3 (Hicken et al. 2009b). In instances where we have data for the same SN from multiple samples, we use the light curve that is most densely sampled and best caputres the light-curve evolution. We also include light curves for SNe 1999aw (Strolger et al. 2002), 1999ee, 2000bh, 2000ca, 2001ba (Krisciunas et al. 2004a), 2001bt, 2001cn, and 2001cz (Krisciunas et al. 2004b). Our final photometry sample consists of 335 multi-color light curves, though we note that not all the

objects in this sample have corresponding spectroscopy.

Of the data within 5 d of maximum brightness investigated in BSNIP II, 115 SNe have light-curve width or color information and are included in the present study. The redshift range spanned by this sample is $0 < z < 0.1$. A complete list of these SNe Ia, their ages, spectral classifications, and spectral feature measurements can be found in BSNIP II. The photometric parameters of these objects can be found in Ganeshalingam et al. (in preparation).

4.3 Measurement Procedures

4.3.1 Spectral Measurements

The algorithm used to measure each of nine spectral features and the features themselves are described in detail in BSNIP II. Here we give a brief summary of the procedure.

Each spectrum has its host-galaxy recession velocity removed and is corrected for Galactic reddening (according to the values presented in Table 1 of BSNIP I), and it is smoothed using a Savitzky–Golay smoothing filter (Savitzky & Golay 1964). If the signal-to-noise ratio (S/N) is larger than 6.5 pixel^{-1} over the entire spectral range, we attempt to define a pseudo-continuum for each spectral feature. This is done by determining where the local slope changes sign on either side of the feature's minimum. Quadratic functions are fit to each of these endpoints and the peaks of the parabolas (assuming that they are both concave downward) are used as the endpoints of the feature; they are then connected with a line to define the pseudo-continuum. We record the flux at the blue and red endpoints of the feature (F_b and F_r, respectively) as well as the pseudo-equivalent width (pEW; e.g., Garavini et al. 2007).

Once a pseudo-continuum is calculated, a cubic spline is fit to the smoothed data between the endpoints of the spectral feature.[1] From the wavelength at which the spline fit reaches its minimum ($\lambda_{\rm min}$) the expansion velocity (v) is calculated. The flux is then normalized to the pseudo-continuum, and the relative depth of the feature (a) and its full-width at half-maximum (FWHM) are computed. Finally, every spectral feature in every spectrum is visually inspected by more than one person and removed from the study if the spline fit and/or pseudo-continuum do not accurately reflect the spectral feature.

4.3.2 Light-Curve Fitting

A variety of methods have been developed to measure the photometric properties of SN Ia light curves. Here, we describe three different light-curve fitting methods adopted in this chapter to characterise the SN Ia light curves. While the light-curve parameters

[1]No attempt is made to fit any of the Mg II or Fe II features in this manner since these complexes consist of so many blended spectral lines that it is unclear which reference wavelength to use when attempting to define an expansion velocity.

derived from each of these methods are degenerate to some extent, it is useful to perform all three fitting techniques for the purpose of comparing our results to previous results in the literature. There are also cases, for certain spectroscopic subtypes, where one method is superior to the other two.

Template and Polynomial Fitting

Our most direct measurement of light-curve properties makes use of the template-fitting routine introduced by Prieto et al. (2006). For a given photometric bandpass, a set of template light curves is used to construct models which match the light-curve data. The model light curves are linear combinations of the template light curves using the weighting scheme described by Ganeshalingam et al. (2010). A χ^2-minimization fitting routine is used to determine the combination of templates that best fits the data. For band X, we measure the date of maximum brightness, the apparent peak magnitude (m_X), and the light-curve width parametrized as the difference in magnitudes between maximum and fifteen days past maximum, $\Delta m_{15}(X)$. We independently fit the B- and V-band light curves for the SNe in our sample.

In instances where we have a well-sampled light curve, but cannot achieve an acceptable fit with our template-fitting routine, we fit the data with a fourth-order polynomial.

For both the template- and polynomial-fitting routines, we use a Monte Carlo routine to measure the uncertainty in our derived parameters. We simulate realizations of our dataset by randomly perturbing each data point by its 1σ photometric error assuming a Gaussian distribution centered at 0 mag. We fit the dataset realization with our fitting routine and measure light-curve properties for that simulation. We estimate the uncertainty in our derived parameters to be the standard deviation of 50 dataset realizations.

MLCS2k2

The Multi-color Light Curve Shape (MLCS) distance-fitting software was first introduced by Riess et al. (1996) to simultaneously fit all light-curve data for a given SN Ia to produce a distance estimate. This method relies on the observation that brighter SNe Ia have broader light curves (Phillips 1993) and also have bluer colors during the photospheric phase. MLCS parametrizes light-curve width using the parameter Δ, which measures the difference in absolute magnitude of the SN with reference to a fiducial SN Ia. MLCS attempts to disentangle intrinsic color variations from host-galaxy effects to also produce an estimate for host-galaxy extinction, A_V. MLCS2k2.v006 (referred to as simply MLCS2k2 for the rest of this work; Jha et al. 2007) is the the most current publicly available implementation of this fitting routine. It has an expanded set of training templates and improvements in the treatment of host reddening and K-corrections in comparison to the original version.

For our analysis with MLCS2k2 we use the Galactic line of sight prior which models the distribution of host-galaxy extinction values as a decaying exponential with a peak value of 0 mag (Hatano et al. 1998). We also set the host-galaxy $R_V = 1.7$ based on the cosmological

analysis of Hicken et al. (2009a). Their analysis found that a lower host-galaxy R_V reduced the scatter in the Hubble diagram compared to a more typical Galactic value of $R_V = 3.1$. A fit using MLCS2k2 is considered reliable (and thus its parameters are used in the current analysis) only when the reduced $\chi^2 \leq 1.6$.

SALT2

Spectral Adaptive Light curve Template (SALT) was first developed by the SuperNova Legacy Survey (SNLS) (Guy et al. 2005). Calculating distances with SALT is a two-step process. SALT first measures light-curve parameters that are expected to correlate with the intrinsic brightness of individual SNe (i.e., light-curve width and color). Then a model for the corrected apparent magnitude of a SN, $m_{B,\mathrm{corr}}$, is adopted which applies linear corrections for the light-curve width and color to the measured apparent magnitude, m_B. Thus, the corrected apparent magnitude has the form

$$m_{B,\mathrm{corr}} = m_B + \alpha \times (\text{light-curve width}) - \beta \times (\text{color}). \tag{4.1}$$

The constants α and β are found by minimizing χ^2 using distance estimates from a large sample of SNe Ia compared to a cosmological model (see Section 4.3.3 for more details). Unlike MLCS2k2, SALT avoids making assumptions on host-galaxy extinction and the intrinsic reddening of SNe.

SALT2 is an updated version of SALT with an expanded training set of light-curve templates and is the version implemented here. SALT2 is trained on light curves and spectra from low-z SNe compiled from the literature and high-z SNe from the first two years of the SNLS (Guy et al. 2007). SALT2 measures a parametrization of the light-curve width (x_1), the SN color (c), and the apparent B-band magnitude at maximum light (m_B).

In fitting our data, we exclude I-band data, which are not included in the SALT2 template set. We also exclude subluminous SNe Ia, often of the spectral subclass of SN 1991bg-like objects (e.g., Filippenko et al. 1992b), since SALT2 was not developed to fit this particular subtype. This is achieved by using only SNe Ia with $-3 \leq x_1 \leq 2$ (as in Blondin et al. 2011). Finally, the results of SALT2 fits are utilized here only when the reduced $\chi^2 < 2$.

4.3.3 Hubble Diagrams

In this section we present the methodology used to standardize SNe Ia for cosmological application. We use a model that applies linear corrections for light-curve width and color. The width of a light curve correlates with the intrinsic luminosity in the sense that SNe with broader light curves are also more luminous. This correlation has been well-established (Phillips 1993). The color parameter combines the effects of intrinsic color variations and host-galaxy reddening. We use the SALT2 parameters x_1 and c as the parametrizations of light-curve width and SN color, respectively. We will also generalize this approach to allow for linear corrections using spectroscopic parameters.

The distance modulus for each SN can be estimated from its redshift by $\mu(z) = 25 + 5\log_{10}[D_L(z)]$, where D_L is the luminosity distance expressed in units of Mpc. The distance modulus including linear corrections for light-curve width and color can be expressed as

$$\mu_{\rm SN} = m_B - M + \alpha x_1 - \beta c. \tag{4.2}$$

The variables α, β, and M (the fiducial absolute magnitude of a SN Ia) are determined by using a custom version of `cosfitter` (A. Conley 2011, priv. comm.) based on the `Minuit` minimization package (James & Roos 1975). The software minimizes the function

$$\chi^2 = \sum_{s=1}^{N} \frac{(\mu(z_s) - \mu_{{\rm SN},s})^2}{\sigma^2_{{\rm m},s} + \sigma^2_{{\rm pec},s} + \sigma^2_{\rm int}}, \tag{4.3}$$

where $\mu(z)$ is the distance modulus of the galaxy in the CMB rest-frame redshift z, $\sigma_{\rm m}$ is the measurement error in light-curve properties accounting for covariances between measured parameters, $\sigma_{\rm pec}$ is the uncertainty due to deviations from Hubble's law induced by gravitational interactions from neighbouring galaxies, and $\sigma_{\rm int}$ is a constant intrinsic scatter added to each SN to achieve a reduced $\chi^2 \approx 1$. We adopt 300 km s^{-1} as the peculiar velocity for each SN. The intrinsic scatter, $\sigma_{\rm int}$, can be considered as the uncertainty associated with a model that attempts to standardize SNe using the parameters x_1 and c.

Only objects with $z_{\rm helio} > 0.01$ are used in the Hubble diagrams in order to avoid including SNe with motions dominated by peculiar velocities. We also adopt the same Hubble diagram color cut as Blondin et al. (2011) who exclude objects with $c > 0.50$. Finally, as mentioned above, all analysis using SALT2 fits is restricted to objects with a reduced $\chi^2 < 2$.

In this work we consider nearby SNe (median $z_{\rm cmb} \approx 0.021$) and are not attempting to find a best-fitting cosmology. A goal of this study is to combine photometric and spectroscopic properties such that SNe Ia become more accurate standardizable candles. We also aim to quantify the amount of improvement when using a variety of observed measurements. To that end, we adopt the standard ΛCDM cosmology with $\Omega_{\rm m} = 0.27$, $\Omega_\Lambda = 0.73$, and $w = -1$ when calculating $\mu(z)$.

Models for Predicting SN Ia Distances

Here we describe the generalization of our calculation of the distance modulus for each SN to allow for linear corrections using measured spectral parameters (such as velocity and pEW; see Sections 4.4.2 and 4.4.4) or the ratios of pEWs and fluxes (such as $\Re$(Si II) and $\mathcal{R}$; see Sections 4.4.5 and 4.4.10). We consider 5 models for predicting distances to SNe Ia using combinations of the SALT2 measured light-curve parameters (x_1 and c) and spectral

measurements:

$$\mu_{\rm SN} = m_B - M + \gamma\mathcal{S}, \tag{4.4}$$
$$\mu_{\rm SN} = m_B - M + \alpha x_1 + \gamma\mathcal{S}, \tag{4.5}$$
$$\mu_{\rm SN} = m_B - M - \beta c + \gamma\mathcal{S}, \tag{4.6}$$
$$\mu_{\rm SN} = m_B - M + \alpha x_1 - \beta c + \gamma\mathcal{S}, \tag{4.7}$$
$$\mu_{\rm SN} = m_B - M + \alpha x_1 - \beta c. \tag{4.8}$$

Here, $\mathcal{S}$ represents any spectral measurement: v, pEW, $\Re$(Si II), $\mathcal{R}$, etc. The last model included in our study was already mentioned above (Equation 4.2) and is the model usually adopted in cosmology studies of SNe Ia using only light-curve parameters (e.g., Astier et al. 2006; Kowalski et al. 2008; Hicken et al. 2009a; Amanullah et al. 2010). In the following analysis the so-called (x_1, c) model will be the one to which we compare the other cosmological models that include spectral information.

Cross-Validation

Ideally, with a sufficiently large sample, the predictive abilities of a model could be inferred by inspecting the dispersion of the residuals. However, for samples of limited size, the dispersion of the residuals is prone to statistical fluctuations and may not accurately reflect the true predictive nature of the model. Furthermore, for a fixed sample, one can always reduce the dispersion of the residuals by adding more variables to the model. However, it is not clear whether the added variables are actually improving the model itself or simply fitting to the noise inherent in the observables. For analyzing the predictive nature of a model, it is useful to perform some form of cross-validation (CV) in which a subset of the entire sample is used to train the model and another subset is used to validate the predictive ability of that model.

Bailey et al. (2009) use a sample of 58 SNe, 28 of which are adopted as a training set to train a model and the other 30 are used as a validation set to assess the predictivity of the model. Using a smaller sample of 26 SNe, Blondin et al. (2011) use a K-fold CV method that allows all of the SNe to be used in the training and validation procedure. For this study, and following Blondin et al. (2011), we adopt the K-fold CV with $K = 10$. We also tested CV with K =2, 5, and 69 and find that our final results are unchanged. The basics of the procedure are best illuminated by an example, as follows.

Let us begin with a sample of 60 SNe. 10-fold CV starts by randomly dividing the sample into 10 subgroups of 6 SNe each. The first subgroup is set aside; this will be our first validation set. We combine the remaining 9 subgroups and train our model on the 54 other SNe to determine the best-fitting parameters (i.e., α, β, γ, and M). Using the best-fitting parameters found with the training set, we apply our model to the validation set and calculate the Hubble residual for each of the 6 SNe in our validation set. We repeat this process using the second subgroup as the validation set and the union of the other 9

subgroups as the training set. This process is repeated a total of 10 times (once for each subgroup as a validation set) until we have calculated a residual for every SN in the sample.

Comparing the Models

As in Blondin et al. (2011), the dispersion in each model is estimated using the weighted root-mean-square (WMRS),

$$\mathrm{WRMS}^2 = \frac{\sum_{s=1}^{N} w_s[\mu(z_s) - \mu_{\mathrm{SN},s}]^2}{\sum_{s=1}^{N} w_s}, \tag{4.9}$$

where the weights, w_s, are given by

$$w_s = \sigma_{\mathrm{m},s}^2 + \sigma_{\mathrm{pec},s}^2 + \sigma_{\mathrm{int}}^2. \tag{4.10}$$

The varaince in WRMS is estimated as

$$\mathrm{Var}[\mathrm{WRMS}] = \Big[\sum_{s=1}^{N} w_s\Big]^{-1}. \tag{4.11}$$

The 1σ uncertainty is found by taking the square root of the variance. This is a more appropriate estimator of the dispersion in the model then simply taking the standard deviation in the residuals since we are not guaranteed that the mean residual will be zero (Blondin et al. 2011).

Following Blondin et al. (2011), for each model which uses a spectral measurement (Equations 4.4–4.7) we also calculate the intrinsic prediction error (σ_{pred}), the intrinsic correlation ($\rho_{x_1,c}$) of the residuals with residuals using the (x_1, c) model (Equation 4.8), and the difference ($\Delta_{x_1,c}$) in intrinsic prediction error with respect to the (x_1, c) model. An uncertainty can be computed for $\Delta_{x_1,c}$ (Appendix B of Blondin et al. 2011), and thus the significance of the difference between a given model and the standard (x_1, c) model can also be computed. This parameter is the most direct comparison of how much better (or worse) a model which utilizes a spectral measurement is compared to the (x_1, c) model, and how significant the change is. Note that $\Delta_{x_1,c} < 0$ represents an improvement over the (x_1, c) model.

4.4 Analysis

4.4.1 Velocity Gradients

Benetti et al. (2005) defined the velocity gradient, $\dot{v} = -\Delta v/\Delta t$, as the "average daily rate of decrease of the expansion velocity" of the Si II λ6355 feature and used this parameter to place each of their 26 SNe Ia into one of three categories. The high velocity gradient

(HVG) group had the largest velocity gradients ($\dot{v} \gtrsim 70$ km s^{-1} d^{-1}) and the low velocity gradient (LVG) group had the smallest velocity gradients. The third subclass (FAINT) had the lowest expansion velocities, yet moderately large velocity gradients, and consisted of subluminous SNe Ia with the narrowest light curves ($\Delta m_{15}(B) \gtrsim 1.6$ mag).

Even though the BSNIP sample is not well-suited to velocity gradient measurements (the average number of spectra per object is $\sim$2, shown in BSNIP I), we are still able to calculate a $\dot{v}$ value for 44 SNe Ia. Figure 4.1 shows the $\dot{v}$ measurements of the BSNIP data plotted against their $\Delta m_{15}(B)$ values. The points are color-coded by their near-maximum Si II λ6355 velocity, with red points representing normal-velocity objects and blue points representing high-velocity (HV) objects. These so-called "Wang types" were first presented by Wang et al. (2009a), and in BSNIP II we discuss our definition of these subclasses in more detail. The data are also shape-coded by the aforementioned "Benetti types" (FAINT are stars, LVG are squares, and HVG are triangles). The top panel of Figure 4.1 shows all objects for which a $\dot{v}$ and $\Delta m_{15}(B)$ are measured, while the bottom panel shows a close-up view of the same data such that the axis ranges match those of Figure 3b of Benetti et al. (2005).

As a result of the definitions of the different subclasses, the FAINT SNe are found to the right in Figure 4.1 (i.e., large $\Delta m_{15}(B)$ values) and the HVG SNe are found in the upper part of the Figure (i.e., large $\dot{v}$ values), though there is no obvious break between the various classes. As pointed out in BSNIP II and confirmed in Figure 4.1, the HVG and LVG objects have similar average $\Delta m_{15}(B)$ values and ranges of values.

It was stated by Benetti et al. (2005) that $\dot{v}$ is weakly correlated with $\Delta m_{15}(B)$ though there is no evidence of such a correlation in the BSNIP data. They also claim that there are three distinct families of SNe Ia (LVG, HVG, and FAINT) based partially on their plot of $\dot{v}$ versus $\Delta m_{15}(B)$. With almost 70% more objects, the BSNIP data fill in this parameter space and cast serious doubt on the existence of truly distinct families of SNe Ia based on velocity-gradient measurements. (see Table 4 of BSNIP II for the median values of $\dot{v}$ and $\Delta m_{15}(B)$ for each of these three sublcasses).

4.4.2 Expansion Velocities

Velocities at Maximum Brightness

Expansion velocities of SNe Ia are calculated from the minima of various absorption features (see BSNIP II for more information on how this measurement is performed on the data presented here). These velocities have been compared to light-curve width measurements and photometric colors in a variety of ways (e.g., Hachinger et al. 2006; Blondin et al. 2011; Nordin et al. 2011b). As discussed in BSNIP II, Hachinger et al. (2006) interpolate/extrapolate their expansion velocities to the time of maximum brightness (i.e., $t = 0$ d), and v_0 was defined as the expansion velocity of Si II λ6355 at maximum brightness. They then compare these velocities to the light-curve shape parameter $\Delta m_{15}(B)$. Figure 4.2 presents the 44 SNe in the BSNIP data for which both v_0 and $\Delta m_{15}(B)$ is calculated. As

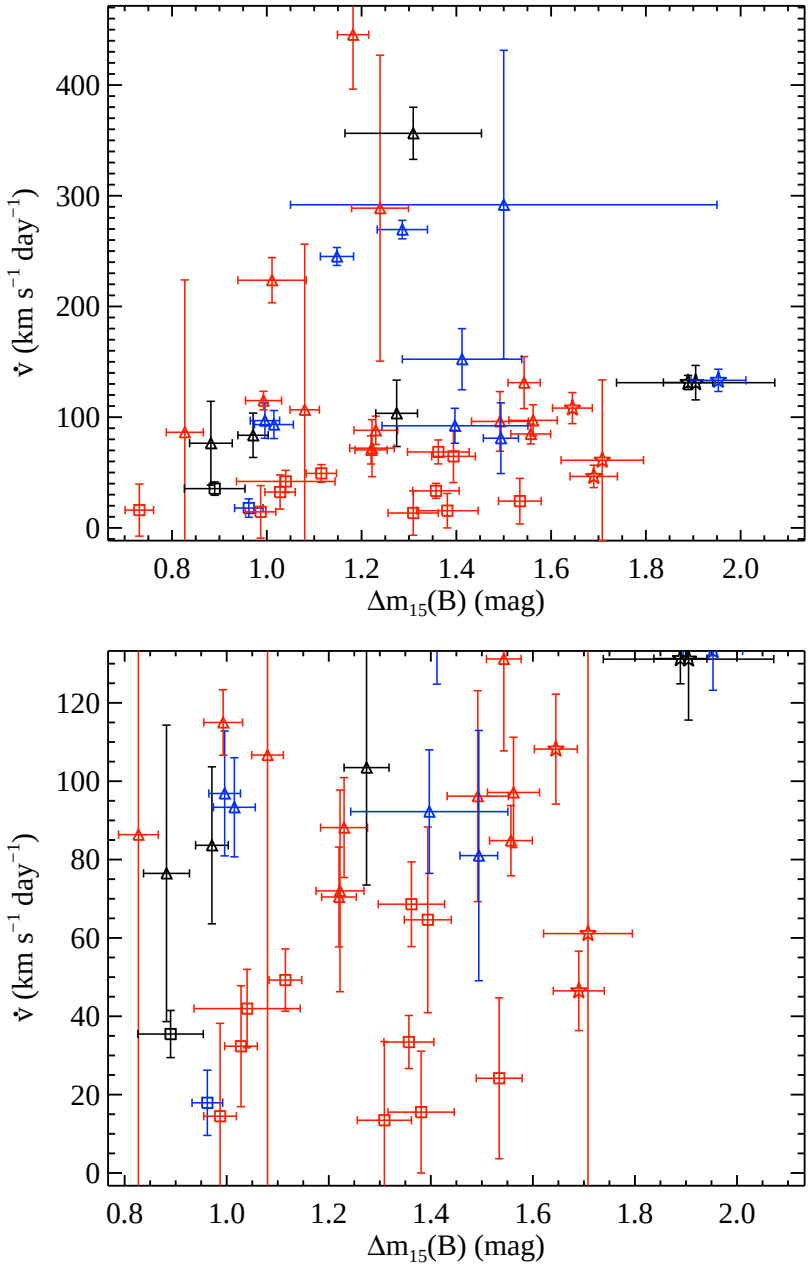

Figure 4.1: The velocity gradient versus $\Delta m_{15}(B)$ of 44 SNe (*top*) and a close-up view of the low-$\dot{v}$ objects (*bottom*). Blue points are high-velocity (HV) objects, red points are normal-velocity objects, and black points are objects for which we could not determine whether the SN was normal or high velocity (see BSNIP II for further details regarding how HV SNe are defined). Stars are FAINT objects, squares are low velocity gradient (LVG) objects, and triangles are high velocity gradient (HVG) objects (see BSNIP II for further details regarding how these subclasses are defined).

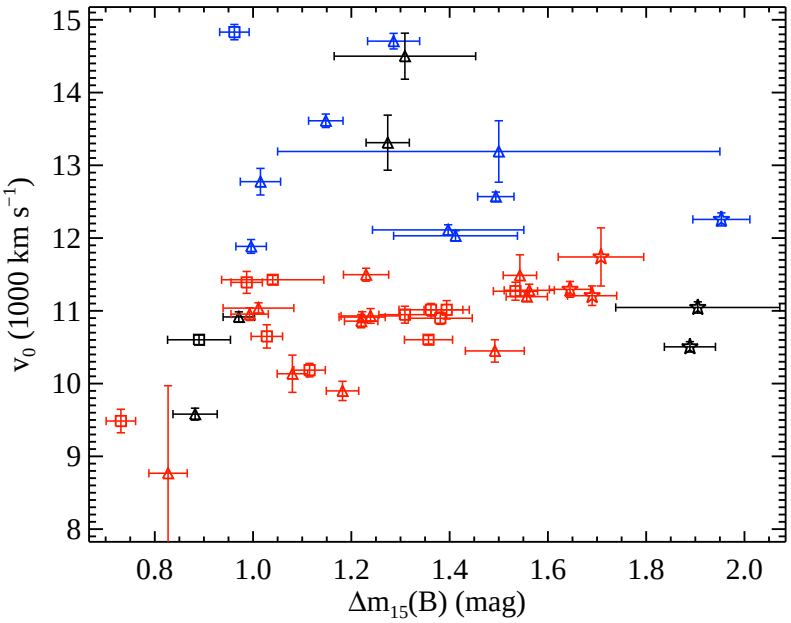

Figure 4.2: The velocity at maximum brightness of the Si II λ6355 feature versus $\Delta m_{15}(B)$ of 44 SNe. Colors and shapes of data points are the same as in Figure 4.1.

above, the points are color-coded by "Wang type" and shape-coded by "Benetti type."

As in Figure 4.1, the FAINT objects are (by definition) found at the right edge of Figure 4.2. Similarly, the HV objects are all in the upper half of the Figure. All of the objects, save for a few of the highest velocity SNe and the object with the lowest velocity in the Figure, are within $\sim$1500 km s^{-1} of 11,000 km s^{-1}. This is remarkably similar to what was found by Hachinger et al. (2006), except the BSNIP data have a slightly larger scatter around the typical velocity of $\sim$11,000 km s^{-1}. Hachinger et al. (2006) also note that the majority of the scatter in velocity comes from the HVG objects, which is also true for Figure 4.2. There is a major difference between the two results, however. The BNSIP data in Figure 4.2 show that HVG SNe have a huge range of v_0, spanning well above average to significantly below average values, whereas the data presented by Hachinger et al. (2006) show evidence of the (oft-quoted) one-to-one relationship between HVG and HV SNe Ia. As mentioned in BSNIP II, while most HVG objects are found to have expansion velocities above the LVG objects, this is not an exclusive feature of HVG SNe Ia.

A weak relationship between the "pseudocolor" $B_{\rm max} - V_{\rm max}$ (i.e., the B-band magnitude at B-band maximum minus the V-band magnitude at V-band maximum) and v_0 has been seen previously (Foley et al. 2011). Figure 4.3 shows 39 BSNIP SNe for which we measure v_0 and the difference between B-band magnitude and V-band magnitude at the time of B-band maximum brightness (i.e., $(B-V)_{B_{\rm max}}$). While these two measurements of color are not exactly equal, no significant difference is found between the two when performing

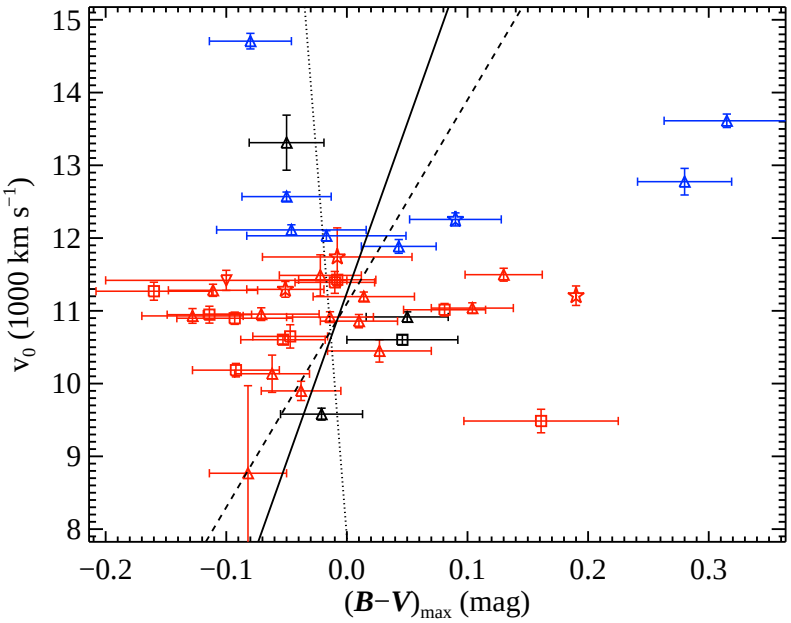

Figure 4.3: The velocity at maximum brightness of the Si II λ6355 feature versus $(B-V)_{B_{\rm max}}$ (i.e., the difference between B-band magnitude and V-band magnitude at the time of B-band maximum brightness) of 39 SNe. Colors and shapes of data points are the same as in Figure 4.1. The solid line is the fit to all of the data while the dotted line is the fit only to objects with $(B-V)_{\rm max} < 0.25$ mag. The dashed line is the relationship between v_0 and $B_{\rm max} - V_{\rm max}$ from the model spectra of Kasen & Plewa (2007), as shown by Foley & Kasen (2011).

cosmological fits. We opt to use $(B-V)_{B_{\rm max}}$ since it is an actual, physical color of the SN at a discrete period of time. Following Foley et al. (2011), we are only presenting SNe Ia with $(B-V)_{\rm max} < 0.319$ mag in Figure 4.3.

The linear least-sqaures fit to all of the points is shown by the solid line. We see only marginal evidence for any overall correlation (Pearson correlation coefficient of 0.23), and the relationship seems to be driven solely by the two outliers with $(B-V)_{\rm max} > 0.25$ mag. If those two objects are removed, the correlation coefficient drops to -0.06 (the best-fitting line to the remaining data is shown by the dotted line). Finally, the dashed line is the relationship between v_0 and $B_{\rm max} - V_{\rm max}$ from the model spectra of Kasen & Plewa (2007), as shown in Foley & Kasen (2011). When including all of the data in Figure 4.3, the correlation between v_0 and $(B-V)_{B_{\rm max}}$ is almost as significant as what was seen by Foley et al. (2011), where they derive correlation coefficients of 0.28 and 0.39 for two different datasets.[2] However,

[2]The first dataset, yielding a correlation coefficient of 0.28, comes from Wang et al. (2009a) and includes some of the data used here. However, the two samples *are* distinct and the method of velocity determination is significantly different.

no correlation is present whatsoever if the two significant outliers are removed. Thus, it is unclear whether a relationship exists between velocity at maximum brightness and color.

Velocities Near Maximum Brightness

If instead of v_0 we plot the actual measured velocity of the Si II λ6355 feature for each object having a spectrum within 5 d of maximum brightness versus $\Delta m_{15}(B)$, the same basic trends are seen (but with nearly twice as many data points). A comparison of the velocity of the Si II λ5972 feature (within 5 d of maximum brightness) with $\Delta m_{15}(B)$ yields nearly identical results. The biggest difference is that the velocities are clustered around 10,300 km s^{-1}, lower than that of the Si II λ6355 feature. This difference between these features has been seen in previous studies as well (Hachinger et al. 2006). The same analysis using the velocity of the S II "W" once again shows the same behavior, but with an even lower typical velocity ($\sim$9000 km s^{-1}). This has also been pointed out in earlier work (Hachinger et al. 2006). The velocity of the S II "W" feature is further discussed below.

Blondin et al. (2011) present a Hubble diagram that is corrected by SALT2 light-curve width parameter x_1 and color parameter c *in addition to* the velocity of the Si II λ6355 feature. This yielded approximately a 10% decrease in the scatter of their Hubble diagram. It has also been shown that the Si II λ6355 velocity is uncorrelated with both x_1 and c, and thus it gives information beyond light-curve width and color. However, the anti-correlation of this velocity with Hubble residuals (corrected for light-curve width and color) is relatively small (Blondin et al. 2011).

Plotted in Figure 4.4 are the 66 SNe Ia in the BSNIP sample which have SALT2 fits and measured Si II λ6355 velocities within 5 d of maximum brightness. The velocities are plotted against x_1, c, and Hubble residuals corrected for light-curve width and color (only for objects which are used to make the Hubble diagram). As above, the points are color-coded by "Wang type." In Figure 4.4 the data are shape-coded by what is referred to in BSNIP II as the "SNID type." The SuperNova IDentification code (SNID; Blondin & Tonry 2007), as implemented in BSNIP I, was used to determine the spectroscopic subtype of each SN used in BSNIP II (as well as this study). SNID compares an input spectrum to a library of spectral templates in order to determine the most likely spectroscopic subtype. Spectroscopically normal objects are objects classified as "Ia-norm" by SNID.

The spectroscopically peculiar SNID subtypes used here include the often underluminous SN 1991bg-like objects ("Ia-91bg," e.g., Filippenko et al. 1992b; Leibundgut et al. 1993), and the often overluminous SN 1991T-like objects ("Ia-91T," e.g., Filippenko et al. 1992a; Phillips et al. 1992) and SN 1999aa-like objects ("Ia-99aa," Li et al. 2001b; Strolger et al. 2002; Garavini et al. 2004). See BSNIP I for more information regarding our implementation of SNID and the various spectroscopic subtype classifications. In Figure 4.4, Ia-norm objects are plotted as squares, Ia-91T objects are shown as upward-pointing triangles, Ia-99aa objects are displayed as downward-pointing triangles, and objects with no determined SNID subtype are circles.

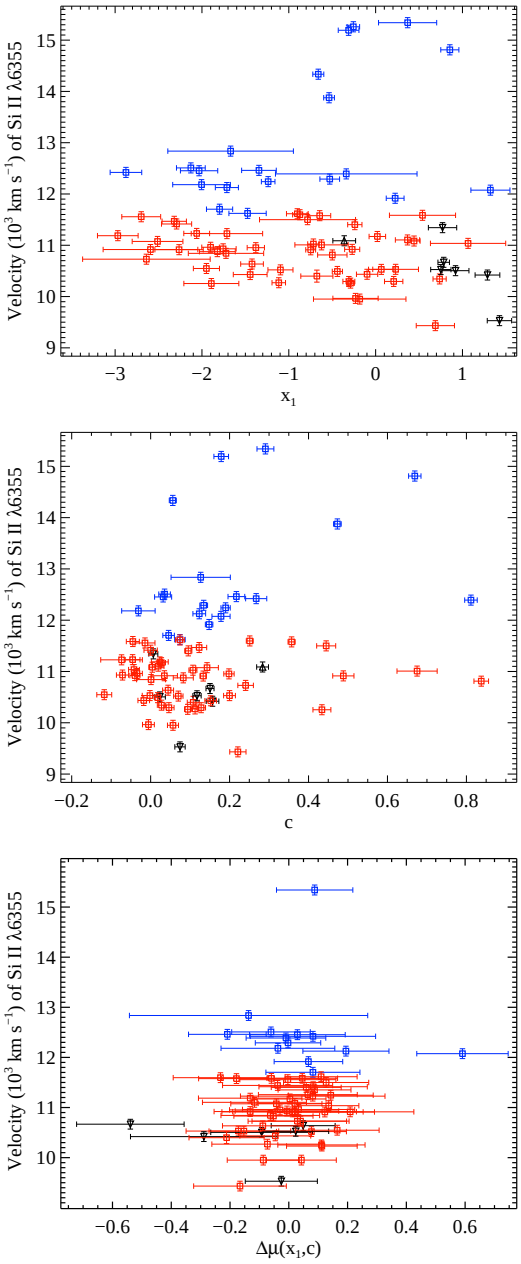

Figure 4.4: The velocity of the Si II λ6355 feature versus SALT2 light-curve width parameter x_1, SALT2 color parameter c, and Hubble residuals corrected for light-curve width and color. As in previous figures, blue points are HV objects, red points are normal-velocity objects, and black points are objects for which we could not determine whether the SN was normal or high velocity. Squares are Ia-norm objects, upward-pointing triangles are Ia-91T objects, downward-pointing triangles are Ia-99aa objects, and circles are objects which do not have a SNID subtype (see BSNIP I for further details regarding how these subclasses are defined).

The data in Figure 4.4 are extremely similar to those of Blondin et al. (2011) and show the same correlations (or lack thereof). The velocity of the Si II λ6355 feature as measured from the BSNIP data is uncorrelated with x_1 (Pearson correlation coefficient of only -0.05). This velocity is also uncorrelated with c, as seen in Blondin et al. (2011). Removing SNe with $c > 0.5$ from the BSNIP data (which is done when Hubble diagrams are produced using this parameter) yields a Pearson correlation coefficient of 0.24 between Si II λ6355 velocity and c.

The bottom panel of Figure 4.4 shows the velocity of the Si II λ6355 feature versus the (x_1, c)-corrected Hubble residuals. If the correction term in a given model (here, the velocity of Si II λ6355) is well-correlated with the SALT2-corrected Hubble residuals, then the extra term is likely providing new information that is actually in the data. Thus, the model is improving the fit not by fitting to noise, but to physical information contained in the data. However, the correction term here is uncorrelated with the residuals (Pearson correlation coefficient of 0.20).

No improvement is found (i.e., the WRMS increases) when adding the Si II λ6355 velocity to the standard (x_1, c) model ($\Delta_{x_1,c} = 0.0083 \pm 0.0084$). Blondin et al. (2011) found that there was a $\lesssim$10% decrease in the WRMS when using the x_1, c, and Si II λ6355 velocity, but their $\Delta_{x_1,c}$ is consistent with 0 (as is ours). They also find only a "modest" correlation between Si II λ6355 velocity and (x_1, c)-corrected residuals (absolute Pearson correlation coefficient of 0.4; Blondin et al. 2011). Therefore, it seems that adding the Si II λ6355 velocity to the standard (x_1, c) model does *not* improve the precision of SN Ia distance calculations.

As mentioned in Section 4.4.2, the models of Kasen & Plewa (2007) imply a correlation between $(B-V)_{\rm max}$ and near-maximum brightness expansion velocity. This was elegantly pointed out by Foley & Kasen (2011) and plotted therein for velocities of both Si II λ6355 and Ca II H&K at maximum brightness. Foley et al. (2011) showed marginal evidence for such a relationship, but Figure 4.3 showed that the BSNIP data do not support this claim. We now expand this investigation to include all Si II λ6355 velocities within 5 d of maximum brightness (as opposed to using only objects for which we could calculate an exact value of v_0).

In Figure 4.5 the velocity of the Si II λ6355 feature is plotted against $(B-V)_{\rm max}$. The top panel shows all 77 SNe from the BSNIP data for which both of these values have been measured and the bottom panel shows a close-up of objects with $(B-V)_{\rm max} < 0.319$ mag (in order to match the sample fit by Foley et al. 2011). The linear least-sqaures fit to all of the points is shown by the solid line and the fit to SNe with $(B-V)_{\rm max} < 0.319$ mag is shown by the dotted line; the Pearson correlation coefficients are 0.37 and 0.32, respectively, and are similar to the value found by Foley et al. (2011), 0.39. While there is evidence for a correlation here, and in fact one that matches well to what was found by Foley et al. (2011), there is a large amount of scatter around the linear fit.

The typical $(B-V)_{\rm max}$ for HV objects is larger than for Ia-norm and Ia-91T/99aa, but smaller than that of Ia-91bg (which appear in the Figure as highly reddened, significant out-

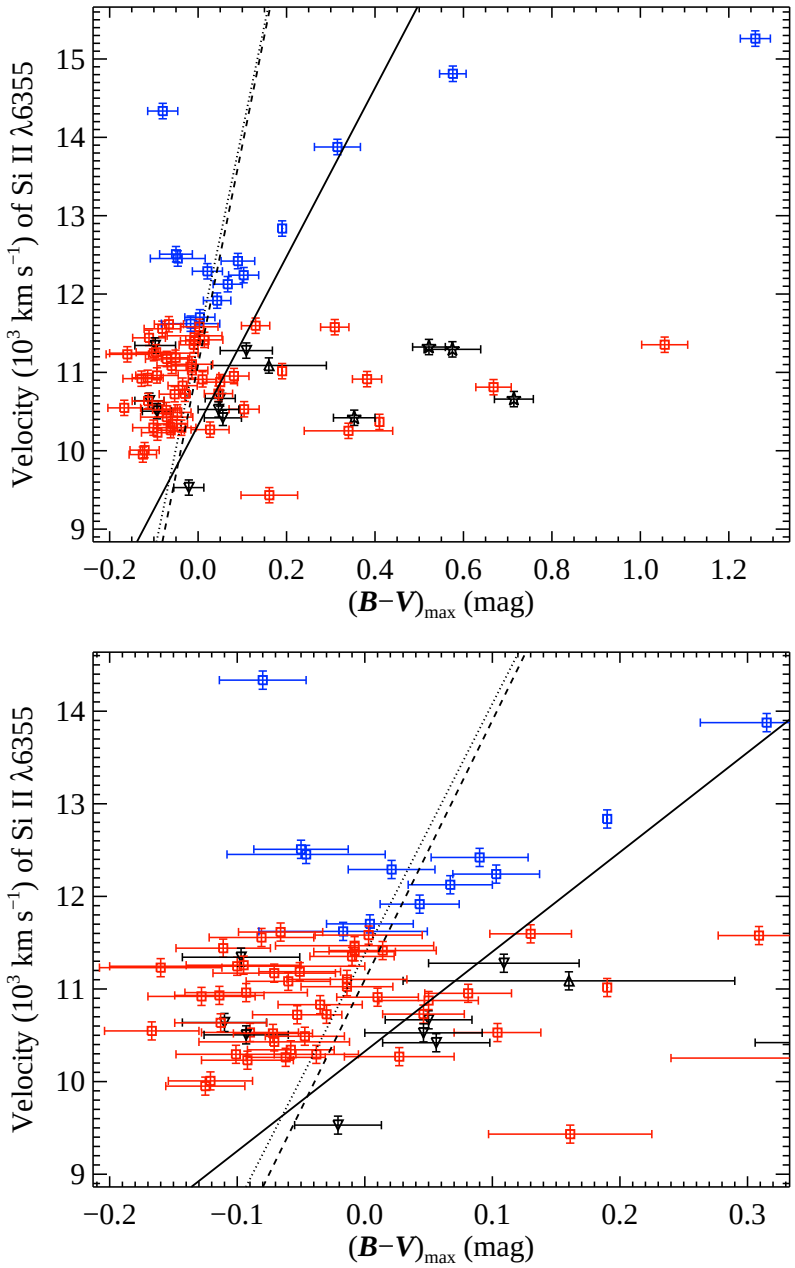

Figure 4.5: The velocity of the Si II λ6355 feature versus $(B-V)_{B_{\max}}$ (*top*) and a close-up of objects with $(B-V)_{\max} < 0.319$ mag (*bottom*). Squares are Ia-norm objects, stars are Ia-91bg objects, upward-pointing triangles are Ia-91T objects, downward-pointing triangles are Ia-99aa objects, and circles are objects which do not have a SNID subtype (see BSNIP I for further details regarding how these subclasses are defined). The solid line is the fit to all of the data while the dotted line is the fit only to objects with $(B-V)_{\max} < 0.319$ mag. The dashed line is the relationship between v_0 and $B_{\max} - V_{\max}$ from the model spectra of Kasen & Plewa (2007), as shown by Foley & Kasen (2011).

liers). However, the range of $(B-V)_{\rm max}$ spanned by Ia-norm and HV objects is similar, with a significant amount of overlap. The scatter in $(B-V)_{B_{\rm max}}$ of the HV objects (0.098 mag) is effectively equal to that of the other objects in the bottom panel of Figure 4.5 (0.101 mag). While this matches the scatter in the HV objects found previously (0.095 mag; Foley et al. 2011), it differs from the SNe with velocities $< 11,800$ km s^{-1} which they found to have a smaller intrinsic color scatter (0.072 mag).

The dashed line in Figure 4.5 is once again the relationship between v_0 and $B_{\rm max} - V_{\rm max}$ from the model spectra of Kasen & Plewa (2007), as shown in Figure 8 of Foley & Kasen (2011). As in Foley et al. (2011), the BSNIP data match extremely well to these predictions. One difference between Figure 4.5 and Figure 8 of Foley & Kasen (2011) is that the BSNIP data contain a handful of objects that are extremely reddened (i.e., they have relatively large values of $(B-V)_{\rm max}$). However, this can easily be explained. All of the Ia-norm and HV SNe in Figure 4.5 with $(B-V)_{\rm max} > 0.31$ mag have been observed to have significant reddening from their host galaxies (which is not taken into account in the models of Kasen & Plewa 2007). The other objects with $(B-V)_{\rm max} > 0.31$ mag are Ia-91bg, which were also not discussed in the models of Kasen & Plewa (2007).

Figure 8 of Foley & Kasen (2011) also presents the theoretical relationship between velocity of the Ca II H&K feature and $(B-V)_{\rm max}$. A comparison of these two values measured from the BSNIP data is shown in Figure 4.6. 31 SNe with $(B-V)_{\rm max} < 0.319$ mag are plotted and show a very weak correlation (solid line). The Pearson coefficient is 0.12, which is half of what was seen previously (Foley et al. 2011). Again, the scatter in $(B-V)_{\rm max}$ is similar for the HV and normal-velocity objects. However, this is unsurprising since, as pointed out in BSNIP II, the Ca II H&K velocities of HV and normal-velocity objects (determined using the Si II λ6355 velocity) are highly overlapping. Finally, as also seen in Foley et al. (2011), the predicted relationship from Kasen & Plewa (2007) has a much shallower slope than the data indicate.

A distance model involving x_1, c, and the velocity of the Ca II H&K feature was calculated, and while the WRMS technically decreased with the addition of this velocity, it was not found to be significant ($\Delta_{x_1,c} = -0.0085 \pm 0.0141$). Other models involving this velocity were all found to degrade the accuracy of distance measurements when compared to the standard (x_1, c) model.

Furthermore, we used Equations 4.4–4.7 along with velocities of all seven spectral features for which velocities were measured and compared the results to the (x_1, c) model. The vast majority of these models predicted a larger scatter than the standard model corrected for light-curve width and color. However, both the O I triplet and the Ca II near-IR triplet, when combined with x_1 and c, were found to perform equally as well as when using just x_1 and c. Thus, adding either of these velocities did not degrade the distances calculated, but they did not significantly improve them either.

On the other hand, the velocity of the S II "W," when used in conjunction with x_1 and c, decreased the WRMS by $\sim$3% and the $\sigma_{\rm pred}$ by $\sim$14%, at the 1.8σ level ($\Delta_{x_1,c} = -0.0119 \pm 0.0066$). Figure 4.7 shows the 64 SNe Ia in the BSNIP sample which have SALT2

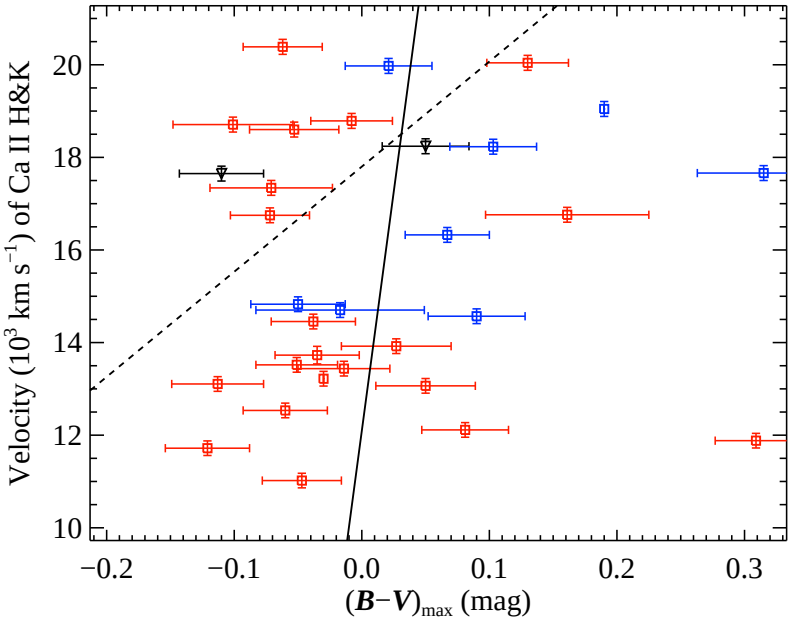

Figure 4.6: The velocity of the Ca II H&K feature versus $(B-V)_{B_{\max}}$ for objects with $(B-V)_{\max} < 0.319$ mag. Colors and shapes of data points are the same as in Figure 4.5. The solid line is the fit to all of the data shown. The dashed line is the relationship between v_0 and $B_{\max} - V_{\max}$ from the model spectra of Kasen & Plewa (2007), as shown by Foley & Kasen (2011).

fits and measured S II "W" velocities within 5 d of maximum brightness. The velocities are again plotted against x_1, c, and Hubble residuals corrected for light-curve width and color (only for SNe that are part of the Hubble diagram).

Neither x_1 nor c show any correlation with the velocity of the S II "W" (correlation coefficients of 0.10 and 0.17, respectively). Even when removing SNe with $c > 0.5$ from the BSNIP data (as done for the Hubble diagrams), the Pearson correlation coefficient becomes only -0.16. The bottom panel of Figure 4.7 shows the velocity of the S II "W" versus the (x_1, c)-corrected Hubble residuals. Once again, the correction term is uncorrelated with the residuals (correlation coefficient of 0.06). Figure 4.8 shows the Hubble diagram residuals for this model as well as the standard (x_1, c) model (using the same set of objects) versus redshift. Also shown, as the gray band, is the WRMS for both models.

While the relative depth of this feature has been seen to improve Hubble diagrams (Blondin et al. 2011, and Section 4.4.3 of this work), the velocity of this feature has not previously been shown to do this. When adding the velocity of the S II "W" feature to the standard (x_1, c) model, the overall decrease in WRMS is relatively small, but the effect appears to be fairly significant. This distance model should be explored further using future, larger datasets.

4.4.3 Relative Depths

The depth of the *bluer absorption* of the S II "W" feature relative to the pseudo-continuum has been shown to decrease the scatter of Hubble residuals by about 10% (Blondin et al. 2011). The relative depth (a) of this feature was found to be uncorrelated with both x_1 and c by Blondin et al. (2011), and its correlation with Hubble residuals (corrected for light-curve width and color) is relatively small. Figure 4.9 presents the 64 BSNIP SNe Ia which have SALT2 fits and measured relative depths of the *redder absorption* of the S II "W" feature within 5 d of maximum brightness. The depths are plotted against x_1, c, and Hubble residuals corrected for light-curve width and color (for objects that are in the Hubble diagram). It should be noted that while Blondin et al. (2011) measure the bluer absorption of this feature (λ5454), we measure only the redder absorption (λ5624) in BSNIP II. While these absorptions are separated by < 200 Å, there may be differences between the relative depths of the two. Nevertheless, we will compare the results presented here to those of Blondin et al. (2011) with the caveat that we may be comparing "Red Delicious apples" to "Granny Smith apples."

The BSNIP data show a fairly significant correlation between the relative depth of S II "W" and x_1 (a Pearson correlation coefficient of -0.47). This is in stark contrast to Blondin et al. (2011), who found no evidence of such a correlation (Pearson correlation coefficient of -0.04). As opposed to x_1, both studies agree that c is uncorrelated with a of the S II "W" feature (the BSNIP data having a Pearson correlation coefficient of 0.09). The Hubble residuals corrected for x_1 and c show no evidence of a correlation with the relative depth of the S II "W" (correlation coefficient of 0.08), which is even weaker than what was found by

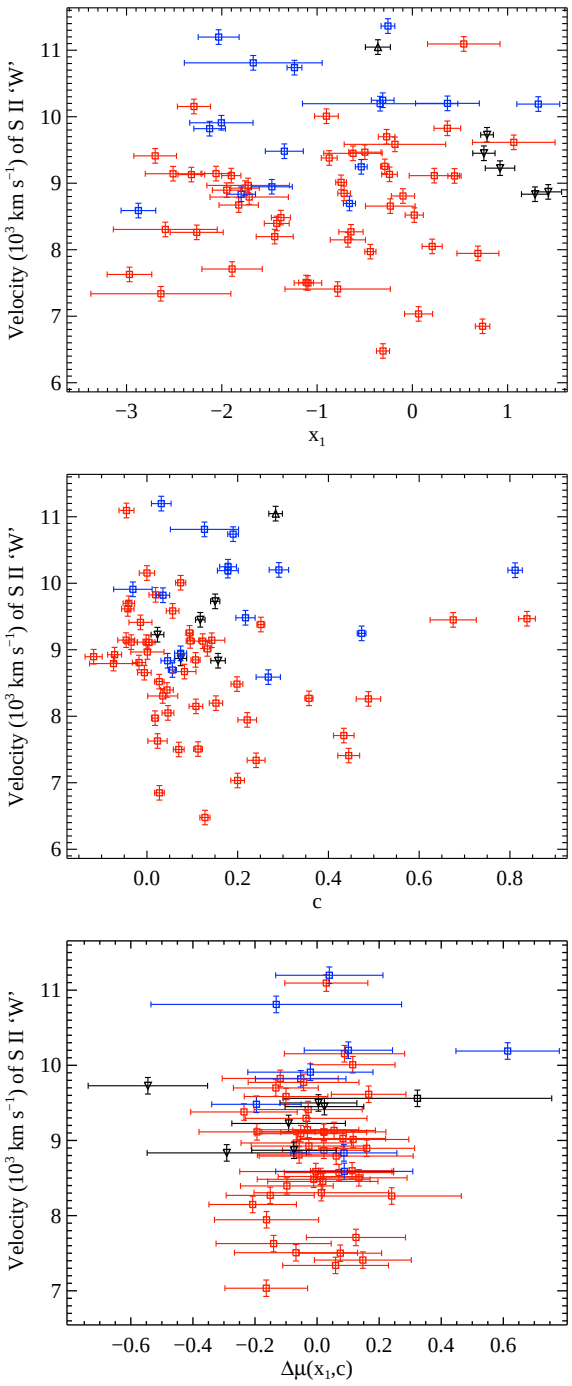

Figure 4.7: The velocity of the S II "W" feature versus SALT2 light-curve width parameter x_1, SALT2 color parameter c, and Hubble residuals corrected for light-curve width and color. Colors and shapes of data points are the same as in Figure 4.5.

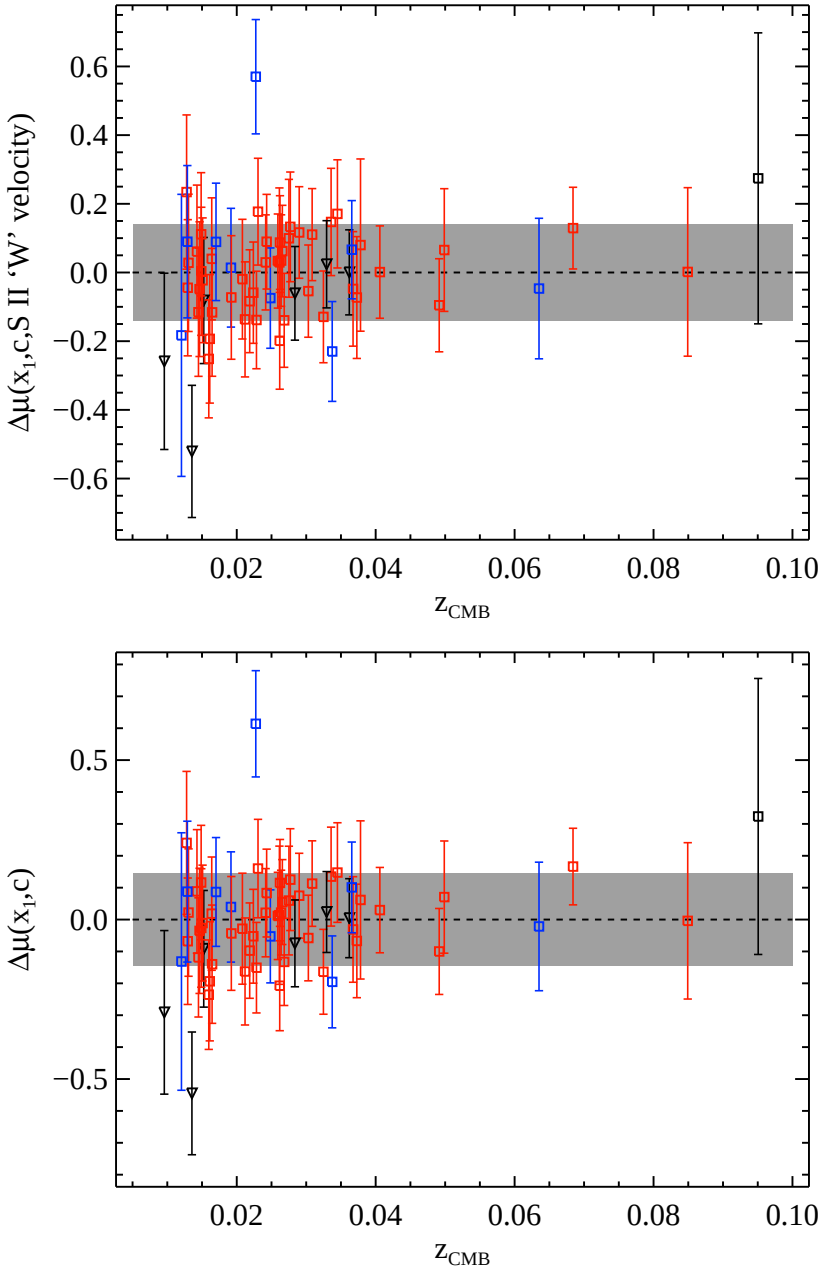

Figure 4.8: Hubble diagram residuals versus $z_{\rm cmb}$ for the (x_1, c, S II "W" velocity) model and the standard (x_1, c) model (Equation 4.8). The gray band is the WRMS for each model. Colors and shapes of data points are the same as in Figure 4.5.

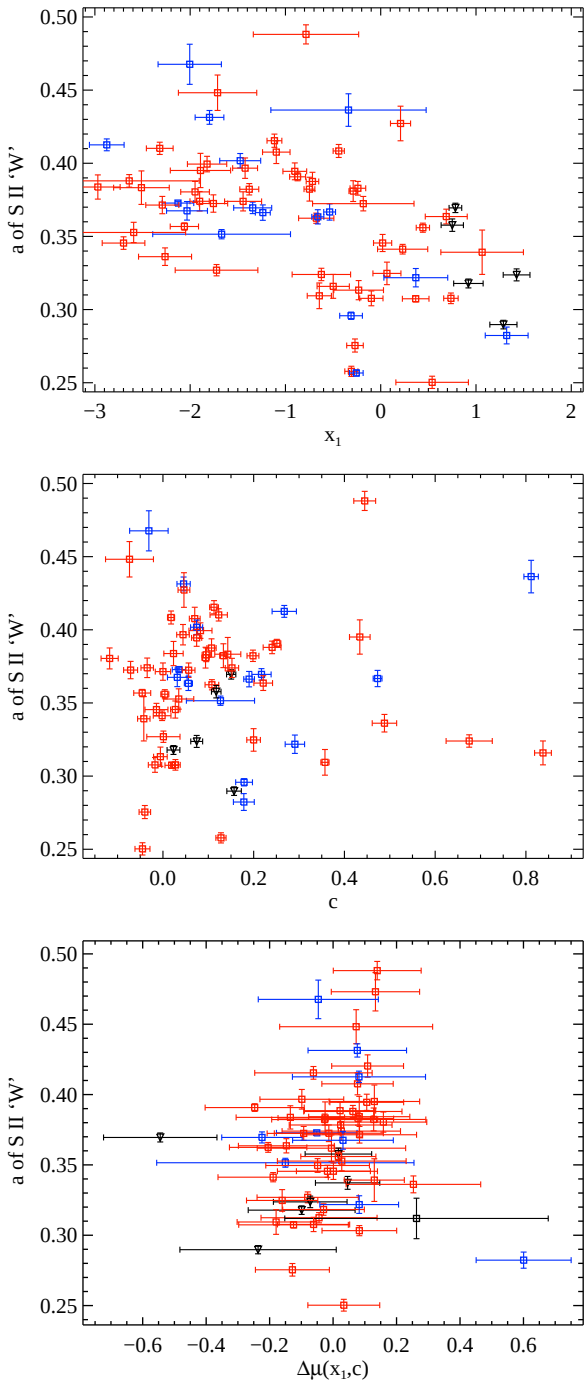

Figure 4.9: The relative depth of the S II "W" feature versus SALT2 light-curve width parameter x_1, SALT2 color parameter c, and Hubble residuals corrected for light-curve width and color. Colors and shapes of data points are the same as in Figure 4.5.

Blondin et al. (2011). They find that a model which includes x_1, c, and a of the S II "W" will decrease the WRMS by $\lesssim$10% while we find the WRMS to be effectively unchanged whether or not one adds in the relative depth of S II "W" ($\Delta_{x_1,c} = 0.0012 \pm 0.0047$).

All other spectral features' relative depths were used, along with Equations 4.4–4.7, to create Hubble diagrams. No model significantly decreased the residuals over the standard (x_1, c) model. Models involving the relative depth of Ca II H&K, Si II λ6355, and the O I triplet, each in combination with x_1 and c, were found to be as accurate as the (x_1, c) model.

4.4.4 Pseudo-Equivalant Widths

Nordin et al. (2011b) fit the temporal evolution of their pEW measurements to attempt to "remove" the age dependence of the pEW values. To do this, an epoch-independent quantity called the "pEW difference" (ΔpEW) was defined which is simply the measured pEW minus the expected pEW at the same epoch using the linear or quadratic fit. In BSNIP II we calculated ΔpEW for the BSNIP sample. However, the relationships seen in BSNIP II involving ΔpEW values were also seen when simply using the pEW values (within 5 d of maximum brightness). This is due to the fact that pEWs do not evolve much within a few days of maximum. Furthermore, the ΔpEW values rely on defining a fit to the measurements which adds another assumption to the analysis. Thus, the current study will focus solely on pEW values within 5 d of maximum brightness and will not further investigate ΔpEW values. Note that comparisons to Nordin et al. (2011b) will be made, despite the fact that their study uses ΔpEW values almost exclusively.

Si II λ4000

The pEW of the Si II λ4000 feature has recently been found to be an indicator of light-curve width due its relatively tight anti-correlation with the SALT2 x_1 parameter (Arsenijevic et al. 2008; Walker et al. 2011; Blondin et al. 2011; Nordin et al. 2011b; Chotard et al. 2011). Curiously, in BSNIP II, no correlation was found between this pEW and another often-used SN Ia luminosity indicator, the so-called "Si II ratio", $\Re$(Si II) (originally defined by Nugent et al. 1995; see also BSNIP II and Section 4.4.5 for more information on this spectral parameter). Here the pEW of Si II λ4000 is compared directly to photometric parameters.

In Figure 4.10 we present the 57 BSNIP SNe which have SALT2 fits and measured pEW values for the Si II λ4000 feature within 5 d of maximum brightness. The pEWs are plotted against x_1, c, and Hubble residuals corrected only for color (for SNe Ia that are used when constructing the Hubble diagram).

The pEW of Si II λ4000 is highly correlated with x_1 (Figure 4.10, top plot) with a Pearson correlation coefficient of -0.85. This is in agreement with many previous studies and is actually a stronger correlation than has been seen before (e.g., Arsenijevic et al. 2008; Walker et al. 2011; Blondin et al. 2011; Nordin et al. 2011b; Chotard et al. 2011). The least-squares linear fit to the data is shown as the solid line in the top plot of Figure 4.10

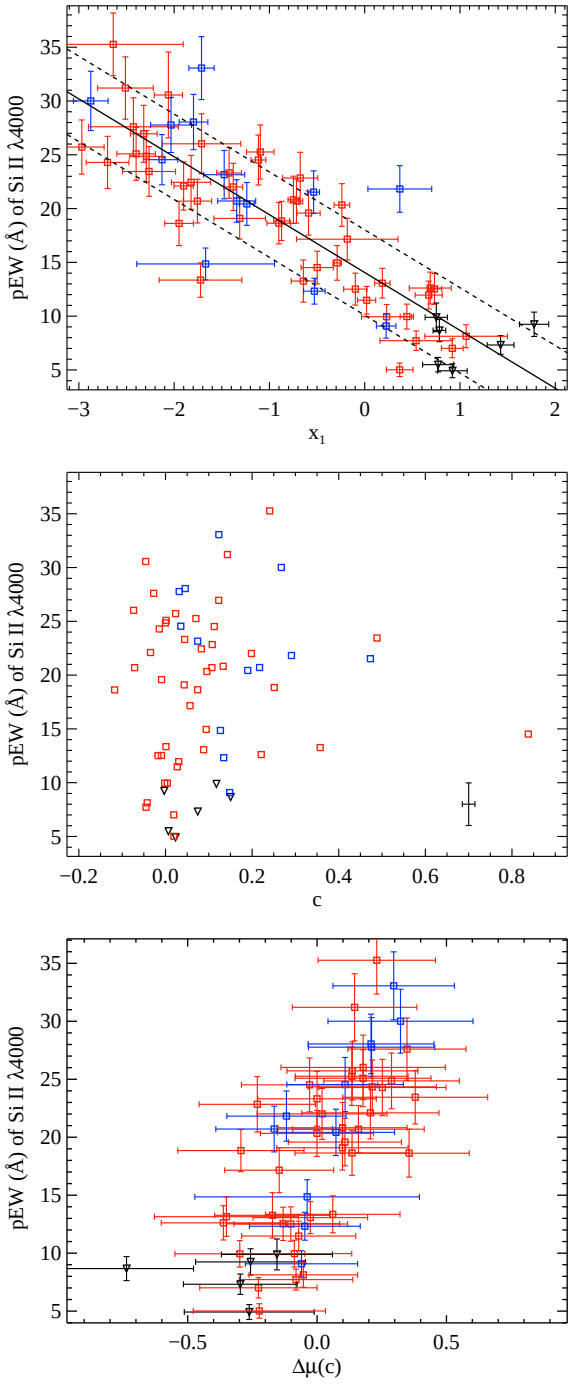

Figure 4.10: The pEW of the Si II λ4000 feature versus SALT2 light-curve width parameter x_1, SALT2 color parameter c, and Hubble residuals corrected for color only. Colors and shapes of data points are the same as in Figure 4.5. In the top plot, the solid line is the linear least-squares fit and the dashed lines are the standard error of the fit. In the middle plot, the median uncertainty in both directions is shown in the lower-right corner.

(the dashed lines are the standard error of the fit). Note that the Ia-99aa objects in the figure also lie along the relationship.

Arsenijevic et al. (2008) plotted x_1 versus the pEW of Si II λ4000 and coded each low-redshift point based on its "Benetti type," and they found that the FAINT objects fell below the linear relationship (i.e., they had smaller than expected pEW values). In BSNIP II it was shown that FAINT (and similarly, Ia-91bg) objects have, if anything, *larger* than average pEW values (especially for the Si II λ4000 feature). Figure 4.10 shows no Ia-91bg objects since SALT/2 is unable to fit that spectral subtype. However, when the BSNIP values of x_1 are plotted against the pEW of Si II λ4000 and coded by "Benetti type," the two FAINT objects fall at the upper-left end of the linear correlation. The cause of this discrepancy between the two studies is unclear.

The middle plot of Figure 4.10 shows no real evidence that the pEW of the Si II λ4000 feature is correlated with c. The Pearson correlation coefficient we find for all of the objects is 0.07, but when removing objects with $c > 0.5$, the coefficient increases to 0.15. This is slightly smaller than what was found by Blondin et al. (2011), and significantly smaller than what was found by Nordin et al. (2011a). While the former claim no observed correlation, the latter do claim that the pEW of Si II λ4000 is correlated with c.

The bottom panel of Figure 4.10 shows the Hubble residuals when corrected for SALT2 color only versus the pEW of Si II λ4000. Blondin et al. (2011) saw a relatively weak correlation between these parameters and found that a distance model involving c and the pEW of the Si II λ4000 feature led to a "marginal improvement" over the standard (x_1, c) model. We find a strong correlation (coefficient of 0.74), and the (c, Si II λ4000 pEW) model performs nearly as well as the (x_1, c) model ($\Delta_{x_1,c} = 0.012 \pm 0.036$). Thus, the BSNIP data are in agreement with the finding of Blondin et al. (2011) that the pEW of the Si II λ4000 feature is essentially a replacement for the x_1 parameter and is an accurate measurement of light-curve width. Figure 4.11 shows the Hubble diagram residuals for the (c, Si II λ4000 pEW) model and the color-corrected-only model verus redshift, with the WRMS for each model as the gray band.

Interestingly, we found that a model involving c, x_1, *and* pEW of the Si II λ4000 feature actually leads to a $\sim$10% decrease in WRMS and a $\sim$28% decrease in $\sigma_{\rm pred}$. For this model, $\Delta_{x_1,c} = -0.026 \pm 0.15$, which implies that the improvement has a significance of about 1.8σ. The correlation between pEW of Si II λ4000 and Hubble residuals corrected for color and light-curve width is only 0.29, and thus perhaps the combination of c, x_1, and pEW of the Si II λ4000 feature is not actually adding much new information. However, the usefulness of a model including all three of these parameters should be investigated with other SN samples. Figure 4.12 contains Hubble residuals for the (x_1, c, Si II λ4000 pEW) model as well as the standard (x_1, c) model (using the same set of objects) versus redshift. Also shown, as the gray band, is the WRMS for each model.

While the above investigation focused on the SALT2 light-curve fitter, we can investigate correlations between pEW of the Si II λ4000 feature and photometric parameters from MLCS2k2. Figure 4.13 shows the 63 BSNIP SNe which have MLCS2k2 fits and measured

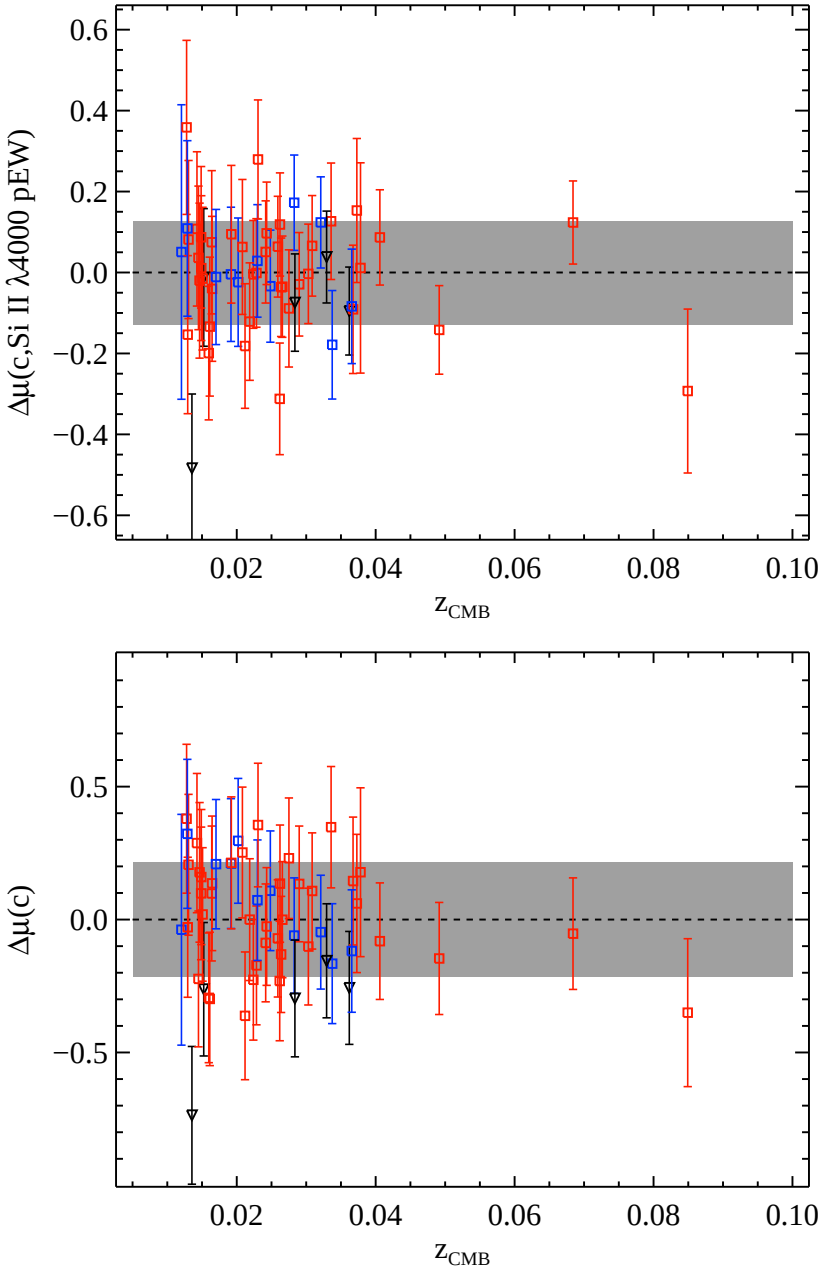

Figure 4.11: Hubble diagram residuals versus $z_{\rm cmb}$ for the (c, Si II λ4000 pEW) model and the color-corrected-only model. The gray band is the WRMS for each model. Colors and shapes of data points are the same as in Figure 4.5.

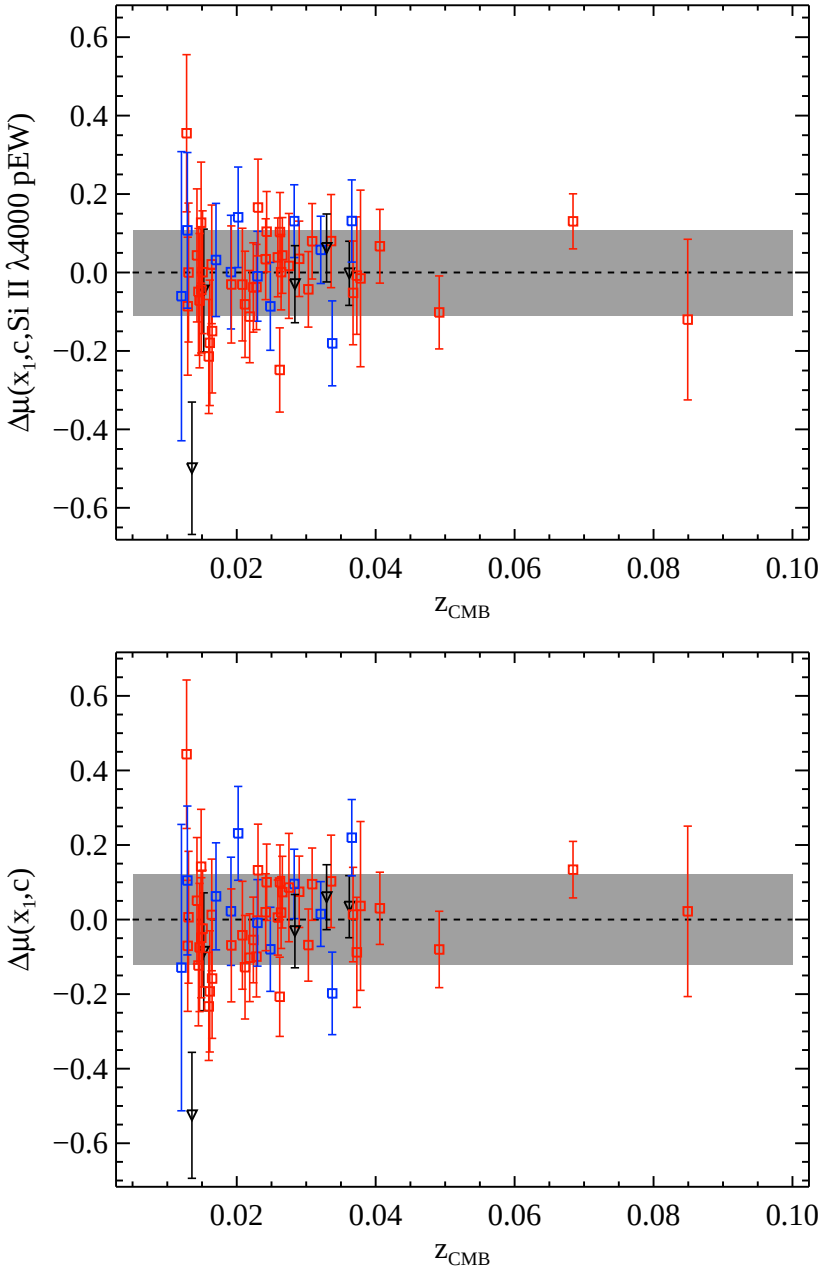

Figure 4.12: Hubble diagram residuals versus $z_{\rm cmb}$ for the (x_1, c, Si II λ4000 pEW) model and the standard (x_1, c) model. The gray band is the WRMS for each model. Colors and shapes of data points are the same as in Figure 4.5.

pEW values for the Si II λ4000 feature within 5 d of maximum brightness. The pEWs are plotted against Δ and A_V.

The Pearson correlation coefficient between pEW of Si II λ4000 and Δ is 0.74, which is larger than previously observed (Nordin et al. 2011b) and implies that these parameters are highly correlated. This is expected based on the high degree of correlation between pEW of Si II λ4000 and x_1 since both Δ and x_1 are measurements of the width of SN Ia light curves. In Figures 4.13 and 4.10 the Ia-99aa objects lie at the extreme low-pEW end of the relationship, though perhaps they are slightly systematically below the trend in the top panel of Figure 4.13. On the other hand, the Ia-91bg objects in the top panel of Figure 4.13 fall significantly below the linear trend.

As in Nordin et al. (2011b), there is no significant correlation between pEW of Si II λ4000 and A_V, even when objects with $A_V > 0.5$ mag are removed (correlation coefficients of < 0.13 in both cases using the BSNIP data). In all of the plots presented in this section, HV and Ia-norm objects overlap significantly. This is expected since in BSNIP II it was shown that the pEW of the Si II λ4000 feature is extremely similar for these two subclasses. We also note that the plot of $\Delta m_{15}(B)$ versus pEW of Si II λ4000 looks nearly identical to the top panel of Figure 4.13 and has a larger Pearson correlation coefficient of 0.85.

Fe II and Mg II

Nordin et al. (2011b) found that the ΔpEW of Fe II within 3 d of maximum brightness is well-correlated with SALT color. In Figure 4.14 we present the 63 SNe in the BSNIP sample which have SALT2 fits and a measurement of the pEW of the Fe II complex within 5 d of maximum brightness. The two observables plotted have a Pearson correlation coefficient of 0.41, but it increases to 0.53 for objects with $c < 0.5$. If, however, only spectra within 3 d of maximum brightness are used, the correlation increases slightly but the sample size decreases by nearly one-quarter. The strength of this correlation is slightly higher than that found by Nordin et al. (2011b), though we point out that they used SALT color while we use SALT2 color, and they used ΔpEW (i.e., the difference between the measured pEW and the average pEW evolution) while we use the actual measured pEW. Ia-99aa objects appear to have typical values of both pEW of Fe II and c, though there are a very small number of objects of this spectral subtype. On the other hand, HV SNe seem to be both redder and have larger pEWs, but as before, there is significant overlap with Ia-norm objects as well.

The pEW of the Mg II complex is almost as correlated with c, as seen in Figure 4.15. In that figure, 64 SNe within 5 d of maximum brightness are plotted, and they have a Pearson correlation coefficient of 0.42 (for objects with $c < 0.5$). Once again, when using only spectra within 3 d of maximum brightness the correlation becomes slightly stronger at the expense of significant decrease in the sample size. This correlation has been observed previously, though at slightly lower significance and with almost one-third the number of low-z SNe (Walker et al. 2011). The data presented in Figure 4.15 match well with what was shown in Walker et al. (2011) for low-z objects, but their high-z sample spans a much larger range of

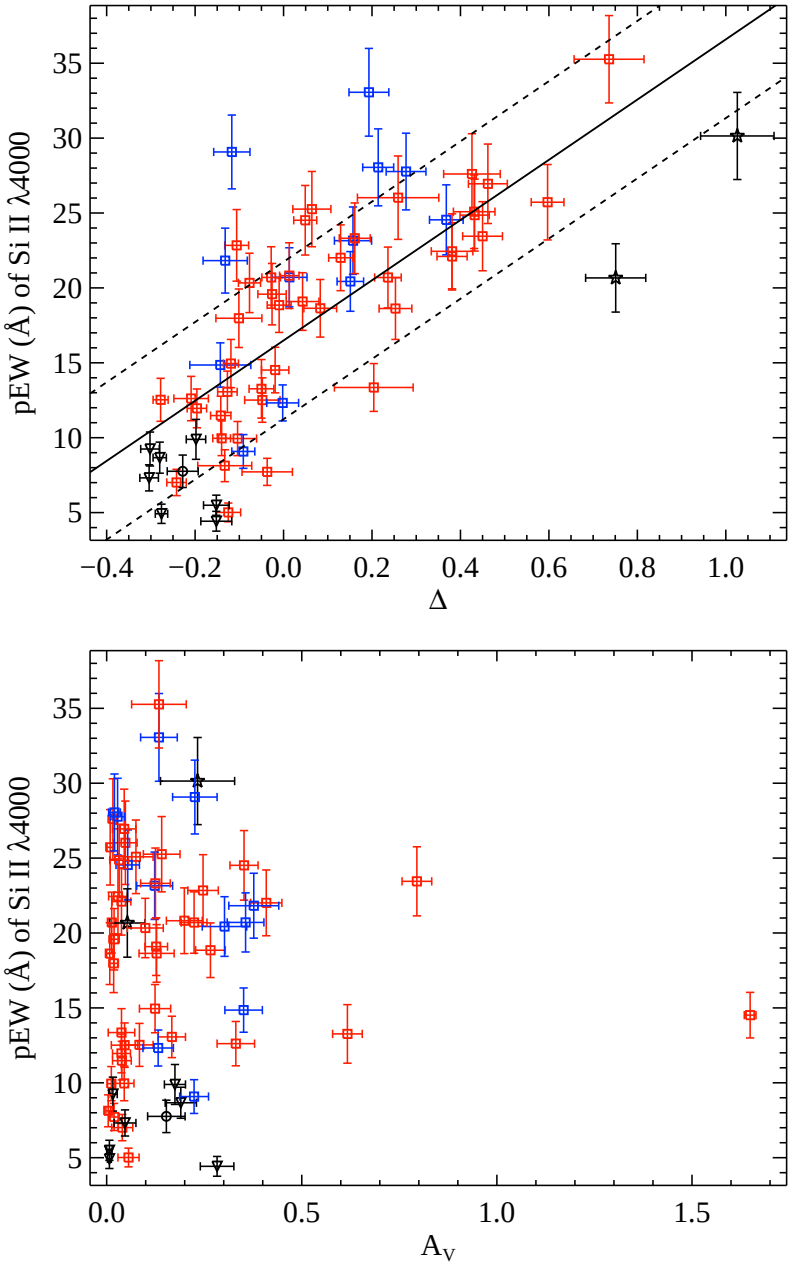

Figure 4.13: The pEW of the Si II λ4000 feature versus MLCS2k2 light-curve width parameter Δ and MLCS2k2 reddening parameter A_V. Colors and shapes of data points are the same as in Figure 4.5. In the top plot, the solid line is the linear least-squares fit and the dashed lines are the standard error of the fit.

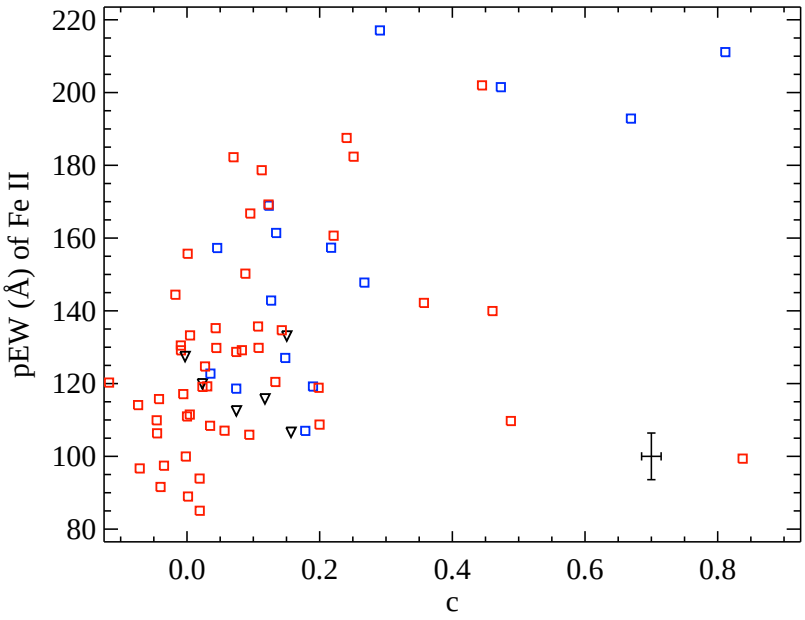

Figure 4.14: The pEW of the Fe II complex versus the SALT2 color parameter c. Colors and shapes of data points are the same as in Figure 4.5. The median uncertainty in both directions is shown in the lower-right corner.

Mg II pEW values and show nearly no correlation with c. There seems to be effectively no difference between the various spectroscopic subtypes in this parameter space.

The significant correlations between c and both pEWs of Fe II and Mg II are promising. Measuring a pEW of a broad feature in a single spectrum near maximum brightness is much simpler than obtaining photometric data for a full light curve that needs to then be modeled by a light-curve fitter (such as SALT2). The fact that a significant amount of scatter is seen in these relationships, however, means that one should probably not simply measure a pEW and use a linear fit to either Figure 4.14 or Figure 4.15 to convert directly to a value for c (which could then be used in a Hubble diagram).

It would likely be more accurate to use a correction term involving the pEW value itself *in lieu of* a term involving c. As with all other spectral measurements discussed in this work, we tested this hypothesis by constructing Hubble diagrams using the pEW of Fe II and Mg II and models of the form shown in Equations 4.4–4.7. All but one of these models performed worse than the standard (x_1, c) model. The model including x_1, c, and the pEW of Mg II was only as accurate as the standard model ($\Delta_{x_1,c} = -0.004 \pm 0.004$). While this is somewhat disheartening, using the pEW of Fe II or Mg II as a replacement for c or in addition to c (along with x_1) is a tantalizing possibility that should be explored using future datasets.

Furthermore, we attempt two other Hubble diagrams using no light-curve information

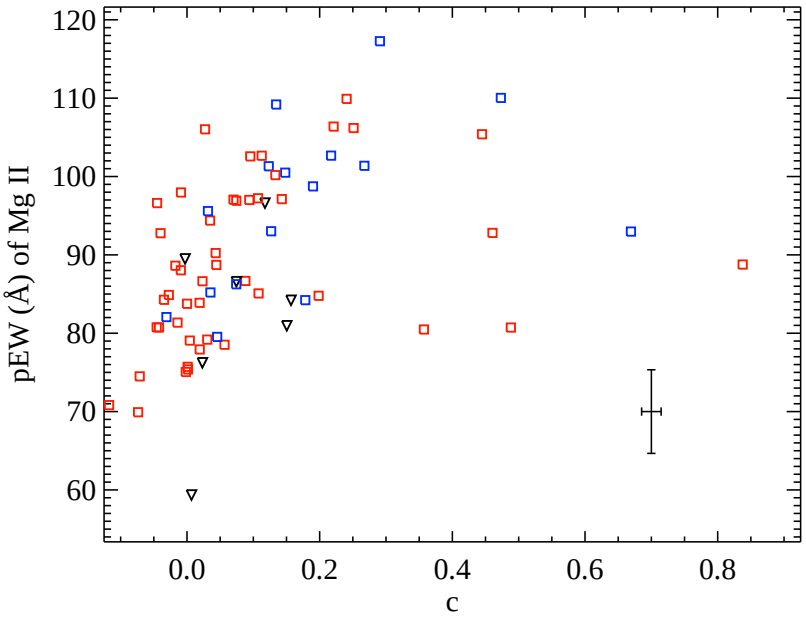

Figure 4.15: The pEW of the Mg II complex versus the SALT2 color parameter c. Colors and shapes of data points are the same as in Figure 4.5. The median uncertainty in both directions is shown in the lower-right corner.

whatsoever. One uses only the pEWs of the Si II λ4000 feature and the Fe II complex and the other uses only the pEWs of the Si II λ4000 feature and the Mg II complex. The idea is that the pEW of Si II λ4000 is a good proxy for x_1, and the pEWs of the Fe II and Mg II features are reasonably good proxies for c. However, both of these models performed significantly worse than the usual (x_1, c) model.

S II "W"

As discussed in Section 4.4.3, the depth of the *bluer absorption* of the S II "W" feature relative to the pseudo-continuum was shown by Blondin et al. (2011) to decrease the scatter of Hubble residuals by about 10%. In that section we showed that the relative depths of the *redder absorption* of the S II "W" in the BSNIP data were marginally correlated with x_1, opposite to what was seen by Blondin et al. (2011). However, both studies agree that c and the color- and width-corrected Hubble residual are uncorrelated with the relative depth of the S II "W".

As discussed in BSNIP II, the relative depth of a spectral feature relies on a spline fit to the spectra and can fairly easily be contaminated by local noise. The pEW, however, is less prone to this type of contamination, relies only on the definition of the pseudo-continuum (and not any additional fit to the data), and often contains the same information as the relative depth. For these reasons the pEW values were used in favor of the a values in the

analysis performed in BSNIP II. Furthermore, both Blondin et al. (2011) and BSNIP II measure the pEW of the *entire* S II "W" feature, and thus pEW values are a more fair comparison between the two studies than are a values.

In Figure 4.16 we present the 64 BSNIP SNe which have SALT2 fits and measured pEW values for the S II "W" feature within 5 d of maximum brightness. The pEWs are plotted against x_1 and c.

As in Figure 4.9, c is is uncorrelated with the pEW of the S II "W" (Pearson correlation coefficient of 0.11 for objects with $c < 0.5$). Opposite to Figure 4.9, however, x_1 is *also* relatively uncorrelated with the pEW of the S II "W" (Pearson correlation coefficient of -0.22). This is significantly weaker than the correlation between x_1 and the relative depth of this feature found in Section 4.4.3. Equations 4.4–4.7 were used to create Hubble diagrams involving the pEW of the S II "W," but none of these models led to an improvement in the WRMS.

Si II λ5972

In BSNIP II it was shown that the pEW of the Si II λ5972 feature correlated well with the spectral luminosity indicator $\Re$(Si II) (see Section 4.4.5 for more information on this parameter). Thus, one might expect this pEW to be an accurate luminosity indicator as well, and in fact evidence for a correlation between the pEW of Si II λ5972 and x_1 and $\Delta m_{15}(B)$ has been seen in previous work (Nordin et al. 2011b; Hachinger et al. 2006, respectively).

Figure 4.17 shows the 55 SNe which have a SALT2 fit as well as a measured pEW for the Si II λ5972 feature. We find a Pearson correlation coefficient of -0.65, which is stronger than what was found by Nordin et al. (2011b). As in the relationship between x_1 and pEW of Si II λ4000, the Ia-99aa objects appear to follow the relation.

Similarly, a strong linear correlation has been observed between the pEW of Si II λ5972 and $\Delta m_{15}(B)$ (Hachinger et al. 2006). This relationship is also found in the BNSIP data, as shown in Figure 4.18. In that plot there are 62 SNe, the parameters have a Pearson correlation coefficient of 0.74, and as with the relationship with x_1, Ia-99aa objects occupy the bottom of the correlation while the Ia-norm and HV objects are highly overlapping. Hachinger et al. (2006) denote the "Benetti type" of each object on their plot of pEW of Si II λ5972 versus $\Delta m_{15}(B)$ and note that FAINT objects are found at the top of the correlation while LVG SNe are found at the bottom (with most HVG objects occupying the middle of the trend). The BSNIP data show a similar behavior for the FAINT objects (again, much like the Ia-91bg objects in Figure 4.18); however, our data show no differentiation between the LVG and HVG objects in this parameter space. Finally, we note that when plotting the pEW of the Si II λ5972 feature against the MLCS2k2 Δ parameter, nearly the exact same results are seen as those in Figure 4.18.

As with the S II "W," no distance model utilizing the pEW of the Si II λ5972 led to an improvement in the Hubble residuals.

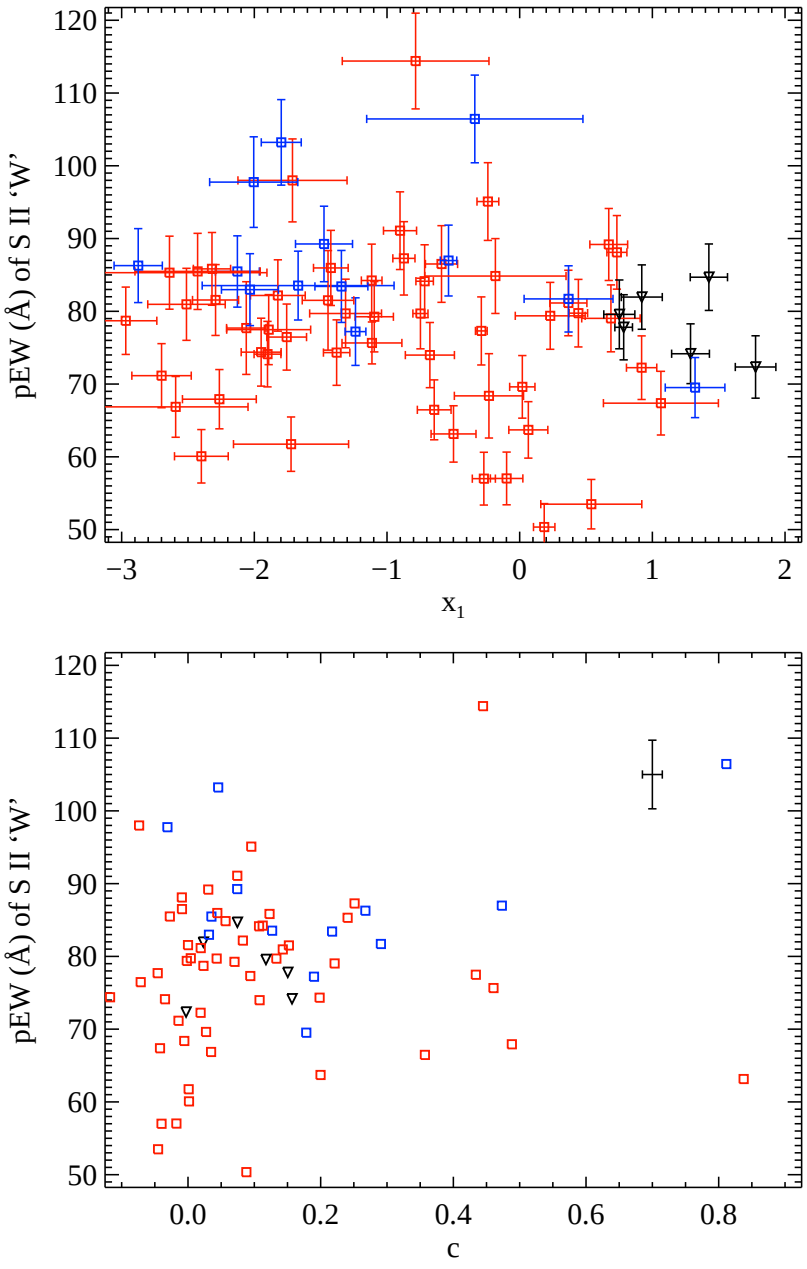

Figure 4.16: The pEW of the S II "W" feature versus SALT2 light-curve width parameter x_1 and SALT2 color parameter c. Colors and shapes of data points are the same as in Figure 4.5. In the bottom plot, the median uncertainty in both directions is shown in the upper-right corner.

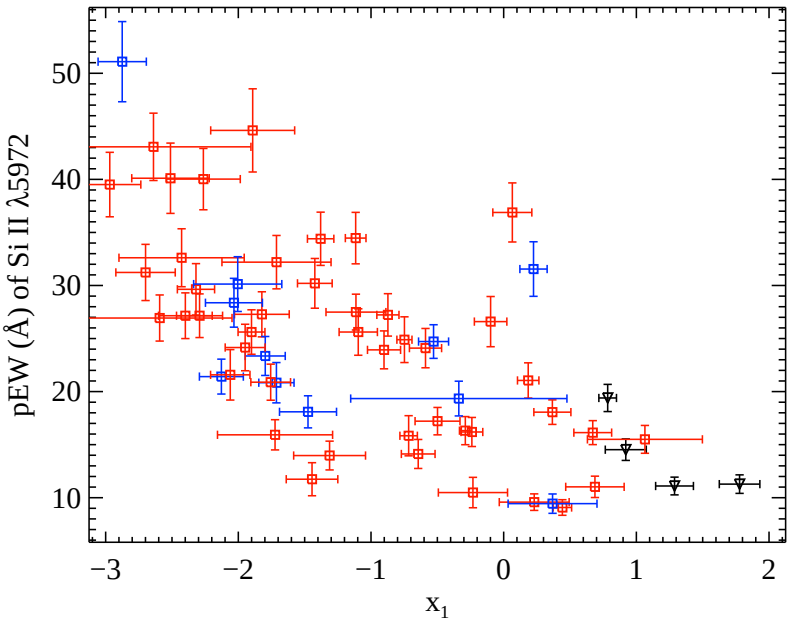

Figure 4.17: The pEW of Si II λ5972 versus the SALT2 light-curve width parameter x_1. Colors and shapes of data points are the same as in Figure 4.5.

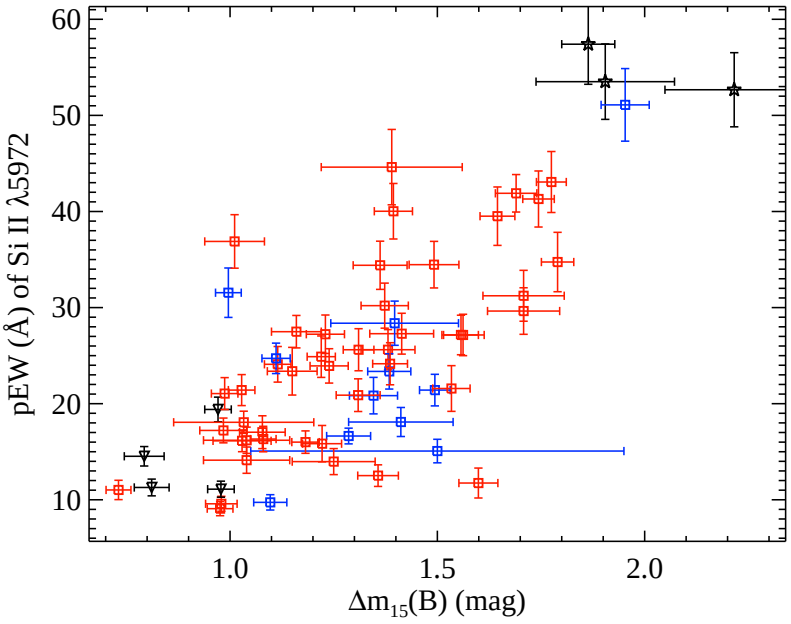

Figure 4.18: The pEW of the Si II λ5972 feature versus $\Delta m_{15}(B)$. Colors and shapes of data points are the same as in Figure 4.5.

Si II λ6355

Much like the pEW of Si II λ5972, the pEW of Si II λ6355 has been seen to correlate marginally well with x_1 and separate various spectral subtypes when compared to $\Delta m_{15}(B)$ (Nordin et al. 2011b; Hachinger et al. 2006, respectively).

In Figure 4.19 the 66 SNe with SALT2 fits and pEW values for the Si II λ6355 feature are shown. The pEW values are plotted against x_1, c, and Hubble residuals corrected for light-curve width and color (for objects that are part of the Hubble diagram). A Pearson correlation coefficient of -0.57 is calculated for the top panel. This is consistent with what was observed in the data studied by Nordin et al. (2011b). As in the previous two relationships between x_1 and the pEW of Si II features, the Ia-99aa objects follow the linear relation.

We find that c is somewhat correlated with the pEW of Si II λ6355 (correlation coefficient of 0.43) for objects with $c < 0.5$. This pEW is even less correlated with Hubble residuals corrected for x_1 and c (correlation coefficient of 0.22). However, a distance model which includes x_1, c, and the pEW of the Si II λ6355 feature leads to a 4% decrease in WRMS, a 6% decrease in $\sigma_{\rm pred}$, and is significant at the 1.2σ level. So while this is technically an improvement over the standard (x_1, c) model, it may not actually be all that helpful.

Plotting the pEW of Si II λ6355 versus $\Delta m_{15}(B)$, Hachinger et al. (2006) are able to separate FAINT, LVG, and HVG objects relatively accurately. This is also seen, though at a lower significance, in the BNSIP data. In Figure 4.20 we plot 80 SNe; the parameters have a Pearson correlation coefficient of 0.46 but the Ia-91bg, Ia-99aa, and the lone Ia-91T objects are all reasonably well separated from the bulk of the SNe. There is even some evidence for a difference between HV and Ia-norm objects in this parameter space. As mentioned above, Hachinger et al. (2006) denote the "Benetti type" of each object on their plot of pEW of Si II λ6355 versus $\Delta m_{15}(B)$ and state that the three subtypes are well separated. Again the BSNIP data support this conclusion, but at a weaker significance. FAINT objects are found in the same part of parameter space as the Ia-91bg objects, while HVG and HV SNe tend to occupy a different part of parameter space compared with the LVG and Ia-norm/91T/99aa objects. However, there is quite a lot of overlap among all of the non-FAINT (and non-Ia-91bg) SNe.

Figure 4.21 presents the pEW of the Si II λ6355 feature plotted against $(B-V)_{\rm max}$. The top panel shows all 78 SNe from the BSNIP dataset for which both of these values have been measured and the bottom panel shows a close-up of objects with $(B-V)_{\rm max} < 0.319$ mag. The linear least-sqaures fit to all of the points is shown by the solid line and the fit to SNe with $(B-V)_{\rm max} < 0.319$ mag is shown by the dotted line.

The correlations for the full sample and the less reddened sample are weak (Pearson coefficients 0.12 and 0.16, respectively), somewhat lower than the correlation coefficient of 0.28 found by Foley et al. (2011). Qualitatively, however, the two studies match, although the slope found in the BSNIP data is steeper than that of Foley et al. (2011). The pEW of the Si II λ6355 feature is less correlated with $(B-V)_{B_{\rm max}}$ than the velocity near maximum brightness of that same spectral feature. Thus, we disagree with the statement of Foley et al.

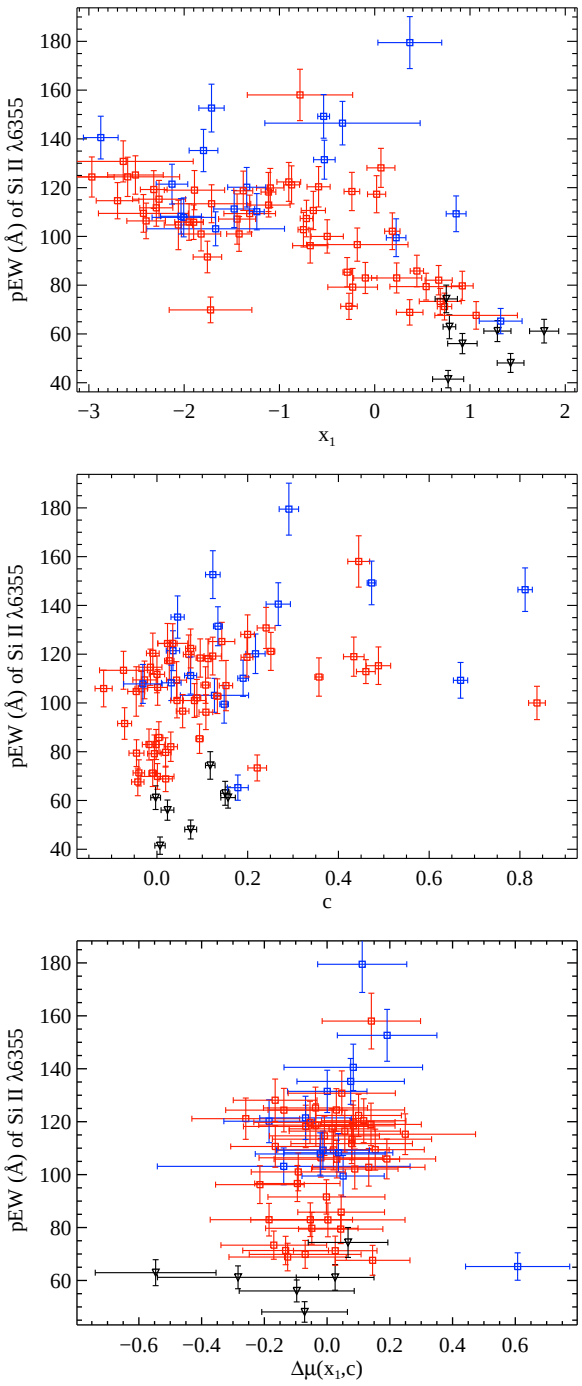

Figure 4.19: The pEW of the Si II λ6355 feature versus SALT2 light-curve width parameter x_1, SALT2 color parameter c, and Hubble residuals corrected for light-curve width and color. Colors and shapes of data points are the same as in Figure 4.5.

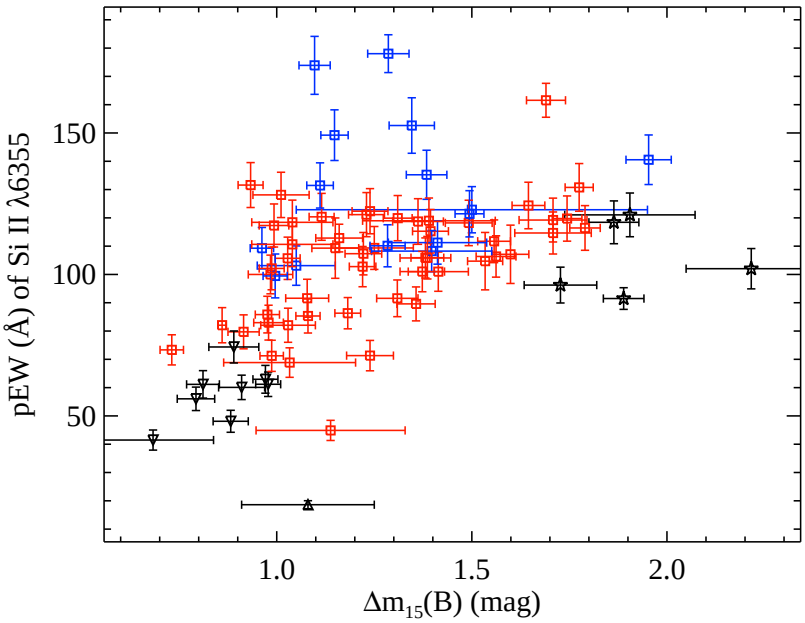

Figure 4.20: The pEW of Si II λ6355 versus $\Delta m_{15}(B)$. Colors and shapes of data points are the same as in Figure 4.5.

(2011) that both the velocity and pEW of Si II λ6355 can be used to derive the intrinsic color of SNe Ia.

Ca II and O I

Much like Hachinger et al. (2006), we searched for possible correlations between pEWs of each spectral feature investigated and various photometric parameters. Many of the strongest and most interesting of these possible correlations have been discussed in the preceding sections. For Ca II H&K as well as the O I triplet, no pairs of pEWs and photometric parameters were found to have Pearson correlation coefficients > 0.4.

However, the pEW of the Ca II near-IR triplet is found to correlate with Δ (with a Pearson correlation coefficient of 0.66) and with c (with a Pearson correlation coefficient of 0.50 for SNe with $c < 0.5$). These two relationships are shown in Figure 4.22, where we plot 59 SNe with pEWs of the Ca II near-IR triplet and Δ (top panel) as well as 53 SNe with pEWs of the Ca II near-IR triplet and c (bottom panel).

Both correlations are marginal at best; however, this spectral region has been studied very little in the past. One of the strengths of the BSNIP data are that the average wavelength coverage (3300–10,400 Å) is significantly wider than that of most other SN Ia spectral datasets. For example, one of the largest previously published SN Ia spectral datasets had an average wavelength coverage of 3700–7400 Å (Matheson et al. 2008). Thus, the Ca II H&K feature, the O I triplet, and the Ca II near-IR triplet have been ignored almost entirely in

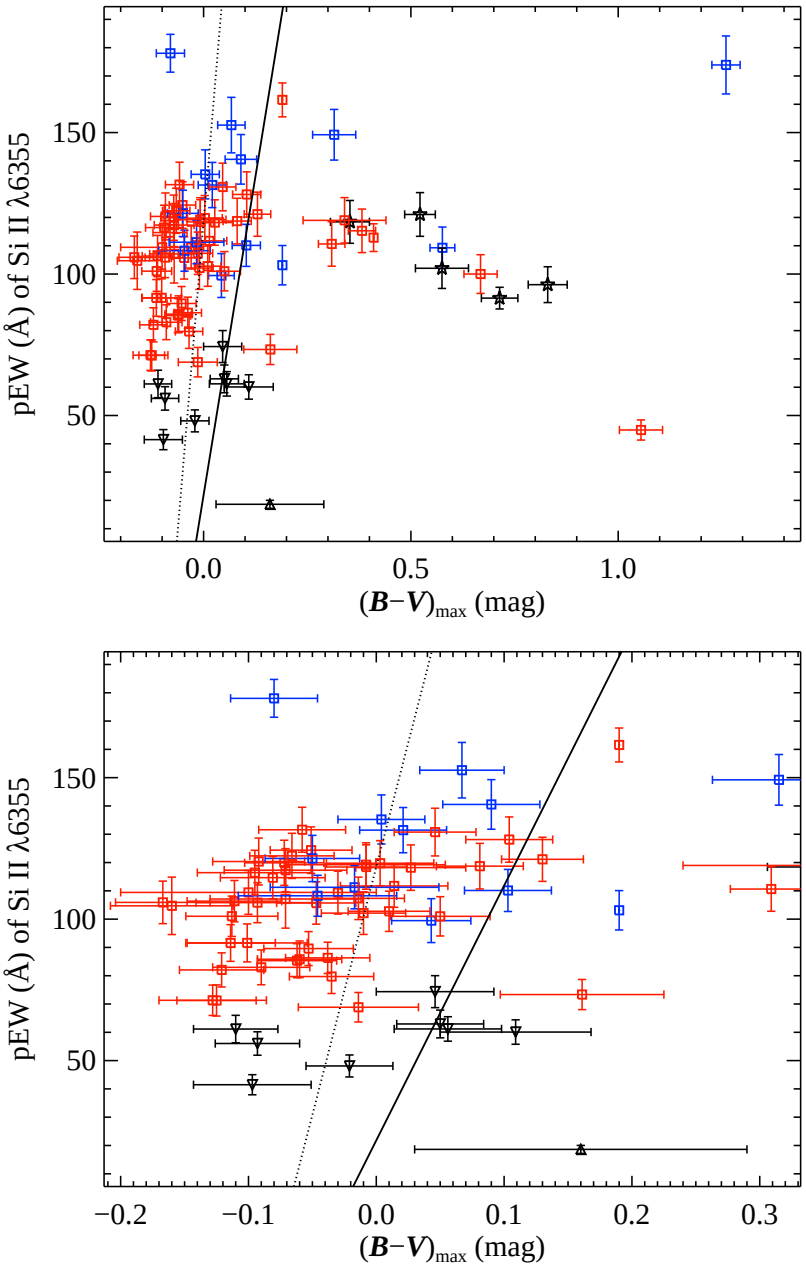

Figure 4.21: The pEW of the Si II λ6355 feature versus $(B-V)_{B_{\max}}$ (*top*) and a close-up view of objects with $(B-V)_{\max} < 0.319$ mag (*bottom*). Colors and shapes of data points are the same as in Figure 4.5. The solid line is the fit to all of the data while the dotted line is the fit only to objects with $(B-V)_{\max} < 0.319$ mag.

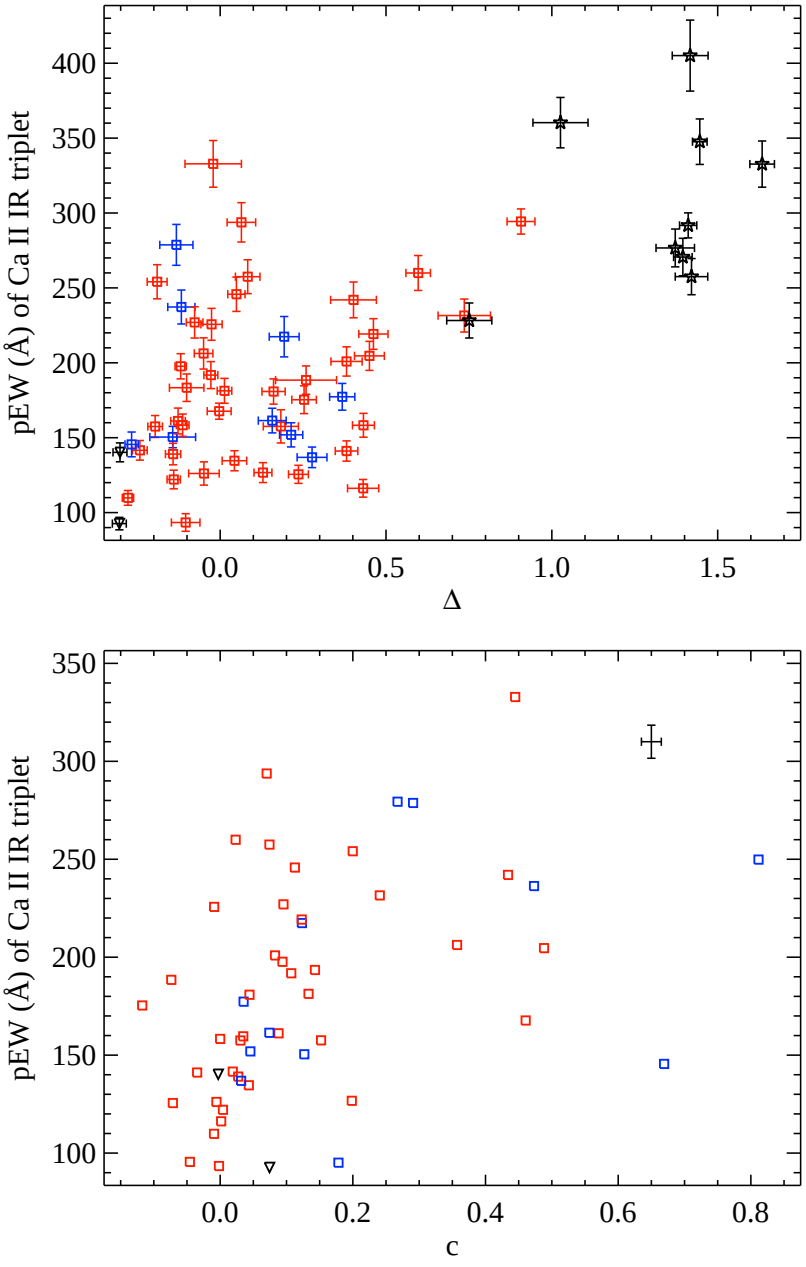

Figure 4.22: The pEW of the Ca II near-IR triplet versus MLCS2k2 light-curve width parameter Δ (*top*) and SALT2 color parameter c (*bottom*). Colors and shapes of data points are the same as in Figure 4.5. In the bottom plot, the median uncertainty in both directions is shown in the upper-right corner.

past spectral analyzes like the one presented here.

We once again constructed Hubble diagrams from Equations 4.4–4.7 and using pEW values of Ca II H&K, the O I triplet, and the Ca II near-IR triplet. All but two models were significantly worse at measuring distances than the standard (x_1, c) model. The $(x_1, c$, Ca II H&K pEW) and $(x_1, c$, O I triplet pEW) models both slightly decreased the WRMS, but at almost imperceptible levels ($\Delta_{x_1,c} = -0.0023 \pm 0.0096$ and $\Delta_{x_1,c} = -0.0063 \pm 0.0148$, respectively).

4.4.5 The Si II Ratio

One of the first spectral luminosity indicators investigated was the Si II ratio, $\Re$(Si II), defined by Nugent et al. (1995) as the ratio of the depth of the Si II λ5972 feature to the depth of the Si II λ6355 feature. Hachinger et al. (2006) redefined the Si II ratio as the pEW of Si II λ5972 divided by the pEW of Si II λ6355. In BSNIP II it was shown that these are nearly equivalent definitions, so in order to be consistent with that work we define the Si II ratio for the present study to be

$$\Re\,(\text{Si II}) \equiv \frac{\text{pEW}\,(\text{Si II}\ \lambda5972)}{\text{pEW}\,(\text{Si II}\ \lambda6355)}. \tag{4.12}$$

The Si II ratio has been shown to correlate with maximum absolute B-band magnitude and $\Delta m_{15}(B)$, which is why it has been used as a spectral luminosity indicator (e.g., Nugent et al. 1995; Benetti et al. 2005; Hachinger et al. 2006). Figure 4.23 shows 62 SNe Ia with both $\Delta m_{15}(B)$ and $\Re$(Si II). The data are correlated with a Pearson correlation coefficient of 0.59. Ia-91bg objects appear at the upper right of the plot and form a continuous relationship with the Ia-norm objects. Ia-99aa objects appear to lie above the main trend (though there are only a handful of these SNe in the figure), while HV objects lie below the main trend. When removing the Ia-99aa objects, the correlation increases slightly (coefficient of 0.65).

If we instead tag each data point in Figure 4.23 by its "Benetti type," we find that the FAINT objects are found in the upper right of the main trend (similar to the Ia-91bg objects and as seen in previous studies, e.g., Benetti et al. 2005; Hachinger et al. 2006). The LVG and HVG objects are found in the lower-left portion of the plot with a significant level of overlap between the two subclasses. This is different than previous work, where there have been claims that LVG objects have larger Si II ratios and lie above the main trend (Benetti et al. 2005; Hachinger et al. 2006), though these studies and the BSNIP data both observe larger scatter in $\Re$(Si II) values in the lower $\Delta m_{15}(B)$ objects. When removing the LVG objects, the correlation is effectively unchanged. Comparing $\Re$(Si II) to the MLCS2k2 Δ parameter yields similar results to those seen in Figure 4.23.

The BSNIP distribution of $\Delta m_{15}(B)$ values, while not evenly distributed, is more continuous than in previous studies similar to the present one. For example, the data in Hachinger et al. (2006) contained only one object with $\Delta m_{15}(B)$ between 1.5 and 1.7 mag, while the BSNIP data has 7 objects in that range. A more continuous distribution of

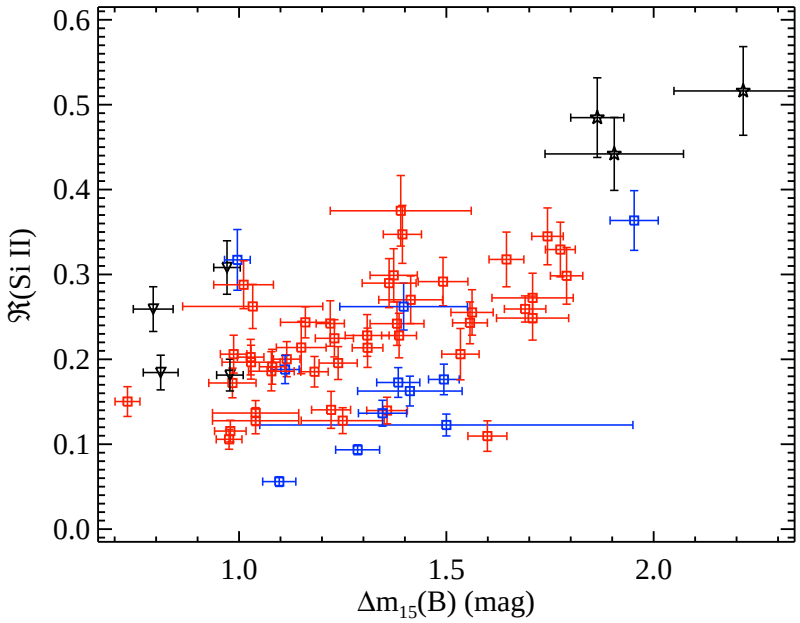

Figure 4.23: The Si II ratio versus $\Delta m_{15}(B)$. Colors and shapes of data points are the same as in Figure 4.5.

$\Delta m_{15}(B)$ values, combined with the spectroscopic subclasses presented in Figure 4.23, complicates the relatively simplistic view that underpins the basic "Phillips relation." For $0.95 \lesssim \Delta m_{15}(B) \lesssim 1.0$ mag there are Ia-99aa, Ia-norm, *and* HV objects. On the other end of the $\Delta m_{15}(B)$ distribution, between $\sim$1.75 and $\sim$1.95 mag there are Ia-91bg, Ia-norm, *and again* HV objects. Thus, for a given light-curve width (or decline rate), there exist SNe Ia of significantly different subclasses.

As discussed in BSNIP II, objects tagged by SNID as Ia-91bg or Ia-99aa are the most spectroscopically peculiar objects and probably only represent the extreme ends of a continuous distribution of spectra. If true, this means that the most spectroscopically peculiar objects *may not* have the most extreme light curves. The reverse may also be true, namely that the SNe with the most extreme light curves may not be the most spectroscopically peculiar. This is further supported by the relatively wide scatter in the main trend of Figure 4.23. At any value of $\Delta m_{15}(B)$ (with a significant number of objects) there is a broad range in $\Re$(Si II) values.

In BSNIP II, it was pointed out that the relative strength of the two Si II features that go into calculating $\Re$(Si II) is fairly robust at differentiating between the various "SNID types" and "Wang types," Thus, from a spectrum, either using SNID or pEWs of Si II features, one may declare an object to be Ia-91bg or Ia-99aa whereas based on the light curve of the same object it might be considered relatively normal. The significant amount of scatter in the correlation between the Si II ratio and $\Delta m_{15}(B)$ also cautions one against simply measuring

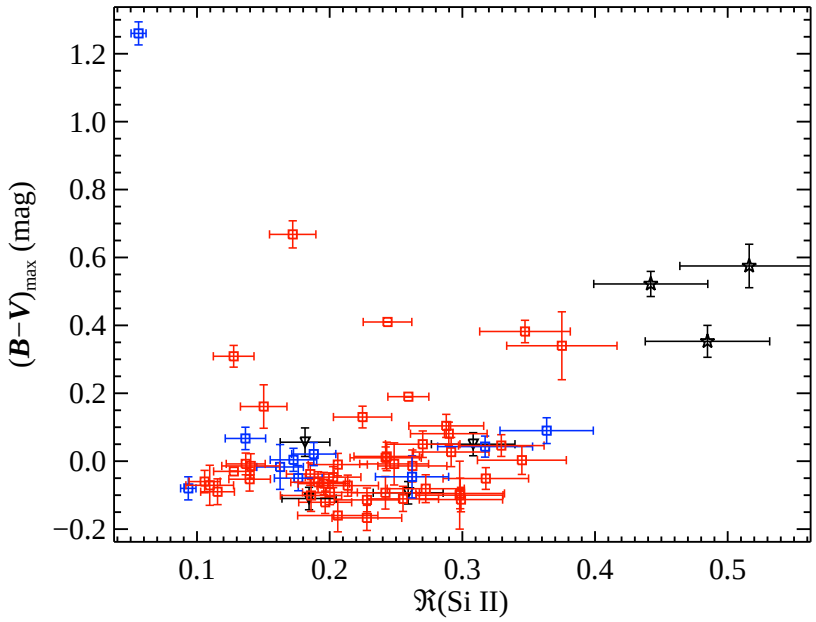

Figure 4.24: $(B-V)_{\rm max}$ (the difference between B-band magnitude and V-band magnitude at the time of B-band maximum brightness) versus the Si II ratio. Colors and shapes of data points are the same as in Figure 4.5.

$\Re$(Si II) from a single spectrum and then using that value and a fit to the data in Figure 4.23 to calculate a $\Delta m_{15}(B)$ value.

A relationship between Si II ratio and $(B-V)_{\rm max}$ has also been seen (Altavilla et al. 2009). 61 SNe from the BSNIP sample are shown in Figure 4.24, where $\Re$(Si II) is plotted against $(B-V)_{\rm max}$ for spectra within 5 d of maximum brightness. The figure matches well with what has been seen before, though our sample also contains a handful of highly reddened objects ($(B-V)_{\rm max} \gtrsim 0.3$ mag) that were not seen in previous work (Altavilla et al. 2009); the significant outlier in the upper-left corner of the plot is the highly reddened, HV object SN 2006X (e.g., Wang et al. 2008). The Ia-91bg objects are found at the upper-right end of the main correlation while the other subclasses are highly mixed (similar to previous work, e.g., Altavilla et al. 2009).

In Figure 4.25 we show the 51 BSNIP SNe which have SALT2 fits and Si II ratios within 5 d of maximum brightness. $\Re$(Si II) is plotted against x_1, c, and Hubble residuals corrected for color only (for SNe which are used in the Hubble diagram).

From the BSNIP data we find that the Si II ratio is only marginally correlated with x_1 (top plot of Figure 4.25) with a Pearson correlation coefficient of -0.40. This is a weaker relationship than what has been found before (Blondin et al. 2011). The Ia-99aa objects appear to be above the main trend and most of the HV objects seem to be below it.

The middle plot of Figure 4.25 shows no evidence for a correlation between $\Re$(Si II) and

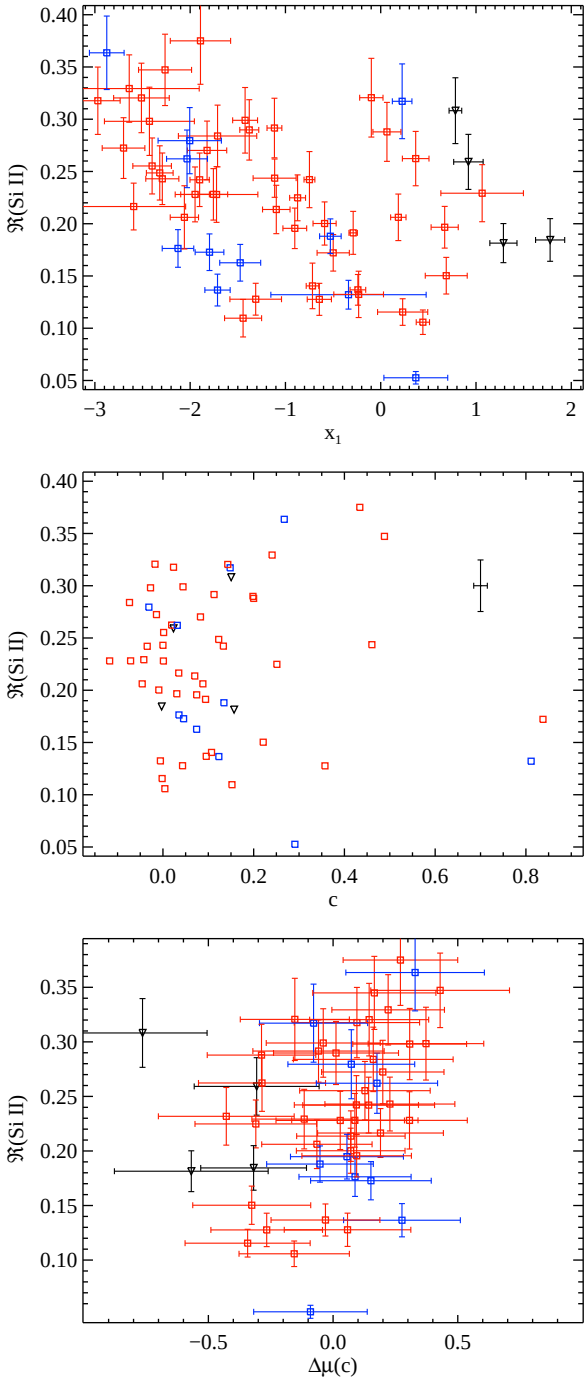

Figure 4.25: The Si II ratio versus SALT2 light-curve width parameter x_1, SALT2 color parameter c, and Hubble residuals corrected for color only. Colors and shapes of data points are the same as in Figure 4.5. In the middle plot, the median uncertainty in both directions is shown in the upper-right corner.

c, with a Pearson correlation coefficient of -0.14 for objects with $c < 0.5$.

Finally, the bottom plot of Figure 4.25 shows a possible correlation between the Si II ratio and Hubble residuals corrected for color only (coefficient of 0.30), and it is again significantly weaker than what has been found before (Blondin et al. 2011). In fact, Blondin et al. (2011) go so far as to say that $\Re$(Si II) acts as a replacement for x_1, but the BSNIP data do not support such a claim. Using the current sample, the best model which includes the Si II ratio also includes both x_1 *and* c, but it is only about as accurate as the standard (x_1, c) model ($\Delta_{x_1,c} = 0.0199 \pm 0.0199$).

Interestingly, Blondin et al. (2011) found that the subluminous (but Ia-norm) SN 2000k is a 2σ outlier in their plot of $\Re$(Si II) versus c, but part of the main correlation of $\Re$(Si II) versus x_1. This object is in the BSNIP dataset and, while we agree that it is subluminous and spectroscopically normal, it is not a significant outlier in any of the three plots in Figure 4.25.

4.4.6 The Ca II Ratio

The Ca II ratio was defined by Nugent et al. (1995) as the ratio of the flux at the red edge of the Ca II H&K feature to the flux at the blue edge of that feature. In the notation from BSNIP II this is

$$\Re\,(\text{Ca II}) \equiv \frac{F_r\,(\text{Ca II H\&K})}{F_b\,(\text{Ca II H\&K})}. \tag{4.13}$$

Like the Si II ratio, it has been found to correlate with maximum absolute B-band magnitude (Nugent et al. 1995).

In BSNIP II it was shown that the Ca II ratio and the Si II ratio are uncorrelated, even though both of them have been used as spectral luminosity indicators. In Section 4.4.5 it was shown that $\Re$(Si II) is correlated with $\Delta m_{15}(B)$. Figure 4.26 shows that $\Re$(Ca II) is even more correlated with $\Delta m_{15}(B)$ (Pearson correlation coefficient of 0.71). The plot contains 65 SNe; the least-squares linear fit to the data is shown as the solid line in Figure 4.26 and the dashed lines are the standard error.

Interestingly, the HV objects seem to occupy a relatively narrow region of parameter space that is surrounded on all sides by mainly Ia-norm SNe. Ia-99aa objects mostly make up the lowest end of the linear trend, while one of the two Ia-91bg objects in the plot perhaps does not follow the main relationship. Unsurprisingly, comparing Δ to $\Re$(Ca II) results in the same trends seen in Figure 4.26.

Figure 4.27 displays the 64 BSNIP SNe which have SALT2 fits as well as Ca II ratios within 5 d of maximum brightness. $\Re$(Ca II) is plotted against x_1, c, and Hubble residuals corrected for light-curve width and color (for objects used when constructing the Hubble diagram).

The Ca II ratio appears to be moderately well anti-correlated with x_1 (correlation coefficient of -0.53) and correlated with c (coefficient of 0.46). The bottom plot of Figure 4.27 shows that the x_1 and c corrected Hubble residuals versus $\Re$(Ca II) are even less correlated with each other (coefficient of 0.27). However, a model that uses x_1, c, *and* the Ca II ratio

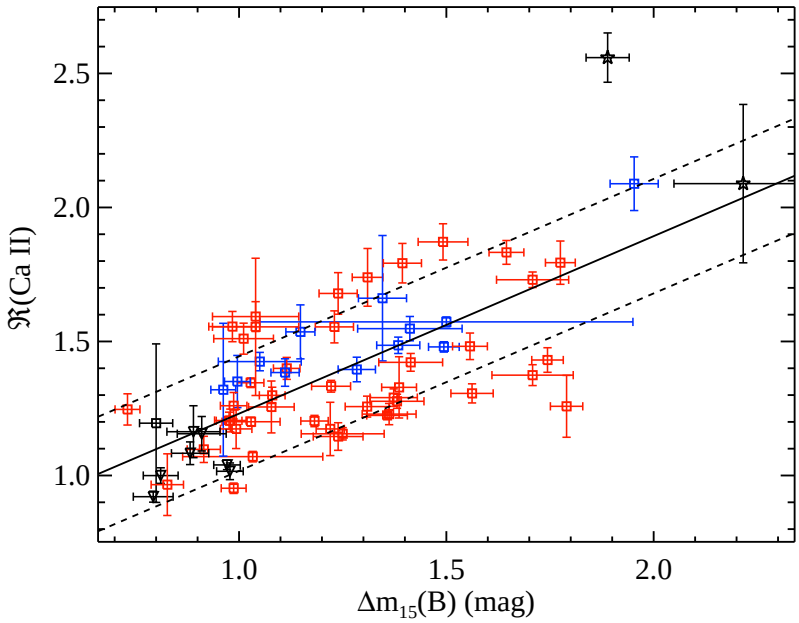

Figure 4.26: The Ca II ratio versus $\Delta m_{15}(B)$. Colors and shapes of data points are the same as in Figure 4.5. The solid line is the linear least-squares fit and the dashed lines are the standard error of the fit.

decreases the WRMS by ∼6% and the $\sigma_{\rm pred}$ by ∼33%. The significance of this improvement is only at the 1.1σ level ($\Delta_{x_1,c} = -0.0207 \pm 0.0191$), though.

4.4.7 The "SiS" Ratio

Analogous to the Ca II ratio, the "SiS ratio" was introduced by Bongard et al. (2006) as the ratio of the flux at the red edge of the S II "W" feature to the flux at the red edge of the Si II λ6355 feature. In the notation used in BSNIP II this is

$$\Re\,(\text{SiS}) \equiv \frac{F_r\,(\text{S II "W"})}{F_r\,(\text{Si II } \lambda 6355)}. \tag{4.14}$$

In a sample of 8 SNe, ℜ(SiS) has been seen to correlate with maximum absolute B-band magnitude in the same way as ℜ(Ca II) (Bongard et al. 2006).

The SiS ratio and the Si II ratio were found to be only marginally correlated in BSNIP II, and Figure 4.28 (which contains 72 SNe) shows that ℜ(SiS) is anti-correlated with $\Delta m_{15}(B)$ (Pearson correlation coefficient of −0.49). The least-squares linear fit to the data is shown as the solid line in Figure 4.28 and the dashed lines are the standard error. Note that this relationship is in the opposite sense of the one between the Ca II ratio and $\Delta m_{15}(B)$. Here Ia-99aa/91T objects lie above the main relationship while the Ia-norm and HV SNe are well

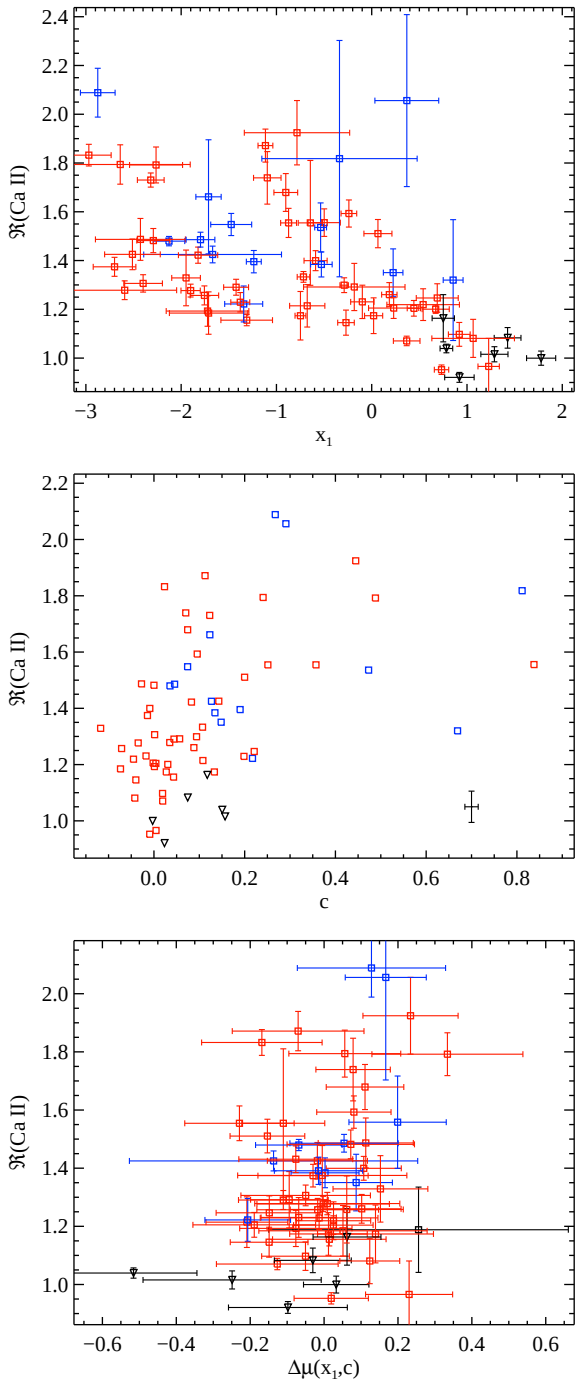

Figure 4.27: The Ca II ratio versus SALT2 light-curve width parameter x_1, SALT2 color parameter c, and Hubble residuals corrected for light-curve width and color. Colors and shapes of data points are the same as in Figure 4.5. In the middle plot, the median uncertainty in both directions is shown in the lower-right corner.

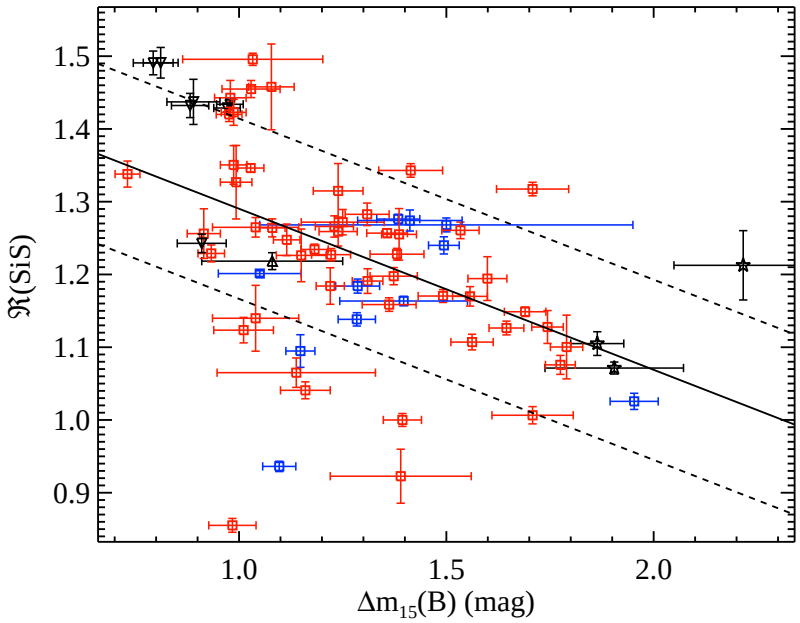

Figure 4.28: The SiS ratio versus $\Delta m_{15}(B)$. Colors and shapes of data points are the same as in Figure 4.5. The solid line is the linear least-squares fit and the dashed lines are the standard error of the fit. The Pearson correlation coefficient is -0.49.

mixed. Once again, comparing Δ or x_1 to $\Re$(SiS) yields similar results to what is seen in Figure 4.28.

The SiS ratio appears to be well-correlated with c, when including the most reddened objects. In Figure 4.29 are 71 SNe, and the Pearson correlation coefficient is -0.61. However, if one removes the most highly reddened objects with $c > 0.5$, the correlation weakens slightly to -0.56. No distance model involving the SiS ratio is more accurate than the (x_1, c) model. However, when $\Re$(SiS) is combined with just c or both x_1 and c, the accuracy is on par with the standard (x_1, c) model ($\Delta_{x_1,c} = 0.0209 \pm 0.0223$ and $\Delta_{x_1,c} = 0.0074 \pm 0.0105$, respectively). While Blondin et al. (2011) find that this ratio does significantly worse than the usual (x_1, c) model, we find (in Section 4.4.10) that out of 17,822 flux ratios combined with c, the most accurate distances are calculated using flux ratios that are approximately equivalent to the SiS ratio (although it is only a marginal improvement over the (x_1, c) model).

4.4.8 The "SSi" Ratio

Yet another possible spectroscopic luminosity indicator is the ratio of the pEW of the S II "W" to that of the Si II λ5972 feature (Hachinger et al. 2006). This SSi ratio is defined in BSNIP II as

$$\Re\,(\text{S,Si}) \equiv \frac{\text{pEW}\,(\text{S II "W"})}{\text{pEW}\,(\text{Si II } \lambda 5972)}. \tag{4.15}$$

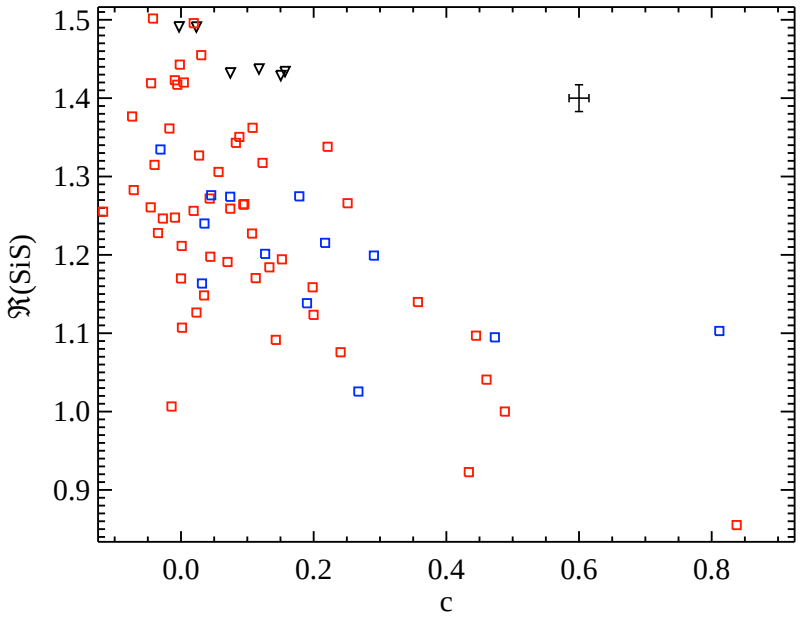

Figure 4.29: The SiS ratio versus c. Colors and shapes of data points are the same as in Figure 4.5. The median uncertainty in both directions is shown in the upper-right corner.

Hachinger et al. (2006) found that the SSi ratio is linearly anti-correlated with Δm_{15} (which is opposite to the relationship between $\Re$(Si II) and Δm_{15}). The analysis in BSNIP II seemed to confirm this observation by showing that the SSi ratio was strongly anti-correlated (non-linearly) with the Si II ratio.

$\Re$(S,Si) is plotted against $\Delta m_{15}(B)$ for 59 SNe in Figure 4.30. The results of Hachinger et al. (2006) and the speculation in BSNIP II are confirmed: the SSi ratio is strongly anti-correlated with $\Delta m_{15}(B)$ (Pearson correlation coefficient of -0.65). Here, the Ia-91bg and Ia-99aa objects follow the main trend and are found at the lower and upper ends of the correlation, respectively. There are only a few HV objects in Figure 4.30, but there is some evidence that they have larger than average $\Re$(S,Si) values (which was also seen in Fig. 34 of BSNIP II).

Plots of Δ and x_1 versus $\Re$(S,Si) display trends like that of Figure 4.30. However, the Ia-99aa objects fall off of the main correlation in both of these parameter spaces. In both cases these SNe have lower $\Re$(S,Si) values than one would expect from the main correlation.

4.4.9 The "SiFe" Ratio

Analogous to the SSi ratio, the "SiFe ratio" was defined as the ratio of the pEW of the Si II λ5972 feature to that of the Fe II complex, and it was shown to be an accurate spectroscopic luminosity indicator (Hachinger et al. 2006). In BSNIP II, $\Re$(Si,Fe) was defined

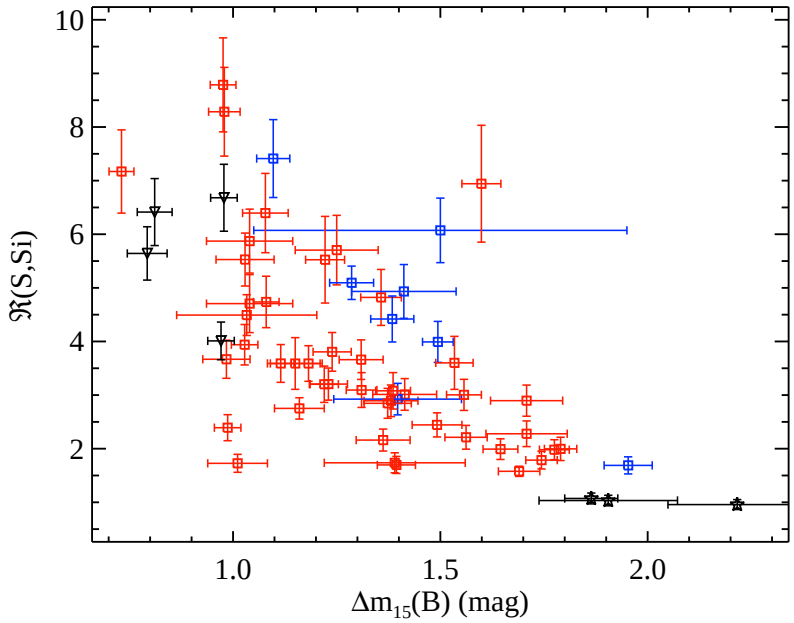

Figure 4.30: The SSi ratio versus $\Delta m_{15}(B)$. Colors and shapes of data points are the same as in Figure 4.5.

as

$$\Re\,(\text{Si,Fe}) \equiv \frac{\text{pEW}\,(\text{Si II}\ \lambda 5972)}{\text{pEW}\,(\text{Fe II})}, \tag{4.16}$$

and found to be strongly correlated with the Si II ratio.

We plot $\Re$(Si,Fe) versus $\Delta m_{15}(B)$ for 53 SNe in Figure 4.31. The results of Hachinger et al. (2006) and the speculation in BSNIP II are again confirmed: the SiFe ratio is strongly (linearly) correlated with $\Delta m_{15}(B)$, with a Pearson correlation coefficient of 0.65. The solid line in the Figure is the linear least-squares fit and the dashed lines are the standard error of the fit.

Similar to $\Re$(Si II), Ia-99aa objects are found at the lowest end of the linear trend while the Ia-91bg objects in the plot appear to be above the main relationship. In Figure 4.31 there are only a few HV SNe, but they appear to have smaller than average $\Re$(S,Si) values (which was also seen in Fig. 35 of BSNIP II). When comparing Δ and x_1 to $\Re$(Si,Fe), the basic trend seen in Figure 4.31 is recovered, but with larger scatter (even though the correlation coefficients are similar).

4.4.10 Arbitrary Flux Ratios

Bailey et al. (2009) found that by using ratios of fluxes from a single, binned SN Ia spectrum they could decrease the scatter in their Hubble diagrams. These ratios are defined

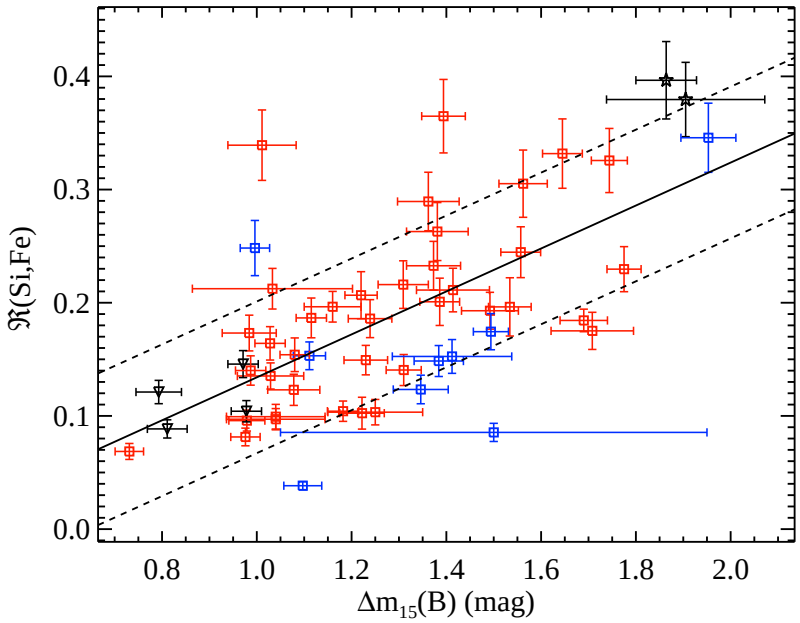

Figure 4.31: The SiFe ratio versus $\Delta m_{15}(B)$. Colors and shapes of data points are the same as in Figure 4.5. The solid line is the linear least-squares fit and the dashed lines are the standard error of the fit.

as $\mathcal{R}(\lambda_y/\lambda_x) \equiv F(\lambda_y)/F(\lambda_x)$, where λ_y and λ_x are the rest-frame central wavelengths of given bins.[3] The spectra are forced to cover a wavelength range of exactly 3500–8500 Å and are binned into 134 equal-sized (in $\ln \lambda$) bins. The data are also deredshifted and dereddened using the redshift and reddening values presented in Table 1 of BSNIP I and assuming that the extinction follows the Cardelli et al. (1989) extinction law modified by O'Donnell (1994). As in Bailey et al. (2009) and Blondin et al. (2011), a color-corrected version of this flux ratio ($\mathcal{R}^c(\lambda_y/\lambda_x)$) is also used, and it is defined as the ratio of fluxes as measured from a spectrum that has been corrected for SALT2 c using the color law from Guy et al. (2007). We use these color-corrected flux ratios when testing models that also use the SALT2 color parameter (i.e., Equations 4.6 and 4.7).

As with the rest of the current study, we only investigate spectra within 5 d of maximum brightness since it was shown in BSNIP II that the spectra do not evolve significantly during these epochs. Since we are utilizing SALT2 fits and Hubble diagrams, we again require that SNe have $z_{\rm helio} > 0.01$, $c < 0.50$, and reduced $\chi^2 < 2$. Blondin et al. (2011) also require that the absolute difference between $B - V$ color at maximum derived from the spectrum

[3]This is similar to the definition of Bailey et al. (2009), but is the reciprocal of the definition used by Blondin et al. (2011). However, this only really matters for the plots of λ_y versus λ_x, such as Figure 4.34. Thus, Figure 7 of Blondin et al. (2011) is the transpose of Figure 4.34. When using either definition, note that the first wavelength listed for a given $\mathcal{R}$ is the numerator in the actual ratio of fluxes.

and derived from the photometry be less than 0.1 mag. This is used as a proxy for their relative spectrophotometric accuracy. In BSNIP I it was shown (in Table 3) that the relative spectrophotometric accuracy is often < 0.1 mag for the BSNIP data. In fact, $B - V$ color is only inaccurate at the 0.1 mag level for the oldest ($t > 20$ d) and noisiest (S/N < 20) BSNIP spectra. Therefore, the spectra investigated here should all be spectrophotometrically accurate enough for the flux-ratio analysis.

Of the data studied here, 69 objects have flux ratios calculated for the entire wavelength range mentioned above and reliable SALT2 fits that pass our Hubble diagram criteria (see Section 4.3.3). We randomly divide our sample into 9 groups of 7 SNe and 1 group with 6 SNe when doing 10-fold CV.

Flux-Ratio Results

The "best" flux ratios for each model are chosen to be the ones with the lowest WRMS values. As discussed in Section 4.3.3, for each model involving a flux ratio (Equations 4.4–4.7) we calculate, in addition to the WRMS, the intrinsic prediction error ($\sigma_{\rm pred}$), the intrinsic correlation ($\rho_{x_1,c}$) of the residuals with residuals using the (x_1, c) model (Equation 4.8), and the difference ($\Delta_{x_1,c}$) in intrinsic prediction error with respect to the (x_1, c) model and its significance. These parameters, along with the wavelengths, of the top 5 ratios for each model which includes a flux ratio (Equations 4.4–4.7) are shown in Table 4.1.

Table 4.1: Top 5 Flux Ratios for Each Model

Rank	λ_y	λ_x	WRMS (mag)	$\sigma_{\rm pred}$ (mag)	$\rho_{x_1,c}$	$\Delta_{x_1,c}$
				$\mathcal{R}$		
1	6330	5360	0.250 ± 0.018	0.220 ± 0.025	-0.09	0.149 ± 0.033 (4.5σ)
2	6370	5360	0.252 ± 0.018	0.225 ± 0.026	-0.02	0.157 ± 0.033 (4.8σ)
3	6330	5550	0.258 ± 0.019	0.224 ± 0.027	0.09	0.153 ± 0.033 (4.6σ)
4	6330	4890	0.260 ± 0.018	0.234 ± 0.027	0.51	0.153 ± 0.029 (5.2σ)
5	6540	4890	0.262 ± 0.019	0.233 ± 0.029	0.53	0.152 ± 0.031 (4.8σ)
				$(x_1, \mathcal{R})$		
1	6330	4310	0.234 ± 0.017	0.207 ± 0.025	0.42	0.181 ± 0.031 (5.9σ)
2	6290	4310	0.234 ± 0.018	0.203 ± 0.025	0.47	0.172 ± 0.030 (5.7σ)
3	6250	4310	0.234 ± 0.019	0.192 ± 0.026	0.32	0.138 ± 0.031 (4.5σ)
4	6590	4920	0.238 ± 0.019	0.196 ± 0.028	0.15	0.135 ± 0.033 (4.2σ)
5	6540	4700	0.238 ± 0.018	0.206 ± 0.028	0.17	0.144 ± 0.033 (4.3σ)
				$(c, \mathcal{R}^c)$		
1	5580	6330	0.143 ± 0.019	0.078 ± 0.022	0.31	-0.011 ± 0.020 (0.5σ)
2	5580	6420	0.145 ± 0.019	0.084 ± 0.021	0.26	-0.007 ± 0.021 (0.3σ)
3	6330	5580	0.146 ± 0.018	0.082 ± 0.022	0.30	-0.000 ± 0.020 (0.0σ)

Continued on Next Page...

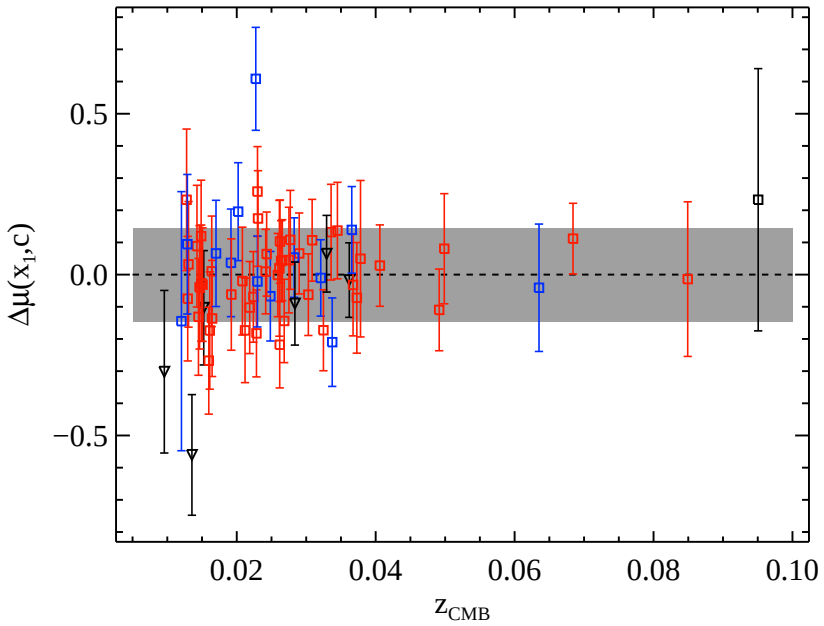

Figure 4.32: Hubble diagram residuals versus $z_{\rm cmb}$ for the standard (x_1, c) model (Equation 4.8). The gray band is the WRMS for the model. Colors and shapes of data points are the same as in Figure 4.5.

Table 4.1 – Continued

Rank	λ_y	λ_x	WRMS (mag)	$\sigma_{\rm pred}$ (mag)	$\rho_{x_1,c}$	$\Delta_{x_1,c}$
4	5580	6370	0.148 ± 0.019	0.091 ± 0.020	0.33	0.003 ± 0.020 (0.2σ)
5	6370	5580	0.148 ± 0.018	0.089 ± 0.020	0.29	0.007 ± 0.021 (0.4σ)
				$(x_1, c, \mathcal{R}^c)$		
1	3580	4280	0.130 ± 0.019	0.044 ± 0.028	0.80	-0.033 ± 0.014 (2.4σ)
2	3580	4230	0.132 ± 0.019	0.051 ± 0.025	0.81	-0.029 ± 0.012 (2.3σ)
3	3560	4090	0.133 ± 0.019	0.051 ± 0.026	0.69	-0.029 ± 0.015 (2.0σ)
4	3610	4400	0.133 ± 0.019	0.056 ± 0.024	0.83	-0.023 ± 0.010 (2.3σ)
5	5690	6590	0.133 ± 0.019	0.028 ± 0.045	0.61	-0.032 ± 0.020 (1.6σ)
				(x_1, c)		
...	...	...	0.146 ± 0.019	0.075 ± 0.023	...	...

Also displayed in Table 4.1 is the WRMS and $\sigma_{\rm pred}$ of our benchmark (x_1, c) model. Figure 4.32 shows the Hubble diagram residuals for this model versus redshift for the 69 SNe Ia mentioned above. The gray band indicates the WRMS for the model.

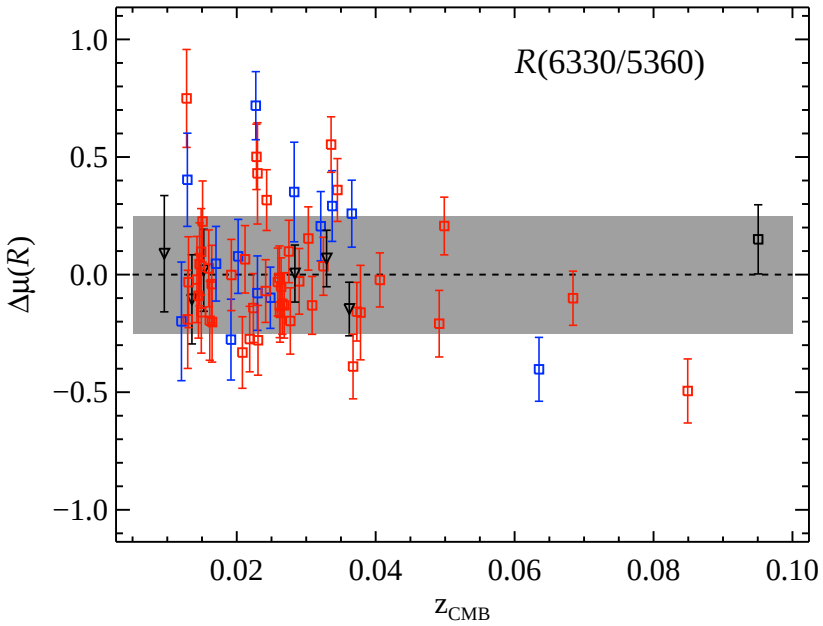

Figure 4.33: Hubble diagram residuals versus $z_{\rm cmb}$ for the best flux ratio, $\mathcal{R}\,(6330/5360)$, using the $\mathcal{R}$-only model (Equation 4.4). The gray band is the WRMS for the model. Colors and shapes of data points are the same as in Figure 4.5.

Model 1: $\mathcal{R}$ Only

Using only a flux ratio (Equation 4.4) leads to no improvement over the usual (x_1, c) model (Equation 4.8). In fact, this model seems to perform significantly worse, as can be seen by the relatively large $\Delta_{x_1,c}$ values. The WRMS and $\sigma_{\rm pred}$ of the "best" ratios are quite a bit larger than those of the (x_1, c) model. This is different than the conclusion of previous work, which found that models using a flux ratio alone could perform as well as the (x_1, c) model (Bailey et al. 2009; Blondin et al. 2011).

Figure 4.33 shows the Hubble diagram residuals for the $\mathcal{R}$-only model versus redshift using the best ratio, $\mathcal{R}\,(6330/5360)$. The gray band is once again the WRMS for the top-ranked model. Figure 4.34 shows the WRMS (top) and absolute Pearson correlation coefficient of the correction term (in this case, $\gamma\mathcal{R}$) with the uncorrected Hubble residuals (bottom) for all 17,822 ($= 134 \times 133$) flux ratios. The colors associated with the WRMS values have been scaled such that $0.13 \leq \text{WRMS} \leq 0.30$; there are no values of WRMS < 0.13 mag for any of the models in this study, and all values of WRMS > 0.30 mag are simply assigned the same color as those with WRMS $= 0.30$ mag.

The top panel of Figure 4.34 is a proxy for the overall scatter in the model while the bottom panel indicates how much "new" information is gained by adding in the correction term $\gamma\mathcal{R}$. In general, a model may have a low WRMS (or $\sigma_{\rm pred}$), meaning that the model is fitting the data well, but since the data have uncertainties associated with them, the model

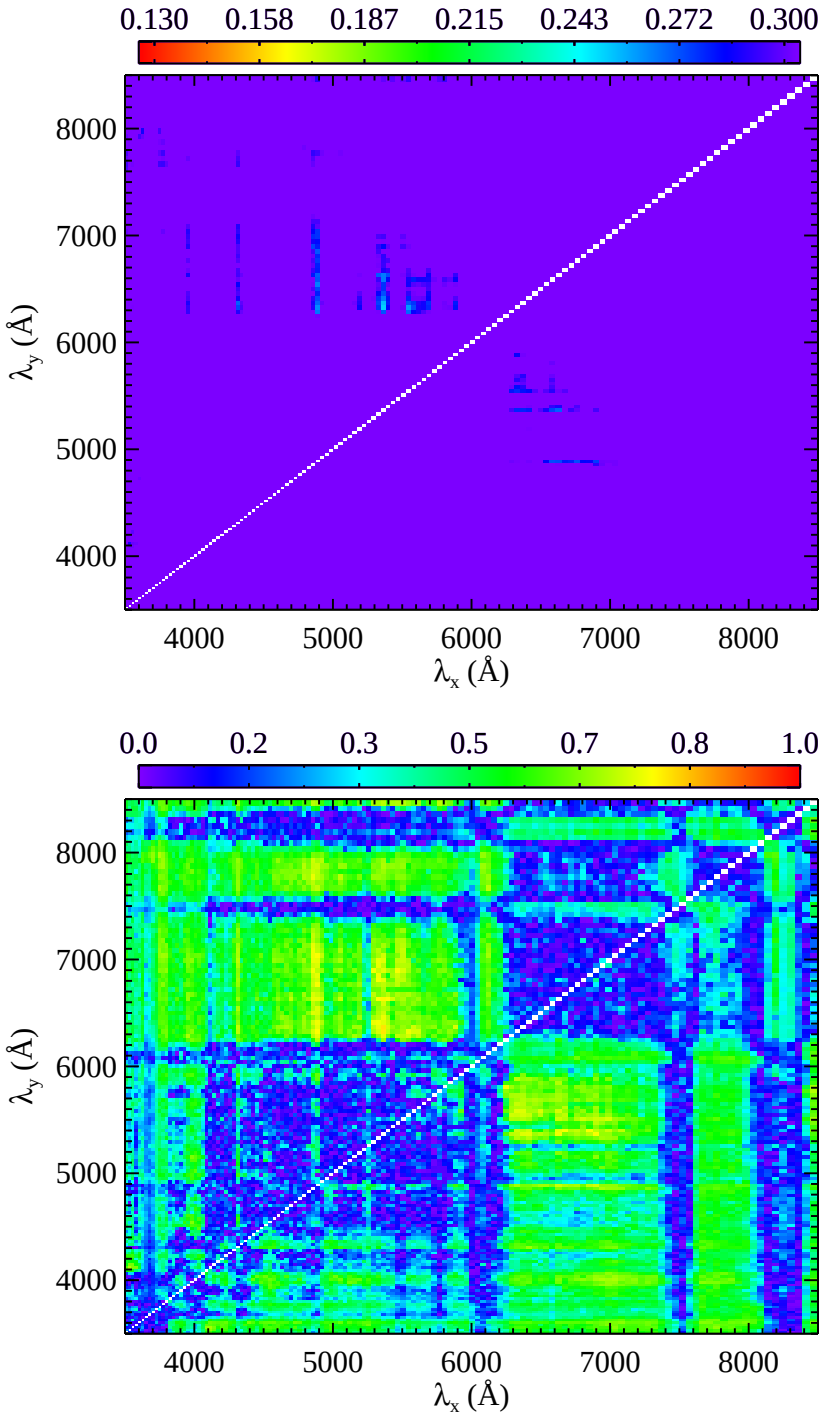

Figure 4.34: A map of all 17,822 flux ratios used in the $\mathcal{R}$-only model, color-coded by WRMS (*top*) and absolute Pearson correlation coefficient of the correction term with the uncorrected Hubble residuals (*bottom*). The WRMS colors are scaled to values between 0.13 mag and 0.30 mag. No WRMS values are < 0.13 mag in any of the models investigated, and all values of WRMS > 0.30 mag are simply assigned the same color as those with WRMS $= 0.30$ mag.

might be *overfitting* the data and actually end up fitting noise.

One way to discern whether or not this is the case is to see how well the correction terms correlate with the uncorrected Hubble residuals. As described in Section 4.4.2, if the terms that do not contain x_c or c (in this case, $\gamma\mathcal{R}$) are well-correlated with the uncorrected Hubble residuals, then the measured observable is fitting information that actually exists in the data (as opposed to noise). However, a large correlation does not necessarily imply a good model. This is obvious in Figure 4.34, where most flux ratios have large WRMS values, including ones that also have quite high correlations between the correction term and the uncorrected Hubble residuals.

Figure 4.35 shows the best flux ratio using the $\mathcal{R}$-only model, $\mathcal{R}\,(6330/5360)$, versus the SALT2 parameters x_1 and c. The ratio is anti-correlated with x_1 (Pearson correlation coefficient of -0.67) and correlated with c (correlation coefficient of 0.64), though both relationships show a significant amount of scatter. This implies that $\mathcal{R}\,(6330/5360)$ is some combination of a color and stretch indicator, but is not as accurate as measuring x_1 and c separately.

The best ratio using this model seen by Blondin et al. (2011), $\mathcal{R}\,(6630/4400)$, was similarly correlated with SALT2 parameters, though they observed a stronger correlation with c and they also found that it improved the Hubble diagram residuals over using the (x_1, c) model (albeit at a low significance). Bailey et al. (2009) also saw an overall improvement when using their top ratio for this model, $\mathcal{R}\,(6420/4430)$. The wavelength whose flux is in the numerator of both of these ratios is quite similar to the top five ratios found in the BSNIP data. However, the denominator is significantly different from all five of our best ratios. The WRMS for both of these ratios using the BSNIP data is $\sim$0.37 mag, which is much larger than the WRMS values seen for our best ratios.

Model 2: $\mathcal{R}$ and x_1

Combining a flux ratio with the SALT2 stretch parameter x_1 (Equation 4.5) also leads to no improvement over the (x_1, c) model. The WRMS and σ_{pred} values are slightly smaller than when using the $\mathcal{R}$-only model, but they are still significantly larger than those from the standard (x_1, c) model. The $\Delta_{x_1,c}$ values are larger for the $(x_1, \mathcal{R})$ model than they are for the $\mathcal{R}$-only model, and thus $(x_1, \mathcal{R})$ is a less accurate model. While Blondin et al. (2011) again found that the $(x_1, \mathcal{R})$ model did better than the (x_1, c) model, we agree with their result that the $(x_1, \mathcal{R})$ model usually performed worse than the $\mathcal{R}$-only model.

The Hubble diagram for the top-ranked flux ratio using the $(x_1, \mathcal{R})$ model, $\mathcal{R}\,(6330/4310)$, is shown in Figure 4.36, along with the WRMS for the best model. Figure 4.37 shows the two-dimensional map of every flux ratio and its associated WRMS and correlation of correction terms with uncorrected residuals. The color scale is the same as in Figure 4.34.

While more ratios have lower WRMS values for this model than for the $\mathcal{R}$-only model and many ratios have even higher correlations between the correction terms and the uncorrected residuals, this model is (at best) comparable to the $\mathcal{R}$-only model and definitely worse

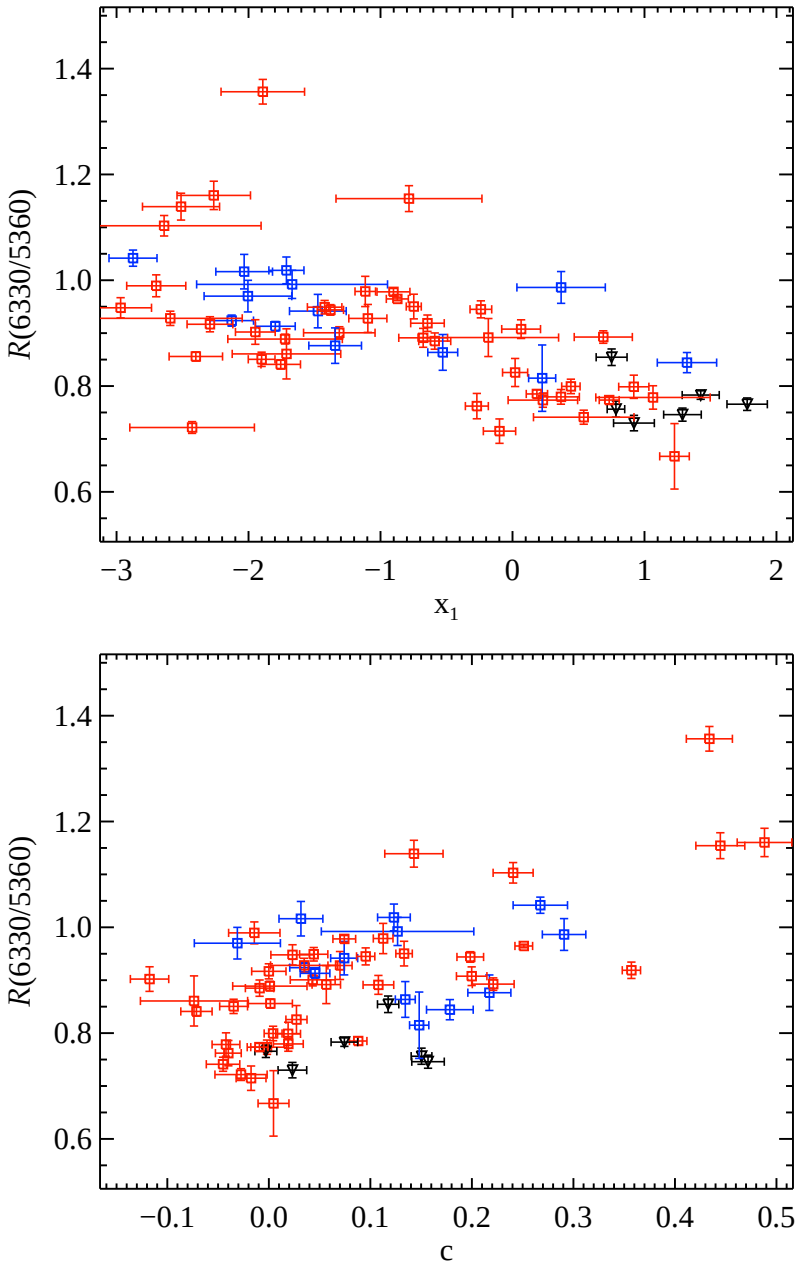

Figure 4.35: The top-ranked flux ratio, $\mathcal{R}\,(6330/5360)$, using the $\mathcal{R}$-only model (Equation 4.4) versus the SALT2 parameters x_1 and c. Colors and shapes of data points are the same as in Figure 4.5.

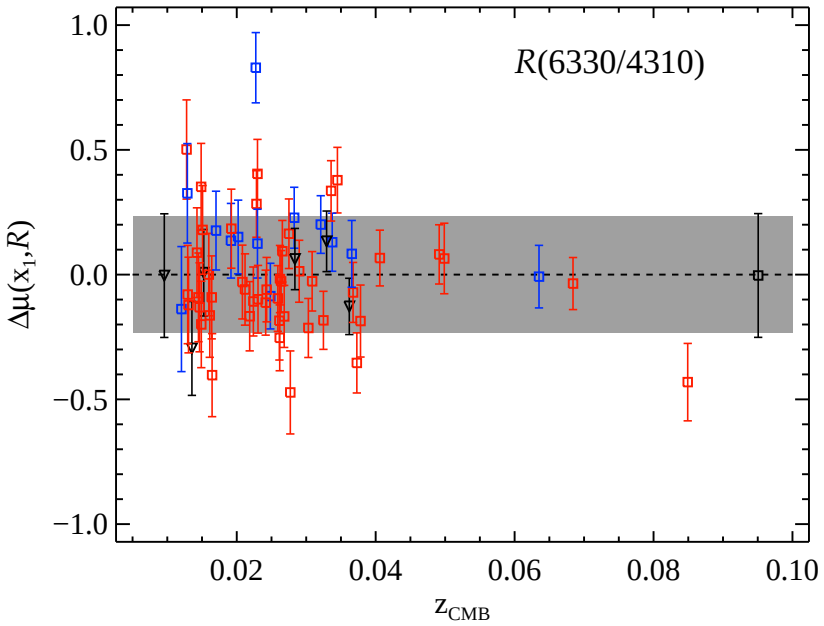

Figure 4.36: Hubble diagram residuals versus $z_{\rm cmb}$ for the best flux ratio, $\mathcal{R}\,(6330/4310)$, using the $(x_1, \mathcal{R})$ model (Equation 4.5). The gray band is the WRMS for the model. Colors and shapes of data points are the same as in Figure 4.5.

than the standard (x_1, c) model.

Figure 4.38 shows the best flux ratio using the $(x_1, \mathcal{R})$ model, $\mathcal{R}\,(6330/4310)$, versus the SALT2 parameters x_1 and c. There is some evidence that the ratio is anti-correlated with x_1 (correlation coefficient of -0.36), but it is strongly correlated with c (coefficient of 0.72). The ratio $\mathcal{R}\,(6330/4310)$ is therefore a proxy for c, and so it is unsurprising that this is the top-ranked ratio in a model using only a ratio and x_1.

All of the top five ratios for the $(x_1, \mathcal{R})$ model have very similar numerator and denominator wavelengths, and the difference in wavelength between the two fluxes is significant (1700–2000 Å). This again supports the idea presented above that the top-ranked flux ratios for the $(x_1, \mathcal{R})$ model are effectively proxies for color.

Using this model Blondin et al. (2011) again found that the ratio $\mathcal{R}\,(6630/4400)$ was best and, as mentioned above, it was similarly correlated with SALT2 parameters. The best ratio found for the BSNIP data is comprised of wavelengths very close to these, although the WRMS for this ratio using our data is ∼0.32 mag.

Model 3: $\mathcal{R}^c$ and c

Using some of the top-ranked flux ratios with the SALT2 color parameter c (Equation 4.6) technically improves the fit when compared to the (x_1, c) model, though the significance is extremely small ($\sim 0.5\sigma$ for the best ratio). Using the best ratio, $\mathcal{R}^c\,(5580/6330)$,

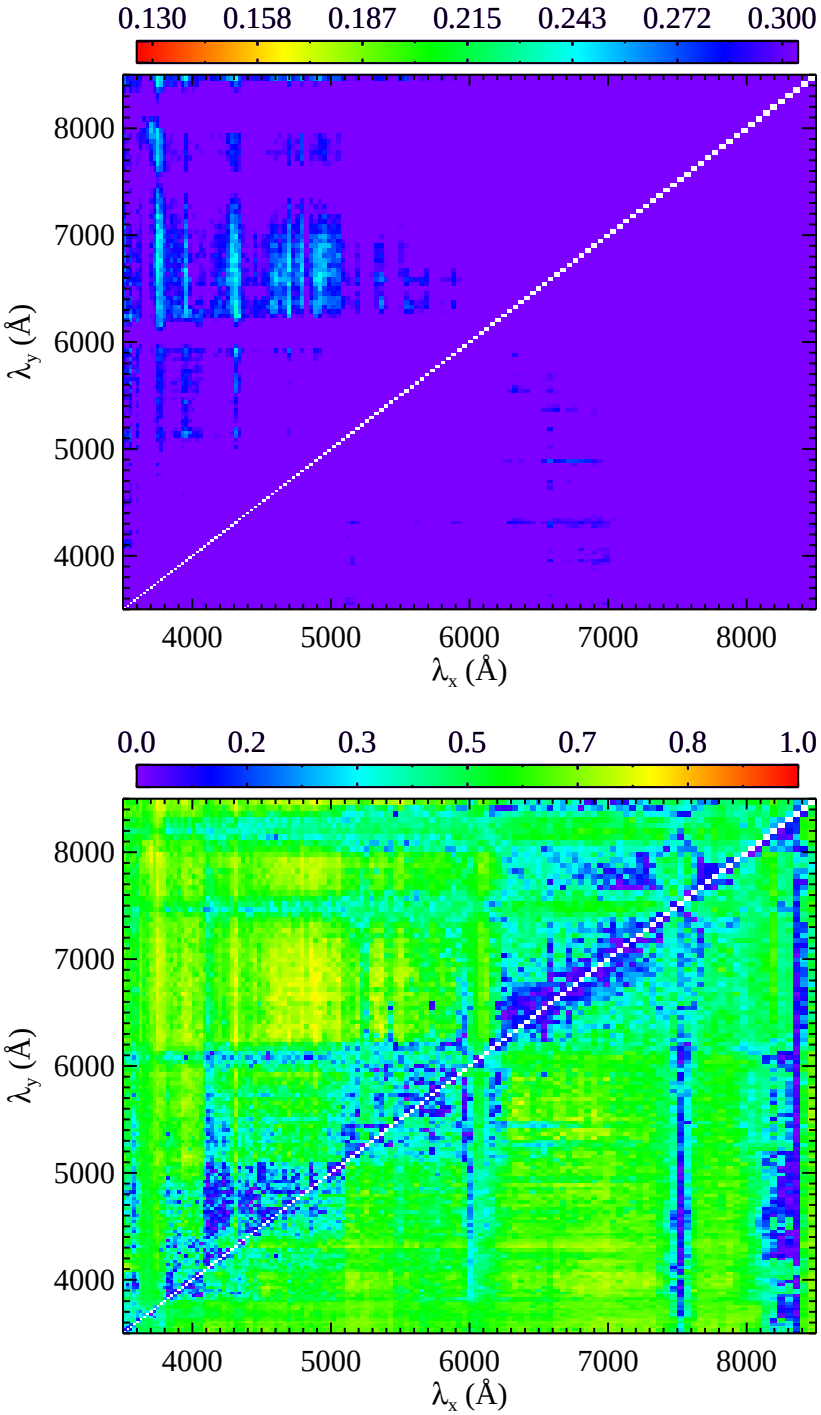

Figure 4.37: A map of all flux ratios used in the $(x_1, \mathcal{R})$ model, color-coded by WRMS (*top*) and absolute Pearson correlation coefficient of the correction terms with the uncorrected Hubble residuals (*bottom*). The colors are the same as in Figure 4.34.

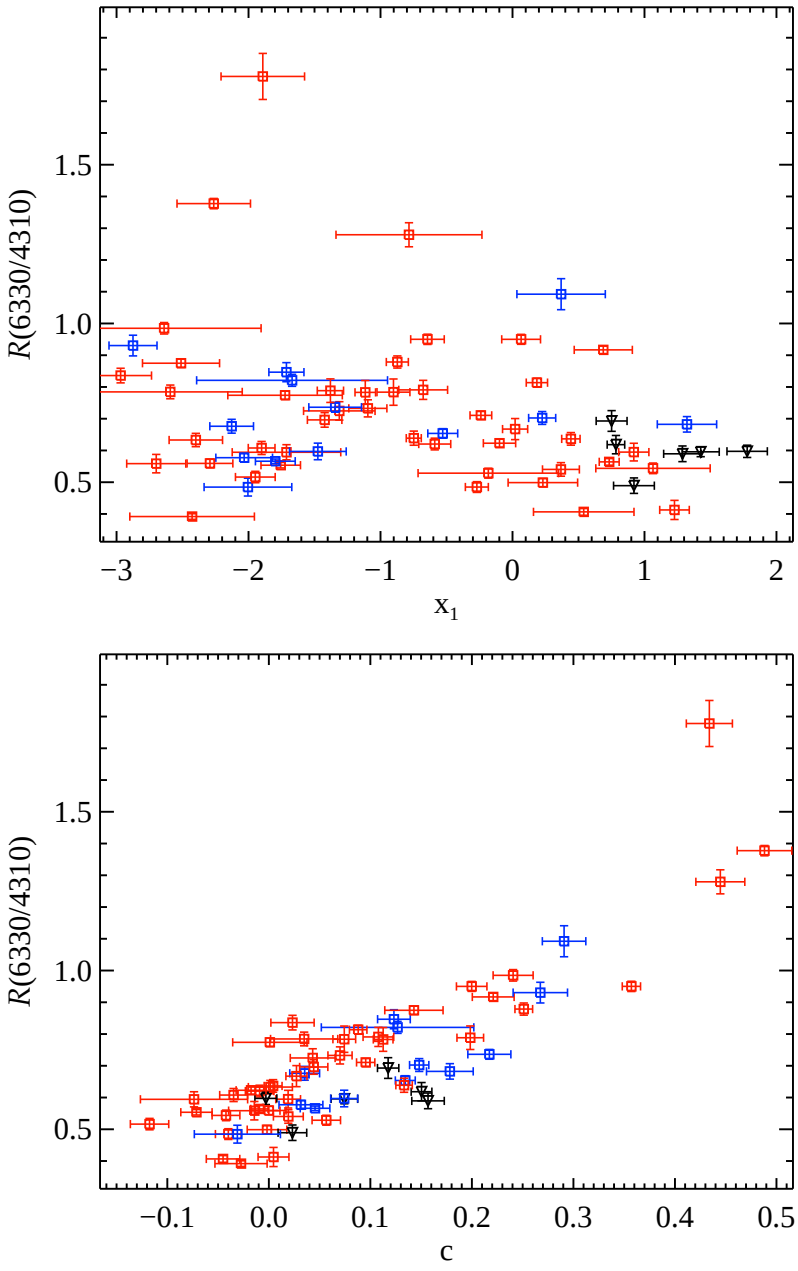

Figure 4.38: The top-ranked flux ratio, $\mathcal{R}(6330/4310)$, using the $(x_1, \mathcal{R})$ model (Equation 4.5) versus the SALT2 parameters x_1 and c. Colors and shapes of data points are the same as in Figure 4.5.

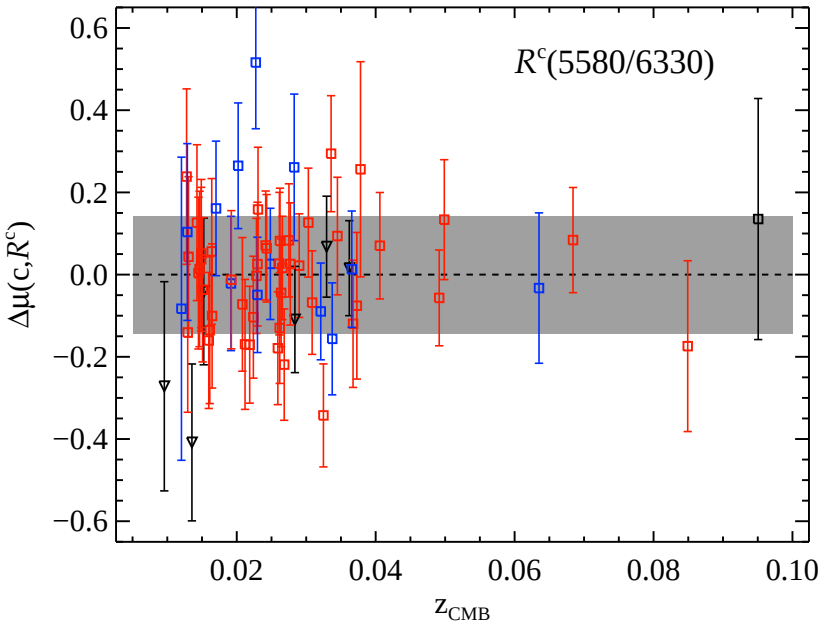

Figure 4.39: Hubble diagram residuals versus $z_{\rm cmb}$ for the best flux ratio, $\mathcal{R}^c\,(5580/6330)$, using the $(c, \mathcal{R}^c)$ model (Equation 4.6). The gray band is the WRMS for the model. Colors and shapes of data points are the same as in Figure 4.5.

the WRMS is reduced by only $\sim$2%, while $\sigma_{\rm pred}$ is actually increased by $\sim$4%. This is a much smaller improvement using this model than what has been seen before (Blondin et al. 2011).

The Hubble diagram for the top-ranked flux ratio using the $(c, \mathcal{R}^c)$ model is shown in Figure 4.39, along with the WRMS for the best model. Figure 4.40 illustrates the two-dimensional map of every flux ratio and its associated WRMS and correlation of correction terms with uncorrected residuals. The color scale is the same as in Figure 4.34.

Many ratios appear to have large correlations between the correction terms and uncorrected residuals, but the lowest WRMS values are tightly clustered in wavelength space. This is also apparent in Table 4.1, where the top five ratios for the $(c, \mathcal{R}^c)$ model involve only 4 different wavelength bins (three of which are effectively the same, within 90 Å of each other). This clustering was seen (although to a lesser extent) by Blondin et al. (2011).

Figure 4.41 shows the best flux ratio using the $(c, \mathcal{R}^c)$ model, $\mathcal{R}^c\,(5580/6330)$, versus the SALT2 parameters x_1 and c. This ratio is strongly correlated with x_1 (correlation coefficient of 0.85) and effectively uncorrelated with c (correlation coefficient of -0.22). Similar to the last section, the top-ranked ratio for this model can be thought of as a proxy for x_1, and it is reasonable that this is the best ratio in a model using only a ratio and c. Furthermore, the lack of correlation between $\mathcal{R}^c\,(5580/6330)$ and c implies that dereddening the data using the SALT2 c and color law is working as intended.

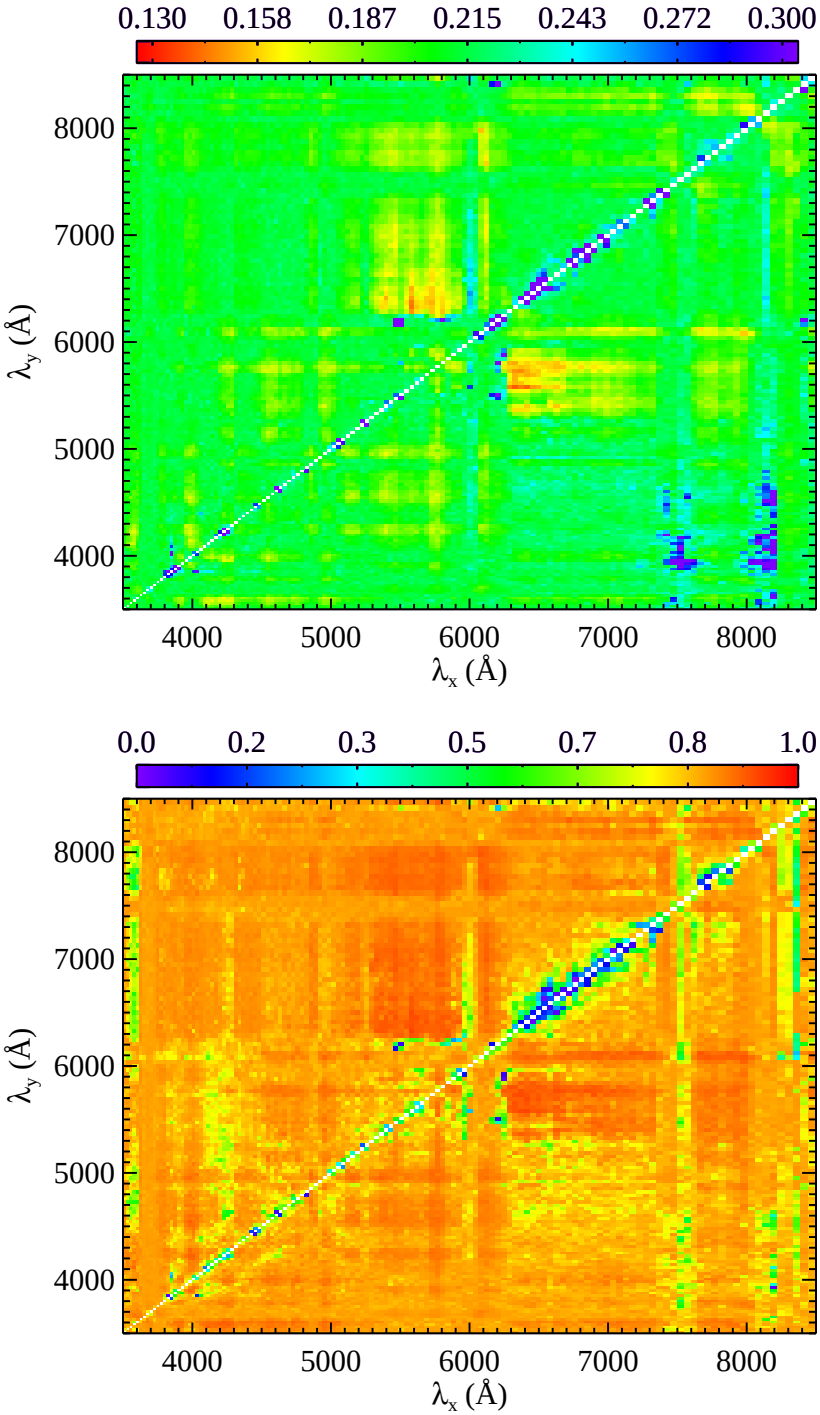

Figure 4.40: A map of all flux ratios used in the $(c, \mathcal{R}^c)$ model, color-coded by WRMS (*top*) and absolute Pearson correlation coefficient of the correction terms with the uncorrected Hubble residuals (*bottom*). The colors are the same as in Figure 4.34.

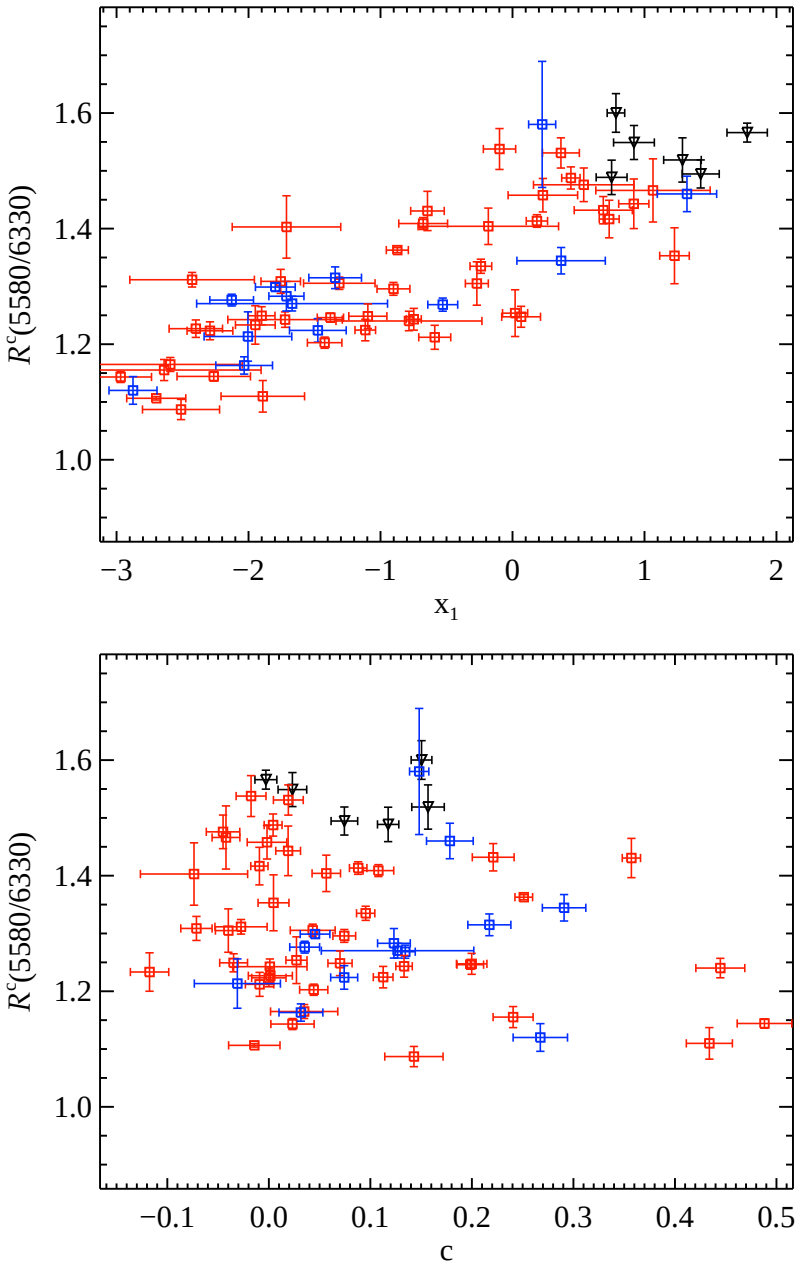

Figure 4.41: The top-ranked flux ratio, $\mathcal{R}^c\,(5580/6330)$, using the $(c, \mathcal{R}^c)$ model (Equation 4.6) versus the SALT2 parameters x_1 and c. Colors and shapes of data points are the same as in Figure 4.5.

The flux ratio $\mathcal{R}^c\,(5580/6330)$ being an accurate proxy for x_1, as well the fact that the top five flux ratios for the $(c, \mathcal{R}^c)$ model all involve a fluxes near ∼5600 Å and ∼6400 Å, could mean that one (or both) of these spectral regions is also a proxy for light-curve width. The region near 6400 Å is usually at (or slightly redward of) the red edge of the Si II λ6355 feature and most likely probes the color-corrected continuum level of a SN Ia spectrum. On the other hand, 5600 Å is often the boundary between the S II "W" and Si II λ5972 features. In Sections 4.4.3 and 4.4.4 we showed that the relative depth of the S II "W" and the pEW of the Si II λ5972 feature are both *anti*-correlated with x_1. This is completely self-consistent. When either of those features are stronger (a larger depth or pEW, resulting in a lower flux), the SN will have a smaller x_1 value.

In fact, $\mathcal{R}^c$(∼5600/∼6400) is almost exactly equal to the SiS ratio, which is defined as the flux at the red edge of the S II "W" divided by the flux at the red edge of the Si II λ6355 feature. In Section 4.4.7 it was shown that $\Re$(SiS) is correlated with x_1 and only marginally correlated with c. We also found that this ratio, in conjunction with c alone or x_1 and c together, yields a WRMS that is consistent with the standard (x_1, c) model. Thus, it seems that both $\mathcal{R}^c$(∼5600/∼6400) and $\Re$(SiS) are acting as accurate replacements for x_1.

With the $(c, \mathcal{R}^c)$ model, Blondin et al. (2011) showed that their top-ranked ratio was $\mathcal{R}^c\,(6420/5290)$. This is very similar to the reciprocal of the best ratio found with the BSNIP data; thus, it is not surprising that they find a strong *anti*-correlation between $\mathcal{R}^c\,(6420/5290)$ and x_1. Their ratio also leads to a larger decrease in WRMS (∼15%, Blondin et al. 2011). Bailey et al. (2009) again showed an improvement when using their top ratio for this model, $\mathcal{R}^c\,(6420/5190)$, which is also very close to the best ratio of Blondin et al. (2011), as well as the reciprocal of the best ratio presented here. Despite this nearness in wavelength space, the top-ranked ratios for this model from Bailey et al. (2009) and Blondin et al. (2011) yield WRMS values of ∼0.21 mag when using the BSNIP data. Furthermore, it is interesting to note that Blondin et al. (2011) found that the SiS ratio leads to a significant *increase* in the WRMS as compared to the (x_1, c) model.

Model 4: $\mathcal{R}^c$, x_1, and c

Quite significant improvements over the standard (x_1, c) model are seen when using the top-ranked flux ratios along with both x_1 and c (Equation 4.7). In fact, the top five ratios lead to improvements at the 1.6–2.4σ level (see Table 4.1). The $(x_1, c, \mathcal{R}^c)$ model and its best ratio, $\mathcal{R}^c\,(3580/4280)$, decrease the WRMS by ∼12% and $\sigma_{\rm pred}$ by ∼40% from the (x_1, c) model. The decrease in WRMS is smaller than previously seen, but the decrease in $\sigma_{\rm pred}$ is larger and the overall improvement is at a higher significance; Blondin et al. (2011) found a 20% decrease in WRMS with a 1.6σ significance. The fact that the current dataset has nearly three times as many objects as the sample studied by Blondin et al. (2011) is likely the reason why the models using BSNIP spectra are showing less overall improvement over the standard (x_1, c) model, but for the $(x_1, c, \mathcal{R}^c)$ model the improvements are more significant.

The Hubble diagram for the top-ranked flux ratio using the $(x_1, c, \mathcal{R}^c)$ model is shown

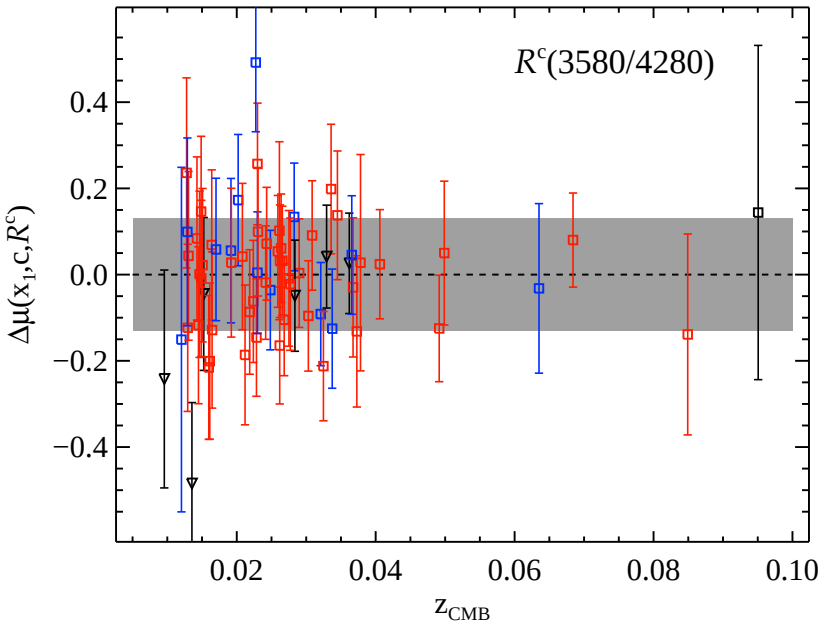

Figure 4.42: Hubble diagram residuals versus $z_{\rm cmb}$ for the best flux ratio, $\mathcal{R}^c$ (3580/4280), using the $(x_1, c, \mathcal{R}^c)$ model (Equation 4.7). The gray band is the WRMS for the model. Colors and shapes of data points are the same as in Figure 4.5.

in Figure 4.42, along with the WRMS for the best model. Figure 4.43 shows the two-dimensional map of every flux ratio and its associated WRMS and correlation of correction terms with uncorrected residuals. The color scale is the same as in Figure 4.34.

Most ratios have low values of WRMS and extremely large correlations between the correction terms and uncorrected residuals, implying that the $(x_1, c, \mathcal{R}^c)$ model is performing better overall than any of the other models investigated. This is consistent with previous work (Blondin et al. 2011), although they found no flux ratio to have a strong correlation between the correction terms and the uncorrected Hubble residuals.

Figure 4.44 shows the best flux ratio using the $(x_1, c, \mathcal{R}^c)$ model, $\mathcal{R}^c$ (3580/4280), versus the SALT2 parameters x_1 and c. There is a moderate correlation of this ratio with x_1 (correlation coefficient of 0.54) and effectively no correlation with c (correlation coefficient of 0.15). Since this ratio is less correlated with SALT2 parameters than the top-ranked ratios of other models, it is more likely to yield useful information about each SN, in addition to light-curve stretch and color.

The wavelengths that make up the top four ratios for this model are all near $\mathcal{R}^c$(∼3600/∼4250) with wavelength baselines of 500–800 Å. These approximately correspond to the blue edge of the Ca II H&K feature and the midpoint of the Mg II complex. In Section 4.4.6 it was shown that the Ca II ratio is anti-correlated with x_1 and somewhat correlated with c. This means that if the flux of the red edge of the Ca II H&K feature is relatively constant

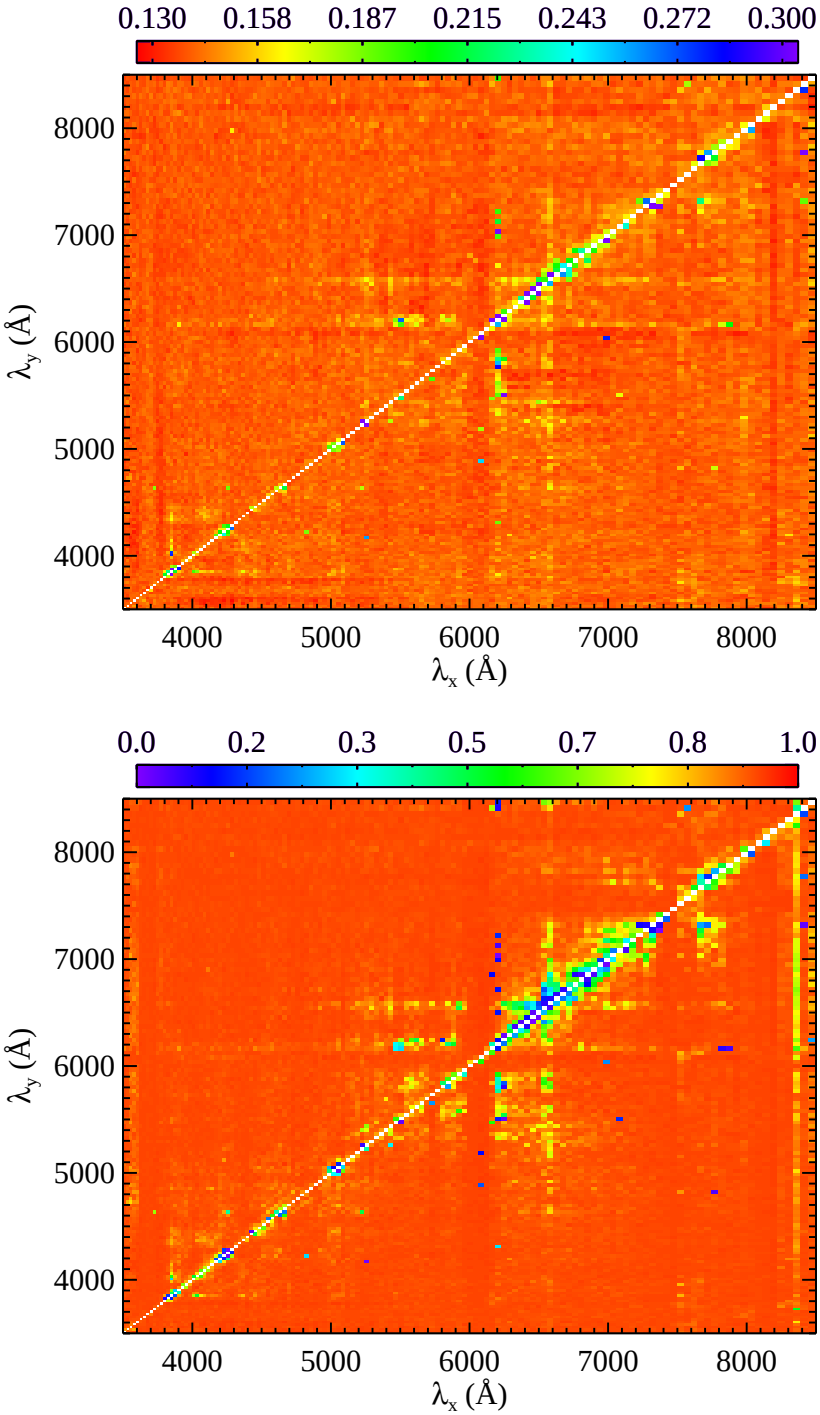

Figure 4.43: A map of all flux ratios used in the $(x_1, c, \mathcal{R}^c)$ model, color-coded by WRMS (*top*) and absolute Pearson correlation coefficient of the correction terms with the uncorrected Hubble residuals (*bottom*). The colors are the same as in Figure 4.34.

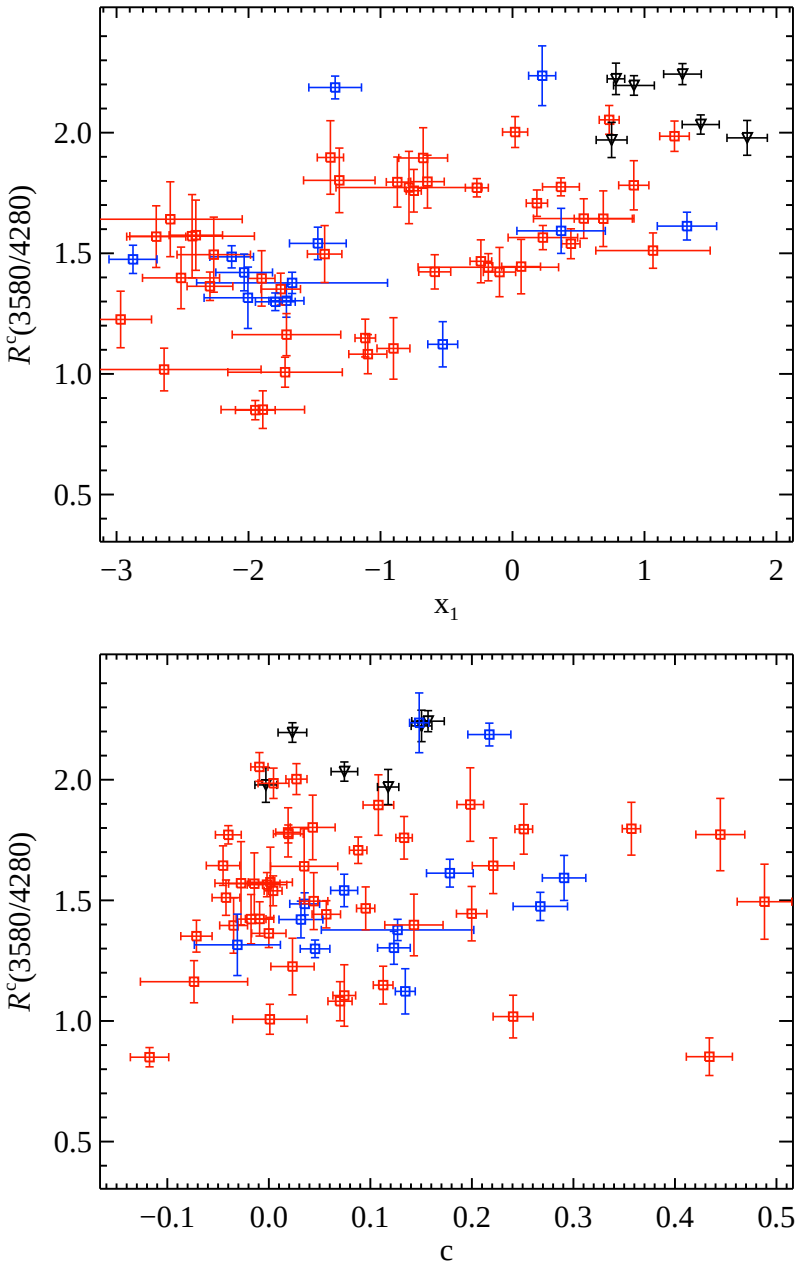

Figure 4.44: The top-ranked flux ratio, $\mathcal{R}^c\,(3580/4280)$, using the $(x_1, c, \mathcal{R}^c)$ model (Equation 4.7) versus the SALT2 parameters x_1 and c. Colors and shapes of data points are the same as in Figure 4.5.

from SN to SN (or, more likely, standardized by the SALT2 c parameter), then the *blue* edge of that feature is likely *correlated* with x_1 and *anti-correlated* with c. Furthermore, it was also shown in Section 4.4.6 that the Ca II ratio (when used in conjunction with x_1 and c) leads to an improvement in WRMS. Interestingly, the improvement attained using the $(x_1, c, \Re(\text{Ca II}))$ model is not quite as great as when the $(x_1, c, \mathcal{R}^c)$ model is used.

On the other hand, in Section 4.4.4 the correlation between the pEW of the Mg II complex and c was discussed. Thus the *flux* near the Mg II feature should be *anti-correlated* with c. Combining all this, ones discovers that the numerator of $\mathcal{R}^c(\sim 3600/\sim 4250)$ should be weakly correlated with x_1 and anti-correlated with c while the denominator should *also* be anti-correlated with c, and thus the ratio itself should show a weak correlation with x_1 and no correlation with c, which is exactly what we observe in Figure 4.44. Since the addition of this ratio decreased the WRMS at the 2.4σ level, it is very likely that there is more information encoded in SN Ia spectra and photometry than just simply light-curve width and SN color.

Note that Blondin et al. (2011) found that flux ratios with wavelengths near $\sim$5300 Å and baselines of < 400 Å gave the best results for the $(x_1, c, \mathcal{R}^c)$ model. Using the best ratio from their study, $\mathcal{R}^c\,(5690/5360)$, the BSNIP data yield a WRMS of $\sim$0.14 mag.While this is better than the (x_1, c) model, it is still not as good as our top five ratios.

4.5 Conclusions

This is the third chapter in the BSNIP series and presents a comparison between spectral feature measurements and photometric properties of 115 low-redshift ($z < 0.1$) SNe Ia within 5 d of maximum brightness. The spectral data all come from BSNIP I, and the photometric data come mainly from the LOSS sample and are published by Ganeshalingam et al. (2010). The details of the spectral measurements can be found in BSNIP II, and the light-curve fits and photometric parameters are in Ganeshalingam et al. (in preparation). A combination of light-curve parameters (specifically the SALT2 stretch and color parameters x_1 and c) and spectral measurements are used to calculate distances to SNe Ia. We then compare the residuals from these models to the standard model which only uses light-curve stretch and color. Future BSNIP papers will incorporate host-galaxy properties and SN spectra at later epochs into the analysis presented here.

4.5.1 Summary of Investigated Correlations

The velocity gradient (Benetti et al. 2005) is compared to the light-curve width, and it is shown that, as in BSNIP II, the various classifications based on the value of $\dot{v}$ overlap significantly. Similarly, velocities at maximum brightness (v_0) are compared to photometric observables and classifications based on velocity gradient, and there is a large amount of overlap in all of these parameters as well. In earlier work, HV and HVG objects have been used almost interchangeably, as have normal velocity and LVG objects (e.g., Hachinger et al. 2006; Pignata et al. 2008; Wang et al. 2009a). However, the analyses of BSNIP II and this

work show that these associations are not as distinct as previously thought. In contrast to the theoretical work of Kasen & Plewa (2007) and the data shown by Foley et al. (2011), v_0 for the BSNIP sample is not well-correlated with $(B-V)_{B_{\max}}$.

Similarly, the actual, measured velocities of the Si II λ6355 and Si II λ5972 features near maximum brightness are uncorrelated with $(B-V)_{B_{\max}}$. When distances to SNe Ia are computed using light-curve width (x_1) and color (c) parameters, in addition to the velocity of the Si II λ6355 feature, no significant improvement in the accuracy of the distances is found. This is opposite to what was seen by Blondin et al. (2011). Furthermore, models involving x_1, c, and the velocity of the Ca II H&K feature fare as poorly. However, the velocity of the S II "W", when used in conjunction with x_1 and c, leads to a decrease in the WRMS of the distances at the 1.8σ level. Despite what was seen in the analysis of Blondin et al. (2011), the use of relative depths of none of the features analyzed here leads to an improvement in the Hubble residuals.

The pEW of the Si II λ4000 feature is strongly anti-correlated with x_1, which confirms many previous studies (Arsenijevic et al. 2008; Walker et al. 2011; Blondin et al. 2011; Nordin et al. 2011b; Chotard et al. 2011). Furthermore, when using a model that includes x_1, c, and the pEW of this feature, the residuals are as low as when using the standard (x_1, c) model. The pEWs of the Mg II and Fe II complexes are both correlated with c, yet when using either of these (as a proxy for c) combined with the pEW of the Si II λ4000 feature (as a proxy for x_1), the Hubble diagram residuals are significantly larger than when simply using x_1 and c.

Both the pEWs of Si II λ5972 and Si II λ6355 are well-correlated with x_1 and correlated with c, but the use of the Si II λ5972 pEW does not improve distance calculations. However, using the Si II λ6355 pEW (along with x_1 and c) leads to an improvement in the WRMS residuals at the 1.2σ level. The pEW of this feature is also found to be uncorrelated with $(B-V)_{B_{\max}}$, and thus should not be used as a proxy for SN color, which differs from the findings of Foley et al. (2011). Finally, the Ca II near-IR triplet is correlated with c and MLCS2k2 light-curve width parameter Δ. This feature and the O I triplet have not been investigated thoroughly in studies similar to this one since other large SN Ia spectral datasets often do not include these spectral regions.

The Si II ratio, used as a luminosity indicator previously (e.g., Nugent et al. 1995; Benetti et al. 2005; Hachinger et al. 2006), is found to be well-correlated with Δm_{15}. However, we caution that at a given value of Δm_{15}, there can exist various spectroscopically classified subtypes of SN Ia. This ratio is also found to be correlated with $(B-V)_{B_{\max}}$, which has been seen in other work (Altavilla et al. 2009). We also show that the Si II ratio is *not* an accurate proxy for x_1 when calculating distance moduli. A model using c and $\Re$(Si II) performs significantly worse than the usual (x_1, c) model, which is different from the results of Blondin et al. (2011).

On the other hand, the Ca II ratio is found to be a good indicator of light-curve width, as it is well-correlated with the MLCS2k2 Δ parameter as well as Δm_{15}. In fact, a model using x_1, c, and $\Re$(Ca II) leads to a 1.1σ decrease in Hubble residuals. The BSNIP data also

indicate that the SiS ratio is correlated with both x_1 and c. Models using $\Re$(SiS) with just c or with both c and x_1 perform as well as the standard (x_1, c) model. Finally, we confirm the results of Hachinger et al. (2006) that the SSi and SiFe ratios are both accurate luminosity indicators, as they are both well-correlated with Δm_{15}.

Following Bailey et al. (2009) and Blondin et al. (2011), we calculate Hubble diagram residuals using models which include combinations of the usual light-curve parameters (width and color) and arbitrary sets of flux ratios. 17,822 different ratios of fluxes are used alone, with x_1, with c, and with both x_1 and c to investigate whether any of these models might improve the accuracy of SN Ia distance measurements. No models utilizing only a flux ratio or a flux ratio and x_1 are found to decrease the Hubble residuals. A handful of models using a flux ratio and c are seen to perform as well as the standard (x_1, c) model. Interestingly, most of these best ratios are extremely close to the SiS ratio mentioned above.

These results differ from the previous work of Bailey et al. (2009) and Blondin et al. (2011), both of whom found that flux ratios alone or in conjunction with light-curve information would usually perform better than the (x_1, c) model. This is perhaps due to the fact that the number of objects used in the current analysis is 2–3 times larger than what was used in these past studies. This could also be caused by the larger number of spectroscopically peculiar SNe Ia in the BSNIP sample.

Finally, when combining a flux ratio with both x_1 and c, our top performing ratio, $\mathcal{R}^c\,(3580/4280)$, decreases the Hubble residuals by 12%, which is significant at the 2.4σ level. The WRMS of the residuals using this model is 0.130 ± 0.019 mag, as compared to 0.146 ± 0.019 mag when using the same sample with the standard (x_1, c) model. This Hubble diagram fit has one of the smallest scatters ever published and at the highest significance ever seen in such a study.

4.5.2 The Future...?

New large-scale surveys are already obtaining SN Ia data, and they are observing to higher redshifts and gathering larger amounts of data than what is in the BSNIP sample (e.g., Rau et al. 2009; Law et al. 2009; Kaiser et al. 2002). Even larger surveys at even higher redshifts are also planned (e.g., LSST, WFIRST). Many more SNe Ia will be discovered than can be rigorously observed; we are quickly entering the age of SN research where we are follow-up limited. Thus, there must be significant effort put forth to determine what is the most efficient way to monitor and utilize such vast quantities of objects. That is one of the major goals of BSNIP.

Soon, for the vast majority of objects, there will only be (at best) a handful of photometric observations near maximum brightness. Those, combined with a relatively low S/N spectrum near maximum, will likely be all the follow-up observations we get. From the work presented here (and in BSNIP II) we have shown that there is still hope.

The pEW of the Si II λ4000 feature is a good indicator of light-curve width and the pEWs of the Mg II and Fe II complexes are relatively good proxies for color. Unfortunately,

the correlations between these spectral measurements and the corresponding photometric properties is not perfect, and distance calculations that employ only those spectroscopic measurements do not perform as well as the standard model which uses light-curve width and color. However, this is still a promising avenue for further investigation using new datasets that are even larger than BSNIP. Other correlations that appear marginal in the BSNIP dataset, or models tested here that performed only equally as well as the usual (x_1, c) model, should also be reexamined in the future.

Occasionally, one will be fortunate enough to have sufficient photometric observations to produce a light curve for which SALT2 (or another light-curve fitter) is able to determine a width and color. In these cases it appears that the light-curve parameters can be combined with a flux ratio from a spectrum near maximum brightness to improve the accuracy of SN Ia distances. The best ratios for this, as determined from the BSNIP data, are all near $\mathcal{R}^c(\sim3600/\sim4250)$.

This is all somewhat heartening for surveys that will discover and monitor SNe Ia at higher redshifts. Si II $\lambda4000$, the Mg II and Fe II complexes, and $\mathcal{R}^c(\sim3600/\sim4250)$ all involve spectral features which are toward the blue end of the optical range. This is critical for higher-z surveys since, as pointed out in BSNIP II, the red wing of the typical, near-maximum Si II $\lambda6355$ feature becomes redshifted beyond $\sim1\mu$m for $z \gtrsim 0.6$. Furthermore, as discussed multiple times in BSNIP II, measuring fluxes and pEWs directly from a spectrum is much easier and less reliant on smoothing models or functional form assumptions than velocities, for example.

To quote the concluding paragraph of Blondin et al. (2011), "Do spectra improve distance measurements of SN Ia? Yes, but not as much as we had hoped." "Good" scientists are not supposed to let personal feelings or hopes interfere with their work. However, we have to agree with the authors of this quote both on the objective part (i.e., spectra *do* improve distance measurements), as well as on the subjective part (i.e., we hoped they would improve things *even more*).

Chapter 5

Fourteen Months of Observations of the Possible Super-Chandrasekhar Mass Type Ia Supernova 2009dc

The barrier has begun to yield.
—John Frederick William Herschel

5.1 Introduction

Type Ia supernovae (SNe Ia) are differentiated from other types of SNe by the absence of hydrogen and the presence of broad absorption from Si II λ6355 in their optical spectra (for a review see Filippenko 1997). SNe Ia have been used to measure cosmological parameters to high precision (e.g., Kowalski et al. 2008; Hicken et al. 2009b; Kessler et al. 2009; Amanullah et al. 2010), as well as to discover the accelerating expansion of the Universe (Riess et al. 1998; Perlmutter et al. 1999). Broadly speaking, SNe Ia are the result of thermonuclear explosions of C-O white dwarfs (WDs) resulting from either the accretion of matter from a nondegenerate companion star (e.g., Whelan & Iben 1973) or the merger of two degenerate objects (e.g., Iben & Tutukov 1984; Webbink 1984). However, the nature of the companion and the details of the explosion itself are both still quite uncertain.

The cosmological utility of SNe Ia comes from the fact that they are standardizable candles (i.e., their luminosities at peak can be calibrated). This naively seems reasonable since SNe Ia should all have the same amount of fuel and the same trigger point: they should all explode when a WD nearly reaches the Chandrasekhar mass of $\sim$1.4 $M_\odot$.

In 2003, SNLS-03D3bb (also known as SN 2003fg) was discovered (Howell et al. 2006) and was shown to be a SN Ia that was overluminous by about a factor of 2, and had a slowly declining light curve, quite low expansion velocities, and unburned material present in near-maximum light spectra. This last observation implies that a layer of carbon and oxygen from the progenitor existed on top of the burned silicon layer. In SNe Ia, carbon

is usually extremely weak or completely absent (even at very early times) in optical and infrared (IR) spectra, although it has been (sometimes tentatively) identified in a few other cases (e.g., Branch et al. 2003; Marion et al. 2006; Thomas et al. 2007; Foley et al. 2010b). Howell et al. (2006) suggest that all of the oddities seen in SN 2003fg could be explained if its progenitor WD had a mass greater then the canonical upper limit for WDs of $\sim$1.4 $M_{\odot}$, a so-called "super-Chandrasekhar mass" (SC) WD.

Hicken et al. (2007) then presented data on SN 2006gz which shared some of the strange properties of SN 2003fg, and they concluded that SN 2006gz must have come from a WD merger leading to a SC SN Ia. Recently, Scalzo et al. (2010) published observations of SN 2007if which is yet another example of this emerging class of possible SC SNe Ia. They not only observed low expansion velocities, but they also saw a plateau in the expansion velocity near maximum-brightness which they interpret as evidence for the SN ejecta running into a shell of material. The accurately determined total mass of the SN 2007if system is well above the Chandrasekhar mass.

Recently, it was pointed out that there might be another member of this SC SN Ia class, SN 2009dc (Harutyunyan et al. 2009; Marion et al. 2009; Yamanaka et al. 2009). SN 2009dc was discovered $15\farcs8$ west and $20\farcs8$ north of the nucleus of the S0 galaxy UGC 10064 by Puckett et al. (2009) on 2009 Apr. 9.31 (UT dates are used throughout this chapter), though in §5.3.1 we will show a detection of the SN $\sim$5 d earlier. It is located at $\alpha_{\rm J2000} = 15^{\rm h}51^{\rm m}12^{\rm s}12$ and $\delta_{\rm J2000} = +25^{\circ}42'28\farcs0$; the SN and its host are shown in Figure 5.1. No object was visible in our data at the position of the SN on 2009 Mar. 28 to a limiting magnitude of $\sim$19.5, so the actual explosion date was almost certainly between Mar. 28 and Apr. 4.

Harutyunyan et al. (2009) obtained a spectrum of SN 2009dc one week after the announced discovery date and showed it to be a SN Ia before maximum light. They also noted that SN 2009dc spectroscopically resembled the SC SN Ia candidate SN 2006gz (Hicken et al. 2007) at this time, but with a much lower expansion velocity as derived from the Si II λ6355 absorption feature. Three days later, nearly simultaneous optical and IR spectra were obtained by Marion et al. (2009), covering a wavelength range of 0.36 to 1.3 μm. They again note some similarities to (as well as differences from) SN 2006gz, as well as similarities with the possible SC SN Ia 2003fg (Howell et al. 2006).

Yamanaka et al. (2009) presented early-time optical and near-IR observations of SN 2009dc and showed that it did indeed share many of the properties seen in both SN 2003fg and SN 2006gz, suggesting that it too is a possible SC SN Ia. Furthermore, Tanaka et al. (2010) published spectropolarimetry of SN 2009dc which indicated that the explosion was quite spherically symmetric.

In this chapter we present and analyze our own optical photometric and spectroscopic data for SN 2009dc (as well as spectra of SN 2007if) with the goal of more definitively answering the question of whether SN 2009dc and SN 2007if were truly SC SNe Ia. We show some of the most precise data on the rise time of a possible SC SN Ia ever published, as well as some of the latest-time photometric and spectral observations of a member of this class. In §5.2 we describe our observations and data reduction, and in §5.3 we discuss our

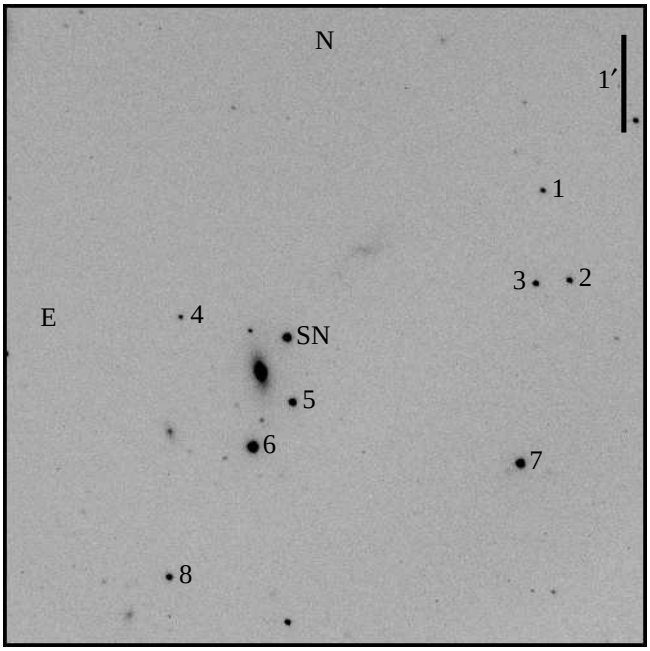

Figure 5.1: KAIT image of SN 2009dc and its host galaxy, UGC 10064. The field of view is $6.7' \times 6.7'$. SN 2009dc is labelled along with the comparison stars used for differential photometry. The scale of the image is marked in the top right; north is up and east is to left. The SN is sufficiently far from its host galaxy that template subtraction was not performed when conducting photometry.

analysis of the photometry and spectra of SN 2009dc (and its host galaxy) and SN 2007if. We attempt to robustly calculate physical parameters of SN 2009dc using a variety of methods and compare them to theoretical predictions in §5.4. Finally, in §5.5, we summarize our conclusions and ruminate about the future.

5.2 Observations and Data Reduction

5.2.1 Photometry

Observations of SN 2009dc began on 2009 Apr. 17, about one week before maximum B-band brightness, in $BVRI$ filters using the 0.76-m Katzman Automatic Imaging Telescope (KAIT; Filippenko et al. 2001) and the 1-m Nickel telescope, both at Lick Observatory. We continued to follow SN 2009dc for over 5 months until 2009 Sep. 26, when it reached the western limit of both telescopes in the early evening. We obtained late-time $gVRI$ images of SN 2009dc using the dual-arm Low-Resolution Imaging Spectrometer (LRIS; Oke et al. 1995) with the 10 m Keck I telescope on 6 Feb. 2010 (281 d past maximum), BRI images using the DEIMOS spectrograph (Faber et al. 2003) mounted on the 10 m Keck II telescope on 12 June 2010 (403 d past maximum), and V-band images again using LRIS on 13 June 2010.

Our optical photometry is complemented with data taken from the UltraViolet Optical Telescope (UVOT) on the *Swift* Observatory in the U, B, V, $UVW1$, $UVM2$, and $UVW2$ filters. We downloaded 7 epochs of observations from the *Swift* archives.

Our early-time optical images were reduced using a pipeline developed for KAIT and Nickel data (Ganeshalingam et al. 2010). The images were bias subtracted and flatfielded at the telescope. Given the distance of SN 2009dc from the host galaxy, we did not find it necessary to attempt galaxy subtraction. We performed differential photometry using point-spread function (PSF) fitting photometry on SN 2009dc and several comparison stars in the field with the DAOPHOT package in IRAF.[1] The output instrumental magnitudes were calibrated to the standard Johnson BV and Cousins RI system using color terms derived from many photometric nights. The comparison stars were calibrated against Landolt (1992) standard stars using 13 photometric epochs to achieve a root-mean square (rms) of < 0.01 mag. The comparison stars are identified in Figure 5.1 with corresponding photometry in Table 5.1. To estimate the uncertainty in our photometry pipeline, we add artificial stars with the same magnitude and PSF as the SN to each data image at positions of similar background brightness; the rms of doing this procedure 20 times is taken as the uncertainty. The photometric uncertainty is added in quadrature to the calibration error to produce our final uncertainty, adopting an error floor of 0.03 mag for B and I and 0.02 mag for V and R to account for slight systematic differences between the KAIT and Nickel photometry. Our final photometry of SN 2009dc is presented in Table 5.2.

[1]IRAF: The Image Reduction and Analysis Facility is distributed by the National Optical Astronomy Observatory, which is operated by the Association of Universities for Research in Astronomy (AURA) under cooperative agreement with the National Science Foundation (NSF).

Table 5.1: Comparison Stars for the SN 2009dc Field

Star	$\alpha_{\rm J2000}$	$\delta_{\rm J2000}$	B (mag)	V (mag)	R (mag)	I (mag)	$N_{\rm cal}$
SN	15:51:12.12	+25:42:28.0					
1	15:51:00.40	+25:44:00.1	18.769 (010)	17.418 (006)	16.503 (005)	15.744 (011)	9
2	15:50:59.16	+25:43:04.7	17.501 (008)	16.957 (006)	16.608 (004)	16.236 (008)	12
3	15:51:00.72	+25:43:02.5	18.126 (009)	16.816 (004)	15.940 (004)	15.228 (008)	10
4	15:51:16.96	+25:42:40.6	18.671 (006)	17.805 (005)	17.249 (006)	16.734 (011)	11
5	15:51:11.83	+25:41:48.3	16.661 (007)	15.872 (004)	15.406 (003)	14.984 (009)	13
6	15:51:13.64	+25:41:20.5	15.383 (007)	14.471 (004)	13.935 (003)	13.460 (009)	13
7	15:51:01.38	+25:41:11.2	15.892 (007)	15.200 (005)	14.808 (003)	14.420 (010)	13
8	15:51:17.44	+25:39:59.6	17.156 (006)	16.534 (004)	16.174 (004)	15.790 (008)	13

1σ uncertainties are in parentheses, in units of 0.001 mag.

Table 5.2: Early-time $BVRI$ photometry of SN 2009dc

JD	B (mag)	V (mag)	R (mag)	I (mag)	Telescope
2454925.95	···	···	18.824 (177)	···	KAIT
2454938.98	15.670 (030)	15.638 (020)	15.596 (020)	15.718 (030)	KAIT
2454939.95	15.549 (030)	15.541 (020)	15.500 (020)	15.577 (030)	Nickel
2454940.92	15.474 (030)	15.472 (030)	15.430 (030)	15.524 (030)	Nickel
2454940.93	15.511 (030)	15.495 (020)	15.475 (020)	15.608 (030)	KAIT
2454942.95	15.455 (030)	15.409 (020)	15.376 (020)	15.529 (030)	KAIT
2454946.97	15.383 (030)	15.327 (020)	15.272 (020)	15.450 (030)	KAIT
2454948.87	15.369 (030)	15.350 (020)	15.288 (020)	15.454 (030)	KAIT
2454951.92	15.449 (030)	15.386 (020)	15.311 (020)	15.449 (030)	KAIT
2454957.97	15.770 (030)	15.535 (020)	15.423 (020)	15.537 (030)	KAIT
2454959.85	15.930 (030)	15.610 (020)	15.464 (020)	15.554 (030)	KAIT
2454960.92	16.004 (030)	15.591 (020)	15.476 (020)	15.593 (030)	KAIT
2454962.93	16.137 (036)	15.656 (024)	15.543 (026)	15.633 (084)	KAIT
2454964.90	16.322 (030)	15.762 (020)	15.584 (020)	15.568 (030)	KAIT
2454966.93	16.528 (030)	15.846 (020)	15.642 (020)	15.562 (030)	KAIT
2454966.95	16.478 (030)	15.839 (020)	15.611 (020)	15.481 (030)	Nickel
2454968.89	16.677 (030)	15.926 (020)	15.675 (020)	15.565 (030)	KAIT
2454970.88	···	16.029 (086)	15.696 (053)	···	KAIT
2454971.92	16.880 (030)	16.054 (020)	15.701 (024)	15.500 (030)	Nickel
2454972.89	16.972 (030)	16.106 (020)	15.748 (020)	15.579 (030)	KAIT
2454974.88	17.154 (030)	16.202 (020)	15.799 (020)	15.557 (030)	KAIT
2454975.87	17.188 (030)	16.239 (020)	15.797 (020)	15.526 (030)	Nickel
2454977.90	17.384 (030)	16.334 (020)	15.874 (020)	15.659 (030)	KAIT
2454981.89	17.650 (047)	16.488 (020)	16.009 (020)	15.707 (030)	KAIT
2454989.83	18.045 (078)	16.893 (027)	16.364 (020)	15.979 (034)	KAIT
2454989.87	17.891 (062)	16.855 (030)	16.333 (030)	15.951 (030)	Nickel
2454993.85	18.128 (080)	16.943 (041)	16.480 (021)	16.167 (030)	KAIT
2454993.90	18.032 (042)	16.960 (022)	16.483 (020)	16.093 (030)	Nickel

Continued on Next Page...

Table 5.2 — Continued

JD	B (mag)	V (mag)	R (mag)	I (mag)	Telescope
2454999.81	18.188 (057)	17.083 (026)	16.696 (020)	···	KAIT
2454999.83	18.153 (037)	17.102 (020)	16.675 (027)	16.315 (030)	Nickel
2455004.78	18.208 (033)	17.180 (033)	16.835 (028)	16.478 (034)	Nickel
2455007.84	18.265 (030)	17.289 (022)	16.913 (027)	16.540 (031)	Nickel
2455009.80	18.254 (089)	17.277 (029)	16.944 (022)	16.677 (039)	KAIT
2455014.83	18.449 (084)	17.344 (057)	17.151 (021)	16.761 (038)	KAIT
2455015.83	18.370 (046)	17.427 (022)	17.132 (031)	16.794 (042)	Nickel
2455019.85	18.377 (106)	17.432 (043)	17.247 (040)	16.937 (036)	Nickel
2455022.74	18.271 (097)	17.581 (047)	17.295 (025)	16.890 (050)	KAIT
2455025.83	18.585 (049)	17.607 (069)	17.431 (059)	17.176 (053)	Nickel
2455027.69	18.502 (054)	17.625 (041)	17.439 (035)	17.243 (036)	KAIT
2455032.69	18.512 (089)	17.770 (043)	17.570 (020)	17.343 (036)	KAIT
2455032.85	18.607 (032)	17.726 (020)	17.588 (025)	17.317 (043)	Nickel
2455034.73	18.678 (030)	17.779 (036)	17.643 (028)	17.425 (046)	Nickel
2455037.69	18.686 (053)	17.805 (045)	17.725 (023)	17.455 (035)	KAIT
2455040.77	18.756 (030)	17.902 (023)	17.800 (021)	17.504 (030)	Nickel
2455042.68	18.646 (062)	18.060 (077)	17.908 (066)	17.690 (111)	KAIT
2455042.77	18.844 (060)	17.912 (037)	17.886 (035)	17.586 (037)	Nickel
2455044.73	18.788 (041)	17.971 (043)	17.946 (028)	17.666 (053)	Nickel
2455047.68	19.035 (151)	17.965 (055)	18.007 (116)	17.646 (057)	KAIT
2455047.73	18.900 (142)	18.075 (076)	18.026 (049)	17.825 (119)	Nickel
2455052.68	18.992 (115)	18.208 (050)	18.178 (040)	17.860 (140)	KAIT
2455054.77	···	18.231 (083)	18.256 (132)	17.909 (133)	Nickel
2455057.69	18.967 (174)	18.233 (136)	18.198 (170)	18.064 (176)	KAIT
2455059.71	19.026 (048)	18.241 (036)	18.309 (041)	18.065 (044)	Nickel
2455062.67	19.087 (120)	18.323 (049)	18.364 (135)	18.227 (174)	KAIT
2455064.70	19.070 (051)	18.339 (045)	18.484 (038)	18.093 (050)	Nickel
2455067.66	19.061 (086)	18.324 (067)	18.462 (068)	18.307 (172)	KAIT
2455068.69	19.144 (045)	18.368 (024)	18.559 (065)	18.285 (080)	Nickel
2455071.69	19.166 (052)	18.427 (033)	18.632 (039)	18.283 (090)	Nickel
2455072.66	19.164 (142)	18.512 (075)	18.653 (085)	18.437 (130)	KAIT
2455074.69	19.249 (098)	18.497 (044)	18.717 (061)	18.313 (082)	Nickel
2455077.65	···	18.725 (082)	···	···	KAIT
2455082.65	19.163 (089)	18.789 (088)	19.011 (188)	18.618 (143)	KAIT
2455087.64	···	18.919 (171)	···	···	KAIT
2455090.68	19.444 (052)	18.765 (037)	19.219 (091)	18.800 (081)	Nickel
2455093.66	19.528 (078)	18.820 (043)	19.176 (086)	18.867 (144)	Nickel
2455100.66	19.665 (061)	18.954 (095)	19.441 (151)	···	Nickel

1σ uncertainties are in parentheses, in units of 0.001 mag.

Late-time data obtained at the Keck I and Keck II telescopes were bias subtracted and flatfielded using standard imaging techniques. Differential photometry was performed using PSF fitting photometry on the SN and comparison stars that were not saturated, but also detected in our calibration images obtained with the Nickel telescope. Calibrations for the

Table 5.3: Late-time Photometry of SN 2009dc

JD	Phase[a]	Telescope	Filter	Exposure (s)	Mag	σ
2455202.07	250	Nickel	B	600	21.868	0.268
	250	Nickel	V	360	21.016	0.320
2455233.10	281	Keck/LRIS	g	180	21.894	0.050
	281	Keck/LRIS	V	180	21.988	0.042
	281	Keck/LRIS	R	60	22.600	0.084
	281	Keck/LRIS	I	120	21.483	0.060
2455359.05	403	Keck/DEIMOS	B	360	25.010	0.120
	403	Keck/DEIMOS	R	450	24.987	0.143
	403	Keck/DEIMOS	I	450	23.746	0.185
2455360.10	404	Keck/LRIS	V	540	24.834	0.152

[a]Rest-frame days relative to the date of B-band maximum brightness.

g band were obtained using the transformations presented by Jester et al. (2005). In cases where all of the field stars from our Nickel calibration were saturated, calibrations for fainter stars in the field were obtained from the Sloan Digital Sky Survey (SDSS) and transformed into $BVRI$ using transformations for stars from Jester et al. (2005). Color-term corrections were not applied. We include a systematic error of 0.03 mag in all bands. Our final late-time photometry of SN 2009dc is presented in Table 5.3, which also includes an epoch of photometry obtained with the Nickel.

We downloaded the Level-2 UVOT data from the *Swift* archive. Images taken during the same pointing were registered and stacked to produce deeper images. We performed aperture photometry using the recipes prescribed by Li et al. (2006) for the optical data and Poole et al. (2008) for the UV data. We modified the U-band data to be in the Johnson-Cousins system using the color corrections found in Li et al. (2006). In general, the UVOT B and V photometry is in good agreement with the photometry from our ground-based telescopes to within ± 0.05 mag. The UVOT B-band data are systemically brighter, which could possibly be attributed to galaxy light falling within our aperture. Our results are given in Table 5.4.

We did not follow the photometric behavior of SN 2007if, another SC SN Ia candidate, but we do present spectroscopic observations (see §5.2.2). Throughout the rest of the chapter we adopt 2007 Sep. 5.4 as the date of B-band maximum brightness and 0.07416 as the redshift (z) of SN 2007if, both taken from Scalzo et al. (2010).

5.2.2 Spectroscopy

Beginning about a week before maximum brightness, optical spectra of SN 2009dc were obtained mainly using the dual-arm Kast spectrograph (Miller & Stone 1993) on the Lick 3 m Shane telescope. Two spectra were also obtained using LRIS on Keck I. Our last spectral

Table 5.4: UVOT Photometry of SN 2009dc

JD	Filter	Mag	σ	JD	Filter	Mag	σ
2454946.57	UVW2	17.338	0.044	2454946.57	U	14.720	0.017
2454951.85	UVW2	17.756	0.079	2454952.21	U	15.124	0.010
2454952.22	UVW2	17.987	0.073	2454955.72	U	15.506	0.022
2454955.72	UVW2	18.246	0.053	2454960.61	U	16.016	0.027
2454960.61	UVW2	18.741	0.066	2454980.35	U	17.890	0.066
2454980.35	UVW2	20.220	0.146	2454984.44	U	18.070	0.088
2454984.44	UVW2	20.314	0.177	2454946.57	B	15.324	0.017
2454946.58	UVM2	17.261	0.027	2454955.72	B	15.630	0.017
2454955.73	UVM2	18.346	0.058	2454960.61	B	15.935	0.019
2454960.61	UVM2	18.884	0.075	2454980.35	B	17.542	0.042
2454980.35	UVM2	19.986	0.135	2454984.44	B	17.739	0.055
2454984.45	UVM2	19.586	0.138	2454946.58	V	15.286	0.028
2454946.53	UVW1	16.041	0.032	2454955.73	V	15.489	0.027
2454951.71	UVW1	16.537	0.035	2454960.61	V	15.587	0.028
2454955.65	UVW1	16.965	0.035	2454980.35	V	16.550	0.044
2454960.27	UVW1	17.404	0.042	2454984.45	V	16.714	0.058
2454980.20	UVW1	18.644	0.077				
2454984.17	UVW1	18.812	0.099				

Table 5.5: Journal of Spectroscopic Observations of SN 2009dc

UT Date	Age[a]	Range (Å)	Airmass[b]	Exp (s)
2009 Apr. 18.5	−7	3500–9900	1.06	1500
2009 May 31.3	35	3500–10200	1.03	1500
2009 Jun. 17.5[c]	52	3400–10200	1.56	250/200[d]
2009 Jun. 29.3	64	3500–10200	1.08	2100
2009 Jul. 16.3	80	3500–10200	1.29	2100
2009 Jul. 23.2	87	3500–10200	1.10	2100
2009 Jul. 28.3	92	3500–10200	1.33	2100
2009 Aug. 14.2	109	3500–10000	1.31	2400
2010 Feb. 6.6[c]	281	3500–10200	1.19	3×(630/600)[d]

[a]Rest-frame days relative to the date of B-band brightness maximum, 2009 Apr. 25.4 (see §5.3.1).
[b]Airmass at midpoint of exposure.
[c]These observations used LRIS (Oke et al. 1995) on the 10 m Keck I telescope. The others used the Kast spectrograph on the Lick 3 m Shane telescope (Miller & Stone 1993).
[d]The blue side was exposed longer than the red side due to the relatively long readout time of the red-side CCD in LRIS.

observation occurred 281 d after B-band maximum.

The Kast spectra all used a 2″ wide slit, a 600/4310 grism on the blue side, and a 300/7500 grating on the red side, yielding full-width at half-maximum (FWHM) resolutions of ∼4 Å and ∼10 Å, respectively. The LRIS spectrum was obtained with a 1″ slit, a 600/4000 grism on the blue side, and a 400/8500 grating on the red side, resulting in FWHM resolutions of ∼4 Å and ∼6 Å, respectively. All observations were aligned along the parallactic angle to reduce differential light losses (Filippenko 1982). Table 5.5 summarizes the spectral data of SN 2009dc presented in this chapter.

We obtained three spectra of SN 2007if using LRIS. For the first two LRIS spectra, we used a 400/3400 grism on the blue side and a 400/8500 grating on the red side, resulting in FWHM resolutions of ∼6 Å on both sides, while the final spectrum of SN 2007if was obtained with a 600/4000 grism on the blue side, giving a resolution of ∼4 Å. In all cases, the long, 1″-wide slit was aligned along the parallactic angle to reduce differential light losses. Table 5.6 summarizes the spectral data on SN 2007if presented here. We also note that our last spectrum of SN 2007if (from 2007 Dec. 13) was taken under nonideal observing conditions (clouds were present and the atmospheric seeing was poor), and thus its spectrophotometric accuracy is not as good as that of the other observations.

All spectra were reduced using standard techniques (e.g., Foley et al. 2003). Routine CCD processing and spectrum extraction were completed with IRAF, and the data were

Table 5.6: Journal of Spectroscopic Observations of SN 2007if

UT Date	Age[a]	Range (Å)	Airmass[b]	Exp. (s)
2007 Oct. 15.4	37	3300–9200	1.03	1200
2007 Nov. 12.2	63	3300–9150	1.49	1200
2007 Dec. 13.2[c]	92	3300–9150	1.01	1200

[a]Rest-frame days relative to the date of B-band maximum brightness, 2007 Sep. 5.4 (Scalzo et al. 2010).
[b]Airmass at midpoint of exposure.
[c]This observation used a slightly higher resolution grism for the blue side.

extracted with the optimal algorithm of Horne (1986). We obtained the wavelength scale from low-order polynomial fits to calibration-lamp spectra. Small wavelength shifts were then applied to the data after cross-correlating a template sky to the night-sky lines that were extracted with the SN. Using our own IDL routines, we fit spectrophotometric standard-star spectra to the data in order to flux calibrate our spectra and to remove telluric lines (Wade & Horne 1988; Matheson et al. 2000). Information regarding both our photometric and spectroscopic data (such as observing conditions, instrument, reducer, etc.) was obtained from our SN database (SNDB). The SNDB uses the popular open-source software stack known as LAMP: the Linux operating system, the Apache webserver, the MySQL relational database management system, and the PHP server-side scripting language (see Silverman et al. in preparation for further details).

5.3 Analysis

5.3.1 Light Curves

We present our final optical $BVRI$ light curves of SN 2009dc in Figure 5.2. We include for comparison a "normal" Type Ia SN 2005cf (Wang et al. 2009b), another SC SN Ia candidate SN 2006gz (Hicken et al. 2007), the "standard overluminous" Type Ia SN 1991T (Lira et al. 1998), and the peculiar SN 2002cx-like SN 2005hk (Phillips et al. 2007).

The light curves of SN 2009dc have many features which are noticeably distinct from most other SNe Ia. The light curves are much broader than those of spectroscopically normal SNe Ia such as SN 2005cf. Even in comparison to the overluminous SN 1991T, SN 2009dc evolves significantly more slowly.The light curve of SN 2006gz presented by Hicken et al. (2007) provides an good match, although SN 2009dc appears to have a slower rise time *and* a slower decline.

The absence of a prominent second maximum in the R and I bands is particularly striking. The secondary maximum in I has been attributed to the propagation of an ionization

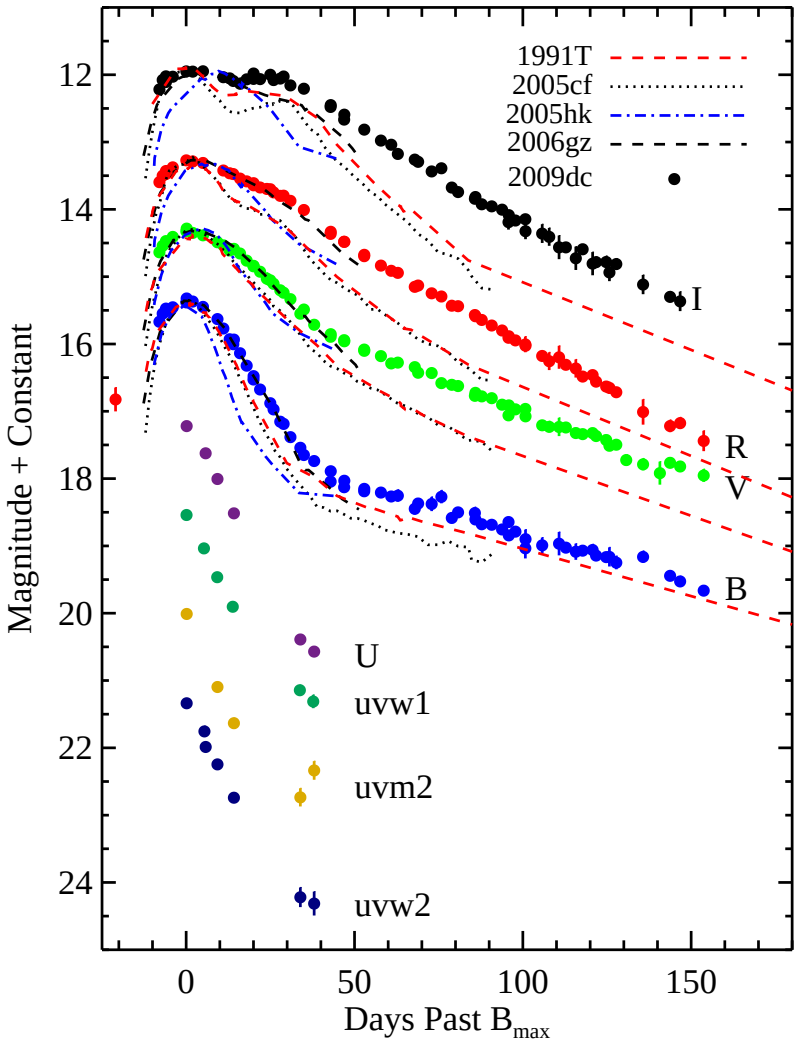

Figure 5.2: Optical and UV light curves of SN 2009dc from KAIT and the 1-m Lick Nickel telescope. For comparison we also plot the optical light curves of the overluminous Type Ia SN 1991T, the normal SN 2005cf, the peculiar SN 2002cx-like SN 2005hk, and another SC SN Ia candidate SN 2006gz. The light curves of each SN are shifted so that $t = 0$ d corresponds to the time of $B_{\rm max}$ and reach the same peak magnitude for a given filter. The evolution of SN 2009dc is atypical compared to other SNe Ia. SN 2009dc evolves much more slowly and exhibits only a muted secondary maximum in the I band. We include in our R-band light curve an early detection of SN 2009dc (*red open circle*) in an unfiltered image from the Lick Observatory SN Search (LOSS), about 3 weeks before maximum brightness. The data sources for the other SNe are cited in the text.

front through iron-group elements (IGEs) as they transition from being doubly ionized to singly ionized (Kasen 2006). Observationally, the strength of the secondary maximum has been found to correlate with peak luminosity, powered by Ni decay, with luminous SNe exhibiting more prominent secondary peaks (Hamuy et al. 1996a; Nobili et al. 2005). However, this feature is weak in SN 2009dc, even though it is more luminous than a typical SN Ia. Kasen (2006) found that significant mixing of ^{56}Ni in the composition of a SN Ia can lead to a blending of the two I-band peaks, possibly explaining why a secondary peak is weak in SN 2009dc.

After correcting for Milky Way (MW) extinction (from the dust maps of Schlegel et al. 1998), we fit a polynomial to the B-band light curve to find that SN 2009dc peaked on JD $2,454,946.93 \pm 0.2$ (on 2009 Apr. 25.4) at $B_{\rm max} = 15.05 \pm 0.04$ mag. These values are consistent with those derived by Yamanaka et al. (2009).

We also measure $\Delta m_{15}(B)$, the decline in flux from maximum light to 15 d past maximum in the B band. Correcting for time dilation, we find $\Delta m_{15}(B) = 0.72 \pm 0.03$ mag, making SN 2009dc one of the most slowly evolving SNe ever discovered and comparable to other SC SN Ia candidates in the literature. Interestingly, Yamanaka et al. (2009) measure $\Delta m_{15}(B) = 0.65 \pm 0.03$ mag. Comparing the two photometric datasets, we find discrepancies between measurements of local standard stars of $\sim$0.15 mag. With over 10 calibrations of the field on photometric nights, we are confident in our measurements of the field standards presented in Table 5.1. While these differences are troubling, they do not alter the conclusion that SN 2009dc is a slowly evolving SN with an extreme value of $\Delta m_{15}(B)$.

The host galaxy of SN 2009dc is part of the Lick Observatory Supernova Search (LOSS; Li et al. 2000; Filippenko et al. 2001), allowing us to put strict constraints on the rise time of SN 2009dc. Our first detection of SN 2009dc is from an unfiltered image on 2009 Apr. 4, when the SN is seen at $R = 18.82 \pm 0.18$ mag, indicating a rise time > 21 d. This first detection is included in Figure 5.2 as part of our R-band data (Li et al. 2003a, show that KAIT unfiltered data approximate the R band). In an image taken on 2009 Mar. 28, there is no detection of SN 2009dc down to $R \approx 19.3$ mag. With these constraints we conservatively estimate a rise time of 23 ± 2 d. Hayden et al. (2010) recently found an average SN Ia rise time of 17.38 ± 0.17 d using 105 SDSS-II SNe Ia, with slowly declining SNe tending to have shorter rise times. The rise time of SN 2009dc is significantly longer than the average SN Ia in their sample, despite being a slowly declining SN, and therefore does not follow the trend found for normal SNe Ia in their sample. Riess et al. (1999a), on the other hand, found an average rise time of 19.5 ± 0.2 d for a "typical" SN Ia ($\Delta m_{15}(B) = 1.1$ mag), with slowly declining SNe having slower rise times. Their sample of 10 objects lacks SNe Ia with $\Delta m(15)_B < 0.95$ mag, making an extrapolation to $\Delta m_{15}(B) = 0.72$ mag to compare with the rise time of SN 2009dc unreliable.

The cosmological application of SNe Ia as precise distance indicators relies on being able to standardize their luminosity. Phillips (1993) showed that $\Delta m_{15}(B)$ is well correlated with luminosity at peak brightness for most SNe Ia, the so-called "Phillips relation". In Figure 5.3, we plot absolute V magnitude as a function of $\Delta m_{15}(B)$ for 71 SNe Ia with $z_{\rm Virgo\ infall} > 0.01$

from the LOSS photometry database (Ganeshalingam et al. in preparation) and SN 2009dc to determine whether SN 2009dc follows the Phillips relation. Host-galaxy extinction for the sample of 71 SNe Ia is derived using MLCS2k2.v006 with the *glosz* prior, which assumes that the late-time $(B-V)_{t=+35\ \mathrm{d}}$ color is indicative of the host-galaxy extinction (Jha et al. 2007). For SN 2009dc, the late-time color evolution differs significantly from that of normal SNe Ia; thus, we instead adopt $E(B-V)_{\mathrm{host}} = 0.1$ mag, assuming $R_V = 3.1$ for the host galaxy (see §5.3.5 for details). To place the SNe on an absolute scale, we use the luminosity distance assuming a ΛCDM cosmology with $H_0 = 70$ km s^{-1}Mpc^{-1}. The best-fitting line to SNe with $0.6 < \Delta m_{15}(B) < 1.7$ mag, excluding SN 2009dc, is plotted in Figure 5.3, with the area that falls within 1σ of the relation shaded in gray. SN 2009dc is clearly an overluminous outlier in comparison to SNe Ia having similar values of $\Delta m_{15}(B)$. Events similar to SN 2009dc cannot be standardized using current distance-fitting techniques which rely on parametrizations of light-curve shape (Howell et al. 2006).

We measure the late-time decay of the light curves using a linear least-squares fit to data in the range ∼50–150 d after maximum. We find a decline of 1.47 ± 0.04 mag per 100 d in B, 1.91 ± 0.02 mag per 100 d in V, 2.78 ± 0.03 mag per 100 d in R, and 2.87 ± 0.04 mag per 100 d in I. Leibundgut (2000) find typical decay rates for SNe Ia of 1.4 mag per 100 d in B, 2.8 mag per 100 d in V, and 4.2 mag per 100 d in I. SN 2009dc shows significantly slower decline rates in V and I.

Late-time photometry of SN 2009dc (Table 5.3) taken with the Nickel telescope shows only marginal detections in B and V and upper limits in R and I, while our Keck images, 281 d past maximum, give clear detections in $gVRI$. Figure 5.4 shows the late-time behavior of SN 2009dc in comparison to late-time photometry of SN 2003du, a typical SN Ia, taken from Stanishev et al. (2007), and the linear decay rates found using data ∼50–150 d after maximum. A constant has been added to each SN 2003du light curve in order to match the peak magnitude of SN 2009dc. Compared to the extrapolations based on the measured linear decay rates, at 281 d past maximum SN 2009dc is fainter by ∼ 0.5 mag in B and V, brighter by ∼0.5 mag in R, and ∼1.5 mag brighter in I. In comparison to SN 2003du, SN 2009dc is within ∼0.15 mag of the interpolated values in BVR and ∼0.5 mag brighter in I. We caution that our interpolated values for SN 2003du suffer from a rather large gap in the light curve between 225 d and 366 d after maximum. While the late-time behavior of SN 2009dc does not match the linear decay of SN 2003du exactly in all bands, our detections indicate that it has not undergone an unexpected drop in luminosity, and it is consistent with the late-time light curve being powered by ^{56}Co decay (see §5.4.2).

The data taken ∼400 d past maximum show only marginal detections in all bands, indicating that the SN is still active despite the points lying below interpolated values from SN 2003du. The detections in B and V are clearly below what we would expect from SN 2003du, while R and I are not too far below expectations. We address possible reasons for the drop in flux in §5.4.2.

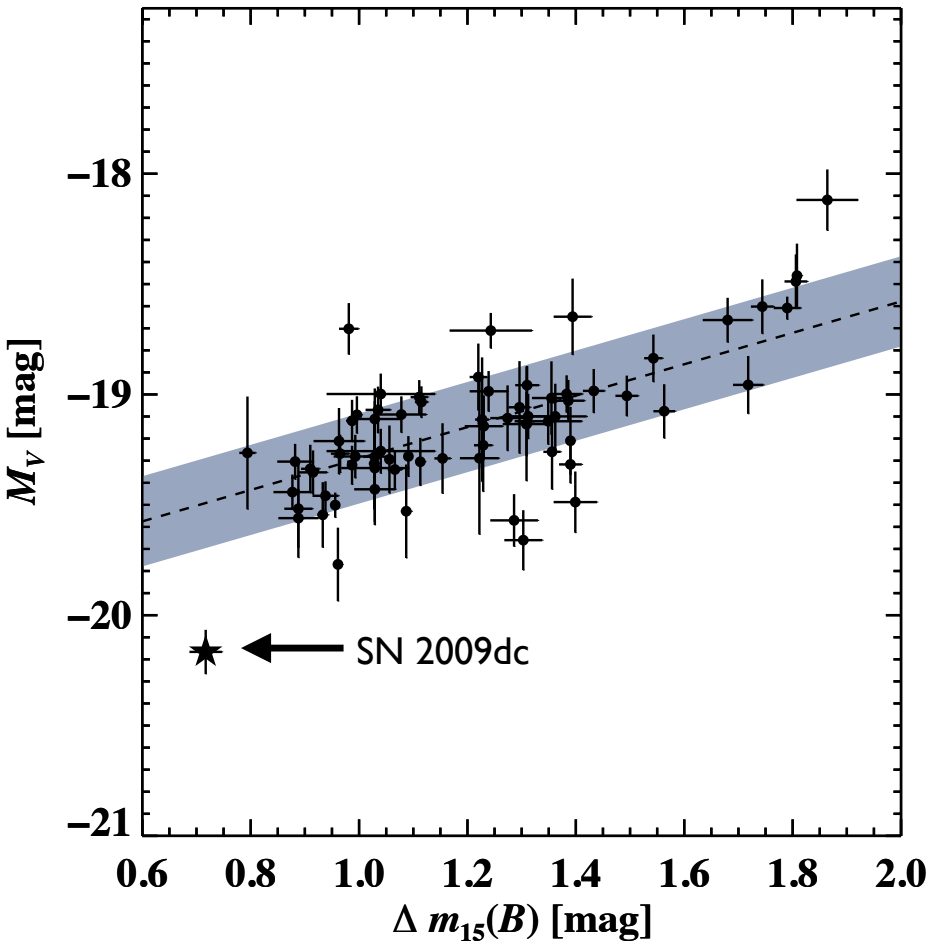

Figure 5.3: M_V as a function of $\Delta m_{15}(B)$ for 71 SNe Ia with $z_{\rm Virgo\ infall} > 0.01$ from the LOSS photometry archive (*filled circles*, Ganeshalingam et al. in preparation), compared with SN 2009dc (*filled star*). Host-galaxy extinction is derived using MLCS2k2.v006 (Jha et al. 2007), except in the case of SN 2009dc where we adopt $E(B-V)_{\rm host} = 0.1$ mag with $R_V = 3.1$ (see §5.3.5 for details). The luminosity distance was calculated using the ΛCDM concordant cosmology with $H_0 = 70$ km s^{-1}Mpc^{-1}, $\Omega_m = 0.27$, and $\Omega_\Lambda = 0.73$ (Spergel et al. 2007). The best-fitting line to the data, excluding SN 2009dc, in the range $0.6 < \Delta m_{15}(B) < 1.7$ mag is plotted as a dashed line, with points that fall within 1σ shaded in gray. SN 2009dc is clearly an outlier that does not follow the luminosity-width relation.

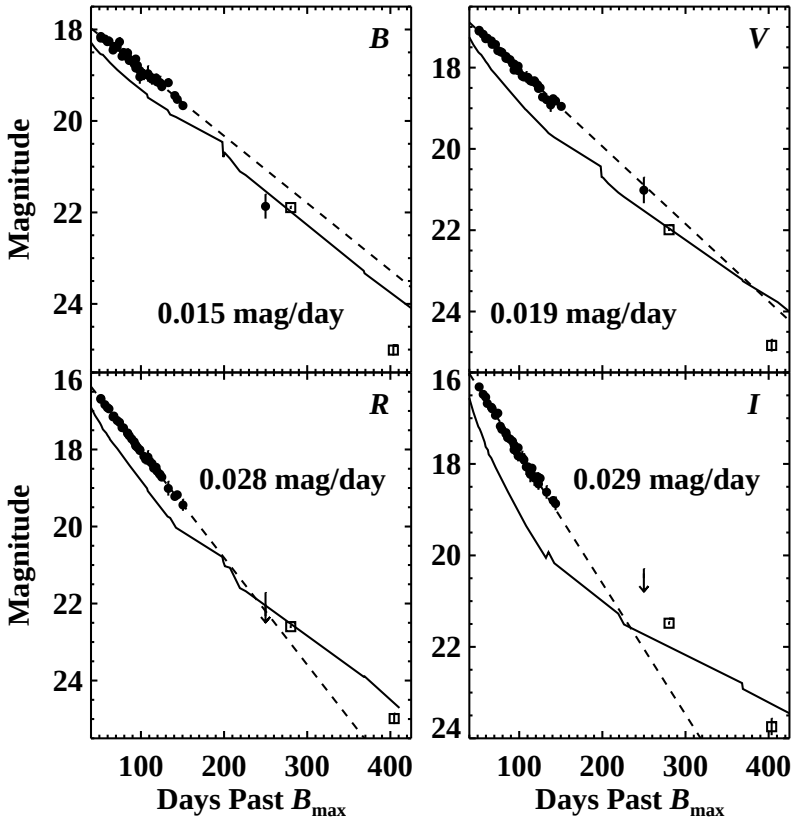

Figure 5.4: The late-time decay of SN 2009dc from 50 to about 400 d past maximum light compared to that of SN 2003du (*solid line*), a typical SN Ia. The light curves are shifted such that $t = 0$ d corresponds to the time of $B_{\rm max}$, and a constant has been added to each SN 2003du light curve to match the peak magnitude of SN 2009dc. Filled circles are KAIT and Nickel data, whereas open squares are LRIS and DEIMOS data. Upper limits are marked with arrows. The LRIS g-band point is plotted in the B-band light curve panel. We fit the decay in $BVRI$, plotted as a dashed line, using a linear least-squares fit to our well-sampled data between 50–150 d past maximum, before the SN became projected too close to the Sun. Late-time photometry obtained with LRIS at 281 d past maximum indicates that the flux in B and V is below what is expected from linear extrapolations, but mostly agrees with expectations from SN 2003du. However, the flux in R and I is larger than what is expected compared to the extrapolations. Our R-band detection falls on the comparison light curve, while the I-band detection is brighter than what is expected. SN 2009dc is detected in all bands at $\sim$400 d past maximum, indicating that the SN is still active despite the points lying below interpolated values from SN 2003du. The data for SN 2003du were taken from Stanishev et al. (2007).

5.3.2 Color Evolution

The color evolution in $B-V$, $V-R$, and $R-I$ for SN 2009dc in comparison to SNe 2006gz, 2005cf, 1991T, and 2005hk is displayed in Figure 5.5. All SNe have been corrected for MW extinction using reddening derived from the dust maps of Schlegel et al. (1998). We have also corrected for host-galaxy extinction, assuming $R_V = 3.1$, using the following reported values of $E(B-V)_{\rm host}$: 0.13 mag for SN 1991T (Lira et al. 1998), 0.10 mag for SN 2005cf (Wang et al. 2009b), 0.09 mag for SN 2005hk (Phillips et al. 2007), 0.18 mag for SN 2006gz (Hicken et al. 2007), and 0.10 mag for SN 2009dc.

The color curves indicate that SN 2009dc was a particularly blue SN Ia even compared to the prototypical overluminous SN 1991T. In $B-V$, SN 2009dc remains bluer than SNe 1991T, 2005cf, and 2005hk until $\sim$50 d past maximum light. The color curves for SN 2009dc are most similar to those of SN 2006gz, another SC SN Ia candidate. At $t > 50$ d, the $B-V$ color of SN 2009dc becomes redder than that of SN 1991T and SN 2005cf.

Lira (1996) showed that SNe with low host-galaxy extinction had similar $B-V$ color evolution between $t = +30$ to $+90$ d independent of light-curve shape (the "Lira-Phillips relation"). Hicken et al. (2007) used this relationship to derive the host-galaxy extinction for SN 2006gz. However, a comparison between the slope of the Lira-Phillips relation and the $B-V$ color evolution of SN 2009dc shows disagreement. Adopting the relation derived using 6 low-reddening SNe Ia by Phillips et al. (1999) and fitting for a constant $E(B-V)_{\rm host}$ between $t = +35$ and $+90$ d, we find $E(B-V)_{\rm host} = 0.26 \pm 0.04$ mag, with $\chi^2 = 41$ for 15 degrees of freedom. If we restrict our fit to between $t = +35$ and $+70$ d, we find a better fit with $E(B-V)_{\rm host} = 0.19 \pm 0.04$ mag; $\chi^2 = 5$ for 7 degrees of freedom. We include the fit to the Lira-Phillips relation in Figure 5.5.

5.3.3 Pre-Maximum Spectrum

On 2009 Apr. 16.22, $\sim$9 d before B-band maximum, Harutyunyan et al. (2009) obtained a spectrum of SN 2009dc which showed "prominent C II lines and a blue continuum", and they noted that the spectrum resembled pre-maximum spectra of SN 2006gz (Hicken et al. 2007), but with a much lower expansion velocity. We obtained a spectrum $\sim$2 d later which confirmed the spectral peculiarities noted by Harutyunyan et al. (2009).

Our pre-maximum spectrum is shown in Figure 5.6, where we compare SN 2009dc to other possible SC SNe Ia: SN 2006gz (Hicken et al. 2007), SN 2003fg (Howell et al. 2006), and SN 2004gu (Contreras et al. 2010, though the displayed spectrum is from our own database). In addition, we show for comparison spectra from similar epochs of the "standard overluminous" Type Ia SN 1991T (Filippenko et al. 1992a), the SN 2002cx-like peculiar SN 2005hk (Chornock et al. 2006), and the "standard normal" Type Ia SN 2005cf (Wang et al. 2009b).

SN 2009dc has strong Si II and S II lines, and appears to also contain O I, all of which are usually found in near-maximum spectra of SNe Ia. However, there are also two apparent C II lines (labelled in Fig. 5.6 and discussed in §5.3.3) seen in SN 2009dc. The existence

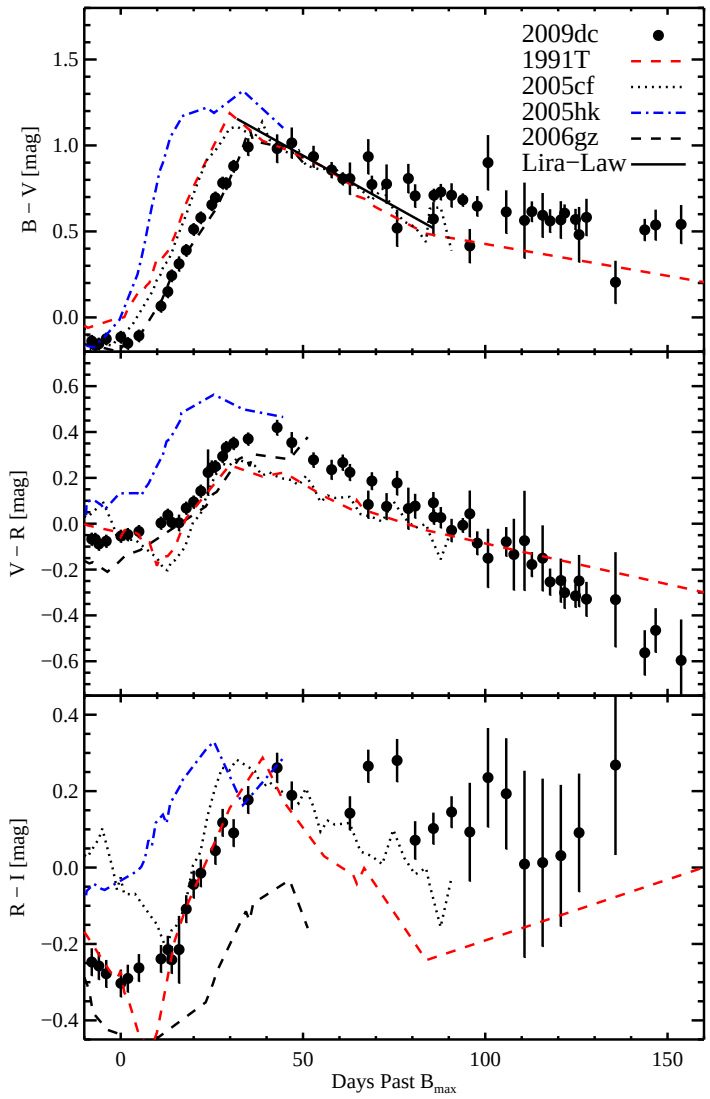

Figure 5.5: $B-V$ (*top*), $V-R$ (*middle*), and $R-I$ (*bottom*) color curves of SN 2009dc. Plotted for comparison are the color curves of SNe 1991T, 2005cf, 2005hk, and 2006gz. All curves have been corrected for MW reddening and host-galaxy extinction. We have not included errors in derived host-galaxy extinction for SN 2009dc which will systematically shift curves in one direction. At early times, SN 2009dc is bluer than SNe 1991T, 2005cf, and 2005hk. The evolution most clearly resembles that of SN 2006gz. We plot the Lira law as a solid line in the range $35 < t < 85$ d. SN 2009dc shows a slower red to blue color evolution compared to the Lira-Phillips relation, especially after $t = 70$ d. The data sources are cited in the text.

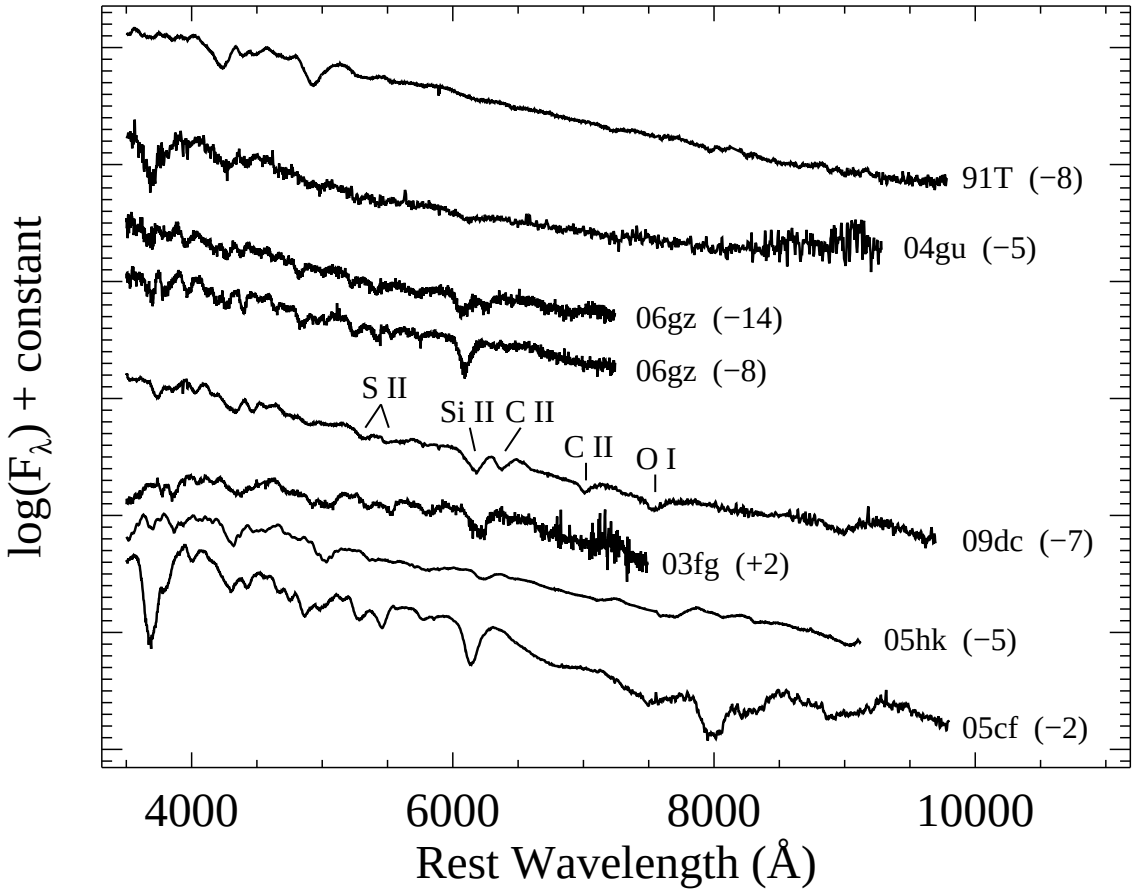

Figure 5.6: Our pre-maximum spectrum of SN 2009dc (and various comparison SNe) with a few major lines identified and days relative to maximum light indicated for each spectrum (in parentheses). From top to bottom, the SNe are the "standard overluminous" Type Ia SN 1991T (Filippenko et al. 1992a), a possible SC SN Ia SN 2004gu (Contreras et al. 2010, though this spectrum is from our own database), another possible SC SN Ia SN 2006gz (Hicken et al. 2007) at two different epochs, SN 2009dc (this chapter), yet another possible SC SN Ia SN 2003fg (Howell et al. 2006), the SN 2002cx-like peculiar SN 2005hk (Chornock et al. 2006), and finally the "standard normal" Type Ia SN 2005cf (Wang et al. 2009b). All spectra have had their host-galaxy recession velocities removed and have been dereddened according to the values presented in their respective references. Note that Si II, S II, and O I are often found in near-maximum spectra of SNe Ia, but C II is not.

(and strength) of these features is one reason that SN 2009dc was immediately classified as a possible SC SN Ia (Harutyunyan et al. 2009), and one way used to distinguish it from other subtypes of SNe Ia.

Spectroscopically, SN 2009dc does not seem to resemble any of SNe 1991T, 2005hk, or 2005cf. Although SN 2006gz has weak C II features at 14 d before maximum, by 8 d before maximum they have almost completely disappeared (whereas SN 2009dc has strong C II at 7 d before maximum). In addition, it is apparent from Figure 5.6 that the expansion velocity of SN 2006gz is much larger than that of SN 2009dc (based on the Si II λ6355 feature, for example; see §5.3.3 for further details). Finally, SN 2003fg does seem to resemble SN 2009dc, even though the spectrum of SN 2003fg has low signal-to-noise ratio (S/N) and the C II features are not nearly as prominent in SN 2003fg as they are in SN 2009dc. It is possible that this is due to the fact that the spectrum of SN 2003fg was taken 9 d later (relative to maximum light) than our spectrum of SN 2009dc.

Si II

The tell-tale spectroscopic signature of a SN Ia is broad absorption from Si II λ6355 (e.g., Filippenko 1997), and SN 2009dc is no different. One thing that *is* interesting about the Si II feature in SN 2009dc is its extremely low velocity. The minimum of the Si II λ6355 absorption feature was found to be blueshifted by 8700 km s^{-1} about 9 d before maximum brightness (Harutyunyan et al. 2009), and we measure the feature to be blueshifted by $\sim$8600 km s^{-1} in our spectrum taken 7 d before maximum. Yamanaka et al. (2009) report it to be blueshifted by 8000 km s^{-1} in their spectrum 3 d before maximum, decreasing to 6000 km s^{-1} by 25 d after maximum.

These velocities are much lower than the average photospheric velocity near maximum for SNe Ia of $\sim$11,000 km s^{-1} (Wang et al. 2009a). In fact, according to Wang et al. (2009a), the Si II velocities seen in SN 2009dc are approximately 8σ below the average.[2]

Interestingly, these velocities *are* similar to those of two other possible SC SNe Ia, SN 2003fg and SN 2007if (Howell et al. 2006; Scalzo et al. 2010, respectively). However, two other objects that were claimed to be possible SC SNe Ia show much more normal Si II velocities. Hicken et al. (2007) report expansion velocities near maximum light of about 11,000–13,000 km s^{-1} for SN 2006gz. SN 2004gu, which was compared to SN 2006gz by Contreras et al. (2010), also shows a normal photospheric velocity of $\sim$11,500 km s^{-1} at 5 d before maximum (this chapter) slowing to $\sim$11,000 km s^{-1} at 3 d past maximum.[3]

Figure 4 of Yamanaka et al. (2009) and Figure 4 of Scalzo et al. (2010) both present the velocity evolution of the Si II λ6355 feature for various possible SC SNe Ia and other comparison SNe. Our new early-time data point (i.e., $\sim$8600 km s^{-1} at $t \approx -7$ d) is quite

[2]Note that they consider SNe Ia with photospheric velocities greater than 3σ above the average to be "high-velocity SNe Ia."

[3]This second velocity has a large uncertainty since it was measured by approximating the minimum of the Si II absorption feature by eye from Figure 3 of Contreras et al. (2010).

consistent with the rest of the published SN 2009dc data. Moreover, we detect Si II λ6355 in our next spectrum taken 35 d past maximum at a blueshifted velocity of about 5500 km s^{-1} (see §5.3.4 for further details). This yields a velocity gradient of ∼74 km s^{-1} d^{-1}, which is over twice as large as that found for SN 2007if (34 km s^{-1} d^{-1}; Scalzo et al. 2010). Furthermore, combining our measurements with all previously published values of the expansion velocity of SN 2009dc (Harutyunyan et al. 2009; Yamanaka et al. 2009; Tanaka et al. 2010), we see no strong evidence for a velocity "plateau" near maximum light like the one seen in SN 2007if (Scalzo et al. 2010).

We measure the equivalent width (EW) of the Si II λ6355 feature to be ∼40 Å in our spectrum of SN 2009dc obtained 7 d before maximum. This is similar to the EW of the same line in SN 2006gz at similar epochs (Hicken et al. 2007), and both are well below the average Si II EW for normal SNe Ia (though they are comparable to the overluminous SN 1991T-like SNe Ia, e.g., Hachinger et al. 2006; Wang et al. 2009a).

C II

As ubiquitous as Si II is in the spectra of SNe Ia, C II is nearly as rare. In a few cases, mainly at very early times, weak C II has been detected in optical spectra of SNe Ia (e.g., Branch et al. 2003; Thomas et al. 2007; Tanaka et al. 2008; Foley et al. 2010b). Candidate SC SNe Ia, on the other hand, exhibit strong C II in their near-maximum spectra (Howell et al. 2006; Hicken et al. 2007; Scalzo et al. 2010).

In our spectrum of SN 2009dc obtained 7 d before maximum brightness, we detect absorption from C II λ6580 and λ7234 (both of which were also detected in a spectrum obtained the same day by Marion et al. 2009). The minimum of the absorption from C II λ6580 is blueshifted by about 9500 km s^{-1} in our pre-maximum spectrum. The expansion velocity of this feature is ∼8500 km s^{-1} at 3 d before maximum, slowing to about 7000 km s^{-1} at 3 d after maximum, and ∼6700 km s^{-1} by 6 d after maximum (Yamanaka et al. 2009; Tanaka et al. 2010). By about 18 d past maximum this feature seems to have completely disappeared, though it is difficult to be sure given the low S/N spectrum seen in Figure 3 of Yamanaka et al. (2009). However, it is clear from the same figure that by 25 d after maximum, the feature is most definitely gone. It is also undetected in our spectrum obtained 35 d past maximum (see §5.3.4).

Also, from our pre-maximum spectrum of SN 2009dc, we measure the minimum of the C II λ7234 absorption to be ∼9400 km s^{-1}, which is in good agreement with the velocity of the C II λ6580 feature that we calculate above. This feature is still apparent at about 6 d past maximum, near a velocity of ∼6600 km s^{-1} (see Fig. 1 of Tanaka et al. 2010, though the feature is not marked), but it has also likely disappeared by 18 d past maximum (Yamanaka et al. 2009, Fig. 3) and is certainly gone by 35 d past maximum (see §5.3.4).

For C II, the velocities seen in SN 2009dc once again match those of SN 2003fg at ∼2 d past maximum (Howell et al. 2006, Fig. 3 and Supplementary Information), though only the C II λ4267 line (at an expansion velocity of ∼8300 km s^{-1}) is clearly detected. On the other

hand, SN 2007if appears to have both the C II λ6580 and λ7234 features in its spectrum from 5 d past maximum (Scalzo et al. 2010).

A spectrum of SN 2006gz at 13 d before maximum shows both the C II λ6580 and C II λ7234 lines with expansion velocities near 15,500 km s^{-1}. However, both features are effectively undetectable 4 d later (Hicken et al. 2007). We also note that neither line is seen in spectra of SN 2004gu at 5 d before maximum (see Fig. 5.6, although this spectrum has low S/N) or at 3 d after maximum (Contreras et al. 2010).[4]

For SN 2009dc, Marion et al. (2009) reported no detectable absorption from C II λ4745 in their spectrum obtained 7 d before maximum. However, in our spectrum taken on the same day, we *do* see evidence for absorption from this transition, as well as absorption from C II λ4267 (see §5.3.3). Note that both of these features are slightly blended with absorption from other species, which is what most likely led Marion et al. (2009) to conclude that the features were not present.

The EW of the C II λ6580 and λ7234 absorptions, as calculated from our spectrum taken 7 d before maximum, are $\sim$19 Å and $\sim$13 Å, respectively. Hicken et al. (2007) report that the C II λ6580 feature in SN 2006gz 14 d before maximum had an EW that was slightly higher than these values (25 Å). Both of these SNe have much stronger C II lines than typical SNe Ia. For example, one of the strongest C II features ever seen in a normal SN Ia was in SN 2006D, where C II λ6580 was detected with an EW of merely 7 Å (Thomas et al. 2007).

Ca II

In our pre-maximum spectrum (as well as most of our post-maximum spectra; see §5.3.4) we detect narrow, as well as broad, absorption from Ca II H&K. The narrow components are at the redshift of SN 2009dc and its host galaxy. At all epochs these lines are just at our instrumental resolution limit; thus, calculating an accurate FWHM is nearly impossible. In addition, the H&K lines occur in a part of the spectrum where numerous broad absorption features blend together, so defining a local continuum is difficult, exacerbating the problem of measuring reliable line strengths. Despite all this, we attempt to measure the strength of this narrow feature. We calculate that the Ca II H&K lines appear to have FWHM ranging from about 100–300 km s^{-1}. However, the line strengths are consistent with no change during these epochs, given our rather large uncertainties.

Some SNe Ia exhibit narrow, time-variable Na I D absorption lines with unchanging, narrow Ca II H&K absorption (e.g., Simon et al. 2009). However, time-variable Ca II H&K absorption has not been seen. SN 2009dc does show weak, narrow absorption from Na I D, but it is far too weak to determine if variability in the line strengths exists (see §5.3.5). We cannot claim to have detected narrow, time-variable Ca II H&K absorption in SN 2009dc, but such variability should be searched for in other, future SC SNe Ia.

The narrow Ca II H&K may arise from calcium-rich interstellar material (ISM) in the host galaxy of SN 2009dc, UGC 10064, and in fact this feature is strong in a spectrum of the

[4]The C II λ7234 line, if present, would be at the red end of this spectrum.

core of the galaxy (Abazajian et al. 2009). However, since SN 2009dc is relatively far from the host's nucleus, this seems somewhat unlikely. The alternative is that the calcium-rich material which gives rise to the strong Ca II H&K line is in close proximity to the SN site. This means that SN 2009dc likely exploded in a region of calcium-rich ISM, or that the progenitor star of SN 2009dc itself had calcium-rich circumstellar material. However, which of these two possibilities best reflects the true situation and how this may affect the SN itself are beyond the scope of this chapter.

Another Ca II feature commonly seen in SNe Ia is the broad Ca II near-IR triplet. However, we see no hint of this line in our spectrum obtained 7 d before maximum. On the other hand, Tanaka et al. (2010) clearly detect this feature near 8400 Å in their spectropolarimetric observations taken ∼6 d after maximum. Not only is the line apparent in their total-flux spectrum, but it is the most polarized spectral feature they detect, with a total polarization of $\sim 0.7\%$. This, along with the high polarization of Si II λ6355 and the relatively low continuum polarization, led Tanaka et al. (2010) to conclude that SN 2009dc had a roughly spherical photosphere (as is the case for most normal SNe Ia, e.g., Leonard et al. 2005; Chornock & Filippenko 2008) with a somewhat clumpy distribution of intermediate-mass elements (IMEs).

Other Species and the SYNOW Fit

To determine which other species are present in our pre-maximum spectrum of SN 2009dc, we use the spectrum-synthesis code SYNOW (Fisher et al. 1997). SYNOW is a parametrized resonance-scattering code which allows for the adjustment of optical depths, temperatures, and velocities in order to help identify spectral features seen in SNe.

Before fitting, we deredden our pre-maximum spectrum of SN 2009dc using $E(B-V)_{\rm MW} = 0.070$ mag, $E(B-V)_{\rm host} = 0.1$ mag (see §5.3.5 for more information on how we derive these values), $R_V = 3.1$, and the reddening curve of Cardelli et al. (1989). We also remove the host-galaxy recession velocity ($cz = 6300 \pm 300$ km s^{-1}, as determined from the narrow Ca II H&K absorption in our spectrum) before comparing with the output of SYNOW.

Our derived SYNOW fit is compared to our actual pre-maximum spectrum in Figure 5.7. Also shown are the spectral features from each of the individual species that were used in the final fit. Our SYNOW fit faithfully reproduces the vast majority of the features seen in our pre-maximum spectrum of SN 2009dc, but a few features are not matched exactly (specifically, the ones near 3700 Å, 4100 Å, and 4600 Å).

In addition to the species mentioned above (Si II, C II, and weak Ca II), we detect O I, S II, Mg II, Si III, Si IV, Fe II, Co II, and Co III. All of these ions (except C II, as mentioned previously) are often found in early-time spectra of SNe Ia, though O I may be weak in some overluminous SNe Ia (e.g., Filippenko 1997). The detection of C II in the spectra of SN 2009dc (see §5.3.3) implies that it had a significant amount of unburned material in its ejecta, and thus the oxygen seen in SN 2009dc is most likely from this unburned material as well.

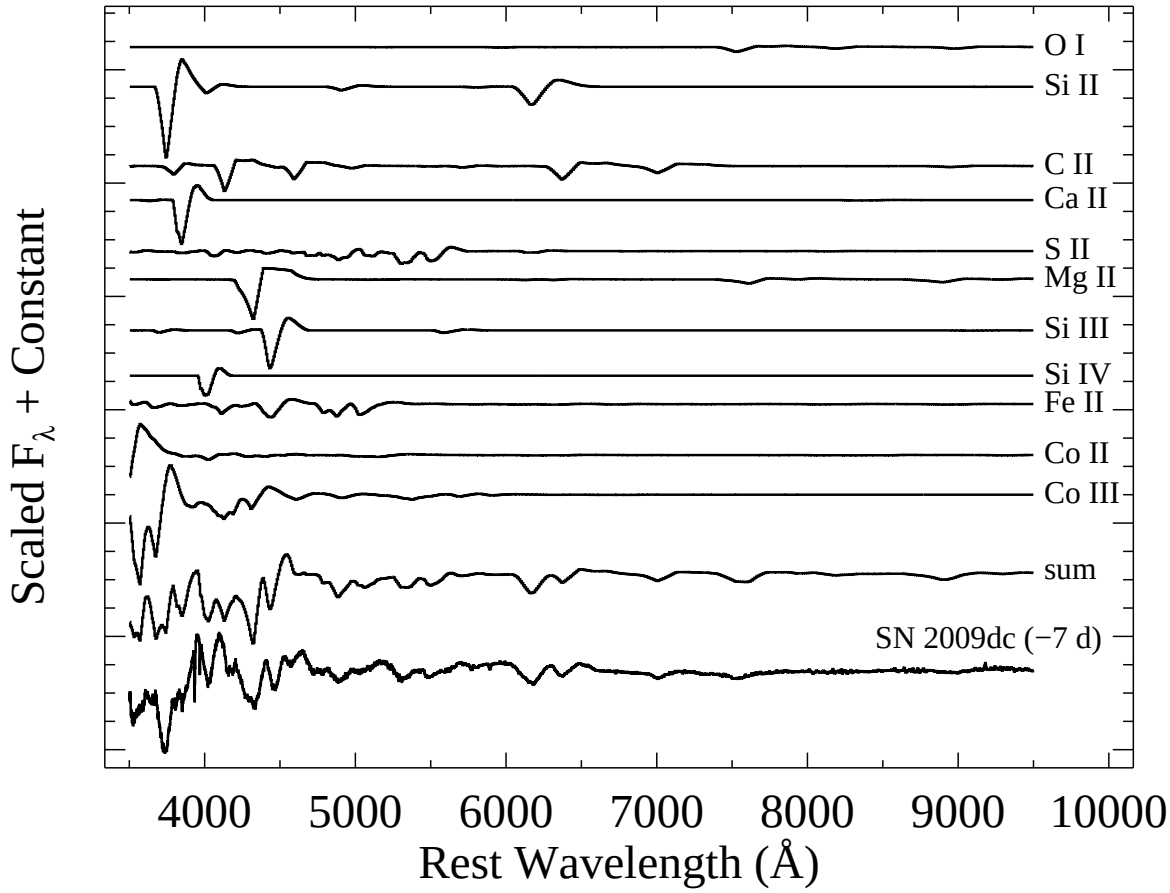

Figure 5.7: The top eleven spectra show the constituent species in our SYNOW fit. The second from bottom spectrum is the sum of the top eleven spectra. The bottom spectrum is our pre-maximum spectrum of SN 2009dc (dereddened by $E(B-V)_{\rm MW} = 0.070$ mag and $E(B-V)_{\rm host} = 0.1$ mag with $R_V = 3.1$). We also remove the host-galaxy recession velocity ($cz = 6300 \pm 300$ km s^{-1}). Finally, we remove the underlying 20,000 K blackbody continuum from all spectra shown.

Our SYNOW fit has a photospheric velocity of 9000 km s^{-1}, with maximum velocities of 10,000–15,000 km s^{-1} depending on the ion. This value matches our derived velocities from the Si II and C II absorption features (see §5.3.3 and §5.3.3, respectively). Since the early-time spectra of SN 2009dc and SN 2003fg greatly resemble each other, it is not surprising that these parameters are similar to those found in a SYNOW fit of SN 2003fg (Howell et al. 2006, Supplementary Information). Our fit requires a slightly higher photospheric velocity (they use 8000 km s^{-1}), but this seems reasonable since our spectrum was obtained 7 d *before* maximum and the spectrum of SN 2003fg fit by Howell et al. (2006) is from ∼2 d *after* maximum.

All ions in our SYNOW fit had an excitation temperature around 10,000 K except C II, which was raised to 20,000 K in order to get the relative line strengths to match the data. This is lower than what was calculated by Howell et al. (2006) for SN 2003fg. They required an excitation temperature for C II of 35,000 K to match their spectrum, while we obtain a temperature that is less than 60% of that value.

Finally, we require an underlying blackbody temperature of 20,000 K in order to reproduce the overall continuum shape of SN 2009dc. This is hot for a SN Ia, even at early times, and is indicative of the production of a large amount of ^{56}Ni (Nugent et al. 1995). Blackbody temperatures in the range of 10,000–15,000 K seem to be more common for normal SNe Ia (e.g., Patat et al. 1996), with the overluminous Type Ia SN 1991T having temperatures at the high end of that range (Mazzali et al. 1995). Howell et al. (2006) used a blackbody temperature of 9000 K to fit SN 2003fg, which does not seem abnormally high for a SN Ia 2 d past maximum. Even though this value is a bit lower than our derived blackbody temperature, it is not too surprising since our spectrum of SN 2009dc was obtained about 9 d earlier (relative to maximum light) than their spectrum of SN 2003fg.

5.3.4 Post-Maximum Spectra

The rest of our spectral data of SN 2009dc (i.e., all of our post-maximum spectra) are presented in Figure 5.8. Note that during our observation on 2009 Aug. 14.2 (day 109), there was smoke and ash in the sky throughout the night (from a fire near the observatory), and thus the continuum shape is less accurate (due to the nonstandard extinction caused by the smoke) than in the other observations.

1 Month After Maximum

Our day 35 (2009 May 31.3) spectrum of SN 2009dc is shown in Figure 5.9, along with spectra of the peculiar SN 2002cx (Li et al. 2003b), another possible SC SN Ia SN 2007if (Scalzo et al. 2010, though the displayed spectrum is from our own database), and the "standard normal" Type Ia SN 2005cf (Wang et al. 2009b). While there are some spectroscopic similarities between SN 2009dc and SN 2005cf at this epoch, there are obvious differences as well. Most notably, there are many more medium-width features in the spectrum of SN 2009dc compared with SN 2005cf, and the features that do clearly match are at much

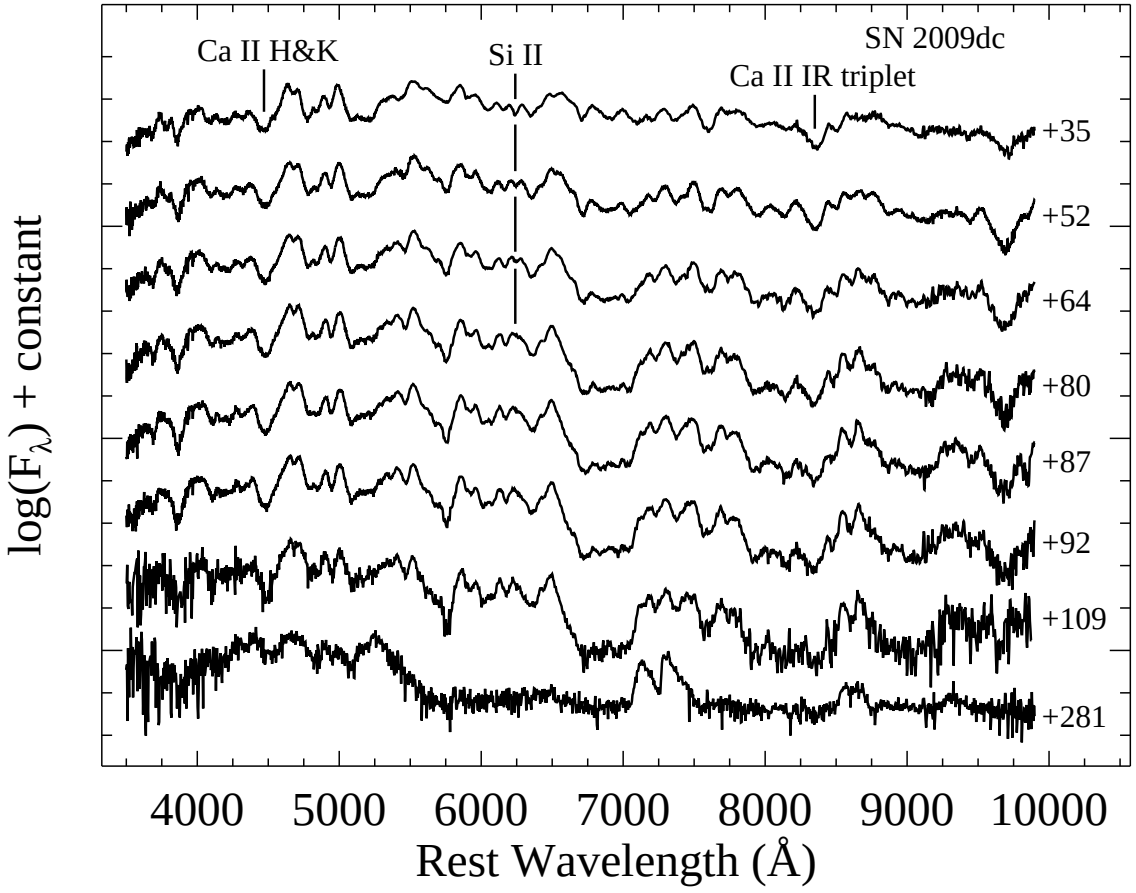

Figure 5.8: Our post-maximum spectra of SN 2009dc, with days relative to maximum light indicated for each spectrum. Important features discussed in the text are labelled. All spectra have been dereddened by $E(B-V)_{\rm MW} = 0.070$ mag and $E(B-V)_{\rm host} = 0.1$ mag with $R_V = 3.1$. We have also removed the host-galaxy recession velocity ($cz = 6300 \pm 300$ km s^{-1}).

lower velocities in SN 2009dc. This is the same as what was seen in the pre-maximum spectra (§5.3.3). Furthermore, the Ca II H&K feature as well as the Ca II near-IR triplet are much stronger in SN 2005cf than they are in SN 2009dc, again consistent with the pre-maximum spectrum of SN 2009dc (§5.3.3).

The possible SC SN Ia SN 2007if appears to be a reasonable match to the spectrum of SN 2009dc, but there are some significant differences. Even though weak Ca II features are detected in both of these objects, there are still a few medium-width features in SN 2009dc that are not seen in SN 2007if. In addition, the velocities of some (but not all) of the features in SN 2007if are larger than those in SN 2009dc by $\sim$1000 km s^{-1}. However, SN 2007if appears to match SN 2005cf well at this epoch, even though its expansion velocity is still not as large as that of SN 2005cf, and SN 2007if is missing the Si II λ6355 absorption seen in SN 2005cf.

The best match to SN 2009dc at this epoch appears to be the peculiar SN 2002cx at an age about 5–10 d younger than SN 2009dc. A detailed discussion of the comparison between peculiar SN 2002cx-like SNe and SN 2009dc can be found in §5.3.4. Since nearly every single spectral feature of SN 2009dc at this epoch matches those in SN 2002cx, we use the line identifications of Li et al. (2003b) (which mainly came originally from Mazzali et al. 1997) for SN 2009dc. The spectra at this time are dominated by various multiplets of Fe II, although Ca II (as mentioned above), Co II, and Na I are also present. There is evidence for O I λ7773 and O I λ9264 (which may give rise to the features seen near 7600 Å and 9100 Å, respectively), though Branch et al. (2004) claim that a mixture of Fe II and Co II transitions can account for these parts of the spectrum without the need for oxygen. Possible detections of Ti II (Li et al. 2003b) and Cr II (Branch et al. 2004) have been claimed for SN 2002cx, but it is extremely difficult to disentangle the individual contributions of each of these IGEs in SN 2009dc.

The one clear difference between the spectrum of SN 2009dc and that of SN 2002cx (and SN 2005hk as well) is that SN 2009dc has a strong absorption feature centered at 6250 Å that is not seen in either of these other peculiar SNe Ia. This line is also not present in our spectrum of SN 2007if from a similar epoch. In Figure 5.10 we present a SYNOW fit to our spectrum of SN 2009dc from 35 d past maximum based originally on a fit to the spectrum of SN 2002cx from 25 d past maximum (Li et al. in preparation). Both SYNOW fits reproduce the majority of the strongest features in SN 2009dc, and the only difference between the two is the addition of Si II at an expansion velocity and excitation temperature similar to other ions in the fit. Based on the comparison of our two fits, we attribute this mysterious absorption in SN 2009dc to Si II λ6355 (blueshifted by $\sim$5500 km s^{-1}). Note that the spectrum of SN 2005cf from 28 d past maximum, shown in Figure 5.9, has strong Si II λ6355 absorption as well. The main difference between these two features is that the absorption in SN 2005cf is blueshifted by $\sim$9100 km s^{-1}, nearly twice the velocity seen in SN 2009dc. We discuss this feature further in §5.3.4.

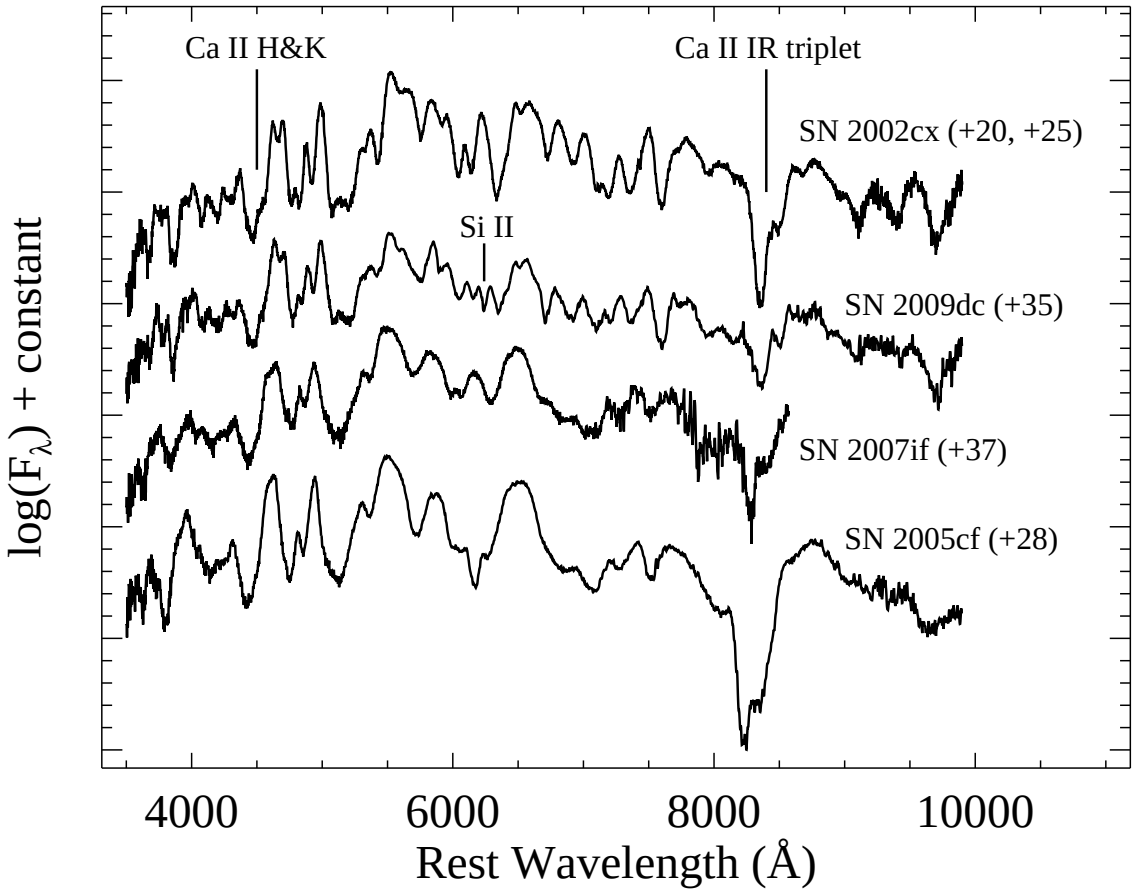

Figure 5.9: Our spectrum of SN 2009dc 35 d past maximum and a few comparison SNe, with days relative to maximum light indicated for each spectrum (in parentheses). From top to bottom, the SNe are the peculiar SN 2002cx (Li et al. 2003b, where we have combined their spectra from 20 and 25 d past maximum), SN 2009dc (this chapter), another possible SC SN Ia SN 2007if (Scalzo et al. 2010, though the spectrum shown is from our own database), and the "standard normal" Type Ia SN 2005cf (Wang et al. 2009b). Important features discussed in the text are labelled. All spectra have had their host-galaxy recession velocities removed and have been dereddened according to the values presented in their respective references.

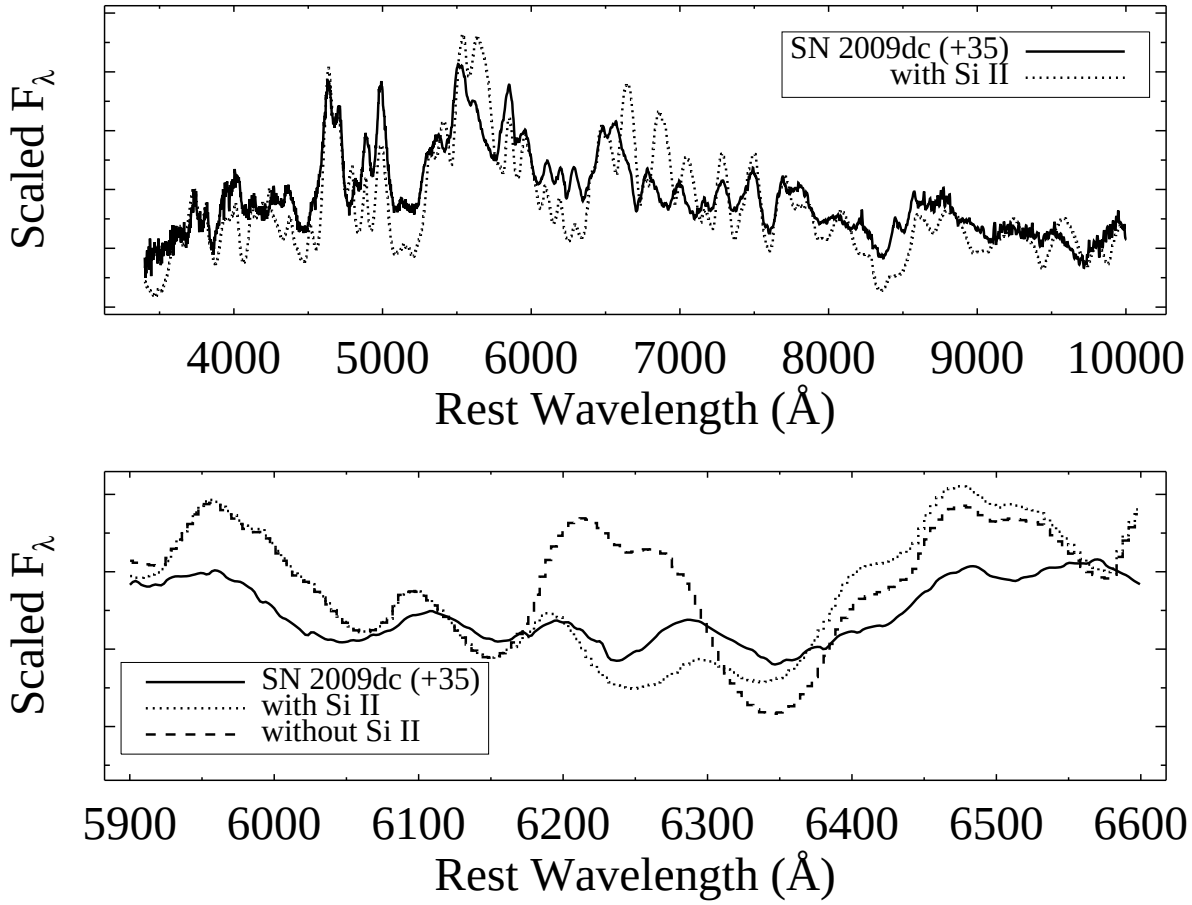

Figure 5.10: The top panel shows our spectrum of SN 2009dc from 35 d past maximum (*solid line*) overplotted with our best SYNOW fit which includes Si II (*dotted line*). The bottom panel is the same as the top panel but zoomed in and centered on the absorption feature in SN 2009dc near 6250 Å; it also shows the same SYNOW fit but with no Si II (*dashed line*). The SYNOW fit *with* Si II appears to reproduce the data better, and thus we attribute this absorption to Si II λ6355 (blueshifted by $\sim$5500 km s^{-1}). We have dereddened our data by $E(B-V)_{\rm MW} = 0.070$ mag and $E(B-V)_{\rm host} = 0.1$ mag with $R_V = 3.1$. We have also removed the host-galaxy recession velocity ($cz = 6300 \pm 300$ km s^{-1}) from the data.

2 Months After Maximum

Our day 52 (2009 Jun. 17.5) and day 64 (2009 Jun. 29.3) spectra of SN 2009dc are shown in Figure 5.11, along with spectra of SN 2002cx (Li et al. 2003b) and SN 2007if (Scalzo et al. 2010, but the displayed spectrum is from our own database). Note that SN 2009dc does not evolve much spectroscopically between days 52 and 64, though there are a few differences which will be discussed in §5.3.4.

As was the case a month earlier, the spectrum of SN 2009dc at 2 months past maximum matches that of SN 2002cx at a similar epoch. Again, the overall shape and line profiles look extremely similar between these two objects for the most part, and both look similar to SN 2007if as well as SN 2005hk (Phillips et al. 2007). At this epoch there remain a handful of medium-width features in SN 2009dc that are not seen in SN 2007if, and once again the velocities of some features in SN 2007if appear to be larger than those of SN 2009dc by about 1000 km s^{-1}.

As mentioned above, the Si II λ6355 absorption that was seen in our day 35 spectrum is still present in our day 52 and day 64 spectra of SN 2009dc. However, it decreases in strength significantly during these three observations and disappears almost completely by 80 d past maximum (see §5.3.4). Another major difference between SN 2009dc and SN 2002cx is that even though the Ca II H&K features are similar in strength, emission from the Ca II near-IR triplet is weaker in SN 2009dc and has a complex profile with multiple peaks. We discuss this feature further in the following section.

3–4 Months After Maximum

Figure 5.8 shows all of our post-maximum spectra of SN 2009dc. Overall, the spectra do not change very much from 35 to 109 d past maximum (see §5.3.4 for more information on our spectrum obtained 281 d past maximum). Most of the major spectral features remain constant during these epochs (except for a few notable examples discussed below) and their profile shapes are largely unaltered as well. The profiles of the features that do change with time mainly seem to weaken in a symmetric manner. That is, there is no compelling evidence for a preferential increase or decrease of flux in the blue or red wings of any feature.

One of the most striking aspects of the spectral evolution of SN 2009dc over these epochs is the disappearance of the broad emission near 5400 Å and in the ranges 6500–7200 Å, 7800–8300 Å, and (to a lesser extent) 8800–9200 Å. The first two of the ranges mainly fall into the R and I bands, respectively. The emission from these features, which is strong through about 1 month past maximum and then begins to decrease with time, is possibly responsible for the plateau-like broad peak in the R and I bands near maximum brightness and their slow late-time decline (as compared to more normal SNe Ia, see Fig. 5.2).

Li et al. (2003b) also saw these features in SN 2002cx, and their temporal evolution and the effect they had on the near-maximum R and I-band light curves is nearly identical to what we find in SN 2009dc. However, Li et al. (2003b) were unable to determine which ions were responsible for some of the features in these ranges in SN 2002cx, and we are likewise

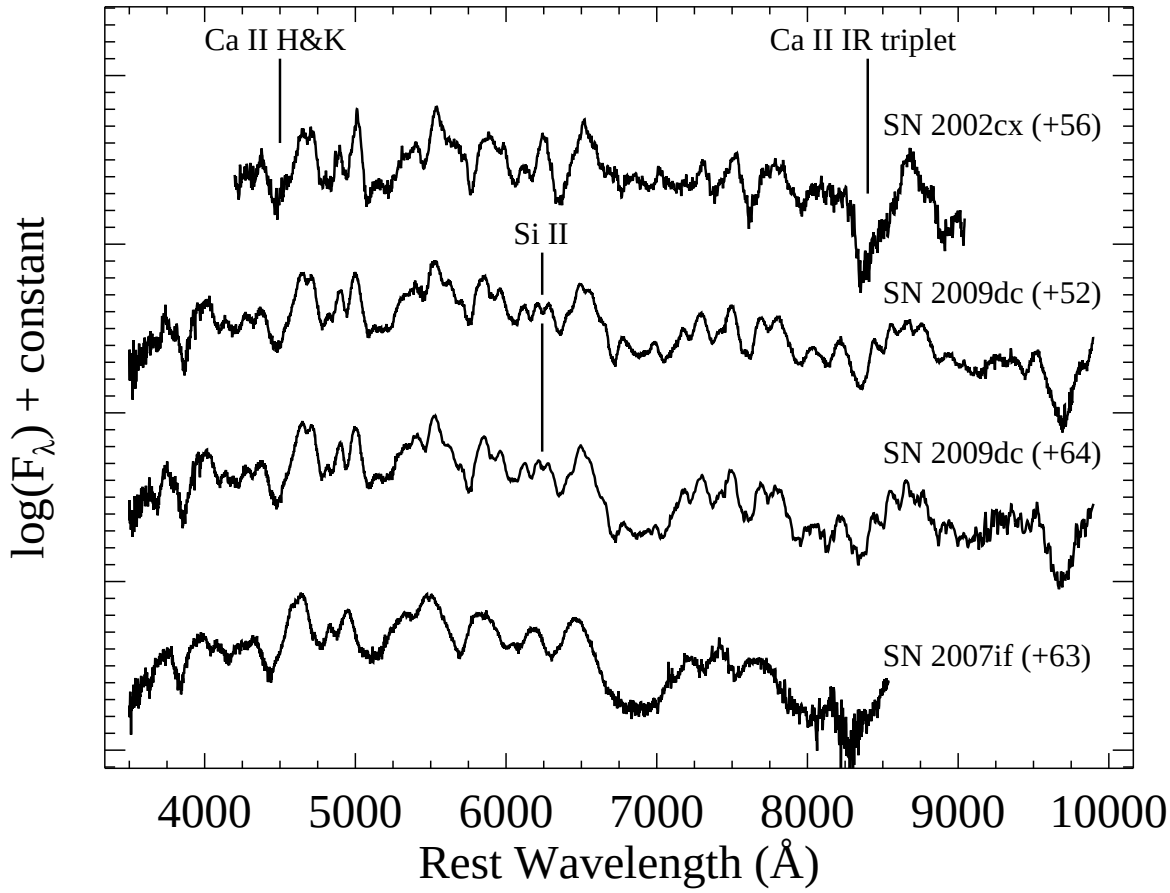

Figure 5.11: Our spectra of SN 2009dc about 52 and 64 d past maximum, and a few comparison SNe with days relative to maximum light indicated for each spectrum (in parentheses). The top SN is the peculiar SN 2002cx (Li et al. 2003b), the next two spectra are SN 2009dc (this chapter), and the bottom spectrum is another possible SC SN Ia SN 2007if (Scalzo et al. 2010, though the displayed spectrum is from our own database). Important features discussed in the text are labelled. All spectra have had their host-galaxy recession velocities removed and have been dereddened according to the values presented in their respective references.

unsure of their origin. The detailed spectral modeling required to definitively determine their identity is beyond the scope of this chapter.

As noted previously, we detect strong Si II λ6355 absorption in our day 35 spectrum of SN 2009dc. This feature is still present, but weakens, in our spectra from 52 and 64 d past maximum. In our observation of SN 2009dc at 80 d past maximum there remains a hint of absorption from Si II λ6355, but it is almost nonexistent and it is effectively undetected in any of our later spectra. It is unusual to see such strong absorption from Si II λ6355 in a SN Ia at such late times. For example, at 46 d past maximum the spectrum of SN 2005cf has only a barely perceptible Si II λ6355 feature (Wang et al. 2009b, Fig. 17).

The relative strength of this Si II line at late times in SN 2009dc is possibly due to its large ejecta mass. In §5.4.2 we find that SN 2009dc has one of the largest ^{56}Ni masses ever produced by a SN Ia, and thus one of the largest total ejecta masses as well. The massive ejecta may imply that a greater than average amount of silicon was synthesised in the explosion of SN 2009dc, which could give rise to the rather long-lived Si II λ6355 line that we detect. However, it is also possible that the Si-rich ejecta have an aspherical or clumpy distribution, and thus the longevity of the observed Si II λ6355 line is simply a viewing angle effect.

As stated earlier, another major difference between SN 2009dc and SN 2002cx is that emission from the Ca II near-IR triplet is weaker in SN 2009dc and has a complex profile with multiple peaks, even though the Ca II H&K features are similar in strength. A SYNOW fit indicates that we are actually resolving the individual components of the Ca II near-IR triplet along with shallow absorption possibly from Mg I and another, unidentified ion. The Ca II and Mg I features are blueshifted by $\sim$6000 km s^{-1}, which matches fairly well with our previously calculated post-maximum expansion velocities (see §5.3.4). Thus, it seems that the complex structure seen in our post-maximum spectra of SN 2009dc near 8600 Å is a mixture of the Ca II near-IR triplet, Mg I, and probably another ion whose identity we are unable to definitively determine.

9 Months After Maximum

On 2010 Feb. 6.6 (281 d after maximum), we obtained our final spectrum of SN 2009dc, shown in Figure 5.12 along with late-time spectra of the normal Type Ia SN 1998bu (Jha et al. 2006a), SN 2006gz (Maeda et al. 2009), another normal Type Ia SN 1990N (Gómez & López 1998, via the online SUSPECT database[5]), and SN 2002cx (Jha et al. 2006a).

At over 9 months past maximum light, SN 2009dc appears to have completely transitioned to the nebular phase. The SN ejecta are now optically thin and the spectrum shows various emission features. The broad peaks in the range 3800–5500 Å are usually attributed to blends of various features from [Fe II] and [Fe III] (e.g., Mazzali et al. 1998). These blends appear slightly weaker in SN 2009dc as compared to the normal Type Ia SNe 1998bu and

[5]http://suspect.nhn.ou.edu/$\sim$suspect

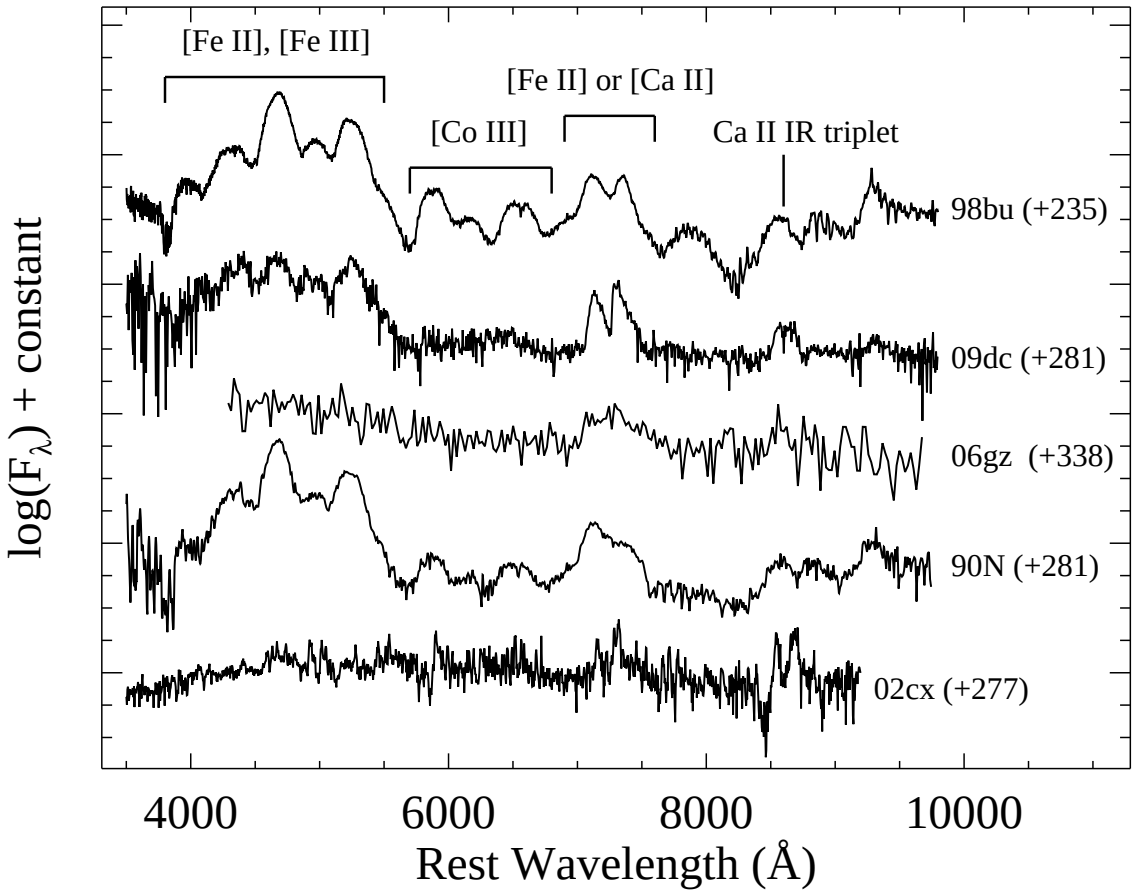

Figure 5.12: Our spectrum of SN 2009dc about 281 d past maximum, and a few comparison SNe with days relative to maximum light indicated for each spectrum (in parentheses). The spectra from top to bottom are the normal Type Ia SN 1998bu (Jha et al. 2006a), SN 2009dc, SN 2006gz (Maeda et al. 2009), SN 1990N (via SUSPECT), and the peculiar Type Ia SN 2002cx (Jha et al. 2006a). Major spectral features are labelled. All spectra have had their host-galaxy recession velocities removed and have been dereddened according to the values presented in their respective references.

1990N at similar epochs. Interestingly, Maeda et al. (2009) found that SN 2006gz completely lacks these features, though their spectrum has a low S/N.

The Ca II near-IR triplet is detected in both of the normal SNe Ia presented in Figure 5.12 as well as in SN 2009dc and possibly SN 2006gz (though the spectrum is noisy at these wavelengths). There is essentially no emission in either SN 2009dc or SN 2006gz from ∼5700 Å to ∼6800 Å, a region in which [Co III] emission has been identified in normal SNe Ia (Kuchner et al. 1994; Ruiz-Lapuente et al. 1995). The ratio of emission from the strongest [Fe III] feature (4589–4805 Å) to emission from the strongest [Co III] feature (5801–5995 Å) has been measured in a handful of SNe Ia at late times; it increases with both phase relative to maximum and ejecta temperature (Kuchner et al. 1994).

Using our spectra of SNe 1998bu and 1990N shown in Figure 5.12, we calculate ratios of about 5.6 and 7.7, respectively. These fit nicely with the other data displayed in Figure 2 of Kuchner et al. (1994). However, it is nearly impossible to calculate this ratio for SN 2009dc and SN 2006gz, since they appear to lack almost any putative cobalt emission at this epoch (and the cobalt and iron lines in spectra at earlier epochs are still significantly blended). We attempt to measure the tiny amount of [Co III] emission above the background level from 5801 Å to 5995 Å and calculate a Fe/Co ratio of about 27. This value, which is likely an underestimate, is already well above that of any other SN Ia at this phase presented by Kuchner et al. (1994). It is also above the dotted lines in Figure 2 of Kuchner et al. (1994), implying that the ejecta temperature of SN 2009dc may be $\gtrsim 10,000$ K. Even though this is broadly consistent with our relatively large value of 20,000 K for the blackbody temperature of SN 2009dc before maximum (§5.3.3), 10,000 K is extremely hot for a normal SN Ia 9 months past maximum brightness and the shape of the spectrum at this epoch does not seem to support such a high temperature.

The most well-defined spectral feature in our day 281 spectrum of SN 2009dc is the broad, double-peaked line centered near 7200 Å, which was also the strongest feature detected in a spectrum of SN 2006gz from 338 d past maximum (Maeda et al. 2009). In late-time spectra of SNe Ia this is attributed to blends of various [Fe II] lines, whereas in core-collapse SNe it is associated with [Ca II] $\lambda\lambda$7291, 7324, though in a late-time spectrum of SN 2006gz it has been suggested that the feature is due to a combination of both [Fe II] and [Ca II] lines (Maeda et al. 2009). The shape of the profile in SN 2009dc matches roughly that of SN 1998bu (though the central dip in SN 2009dc is deeper), but differs somewhat significantly from that of SN 1990N. Shapes similar to the one seen in SN 2009dc have, however, been seen by Maeda et al. (2009), who present synthetic late-time spectra of SNe Ia. Their models with more massive progenitors seem to lead to the feature near 7200 Å becoming strong relative to the complex of lines in the range 3800–5500 Å, as seen in SN 2009dc.

SN 2009dc and SN 2002cx-Like Objects

As already mentioned numerous times, SN 2009dc shares some interesting properties with both SN 2002cx and SN 2005hk, which are members of a class of peculiar SNe Ia

(Filippenko 2003; Li et al. 2003b; Jha et al. 2006a). These so-called "SN 2002cx-like" SNe are characterized by low expansion velocities and low peak luminosities, slow late-time declines in R, and Fe III features dominating early-time spectra (Jha et al. 2006a). Many of these criteria hold for SN 2009dc as well, but the very obvious difference is that the peak luminosity of SN 2009dc is much larger than average (see §5.4.1) while those of SN 2002cx-like objects are well below average.

In §5.3.1, we noted the absence of a prominent second maximum in the R and I-band light curves of SN 2009dc. This lack of a secondary maximum has been observed in SN 2002cx-like objects (Li et al. 2003b; Phillips et al. 2007). However, as seen in Figure 5.2, SN 2005hk (a SN 2002cx-like object) evolves much faster than SN 2009dc in all bands and proves to be a poor match photometrically. The color indices of SN 2009dc and SN 2005hk are again a poor match as shown in Figure 5.5.

Spectroscopically, SN 2009dc does not really resemble SN 2002cx-like objects before maximum (see Fig. 5.6), nor about 9 months after maximum (see Fig. 5.12). At these latest times, the spectrum of SN 2009dc consists of broad emission from forbidden iron lines while the spectrum of SN 2002cx is made up of many *narrow permitted* lines of Fe II, Na II, Ca II, and (tentatively) O I (Jha et al. 2006a). This is supported by the fact that the narrow spectral features of SN 2002cx do not simply appear to correspond to resolved versions of the blends seen in SN 2009dc.

Despite all of these differences, we have shown that at 1–2 months past maximum brightness the spectra of SN 2009dc and SN 2002cx are surprisingly similar. In Figure 5.9 we have combined the day 20 and 25 spectra of SN 2002cx from Li et al. (2003b) in order to improve the S/N and the wavelength coverage. Not only are the overall shapes of these two spectra nearly identical, but the width, strength, and existence of almost all of the individual spectral features match extremely well (with one significant exception, the Si II λ6355 absorption as mentioned in §5.3.4). Both objects, after being dereddened and deredshifted, appear to have an underlying blackbody continuum of about 5500 K (Branch et al. 2004).

About a month past maximum, Li et al. (2003b) and Branch et al. (2004) calculate expansion velocities of $\sim$5000–6000 km s^{-1} for SN 2002cx, and Phillips et al. (2007) determine expansion velocities in nearly the same range for SN 2005hk. For SN 2009dc we also derive velocities in this range for a few ions (O I, Ca II, Fe II, and Si II) with significant uncertainty since not only are many of these features blended, but the line identifications themselves are not definitive. These values also match well with the expansion velocity of $\sim$6000 km s^{-1} derived by Yamanaka et al. (2009) from their spectrum of SN 2009dc from 25 d past maximum.

Both Li et al. (2003b) and Branch et al. (2004) determine an expansion velocity for SN 2002cx at 56 d past maximum of $\sim$4700 km s^{-1} based on the Fe II λ4555 feature and a SYNOW fit. Phillips et al. (2007) calculate a slightly higher value of about 6000 km s^{-1} for SN 2005hk at 55 d past maximum (also using the Fe II λ4555 line). Based on this Fe II feature, we determine an expansion velocity of $\sim$5500 km s^{-1} for our spectra of SN 2009dc from 52 and 64 d past maximum. If we use the Si II λ6355 line, which is still present in

SN 2009dc but not seen in the SN 2002cx-like objects, we derive similar expansion velocities for both our day 52 and day 64 spectra. In general, it appears that the post-maximum expansion velocities of the spectral features of SN 2009dc are slightly greater than those seen in SN 2002cx by a few hundred km s^{-1} depending on the feature (Li et al. 2003b; Branch et al. 2004), whereas they are about equal to those of SN 2005hk (Phillips et al. 2007).

In conclusion, SN 2009dc and SN 2002cx-like objects have quite different photometric properties but are nearly identical spectroscopically *only* at 1–2 months past maximum brightness. The expansion velocity, the blackbody temperature, and the chemical composition match extremely well at these epochs, but the evolution of these observables from pre-maximum to nearly a year after maximum is quite different between SN 2009dc and SN 2002cx-like objects.

SN 2007if

In Figure 5.13 we present our late-time spectra of another possible SC SN Ia, SN 2007if. As noted earlier, the spectra of SN 2007if generally look similar to those of SN 2009dc, SN 2002cx, and even SN 2005cf at comparable epochs. The most significant spectral differences between SN 2007if and SN 2009dc are, as stated previously, that the expansion velocities seen in SN 2007if are ∼1000 km s^{-1} larger than those in SN 2009dc and SN 2002cx at comparable phases. This larger velocity is likely causing some of the medium-width features seen in SN 2009dc and SN 2002cx to be "smoothed out", and hence we do not detect many of these features in SN 2007if. It also has velocities which are smaller than those seen in SN 2005cf, but otherwise the spectra match well.

We have also stated previously that SN 2007if does not show the strong Si II λ6355 absorption after maximum that is visible in spectra of SN 2009dc (as well as in SN 2005cf). Unfortunately, our observations of SN 2007if do not extend to sufficiently long wavelengths for us to inspect whether the Ca II near-IR triplet of SN 2007if shows the complex structure seen in SN 2009dc.

The main aspects of the spectral evolution of SN 2007if over our three epochs is the disappearance of broad emission near 5500 Å and in the ranges 6700–7100 Å and possibly 7800–8100 Å (though our data are noisy in this second range of wavelengths). These match nearly exactly with the spectral features of SN 2009dc that were seen to decrease in strength over similar epochs.[6]

5.3.5 Reddening and Extinction

As mentioned above, we detect weak (but noticeable), narrow absorption from Na I D in all of our spectra of SN 2009dc, both at zero redshift and at the recession velocity of the

[6]The third wavelength range which possibly decreased in strength in SN 2009dc, 7800–8100 Å, is outside of our spectral coverage of SN 2007if.

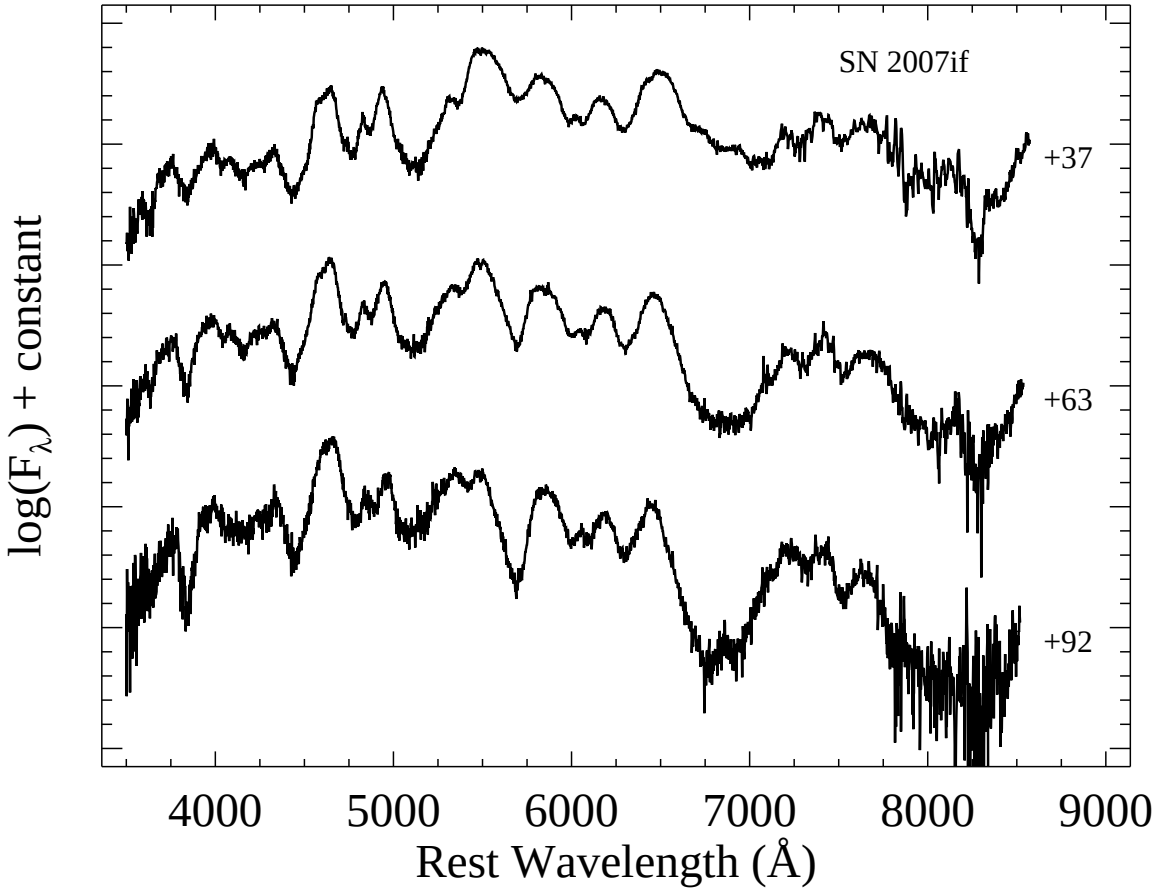

Figure 5.13: Our spectra of SN 2007if with days relative to maximum light indicated in each case. We have removed the host-galaxy recession velocity (cz = 22,200 ±250 km s^{-1}, Scalzo et al. 2010).

SN itself ($cz = 6300 \pm 300$ km s^{-1}). Even though there are clear notches in all of our spectra at the correct wavelengths for Na I D in the MW and in the host of SN 2009dc (UGC 10064), they are not broader than our spectral resolution.

We attempt to measure an EW of both absorption features in each of our observations, and we calculate average values of $\sim$0.7$\pm$0.1 Å for the MW and $\sim$1.0$\pm$0.1 Å for UGC 10064. These are close to the values of 0.7 Å and 1.2 Å reported by Marion et al. (2009) and 0.5 Å and 1.0 Å found by Tanaka et al. (2010).

There is some uncertainty in how exactly to convert the EW of Na I D absorption into extinction, but a few (mainly empirical) relations do exist (e.g., Barbon et al. 1990; Munari & Zwitter 1997; Turatto et al. 2003). Using these conversions, we determine a range of values for $E(B-V)$ both in the MW ($0.1 \lesssim E(B-V)_{\rm MW} \lesssim 0.18$ mag) and in UGC 10064 ($0.15 \lesssim E(B-V)_{\rm host} \lesssim 0.3$ mag).

For the extinction from the MW, we compare our calculated values of $E(B-V)$ to the value from the Galactic dust maps of Schlegel et al. (1998). Their maps give $E(B-V)_{\rm MW} = 0.070$ mag for the position of SN 2009dc, slightly lower than our range of values. However, since the accuracy of the Schlegel et al. (1998) dust maps is almost certainly higher than that of our EW measurements, we adopt $E(B-V)_{\rm MW} = 0.070$ mag for our analysis.

The extinction from UGC 10064 is a bit more complicated to determine accurately. If the Lira-Phillips relation holds for SN 2009dc, then we expect an extinction of $E(B-V)_{\rm host} \approx 0.26$ mag (see §5.3.2 for details on our application of the Lira-Phillips relation), which is within our range of values calculated from the spectra. Furthermore, if we assume that the EW of Na I D is directly proportional to $E(B-V)$, as Tanaka et al. (2010) do, then we derive $E(B-V)_{\rm host} \approx \left(1.0 \text{ Å}/0.7 \text{ Å}\right) \times 0.070 \approx 0.1$ mag. Taking into account all of these values, their uncertainties, and the method by which they were derived, we adopt $E(B-V)_{\rm host} = 0.1$ mag for our analysis, which is our lowest plausible, nonzero reddening. However, we note that the reddening could be as large as 0.3 mag.

5.3.6 Host-Galaxy Properties

SN 2009dc occurred $\sim$27″ away from the center of the S0 galaxy UGC 10064. We adopt the luminosity distance (d_L) as the distance to the SN, again assuming a ΛCDM Universe with $H_0 = 70$ km s^{-1} Mpc^{-1}, $\Omega_m = 0.27$, and $\Omega_\Lambda = 0.73$ (Spergel et al. 2007) and $z = 0.022 \pm 0.001$, where the redshift has been corrected for infall into the Virgo cluster and we have adopted an uncertainty of $cz = 300$ km s^{-1} to allow for a peculiar velocity induced by the gravitational interaction of neighboring galaxies. At $d_L = 97 \pm 7$ Mpc, SN 2009dc is a projected distance of $\sim$13 kpc from the center of UGC 10064. A useful galactic scale is the radius containing 50% of the flux (Petrosian 1976), which for UGC 10064 is about $4\farcs71 \pm 0\farcs21$ in the R band (Abazajian et al. 2009). This puts SN 2009dc about 5.7 Petrosian radii (in projection) from the center of its host. For comparison, SN 2003fg was found to be projected 0.9 kpc from the core of its low-mass star-forming host (Howell et al. 2006) and SN 2007if was discovered effectively directly on top of its low-mass and low-metallicity host

(Scalzo et al. 2010). The host of SN 2006gz is an Scd galaxy, and the SN was projected 14.4 kpc from the nucleus (Hicken et al. 2007), while SN 2004gu was projected 2.21 kpc from its host's nucleus (Monard et al. 2004). It seems that host-galaxy type and distance from the nucleus vary widely among candidate SC SN Ia (though the distance comparison is difficult given projection effects). However, SN 2003fg, SN 2007if, and possibly SN 2009dc (see below) were all associated with regions of recent star formation.

Wegner & Grogin (2008) inspected an optical spectrum of the core of UGC 10064 and derived an age of 4.0 ± 3.0 Gyr, a metallicity $[Z/\mathrm{H}] = 0.45 \pm 0.07$, and a chemical abundance $[\alpha/\mathrm{Fe}] = 0.13 \pm 0.09$. This value for metallicity is about 1σ above the average found for 26 S0/E void galaxies by Wegner & Grogin (2008), whereas the chemical abundance is just about the same as their average value. Optical spectra of the nucleus of UGC 10064 show no strong emission lines (Wegner & Grogin 2008; Abazajian et al. 2009), implying very little ongoing star formation ($\lesssim 0.2$ $\mathrm{M}_\odot$ yr^{-1}) in the core of the galaxy.

However, recent deep H I surveys of S0 galaxies have shown that the majority of non-cluster early-type galaxies contain substantial reservoirs (10^6–10^9 $\mathrm{M}_\odot$) of neutral gas that extend to large galactocentric radii (Morganti et al. 2006), whose morphology and kinematics suggest external origins. On the other hand, in the majority of these galaxies the column density of this gas is too low to support star formation at large radii, and thus the stellar populations throughout the galaxy are old.

Interestingly, in a fraction of the early-type galaxies rich in H I, a dynamical feature such as a prominent bar can create relatively dense ring-like accumulations of neutral gas at large radii (e.g., Schinnerer & Scoville 2002; Weijmans et al. 2008). In these regions of enhanced H I, low-level star formation ($\sim$0.1 $\mathrm{M}_\odot$ yr^{-1}) is observed (Jeong et al. 2007; Shapiro et al. 2010). Since SN 2009dc exploded in the outskirts of an S0 galaxy, it seems difficult to say with certainty whether SN 2009dc came from an old or young stellar population.

In the Supplementary Information of Howell et al. (2006), the age of the host galaxy of SN 2003fg is estimated to be $\sim$700 Myr (with significant uncertainty) and the star-formation rate to be $1.26^{+0.02}_{-1}$ $\mathrm{M}_\odot$ yr^{-1}, averaged over 0.5 Gyr. This star-formation rate is nearly an order of magnitude greater that the value derived by Wegner & Grogin (2008) for the core of UGC 10064 as well as the residual star-formation rate seen in rings of enhanced neutral gas at large galactocentric radii (Jeong et al. 2007; Shapiro et al. 2010). SC SNe Ia are expected to be found preferentially in young stellar populations (e.g., Howell et al. 2006; Chen & Li 2009, and references therein), but they are not necessarily restricted to them. If SC SNe Ia are the result of the merger of two degenerate objects, then the merger time-scale can be set by the emission of gravitational waves (e.g., Iben & Tutukov 1984). Depending on the particular orbital parameters of the binary, there may be a significant delay between the formation of the constituent degenerate objects and their eventual merger. Thus, SC SNe Ia *could* occur in older stellar populations.

Even though there is a significant difference between the average star-formation rates near the sites of SN 2009dc and SN 2003fg, there is still a possibility that they both come from relatively young stellar populations. As mentioned above, an age of $\sim$700 Myr was calculated

for the environment of SN 2003fg (Howell et al. 2006, Supplementary Information), while an age of ∼4.0 Gyr was calculated for the *core* of the host of SN 2009dc (Wegner & Grogin 2008). The fact that SN 2009dc is a few effective radii away from the nucleus of its host, coupled with the observations of low levels of residual star formation in other early-type galaxies at such galactocentric radii, imply that it is possible that SN 2009dc also came from a relatively small, but young, stellar population on the edge of UGC 10064, and that the age calculated for the core of the galaxy is not actually representative of the local environment of SN 2009dc.

Furthermore, in the SDSS Data Release 7, an extended, blue source appears 99.″3 (which is a projected distance of 43.6 kpc) to the northwest of UGC 10064 (Abazajian et al. 2009). This SBdm galaxy is known as SDSS J155108.42+254321.3 or UGC 10063 (de Vaucouleurs et al. 1991). *Swift*/UVOT images of the SN 2009dc field (shown in Fig. 5.14) indicate that UGC 10063 is significantly bluer than UGC 10064. The irregularly shaped UGC 10063 is barely visible in the KAIT R-band image to the northwest of SN 2009dc in Figure 5.1. Stacked UVOT images show that UGC 10063 increases in prominence in progressively bluer bands. As seen in Figure 5.14, UGC 10063 seems to have a tidal tail extending toward UGC 10064, pointed roughly at the site of SN 2009dc.

On 2010 Feb. 7 we obtained a spectrum of UGC 10063 using LRIS on the Keck I telescope (with a 1″-wide slit, a 600/4000 grism on the blue side, and a 400/8500 grating on the red side, resulting in FWHM resolutions of ∼4 Å and ∼6 Å, respectively). It has a blue continuum with few spectral features, but there is strong and narrow absorption from the Balmer series (though Hα is undetected). Strong Balmer lines and the lack of obvious emission lines are the hallmarks of so-called "post-starburst" galaxies in which vigorous star-formation activity ended between ∼50 Myr and 1.5 Gyr ago (Poggianti et al. 2009, and references therein). This is consistent with UGC 10063 being a SBdm galaxy (de Vaucouleurs et al. 1991). From the seven Balmer absorption lines marked in Figure 5.15, we calculate the redshift of UGC 10063 to be 0.021 ± 0.001, consistent with the redshift derived from the 21-cm H I line ($z = 0.02158 \pm 0.00003$, Schneider et al. 1990). This also exactly matches the redshift of UGC 10064 and SN 2009dc (as determined from narrow Ca II H&K absorption).

Based on the spectrum of UGC 10063 and its position relative to UGC 10064, we propose that these two galaxies had a close encounter in the relatively recent past. If UGC 10063 passed near the nucleus of UGC 10064, gas from UGC 10063 could have been stripped off and become gravitationally bound to UGC 10064 (which has been seen in both simulations and observations, e.g., Barnes & Hernquist 1991; Falcón-Barroso et al. 2004). This newly acquired gas (some of which could be at large galactocentric radii) would have likely undergone a burst of star formation soon after the two galaxies had their closest encounter (Mihos & Hernquist 1994; Barnes & Hernquist 1996), and this might be how and when the progenitor of SN 2009dc formed. Both SN 2007if and SN 2003fg were also found in hosts with recent star formation (Scalzo et al. 2010); in fact, SN 2003fg was discovered in a tidal feature (Howell et al. 2006) reminiscent of SN 2009dc and UGC 10063.

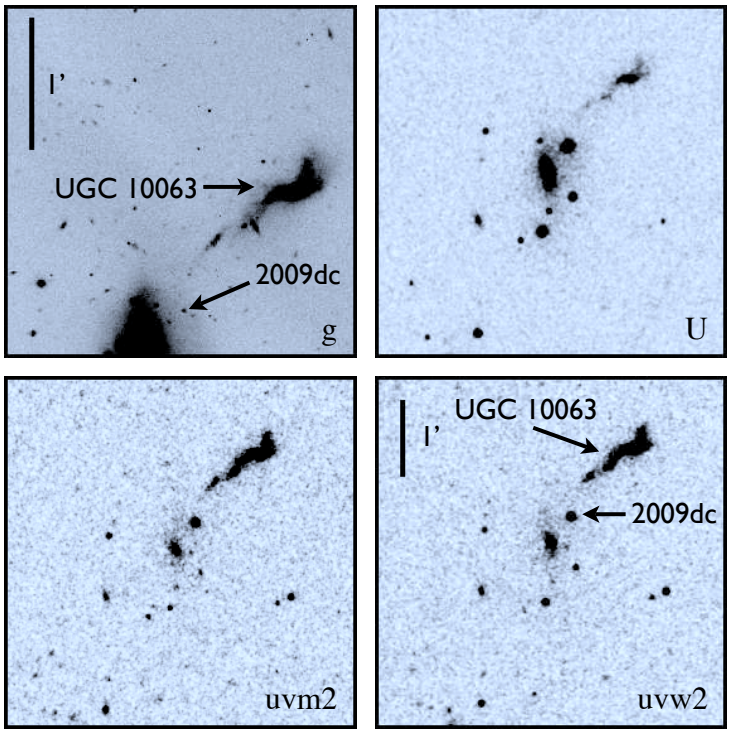

Figure 5.14: Keck g-band image and stacked UVOT U, $uvm2$, and $uvw2$ images of UGC 10063 (SDSS J155108.42+254321.3). UGC 10063 and SN 2009dc are labelled in the upper-left and lower-right panels. The upper-left panel is $2.69' \times 2.69'$, and the remaining panels are $4.67' \times 4.67'$; north is up and east is to the left in all four images. UGC 10063 increases in prominence in progressively bluer bands, and is much bluer than UGC 10064 (compare its appearance here with that in Fig. 5.1). It also seems to have a tidal tail extending toward UGC 10064, pointed roughly in the direction of the site of SN 2009dc.

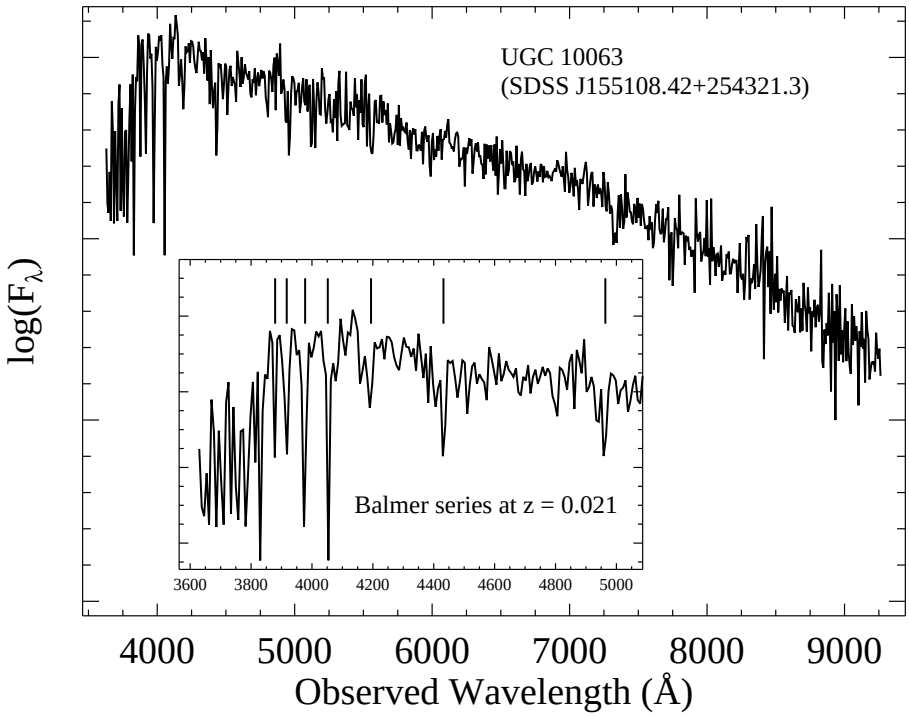

Figure 5.15: An optical spectrum of UGC 10063 (SDSS J155108.42+254321.3). The inset is a zoom-in of the full spectrum. Narrow Balmer-series absorption (Hβ through Hθ) is marked, and these features yield $z = 0.021 \pm 0.001$, equal to the redshift of UGC 10064 and SN 2009dc. Note that Hα is undetected at an expected wavelength of $\sim$6700 Å; perhaps Hα emission from residual H II regions fills in the absorption line.

5.4 Discussion

5.4.1 Bolometric Luminosity

To estimate the bolometric luminosity of SN 2009dc, we follow the method outlined by Howell et al. (2009). Using spectra of SN 2009dc presented here and spectra of the similar SC SN Ia candidate SN 2007if from Scalzo et al. (2010), we take each simultaneous epoch of *BVRI* photometry and warp the spectrum closest in phase to match the photometry using a smooth third-order spline. We then integrate the warped spectrum over wavelengths of 4000–8800 Å (i.e., from the blue edge of the *B*-band filter to the red edge of *I*-band filter.) We convert the flux into a luminosity using the luminosity distance ($d_L = 97 \pm 7$ Mpc) adopted in §5.3.6.

The above method will only give us the optical bolometric luminosity. To derive the total bolometric luminosity from UV to IR, we use bolometric corrections from Wang et al. (2009b), who found that *BVRI* only accounts for $\sim 60\%$ of the total luminosity in the case of SN 2005cf, a normal SN Ia. They also found that an additional 20% is emitted in the UV and *U* band, and the final 20% in the near-IR. We test to see if the tabulated corrections for the UV and *U* band are reasonable for SN 2009dc by first calculating the bolometric luminosity using optical and UV photometry at $t = 0$ d (using our optical ground-based photometry combined with UVOT photometry of SN 2009dc). We find that our results are consistent with a correction of 20%. Yamanaka et al. (2009) found that their near-IR data for SN 2009dc represented $\sim$20% of the bolometric luminosity. With this, we cautiously adopt a 40% correction for our bolometric luminosity using our well-sampled *BVRI* photometry. Overall, SN 2005cf is a much different SN than SN 2009dc, so we include a systematic uncertainty of 20% for our bolometric luminosity.

Figure 5.16 shows our final bolometric light curves for the various levels of host-galaxy extinction we have adopted throughout this chapter. We also plot the bolometric light curve of SN 2005cf for comparison.

If we use our fiducial nonzero value for the host-galaxy reddening, $E(B-V)_{\rm host} = 0.1$ mag, and our largest reasonable value for the host reddening, $E(B-V)_{\rm host} = 0.3$ mag, then we get $M_V = -20.16 \pm 0.1$ mag ($L_{\rm bol} = (3.3 \pm 0.6) \times 10^{43}$ erg s^{-1}) and $M_V = -20.82 \pm 0.10$ mag ($L_{\rm bol} = (7.3 \pm 1.0) \times 10^{43}$ erg s^{-1}), respectively. We note that assuming no host-galaxy extinction we find $M_V = -19.83 \pm 0.10$ mag ($L_{\rm bol} = (2.4 \pm 0.5) \times 10^{43}$ erg s^{-1}). A summary of these results can be found in Table 5.7. Our range of values of $L_{\rm bol}$ for SN 2009dc matches quite well that of Yamanaka et al. (2009): (2.1–3.3) $\times 10^{43}$ erg s^{-1}. The most significant difference between the two analyzes comes from using a different range of values for $E(B-V)_{\rm host}$ and R_V.

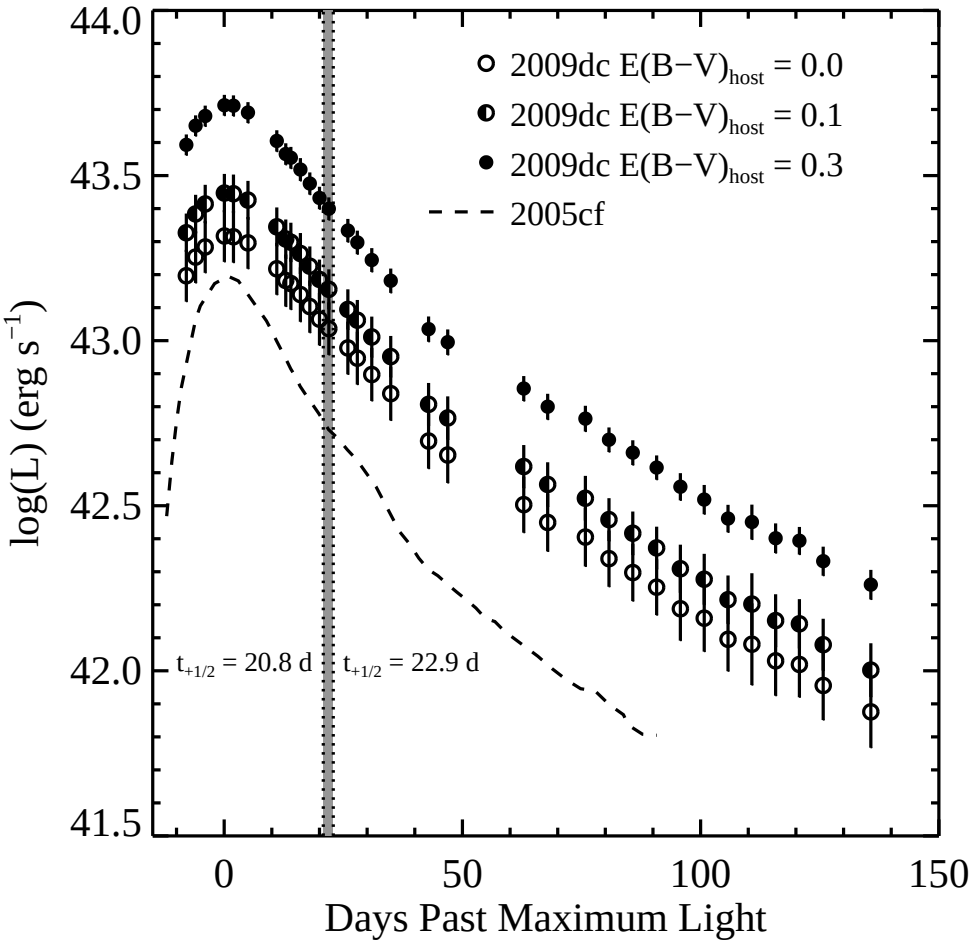

Figure 5.16: Bolometric light curve of SN 2009dc assuming various levels of extinction, in comparison with that of SN 2005cf. The curve plotted with empty circles assumes no host-galaxy extinction, the half-filled circles assume $E(B-V)_{\rm host} = 0.1$ mag with $R_V = 3.1$, and the filled circles assume $E(B-V)_{\rm host} = 0.3$ mag with $R_V = 3.1$. For comparison, we include the bolometric light curve of SN 2005cf as a dashed line (Wang et al. 2009b). We indicate our calculated range of values of $t_{+1/2}$ (i.e., the number of days after maximum bolometric luminosity when the bolometric luminosity has decreased to half its maximum value) for SN 2009dc within the shaded gray region bounded by dotted lines. The lower bound of $t_{+1/2} = 20.5$ d is calculated using a host reddening of $E(B-V)_{\rm host} = 0.3$ mag and the upper limit of $t_{+1/2} = 22.8$ d assumes no host-galaxy extinction.

Table 5.7: Bolometric Luminosity for Various Reddenings

$E(B-V)_{\rm host}$ (mag)	$L_{\rm bol,max}$ (10^{43} erg s^{-1})	$M_{V,\rm max}$ (mag)
0.0	2.4 ± 0.5	-19.83 ± 0.10
0.1	3.3 ± 0.6	-20.16 ± 0.10
0.3	7.3 ± 1.0	-20.82 ± 0.10

5.4.2 ^{56}Ni Masses and Energetics

^{56}Ni Masses from Arnett's Law

The vast majority of the bolometric luminosity of SNe Ia comes from the decay of ^{56}Ni to ^{56}Co (and subsequently the decay of ^{56}Co to ^{56}Fe), so we can calculate how much ^{56}Ni was created in SN 2009dc by using "Arnett's law", which asserts that the luminosity of a SN Ia at maximum light is proportional to the instantaneous rate of radioactive decay of ^{56}Ni (e.g., Arnett 1982; Stritzinger & Leibundgut 2005). Arnett's law is often written

$$M_{\rm Ni} = \frac{L_{\rm bol}}{\alpha \dot{S}(t_R)}, \tag{5.1}$$

where $M_{\rm Ni}$ is the mass of ^{56}Ni present in the ejecta, $L_{\rm bol}$ is the bolometric luminosity at maximum light, α is the ratio of bolometric to radioactive luminosities (which is of order unity), and $\dot{S}(t_R)$ is the radioactive luminosity per mass of ^{56}Ni as a function of the rise time, t_R.

For SN 2009dc, we have tight constraints on the rise time from our photometric data and, as described in §5.3.1, we find a value of 23 ± 2 d. Substituting this into the equation for $\dot{S}(t_R)$ from Stritzinger & Leibundgut (2005), we get $\dot{S}(t_R) \approx (1.65 \pm 0.13) \times 10^{43}$ erg s^{-1} M$_\odot{}^{-1}$. Stritzinger & Leibundgut (2005) find $\alpha = 1.2 \pm 0.2$, which we use for our analysis, though we note that this is an upper limit (which leads to a lower limit on the ^{56}Ni mass) since any ^{56}Ni that is *above* the photosphere will not contribute to the SN luminosity.

Using these values, along with our most likely estimate of the bolometric luminosity mentioned above, we calculate that SN 2009dc synthesised about 1.7 ± 0.4 M$_\odot$ of ^{56}Ni. If we adopt the bolometric luminosity assuming no host-galaxy reddening and our largest reasonable host-galaxy reddening, along with our calculated rise time and $\alpha = 1.2$, we get $\sim$1.2 M$_\odot$ and $\sim$3.7 M$_\odot$ of ^{56}Ni, respectively.

^{56}Ni Masses from Late-Time Photometry

The detection of SN 2009dc in late-time images at levels similar to those of normal SNe Ia offers a stark contrast to SN 2006gz, another SC SN Ia candidate. Late-time photometry obtained by Maeda et al. (2009) $\sim$360 d after maximum found that SN 2006gz had faded

significantly faster than normal SNe Ia, casting doubt on the amount of ^{56}Ni synthesised in the explosion. The authors constrain $M_{\rm Ni} \lesssim 0.3$ M$_\odot$ assuming that the positrons are nearly completely trapped in the ejecta. This is at odds with the $\sim$1 M$_\odot$ of ^{56}Ni calculated to power the light curve at early times (Hicken et al. 2007).[7] To reconcile this difference in nickel mass, it was suggested that perhaps SN 2006gz was a highly asymmetric explosion, and due to the exact viewing angle more ^{56}Ni was inferred at early times than was actually present (Maeda et al. 2009). However, SN 2009dc appears to be spherically symmetric at early times (Tanaka et al. 2010). Furthermore, Maeda et al. (2009) posit that dust might have formed in the ejecta of SN 2006gz by this time, which would reprocess much of the optical light to longer wavelengths. However, we do not see strong evidence for dust formation in SN 2009dc since the spectral features all appear to evolve symmetrically.

To constrain the nickel mass produced by SN 2009dc from late-time photometry, we write out the SN luminosity as a function of time (e.g., Clocchiatti & Wheeler 1997; Maeda et al. 2003, 2009),

$$L(t) = M_{\rm Ni} \left(\varepsilon_\gamma (1 - e^{-\tau(t)}) + f_{\rm e^+} \varepsilon_{\rm e^+}\right) e^{-t/111.3}, \tag{5.2}$$

where t is the number of days from the explosion date, $M_{\rm Ni}$ is the initial amount of ^{56}Ni synthesised, $\varepsilon_\gamma = 6.8 \times 10^9$ erg s^{-1} g^{-1}, $\tau(t)$ is the time-dependent optical depth to γ-rays, $f_{\rm e^+}$ is the fraction of positrons trapped in the ejecta, $\varepsilon_{\rm e^+} = 2.4 \times 10^8$ erg s^{-1} g^{-1}, and 111.3 d is the e-folding time of ^{56}Co decay. Evaluating $\tau(t)$ requires defining a model with estimates for the kinetic energy of the explosion and the total mass of the white dwarf.

We can place constraints on the ^{56}Ni mass by only considering the luminosity powered by the trapped positrons; to do this we set $\tau(t) = 0$ in Eqn. (5.2). Using only the optical contribution to the bolometric luminosity over the range 4000–8000 Å from our Keck data taken 281 d past maximum (which is 304 d after explosion), we calculate the ^{56}Ni mass for a number of reddening and $f_{\rm e^+}$ values which can be found in Table 5.8. Our calculation of the bolometric luminosity does not include a bolometric correction for any possible contribution to the bolometric luminosity in the NIR. For our nominal values of $E(B-V)_{\rm host} = 0.1$ mag, $R_V = 3.1$, and $f_{\rm e^+} = 1$, we calculate a ^{56}Ni mass of 1.4 ± 0.3 M$_\odot$, consistent with the ^{56}Ni mass derived from Arnett's law and our data at $B_{\rm max}$ (§5.4.2).

We also determine the ^{56}Ni mass using our epoch of photometry from 403 d past maximum (which is 426 d after explosion). However, without a spectrum to model the spectral energy distribution at this phase, we had to use our last spectrum taken 281 d past $B_{\rm max}$, which could lead to an inaccurate measure of the bolometric luminosity. Furthermore, the detection of the SN was marginal in all bands. Using our nominal values of $E(B-V)_{\rm host} = 0.1$ mag, $R_V = 3.1$, and $f_{\rm e^+} = 1$, we calculate a ^{56}Ni mass of 0.34 ± 0.06 M$_\odot$, clearly much lower than previous estimates of the ^{56}Ni mass. We summarise ^{56}Ni masses for a range of parameters in Table 5.8.

The drop in derived ^{56}Ni mass and expected luminosity could indicate the formation of dust between $t = 281$ and 426 d past maximum light, although this cannot be substantiated

[7] Note that this value was derived by assuming a high value for the host-galaxy reddening of SN 2006gz, which might have been an overestimate.

Table 5.8: Ni Mass Estimates from Late-Time Photometry

Days past Explosion	f_{e^+}	$E(B-V)_{host}$ (mag)	L^a_{bol} (10^{40} erg s^{-1})	^{56}Ni ($M_\odot$)
304	0.75	0	3.1 ± 0.7	1.4 ± 0.3
304	1	0	3.1 ± 0.7	1.0 ± 0.2
304	0.75	0.1	4.2 ± 0.8	1.8 ± 0.3
304	1	0.1	4.2 ± 0.8	1.4 ± 0.3
304	0.75	0.3	7.9 ± 1.5	3.4 ± 0.6
304	1	0.3	7.9 ± 1.5	2.5 ± 0.6
426	0.75	0	0.26 ± 0.05	0.33 ± 0.06
426	1	0	0.26 ± 0.05	0.25 ± 0.05
426	0.75	0.1	0.35 ± 0.07	0.45 ± 0.08
426	1	0.1	0.35 ± 0.07	0.34 ± 0.06
426	0.75	0.3	0.64 ± 0.12	0.82 ± 0.15
426	1	0.3	0.64 ± 0.12	0.62 ± 0.12

[a]Bolometric luminosity only contains contribution over the range 4000–8800 Å.

without IR data or a relatively high-S/N spectrum. The unexpected drop could also be an indication that the positron trapping fraction at this phase is significantly lower than the nominal value of $f_{e^+} = 1$. To produce the $\sim$1.4 $M_\odot$ of ^{56}Ni found using our photometry from 281 d past maximum, we would need $f_{e^+} \approx 0.25$. SN 2009dc could have undergone an "IR catastrophe" which would cause most of the emission to escape at IR wavelengths (as opposed to the optical; Axelrod 1988) as the temperature of the SN cools to $\sim$1000 K. This would require using a bolometric correction to our derived optical bolometric luminosity. Alternatively, the low derived ^{56}Ni mass could suggest that the late-time light curve of SN 2009dc is not powered by the decay of ^{56}Co. This conclusion, however, is at odds with the ^{56}Ni mass derived from our epoch of photometry from $t = 281$ d past maximum light. Without near-IR data or a spectrum at this epoch, it is difficult to reconcile these differences. We again caution that the spectral energy distribution is ill constrained at this phase.

WD Masses and Kinetic Energies

Using the technique developed by Howell et al. (2006), we attempt to combine our observations of SN 2009dc with properties of WDs and SNe Ia in order to calculate the mass of the progenitor WD as well as the amount of ^{56}Ni produced in the explosion. We note that this method is independent of the one used in the previous section which utilitized the late-time photometry of SN 2009dc. As will be mentioned below, there are a few assumptions and simplifications that go into this analysis, and thus the final values should probably not be

taken literally. However, the sense of the relationships and trends these calculations indicate should be reliable and will show that SN 2009dc likely had a SC WD progenitor.

The ejecta of SNe Ia derive their kinetic energy (E_K) from the energy released during explosive nucleosynthesis (E_n), but the ejecta must first overcome the binding energy (E_b) of the WD progenitor (Branch 1992). Therefore, we can write

$$E_K = \frac{M_{\rm WD} v^2}{2} = E_n - E_b, \tag{5.3}$$

where $M_{\rm WD}$ is the mass of the WD just before explosion and v is a representative velocity of the ejecta. A single value for velocity only relates to the kinetic energy of the SN averaged over the entire ejecta, and thus there has been disagreement as to which actual value should be used for a given SN. Previous studies have used the velocity of the Si II λ6355 feature at 10 and 40 d past maximum (Benetti et al. 2005; Howell et al. 2006).

Since about 70% of IGEs produced in SNe Ia are in the form of ^{56}Ni (Nomoto et al. 1984; Khokhlov et al. 1993), the total mass of the WD can be related to the nickel mass by

$$M_{\rm Ni} = 0.7 M_{\rm WD} f_{\rm IGE}, \tag{5.4}$$

where $f_{\rm IGE}$ is the fractional composition of IGEs in the SN ejecta. However, the exact amount of IGEs that are made up of ^{56}Ni may not be the same for all SNe Ia and likely dependent on other, external factors such as metallicity (e.g., Howell et al. 2009, and references therein).

Furthermore, Branch (1992) found that fusing equal parts carbon and oxygen all the way to iron yields $\varepsilon_{\rm Fe} = 1.55 \times 10^{51}$ erg ${\rm M}_\odot^{-1}$, and burning the same material only up to silicon liberates about 76% of that energy. Thus we can write

$$E_n = \varepsilon_{\rm Fe} M_{\rm WD} \left(f_{\rm IGE} + 0.76 f_{\rm IME} \right), \tag{5.5}$$

where $f_{\rm IME}$ is the fractional composition of IMEs in the ejecta.

Finally, we define the fractional composition of unburned carbon in the SN ejecta as $f_{\rm C}$.[8] Based on our definitions we can write

$$1 = f_{\rm C} + f_{\rm IME} + f_{\rm IGE}. \tag{5.6}$$

Putting all of this together, we relate various properties of the progenitor WD to properties of the SN ejecta it created using

$$v^2 \approx 2\varepsilon_{\rm Fe} \left(\frac{0.34 M_{\rm Ni}}{M_{\rm WD}} - 0.76 f_{\rm C} + 0.76 \right) - \frac{2E_b}{M_{\rm WD}}. \tag{5.7}$$

However, given the assumptions and simplifications that went into this "equation", we stress that it should be used more as an illustration of how the different parameters relate to each other and less as a tool to actually calculate WD and ^{56}Ni masses.

[8] This parameter does not appear in the equation for E_n; it represents the amount of *unburned* material, and thus does not contribute to the energy released by nucleosynthesis.

Values of E_b range from about 0.5×10^{51} erg for a WD with a mass of 1.4 $M_\odot$ to about 1.3×10^{51} erg for a WD with a mass of 2 $M_\odot$ and a central density of 4×10^9 g cm^{-3} (Yoon & Langer 2005). We perform separate calculations for each pair of these values of E_b and $M_{\rm WD}$. Tanaka et al. (2010) measure the Si II λ6355 feature to be blueshifted by 7200 km s^{-1} in their spectrum of SN 2009dc obtained 6 d past maximum, while we find the same feature to be blueshifted by 5000–6000 km s^{-1} in our spectra taken 35, 52, and 64 d past maximum. Since v has been evaluated at 10 and 40 d past maximum for similar analyzes previously (Benetti et al. 2005; Howell et al. 2006), we will use a range of velocities from 7000 km s^{-1} to 5500 km s^{-1} for our analysis. Finally, since there is clear indication of unburned material in the ejecta of SN 2009dc (see §5.3.3), we know that $f_{\rm C}$ must be nonzero. However, based on models of SN Ia ejecta (e.g., Nomoto et al. 1984) and the relative scarcity of carbon detections in SNe Ia (Marion et al. 2006; Thomas et al. 2007), we will only use values in the range 0.05–0.3 for $f_{\rm C}$.

With such large uncertainties and so many parameters, we will clearly calculate a huge range of ^{56}Ni masses, and we realize that a few assumptions and model-dependent values have come into the derivation. However, this is still a useful line of reasoning in our attempt to determine both the mass of the WD progenitor and the amount of ^{56}Ni synthesised by SN 2009dc. We therefore forge ahead and attempt to eliminate at least some of the most extreme situations.

Almost all of parameter space is ruled out when we use a 1.4 $M_\odot$ WD (and its associated binding energy), since we calculate negative nickel masses for these cases. The largest ^{56}Ni mass we can reasonably derive for a 1.4 $M_\odot$ WD (using $f_{\rm C} = 0.3$ and $v = 7000$ km s^{-1}) is 0.06 $M_\odot$, nearly an order of magnitude smaller than the amount of nickel produced by a normal SN Ia (e.g., Nomoto et al. 1984; Kasen et al. 2008). We have also shown that SN 2009dc is much more luminous than the average SN Ia. Therefore, if it did have a 1.4 $M_\odot$ progenitor, then we would need to invoke a large, hitherto unknown energy source to power its light curve, which seems highly unlikely.

The situation changes when we use a 2 $M_\odot$ WD (with a central density of 4×10^9 g cm^{-3}), put forth as a possible SC SN Ia progenitor by Yoon & Langer (2005). Again, a significant part of parameter space is eliminated, since at low values of $f_{\rm C}$ we calculate negative (or extremely small) nickel masses. Assuming that $f_{\rm IME}$ must be $\gtrsim 0.1$ (given that we detect IMEs in the spectra for months after maximum; see, e.g., Nomoto et al. 1984), we calculate nickel masses as high as $\sim$1 $M_\odot$. In order to match our nominal ^{56}Ni mass range of 1.4–1.7 $M_\odot$ *and* satisfy our constraints on the fractional composition of elements mentioned previously, we must resort to using a WD progenitor more massive than 2 $M_\odot$.

Again, the final values calculated above are almost certainly not the true answer. However, the range of plausible values presented, as well as the relationships between the parameters of the SN and its WD progenitor, yet again indicate that the progenitor of SN 2009dc was likely a SC WD.

The various analyzes presented above seem to strongly favor the conclusion that the progenitor of SN 2009dc was a SC WD with a mass of probably greater than $\sim$2 $M_\odot$. These

analyzes also indicate that SN 2009dc most likely produced 1.4–1.7 $M_\odot$ of ^{56}Ni (assuming our nominal value for the host-galaxy reddening and our peak bolometric luminosity). More than 1 $M_\odot$ of ^{56}Ni was almost certainly created by SN 2009dc, and the actual value *could* be as high as $\sim$3.3 $M_\odot$. This matches well with the conclusions of Yamanaka et al. (2009), who calculate a similar range of nickel masses for SN 2009dc (1.2–1.8 $M_\odot$). Part of the difference can be accounted for by the fact that the two studies use different values of host-galaxy reddening (causing the derived bolometric luminosities to differ somewhat; see §5.4.1). However, the majority of the difference in derived ^{56}Ni masses comes from the assumed rise time of SN 2009dc. Yamanaka et al. (2009) adopt a rise time of 20 d based on comparisons to typical SNe Ia and SN 2006gz, while we use a rise time of 23 d based on our pre-maximum photometry. The longer rise time used in this chapter leads to a larger derived nickel mass for SN 2009dc.

SN 2003fg had a derived progenitor mass of $\sim$2.1 $M_\odot$ and produced $\sim$1.3 $M_\odot$ of ^{56}Ni (Howell et al. 2006), and these values are quite similar to those we calculate for SN 2009dc. SN 2006gz was estimated to have produced 1–1.2 $M_\odot$ of ^{56}Ni, which is on the low end of our range for SN 2009dc, and it was also claimed to have a SC WD progenitor (though no attempt was made to further constrain the progenitor mass; Hicken et al. 2007).

5.4.3 Comparison to Theoretical Models

Any theoretical model which is postulated to explain SN 2009dc, with or without a SC WD, *must* be able to reproduce the observed peculiarities for which we have very tight constraints: (*a*) high luminosity even when assuming no host-galaxy reddening, (*b*) relatively long light-curve rise time, (*c*) relatively slow photometric decline and late-time spectroscopic evolution, (*d*) the presence of carbon in spectra near maximum brightness, (*e*) the presence of silicon in spectra as late as a few months past maximum brightness, (*f*) IGEs dominating the spectra at late times, and (*g*) mostly spherically symmetric ejecta near maximum with possible clumpy layers of IMEs (Tanaka et al. 2010).

Below we consider both SC and non-SC models, all of which involve the thermonuclear explosion of a WD. However, the similarities between SN 2009dc and SN 2002cx and its brethren (see §5.3.4) may argue that the progenitor and explosion scenario for these objects are all linked. Could SN 2009dc be a SN 2002cx-like object but with a much higher luminosity? Perhaps, although attempts to explain the origins of even the best-observed SN 2002cx-like objects are still ongoing (e.g., Jha et al. 2006a; Phillips et al. 2007; Valenti et al. 2009).

SC Models

Two- and three-dimensional models of differentially rotating massive WDs have been presented in the literature, and calculations show that SC WDs with masses as large as 2 $M_\odot$ are possible by accretion from a nondegenerate companion, while masses up to $\sim$ 1.5 $M_\odot$ are possible from a double-degenerate merger (Yoon & Langer 2005; Yoon et al. 2007,

respectively). More recent studies of double-degenerate mergers have even shown possible SN Ia progenitors with total masses approaching 2.4 $M_\odot$ (Greggio 2010). This is encouraging for the case of SN 2009dc, since our energetics arguments imply that its progenitor is likely greater than $\sim$2 $M_\odot$. However, calculations by Piro (2008) suggest that differential rotation is unlikely for WDs accreting from a nondegenerate companion, and thus their masses cannot exceed the Chandrasekhar mass by more than a few percent.

Yoon & Langer (2005) also consider how much ^{56}Ni would be produced by a SN Ia whose progenitor is $\sim$2 $M_\odot$, calculating values of 0.4–1.3 $M_\odot$. This large range does encompass the lower end of our range of ^{56}Ni for SN 2009dc. However, only specific kinetic energies (i.e., kinetic energies per unit mass) which are lower than what we find for SN 2009dc by a factor of $\sim$2 were used (Yoon & Langer 2005). Adopting lower specific kinetic energies will tend to decrease the nickel yield for a given WD mass, according to their models. It is possible that increasing the specific kinetic energies used in the models of Yoon & Langer (2005) to values that better match SN 2009dc will in fact reproduce our derived nickel mass, but this may require pushing the models into regimes where they are no longer valid.

Pfannes et al. (2010) use aspects of the WD models of Yoon & Langer (2005) and simulate prompt detonations of massive, rapidly rotating WDs. None of their models appears to reproduce the fact that we detect unburned fuel (i.e., carbon) and IMEs near maximum brightness at low velocities, and subsequently IMEs and IGEs at later times (also at low velocities). Even more at odds with SN 2009dc, Pfannes et al. (2010) predict that the IMEs and unburned material should have similar spatial distributions in the ejecta (specifically, in a torus in the equatorial plane), but this seems unlikely given the strong line polarizations seen by Tanaka et al. (2010) in Si II and Ca II features and the lack thereof in two different C II features. Thus, we conclude that the models of Pfannes et al. (2010) do not seem to reproduce the observations of SN 2009dc.

Models of SC WDs and their evolution in close binary systems with nondegenerate companions can also be found in the literature (Chen & Li 2009). These evolutionary calculations include the effects of varying the orbital period of the binary systems, the metallicity and mass-transfer rate of the binary companion, and (most importantly) the mass of the WD. Chen & Li (2009) find that WDs with initial masses of $\sim$1.2 $M_\odot$, under the right mass-transfer conditions, can accrete up to masses of about 1.4–1.8 $M_\odot$ before exploding as a SN Ia (though they find that most of these WDs explode with masses not much above 1.4 $M_\odot$). Thus it seems somewhat unlikely that these models can explain the progenitor we suggest for SN 2009dc; even if the occasional WD *can* accrete up to 1.8 $M_\odot$, this is at the lowest end of our range of WD progenitor masses.

Spherically symmetric, one-dimensional radiation transport calculations for normal and SC WDs have been carried out by Maeda & Iwamoto (2009). They find that based on the light-curve shapes, photospheric velocities, peak bolometric luminosities, and peak effective temperatures, SN 2006gz likely came from a SC WD[9] while SN 2003fg did not. Since

[9]Maeda & Iwamoto (2009) claim that most of the emission likely shifted to the near-IR and mid-IR at late times in order to explain the relatively faint late-time observations of Maeda et al. (2009).

the observables of SN 2003fg used for their analysis have very similar values to those of SN 2009dc, it would seem that their models imply that SN 2009dc is also not a SC SN Ia. Maeda & Iwamoto (2009) point out that SN 2003fg (and thus probably SN 2009dc as well) could be a SC SN Ia if the progenitor star were highly aspherical, but again this seems unlikely for SN 2009dc from the spectropolarimetric data (Tanaka et al. 2010).

The primary independent variable used in the calculations of Maeda & Iwamoto (2009) is $t_{+1/2}$, the number of days after maximum bolometric luminosity when the bolometric luminosity has decreased to half its maximum value (Contardo et al. 2000). For SN 2006gz they measure $t_{+1/2} = 18$ d from the publicly available photometry, but for SN 2003fg they convert the stretch value published by Howell et al. (2006) to Δm_{15} and then to a $t_{+1/2}$ value of 13.5 d (adopting an empirical linear fit to Δm_{15} and $t_{+1/2}$ values from Contardo et al. 2000). Using their conversions between Δm_{15} and $t_{+1/2}$, we calculate $t_{+1/2} \approx 14$ d (which, unsurprisingly, is nearly the same as the value calculated for SN 2003fg by Maeda & Iwamoto 2009). However, when we measure $t_{+1/2}$ directly from our light curve, we get a minimum value of about 20.5 d (when we use our maximum plausible host-galaxy reddening), which is nearly 50% larger! Furthermore, if one converts the Δm_{15} value of SN 2006gz to $t_{+1/2}$ using the linear fit, one again finds $t_{+1/2} \approx 14$ d, suggesting that the linear conversion derived by Maeda & Iwamoto (2009) is not accurate for such low values of Δm_{15}. This is not wholly unexpected since the Δm_{15} values of SNe 2006gz, 2003fg, and 2009dc (or $t_{+1/2}$ as measured from light curves) are all below (or above) the values used to derive the linear fit (Contardo et al. 2000). In addition, the conversion from stretch to Δm_{15} used by Maeda & Iwamoto (2009) for SN 2003fg did not take into account the fact that the definition of stretch has evolved as new SN Ia light-curve templates have been constructed (e.g., Conley et al. 2008).

We can now compare SN 2009dc to the analysis of Maeda & Iwamoto (2009) using the actual values of $t_{+1/2} \approx 20.5$–22.8 d. Given the large bolometric luminosity and $t_{+1/2}$ value, as well as the extremely low photospheric velocity of SN 2009dc, none of their models (using normal or SC WDs) appears to be viable. Their "normal WD" model with $M_{\rm WD} = 1.39$ M$_\odot$ and $M_{\rm Ni} = 0.6$ M$_\odot$ accounts for the low velocity with large $t_{+1/2}$, but it underpredicts $L_{\rm bol}$ by a factor of a few. Some of the SC WD models ($M_{\rm WD} \geq 2.0$ M$_\odot$ and $M_{\rm Ni} = 1.0$ M$_\odot$) of Maeda & Iwamoto (2009) can almost account for the large values of $L_{\rm bol}$ and $t_{+1/2}$ seen in SN 2009dc, but they then overpredict the photospheric velocity of SN 2009dc by a factor of 2 or so (with the models having the highest mass WDs coming the closest to matching the observed velocities).

While no single model of Maeda & Iwamoto (2009) clearly reproduces our observations of SN 2009dc, its properties seem to be on the outskirts of the parameter space explored by their analysis. This hints at the possibility that more extreme WD and ^{56}Ni masses may be required to match the observational data of SN 2009dc. In addition, it is possible that *multi-dimensional* analyzes are required to truly capture the underlying physics of a SC WD explosion.

Furthermore, a few synthetic late-time spectra of SC SNe Ia have been presented in the literature (e.g., Maeda et al. 2009). Their models take as inputs a WD progenitor mass, a

WD central density, and mass fractions of burning products, and then use a one-dimensional Monte Carlo radiation transport code, along with ionization/recombination equilibrium and rate equations, to calculate synthetic light curves and spectra. Both of their SC SN Ia models roughly match our SN 2009dc photometry. In addition, their late-time spectra are similar to our day 281 spectrum of SN 2009dc. Maeda et al. (2009) note that as they increase their models' progenitor mass, the [Fe II]/[Ca II] feature near 7200 Å becomes stronger relative to the blends of [Fe II] and [Fe III] near 3800–5500 Å. This is seen in SN 2009dc (as compared to SNe Ia with more normal peak luminosity), and it further supports our finding that the progenitor of SN 2009dc was a SC WD. However, it should be noted that the SC SN Ia models of Maeda et al. (2009) only use WDs with masses of 2 and 3 $M_\odot$, and ^{56}Ni masses of only 1 $M_\odot$, which is on the low end of our range of calculated values for the ^{56}Ni yield of SN 2009dc.

Non-SC Models

A number of models which employ Chandrasekhar-mass WDs as the progenitors of super-luminous SNe Ia (ones that we would consider possibly SC SNe Ia) have been proposed (Hillebrandt et al. 2007; Sim et al. 2007; Kasen et al. 2008, 2009). These models usually invoke the off-center ignition of a normal WD progenitor which leads to nuclear burning (and thus ^{56}Ni production) that is peaked away from the center of the WD. This off-center nickel blob would increase the observed luminosity if the blob were offset from the center of the WD toward the observer, with the maximum effect occurring when it is offset directly along the line of sight. These viewing angles also lead to the fastest light-curve rise times in such simulations (Sim et al. 2007; Kasen et al. 2008).

Once again, we can compare our observed values for SN 2009dc to the models. Since the nickel blob is offset from the center, asphericity is introduced into the explosion by construction (Kasen et al. 2008). If there is in fact a blob of ^{56}Ni in SN 2009dc and it is offset from the progenitor's center directly along our line of sight (thus maximizing the measured luminosity), then perhaps there is still azimuthal symmetry in the explosion. This may account for the low levels of continuum polarization measured by Tanaka et al. (2010), as well as the higher levels of IME line polarization, but it seems tenuous at best.

Observing along the axis of the offset blob of ^{56}Ni, Hillebrandt et al. (2007) produce light curves that peak at a bolometric magnitude of $M_{\rm bol} \approx -19.9$ mag, Kasen et al. (2008) show light curves that get as bright as $M_B \approx -20$ mag, and Kasen et al. (2009) claim models with luminosities as high as 2.1×10^{43} erg s^{-1}. These brightest magnitudes and luminosities that can be obtained by off-center explosions are nearly equal to our *lower limits* for SN 2009dc (assuming no host-galaxy reddening), and are likely below the true values. Furthermore, we note that the maximum amount of ^{56}Ni obtained from these explosions is 0.9–1.1 $M_\odot$ (Hillebrandt et al. 2007; Kasen et al. 2009), which is once again at the lowest end of our range of calculated values for SN 2009dc.

Finally, as mentioned above, the viewing angles that maximize the observed peak mag-

nitudes also *minimize* the rise time. We find a relatively long rise time of 23 ± 2 d for SN 2009dc, and our first detection of the SN implies that its rise time *must be* >21 d. This is significantly longer than the rise times for these viewing angles as derived from the models (∼12 d and ∼18 d; Hillebrandt et al. 2007; Kasen et al. 2008, respectively). Thus, it seems that none of these models which include a Chandrasekhar-mass WD is viable for SN 2009dc.

It should be mentioned, however, that these models mostly assume expansion velocities of "normal" SNe Ia (e.g. Sim et al. 2007) and we have shown that the expansion velocity of SN 2009dc is significantly lower. This is evident in the synthetic spectra derived from these models; from all viewing angles, they resemble early-time normal SN Ia spectra much more than the spectra of SN 2009dc near maximum brightness (Kasen et al. 2008). Thus, perhaps it is not too surprising that these specific examples of non-SC models do not match the observations of SN 2009dc.

5.5 Conclusions

In this chapter we have presented and analyzed optical photometry and spectra of SN 2009dc and SN 2007if, both of which are possibly SC SNe Ia. Our photometric and spectral data on SN 2009dc constitute one of the richest datasets ever published on a SC SN Ia candidate. Our well-sampled light curve follows SN 2009dc from about 1 week before maximum brightness until about 5 months past maximum, and shows that SN 2009dc is one of the slowest photometrically evolving SNe Ia ever observed. We derive a rise time of 23 d and $\Delta m_{15}(B) = 0.72$ mag, which are two of the most extreme values for these parameters ever seen in a SN Ia. Assuming no host-galaxy reddening, we derive a peak bolometric luminosity of about 2.4×10^{43} erg s^{-1}, though this is almost certainly an underestimate since we observe strong evidence for at lease *some* host reddening. Using our nonzero values for $E(B-V)_{\rm host}$, the peak bolometric luminosity increases by about 40%–200%.

Spectroscopically, SN 2009dc also evolves relatively slowly. Strong C II absorption features (which are rarely observed in SNe Ia) are seen in the spectra near maximum brightness, implying a significant amount of unburned fuel from the progenitor WD in the outer layers of the SN ejecta. Si II absorption also appears in our spectra of SN 2009dc and remains visible even 2 months past maximum. Our post-maximum spectra are dominated by a forest of IGE features and, interestingly, resemble spectra of the peculiar SN Ia 2002cx. Finally, the spectra of SN 2009dc all show very low expansion velocities at all layers (i.e., unburned carbon, IMEs, and IGEs) as compared to other SNe Ia. This may be explained by a massive WD progenitor which consequently has a large binding energy. Even though the expansion velocities are small, we see no strong evidence in SN 2009dc for a velocity "plateau" near maximum light like the one seen in SN 2007if (Scalzo et al. 2010).

Using various luminosity and energy arguments, we calculate that the progenitor of SN 2009dc is possibly a SC WD with a mass greater than ∼2 $M_\odot$, and that at least ∼1 $M_\odot$ of ^{56}Ni was likely formed in the explosion (though the most probable value is in the range 1.4–1.7 $M_\odot$). These values are larger than (or about as large as) those calculated for any

other SN Ia ever observed. We propose that the host galaxy of SN 2009dc underwent a gravitational interaction with a nearby galaxy (UGC 10063) in the relatively recent past, and that this could have induced a sudden burst of star formation which may have given rise to the progenitor of SN 2009dc and turned UGC 10063 into the "post-starburst" galaxy that we observe today. We also compare our observed quantities for SN 2009dc to theoretical models, and while no model seems to match or explain every aspect of SN 2009dc, simulations show that SC WDs with masses near what we calculate for the progenitor of SN 2009dc can possibly form, likely from the merger of two WDs. Furthermore, models of extremely luminous SNe Ia which employ a Chandrasekhar-mass WD progenitor cannot explain our observations of SN 2009dc.

Thus, taking all of these extreme values into account, we conclude that SN 2009dc is very likely a SC SN Ia. As mentioned previously, many of the observed peculiarities of SN 2009dc are also seen in SN 2003fg and SN 2007if. Therefore, we concur with Howell et al. (2006) and Scalzo et al. (2010) that both SN 2003fg and SN 2007if (respectively) are also probably SC SNe Ia. However, given their fairly normal expansion velocities and relative weakness (or even absence) of C II features near maximum brightness, it seems that SN 2006gz and SN 2004gu are less likely to be SC SNe Ia.

New large transient searches such as Pan-STARRS (Kaiser et al. 2002) and the Palomar Transient Factory (Rau et al. 2009; Law et al. 2009) will probably find many SC or other super-luminous SNe Ia in the near future. Since it seems that they cannot be standardized in the same way as most SNe Ia, they will need to be handled separately or ignored in cosmological surveys which will use large numbers of SNe Ia. However, the simulations of Chen & Li (2009) show that donor stars with lower metallicities (e.g., Population II stars) are less likely to form WDs with masses greater than 1.7 $M_{\odot}$ than higher metallicity stars. Thus, it is possible that contamination levels from SC SNe Ia, which are already rare at low redshifts (i.e., average metallicity), may be relatively small in medium or high-redshift surveys.

Bibliography

Abazajian, K. N. et al. 2009, ApJS, 182, 543
Adelman-McCarthy, J. K. et al. 2008, ApJS, 175, 297
Aldering, G., , et al. 2002, in Proceedings of the Society of Photo-Optical Instrumentation Engineers (SPIE) Conference., ed. J. A. Tyson & S. Wolff, Vol. 4836, 61
Altavilla, G. et al. 2009, ApJ, 695, 135
Amanullah, R. et al. 2010, ApJ, 716, 712
Arnett, W. D. 1982, ApJ, 253, 785
Arsenijevic, V., Fabbro, S., Mourão, A. M., & Rica da Silva, A. J. 2008, A&A, 492, 535
Astier, P. et al. 2006, A&A, 447, 31
Axelrod, T. S. 1988, in Atmospheric Diagnostics of Stellar Evolution. Lecture Notes in Physics., ed. K. Nomoto, 375
Bailey, S. et al. 2009, A&A, 500, L17
Barbon, R., Benetti, S., Rosino, L., Cappellaro, E., & Turatto, M. 1990, A&A, 237, 79
Barnes, J. E. & Hernquist, L. E. 1991, ApJ, 370, L65
—. 1996, ApJ, 471, 115
Benetti, S. et al. 2004, MNRAS, 348, 261
—. 2005, ApJ, 623, 1011
Bessell, M. S. 1990, PASP, 102, 1181
Blanton, M. R. & Roweis, S. 2007, AJ, 133, 734
Blanton, M. R. et al. 2003, AJ, 125, 2348
Blondin, S. & Calkins, M. 2008, Central Bureau Electronic Telegrams, 1246, 1
Blondin, S., Mandel, K. S., & Kirshner, R. P. 2011, A&A, 526, A81
Blondin, S. & Tonry, J. L. 2007, ApJ, 666, 1024
Blondin, S. et al. 2006, AJ, 131, 1648
—. 2008, ApJ, 682, 724
Boles, T. & Li, W. 2008, Central Bureau Electronic Telegrams, 1256, 1
Bongard, S., Baron, E., Smadja, G., Branch, D., & Hauschildt, P. H. 2006, ApJ, 647, 513
Brahe, T. 1573, De Nova Stella
Branch, D. 1992, ApJ, 392, 35
Branch, D., Baron, E., Hall, N., Melakayil, M., & Parrent, J. 2005, PASP, 117, 545
Branch, D., Baron, E., Thomas, R. C., Kasen, D., Li, W., & Filippenko, A. V. 2004, PASP, 116, 903

Branch, D., Dang, L. C., & Baron, E. 2009, PASP, 121, 238
Branch, D., Dang, L. C., Hall, N., Ketchum, W., Melakayil, M., Parrent, J., Troxel, M. A., Casebeer, D., Jeffery, D. J., & Baron, E. 2006, PASP, 118, 560
Branch, D. & van den Bergh, S. 1993, AJ, 105, 2231
Branch, D. et al. 2003, AJ, 126, 1489
—. 2008, PASP, 120, 135
Bronder, T. J. et al. 2008, A&A, 477, 717
Cardelli, J. A., Clayton, G. C., & Mathis, J. S. 1989, ApJ, 345, 245
Chen, W. & Li, X. 2009, ApJ, 702, 686
Chornock, R. & Filippenko, A. V. 2008, AJ, 136, 2227
Chornock, R., Filippenko, A. V., Branch, D., Foley, R. J., Jha, S., & Li, W. 2006, PASP, 118, 722
Chotard, N. et al. 2011, A&A, 529, L4
Clocchiatti, A. & Wheeler, J. C. 1997, ApJ, 491, 375
Colgate, S. A. & McKee, C. 1969, ApJ, 157, 623
Conley, A. et al. 2008, ApJ, 681, 482
Contardo, G., Leibundgut, B., & Vacca, W. D. 2000, A&A, 359, 876
Contreras, C. et al. 2010, AJ, 139, 519
de Vaucouleurs, G. et al. 1991, Third Reference Catalogue of Bright Galaxies (New York: Springer)
Domínguez, I., Höflich, P., & Straniero, O. 2001, ApJ, 557, 279
Elias-Rosa, N. et al. 2008, MNRAS, 384, 107
Faber, S. M. et al. 2003, in Proceedings of the Society of Photo-Optical Instrumentation Engineers (SPIE) Conference., ed. M. Iye & A. F. M. Moorwood, Vol. 4841, 1657
Falco, E. E. et al. 1999, PASP, 111, 438
Falcón-Barroso, J. et al. 2004, MNRAS, 350, 35
Filippenko, A. V. 1982, PASP, 94, 715
—. 1988, AJ, 96, 1941
—. 1997, ARA&A, 35, 309
Filippenko, A. V. 2003, in From Twilight to Highlight, ed. W. Hillebrandt & B. Leibundgut (Berlin: Springer-Verlag), 171
Filippenko, A. V. & Coil, A. L. 2000, IAU Circ., 7381
Filippenko, A. V., Li, W. D., Treffers, R. R., & Modjaz, M. 2001, in Small-Telescope Astronomy on Global Scales., ed. B. Paczyński, W. P. Chen, & C. Lemme (San Francisco: Astron. Soc. Pac.), 121
Filippenko, A. V., Matheson, T., & Ho, L. C. 1993, ApJ, 415, L103
Filippenko, A. V. et al. 1992a, ApJ, 384, L15
—. 1992b, AJ, 104, 1543
Fisher, A., Branch, D., Nugent, P., & Baron, E. 1997, ApJ, 481, L89
Folatelli, G. 2004, New Astronomy Reviews, 48, 623
Foley, R. J., Filippenko, A. V., & Jha, S. W. 2008, ApJ, 686, 117

Foley, R. J. & Kasen, D. 2011, ApJ, 729, 55
Foley, R. J., Sanders, N. E., & Kirshner, R. P. 2011, ApJ, accepted (arXiv:1107.3555)
Foley, R. J., Smith, N., Ganeshalingam, M., Li, W., Chornock, R., & Filippenko, A. V. 2007, ApJ, 657, L105
Foley, R. J. et al. 2003, PASP, 115, 1220
—. 2009a, AJ, 138, 376
—. 2009b, AJ, 137, 3731
—. 2010a, ApJ, submitted (arXiv:1010.2749)
—. 2010b, ApJ, 708, L61
—. 2010c, AJ, 140, 1321
Gal-Yam, A., Sand, D., & Leonard, D. 2005, The Astronomer's Telegram, 581, 1
Gallagher, J. S., Garnavich, P. M., Caldwell, N., Kirshner, R. P., Jha, S. W., Li, W., Ganeshalingam, M., & Filippenko, A. V. 2008, ApJ, 685, 752
Ganeshalingam, M. et al. 2010, ApJS, 190, 418
Garavini, G. et al. 2004, AJ, 128, 387
—. 2007, A&A, 470, 411
Gerardy, C. L., Roman, B., & Deglman, F. 2004, IAU Circ., 8343, 3
Germany, L., Sabine, S., Chan, S., Filippenko, A. V., Leonard, D. C., Modjaz, M., & Eastman, R. G. 1998, IAU Circ., 6943, 2
Gómez, G. & López, R. 1998, AJ, 115, 1096
Graham, J. & Foley, R. J. 2004, IAU Circ., 8340, 1
Greggio, L. 2010, MNRAS, 906
Guy, J., Astier, P., Nobili, S., Regnault, N., & Pain, R. 2005, A&A, 443, 781
Guy, J. et al. 2007, A&A, 466, 11
Hachinger, S., Mazzali, P. A., & Benetti, S. 2006, MNRAS, 370, 299
Hamuy, M., Phillips, M. M., Suntzeff, N. B., Schommer, R. A., Maza, J., Smith, R. C., Lira, P., & Aviles, R. 1996a, AJ, 112, 2438
Hamuy, M. et al. 1996b, AJ, 112, 2408
Harutyunyan, A., Elias-Rosa, N., & Benetti, S. 2009, CBET, 1768, 1
Hatano, K., Branch, D., & Deaton, J. 1998, ApJ, 502, 177
Hatano, K., Branch, D., Lentz, E. J., Baron, E., Filippenko, A. V., & Garnavich, P. M. 2000, ApJ, 543, L49
Hayden, B. T. et al. 2010, ApJ, 712, 350
Hicken, M., Garnavich, P. M., Prieto, J. L., Blondin, S., DePoy, D. L., Kirshner, R. P., & Parrent, J. 2007, ApJ, 669, L17
Hicken, M., Wood-Vasey, W. M., Blondin, S., Challis, P., Jha, S., Kelly, P. L., Rest, A., & Kirshner, R. P. 2009a, ApJ, 700, 1097
Hicken, M. et al. 2009b, ApJ, 700, 331
Hillebrandt, W. & Niemeyer, J. C. 2000, ARA&A, 38, 191
Hillebrandt, W., Sim, S. A., & Röpke, F. K. 2007, A&A, 465, L17
Ho, W. C. G., Van Dyk, S. D., Peng, C. Y., Filippenko, A. V., Leonard, D. C., Matheson,

T., Treffers, R. R., & Richmond, M. W. 2001, PASP, 113, 1349
Hook, I. M. et al. 2005, AJ, 130, 2788
Horne, K. 1986, PASP, 98, 609
Howell, D. A. et al. 2006, Nature, 443, 308
—. 2009, ApJ, 691, 661
Hoyle, F. & Fowler, W. A. 1960, ApJ, 132, 565
Iben, Jr., I. & Tutukov, A. V. 1984, ApJS, 54, 335
Ilbert, O. et al. 2006, A&A, 457, 841
James, F. & Roos, M. 1975, Computer Physics Communications, 10, 343
Jeong, H., Bureau, M., Yi, S. K., Krajnović, D., & Davies, R. L. 2007, MNRAS, 376, 1021
Jester, S. et al. 2005, AJ, 130, 873
Jha, S., Branch, D., Chornock, R., Foley, R. J., Li, W., Swift, B. J., Casebeer, D., & Filippenko, A. V. 2006a, AJ, 132, 189
Jha, S., Riess, A. G., & Kirshner, R. P. 2007, ApJ, 659, 122
Jha, S. et al. 2006b, AJ, 131, 527
Kaiser, N. et al. 2002, in Proceedings of the Society of Photo-Optical Instrumentation Engineers (SPIE) Conference., ed. J. A. Tyson & S. Wolff, Vol. 4836, 154
Kasen, D. 2006, ApJ, 649, 939
Kasen, D. & Plewa, T. 2007, ApJ, 662, 459
Kasen, D., Röpke, F. K., & Woosley, S. E. 2009, Nature, 460, 869
Kasen, D., Thomas, R. C., Röpke, F., & Woosley, S. E. 2008, Journal of Physics Conference Series, 125, 012007
Kessler, R. et al. 2009, ApJS, 185, 32
Khokhlov, A., Mueller, E., & Höflich, P. 1993, A&A, 270, 223
Kimeridze, G. N. & Tsvetkov, D. Y. 1991, AZh, 68, 341
Konishi, K. et al. 2011, AJ, submitted (arXiv:1103.2497)
Kowalski, M. et al. 2008, ApJ, 686, 749
Krisciunas, K. et al. 2004a, AJ, 127, 1664
—. 2004b, AJ, 128, 3034
Kuchner, M. J., Kirshner, R. P., Pinto, P. A., & Leibundgut, B. 1994, ApJ, 426, L89
Landolt, A. U. 1983, AJ, 88, 439
—. 1992, AJ, 104, 340
Law, N. M. et al. 2009, PASP, 121, 1395
Leaman, J., Li, W., Chornock, R., & Filippenko, A. V. 2011, MNRAS, 412, 1419
Leibundgut, B. 2000, A&A Rev., 10, 179
Leibundgut, B. et al. 1993, AJ, 105, 301
Leonard, D. C., Li, W., Filippenko, A. V., Foley, R. J., & Chornock, R. 2005, ApJ, 632, 450
Leonard, D. C. et al. 2002, PASP, 114, 35
Li, W. 2001, IAU Circ., 7729
Li, W., Filippenko, A. V., Chornock, R., & Jha, S. 2003a, PASP, 115, 844
Li, W., Filippenko, A. V., & Riess, A. G. 2001a, ApJ, 546, 719

Li, W., Filippenko, A. V., Treffers, R. R., Riess, A. G., Hu, J., & Qiu, Y. 2001b, ApJ, 546, 734
Li, W., Jha, S., Filippenko, A. V., Bloom, J. S., Pooley, D., Foley, R. J., & Perley, D. A. 2006, PASP, 118, 37
Li, W. et al. 2000, in Cosmic Explosions., ed. S. S. Holt & W. W. Zhang (New York: American Institute of Physics), 103
Li, W. et al. 2001c, PASP, 113, 1178
—. 2003b, PASP, 115, 453
—. 2011a, MNRAS, 412, 1441
—. 2011b, MNRAS, 412, 1473
Lira, P. 1996, Master's thesis, Univ. Chile
Lira, P. et al. 1998, AJ, 115, 234
Maeda, K. & Iwamoto, K. 2009, MNRAS, 394, 239
Maeda, K., Kawabata, K., Li, W., Tanaka, M., Mazzali, P. A., Hattori, T., Nomoto, K., & Filippenko, A. V. 2009, ApJ, 690, 1745
Maeda, K., Mazzali, P. A., Deng, J., Nomoto, K., Yoshii, Y., Tomita, H., & Kobayashi, Y. 2003, ApJ, 593, 931
Maeda, K. et al. 2010, Nature, 466, 82
Marion, G. H., Höflich, P., Wheeler, J. C., Robinson, E. L., Gerardy, C. L., & Vacca, W. D. 2006, ApJ, 645, 1392
Marion, H., Garnavich, P., Challis, P., Calkins, M., & Peters, W. 2009, CBET, 1776, 1
Matheson, T., Filippenko, A. V., Ho, L. C., Barth, A. J., & Leonard, D. C. 2000, AJ, 120, 1499
Matheson, T. et al. 2008, AJ, 135, 1598
Maund, J. R. et al. 2010, ApJ, 725, L167
Mazzali, P. A., Cappellaro, E., Danziger, I. J., Turatto, M., & Benetti, S. 1998, ApJ, 499, L49
Mazzali, P. A., Chugai, N., Turatto, M., Lucy, L. B., Danziger, I. J., Cappellaro, E., Della Valle, M., & Benetti, S. 1997, MNRAS, 284, 151
Mazzali, P. A., Danziger, I. J., & Turatto, M. 1995, A&A, 297, 509
Mazzali, P. A. et al. 2005, ApJ, 623, L37
Mihos, J. C. & Hernquist, L. 1994, ApJ, 431, L9
Miknaitis, G. et al. 2007, ApJ, 666, 674
Miller, J. S. & Stone, R. P. S. 1987, Lick Obs. Tech. Rep. 48 (Santa Cruz: Lick Obs.)
—. 1993, Lick Obs. Tech. Rep. 66 (Santa Cruz: Lick Obs.)
Misra, K., Sahu, D. K., Anupama, G. C., & Pandey, K. 2008, MNRAS, 389, 706
Monard, L. A. G., Quimby, R., Gerardy, C., Höflich, P., Wheeler, J. C., Chen, Y., Smith, H. J., & Bauer, A. 2004, IAU Circ., 8454, 1
Moore, M. & Li, W. 2005, Central Bureau Electronic Telegrams, 196, 1
Morganti, R. et al. 2006, MNRAS, 371, 157
Mueller, J. & Filippenko, A. V. 1991, IAU Circ., 5233, 1

Mulchaey, J. & Gladders, M. 2005, LDSS-3 User's Guide (Pasadena: The Carnegie Observatories)
Munari, U. & Zwitter, T. 1997, A&A, 318, 269
Nobili, S. et al. 2005, A&A, 437, 789
Nomoto, K., Thielemann, F.-K., & Yokoi, K. 1984, ApJ, 286, 644
Nordin, J. et al. 2011a, ApJ, 734, 42
—. 2011b, A&A, 526, A119
Nugent, P., Phillips, M., Baron, E., Branch, D., & Hauschildt, P. 1995, ApJ, 455, L147
O'Donnell, J. E. 1994, ApJ, 422, 158
Oke, J. B. 1990, AJ, 99, 1621
Oke, J. B., Cohen, J. G., Carr, M., et al. 1995, PASP, 107, 375
Oke, J. B. & Gunn, J. E. 1982, PASP, 94, 586
—. 1983, ApJ, 266, 713
Östman, L. et al. 2011, A&A, 526, A28
Patat, F., Benetti, S., Cappellaro, E., Danziger, I. J., Della Valle, M., Mazzali, P. A., & Turatto, M. 1996, MNRAS, 278, 111
Patat, F. et al. 2007, Science, 317, 924
Peek, J. E. G. & Graves, G. J. 2010, ApJ, 719, 415
Perlmutter, S. et al. 1999, ApJ, 517, 565
Petrosian, V. 1976, ApJ, 209, L1
Pfannes, J. M. M., Niemeyer, J. C., & Schmidt, W. 2010, A&A, 509, 75
Phillips, A. C., Miller, J., Cowley, D., & Wallace, V. 2006, in Society of Photo-Optical Instrumentation Engineers (SPIE) Conference Series, Vol. 6269, Society of Photo-Optical Instrumentation Engineers (SPIE) Conference Series
Phillips, M. M. 1993, ApJ, 413, L105
Phillips, M. M., Lira, P., Suntzeff, N. B., Schommer, R. A., Hamuy, M., & Maza, J. 1999, AJ, 118, 1766
Phillips, M. M., Wells, L. A., Suntzeff, N. B., Hamuy, M., Leibundgut, B., Kirshner, R. P., & Foltz, C. B. 1992, AJ, 103, 1632
Phillips, M. M. et al. 2007, PASP, 119, 360
Pignata, G. et al. 2008, MNRAS, 388, 971
Piro, A. L. 2008, ApJ, 679, 616
Poggianti, B. M. et al. 2009, ApJ, 693, 112
Pollas, C., Filippenko, A. V., & Matheson, T. 1993, IAU Circ., 5871, 1
Poole, T. S. et al. 2008, MNRAS, 383, 627
Poznanski, D., Gal-Yam, A., Maoz, D., Filippenko, A. V., Leonard, D. C., & Matheson, T. 2002, PASP, 114, 833
Prieto, J. L., Rest, A., & Suntzeff, N. B. 2006, ApJ, 647, 501
Prieto, J. L. et al. 2007, AJ, submitted (arXiv: 0706.4088)
Puckett, T., Gagliano, R., & Orff, T. 2008, Central Bureau Electronic Telegrams, 1241, 1
Puckett, T., George, D., Rest, A., & Krisciunas, K. 2000, IAU Circ., 7362

Puckett, T. & Langoussis, A. 2002, IAU Circ., 7847
Puckett, T., Moore, R., Newton, J., & Orff, T. 2009, CBET, 1762, 1
Rau, A. et al. 2009, PASP, 121, 1334
Riess, A. G., Filippenko, A. V., Li, W., & Schmidt, B. P. 1999a, AJ, 118, 2668
Riess, A. G., Press, W. H., & Kirshner, R. P. 1996, ApJ, 473, 88
Riess, A. G. et al. 1997, AJ, 114, 722
—. 1998, AJ, 116, 1009
—. 1999b, AJ, 117, 707
—. 2007, ApJ, 659, 98
Ruiz-Lapuente, P., Kirshner, R. P., Phillips, M. M., Challis, P. M., Schmidt, B. P., Filippenko, A. V., & Wheeler, J. C. 1995, ApJ, 439, 60
Salvo, M., Schmidt, B., Davis, T., & Sankarankutty, S. 2005, Central Bureau Electronic Telegrams, 199, 1
Savitzky, A. & Golay, M. J. E. 1964, Analytical Chemistry, 36, 1627
Scalzo, R. A. et al. 2010, ApJ, 713, 1073
Schinnerer, E. & Scoville, N. 2002, ApJ, 577, L103
Schlegel, D. J., Finkbeiner, D. P., & Davis, M. 1998, ApJ, 500, 525
Schneider, S. E. et al. 1990, ApJS, 72, 245
Shapiro, K. L. et al. 2010, MNRAS, 92
Sheinis, A. I., Bolte, M., Epps, H. W., Kibrick, R. I., Miller, J. S., Radovan, M. V., Bigelow, B. C., & Sutin, B. M. 2002, PASP, 114, 851
Silverman, J. M., Steele, T. N., Ganeshalingam, M., Lee, N., & Filippenko, A. V. 2008, Central Bureau Electronic Telegrams, 1264, 1
Sim, S. A., Sauer, D. N., Röpke, F. K., & Hillebrandt, W. 2007, MNRAS, 378, 2
Simon, J. D. et al. 2009, ApJ, 702, 1157
Spergel, D. N. et al. 2007, ApJS, 170, 377
Stanishev, V. et al. 2007, A&A, 469, 645
Stritzinger, M. & Leibundgut, B. 2005, A&A, 431, 423
Strolger, L. et al. 2002, AJ, 124, 2905
Suzuki, N. et al. 2011, ApJ, submitted (arXiv:1105.3470)
Tanaka, M. et al. 2008, ApJ, 677, 448
—. 2010, ApJ, 714, 1209
Thomas, R. C. et al. 2007, ApJ, 654, L53
Timmes, F. X., Brown, E. F., & Truran, J. W. 2003, ApJ, 590, L83
Tsvetkov, D. I., Volkov, I. M., Bartunov, O. S., Ikonnikova, N. P., & Kimeridze, G. N. 1990, A&A, 236, 133
Turatto, M. 2003, in Supernovae and Gamma-Ray Bursters., ed. K. Weiler (Berlin: Springer-Verlag), 21
Turatto, M., Benetti, S., & Cappellaro, E. 2003, in From Twilight to Highlight: The Physics of Supernovae., ed. W. Hillebrandt & B. Leibundgut (Berlin: Springer), 200
Turatto, M., Benetti, S., Cappellaro, E., Danziger, I. J., Della Valle, M., Gouiffes, C.,

Mazzali, P. A., & Patat, F. 1996, MNRAS, 283, 1
Valenti, S. et al. 2009, Nature, 459, 674
van der Marel, R. P. & Franx, M. 1993, ApJ, 407, 525
Voss, R. & Nelemans, G. 2008, Nature, 451, 802
Wade, R. A. & Horne, K. 1988, ApJ, 324, 411
Walker, E. S. et al. 2011, MNRAS, 410, 1262
Wang, L., Baade, D., Höflich, P., Wheeler, J. C., Kawabata, K., Khokhlov, A., Nomoto, K., & Patat, F. 2006, ApJ, 653, 490
Wang, L., Baade, D., & Patat, F. 2007, Science, 315, 212
Wang, X. et al. 2008, ApJ, 675, 626
—. 2009a, ApJ, 699, L139
—. 2009b, ApJ, 697, 380
Webbink, R. F. 1984, ApJ, 277, 355
Wegner, G. & Grogin, N. A. 2008, AJ, 136, 1
Weijmans, A., Krajnović, D., van de Ven, G., Oosterloo, T. A., Morganti, R., & de Zeeuw, P. T. 2008, MNRAS, 383, 1343
Wells, L. A. et al. 1994, AJ, 108, 2233
Whelan, J. & Iben, Jr., I. 1973, ApJ, 186, 1007
Wood-Vasey, W. M. et al. 2007, ApJ, 666, 694
—. 2008, ApJ, 689, 377
Yamanaka, M. et al. 2009, ApJ, 707, L118
Yoon, S. & Langer, N. 2005, A&A, 435, 967
Yoon, S., Podsiadlowski, P., & Rosswog, S. 2007, MNRAS, 380, 933
Zhang, T. et al. 2010, PASP, 122, 1